

GEOPHYSICAL FLUID MECHANICS

VOLUME 2

MECHANICS AND THERMODYNAMICS OF FLUID FLOWS

Stephen.M.Griffies@gmail.com

Princeton University Atmospheric and Oceanic Sciences

Draft from January 12, 2026



COPYRIGHT ©2025 BY STEPHEN M. GRIFFIES

ALL RIGHTS RESERVED

GRIFFIES, STEPHEN M., 1962-

GEOPHYSICAL FLUID MECHANICS

THIS BOOK WAS TYPESET USING LATEX.

CONTENTS

	Page
PREFACE	vii
GUIDE TO THIS BOOK	xvii
o PROLOGUE: CONTINUUM APPROXIMATION	1
Part I. Kinematics	13
1 FUNDAMENTALS OF FLUID KINEMATICS	17
2 MOTION AND DEFORMATION	47
3 MASS CONSERVATION	87
4 MATERIAL TRACER CONSERVATION	115
5 NON-DIVERGENT FLOWS	139
Part II. Thermodynamics	161
6 EQUILIBRIUM THERMODYNAMICS	165
7 THERMODYNAMICS WITH A GEOPOTENTIAL	209
Part III. Dynamics	231
8 MOMENTUM	235
9 STRESS	261
10 ENERGY AND ENTROPY	301
11 HYDROSTATIC FLOWS	349
12 PRESSURE FORM STRESS	381
13 BOUSSINESQ OCEAN	407
14 BUOYANCY	461
15 GEOSTROPHY AND THERMAL WIND	503
16 TANGENT PLANE FLOWS	531
17 EKMAN MECHANICS	547

Part IV. End matter	573
A GLOSSARY OF CONCEPTS AND TERMS	575
B LIST OF ACRONYMS	621
C LIST OF SYMBOLS	623
BIBLIOGRAPHY	633
INDEX	647

CONTENTS

PREFACE

Geophysical fluid mechanics (GFM) is a branch of theoretical physics concerned with natural fluid motion on a rotating and gravitating planet or star. The subject makes use of concepts from classical continuum mechanics and thermodynamics, along with the corresponding methods of mathematical physics. The primary inspiration for our study comes from the motion of fluids in the earth's atmosphere and ocean, though the principles and methods are also applicable to extra-terrestrial fluid flows. Geophysical fluids are in near rigid-body motion with the rotating planet, thus prompting a description from the rotating (non-inertial) planetary reference frame. Body forces from gravity plus planetary rotation (Coriolis and centrifugal) are fundamental features of the motion, as are contact forces from stresses (pressure and friction). In this book, we limit attention to the motion of a single phase of matter (gas or liquid), with the study of multiphase geophysical fluid mechanics, which is relevant to a moist atmosphere, outside our scope. Electromagnetic forces, important for the study of astrophysical fluid motions, are also ignored. We also ignore chemical reactions (which transform matter from one form to another), and nuclear reactions (which convert between matter and nuclear energy).

Geophysical fluid flows manifest over a huge range of space and time scales, with linear and nonlinear interactions transferring information across these scales. Physical insights into such flows typically result from examining a hierarchy of conceptual models using a variety of methods and perspectives. Some of the models we consider are formulated within the context of a **perfect fluid** comprising a single material constituent with fundamental processes limited to the reversible and mechanical. Other models are posed using a **real fluid** that is comprised of multiple matter constituents exposed to an **irreversible process** such as mixing of momentum through viscous friction, mixing of matter through matter diffusion, and/or the mixing of enthalpy through conduction. Some models consider constant density fluids, as commonly considered in classical **hydrodynamics**. And some models ignore rotation, thus tacitly applying to flows with length scales too short to feel the planetary Coriolis acceleration, whereas others ignore buoyancy to thus focus on the dynamics of a homogeneous fluid in a rotating reference frame.

We develop geophysical fluid mechanics from a mathematical physics perspective, with a grounding in fundamentals offering a robust and versatile framework for exploring a gamut of special cases and approximations. Topics are approached by establishing general principles prior to the examination of case studies. Consistent with this approach, our treatment focuses on developing the mechanics of geophysical fluid motion, with that focus supporting theoretical explorations that often extend beyond that required for phenomenological purposes. Correspondingly, we embrace the opportunity to examine physics through multiple lenses that render a variety of complementary insights. In a nutshell, if a physical system can be formulated and analyzed in more than one way, then we do so if it enhances pedagogy and exposes layers of understanding. As a result, brevity is sacrificed to support exposition and exploration, with this perspective leading to a book with multiple volumes.

The presentation is based on the premise that skills in theoretical physics are optimally taught by nurturing physical reasoning, with physical reasoning supported by mathematical precision coupled to the elucidation of concepts using words and pictures. Correspondingly, the presentation is both deductive and descriptive. The deductive approach supports a precise understanding through the use of elementary physical notions that are expressed mathematically. The descriptive approach builds skills in reasoning along with the ability to articulate physical ideas using words and pictures that complement the maths. Readers are supported by development of salient physical concepts and mathematical methods in the process of building understanding. With sufficient study, the material in this book should be accessible to the advanced undergraduate student or entering graduate student in fields such as applied mathematics, astrophysics, atmospheric physics, engineering, geophysics, ocean physics, planetary physics, and theoretical physics.

We generally offer details to mathematical derivations. Doing so nurtures the mathematical skills required for the budding theorist, with the reader strongly encouraged to work through the various derivations and exercises to fully embrace each detail and concept. Exposing mathematical details also helps to unpack many of the physical concepts encapsulated by equations. It is notable that the concepts encountered in this book generally accord with common experience (we are doing classical physics), thus affording a means to check on the validity of the maths. Even so, it does take time to wrap one's head around the physics of large-scale ocean and atmosphere circulations, so patience and persistence are required. Furthermore, as we are studying physics, all mathematical equations must satisfy dimensional consistency, with this constraint offering the physicist a powerful tool for exposing spurious mathematical statements.

We consider this book to be an intellectual journey taken together by the author and reader, thus motivating use of the first person plural pronouns *we* and *us*. Furthermore, we cultivate the deductive and descriptive approaches by embracing the synergism between physics and maths, whereby physics informs the maths and maths reveals the physics. This synergism is facilitated by a presentation style inspired by [Mermin \(1989\)](#), who identified the following characteristics for clear presentations of mathematical physics.

- RULE 1: All displayed equations are given numbers to facilitate cross-referencing. Additionally, any equation supporting another equation or a discussion is itself afforded an equation number.
- RULE 2: Cross-referenced equations are referred to by their equation number as well as descriptive phrases or names (e.g., “as seen by the vector-invariant velocity equation XX.YY” rather than just “as seen by equation XX.YY”). Coupling maths to words supports learning and reduces the need to flip pages to view the cited equation.
- RULE 3: Equations are part of the prose and are thus subject to punctuation.

Concerning the book’s title

The study of rotating and stratified geophysical fluid motion largely started in the first half of the 20th century. During recent decades, the study has seen particular evolution through deepening physical foundations, refining mathematical formulations, increasing the intellectual and predictive value of numerical simulations, extending applications across terrestrial and planetary systems, and expanding observational and laboratory measurements and techniques.

What has emerged is a recognition that a fruitful study of rotating and stratified fluid flows makes use of ideas that go beyond the traditional notions of **geophysical fluid dynamics** (GFD). Rather, the contemporary practitioner develops insights by weaving together concepts and tools from mathematics, Newtonian mechanics, analytical mechanics, fluid mechanics, thermodynamics, classical scalar field theory, numerical simulations, laboratory experiments, field measurements, and data science. Acknowledging this broadening of the practice motivates the term *mechanics* in this book's title, rather than the more focused *dynamics*. It is a minor change in verbiage that reflects a broadening of the perspectives and goals pursued here.

Two pillars of theoretical geophysical fluid mechanics

We conceive of two pillars to theoretical geophysical fluid mechanics that are synergistic, thus offering lessons, guidance, and feedback to the other. The **elements pillar** of geophysical fluid mechanics comprises the physical and mathematical formulation of conceptual models used to garner insight into rotating and stratified fluid motion. This pillar is concerned with setting the stage by deductively and descriptively exposing how physical concepts are mathematically expressed to describe geophysical fluid flows. We provide a thorough treatment of the element pillar given its foundational importance, and since it is commonly offered only a terse treatment in other presentations. We emphasize that the elements pillar is far more than equation manipulation, although one certainly must become adept at that task. Instead, at its core, the elements pillar allows the physicist to reveal the fundamental physical concepts in a precise mathematical manner. Doing so supports understanding while building the foundations for the **emergent phenomena pillar**. The emergent phenomena pillar of geophysical fluid mechanics studies solutions to equations that describe phenomena, such as waves, instabilities, turbulence, and general circulation, all of which emerge from the fundamental equations. Phenomena can emerge in manners that are far from simple to understand deductively, particularly when considering nonlinear behavior such as turbulence. Our treatment of the emergent pillar is limited to waves and instabilities, whereas turbulence and general circulation are beyond our scope, though we do touch upon these topics where suited to the discussion.¹

Some themes found in this book

This multi-volume book covers a number of topics in theoretical geophysical fluid mechanics. Throughout, we encounter a number of themes that appear in various guises, with the following offering a brief survey.

Causation and budgets

A great deal of this book is concerned with deriving and understanding equations that describe the evolution of fluid properties, with such equations (differential or integral) derived from physical principles such as Newton's laws of motion, Hamilton's principle of stationary action, Noether's theorem, thermodynamic laws, mass conservation, and vorticity mechanics. These **budget equations** form the theoretical foundation of continuum mechanics. As part of this development we often seek information about what *causes* fluid motion, making use of a variety of kinematic and mathematical frameworks. The causality question is nicely posed by Newton's

¹The further one moves along the axis of nonlinearity, the more Sisyphean the task of connecting fundamental processes to emergent phenomena. This perspective is lucidly discussed by [Anderson \(1972\)](#).

equation of motion, which says that acceleration (motion) arises from a net force (the cause of motion). Even though seemingly a clear decomposition of cause and effect, this fundamental statement of Newtonian mechanics offers little more than the definition of a force. We break the self-referential loop, and thus make physical progress, after specifying the nature of the force (e.g., gravitational, frictional), as well as by offering properties of these forces as per Newton's third law (the action/reaction law).²

In geophysical fluid mechanics, we sometimes refer to a time evolving budget equation as an **evolution equation** or, more commonly, a **prognostic equation**, with each term in the prognostic equation referred to as a **time tendency**.³ For prognostic equations, knowledge of the processes contributing to the net time tendency enables a prediction of flow properties. The question arises how to practically determine the tendencies acting in the fluid, particularly when tendencies are generally dependent on the flow itself. This question is often very difficult to answer. Such is the complexity and beauty inherent in nonlinear field theories such as fluid mechanics, where cause and effect are intrinsically coupled.

We can sometimes make progress by turning the problem around, whereby kinematic knowledge of the motion offers inferential knowledge of the dynamical processes contributing to the motion. This situation is exemplified by pressure forces acting within a non-divergent flow whereby pressure provides the force that acts, instantaneously and globally, to maintain the constraint that the velocity is non-divergent.⁴ We may also make use of constraints that restrict the flow in manners that assist in prediction and understanding.

Constraints

Determining the forces, either directly or indirectly, provides physical insight into the cause of fluid flow and its changes. This approach is sometimes referred to a **momentum based viewpoint** since it is based on working directly with the momentum equation (i.e., Newton's second law of motion). However, we are commonly unable to deduce the forces due to complexities inherent in nonlinear field theories. Furthermore, there are many occasions when we are simply uninterested in the forces. In these cases, we are motivated to use constraints that can allow us to sidestep forces but still garner insights into the motion.

One example of a constraint concerns the inability of fluid to flow through a solid static material boundary, such as the solid-earth boundary encountered by geophysical flows. To understand how this constraint impacts the macroscopic fluid motion, we do not need to understand details of the atomic forces that underlie the resistance to macroscopic motion. Instead, we simply impose the kinematic boundary condition whereby the component of the velocity that is normal to the boundary vanishes at the boundary. The forces active within the fluid, no matter what flavor they may take, are constrained to respect the kinematic boundary condition. Another example concerns the study of vorticity. A variety of vorticity constraints offer the means to deduce flow properties without determining forces. Indeed, the **vorticity based viewpoint** often provides a framework that is more versatile in practice than the momentum-based approach, thus prompting the importance of vortex mechanics in the study of geophysical fluid flows.

²For more on this perspective of Newton's laws, see Chapter 1 of *Symon* (1971) or Chapter 2 of *Marion and Thornton* (1988).

³This language has its origins in weather forecasting.

⁴For non-divergent flow, pressure acts as the *Lagrange multiplier* enforcing flow non-divergence.

Associations and balances

Besides seeking causal relations pointing toward the future, many basic questions of fluid mechanics arise either instantaneously, as in the constraints maintaining non-divergent flows, or when the flow is steady, in which case properties at each point in space have no time dependence. In steady flows, the net acceleration, and hence the net force, vanish at each point within the fluid, although the fluid itself can still be moving (steady flows are not necessarily static). For steady flows we are unconcerned with causality since time changes have been removed. In this manner, a steady state equation is a [diagnostic equation](#) rather than a [prognostic equation](#). Diagnostic equations thus provide mechanical statements about associations between physical processes that manifest as balances. The [geostrophic balance](#) is the canonical association in geophysical fluid mechanics, where the horizontal Coriolis force is balanced by the horizontal pressure gradient force. Another balance concerns the vertical pressure gradient and its near balance with the weight of fluid above a point in the fluid, with this [hydrostatic balance](#) approximately maintained at the large scale even for moving geophysical fluids. Further associations arise when studying steady vorticity balances, with the [Sverdrup balance](#) a key example that is commonly used in ocean circulation theory.

We summarize the above by saying that diagnostic equations are concerned with the way things are, whereas prognostic equations point to how things will be. So although a predictive theory requires prognostic equations that manifest causal relations, an understanding of how fluid motion appears, and in particular how it is constrained, is revealed by studying diagnostic relations that expose associations through balances.

Mathematical transformations between kinematic perspectives

Geophysical fluid flows are complex. Hence, it proves useful to avail ourselves of a variety of methods and perspectives that support a mechanistic description of the motion. Many methods are associated with distinct kinematic lenses that reveal particular facets of the flow that might be less visible using alternative lenses. Examples include the Eulerian (spatial) and Lagrangian (material) kinematics used throughout fluid mechanics; the dual position space (x -space) and wavevector space (k -space) used for wave mechanics; the variety of vertical coordinates used for vertically stratified flows; and the analysis of motion in property spaces exemplified by watermass or thermodynamic analysis. We make use of these perspectives throughout this book, and offer the mathematical tools (e.g., tensor methods) needed to transform between them.

Newtonian mechanics and Hamilton's principle

Throughout this book we pursue the maxim

PURSUE ALL WAYS TO FORMULATE AND TO SOLVE A PROBLEM.

A canonical example concerns the complementary perspectives available from Newtonian mechanics and Hamilton's principle of stationary action. Each offers logically consistent results yet approaches mechanics from fundamentally distinct conceptual and operational perspectives. In a Newtonian approach to fluid mechanics, governing differential equations are formulated using a continuum version of Newton's law of motion, in which forces (causes) and accelerations (effects) are articulated as a means to understand and predict the flow. The alternative approach of Hamilton's principle of stationary action approaches mechanics via a variational formulation involving the [action](#). Hamilton's principle says that the action functional is extremized by

the physically realized system. The action is the space-time integral of the difference between kinetic and potential/internal energies, and by extremizing the action we reveal the governing Euler-Lagrange differential equations. The Euler-Lagrange equations are identical to Newton's equations for those cases where Newton's equations are available,⁵ and yet the route to deriving these equations is very distinct. It is by pursuing these distinct paths that we uncover new insights and develop distinct tools for analysis.

Hamilton's principle is not typically covered in fluid mechanics books. This absence contrasts to the ubiquity of Hamilton's principle in other areas of physics. We include facets of Hamilton's principle in this book with the hope that doing so partially remedies the disconnect.⁶ Furthermore, we include Hamilton's principle since it provides novel perspectives on the fundamental equations of geophysical fluid mechanics, and renders insights and tools for the study of emergent phenomena such as waves and instabilities. The reader interested in a serious pursuit of theoretical mechanics should, at some point, make friends with Hamilton's principle. The effort is nontrivial as it requires brain muscles not exercised when studying Newtonian mechanics. But the conceptual and technical payoff is significant.

Non-dimensionalization and scale analysis

Mathematical symbols describing a physical system generally have physical dimensions. Examining the physical dimensions of an equation supports an understanding of the physical content of the equation, and provides a powerful means to identify errors in mathematical manipulations. It is for this reason that we prefer to expose physical dimensions throughout this book, rather than the alternative approach of working predominantly with non-dimensional equations. Even so, scale analysis, as realized through [non-dimensionalization](#), offers an essential tool for deriving mathematical equations used to describe particular flow regimes.

There are two general types of dimensional scales that we use to non-dimensionalize a mathematical physics equation. The first is the [external scale](#), with examples in this book being the gravitational acceleration, Coriolis parameter, and specified properties of the background state such as the buoyancy frequency or prescribed flow. External scales are set by the geophysical parameter regime in which the flow occurs, and as such they are under direct control of the theorist or experimentalist. The second is the [emergent scale](#), which emerges from the flow itself. Emergent scales, such as the length scale and velocity scale of the flow, are specified by the subjective interest of the theorist though these scales are not under direct control. That is, we choose to focus on flows with a particular scale for purposes of examining the corresponding equations that describe that flow regime. A key example concerns our study of planetary geostrophy and quasi-geostrophy, where we choose to focus on flows of a particular scale where the Coriolis acceleration is of leading order importance.

We thus consider the operational aspects of scale analysis to be largely subjective in nature. Namely, we approach the analysis with a subjective bias towards the flow regime of interest, which in turn affects choices for non-dimensional parameters that lead to the corresponding

⁵Hamilton's principle yields the Maxwell's equations of electromagnetism, and yet Maxwell's equations are distinct from Newton's equations. Indeed, Hamilton's principle is used throughout modern physics in areas far beyond Newtonian mechanics.

⁶There certainly are examples where Hamilton's principle is discussed in fluid mechanics books, with [Salmon \(1998\)](#), [Olbers et al. \(2012\)](#), and [Badin and Crisciani \(2018\)](#) notable examples that have inspired this author. Even so, these books remain the exception rather than the norm. As a result, the broader geophysical fluid mechanics community, even those pursuing theoretical aspects, are largely unaware of the beauty and power of Hamilton's principle. This situation contrasts to nearly every other area of mechanics, in which Hamilton's principle is central to both theory and application.

asymptotic equations that describe the regime. Hence, scale analysis is deductive while being strongly guided by our subjective interests.

Geophysical Fluid Mechanics and Climate Science

Fluid mechanics has a history of applications that span science and engineering, from blood flow to the evolution of galaxies. A key 21st century application of geophysical fluid mechanics concerns the questions of earth system science associated with the uncontrolled greenhouse gas experiment pursued by industrialized civilization's carbon centered energy use. Leading order science questions about climate warming have been sufficiently addressed to recognize that the planet has reached a crisis point threatening many features of the biosphere. Even so, mechanistic answers to a number of questions remain at the cutting edge of research. What will happen to the atmospheric jet stream and storm tracks in a world without summer Arctic sea ice? Will tropical storms be more powerful in a warmer world? What are the patterns for coastal sea level rise and their connections to large-scale ocean circulation? What are the key processes acting to bring relatively warm ocean waters to the base of high latitude ice shelves? How stable are the ocean and atmosphere's large-scale overturning circulations and their associated heat transport? Are there feasible and sustainable climate intervention options that equitably reduce the negative impacts of climate warming without introducing new problems? These questions, and countless others, constitute key intellectual challenges of climate science in particular and Earth system science more generally.

Numerical circulation models, observational field campaigns (both *in situ* and remote), and laboratory experiments, are core platforms for Earth system science. Many of these platforms have reached a level of maturity allowing them to vividly reveal details of the complex and multi-scaled nature of planetary fluid flow. Geophysical fluid mechanics is key to the design of observational field campaigns and novel laboratory and numerical experiments, and it provides the intellectual framework for developing mechanistic analyses and robust interpretations of measurements and simulations. In this way, geophysical fluid mechanics furthers predictive capability for weather and climate forecast systems and it enhances confidence in projections for future climate. In a world of increasingly large volumes of simulated and measured data, we conjecture that the marriage of fundamental physical theory to data science tools will enable the significant science and engineering advances needed to address key questions of Earth system science.

About the cover

I took the cover photo of an iceberg, ocean, clouds, and sea bird (can you find the bird?) in the Orkney Passage region of the Southern Ocean during a research cruise from March-May 2017 aboard the British ship James Clark Ross. I am grateful to Alberto Naveira Garabato, the chief scientist on this cruise, for taking me to this amazing part of the planet. Although I largely pursue theoretical research, experiences with seagoing field research have greatly enhanced my scientific viewpoint and profoundly deepened a connection to the natural forces and phenomena that are in part described by geophysical fluid mechanics.

Gratitudes

This book greatly benefited from interactions with students in the Princeton University Atmospheric and Oceanic Sciences Program. In particular, parts of this book served as the basis for my teaching, over many years, a two-semester graduate course, AOS 571 and AOS 572. It also supported a variety of special topic classes (AOS/GEO 585) and lecture series. Further inspiration was offered by students, postdocs, and fellow researchers and scholars encountered on my path. I also thank those who provided specific suggestions, corrections, and comments on various drafts of this book, whose names are too many to list.

I am grateful for having been part of the unique research and learning environment cultivated by three of the world's best examples of scientific enterprises. First and foremost, I am the product of NOAA's Geophysical Fluid Dynamics Laboratory (GFDL), where I worked as a research physicist from 1996 until 2025. As part of my life as a US federal research scientist, I was fortunate to also be associated with Princeton University's Atmospheric and Oceanic Sciences (AOS) program, where I was a postdoc from 1993-1996 and then a faculty member from 2014-2026. As of 2026, I entered the most recent (hopefully not the final!) part of my career journey as a CNRS research scientist in Paris, a position offering an amazing, and humbling, level of intellectual freedom. Throughout my career, I have focused research concerns on ocean physics and the ocean's role in climate, and I have pursued this research from the perspective garnered from the theoretical physics, applied maths, and chemical engineering training of my undergraduate and graduate education.

The communities at GFDL, Princeton AOS, and CNRS provide an ideal setting for those interested in broadening scientific perspectives while diving deep into particular research areas. As part of my research and mentoring in this community, I have encountered thinkers whose style, questions, and insights have taken root in my work. This work has also afforded me the opportunity to travel the world to interact with colleagues whose wisdom and love of the scientific endeavor are infectious and inspiring. Throughout these interactions, I have entered into trusting and non-judgmental spaces where deep learning and understanding arise. Partaking in these spaces, where heart and mind meld, has been among the most fulfilling experiences of my life.

Developing a book of this nature is not a simple endeavor. It starts modestly, grows over time, and eventually becomes a passion and obsession. I was particularly drawn to writing during the COVID-19 pandemic that kept the world largely sequestered at home, and I am grateful that my life situation allowed for this work to safely flourish during what were otherwise very difficult times for civilization. Writing this book has been an exercise in rational thought that exemplifies the maxim "to write is to learn", as articulated by [Zinnser \(1993\)](#). It was furthermore fed by spiritual food from meditation, yoga, family, and community. In particular, each step was supported by my wife, Adi, and our son, Francisco. I am deeply grateful for their patience and trust as I satisfied the goal of writing this book through countless nights, weekends, and holidays. I treasure being part of our family and I dedicate this work to you two amazing human beings.

Caveats and limitations

This book remains a work in progress that is not yet ready for publication. There are many loose threads detailed at the start of various chapters. In addition, here are items targeted for completion prior to release of this book to a publisher.

-
- Wave mechanics
 - equatorial shallow water waves
 - Rossby wave packets and motion in non-homogeneous background
 - Shallow water waves on a rotating sphere, including Laplace's tidal equations, Hough functions, and spherical harmonics
 - Ray theory using Hamilton's principle as in [Tracy et al. \(2014\)](#)
 - Flow stability
 - Charney problem of baroclinic instability
 - Arnold's stability theorem
 - Rayleigh-Benard convection
 - Application of Hamilton's principle
 - Referential flow using Hamilton's principle
 - shallow water and Hamilton's principle
 - semi-geostrophy and Hamilton's principle
 - quasi-geostrophy and Hamilton's principle
 - waves and mean flow interactions
 - Mathematical topics
 - Lie derivative following Section F.3 of [Tromp \(2025a\)](#)



GUIDE TO THIS BOOK

No book is an island, with this book generously making use of other books, review articles, research papers, and online tutorials. Many readers find value in studying a subject from a variety of perspectives and voices, thus justifying the proliferation of books with overlapping subject matter. Sometimes it is merely one or two sentences that allow for an idea or concept to click within the reader's brain, whereas other topics require the full gamut of detailed derivations and discussions coming from multiple voices. For these reasons we provide pointers to written and/or video presentations that offer supportive views on material in this book. Many further resources are available through a quick internet search or consultation with artificial intelligence (AI).

There is no pretense that any reader will study all topics in this multi-volume book. This recognition is particularly apparent in a world where research and educational agendas often spread rather than focus attention. Hence, an attempt has been made to facilitate picking up each book at a variety of starting points. For that purpose, each chapter is written in a reasonably self-contained manner and with a brief guide at the start of each chapter listing pre-requisite material. As such, some equations and derivations are reproduced in more than one place, thus obviating the need to back reference. Certainly each chapter cannot be fully self-contained, since this is a book with material building from other chapters across the volumes. We thus make generous use of cross-referencing to point out allied material treated elsewhere. We also make extensive use of the glossary to help define concepts accessed in one volume that might be more thoroughly treated in another volume.



Organization

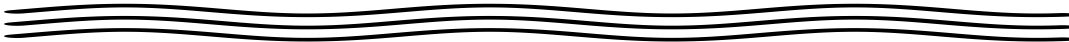
This book contains five volumes, each of which comprises parts that have multiple chapters. Parts and chapters start with a brief guide to the material along with pointers to dependencies. The book's end matter includes a glossary of key concepts and terms. Items highlighted within the text identify terms with a glossary entry. The glossary also serves as an annotated index, with page numbers pointing to where the terms and concepts are examined within a particular volume. Indeed, the glossary is an essential means to navigate this multi-volume book, reducing (though not eliminating) the need to have more than one volume open at a time. The glossary is then followed by a list of acronyms⁷ and then by a list of symbols. A bibliography follows, with pages listed for where the book or paper is cited. We close the book with an index.

Not all topics are treated equally, with some probed deeply whereas others are given relatively superficial treatment. Indeed, there are many topics omitted that arguably should

⁷We generally try to avoid acronyms, but some are inevitable.

find a home here. Each shortcoming reflects on the author's limited energy and experience rather than a judgement of relative importance.

Cross-referencing to specific sections and equations is provided when pointing to material within the same volume. Cross-referencing material in other volumes is less specific. In many cases, a cross-reference concerns an item in the glossary and/or index, which can be consulted across volumes to help make the connection.



Volume 1

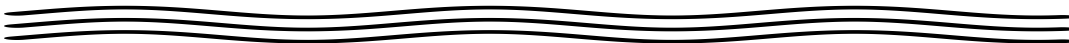
VOLUME 1 establishes foundations in mathematical physics and classical mechanics.

Mathematical physics

We start the book with a suite of mathematical methods chapters. Many readers can skim these chapters without sacrificing too much from later chapters, assuming they have a working knowledge of Cartesian tensors as well as vector differential and integral calculus. Where unfamiliar mathematics topics arise in later chapters, the reader is encouraged to return to this part of the book to help develop the necessary skills.

Classical mechanics

We here survey salient topics from classical mechanics with a geophysical perspective, and in turn develop concepts and methods that have direct relevance to the continuum physics of geophysical fluid flows. Of particular note, this part develops an understanding of physics as viewed from a rotating reference frame. Doing so allows for the sometimes non-intuitive results of rotating physics to be developed within the context of a particle system as a pedagogical preface to later developments for geophysical fluid motion.



Volume 2

VOLUME 2 treats the fundamentals of fluid mechanics with an emphasis on geophysical fluid mechanics.

Kinematics of fluid flow

Mechanics is comprised of kinematics (the study of intrinsic properties of motion) and dynamics (the study of forces and energies causing motion). In the fluid kinematics part of this book, we initiate a study of fluid mechanics by focusing on the kinematics of fluid flow and matter transported by that flow. Our treatment exposes both the Eulerian and Lagrangian viewpoints and emphasizes the variety of kinematic notions and tools key to describing fluid motion. We also encounter facets of material transport as described by the tracer equation. We emphasize that fluid flow, and the transport of matter within that flow, have many features that are fundamentally distinct from point particle and rigid body motion. It takes practice to intellectually digest these differences.

Some kinematic topics can seem esoteric on first encounter, particularly the study of Lagrangian kinematics. However, an incomplete understanding of fluid kinematics can lead to difficulties appreciating facets of fluid dynamics. The reader is thus encouraged to fully study the kinematics chapters, and to revisit the material as the needs arise in later chapters.

Thermodynamics

We study the rudiments of thermodynamics with a focus on topics arising in the study of geophysical fluids. We pay particular attention to the role of gravity in modifying the treatment of thermodynamic equilibrium states, with gravity an essential facet of geophysical fluids and yet a force that is commonly ignored in standard treatments of thermodynamics. We ignore phase transitions, which is a notable limitation of our treatment, thus making this part of the book a mere introduction to the study of a moist atmosphere or an ocean with sea ice.

Dynamics of geophysical fluid flow

In this lengthy part of the book, we study how Newton's laws of mechanics and the principles of thermodynamics are applied to continuum fluid motion on a rotating and gravitating planet. We approach the subject by focusing on how forces that act on fluid elements lead to accelerations and thus to motion. In particular, we examine **body forces** that act throughout the volume of a fluid element (e.g., planetary gravity, planetary Coriolis, and planetary centrifugal) as well as **contact forces** that act on the boundary of a fluid element (e.g., pressure and friction).



Volume 3

Shallow water mechanics

A shallow water fluid is comprised of hydrostatically balanced homogeneous fluid layers. The layers are also typically assumed to be immiscible, so that interactions between layers occur only via mechanical forces from pressure acting at the layer interfaces. The shallow water fluid allows us to focus on planetary rotation and vertical stratification without the complexities of vertically continuous stratification and thermodynamics. Many physical insights garnered by studying shallow water fluids extend to more realistic fluids, thus making the shallow water model very popular among theorists and teachers. Indeed, [Zeitlin \(2018\)](#) provides an example of just how far one can go in understanding geophysical fluids with shallow water theory.

Vorticity

Vorticity plays a role in the motion of all geophysical fluids since motion on a rotating planet provides a nonzero **planetary vorticity** even to fluids at rest on the planet. This feature of geophysical fluids contrasts to many other areas of fluid mechanics, where irrotational flows are commonly encountered. **Potential vorticity** is a strategically chosen component of the vorticity vector that melds mechanics (vorticity) to thermodynamics (stratification). Material conservation properties of potential vorticity are striking and render important constraints on fluid motion. Indeed, perhaps the most practical reason to study vorticity concerns the various constraints imposed on the flow moving on a rotating and gravitating planet. These constraints provide conceptual insights and predictive power.

Nearly geostrophic balanced flows

Balanced models generally remove the horizontally divergent motions associated with gravity waves, thus allowing a focus on the large-scale vortical motions. Balanced models have a rich history among theoretical geophysical fluid studies, providing insights into both laminar oceanic flows through planetary geostrophy, and wave-turbulent atmospheric and oceanic flows through quasi-geostrophy. When studying balanced models, we focus on the shallow water and continuously stratified versions of quasi-geostrophy and planetary geostrophy.



Volume 4

Generalized vertical coordinates

The chapters on **generalized vertical coordinate (GVC)s (GVC)** dive into the maths, kinematics, dynamics, and applications of such coordinates for the study of geophysical fluid mechanics. This material is central to many current research activities, including subgrid scale parameterizations and the design of numerical atmosphere and ocean models. The mathematics in this part leans heavily on the general tensors studied in VOLUME 1. Even so, many readers can make the most of these chapter without the full gamut of general tensors.

Scalar fields

Many chapters target the mechanics of scalar fields with a focus mostly on the ocean. Here we consider active tracers (temperature and salinity), passive tracers, and buoyancy. Much of this study forms the basis of tracer mechanics, which has proven very important for the ocean since it is generally very difficult to measure vector fields such as velocity and vorticity, whereas tracer distributions are far more readily measured. We also consider facets of sea level analysis in this part of the book.

Hamilton's principle for geophysical flows

We study the analytical mechanics of geophysical flows using Hamilton's principle. This material forms the heart of field theory, both classical and quantum. It requires a different set of techniques than used in the study of Newtonian fluid mechanics used elsewhere in this book. Hence, it offers complementary insights that deepen our understanding of geophysical fluid flows in particular.



Volume 5

Linear wave mechanics

We study a variety of geophysical waves and associated mathematical methods used for their characterization. Notably, we consider waves not commonly included in a book on geophysical fluids, such as sound and capillary waves, with these waves included due to their ubiquity in the natural environment as well as their pedagogical value. Most focus, however, is given to waves arising from the Coriolis acceleration (inertial waves, planetary Rossby waves, topographic

Rossby waves) and gravitational acceleration (surface gravity waves, internal gravity waves). Furthermore, we study linear waves and their corresponding wave packets, first studying their behavior in a homogeneous background environment where Fourier methods are available. Thereafter, we introduce methods needed to study linear waves on a gently varying background, including the methods of geometrical optics and wave action, with these methods of use particularly when Fourier methods are not suited.

Flow instabilities

We study instabilities that arise in geophysical fluid motions, distinguishing two classes of fluid instabilities: **local instabilities** or **parcel instabilities** versus **global instabilities** or **wave instabilities**. Local instabilities are afforded a local necessary and sufficient condition to determine whether the fluid base state is unstable to perturbations. In contrast, global instabilities arise from the constructive interference of waves and so involve the solution of an eigenvalue problem to determine properties of unstable waves. At most, a necessary condition can be derived to determine whether a global instability exists. Our study of fluid instabilities introduces a suite of case studies that foster analysis and conceptual methods to establish a foundation for further study. Geophysical fluid instability analysis remains an active area of research, with insights into the suite of primary and secondary instabilities providing compelling stories for how the ocean and atmosphere work.



Pointers on written and spoken communication

To thrive in research and teaching requires one to master elements of both written and spoken communication. Here are a few pointers for the student interested in furthering these skills.

CLEAR THINKING LEADS TO CLEAR COMMUNICATION

Clear communication is the sign of clear thinking. Some people communicate better in writing, where one has the opportunity to carefully organize thoughts and refine the writing. Others are better at speaking, where spontaneous and interactive reflections and experiences can bolster the clarity of a presentation.

As inspiration for both the clear and obscure, pick up a textbook or lecture notes and analyze the presentation for clarity. Where is the presentation confusing? Where is the material crystal clear? Then pick up a journal article and perform the same analysis. What is appealing? What is unappealing? Then go to the internet and find a science or engineering lecture, old or new. What makes the speaker engaging and clear, or boring and obscure?

EMPATHY IS KEY

Empathy is a basic facet of effective communication and teaching, where the writer, speaker, or teacher places their mind inside that of an interested and smart reader or listener. Identify with their quest to understand new ideas and to comprehend the foundations and assumptions. Are the assumptions justified based on the audience? How compelling is the scientific story? Are missing steps crucial to understanding or easily dispensed with for streamlining the presentation?

Although poor communication hinders our ability to digest new ideas and concepts, it is also important to appreciate that some material is tough no matter how well it is communicated. We should aim to make a subject matter as simple as possible, but not simpler (paraphrasing Einstein). Furthermore, it sometimes takes a few generations of teaching before some scientific material can be sufficiently digested to allow for the core conceptual nuggets to be revealed. As an example, try reading Newton or Maxwell's original works as compared to a modern presentation of Classical Mechanics or Electromagnetism. So as we strive for clear communication, we cannot presume that clarity is sufficient to remove the struggles everyone experiences when learning.

Additionally, it is essential to recognize that everyone makes mistakes, either in fundamentals or practices. The toughest part of making mistakes is often the self-imposed shame and embarrassment. However, mistakes offer significant opportunities for learning and advancing, with honesty and humility critical for identifying weaknesses, both in our own work and those of others.



Pointers on physics problem solving

We conclude each chapter with a suite of exercises. Working through these exercises, in full detail, is an integral part of learning and doing physics. Indeed, there is no replacement for struggle and head-scratching to support the physics problem-solving brain muscle. However, with the advent of AI tools, one can readily access AI generated solutions. It goes without saying that over-reliance on AI tools greatly compromises one's ability to develop the skills necessary to know whether the AI solution is correct. In light of this situation, we provide some worked solutions, which generally go beyond what is expected from a student learning the material for the first time, as we aim for the solutions to be instructional as well as utilitarian. For this reason, we expose many of the intermediate steps needed to derive a solution, further supporting an in-depth learning of how to independently solve physics problems. Additionally, it helps to identify when an incorrect result follows from a physical/conceptual error (e.g., incorrect setup of the problem solution) or a mathematical error (e.g., sign error).

We observe that most people are not born with *a priori* physics problem solving skills. Rather, it takes extensive practice to develop the necessary brain muscle. The student who values the ability to solve physics problems should resist the temptation to quickly flip pages to read solutions. Time pondering an exercise is time well spent learning how to do theoretical physics in a manner needed to pursue novel research. In the remainder of this section we offer specific pointers of use when diving into a physics problem.

CHECK FOR DIMENSIONAL CONSISTENCY

The symbols we use in mathematical physics correspond to geometrical objects (e.g., points, vectors, tensors) describing a physical concept (e.g., position in space, velocity, temperature, angular momentum, stress). Hence, the symbols generally carry physical dimensions. The physical dimensions we are concerned with in this book are length (L), time (T), mass (M), and temperature. We do not consider electromagnetism or the quantum mechanical world. Physical dimensions of the equations must be self-consistent. For example, if one writes an equation $A = B$, where A and B have different physical dimensions, then the equation makes no physical

sense. Something is wrong. Although not always sufficient to uncover errors, dimensional analysis is an incredibly powerful necessary step in debugging the maths.

CHECK FOR TENSORIAL CONSISTENCY

In the same way that mathematical equations in physics need to maintain dimensional consistency, they must also respect tensor rules. For example, the equation $A = B$ makes mathematical sense if A and B are both scalars. Likewise, $\mathbf{A} = \mathbf{B}$ makes sense if \mathbf{A} and \mathbf{B} are both vectors. However, if both \mathbf{A} and \mathbf{B} are vectors, then the equation $\mathbf{A} = \nabla \cdot \mathbf{B}$ does not make sense because the left hand side is a vector and the right hand side is a scalar. A more subtle example is when \mathbf{A} is a vector yet \mathbf{B} is an axial vector. In this case, \mathbf{A} remains invariant under a change from right hand to left hand coordinates whereas \mathbf{B} flips sign. Maintaining basic tensorial rules can be considered the next level of sophistication beyond dimensional analysis.

USE WORDS AND PICTURES

Words and pictures are important elements in explaining a physical concept and/or a problem in physics. Hence, it is good practice to liberally sprinkle sentences in between the key equations for the purpose of explaining what the maths means using clear English. Here are some practical payoffs to the student for this style of presentation.

- The process of explaining the maths using words and pictures requires one to dive deeper into the logic of a physics problem. Doing so often reveals weak points, incomplete or unmentioned assumptions, and errors. This process is a very important learning stage in preparing to stand in front of an audience to present results and to answer questions. It is a key facet of research and teaching.
- Physics teachers are often more forgiving of math errors if you convince the teacher that you have a sensible physical understanding of the problem. Plain English and pictures are very useful means for this purpose.

THERE IS OFTEN MORE THAN ONE PATH TO A SOLUTION

In physics, there is often more than one path to a problem solution or to the formulation of a concept. Pursuing distinct paths offers novel physical and mathematical insights, exposes otherwise hidden assumptions, and allows one to double-check the veracity of a solution. Some of the most profound advances in physics came from pursuing distinct formulations. One example concerns the distinct formulation of mechanics offered by Newton (1642-1746), and then later by Lagrange (1736-1813) and then Hamilton (1805-1865). Had Lagrange or Hamilton rested on the merits of their predecessors, we may well have had a very different intellectual evolution of 19th and 20th century physics.



Chapter 0

PROLOGUE: CONTINUUM APPROXIMATION

In this chapter we briefly motivate the use of a space and time continuous description of fluid mechanics, thus supporting the continuum approximation for the study of macroscopic phenomena. Section 2.4 of [Pride \(2025\)](#) proposes that the “continuously distributed macroscopic fields of continuum mechanics are defined by going to any point, \mathbf{x} , and adding up (averaging) the molecular behavior in a volumetric region that surrounds that point.” In contrast, the pre-atomic interpretation of continuum mechanics is based on considering matter as a space-filling material media that is smooth and continuously divisible. Although the molecular interpretation adds insights into the nature of forces in many areas of continuum mechanics, such as elasticity (e.g., see [Pride \(2025\)](#)), we retain space-filling perspective in our formulations of geophysical fluid mechanics.

READER’S GUIDE TO THIS CHAPTER

One goal in this chapter is to unpack the dictum *macroscopically small yet microscopically large*, which summarizes the regime assumed when formulating the equations of continuum mechanics. For this purpose, we borrow from the kinetic theory of gases as treated in statistical physics books such as [Reif \(1965\)](#) and [Huang \(1987\)](#). Alternative treatments are given in chapter 1 of [Salmon \(1998\)](#) and chapter 2 of [Pride \(2025\)](#). Our treatment is heuristic and brief, with a more deductive treatment falling outside our scope. We return to elements of this chapter in VOLUME 2 when studying [local thermodynamic equilibrium](#). Together, the continuum approximation and the hypothesis of local thermodynamic equilibrium form two foundational elements of continuum mechanics.

0.1	Introduction to the continuum approximation	2
0.2	A variety of length scales	3
0.2.1	Macroscopic and microscopic length scales	3
0.2.2	Fields at each space point	4
0.2.3	Reynolds number and the macroscopic length scale	5
0.2.4	Resolution of measurements and simulations	6
0.2.5	Fields at each time instance	6
0.2.6	The Deborah number	6
0.2.7	Comments	7
0.3	Results from kinetic theory	7
0.3.1	A mole and Avogadro’s number	7
0.3.2	Ideal gas law	8
0.3.3	Molecular mean free path	9
0.3.4	Root mean square molecular speed	9
0.3.5	Time scales for molecular collisions	10

0.3.6	Macroscopically small and microscopically large	10
0.3.7	Further study	11

0.1 Introduction to the continuum approximation

Ordinary gases and liquids are canonical examples of fluids, with gases filling any container with its molecules widely separated, whereas molecules in liquids are much closer together so that liquids are far less compressible than gases. Viewed macroscopically, a fluid is mechanically characterized by deforming continuously when applying a tangential or shearing stress, so that a fluid has no preferred shape.¹ Consequently, a fluid responds to a shearing stress by flowing. Even so, fluids can maintain their shape when experiencing a bulk compression, otherwise known as a **normal stress**, with liquids and gases generally distinguished by their very different compressibilities.

For geophysical fluid mechanics, we are concerned with the atmosphere (mostly a gas) and the ocean (mostly a liquid). We are furthermore interested in macroscopic properties of fluid motion, with no interest in describing molecular degrees of freedom. Nor do we consider rarefied gas dynamics, which is a subject appropriate for the upper bounds of the atmosphere where pressures are relatively low and the molecular mean free path relatively large. For these reasons we pursue a phenomenological approach that makes use of conservation laws describing the motion of a continuous fluid media. This treatment is based on the **continuum approximation**, which assumes that mathematical limits for fluid volumes tending to zero are reached on length and time scales very large compared to molecular space and time scales. The temporal realization of the continuum approximation is based on recognizing that macroscopic motion associated with fluid flows (e.g., advection, waves, and mixing) evolves with time scales far longer than the time scales of molecular motions. Hence, from a macroscopic perspective, we assume that all fluid motions are continuous in both space and time.

The huge space and time scale separation that supports the continuum approximation allows us to make use of differential calculus for describing the mechanics of fluid motion. That is, the continuum approximation makes fluid mechanics a continuous field theory, thus sitting within the broader discipline of **continuum mechanics**. Correspondingly, the differential laws describing fluid motion are partial differential equations. Even so, it must be admitted that the equations of continuum mechanics are motivated by the continuum approximation rather than deductively resulting from it. That is, a deductive derivation of continuum field theory, starting from molecular dynamics, is nontrivial even for an ideal gas, and largely non-existent for liquids. For our purpose, we remain satisfied to postulate that a continuum description is suited for the fluid mechanics of atmosphere and ocean flows, and to examine the postulate *a posteriori* via experimental measurements. Centuries of experiments with fluid motions in the environment and laboratory lend credence to the continuum description. We consider these tests to offer sufficient motivation to use continuum mechanics as the foundation for our study of geophysical fluid mechanics.

¹A stress is a force per area, and a shearing or tangential stress gives rise to fluid acceleration that causes fluid elements to deform.

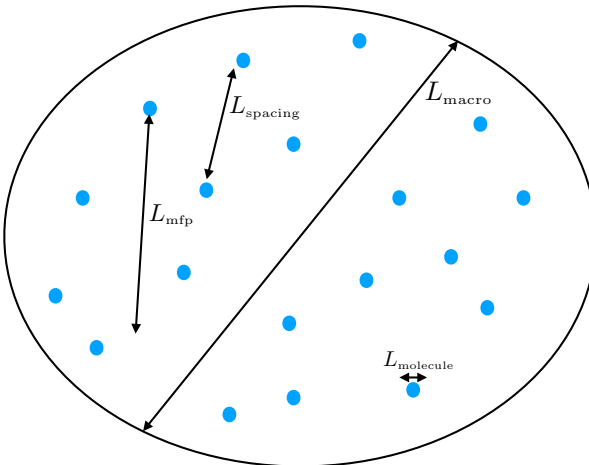


FIGURE 0.1: Schematic to illustrate the length scales considered when making the continuum approximation. The blue circles represent molecules with diameter L_{molecule} . On average, molecules are separated by a spacing, L_{spacing} , that is much larger than the size of the molecule. The mean free path, L_{mfp} , is the average distance a molecule travels between collisions with other molecules, with L_{mfp} generally larger than L_{molecule} since the mean free path takes into account the trajectory of a molecule between collisions, rather than just its immediate neighbors. The smallest macroscopic length scale for fluid flow is denoted L_{macro} . There is no objective value for L_{macro} , though for our purposes we assume it is on the order of $L_{\text{macro}} \sim 10^{-4}$ m, which corresponds roughly to the precision of a flow measurement using typical fluid mechanical laboratory instruments. In this case, $L_{\text{macro}} \approx 10^3 L_{\text{mfp}}$ for an ideal gas at standard conditions. A region of air with volume L_{macro}^3 contains roughly 10^{13} air molecules, whereas that same volume contains roughly 10^{16} water molecules. For either case, the Law of Large Numbers greatly helps in taking the continuum limit. Note that this schematic is not drawn to scale!

0.2 A variety of length scales

Matter is comprised of molecules. However, fluid mechanics is not concerned with the motion of individual molecular degrees of freedom. Rather, fluid mechanics is concerned with phenomenological conservation laws describing the flow of a continuous fluid material. In this section we outline certain properties of matter that motivate the continuum approximation and the corresponding study of continuum mechanics. More details are offered in Section 0.3, although a full discussion is outside the purview of fluid mechanics, with interested readers encouraged to penetrate the literature in statistical physics and kinetic theory.

0.2.1 Macroscopic and microscopic length scales

In fluid mechanics, as in other areas of continuum mechanics, we are concerned with the motion of matter over geometric scales that have a lower bound that is macroscopically small (e.g., $L_{\text{macro}} \sim 10^{-4}$ m) yet microscopically large (e.g., $L_{\text{macro}} \gg L_{\text{mfp}} \sim 10^{-7}$ m, where L_{mfp} is the molecular mean free path). For example, a region of air with volume L_{macro}^3 contains roughly 10^{13} air molecules at standard temperature ($T_{\text{stand}} = 0^\circ\text{C} = 273.15$ K) and standard atmospheric pressure ($p_{\text{stand}} = 101.325 \times 10^3$ Pa), whereas that same volume contains roughly 10^{16} water molecules. These numbers illustrate the notions of macroscopically small yet microscopically large. That is, a macroscopically small region, which provides a lower bound for the precision of flow measurements, generally contains an enormous number of microscopic molecules. It is only when reaching length scales on the order of the molecular mean free path that we need to be concerned with the discrete nature of matter. Figure 0.1 offers a schematic to illustrate these distinct length scales.

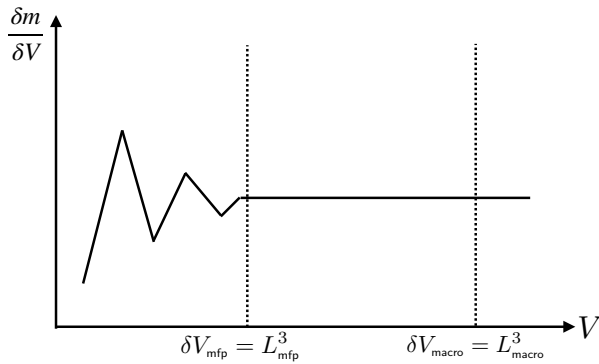


FIGURE 0.2: The measurement of mass density of a fluid becomes erratic for volumes smaller than that determined by the molecular mean free path, L_{mfp}^3 . For the fluid mechanical study of fluid motion, we are concerned with length scales much larger than the mean free path, $L_{\text{macro}} \gg L_{\text{mfp}}$, in which case the mass density is a smooth function of space and time. This figure is adapted from Figure 1.2.1 of [Batchelor \(1967\)](#).

0.2.2 Fields at each space point

When measured on length scales of the mean free path, material properties exhibit very large fluctuations on time scales of order $L_{\text{mfp}}/v_{\text{rms}}$, where v_{rms} is the root-mean-square speed of a fluid molecule (see Section 0.3.4). However, on macroscopic scales encompassing many molecular degrees of freedom, fluid matter appears continuous in both space and time. The incredibly large number of molecules within a macroscopically tiny region motivates our assumption that physical properties are homogeneous over regions of size L_{macro} . For our purposes, this **continuum approximation** works with macroscopically small but finite sized fluid elements whose mean dynamical properties (e.g., velocity, vorticity) and thermodynamical properties (e.g., mass density, matter concentration, temperature, pressure, specific entropy) are defined at each point within the continuous fluid media and at each time instance. As a result, we assume that any differential space increment, δx , has a magnitude on the order of L_{macro} , even though we make use of differential calculus and its associated infinitesimals.

Let us be a bit more precise by considering the measurement of mass density for a prescribed region of fluid, δV . To compute the mass density we take the ratio of the mass of fluid in the region, δm , to the region volume. When the region volume is macroscopic, and thus contains many molecules, we can maintain a relatively fixed mass for this region since molecular fluctuations have a relatively tiny effect on δm . Correspondingly, we can maintain a precise measurement of the mass density, $\delta m/\delta V$. However, when the volume of the region becomes microscopic, whereby it has a volume on the order of $\delta V \sim L_{\text{mfp}}^3$, then molecular fluctuations generally lead to a relatively large fluctuation in the region's mass. We thus lose the notion of a smooth and continuous mass density when the volume approaches that set by the molecular mean free path. This situation is depicted in Figure 0.2.

The ratio of the molecular mean free path to the macroscopic length scale is known as the **Knudsen number**

$$\text{Kn} = \frac{L_{\text{mfp}}}{L_{\text{macro}}}. \quad (0.1)$$

For this book, we are concerned with fluid conditions where the mean free path is microscopic so that the Knudsen number is tiny

$$\text{Kn} \ll 1. \quad (0.2)$$

For tiny Knudsen numbers, we are led to make use of the continuum approximation. The continuum approximation allows us to employ fluid properties that take values at each point

within a space and time continuum, (\mathbf{x}, t) . For example, we make use of the mass density, $\rho(\mathbf{x}, t)$, fluid velocity, $\mathbf{v}(\mathbf{x}, t)$, pressure $p(\mathbf{x}, t)$, temperature $T(\mathbf{x}, t)$, tracer concentration, $C(\mathbf{x}, t)$, and other fields.

We contrast the above to the study of a rarefied gas, such as in the outer reaches of the earth's atmosphere. With a relatively small number density of molecules, rarefied gases have macroscopic mean free paths so that there are relatively few molecular collisions in a given time increment. Correspondingly, a rarefied gas is far from thermodynamic equilibrium and the continuum approximation is not well suited to its description.

0.2.3 Reynolds number and the macroscopic length scale

The continuum field equations of fluid mechanics are formally established for fluid motions with length scales on the order of L_{macro} and larger. We stated earlier that L_{macro} is on the order of 10^{-4} m, with that length loosely based on noting that most macroscopic measurements in a fluid cannot distinguish flow features smaller than a millimetre. We here describe another means to determine L_{macro} .

Namely, we set L_{macro} to the length scale at which the Reynolds number is order unity

$$\text{Re}_{\text{macro}} = \frac{U L_{\text{macro}}}{\nu} \sim 1. \quad (0.3)$$

In this equation, $\nu > 0$ is the kinematic viscosity (with dimensions squared length per time), which is a property of the fluid. The velocity scale, U , is set by the scale for a macroscopic fluid velocity fluctuation relative to some mean flow velocity. The Reynolds number measures the ratio of inertial accelerations (accelerations felt by fluid elements) to frictional accelerations from viscous forces (forces due to the rubbing of fluid elements against one another in the presence of viscosity). When the Reynolds number is on the order of unity, viscous forces play a leading role in the acceleration of the fluid. Furthermore, at this scale the viscous accelerations serve to dissipate kinetic energy of the macroscopic motion, with this dissipation a particularly important process in fluid turbulence. We are thus motivated to define L_{macro} as the length scale where viscosity is of leading order importance.

The **kinematic viscosity** is the ratio of the **dynamic viscosity** and the mass density. For air, the kinematic viscosity is (page 75 of [Gill \(1982\)](#))

$$\nu_{\text{air}} = \frac{1.7 \times 10^{-5} \text{ kg m}^{-1} \text{ s}^{-1}}{1.3 \text{ kg m}^{-3}} = 1.3 \times 10^{-5} \text{ m}^2 \text{ s}^{-1}, \quad (0.4)$$

and a typical fluid velocity fluctuation has a scale 10^{-1} m s $^{-1}$, so that

$$L_{\text{macro}} \approx 10^{-4} \text{ m} = 0.1 \text{ mm}. \quad (0.5)$$

Water has a kinematic viscosity (page 75 of [Gill \(1982\)](#))

$$\nu_{\text{water}} = \frac{10^{-3} \text{ kg m}^{-1} \text{ s}^{-1}}{1000 \text{ kg m}^{-3}} \approx 10^{-6} \text{ m}^2 \text{ s}^{-1}, \quad (0.6)$$

and a fluid velocity fluctuation about 10 times smaller than air. Hence, the macroscopic length scale for water is on the order of that for air, both of which are roughly 10^{-4} m. We are thus further compelled to consider the macroscopic length scale to be on the order 10^{-4} m and larger.

0.2.4 Resolution of measurements and simulations

When we measure fluid motions in the laboratory or field, we generally do not measure the motions at scales on the order of $L_{\text{macro}} \approx 10^{-4}$ m. Rather, our measurement devices generally have a spatial resolution coarser than L_{macro} , so that $L_{\text{measure}} \gg L_{\text{macro}}$. Likewise, numerical simulations are generally designed using discrete grids with length scales $L_{\text{numerical}} \gg L_{\text{macro}}$. The equations describing motions at the measurement/simulation length scales involve effects from fluctuations occurring at the smaller (unmeasured) scales. The reason for this coupling is that the fluid equations are nonlinear, and with the nonlinearities leading to an interaction across spatial scales. These fluctuations, generally associated with turbulent or chaotic motions, have statistical correlations that can play a role, sometimes a dominant role, in the evolution of flow features at the measured/simulated scales. The parameterization of these correlations in terms of measured/simulated motions constitutes the **turbulence closure** problem. We do not study turbulence closure in this book though we do identify the role of turbulence at certain points.

It is important to acknowledge the limited ability of macroscopic measurements to accurately characterize fine scale motions. For this purpose define a gradient length scale

$$L_{\text{gradient}} = \frac{|\mathbf{v}|}{|\nabla \mathbf{v}|}, \quad (0.7)$$

where \mathbf{v} is the velocity of a fluid element relative to some mean velocity, and $|\nabla \mathbf{v}|$ is the magnitude of velocity gradients. Decomposing fluctuations into Fourier modes allows us to see that an accurate measurement of velocity fluctuations with length scales L_{gradient} requires a measurement length scale that satisfies

$$2\pi L_{\text{measure}} \leq L_{\text{gradient}}. \quad (0.8)$$

This constraint means that to measure velocity fluctuations on a scale L_{gradient} requires a finer measurement sampling with $L_{\text{measure}} = L_{\text{gradient}}/(2\pi)$. Note that this discussion of length scales transfers seamlessly over to time scales through dividing the length scale by the velocity scale. Correspondingly, fluctuations with time scales shorter than $2\pi T_{\text{measure}}$ cannot be accurately measured.

0.2.5 Fields at each time instance

The continuum approximation means that fields are defined at every point in the space continuum and at each time in the time continuum. As motivation for the time continuum, we note that there are a huge number of molecular collisions per second, with molecules moving at incredibly high speeds (see Section 0.3 for some numbers). There are added features of the continuous time assumption that are best studied as part of the hypothesis of **local thermodynamic equilibrium** in VOLUME 2.

0.2.6 The Deborah number

Although the focus of this book concerns the atmosphere and ocean, which are clearly fluids, it is useful to mention that not all materials clearly fit into the category of solid or fluid. For example, in geophysics we encounter frozen materials within the cryosphere and rocky material as part of the crust and deeper earth interior. Both materials appear quite hard and solid from human perspectives, and yet they flow over longer time scales and as such they are not rigid solids.

We are led to recognize that the characterization of whether a material is a solid or fluid depends on the time scale of the macroscopic observation, t_{observe} , versus the time scale for the internal relaxations within the material, t_{relax} . The ratio of these two time scales is referred to as the **Deborah number**²

$$\text{Db} = \frac{t_{\text{relax}}}{t_{\text{observe}}}. \quad (0.9)$$

For the fluid mechanics considered in this book, we are concerned with tiny Deborah numbers, in which the relaxation time scales are determined by the relatively rapid molecular collisions that take place on time scales of order 10^{-10} s (see Section 0.3.5), whereas the observation time scales are determined by macroscopic deformations that are $\approx 10^0$ s, so that

$$\text{Db} \ll 1 \implies \text{viscous fluid.} \quad (0.10)$$

In contrast, for many geophysical materials, as well as polymers encountered in material science, the relaxation time scales are relatively large, in which case the Deborah number can be order unity or even larger

$$\text{Db} = \begin{cases} \mathcal{O}(1) & \implies \text{viscoelastic material} \\ \gg 1 & \implies \text{elastic solid.} \end{cases} \quad (0.11)$$

0.2.7 Comments

Alternative methods to compute the length scales are provided In Section 1.2 of [Lautrup \(2005\)](#), thus pointing to the somewhat non-specific nature of these estimates. Even so, the main point for purposes of the continuum approximation remains unchange. Namely, there is a vast scale difference between microscopic and macroscopic, with interests in the macroscopic behavior of matter fully motivating use of the continuum approximation.

0.3 Results from kinetic theory

This section outlines results from the kinetic theory of ideal gases to support the continuum approximation. Deductive treatments that transition from molecular mechanics to macroscopic fluid mechanics is a topic of the kinetic theory of gases and liquids, which is outside our scope. In Section 0.3.7, we provide literature pointers for those wishing more rigor.

0.3.1 A mole and Avogadro's number

There are a tremendous number of molecules in the tiniest drop of water or puff of air. Just how many? To answer this question, we introduce the notion of a **mole** of matter, where a mole is defined as the mass of a material substance that contains **Avogadro's number** of that substance, with

$$A^v = 6.022 \times 10^{23} \text{ mole}^{-1}. \quad (0.12)$$

Avogadro's number, A^v , is the proportionality constant converting from one molar mass of a substance to the mass of a substance. Avogadro's number is conventionally specified so that one mole of the carbon isotope, ^{12}C , contains exactly 12 grams. Hence, 12 grams of ^{12}C contains 6.022×10^{23} atoms of ^{12}C . Avogadro's number provides a connection between scales active in the microscopic world of atoms and molecules to the macroscopic world.

²See [Reiner \(1964\)](#) for the Biblical origins of the Deborah number.

Dry air (air with no water vapor) is comprised of oxygen molecules, O_2 , at roughly 22% by molecular mass, and nitrogen molecules, N_2 , at roughly 78% molecular mass.³ The molar mass of dry air is thus

$$M^{\text{air}} = 0.22 * 32 \text{ g mole}^{-1} + 0.78 * 28 \text{ g mole}^{-1} \approx 28.8 \text{ g mole}^{-1}. \quad (0.13)$$

Pure (fresh) water is comprised of two hydrogen atoms and one oxygen atom. The molar mass of pure water is thus given by

$$M^{\text{water}} = 2 * 1 \text{ g mole}^{-1} + 16 \text{ g mole}^{-1} = 18 \text{ g mole}^{-1}. \quad (0.14)$$

0.3.2 Ideal gas law

The **ideal gas law** is given by

$$pV = n^{\text{mole}} R^g T, \quad (0.15)$$

where p is the pressure, V is the volume, n^{mole} is the number of moles, R^g is the universal gas constant,⁴ and T is the absolute or thermodynamic temperature (temperature relative to absolute zero). Measuring the temperature in Kelvin leads to the universal gas constant

$$R^g = 8.314 \text{ J mole}^{-1} \text{ K}^{-1} = 8.314 \text{ kg m}^2 \text{ s}^{-2} \text{ mole}^{-1} \text{ K}^{-1}, \quad (0.16)$$

where the second equality replaced the energy unit, Joule, by its MKS equivalent,

$$\text{J} = \text{kg m}^2 \text{ s}^{-2}. \quad (0.17)$$

Use of the ideal gas law (0.15) says that one mole of ideal gas at standard temperature ($T_{\text{stand}} = 0^\circ\text{C} = 273.15 \text{ K}$) and standard atmospheric pressure ($p_{\text{stand}} = 101.325 \times 10^3 \text{ Pa}$) occupies the following volume

$$V = \frac{n^{\text{mole}} R^g T_{\text{stand}}}{p_{\text{stand}}} \quad (0.18a)$$

$$= \frac{(1 \text{ mole})(8.314 \text{ kg m}^2 \text{ s}^{-2} \text{ mole}^{-1} \text{ K}^{-1})(273.15 \text{ K})}{101.325 \times 10^3 \text{ kg m}^{-1} \text{ s}^{-2}} \quad (0.18b)$$

$$\approx 2.25 \times 10^{-2} \text{ m}^3, \quad (0.18c)$$

where we introduced the MKS units for pressure (force per unit area)

$$\text{Pa} = \text{N m}^{-2} = \text{kg m}^{-1} \text{ s}^{-2}. \quad (0.19)$$

Hence, the number density (number of molecules per volume) for a mole of ideal gas is given by

$$n^{\text{gas}} = \frac{\text{number per mole}}{\text{volume per mole}} \quad (0.20a)$$

$$= \frac{A^v}{V} \quad (0.20b)$$

³We here ignore the presence of other trace gases, such as CO_2 and H_2O , although these gases are critical for understanding atmospheric radiation and hence the earth's energy budget.

⁴We write R^g rather than the more conventional, R , to distinguish from R commonly used in this book for the radius of a sphere.

$$= \frac{6.022 \times 10^{23}}{2.25 \times 10^{-2} \text{ m}^3} \quad (0.20\text{c})$$

$$= 2.68 \times 10^{25} \text{ m}^{-3}. \quad (0.20\text{d})$$

Specializing to air, we compute the mass density of air at standard temperature and pressure as

$$\rho^{\text{air}} = \frac{M^{\text{air}}}{V} = \frac{28.8 \times 10^{-3} \text{ kg}}{2.25 \times 10^{-2} \text{ m}^3} = 1.28 \text{ kg m}^{-3}, \quad (0.21)$$

where we set $M^{\text{air}} = 28.8 \times 10^{-3}$ kg according to equation (0.13). This ideal gas density is close to the 1.225 kg m^{-3} density measured for air at standard conditions, thus supporting use of the ideal gas law for dry air. Differences arise from trace constituents in air as well as inter-molecular forces (an ideal gas assumes zero inter-molecular forces).

0.3.3 Molecular mean free path

We are in search of length scales relevant for molecular motion. One length scale is that of the molecule itself. Another is set by the average distance between molecules. Finally, we may consider the distance between molecular collisions, with the molecular mean free path the mean distance that a molecule travels before colliding with another molecule. The mean free path is generally larger than the average molecular distance since for molecules to collide requires their trajectories to intersect, and that generally happens over a distance larger than the averaged molecular distance.

Arguments from kinetic theory of gases, applied to an ideal gas, lead to the expression

$$L_{\text{mfp}} = \frac{1}{\pi \sqrt{2} n^{\text{gas}} d^2} \quad (0.22)$$

where d is the diameter of the molecule. The mean diameter of air molecules is roughly

$$d_{\text{molecule air}} \approx 2 \times 10^{-10} \text{ m}. \quad (0.23)$$

Hence, the mean free path for air molecules at standard temperature and pressure is

$$L_{\text{mfp}} = \frac{1}{\pi \sqrt{2} n^{\text{gas}} d_{\text{molecule air}}^2} \quad (0.24\text{a})$$

$$= \frac{1}{\pi \sqrt{2} (2.68 \times 10^{25} \text{ m}^{-3}) (2 \times 10^{-10} \text{ m})^2} \quad (0.24\text{b})$$

$$= 2 \times 10^{-7} \text{ m}. \quad (0.24\text{c})$$

The mean free path for an air molecule is roughly 1000 times larger than the molecular diameter (e.g., Figure 0.1).

0.3.4 Root mean square molecular speed

What is the mean speed for molecules moving through a gas? Again, kinetic theory for ideal gases offers an explicit expression, here written in terms of the pressure and density of the gas

$$v_{\text{rms}} = \sqrt{\frac{3p}{\rho}} = \sqrt{\frac{3R^g T}{M}}. \quad (0.25)$$

Note the direct relation between pressure, temperature, and speed. That is, molecules move faster at higher temperature, and thus impart larger pressure on their surrounding environment. At standard pressure and temperature, the root-mean-square speed for an air molecule is given by

$$v_{\text{rms}} = \sqrt{\frac{3 p_{\text{stand}}}{\rho^{\text{air}}}} \quad (0.26\text{a})$$

$$= \sqrt{\frac{3 (101.325 \times 10^3 \text{ kg m}^{-1} \text{ s}^{-2})}{1.28 \text{ kg m}^{-3}}} \quad (0.26\text{b})$$

$$= 487 \text{ m s}^{-1}. \quad (0.26\text{c})$$

To get a sense for the relative scale of this speed, note that the speed of sound in air at standard temperature and pressure is 331 m s^{-1} . So these molecules are moving faster than sound! These speeds are correspondingly much higher than the speeds typical for fluid elements in the atmosphere and ocean.

0.3.5 Time scales for molecular collisions

Assuming one collision occurs within a mean free path, and the molecules are moving at the root-mean-square speed, we can estimate the time between collision according to

$$t_{\text{collision}} = \frac{L_{\text{mfp}}}{v_{\text{rms}}} \quad (0.27)$$

The corresponding time for air is given by

$$t_{\text{air}} = \frac{2 \times 10^{-7} \text{ m}}{487 \text{ m s}^{-1}} = 4.1 \times 10^{-10} \text{ s}. \quad (0.28)$$

Inverting this number, we see that there are roughly $t_{\text{air}}^{-1} = 2.5 \times 10^9 \text{ s}^{-1}$ collisions per second. The huge number of molecular collisions per second means that for all macroscopic processes, including highly turbulent geophysical fluid flow, the dynamical time scales for the macroscopic motion are many orders of magnitude longer than the time scales for molecular motions.

0.3.6 Macroscopically small and microscopically large

For environmental measurements of the atmosphere and ocean, or for conventional measurements in laboratories, we can detect differences in fluid properties (e.g., mass density, velocity, tracer concentration, thermodynamic state properties) for length scales no smaller than

$$L_{\text{macro}} = 10^{-4} \text{ m}. \quad (0.29)$$

For macroscopic purposes, fluid properties are homogeneous over regions with length scales on the order of L_{macro} . Although macroscopically rather tiny, a fluid region of volume L_{macro}^3 is huge microscopically. We can see so by computing the number of molecules in this region.

At standard conditions, a volume of air of size L_{macro}^3 contains

$$N^{\text{molecules}} = V n^{\text{gas}} = (10^{-4} \text{ m})^3 (2.68 \times 10^{25} \text{ m}^{-3}) \approx 3 \times 10^{13} \text{ air molecules}. \quad (0.30)$$

To compute the number of water molecules in this same volume, we first use the water mass

density of

$$\rho^{\text{water}} \approx 10^3 \text{ kg m}^{-3} \quad (0.31)$$

to determine the water mass in this region

$$M^{\text{water}} = \rho^{\text{water}} V = (1000 \text{ kg m}^{-3}) (10^{-12} \text{ m}^3) = 10^{-9} \text{ kg}. \quad (0.32)$$

Water has a molar mass of $0.018 \text{ kg mole}^{-1}$, so a volume of $(10^{-4} \text{ m})^3$ contains

$$N^{\text{water}} = \left(\frac{10^{-9} \text{ kg}}{0.018 \text{ kg mole}^{-1}} \right) \times 6.022 \times 10^{23} \text{ molecules mole}^{-1} = 3 \times 10^{16} \text{ water molecules.} \quad (0.33)$$

Water thus has roughly 10^3 more molecules in this volume than air at standard pressure, which reflects the roughly 10^3 times larger mass density for water. Evidently, both water and air contain a huge number of molecules in this macroscopically tiny region.

0.3.7 Further study

Pedagogical treatments of the ideal gas law and kinetic theory can be found in most books on introductory physics or chemistry. [Vallis \(2017\)](#) provides extensions of the ideal gas law for an atmosphere with moisture.

For discussions of the continuum approximation reflecting that given here, see the discussion on page 1 of [Olbers et al. \(2012\)](#), or the more thorough treatments in Section 1.2 of [Batchelor \(1967\)](#), Section 2.1 of [Pope \(2000\)](#), or Section 1.4 of [Kundu et al. \(2016\)](#). Chapter 1 of [Salmon \(1998\)](#) touches on elements from kinetic theory and details for how to coarse grain average over molecular degrees of freedom (see his pages 3 and 4 and Sections 9, 10, and 11). An analogous treatment is given by exercise 2.1 of [Pope \(2000\)](#). A rigorous account of kinetic theory is offered in many treatments of statistical mechanics. That given by [Reif \(1965\)](#) and [Huang \(1987\)](#) are accessible to those with a physics undergraduate training. When reading the statistical mechanics literature, look for discussions of the “hydrodynamical limit,” which concerns the transition from discrete particle mechanics to continuum mechanics.



Part I

Kinematics

In this part of the book we focus on the kinematics of a classical and non-relativistic continuous fluid flows. We take inspiration from treatments given in the continuum mechanics literature (e.g., chapter 4 of [Malvern \(1969\)](#) and Part I of [Tromp \(2025a\)](#)), though with a bias towards elements particularly useful in fluid mechanics (e.g., chapter 2 of [Truesdell \(1954\)](#)). There are a variety of rather subtle points connected with fluid flow kinematics, and such subtleties can lead to confusion (it certainly has for this author!). The present treatment aims for a reasonably deductive level of rigor while appealing to the physicist. The interested student is encouraged to read a variety of treatments to survey the presentations, as each author stresses unique nuances that can be important both for understanding and for applications.

Kinematic properties of fluid flows in an inertial reference frame also hold for flow on steady rotating reference frames such as considered in this book. The reason is that steady rigid-body rotation does not directly impart strain to the flow, where strain refers to the relative motion between fluid particles (Chapter 1). Rotation does impart a planetary component to the vorticity of geophysical fluids, with important implications for the study of vorticity in VOLUME 3. However, we can safely ignore planetary rotation for the purpose of fluid kinematics studied in this part of the book.

EULERIAN AND LAGRANGIAN REFERENCE FRAMES

The Eulerian reference frame and Lagrangian reference frame provide dual kinematic descriptions of fluid flows. The Eulerian frame describes fluid motion relative to a frame fixed in the laboratory, whereas the Lagrangian frame follows a moving material fluid particle. The Eulerian frame is inertial (when the laboratory is not accelerating), whereas the Lagrangian frame is non-inertial since fluid particles generally accelerate. Having two descriptions of the same motion provides a synergy that is extensively used in fluid mechanics. Fully realizing this synergy requires skills to move between the Eulerian and Lagrangian descriptions, with tools from tensor analysis in VOLUME 1 used for this purpose. Whereas Cartesian coordinates offer a complete description for Eulerian kinematics, Lagrangian kinematics requires general tensor analysis since fluid particles deform with the fluid motion and thus render a non-orthogonal coordinate description. Elements of Eulerian and Lagrangian kinematics are the focus of Chapter 1, and Chapter 2 further develops the formal theory of fluid kinematics with applications to the study of material lines, areas, and volumes.

For nearly all flows encountered in geophysical fluid mechanics, a Lagrangian description has practical limitations. These limitations arise from the chaotic and turbulent nature of the flow that render a description based on fluid particle trajectories of little use after even a brief time. This is perhaps the key reason that Eulerian approaches are far more common in fluid mechanics, whereas Lagrangian approaches are more common in solid mechanics where materials maintain their shape far longer. Nevertheless, Lagrangian formulations of continuum mechanics offer insights to the fundamental theorems of fluid flows, thus motivating the Lagrangian approach in tandem with the Eulerian.

A historical note is appropriate here. As emphasized by [Truesdell \(1953\)](#), as well as Section 14 of [Truesdell \(1954\)](#), it was Euler who first introduced the material coordinates used with the Lagrangian reference frame. In recognition of this historical error, we sometimes use “material” in place of “Lagrangian”. Even so, we do make use of “Lagrangian” in most places, thus according with its common usage in geophysical fluid mechanics. Relatedly, again according to [Truesdell \(1953\)](#), it was d’Alembert who introduced the spatial coordinates used for the Eulerian description.

The conservation of mass plays a central role in physics. For fluids, mass conservation constrains the flow regardless what forces act on the fluid. Hence, we include mass conservation as a part of fluid kinematics rather than fluid dynamics. Mass conservation, and its expression as volume conservation for non-divergent flows, are the topics of Chapters 3 and 5. Chapter 4 develops the allied study of matter conservation and matter flow, with this study forming the foundations for the study of scalar fields in VOLUME 4.

$$\text{FLUID KINEMATICS} + \text{FLUID DYNAMICS} = \text{FLUID MECHANICS}$$

Kinematics is concerned with the intrinsic properties of motion, including properties of the space and time in which motion occurs. It is the complement to dynamics, which is concerned with the causes of motion that arise through the action of forces. In one sense, kinematics deduces the acceleration whereas dynamics deduces the forces, with Newton's second law linking the two via the equation of motion: $\mathbf{F} = m \mathbf{a}$. Fluid kinematics studies the flow of a fluid and its matter constituents, whereas fluid dynamics studies the forces causing the motion. Furthermore, symmetries of a mechanical system lead, through Noether's theorem, to dynamical conservation laws. That is, symmetries, which embody kinematic properties, lead to dynamical invariants maintained by the motion, with these invariants constraining the motion. The intellectual avenues pursued in developing a mechanical description of fluid motion are many and varied, with fluid kinematics and fluid dynamics intimately woven into the fabric of that description.

A KINEMATICAL RESULT IS VALID FOREVER

As motivation for studying this part of the book, we offer the following quote from page 2 of [Truesdell \(1954\)](#), with Clifford Truesdell one the giants of 20th century continuum mechanics who was clearly fond of kinematics.

All dynamical statements I have relegated to parenthetical sections, appendices, or footnotes, not in a foolish attempt to diminish their physical importance, but rather to let the argument course freely, uninterrupted by merely interpretative remarks, and to leave the propositions free for application to such special dynamical situations as may be of interest either now or in the future—for I cannot too strongly urge that a kinematical result is a result valid forever, no matter how time and fashion may change the “laws” of physics.

MATHEMATICS IN THIS PART

We mostly make use of Cartesian tensor analysis and vector calculus from VOLUME 1. However, for treating Lagrangian coordinates in Chapter 2 we make extensive use of general tensor methods, also from VOLUME 1. Doing so allows us to seamlessly move between Eulerian and Lagrangian coordinate descriptions.

Chapter 1

FUNDAMENTALS OF FLUID KINEMATICS

In describing fluid motion, we use a variety of kinematic lenses, including the dual lenses offered by the Eulerian reference frame and the Lagrangian reference frame reference frames.¹ The Eulerian reference frame (\mathbf{x} -space) uses a spatial description with coordinates that are fixed in Euclidean space, whereas the Lagrangian reference frame (\mathbf{a} -space) uses a material description with coordinates that are fixed on fluid particles. These dual descriptions (spatial versus material) form the foundation for fluid kinematics. We give attention to the needs of both Eulerian and Lagrangian kinematics in this chapter and elsewhere in this book, and how to transform between the two.²

The Eulerian description is more commonly used in fluid mechanics since the kinematic property of central focus is the fluid velocity as a vector field, $\mathbf{v}(\mathbf{x}, t)$, whereas trajectories for fluid particles are not needed for most purposes. In contrast, the Lagrangian approach is more commonly used in solid mechanics, in which one is concerned with motion of material particles relative to a reference or base configuration (typically the initial state). The two descriptions are mathematically related by a one-to-one invertible mapping. To transform from the Lagrangian to Eulerian description requires taking the time derivative of the trajectory to produce the velocity, whereas to transform from the Eulerian to Lagrangian description requires solving a set of ordinary differential equations to compute a trajectory from the time integral of the velocity. The Eulerian description requires less information than the Lagrangian since it does not determine trajectories. However, there is a price to pay for reducing the information, in which case the mechanical foundations can be somewhat obscured using the Eulerian approach.

READER'S GUIDE TO THIS CHAPTER

This chapter introduces concepts and tools used in nearly every subsequent chapter of this book that concerns a description of fluid motion.

1.1	Loose threads	18
1.2	Introduction to fluid kinematics	18
1.2.1	Strong and weak formulations	19
1.2.2	Lagrangian and Eulerian descriptions	19

¹The generalized vertical coordinate approach from VOLUME 3 provides a third kinematic perspective favored in our study of geophysical fluid mechanics. This approach is neither purely Eulerian nor purely Lagrangian, so that it offers somewhat distinct challenges in its mathematical formulation.

²As noted by [Truesdell \(1953\)](#), as well as the long footnote on pages 30-31 of [Truesdell \(1954\)](#), the Lagrangian reference frame originates from the work of Leonard Euler (1707-1783), so that the term "Lagrangian reference frame" is a historical error. Even so, we continue this error given the near ubiquitous terminology used in the geophysical fluid mechanics literature, thus referring to the material frame as the Lagrangian frame.

1.3	Conceptually partitioning the continuum	20
1.3.1	Fluid particles	20
1.3.2	Material fluid parcels in perfect fluids	21
1.3.3	Finite sized material objects in perfect fluids	22
1.3.4	Fluid elements in real fluids	22
1.3.5	Test fluid element in real fluids	23
1.3.6	Finite sized fluid region in real fluids	23
1.3.7	Comments	23
1.4	Material and spatial coordinates	23
1.4.1	Fluid particle trajectories	24
1.4.2	Example material coordinates	25
1.5	Lagrangian and Eulerian time derivatives	26
1.5.1	Infinitesimal space-time increment of a function	26
1.5.2	Total time derivative of a function	26
1.5.3	Eulerian: evolution measured in the spatial frame	27
1.5.4	Lagrangian: evolution measured in the material frame	27
1.5.5	Example material time derivative operations	28
1.5.6	Material time derivative of a vector field	29
1.5.7	Summarizing some terminology	30
1.6	Galilean invariance	30
1.6.1	Specifying the Galilean transformation	31
1.6.2	Transformation matrix	31
1.6.3	Transforming the differential operators	32
1.6.4	Comments	33
1.7	Transforming the material time derivative	33
1.7.1	Definition of the material time derivative	34
1.7.2	Example: a rotating reference frame	34
1.7.3	Invariance using space-time tensors	36
1.7.4	Comments	37
1.8	Fluid flow lines	37
1.8.1	Material pathlines from fluid particle trajectories	37
1.8.2	Fluid streamlines and streamtubes	38
1.8.3	Distinguishing streamlines and pathlines	39
1.8.4	Fluid streaklines	39
1.8.5	An analytic example of flow lines	40
1.8.6	Further study	42
1.9	Exercises	42

1.1 Loose threads

- Draw space-time particle trajectory for Exercise 1.1.
- Draw space-time particle trajectory for Exercise 5.3.

1.2 Introduction to fluid kinematics

We here introduce some basic concepts that form the foundation for fluid kinematics as discussed in this chapter.

1.2.1 Strong and weak formulations

The [continuum approximation](#) allows us to consider fluid flow from a field theoretic perspective, whereby physical properties are described by fields that take on values at each point of a space and time continuum. Consequently, we make use of a differential equation formulation of the governing continuum equations and an integral formulation for describing finite regions. The differential formulation is sometimes referred to as the *strong* formulation. This name is motivated by the need to make assumptions about the smoothness of the continuum fields. Absent such smoothness assumptions, the differential equations lack predictive skill. Some phenomena (e.g., shocks in fluids and faults in solids) do not satisfy the necessary smoothness assumptions, thus making the strong formulation unsuitable. In those cases it can be useful to employ an integral formulation, with the integral formulation known as the *weak* formulation since it requires fewer assumptions about smoothness.

In this book, we are not concerned with shocks or other discontinuities in the fluid flow. Consequently, we make use of both the strong and weak formulations. We are afforded a connection between these formulations through the [Leibniz-Reynolds transport theorem](#) derived in Section 4.2.4. The two formulation are suited for particular needs. For example, the strong formulation provides a concise view of the fluid equations and allows for manipulations and transformations based on the rules of tensor analysis studied in VOLUME 1. In contrast, the weak formulation is used to develop budgets over finite fluid regions. Correspondingly, the weak formulation provides a starting point for the derivation of finite volume budgets that serve as the basis for analysis methods and numerical methods (e.g., [Griffies et al. \(2020\)](#)).

1.2.2 Lagrangian and Eulerian descriptions

There are two reference frames commonly used as the basis for describing motion of a continuum. For the continuous fluid motions considered in this book, these two reference frames retain a 1-to-1 and invertible relation that allows for the mathematical and conceptual transformation between the frames.

- **LAGRANGIAN OR MATERIAL DESCRIPTION:** This description makes use of the [Lagrangian reference frame](#) that is defined by motion of material fluid particles (Section 1.3.1), so that the Lagrangian reference frame is comoving with the continuum of fluid particles. The mechanical description aims to determine the continuum of trajectories, with each trajectory delineated by a continuous material coordinate that labels each fluid particle. The Lagrangian reference frame is non-inertial since fluid particles generally experience accelerations via changes to their speed and/or direction.
- **EULERIAN OR LABORATORY DESCRIPTION:** This description makes use of the [Eulerian reference frame](#) that observes fluid motion relative to fixed spatial positions with coordinate, \mathbf{x} , within a “laboratory”. This *Eulerian* description measures fluid properties as the fluid streams by a fixed observer. It is not concerned with determining trajectories. Instead, Eulerian kinematics focuses on fluid properties as continuous fields that are functions of spatial position with coordinate, \mathbf{x} , and time, t .

The Eulerian and Lagrangian descriptions complement one another. The Lagrangian description renders insights partly due to its direct analog to point particle mechanics of VOLUME 1 in this book. Alternatively, the Eulerian description is commonly more straightforward when developing numerical methods for simulations, or when making laboratory or field measurements. Throughout this book, we make use of both Eulerian and Lagrangian kinematic descriptions.

A goal of this chapter is to provide the foundation for these two descriptions and to develop tools for transforming between them.

In non-geophysical treatments of fluid mechanics, it is typical to assume that the laboratory reference frame of the Eulerian observer is fixed in space, and thus is an inertial reference frame. However, for geophysical fluid mechanics we generally consider an Eulerian reference frame fixed with respect to the rotating planet (a rotating laboratory frame), and the earth laboratory frame is not inertial. However, the discussion in this chapter is not concerned with the non-inertial features that give rise to planetary centrifugal and planetary Coriolis accelerations (see VOLUME 1). Instead, we note that the constant rotation of the planet does not impart any strain to the fluid.³ Consequently, non-rotating fluid kinematics is sufficient for most purposes of geophysical fluid kinematics.

1.3 Conceptually partitioning the continuum

As part of a continuum description of fluid motion, we make use of conceptual physical systems to frame the mechanics and to describe the motion. We start by describing the material fluid particle in Section 1.3.1, which is a zero-dimensional point moving with the fluid flow, and then expand to infinitesimal fluid regions (fluid parcels and fluid elements) that are bounded by imagined partitions. The boundaries of fluid regions can be either open or closed to matter and energy exchange depending on the character of the fluid. Importantly, there is no pretense that the partitions used to define fluid parcels and fluid elements can be experimentally determined. Rather, partitions are drawn within the continuum fluid by the theorist for purposes of formulation and conceptualization. We are afforded the ability to draw these partitions through the continuum description of fluid mechanics.⁴

1.3.1 Fluid particles

A point in Euclidean space is specified by a spatial coordinate, \mathbf{x} , and an instant in Newtonian time is specified by the time, t . Euclidean space plus Newtonian time is referred to as a Galilean space-time. Each point within a matter continuum undergoes motion according to the laws of continuum mechanics. We define a fluid particle as a zero dimensional mathematical point that follows motion of the continuous material fluid, with that motion specified by the velocity field (left panel in Figure 1.1). Since it has zero spatial extent, a fluid particle has no impact on the flow. Notably, a fluid particle is not a molecule or atom since even molecules and atoms have nonzero spatial extent and so impact their surroundings. Even so, a fluid particle does represent a point in the material fluid continuum rather than just a point in space.

The position of a fluid particle in space and time is uniquely specified by its material coordinate plus time (we discuss material coordinates in Section 1.4.1). The trajectory or pathline of a fluid particle is an integral curve of the velocity field, where each point along a trajectory has a tangent that defines the velocity vector (Section 1.8).⁵ The accumulation of a continuum of fluid particle trajectories define the pathlines that form the Lagrangian or material reference frame (Section 1.2.2).

³This point is made more formally when studying the kinematics of fluid strain in Section 2.7.

⁴This conceptual formulation of fluid mechanics, namely as a continuous collection of infinitesimally small fluid elements, originates from the work of Leonard Euler (1707-1783). For an insightful and authoritative discussion on this topic, see [Truesdell \(1953\)](#) as well as the long footnote on pages 30-31 of [Truesdell \(1954\)](#).

⁵When orienting time along the vertical axis, then the tangent to the trajectory is actually the inverse velocity: slope = $dt/dx = 1/u$. We follow the convention used in special relativity, where the trajectory is known as the *world line*, and world lines live within the cone bounded by the world line of photons.

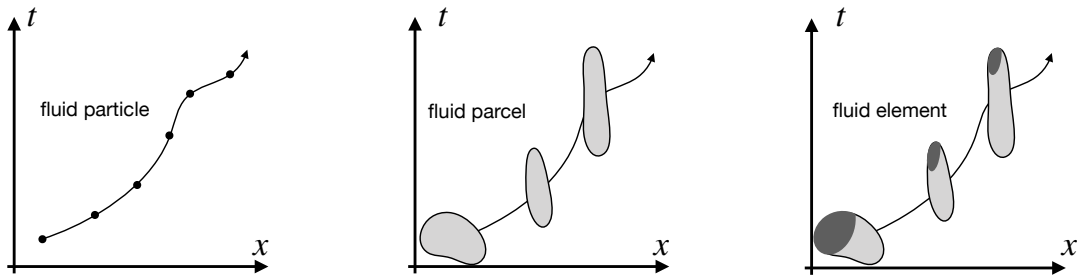


FIGURE 1.1: Schematic of the motion in space-time for the conceptual systems used in our considerations of fluid kinematics. Left panel: a fluid particle has zero spatial extent and has zero impact on the flow. Its motion in space-time defines a path/trajetory as determined by integral curves of the velocity field, $\mathbf{v}(\mathbf{x}, t)$. Note that slope of the curve on this space-time diagram is the inverse of the velocity: slope = $dt/dx = 1/u$. The trajectories of fluid particles define the Lagrangian reference frame. Middle panel: a material fluid parcel is comprised of a fixed material content (and thus a fixed mass) and fixed thermodynamic properties. Fluid parcels are infinitesimal deformable regions of a perfect fluid whose motion within a straining velocity field changes the parcel's shape. The center of mass for the fluid parcel follows a path that is approximated by that of a fluid particle at the center of mass. Right panel: a fluid element is comprised of a fixed mass but with matter and thermodynamic properties exchanged across its boundary, here depicted by the loss of dark gray matter and increase of light gray matter through exchanges with the surrounding fluid. The fluid element moves with the barycentric velocity (see Section 4.1), which is the center of mass velocity for the constituents contained in the fluid element. Both fluid parcels and fluid elements change their shape in the presence of fluid strain. Over time, a fluid parcel and a fluid element change their shape, with realistic flows requiring the reinitialization of parcel/element boundaries in order to maintain coherency as identifiable fluid regions.

Fluid particles are directly analogous to *test mass particles* in Newtonian gravitation that are used to map gravitational field lines, and *test electric charges* in electromagnetism used for mapping the electromagnetic field. However, fluid particles have zero mass and are fully defined kinematically through specifying the velocity field. Fluid particles can be used to study perfect fluids, which necessarily have a single matter constituent, as well as real fluids with multiple matter constituents. For the perfect fluid, fluid particles trace out *integral curves* of the velocity field, whereas for a real fluid the fluid particles provide integral curves for the *barycentric velocity* studied in Section 4.1.

Some books define fluid particles as finite sized fluid regions, much like the fluid parcel described in Section 1.3.2 or the fluid element in Section 1.3.4. Some treatments also suggest that a fluid particle is akin to a fluid molecule. We instead find it conceptually clearer to define a fluid particle as a mathematical point with zero spatial extent and zero mass, thus serving solely as a conceptual probe for the fluid flow and as a means to define the Lagrangian reference frame.⁶

1.3.2 Material fluid parcels in perfect fluids

For many purposes we find it useful to study fluid mechanics in the absence of irreversible processes such as friction, heat exchange, and diffusive mixing. In this case the fluid is referred to as an *ideal fluid* or equivalently a *perfect fluid*. We prefer the term *perfect fluid* to avoid confusions with an ideal gas often found useful in studying the atmosphere. Namely, ideal gases can possess irreversible processes so that they need not be perfect fluids.

Perfect fluid mechanics is concerned with motion of a homogeneous fluid (e.g., pure water or pure air) with zero viscosity (no friction), and in the absence of any heat exchange (adiabatic). In describing perfect fluids we commonly make use of material *fluid parcels*, which are infinitesimal deformable fluid regions (middle panel in Figure 1.1). A material fluid parcel maintains a fixed

⁶Our definition of fluid particle agrees with Section 2.2 of [Pope \(2000\)](#).

matter content so that it has a fixed mass. Furthermore, it does not experience irreversible exchanges of momentum arising from friction since the perfect fluid has zero viscosity. Hence, its only interaction with the surrounding fluid environment is through reversible mechanical exchanges from pressure. The material fluid parcel is thus a closed thermodynamic system that is exposed to reversible mechanical interactions.

A material parcel is not a point. Rather, it has an infinitesimal volume that deforms with the flow. Conceptually we can imagine the material fluid parcel as a tiny region of fluid surrounded by a perfectly slippery bag that is also perfectly insulating. This bag is closed to matter exchange so that its enclosed fluid particles are not exchanged with surrounding environment. Even so, the fluid parcel deforms in response to mechanical interactions mediated by pressure. Additionally, the bag expands or contracts according to the density of the fluid within the bag. This conceptual picture is qualified by noting that we never have occasion or need to precisely specify the boundary of a material fluid parcel. Rather, we make use of the conceptual framework provided by fluid parcels as a means to formulate the differential equations of perfect fluid mechanics.

1.3.3 Finite sized material objects in perfect fluids

Any extended region in a perfect fluid, either infinitesimal or finite, remains exactly coherent (fixed matter content) as the region moves through the fluid. The reason for such coherency is that a perfect fluid supports no mixing or other irreversible processes that would otherwise act to diffuse the matter content. A closed material region in a perfect fluid is a finite volume generalization of a material fluid parcel. Conversely, a material fluid parcel is the infinitesimal limit of a closed material fluid region. Likewise, we can define finite sized material regions of any shape, each of which retains a fixed mass and fixed matter content as it moves through a perfect fluid. We study the kinematics of perfect fluid material lines, surfaces, and volumes in Chapter 2.

1.3.4 Fluid elements in real fluids

A **fluid element** is an infinitesimal and deformable fluid region of fixed mass yet non-fixed matter and non-fixed thermodynamic properties (right panel in Figure 1.1). For a homogeneous fluid comprised of a single matter constituent and no irreversible processes, then a fluid element reduces to a material fluid parcel. However, there is a distinction for real fluids such as the ocean and atmosphere, both of which have multiple constituents and support irreversible processes.

The exchange of matter across the boundary of a fluid element arises from the irreversible mixing of matter constituents within the fluid. As detailed in Section 4.1, diffusive matter exchange leaves the mass of the fluid element unchanged since the fluid element velocity is determined by its center of mass (*barycentric velocity*). Just as for a material fluid parcel, we have no need to experimentally specify the boundary of a fluid element. Instead, fluid elements are conceptual systems used to formulate the differential equations of a real fluid. Much of the kinematics in the current chapter holds for both material fluid parcels and fluid elements. However, in Chapter 3 and elsewhere, we make the distinction when studying the kinematics of multi-constituent fluids.

Many authors do not distinguish between material fluid parcels and fluid elements, choosing instead to retain a single overloaded term for both a perfect fluid and real fluid. However, this overloaded terminology can lead to confusion. We are thus motivated to maintain a distinction between fluid parcel (single component perfect fluid with no mixing) and fluid

element (multi-component real fluid with mixing). The distinction offers an added signal for when the fluid under study is perfect (fluid parcel) or real (fluid element).

1.3.5 Test fluid element in real fluids

A **test fluid element** is a fluid element that has no effect on the surrounding fluid environment and is used as a conceptual probe of the fluid much like the fluid particle in Section 1.3.1. Yet unlike the fluid particle, the test fluid element has nonzero spatial extent and it can exchange matter and energy with its surrounding environment. The test fluid element is of particular use when studying buoyancy.

1.3.6 Finite sized fluid region in real fluids

A finite sized region within a real fluid is the most general subsystem we consider, with the region having boundaries that are open to the exchange of matter, mechanical forces, and thermodynamic properties with the surrounding environment. Here, we are often concerned with details of the region boundary and study the transport of properties across that boundary.

1.3.7 Comments

Throughout the study of fluid kinematics, it is important to maintain an appreciation for the continuum approximation. In particular, the continuum approximation affords information about the continuous velocity field at each point of space and each instance of time. The velocity field allows us to determine fluid particle trajectories (via time integration), as well as the motion of fluid parcels in perfect fluids and fluid elements in real fluids. As part of a diagnostic framework for laboratory or field experiments, it can be useful to seed the fluid flow with a large number of tiny objects that approximate fluid particles whose motion approximates fluid particle trajectories. Similarly, in numerical experiments we may seed the flow with numerical fluid particles and compute their trajectories (*van Sebille et al., 2018*). If we initially seed these particles in a tiny region, then deformation of the region provides the means to study deformation of fluid parcels and fluid elements as they move through the fluid. Likewise, seeding particles over larger regions allows one to study how finite sized regions are deformed.

When thinking about fluids parcels and fluid elements, we should acknowledge that they are convenient concepts, and yet we do not delineate their boundaries either conceptually or in practice. This situation contrasts to certain other areas of continuum mechanics, where discrete regions of the media are identifiable. For a fluid, the notion of identifying a fluid element, such as by wrapping a tiny region of fluid with an imaginary permeable sack, is a fiction that works for some thought experiments, but it is not taken literally. The perspective leads us to discount (i.e., consider incorrect) a description of continuum mechanics that depends on fluid elements as distinct and identifiable objects. Rather, we aim for a theoretical description that is independent of details for the fluid element boundaries. In this case, we are afforded the ability to describe a fluid as continuum matter with properties that are unambiguously defined at every point in the fluid.

1.4 Material and spatial coordinates

A material description is afforded by the Lagrangian reference frame, whereby each fluid particle is labeled with a continuous material coordinate, a , along with a material time coordinate, T ,

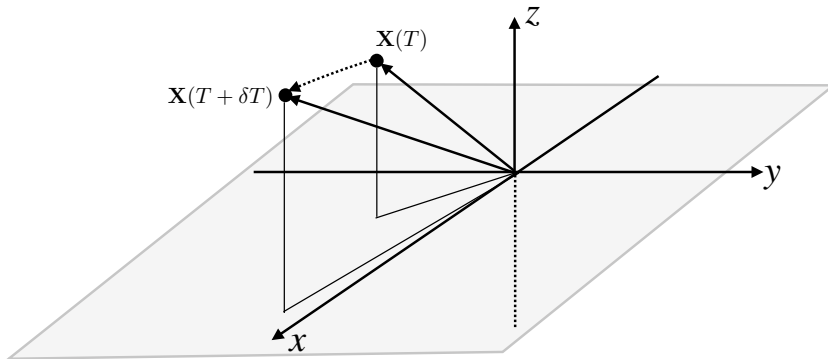


FIGURE 1.2: A short segment of a fluid particle trajectory in Euclidean space. The trajectory passes through the point $\mathbf{x} = \mathbf{X}(T)$ at time T and $\mathbf{x} + \delta\mathbf{x} = \mathbf{X}(T + \delta T)$ at time $T + \delta T$. Eulerian kinematics describes the fluid flow from the perspective of an observer fixed with respect to the laboratory frame. Lagrangian kinematics describes the fluid flow from the perspective of an observer comoving with fluid particles. Note that we have here chosen an origin for use in defining the fluid particle trajectory. If we only cared about the velocity, which is the difference of the trajectory between two infinitesimally close time instants, then there is no need to prescribe a particular origin. The reason is that in the process of computing the time difference, we remove dependence on the origin.

thus leading to the \mathbf{a} -space or material space description.⁷ This description complements the Eulerian or \mathbf{x} -space description, whereby each point in Euclidean space, \mathbf{x} , is labeled by its position relative to a fixed origin and with time, t . The \mathbf{a} -space description determines the history of each material fluid particle’s trajectory, whereas the \mathbf{x} -space description determines the fluid velocity as viewed at each spatial point, \mathbf{x} . Note that $t = T$ since we are working with universal Newtonian time. However, it is very useful to distinguish the two times, since when taking time derivatives it is important to know whether the time derivative is computed holding \mathbf{x} fixed or \mathbf{a} fixed.

1.4.1 Fluid particle trajectories

In describing the motion of a classical point particle in VOLUME 1, we specify its spatial position according to a time dependent position, $\mathbf{X}(T)$, that is relative to a chosen origin. At a given time, T , the position points to the spatial point \mathbf{x} , in which case we write

$$\mathbf{x} = \mathbf{X}(T) \quad \text{point particle.} \quad (1.1)$$

A sample trajectory is shown in Figure 1.2. We emphasize the notation convention used here, which may seem pedantic but in later discussions proves essential. Namely, the time dependent spatial position of a particle is denoted by $\mathbf{X}(T)$, whose instantaneous space position is denoted by the lowercase, \mathbf{x} . This convention aims to distinguish time dependent functions, such as $\mathbf{X}(T)$, from the value of these functions, \mathbf{x} , evaluated at a particular time instance. In Section 2.2 we introduce the fluid *motion*, which serves as a slightly more formal, and general, means to distinguish points on a particle trajectory from points in space.

When there are N discrete particles, we distinguish the various particle trajectories by introducing a discrete label for each of the trajectories. The spatial position of particle i at

⁷The continuum mechanics literature often writes \mathbf{X} rather than \mathbf{a} for the material particle label. That nomenclature is motivated since \mathbf{X} is commonly chosen as the initial Cartesian position at a referential time. We instead write the material coordinate as \mathbf{a} . The reason for our notation is that, as noted in Section 1.4.2, there are examples where one, two, or three of the \mathbf{a} coordinates are not positions in Euclidean space, but instead are determined by a property such as Archimedean buoyancy, specific entropy, or tracer concentration.

time T is thus written

$$\mathbf{x} = \mathbf{X}_{(i)}(T). \quad (1.2)$$

When the matter is a continuum, then the discrete label becomes a continuous coordinate, \mathbf{a} , which is referred to as the *material* coordinate along with material time, T . At time T , the spatial coordinate of a fluid particle labelled by the material coordinate, \mathbf{a} , is written⁸

$$\mathbf{x} = \mathbf{X}(\mathbf{a}, T) \quad \text{coordinates for matter continuum.} \quad (1.3)$$

The continuous material coordinate, \mathbf{a} , labels a point of matter within the continuum fluid. Correspondingly, by allowing time to progress, the function, $\mathbf{X}(\mathbf{a}, T)$, provides the trajectory for the fluid particle labelled by the material coordinate, \mathbf{a} .

In this book we ignore special relativistic effects, so that both the material reference frame and the laboratory reference frame measure the same universal Newtonian time, $t = T$. In contrast, the spatial coordinates are distinct for the Eulerian and Lagrangian references frames. Again, the spatial coordinates for the Eulerian frame are given by the position in Euclidean space relative to a fixed laboratory frame, with this specification making use of any convenient set of coordinates, such as Cartesian, spherical, cylindrical-polar. The three components of a material Lagrangian coordinate, \mathbf{a} , remain fixed according to the value assigned to each fluid particle. Additionally, the three coordinates for both the Eulerian and Lagrangian description must be linearly independent to allow for a unique specification of the fluid particle.

1.4.2 Example material coordinates

One common choice for material coordinate is the Cartesian coordinate for each fluid particle at the referential time,

$$\mathbf{a} = (a, b, c) = (\dot{x}, \dot{y}, \dot{z}) = \text{Cartesian position at } T = \dot{t} \text{ for particle labelled by } \mathbf{a}. \quad (1.4)$$

Even if not making this choice, initial position coordinates are quite useful conceptually as a grounding in the maths of material coordinates.

Now consider a perfect fluid (single material component with no irreversible processes). For this fluid, the specific entropy of each fluid parcel remains fixed at its initial value. When the fluid is placed in a gravitational field, layers of constant specific entropy are generally found to be monotonically stacked, or *stratified*, in the vertical direction. As a result, we can uniquely specify a fluid parcel by giving its horizontal coordinate position, (x, y) , as well as the specific entropy. The material coordinates for a parcel can thus be written as

$$\mathbf{a} = (a, b, c) = (\dot{x}, \dot{y}, \theta) = \text{Cartesian horizontal and } \theta \text{ at } T = t_0, \quad (1.5)$$

where θ is a measure of the specific entropy (or potential temperature as discussed in our study of thermodynamics in VOLUME 2). In this example, the physical dimensions of the individual material coordinates can generally differ. It is this generality that necessitates the use of general tensor methods when developing the mechanical equations using arbitrary Lagrangian coordinates. The case of a single Lagrangian coordinate combined with two horizontal Eulerian coordinates is commonly used for geophysical fluid mechanics, with the mathematical physics

⁸Following the notation from VOLUME 1, we distinguish an upright symbol, such as \mathbf{X} , when not tied to specific coordinates, whereas slanted symbols, \mathbf{X} , are coordinate specific statements. Equation (1.3) refers to coordinates, hence the slanted notation.

of generalized vertical coordinates detailed in VOLUME 3.

In combination with using specific entropy as a generalized vertical coordinate, we might further choose to specify a horizontal position according to the value of tracer concentration. So long as there is a one-to-one mapping between tracer space and geographic space, then we can consider a tracer concentration as a viable Lagrangian coordinate. This approach is less common than the generalized vertical coordinate approach, since tracers are rarely monotonically organized in any particular horizontal direction.

1.5 Lagrangian and Eulerian time derivatives

As noted in Section 1.4.2, we assume non-relativistic motion so that the Lagrangian reference frame and the Eulerian reference frame both measure the same universal Newtonian time, t . However, when computing time derivatives, the Eulerian frame does so by fixing the space coordinate, \mathbf{x} , whereas the Lagrangian frame does so by fixing the material coordinate, \mathbf{a} . These two time derivatives generally measure distinct changes in the fluid since one is computed in the laboratory frame and the other in the material frame. Relating their changes constitutes a key result of fluid kinematics. We derive an expression for the relation by first focusing on time derivatives acting on scalar fields, such as the temperature, and then derive the relation for vector fields, such as the velocity.

1.5.1 Infinitesimal space-time increment of a function

Consider a fluid property as represented by a space-time dependent scalar field, F . For example, F could be the temperature, kinetic energy per mass, or the mass density. When measured at a point in space using coordinates \mathbf{x} , this fluid property is written mathematically as the functional relation

$$F = F(\mathbf{x}, t). \quad (1.6)$$

The difference between $F(\mathbf{x}, t)$ and $F(\mathbf{x} + d\mathbf{x}, t + dt)$ delivers the differential space and time increment, computed to leading order via a Taylor series expansion

$$dF = F(\mathbf{x} + d\mathbf{x}, t + dt) - F(\mathbf{x}, t) \quad (1.7a)$$

$$= dt \partial_t F + d\mathbf{x} \cdot \nabla F. \quad (1.7b)$$

In this equation, dt is the infinitesimal time increment, and $d\mathbf{x}$ is the vector of infinitesimal space increments using a particular coordinate choice. For example, making use of Cartesian coordinates leads to the increment

$$d\mathbf{x} = \hat{\mathbf{x}} dx + \hat{\mathbf{y}} dy + \hat{\mathbf{z}} dz. \quad (1.8)$$

We ignore higher order terms in equation (1.7b) since the space and time increments are infinitesimal.⁹

1.5.2 Total time derivative of a function

In fluid mechanics, it is often useful to sample properties of the fluid from moving reference frames. In this case, the sampling position is a function of time. Determining how a field

⁹Mathematically, equation (1.7b) defines the *exterior derivative* of a scalar field.

evolves when sampled in this moving reference frame requires us to allow the sampling position to itself be a function of time. Operationally, we have the total time derivative of F determined by dividing both sides of equation (1.7b) by the infinitesimal time increment

$$\frac{dF}{dt} = \frac{\partial F}{\partial t} + \frac{dx}{dt} \cdot \nabla F. \quad (1.9)$$

The first term measures the time derivative of F at the specific space point using the coordinate, \mathbf{x} , and as such it measures the Eulerian time derivative. The second term accounts for changes in F arising from movement of the reference frame relative to a point, \mathbf{x} , according to the velocity, $d\mathbf{x}/dt$. Equation (1.9) holds regardless the velocity of the moving frame. Even so, we find it useful to specialize to the two common reference frames used in fluid mechanics.

1.5.3 Eulerian: evolution measured in the spatial frame

The Eulerian time derivative considers the evolution of a fluid property when sampled at a fixed space point with coordinate, \mathbf{x}

$$\text{Eulerian time derivative} = \frac{\partial F(\mathbf{x}, t)}{\partial t}. \quad (1.10)$$

This result follows from specializing the total time derivative in equation (1.9) to the case of fixed spatial points, so that $d\mathbf{x}/dt = 0$. In the geophysical fluids literature, the Eulerian time derivative is often termed the *time tendency* and flows with a nonzero time tendency are said to be *developing flows* or *evolving flows*. When the Eulerian time derivative vanishes everywhere the flow is said to be in a *steady state* or in a *steady flow* condition, with all points in the laboratory frame measuring a zero time change for fluid properties. Note that steady flows are not generally static; rather, they are simply unchanging locally.

1.5.4 Lagrangian: evolution measured in the material frame

The Lagrangian time derivative, also referred to as the material time derivative, measures the evolution of a fluid property sampled along the trajectory of a moving fluid particle. The Lagrangian time derivative for a scalar property is

$$\text{Lagrangian time derivative} = \frac{DF}{Dt} = \frac{\partial F}{\partial t} + \mathbf{v} \cdot \nabla F. \quad (1.11)$$

The second equality follows by setting $d\mathbf{x}/dt = \mathbf{v}$ in equation (1.9) since we are sampling points along the fluid particle trajectory, $\mathbf{x} = \mathbf{X}(\mathbf{a}, t)$. The operator, $\partial/\partial t$, is the Eulerian time derivative from equation (1.10), whereas the operator, $\mathbf{v} \cdot \nabla$, is referred to as the *advection* operator. Use of the capital D for the material time operator

$$\frac{D}{Dt} = \frac{\partial}{\partial t} + \mathbf{v} \cdot \nabla \quad (1.12)$$

signals that the time derivative is computed along a fluid particle trajectory. This notation distinguishes the material time derivative from the more generic total time derivative of equation (1.9). In some texts the material time derivative is referred to as the *convective time derivative*, since the term “convection” is often used rather than “advection”.¹⁰ It is also sometimes

¹⁰In the geophysical fluids literature, “convection” generally refers to vertical motion induced by gravitational instability, such as when heavy fluid is above light fluid. In contrast, the engineering literature often refers to

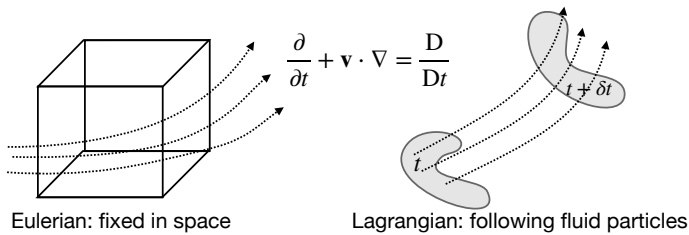


FIGURE 1.3: Illustrating the distinctions between the Eulerian (laboratory) and Lagrangian (material) reference frames for describing fluid motion. For the Eulerian description we consider a fixed control volume in the laboratory frame and measure properties as the fluid moves through the volume. For the Lagrangian description we tag fluid particles and measure fluid properties as sampled along the particle trajectories. When acting on a scalar field, the Eulerian representation of the material time derivative has two terms, one due to time changes local to the fixed laboratory point, and one due to the advection of properties that are swept by the local position.

referred to as the *substantial time derivative* since it refers to the time changes following a material substance.

Equation (1.12) provides an Eulerian expression (right hand side) to the material time derivative, D/Dt . There are two Eulerian contributions: the local (fixed space point) time tendency $\partial/\partial t$ and advection, $\mathbf{v} \cdot \nabla$. Advection arises in the Eulerian reference frame due to the fluid passing by the fixed laboratory observer, whereas it is absent from the material reference frame since the material frame moves with the fluid particles. Figure 1.3 illustrates the differences between the Eulerian and Lagrangian perspectives.

A *steady flow* is one with zero Eulerian time derivatives so that a steady flow does not imply a vanishing Lagrangian time derivative. Rather, a steady flow is a statement that the flow is time independent when viewed from the Eulerian (laboratory) reference frame. Hence, a steady flow generally has changing properties when sampled along a fluid particle trajectory. That is, there can be a nonzero Lagrangian evolution (via advection) even when the Eulerian time tendency vanishes.

1.5.5 Example material time derivative operations

The material time derivative operator is perhaps the most important operator in fluid mechanics, and its relation to the Eulerian time derivative plus advection is a key result of fluid kinematics. Therefore, it is critical to develop experience with this operator and its generalizations. The examples here offer a starting point.

Material invariant/constant

Consider a scalar property, F , that remains constant on a material trajectory. Consequently, any functional representation of this property, $F(\mathbf{x}, t)$, has a vanishing material time derivative

$$\frac{DF}{Dt} = 0. \quad (1.13)$$

Material constancy is sometimes referred to as *material invariance*. At a fixed point in space, a materially invariant property has its Eulerian time derivative arising only via advection

$$\frac{\partial F}{\partial t} = -\mathbf{v} \cdot \nabla F. \quad (1.14)$$

^{“convection” in the same manner as we use the term “advection.”}

For geometric insight into relation (1.14), introduce the unit normal vector to the surface of constant F

$$\hat{\mathbf{n}} = \frac{\nabla F}{|\nabla F|}. \quad (1.15)$$

Material invariance of F thus means that the normalized Eulerian time tendency equals to the negative of the projection of the fluid velocity into the direction normal to constant F surfaces

$$\frac{\partial F / \partial t}{|\nabla F|} = -\mathbf{v} \cdot \hat{\mathbf{n}}. \quad (1.16)$$

That is, the normal projection of the fluid velocity, \mathbf{v} , is matched precisely to the moving surface of constant F . No fluid particles cross the surface. We return to this result in Section 3.6.2 when studying the kinematic boundary conditions at a variety of surfaces.

Time derivative measured in an arbitrary moving frame

Now consider a reference frame moving at an arbitrary velocity, $\mathbf{v}^{(s)}$. Examples include the quasi-Lagrangian reference frames of a float in the ocean or balloon in the atmosphere. Due to their finite size and associated drag effects, these objects only approximate material particle motion, so that $\mathbf{v}^{(s)} \neq \mathbf{v}$. Returning to the general expression (1.9) for the total time derivative, we have the time derivative operator as measured in this non-material moving reference frame

$$\frac{D^{(s)}}{Dt} = \frac{\partial}{\partial t} + \mathbf{v}^{(s)} \cdot \nabla. \quad (1.17)$$

A function that remains constant within this general moving frame thus satisfies

$$\frac{D^{(s)}F}{Dt} = 0 \implies \frac{\partial F}{\partial t} = -\mathbf{v}^{(s)} \cdot \nabla F. \quad (1.18)$$

Introducing the normal direction $\hat{\mathbf{n}} = |\nabla F|^{-1} \nabla F$ leads to

$$\frac{\partial F / \partial t}{|\nabla F|} = -\mathbf{v}^{(s)} \cdot \hat{\mathbf{n}}, \quad (1.19)$$

which is an analog to the material invariance condition (1.16).

1.5.6 Material time derivative of a vector field

We now develop the material time derivative of a vector field (a $(1, 0)$ tensor), such as the velocity. We expect there to be a bit more baggage to carry around since a coordinate representation of a vector field requires basis vectors, with such vectors generally a function of space. Even so, the work has already been done through deriving the covariant derivative of a vector field in VOLUME 1.¹¹

To start, consider Cartesian coordinates in Euclidean space. There is no special treatment needed in this case, in which each component of a vector field, $\mathbf{G} = \hat{\mathbf{x}} G^1 + \hat{\mathbf{y}} G^2 + \hat{\mathbf{z}} G^3$, has a material time derivative

$$DG^m / Dt = (\partial_t + \mathbf{v} \cdot \nabla) G^m = (\partial_t + v^n \partial_n) G^m. \quad (1.20)$$

¹¹We are here concerned with the material time derivative as represented using Eulerian coordinates, with Eulerian coordinate basis vectors time independent. More work is needed when the basis vectors are time dependent, such as for the generalized vertical coordinates in VOLUME 3.

That is, for Cartesian coordinates in Euclidean space, each component of a vector field has a material time derivative with the same form as that for a scalar field. Extending to arbitrary Eulerian coordinates requires us to take into account the space dependence of the basis vectors used to represent a vector. Doing so requires us to make use of the covariant derivative, so that the advection operator written in Cartesian coordinates is generalized to the form

$$(\mathbf{v} \cdot \nabla) \mathbf{G} = (v^n G^m_{;n}) \mathbf{e}_m = (v^n \nabla_n G^m) \mathbf{e}_m, \quad (1.21)$$

where we used results from VOLUME 1 for the covariant derivative of a vector. We thus have the material time derivative of a vector field using arbitrary Eulerian coordinates,

$$\frac{D\mathbf{G}}{Dt} = \partial_t \mathbf{G} + (\mathbf{v} \cdot \nabla) \mathbf{G} = \mathbf{e}_m (\partial_t + v^n \nabla_n) G^m, \quad (1.22)$$

where the covariant derivative is given by

$$\nabla_n G^m = G^m_{;n} = \partial_n G^m + \Gamma_{na}^m G^a. \quad (1.23)$$

1.5.7 Summarizing some terminology

We here summarize some terminology referring to the variety of equations found in geophysical fluid mechanics. Some of this terminology was already introduced in this chapter, whereas others will be encountered later.

- PROGNOSTIC: A [prognostic equation](#) determines the time tendency (Eulerian evolution) of a quantity such as the temperature or velocity.
- DIAGNOSTIC: A [diagnostic equation](#) determines the value of a field at a particular time instance. An example is the non-divergence condition satisfied by velocity in an incompressible flow (Chapter 5). There are generally no time derivatives appearing in diagnostic equations, though this property is generally a function of the chosen coordinate system.
- STEADY STATE: A [steady state](#) is characterized by having the Eulerian time derivative vanish for all fields, so that all fluid properties are time independent when measured in the laboratory frame.
- MATERIAL INVARIANCE: The Lagrangian time derivative vanishes for a property that is a [material invariant](#).

1.6 Galilean invariance

Recall from VOLUME 1 that Galilean invariance for a point particle means that the equations of motion are the same in all inertial reference frames; i.e., they are invariant under a [Galilean transformation](#). Correspondingly, two inertial reference frames can only be moving with a constant velocity relative to one another. A necessary condition for Galilean invariance of a fluid requires the material acceleration to remain the same when viewed in all inertial reference frames. This statement is manifest for Lagrangian kinematics, given the focus on material fluid particles and correspondence with point particles. However, care is required with Eulerian kinematics, with details presented here. Our considerations provide a useful warmup to the

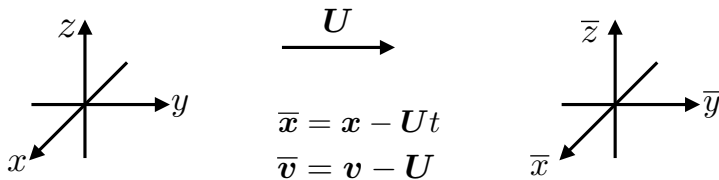


FIGURE 1.4: Illustrating the Galilean transformation between two inertial reference frames. The time coordinate is unchanged, $\bar{t} = t$, whereas space coordinates (assuming Cartesian) are related by $\bar{x} = x - \mathbf{U}t$ with \mathbf{U} a constant boost velocity. We refer to the barred frame as the boosted reference frame and the unbarred frame as the rest frame, though since both frames are inertial there is no unique rest frame.

more general discussion in Section 1.7, where we transform space and time derivative operators between an inertial frame and a rotating frame.

We observe that boundary conditions and initial conditions generally break Galilean invariance, since they reduce the symmetry of space and time. So what is of interest when investigating Galilean invariance of a physical system is whether the dynamics (i.e., forces) and kinematics (i.e., accelerations), as reflected in the differential operators, respect Galilean invariance. Hence, the study of Galilean invariance is a study of the symmetry of the mechanical equations sans the boundary and initial conditions, and in this section we focus just on the material time derivative operator.

1.6.1 Specifying the Galilean transformation

A Galilean transformation is illustrated in Figure 1.4 and it is given mathematically by the linear space-time transformation (here assuming Cartesian coordinates)

$$\bar{t} = t \quad \text{and} \quad \bar{x} = x - \mathbf{U}t \quad \text{and} \quad \bar{v} = v - \mathbf{U}. \quad (1.24)$$

We say that the barred coordinates measure space and time in the moving (boosted) reference frame and the unbarred coordinates measure space and time in the rest (unboosted) frame. As time increases, fixing a position, \bar{x} , in the boosted frame, so that $\bar{v} = 0$, is equivalent to moving with velocity $v = \mathbf{U}$ in the unboosted frame. Conversely, fixing a position, x , in the rest frame, so that $v = 0$, is equivalent to movement with velocity $\bar{v} = -\mathbf{U}$ in the boosted frame.

Since both reference frames are inertial, there is no experiment on a Galilean invariant physical system that can determine which frame is at rest or which is moving. Instead, what is relevant is that the two inertial frames are moving relative to one another. Furthermore, note that time remains unchanged (universal Newtonian time), whereas the position of a point in the new frame equals to that in the original reference frame plus a contribution from the constant velocity, \mathbf{U} . The inverse transformation is trivially given by

$$t = \bar{t} \quad \text{and} \quad x = \bar{x} + \mathbf{U}\bar{t} \quad \text{and} \quad v = \bar{v} + \mathbf{U}. \quad (1.25)$$

1.6.2 Transformation matrix

We make use of the [transformation matrix](#) formalism from the tensor analysis in VOLUME 1 to derive relations between the partial differential operators. The reader having skipped that section should still be able to understand the gist of the following. For simplicity we work in the 1+1 dimensional case (time plus one space dimension).

Writing the space and time coordinates as

$$(t, x) = (x^0, x^1) \quad \text{and} \quad (\bar{t}, \bar{x}) = (x^{\bar{0}}, x^{\bar{1}}) \quad (1.26)$$

renders the transformation of partial derivatives (following the chain rule)

$$\frac{\partial}{\partial x^{\bar{\alpha}}} = \frac{\partial x^\alpha}{\partial x^{\bar{\alpha}}} \frac{\partial}{\partial x^\alpha}, \quad (1.27)$$

where $\alpha = 0, 1$ is a tensor index that has $\alpha = 0$ for the time coordinate. The transformation matrix for the Galilean transformation is thus given by the 2×2 matrix

$$\frac{\partial x^{\bar{\alpha}}}{\partial x^\alpha} = \begin{bmatrix} \partial x^{\bar{0}}/\partial x^0 & \partial x^{\bar{0}}/\partial x^1 \\ \partial x^{\bar{1}}/\partial x^0 & \partial x^{\bar{1}}/\partial x^1 \end{bmatrix} = \begin{bmatrix} 1 & 0 \\ -U & 1 \end{bmatrix}, \quad (1.28)$$

and the inverse transformation matrix is

$$\frac{\partial x^\alpha}{\partial x^{\bar{\alpha}}} = \begin{bmatrix} 1 & 0 \\ U & 1 \end{bmatrix}. \quad (1.29)$$

The determinant of the transformation matrix (Jacobian) is unity, so that the Galilean transformation always has an inverse.

1.6.3 Transforming the differential operators

Given the transformation matrix, we can compute the Eulerian time derivative as measured in the moving frame by using the chain rule

$$\frac{\partial}{\partial x^{\bar{0}}} = \frac{\partial x^0}{\partial x^{\bar{0}}} \frac{\partial}{\partial x^0} + \frac{\partial x^1}{\partial x^{\bar{0}}} \frac{\partial}{\partial x^1} = \frac{\partial}{\partial x^0} + U \frac{\partial}{\partial x^1} = \frac{\partial}{\partial t} + U \frac{\partial}{\partial x}. \quad (1.30)$$

In words, this identity says that the time derivative computed between two inertial reference frames differs due to an advective term (with the constant Galilean boost velocity) arising from the relative motion of the two inertial observers. A time derivative measured in the boosted reference frame keeps the position, \bar{x} , fixed, so that even if ∂_t is zero, we can still have a nonzero $\partial_{\bar{t}}$ due to advection, $U \partial_{\bar{x}}$.

In the same manner we find that the space derivatives are related by

$$\frac{\partial}{\partial x^{\bar{1}}} = \frac{\partial x^0}{\partial x^{\bar{1}}} \frac{\partial}{\partial x^0} + \frac{\partial x^1}{\partial x^{\bar{1}}} \frac{\partial}{\partial x^1} = \frac{\partial}{\partial x^1}. \quad (1.31)$$

Evidently, the space derivative operator remains form invariant under a Galilean transformation. This result holds also for the other two space dimensions.

Bringing pieces together we find that the material time derivative operator is form invariant under a Galilean transformation

$$\frac{D}{Dt} = \frac{\partial}{\partial t} + \mathbf{v} \cdot \nabla \quad (1.32a)$$

$$= \frac{\partial}{\partial \bar{t}} - \mathbf{U} \cdot \bar{\nabla} + (\bar{\mathbf{v}} + \mathbf{U}) \cdot \bar{\nabla} \quad (1.32b)$$

$$= \frac{\partial}{\partial \bar{t}} + \bar{\mathbf{v}} \cdot \bar{\nabla} \quad (1.32c)$$

$$= \frac{\overline{D}}{Dt}, \quad (1.32d)$$

where we used the shorthand

$$\bar{v} \cdot \bar{\nabla} = \bar{u} \frac{\partial}{\partial x^1} + \bar{v} \frac{\partial}{\partial x^2} + \bar{w} \frac{\partial}{\partial x^3}. \quad (1.33)$$

So although the individual pieces to the material time operator are modified by a Galilean transformation, the material time derivative operator is form invariant. Hence, if a scalar function has a material time derivative in one inertial reference frame, it has the same material time operator in any other inertial reference frame. To be more precise, let F represent some scalar property. When measured at a space-time point (\mathcal{P}, t) using the coordinate system, $x^\alpha = (\mathbf{x}, t)$, we write

$$F(\mathcal{P}, t) = F(\mathbf{x}, t), \quad (1.34)$$

and its material time derivative is

$$\frac{DF(\mathbf{x}, t)}{Dt} = (\partial_t + v^m \partial_m) F. \quad (1.35)$$

Likewise, when evaluated at the same point but using the boosted coordinates, $x^{\bar{\alpha}} = (\bar{\mathbf{x}}, \bar{t})$, then

$$F(\mathcal{P}) = \bar{F}(\bar{\mathbf{x}}, \bar{t}), \quad (1.36)$$

with its material time derivative

$$\frac{DF(\mathcal{P})}{D\bar{t}} = (\partial_{\bar{t}} + v^{\bar{m}} \partial_{\bar{m}}) \bar{F}. \quad (1.37)$$

We provide an explicit example in Exercise 1.7.

1.6.4 Comments

There are many features of geophysical fluid flows that break Galilean invariance. For example, a solid boundary breaks Galilean invariance since it establishes a special reference frame and thus breaks the symmetry of unbounded space. Additionally, a rotating planet distinguishes between longitude and latitude even if the planet is perfectly smooth. Nonetheless, as a starting point in our study of the equations of fluid mechanics it is useful to establish their properties under a Galilean transformation. In general, if space is Galilean invariant and yet the equations of motion are not, then we question the physical relevance of the equations.

There are further symmetries of the equations of fluid mechanics, especially when there is no dissipation (inviscid). Section 2.2 of [Frisch \(1995\)](#), Section 2.9 of [Pope \(2000\)](#), and Section 1.4 of [Badin and Crisciani \(2018\)](#) provide a discussion of these further symmetries.

1.7 Transforming the material time derivative

In the discussion of Galilean invariance in Section 1.6, we showed that the material time derivative operator remains form invariant under changes to the inertial reference frame. Here, we consider an arbitrary transformation, with a focus on its action on a scalar field. The development offers a case study for how to transform from one reference frame to another.

1.7.1 Definition of the material time derivative

We first determine the transformation by focusing on the conceptual definition of the material time derivative. Namely, the material time derivative measures time changes of a fluid property in the reference frame comoving with a fluid particle. The Lagrangian reference frame follows fluid particles, so it is the natural reference frame for measuring material time changes. In contrast, the Eulerian reference frame is fixed in a laboratory. The material time derivative acting on a scalar when computed from the laboratory reference frame consists of an Eulerian time tendency plus an advection operator

$$\frac{D}{Dt} = \frac{\partial}{\partial t} + \mathbf{v} \cdot \nabla. \quad (1.38)$$

Importantly, this expression holds regardless the choice of laboratory reference frame, either inertial or non-inertial. The fluid particle reference frame is unconcerned with the subjective choice made by the observer in the laboratory reference frame. Our choice of laboratory frame only impacts on the form of the Eulerian time derivative and on the advection operator. The sum of the two terms returns the same material time derivative operator, no matter what laboratory frame is chosen.

1.7.2 Example: a rotating reference frame

Consider two reference frames. The first is at rest and so serves as an inertial frame, whereas the second is rotating (and thus non-inertial) with rotational axis aligned with the vertical direction. Introduce Cartesian coordinates for the inertial frame, with corresponding basis vectors $(\hat{\mathbf{x}}, \hat{\mathbf{y}}, \hat{\mathbf{z}})$. Let these inertial frame unit vectors be related to rotating frame unit vectors according to

$$\hat{\mathbf{x}} = \hat{\mathbf{x}} \cos \vartheta - \hat{\mathbf{y}} \sin \vartheta \quad (1.39a)$$

$$\hat{\mathbf{y}} = \hat{\mathbf{x}} \sin \vartheta + \hat{\mathbf{y}} \cos \vartheta \quad (1.39b)$$

$$\hat{\mathbf{z}} = \hat{\mathbf{z}}, \quad (1.39c)$$

and let time be the same in the two reference frames. The angle ϑ measures the counter-clockwise angle between the inertial frame direction $\hat{\mathbf{x}}$ and the moving frame direction $\hat{\mathbf{x}}$, with this angle assumed to be a linear function of time

$$\vartheta = \Omega t, \quad (1.40)$$

with Ω the angular speed. The above relations between the two sets of basis vectors, since they are linear relations, translates into the same relations between the corresponding coordinate representations for an arbitrary vector. Including time, we have the relation between inertial coordinates (the barred frame) and rotating coordinates (unbarred frame)

$$\bar{t} = t \quad (1.41a)$$

$$\bar{x} = x \cos \vartheta - y \sin \vartheta \quad (1.41b)$$

$$\bar{y} = x \sin \vartheta + y \cos \vartheta \quad (1.41c)$$

$$\bar{z} = z, \quad (1.41d)$$

along with the inverse transformation

$$t = \bar{t} \quad (1.42a)$$

$$x = \bar{x} \cos \vartheta + \bar{y} \sin \vartheta \quad (1.42b)$$

$$y = -\bar{x} \sin \vartheta + \bar{y} \cos \vartheta \quad (1.42c)$$

$$z = \bar{z}. \quad (1.42d)$$

We are now prepared to make use of the transformation formalism from tensor analysis developed in VOLUME 1, and as applied to the Galilean transformation in Section 1.6. As for the Galilean transformation, we here include time as part of the formalism by introducing the Greek label $\alpha = 0, 1, 2, 3$ so that the transformation matrix between the inertial frame and rotating frame is given by

$$\frac{\partial x^{\bar{\alpha}}}{\partial x^{\alpha}} = \begin{bmatrix} \partial x^{\bar{0}}/\partial x^0 & \partial x^{\bar{0}}/\partial x^1 & \partial x^{\bar{0}}/\partial x^2 & \partial x^{\bar{0}}/\partial x^3 \\ \partial x^{\bar{1}}/\partial x^0 & \partial x^{\bar{1}}/\partial x^1 & \partial x^{\bar{1}}/\partial x^2 & \partial x^{\bar{1}}/\partial x^3 \\ \partial x^{\bar{2}}/\partial x^0 & \partial x^{\bar{2}}/\partial x^1 & \partial x^{\bar{2}}/\partial x^2 & \partial x^{\bar{2}}/\partial x^3 \\ \partial x^{\bar{3}}/\partial x^0 & \partial x^{\bar{3}}/\partial x^1 & \partial x^{\bar{3}}/\partial x^2 & \partial x^{\bar{3}}/\partial x^3 \end{bmatrix} = \begin{bmatrix} 1 & 0 & 0 & 0 \\ -\Omega \bar{y} & \cos \vartheta & -\sin \vartheta & 0 \\ \Omega \bar{x} & \sin \vartheta & \cos \vartheta & 0 \\ 0 & 0 & 0 & 1 \end{bmatrix}. \quad (1.43)$$

Similarly, the inverse transformation is given by

$$\frac{\partial x^{\alpha}}{\partial x^{\bar{\alpha}}} = \begin{bmatrix} \partial x^0/\partial x^{\bar{0}} & \partial x^0/\partial x^{\bar{1}} & \partial x^0/\partial x^{\bar{2}} & \partial x^0/\partial x^{\bar{3}} \\ \partial x^1/\partial x^{\bar{0}} & \partial x^1/\partial x^{\bar{1}} & \partial x^1/\partial x^{\bar{2}} & \partial x^1/\partial x^{\bar{3}} \\ \partial x^2/\partial x^{\bar{0}} & \partial x^2/\partial x^{\bar{1}} & \partial x^2/\partial x^{\bar{2}} & \partial x^2/\partial x^{\bar{3}} \\ \partial x^3/\partial x^{\bar{0}} & \partial x^3/\partial x^{\bar{1}} & \partial x^3/\partial x^{\bar{2}} & \partial x^3/\partial x^{\bar{3}} \end{bmatrix} = \begin{bmatrix} 1 & 0 & 0 & 0 \\ \Omega y & \cos \vartheta & \sin \vartheta & 0 \\ -\Omega x & -\sin \vartheta & \cos \vartheta & 0 \\ 0 & 0 & 0 & 1 \end{bmatrix}. \quad (1.44)$$

The derivative operators transform according to

$$\frac{\partial}{\partial x^{\alpha}} = \frac{\partial x^{\bar{\alpha}}}{\partial x^{\alpha}} \frac{\partial}{\partial x^{\bar{\alpha}}}, \quad (1.45)$$

in which case

$$\frac{\partial}{\partial t} = \frac{\partial}{\partial \bar{t}} + (\boldsymbol{\Omega} \times \bar{\boldsymbol{x}}) \cdot \bar{\nabla} \quad (1.46a)$$

$$\frac{\partial}{\partial x} = \cos \vartheta \frac{\partial}{\partial \bar{x}} + \sin \vartheta \frac{\partial}{\partial \bar{y}} \quad (1.46b)$$

$$\frac{\partial}{\partial y} = -\sin \vartheta \frac{\partial}{\partial \bar{x}} + \cos \vartheta \frac{\partial}{\partial \bar{y}} \quad (1.46c)$$

$$\frac{\partial}{\partial z} = \frac{\partial}{\partial \bar{z}}. \quad (1.46d)$$

The velocity vector components transform according to

$$v^{\alpha} = \frac{\partial x^{\alpha}}{\partial x^{\bar{\alpha}}} v^{\bar{\alpha}}, \quad (1.47)$$

so that

$$v^0 = v^{\bar{0}} \quad (1.48a)$$

$$u = \Omega y + \bar{u} \cos \vartheta + \bar{v} \sin \vartheta \quad (1.48b)$$

$$v = -\Omega x - \bar{u} \sin \vartheta + \bar{v} \cos \vartheta \quad (1.48c)$$

$$w = \bar{w}, \quad (1.48d)$$

where

$$v^0 = v^{\bar{0}} = 1. \quad (1.49)$$

Bringing these result together leads to the transformation of the horizontal advection operator

$$u \frac{\partial}{\partial x} + v \frac{\partial}{\partial y} = (\bar{\mathbf{u}} - \boldsymbol{\Omega} \times \bar{\mathbf{x}}) \cdot \bar{\nabla}. \quad (1.50)$$

Combining this result with the transformed Eulerian time derivative leads to the material time derivative

$$\frac{D}{Dt} = \frac{\partial}{\partial t} + \mathbf{v} \cdot \nabla \quad (1.51a)$$

$$= \frac{\partial}{\partial t} + u \frac{\partial}{\partial x} + v \frac{\partial}{\partial y} + w \frac{\partial}{\partial z} \quad (1.51b)$$

$$= \frac{\partial}{\partial \bar{t}} + (\boldsymbol{\Omega} \times \bar{\mathbf{x}}) \cdot \bar{\nabla} + (\bar{\mathbf{u}} - \boldsymbol{\Omega} \times \bar{\mathbf{x}}) \cdot \bar{\nabla} + \bar{w} \frac{\partial}{\partial \bar{z}} \quad (1.51c)$$

$$= \frac{\partial}{\partial \bar{t}} + \bar{\mathbf{v}} \cdot \bar{\nabla}. \quad (1.51d)$$

As advertised, the operator is form invariant under time dependent transformations to a non-inertial reference frame.

1.7.3 Invariance using space-time tensors

We can generalize the previous result by writing the material time derivative operator using space-time tensor notation from VOLUME 1, in which case

$$\frac{D}{Dt} = \frac{\partial}{\partial t} + \mathbf{v} \cdot \nabla = \frac{\partial}{\partial x^0} + v^m \frac{\partial}{\partial x^m} = v^\alpha \frac{\partial}{\partial x^\alpha}, \quad (1.52)$$

where we introduced the velocity 4-vector

$$(v^0, v^1, v^2, v^3) = (1, v^1, v^2, v^3). \quad (1.53)$$

All space-time indices are contracted in equation (1.52), which means the material time derivative is a space-time scalar. Consequently, we can change coordinates or change reference frames without changing the material time operator.

We verify the above conclusion via the following manipulations using the chain rule

$$\frac{D}{Dt} = \partial_0 + v^m \partial_m \quad (1.54a)$$

$$= \Lambda^{\bar{\alpha}}_0 \partial_{\bar{\alpha}} + \Lambda^a_{\bar{\alpha}} v^{\bar{\alpha}} \Lambda^{\bar{\beta}}_a \partial_{\bar{\beta}} \quad (1.54b)$$

$$= \Lambda^{\bar{\alpha}}_0 \partial_{\bar{\alpha}} + \Lambda^a_{\bar{\alpha}} \Lambda^{\bar{\beta}}_a v^{\bar{\alpha}} \partial_{\bar{\beta}}, \quad (1.54c)$$

where we wrote the transformation matrix and its inverse in the form

$$\Lambda^\alpha_{\bar{\alpha}} \equiv \frac{\partial x^\alpha}{\partial x^{\bar{\alpha}}} \quad \text{and} \quad \Lambda^{\bar{\alpha}}_\alpha \equiv \frac{\partial x^{\bar{\alpha}}}{\partial x^\alpha}. \quad (1.55)$$

Next make use of the identity

$$\Lambda^a_{\bar{\alpha}} \Lambda^{\bar{\beta}}_a = \Lambda^{\alpha}_{\bar{\alpha}} \Lambda^{\bar{\beta}}_{\alpha} - \Lambda^0_{\bar{\alpha}} \Lambda^{\bar{\beta}}_0 \quad a = 1, 2, 3 \text{ and } \alpha = 0, 1, 2, 3 \quad (1.56a)$$

$$= \delta^{\bar{\beta}}_{\bar{\alpha}} - \Lambda^0_{\bar{\alpha}} \Lambda^{\bar{\beta}}_0 \quad \Lambda^{\alpha}_{\bar{\alpha}} \Lambda^{\bar{\beta}}_{\alpha} = \delta^{\bar{\beta}}_{\bar{\alpha}} \text{ by chain rule} \quad (1.56b)$$

$$= \delta^{\bar{\beta}}_{\bar{\alpha}} - \delta^0_{\bar{\alpha}} \Lambda^{\bar{\beta}}_0 \quad \Lambda^0_{\bar{\alpha}} = \delta^0_{\bar{\alpha}} \text{ for Newtonian time.} \quad (1.56c)$$

Use of this identity in equation (1.54c) renders

$$\frac{D}{Dt} = \Lambda^{\bar{\alpha}}_0 \partial_{\bar{\alpha}} + \left[\delta^{\bar{\beta}}_{\bar{\alpha}} - \delta^0_{\bar{\alpha}} \Lambda^{\bar{\beta}}_0 \right] v^{\bar{\alpha}} \partial_{\bar{\beta}} \quad (1.57a)$$

$$= \Lambda^{\bar{\alpha}}_0 \partial_{\bar{\alpha}} + v^{\bar{\alpha}} \partial_{\bar{\alpha}} - v^{\bar{0}} \Lambda^{\bar{\beta}}_0 \partial_{\bar{\beta}} \quad (1.57b)$$

$$= v^{\bar{\alpha}} \partial_{\bar{\alpha}} \quad (1.57c)$$

$$= \partial_{\bar{t}} + v^{\bar{\alpha}} \partial_{\bar{\alpha}}, \quad (1.57d)$$

where we used $v^{\bar{0}} = 1$. This proof means that the material time derivative remains form invariant no matter what coordinate choice is made for the laboratory reference frame.

1.7.4 Comments

As argued at the start of this section, there is no reason for a time derivative computed in a material frame to be concerned with the coordinates chosen for the laboratory frame. Hence, we expect there to be form invariance across all chosen laboratory coordinates. It is thus satisfying to see the tools of coordinate transformations put to use in verifying this result.

1.8 Fluid flow lines

There are three types of flow lines commonly used to visualize fluid motion: **pathlines** (also known as **fluid particle trajectories**), **streamlines**, and **streaklines**. These flow lines are identical for time independent (steady) flow, where steady flow means that all fields are constant in time when observed in the Eulerian reference frame. However, these flow lines differ for unsteady flow. They each offer unique information about the flow field, and have uses in both theoretical and experimental contexts. We have use for pathlines and streamlines in this book, yet also introduce streaklines for completeness.

1.8.1 Material pathlines from fluid particle trajectories

As introduced in Section 1.4.1, a fluid particle traces out a trajectory as it moves through space and as time progresses (Figure 1.2). We refer to **pathlines** for **fluid particle trajectories**, with a collection of pathlines providing a means to visualize fluid particle motion throughout the flow. In this book we are only concerned with smooth velocity fields, which allow for an unambiguous specification of the pathline at each point of the fluid.

We consider a fluid particle trajectory as a curve in space, $\boldsymbol{\varphi}(\mathbf{a}, T)$, that is traced by fixing the material coordinate, \mathbf{a} , and letting time, T , advance.¹² Trajectories are computed by time

¹²As studied in Chapter 2, trajectories are the Euclidean space manifestation of the **flow map**, which acts to smoothly deform the matter continuum through space as the fluid moves. For this reason, we sometimes write $\boldsymbol{\varphi}(\mathbf{a}, T) = \mathbf{X}(\mathbf{a}, T)$ to correspond to the particle mechanics studied in VOLUME 1.

integrating the ordinary differential equation

$$\frac{\partial \boldsymbol{\varphi}(\mathbf{a}, T)}{\partial T} = \mathbf{v}[\boldsymbol{\varphi}(\mathbf{a}, T), T] \quad (1.58a)$$

$$\boldsymbol{\varphi}(\mathbf{a}, T = t_0) = \mathbf{a}, \quad (1.58b)$$

where the Lagrangian velocity of the fluid particle is written as the Eulerian velocity when evaluated on a trajectory¹³

$$\mathbf{v}^L(\mathbf{a}, T) = \mathbf{v}[\mathbf{x} = \boldsymbol{\varphi}(\mathbf{a}, T), t = T], \quad (1.59)$$

and we have assumed the material coordinates are known at some arbitrary initial time, $T = t_0$. Again, the partial time derivative is computed with the material coordinate held fixed, so that the material coordinate distinguishes between particle trajectories.

Since the trajectory is determined by integrating the ordinary differential equation (1.58a), the fluid particle trajectory provides an *integral curve* for the velocity vector. Correspondingly, the particle velocity is tangent to its corresponding trajectory at each point. Furthermore, since we are concerned with continuous media, there is a trajectory that passes through each point of space at each time instance.

In the laboratory, we can insert tiny particles into the fluid to offer a means for visualizing the flow, with a time exposed photograph providing an estimate of fluid particle pathlines. As another example, consider cars moving at night with a time exposed photograph revealing pathlines formed by car head and tail lights. Like cars, the material pathlines in a fluid can intersect, cross, and become quite complex, particularly when the flow is turbulent.

1.8.2 Fluid streamlines and streamtubes

Streamlines are curves whose tangent is parallel to the instantaneous fluid velocity field. Streamlines can intersect only at a stagnation point; i.e., a point where the fluid is not moving. Let

$$d\mathbf{x} = \hat{\mathbf{x}} dx + \hat{\mathbf{y}} dy + \hat{\mathbf{z}} dz \quad (1.60)$$

be an infinitesimal increment along a streamline written using Cartesian coordinates. The family of streamlines at a given time, t , satisfies the tangent constraint

$$\mathbf{v} \times d\mathbf{x} = 0, \quad (1.61)$$

which is equivalent to

$$\frac{dx}{u(\mathbf{x}, t)} = \frac{dy}{v(\mathbf{x}, t)} = \frac{dz}{w(\mathbf{x}, t)}. \quad (1.62)$$

Alternatively, we can introduce a pseudo-time parameter, s , that determines a position along a streamline. Streamlines are the curves, $\mathbf{x} = \boldsymbol{\varphi}(s; \mathbf{a}, T)$, computed with (\mathbf{a}, T) held fixed, but with the pseudo-time varied

$$\frac{\partial \boldsymbol{\varphi}(s; \mathbf{a}, T)}{\partial s} = \mathbf{v}[\boldsymbol{\varphi}(s; \mathbf{a}, T), T] \quad (1.63a)$$

$$\boldsymbol{\varphi}(s = 0; \mathbf{a}, T) = \mathbf{a}. \quad (1.63b)$$

¹³We have more to say about equation (1.59) in Chapter 2.

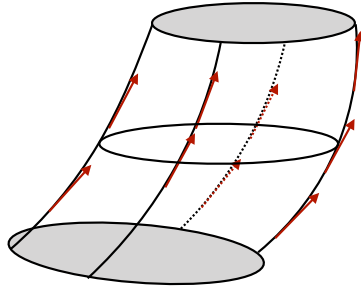


FIGURE 1.5: This image shows an example streamtube. The side boundaries of a streamtube consist of streamlines. At each point of a streamline, the local tangent vector equals to the velocity field (see equation (1.61)). Streamlines are identical to pathlines only for steady flow; they differ for unsteady flows. Hence, for unsteady flows, particle trajectories generally cross through the streamtube boundary.

Again, both the material coordinate, \mathbf{a} , and time, T , are held fixed when determining streamlines, so that (\mathbf{a}, T) act as parameters to distinguish streamlines. Streamlines thus do not know about the time evolution of unsteady flow. Instead, streamlines only sample a snapshot of the velocity field and so they are freshly computed at each time instance.

A **streamtube** is a bundle of streamlines crossing through an arbitrary closed curve as depicted in Figure 1.5. At each time instance, the flow velocity is tangent to the streamtube sides. Furthermore, when the flow is steady then streamlines are identical to material particle pathlines. Hence, a streamtube is a material tube for steady flow, in which case no fluid particles cross the streamtube boundary.

1.8.3 Distinguishing streamlines and pathlines

The tangent to a streamline gives the velocity at a single point in time, whereas the tangent to a material pathline gives the velocity at all times. These tangents are identical when the flow is steady. However, if the flow is time dependent (unsteady), then streamlines differ from material pathlines. Furthermore, for unsteady flow, the pseudo-time parameter, s , determining the streamlines in equation (1.63a) is not equal to the time, t , used to compute fluid particle trajectories in equation (1.58a). Consequently, the condition $\mathbf{v} \cdot \hat{\mathbf{n}} = 0$ satisfied at each time instance by a streamline still allows fluid particles to cross streamlines. The reason is that a material pathline moves with the fluid in such a way that

$$(\mathbf{v} - \mathbf{v}^{\text{line}}) \cdot \hat{\mathbf{n}} = 0 \implies \mathbf{v} \cdot \hat{\mathbf{n}} = \mathbf{v}^{\text{line}} \cdot \hat{\mathbf{n}} \quad \text{material lines,} \quad (1.64)$$

where \mathbf{v}^{line} is the velocity of a point on the material pathline. The material pathline thus moves so that no fluid particles cross it. Only when the flow is steady, so that $\mathbf{v}^{\text{line}} \cdot \hat{\mathbf{n}} = 0$, will material pathlines and streamlines be equal. That is, the streamline constraint $\mathbf{v} \cdot \hat{\mathbf{n}} = 0$ is not a material constraint when $\mathbf{v}^{\text{line}} \cdot \hat{\mathbf{n}} \neq 0$. The key point is that streamlines do not probe the time behavior of the flow, so they do not know whether the velocity is steady or unsteady.

1.8.4 Fluid streaklines

Fluid **streaklines** are those curves obtained by connecting the positions for all fluid particles that emanate points fixed in space (see Figure 1.6). Streaklines are straightforward to define conceptually and to realize experimentally. However, they are a bit convoluted to specify mathematically. We present two formulations.

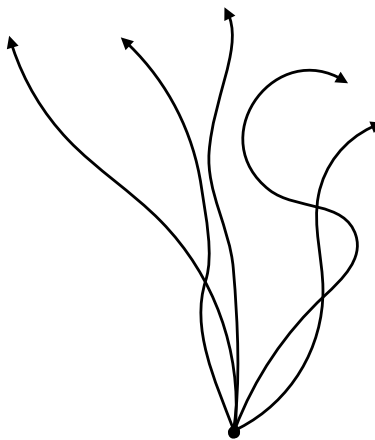


FIGURE 1.6: A suite of trajectories emanating from a single point. Common approximate realizations include the paths of fluid particles that leave a chimney, or the smoke from a source like a burning stick or torch. A streakline is defined as the accumulation of positions at time T of particles that passed through the common point at some earlier time $s < T$.

At any time T , the streakline passing through a fixed point, \mathbf{y} , is a curve going from \mathbf{y} to $\boldsymbol{\varphi}(\mathbf{y}, T)$, the position reached by the particle initialized at $T = 0$ at the point \mathbf{y} . A particle is on the streakline if it passed the fixed point \mathbf{y} at some time between 0 and T . If this time was s , then the material coordinate of the particle would be given by $\mathbf{a}(\mathbf{y}, s)$ relating the material coordinate to its corresponding laboratory position. Furthermore, at time T , this particle is at \mathbf{x} , so that the equation of the streakline at time T is

$$\mathbf{x} = \boldsymbol{\varphi}[\mathbf{a}(\mathbf{y}, s), T] \quad 0 \leq s \leq T. \quad (1.65)$$

We can connect the streakline specification to that given for a pathline and streamline through the following. A streakline at some time instance, \tilde{T} , is a curve defined by fixing \tilde{T} and varying s over $s \leq \tilde{T}$ in the function $\boldsymbol{\varphi}(s; \mathbf{a}, \tilde{T})$. We determine the curves, $\mathbf{x} = \boldsymbol{\varphi}(s; \mathbf{a}, \tilde{T})$, by solving the following set of initial value problems for trajectories with initial conditions imposed at $T = s$ rather than $T = 0$

$$\frac{\partial \boldsymbol{\varphi}(s; \mathbf{a}, T)}{\partial T} = \mathbf{v}[\boldsymbol{\varphi}(s; \mathbf{a}, T), T] \quad (1.66a)$$

$$\boldsymbol{\varphi}(T = s; \mathbf{a}, T) = \mathbf{a}. \quad (1.66b)$$

Note that \mathbf{a} remains fixed, as we start all trajectories determining a streakline from the same initial point (e.g., the chimney does not move). A streakline can thus be generated by emitting a dye from a point over a time interval equal to the range of s , with the dye following fluid particle trajectories.

1.8.5 An analytic example of flow lines

Consider the following two-dimensional example as taken from Section 4.13 of [Aris \(1962\)](#). Let the Eulerian velocity field be given by

$$u = \frac{x}{\tau + t} \quad \text{and} \quad v = \frac{y}{\tau} \quad \text{and} \quad w = 0, \quad (1.67)$$

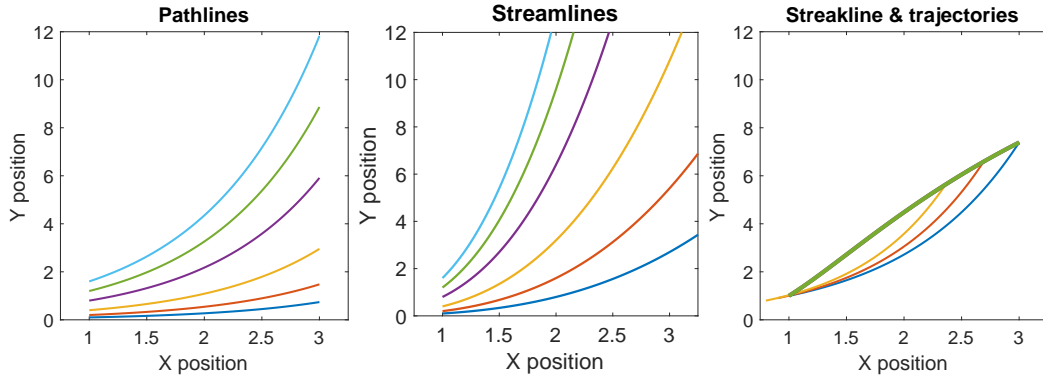


FIGURE 1.7: Left panel: sample pathlines $X(T) = X_0 (1 + T/\tau)$ and $Y(T) = Y_0 e^{T/\tau}$ (see equations (1.69a) and (1.69b)) during times $T \in [0, 2\tau]$. The trajectories drawn here all start at $X_0 = 1$ (in some arbitrary length unit) and set the parameter $\tau = 1$ (in some arbitrary time unit). Note that those pathlines with $X_0 = 0$ remain on the y-axis, and those with $Y_0 = 0$ remain on the x-axis. Middle panel: Sample streamlines $X(s; T) = X_0 e^{s/(\tau+T)}$ and $Y(s; T) = Y_0 e^{s/\tau}$ (see equations (1.72a) and (1.72b)). We set $T = 2$ and let the pseudo-time run from $s \in [0, 4]$. All streamlines shown here start at $X_0 = 1$. Note that those that start with $X_0 = 0$ remain on the y-axis, and those that start with $Y_0 = 0$ remain on the x-axis. Right panel: sample analytic streakline (dark bold line) at $T = 2$ according to equations (1.75a) and (1.75b). This streakline is determined by the position of particles at $T = 2$ that pass through $(X, Y) = (1, 1)$ during times $t \in (-\infty, 2)$. We show three sample trajectories that fall onto the streakline. The longest trajectory starts at $(X, Y) = (1, 1)$ at $T = 0$, whereas the two shorter trajectories pass through $(X, Y) = (1, 1)$ at some time $0 < T < 2$. Notice the distinction between all three flow lines, which is to be expected since the flow field is unsteady.

where $\tau > 0$ is a constant with the dimensions of time. Also write $\mathbf{X}(\mathbf{a}, T) = \varphi(\mathbf{x}, T)$ for the trajectories, with $t = T$ the time coordinate.

Pathlines

Pathlines are determined by solving the trajectory equations

$$\frac{dX(T)}{dT} = \frac{X(T)}{\tau + T} \quad \text{and} \quad \frac{dY(T)}{dT} = \frac{Y(T)}{\tau} \quad \text{and} \quad \frac{dZ(T)}{dT} = 0, \quad (1.68)$$

which are found to be

$$X(T) = X_0 (1 + T/\tau) \quad (1.69a)$$

$$Y(T) = Y_0 e^{T/\tau} \quad (1.69b)$$

$$Z(T) = Z_0, \quad (1.69c)$$

where $\mathbf{X}(T = 0) = \mathbf{X}_0$. Sample trajectories are shown in Figure 1.7 over time $T \in [0, 2]$ (in arbitrary time units). We can eliminate time to yield a curve in the horizontal (x, y) plane

$$y = Y_0 e^{(x-X_0)/X_0}. \quad (1.70)$$

Streamlines

Streamlines are determined by solving the differential equations

$$\frac{dX(s; T)}{ds} = \frac{X(s; T)}{\tau + T} \quad \text{and} \quad \frac{dY(s; T)}{ds} = \frac{Y(s; T)}{\tau} \quad \text{and} \quad \frac{dZ(s; T)}{ds} = 0, \quad (1.71)$$

where time, T , is a fixed parameter whereas the pseudo-time, s , is varied. Integration renders the streamlines

$$X(s; T) = X_0 e^{s/(\tau+T)} \quad (1.72\text{a})$$

$$Y(s; T) = Y_0 e^{s/\tau} \quad (1.72\text{b})$$

$$Z(s; T) = Z_0. \quad (1.72\text{c})$$

Sample streamlines are shown in Figure 1.7. Note that we can eliminate the pseudo-time s to render a curve in the horizontal (x, y) plane

$$y = Y_0 \left[\frac{x}{X_0} \right]^{(\tau+T)/\tau} \quad (1.73\text{a})$$

$$z = Z_0. \quad (1.73\text{b})$$

Streaklines

For streaklines, invert the trajectory expressions (1.69a)-(1.69b) to find the material coordinates $\mathbf{a}(\mathbf{y}, s)$ in the form

$$a_1 = \frac{y_1}{1 + s/\tau} \quad \text{and} \quad a_2 = y_2 e^{-s/\tau} \quad \text{and} \quad a_3 = y_3. \quad (1.74)$$

We next evaluate the trajectory expressions (1.69a)-(1.69b) with \mathbf{a} as the initial positions to find the streaklines

$$X(s; \mathbf{a}, T) = \frac{y_1 (1 + T/\tau)}{1 + s/\tau} \quad (1.75\text{a})$$

$$Y(s; \mathbf{a}, T) = y_2 e^{(T-s)/\tau} \quad (1.75\text{b})$$

$$Z(s; \mathbf{a}, T) = y_3. \quad (1.75\text{c})$$

Figure 1.7 illustrates the streakline for a particular point $(X, Y) = (1, 1)$.

1.8.6 Further study

A discussion of flow lines can be found in most books on fluid mechanics. The presentation here borrows from Sections 4.11-4.13 of *Aris* (1962), Section 3.3 of *Kundu et al.* (2016), and online lecture notes on fluid kinematics from Professor McIntyre of Cambridge University.



1.9 Exercises

EXERCISE 1.1: FLUID VELOCITY AND ACCELERATION DERIVED FROM A TRAJECTORY

Following example 3.2 from *Kundu et al.* (2016), consider a one-dimensional fluid motion whereby the trajectory of a fluid particle is given in Cartesian coordinates by

$$\mathbf{X}(T) = \hat{\mathbf{x}} X(T) = \hat{\mathbf{x}} [K(T - T_0) + X_0^3]^{1/3}, \quad (1.76)$$

where K is a constant with dimensions volume per time and X_0 is the particle position at time $T = T_0$.

- (a) Determine the particle velocity.
- (b) Determine the particle acceleration.
- (c) Determine the Eulerian velocity field.
- (d) Determine the Eulerian acceleration field.

EXERCISE 1.2: FLUID VELOCITY AND ACCELERATION DERIVED FROM A TRAJECTORY

This exercise is based on Q1.6 of [Johnson \(1997\)](#), and it is similar to Exercise 1.1. As described in this chapter, Eulerian kinematics focuses on the velocity field, $\mathbf{v}(\mathbf{x}, t)$, which provides the fluid velocity as a function of space and time. The complementary Lagrangian kinematics is based on describing fluid motion from the perspective of a moving fluid particle labeled by a material coordinate, \mathbf{a} . For definiteness, let the material coordinate be the position of a fluid particle at some arbitrary initial time, $\mathbf{a} = \mathbf{X}_0$.

Consider the following Cartesian coordinate expression for the trajectory of a fluid particle

$$\mathbf{X}(T) = X(T) \hat{\mathbf{x}} + Y(T) \hat{\mathbf{y}} + Z(T) \hat{\mathbf{z}} = X_0 e^{(T/\tau)^2} \hat{\mathbf{x}} + Y_0 e^{-(T/\tau)^2} \hat{\mathbf{y}} + Z_0 e^{-(T/\tau)^2} \hat{\mathbf{z}}, \quad (1.77)$$

where τ is a constant with dimensions of time.

- (a) Derive an expression for the Lagrangian velocity (i.e., velocity of the fluid particle), $\mathbf{V} = \dot{\mathbf{X}} = d\mathbf{X}/dT$.
- (b) Derive an expression for the Eulerian velocity field, $\mathbf{v}(\mathbf{x}, t)$.
- (c) Derive an expression for the Lagrangian acceleration, $\mathbf{A} = \ddot{\mathbf{V}} = d\mathbf{V}/dT$. To simplify the expression, write \mathbf{A} in terms of \mathbf{V} , $\dot{\mathbf{X}}$, $\dot{\mathbf{Y}}$, and $\dot{\mathbf{Z}}$.
- (d) Derive an expression for the Eulerian acceleration, which is given by the material time derivative of the Eulerian velocity field,

$$\frac{D\mathbf{v}}{Dt} = (\partial_t + \mathbf{v} \cdot \nabla) \mathbf{v}. \quad (1.78)$$

- (e) Show that the Lagrangian acceleration and Eulerian acceleration are the same when evaluated at the same point in space and time,

$$\frac{D\mathbf{v}}{Dt} = \mathbf{A} \quad \text{if } t = T \text{ and } \mathbf{x} = \mathbf{X}(T). \quad (1.79)$$

EXERCISE 1.3: FLUID VELOCITY AND ACCELERATION DERIVED FROM A TRAJECTORY

This exercise is just like Exercises 1.1 and 1.2, only with a different expression for the trajectory, and here considering only a single space dimension. Consider the one-dimensional fluid particle trajectory written using Cartesian coordinates

$$\mathbf{X}(T) = \hat{\mathbf{x}} X(T) = \hat{\mathbf{x}} [k(T - T_0)^2 + X_0^3]^{1/3}, \quad (1.80)$$

where k is a constant with dimensions $L^3 T^{-2}$, X_0 is the particle position at time $T_0 = t_0$, and $\hat{\mathbf{x}}$ is the fixed Cartesian unit vector.

- (a) Determine the velocity of the fluid particle.
- (b) Determine the acceleration of the fluid particle.
- (c) Determine the Eulerian velocity field.
- (d) Determine the Eulerian acceleration field and show that it equals to the particle acceleration when evaluated at the spatial point, $\mathbf{x} = \mathbf{X}(T)$.

EXERCISE 1.4: STREAMLINES AND PATHLINES

Consider the spatially constant oscillating horizontal velocity field written using Cartesian coordinates

$$\mathbf{u} = U [\hat{\mathbf{x}} \cos(\omega t) + \hat{\mathbf{y}} \sin(\omega t)], \quad (1.81)$$

where U is the constant flow speed and ω is the angular frequency of the oscillating flow. In this example we determine the streamlines and pathlines, which serves to clearly illustrate their distinction for this spatially constant time dependent flow.

- (a) Derive the equation $y = y(x)$ for the streamline that passes through the origin at time $t = 0$.
- (b) Derive the equation for the pathline that passes through the origin at time $t = 0$. Write the equation in a form that eliminates time, so to reveal the geometric shape of the pathlines.

EXERCISE 1.5: MATERIAL EVOLUTION OF THE PARTIAL DERIVATIVE OF A FUNCTION

In this exercise we establish some properties of the material time derivative operator when acting on spatial derivatives of a scalar field. Use Cartesian tensors throughout this exercise.

- (a) If a scalar field Π is materially constant, prove that the material evolution of its spatial derivative is given by

$$\frac{D(\partial_i \Pi)}{Dt} = -\partial_i \mathbf{v} \cdot \nabla \Pi. \quad (1.82)$$

For example, if $D\Pi/Dt = 0$, then the zonal partial derivative $\partial_x \Pi$ has a material time derivative given by

$$\frac{D(\partial \Pi / \partial x)}{Dt} = -\frac{\partial \mathbf{v}}{\partial x} \cdot \nabla \Pi. \quad (1.83)$$

- (b) What is the material time derivative of $\nabla \Pi$ for the case that Π is not materially constant? Write your answer in a manner that clearly shows that the partial space derivative does not commute with the material time derivative. That is,

$$\frac{D(\partial_i \Pi)}{Dt} \neq \partial_i \frac{D\Pi}{Dt}. \quad (1.84)$$

Show what term appears on the right hand side to produce an equality.

Hint: Some might find it more suitable to first solve the general case.

EXERCISE 1.6: SURFACE MOVING WITH THE FLUID

This exercise is based on Q1.5 of [Johnson \(1997\)](#). Consider a non-dimensional velocity field (all symbols are non-dimensional in this exercise and all coordinates are Cartesian)

$$\mathbf{v}(x, y, z, t) = t(2x\hat{\mathbf{x}} - y\hat{\mathbf{y}} - z\hat{\mathbf{z}}) \quad (1.85)$$

and a surface defined by the function

$$F(x, y, z, t) = x^2 e^{-2t^2} + (y^2 + 2z^2) e^{t^2} = \text{constant}. \quad (1.86)$$

Show that

$$\frac{DF}{Dt} = (\partial_t + \mathbf{v} \cdot \nabla) F = 0, \quad (1.87)$$

which means that the surface follows fluid particles.

EXERCISE 1.7: TRACER CONCENTRATION AND A GALILEAN TRANSFORMATION

Consider a tracer concentration written using (x, t) coordinates¹⁴

$$\Pi(x, t) = \Pi_0 e^{-x^2/(4\kappa t)}, \quad (1.88)$$

where Π_0 is a constant and where κ is a constant diffusivity with dimensions of $L^2 T^{-1}$.

- (a) Compute the material time derivative, $D\Pi/Dt$, with an assumed zero fluid flow.
- (b) Perform a Galilean boost to a reference frame moving with constant velocity, $U \hat{x}$. In this frame the fluid velocity is no longer static, but is now seen to be moving. Compute the material time derivative of $\bar{\Pi}(\bar{x}, \bar{t})$ in this reference frame. Hint: you should find that

$$\frac{D\bar{\Pi}(\bar{x}, \bar{t})}{D\bar{t}} = \frac{D\Pi(x, t)}{Dt}, \quad (1.89)$$

where (x, t) are space-time coordinates in the rest frame, (\bar{x}, \bar{t}) are coordinates in the boosted frame, and $\bar{\Pi}(\bar{x}, \bar{t})$ is the functional representation of the tracer concentration in the boosted frame.

Hint: make use of ideas detailed in Section 1.6

EXERCISE 1.8: UNSTATED ASSUMPTION IN LUMLEY'S VIDEO

[This 27-minute video on Eulerian and Lagrangian descriptions](#) from Prof. Lumley offers a pedagogical discussion of these two kinematic perspectives on fluid motion. However, there is one unstated assumption in this video that limits the applicability of his expressions for the material time derivative. What is that assumption? Hint: read Section 1.5.6.



¹⁴We study tracers in Chapter 4. No prior knowledge of tracers is needed for this exercise.

Chapter 2

MOTION AND DEFORMATION

Motion of the matter continuum provides a [flow map](#) that continuously and smoothly reshapes the continuum as time evolves. In this chapter we develop an understanding of how this [motion field](#) that transforms the continuum so to modify geometric objects and shapes placed in the flow. The kinematics of this modification is directly connected to flow [deformation](#), and we consider two methods to characterize deformation. One is based on the [motion field](#) that produces a [flow map](#) of the continuum. This method makes use of the [deformation matrix](#) (computed from derivatives of the flow map) that deforms material objects. The second method (which is dual to the first) is based on the [velocity gradient tensor](#), which is conveniently decomposed into its symmetric component, the [strain rate tensor](#) (also called the [deformation rate tensor](#)), and its anti-symmetric component known as the [rotation tensor](#).

The kinematic ideas in this chapter make extensive use of the material [fluid particle](#) as introduced in Section 1.3.1. Fluid particles are mathematical points that move with the fluid flow, and there is a continuum of such particles comprising any continuous region of fluid. We do not ask questions about the number of such particles on a material object, nor do we question whether particles are created or destroyed as a material object changes its length, area, or volume. Instead, we make use of fluid particles as a conceptual construct to describe motion of the continuum, and we use their trajectories to define the [Lagrangian reference frame](#). Point fluid particles are not approximations to molecules. Instead, they are mathematical constructs that offer a lens to view motion of the matter continuum.

As part of a study of flow kinematics, we commonly consider thought experiments by drawing an imaginary geometric object within a fluid and following the object as the fluid flows. A particularly relevant object is one whose material points follow a fluid particle trajectory. We study the kinematics of such material fluid objects by using rudimentary Lagrangian and Eulerian methods. Extra attention is given to the kinematics of two-dimensional flow due to the relative mathematical ease and the associated intuition that proves useful for more general three dimensional flows.

READER'S GUIDE FOR THIS CHAPTER

This chapter builds from the kinematics of Chapter 1, and makes extensive use of both the Eulerian and Lagrangian references frames. We assign the Latin labels i, j, k for the spatial (Eulerian) description in \mathbf{x} -space, whereas material (Lagrangian) labels use the capital letters, I, J, K for \mathbf{a} -space. Coordinates in both \mathbf{x} -space and \mathbf{a} -space sometimes assumed to be arbitrary, so that we make use of notions from general tensor analysis from VOLUME 1, with distinctions made between covariant and contravariant labels and adherence to the Einstein summation convention.

We require tensor analysis to systematically transform between the Eulerian and Lagrangian descriptions, and we review the salient formalism in this chapter as applied to x -space and a -space. Even so, at certain points we make use of Cartesian coordinates for the Eulerian space since doing so allows for the use of familiar notions from Cartesian tensor analysis when studying how points in the flow move relative to one another. Extending certain of these kinematic concepts to general coordinates requires more mathematical apparatus than considered in this book (e.g., Lie derivatives).

References for this chapter include the text by [Salmon \(1998\)](#), who provides an accessible treatment of Eulerian and Lagrangian fluid mechanics. Chapter 4 of [Aris \(1962\)](#) treats fluid kinematics in the context of tensor analysis. Chapter 4 of [Malvern \(1969\)](#), Chapters 1 and 2 of [Tromp \(2025a\)](#), and [Tromp \(2025b\)](#) provide insightful summaries of continuum kinematics, with Eulerian (spatial) and Lagrangian (material) two of the four descriptions that have found use in continuum mechanics. The other two descriptions are the *referential description* and the *relative description*. We make some use of the referential description in Section 2.2, which is commonly used in solid mechanics.

2.1	Loose threads	49
2.2	Motion generates the flow map	49
2.2.1	Defining the motion field and its flow map	50
2.2.2	Depicting the motion and its inverse	51
2.2.3	Comments	52
2.3	Material and spatial representations	52
2.3.1	Notation	52
2.3.2	The flow map as a coordinate transformation	52
2.3.3	Material time derivative of a scalar field	53
2.3.4	The flow map is a function, not a tensor	54
2.4	The deformation matrix as a transformation matrix	55
2.4.1	The deformation (transformation) matrix $F^i{}_I$	55
2.4.2	The inverse deformation matrix $F^I{}_i \equiv (F^{-1})^I{}_i$	56
2.4.3	A terse notation for the deformation matrix and its inverse	56
2.4.4	Jacobian determinant of the deformation matrix $F^i{}_I$	56
2.4.5	A discrete algorithm for the deformation matrix	57
2.4.6	Lagrangian coordinate representation of the velocity vector	57
2.4.7	Comments and further study	59
2.5	The metric tensor	59
2.5.1	Representing the metric tensor with x -coordinates	59
2.5.2	Representing the metric tensor with a -coordinates	60
2.5.3	Exposing the functional dependencies	61
2.5.4	Determinant of the metric tensor and deformation matrix	61
2.5.5	Diffusion operator in Lagrangian coordinates	62
2.6	An example of linear hyperbolic flow	62
2.6.1	Fluid particle trajectories and the motion field	63
2.6.2	Deformation matrix and metric tensor	64
2.6.3	Diffusion operator	64
2.6.4	Further reading	64
2.7	Kinematic description of relative motion	65
2.7.1	Differential increment for a -space and x -space	65
2.7.2	A role for the deformation matrix	66
2.7.3	Kinematic evolution equation	66

2.7.4	Cauchy's solution for evolution of the relative vector	67
2.8	The volume element	68
2.8.1	Arbitrary Eulerian and Lagrangian coordinates	69
2.8.2	Cartesian Eulerian coordinates	69
2.8.3	The volume of a fixed region of a -space	70
2.9	The velocity gradient tensor and relative velocity	70
2.9.1	Evolution of the relative velocity	71
2.9.2	Velocity gradient tensor	71
2.9.3	Stretching and tilting of material lines	72
2.9.4	Evolution of squared line element is affected by the strain rate .	72
2.9.5	Rigid rotation of the line element	73
2.9.6	Cauchy-Stokes decomposition	74
2.9.7	Evolution of the deformation matrix	74
2.9.8	Evolution of the Cauchy-Green strain tensor	75
2.10	Evolution of material surfaces	76
2.10.1	Surfaces in three-dimensional flow	76
2.10.2	Evolution of the material surface area	77
2.10.3	Evolution of the unit normal	78
2.10.4	Material area in two-dimensional flow	79
2.11	Volume, thickness, and the Jacobian	79
2.11.1	Material parcel volume	80
2.11.2	Evolution of the column thickness	81
2.11.3	Evolution of the Jacobian of transformation	81
2.12	Kinematics of two-dimensional flow	82
2.12.1	Diverging flow	83
2.12.2	Flow with nonzero deformation	83
2.12.3	Rotational flow with nonzero vorticity	83
2.12.4	Tension strain and shearing strain	84
2.12.5	Further study	84
2.13	Exercises	84

2.1 Loose threads

- Clarify footnote in Section 2.7.2.
- Introduce the Lie derivative and covariant derivative to generalize the work in this chapter. See Section F.3 of [Tromp \(2025a\)](#). In particular, make use of the Lie derivative for the differential increments in Section 2.7 and covariant derivative for the velocity gradient tensor. Should $\partial_I \varphi^i$ instead be $\nabla_I \varphi^i$, so that we are working with covariant derivatives in the Lagrangian frame?

2.2 Motion generates the flow map

The discussion in Section 1.4 serves to emphasize the primary role of fluid particle trajectories for use in describing fluid motion through Euclidean space. In this section we provide a more in-depth treatment, with a particular aim to develop a mathematical structure for describing the motion of continuum matter.

2.2.1 Defining the motion field and its flow map

In classical continuum mechanics, we conceive of a matter continuum that moves through Euclidean space as Newtonian time progresses. We define the **motion field**, $\boldsymbol{\varphi}$, as the mathematical object that generates a nonlinear time dependent and invertible *flow map*. The flow map moves between the continuous matter distribution in a reference (or base) state and the continuous matter distribution in a future state. That is, the motion field is the reason there is a flow map, so that the nomenclature “motion field” and “flow map” are used interchangeably in this book since they both refer to movement of the continuum.

Making use of Cartesian coordinates for \mathbf{x} -space, we write the motion field or flow map as

$$\mathbf{x} = \boldsymbol{\varphi}(\mathbf{a}, T) \quad \text{and} \quad x^i = \varphi^i(\mathbf{a}, T) \quad \text{for } i = 1, 2, 3. \quad (2.1)$$

The function, $\boldsymbol{\varphi}$, has a nonlinear dependence on the material coordinate, a^I (labeling a material point in the continuum), as well as the material time, T . The uppercase index, $I = 1, 2, 3$, is used for material coordinates. Equation (2.1) says that the spatial point, \mathbf{x} , for a fluid particle in the spatial manifold, \mathcal{S} , is determined once we specify the material coordinate, \mathbf{a} , and the time, $T = t$. We thus conceive of the motion through Euclidean space of the material continuum as providing the map that continuously and smoothly reshapes the material configuration. We are only concerned in this book with evolution that renders no holes or rips in the matter continuum; i.e., no discontinuities such as shocks in fluids or faults in solids.¹ Hence, the flow map (2.1) is smooth, one-to-one, and invertible.²

We encountered the idea of motion creating a flow map when studying flow lines in Section 1.8. Namely, by fixing a particular material coordinate, \mathbf{a} , and letting time progress, the flow map, $\boldsymbol{\varphi}(\mathbf{a}, T)$, defines a fluid particle trajectory moving through Euclidean space

$$\boldsymbol{\varphi}(\mathbf{a}, T) = \mathbf{X}(\mathbf{a}, T). \quad (2.2)$$

Given this identity, we could have maintained the notation for trajectories introduced in Section 1.4, rather than introduce the new symbol, $\boldsymbol{\varphi}$. Indeed, in many cases in this book it is convenient to use the notation $\mathbf{X}(\mathbf{a}, T)$ to connect to trajectories of point particles moving through Euclidean space, as studied in VOLUME 1. However, the $\boldsymbol{\varphi}$ notation is more general, allowing for the consideration of motion without presuming it is embedded within Euclidean space. Even though such generalities are not essential for this book, it is of use for more general treatments of continuum mechanics (e.g., [Tromp \(2025a\)](#) and [Tromp \(2025b\)](#)). Furthermore, it is effective nomenclature for our use when interpreting the flow map as a coordinate transformations between \mathbf{a} -space and \mathbf{x} -space, as we do in Section 2.3.2.

As depicted in Figure 2.1, the \mathbf{a} -space coordinates can be specified by the Cartesian positions of the fluid particles at a specified reference time, $T = t_R$. Indeed, this choice is common in the continuum mechanics literature. The continuum matter deforms as it evolves according to the motion field, $\boldsymbol{\varphi}(\mathbf{a}, T)$, with this deformation typically leading to rather complex coordinate lines. Hence, a coordinate description of fluid motion using Lagrangian kinematics necessarily

¹ [Tromp \(2025a\)](#) and [Tromp \(2025b\)](#) further generalizes the motion by working fully within the context of manifolds and differential geometry, thus removing the need to conceive of the motion of particles in Euclidean space. Besides allowing for the power of differential geometry, that level of abstraction allows [Tromp \(2025a\)](#) and [Tromp \(2025b\)](#) to consider rips in matter continuum, thus opening up the formalism to treating faults and earthquakes. For the present book, we do not employ that level of abstraction since the geophysical fluid motion of concern this book concerns the smooth motion of fluid particles through Euclidean space.

²Invertibility of the flow map holds even in the presence of irreversible mixing. The reason is that mixing retains the notion of distinct fluid particles, even though the mixing of fluid particles generates entropy.

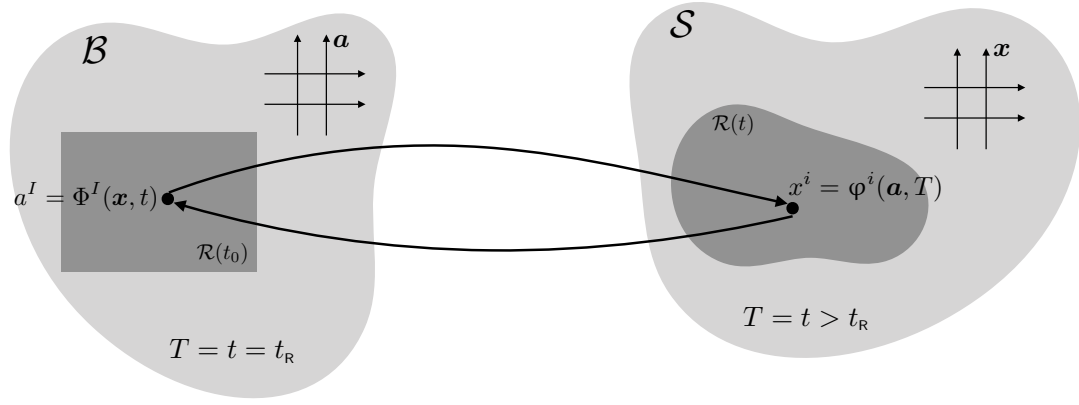


FIGURE 2.1: In the left panel, the matter continuum at reference time, $T = t_{\text{R}}$, defines a reference or base manifold, \mathcal{B} . Each point in \mathcal{B} is specified by its material (Lagrangian) coordinate, \mathbf{a} , thus providing the roots to the \mathbf{a} -space (Lagrangian) kinematic description of the motion. Within the base manifold we also depict a subregion, $\mathcal{R}(t_{\text{R}})$. The motion field, $\varphi(\mathbf{a}, T)$, acts as a one-to-one invertible flow map that smoothly evolves the matter continuum from the base manifold, \mathcal{B} , to the deformed or spatial manifold, \mathcal{S} , at Newtonian time, $t = T > t_{\text{R}}$. The motion field also maps the subregion, $\mathcal{R}(t_{\text{R}})$, of the base manifold, \mathcal{B} , to the subregion, $\mathcal{R}(t)$, of the spatial manifold, \mathcal{S} . The inverse motion or inverse flow map, Φ , defines the one-to-one inverse flow map going from \mathcal{S} to \mathcal{B} . A point on the spatial manifold is specified by the coordinate, \mathbf{x} , for points in space, thus providing the roots to the Eulerian \mathbf{x} -space kinematic description. We here depict the \mathbf{a} -space and \mathbf{x} -space coordinates as orthogonal Cartesian coordinates, yet they can be arbitrary coordinates by making use of the general tensor formalism in VOLUME 1. Indeed, it is common for the Lagrangian coordinates to have arbitrary physical dimensions (i.e., not length), as discussed in Section 1.4.2.

involves the general tensor analysis from VOLUME 1.

2.2.2 Depicting the motion and its inverse

In Figure 2.1 we depict the motion field and the corresponding flow map of the matter continuum. The base or reference state of the continuum is referred to as \mathcal{B} , and it defines a smooth **reference manifold** or **base manifold** on which we can perform differential calculus (again, we assume there are no rips or discontinuities in the fluid continuum). Each point of \mathcal{B} is specified by a value for the material (also Lagrangian) coordinate, \mathbf{a} . As time progresses, the motion field smoothly and invertibly maps each point of \mathcal{B} to a deformed state of the matter continuum. A point in the deformed fluid state is described by a point in the manifold, \mathcal{S} . We measure a position on \mathcal{S} using the spatial (or Eulerian) coordinates, \mathbf{x}^i , according to the flow map (2.1), thus motivating the name **spatial manifold** for \mathcal{S} .

Since the flow map provided by the motion is invertible, there is an inverse flow map, Φ . The inverse flow map takes each point occupied by fluid in the spatial manifold, \mathcal{S} , to a unique point on the reference manifold, \mathcal{B} . That is, given the Eulerian coordinate position of available to a fluid particle, \mathbf{x} , we have a unique material coordinate \mathbf{a} , which is specified by the inverse flow map

$$\mathbf{a} = \Phi(\mathbf{x}, t) \quad \text{and} \quad \mathbf{a}^I = \Phi^I(\mathbf{x}, t). \quad (2.3)$$

The invertible nature of the flow map means that a fluid particle trajectory does not split, nor do two trajectories occupy the same point at the same time. We acknowledge that fluid particle trajectories generally become increasingly complex in turbulent flow (indeed, even for some laminar flows). Consequently, the Lagrangian description is less convenient after a certain time has elapsed, thus motivating the reinitialization of fluid particle trajectories for practical calculations. Even so, as long as trajectories do not split or merge, the trajectories are well

defined in principle, and so is the corresponding Lagrangian formulation.

2.2.3 Comments

We mostly interpret the flow map as a coordinate transformation, as discussed in Section 2.3.2. Even so, it is useful to appreciate the complementary view in terms of motion as a flow map between distinct manifolds, as presented in this section. This kinematic perspective is commonly taken in solid mechanics.

2.3 Material and spatial representations

According to the presentation in Section 2.2, we specify a point of matter on the reference (or base) manifold, \mathcal{B} , by providing its material coordinate, \mathbf{a} . Similarly, a point on the spatial manifold, \mathcal{S} , is specified by the Eulerian coordinate in space, \mathbf{x} . The motion field generates a one-to-one and invertible flow map, $\boldsymbol{\varphi}(\mathbf{a}, T)$, which affords the ability to move seamlessly between the base manifold and the spatial manifold for any particular Newtonian time, $t = T$. For example, by specifying the material coordinate, \mathbf{a} , on \mathcal{B} , then that information uniquely specifies the fluid particle's spatial coordinate, \mathbf{x} , on \mathcal{S} , according to

$$\mathbf{x} = \boldsymbol{\varphi}(\mathbf{a}, T) \quad \text{and} \quad t = T. \quad (2.4)$$

Alternatively, by specifying the spatial point of a fluid particle, \mathbf{x} , on \mathcal{S} , then we uniquely specify the material point \mathbf{a} on \mathcal{B} , via the inverse motion

$$\mathbf{a} = \boldsymbol{\Phi}(\mathbf{x}, t) \quad \text{and} \quad T = t. \quad (2.5)$$

2.3.1 Notation

We write $d\mathbf{x}$ for the differential increment between two Eulerian positions in \mathbf{x} -space. Likewise, $d\mathbf{a}$ is the differential increment between two positions in \mathbf{a} -space.³ Finally, we write $\delta\mathbf{x}$ for the differential distance in \mathbf{x} -space between two material fluid particles specified by \mathbf{a} and $d\mathbf{a}$.

2.3.2 The flow map as a coordinate transformation

Equation (2.4) has the appearance of an invertible coordinate transformation between spatial and material coordinates. However, the coordinate transformations studied in VOLUME 1 concern two alternative coordinate representations for points on a single manifold. As illustrated by Figure 2.1, equation (2.4) provides a flow map between two points on two manifolds, with one point on the reference manifold and one point on the spatial manifold. Even so, the motion field provides a smooth, one-to-one and invertible mapping between these points. Consequently, we are afforded an alternative interpretation of the motion field as a coordinate transformation via equation (2.4). That is, the flow map defines a *point transformation* between a spatial representation of a fluid particle (fixed laboratory frame; Eulerian) and a material representation of the same fluid particle (moving reference frame co-moving with fluid particles; Lagrangian), with Figure 2.2 providing a schematic.⁴ We make use of general tensor analysis from VOLUME 1 to enable the mathematical transformation between the two coordinate systems.

³Mathematically, $d\mathbf{x}$ and $d\mathbf{a}$ are exterior derivatives.

⁴The point transformation perspective follows from Section 4.11 of [Aris \(1962\)](#) and is commonly considered in fluid mechanics.

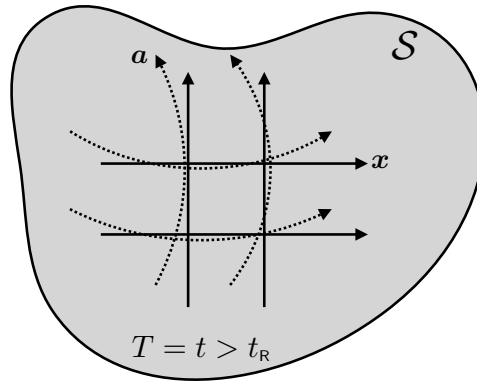


FIGURE 2.2: Two coordinate systems used to represent the spatial manifold, \mathcal{S} . The first is the spatial (Eulerian) representation, \mathbf{x} , which is fixed in space. The second is the material (Lagrangian) representation, \mathbf{a} , which is fixed on material particles. When projected onto the spatial manifold, the lines of constant \mathbf{a} are deformed as the fluid evolves, although they are typically assumed orthogonal on the base manifold as in Figure 2.1. The transformation between these two sets of coordinates is facilitated by the motion field, $\boldsymbol{\varphi}$, as given by equation (2.1). The coordinate transformation perspective complements the mapping perspective from Figure 2.1.

The velocity of a fluid particle is given by the time derivative of the flow map

$$\mathbf{v}^L(\mathbf{a}, T) = \partial_T \boldsymbol{\varphi}(\mathbf{a}, T) \iff (v^L)^i = \partial_T \varphi^i, \quad (2.6)$$

where the L superscript indicates that the velocity is written as a function of the material coordinates and time.⁵ This expression for the fluid particle velocity equals to the Eulerian velocity field as sampled along the fluid particle trajectory

$$\mathbf{v}^L(\mathbf{a}, T) = \mathbf{v}[\mathbf{x} = \boldsymbol{\varphi}(\mathbf{a}, T), t = T]. \quad (2.7)$$

Equivalently, we can produce the Eulerian expression for the velocity by inverting the expression for the flow map, $\boldsymbol{\varphi}(\mathbf{a}, T)$, as per equation (2.5) to obtain the material coordinate, $\mathbf{a}(\mathbf{x}, t)$, thus rendering

$$\mathbf{v}^L(\mathbf{a}, T) = \mathbf{v}^L[\mathbf{a}(\mathbf{x}, t), T]. \quad (2.8)$$

The right hand expression is defined at all spatial points, \mathbf{x} , so that we can define the Eulerian velocity field according to

$$\mathbf{v}(\mathbf{x}, t) = \mathbf{v}^L[\mathbf{a}(\mathbf{x}, t), T = t]. \quad (2.9)$$

In the converse situation we have the Eulerian velocity field, $\mathbf{v}(\mathbf{x}, t)$ at all points in space. The flow map, and hence the Lagrangian description, can be determined by integrating the first order ordinary differential equation

$$\partial_T \boldsymbol{\varphi}(\mathbf{a}, T) = \mathbf{v}[\mathbf{x} = \boldsymbol{\varphi}(\mathbf{a}, T), t]. \quad (2.10)$$

This is a nonlinear differential equation since the flow map appears on the left hand side as its time derivative, as well as within the argument to the velocity on the right hand side.

2.3.3 Material time derivative of a scalar field

To further help understand the role of the motion field, as well as the time derivative following a fluid particle trajectory, consider a scalar fluid property, Π , and measure it along the fluid

⁵The L superscript is *not* a tensor index.

particle trajectory

$$\Pi^L(\mathbf{a}, T) = \text{property II following the trajectory } \boldsymbol{\varphi}(\mathbf{a}, T). \quad (2.11)$$

As a complement, measuring the property at a spatial point renders the Eulerian representation⁶

$$\Pi^E(\mathbf{x}, t) = \text{property II at a spatial point } \mathbf{x} \text{ at time } t. \quad (2.12)$$

Since the arguments differ, the two functions, Π^L and Π^E , are generally distinct. The Eulerian and Lagrangian values for the fluid property agree when they are evaluated at the same point in space and time, hence

$$\Pi^L(\mathbf{a}, T) = \Pi^E[\mathbf{x} = \boldsymbol{\varphi}(\mathbf{a}, T), t = T]. \quad (2.13)$$

The time derivative of $\Pi^L(\mathbf{a}, T)$ following the fluid particle motion is given by the partial derivative

$$\frac{\partial \Pi^L(\mathbf{a}, T)}{\partial T} = \text{time derivative following fluid particle motion,} \quad (2.14)$$

which is computed while holding the material coordinates fixed. The chain rule renders the Eulerian expression for the same time derivative

$$\frac{\partial \Pi^L(\mathbf{a}, T)}{\partial T} = \frac{\partial \Pi^E[\mathbf{x} = \boldsymbol{\varphi}(\mathbf{a}, T), t = T]}{\partial T} \quad (2.15a)$$

$$= \frac{\partial \Pi^E(\mathbf{x}, t)}{\partial t} + \frac{\partial \boldsymbol{\varphi}(\mathbf{a}, T)}{\partial T} \cdot \nabla \Pi^E(\mathbf{x}, t) \quad (2.15b)$$

$$= (\partial_t + \mathbf{v}^L(\mathbf{a}, T) \cdot \nabla) \Pi^E(\mathbf{x}, t), \quad (2.15c)$$

$$= (\partial_t + \mathbf{v}^E(\mathbf{x}, t) \cdot \nabla) \Pi^E(\mathbf{x}, t). \quad (2.15d)$$

In equation (2.15c) we introduced the Lagrangian expression for the fluid particle velocity from Section 2.3.2

$$\mathbf{v}^L(\mathbf{a}, T) \equiv \mathbf{v}[\mathbf{x} = \boldsymbol{\varphi}(\mathbf{a}, T), t = T] = \partial_T \boldsymbol{\varphi}(\mathbf{a}, T), \quad (2.16)$$

where, again, the time derivative of the motion field is computed while holding the material coordinate, \mathbf{a} , fixed. For equation (2.15d) we equated the Lagrangian and Eulerian expressions for the particle velocity when they are evaluated at the same point in space and time, as given by equation (1.59). Equation (2.15d) accords with equation (1.11) derived using distinct methods.

2.3.4 The flow map is a function, not a tensor

The flow map is a function that assigns the position in space for fluid particles at a particular time instance. As such, the flow map generalizes to the continuum the notion of position for a continuum of point fluid particles, with the position defined relative to a chosen origin. In VOLUME 1 we emphasized that the point particle position is not a tensor, reserving the term “tensor” for geometric objects that are independent of coordinates and coordinate origins. We thus eschew the term “position vector.” For the same reason, the flow map is not a tensor since it is based on a chosen origin. So although the flow map is written with the boldface notation and it carries indices, we eschew the term “flow map vector” or “motion vector field.”

⁶In most occasions throughout this book, we do not expose the E superscript to denote an Eulerian expression for a fluid property. But for the present purposes it is useful to be somewhat pedantic in order to clearly distinguish the two functional representations of the scalar property, Π .

As for the position, the time derivative of the flow map defines a tensor, namely the velocity of the flow. The velocity is indeed a tensor since by taking the time derivative of the flow map, we remove dependence on the arbitrary origin of any chosen coordinate system.

2.4 The deformation matrix as a transformation matrix

In an analysis of fluid flow, we make routine use of the spatial coordinates (\mathbf{x} -space) of an Eulerian description and material coordinates (\mathbf{a} -space) of a Lagrangian description. Following the interpretation in Section 2.3.2 of the flow map as a coordinate transformation, we here introduce the *transformation matrix* that facilitates the coordinate transformation of physical objects between the Eulerian and Lagrangian kinematic descriptions. Since the flow map is invertible, so too is the transformation matrix, which means that its determinant, the *Jacobian*, remains nonzero and hence is single signed. We refer to the transformation matrix as the *deformation matrix*, for reasons motivated below.

2.4.1 The deformation (transformation) matrix $F^i{}_I$

We introduced the *transformation matrix* in VOLUME 1 for enabling a coordinate transformation of tensors. We here write the transformation matrix as the matrix of partial derivatives of the flow map and organize the elements to this matrix according to the following convention

$$F^i{}_I = \frac{\partial \varphi^i}{\partial a^I} \equiv \begin{bmatrix} \partial \varphi^1 / \partial a^1 & \partial \varphi^1 / \partial a^2 & \partial \varphi^1 / \partial a^3 \\ \partial \varphi^2 / \partial a^1 & \partial \varphi^2 / \partial a^2 & \partial \varphi^2 / \partial a^3 \\ \partial \varphi^3 / \partial a^1 & \partial \varphi^3 / \partial a^2 & \partial \varphi^3 / \partial a^3 \end{bmatrix}. \quad (2.17)$$

The upper Eulerian label, i , denotes the row and the lower material label, I , denotes the column. The transformation matrix, $F^i{}_I$, provides a means to measure how trajectories are deformed by the flow. Namely, each element of $F^i{}_I$ measures how much the i -component of a fluid particle trajectory is modified when altering the I -component of the material coordinate.

Malvern (1969) refers to $F^i{}_I$ as a two-point tensor, given that it connects points in \mathbf{x} -space to points in \mathbf{a} -space as per Figure 2.1. However, the transformation matrix is *not* a tensor, so we do not refer to $F^i{}_I$ as a tensor.⁷ Rather, we refer to the transformation matrix, $F^i{}_I$, as the *deformation matrix* in deference to its role as the transformation matrix between spatial and material coordinates as per Figure 2.2, and given its measure of how trajectories are deformed by the flow of matter.

In Section 2.7 we study how the deformation matrix leads to the evolution of the vector connecting two material points in the fluid. As a preface to that discussion, consider the special case where the material coordinate is the reference spatial position. In this case, the partial derivatives measure how particle trajectories are modified when altering the reference position of the particles. If the fluid has no deformation, then particle trajectories remain unaffected if changing the material coordinate (i.e., the reference position), in which case the deformation matrix is the identity tensor

$$F^i{}_I = \delta^i{}_I \quad \text{if there is no flow deformation.} \quad (2.18)$$

Generally each component of the deformation matrix is nonzero so that trajectories are deformed by the flow and as such they are dependent on the reference position.

⁷In VOLUME 1 we discuss the distinction between a second order tensor and a matrix.

2.4.2 The inverse deformation matrix $F^I{}_i \equiv (F^{-1})^I{}_i$

Since the transformation between \mathbf{a} -space and \mathbf{x} -space is invertible, we sometimes have occasion to consider the inverse transformation matrix, which we write as

$$F^I{}_i \equiv (F^{-1})^I{}_i = \frac{\partial \Phi^I}{\partial x^i} \equiv \begin{bmatrix} \partial \Phi^1 / \partial x^1 & \partial \Phi^1 / \partial x^2 & \partial \Phi^1 / \partial x^3 \\ \partial \Phi^2 / \partial x^1 & \partial \Phi^2 / \partial x^2 & \partial \Phi^2 / \partial x^3 \\ \partial \Phi^3 / \partial x^1 & \partial \Phi^3 / \partial x^2 & \partial \Phi^3 / \partial x^3 \end{bmatrix}, \quad (2.19)$$

where $a^I = \Phi^I(\mathbf{x}, t)$ defines the mapping from \mathbf{x} -space to \mathbf{a} -space according to equation (2.3). As the inverse matrix, we are afforded the identities

$$F^I{}_i F^i{}_J = \delta^I{}_J \quad \text{and} \quad F^I{}_i F^j{}_I = \delta^j{}_i. \quad (2.20)$$

2.4.3 A terse notation for the deformation matrix and its inverse

The deformation appears throughout our study of fluid mechanics given its role as the transformation matrix between material and position coordinates. Here we summarize the notation

$$F^i{}_I = \frac{\partial \varphi^i(\mathbf{a}, T)}{\partial a^I} = \frac{\partial x^i}{\partial a^I} \quad \text{deformation matrix} \quad (2.21a)$$

$$F^I{}_i = (F^{-1})^I{}_i = \frac{\partial \Phi^I(\mathbf{x}, t)}{\partial x^i} = \frac{\partial a^I}{\partial x^i} \quad \text{inverse deformation matrix.} \quad (2.21b)$$

The final equality in each of the above two equations introduces a shorthand whose definition is given by the preceding equality. This shorthand is suited to manipulations with the deformation matrix and its determinant. Furthermore, note that use of the symbol, x^i , does not imply that the Eulerian coordinates are Cartesian.

2.4.4 Jacobian determinant of the deformation matrix $F^i{}_I$

The Jacobian determinant of the deformation matrix can be written in either of the following ways

$$\det(F^i{}_I) = \frac{\partial \mathbf{x}}{\partial \mathbf{a}} = \frac{\partial \boldsymbol{\varphi}}{\partial \mathbf{a}} = \det \begin{bmatrix} \partial \varphi^1 / \partial a^1 & \partial \varphi^1 / \partial a^2 & \partial \varphi^1 / \partial a^3 \\ \partial \varphi^2 / \partial a^1 & \partial \varphi^2 / \partial a^2 & \partial \varphi^2 / \partial a^3 \\ \partial \varphi^3 / \partial a^1 & \partial \varphi^3 / \partial a^2 & \partial \varphi^3 / \partial a^3 \end{bmatrix}. \quad (2.22)$$

The notation $\partial \boldsymbol{\varphi} / \partial \mathbf{a} = \partial \mathbf{x} / \partial \mathbf{a}$ offers a useful means to distinguish between the determinant of the deformation matrix (2.17), versus the determinant of the inverse deformation matrix, written as

$$\det(F^I{}_i) = \frac{\partial \mathbf{a}}{\partial \mathbf{x}} = \frac{\partial \boldsymbol{\Phi}}{\partial \mathbf{x}} = \det \begin{bmatrix} \partial \Phi^1 / \partial x^1 & \partial \Phi^1 / \partial x^2 & \partial \Phi^1 / \partial x^3 \\ \partial \Phi^2 / \partial x^1 & \partial \Phi^2 / \partial x^2 & \partial \Phi^2 / \partial x^3 \\ \partial \Phi^3 / \partial x^1 & \partial \Phi^3 / \partial x^2 & \partial \Phi^3 / \partial x^3 \end{bmatrix}. \quad (2.23)$$

The Jacobian is single-signed since the mapping between \mathbf{a} -space and \mathbf{x} -space is one-to-one invertible.

2.4.5 A discrete algorithm for the deformation matrix

To help further understanding of the deformation matrix (2.17), we here sketch an algorithm for its discrete approximation. For this purpose, consider two-dimensional flow and write the trajectory of a particular fluid particle using Cartesian coordinates

$$\mathbf{X}(T) = X^1(T) \hat{\mathbf{x}} + X^2(T) \hat{\mathbf{y}}, \quad (2.24)$$

and use a Cartesian representation for the corresponding material coordinate

$$\mathbf{a} = a^1 \hat{\mathbf{x}} + a^2 \hat{\mathbf{y}}. \quad (2.25)$$

Now lay down a two-dimensional lattice with discrete indices (e, f) for each of the nodal points (grid points) on the lattice, and with corresponding spatial coordinates

$$\mathbf{x}(e, f) = x(e, f) \hat{\mathbf{x}} + y(e, f) \hat{\mathbf{y}}. \quad (2.26)$$

This lattice discretizes the two-dimensional space and so provides a discrete approximation to the Eulerian reference frame. Initialize fluid particles at each of the lattice grid points,

$$\mathbf{X}(e, f; T = 0) = \mathbf{x}(e, f) = \mathbf{a}(e, f), \quad (2.27)$$

with the discrete material coordinates defined by the initial positions. Then time step the trajectories using the velocity field to compute the particle pathlines, $\mathbf{X}[\mathbf{a}(e, f); T]$, as illustrated in Figure 2.3. At any particular time, the Eulerian position of a fluid particle is found by interpolating from the lattice grid points. Setting the material coordinates equal to the initial position then leads to the finite difference approximation to the deformation matrix

$$F^i_I = \begin{bmatrix} F^1_1 & F^1_2 \\ F^2_1 & F^2_2 \end{bmatrix} \approx \begin{bmatrix} \frac{X^1(e+1,f;T) - X^1(e-1,f;T)}{X^1(e+1,f;0) - X^1(e-1,f;0)} & \frac{X^1(e,f+1;T) - X^1(e,f-1;T)}{X^2(e,f+1;0) - X^2(e,f-1;0)} \\ \frac{X^2(e+1,f;T) - X^2(e-1,f;T)}{X^1(e+1,f;0) - X^1(e-1,f;0)} & \frac{X^2(e,f+1;T) - X^2(e,f-1;T)}{X^2(e,f+1;0) - X^2(e,f-1;0)} \end{bmatrix}. \quad (2.28)$$

If the grid is regular in both directions, then the initial positions have a separation, Δ , given by the grid spacing so that

$$F^i_I \approx \frac{1}{2\Delta} \begin{bmatrix} X^1(e+1,f;T) - X^1(e-1,f;T) & X^1(e,f+1;T) - X^1(e,f-1;T) \\ X^2(e+1,f;T) - X^2(e-1,f;T) & X^2(e,f+1;T) - X^2(e,f-1;T) \end{bmatrix}. \quad (2.29)$$

This expression illustrates how the deformation matrix provides a measure of trajectory spreading as fluid particles move away from their initial positions. As a check on the formulation, consider the case without any deformation. In this case $X^1(e, f; T) = X^1(e; T)$ and $X^2(e, f; T) = X^2(f; T)$ so that the transformation matrix is diagonal, and furthermore, $X^1(e+1; T) - X^1(e-1; T) = 2\Delta$ and $X^2(f+1; T) - X^2(f-1; T) = 2\Delta$, so that the transformation matrix is the identity.

2.4.6 Lagrangian coordinate representation of the velocity vector

In Section 2.3.2 we studied the flow map, φ , and showed that its material time derivative yields the Eulerian representation of the velocity vector for a fluid particle, as per equation (2.6)

$$\mathbf{v}^L(\mathbf{a}, T) = \partial_T \varphi(\mathbf{a}, T) \iff (v^L)^i = \partial_T \varphi^i. \quad (2.30)$$

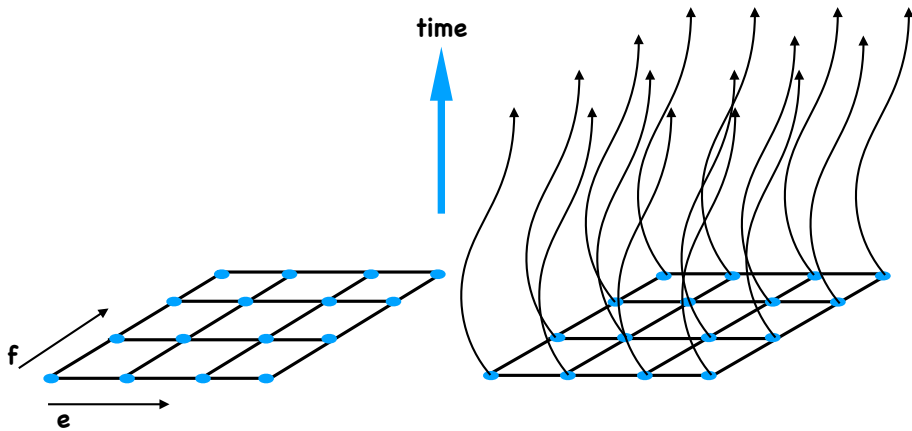


FIGURE 2.3: Illustrating the discrete algorithm of Section 2.4.5 to approximate the deformation matrix, F^I . The left panel shows the two-dimensional grid with nodal points defining the initial positions for fluid particles. Each position on the grid is labeled by a unique integer pair, (e, f) . The initial position of each particle is taken as the material coordinate, with the discrete label (e, f) maintained by the particles as they evolve. The right panel shows the pathlines for the fluid particles after time $T > 0$. When working on a discrete grid, the position of the fluid particles is not generally at a nodal point. Hence, the position must be found by interpolating between the node points.

Recall we make use of the L , superscript when measuring the velocity of a fluid particle trajectory, whereas it is the unadorned Eulerian velocity field, $\mathbf{v}(\mathbf{x}, t)$, when sampled at a point in space. But in both cases this velocity carries Eulerian labels, which prompts us to refer to it as the Eulerian coordinate representation of the fluid particle velocity vector.

We can derive a corresponding Lagrangian coordinate representation through use of the deformation matrix and its inverse. Namely, we write the Lagrangian coordinate representation of the fluid particle velocity via the transformation

$$v^I(\mathbf{a}, T) = (F^{-1})^I{}_i (v^{\text{L}})^i = \partial_i \Phi^I \partial_T \varphi^i. \quad (2.31)$$

We can derive a particularly elegant expression by writing the inverse map

$$a^I = \Phi^I(x^i, t) \quad (2.32)$$

and noting that its T derivative vanishes, $\partial_T a^I = \partial_T \Phi^I = 0$, since the material coordinates are independent of the material time. We thus find that

$$0 = \partial_T \Phi^I(x^i, t) = \frac{\partial \varphi^i}{\partial T} \partial_i \Phi^I + \frac{\partial t}{\partial T} \partial_t \Phi^I = (v^{\text{L}})^i \partial_i \Phi^I + \partial_t \Phi^I = (v^{\text{L}})^i (F^{-1})^I{}_i + \partial_t \Phi^I. \quad (2.33)$$

In the final equality we recognize $(v^{\text{L}})^i (F^{-1})^I{}_i = v^I$, which then leads us to conclude that the Lagrangian coordinate representation of the fluid particle velocity is given by minus the Eulerian time derivative of the inverse motion

$$v^I = -\partial_t \Phi^I, \quad (2.34)$$

which provides a complement to the Eulerian coordinate representation of the velocity, $v^i = \partial_T \varphi^i$. As a check on the self-consistency of this result, write the material time derivative acting on a scalar field as

$$(\partial_t + v^i \partial_i) C = (\partial_t T \partial_T + \partial_t \Phi^I \partial_I + v^I \partial_I) C = \partial_T C. \quad (2.35)$$

2.4.7 Comments and further study

When transforming between Eulerian and Lagrangian coordinates, it is the deformation matrix,

$$F^i{}_I = \partial \varphi^i / \partial a^I, \quad (2.36)$$

and its Jacobian determinant,

$$\det(F^i{}_I) = \partial \mathbf{x} / \partial \mathbf{a} = \partial \boldsymbol{\varphi} / \partial \mathbf{a}, \quad (2.37)$$

that encapsulates information about the transformation between Eulerian (\mathbf{x} -space) coordinates and Lagrangian (\mathbf{a} -space) coordinates. In particular, it is the deformation matrix (and its inverse) that transforms the representation of tensors between Eulerian coordinates and Lagrangian coordinates. The rules of coordinate transformation between Eulerian and Lagrangian representations are identical to those between any other set of coordinates considered in our study of tensor analysis in VOLUME 1. However, for continuum mechanics the transformation between Eulerian and Lagrangian coordinates is given special treatment due to the central roles played by Eulerian and Lagrangian kinematics.

This video from the *National Committee for Fluid Mechanics Films* offers insightful visualizations to help understand Eulerian and Lagrangian fluid descriptions. This lecture from Prof. Brunton discusses fluid kinematics related to finite time Lyapunov exponents, whose calculation requires estimating the transformation matrix in Section 2.4.5 along with its eigenvalues and eigenvectors.

2.5 The metric tensor

Throughout this book, we are concerned with the motion of continuum matter through Euclidean space. Euclidean space is endowed with a metric tensor as a means to measure the distance between points in space. When using Cartesian coordinates to describe Euclidean space, the metric tensor has a Cartesian coordinate representation equal to the identity tensor. However, for fluid mechanics we are interested in a variety of coordinates, both for Eulerian and Lagrangian descriptions. In particular, the material coordinates used for the Lagrangian description follow fluid particles. As such, these coordinates deform with the flow and so do not remain Cartesian even if initialized as Cartesian. Consequently, we require general tensor analysis as detailed in VOLUME 1. Having introduced the deformation matrix as the transformation matrix between \mathbf{x} -space and \mathbf{a} -space, we here introduce the metric tensor, \mathbf{g} , and its representations using Eulerian and Lagrangian coordinates.

2.5.1 Representing the metric tensor with x -coordinates

Consider two very close points in Euclidean space as represented by arbitrary Eulerian coordinates,⁸ x^a and $x^a + dx^a$. The squared arc-distance, $ds^2 = (ds)^2$, between these points is given by

$$ds^2 = g_{ij} dx^i dx^j, \quad (2.38)$$

⁸We here use x^a as any arbitrary Eulerian coordinates, either Cartesian or more general.

with g_{ij} the components to the metric tensor. Invertible transformations between two sets of arbitrary Eulerian coordinates,

$$\bar{\mathbf{x}} = \bar{\mathbf{x}}(\mathbf{x}) \quad \text{or component-wise} \quad \bar{x}^i = x^i(\bar{x}^i), \quad (2.39)$$

are facilitated by the transformation matrix built from the partial derivatives of the coordinate transformation. For example, the metric tensor transforms as a second order (0, 2) tensor

$$g_{\bar{i}\bar{j}} = g_{ij} \frac{\partial x^i}{\partial \bar{x}^i} \frac{\partial x^j}{\partial \bar{x}^j}, \quad (2.40)$$

which has an inverse transformation

$$g_{ij} = g_{\bar{i}\bar{j}} \frac{\partial x^i}{\partial \bar{x}^i} \frac{\partial x^j}{\partial \bar{x}^j}. \quad (2.41)$$

The Eulerian coordinates are independent of time, t . Consequently, the metric tensor represented using Eulerian coordinates is time independent

$$\partial_t g_{ij} = 0 \implies g_{ij} = g_{ij}(\mathbf{x}). \quad (2.42)$$

Note that if the coordinates, x^i , are Cartesian, then the Euclidean space metric tensor is represented by the Kronecker delta

$$g_{ij} = \delta_{ij} \quad \text{Euclidean space with Cartesian coordinates.} \quad (2.43)$$

2.5.2 Representing the metric tensor with a -coordinates

In a directly analogous fashion to the transformation (2.40) between two Eulerian coordinates, we use the deformation matrix from Section 2.4.1 to transform the metric tensor from general Eulerian coordinates to general Lagrangian coordinates via

$$g_{IJ} = g_{ij} \frac{\partial x^i}{\partial a^I} \frac{\partial x^j}{\partial a^J} = g_{ij} F^i{}_I F^j{}_J. \quad (2.44)$$

This representation of the metric tensor is useful when measuring the length of material line elements⁹

$$\delta s^2 = g_{ij} d\varphi^i d\varphi^j = g_{ij} \frac{\partial \varphi^i}{\partial a^I} \frac{\partial \varphi^j}{\partial a^J} da^I da^J = g_{ij} F^i{}_I F^j{}_J da^I da^J = g_{IJ} da^I da^J. \quad (2.45)$$

This expression is directly analogous to the squared differential length (2.38) found in \mathbf{x} -space. Although the Eulerian representation of the metric tensor is time independent as per equation (2.42), the Lagrangian representation is time dependent due to the time dependence of the deformation matrix, so that

$$g_{IJ} = g_{IJ}(\mathbf{a}, T). \quad (2.46)$$

When the Eulerian coordinates are Cartesian, so that $g_{ij} = \delta_{ij}$, then the Lagrangian form of the metric tensor is known as **Cauchy-Green strain tensor**

$$g_{IJ} = F^i{}_I F^j{}_J \delta_{ij} \quad \text{Cauchy-Green strain tensor.} \quad (2.47)$$

⁹To help understand equation (2.45), it can be useful to be reminded of the notation conventions summarized in Sections 2.3.1, 2.4.3, and 2.4.4.

Note that in Section 1.6 of [Tramp \(2025a\)](#), g_{IJ} in equation (2.47) is referred to as the *right Cauchy-Green deformation rate tensor*, which is the term also used in [Malvern \(1969\)](#). We use the term “strain” rather than “deformation” to help reduce confusion with the deformation matrix, $F^i{}_I$.

2.5.3 Exposing the functional dependencies

In equation (2.46) we noted that the metric tensor represented using Lagrangian coordinates is a function of (\mathbf{a}, T) . Likewise, the metric tensor represented using Eulerian coordinates is written in terms of the Eulerian coordinates, $g_{ij}(\mathbf{x})$. Written in terms of their transformations we have

$$g_{ij}(\mathbf{x}) = F^I{}_i(\mathbf{x}, t) F^J{}_j(\mathbf{x}, t) g_{IJ}(\mathbf{a} = \Phi(\mathbf{x}, t), T = t) \quad (2.48a)$$

$$g_{IJ}(\mathbf{a}, T) = F^i{}_I(\mathbf{a}, T) F^j{}_J(\mathbf{a}, T) g_{ij}(\mathbf{x} = \varphi(\mathbf{a}, T)). \quad (2.48b)$$

In these equations we inserted the motion field, $\varphi(\mathbf{a}, T)$, and its inverse, $\Phi(\mathbf{x}, t)$, when written on the right hand sides to these equations.

As noted in Section 2.5.1, the Eulerian representation of the metric tensor has no dependence on the Eulerian time, t . In contrast, the Lagrangian representation is generally a function of Lagrangian time, T . This distinction becomes less clear, however, when using coordinates commonly used in geophysical fluid mechanics, in which the set of coordinates are neither fully Eulerian nor fully Lagrangian, with the primary example being the generalized vertical coordinates studied in VOLUME 3. In that case, we generally have a metric tensor that is time dependent, even though some of the coordinates are Eulerian.

2.5.4 Determinant of the metric tensor and deformation matrix

The determinant of the metric tensor appears in the covariant volume element derived in VOLUME 1 and extended to Eulerian and Lagrangian coordinates in Section 2.8. Furthermore, the metric tensor is a positive-definite tensor, so that we know its determinant is positive. As a shorthand, we find it useful to introduce the following notation for the square root of the determinant as represented using Eulerian and Lagrangian coordinates

$$g^E = \sqrt{\det[g(\mathbf{x})]} \quad \text{and} \quad g^L = \sqrt{\det[g(\mathbf{a}, T)]}. \quad (2.49)$$

With this notation, we take the determinant of equation (2.44) to render

$$(g^L)^2 = \det(F^i{}_I) \det(F^j{}_J) (g^E)^2 = \left[\frac{\partial \mathbf{x}}{\partial \mathbf{a}} \right]^2 (g^E)^2. \quad (2.50)$$

Rearrangement leads to

$$\frac{\partial \mathbf{x}}{\partial \mathbf{a}} = \frac{\partial \varphi}{\partial \mathbf{a}} = \frac{g^L}{g^E}, \quad (2.51)$$

where we assumed the Jacobian determinant is positive. Note that if the Eulerian coordinates are Cartesian, then $g^E = 1$ so that

$$\frac{\partial \mathbf{x}}{\partial \mathbf{a}} = \frac{\partial \varphi}{\partial \mathbf{a}} = g^L \quad \text{Cartesian Eulerian coordinates.} \quad (2.52)$$

2.5.5 Diffusion operator in Lagrangian coordinates

As an application of the formalism, we here express the diffusion operator in Lagrangian coordinates.¹⁰ The diffusion operator is a scalar that is given by the covariant convergence of the diffusive flux

$$-\nabla \cdot \mathbf{J} = -g^{-1} \partial_a (g J^a), \quad (2.53)$$

with the right hand side taken from our study of general tensors in VOLUME 1. The square root of the metric determinant is unity for Cartesian coordinates, $g = 1$, yet it is nonzero for Lagrangian coordinates. As a scalar, the diffusion operator is coordinate invariant, and so our task is to identify the Lagrangian coordinate expression for the diffusive flux, \mathbf{J} . The diffusive flux is written in terms of a second order symmetric and positive-definite diffusion tensor, \mathbf{K} , according to

$$\mathbf{J} = -\mathbf{K} \cdot \nabla C \iff J^i = -K^{ij} \partial_j C, \quad (2.54)$$

with C the scalar tracer concentration and the right hand side uses Eulerian coordinates. We transform the Eulerian flux to Lagrangian coordinates according to

$$J^I = (F^{-1})^I{}_i J^i = -(F^{-1})^I{}_i K^{ij} \partial_j C = -(F^{-1})^I{}_i K^{ij} \partial_j C = -K^{IJ} \partial_J C. \quad (2.55)$$

This expression directly compares to the Eulerian form (2.54), only here with Lagrangian tensor indices rather than Eulerian. Correspondingly, the diffusion operator (2.53) is written using Lagrangian coordinates

$$-\nabla \cdot \mathbf{J} = -g^{-1} \partial_I (g J^I) = g^{-1} \partial_I (g K^{IJ} \partial_J C). \quad (2.56)$$

Note that when the diffusion tensor is isotropic in Eulerian Cartesian coordinates, as per the case of molecular diffusion, then

$$K^{ij} = \kappa \delta^{ij} \quad \text{and} \quad K^{IJ} = \kappa g^{IJ}, \quad (2.57)$$

in which case the Lagrangian coordinate representation of the diffusion operator takes the form

$$-\nabla \cdot \mathbf{J} = g^{-1} \partial_I (g \kappa g^{IJ} \partial_J C), \quad (2.58)$$

with g the square root of the metric tensor determinant using Lagrangian coordinates.

2.6 An example of linear hyperbolic flow

To help ground some of the formalism developed thus far, we work through an example where the fluid particle trajectories can be analytically computed, which then allows us to analytically compute the motion field, the deformation matrix, and the metric tensor. The flow we consider is generated by the following non-divergent horizontal Eulerian velocity field

$$\mathbf{u} = \alpha (\hat{\mathbf{x}} x - \hat{\mathbf{y}} y) = \alpha (\mathbf{e}_1 x^1 - \mathbf{e}_2 x^2), \quad (2.59)$$

where $\alpha > 0$ is a constant with dimensions inverse time, and the second equality introduced Eulerian tensor labels for the Eulerian coordinates, x^i , and corresponding Cartesian basis

¹⁰We provide mathematical and physical details about tracer diffusion in VOLUME 4. For present purposes, we are just focused on the mathematics of the transformation to Lagrangian coordinates.

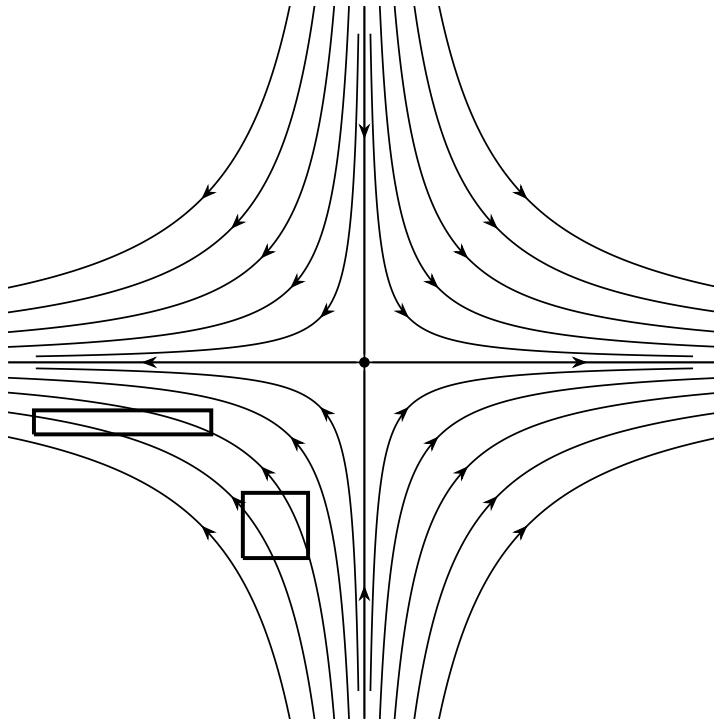


FIGURE 2.4: An ensemble of hyperbolic fluid particle trajectories defined from the horizontally non-divergent velocity field, $\mathbf{u} = \alpha(\hat{x}x - \hat{y}y)$, and the corresponding motion field, $\varphi(a^I, T) = \hat{x}a^1 e^{\alpha T} + \hat{y}a^2 e^{-\alpha T}$. The deformation matrix is diagonal, so that the flow both conserves area (since $\nabla \cdot \mathbf{u} = 0$), and preserves angles. Namely, this map stretches along the x direction and compresses along the y direction. Angular distortion requires off-diagonal elements to the deformation matrix. Note that units are arbitrary.

vectors, \mathbf{e}_i .

2.6.1 Fluid particle trajectories and the motion field

The fluid particle trajectories can be computed by time integration

$$\frac{dX}{dt} = \alpha X \implies X(t) = X(0) e^{\alpha t} \quad (2.60a)$$

$$\frac{dY}{dt} = -\alpha Y \implies Y(t) = Y(0) e^{-\alpha t}. \quad (2.60b)$$

We define the Lagrangian coordinates according to the initial particle positions so that

$$a^1 = X(0) \quad \text{and} \quad a^2 = Y(0). \quad (2.61)$$

We thus have the motion, φ , given by

$$x^1 = \varphi^1(a^I, T) = a^1 e^{\alpha T} \quad \text{and} \quad x^2 = \varphi^2(a^I, T) = a^2 e^{-\alpha T}, \quad (2.62)$$

and its inverse

$$a^1 = \Phi^1(x^i, t) = x^1 e^{-\alpha t} \quad \text{and} \quad a^2 = \Phi^2(x^i, t) = x^2 e^{\alpha t}. \quad (2.63)$$

2.6.2 Deformation matrix and metric tensor

The deformation matrix is given by

$$F^i{}_I = \frac{\partial \varphi^i}{\partial a^I} \equiv \begin{bmatrix} \partial \varphi^1 / \partial a^1 & \partial \varphi^1 / \partial a^2 \\ \partial \varphi^2 / \partial a^1 & \partial \varphi^2 / \partial a^2 \end{bmatrix} = \begin{bmatrix} e^{\alpha T} & 0 \\ 0 & e^{-\alpha T} \end{bmatrix}. \quad (2.64)$$

The diagonal nature of the deformation matrix means that it stretches and compresses along the coordinate axes, thus preserving angles. More general distortion arises from motion fields that generate off-diagonal terms in the deformation matrix. Additionally, the determinant is unity,

$$\det(F^i{}_I) = 1, \quad (2.65)$$

which means that the flow conserves area, as we already know since $\nabla \cdot \mathbf{u} = 0$. We thus find that a square deforms to a rectangle with the same area, as seen in Figure 2.4.

The Lagrangian coordinate representation of the metric tensor, g_{IJ} , is given by the coordinate transformation equation (2.44). Assuming the Eulerian coordinates are Cartesian, we have

$$g_{IJ} = \delta_{ij} F^i{}_I F^j{}_J. \quad (2.66)$$

The deformation matrix takes on the diagonal form (2.64), which readily yields the Lagrangian coordinate representation of the metric tensor and its inverse

$$g_{IJ} = \begin{bmatrix} e^{2\alpha T} & 0 \\ 0 & e^{-2\alpha T} \end{bmatrix} \quad \text{and} \quad g^{IJ} = \begin{bmatrix} e^{-2\alpha T} & 0 \\ 0 & e^{2\alpha T} \end{bmatrix}. \quad (2.67)$$

Note how the (1, 1) component grows in time whereas the (2, 2) component decays. Their product, which is the determinant of the metric, equals to unity,

$$\det(g(\mathbf{a}, T)) = 1, \quad (2.68)$$

which means that expansion of material regions in the x direction is exactly compensated by compression in the y direction.

2.6.3 Diffusion operator

Assuming isotropic molecular diffusion, the diffusion operator (2.58) is given by

$$-\nabla \cdot \mathbf{J} = \partial_I (\kappa g^{IJ} \partial_J C) = \kappa e^{-2\alpha T} \partial_{a^1 a^1} C + \kappa e^{2\alpha T} \partial_{a^2 a^2} C, \quad (2.69)$$

in which case the diffusion equation in Lagrangian coordinates is given by

$$\partial_T C = \kappa e^{-2\alpha T} \partial_{a^1 a^1} C + \kappa e^{2\alpha T} \partial_{a^2 a^2} C. \quad (2.70)$$

2.6.4 Further reading

This section made use of material in Section 4.3 of [Young \(1999\)](#).

2.7 Kinematic description of relative motion

Material curves are one-dimensional geometric objects that follow fluid particles. We initialize a material curve by drawing a line in the fluid and then following the curve as it deforms according to the trajectories of the fluid particles. The material curve is stretched and folded by the fluid flow as illustrated in Figure 2.5. We here develop the rudimentary kinematics of such motion by considering evolution of the relative vector connecting two fluid particles in Euclidean space. We specialize to Eulerian Cartesian coordinates to simplify comparison of the particle position vectors. That is, we assume the flow map generated by the motion, $\boldsymbol{\varphi}(\mathbf{a}, T)$, is represented by the Cartesian position of the fluid particles. As we will see, evolution of these two points is determined by the deformation matrix introduced in Section 2.4.

2.7.1 Differential increment for a -space and x -space

We start by developing expressions for the differential increment of a function in x -space and in material a -space.¹¹ These relations are useful when manipulating relations in either x -space or a -space.

Spatial increments

Consider a scalar fluid property, Π , and represent it with the spatial coordinates of an Eulerian description, $\Pi(\mathbf{x}, t)$. In Section 1.5.1, we considered the space and time increment of a scalar function. Here we consider just the space increment, as defined by the differential increment of a function evaluated at the same time but at two infinitesimally close points in space. Writing this increment for a scalar renders

$$d\Pi(\mathbf{x}, t) = \Pi(\mathbf{x} + d\mathbf{x}, t) - \Pi(\mathbf{x}, t) = (dx^i \partial_i)\Pi(\mathbf{x}, t). \quad (2.71)$$

Material increments

Consider the same fluid property, Π , now evaluated on a material fluid particle trajectory, and write this Lagrangian function as in Section 2.3.3

$$\Pi^L(\mathbf{a}, T) \equiv \Pi[\mathbf{x} = \boldsymbol{\varphi}(\mathbf{a}, T), t = T]. \quad (2.72)$$

Now consider an infinitesimal increment of $\Pi^L(\mathbf{a}, T)$ within material coordinate space. This increment measures the difference of the fluid property, Π , when evaluated on two fluid particles, one labelled by \mathbf{a} and the other by $\mathbf{a} + da$. Just like when working in x -space, we take a Taylor series and truncate to leading order, so that

$$d\Pi^L(\mathbf{a}, T) = \Pi[\boldsymbol{\varphi}(\mathbf{a} + da, T), T] - \Pi[\boldsymbol{\varphi}(\mathbf{a}, T), T] \quad (2.73a)$$

$$= \Pi^L(\mathbf{a} + da, T) - \Pi^L(\mathbf{a}, T) \quad (2.73b)$$

$$= (da^I \partial_I)\Pi^L(\mathbf{a}, T). \quad (2.73c)$$

Duality between Eulerian and Lagrangian perspectives

It is self-evident that the value of a fluid property at a spatial point \mathbf{x} (Eulerian perspective) equals to the property evaluated on a moving fluid particle (Lagrangian perspective) at the

¹¹From a mathematical perspective, we develop the exterior derivatives for a selection of scalar functions, and detail their expressions using both Eulerian and Lagrangian coordinates.

instance the particle passes through \mathbf{x} . Mathematically, this identity takes the form

$$\Pi^L(\mathbf{a}, T) = \Pi[\mathbf{x} = \boldsymbol{\varphi}(\mathbf{a}, T), t = T] = \Pi(\mathbf{x}, t) \quad \text{if } \boldsymbol{\varphi}(\mathbf{a}, T) = \mathbf{x}. \quad (2.74)$$

Likewise, if the infinitesimal increment in space, $\delta\mathbf{x}$, equals to the vector increment of the two fluid particles,

$$d\boldsymbol{\varphi}(\mathbf{a}, T) = \boldsymbol{\varphi}(\mathbf{a} + d\mathbf{a}, T) - \boldsymbol{\varphi}(\mathbf{a}, T), \quad (2.75)$$

then the functional increments are identical

$$d\Pi^L(\mathbf{a}, T) = \delta\Pi(\mathbf{x}, t) \quad \text{if } d\boldsymbol{\varphi}(\mathbf{a}, T) = \delta\mathbf{x}, \quad (2.76)$$

where

$$\delta\Pi(\mathbf{x}, t) = \Pi(\mathbf{x} + \delta\mathbf{x}, t) - \Pi(\mathbf{x}, t) = (\delta x^i \partial_i) \Pi(\mathbf{x}, t) \quad (2.77a)$$

$$d\Pi^L(\mathbf{a}, T) = \Pi^L(\mathbf{a} + d\mathbf{x}, T) - \Pi^L(\mathbf{a}, T) = (da^I \partial_I) \Pi^L(\mathbf{a}, T). \quad (2.77b)$$

These identities allow us to develop relations using either a Lagrangian or an Eulerian description, and then to interpret the resulting equations in their dual perspective.

2.7.2 A role for the deformation matrix

Consider two fluid particles with material coordinates, \mathbf{a} and $\mathbf{a} + d\mathbf{a}$, along with their corresponding trajectories $\boldsymbol{\varphi}(\mathbf{a}, T)$ and $\boldsymbol{\varphi}(\mathbf{a} + d\mathbf{a}, T)$ (see Figure 2.5). Assuming the trajectories are represented using Cartesian coordinates, we can write the vector connecting these two particles (the relative vector) as

$$d\boldsymbol{\varphi}(\mathbf{a}, T) = \boldsymbol{\varphi}(\mathbf{a} + d\mathbf{a}, T) - \boldsymbol{\varphi}(\mathbf{a}, T). \quad (2.78)$$

Expanding to leading order yields an expression of *Cauchy's solution* (further explored in Section 2.7.4)

$$d\boldsymbol{\varphi}(\mathbf{a}, T) = \boldsymbol{\varphi}(\mathbf{a} + d\mathbf{a}, T) - \boldsymbol{\varphi}(\mathbf{a}, T) \approx (da^I \partial_I) \boldsymbol{\varphi}(\mathbf{a}, T). \quad (2.79)$$

Making use of the assumed Cartesian coordinates for the flow map allows us to write the material increment in terms of the deformation matrix¹²

$$d\varphi^i = da^I \partial_I \varphi^i = da^I F^i{}_I, \quad (2.80)$$

where we introduced the deformation matrix from Section 2.4.1, $F^i{}_I \equiv \partial_I \varphi^i$.

2.7.3 Kinematic evolution equation

Now consider the material time derivative of the material increment

$$\frac{\partial[d\boldsymbol{\varphi}(\mathbf{a}, T)]}{\partial T} = \frac{\partial\boldsymbol{\varphi}(\mathbf{a} + d\mathbf{a}, T)}{\partial T} - \frac{\partial\boldsymbol{\varphi}(\mathbf{a}, T)}{\partial T} \quad (2.81a)$$

$$= \mathbf{v}^L(\mathbf{a} + d\mathbf{a}, T) - \mathbf{v}^L(\mathbf{a}, T) \quad (2.81b)$$

$$= d\mathbf{v}^L(\mathbf{a}, T). \quad (2.81c)$$

¹²The connection between differential increment and deformation gradient does not hold when using general coordinates for the flow map. The reason is that we cannot naively compare vectors on a general manifold. More work is needed, with details provided in Chapter 1 of [Tromp \(2025a\)](#) as well as in [Tromp \(2025b\)](#). Is this really the case?? Or perhaps all we need is to use a covariant derivative rather than partial derivative??

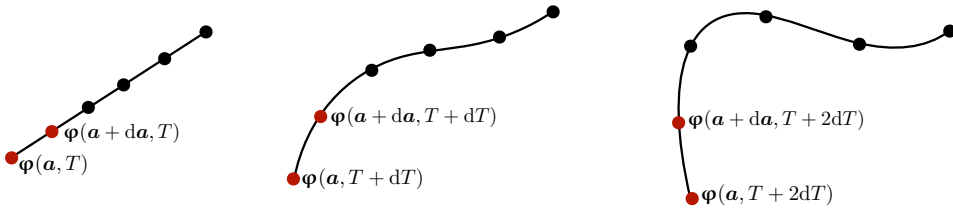


FIGURE 2.5: Three time instances of a material curve, highlighting two fluid particles whose trajectories are $\varphi(\mathbf{a}, T)$ and $\varphi(\mathbf{a} + d\mathbf{a}, T)$. All points along the curve move through the fluid by following the trajectories of the fluid particles. Kinematics of the relative vector separating two fluid particles is determined by properties of the deformation matrix in Section 2.7, or the deformation rate in Section 2.9.

In these equations, we introduced the Lagrangian velocity,

$$\mathbf{v}^L(\mathbf{a}, T) = \mathbf{v}[\mathbf{x} = \varphi(\mathbf{a}, T), t = T], \quad (2.82)$$

as per equation (2.16). As for the manipulations in Section 2.7.2, we can massage the expression (2.81c) by performing a Taylor series expansion and truncating to leading order

$$\frac{\partial[d\varphi(\mathbf{a}, T)]}{\partial T} = d\mathbf{v}^L(\mathbf{a}, T) = (d\mathbf{a}^I \partial_I) \mathbf{v}^L(\mathbf{a}, T). \quad (2.83)$$

Alternatively, we can choose to evaluate this expression using an Eulerian perspective (see Section 2.7.1), in which case

$$\frac{D(\delta\mathbf{x})}{Dt} = \delta\mathbf{v}(\mathbf{x}, t) = (\delta x^i \partial_i) \mathbf{v}(\mathbf{x}, t). \quad (2.84)$$

In Section 2.7.4 we examine this equation according to Cauchy, thus furthering our understanding of how the relative displacement vector evolves.

2.7.4 Cauchy's solution for evolution of the relative vector

We can determine a general solution to the kinematic evolution equation (2.84), and we do so by following the method used by Cauchy¹³. Indeed, we already encountered the Cauchy solution in Section 2.7.2. We rederive it here as an exercise in the formalism that can be of general use when working with Lagrangian coordinates.

Derivation using the motion field and deformation matrix

For this derivation we make use of the motion field, $\varphi^i(\mathbf{a}, T)$, and the deformation matrix, $\partial_I \varphi^i = F^i{}_I$, in which we start from equation (2.84) yet written using Lagrangian coordinates

$$\partial_T(\delta x^i) = \delta x^j \partial_j(\partial_T \varphi^i) = \delta x^j F^J{}_j \partial_J(\partial_T \varphi^i), \quad (2.85)$$

where the second equality used the deformation matrix to convert from an Eulerian derivative to a Lagrangian derivative: $\partial_j = F^J{}_j \partial_J$. Noting that $\partial_J \partial_T = \partial_T \partial_J$, and introducing the deformation matrix, $\partial_J \varphi^i = F^i{}_J$, we find

$$\partial_T(\delta x^i) = \delta x^j F^J{}_j \partial_T F^i{}_J = -\delta x^j (\partial_T F^J{}_j) F^i{}_J. \quad (2.86)$$

¹³See [Frisch and Villone \(2014\)](#) for an insightful discussion of the enduring impact of Cauchy's solution.

The second equality follows since $F^J{}_j F^i{}_J = \delta^i{}_j$ is time independent. Now contract both sides of this equation with $F^K{}_i$ and note that $F^K{}_i F^i{}_J = \delta^J{}_K$, so that

$$F^K{}_i \partial_T(\delta x^i) = -\delta x^j \partial_T F^K{}_j \implies \partial_T(F^K{}_i \delta x^i) = 0. \quad (2.87)$$

Choosing the material coordinates equal to the reference positions

If we choose the material coordinates as the reference positions of fluid particles,

$$\mathbf{a} = \mathbf{x}(t = t_R) = \dot{\mathbf{x}}, \quad (2.88)$$

then the inverse transformation matrix element at the reference time is given by the unit tensor

$$F^K{}_j = \delta^K{}_j \quad \text{at } t = t_R, \quad (2.89)$$

so that the material invariance in equation (2.87) leads to

$$\delta x^j F^K{}_j = \delta \dot{x}^K. \quad (2.90)$$

Inverting this equation by contracting with $F^i{}_K$ and using $F^i{}_K F^K{}_j = \delta^i{}_j$ leads to *Cauchy's solution*

$$\delta x^i = \delta \dot{x}^K F^i{}_K = \delta \dot{x}^K \partial_K \varphi^i(\mathbf{a}, T). \quad (2.91)$$

Discussion of Cauchy's solution (2.91)

The Cauchy solution (2.91) says that the increment along a line segment defined by fluid particles, $\delta \mathbf{x} = \delta \boldsymbol{\varphi}$, expands or contracts according to the time and space dependent deformation matrix, $F^i{}_K$. This result follows from our assumption that the increment is defined by fixed \mathbf{a} -space coordinates, which then constrains the increment's \mathbf{x} -space evolution. It is also an expression that we wrote down, rather trivially, in Section 2.7.2 when performing a truncated Taylor series expansion of the spatial increment between two material fluid particles that follow the flow. Both approaches offer distinct insights as well as confidence in the validity of the result.¹⁴ The ability to derive kinematic results using either simple (indeed trivial) methods versus more long-winded methods is somewhat exemplary of fluid kinematics.

2.8 The volume element

Consider the volume, dV , of an infinitesimal region of \mathbf{x} -space as depicted in Figure 2.6. The volume has a zero Eulerian time derivative,

$$\partial_t[dV] = 0, \quad (2.92)$$

which trivially follows since the region is Eulerian. The volume has dimensions of L^3 , and it can be represented using either Cartesian coordinates, \mathbf{x}^{cart} , or arbitrary coordinates, \mathbf{x} . We first consider the general case and then specialize to Cartesian.

¹⁴If there is more than one way to solve a problem, then do so, even if one of those ways is much more tedious!

2.8.1 Arbitrary Eulerian and Lagrangian coordinates

Using the invariant volume element from VOLUME 1, we have

$$dV = g^E d^3x, \quad (2.93)$$

where $g^E = \sqrt{\det(g_{ij}(\mathbf{x}))}$ from Section 2.5.4, which is the square root of the metric as written using the arbitrary Eulerian coordinates, \mathbf{x} . Following the interpretation from Section 2.3.2 whereby \mathbf{a} -space is a coordinate transformation of \mathbf{x} -space, we can write the Eulerian volume element using arbitrary material coordinates, \mathbf{a} , just like we did for two sets of Eulerian coordinates in equation (2.93). Namely,

$$dV = g^E(\mathbf{x}) d^3x = g^L(\mathbf{a}, T) d^3a, \quad (2.94)$$

where $g^L = \sqrt{\det(g_{IJ})}$ is the square root of the Euclidean metric using the material coordinates (equation (2.49)), and g^L is a function of material space and time.

2.8.2 Cartesian Eulerian coordinates

Consider the specific case of Eulerian Cartesian coordinates (still written as \mathbf{x}) and material coordinates set by the Cartesian reference positions of fluid particles,

$$\mathbf{a} = \boldsymbol{\varphi}(\mathbf{a}, T = t_R) = \dot{\mathbf{x}}. \quad (2.95)$$

We are led to the coordinate transformed expression for the volume element

$$dV = d^3x = (\partial \mathbf{x} / \partial \dot{\mathbf{x}}) d^3\dot{\mathbf{x}}, \quad (2.96)$$

where $\partial \mathbf{x} / \partial \dot{\mathbf{x}}$ is the Jacobian of transformation between the present Cartesian positions of fluid particles moving with the flow,

$$\mathbf{x} = \boldsymbol{\varphi}(\dot{\mathbf{x}}, T), \quad (2.97)$$

and their reference Cartesian positions

$$\dot{\mathbf{x}} = \boldsymbol{\varphi}(\dot{\mathbf{x}}, T = t_R). \quad (2.98)$$

The material coordinate volume element, $d^3\dot{\mathbf{x}} = d\dot{x} d\dot{y} d\dot{z}$, is the Cartesian expression for the volume of fluid in the reference flow state that fits into the Eulerian volume, $d^3x = dV$, at time $t > t_R$. The Jacobian is a function of time for a moving fluid and so is the volume $d^3\dot{\mathbf{x}}$, but their product is time independent by construction. Furthermore, it is notable that the Jacobian is the ratio of the volume elements

$$\frac{\partial \mathbf{x}}{\partial \dot{\mathbf{x}}} = \frac{d^3x}{d^3\dot{\mathbf{x}}}. \quad (2.99)$$

When material coordinates are given by the reference fluid particle positions, $\mathbf{a} = \dot{\mathbf{x}} = \boldsymbol{\varphi}(\mathbf{a}, T = t_R)$, then the Jacobian is unity at the reference time, $T = t_R$. This choice for material coordinate is commonly made in the solid mechanics literature (e.g., Chapter 1 of [Tromp \(2025a\)](#)), and it is suggested by the referential manifold perspective of Figure 2.12. However, for geophysical fluid mechanics we do not build this assumption into the formalism. The reason is that we often find it useful to set \mathbf{a} to a non-spatial coordinate, such as discussed in Section 1.4.2, in which case the Jacobian is not unity at the reference time.

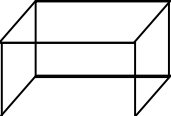
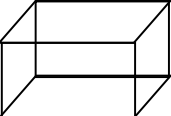
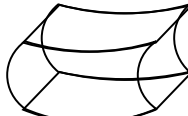
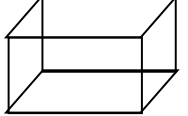
	Eulerian region dV	Material region δV	
Eulerian coordinates 			
Lagrangian coordinates 			

FIGURE 2.6: Depicting the volume of tiny regions of the fluid using Eulerian (x -space) coordinates (top row) and Lagrangian (a -space) coordinates (bottom row). The left column considers an Eulerian region with volume, $dV = g^E d^3x = g^L d^3a$, with this volume independent of Eulerian time, t . The right column depicts the complement material region, in which the material coordinate volume, δV , is assumed to have zero material time derivative, so that it is a function just of a .

2.8.3 The volume of a fixed region of a -space

Now consider a tiny material region that moves through the fluid and whose volume is written δV , as in Figure 2.6, and with the volume independent of material time. The volume has dimensions of L^3 , and it can be represented using either the reference Cartesian positions, $\mathbf{a} = \dot{\mathbf{x}}$, or arbitrary material coordinates, a , which leads to

$$\delta V = g^E \delta^3 x = g^L d^3 a, \quad (2.100)$$

which are the same expressions we derived in Section 2.8.1 for the Eulerian volume element. However, in the present case the material coordinate element, $d^3 a$, is materially constant whereas the Eulerian coordinate element, $\delta^3 x$, is a function of time.

2.9 The velocity gradient tensor and relative velocity

In this section we return to the expression (2.79) of the Cauchy solution for the relative position vector between two fluid particles at the same time instance¹⁵

$$d\boldsymbol{\varphi}(a, T) = \boldsymbol{\varphi}(a + da, T) - \boldsymbol{\varphi}(a, T) = (da^I \partial_I) \boldsymbol{\varphi}(a, T). \quad (2.101)$$

Rather than developing the solution into the form (2.91), which exposes the deformation matrix, we here take a material time derivative, in which case the deformation matrix is seen to determine evolution of the relative velocity.

¹⁵We continue to assume Cartesian coordinates for the Eulerian description, whereas the material description is general.

2.9.1 Evolution of the relative velocity

Taking the material time derivative of the left hand side to equation (2.101) leads to the relative velocity vector

$$\partial_T(d\boldsymbol{\varphi}) = d(\partial_T \boldsymbol{\varphi}) = d\boldsymbol{v}^L, \quad (2.102)$$

where we introduced the velocity vector as evaluated on a fluid particle

$$\boldsymbol{v}^L(\boldsymbol{a}, T) = \partial_T \boldsymbol{\varphi}(\boldsymbol{a}, T). \quad (2.103)$$

Combining equation (2.102) with the material time derivative acting on the right hand side of equation (2.101) renders

$$d\boldsymbol{v}^L = (da^I \partial_I) \partial_T \boldsymbol{\varphi} = (da^I \partial_I) \boldsymbol{v}^L, \quad (2.104)$$

where the material time derivative operator commutes with the material increment operator $da^I \partial_I$, and with equation (2.104) agreeing with the earlier identity (2.77b). Making use of the deformation matrix renders the component form of equation (2.104)

$$(dv^L)^i = (da^I \partial_I) \partial_T \varphi^i = da^I \partial_T \partial_I \varphi^i = da^I \partial_T F^i{}_I. \quad (2.105)$$

Hence, the relative velocity of two fluid particles is directly determined by the material time derivative of the deformation matrix.

2.9.2 Velocity gradient tensor

We make use of the duality developed in Section 2.7.1 to write the Lagrangian expression (2.104) in terms of Eulerian position coordinates

$$\delta\boldsymbol{v}(\boldsymbol{x}, t) = (\delta x^j \partial_j) \boldsymbol{v}(\boldsymbol{x}, t) \iff \delta v^i = (\delta x^j \partial_j) v^i. \quad (2.106)$$

Alternatively, we can return to the identity (2.102), and again make use of the duality to write the material time derivative of the position increment

$$\frac{D(\delta x^i)}{Dt} = \delta v^i = (\delta x^j \partial_j) v^i. \quad (2.107)$$

This equation says that the material evolution of δx^i is determined by the velocity derivatives, $\partial_j v^i$. These derivatives form elements to the Cartesian Eulerian form of the second order velocity gradient tensor

$$G^i{}_j = \partial_j v^i, \quad (2.108)$$

so that equation (2.107) can be written

$$\frac{D(\delta x^i)}{Dt} = G^i{}_j \delta x^j. \quad (2.109)$$

To help understand how the velocity gradient tensor affects the evolution of $\delta\boldsymbol{x}$, it is useful to decompose the tensor into its symmetric and anti-symmetric components. For this purpose we need the transpose of the tensor, which is written

$$(G^T)^i{}_j = G_j{}^i. \quad (2.110)$$

We can thus write the velocity gradient tensor as

$$\mathbf{G} = (\mathbf{G} + \mathbf{G}^T)/2 + (\mathbf{G} - \mathbf{G}^T)/2 \equiv \mathbf{S} + \mathbf{R}, \quad (2.111)$$

where

$$\mathbf{S} = (\mathbf{G} + \mathbf{G}^T)/2 \quad \text{strain (deformation) rate tensor (symmetric)} \quad (2.112a)$$

$$\mathbf{R} = (\mathbf{G} - \mathbf{G}^T)/2 \quad \text{rotation tensor (anti-symmetric).} \quad (2.112b)$$

As seen in the following, the strain rate and rotation tensors affect the motion of a material fluid object in distinct manners. Note that the strain rate tensor is commonly referred to as the *deformation rate* tensor in the literature. We choose the strain rate nomenclature to help reduce confusion with the deformation matrix, $F^i{}_I$ from Section 2.4.1.

2.9.3 Stretching and tilting of material lines

Consider a material line element initially aligned with the vertical axis

$$\delta\mathbf{x}_{t=0} = \hat{\mathbf{z}} \delta Z_0. \quad (2.113)$$

The evolution equation (2.109) means that the initial evolution of this material line element takes on the form

$$\frac{D(\delta x)}{Dt} = \underbrace{\delta Z_0 \left[\frac{\partial u}{\partial z} \right]}_{\text{tilting}} \quad \text{and} \quad \frac{D(\delta y)}{Dt} = \underbrace{\delta Z_0 \left[\frac{\partial v}{\partial z} \right]}_{\text{tilting}} \quad \text{and} \quad \frac{D(\delta z)}{Dt} = \underbrace{\delta Z_0 \left[\frac{\partial w}{\partial z} \right]}_{\text{stretching}}. \quad (2.114)$$

In the presence of a vertical derivative in the horizontal velocity field (vertical shear), the first and second terms create a non-zero projection of the material line element onto the horizontal plane. That is, these terms *tilt* the material line element. Additionally, in the presence of a vertical derivative of the vertical velocity, the material line element is expanded or compressed along its initial axis. This term is called *stretching*. We return to the tilting and stretching mechanisms when discussing the dynamics of vorticity in VOLUME 3. There, we see that vortex lines in a perfect fluid flow are material lines. Consequently, vortex lines are also affected by tilting and stretching just like a material line.

2.9.4 Evolution of squared line element is affected by the strain rate

Recall the expression (2.45) for the squared length of a material line element

$$d\boldsymbol{\varphi} \cdot d\boldsymbol{\varphi} = d\varphi^i \delta_{ij} d\varphi^j = (da^I \partial_I) \varphi^i \delta_{ij} (da^J \partial_J) \varphi^j, \quad (2.115)$$

whose material time derivative is given by

$$\partial_T(d\boldsymbol{\varphi} \cdot d\boldsymbol{\varphi}) = 2(da^I \partial_I) \boldsymbol{v}^\perp \cdot (da^J \partial_J) \boldsymbol{\varphi}. \quad (2.116)$$

We can express this result using Eulerian \mathbf{x} -space coordinates through the duality in Section 2.7.1, which leads to

$$(\delta a^I \partial_I) \boldsymbol{v}^\perp = (\delta x^i \partial_i) \boldsymbol{v} \quad \text{and} \quad (\delta a^I \partial_I) \boldsymbol{\varphi} = \delta \mathbf{x}, \quad (2.117)$$

so that

$$\frac{D(\delta\mathbf{x} \cdot \delta\mathbf{x})}{Dt} = 2 \delta x^i \delta x^k \delta_{jk} \partial_i v^j = 2 \delta x^i \delta x^k \delta_{jk} G^j{}_i. \quad (2.118)$$

Since the product $\delta x^i \delta x^k$ is symmetric on the indices i, k , it projects out the symmetric portion of the velocity gradient tensor, which is the strain rate tensor, thus yielding

$$\frac{1}{2} \frac{D(\delta\mathbf{x} \cdot \delta\mathbf{x})}{Dt} = 2 \delta x^i \delta x^k \delta_{jk} S^j{}_i. \quad (2.119)$$

Consequently, the strain rate tensor, \mathbf{S} , determines the rate at which a material curve changes its length.

To further understand the result (2.119), consider two fluid particles initialized very close together. Equation (2.119) says that the distance between the two particles is modified so long as there are nonzero strain rates in the fluid flow. In the special case of a zero strain rate tensor, then the separation between the two fluid particles is fixed. Evidently, in the absence of a strain rate, the two fluid particles move in a locally and instantaneously rigid manner.

Since the strain rate tensor is symmetric, it has six degrees of freedom. Furthermore, it can be diagonalized, with the diagonal elements equal to the eigenvalues (e.g., see section 2.2 of [Segel \(1987\)](#)). Each eigenvalue measures the rate that material lines oriented according to the principle axes (eigenvectors) expand/contract under the impacts of straining motion in the fluid. According to equation (2.119), the expansion/contraction is exponential when aligned along the principle axes, with the exponential rate determined by the eigenvalues of \mathbf{S} . Furthermore, as shown in Section 2.11, the sum of these eigenvalues (given by the trace of the strain rate tensor) measures the rate that a material volume changes through the divergence of the velocity

$$S^i{}_i = \partial_i v^i = \nabla \cdot \mathbf{v}. \quad (2.120)$$

2.9.5 Rigid rotation of the line element

As defined by equation (2.112b), the **rotation tensor** is given by

$$\mathbf{R} = (\mathbf{G} - \mathbf{G}^T)/2. \quad (2.121)$$

Notably, the rotation tensor is anti-symmetric so that

$$\mathbf{R} = -\mathbf{R}^T, \quad (2.122)$$

and as such it has three degrees of freedom. We now introduce the vorticity vector,

$$\boldsymbol{\omega} = \nabla \times \mathbf{v}, \quad (2.123)$$

which is related to the rotation tensor via

$$2 R^i{}_j = -\epsilon^i{}_{jk} \omega^k \iff \mathbf{R} = \frac{1}{2} \begin{bmatrix} 0 & -\omega^3 & \omega^2 \\ \omega^3 & 0 & -\omega^1 \\ -\omega^2 & \omega^1 & 0 \end{bmatrix} \iff \omega^k = -\epsilon^{kij} R_{ij}, \quad (2.124)$$

where the final expression made use of the identity (see VOLUME 1)

$$\epsilon^{ijl} \epsilon_{ijm} = 2 \delta^l{}_m. \quad (2.125)$$

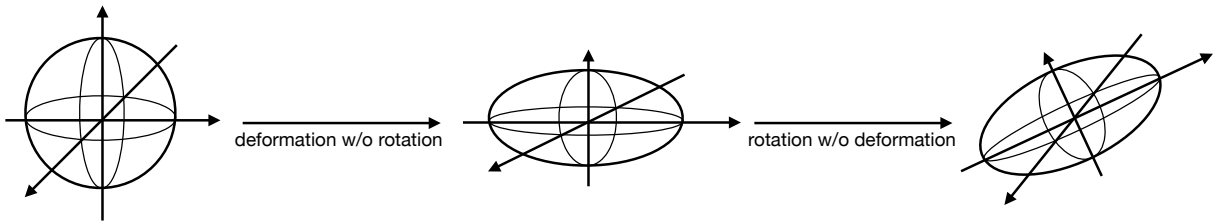


FIGURE 2.7: Schematic illustrating the Cauchy-Stokes decomposition of how fluid flow can modify a spherical material region according to equation (2.128). First the sphere can be deformed without rotation, with this process encompassed by the strain rate tensor, \mathbf{S} . Next it can be rigidly rotated without changing its shape, as encompassed by the rotation tensor, \mathbf{R} . The axes shown represent the principle axes so that deformation corresponds to expansion or contraction along the principle axes directions.

It is furthermore straightforward to show that the doubly contracted rotation tensor equals to half the squared vorticity

$$R^i_j R^j_i = |\boldsymbol{\omega}|^2/2. \quad (2.126)$$

The contribution of the rotation tensor to evolution of the material line element is given by

$$\left[\frac{D(\delta x^i)}{Dt} \right]_{\text{rot}} = R^i_j \delta x^j = -(\epsilon^i_{jk} \omega^k/2) \delta x^j \implies \left[\frac{D(\delta \mathbf{x})}{Dt} \right]_{\text{rot}} = \frac{1}{2} (\boldsymbol{\omega} \times \delta \mathbf{x}). \quad (2.127)$$

This relation is in the form of a pure rotation of the material line element, $\delta \mathbf{x}$, as generated by the vector, $\boldsymbol{\omega}/2$. We thus conclude that the anti-symmetric rotation tensor, \mathbf{R} , provides a rigid rotation to a material line element about the axis defined by the vorticity vector. It rotates the objects without altering the size (length, area, volume).

2.9.6 Cauchy-Stokes decomposition

The above discussion of how fluid motion impacts on a material curve falls under the more general insights from the [Cauchy-Stokes decomposition theorem](#). This theorem says that the arbitrary motion of a region in a continuous media can be decomposed into a uniform translation, dilation along three perpendicular axes, plus a rigid body rotation. Mathematically, this decomposition can be written by expanding equation (2.109) to read

$$v^i(\mathbf{x}, t) = v^i(\mathbf{x}_0, t) + G^i_j \delta x^j = v^i(\mathbf{x}_0, t) + S^i_j \delta x^j + R^i_j \delta x^j. \quad (2.128)$$

Figure 2.7 illustrates the deformation and rotation portion of this decomposition. A more thorough discussion of this theorem can be found in Chapter 4 of [Aris \(1962\)](#) and Section 3.1 of [Segel \(1987\)](#).

2.9.7 Evolution of the deformation matrix

In equation (2.105) we found that the relative velocity of two fluid particles is directly determined by the material time derivative of the deformation matrix. As an exercise in the formalism, we here determine how the deformation matrix evolves materially, in which we compute

$$\partial_T F^i_I = \partial_T \partial_I \varphi^i \quad \text{definition (2.17) of deformation matrix} \quad (2.129a)$$

$$= \partial_I \partial_T \varphi^i \quad \text{Lagrangian space and time derivatives commute} \quad (2.129b)$$

$$= \partial_I (v^l)^i \quad \text{flow velocity (2.16)} \quad (2.129c)$$

$$= \partial_I v^i \quad \text{dual representation of flow velocity} \quad (2.129d)$$

$$= (\partial\varphi^j/\partial a^I) \partial_j v^i \quad \text{chain rule} \quad (2.129e)$$

$$= F^j{}_I G^i{}_j \quad \text{definitions (2.17) and (2.108).} \quad (2.129f)$$

Evidently, material evolution of the deformation matrix is given by

$$\partial_T F^i{}_I = G^i{}_j F^j{}_I, \quad (2.130)$$

so that the deformation matrix experiences larger changes in regions with stronger gradients in the flow, as measured by the velocity gradient tensor, $G^i{}_j$. Making use of equation (2.130) in equation (2.105) thus leads to the expression for the relative velocity increment

$$(dv^L)^i = \partial_T F^i{}_I da^I = G^i{}_j F^j{}_I da^I. \quad (2.131)$$

2.9.8 Evolution of the Cauchy-Green strain tensor

As noted in Section 2.5.1, the Eulerian representation of the metric tensor is independent of Eulerian time, so that $\partial_t g_{ij} = 0$. Following from the discussion in Section 2.9.7 for evolution of the deformation matrix, we here consider the material time evolution of the \mathbf{a} -space representation of the metric tensor

$$\partial_T g_{IJ} = \partial_T [g_{ij} F^i{}_I F^j{}_J] = \partial_T g_{ij} [F^i{}_I F^j{}_J] + g_{ij} \partial_T [\partial_I \varphi^i \partial_J \varphi^j]. \quad (2.132)$$

The first equality made use of equation (2.44) for the metric tensor written in terms of Lagrangian coordinates, and the second equality made use of equation (2.17) for the deformation matrix, $F^i{}_I$. Now use equation (2.16) for velocity of the fluid flow to arrive at

$$\partial_T [\partial_I \varphi^i \partial_J \varphi^j] = \partial_I (\partial_T \varphi^i) \partial_J \varphi^j + \partial_J (\partial_T \varphi^j) \partial_I \varphi^i \quad (2.133a)$$

$$= \partial_I (v^L)^i \partial_J \varphi^j + \partial_J (v^L)^j \partial_I \varphi^i. \quad (2.133b)$$

Examine one of these terms, with the Eulerian metric contracted, to find

$$g_{ij} \partial_I (v^L)^i \partial_J \varphi^j = g_{ij} F^k{}_I \partial_k (v^L)^i F^j{}_J \quad \text{chain rule and deformation matrix (2.17)} \quad (2.134a)$$

$$= g_{ij} F^k{}_I G^i{}_k F^j{}_J \quad \text{introduce gradient tensor (2.108)} \quad (2.134b)$$

$$= g_{ij} G^i{}_I F^j{}_J \quad \text{transformation of } \mathbf{x}\text{-space to } \mathbf{a}\text{-space} \quad (2.134c)$$

$$= G_{JI} F^j{}_J \quad \text{metric tensor to lower } i\text{-index} \quad (2.134d)$$

$$= G_{JI} \quad \text{transformation of } \mathbf{x}\text{-space to } \mathbf{a}\text{-space.} \quad (2.134e)$$

Bringing terms together leads to

$$\partial_T g_{IJ} = \partial_T g_{ij} [F^i{}_I F^j{}_J] + G_{JI} + G_{IJ} = \partial_T g_{ij} [F^i{}_I F^j{}_J] + 2 S_{IJ}, \quad (2.135)$$

where the second equality introduced the Lagrangian representation of the strain rate tensor (2.112a). If we choose Cartesian coordinates for the Eulerian \mathbf{x} -space description so that $g_{ij} = \delta_{ij}$, then g_{IJ} is the Cauchy-Green strain tensor from equation (2.47), with equation (2.135) leading to

$$\partial_T g_{IJ} = 2 S_{IJ} \quad \text{material evolution of Cauchy-Green strain tensor.} \quad (2.136)$$

Evidently, the Cauchy-Green strain tensor has its material time evolution determined by the Lagrangian expression for the strain rate tensor. Namely, regions of large Lagrangian strain rates see a relatively large material evolution of the Cauchy-Green strain tensor.

2.10 Evolution of material surfaces

We here extend the discussion of the material line element in Sections 2.7 and 2.9 to the case of a material surface such as that shown in Figure 2.8. Considerations are given to both three-dimensional and two-dimensional flows. We employ Cartesian tensors throughout this section, though use covariant and contravariant index placement to facilitate use of the Einstein summation convention.

2.10.1 Surfaces in three-dimensional flow

Following from the geometric interpretation of the vector product in VOLUME 1, we here define a material surface by (see Figure 2.8)

$$\delta\mathcal{S} = \delta\mathbf{A} \times \delta\mathbf{B} \quad \text{and in components} \quad \delta\mathcal{S}_i = \epsilon_{ijk} \delta A^j \delta B^k \quad (2.137)$$

where $\delta\mathbf{A}$ and $\delta\mathbf{B}$ are non-parallel infinitesimal material lines. The surface projected onto the unit normal direction, $\hat{\mathbf{n}}$, is given by

$$\hat{\mathbf{n}} \cdot \delta\mathcal{S} = \hat{\mathbf{n}} \cdot (\delta\mathbf{A} \times \delta\mathbf{B}). \quad (2.138)$$

The evolution of the material surface is given by

$$\frac{D(\delta\mathcal{S})}{Dt} = \frac{D(\delta\mathbf{A})}{Dt} \times \delta\mathbf{B} + \delta\mathbf{A} \times \frac{D(\delta\mathbf{B})}{Dt} \quad (2.139a)$$

$$= [(\delta\mathbf{A} \cdot \nabla) \mathbf{v}] \times \delta\mathbf{B} + \delta\mathbf{A} \times [(\delta\mathbf{B} \cdot \nabla) \mathbf{v}], \quad (2.139b)$$

where the second equality made use of the material line evolution equation (2.84). To proceed we expose indices and make use of some tensor identities

$$\frac{D(\delta\mathcal{S}_i)}{Dt} = \epsilon_{ijk} [(\delta A^q \partial_q) v^j] \delta B^k + \epsilon_{ijk} \delta A^j [(\delta B^q \partial_q) v^k] \quad (2.140a)$$

$$= \epsilon_{ijk} [\delta A^q \delta B^k \partial_q v^j + \delta A^j \delta B^q \partial_q v^k] \quad (2.140b)$$

$$= \epsilon_{ijk} \partial_q v^j [\delta A^q \delta B^k - \delta A^k \delta B^q] \quad (2.140c)$$

$$= \epsilon_{ijk} \partial_q v^j \epsilon^{rjk} \delta\mathcal{S}_r \quad (2.140d)$$

$$= (\delta^r_i \delta^q_j - \delta^r_j \delta^q_i) \partial_q v^j \delta\mathcal{S}_r \quad (2.140e)$$

$$= (\nabla \cdot \mathbf{v}) \delta\mathcal{S}_i - (\partial_i \mathbf{v}) \cdot \delta\mathcal{S}. \quad (2.140f)$$

To reach this result we made use of the following identities available for the permutation symbol from VOLUME 1

$$\delta A^q \delta B^k - \delta A^k \delta B^q = \epsilon^{rjk} \delta\mathcal{S}_r \quad (2.141a)$$

$$\delta^r_i \delta^q_j - \delta^r_j \delta^q_i = \epsilon_{ijk} \epsilon^{rjk}. \quad (2.141b)$$

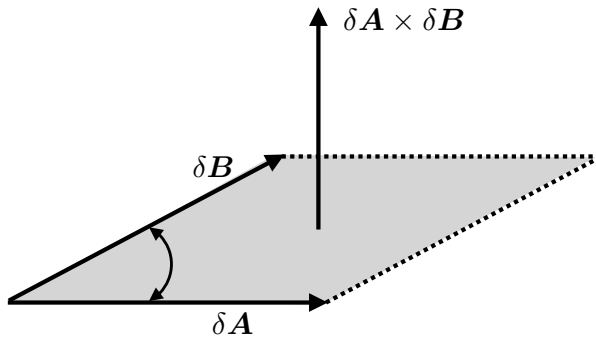


FIGURE 2.8: A material surface as defined by the cross product of two material line elements, $\delta\mathcal{S} = \delta\mathbf{A} \times \delta\mathbf{B}$. In the special case of $\delta\mathbf{A} = \hat{\mathbf{x}} \delta x$ and $\delta\mathbf{B} = \hat{\mathbf{y}} \delta y$, then $\delta\mathcal{S} = \delta x \delta y \hat{\mathbf{z}}$.

2.10.2 Evolution of the material surface area

Now orient the material surface area according to its outward unit normal

$$\delta\mathcal{S} = \hat{\mathbf{n}} \delta\mathcal{S} \quad \text{and in components} \quad \delta\mathcal{S}_i = \hat{n}_i \delta\mathcal{S}, \quad (2.142)$$

where the magnitude of the area element is written

$$\delta\mathcal{S} = |\delta\mathcal{S}|. \quad (2.143)$$

Doing so brings equation (2.140f) to the form

$$\frac{1}{\delta\mathcal{S}} \frac{D(\hat{n}_i \delta\mathcal{S})}{Dt} = (\nabla \cdot \mathbf{v}) \hat{n}_i - (\partial_i \mathbf{v}) \cdot \hat{\mathbf{n}}. \quad (2.144)$$

Evidently, we can develop evolution equations for the surface area, $\delta\mathcal{S}$, and the unit normal, $\hat{\mathbf{n}}$.

For the surface area evolution we take the scalar product of equation (2.144) with \hat{n}_i to yield

$$\frac{1}{\delta\mathcal{S}} \frac{D\delta\mathcal{S}}{Dt} = \nabla \cdot \mathbf{v} - [(\hat{\mathbf{n}} \cdot \nabla) \mathbf{v}] \cdot \hat{\mathbf{n}} \quad (2.145)$$

where we set $\hat{\mathbf{n}} \cdot \hat{\mathbf{n}} = 1$ to find that

$$\hat{\mathbf{n}} \cdot \hat{\mathbf{n}} = 1 \implies \hat{\mathbf{n}} \cdot \frac{D\hat{\mathbf{n}}}{Dt} = 0, \quad (2.146)$$

so that the normal is always perpendicular to its material time derivative. Rearrangement of equation (2.145) then leads to the kinematic evolution equation for the area

$$\frac{1}{\delta\mathcal{S}} \frac{D\delta\mathcal{S}}{Dt} = [\partial_i - \hat{n}_i (\hat{\mathbf{n}} \cdot \nabla)] v^i. \quad (2.147)$$

We next provide some interpretation of this result.

Surface derivative operator

The derivative operator on the right hand side of equation (2.147),

$$\partial_i^{\text{surf}} \equiv \partial_i - \hat{n}_i (\hat{\mathbf{n}} \cdot \nabla), \quad (2.148)$$

is a *surface derivative operator* since it subtracts from the gradient operator the projection onto the local normal, thus leaving a gradient operator just in the tangent plane of the surface. The area evolution equation (2.147) can thus be written in the tidy form

$$\frac{1}{\delta S} \frac{D(\delta S)}{Dt} = \nabla^{\text{surf}} \cdot \mathbf{v}, \quad (2.149)$$

so that the relative area of the material surface changes according to the surface divergence of the velocity field.

Special case of a horizontal surface

To help understand the kinematic equation (2.149), consider the special case of a horizontal surface with a vertical unit normal, $\hat{\mathbf{n}} = \hat{\mathbf{z}}$, so that

$$\frac{1}{\delta S} \frac{D(\delta S)}{Dt} = \nabla \cdot \mathbf{v} - \hat{\mathbf{z}} \cdot \partial_z \mathbf{v} = \nabla_h \cdot \mathbf{u}. \quad (2.150)$$

In this case we see that the area of a horizontal surface increases when the horizontal velocity diverges, and the area decreases when the horizontal velocity converges. We expect this behavior since the surface is material and is thus moving with the flow. We encounter this result again in Section 2.10.4 for two-dimensional flow, in which the area is always horizontal.

As another special case, consider a three dimensional flow that is non-divergent, $\nabla \cdot \mathbf{v} = 0$ (see Chapter 5). In this case the area changes are only due to the projection of the normal gradient onto the normal direction. So again considering a horizontal area with $\hat{\mathbf{n}} = \hat{\mathbf{z}}$, the area evolution in a non-divergent flow is given by

$$\frac{1}{\delta S} \frac{D(\delta S)}{Dt} = -\hat{\mathbf{z}} \cdot (\hat{\mathbf{z}} \cdot \nabla) \mathbf{v} = -\partial_z w, \quad (2.151)$$

which follows from equation (2.150) with $\partial_x u + \partial_y v + \partial_z w = \nabla_h \cdot \mathbf{u} + \partial_z w = 0$.

2.10.3 Evolution of the unit normal

We make use of the area evolution equation (2.149) within equation (2.144) to derive an evolution equation for the unit normal

$$\frac{D\hat{n}_i}{Dt} = -\hat{n}_i \frac{1}{\delta S} \frac{D(\delta S)}{Dt} + (\partial_j v^j) \hat{n}_i - (\partial_i v^j) \hat{n}_j \quad (2.152a)$$

$$= -\hat{n}_i [\partial_j v^j - \hat{n}_j (\hat{\mathbf{n}} \cdot \nabla) v^j] + (\partial_j v^j) \hat{n}_i - (\partial_i v^j) \hat{n}_j \quad (2.152b)$$

$$= -\hat{n}_j [\partial_i - \hat{n}_i \hat{\mathbf{n}} \cdot \nabla] v^j \quad (2.152c)$$

$$= -\hat{n}_j \partial^{\text{surf}} v^j \quad (2.152d)$$

$$= -\hat{\mathbf{n}} \cdot \partial^{\text{surf}} \mathbf{v}. \quad (2.152e)$$

Equation (2.152c) provides a simple means to verify that the kinematic constraint (2.146) is satisfied, in which it is clear that $\hat{\mathbf{n}} \cdot D\hat{\mathbf{n}}/Dt = 0$.

To help understand the evolution equation (2.152e), consider again a horizontal area with its unit normal initially in the vertical. The evolution of this unit normal is thus given by

$$\frac{D\hat{n}_i}{Dt} = -(\partial_i - \hat{z}_i \partial_z) w, \quad (2.153)$$

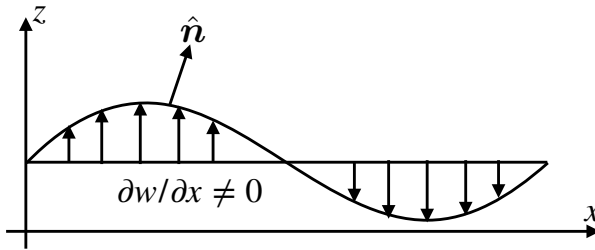


FIGURE 2.9: Horizontal shear in the vertical velocity, $\nabla_z w$, creates undulations in an initially horizontal material surface that leads to a horizontal component in the normal. We here show the case where $\partial w / \partial x \neq 0$, thus leading to a zonal component to the normal according to $D\hat{n}_x/Dt = -\partial_x w$.

with each component evolving according to

$$\frac{D\hat{n}_1}{Dt} = -\partial_x w \quad \text{and} \quad \frac{D\hat{n}_2}{Dt} = -\partial_y w \quad \text{and} \quad \frac{D\hat{n}_3}{Dt} = 0. \quad (2.154)$$

Hence, an initially vertical normal tilts into the horizontal direction according to minus the horizontal shear in the vertical velocity. As illustrated in Figure 2.9, we understand this result by noting that such a shear creates undulations in the initially horizontal surface that render a horizontal component to the normal.

2.10.4 Material area in two-dimensional flow

Now consider a material area for two-dimensional fluid flow with velocity, $\mathbf{v} = (u, v, 0)$, and $\delta\mathbf{A} = \hat{x}\delta x, \delta\mathbf{B} = \hat{y}\delta y$, with zero dependence on z . In this case, the area of an infinitesimal material region is

$$\delta\mathcal{S} = (\delta\mathbf{A} \times \delta\mathbf{B}) \cdot \hat{z} = \delta x \delta y, \quad (2.155)$$

and its evolution is given by

$$\frac{D(\delta\mathcal{S})}{Dt} = (\delta\mathbf{B} \times \hat{z}) \cdot (\delta\mathbf{A} \cdot \nabla) \mathbf{u} + (\hat{z} \times \delta\mathbf{A}) \cdot (\delta\mathbf{B} \cdot \nabla) \mathbf{u} \quad (2.156a)$$

$$= \delta x \delta y \nabla \cdot \mathbf{u}, \quad (2.156b)$$

so that

$$\frac{1}{\delta\mathcal{S}} \frac{D(\delta\mathcal{S})}{Dt} = \nabla \cdot \mathbf{u}. \quad (2.157)$$

Hence, the area of the material region evolves according to the divergence of the horizontal velocity. Correspondingly, the area remains constant in a horizontally non-divergent flow. This result follows from specializing the three-dimensional result (2.140f) to the case of two-dimensional flow by assuming no dependence on the vertical direction.

2.11 Volume, thickness, and the Jacobian

In this section we determine how volume evolves for a material parcel, and as part of that derivation we determine the evolution equation for the Jacobian of transformation between position space and material space. We find that the relative change for both the parcel volume and the Jacobian are determined by divergence of the velocity field. For simplicity we make use of Cartesian tensors throughout this section. Note that some of these results were anticipated in Sections 2.5 and 2.8.

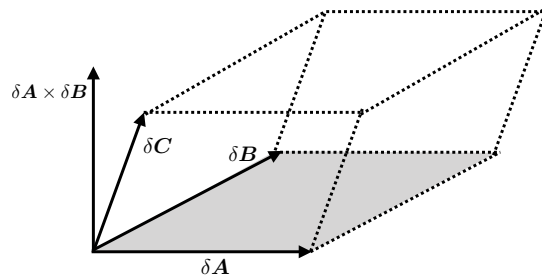


FIGURE 2.10: A parallelepiped defined by three material lines with volume (to within a sign) given by $\delta V = (\delta\mathbf{A} \times \delta\mathbf{B}) \cdot \delta\mathbf{C}$.

2.11.1 Material parcel volume

Consider a material region with a volume, δV , spanned by the infinitesimal material lines $\delta\mathbf{A}$, $\delta\mathbf{B}$, and $\delta\mathbf{C}$ (see Figure 2.10). To within a sign the volume is given by

$$\delta V = (\delta\mathbf{A} \times \delta\mathbf{B}) \cdot \delta\mathbf{C}. \quad (2.158)$$

Making use of the material line evolution equation (2.84) renders

$$\frac{D(\delta V)}{Dt} = (\delta\mathbf{B} \times \delta\mathbf{C}) \cdot (\delta\mathbf{A} \cdot \nabla)\mathbf{v} + (\delta\mathbf{C} \times \delta\mathbf{A}) \cdot (\delta\mathbf{B} \cdot \nabla)\mathbf{v} + (\delta\mathbf{A} \times \delta\mathbf{B}) \cdot (\delta\mathbf{C} \cdot \nabla)\mathbf{v}. \quad (2.159)$$

Now specialize to the case where the parcel is a parallelepiped oriented according to the coordinate axes

$$\delta\mathbf{A} = \hat{\mathbf{x}} \delta x \quad \text{and} \quad \delta\mathbf{B} = \hat{\mathbf{y}} \delta y \quad \text{and} \quad \delta\mathbf{C} = \hat{\mathbf{z}} \delta z, \quad (2.160)$$

so that

$$\delta V = \delta x \delta y \delta z. \quad (2.161)$$

Plugging into equation (2.159) leads to

$$\frac{1}{\delta V} \frac{D(\delta V)}{Dt} = \nabla \cdot \mathbf{v}. \quad (2.162)$$

This result is a three-dimensional generalization of the material area equation (2.157).

We offer an alternative derivation of equation (2.162) in Section 3.2, where no assumptions are made concerning the shape of the material region. That derivation leads us to conclude that the relative volume of a material parcel increases when the parcel moves through a region where the velocity diverges ($\nabla \cdot \mathbf{v} > 0$). We think of a diverging velocity field as “spreading out” the material parcel boundary, thus increasing its volume. In contrast, the volume of a material parcel decreases where the fluid velocity converges ($\nabla \cdot \mathbf{v} < 0$)

$$\nabla \cdot \mathbf{v} > 0 \implies \text{material volume increases in diverging flow} \implies \text{parcel expands} \quad (2.163a)$$

$$\nabla \cdot \mathbf{v} < 0 \implies \text{material volume decreases in converging flow} \implies \text{parcel contracts.} \quad (2.163b)$$

Some authors refer to $\nabla \cdot \mathbf{v}$ as the *dilatation* (e.g., page 15 of [Pope \(2000\)](#)), since the velocity divergence measures the rate that the volume of a fluid element is expanded (dilates) or contracts.

2.11.2 Evolution of the column thickness

A material volume, δV , evolves according to the divergence of the velocity (equation (2.162)), whereas the material area, δS , evolves according to the surface divergence of the velocity (equation (2.149)). Now consider a material volume whose cross-sectional area is δS and whose thickness is δh , with δh measuring the thickness in a direction defined by the unit normal, $\hat{\mathbf{n}}$. We can deduce the evolution of the thickness since we know the evolution of the volume and area

$$\frac{1}{\delta V} \frac{D(\delta V)}{Dt} = \frac{1}{\delta h \delta S} \frac{D(\delta h \delta S)}{Dt} = \frac{1}{\delta h} \frac{D(\delta h)}{Dt} + \frac{1}{\delta S} \frac{D(\delta S)}{Dt}. \quad (2.164)$$

Use of equations (2.162) and (2.149) render

$$\frac{1}{\delta h} \frac{D(\delta h)}{Dt} = \nabla \cdot \mathbf{v} - \nabla^{\text{surf}} \cdot \mathbf{v} = \hat{\mathbf{n}}_i (\hat{\mathbf{n}} \cdot \nabla) v_i. \quad (2.165)$$

For example, consider the special case with $\hat{\mathbf{n}} = \hat{\mathbf{z}}$, in which

$$\frac{1}{\delta h} \frac{D(\delta h)}{Dt} = \frac{\partial w}{\partial z}, \quad (2.166)$$

so that the column thickness evolves according to the vertical derivative of the vertical velocity. This result accords with our discussion of stretching in Section 2.9.3.

2.11.3 Evolution of the Jacobian of transformation

Recall the discussion in Sections 2.8.3 and 2.8.1, where we showed how the Jacobian satisfies

$$d^3x = \frac{\partial \boldsymbol{\varphi}(\mathbf{a}, T)}{\partial \mathbf{a}} d^3a \implies \frac{\partial \boldsymbol{\varphi}(\mathbf{a}, T)}{\partial \mathbf{a}} = \frac{d^3x}{d^3a}, \quad (2.167)$$

where

$$d^3a = da^1 da^2 da^3 \quad (2.168)$$

is the material coordinate volume for the parcel, and d^3x is the Eulerian coordinate volume. The material coordinate volume is a constant following a particle trajectory, whereas the Eulerian coordinate volume is not a constant, so that

$$\frac{D}{Dt} \frac{\partial \boldsymbol{\varphi}}{\partial \mathbf{a}} = \frac{1}{d^3a} \frac{D(d^3x)}{Dt} \quad (2.169a)$$

$$= \frac{d^3x}{d^3a} \nabla \cdot \mathbf{v} \quad (2.169b)$$

$$= \frac{\partial \boldsymbol{\varphi}}{\partial \mathbf{a}} \nabla \cdot \mathbf{v}. \quad (2.169c)$$

The second equality made use of the equation (2.162), which expresses the material time change for the volume of a material fluid parcel, as measured in position space, in terms of the velocity divergence. We thus see that the relative change of the Jacobian is determined by the divergence of the velocity

$$\left[\frac{\partial \boldsymbol{\varphi}}{\partial \mathbf{a}} \right]^{-1} \frac{D}{Dt} \left[\frac{\partial \boldsymbol{\varphi}}{\partial \mathbf{a}} \right] = \nabla \cdot \mathbf{v}. \quad (2.170)$$

This equation is identical to the parcel volume equation (2.162), which is expected given the relation between the Jacobian and the parcel volume. In Exercise 2.5, we derive this result

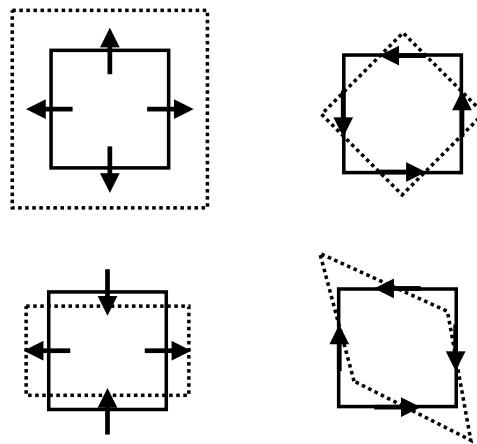


FIGURE 2.11: Illustrating the varieties of changes for an initially square material fluid region in two-dimensional flow. Upper left: purely divergent flow, whereby $\nabla \cdot \mathbf{u} > 0$ yet with zero vorticity, thus leading to an increase in the area. An example flow generating this motion is realized by $\mathbf{u} = \gamma(x\hat{\mathbf{x}} + y\hat{\mathbf{y}}) = \gamma\mathbf{x}$ (with $\gamma > 0$ a constant of dimensions inverse time) so that the divergence is $\nabla \cdot \mathbf{u} = 2\gamma$. Upper right: rotational flow with nonzero vertical vorticity component, $\zeta = \hat{\mathbf{z}} \cdot (\nabla \times \mathbf{u})$, yet zero divergence, thus leading to a pure rotation of the square patch. An example flow generating this motion is realized by $\mathbf{u} = \hat{\mathbf{z}} \times \nabla \psi = \gamma(-y\hat{\mathbf{x}} + x\hat{\mathbf{y}}) = -\gamma\hat{\mathbf{z}} \times \mathbf{x}$ with streamfunction $\psi = (\gamma/2)(x^2 + y^2)$ and vorticity $\zeta = \nabla^2 \psi = 2\gamma$. Lower left: result of a pure tension/compression straining flow (also called a deformation flow) with zero divergence and zero vorticity, leading to compression in one direction and dilation in the orthogonal direction. An example flow is given by $\mathbf{u} = \hat{\mathbf{z}} \times \nabla \psi = \gamma(x\hat{\mathbf{x}} - y\hat{\mathbf{y}})$ with streamfunction $\psi = -\gamma xy$. The deformation of the region is measured by the tension strain, $\partial_x u - \partial_y v = 2\gamma$. Lower right: pure shearing strain flow with zero divergence and zero vorticity. An example flow is given by $\mathbf{u} = -\gamma(y\hat{\mathbf{x}} + x\hat{\mathbf{y}})$ with streamfunction $\psi = -(\gamma/2)(x^2 - y^2)$. The deformation of the region is measured by the shearing strain, $\partial_y u + \partial_x v = -2\gamma$. This figure is adapted from Figure 2.4 of [Hoskins and James \(2014\)](#).

using the explicit expression for the Jacobian in terms of the permutation symbol, ϵ .

2.12 Kinematics of two-dimensional flow

In this section we consider the rudiments of two-dimensional flow as a venue to illustrate topics presented earlier in this chapter such as dilation, rotation, and strains. In so doing we expose kinematic properties commonly used to characterize two-dimensional flow, with generalizations to three-dimensions available with a bit more maths. We retain Cartesian tensors throughout this section.

The starting point is Figure 2.11, which shows a square region of fluid exposed to a variety of flow regimes. We can kinematically describe these changes by making use of the velocity gradient tensor introduced in Section 2.9, here written for the two-dimensional flow with horizontal velocity components, (u, v)

$$[\partial_j v^i] = \begin{bmatrix} \partial u / \partial x & \partial u / \partial y \\ \partial v / \partial x & \partial v / \partial y \end{bmatrix} \quad (2.171a)$$

$$= \begin{bmatrix} \partial u / \partial x & (1/2)(\partial u / \partial y + \partial v / \partial x) \\ (1/2)(\partial u / \partial y + \partial v / \partial x) & \partial v / \partial y \end{bmatrix} + \frac{\zeta}{2} \begin{bmatrix} 0 & -1 \\ 1 & 0 \end{bmatrix} \quad (2.171b)$$

$$= \mathbf{S} + \mathbf{R}, \quad (2.171c)$$

where

$$\zeta = \hat{\mathbf{z}} \cdot \nabla \times \mathbf{v} = \partial v / \partial x - \partial u / \partial y \quad (2.172)$$

is the vertical component to the vorticity.

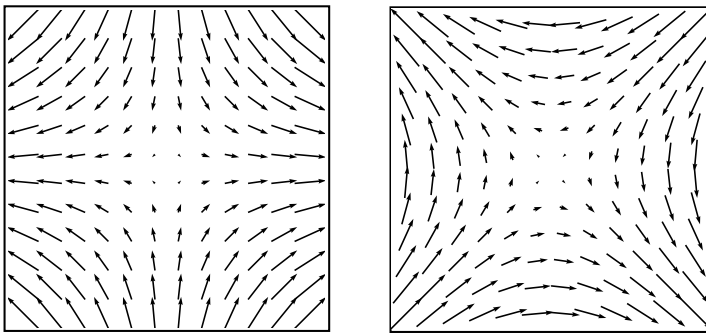


FIGURE 2.12: Two-dimensional horizontally non-divergent and irrotational flow with nonzero deformation/strain. Left panel: pure tension strain as determined by the streamfunction, $\psi = -\gamma xy$, so that the velocity $\mathbf{u} = \hat{\mathbf{z}} \times \nabla \psi = \gamma(x\hat{\mathbf{x}} - y\hat{\mathbf{y}})$. The y-axis orients the direction along which flow contracts (compression) whereas the x-axis is the dilation axis (tension). The lower left panel of Figure 2.11 illustrates the effects from this flow on a square material area. Right panel: pure shearing flow as determined by the streamfunction $\psi = -(\gamma/2)(x^2 - y^2)$ so that the velocity is $\mathbf{u} = \hat{\mathbf{z}} \times \nabla \psi = \gamma(-y\hat{\mathbf{x}} - x\hat{\mathbf{y}})$. The lower right panel of Figure 2.11 illustrates the effects from this flow on a square material area. We set $\gamma = 1$ for both examples.

2.12.1 Diverging flow

Recall from Section 2.10.4 that a material surface in two-dimensional flow changes its area according to the divergence. The upper left panel of Figure 2.11 thus illustrates equation (2.157)

$$\frac{1}{\delta S} \frac{D(\delta S)}{Dt} = \nabla \cdot \mathbf{u} = S^i_i = S^1_1 + S^2_2, \quad (2.173)$$

where δS is the area and S^i_i is the trace of the strain rate tensor. That is, a diverging flow as depicted by this figure, with $\nabla \cdot \mathbf{u} > 0$, leads to an expansion of the area. The opposite occurs for a converging flow, where the area compresses.

2.12.2 Flow with nonzero deformation

The lower left panel of Figure 2.11 shows the square within a deformational flow whereby it contracts along the y -axis and dilates along the x -axis. This flow is non-divergent, $\nabla \cdot \mathbf{u} = 0$, and has zero vorticity, $\zeta = 0$, so that the area remains constant and the orientation is fixed. However, it has shear that acts to deform the area. This particular non-divergent deformational flow is determined by

$$\mathbf{u} = \hat{\mathbf{z}} \times \nabla \psi, \quad (2.174)$$

with the streamfunction, $\psi = -\gamma xy$ where γ is a constant inverse time scale and hence the strength of the strain. The resulting velocity components are $u = -\partial \psi / \partial y = \gamma x$ and $v = \partial \psi / \partial x = -\gamma y$.

2.12.3 Rotational flow with nonzero vorticity

The upper right panel of Figure 2.11 illustrates the effects from flow with a non-zero vorticity, $\zeta = \partial v / \partial x - \partial u / \partial y$. The nonzero vorticity imparts a rotation to an area element, with the flow in the upper right panel of Figure 2.11 bringing about a counter-clockwise rotation. All components of the strain tensor vanish for a purely rotational flow, so that there is no deformation of the square as it rotates.

2.12.4 Tension strain and shearing strain

There are two combinations of the strain rate tensor elements that are useful in describing deformational flows:

$$\text{tension strain rate} = S_T = S^1_1 - S^2_2 = \partial u / \partial x - \partial v / \partial y \quad (2.175\text{a})$$

$$\text{shearing strain rate} = S_S = 2 S^1_2 = \partial u / \partial y + \partial v / \partial x. \quad (2.175\text{b})$$

The tension strain and shearing strain are also known as tension and shearing *deformation rates*. Note that negative tension is known as *compression*. For the deformation flow with streamfunction $\psi = -\gamma x y$, we have

$$S_T = 2\gamma \quad \text{and} \quad S_S = 0, \quad (2.176)$$

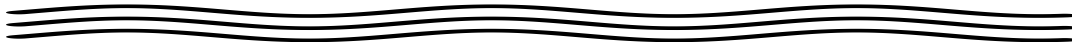
so that this velocity leads to a purely tension straining flow. In contrast, the following non-divergent irrotational flow is a purely shearing strain flow

$$\psi = -(\gamma/2)(x^2 - y^2) \quad u = -\gamma y \quad v = -\gamma x \quad S_T = 0 \quad S_S = -2\gamma, \quad (2.177)$$

as depicted by the right panel of Figure 2.12. This pure shearing flow leads to the deformation of the fluid square shown in the lower right panel of Figure 2.11.

2.12.5 Further study

Elements of this section can be found in Section 2.3 of [Hoskins and James \(2014\)](#). More detailed examinations of two-dimensional flow kinematics are offered by [Weiss \(1991\)](#) and [Lilly \(2018\)](#). Furthermore, we here introduced the streamfunction, ψ , for non-divergent two-dimensional flow, yet provide a more thorough discussion in Section 5.4.



2.13 Exercises

EXERCISE 2.1: MATERIAL EVOLUTION OF THE ACCELERATION DIVERGENCE

Derive the relation

$$\nabla \cdot \frac{D\mathbf{v}}{Dt} = \frac{D(\nabla \cdot \mathbf{v})}{Dt} + S^i_j S^j_i - R^i_j R^j_i, \quad (2.178)$$

where $S^i_j S^j_i$ and $R^i_j R^j_i$ are the doubly contracted strain rate tensor and squared rotation tensor (Sections 2.9.4 and 2.9.5). Make use of Cartesian tensors for your solution.

Note that this exercise is adapted from problem 10(a) from Section 3.1 of [Segel \(1987\)](#).

EXERCISE 2.2: VELOCITY FIELD WITH ZERO STRAIN

If the strain rate tensor vanishes, show that the velocity field can be written

$$\mathbf{v} = \mathbf{U} + \boldsymbol{\Omega} \times \mathbf{x}, \quad (2.179)$$

where $\boldsymbol{\Omega}$ is a constant angular rotation rate and \mathbf{U} is a constant velocity. That is, a fluid velocity equal to a constant rotation plus translation renders zero strain. Hint: if $\mathbf{S} = 0$, what does that imply about the velocity field? You may also wish to make use of the general decomposition (2.128).

Note that this exercise is adapted from exercise 4.41.1 of [Aris \(1962\)](#).

EXERCISE 2.3: STRAIN RATE TENSOR AND ROTATION TENSOR

Following exercise 4.43.3 of [Aris \(1962\)](#), consider a two-dimensional flow with horizontal velocity

$$\mathbf{u} = (F/r)(\hat{\mathbf{x}}y - \hat{\mathbf{y}}x), \quad (2.180)$$

where $F = F(r)$ is an arbitrary function of the radial distance $r = \sqrt{x^2 + y^2}$ and with dimensions of L T^{-1} . Throughout this exercise, be sure your solution is dimensionally consistent.

- (a) Show that the velocity field is non-divergent.
- (b) Determine an analytic expression for the streamlines and draw a picture.
- (c) Determine the elements to the strain rate tensor, \mathbf{S} , given by equation (2.171c). Write the expression using polar coordinates $x = r \cos \varphi$ and $y = r \sin \varphi$ (see VOLUME 1) and the structure function

$$G(r) = r \frac{d(F/r)}{dr} = (F' - F/r)/2 \quad \text{with } F' = dF/dr. \quad (2.181)$$

- (d) Determine elements to the rotation tensor, \mathbf{R} , given by equation (2.171c), also written in polar coordinates.

EXERCISE 2.4: STRAIN RATE TENSOR AND ROTATION TENSOR FOR PARALLEL SHEAR FLOW

Consider a two-dimensional parallel shear flow with horizontal velocity

$$\mathbf{u} = a x \hat{\mathbf{y}}, \quad (2.182)$$

where a is a constant with dimension inverse time.

- (a) Compute the strain rate tensor, \mathbf{S} (equation (2.171c)) for this velocity field.
- (b) Compute the rotation tensor, \mathbf{R} (equation (2.171c)) for this velocity field.
- (c) Decompose the velocity field according to equation (2.128), and show that each of the velocity components is non-divergent. That is, write

$$\mathbf{u} = \mathbf{u}^0 + \mathbf{u}^{(S)} + \mathbf{u}^{(A)} \quad \text{with} \quad \nabla \cdot \mathbf{u}^{(S)} = \nabla \cdot \mathbf{u}^{(A)} = 0, \quad (2.183)$$

with u_i^0 the velocity at the point where $\delta x_i = x_i - x_i^0 = 0$. The velocity $\mathbf{u}^{(S)}$ has a constant strain but no vorticity whereas $\mathbf{u}^{(A)}$ has a constant vorticity but no strain. Hint: both $\mathbf{u}^{(S)}$ and $\mathbf{u}^{(A)}$ have nonzero $\hat{\mathbf{x}}$ and $\hat{\mathbf{y}}$ components.

- (d) Determine the streamfunctions for $\mathbf{u}^{(S)}$ and $\mathbf{u}^{(A)}$.
- (e) Sketch the velocity vectors $\mathbf{u}^{(S)}$ and $\mathbf{u}^{(A)}$.

EXERCISE 2.5: EVOLUTION OF THE JACOBIAN USING ϵ -TENSOR GYMNASTICS

There is another way to derive the identity (2.170) for the evolution of the Jacobian. This other method is somewhat more tedious. However, it exercises some useful methods of index gymnastics involving the ϵ -tensor. It also has a natural generalization to curved spaces. This exercise is only for aficionados of tensor analysis.

An explicit expression for the Jacobian of transformation is given by

$$\frac{\partial \boldsymbol{\varphi}}{\partial \mathbf{a}} = \frac{1}{3!} \epsilon_{mnp} \epsilon^{IJK} \frac{\partial \varphi^m}{\partial a^I} \frac{\partial \varphi^n}{\partial a^J} \frac{\partial \varphi^p}{\partial a^K}. \quad (2.184)$$

Take the material derivative of this expression and show that we get the same expression as

equation (2.170). Hint: make use of the identity

$$\frac{D}{Dt} \frac{\partial \varphi^m}{\partial a^I} = \frac{\partial v^m}{\partial a^I}, \quad (2.185)$$

which holds since the material time derivative is taken with the material coordinates, \mathbf{a} , held fixed. Also make use of the following identity (discussed in VOLUME 1) for the derivative of the Jacobian with respect to one of the matrix elements

$$\frac{\partial \det(\Lambda^a_{\bar{a}})}{\partial \Lambda^d_{\bar{d}}} = \frac{1}{3!} \epsilon^{\bar{a}\bar{b}\bar{c}} \epsilon_{abc} \frac{\partial}{\partial \Lambda^d_{\bar{d}}} [\Lambda^a_{\bar{a}} \Lambda^b_{\bar{b}} \Lambda^c_{\bar{c}}] = \frac{1}{2} \epsilon^{\bar{d}\bar{b}\bar{c}} \epsilon_{dbc} \Lambda^b_{\bar{b}} \Lambda^c_{\bar{c}} = \Lambda^{\bar{d}}_d \det(\Lambda^a_{\bar{a}}), \quad (2.186)$$



Chapter 3

MASS CONSERVATION

Throughout this book, we assume that matter is neither created nor destroyed anywhere within the fluid continuum, and furthermore that the fluid remains in a single phase.¹ These assumptions constrain the fluid motion and as such they form an important facet of fluid kinematics. In this chapter, we derive a variety of mathematical expressions of mass conservation in a single component fluid (materially homogeneous fluid), along with associated kinematic constraints placed on fluid motion. These constraints are examined both in the fluid interior and at boundaries, and from both Eulerian and Lagrangian kinematic viewpoints.

READER'S GUIDE TO THIS CHAPTER

We are here concerned with single-component fluids, with generalizations to multiple-component fluids given in Chapter 4. We build on our understanding of the Eulerian and Lagrangian kinematic descriptions developed in Chapters 1 and 2.

For the bulk of this chapter we make use of general tensors for the Eulerian coordinates to expose the coordinate invariant nature of the mass conservation equations. However, we use Cartesian coordinates when dealing with kinematic boundary conditions. Recall that when acting on scalar fields, the covariant derivative operator, ∇ , is the usual gradient operator built from partial derivatives, yet it is more complicated (involving Christoffel symbols) when acting on vector fields. Furthermore, we use general tensor analysis as summarized in Chapter 2 to transform between Eulerian (x -space) and Lagrangian (a -space).

3.1 Eulerian fluid regions	88
3.1.1 Finite volume expression	88
3.1.2 Flux-form conservation laws	89
3.1.3 Arbitrary Eulerian region	90
3.2 Material fluid parcels	90
3.2.1 Lagrangian expression for mass conservation	91
3.2.2 Summary of material kinematic equations	91
3.3 Material fluid regions	92
3.3.1 Evolution of volume	92
3.3.2 Mass conservation	93
3.4 Mass conservation and the motion field	93
3.4.1 Mass for a fluid parcel	93
3.4.2 Parcel mass conservation and the Jacobian	95

¹Chemical reactions transform matter from one form to another. Nuclear reactions convert between matter and nuclear energy. Phase changes convert matter from one phase to another. These processes are all outside the scope of this book.

3.4.3	Another derivation of mass conservation	95
3.4.4	Mass conservation for material fluid regions	96
3.5	Reynolds transport theorem	97
3.5.1	Derivation of the theorem	97
3.5.2	Comments on notation for the time derivative	98
3.6	Kinematic boundary conditions	99
3.6.1	Static material surface	99
3.6.2	Moving (free) material surface	100
3.6.3	Dynamic and permeable surface	104
3.7	Volume and mass budgets for a bounded fluid column	107
3.7.1	Kinematic free surface equation	107
3.7.2	Budget for mass per horizontal area	109
3.8	Exercises	109

3.1 Eulerian fluid regions

We here develop expressions for the mass budget within an Eulerian region, both infinitesimal and finite. Recall that Eulerian regions are fixed in space and thus have constant volumes. We start by assuming Cartesian coordinates, but then quickly generalize to arbitrary coordinates through converting partial derivatives to covariant derivatives as per the tensor analysis from VOLUME 1.

3.1.1 Finite volume expression

Consider a finite sized cube region that is fixed in space as shown in Figure 3.1. The mass contained within the cube is given by

$$\Delta M = \rho \Delta V = \rho \Delta x \Delta y \Delta z, \quad (3.1)$$

where the cube volume,

$$\Delta V = \Delta x \Delta y \Delta z, \quad (3.2)$$

is constant in time as per an Eulerian region. Since we will be taking the limit as the size of the cube becomes infinitesimal, it is sufficient to approximate the mass density as that at the cube center, $\rho = \rho(x, y, z, t)$. In the absence of mass sources within the fluid, the mass within the cube changes only through the accumulation or depletion of mass transported across the six cube faces.

Focusing on the mass **transport** in the meridional direction as illustrated in Figure 3.1, the accumulation of mass within the cube through this transport is determined by the difference in mass transport crossing the two adjacent cell faces

$$\text{mass change from meridional transport} = (\Delta x \Delta z) [(v \rho)_{y-\Delta y/2} - (v \rho)_{y+\Delta y/2}]. \quad (3.3)$$

Expanding the difference into a Taylor series and truncating after leading order yields

$$\text{mass change from meridional transport} \approx -(\Delta x \Delta y \Delta z) \frac{\partial(v \rho)}{\partial y}. \quad (3.4)$$

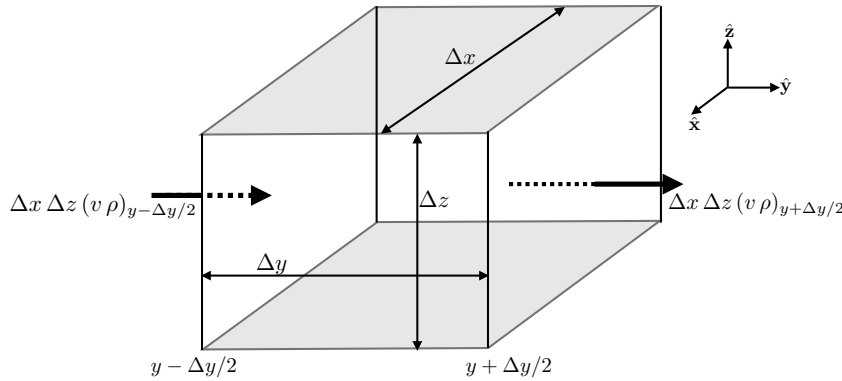


FIGURE 3.1: A finite sized cube or cell region with fixed dimensions and position (an Eulerian region) used to formulate the Eulerian form of mass conservation. We highlight two cell faces with area $\Delta x \Delta z$ and with meridional mass transport (with physical dimensions of mass per time) crossing the faces given by $\Delta x \Delta z (v \rho)_{y-\Delta y/2}$ and $\Delta x \Delta z (v \rho)_{y+\Delta y/2}$. To establish signs we assume the meridional velocity is positive, $v > 0$, so that mass enters the face at $y - \Delta y/2$ and leaves the face at $y + \Delta y/2$. Differences between these two transports leads to an accumulation of mass within the cell. The resulting mass budget holds regardless the direction of the flow velocity.

The same analysis for the zonal and vertical directions leads to the mass budget for the cube

$$\frac{\partial(\rho \Delta V)}{\partial t} = -\Delta V \left[\frac{\partial(u \rho)}{\partial x} + \frac{\partial(v \rho)}{\partial y} + \frac{\partial(w \rho)}{\partial z} \right]. \quad (3.5)$$

Hence, the cube mass changes according to convergence of mass across the cube boundaries. Cancelling the constant volume ΔV (again, the volume is assumed fixed as per an Eulerian region) renders the [flux-form conservation law](#), also referred to as the Eulerian form of the mass [continuity equation](#)

$$\frac{\partial \rho}{\partial t} + \nabla \cdot (\rho \mathbf{v}) = 0. \quad (3.6)$$

This equation is also commonly referred to as the [mass continuity](#) equation. The mass [flux](#), $\rho \mathbf{v}$, with dimensions $M L^{-2} T^{-1}$, measures the mass per time of matter crossing a unit area oriented with an outward normal direction. The corresponding mass [transport](#) is given by the flux multiplied by the area across which the flux passes, so the mass transport has dimensions $M T^{-1}$. If more mass is transported into a region than leaves (i.e., mass converges), then the mass density increases, and vice versa for a mass flux that diverges from a region. It is notable that the mass flux also serves as a measure of the momentum [flux](#).

3.1.2 Flux-form conservation laws

The mass [continuity equation](#) (3.6) is in the form of a [flux-form conservation law](#), in which the local time tendency of a field within an Eulerian reference frame is determined by the convergence of a flux

$$\partial_t \rho = -\nabla \cdot (\rho \mathbf{v}). \quad (3.7)$$

We wrote this equation as a tensor expression to emphasize its coordinate invariant nature, again assuming Eulerian coordinates (so that all basis vectors are time independent).² Namely,

²Following the notation from the tensor analysis in VOLUME 1, we write an upright symbol, such as \mathbf{v} , when not tied to specific coordinates, whereas slanted symbols, \mathbf{v} , are coordinate specific representations of tensors. Additionally, we write ∇ for the covariant derivative as a tensor operator that has ∇ as a particular Eulerian coordinate representation.

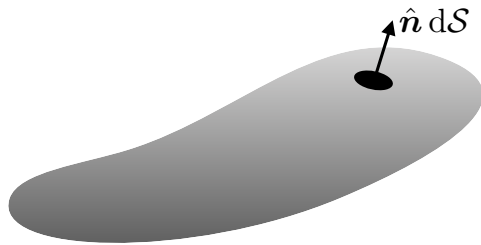


FIGURE 3.2: An arbitrarily shaped simply closed region, \mathcal{R} , within the fluid. If the region is fixed in space, then it represents a general Eulerian region for considering mass budgets. A surface area element, $d\mathcal{S}$, is oriented according to the outward normal, $\hat{\mathbf{n}}$.

equation (3.7) says that the time tendency of the mass density is driven by the covariant convergence of the mass flux, $\rho \mathbf{v}$.

3.1.3 Arbitrary Eulerian region

The discussion for the infinitesimal cube can be generalized by making use of the [divergence theorem](#). For that purpose, consider an arbitrary static and simply closed region within the fluid such as in Figure 3.2. Integrating the continuity equation (3.7) over that region leads to

$$\int_{\mathcal{R}} \frac{\partial \rho}{\partial t} dV = - \int_{\mathcal{R}} \nabla \cdot (\rho \mathbf{v}) dV. \quad (3.8)$$

Since the region is static we can move the partial time derivative outside on the left hand side. Furthermore, the divergence theorem can be applied to the right hand side to convert the volume integral to a surface integral over the boundaries of the static domain. The resulting mass budget is given by

$$\frac{d}{dt} \int_{\mathcal{R}} \rho dV = - \oint_{\partial\mathcal{R}} \rho \mathbf{v} \cdot \hat{\mathbf{n}} d\mathcal{S}, \quad (3.9)$$

where $\hat{\mathbf{n}}$ is the outward unit normal along the closed boundary of the region, and $d\mathcal{S}$ is the surface area element along that boundary. This equation, which holds for arbitrary coordinates, says that the mass within a fixed region of the fluid changes in time (left hand side) according to the accumulation of mass crossing the region boundary (right hand side). The minus sign means that the mass decreases in the region if there is a net mass transport leaving the domain in the direction of the outward normal.

3.2 Material fluid parcels

We here derive the differential expressions for mass conservation of a constant mass fluid parcel within a Lagrangian reference frame. The differential expressions for volume and density arise as a corollary. This discussion complements the Eulerian discussion from Section 3.1. To motivate the derivations we expand the flux-form mass continuity equation (3.7) to have

$$\frac{1}{\rho} \frac{D\rho}{Dt} = -\nabla \cdot \mathbf{v}, \quad (3.10)$$

where

$$D/Dt = \partial_t + \mathbf{v} \cdot \nabla \quad (3.11)$$

is the material time derivative operator from Section 1.5.4. We now derive the mass continuity equation (3.10) using Lagrangian methods.

3.2.1 Lagrangian expression for mass conservation

The mass of an infinitesimal fluid parcel that moves with the fluid flow is written³

$$\delta M = \rho \delta V, \quad (3.12)$$

where δV is the volume and

$$\rho = \delta M / \delta V \quad (3.13)$$

is the mass density of the moving parcel. Mass conservation means that the fluid parcel has a constant mass as it moves with the flow, so that its material time derivative vanishes

$$\frac{D(\delta M)}{Dt} = 0. \quad (3.14)$$

Equation (3.14) is the most basic form of mass conservation for a fluid parcel. However, we often have need to express this result in terms of parcel density and parcel volume

$$\frac{D(\delta M)}{Dt} = \frac{D(\rho \delta V)}{Dt} = \delta M \left[\frac{1}{\rho} \frac{D\rho}{Dt} + \frac{1}{\delta V} \frac{D(\delta V)}{Dt} \right]. \quad (3.15)$$

Making use of equation (2.162)⁴

$$\frac{1}{\delta V} \frac{D(\delta V)}{Dt} = \nabla \cdot \mathbf{v}, \quad (3.16)$$

leads to

$$\frac{1}{\delta M} \frac{D(\delta M)}{Dt} = \frac{1}{\rho} \frac{D\rho}{Dt} + \nabla \cdot \mathbf{v}. \quad (3.17)$$

Setting $D(\delta M)/Dt = 0$ renders the continuity equation (3.10) derived from the Eulerian expression

$$\frac{1}{\rho} \frac{D\rho}{Dt} = -\nabla \cdot \mathbf{v}. \quad (3.18)$$

The parcel volume contracts in regions where the velocity converges (we prove that property in Sections 2.11.1 and 3.3.1). The continuity equation (3.18) then says that regions of volume contraction are where the parcel density increases whereas the opposite occurs for regions where the velocity diverges.

3.2.2 Summary of material kinematic equations

Let us now summarize the variety of differential evolution equations for mass, volume, and density as viewed from a material reference frame

$$\frac{D(\delta M)}{Dt} = 0 \quad \text{parcel mass is constant} \quad (3.19)$$

$$\frac{1}{\delta V} \frac{D(\delta V)}{Dt} = \nabla \cdot \mathbf{v} \quad \text{parcel volume increases in divergent flow} \quad (3.20)$$

³Recall that we use the δ symbol to signal a property measured in the Lagrangian reference frame.

⁴We derive equation (3.16) in Section 3.3 using finite volume methods that are more general than those used to derive equation (2.162) in Section 2.11.1.

$$\frac{1}{\rho} \frac{D\rho}{Dt} = -\nabla \cdot \mathbf{v} \quad \text{parcel density increases in convergent flow.} \quad (3.21)$$

To help remember the signs on the right hand side, recall that as the fluid diverges from a point ($\nabla \cdot \mathbf{v} > 0$), it expands the boundaries of the material parcel and so increases the parcel volume as per equation (3.20). Since the parcel has a fixed mass, the diverging velocity field causes the material parcel density to decrease ($-\nabla \cdot \mathbf{v} < 0$) as per equation (3.21).

3.3 Material fluid regions

We now extend the kinematics of material fluid parcels in Section 3.2 to finite sized material fluid regions. Just as for material fluid parcels, the finite sized material fluid region retains the same matter content, and thus maintains a constant mass.⁵ We contrast the discussion here with that for Eulerian regions (fixed in space) considered in Section 3.1. One key operational distinction between the Eulerian and Lagrangian domains is that partial time derivative, ∂_t , commutes with integration over a fixed Eulerian domain, whereas material time derivative, ∂_T , commutes with integration over a Lagrangian domain as per Reynolds transport theorem derived in Section 3.5.

3.3.1 Evolution of volume

Consider a finite material region, $\mathcal{R}(\mathbf{v})$, whose volume is given by the integral

$$V = \int_{\mathcal{R}(\mathbf{v})} dV, \quad (3.22)$$

with dV the volume element. The region changes its shape according to motion of the fluid particles fixed to the boundary of the material region. We designate this region as

$$\mathcal{R}(\mathbf{v}) = \text{region following flow}, \quad (3.23)$$

with the \mathbf{v} argument emphasizing that the region moves with the flow velocity. The material region expands when the flow moves outward and contracts when the flow moves inward. These statements take on the following mathematical expression

$$\frac{d}{dt} \int_{\mathcal{R}(\mathbf{v})} dV = \oint_{\partial\mathcal{R}(\mathbf{v})} \mathbf{v} \cdot \hat{\mathbf{n}} d\mathcal{S}, \quad (3.24)$$

where $\hat{\mathbf{n}}$ is the outward normal on the region's closed boundary, $d\mathcal{S}$ is the area element on the boundary, and

$$\mathbf{v} \cdot \hat{\mathbf{n}} d\mathcal{S} = \text{volume transport (volume per time) at the boundary } \partial\mathcal{R}. \quad (3.25)$$

Use of the divergence theorem then leads to the equivalent expression

$$\frac{d}{dt} \int_{\mathcal{R}(\mathbf{v})} dV = \int_{\mathcal{R}(\mathbf{v})} \nabla \cdot \mathbf{v} dV. \quad (3.26)$$

⁵Recall that throughout this chapter we are focused on single-component fluids, so there is no diffusion of matter considered here. We relax this restriction in Chapter 4.

We now take the limit as the material region becomes a material parcel, in which case we recover the differential expression

$$\frac{1}{\delta V} \frac{D(\delta V)}{Dt} = \nabla \cdot \mathbf{v}, \quad (3.27)$$

where we make use of D/Dt since the infinitesimal volume is moving with the fluid. This equation is also derived in Section 2.11.1 using different (somewhat more restrictive) methods.

3.3.2 Mass conservation

The mass of fluid contained in a finite material region is given by

$$M = \int_{\mathcal{R}(\mathbf{v})} \rho dV. \quad (3.28)$$

As a material fluid region, it maintains a constant mass as it moves through the fluid so that

$$\frac{d}{dt} \int_{\mathcal{R}(\mathbf{v})} \rho dV = 0. \quad (3.29)$$

Just as for the volume in Section 3.3.1, taking the limit as the material region becomes infinitesimally small, the region mass conservation statement (3.29) becomes the parcel mass conservation statement (3.14)

$$\frac{D(\delta M)}{Dt} = \frac{D(\rho \delta V)}{Dt} = 0. \quad (3.30)$$

3.4 Mass conservation and the motion field

In Sections 2.2 and 2.3 we described motion of the matter continuum in terms of the motion field, $\varphi(\mathbf{a}, T)$. The motion field smoothly and continuously maps the reference or base manifold, \mathcal{B} , to the spatial manifold, \mathcal{S} , as time evolves. In that manner, the motion field provides a flow map. Here we frame mass conservation in this language of Lagrangian fluid kinematics, with Figure 3.3 providing a summary of the ideas.

3.4.1 Mass for a fluid parcel

Following the discussion of material volume elements in Section 2.8.3, write the mass of a fluid parcel on the base manifold, \mathcal{B} , as (see equation (2.100))

$$\delta M = \rho^L(\mathbf{a}, T = t_R) \sqrt{\det[\mathbf{g}^L(\mathbf{a}, T = t_R)]} d^3a = \hat{\rho}^L(\mathbf{a}) \hat{\mathbf{g}}^L(\mathbf{a}) d^3a. \quad (3.31)$$

In this equation, d^3a is the region of material space that is occupied by the parcel, with this region specified on the base manifold so that it does not change as the parcel evolves via the motion field. We use the shorthand

$$\hat{\mathbf{g}}^L(\mathbf{a}) = \mathbf{g}^L(\mathbf{a}, T = t_R) = \sqrt{\det[\mathbf{g}^L(\mathbf{a}, T = t_R)]} \quad (3.32)$$

for the square root of the Euclidean metric using the Lagrangian coordinates, computed at the reference time, $T = t_R$, and written as per equation (2.49). The mass density, $\hat{\rho}^L(\mathbf{a}) = \rho^L(\mathbf{a}, T = t_R)$, is the density of the fluid parcel computed at the base time, $T = t_R$.

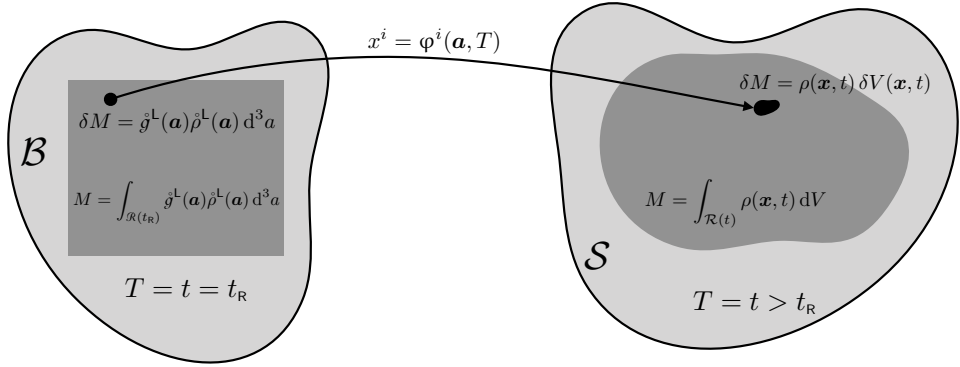


FIGURE 3.3: Following from Figure 2.1, we here depict conservation of mass in terms of the mapping between the referential or base manifold, \mathcal{B} , at time $T = t = t_R$, and the spatial manifold, \mathcal{S} , at some future time. The mapping is affected by the motion field, $\varphi(\mathbf{a}, T)$, which provides a flow map for the matter continuum. Mass conservation means that each infinitesimal fluid parcel within the matter continuum has a constant mass as it evolves from the base manifold to the spatial manifold. When represented using material coordinates on the base manifold, the parcel (small black circular region) has a mass given by $\delta M = \dot{\rho}(\mathbf{a}) d^3 a$, and mass within a finite subregion, $\mathcal{R}(t_R)$ of the base manifold (dark gray region) is given by the integral, $M = \int_{\mathcal{R}(t_R)} \dot{\rho}(\mathbf{a}) d^3 a$. When represented using Eulerian coordinates on the spatial manifold, the parcel has a mass, $\delta M = \rho(\mathbf{x}, t) \delta V(\mathbf{x}, t)$, and the mass within the finite subregion, $\mathcal{R}(t)$, that moves with the motion field, is given by the integral, $M = \int_{\mathcal{R}(t)} \rho(\mathbf{x}, t) dV$. Mass conservation for parcels, according to equation (3.42), means that the mass densities are related by $\dot{\rho}(\mathbf{a}) \dot{\mathbf{g}}^L(\mathbf{a}) = \rho^L(\mathbf{a}, T) \mathbf{g}^L(\mathbf{a}, T)$, or when using Cartesian Eulerian coordinates we have $\dot{\rho}(\mathbf{a}) = \rho^L(\mathbf{a}, T) \partial \varphi(\mathbf{a}, T) / \partial \mathbf{a}$. In either case, $\dot{\rho}(\mathbf{a})$ is independent of the material time, T .

As the fluid evolves, the motion field maps the base manifold, \mathcal{B} , to the spatial manifold, \mathcal{S} , as depicted in Figure 3.3. Mass conservation means that mass of the fluid parcel, δM , remains unchanged as its center of mass moves along a fluid particle trajectory, so that

$$\delta M = \rho^L(\mathbf{a}, T) \mathbf{g}^L(\mathbf{a}, T) d^3 a = \dot{\rho}(\mathbf{a}) \dot{\mathbf{g}}^L(\mathbf{a}) d^3 a. \quad (3.33)$$

When measured using Eulerian coordinates on the spatial manifold, the parcel mass is written

$$\delta M = \rho(\mathbf{x}, t) \delta V(\mathbf{x}, t). \quad (3.34)$$

In this equation, $\delta V(\mathbf{x}, t)$ is the parcel volume measured using \mathbf{x} coordinates, with this volume having dimensions L^3 , and being a function of space and time. The mass density, $\rho(\mathbf{x}, t)$, is the mass of the parcel per unit volume, $\delta V(\mathbf{x}, t)$. Writing the parcel mass using arbitrary Eulerian coordinates renders

$$\delta M = \rho(\mathbf{x}, t) \delta V = \rho(\mathbf{x}, t) \mathbf{g}^E(\mathbf{x}) d^3 x, \quad (3.35)$$

where $\mathbf{g}^E(\mathbf{x}) = \sqrt{\det[\mathbf{g}^E(\mathbf{x})]}$ is the square root of the metric determinant when using arbitrary Eulerian coordinates.⁶ Equating the Lagrangian expression (3.33) to the Eulerian expression (3.35) yields the identity

$$\rho^L(\mathbf{a}, T) \mathbf{g}^L(\mathbf{a}, T) d^3 a = \rho(\mathbf{x}, t) \mathbf{g}^E(\mathbf{x}) d^3 x. \quad (3.36)$$

If the Eulerian coordinates are taken to be Cartesian, then equation (2.52) means that the Jacobian of the transformation between \mathbf{x} -space and \mathbf{a} -space can be written in terms of the

⁶Recall from Section 2.5.1 that the Eulerian representation of the metric tensor is independent of the Eulerian time coordinate, t .

Lagrangian metric tensor determinant,

$$\frac{\partial \boldsymbol{\varphi}}{\partial \mathbf{a}} = \mathbf{g}^L(\mathbf{a}, T) \quad \text{Cartesian Eulerian coordinates.} \quad (3.37)$$

With this choice, the parcel mass can be written as

$$\delta M = \rho^L(\mathbf{a}, T) (\partial \boldsymbol{\varphi} / \partial \mathbf{a}) d^3 a \quad \text{Cartesian Eulerian coordinates.} \quad (3.38)$$

3.4.2 Parcel mass conservation and the Jacobian

The coordinate volume in material space is a material constant, so that

$$\partial_T(d^3 a) = 0. \quad (3.39)$$

Consequently, setting $\partial_T(\delta M) = \partial_T(\rho \delta V) = 0$ in equation (3.33) leads to the expression of mass conservation

$$\frac{\partial}{\partial T} [\rho^L(\mathbf{a}, T) \mathbf{g}^L(\mathbf{a}, T)] = 0. \quad (3.40)$$

Evidently, the product of the mass density times the square root of the metric determinant remains constant when following the trajectory of a fluid particle. Specializing to the case of Cartesian Eulerian coordinates allows us to replace the metric determinant with the Jacobian as per equation (2.52), so that

$$\frac{\partial}{\partial T} \left[\rho^L(\mathbf{a}, T) \frac{\partial \boldsymbol{\varphi}(\mathbf{a}, T)}{\partial \mathbf{a}} \right] = 0 \quad \text{Cartesian Eulerian coordinates.} \quad (3.41)$$

Equation (3.31) for mass conservation leads to

$$\dot{\rho}^L(\mathbf{a}) \dot{\mathbf{g}}^L(\mathbf{a}) = \rho^L(\mathbf{a}, T) \mathbf{g}^L(\mathbf{a}, T) \stackrel{\text{Cartesian Eulerian}}{=} \rho^L(\mathbf{a}, T) \frac{\partial \boldsymbol{\varphi}(\mathbf{a}, T)}{\partial \mathbf{a}}. \quad (3.42)$$

Defining material coordinates as the base manifold particle positions is commonly made in the solid mechanics literature (e.g., Chapter 1 of [Tromp \(2025a\)](#)). However, for geophysical fluid mechanics we do not build this assumption into the formalism. The reason is that we often find it useful to set \mathbf{a} to non-spatial coordinates, such as discussed in Section 1.4.2.

3.4.3 Another derivation of mass conservation

Yet another derivation of mass conservation follows from the identity (2.170), in which

$$\frac{D}{Dt} [\rho(\mathbf{x}, t) \delta V(\mathbf{x}, t)] = \frac{D}{Dt} \left[\rho \frac{\partial \boldsymbol{\varphi}}{\partial \mathbf{a}} d^3 a \right] \quad (3.43a)$$

$$= \left[\frac{D\rho}{Dt} + \rho \nabla \cdot \mathbf{v} \right] \left[\frac{\partial \boldsymbol{\varphi}}{\partial \mathbf{a}} \right] d^3 a \quad (3.43b)$$

$$= \left[\frac{D\rho}{Dt} + \rho \nabla \cdot \mathbf{v} \right] \delta V(\mathbf{x}, t). \quad (3.43c)$$

The Eulerian form of mass conservation given by equation (3.18) is recovered when noting that the mass of a material parcel is constant, so that $D\rho/Dt = -\rho \nabla \cdot \mathbf{v}$.

3.4.4 Mass conservation for material fluid regions

Now consider a finite region of the base manifold, $\mathcal{R}(t_R)$, as depicted in Figure 3.3. The mass of matter in this region is given by the integral

$$M = \int_{\mathcal{R}(t_R)} \rho^L(\mathbf{a}) \dot{\mathbf{g}}^L(\mathbf{a}) d^3a. \quad (3.44)$$

If the region follows the fluid flow so that $\mathcal{R}(t > t_R)$ is comprised of the same fluid particles, then the domain in \mathbf{a} -space remains unchanged, in which case we write it as $\mathcal{R}(\mathbf{a})$. Furthermore, a region that moves with fluid particles has a mass given by

$$M = \int_{\mathcal{R}(\mathbf{a})} \rho^L(\mathbf{a}, T) g^L(\mathbf{a}, T) d^3a \stackrel{\text{Cartesian Eulerian}}{=} \int_{\mathcal{R}(\mathbf{a})} \rho^L(\mathbf{a}, T) \frac{\partial \varphi(\mathbf{a}, T)}{\partial \mathbf{a}} d^3a. \quad (3.45)$$

When measured on the spatial manifold using Eulerian coordinates, the mass is given by

$$M = \int_{\mathcal{R}(t)} \rho(\mathbf{x}, t) dV \stackrel{\text{Cartesian Eulerian}}{=} \int_{\mathcal{R}(t)} \rho(\mathbf{x}, t) d^3x, \quad (3.46)$$

with the Eulerian domain, $\mathcal{R}(t)$, a function of time.

A one-dimensional example

To help understand the equality between equations (3.44)–(3.46), consider a one-dimensional example, in which the mass on a material line is given by

$$\int_{x_1(t)}^{x_2(t)} \rho(x, t) dx = \int_{a[x_1(t)]}^{a[x_2(t)]} \rho^L(a, T) \frac{\partial \varphi(a, T)}{\partial a} da \quad (3.47a)$$

$$= \int_{a_1}^{a_2} \rho^L(a, T) \frac{\partial \varphi(a, T)}{\partial a} da \quad (3.47b)$$

$$= \int_{a_1}^{a_2} \dot{\rho}^L(a) \dot{\mathbf{g}}^L(a) da. \quad (3.47c)$$

The equality (3.47a) introduced the Jacobian, $\partial \varphi / \partial a$, for the one-dimensional coordinate transformation from \mathbf{x} -space to \mathbf{a} -space, with corresponding changes to the integration limits. We can make this coordinate transformation since there is an assumed 1-to-1 relation between the \mathbf{a} -space and \mathbf{x} -space representation of a material fluid parcel. We also introduced the Lagrangian expression for the mass density following a fluid particle

$$\rho^L(a, T) = \rho[x = \varphi(a, T), t = T]. \quad (3.48)$$

The equality (3.47b) wrote the integral bounds in terms of the material coordinate. Since we are considering a material region that follows fluid particles, the integral bounds have fixed material coordinate values, $a[x_1(t)] = a_1$ and $a[x_2(t)] = a_2$. The final equality given by equation

(3.47c) introduced base manifold density and metric determinant,

$$\dot{\rho}^L(a) \dot{g}^L(a) = \rho^L(a, T) \frac{\partial \varphi(a, T)}{\partial a}, \quad (3.49)$$

which is independent of time, as required for mass conservation for a material fluid parcel as given by equation (3.41).

An exercise in the formalism

As an exercise using the Lagrangian formalism, consider the time derivative of the mass within a material fluid region and assume Cartesian \mathbf{x} -space so that

$$\frac{d}{dt} \left[\int_{\mathcal{R}[\mathbf{v}(\mathbf{x}, t)]} \rho dV \right] = \frac{d}{dt} \left[\int_{\mathcal{R}[\mathbf{v}(\mathbf{x}, t)]} \rho d^3x \right] \quad dV = d^3x \text{ for Cartesian } \mathbf{x} \quad (3.50a)$$

$$= \frac{\partial}{\partial T} \left[\int_{\mathcal{R}(\mathbf{a})} \rho^L \frac{\partial \varphi}{\partial \mathbf{a}} d^3a \right] \quad \text{transform } \mathbf{x} \text{ to } \mathbf{a} \quad (3.50b)$$

$$= \int_{\mathcal{R}(\mathbf{a})} \frac{\partial}{\partial T} \left[\rho^L \frac{\partial \varphi}{\partial \mathbf{a}} d^3a \right] \quad \partial_T \text{ commutes w/ integral} \quad (3.50c)$$

$$= \int_{\mathcal{R}[\mathbf{v}(\mathbf{x}, t)]} \frac{D}{Dt} [\rho d^3x] \quad \text{transform } \mathbf{a} \text{ to } \mathbf{x} \quad (3.50d)$$

$$= \int_{\mathcal{R}[\mathbf{v}(\mathbf{x}, t)]} \left[\frac{D\rho}{Dt} + \rho \nabla \cdot \mathbf{v} \right] dV \quad \text{chain rule + eq. (2.162)} \quad (3.50e)$$

$$= \int_{\mathcal{R}[\mathbf{v}(\mathbf{x}, t)]} \left[\frac{1}{\rho} \frac{D\rho}{Dt} + \nabla \cdot \mathbf{v} \right] \rho dV \quad \text{rearrange.} \quad (3.50f)$$

When expressing the integral bounds using \mathbf{a} -space coordinates, the integral bounds have no material T -dependence since they are fixed on fluid particles. We can thus move the ∂_T derivative inside of the integral sign to reach equality (3.50c). The equality (3.50d) made use of mass conservation in the form of equations (3.43a)-(3.43c) and converted back to \mathbf{x} -space. In this manner, upon entering the integral and using Eulerian coordinates, the time derivative is written as a material time derivative, D/Dt , since it is a time derivative computed by following the fluid particles that define the material region. As the material region, \mathcal{R} , has a materially constant mass, and it is an arbitrary shape, we recover the mass continuity equation (3.18) by setting the integrand in equation (3.50f) to zero.

3.5 Reynolds transport theorem

On first encounter, the method from Section 3.4.4 that involves moving between Eulerian (\mathbf{x} -space) and Lagrangian (\mathbf{a} -space) representations is clumsy at best and a black box at worse. However, with some practice it becomes an elegant means to study the time evolution of fluid properties integrated over a material region. The method is formalized by the *Reynolds transport theorem*.

3.5.1 Derivation of the theorem

Manipulations leading to the mass conservation statement (3.50f) can be generalized by considering the material time derivative of a mass-weighted field ψ (e.g., a tracer concentration

as in Section 4.1)

$$\frac{D(\psi \rho \delta V)}{Dt} = \frac{D\psi}{Dt} \rho \delta V + \psi \frac{D(\rho \delta V)}{Dt} \quad (3.51a)$$

$$= \rho \delta V \left[\frac{D\psi}{Dt} + \frac{\psi D\rho}{\rho} + \psi \nabla \cdot \mathbf{v} \right] \quad (3.51b)$$

$$= \delta V \left[\frac{\partial(\rho \psi)}{\partial t} + \nabla \cdot (\rho \psi \mathbf{v}) \right]. \quad (3.51c)$$

The first equality used the product rule, which holds for material time derivatives. Mass conservation means that the material derivative $D(\rho \delta V)/Dt = 0$. However, we choose to write mass conservation in the form of equation (3.43c), which allows us to introduce the flux-form Eulerian expression after replacing the material time derivative with its Eulerian form from equation (1.11). Another means to derive this result is to write

$$\rho \frac{D\psi}{Dt} = \rho \left[\frac{\partial \psi}{\partial t} + \mathbf{v} \cdot \nabla \psi \right] \quad (3.52a)$$

$$= \rho \left[\frac{\partial \psi}{\partial t} + \mathbf{v} \cdot \nabla \psi \right] + \psi \left[\frac{\partial \rho}{\partial t} + \nabla \cdot (\mathbf{v} \rho) \right] \quad (3.52b)$$

$$= \frac{\partial(\rho \psi)}{\partial t} + \nabla \cdot (\rho \mathbf{v} \psi). \quad (3.52c)$$

Following the discussion in Section 3.4.4, we can extend the material parcel result (3.51c) to a finite size material region. Again, each point in the material region is following a fluid particle. The result is known as the *Reynolds transport theorem*, which can be written in the following equivalent manners

$$\frac{d}{dt} \int_{\mathcal{R}(\mathbf{v})} \psi \rho dV = \int_{\mathcal{R}(\mathbf{v})} \frac{D\psi}{Dt} \rho dV \quad \text{material region} \quad (3.53a)$$

$$= \int_{\mathcal{R}(\mathbf{v})} \left[\frac{\partial(\rho \psi)}{\partial t} + \nabla \cdot (\rho \psi \mathbf{v}) \right] dV \quad \text{identity (3.52c)} \quad (3.53b)$$

$$= \int_{\mathcal{R}(\mathbf{v})} \frac{\partial(\rho \psi)}{\partial t} dV + \oint_{\partial \mathcal{R}(\mathbf{v})} \rho \psi \mathbf{v} \cdot \hat{\mathbf{n}} d\mathcal{S} \quad \text{divergence theorem.} \quad (3.53c)$$

Note that we returned to the notation $\mathcal{R}(\mathbf{v})$ for material region as introduced in Section 3.3.1. This notation is sufficient to designate that the region is following fluid particles whose velocity is the fluid velocity, \mathbf{v} . The surface integral term, $\mathbf{v} \cdot \hat{\mathbf{n}}$, generally does not vanish. Rather, it is given by $\mathbf{v} \cdot \hat{\mathbf{n}} = \mathbf{v}^{(s)} \cdot \hat{\mathbf{n}}$, where $\mathbf{v}^{(s)}$ is the velocity of a point on the boundary of the material region. Only when the material boundary is static can we set $\mathbf{v} \cdot \hat{\mathbf{n}} = 0$. We further consider this issue in Section 3.6 when studying kinematic boundary conditions.

3.5.2 Comments on notation for the time derivative

In this book we write d/dt for the time derivative operator. Furthermore, when the domain is specialized to follow fluid particles, we identify the special nature of such domains by introducing the fluid velocity argument to the domain name, $\mathcal{R}(\mathbf{v})$. This notation designates that all points in the domain, \mathcal{R} , move with the fluid velocity, \mathbf{v} , since all points have fluid particles attached. However, many authors choose an alternative notation by using the material time derivative, D/Dt , when acting on an integral over a material region. We thus have the following equality

across the two notational conventions

$$\frac{D}{Dt} \int_{\mathcal{R}} \psi \rho dV = \frac{d}{dt} \int_{\mathcal{R}(\mathbf{v})} \psi \rho dV. \quad (3.54)$$

The use of one convention versus the other is a matter of taste. We follow Section 2.1 of [Batchelor \(1967\)](#) by restricting the D/Dt operator to act only on space-time fields, such as $\psi(\mathbf{x}, t)$. Hence, the D/Dt operator is not used when acting on integrals over spatial regions. Following this convention leads us to write $\mathcal{R}(\mathbf{v})$ for a region that moves with the fluid flow and to retain d/dt when acting on the integral over that region.

The $\mathcal{R}(\mathbf{v})$ notation is not generally used in the literature, with many authors dropping the \mathbf{v} and thus letting words designate whether a region follows the flow or otherwise. As we have occasion in this book to consider a variety of fluid regions, we find it essential to introduce the somewhat more explicit notation, $\mathcal{R}(\mathbf{v})$, to denote a region moving with the flow velocity, \mathbf{v} . This usage aims to help the reader freely swim along with the mathematical flow rather than struggling to stay afloat in an ocean of confused or non-specific notation.

3.6 Kinematic boundary conditions

When a fluid encounters a boundary, either at the edge of the fluid region or an imaginary boundary within the fluid itself, the flow must accommodate the boundary and/or the boundary must accommodate the flow. Some boundaries are permeable, thus allowing matter to cross. Other boundaries are impermeable, so that no matter crosses the boundary. For material boundaries, any fluid originally in contact with the boundary stays in contact; at most the fluid can move tangential to the boundary without leaving it. We can understand this rather remarkable constraint placed on material boundaries by noting that no two fluid particles can occupy the same point along the material boundary, nor can there be a cavity next to the boundary as the boundary moves through the fluid. In this section we develop **kinematic boundary conditions** appropriate for the variety of cases encountered in fluid mechanics.

3.6.1 Static material surface

Consider a moving fluid that encounters a static material surface, such as the solid-earth. At the boundary, we can decompose the fluid velocity into a component that moves in the plane locally tangent to the boundary and another component that is normal to the boundary. To ensure that no fluid crosses the static boundary, the normal component must vanish at the boundary surface. Hence, the kinematic boundary condition for a moving fluid that encounters a static material boundary is (see Figure 3.4)

$$\mathbf{v} \cdot \hat{\mathbf{n}} = 0 \quad \text{no-normal flow condition on static material boundary.} \quad (3.55)$$

Recall our discussion of streamlines in Section 1.8.2, where $\mathbf{v} \cdot \hat{\mathbf{n}} = 0$ along a streamline. Evidently, the static material boundary is a flow streamline so that fluid that is in contact with the boundary remains in contact. This result holds even in the case of a time dependent flow.⁷

For many cases in practice, the material surface has its outward normal having a nonzero component in the vertical direction, which means there are no overturns in the surface. In this

⁷Specification of the tangential velocity along a material boundary requires dynamical information, such as the no-slip boundary that is unavailable from purely kinematic considerations.

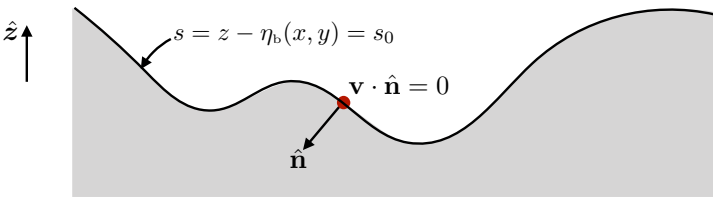


FIGURE 3.4: Illustrating the no-normal flow boundary condition maintained for a solid material boundary, on which $\mathbf{v} \cdot \hat{\mathbf{n}} = 0$ (equation (3.55)). When the solid boundary denotes the solid-earth (ground or ocean bottom), and when the boundary does not overturn (i.e., $\hat{\mathbf{n}} \cdot \hat{z}$ is single-signed), then the position of the interface can be written $s(x, y, z) = z - \eta_b(x, y) = s_0$, with s_0 a constant (equation (3.56)). Correspondingly, the outward unit normal is given by $\hat{\mathbf{n}} = -\nabla s/|\nabla s| = -(\hat{z} - \nabla \eta_b)/\sqrt{1 + |\nabla \eta_b|^2}$ as given by equation (3.57).

case, it is useful to introduce some differential geometry (at the level of introductory calculus) to unpack the boundary condition (3.55). Doing so helps to develop a geometric formalism especially useful for the more complicated moving boundary conditions in Sections 3.6.2 and 3.6.3. For this purpose, introduce a Cartesian coordinate expression for the boundary according to

$$s(x, y, z) = z - \eta_b(x, y) = s_0 \quad \text{static material boundary}, \quad (3.56)$$

with $z = \eta_b(x, y)$ the vertical position of the boundary and s_0 a constant. The outward unit normal vector at the boundary is thus given by

$$\hat{\mathbf{n}} = -\frac{\nabla s}{|\nabla s|} = -\frac{\nabla(z - \eta_b)}{|\nabla(z - \eta_b)|} = -\frac{\hat{z} - \nabla \eta_b}{\sqrt{1 + |\nabla \eta_b|^2}}. \quad (3.57)$$

Consequently, the no-flux boundary condition (3.55) takes the form (now using Cartesian coordinates)

$$\nabla(z - \eta_b) \cdot \mathbf{v} = w - \mathbf{u} \cdot \nabla_h \eta_b = 0 \quad \text{at } z = \eta_b(x, y), \quad (3.58)$$

where the velocity is decomposed into its horizontal and vertical components, $\mathbf{v} = (\mathbf{u}, w)$, using Cartesian coordinates. Hence, to maintain the no-flux boundary condition requires the vertical velocity component to precisely balance the projection of the horizontal velocity onto the slope of the material surface. If the material surface is flat, so that $\nabla_h \eta_b = 0$, then the kinematic boundary condition reduces to $w = 0$. Alternatively, if the flow is purely horizontal and thus moves along a constant η_b isoline, then $\mathbf{u} \cdot \nabla_h \eta_b = 0$ so that $w = 0$.

3.6.2 Moving (free) material surface

We next consider the kinematic constraints imposed by a moving surface that does not allow matter to cross the surface.⁸

General expression of the kinematic boundary condition

To ensure that no matter crosses the surface, the normal component of the velocity for a point on the surface must match the normal component of the fluid at the surface. We are thus led

⁸As we discuss in Chapter 4, with multiple matter components a surface that follows the barycentric velocity, and so allows for zero net mass to cross it, can still allow for the exchange of matter constituents (i.e., tracers) when there is matter diffusion. In the current chapter, we only consider a single matter constituent, so that zero mass crossing a surface also means there are no fluid particles crossing the surface.

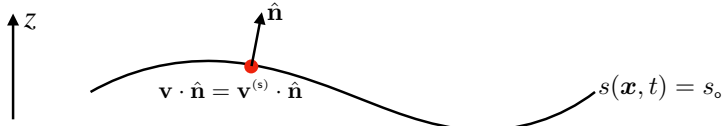


FIGURE 3.5: Illustrating the boundary condition for a moving material surface, on which $\hat{\mathbf{n}} \cdot (\mathbf{v} - \mathbf{v}^{(s)}) = 0$ (equation (3.59)), so that no fluid particles cross the surface. The boundary condition means that the velocity of the surface, $\mathbf{v}^{(s)}$, has the same normal component as the velocity of a fluid particle, \mathbf{v} . The material nature of the surface is not compromised if $\mathbf{v} \neq \mathbf{v}^{(s)}$, so long as their normal components are identical, $\hat{\mathbf{n}} \cdot \mathbf{v} = \hat{\mathbf{n}} \cdot \mathbf{v}^{(s)}$. For many cases, we can specify the surface by the value of a function that is a constant on the surface: $s(\mathbf{x}, t) = s_0$ for some constant s_0 (equation (3.60)). In such cases, the unit normal direction is given by $\hat{\mathbf{n}} = |\nabla s|^{-1} \nabla s$ (equation (3.61)). For example, s could represent a surface of constant temperature, or a constant Archimedean buoyancy in a buoyancy stratified fluid.

to the kinematic boundary condition for a moving material surface

$$(\mathbf{v} - \mathbf{v}^{(s)}) \cdot \hat{\mathbf{n}} = 0 \quad \text{moving material boundary condition.} \quad (3.59)$$

We illustrate this boundary condition in Figure 3.5, where $\mathbf{v}^{(s)}$ is the velocity of a point fixed on the moving material surface and \mathbf{v} is the velocity of the fluid particles.

As for the static material boundary, there is no constraint on the tangential component of the velocities, since it is only the normal component that measures the flow of matter across the boundary. Hence, the boundary condition (3.59) does not mean \mathbf{v} and $\mathbf{v}^{(s)}$ are identical. It only says that their normal components are the same when evaluated on the material surface. As a Corollary, we see that $\mathbf{v} \cdot \hat{\mathbf{n}}$ is not generally zero so that a moving material boundary does *not* coincide with a flow streamline (see discussion in Sections 1.8.2 and 1.8.3).

Specialized expression of the boundary condition

Now specialize the kinematic condition (3.59) to the case of a material surface, \mathcal{S} , as specified by a scalar function whose value remains a fixed constant when it is evaluated on the surface⁹

$$s(\mathbf{x}, t) = s_0 \quad \text{when } \mathbf{x} \in \mathcal{S}. \quad (3.60)$$

An example of such a function is the Archimedean buoyancy or the Conservative Temperature. Correspondingly, the surface unit normal is given by

$$\hat{\mathbf{n}} = |\nabla s|^{-1} \nabla s. \quad (3.61)$$

From Section 1.5.5, we know that a point fixed on an arbitrary surface has a velocity that satisfies (see equation (1.19))¹⁰

$$\partial_t s + \mathbf{v}^{(s)} \cdot \nabla s = 0 \quad \text{on an iso-surface } s(\mathbf{x}, t) = s_0. \quad (3.62)$$

Use of the identity

$$\frac{\partial s}{\partial t} = \frac{Ds}{Dt} - \mathbf{v} \cdot \nabla s \quad (3.63)$$

renders

$$\frac{Ds}{Dt} - \mathbf{v} \cdot \nabla s + \mathbf{v}^{(s)} \cdot \nabla s = \frac{Ds}{Dt} + (\mathbf{v}^{(s)} - \mathbf{v}) \cdot \nabla s = 0. \quad (3.64a)$$

⁹We use Cartesian coordinates in the remainder of this subsection.

¹⁰We offer another derivation of equation (3.62) later in this subsection.

Since $(\mathbf{v}^{(s)} - \mathbf{v}) \cdot \nabla s = 0$ from the boundary condition (3.59), we are left with the material constancy condition

$$\frac{Ds}{Dt} = \frac{\partial s}{\partial t} + \mathbf{v} \cdot \nabla s = 0 \quad \text{on material surface } s(\mathbf{x}, t) = s_o. \quad (3.65)$$

Consequently, matter does not cross a surface of constant s so long as s is materially constant. This is an important kinematic property that reappears in many forms throughout fluid mechanics.¹¹

Boundary condition for a material interface

Consider the interface between two immiscible fluids. Assume this interface has an outward normal that has a nonzero vertical component, so that there are no overturning or breaking waves. In this case we can express the vertical position of a point on the interface as

$$s(x, y, z, t) = z - \eta(x, y, t) = s_o. \quad (3.66)$$

The function $\eta(x, y, t)$ is the vertical deviation of the interface relative to the horizontal. The kinematic boundary condition (3.65) thus takes the form

$$\frac{Ds}{Dt} = \frac{D(z - \eta)}{Dt} = 0. \quad (3.67)$$

Hence, the vertical velocity component at the interface equals to the material time derivative of the interface displacement

$$\frac{Dz}{Dt} = \frac{D\eta}{Dt} \implies w = \frac{\partial \eta}{\partial t} + \mathbf{u} \cdot \nabla \eta \quad \text{material b.c. at interface } z = \eta(x, y, t). \quad (3.68)$$

This boundary condition can be equivalently written in the form

$$\mathbf{v} \cdot \hat{\mathbf{n}} = \frac{\partial \eta / \partial t}{\sqrt{1 + |\nabla \eta|^2}}, \quad (3.69)$$

where

$$\hat{\mathbf{n}} = \frac{\nabla(z - \eta)}{|\nabla(z - \eta)|} = \frac{-\nabla \eta + \hat{\mathbf{z}}}{\sqrt{1 + |\nabla \eta|^2}} \quad (3.70)$$

is the outward unit normal at the material surface. These equations provide kinematic relation for the motion of a surface within a perfect fluid. It also provides the kinematic relation for the interface separating two immiscible fluid layers. A particular example concerns the boundary condition placed on the ocean free surface in the special case of no water penetrating the surface (i.e., no rain or evaporation).

A geometric derivation of the material boundary condition

The material invariance condition, $Ds/Dt = 0$, is a key kinematic result. We thus offer an alternative derivation to help further establish its meaning. As before, define the surface according to

$$s(\mathbf{x}, t) = z - \eta(x, y, t) = s_o, \quad (3.71)$$

¹¹As noted on page 137 of [Serrin \(1959\)](#), the kinematic condition (3.65) originates from Kelvin in 1848 and Lagrange in 1781.

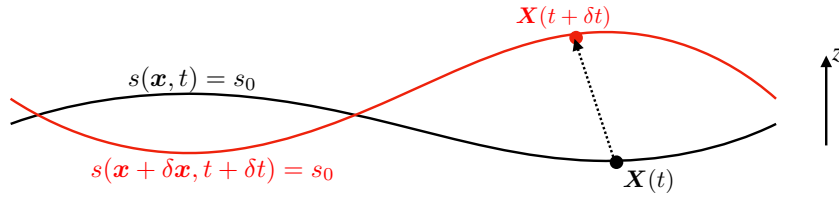


FIGURE 3.6: A surface within a fluid at two time instants, along with the position of a fluid particle on the surface at $\mathbf{X}(t)$ and $\mathbf{X}(t + \delta t)$. The velocity of a point on the surface is given by $\mathbf{v}^{(s)} = [\mathbf{X}(t + \delta t) - \mathbf{X}(t)]/\delta t = \delta \mathbf{X}/\delta t$. The equation, $s(\mathbf{x}, t) = z - \eta(\mathbf{x}, y, t) = s_0$, specifies the vertical position for points on the surface as a function of horizontal position and time. At both time instances the vertical position is determined by $s(\mathbf{x}, t) = s(\mathbf{x} + \delta \mathbf{x}, t + \delta t) = s_0$.

which specifies the vertical position of a point on the surface at time t . Now consider the position of the surface after a small time interval, $t + \delta t$ (see Figure 3.6). The vertical position of the surface at the new time is determined by the same condition

$$s(\mathbf{x} + \delta \mathbf{x}, t + \delta t) = s_0, \quad (3.72)$$

where $\mathbf{X}(t + \delta t) = \mathbf{x} + \delta \mathbf{x}$ is the displaced position of a point on the surface that started at $\mathbf{X}(t) = \mathbf{x}$, and

$$\mathbf{v}^{(s)} = [\mathbf{X}(t + \delta t) - \mathbf{X}(t)]/\delta t = \delta \mathbf{x}/\delta t \quad (3.73)$$

is the velocity of a point stuck to the surface. Expanding equation (3.72) in a Taylor series to leading order yields

$$s(\mathbf{x}, t) + \delta \mathbf{x} \cdot \nabla s + \delta t \partial_t s = s_0. \quad (3.74)$$

Since $s(\mathbf{x}, t) = s_0$ from equation (3.71) we thus have

$$\frac{\partial s}{\partial t} + \frac{\delta \mathbf{x}}{\delta t} \cdot \nabla s = \frac{\partial s}{\partial t} + \frac{\delta \mathbf{x}}{\delta t} \cdot \hat{\mathbf{n}} |\nabla s| = 0, \quad (3.75)$$

where $\hat{\mathbf{n}} = |\nabla s|^{-1} \nabla s$ is the surface unit normal direction. This result means that when positioned at a fixed point in space, it is the normal component of the displacement that corresponds to a temporal modification of $s(\mathbf{x}, t)$

$$\partial_t s = -\mathbf{v}^{(s)} \cdot \hat{\mathbf{n}} |\nabla s|. \quad (3.76)$$

In contrast, any tangential displacement along an s -isosurface leaves $s(\mathbf{x}, t)$ unchanged. Hence, when following motion of points on the surface, we are only concerned with motion along the direction set by the normal component of the velocity of that point, $\hat{\mathbf{n}} (\mathbf{v}^{(s)} \cdot \hat{\mathbf{n}})$. It is this velocity component that corresponds to movement of the surface normal to itself, thus leading to nonzero motion through space.

Writing equation (3.76) in a more conventional form leads to the differential equation satisfied by a point fixed on the moving surface

$$\partial_t s + \mathbf{v}^{(s)} \cdot \nabla s = 0. \quad (3.77)$$

Again, assuming the surface is material means that

$$\mathbf{v}^{(s)} \cdot \hat{\mathbf{n}} = \mathbf{v} \cdot \hat{\mathbf{n}}, \quad (3.78)$$

so that motion of the surface normal to itself is identical to that of the fluid in the same direction.

Use of the boundary condition (3.78) in equation (3.77) renders the material invariance condition

$$\frac{Ds}{Dt} = \frac{\partial s}{\partial t} + \mathbf{v} \cdot \nabla s = 0. \quad (3.79)$$

3.6.3 Dynamic and permeable surface

We now consider the kinematic boundary condition for a moving permeable surface that separates two fluid media (e.g., ocean and atmosphere) or two regions within a single media (e.g., surface of constant buoyancy within the ocean or within the atmosphere). As before, the kinematic boundary condition is a statement about the mass transport through the boundary. Whereas the previous conditions enforced a zero mass transport through the boundary at each point of the boundary, here we allow for a generally non-zero transport (mass per time). We write this transport condition as

$$\rho(\mathbf{v} - \mathbf{v}^{(s)}) \cdot \hat{\mathbf{n}} dS = -Q_m dS \quad \text{moving non-material boundary condition.} \quad (3.80)$$

In this equation, dS is an infinitesimal area element on the surface, and Q_m measures the mass per time per surface area (mass flux) crossing the boundary. The minus sign is a convention to be motivated in the following. We now massage this kinematic boundary condition into alternative forms.¹²

Coordinate representation of the permeable surface

The expression (3.62) for $\mathbf{v}^{(s)} \cdot \hat{\mathbf{n}}$ holds for a point on an arbitrary surface, even if that surface is permeable, so that

$$\mathbf{v}^{(s)} \cdot \hat{\mathbf{n}} = -\frac{\partial s / \partial t}{|\nabla s|}. \quad (3.81)$$

Furthermore, the projection of the fluid velocity onto the normal direction can be written

$$\frac{Ds}{Dt} = \frac{\partial s}{\partial t} + \mathbf{v} \cdot \nabla s \implies \mathbf{v} \cdot \hat{\mathbf{n}} = \frac{1}{|\nabla s|} \left[\frac{Ds}{Dt} - \frac{\partial s}{\partial t} \right]. \quad (3.82)$$

Bringing these results together leads to

$$\rho(\mathbf{v} - \mathbf{v}^{(s)}) \cdot \hat{\mathbf{n}} dS = \frac{\rho dS}{|\nabla s|} \frac{Ds}{Dt} \implies Q_m = -\frac{\rho}{|\nabla s|} \frac{Ds}{Dt}. \quad (3.83)$$

This equation says that the mass transport crossing the surface is proportional to the material time derivative of the surface coordinate. The material time derivative vanishes when there is no mass transport across the surface, which is a result already seen in Section 3.6.2.

In terms of the horizontal projection of the surface area

Assume that the surface is not vertical, so that its normal direction has a nonzero component in the vertical (e.g., waves that do not overturn). This assumption means that

$$\frac{\partial s}{\partial z} \neq 0, \quad (3.84)$$

¹²We use Cartesian coordinates in the remainder of this subsection for purposes of deriving various coordinate invariant expressions.

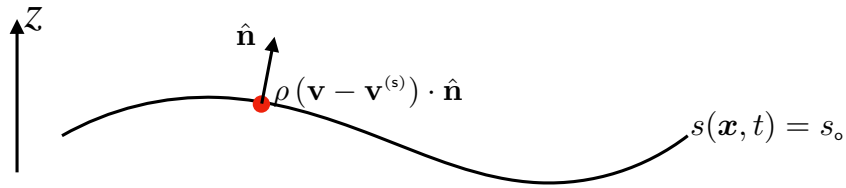


FIGURE 3.7: Illustrating the boundary condition for a moving permeable surface, such as the interface between two miscible fluid layers. On this surface, the boundary condition states that $\rho(\mathbf{v} - \mathbf{v}^{(s)}) \cdot \hat{\mathbf{n}} d\mathcal{S} = -Q_m d\mathcal{S}$ (as per equation (3.80)). In the special case of an ocean free surface with no overturns, this boundary condition reduces to the surface kinematic boundary condition (3.96).

so that we can further massage the boundary condition (3.83) by writing the area factor in the form

$$\frac{d\mathcal{S}}{|\nabla s|} = \frac{d\mathcal{S}}{\sqrt{(\partial s/\partial x)^2 + (\partial s/\partial y)^2 + (\partial s/\partial z)^2}} \quad (3.85a)$$

$$= \frac{d\mathcal{S}}{|\partial s/\partial z| \sqrt{[(\partial s/\partial x)/(\partial s/\partial z)]^2 + [(\partial s/\partial y)/(\partial s/\partial z)]^2 + 1}} \quad (3.85b)$$

$$= \frac{d\mathcal{S}}{|\partial s/\partial z| \sqrt{1 + \tan^2 \vartheta}} \quad (3.85c)$$

$$= \left| \frac{\partial z}{\partial s} \right| |\cos \vartheta| d\mathcal{S} \quad (3.85d)$$

$$= \left| \frac{\partial z}{\partial s} \right| dA. \quad (3.85e)$$

The equality (3.85c) introduced the angle, ϑ , between the boundary surface and the horizontal plane. The squared slope of this surface is given by

$$\tan^2 \vartheta = \frac{\nabla_h s \cdot \nabla_h s}{(\partial s/\partial z)^2} = \nabla_{hs} z \cdot \nabla_{hs} z \quad (3.86)$$

with

$$\nabla_h = \hat{x} \left[\frac{\partial}{\partial x} \right]_{y,z} + \hat{y} \left[\frac{\partial}{\partial y} \right]_{x,z} \quad (3.87)$$

the horizontal gradient operator on constant z surfaces, and

$$\nabla_{hs} = \hat{x} \left[\frac{\partial}{\partial x} \right]_{y,s} + \hat{y} \left[\frac{\partial}{\partial y} \right]_{x,s} \quad (3.88)$$

the horizontal gradient operator on constant s surfaces, along with $z(x, y, s, t)$ for the vertical position of the constant s surface.¹³ The equality (3.85d) made use of a trigonometric identity, and the equality (3.85e) introduced the horizontal projection of the area,

$$dA = |\cos \vartheta| d\mathcal{S}. \quad (3.89)$$

See Figure 3.8 for an illustration.

¹³We make use of such operators in VOLUME 3 as part of the mathematical development of generalized vertical coordinates.

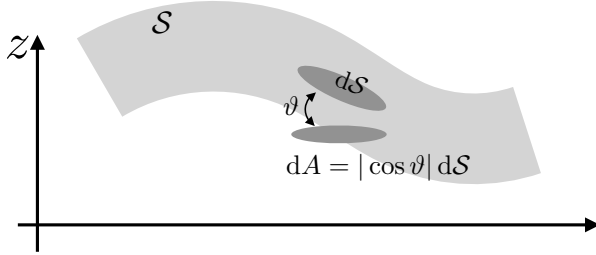


FIGURE 3.8: Illustrating the relation between an infinitesimal area element on a surface, $d\mathcal{S}$, to its horizontal projection, $dA = |\cos \vartheta| d\mathcal{S}$, according to equation (3.89). The angle, ϑ , must be bounded away from $\pm\pi/2$, thus enabling a nonzero horizontal area projection. For the specific case of a surface defined by $s = z - \eta(x, y, t)$, then $\partial s / \partial z = 1$ and $d\mathcal{S} = \sqrt{1 + (\nabla \eta)^2} dA$ (equation (3.93)).

These results bring the kinematic boundary condition (3.83) into the form

$$\rho (\mathbf{v} - \mathbf{v}^{(s)}) \cdot \hat{\mathbf{n}} d\mathcal{S} = -Q_m d\mathcal{S} \quad (3.90a)$$

$$= \rho \frac{Ds}{Dt} \left| \frac{\partial z}{\partial s} \right| dA \quad (3.90b)$$

$$\equiv -Q_m dA. \quad (3.90c)$$

As defined, the flux Q_m is the net mass per time per horizontal area crossing the boundary surface

$$Q_m = -\rho (\mathbf{v} - \mathbf{v}^{(s)}) \cdot \hat{\mathbf{n}} \frac{d\mathcal{S}}{dA} = -\rho \frac{Ds}{Dt} \left| \frac{\partial z}{\partial s} \right|. \quad (3.91)$$

We motivate the minus sign through the ocean free surface case in the following.

Kinematic boundary condition at the ocean free surface

Consider the ocean free surface located at

$$s(x, y, z, t) = z - \eta(x, y, t) = 0 \quad \text{ocean free surface.} \quad (3.92)$$

For this boundary, $\partial s / \partial z = 1$ so that the area elements are related by

$$d\mathcal{S} = |\nabla(z - \eta)| dA = \sqrt{1 + |\nabla\eta|^2} dA. \quad (3.93)$$

The normal projection for the velocity of a point fixed on the free surface is given by

$$\mathbf{v}^{(\eta)} \cdot \hat{\mathbf{n}} = -\frac{\partial s / \partial t}{|\nabla s|} = \frac{\partial \eta / \partial t}{|\nabla(z - \eta)|} = \frac{\partial \eta / \partial t}{\sqrt{1 + |\nabla\eta|^2}} \implies \mathbf{v}^{(\eta)} \cdot \hat{\mathbf{n}} d\mathcal{S} = \partial_t \eta dA, \quad (3.94)$$

so that the mass flux crossing the free surface is

$$-Q_m = \rho (\mathbf{v} - \mathbf{v}^{(\eta)}) \cdot \hat{\mathbf{n}}. \quad (3.95)$$

The boundary condition (3.91) thus takes the form

$$\rho (\mathbf{v} - \mathbf{v}^{(\eta)}) \cdot \hat{\mathbf{n}} \frac{d\mathcal{S}}{dA} = \rho \left[\frac{D(z - \eta)}{Dt} \right] = -Q_m \implies w + \rho^{-1} Q_m = \frac{\partial \eta}{\partial t} + \mathbf{u} \cdot \nabla \eta. \quad (3.96)$$

We now motivate the sign convention chosen for equation (3.90c) by considering the special case of a flat free surface and a resting fluid with $\mathbf{v} = 0$. Adding mass to the ocean raises the free surface, so that $\partial\eta/\partial t > 0$. Hence, the chosen sign convention means that $Q_m > 0$ corresponds to mass added to the ocean.

Kinematic boundary condition on a buoyancy surface

Now consider the interface to be a surface of constant potential density in the ocean (or analogously a surface of constant specific entropy in the atmosphere). These buoyancy isosurfaces are also known as isopycnals, and we use the symbol¹⁴

$$s = \sigma(x, y, z, t) \quad (3.97)$$

for a particular isopycnal, σ . The mass transport crossing the isopycnal is written

$$Q_m = \rho \frac{D\sigma}{Dt} \left| \frac{\partial z}{\partial \sigma} \right| \equiv \rho w^{(\dot{\sigma})}, \quad (3.98)$$

where we introduced the *diapycnal transport velocity*

$$w^{(\dot{\sigma})} \equiv \frac{D\sigma}{Dt} \left| \frac{\partial z}{\partial \sigma} \right|. \quad (3.99)$$

A key aspect of ocean physics concerns the development of theories for processes that cause a non-zero diapycnal transport. Examples include breaking waves, which act to mix matter across density surfaces; i.e., to **entrain** water from one density class to another.

3.7 Volume and mass budgets for a bounded fluid column

We close this chapter by deriving the budget for the volume per horizontal area in a column of a bounded fluid, as well as the budget for the mass per horizontal area in this as shown in Figure 3.9. Such fluid columns are relevant to the study of mass budgets over the full depth of the ocean. Since the upper boundary of the domain is the free surface, and since the free surface is a function of time, the region is not strictly Eulerian even though the sides are fixed in space. Furthermore, the free surface is permeable, as are the sides, so that the region is not material. The derivation offers experience working with the kinematic boundary conditions, as well as some exposure to the use of **Leibniz's rule** from calculus. We make use of Cartesian coordinates throughout.

3.7.1 Kinematic free surface equation

We here derive an equation for the free surface evolution, with this equation providing a budget for the volume per horizontal area in the column. The derivation proceeds by vertically integrating the mass continuity equation (3.18) over the depth of an ocean column, from $z = \eta_b(x, y)$ at the bottom to $z = \eta(x, y, t)$ at the free surface. Use of the bottom and surface kinematic boundary conditions renders a kinematic expression for the free surface time tendency.

¹⁴In this book, we use σ as an arbitrary generalized vertical coordinate, here chosen to be an isopycnal.

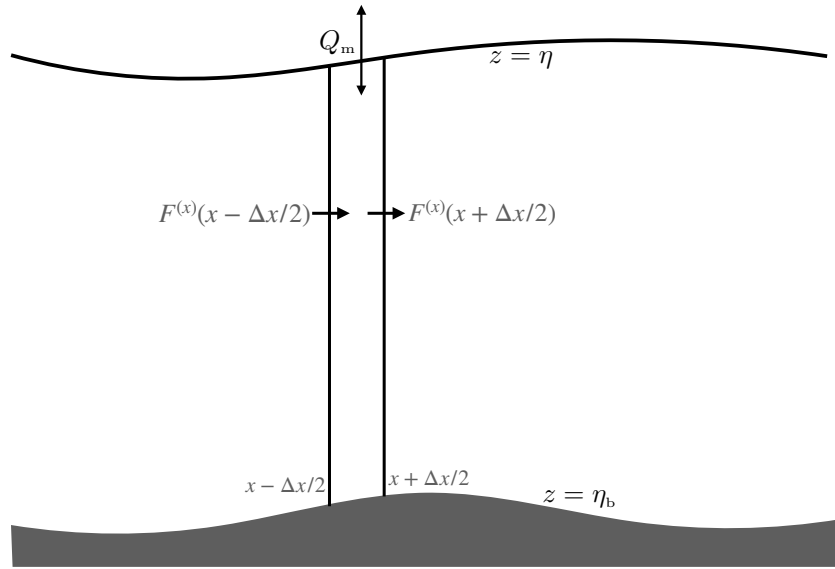


FIGURE 3.9: A longitudinal-vertical slice of ocean fluid from the surface at $z = \eta(x, y, t)$ to bottom at $z = \eta_b(x, y)$. The horizontal boundaries of the column at $x - \Delta x/2$ and $x + \Delta x/2$ are static and are penetrated by zonal mass transport, $F^{(x)}$. The zonal mass transport is computed by integrating the zonal mass flux, ρu over the area of the column sides. A similar transport acts in the meridional direction as well. The ocean bottom at the solid-earth boundary, $z = \eta_b(x, y)$, is static with no mass crossing this interface. The ocean surface at $z = \eta(x, y, t)$ is time dependent with mass flux, Q_m , crossing this interface.

Vertically integrating the continuity equation (3.18) renders

$$-\int_{\eta_b}^{\eta} \frac{1}{\rho} \frac{D\rho}{Dt} dz = \int_{\eta_b}^{\eta} \nabla \cdot \mathbf{v} dz \quad (3.100a)$$

$$= w(\eta) - w(\eta_b) + \int_{\eta_b}^{\eta} \nabla_h \cdot \mathbf{u} dz \quad (3.100b)$$

$$= w(\eta) - w(\eta_b) + \nabla_h \cdot \left[\int_{\eta_b}^{\eta} \mathbf{u} dz \right] - \mathbf{u}(\eta) \cdot \nabla_h \eta + \mathbf{u}(\eta_b) \cdot \nabla_h \eta_b \quad (3.100c)$$

$$= [w(\eta) - \mathbf{u}(\eta) \cdot \nabla_h \eta] - [w(\eta_b) - \mathbf{u}(\eta_b) \cdot \nabla_h \eta_b] + \nabla_h \cdot \left[\int_{\eta_b}^{\eta} \mathbf{u} dz \right], \quad (3.100d)$$

where we made use of [Leibniz's rule](#) from calculus in order to move the horizontal divergence outside of the integral. Also note that $\nabla \cdot \mathbf{u} = \nabla_h \cdot \mathbf{u}$ since \mathbf{u} is the horizontal velocity, and likewise for $\nabla \eta_b$ and $\nabla \eta$ since η_b and η are both functions of horizontal space and time, and so have no z dependence.

Use of the surface kinematic boundary condition (3.96) and no-normal flow bottom boundary condition yield

$$\frac{\partial \eta}{\partial t} = \frac{Q_m}{\rho(\eta)} - \nabla \cdot \mathbf{U} - \int_{\eta_b}^{\eta} \frac{1}{\rho} \frac{D\rho}{Dt} dz \quad (3.101)$$

where

$$\mathbf{U} = \int_{\eta_b}^{\eta} \mathbf{u} dz \quad (3.102)$$

is the depth integrated horizontal transport. Hence, as deduced from the mass continuity equation, the ocean free surface time tendency is affected by the passage of mass across the surface boundary (as normalized by the surface density), the convergence of depth integrated flow, and the depth integral of the material changes in density. The density term contributes

to a positive sea surface height tendency when density decreases, and vice versa when density increases. [Griffies and Greatbatch \(2012\)](#) provide a more complete analysis of the sea surface height budget (3.101) by unpacking the physical processes leading to the material evolution of density, which they refer to as the *non-Boussinesq steric effect*.

3.7.2 Budget for mass per horizontal area

The mass per horizontal area in the fluid column is given by $\int_{\eta_b}^{\eta} \rho dz$. Use of Leibniz's rule, the bottom kinematic boundary condition, (3.58), surface kinematic boundary condition (3.96), and the mass continuity equation (3.6), leads to

$$\frac{d}{dt} \left[\int_{\eta_b}^{\eta} \rho dz \right] = \rho(\eta) \frac{\partial \eta}{\partial t} + \int_{\eta_b}^{\eta} \frac{\partial \rho}{\partial t} dz \quad (3.103a)$$

$$= \rho(\eta) \frac{\partial \eta}{\partial t} - \int_{\eta_b}^{\eta} \nabla \cdot (\rho \mathbf{v}) dz \quad (3.103b)$$

$$= \rho(\eta) \left[\frac{\partial \eta}{\partial t} - w(\eta) \right] + \rho(\eta_b) w(\eta_b) - \int_{\eta_b}^{\eta} \nabla_h \cdot (\rho \mathbf{u}) dz \quad (3.103c)$$

$$= \rho(\eta) \left[\frac{\partial \eta}{\partial t} + \mathbf{u} \cdot \nabla \eta - w(\eta) \right] + \rho(\eta_b) [w(\eta_b) - \mathbf{u}(\eta_b) \cdot \nabla \eta_b] - \nabla_h \cdot \mathbf{U}^\rho \quad (3.103d)$$

$$= Q_m - \nabla_h \cdot \mathbf{U}^\rho, \quad (3.103e)$$

where

$$\mathbf{U}^\rho = \int_{\eta_b}^{\eta} \rho \mathbf{u} dz. \quad (3.104)$$

Hence, the mass per horizontal area within a column evolves according to

$$\frac{d}{dt} \left[\int_{\eta_b}^{\eta} \rho dz \right] = Q_m - \nabla \cdot \mathbf{U}^\rho, \quad (3.105)$$

with terms on the right hand side representing the convergence of mass onto the column either through the sides or upper surface. We consider an alternative derivation of this budget in Exercise 3.3.



3.8 Exercises

EXERCISE 3.1: VELOCITY THAT DOES NOT PENETRATE A CURVE

Consider a static curve defined by the Cartesian coordinate expression

$$s(x, y) = x y = \text{constant}. \quad (3.106)$$

Provide an example velocity, $\mathbf{v} = u \hat{x} + v \hat{y} + w \hat{z}$, that has nonzero horizontal components and that satisfies $\mathbf{v} \cdot \hat{n} = 0$, where \hat{n} is the unit normal to the curve. Be sure that your answer has the proper dimensions for a velocity.

EXERCISE 3.2: CENTER OF MASS MOTION

Consider a material fluid region, $\mathcal{R}(\mathbf{v})$, with constant mass written as

$$M = \int_{\mathcal{R}(\mathbf{v})} \rho dV. \quad (3.107)$$

Assume Cartesian coordinates throughout this exercise.¹⁵

- (a) Show mathematically that the center of mass for the region moves with the region's total linear momentum

$$\frac{d}{dt} \left[\frac{1}{M} \int_{\mathcal{R}(\mathbf{v})} \mathbf{x} \rho dV \right] = \frac{1}{M} \int_{\mathcal{R}(\mathbf{v})} \frac{D\mathbf{x}}{Dt} \rho dV = \frac{1}{M} \int_{\mathcal{R}(\mathbf{v})} \mathbf{v} \rho dV. \quad (3.108)$$

Precisely describe the reasoning behind each step. Note: a brief solution is sufficient, so long as the reasoning is sound.

- (b) Show mathematically (or precisely describe why) that the time change in the linear momentum for the region is given by

$$\frac{d}{dt} \left[\int_{\mathcal{R}(\mathbf{v})} \rho \mathbf{v} dV \right] = \int_{\mathcal{R}(\mathbf{v})} \frac{D\mathbf{v}}{Dt} \rho dV. \quad (3.109)$$

Precisely describe the reasoning behind each step. Note: a brief solution is sufficient, so long as the reasoning is sound.

EXERCISE 3.3: MASS BUDGET FOR A FLUID COLUMN

We here provide an alternative derivation of equation (3.105), the budget for the mass per horizontal area over a column of fluid.

The mass within an arbitrary fluid region is given by

$$M = \int_{\mathcal{R}} \rho dV. \quad (3.110)$$

Consider the fluid mass within the column shown in Figure 3.9. In this column, the vertical side-walls are fixed in time, the bottom surface, $z = \eta_b(x, y)$, is at the solid-earth boundary, and the top, $z = \eta(x, y, t)$, is the fluctuating ocean free surface. Convince yourself that the mass for this column can be written

$$M = \iint \left[\int_{\eta_b(x, y)}^{\eta(x, y, t)} \rho dz \right] dx dy, \quad (3.111)$$

where the horizontal (x, y) integrals extend over the horizontal extent of the column. Mass conservation for this column means that the change in mass arises just through boundary fluxes, so that

$$\frac{dM}{dt} = - \int \rho \Delta \mathbf{v} \cdot \hat{\mathbf{n}} d\mathcal{S}, \quad (3.112)$$

where $\hat{\mathbf{n}}$ is the outward normal to the surface of the fluid region, $d\mathcal{S}$ is the area of an infinitesimal element on the surface, and the minus sign means that fluid leaving the region contributes to a

¹⁵Note the for a general manifold, the addition of vectors is only defined locally within a tangent space. This limitation prevents us from integrating general tensors over a volume. However, for Cartesian tensors we can perform integration in a naive manner just as for scalars.

reduction in mass within the region. The term

$$\Delta \mathbf{v} = \mathbf{v} - \mathbf{v}^{(s)} \quad (3.113)$$

is the velocity of the fluid relative to the velocity of the boundary; e.g., see the kinematic boundary condition discussion in Section 3.6.3. We also derive a general form of this relation in equation (4.47), though this exercise can be solved without knowing the details of that derivation.

- (a) Mass transported in the zonal direction ($\hat{\mathbf{x}}$) that crosses the column's vertical boundary at x is given by

$$F^{(x)}(x, y, t) = \int_{y-\Delta y/2}^{y+\Delta y/2} \left[\int_{\eta_b(x, y')}^{\eta(x, y', t)} u(x, y', z', t) \rho(x, y', z', t) dz' \right] dy' \quad (3.114a)$$

$$\equiv \int_{y-\Delta y/2}^{y+\Delta y/2} U^\rho(x, y', t) dy', \quad (3.114b)$$

and similarly for mass transport in the meridional direction

$$F^{(y)}(x, y, t) = \int_{x-\Delta x/2}^{x+\Delta x/2} \left[\int_{\eta_b(x', y)}^{\eta(x', y, t)} v(x', y, z', t) \rho(x', y, z', t) dz' \right] dx' \quad (3.115a)$$

$$\equiv \int_{x-\Delta x/2}^{x+\Delta x/2} V^\rho(x', y, t) dx', \quad (3.115b)$$

where

$$\mathbf{U}^\rho(x, y, t) = \int_{\eta_b(x, y)}^{\eta(x, y, t)} \mathbf{u}(x, y, z', t) \rho(x, y, z', t) dz' = \hat{\mathbf{x}} U^\rho + \hat{\mathbf{y}} V^\rho. \quad (3.116)$$

What are the physical dimensions [in terms of length (L), mass (M), and time (T)] for the mass transports, $F^{(x)}$ and $F^{(y)}$?

- (b) Using these expressions for the mass crossing the vertical side boundaries of a fluid column, take the limit as the horizontal cross-sectional area of the column becomes infinitesimally small to show that the evolution equation for the mass per unit area of the column is given by

$$\frac{d}{dt} \left[\int_{\eta_b}^{\eta} \rho dz \right] = -\nabla \cdot \mathbf{U}^\rho + Q_m, \quad (3.117)$$

where Q_m is the mass transport entering the ocean through the surface, per horizontal area, as defined by equation (3.90c), so that

$$\int Q_m dA = - \int \rho \Delta \mathbf{v} \cdot \hat{\mathbf{n}} dS \quad \text{at } z = \eta. \quad (3.118)$$

The derivation of equation (3.117) is part of this exercise, using methods distinct from those used in Section 3.7.2.

- (c) In words, the mass budget in equation (3.117) says that mass changes in a column of fluid if there is a convergence of mass into the column across its vertical boundaries (first term on right hand side), and a mass flux entering the column across the ocean surface (second term on right hand side). What are the physical dimensions of all terms in equation

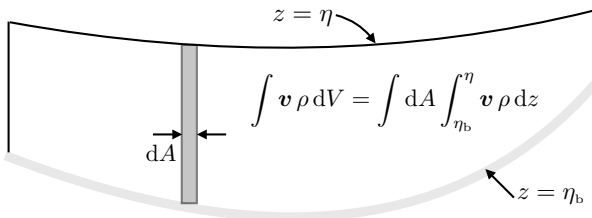


FIGURE 3.10: Cross-section of the integration region for Exercise 3.4, with the region extending from the ocean bottom at $z = \eta_b(x, y)$ and the free surface at $z = \eta(x, y, t)$. The sides are assumed to be vertical and rigid. An infinitesimal column is shown with cross-sectional area dA , extending from the bottom to the surface. The cross-sectional area for the column is time independent, so that a time derivative passes across the area integral to act only on the upper limit $z = \eta$ and the integrand in equation (3.121).

(3.117)?

EXERCISE 3.4: CHANGE IN LINEAR MOMENTUM OF A FLUID REGION

Consider a closed ocean basin with zero boundary fluxes of matter; i.e., zero precipitation/e-vaporation and zero mass fluxes through the solid-earth bottom. Consequently, this region is bounded by material surfaces and so it maintains constant matter content with fixed mass

$$M = \int_{\mathcal{R}} \rho dV. \quad (3.119)$$

Show that the time change in the linear momentum for this ocean basin is given by

$$\frac{d}{dt} \left[\int_{\mathcal{R}} \rho \mathbf{v} dV \right] = \int_{\mathcal{R}} \frac{D\mathbf{v}}{Dt} \rho dV. \quad (3.120)$$

This result is identical to that derived in Exercise 3.2. Rather than just repeating the solution method used there, make use of [Leibniz's rule](#), the kinematic boundary condition detailed in Section 3.6.2, and mass conservation.

As noted in the footnote for Exercise 3.2, addition of vectors is only defined locally within a tangent space when working on a general manifold. This limitation prevents us from integrating vectors over an arbitrary manifold. However, for Cartesian tensors in Euclidean space, we can perform integration in a naive manner just as for scalars, thus enabling us to perform the integration in equation (3.120). Hence, throughout this exercise we use Cartesian tensors in Euclidean space.

Hint: Refer to Figure 3.10 for a schematic of the integration where we have expanded the volume integral into the form

$$\frac{d}{dt} \left[\int_{\mathcal{R}} \rho \mathbf{v} dV \right] = \frac{d}{dt} \left[\int \left(\int_{\eta_b}^{\eta} \rho \mathbf{v} dz \right) dA \right], \quad (3.121)$$

where the horizontal integral extends over the rigid and fixed horizontal area of the basin, $dA = dx dy$ is the time independent horizontal area element, $z = \eta_b(x, y)$ is the solid-earth bottom and $z = \eta(x, y, t)$ is the ocean free surface. Time dependence appears in the upper boundary at $z = \eta$ and within the integrand. Perform the time derivative operation and make use of mass continuity and the kinematic boundary condition. Also make use of the trigonometry presented in Section 3.6.3 (in particular equation (3.89)). Unlike the formulation in Exercise 3.2, there is no use of a material time derivative in this approach. Rather, it is a straightforward (albeit tedious) use of integration over a domain with fixed horizontal/bottom

boundaries and a time dependent free surface boundary.



Chapter 4

MATERIAL TRACER CONSERVATION

As seen in Chapter 3, the assumption of mass conservation has many implications for the motion of single-component fluids. In this chapter we extend that discussion to the case of a fluid comprised of multiple matter constituents referred to as material tracers. Material tracers are particular forms of tracers, with ocea examples including feshwater, salt, nitrogen, oxygen, carbon, nutrients, radioactive isotopes, biogeochemicals, and atmospheric examples including oxygen, nitrogen, water vapor, radioactive isotopes, and carbon dioxide. In so doing, we develop integral finite-volume budget equations for extensive properties, such as mass or tracer content, along with a differential continuity equation for each of the intensive properties, such as mass density and tracer concentration. The continuity equation describing material tracer concentration is referred to as the tracer equation, with the Leibniz-Reynolds transport theorem providing the link between integral and differential formulations.

The barycentric velocity is the center of mass velocity for a fluid element. It plays a central role in the formulation of continuity equations and integral mass budgets for fluids with multiple matter constituents. The barycentric velocity plays the same role for multi-component fluids as the fluid parcel velocity does for single-component fluids. Differences between the barycentric velocity and the velocity of a specific fluid constituent leads to the exchange of matter across the boundary of the fluid element, with that exchange typically parameterized as diffusion.

READER'S GUIDE TO THIS CHAPTER

Our formulation of the material tracer equation is inspired by similar treatments in the chemical engineering and chemical physics literature (e.g., Section 16.1 of *Bird et al. (1960)*, Chapter 11 of *Aris (1962)*, Section 2.1 of *Kreuzer (1981)*, and Chapter II of *DeGroot and Mazur (1984)*), who develop the equations for mass transport in multi-component fluids. For this chapter, we assume an understanding of the Eulerian and Lagrangian kinematic descriptions detailed in Chapter 1 and the mass conservation analysis in Chapter 3. Much of what we cover in this chapter is used for the study of scalar fields throughout this book. Furthermore, the Leibniz-Reynolds transport theorem of Section 4.2.4 is a kinematic result central to all finite volume budgets in fluid mechanics.

4.1 The tracer equation	116
4.1.1 Mass continuity for each matter constituent	116
4.1.2 Total mass conservation	118
4.1.3 The tracer equation	118
4.1.4 Compatibility between mass and tracer continuity	120
4.1.5 Passive tracers	120

4.1.6	Summary of some conceptual points	121
4.1.7	Further study	122
4.2	Budgets for arbitrary fluid regions	123
4.2.1	Extensive and intensive fluid properties	123
4.2.2	General form of the finite domain integral	124
4.2.3	Eulerian (static) domain	125
4.2.4	Deriving the Leibniz-Reynolds transport theorem	125
4.2.5	Interpreting the Leibniz-Reynolds transport theorem	127
4.2.6	Revisiting Reynolds transport theorem	129
4.2.7	Summary of the time derivatives acting on integrals	131
4.3	Brute force illustration of Leibniz-Reynolds	131
4.3.1	Leibniz's rule plus kinematic boundary conditions	131
4.3.2	Summarizing the result	133
4.4	Boundary conditions	133
4.4.1	Interior layer boundary conditions	134
4.4.2	Solid-earth boundary conditions	134
4.4.3	Upper ocean surface boundary conditions	135
4.5	Exercises	136

4.1 The tracer equation

As defined in Section 1.3, a **fluid element** is an infinitesimal region of constant mass that lives within the moving fluid continuum. Although possessing a constant mass, it generally has a non-constant material composition, so that a fluid element is a non-material fluid **parcel**. Fluid element boundaries are open to the exchange of matter (i.e., tracers) with adjacent fluid elements. They are also open to the exchange of thermodynamic properties such as temperature and specific entropy.

The kinematics of fluid elements share certain features with material fluid parcels. For example, we can uniquely specify the position of a fluid element's center of mass by providing a material coordinate and time. Correspondingly, we can generalize the Reynolds transport theorem for integration over a constant mass fluid region (Section 4.2.4). We make use of fluid elements to develop the mass budgets for multi-component fluids such as the ocean and atmosphere. The differential equation for the concentration of a constituent is commonly referred to as the **tracer equation**.

4.1.1 Mass continuity for each matter constituent

In this subsection we formulate the mass continuity equation for each matter constituent within the fluid. The mass equation is formulated by taking an integral (weak formulation) over a fixed (Eulerian) region.

Density and velocity for each matter constituent

Consider a fluid with $n = 1, N$ matter constituents. For example, seawater has $N = 2$ when concerned just with its freshwater and salt content, whereas $N > 2$ when also concerned with other material constituents such as carbon dioxide and biogeochemical species. Now focus on a fixed (Eulerian) region of the fluid with volume, V , and total mass, M . Inside of the region, assume we can, at each time instance, count the number of molecules of each constituent and determine their corresponding velocities. This information can be used to construct the

molecular center of mass velocity for each constituent, $\mathbf{v}^{(n)}$, as well as the mass density,

$$\rho^{(n)} = V^{-1} M^{(n)}. \quad (4.1)$$

In the continuum limit, the volume and mass in the region get tiny ($V \rightarrow dV$ and $M \rightarrow dM$), yet the mass density remains smooth and finite.¹ Hence, the constituent velocity and mass density are continuous fields whose values are available at each point within the continuum fluid.

Integral formulation of the constituent mass budget

Consider an arbitrary region, \mathcal{R} , assumed to be fixed in space (an Eulerian region). The mass of component n within \mathcal{R} is given by the integral

$$M^{(n)} = \int_{\mathcal{R}} \rho^{(n)} dV, \quad (4.2)$$

and it changes in time according to the finite volume budget equation (there is no implied summation on the right hand side)

$$\frac{d}{dt} \int_{\mathcal{R}} \rho^{(n)} dV = - \oint_{\partial\mathcal{R}} \rho^{(n)} \mathbf{v}^{(n)} \cdot \hat{\mathbf{n}} dS. \quad (4.3)$$

This equation is a constituent form of the finite volume mass budget given for a single-component fluid by equation (3.9). It says that the mass of constituent, n , within the finite region, \mathcal{R} , changes in time according to the transport of this constituent across the region boundary, $\partial\mathcal{R}$. This budget assumes no source or sink of matter constituent n within the region. Since the region, \mathcal{R} , is assumed to be fixed in space, we can move the time derivative across the integral to reveal

$$\int_{\mathcal{R}} \left[\frac{\partial \rho^{(n)}}{\partial t} + \nabla \cdot (\rho^{(n)} \mathbf{v}^{(n)}) \right] dV = 0, \quad (4.4)$$

where we also used the divergence theorem to convert the surface integral to a volume integral. Arbitrariness of the Eulerian region means that this integral expression must be satisfied at each point of the continuum, thus leading to the Eulerian form of the constituent mass continuity equation

$$\partial_t \rho^{(n)} + \nabla \cdot (\rho^{(n)} \mathbf{v}^{(n)}) = 0. \quad (4.5)$$

This equation can also be written using a material time derivative

$$\frac{D^{(n)} \rho^{(n)}}{Dt} = -\rho^{(n)} \nabla \cdot \mathbf{v}^{(n)} \quad \text{for each of the } n = 1, N \text{ constituents,} \quad (4.6)$$

where the constituent material time derivative is given by

$$\frac{D^{(n)}}{Dt} = \frac{\partial}{\partial t} + \mathbf{v}^{(n)} \cdot \nabla. \quad (4.7)$$

We thus have N statements of mass conservation corresponding to each constituent material fluid parcel moving according to the velocity, $\mathbf{v}^{(n)}$.

¹For more on this point, see Figure 0.2 and corresponding discussion of the continuum approximation, with the continuum approximation providing a conceptual foundation to the formulation of fluid mechanical differential and integral relations.

4.1.2 Total mass conservation

Summing the Eulerian mass continuity equation (4.5) over all constituents leads to the continuity equation for the total mass

$$\partial_t \rho + \nabla \cdot (\rho \mathbf{v}) = 0, \quad (4.8)$$

where the total mass density and barycentric velocity are given by

$$\rho = \sum_{n=1}^N \rho^{(n)} \quad \text{and} \quad \mathbf{v} = \rho^{-1} \sum_{n=1}^N \rho^{(n)} \mathbf{v}^{(n)}. \quad (4.9)$$

Introducing the material time derivative following the barycentric velocity leads to the equivalent material form for the mass conservation equation

$$\frac{D}{Dt} = \partial/\partial t + \mathbf{v} \cdot \nabla \implies \frac{D\rho}{Dt} = -\rho \nabla \cdot \mathbf{v}. \quad (4.10)$$

The barycenter of a distribution of matter is the center of inertia for that matter. We choose the term barycentric velocity for \mathbf{v} to distinguish it from the molecular *center of mass velocity*, $\mathbf{v}^{(n)}$, of each material constituent. The barycentric velocity plays a key role in conservation laws for multi-component fluids, since equations (4.8) and (4.10) are identical to the mass conservation equations that hold for the homogeneous fluid derived in Section 3.2.

4.1.3 The tracer equation

Rather than keep track of each constituent velocity, $\mathbf{v}^{(n)}$, and the corresponding material parcels, it is generally more convenient to focus on the fluid element that moves with the barycentric velocity. For this purpose, consider again the constituent mass continuity equation (4.5)

$$(\partial_t + \mathbf{v}^{(n)} \cdot \nabla) \rho^{(n)} = -\rho^{(n)} \nabla \cdot \mathbf{v}^{(n)}, \quad (4.11)$$

and insert the barycentric velocity to both sides by adding $0 = \mathbf{v} - \mathbf{v}$

$$[\partial_t + (\mathbf{v} - \mathbf{v} + \mathbf{v}^{(n)}) \cdot \nabla] \rho^{(n)} = -\rho^{(n)} \nabla \cdot [\mathbf{v} - \mathbf{v} + \mathbf{v}^{(n)}]. \quad (4.12)$$

Rearrangement leads to

$$(\partial_t + \mathbf{v} \cdot \nabla) \rho^{(n)} = -\rho^{(n)} \nabla \cdot \mathbf{v} - \nabla \cdot [\rho^{(n)} (\mathbf{v}^{(n)} - \mathbf{v})], \quad (4.13)$$

which can be written

$$\frac{D\rho^{(n)}}{Dt} = -\rho^{(n)} \nabla \cdot \mathbf{v} - \nabla \cdot \mathbf{J}^{(n)}, \quad (4.14)$$

where we defined the constituent *tracer mass flux*

$$\mathbf{J}^{(n)} = \rho^{(n)} (\mathbf{v}^{(n)} - \mathbf{v}), \quad (4.15)$$

which arises from the difference between the constituent velocity and the barycentric velocity. The dimensions of $\mathbf{J}^{(n)}$ are mass of constituent, n , per time per area.

The material mass conservation equation (4.14) takes on the Eulerian form

$$\partial_t \rho^{(n)} + \nabla \cdot (\mathbf{v} \rho^{(n)}) = -\nabla \cdot \mathbf{J}^{(n)}. \quad (4.16)$$

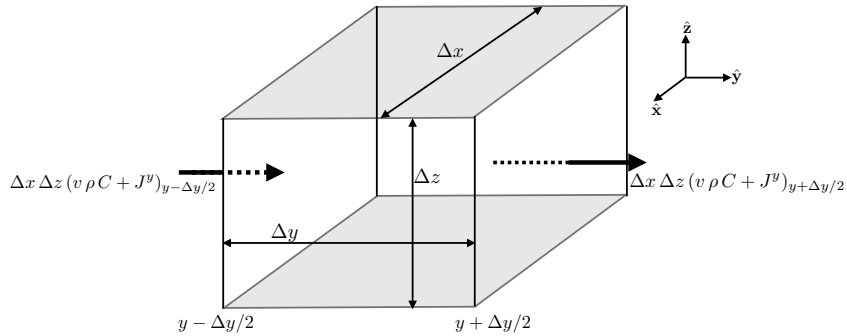


FIGURE 4.1: A finite sized cube as in Figure 3.1, here used to illustrate the budget of tracer mass over an Eulerian region (fixed in space) using Cartesian coordinates. In addition to the advective flux of tracer moving with the barycentric velocity, \mathbf{v} , there is a flux, \mathbf{J} , that arises from differences between the barycentric velocity and the constituent velocity. We here only show fluxes in the $\hat{\mathbf{y}}$ direction, with corresponding fluxes in the $\hat{\mathbf{x}}$ and $\hat{\mathbf{z}}$ directions also contributing to the tracer budget.

Introducing the material tracer concentration, $C^{(n)}$, according to

$$C^{(n)} = \frac{\rho^{(n)}}{\rho} = \frac{\delta M^{(n)}}{\delta M} = \frac{\text{mass of constituent } n \text{ in fluid element}}{\text{mass of fluid element}}, \quad (4.17)$$

leads to the tracer flux

$$\mathbf{J}^{(n)} = \rho C^{(n)} (\mathbf{v}^{(n)} - \mathbf{v}), \quad (4.18)$$

and the flux-form tracer budget

$$\partial_t(\rho C^{(n)}) + \nabla \cdot (\mathbf{v} \rho C^{(n)} + \mathbf{J}^{(n)}) = 0. \quad (4.19)$$

In Figure 4.1 we illustrate the contributions to the tracer evolution.

Eulerian and Lagrangian forms of the tracer equation

The flux-form equation (4.19) has a corresponding material time derivative form derived by expanding the derivatives

$$\begin{aligned} C^{(n)} \partial_t \rho + \rho \partial_t C^{(n)} + \rho \mathbf{v} \cdot \nabla C^{(n)} + C^{(n)} \nabla \cdot (\rho \mathbf{v}) \\ = C^{(n)} (\partial_t \rho + \nabla \cdot (\rho \mathbf{v})) + \rho (\partial_t + \mathbf{v} \cdot \nabla) C^{(n)}. \end{aligned} \quad (4.20)$$

The first term on the right hand side vanishes through mass continuity in the form of equation (4.8). The second term on the right hand side is the material time derivative of the tracer concentration. We are thus led to the equivalent forms for the tracer equation

$$\partial_t(\rho C^{(n)}) + \nabla \cdot [\mathbf{v} \rho C^{(n)}] = \rho \frac{DC^{(n)}}{Dt} = -\nabla \cdot \mathbf{J}^{(n)}. \quad (4.21)$$

The same result was also derived in equation (3.52c) when discussing Reynolds transport theorem for a single-component fluid.

Advective plus non-advective (diffusive) tracer fluxes

The above definitions allow us to decompose the advective tracer flux, defined according to the tracer velocity, into an advective flux based on the barycentric velocity plus a non-advective

flux

$$\rho C^{(n)} \mathbf{v}^{(n)} = \rho C^{(n)} (\mathbf{v}^{(n)} - \mathbf{v} + \mathbf{v}) = \mathbf{J}^{(n)} + \rho C^{(n)} \mathbf{v}. \quad (4.22)$$

The non-advection flux, $\mathbf{J}^{(n)} = \rho C^{(n)} (\mathbf{v}^{(n)} - \mathbf{v})$ (equation (4.18)), vanishes when the tracer velocity equals to the barycentric velocity, $\mathbf{v}^{(n)} = \mathbf{v}$. Correspondingly, the non-advection flux also vanishes for a single-component fluid, since in that case there is only one matter component and so the constituent velocity equals to the barycentric velocity. We sometimes refer to the non-advection flux as a **diffusive flux** since it is common in practice to parameterize this term as a downgradient diffusive flux. However, as seen in our study in VOLUME 2 of the entropy budget for a continuum fluid, not all non-advection processes are downgradient.

4.1.4 Compatibility between mass and tracer continuity

By construction, the flux-form of the tracer equation (4.19) (i.e., tracer continuity) exhibits the **compatibility** property with the flux-form mass continuity equation

$$\partial_t(\rho C^{(n)}) + \nabla \cdot [\rho \mathbf{v} C^{(n)} + \mathbf{J}^{(n)}] = 0 \iff \partial_t \rho + \nabla \cdot (\rho \mathbf{v}) = 0. \quad (4.23)$$

Namely, compatibility is manifest by summing the tracer equation over all constituents and using the identities

$$\sum_{n=1}^N C^{(n)} = 1 \quad \text{and} \quad \sum_{n=1}^N \mathbf{J}^{(n)} = 0. \quad (4.24)$$

Furthermore, through use of the barycentric velocity (4.9), we are ensured that the continuity equation (4.8) for the total density of a fluid element contains just the barycentric velocity. There is no contribution from $\mathbf{J}^{(n)}$ since $\sum_{n=1}^N \mathbf{J}^{(n)} = 0$.

4.1.5 Passive tracers

As defined in equation (4.17), the concentration of a material tracer is the mass of the trace constituent per mass of a fluid element. Such material tracers modify the barycentric velocity (4.9) since they carry mass and thus affect the mass density. We here define the theoretical construct known as a **passive tracer**. A passive tracer satisfies the advection-diffusion equation, but it has zero impact on the velocity and is thus dynamically passive. The passive tracer is analogous to the massless fluid particle of Section 1.3 whose trajectories define the Lagrangian reference frame. However, the passive tracer is transported both via advection and diffusion. Hence, we make use of passive tracers to probe the advective and diffusive features of the flow without modifying the flow. For example, a passive tracer can be used to define tracer pathways and time scales for transport between fluid regions. As reviewed by [Haine et al. \(2025\)](#), passive tracers enable use of **Green's function** methods for describing their evolution.

In Chapter 2 and Section 3.6.2, we discussed the notion of a material fluid object, which is an object comprised of fluid particles that follow the velocity, \mathbf{v} . In a single-component fluid, such material objects are impenetrable to matter, by construction. For a multi-component fluid, we can also consider objects that move with the barycentric velocity. However, trace matter generally crosses the material object through diffusion since $\mathbf{v}^{(n)} \neq \mathbf{v}$. Hence, there is no perfectly impenetrable fluid object in a fluid with any form of diffusion. Even so, we can consider a passive tracer that follows the barycentric velocity, and selectively decide whether that passive tracer is affected by diffusion or not. Such theoretical options are afforded the passive tracer given that it is a conceptual idealization used to probe the fluid flow properties.

Hence, the passive tracer is not subject to the same physical constraints as a material tracer.

4.1.6 Summary of some conceptual points

What is a fluid element? How does it maintain constant mass but not constant matter? Here we aim to review some of the conceptual points that answer these questions, building from our initial specification of fluid elements and fluid parcels in Section 1.3.

Revisiting the concept of a fluid element

The mass continuity equation (4.10) motivates us to define a fluid element as an infinitesimal fluid parcel that moves with barycentric velocity, \mathbf{v} , and maintains a constant total mass

$$\delta M = \sum_{n=1}^N \delta M^{(n)}. \quad (4.25)$$

The fluid element does not maintain a constant mass for each constituent, since the fluid element moves at the barycentric velocity, \mathbf{v} , which generally differs from the constituent velocities, $\mathbf{v}^{(n)}$. Consequently, a fluid element boundary is permeable to matter transport that leaves its mass constant but allows for exchanges of matter constituents with adjacent fluid elements. Hence, if some matter leaves the fluid element, then an equal amount must enter the element in order to maintain a constant mass.

The exchange of matter across a fluid element's boundary can arise from direct motion of matter crossing the boundary, or from the motion of the fluid element boundary relative to the matter. This point is central to resolving conundrums associated with the notion of constituent matter exchange constrained to retain constant mass.

Conceptual summary of the formulation

Our formulation is based on considering the multi-component fluid to be a continuum with distinct matter constituents (e.g., salt and freshwater for the ocean or water vapor and dry air for the atmosphere). Furthermore, the mass concentration for each constituent is represented by a scalar field whose value at any point in space-time gives the mass of tracer per mass of fluid. We then formulate mass continuity equations for each matter constituent (as well as the net mass) following methods used for the single-component fluid in Chapter 3. By choosing to use the [barycentric velocity](#) (center of mass velocity) for describing fluid flow, the mass continuity equation for the total density of a fluid element takes on the same form as for a single-component fluid. The resulting constituent continuity equations (i.e., tracer equations) have [non-advection flux](#) (diffusive) fluxes since the velocity of each matter constituent is generally distinct from the barycentric velocity.

To expose a bit of the details, we saw in this section that the tracer equation expresses the balance of mass for each trace constituent in the fluid. Furthermore, a nonzero tracer flux, $\mathbf{J}^{(n)} = \rho C^{(n)} (\mathbf{v}^{(n)} - \mathbf{v})$, arises when the barycentric velocity, \mathbf{v} , differs from the constituent velocity, $\mathbf{v}^{(n)}$. In that case, matter and thermodynamic properties are exchanged between fluid elements, with the exchange made without altering the mass of a fluid element. In the presence of random motion within a turbulent fluid, or in the presence of random interactions with molecular degrees of freedom, tracer exchange is akin to a random walk. Such exchange is commonly parameterized by a diffusion process. Correspondingly, the mass of tracers in a fluid

element is altered in the presence of differences in tracer concentration between fluid elements (i.e., tracer concentration gradients). However, the total mass of the element remains fixed.

How to maintain constant mass

As defined, a fluid element provides a generalization to multi-component fluids of the constant mass material fluid parcel we used in describing a single-component fluid (see Section 1.3). Later in this chapter we encounter a finite volume extension of the fluid element, which we refer to as a [Lagrangian region](#). A Lagrangian region has boundaries that follow the barycentric velocity so that the region maintains constant mass as per our discussion of Reynolds transport theorem in Section 4.2.6.

To maintain constant mass, any matter that leaves the fluid element by crossing its boundary is compensated by an equal mass that enters the boundary. Kinematically, there are two means for matter to cross a boundary. First, the matter itself can move across the boundary, with the limiting case being a stationary boundary with matter moving across. Second, the boundary can move relative to the matter, with the limiting case being stationary matter with the boundary moving. In either case, by choosing to follow the barycentric velocity, a fluid element's boundary (or a corresponding Lagrangian region's boundary) adjusts so that mass remains constant.

The strategic choice to formulate the kinematics of multi-component fluids using the barycentric velocity is directly analogous to the choice in Newtonian mechanics. Namely, in describing motion of many moving objects such as planets or point particles, we generally determine that motion relative to the [center of mass](#) for a system. In particular, by describing the motion of a multi-component fluid using the barycentric velocity, we simplify the kinematics by linking to the kinematics of single-component fluids while also supporting a generalization in the form of constituent tracer equations.

The importance of compatibility

In Section 4.1.4, we introduced the notion of compatibility between the tracer equation and mass continuity equation. Mathematically, this compatibility is rather trivial, as it directly follows from our choice to describe motion according to the barycentric velocity. However, it is a notion that can sometimes be overlooked when in the midst of a formulation that decomposes the flow into mean components and deviations, as occurs with studies of turbulent flows. The key point to remember is that whatever form the mean-field mass continuity equation takes, one must retain a clear formulation of mass conservation. Doing so may require modification of the effective barycentric velocity in the presence of turbulent fluctuations, such as through the density weighted averaged velocity introduced in Exercise 4.3.

4.1.7 Further study

We used many words in this section to develop the mass budget for fluid elements in a multi-component fluid. The reason for such verbosity is that the formulation can be confusing on first encounter. Even so, it is important to keep in mind that the basic notions are quite simple. Further extension of these ideas incorporates chemical reactions that transfer mass from one matter constituent to others, while retaining fixed net mass. This extension is relevant for studies of atmospheric chemistry and ocean biogeochemistry. Development of these extensions, using nomenclature similar to that used here, is provided in Chapter 11 of [Aris \(1962\)](#), Chapter II of [DeGroot and Mazur \(1984\)](#), and Section 2.1 of [Kreuzer \(1981\)](#).

The tracer fluxes introduced when formulating the tracer equation are typically parameterized by downgradient diffusion. However, as discussed in our study of the ocean entropy budget in VOLUME 2, the transport of a scalar field can arise both from spatial gradients in that field as well as gradients in other fluid properties. These fluxes arise as a result of fundamental constraints from the [second law of thermodynamics](#), and as such they are part of the suite of processes contributing to the transport of scalar properties in a multi-component fluid.

4.2 Budgets for arbitrary fluid regions

Thus far in this chapter we have considered the evolution of mass within a variety of fluid regions, including infinitesimal and finite domains either moving with the fluid or fixed in space. We have also considered similar domains in Chapter 3 where the fluid domains were typically material regions. In this section we synthesize these presentations by considering mass budgets over an arbitrary finite sized domain within multi-component fluids. The resulting mass equations form the basis for matter budgets used in geophysical fluid mechanics.

4.2.1 Extensive and intensive fluid properties

Consider a bucket of seawater that has homogeneous [Conservative Temperature](#) and salinity. Removing a cup of water from this bucket does not alter the [Conservative Temperature](#) or salinity, but it does alter the enthalpy, salt mass, and freshwater mass. We are thus motivated to characterize whether a physical property is an [extensive property](#) or [intensive property](#). [Conservative Temperature](#) and salinity are intensive quantities for the bucket of seawater, since their value does not change when removing seawater from the bucket. Further intensive properties include number density (number of particles per volume), mass density (mass of substance per volume), tracer concentration (mass of tracer per mass of fluid), temperature, velocity (linear momentum per mass), kinetic energy per mass, entropy per mass, and enthalpy per mass. An extensive property changes when the size of the sample changes, with examples including particle number, mass, length, volume, kinetic energy, entropy, enthalpy, and linear momentum.²

We are concerned in this section with how scalar extensive properties change as a function of time. Determining the evolution of such properties constitutes a budget analysis for the scalar property. What are the processes responsible for these changes? Where are the changes coming from? Those are basic questions asked when performing a budget analysis. In addition to physical and biogeochemical processes active within the fluid, details of the region over which one performs a budget have an important impact on the budget. Is the region open to matter and energy transport, or is it closed? Is the region static (Eulerian) or do boundaries move? If the boundaries move, do they move with the barycentric velocity (Lagrangian) or are they moving in some other manner?

In the following, let Π represent an intensive scalar property of a fluid element so that $\Pi \rho \delta V$ is the corresponding extensive property

$$\Pi = \text{intensive fluid property such as tracer concentration} \quad (4.26a)$$

$$\Pi \rho \delta V = \text{extensive fluid property such as tracer mass.} \quad (4.26b)$$

²Intensive and extensive properties play a role in formulating the equations for equilibrium thermodynamics studied in VOLUME 2.

For example, if Π is the tracer concentration in a fluid element (i.e., mass of tracer per mass of fluid), then the corresponding extensive property, $\Pi \rho \delta V$, is the mass of tracer in the fluid element. If Π is the [Conservative Temperature](#), Θ , of a fluid element, then the corresponding extensive property, $\Theta c_p \rho \delta V$, is the potential enthalpy with c_p a standard (constant) specific heat capacity.

We furthermore assume that Π satisfies the scalar conservation equation, written here in both its material (or advective) form and [flux-form conservation law](#)

$$\rho \frac{D\Pi}{Dt} = -\nabla \cdot \mathbf{J} \quad \Longleftrightarrow \quad \frac{\partial(\rho\Pi)}{\partial t} + \nabla \cdot (\rho\Pi \mathbf{v} + \mathbf{J}) = 0, \quad (4.27)$$

where \mathbf{J} is a flux such as that associated with the tracer equation derived in Section 4.1.3. Notably, satisfaction of a conservation law does not mean that Π is constant either at a point in space nor following a fluid particle. Instead, there are two cases of “constancy” that naturally arise. First, with $-\nabla \cdot \mathbf{J} = 0$, the scalar field is constant following a material fluid particle

$$-\nabla \cdot \mathbf{J} = 0 \implies \frac{D\Pi}{Dt} = 0. \quad (4.28)$$

In this case we say that Π is a [material invariant](#) or a [material constant](#). Second, if the Eulerian time derivative vanishes for all fields, then Π and ρ remain constant at a fixed spatial point in the fluid and we say that the fields are in a [steady state](#). Furthermore, recall that the Eulerian reference frame is stationary with respect to a laboratory frame. If the laboratory frame is inertial, then steady flow in one laboratory frame is steady in all inertial frames.³

4.2.2 General form of the finite domain integral

We are concerned here with the evolution of extensive fluid properties integrated over an arbitrary region. Let us make use of the following notation for such integrals

$$\mathcal{I}[\mathcal{R}(t), t] = \int_{\mathcal{R}(t)} \Pi \rho dV \equiv \int_{\mathcal{R}(t)} \varphi dV, \quad (4.29)$$

where we introduced the shorthand

$$\varphi = \rho \Pi. \quad (4.30)$$

The integrand in equation (4.29) is a function of space and time, $\varphi = \varphi(\mathbf{x}, t)$, and the integration region is generally a function of time, $\mathcal{R}(t)$. In previous sections, \mathcal{R} was a material region of fixed matter content (Section 3.3) or a constant mass fluid region open to the exchange of matter with the surroundings (Section 4.1). In both of these cases the region was denoted by $\mathcal{R}(\mathbf{v})$ since it moved with the fluid flow. Here we make no *a priori* assumption about the region.

The total time derivative of \mathcal{I} can be written as

$$\frac{d\mathcal{I}}{dt} = \left[\frac{\partial \mathcal{I}}{\partial t} \right]_{\mathcal{R}} + \frac{d\mathcal{R}}{dt} \left[\frac{\partial \mathcal{I}}{\partial \mathcal{R}} \right]_t. \quad (4.31)$$

The first term on the right hand side is the time derivative of the integral when holding the region fixed in space as per an Eulerian time derivative. The second term accounts for changes due to evolution of the region as weighted by dependence of the integral on the region itself. How the integral changes in time depends on both the evolution of the fluid property relative to

³In Exercise 4.2 we prove that the tracer equation is Galilean invariant.

the chosen region and evolution of the fluid region itself. Equation (4.31) is directly analogous to the total time derivative of a field in a moving fluid as given by equation (1.9).

4.2.3 Eulerian (static) domain

We first consider an Eulerian domain, which is fixed in space and thus static so that

$$\frac{d\mathcal{I}}{dt} = \left[\frac{\partial \mathcal{I}}{\partial t} \right]_{\mathcal{R}} = \frac{\partial}{\partial t} \left[\int_{\mathcal{R}} \Pi \rho dV \right] = \int_{\mathcal{R}} \left[\frac{\partial(\rho \Pi)}{\partial t} \right] dV. \quad (4.32)$$

Movement of the time derivative across the integral sign is available since the domain boundaries are static; i.e., the second term on the right hand side of equation (4.31) vanishes. Furthermore, since the domain is static, the volume element, dV , provides a static partition of the total domain volume so that dV does not appear inside the time derivative. This case corresponds to the Eulerian budgets depicted in Figures 3.1, 3.2, and 4.1.

4.2.4 Deriving the Leibniz-Reynolds transport theorem

We now allow the domain boundaries to be time dependent so that both terms in the total time derivative (4.31) contribute. The resulting **Leibniz-Reynolds transport theorem** is a general expression of conservation over an arbitrary region. We derive this theorem here using two methods, one naive and another a bit more rigorous. Interpretation and application of this theorem are then presented in Section 4.2.5.

A rectangular region

Consider a one-dimensional domain with time dependent endpoints. Integrals of this type commonly arise when integrating over the depth of the atmosphere or ocean, in which case the boundary terms are replaced by the kinematic boundary conditions studied in Section 3.6. The chain rule for differentiating integrals is known as **Leibniz's rule**. It results in the time derivative acting on the upper integral limit, the lower limit, and the integrand

$$\frac{d}{dt} \left[\int_{x_1(t)}^{x_2(t)} \varphi(x, t) dx \right] = \int_{x_1(t)}^{x_2(t)} \frac{\partial \varphi}{\partial t} dx + \frac{d}{dt} \left[\int_{x_1(t)}^{x_2(t)} \right] \varphi(x, t) dx \quad (4.33a)$$

$$= \int_{x_1(t)}^{x_2(t)} \frac{\partial \varphi}{\partial t} dx + \frac{dx_2(t)}{dt} \varphi(x_2, t) - \frac{dx_1(t)}{dt} \varphi(x_1, t), \quad (4.33b)$$

with the terms $dx_{1,2}/dt$ the velocities of the endpoints.

We can generalize the one-dimensional result (4.33b) to three dimensions by assuming the three dimensional domain is expressible by Cartesian coordinates whose extents are mutually independent. That is, we assume the domain, $\mathcal{R}(t)$, is rectangular. In this case we can immediately generalize equation (4.33b) to

$$\frac{d}{dt} \left[\int_{\mathcal{R}} \varphi dV \right] = \int_{\mathcal{R}} \frac{\partial \varphi}{\partial t} dV + \oint_{\partial \mathcal{R}} \varphi \mathbf{v}^{(b)} \cdot \hat{\mathbf{n}} d\mathcal{S}, \quad (4.34)$$

where we introduced the shorthand for the velocity of a point on the region boundary

$$\mathbf{v}^{(b)} = \frac{d\mathbf{x}}{dt}. \quad (4.35)$$

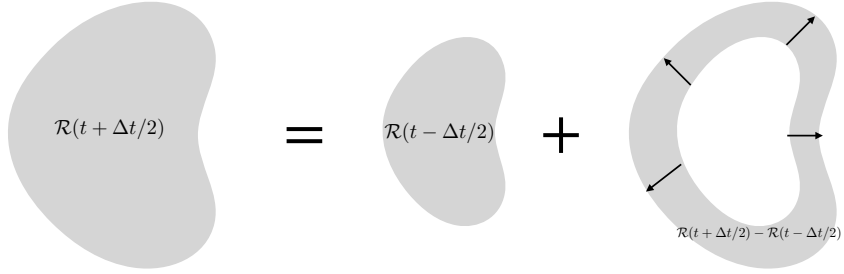


FIGURE 4.2: Illustrating the geometry of the Leibniz-Reynolds transport theorem. The region at time $t + \Delta t/2$, is written as $\mathcal{R}(t + \Delta t/2)$, which results from changing $\mathcal{R}(t - \Delta t/2)$ by the increment $\mathcal{R}(t + \Delta t/2) - \mathcal{R}(t - \Delta t/2)$. We here depict the case with an expanding boundary that renders a larger volume at $t + \Delta t/2$. At each point along the boundary the velocity of the boundary, $\mathbf{v}^{(b)}$, has an outward normal projection, $\mathbf{v}^{(b)} \cdot \hat{\mathbf{n}}$. The product $\mathbf{v}^{(b)} \cdot \hat{\mathbf{n}} \Delta t$ measures the distance that the boundary moves over the time increment, Δt . Hence, area integrating $\mathbf{v}^{(b)} \cdot \hat{\mathbf{n}}$ over the boundary yields the rate that the region volume changes.

The identity (4.34) is the Leibniz-Reynolds transport theorem.

An arbitrary simply connected region

We now present the derivation for an arbitrary simply connected domain, $\mathcal{R}(t)$, thus generalizing the domain geometry while offering further insight into the transport theorem. For this purpose, again let the region boundary, $\partial\mathcal{R}$, have an outward unit normal, $\hat{\mathbf{n}}$, and let points on the boundary move with the velocity, $\mathbf{v}^{(b)}$. In Figure 4.2 we depict the region geometry as it evolves over a time step of size, Δt . In particular, this figure illustrates the identity⁴

$$\mathcal{R}(t + \Delta t/2) = \mathcal{R}(t - \Delta t/2) + [\mathcal{R}(t + \Delta t/2) - \mathcal{R}(t - \Delta t/2)], \quad (4.36)$$

with the corresponding equation for the region volume given by

$$\int_{\mathcal{R}(t+\Delta t/2)} dV = \int_{\mathcal{R}(t-\Delta t/2)} dV + \int_{\mathcal{R}(t+\Delta t/2)-\mathcal{R}(t-\Delta t/2)} dV. \quad (4.37)$$

From Figure 4.2 we see that the volume of the time incremented region, $\mathcal{R}(t+\Delta t/2)-\mathcal{R}(t-\Delta t/2)$, in the limit $\Delta t \rightarrow 0$, is given by

$$\lim_{\Delta t \rightarrow 0} \frac{1}{\Delta t} \int_{\mathcal{R}(t+\Delta t/2)-\mathcal{R}(t-\Delta t/2)} dV = \lim_{\Delta t \rightarrow 0} \frac{1}{\Delta t} \left[\int_{\mathcal{R}(t+\Delta t/2)} dV - \int_{\mathcal{R}(t-\Delta t/2)} dV \right] \quad (4.38a)$$

$$= \frac{d}{dt} \left[\int_{\mathcal{R}(t)} dV \right] \quad (4.38b)$$

$$= \oint_{\partial\mathcal{R}(t)} \mathbf{v}^{(b)} \cdot \hat{\mathbf{n}} d\mathcal{S}. \quad (4.38c)$$

The final equality follows since $\mathbf{v}^{(b)} \cdot \hat{\mathbf{n}}$ measures the rate that the boundary is moving normal to itself, so that its area integral over $\partial\mathcal{R}(t)$ measures the rate that the volume of $\mathcal{R}(t)$ changes. It is the analog to the Lagrangian result (3.24) measuring the change in volume of a material region following the fluid flow.

⁴For those familiar with numerical methods, note that we make use of centered finite time differences in this discussion. Doing so offers a second order accurate expression of the finite difference approximations to the time derivative, whereas forward or backward differences are only first order accurate. Central differences also provides an intuitive centering of the time differences around the central time, t .

The above ideas used to derive the volume budget equation (4.38c) are now applied when $\varphi(\mathbf{x}, t)$ is included within the integral, in which case we consider

$$\frac{d}{dt} \left[\int_{\mathcal{R}(t)} \varphi(t) dV \right] = \lim_{\Delta t \rightarrow 0} \frac{1}{\Delta t} \left[\int_{\mathcal{R}(t+\Delta t/2)} \varphi(t + \Delta t/2) dV - \int_{\mathcal{R}(t-\Delta t/2)} \varphi(t - \Delta t/2) dV \right]. \quad (4.39)$$

Note that for brevity we suppressed the \mathbf{x} functional dependence of $\varphi(\mathbf{x}, t)$. Expanding the first integral on the right hand side around the central time leads to the expression, which is accurate to $\mathcal{O}(\Delta t)^2$,

$$\begin{aligned} & \int_{\mathcal{R}(t+\Delta t/2)} \varphi(t + \Delta t/2) dV \\ &= \int_{\mathcal{R}(t)} \left[\varphi(t) + \frac{\Delta t}{2} \frac{\partial \varphi(t)}{\partial t} \right] dV + \int_{\mathcal{R}(t+\Delta t/2)-\mathcal{R}(t)} \left[\varphi(t) + \frac{\Delta t}{2} \frac{\partial \varphi(t)}{\partial t} \right] dV. \end{aligned} \quad (4.40)$$

We have a similar expansion for the second integral in equation (4.39)

$$\begin{aligned} & \int_{\mathcal{R}(t-\Delta t/2)} \varphi(t - \Delta t/2) dV \\ &= \int_{\mathcal{R}(t)} \left[\varphi(t) - \frac{\Delta t}{2} \frac{\partial \varphi(t)}{\partial t} \right] dV + \int_{\mathcal{R}(t-\Delta t/2)-\mathcal{R}(t)} \left[\varphi(t) - \frac{\Delta t}{2} \frac{\partial \varphi(t)}{\partial t} \right] dV, \end{aligned} \quad (4.41)$$

thus leading to the finite difference

$$\begin{aligned} & \int_{\mathcal{R}(t+\Delta t/2)} \varphi(t + \Delta t/2) dV - \int_{\mathcal{R}(t-\Delta t/2)} \varphi(t - \Delta t/2) dV \\ &= \Delta t \int_{\mathcal{R}(t)} \frac{\partial \varphi(t)}{\partial t} dV + \int_{\mathcal{R}(t+\Delta t/2)-\mathcal{R}(t-\Delta t/2)} \varphi(t) dV, \end{aligned} \quad (4.42)$$

which is again accurate to $\mathcal{O}(\Delta t)^2$. Following our derivation of equation (4.38c) leads us to

$$\int_{\mathcal{R}(t+\Delta t/2)-\mathcal{R}(t-\Delta t/2)} \varphi(t) dV = \Delta t \oint_{\partial\mathcal{R}(t)} \varphi \mathbf{v}^{(b)} \cdot \hat{\mathbf{n}} d\mathcal{S}, \quad (4.43)$$

where all terms on the right hand side surface integral are evaluated at the central time, t . Bringing the pieces together, and taking the limit as $\Delta t \rightarrow 0$, leads to the **Leibniz-Reynolds transport theorem**

$$\frac{d}{dt} \left[\int_{\mathcal{R}(t)} \varphi(t) dV \right] = \int_{\mathcal{R}(t)} \frac{\partial \varphi}{\partial t} dV + \oint_{\partial\mathcal{R}(t)} \varphi \mathbf{v}^{(b)} \cdot \hat{\mathbf{n}} d\mathcal{S}, \quad (4.44)$$

which agrees with the earlier result given by equation (4.34).

4.2.5 Interpreting the Leibniz-Reynolds transport theorem

The **Leibniz-Reynolds transport theorem** (4.34) is a central kinematic result in fluid mechanics. In particular, it forms the starting point for all finite volume budgets. Although we made use of Cartesian coordinates for both derivations, the result is a coordinate invariant measure of how an extensive scalar fluid property evolves within a region. Hence, by the rules of tensor

analysis from VOLUME 1, the result holds for arbitrary Eulerian coordinates. Furthermore, we can extend it to multiply connected domains for which one sums over the distinct sub-domains to render the complete budget. These results confirm our notions regarding extensive scalar properties, such as fluid mass, tracer mass, and enthalpy, and how they are budgeted throughout the fluid. Namely, these quantities are simply counted over the various regions of the fluid.

Comments on the boundary velocity

As defined by equation (4.35), boundary velocity, $\mathbf{v}^{(b)}$, measures the velocity of a point on the domain boundary. Notably, the resulting budget only requires information about the normal component to that velocity, $\mathbf{v}^{(b)} \cdot \hat{\mathbf{n}}$. For example, the domain boundary could be exhibiting arbitrary motion in the direction tangent to the bounding surface. Yet such tangential motion is of no concern for a budget developed over the domain since we are only concerned with transport across the boundary. Indeed, information concerning the tangential component is not available without making dynamical assumptions that go beyond the kinematics considered here. We encountered the same ideas when studying the kinematic boundary conditions in Section 3.6.

Transport theorem for region volume

As part of the derivation of Leibniz-Reynolds in equation (4.44), we derived the expression (4.38c) for the volume changes of the region, which is recovered by setting $\varphi = 1$ in the transport theorem (4.34)

$$\frac{d}{dt} \left[\int_{\mathcal{R}} dV \right] = \oint_{\partial\mathcal{R}} \mathbf{v}^{(b)} \cdot \hat{\mathbf{n}} d\mathcal{S}. \quad (4.45)$$

This result says that the volume for an arbitrary region changes in time so long as there is motion of the region boundary normal to itself. As noted above, we can compare this expression to that for a material region given by equation (3.24), with the expressions identical when $\mathbf{v}^{(b)} \cdot \hat{\mathbf{n}} = \mathbf{v} \cdot \hat{\mathbf{n}}$ for a material region. Furthermore, the volume budget (4.45) holds for both divergent and non-divergent flows, with further specialization to the non-divergent case in Section 5.6.2.

Transport theorem for a scalar field

We now derive a corollary to the transport theorem (4.34) that proves useful for budget analyses over moving regions. For this purpose, make use of the flux-form of the scalar conservation equation (4.27) so that the transport theorem is written

$$\frac{d}{dt} \left[\int_{\mathcal{R}} \rho \Pi dV \right] = - \oint_{\partial\mathcal{R}} [\rho \Pi (\mathbf{v} - \mathbf{v}^{(b)}) + \mathbf{J}] \cdot \hat{\mathbf{n}} d\mathcal{S}. \quad (4.46)$$

Setting $\Pi = 1$ gives an expression for the change in mass for the region

$$\frac{d}{dt} \left[\int_{\mathcal{R}} \rho dV \right] = - \oint_{\partial\mathcal{R}} \rho (\mathbf{v} - \mathbf{v}^{(b)}) \cdot \hat{\mathbf{n}} d\mathcal{S}. \quad (4.47)$$

The transport theorem (4.46) has a straightforward interpretation. Namely, the left hand side is the time tendency for the total Π -stuff within the moving region. The right hand side is the surface area integral of the flux of Π -stuff through the boundary of the region. The first right hand side term arises from the difference between the barycentric fluid velocity and the velocity

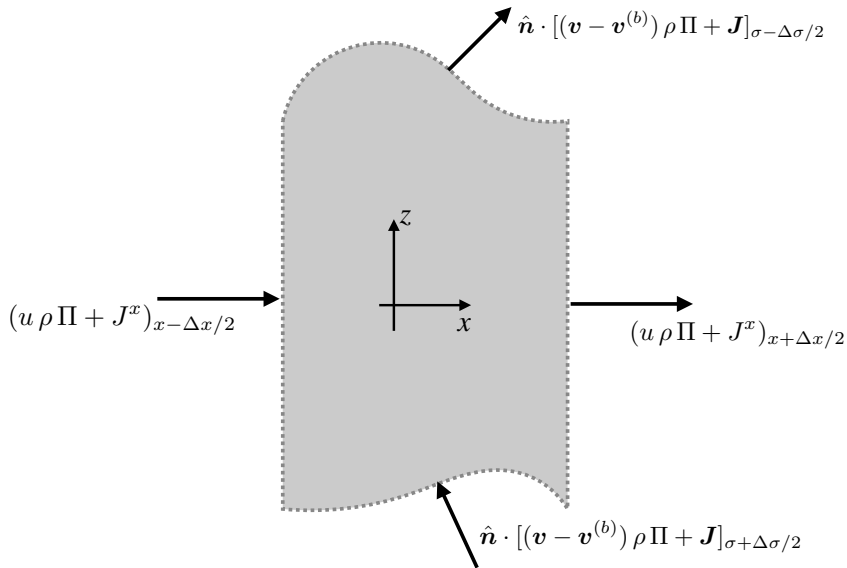


FIGURE 4.3: This figure depicts the contributions to the [Leibniz-Reynolds transport theorem](#) (4.46). The theorem is applied to a domain corresponding to a numerical model grid cell with the top and bottom interfaces defined by generalized vertical coordinates with values $\sigma \pm \Delta\sigma/2$ (see [VOLUME 3](#) for more on [generalized vertical coordinate surfaces](#)). In particular, the vertical cell faces are assumed to have fixed positions, so that $(\mathbf{v} - \mathbf{v}^{(b)}) \cdot \hat{\mathbf{n}} = \mathbf{v} \cdot \hat{\mathbf{n}}$ for these cell faces. Hence, the fluxes crossing these faces are due to advection by the barycentric velocity plus contributions from non-advection (e.g., diffusive) fluxes. However, the top and bottom faces of the cell are allowed to move according to the generalized vertical coordinate surfaces. Hence, transport through these faces must take into account the nonzero velocity of the boundaries. Note that numerical models generally assume the top and bottom interfaces have a nonzero projection in the vertical direction so that they never overturn (e.g., [Griffies et al. \(2020\)](#)).

of the boundary, and the second term arises from the non-advection (e.g., diffusive) flux. Both fluxes are projected onto the outward normal at the boundary and then integrated over the surface area. Hence, the budget is not affected by fluxes tangential to the boundary. Finally, for the mass budget (4.47), the non-advection flux vanishes since the mass of a fluid element moves according to the barycentric velocity of Section (4.1.2).

In Figure 4.3 we illustrate the transport theorem (4.46) for the special case of a discrete numerical model grid cell. This cell has fixed positions for the vertical sides whereas the top and bottom interfaces are time dependent. This application of the transport theorem provides the framework for finite volume methods in numerical models (e.g., [Griffies et al. \(2020\)](#)).

4.2.6 Revisiting Reynolds transport theorem

Consider the special case of a region that is moving with the fluid flow, in which case we provide a more general derivation of the [Reynolds transport theorem](#) than originally given for material regions in Section 3.5. The following results are special cases of the general expression (4.46).

Reynolds Transport Theorem

Let us apply the result (4.34) to a region that follows the fluid flow as defined by the barycentric velocity, \mathbf{v} . For this moving region, the time derivative of the region boundaries in equation (4.34) is given by the fluid velocity

$$\frac{d}{dt} \left[\int_{\mathcal{R}(\mathbf{v})} \varphi dV \right] = \int_{\mathcal{R}(\mathbf{v})} \left[\frac{\partial \varphi}{\partial t} + \nabla \cdot (\mathbf{v} \varphi) \right] dV = \int_{\mathcal{R}(\mathbf{v})} \left[\frac{D\varphi}{Dt} + \varphi \nabla \cdot \mathbf{v} \right] dV. \quad (4.48)$$

This result is the Reynolds transport theorem. The derivation given here is more general than that in Section 3.5, with that derivation assuming the region to be material (i.e., no matter crosses the region boundary). For the present derivation we only assumed that the region boundaries move so that $(\mathbf{v} - \mathbf{v}^{(b)}) \cdot \hat{\mathbf{n}} = 0$, where again \mathbf{v} is the barycentric velocity. We did not assume the region boundaries are material. We can thus make use of Reynolds transport theorem (4.48) for constant mass regions of a multi-component fluid so long as $(\mathbf{v} - \mathbf{v}^{(b)}) \cdot \hat{\mathbf{n}} = 0$. Furthermore, the region boundary is generally permeable via the **non-advection flux** (diffusive) tracer fluxes.

Alternative form of Reynolds Transport Theorem

We can put the Reynolds Transport Theorem (4.48) into another useful form by reintroducing $\varphi = \rho \Pi$ and making use of mass continuity

$$\frac{1}{\rho} \frac{D\rho}{Dt} = -\nabla \cdot \mathbf{v}. \quad (4.49)$$

Doing so yields the rather tidy result

$$\frac{d}{dt} \left[\int_{\mathcal{R}(\mathbf{v})} \Pi \rho dV \right] = \int_{\mathcal{R}(\mathbf{v})} \left[\frac{D\varphi}{Dt} + \varphi \nabla \cdot \mathbf{v} \right] dV \quad \text{Reynolds (4.48)} \quad (4.50a)$$

$$= \int_{\mathcal{R}(\mathbf{v})} \left[\frac{D(\rho \Pi)}{Dt} + \rho \Pi \nabla \cdot \mathbf{v} \right] dV \quad \varphi = \rho \Pi \quad (4.50b)$$

$$= \int_{\mathcal{R}(\mathbf{v})} \left[\Pi \left(\frac{D\rho}{Dt} + \rho \nabla \cdot \mathbf{v} \right) + \rho \frac{D\Pi}{Dt} \right] dV \quad \text{product rule} \quad (4.50c)$$

$$= \int_{\mathcal{R}(\mathbf{v})} \frac{D\Pi}{Dt} \rho dV. \quad \text{continuity (4.10)} \quad (4.50d)$$

Heuristically, this result follows since ρdV is a constant when following the flow, so that passage of the time derivative across the material integral only picks up the material derivative of Π .

We can take the result (4.50d) one more step by inserting the material form of the scalar conservation equation (4.27) so that

$$\frac{d}{dt} \left[\int_{\mathcal{R}(\mathbf{v})} \Pi \rho dV \right] = - \oint_{\partial\mathcal{R}(\mathbf{v})} \mathbf{J} \cdot \hat{\mathbf{n}} d\mathcal{S}, \quad (4.51)$$

which is a special case of the general transport theorem (4.46) found by setting $(\mathbf{v} - \mathbf{v}^{(b)}) \cdot \hat{\mathbf{n}} = 0$ along the region boundary. This result says that the change in Π -stuff within a region moving with the barycentric velocity arises only from the area integrated non-advection flux crossing normal to the boundary. It is a finite volume generalization of the mass conservation statement for a fluid element as discussed in Section 4.1.3. We can set $\Pi = 1$ to render a statement of mass conservation for a Lagrangian region

$$\frac{d}{dt} \left[\int_{\mathcal{R}(\mathbf{v})} \rho dV \right] = 0, \quad (4.52)$$

where the non-advection flux, \mathbf{J} , vanishes for the mass.

4.2.7 Summary of the time derivatives acting on integrals

We here summarize the variety of time derivatives acting on integrals of scalar fields, also writing expressions in their Eulerian coordinate covariant form

$$\frac{d}{dt} \int_{\mathcal{R}} \rho \Pi dV = \begin{cases} \int_{\mathcal{R}} \frac{\partial(\rho \Pi)}{\partial t} dV = -\oint_{\partial\mathcal{R}} (\rho \mathbf{v} \Pi + \mathbf{J}) \cdot \hat{\mathbf{n}} dS & \text{Eulerian } \mathcal{R} \\ \int_{\mathcal{R}(v)} \rho \frac{D\Pi}{Dt} dV = -\oint_{\partial\mathcal{R}(v)} \mathbf{J} \cdot \hat{\mathbf{n}} dS & \text{Lagrangian } \mathcal{R}(\mathbf{v}) \\ -\oint_{\partial\mathcal{R}} [\rho \Pi (\mathbf{v} - \mathbf{v}^{(b)}) + \mathbf{J}] \cdot \hat{\mathbf{n}} dS & \text{arbitrary } \mathcal{R}, \end{cases} \quad (4.53)$$

with the scalar fields assumed to satisfy the flux-form conservation equation

$$\rho \frac{D\Pi}{Dt} = -\nabla \cdot \mathbf{J} \iff \partial_t(\rho \Pi) + \nabla \cdot (\rho \mathbf{v} \Pi + \mathbf{J}) = 0. \quad (4.54)$$

As discussed in Section 1.2.1, the partial differential equation (4.54) is referred to as the **strong formulation** of the scalar budget, whereas the integral expressions in equation (4.53) provide expressions of the **weak formulation**. We thus see how the Leibniz-Reynolds transport theorem provides the operational means to move between the strong form and weak form of the scalar budgets.

4.3 Brute force illustration of Leibniz-Reynolds

The Leibniz-Reynolds transport theorem

$$\frac{d}{dt} \left[\int_{\mathcal{R}} \rho \Pi dV \right] = - \int_{\partial\mathcal{R}} [\rho \Pi (\mathbf{v} - \mathbf{v}^{(b)}) + \mathbf{J}] \cdot \hat{\mathbf{n}} dS, \quad (4.55)$$

is an incredibly useful and elegant expression of the scalar budget over an arbitrary domain. Correspondingly, we make great use of it throughout this book. To further our understanding, we here consider the scalar budget for an ocean domain such as in Figure 4.4. Rather than make direct use of Leibniz-Reynolds, we use a brute force approach by expanding the volume integral using Cartesian coordinates according to

$$\frac{d}{dt} \left[\int_{\mathcal{R}} \rho \Pi dV \right] = \frac{d}{dt} \left[\int_{A(t)} dA \int_{\eta_b}^{\eta} \rho \Pi dz \right]. \quad (4.56)$$

In this equation, $\int_{A(t)} dA$ is an integral over the horizontal area of the domain, with the lateral boundaries of the domain generally a function of time. This exercise requires the use of various kinematic boundary conditions and provides further practice with Leibniz's rule. Additionally, through exposing the many steps, this exercise illustrates the elegance and power of the Leibniz-Reynolds.

4.3.1 Leibniz's rule plus kinematic boundary conditions

Performing the time derivative in equation (4.56) and using Leibniz's rule yields

$$\begin{aligned} \frac{d}{dt} \left[\int_{\mathcal{R}} \rho \Pi dV \right] &= \int_{A(t)} [\partial_t \eta (\rho \Pi)_{z=\eta}] dA + \frac{dA}{dt} \left[\int_{\eta_b}^{\eta} \rho \Pi dz \right]_{\text{bounds}} \\ &\quad + \int_{A(t)} dA \int_{\eta_b}^{\eta} \frac{\partial(\rho \Pi)}{\partial t} dz. \end{aligned} \quad (4.57)$$

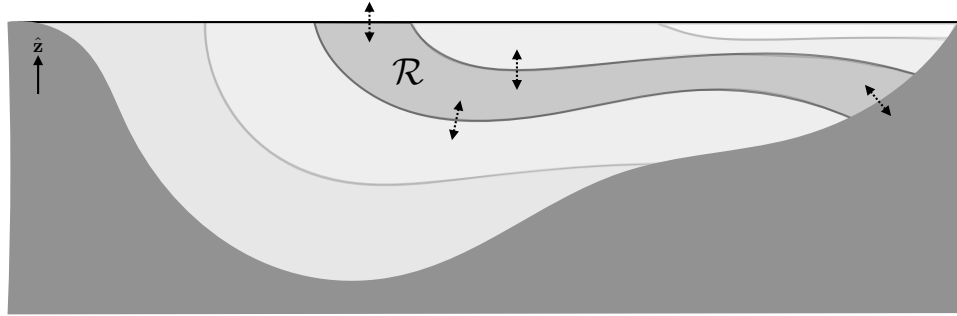


FIGURE 4.4: A depiction of fluid layers in which we formulate the budget for the total mass of scalar (e.g., tracer or potential enthalpy). The scalar mass within the layer, such as that one denoted by \mathcal{R} , is modified by dia-surface transport across interior layer interfaces, as well as transport across the surface and bottom boundaries. Note that an arbitrary layer might never intersect the bottom or surface boundaries. However, the layers depicted here each intersect boundaries, with such layers requiring extra care in formulating their budgets.

The first term on the right hand side arises from time dependence to the free surface. This term is present even if the horizontal boundaries are rigid. The second term on the right hand side is evaluated along the lateral boundaries of the domain. If the boundaries are fixed in time, as in a rectangular box of seawater or a periodic channel, then $dA/dt = 0$. The more general case has a lateral boundary that is time dependent such as along a beach where fluid moves up and down the sloping shoreline. However, in that case the thickness of fluid vanishes at the lateral boundary, $\eta - \eta_b = 0$, thus again revealing that the second term on the right hand side drops from the budget to render

$$\frac{d}{dt} \left[\int_{\mathcal{R}} \rho \Pi dV \right] = \int_{A(t)} [\partial_t \eta (\rho \Pi)_{z=\eta}] dA + \int_{A(t)} dA \int_{\eta_b}^{\eta} \frac{\partial(\rho \Pi)}{\partial t} dz. \quad (4.58)$$

For the second term on the right hand side of equation (4.58) we make use of the scalar equation (4.54) and Leibniz's rule to write

$$\int_{\eta_b}^{\eta} \frac{\partial(\rho \Pi)}{\partial t} dz = - \int_{\eta_b}^{\eta} \nabla_h \cdot (\rho \Pi \mathbf{u} + \mathbf{J}^h) dz - \int_{\eta_b}^{\eta} \frac{\partial(\rho \Pi w + J^z)}{\partial z} dz \quad (4.59a)$$

$$= - \nabla_h \cdot \int_{\eta_b}^{\eta} (\rho \Pi \mathbf{u} + \mathbf{J}^h) dz + \nabla(\eta - z) \cdot (\rho \Pi \mathbf{v} + \mathbf{J})_{z=\eta} \\ + \nabla(z - \eta_b) \cdot (\rho \Pi \mathbf{v} + \mathbf{J})_{z=\eta_b} \quad (4.59b)$$

where we decomposed the non-advectional flux into its horizontal and vertical components, $\mathbf{J} = \mathbf{J}^h + \hat{z} J^z$. The surface terms ($z = \eta$) combine with the $\partial_t \eta$ term appearing in equation (4.58) to yield

$$\rho \Pi \left[\frac{\partial \eta}{\partial t} + \mathbf{u} \cdot \nabla \eta - w \right] = \Pi Q_m, \quad (4.60)$$

where we used the surface kinematic boundary condition (3.96) to introduce the surface boundary mass flux, Q_m . The bottom kinematic boundary condition eliminates the advective contribution at the bottom, $z = \eta_b$, via the no normal flow condition (3.58)

$$\nabla(z - \eta_b) \cdot \mathbf{v} = w - \mathbf{u} \cdot \nabla \eta_b = 0 \quad \text{at } z = \eta_b(x, y). \quad (4.61)$$

Finally, when integrated over the horizontal extent of the domain, the horizontal convergence term from equation (4.59b) vanishes. The reason it vanishes is because either the thickness

of fluid vanishes at the horizontal boundaries (as along a beach); there is a no flux boundary condition if the boundary is a vertical wall; or the domain is periodic.

4.3.2 Summarizing the result

Bringing the results together yields the budget equation

$$\frac{d}{dt} \left[\int_{\mathcal{R}} \rho \Pi dV \right] = \int_{z=\eta} (\Pi Q_m + \nabla(\eta - z) \cdot \mathbf{J}) dA + \int_{z=\eta_b} \nabla(z - \eta_b) \cdot \mathbf{J} dA. \quad (4.62)$$

We now use the identity (3.85e) between horizontal area element, $dA = dx dy$, and area element on the surface

$$\hat{\mathbf{n}} d\mathcal{S} = -\nabla(\eta - z) dA \quad \text{at } z = \eta \quad (4.63a)$$

$$\hat{\mathbf{n}} d\mathcal{S} = -\nabla(z - \eta_b) dA \quad \text{at } z = \eta_b, \quad (4.63b)$$

to write

$$\frac{d}{dt} \left[\int_{\mathcal{R}} \rho \Pi dV \right] = - \int_{z=\eta} (-\Pi Q_m + \hat{\mathbf{n}} \cdot \mathbf{J}) d\mathcal{S} - \int_{z=\eta_b} \hat{\mathbf{n}} \cdot \mathbf{J} d\mathcal{S}, \quad (4.64)$$

where

$$Q_m dA = Q_m d\mathcal{S} = -\rho (\mathbf{v} - \mathbf{v}^{(\eta)}) \cdot \hat{\mathbf{n}} d\mathcal{S} \quad (4.65)$$

according to equation (3.90c). The budget for fluid mass is realized by setting Π to a constant and thus dropping the non-advectional flux

$$\frac{d}{dt} \left[\int_{\mathcal{R}} \rho dV \right] = \int_{z=\eta} Q_m d\mathcal{S} = - \int_{z=\eta} \rho (\mathbf{v} - \mathbf{v}^{(\eta)}) \cdot \hat{\mathbf{n}} d\mathcal{S}. \quad (4.66)$$

The manipulations in this section have succeeded in bringing the scalar and mass budgets into the form of the Leibniz-Reynolds transport theorem (4.55). The process of doing so required far more tedium as compared to the elegance of merely starting from equation (4.55). Even so, our efforts provide a useful means to ground the formalism by unpacking the many steps summarized by Leibniz-Reynolds. Furthermore, many of these steps are encountered in practical calculations of finite volume budgets.

4.4 Boundary conditions

We here study the boundary conditions for scalar fields that hold at the variety of boundaries encountered by a fluid. To be specific, consider Π to be a tracer concentration,

$$\Pi = C, \quad (4.67)$$

though note that the formalism holds for an arbitrary scalar satisfying the tracer equation

$$\partial_t(\rho C) + \nabla \cdot (\rho C \mathbf{v} + \mathbf{J}) = 0. \quad (4.68)$$

We continue to focus on a fluid layer such as shown in Figure 4.4, paying particular interest to fluid layers that intersect the surface boundary (as for the ocean) and/or solid-earth bottom boundary (as for the ocean or atmosphere). We commonly think of this layer as defined by isosurfaces of a **generalized vertical coordinate** whose layers are monotonically stacked in the

vertical.⁵ However, the treatment given here allows for the layers to be non-monotonic in the vertical (e.g., vertical surfaces and surface overturns are allowed), so that these results can be used for the water mass transformation analysis studied in VOLUME 4.

The Leibniz-Reynolds transport theorem (4.46) provides the starting point to our analysis

$$\frac{d}{dt} \left[\int_{\mathcal{R}} \rho C dV \right] = - \int_{\partial \mathcal{R}} [\rho C (\mathbf{v} - \mathbf{v}^{(b)}) + \mathbf{J}] \cdot \hat{\mathbf{n}} dS, \quad (4.69)$$

The left hand side of this equation is the time tendency for the mass of tracer within the finite sized region. This tendency is affected by transport across the region boundaries, with three boundaries considered here. We ignore interior sources, though note that the formalism can be readily extended in their presence.

4.4.1 Interior layer boundary conditions

The boundary transport across interior layer interfaces,

$$\text{interior boundary transport} = [\rho C (\mathbf{v} - \mathbf{v}^{(b)}) + \mathbf{J}] \cdot \hat{\mathbf{n}} dS, \quad (4.70)$$

measures the tracer mass transport due to an advective flux across the moving layer boundaries (first term; dia-surface flux), plus a subgrid scale (typically) **non-advection flux**.

4.4.2 Solid-earth boundary conditions

At the static material bottom boundary, the no-normal flow condition means that

$$\mathbf{v} \cdot \hat{\mathbf{n}} = 0. \quad (4.71)$$

Consider the velocity of a point attached to the layer interface, $\mathbf{v}^{(b)}$, and focus on where the interface intersects the bottom boundary. Here, the velocity, $\mathbf{v}^{(b)}$, tracks the position of the interface as it intersects the solid-earth bottom boundary. By construction, the movement of this intersection point is tangential to the solid-earth boundary so that $\mathbf{v}^{(b)}$ is orthogonal to the boundary outward normal direction

$$\mathbf{v}^{(b)} \cdot \hat{\mathbf{n}} = 0. \quad (4.72)$$

Hence, the only contribution to the tracer budget at the bottom boundary comes through the non-advection flux, \mathbf{J}

$$\text{bottom boundary transport} = -\mathbf{J} \cdot \hat{\mathbf{n}} dS. \quad (4.73)$$

This equation says that if there is any transport through the bottom boundary (left hand side), then it induces a non-advection transport within the adjacent fluid whose normal component at the boundary equals to the bottom transport (right hand side).

Geothermal heating is the canonical solid-earth transport in the ocean. Assuming a known geothermal heat flux, $Q_{\text{geo-heat}}$, it leads to a non-advection ocean boundary flux

$$Q_{\text{geo-heat}} = -c_p \mathbf{J}(\Theta) \cdot \hat{\mathbf{n}}, \quad (4.74)$$

where c_p is the ocean heat capacity and Θ is the **Conservative Temperature**. Furthermore, if we

⁵Monotonically stacked means that the outward normal to the surface, $\hat{\mathbf{n}}$, has a nonzero projection onto the vertical, $\hat{\mathbf{n}} \cdot \hat{\mathbf{z}} \neq 0$, and the sign of this projection remains unchanged. If the surface is vertical then $\hat{\mathbf{n}} \cdot \hat{\mathbf{z}} = 0$, whereas an overturning surface means that $\hat{\mathbf{n}} \cdot \hat{\mathbf{z}}$ changes sign.

assume the non-advection flux is parameterized as the downgradient diffusive flux, then the geothermal boundary condition (4.74) takes the form

$$\mathcal{Q}_{\text{geo}} = c_p \rho (\mathbf{K} \cdot \nabla \Theta) \cdot \hat{\mathbf{n}}, \quad (4.75)$$

where \mathbf{K} is the diffusion tensor.

For those cases where the geothermal heating vanishes, or more generally for tracers that have zero bottom boundary flux, then the tracer must satisfy the following no-normal flux (Neumann) boundary condition

$$\text{no flux bottom boundary} = (\mathbf{K} \cdot \nabla C) \cdot \hat{\mathbf{n}} = 0. \quad (4.76)$$

In the case where diffusion next to the boundary is isotropic, as per molecular diffusion, then we reach the simpler result

$$\text{no flux bottom boundary} = \nabla C \cdot \hat{\mathbf{n}} = 0. \quad (4.77)$$

Namely, in this case, tracer isosurfaces are oriented normal to the boundary as depicted in Figure 4.5. Notably, this kinematic boundary condition holds at each point in time. For the dynamical tracers like temperature and salinity, this boundary condition affects flow near the boundary by modifying the density field and thus the pressure.

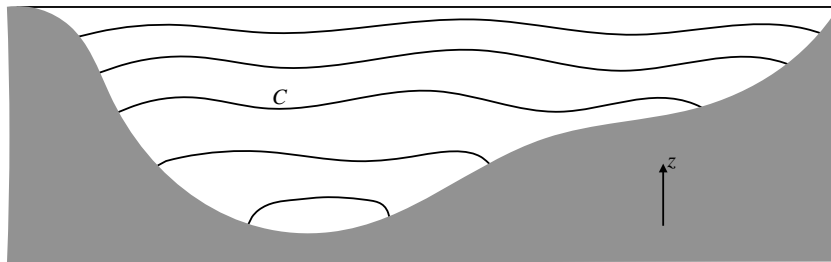


FIGURE 4.5: In the absence of a bottom boundary tracer flux (e.g., geothermal heating), and in the presence of isotropic downgradient diffusion, the isosurfaces of tracer, C , intersect solid boundaries normal to the boundary as per equation (4.77): $\nabla C \cdot \hat{\mathbf{n}} = 0$, where $\hat{\mathbf{n}}$ is the outward normal direction. This constraint holds at each time instance.

4.4.3 Upper ocean surface boundary conditions

Let us write the upper ocean surface boundary tracer transport as

$$\mathcal{Q}_C dS = \text{net tracer mass per time crossing ocean surface}. \quad (4.78)$$

The surface boundary transport is generally comprised of two terms: a non-advection term just like at the solid-earth in Section 4.4.2, plus an advective term arising since the ocean surface is permeable. If we assume that the tracer transported via the advected matter is either a dissolved tracer, such as salinity, or a thermodynamic tracer, such as Conservative Temperature, then we can write the net tracer flux as

$$\mathcal{Q}_C = C_m \mathcal{Q}_m + \mathcal{Q}_C^{\text{non-adv}}, \quad (4.79)$$

where $\mathcal{Q}_C^{\text{non-adv}}$ is the non-advection flux, C_m is the tracer concentration within the mass transported across the surface, and \mathcal{Q}_m the mass per time per surface area of matter that crosses the

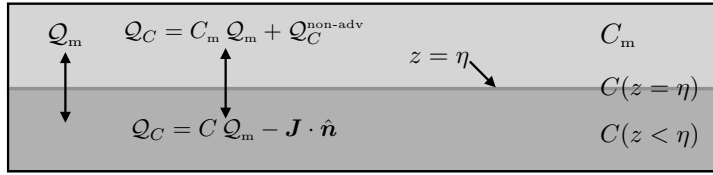


FIGURE 4.6: A schematic of an infinitesimal region of the ocean surface boundary at $z = \eta(x, y, t)$, with $z < \eta$ the ocean region. $\mathcal{Q}_m d\mathcal{S}$ is the mass transport (mass per time) that crosses the interface and carries a tracer concentration, C_m . $\mathcal{Q}_c d\mathcal{S}$ is the tracer mass transport that crosses the ocean surface. Continuity across the $z = \eta$ boundary means that the tracer mass transport at $z = \eta - \epsilon$ (ocean side) equals to that at $z = \eta + \epsilon$ (atmospheric side), with $\epsilon > 0$ a tiny number. The tracer concentration at the interface, $C(z = \eta)$, is not determined by kinematics. Many analyses and numerical model applications approximate $C(z = \eta)$ as the bulk tracer concentration within the upper few meters of the ocean, depending on details of the upper ocean turbulence. However, as vertical grid spacing is refined to be finer than roughly a meter, this assumption must be reconsidered.

boundary, as defined according to the kinematic boundary condition (3.80)

$$\mathcal{Q}_m = -\rho \hat{n} \cdot (\mathbf{v} - \mathbf{v}^{(\eta)}) \quad \text{surface ocean boundary.} \quad (4.80)$$

As for the solid-earth boundary condition, specification of \mathcal{Q}_c requires information concerning the flux of tracer mass into or out of the ocean, and this flux equals to the net flux on the ocean side of the surface

$$\mathcal{Q}_c = C_m \mathcal{Q}_m + \mathcal{Q}_c^{\text{non-adv}} \equiv -[\rho C (\mathbf{v} - \mathbf{v}^{(b)}) + \mathbf{J}] \cdot \hat{n} = C \mathcal{Q}_m - \mathbf{J} \cdot \hat{n}, \quad (4.81)$$

We thus see that the surface transport of tracer mass induces the following non-advectional flux within the ocean at $z = \eta$

$$-\mathbf{J} \cdot \hat{n} = \mathcal{Q}_c - C \mathcal{Q}_m = \mathcal{Q}_c^{\text{non-adv}} + (C_m - C) \mathcal{Q}_m. \quad (4.82)$$

Figure 4.6 offers a schematic to summarize these results.



4.5 Exercises

EXERCISE 4.1: EQUATION FOR TRACER MASS PER FLUID VOLUME

In some treatments it can be suitable to define a volumetric tracer concentration as the mass of tracer per volume of fluid

$$\phi = \frac{\text{mass of constituent } n \text{ in fluid element}}{\text{volume of fluid element}} = C \rho, \quad (4.83)$$

where C is the mass concentration defined by equation (4.17) and satisfying the tracer equation (4.21). Derive the corresponding equation satisfied by ϕ .

EXERCISE 4.2: GALILEAN INVARIANCE OF THE TRACER EQUATION

Prove that the source-free tracer equation is Galilean invariant. Hint: recall our discussion of Galilean invariance in Section 1.6.

EXERCISE 4.3: DENSITY WEIGHTED VELOCITY

Let $\bar{\rho}$ and $\bar{\mathbf{v}}$ be the mean density and mean velocity, where “mean” can represent any number

of averaging operators, and let primes denote deviations from the means. The mass continuity equation for the mean density thus takes the form

$$\partial_t \bar{\rho} + \nabla \cdot (\bar{\rho} \bar{\mathbf{v}}) = 0. \quad (4.84)$$

Now introduce the density-weighted velocity

$$\mathbf{v}^H \equiv \bar{\rho} \bar{\mathbf{v}} / \bar{\rho} = \bar{\mathbf{v}} + \bar{\rho}' \bar{\mathbf{v}}' / \bar{\rho} \quad (4.85)$$

and show that the mean continuity equation can be written

$$\partial_t \bar{\rho} + \nabla \cdot (\bar{\rho} \mathbf{v}^H) = 0. \quad (4.86)$$

The density-weighted velocity, \mathbf{v}^H , is motivated by the work of [Hesselberg \(1926\)](#) and [Favre \(1965\)](#), with further details for its use in the full suite of dynamical equations summarized in Chapter 8 of [Griffies \(2004\)](#). Its introduction illustrates how one may choose to work with averaged equations in a manner that retains a clear sense for mass conservation. Namely, by introducing \mathbf{v}^H , which can be considered a modified barycentric velocity, the mean mass continuity equation (4.86) takes on the same form as the un-averaged continuity equation (4.8). In this manner we see that \mathbf{v}^H , rather than $\bar{\mathbf{v}}$, advects the mean fluid mass density.

EXERCISE 4.4: EVOLUTION OF THE INTEGRATED DENSITY WEIGHTED POSITION

In Exercise 3.2 we developed an evolution equation for the center of mass motion for a region with fixed mass. Here we derive a slightly more general result holding for an arbitrary region, \mathcal{R} , within the fluid. Namely, for Cartesian coordinates, use the Leibniz-Reynolds transport theorem (4.34) as well as the mass continuity equation (3.6) to derive the identity

$$\frac{d}{dt} \int_{\mathcal{R}} \rho \mathbf{x} dV = \int_{\mathcal{R}} \rho \mathbf{v} dV + \oint_{\partial \mathcal{R}} \rho \mathbf{x} [(\mathbf{v} - \mathbf{v}^{(b)}) \cdot \hat{\mathbf{n}}] d\mathcal{S}, \quad (4.87)$$

where \mathbf{x} is the position vector for a point within the fluid. Notice that for a mass conserving Lagrangian region (i.e., a region that moves with the fluid flow), the boundary term vanishes since in this case $(\mathbf{v} - \mathbf{v}^{(b)}) \cdot \hat{\mathbf{n}} = 0$, which then reduces equation (4.87) to equation (3.108) derived in Exercise 3.2.

EXERCISE 4.5: EVOLUTION OF REGION MEAN TRACER

We here consider an application of the formalism developed in this chapter by deriving evolution equations for the averaged tracer concentration as defined by

$$\langle C \rangle = \frac{1}{M} \int_{\mathcal{R}} \rho C dV \quad \text{with} \quad M = \int_{\mathcal{R}} \rho dV, \quad (4.88)$$

where the finite region, \mathcal{R} , is within the fluid but otherwise it is arbitrary.

- (a) Derive the following equation for the evolution of the region averaged tracer concentration

$$M \frac{d\langle C \rangle}{dt} = - \oint_{\partial \mathcal{R}} [\rho (C - \langle C \rangle) (\mathbf{v} - \mathbf{v}^{(b)}) + \mathbf{J}] \cdot \hat{\mathbf{n}} d\mathcal{S}. \quad (4.89)$$

- (b) Specialize equation (4.89) to a region comprised of an ocean model grid cell that is

adjacent to the ocean surface (see Figure 4.3 or 4.6), in which

$$M \frac{d\langle C \rangle}{dt} = \int_{z=\eta} (C - \langle C \rangle) Q_m dA - \int_{\partial R_{int}} \rho (C - \langle C \rangle) (\mathbf{v} - \mathbf{v}^{(b)}) \cdot \hat{\mathbf{n}} dS - \oint_{\partial R} \mathbf{J} \cdot \hat{\mathbf{n}} dS. \quad (4.90)$$



Chapter 5

NON-DIVERGENT FLOWS

In this chapter, we study the kinematics of a **non-divergent flow** as defined by a velocity that satisfies $\nabla \cdot \mathbf{v} = 0$. In many areas of fluid mechanics, a non-divergent flow is said to describe an **incompressible flow**, with this term motivated by the case of flow within a constant density or incompressible fluid. In other areas of fluid mechanics, non-divergent flows are referred to as *solenoidal*, in analog to the non-divergent or solenoidal magnetic field occurring in classical electrodynamics. As seen when studying the Boussinesq ocean, a fluid with a non-divergent flow can still experience compressibility effects and the associated density variations. That is, the study of a Boussinesq ocean concerns the incompressible flow of a compressible fluid, thus exemplifying the important distinction between a **fluid property** versus a **flow property**.

READER'S GUIDE TO THIS CHAPTER

This chapter introduces many concepts and tools of use in the remainder of the book. We presume an understanding of the kinematics of mass conservation from Chapter 3 as well as many of the results from vector calculus in VOLUME 1. Most of the treatment makes use of Cartesian coordinates for simplicity, though the results hold for general Eulerian coordinates.

5.1	Loose threads	140
5.2	Introduction to non-divergent flow	140
5.3	Kinematic boundary conditions	141
5.4	Streamfunction for two-dimensional flow	141
5.4.1	Streamfunction isolines are streamlines	142
5.4.2	Streamfunction is constant on material boundaries	142
5.4.3	The streamfunction and fluid transport	142
5.4.4	Gauge symmetry	143
5.4.5	Exact differential formulation	144
5.4.6	Concerning the Helmholtz decomposition	144
5.4.7	A caveat: transport with curl-free + divergent flow	145
5.5	Vector streamfunction for three-dimensional flow	145
5.5.1	Gauge symmetry	146
5.5.2	The streamfunction and transport through a surface	146
5.5.3	Scalar streamfunctions and transport	146
5.5.4	Concerning a harmonic velocity potential	148
5.5.5	The streamfunction using the vertical gauge	148
5.6	Evolution of volume and area	150
5.6.1	Material volumes and areas	150
5.6.2	Arbitrary volume and area	150
5.7	Meridional-depth circulation	151

5.7.1	The zonally integrated transport is non-divergent	152
5.7.2	Meridional-depth streamfunction	153
5.7.3	Verifying that Ψ is a streamfunction	153
5.7.4	Generalizing to arbitrary domains	154
5.7.5	$\Psi(y, z)$ does not generally delineate particle pathlines	155
5.8	Kinematic free surface equation	155
5.8.1	Derivation	155
5.8.2	Comments	156
5.9	Exercises	157

5.1 Loose threads

- Need more work for the general Ψ in Section 5.7.4 to prove that it is a streamfunction.
- Kinetics of strain, vorticity, and Helmholtz as per the boxed material in Aluie et al review in progress. Perhaps make into an exercise.

5.2 Introduction to non-divergent flow

For many purposes in fluid mechanics, we can make the simplifying assumption regarding the fluid kinematics whereby the volume of a moving fluid element is approximated as a constant. Recalling the expression

$$\frac{1}{\delta V} \frac{D(\delta V)}{Dt} = \nabla \cdot \mathbf{v} \quad (5.1)$$

from Section 2.11.1, we see that a constant volume for a fluid element constrains the velocity field to be non-divergent

$$\frac{1}{\delta V} \frac{D(\delta V)}{Dt} = 0 \implies \nabla \cdot \mathbf{v} = 0. \quad (5.2)$$

Flow satisfying $\nabla \cdot \mathbf{v} = 0$ is said to be *incompressible* since the volume of a fluid element is materially invariant. We illustrate this situation in Figure 5.1.

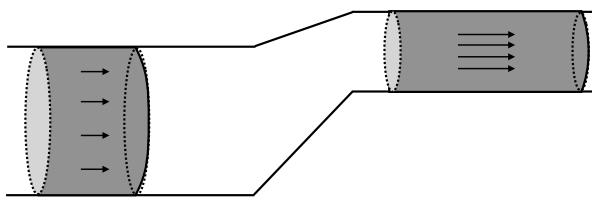


FIGURE 5.1: Illustrating volume continuity for a non-divergent velocity flow in a pipe. On the left the pipe has a relatively large diameter whereas on the right the pipe is narrower. A plug of water on the left moves through the pipe and becomes longer when it moves into the narrower region so that the volume of the plug remains the same. Correspondingly, the speed of the flow increases when moving into the narrower portion of the pipe.

A slightly less onerous constraint arises from the *anelastic approximation*, whereby

$$\nabla \cdot (\rho \mathbf{v}) = 0. \quad (5.3)$$

The anelastic approximation is sometimes motivated for the atmosphere. However, it is less commonly used for atmospheric dynamics than the Boussinesq ocean is used for the ocean. We thus focus on the Boussinesq case here, whereby $\nabla \cdot \mathbf{v} = 0$.

The non-divergence constraint (5.2) reduces by one the number of functional degrees of freedom possessed by the velocity field. What that means in practice is that we need one fewer velocity component to determine the flow since one component can be diagnosed from the other two components. This property manifests by our ability to introduce a streamfunction to specify the velocity, as further developed in this chapter.

5.3 Kinematic boundary conditions

For non-divergent flow, there are slight modifications to the boundary conditions detailed in Section 3.6. Whereas the material conditions remain identical, the non-material conditions are applied with a constant reference density, ρ_0 , rather than the local *in situ* density, ρ . In particular, the boundary condition (3.80) takes on the form

$$\rho_0 (\mathbf{v} - \mathbf{v}^{(s)}) \cdot \hat{\mathbf{n}} dS = -Q_m dS = -Q_m dA \quad \text{moving non-material boundary condition, (5.4)}$$

where the second equality introduced the mass flux per unit horizontal area, Q_m , according to equation (3.90c). Correspondingly, the kinematic boundary condition (3.96) applied at the ocean free surface takes on the form

$$\rho_0 \frac{D(z - \eta)}{Dt} = -Q_m \implies w + \frac{Q_m}{\rho_0} = \frac{\partial \eta}{\partial t} + \mathbf{u} \cdot \nabla \eta. \quad (5.5)$$

Making use of the non-divergence condition on the velocity allows us to write this equation in the equivalent forms¹

$$\partial_t \eta - Q_m / \rho_0 = (\hat{\mathbf{z}} - \nabla \eta) \cdot \mathbf{v} = \nabla(z - \eta) \cdot \mathbf{v} = \nabla \cdot [(z - \eta) \mathbf{v}]. \quad (5.6)$$

In Section 5.8 we derive the kinematic free surface equation (5.81), which also shows that $\partial_t \eta - Q_m / \rho_0$ is a total divergence.

5.4 Streamfunction for two-dimensional flow

Vertical stratification of buoyancy plus the effects from planetary rotation inhibit vertical motion in geophysical flows. Therefore, as an idealization it is sometimes useful to assume the geophysical fluid flow is horizontal (two-dimensional) as well as non-divergent. The non-divergent constraint for two-dimensional flow can be satisfied by writing the horizontal velocity in the form

$$\mathbf{u} = \nabla \times (z \nabla \psi) = \hat{\mathbf{z}} \times \nabla \psi = \hat{\mathbf{z}} \times \nabla_h \psi = -\hat{\mathbf{x}} \partial_y \psi + \hat{\mathbf{y}} \partial_x \psi, \quad (5.7)$$

where

$$\nabla_h = \hat{\mathbf{x}} \partial_x + \hat{\mathbf{y}} \partial_y \quad (5.8)$$

is the horizontal gradient operator. The constraint $\nabla_h \cdot \mathbf{u} = 0$ is satisfied since the partial derivative operators commute

$$\frac{\partial^2 \psi}{\partial x \partial y} = \frac{\partial^2 \psi}{\partial y \partial x}. \quad (5.9)$$

¹In equation (5.6), we set $z = \eta$ after applying the gradient operator in the penultimate expression and the divergence in the final expression.

We refer to ψ as the *streamfunction*, with this name motivated by the following considerations.²

5.4.1 Streamfunction isolines are streamlines

At any fixed time instance, the exact differential of the streamfunction is

$$d\psi = \partial_x \psi dx + \partial_y \psi dy = v dx - u dy, \quad (5.10)$$

where the second equality follows from equation (5.7). Instantaneous lines along which ψ is a constant satisfy

$$d\psi = 0 \implies \frac{dx}{u} = \frac{dy}{v}. \quad (5.11)$$

Furthermore, the direction that is orthogonal to constant ψ lines

$$\hat{\mathbf{n}} = \frac{\nabla_h \psi}{|\nabla_h \psi|} = \frac{v \hat{\mathbf{x}} - u \hat{\mathbf{y}}}{|\mathbf{u}|} \quad (5.12)$$

is itself normal to the velocity

$$\mathbf{u} \cdot \nabla_h \psi = uv - vu = 0. \quad (5.13)$$

Consequently, at each time instance, lines of constant ψ are streamlines, which means (following Section 1.8.2) that curves of constant ψ define integral curves for the instantaneous velocity field. This property motivates referring to ψ as the *streamfunction*. Furthermore, through each point of a two-dimensional non-divergent flow and at any particular time instance, there is one and only one streamline passing through that point.

5.4.2 Streamfunction is constant on material boundaries

As a corollary to the results from Section 5.4.1, we know that the streamfunction is a spatial constant when evaluated along static material boundaries where $\mathbf{u} \cdot \hat{\mathbf{n}} = 0$. This property follows from equation (5.13). We can also see it from

$$\mathbf{u} \cdot \hat{\mathbf{n}} = (\hat{\mathbf{z}} \times \nabla_h \psi) \cdot \hat{\mathbf{n}} = (\hat{\mathbf{n}} \times \hat{\mathbf{z}}) \cdot \nabla_h \psi = \hat{\mathbf{t}} \cdot \nabla_h \psi = 0, \quad (5.14)$$

where $\hat{\mathbf{t}}$ a unit direction that is tangent to the boundary. The operator, $\hat{\mathbf{t}} \cdot \nabla_h \psi$, is the derivative of ψ computed in a direction tangent to the boundary. Hence, $\hat{\mathbf{t}} \cdot \nabla_h \psi = 0$ means that ψ takes on the same value everywhere along the boundary. Note that this property still allows ψ to be a function of time along the boundary.

We emphasize that a constant streamfunction along a boundary, $\hat{\mathbf{t}} \cdot \nabla_h \psi = 0$, is distinct from a vanishing normal derivative at the boundary. Indeed, the streamfunction for a two-dimensional non-divergent flow generally has a nonzero normal derivative at boundaries, $\hat{\mathbf{n}} \cdot \nabla_h \psi \neq 0$.

5.4.3 The streamfunction and fluid transport

Consider an arbitrary curve in the fluid with endpoints represented by the Cartesian coordinates, \mathbf{x}_1 and \mathbf{x}_2 , as depicted in Figure 5.2. At any particular time instance, the difference in

²In this section we could choose to relax notation by dispensing with the h subscript on the horizontal gradient operator, ∇_h , since we are here concerned only with two-dimensional horizontal flow. Even so, we find it useful to be pedantic as doing so clearly distinguishes the two-dimensional formulations in this section from the analogous three-dimensional case considered in Section 5.5.

streamfunction between these two points is given by

$$\psi(\mathbf{x}_2) - \psi(\mathbf{x}_1) = \int_{\mathbf{x}_1}^{\mathbf{x}_2} d\psi = \int_{\mathbf{x}_1}^{\mathbf{x}_2} \left[dx \frac{\partial \psi}{\partial x} + dy \frac{\partial \psi}{\partial y} \right] = \int_{\mathbf{x}_1}^{\mathbf{x}_2} \nabla_h \psi \cdot d\mathbf{x} = \int_{\mathbf{x}_1}^{\mathbf{x}_2} \nabla_h \psi \cdot \hat{\mathbf{t}} ds. \quad (5.15)$$

For the final equality we wrote

$$d\mathbf{x} = \hat{\mathbf{t}} ds, \quad (5.16)$$

where

$$ds = |d\mathbf{x}| \quad (5.17)$$

is the element of arc length along the curve, and $\hat{\mathbf{t}}$ is the unit tangent vector that points in the direction along the curve from \mathbf{x}_1 to \mathbf{x}_2 . Now introduce the unit normal vector along the curve according to

$$\hat{\mathbf{t}} = \hat{\mathbf{n}} \times \hat{\mathbf{z}}, \quad (5.18)$$

where $\hat{\mathbf{n}}$ points to the left when facing in the $\hat{\mathbf{t}}$ direction. We thus have

$$\psi(\mathbf{x}_2) - \psi(\mathbf{x}_1) = \int_{\mathbf{x}_1}^{\mathbf{x}_2} \nabla_h \psi \cdot (\hat{\mathbf{n}} \times \hat{\mathbf{z}}) ds = \int_{\mathbf{x}_1}^{\mathbf{x}_2} (\hat{\mathbf{z}} \times \nabla_h \psi) \cdot \hat{\mathbf{n}} ds = \int_{\mathbf{x}_1}^{\mathbf{x}_2} \mathbf{u} \cdot \hat{\mathbf{n}} ds, \quad (5.19)$$

with the final equality an expression for the net area transport of fluid normal to the curve (dimensions of area per time). As the chosen curve connecting the points is arbitrary, we conclude that the difference in streamfunction values between two points measures the transport across any curve connecting the points. Correspondingly, the stronger the gradient in the streamfunction, the larger the transport since

$$|\mathbf{u}| = |\nabla_h \psi|. \quad (5.20)$$

Given the connection between the transport between two points and the value of the streamfunction at those two points, we are motivated to name ψ the *transport streamfunction*.

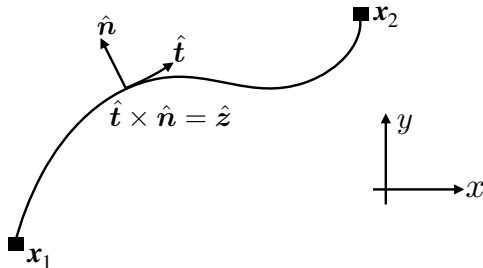


FIGURE 5.2: Depicting the transport between two points in a two-dimensional fluid. The transport is the line integral, $\int_{x_1}^{x_2} \mathbf{u} \cdot \hat{\mathbf{n}} ds$, from point x_1 to x_2 , with the unit normal, $\hat{\mathbf{n}}$, pointing to the left when facing in the direction of the local unit tangent vector, $\hat{\mathbf{t}}$. By construction, $\hat{\mathbf{t}} \times \hat{\mathbf{n}} = \hat{\mathbf{z}}$, where $\hat{\mathbf{z}}$ points vertically out of the page. For a two-dimensionally non-divergent flow, $\nabla_h \cdot \mathbf{u} = 0$, the transport between any two points is the streamfunction difference at these two points, $\int_{x_1}^{x_2} \mathbf{u} \cdot \hat{\mathbf{n}} ds = \psi(x_1) - \psi(x_2)$. This result holds regardless the path taken between these two points, so long as the path remains simple; i.e., it does not intersect itself.

5.4.4 Gauge symmetry

For a two-dimensional non-divergent flow, the constraint, $\nabla_h \cdot \mathbf{u} = 0$, reduces the functional degrees of freedom from two (the two velocity components (u, v)) to one (the streamfunction).

However, the streamfunction is arbitrary up to a constant, k , since

$$\psi' = \psi + k \Rightarrow \mathbf{u}' = \mathbf{u}. \quad (5.21)$$

So the value of the streamfunction at a particular point has no unambiguous physical meaning. Rather, only the difference in streamfunction between two points is physically relevant. The ability to add a constant to the streamfunction represents a form of [gauge symmetry](#).

5.4.5 Exact differential formulation

Consider the differential

$$\mathbf{A} \cdot d\mathbf{x} \equiv (\mathbf{u} \times \hat{\mathbf{z}}) \cdot d\mathbf{x} = v dx - u dy. \quad (5.22)$$

By construction

$$\hat{\mathbf{z}} \cdot (\nabla_h \times \mathbf{A}) = 0 \quad \text{since} \quad \nabla_h \cdot \mathbf{u} = 0, \quad (5.23)$$

which means that $\mathbf{A} \cdot d\mathbf{x}$ is an [exact differential](#). Consequently, we can write

$$\mathbf{A} \cdot d\mathbf{x} = (\mathbf{u} \times \hat{\mathbf{z}}) \cdot d\mathbf{x} = \nabla_h \psi \cdot d\mathbf{x} = d\psi, \quad (5.24)$$

which then leads to the results derived earlier in this section where ψ is the transport streamfunction.

5.4.6 Concerning the Helmholtz decomposition

We close this section by tidying up some mathematical niceties concerning the [Helmholtz decomposition](#). For two-dimensional flows on a simply connected domain, the Helmholtz decomposition takes the form

$$\mathbf{u} = \hat{\mathbf{z}} \times \nabla_h \Gamma + \nabla_h \Phi, \quad (5.25)$$

for some functions Γ and Φ . For non-divergent flows, Φ is constrained to be a harmonic function

$$\nabla \cdot \mathbf{u} = 0 \implies \nabla_h^2 \Phi = \nabla_h \cdot \nabla_h \Phi = 0. \quad (5.26)$$

As summarized in Table 5.1, it is sufficient to make use of just a streamfunction, ψ , for vortical flow and just a [velocity potential](#), ϕ , for irrotational flow. In the following we verify why it is sufficient to make use of this truncated version of the Helmholtz decomposition for non-divergent two-dimensional flows.

NON-DIVERGENT VORTICAL FLOW	NON-DIVERGENT IRROTATIONAL FLOW
$\nabla_h \cdot \mathbf{u} = 0$	$\nabla_h \cdot \mathbf{u} = 0$
$\nabla_h \times \mathbf{u} \neq 0$	$\nabla_h \times \mathbf{u} = 0$
$\mathbf{u} = \hat{\mathbf{z}} \times \nabla_h \psi$	$\mathbf{u} = \nabla_h \phi$
$\hat{\mathbf{z}} \cdot (\nabla_h \times \mathbf{u}) = \nabla_h^2 \psi$	$\nabla_h^2 \phi = 0$

TABLE 5.1: Summarizing some mathematical properties of non-divergent two-dimensional velocity fields, $\nabla_h \cdot \mathbf{u} = 0$. The streamfunction is ψ , whereas ϕ is the velocity potential.

Non-divergent vortical flow

Return to the exact differential formulation from Section 5.4.5. In that formulation we noted that $\nabla_h \cdot \mathbf{u} = 0$ means that the differential $\mathbf{A} \cdot d\mathbf{x} = (\mathbf{u} \times \hat{\mathbf{z}}) \cdot d\mathbf{x}$ is exact. Making use of the Helmholtz decomposition (5.25) renders

$$\mathbf{A} \cdot d\mathbf{x} = (\mathbf{u} \times \hat{\mathbf{z}}) \cdot d\mathbf{x} \quad (5.27a)$$

$$= [(\hat{\mathbf{z}} \times \nabla_h \Gamma) \times \hat{\mathbf{z}} + \nabla_h \Phi \times \hat{\mathbf{z}}] \cdot d\mathbf{x} \quad (5.27b)$$

$$= [\nabla_h \Gamma + \nabla_h \Phi \times \hat{\mathbf{z}}] \cdot d\mathbf{x}. \quad (5.27c)$$

To reveal the exactness of the right hand side requires the harmonic property of Φ so that we can write

$$\hat{\mathbf{z}} \cdot [\nabla_h \times (\nabla_h \Phi \times \hat{\mathbf{z}})] = -\nabla_h^2 \Phi = 0 \implies \nabla_h \Phi \times \hat{\mathbf{z}} \equiv \nabla_h \Upsilon, \quad (5.28)$$

in which case

$$\mathbf{A} \cdot d\mathbf{x} \equiv v dx - u dy = d(\Gamma + \Upsilon) \equiv d\psi. \quad (5.29)$$

We conclude that for non-divergent vortical flow, we lose no generality by working just with the streamfunction, ψ , of Section 5.4.3. There is no need to also include a harmonic function.

Non-divergent irrotational flow

Consider now non-divergent and irrotational flow. The irrotational condition holds so long as Γ is harmonic

$$\hat{\mathbf{z}} \cdot [\nabla_h \times (\hat{\mathbf{z}} \times \nabla_h \Gamma)] = \nabla_h^2 \Gamma = 0. \quad (5.30)$$

Consequently, we can write

$$\hat{\mathbf{z}} \times \nabla_h \Gamma = \nabla_h \gamma, \quad (5.31)$$

in which case

$$\mathbf{u} = \hat{\mathbf{z}} \times \nabla_h \Gamma + \nabla_h \Phi = \nabla_h (\gamma + \Phi) \equiv \nabla_h \phi. \quad (5.32)$$

Hence, for non-divergent irrotational flow, it is sufficient to work just with the harmonic velocity potential, ϕ .

5.4.7 A caveat: transport with curl-free + divergent flow

Consider a horizontal velocity that has a non-zero divergence, $\nabla \cdot \mathbf{u} \neq 0$, and yet it has a zero curl, $\nabla \times \mathbf{u} = 0$. The zero curl allows us to write $\mathbf{u} = \nabla_h \phi$, with ϕ the velocity potential. Hence, $d\Phi = \nabla_h \phi \cdot d\mathbf{x}$ is an exact differential and so its closed loop integral vanishes: $\oint d\Phi = 0$. However, there is no connection between velocity potential and transport. That is, we cannot conclude anything about the net transport across a closed curve based on properties of ϕ .

5.5 Vector streamfunction for three-dimensional flow

A three-dimensional non-divergent velocity, $\nabla \cdot \mathbf{v} = 0$, can be specified by a vector streamfunction

$$\mathbf{v} = \nabla \times \Psi. \quad (5.33)$$

The constraint $\nabla \cdot \mathbf{v} = 0$ is trivially satisfied since the divergence of the curl vanishes

$$\nabla \cdot (\nabla \times \Psi) = 0. \quad (5.34)$$

5.5.1 Gauge symmetry

For three-dimensional non-divergent flow, the constraint $\nabla \cdot \mathbf{v} = 0$ reduces the three functional degrees of freedom down to two, meaning that one of the velocity components can be diagnosed from the other two. Gauge symmetry manifests through the ability to add the gradient of an arbitrary scalar field to the streamfunction, Ψ , without altering \mathbf{v} :

$$\Psi' = \Psi + \nabla \lambda \Rightarrow \mathbf{v}' = \mathbf{v}, \quad (5.35)$$

which follows since $\nabla \times \nabla \lambda = 0$. Hence, the vector streamfunction has no absolute physical meaning since it can be modified by adding an arbitrary gauge function.

5.5.2 The streamfunction and transport through a surface

The volume transport (volume per time) of fluid crossing a surface is measured by the area integral

$$\mathcal{T}(\mathcal{S}) = \int_{\mathcal{S}} \mathbf{v} \cdot \hat{\mathbf{n}} d\mathcal{S}, \quad (5.36)$$

where $\hat{\mathbf{n}}$ is the outward unit normal direction on the surface. Introducing the vector streamfunction and making use of [Stokes' theorem](#) then leads to

$$\mathcal{T}(\mathcal{S}) = \int_{\mathcal{S}} \mathbf{v} \cdot \hat{\mathbf{n}} d\mathcal{S} = \int_{\mathcal{S}} (\nabla \times \Psi) \cdot \hat{\mathbf{n}} d\mathcal{S} = \oint_{\partial\mathcal{S}} \Psi \cdot \hat{\mathbf{t}} ds, \quad (5.37)$$

where $\hat{\mathbf{t}} ds$ is the oriented arc distance increment along the boundary of \mathcal{S} , and $\oint_{\partial\mathcal{S}}$ is the oriented line integral around the boundary $\partial\mathcal{S}$. Hence, the volume transport of fluid through the surface depends only on the vector streamfunction on the perimeter of the surface. Furthermore, if the transport through the surface vanishes (e.g., no-flux material surface such as a solid earth boundary), then on the surface the vector streamfunction can be written as the gradient of an arbitrary scalar field, $\Psi = \nabla \chi$, since

$$\oint_{\partial\mathcal{S}} \Psi \cdot \hat{\mathbf{t}} ds = \oint_{\partial\mathcal{S}} \nabla \chi \cdot \hat{\mathbf{t}} ds = \oint_{\partial\mathcal{S}} \nabla \chi \cdot d\mathbf{x} = \oint_{\partial\mathcal{S}} d\chi = 0. \quad (5.38)$$

Because Ψ has a connection to fluid transport, we sometimes refer to it as the *transport streamfunction*, just as for the streamfunction ψ in two-dimensional non-divergent flows (Section 5.4.3).

5.5.3 Scalar streamfunctions and transport

We can expose the two degrees of freedom of the vector streamfunction by writing it as the product of a scalar field and the gradient of another scalar field

$$\Psi = \gamma \nabla \psi \quad (5.39)$$

so that the velocity is given by³

$$\mathbf{v} = \nabla \times \Psi = \nabla \gamma \times \nabla \psi. \quad (5.40)$$

³Equation (5.40) is sometimes referred to as *Euler's form*, for, as noted on page 21 of [Truesdell \(1954\)](#), it was Euler who originally proved its validity.

By construction the velocity satisfies

$$\mathbf{v} \cdot \nabla \gamma = \mathbf{v} \cdot \nabla \psi = 0, \quad (5.41)$$

so that the velocity is parallel to surfaces of constant γ as well as to surfaces of constant ψ . Correspondingly, the velocity streamlines are intersections of the γ and ψ isosurfaces, as depicted in Figure 5.3. We thus refer to γ and ψ as the two *scalar streamfunctions* for the three dimensional non-divergent flow. However, note that γ and ψ have different dimensions. By convention, we choose γ to have dimensions of length, so that it is not a traditional streamfunction, whereas ψ has the traditional streamfunction dimensions of length squared per time.

As a check that the formalism is sensible, consider the special case of two-dimensional flow so that all streamlines are in the horizontal x - y plane. Taking $\gamma = z$ then renders

$$\Psi = z \nabla \psi \quad \text{and} \quad \mathbf{v} = \nabla \times \Psi = \hat{z} \times \nabla \psi, \quad (5.42)$$

which agrees with the scalar streamfunction in equation (5.7) for two dimensional non-divergent flow.

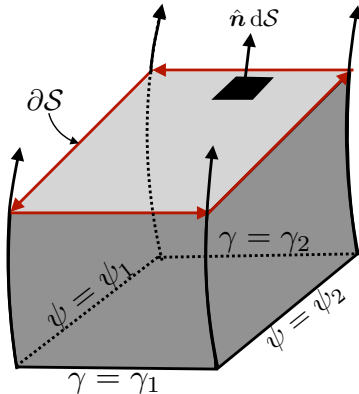


FIGURE 5.3: Isosurfaces of constant scalar streamfunctions, γ and ψ , for a three dimensional non-divergent flow. Streamlines are defined by the intersections of the γ and ψ isosurfaces, as shown by four streamlines along the corners of this particular volume. The volume transport of fluid through the surface, \mathcal{S} , is determined by the line integral, $\oint_{\partial\mathcal{S}} \gamma \, d\psi = -\oint_{\partial\mathcal{S}} \psi \, d\gamma = (\gamma_1 - \gamma_2)(\psi_2 - \psi_1)$, around the boundary circuit.

The volume transport through a surface defined by the two streamfunction isosurfaces takes the form

$$\mathcal{T}(\mathcal{S}) = \int_{\mathcal{S}} \mathbf{v} \cdot \hat{\mathbf{n}} \, d\mathcal{S} = \oint_{\partial\mathcal{S}} \Psi \cdot \hat{\mathbf{t}} \, ds = \oint_{\partial\mathcal{S}} \gamma \nabla \psi \cdot \hat{\mathbf{t}} \, ds = \oint_{\partial\mathcal{S}} \gamma \, d\psi = -\oint_{\partial\mathcal{S}} \psi \, d\gamma. \quad (5.43)$$

To reach the penultimate step we set

$$d\psi = \nabla \psi \cdot dx = \nabla \psi \cdot \hat{\mathbf{t}} \, ds, \quad (5.44)$$

and for the final step we used the identity

$$\oint_{\partial\mathcal{S}} \gamma \, d\psi = \oint_{\partial\mathcal{S}} d(\gamma \psi) - \oint_{\partial\mathcal{S}} \psi \, d\gamma = -\oint_{\partial\mathcal{S}} \psi \, d\gamma. \quad (5.45)$$

This identity follows from

$$\oint_{\partial S} d(\gamma \psi) = 0, \quad (5.46)$$

which holds since $d(\gamma \psi)$ is an exact differential and its line integral vanishes when computed around a closed path.⁴ The volume transport for the particular surface shown in Figure 5.3 is given by

$$\mathcal{T}(S) = \oint_{\partial S} \gamma d\psi = \gamma_1 (\psi_2 - \psi_1) + \gamma_2 (\psi_1 - \psi_2) = (\gamma_1 - \gamma_2) (\psi_2 - \psi_1). \quad (5.47)$$

Hence, the volume transport through a streamtube defined by isosurfaces of γ and ψ is given by the product of the difference between the isosurfaces.

5.5.4 Concerning a harmonic velocity potential

As for the two-dimensional case discussed in Section 5.4.6, we consider the relevance of an arbitrary harmonic velocity potential, χ , so that the velocity takes the form

$$\mathbf{v} = \nabla \times \boldsymbol{\Gamma} + \nabla \chi \quad \text{with} \quad \nabla^2 \chi = 0. \quad (5.48)$$

Since $\nabla \cdot \nabla \chi = 0$ we can write $\nabla \chi$ as the curl of another vector

$$\nabla \cdot \nabla \chi = 0 \implies \nabla \chi = \nabla \times \boldsymbol{\Lambda}, \quad (5.49)$$

in which case the velocity takes the form

$$\mathbf{v} = \nabla \times \boldsymbol{\Gamma} + \nabla \chi = \nabla \times (\boldsymbol{\Gamma} + \boldsymbol{\Lambda}) \equiv \nabla \times \boldsymbol{\Psi}. \quad (5.50)$$

Consequently, just as for the two-dimensional case, we are at liberty to work with the transport streamfunction, $\boldsymbol{\Psi}$, if that suits our needs. Otherwise, we can work with the harmonic potential, χ , which is commonly used when the velocity is both non-divergent and irrotational.

5.5.5 The streamfunction using the vertical gauge

To explicitly reveal the two functional degrees of freedom possessed by the non-divergent velocity field, we establish that the velocity field can be constructed from the following *vertical gauge* streamfunction⁵

$$\boldsymbol{\Psi}^{vg} = \hat{x} \Psi_1^{vg} + \hat{y} \Psi_2^{vg}, \quad (5.51)$$

which has a zero vertical component, $\Psi_3^{vg} = 0$. In addition to proving that $\mathbf{v} = \nabla \times \boldsymbol{\Psi}^{vg}$, we show that $\boldsymbol{\Psi}^{vg}$ provides a measure of the horizontal volume transport of fluid beneath a chosen depth.

⁴The identity (5.46) follows from the fundamental theorem of calculus, whereby the closed loop integral of an exact differential vanishes.

⁵There are occasions in which it is suitable to use either $\boldsymbol{\Psi} = \hat{x} \Psi_1 + \hat{z} \Psi_3$ or $\boldsymbol{\Psi} = \hat{y} \Psi_2 + \hat{z} \Psi_3$. In this section we focus on the vertical gauge (5.51) since that is more commonly used in applications.

Proof that $v = \nabla \times \Psi^{\text{vg}}$

In terms of the vertical gauge streamfunction, the velocity components are given by

$$u = -\frac{\partial \Psi_2^{\text{vg}}}{\partial z} \quad \text{and} \quad v = \frac{\partial \Psi_1^{\text{vg}}}{\partial z} \quad \text{and} \quad w = \frac{\partial \Psi_2^{\text{vg}}}{\partial x} - \frac{\partial \Psi_1^{\text{vg}}}{\partial y}. \quad (5.52)$$

Vertically integrating the u, v equations from the bottom at $z = \eta_b(x, y)$ up to an arbitrary vertical position leads to⁶

$$\Psi^{\text{vg}}(x, y, z, t) = \int_{\eta_b(x, y)}^z \mathbf{u}(x, y, z', t) dz' \times \hat{\mathbf{z}} \equiv \mathbf{U}(x, y, z, t) \times \hat{\mathbf{z}}, \quad (5.53)$$

where

$$\mathbf{U}(x, y, z, t) = \int_{\eta_b(x, y)}^z \mathbf{u}(x, y, z', t) dz' \quad (5.54)$$

is the horizontal transport of fluid from the bottom up to a chosen vertical position above the bottom. We trivially see that $u = -\partial \Psi_2^{\text{vg}}/\partial z$ and $v = \partial \Psi_1^{\text{vg}}/\partial z$. It takes a bit more work to verify that this streamfunction also renders w through noting that

$$\frac{\partial \Psi_2^{\text{vg}}}{\partial x} = u(\eta_b) \partial_x \eta_b - \int_{\eta_b}^z \partial_x u dz' \quad \text{and} \quad \frac{\partial \Psi_1^{\text{vg}}}{\partial y} = \int_{\eta_b}^z \partial_y v dz' - v(\eta_b) \partial_y \eta_b, \quad (5.55)$$

so that

$$\frac{\partial \Psi_2^{\text{vg}}}{\partial x} - \frac{\partial \Psi_1^{\text{vg}}}{\partial y} = \mathbf{u}(\eta_b) \cdot \nabla \eta_b - \int_{\eta_b}^z \left[\frac{\partial u}{\partial x} + \frac{\partial v}{\partial y} \right] dz' = w(\eta_b) + \int_{\eta_b}^z \frac{\partial w}{\partial z'} dz' = w(z), \quad (5.56)$$

where we used the bottom kinematic boundary condition (3.58) to write $\mathbf{u}(\eta_b) \cdot \nabla \eta_b = w(\eta_b)$. We conclude that knowledge of the vector streamfunction (5.53), which just has two functional degrees of freedom, contains all the information of the three velocity components, including the kinematic boundary conditions.

We close by noting that the transport through the solid-earth bottom, $z = \eta_b(x, y)$, vanishes according to equation (5.37) discussed below. We can trivially verify this result for the vertical gauge since

$$\Psi^{\text{vg}}(z = \eta_b) = 0, \quad (5.57)$$

so that $\oint_{\partial S} \Psi^{\text{vg}} \cdot \hat{\mathbf{t}} ds = 0$ on the bottom.

Comments on the vertical gauge streamfunction

Consider a streamfunction with nonzero components in all three directions

$$\bar{\Psi} = \hat{\mathbf{x}} \bar{\Psi}_1 + \hat{\mathbf{y}} \bar{\Psi}_2 + \hat{\mathbf{z}} \bar{\Psi}_3. \quad (5.58)$$

Following Section 5.5.1, introduce a gauge transformation so that

$$\Psi = \bar{\Psi} + \nabla \lambda. \quad (5.59)$$

⁶We expose the functional dependencies in equations (5.53) and (5.54), as it can be useful when first encountering these equations. Otherwise, we typically use a more terse notation.

Is it possible to remove one of the components of $\bar{\Psi}$? For example, can we find a λ so that Ψ is a horizontal vector and is thus a vertical gauge streamfunction? For that to occur we need, at each time instance, to satisfy

$$\nabla \lambda(x, y, z) = -\hat{z} \bar{\Psi}_3(x, y, z). \quad (5.60)$$

This equation is not generally solvable since the gradient of a function, $\lambda(x, y, z)$, has vector components in all three directions rather than just in the vertical. We conclude that the vertical gauge streamfunction is not the result of a gauge transformation from a streamfunction of the form (5.58). Even so, it is a legitimate streamfunction, as noted by the above proof that $\mathbf{v} = \nabla \times \Psi^{\text{vg}}$.

5.6 Evolution of volume and area

In this section we develop kinematic equations for the evolution of volume and area within a non-divergent flow, starting with a material region and then considering an arbitrary region.

5.6.1 Material volumes and areas

As shown by equation (5.2), the volume of a fluid element remains constant in a non-divergent flow. Correspondingly, a fluid region moving with the velocity field maintains a constant volume

$$\frac{d}{dt} \int_{\mathcal{R}(\mathbf{v})} dV = \int_{\mathcal{R}(\mathbf{v})} \frac{D(\delta V)}{Dt} = \int_{\mathcal{R}(\mathbf{v})} (\nabla \cdot \mathbf{v}) dV = \oint_{\partial \mathcal{R}(\mathbf{v})} \mathbf{v} \cdot \hat{\mathbf{n}} dS = 0. \quad (5.61)$$

The appearance of a material time derivative on the inside of the integral arises since the integral is computed following fluid particles whose trajectories define integral curves of the flow (see Section 4.2.7). Likewise, following from the area element equation (2.157), the area of a region moving with a two-dimensional non-divergent flow remains materially constant

$$\frac{d}{dt} \int_{\mathcal{S}(\mathbf{v})} dS = \int_{\mathcal{S}(\mathbf{v})} \frac{D(\delta S)}{Dt} = \int_{\mathcal{S}(\mathbf{v})} (\nabla \cdot \mathbf{u}) dS = \oint_{\partial \mathcal{S}(\mathbf{v})} \mathbf{u} \cdot \hat{\mathbf{n}} ds = 0. \quad (5.62)$$

This area preservation property is illustrated in Figure 5.4, in which a two-dimensional non-divergent flow is seen to deform an initially square patch of fluid while retaining a constant area for the patch.

5.6.2 Arbitrary volume and area

We make use of the Leibniz-Reynolds transport theorem from Section 4.2.4 to develop the evolution equation for the volume of an arbitrary region. In particular, equation (4.45) gives

$$\frac{d}{dt} \left[\int_{\mathcal{R}} dV \right] = \oint_{\partial \mathcal{R}} \mathbf{v}^{(b)} \cdot \hat{\mathbf{n}} dS. \quad (5.63)$$

This result holds for both divergent and non-divergent flows. But for non-divergent flows we can go one step further by noting that

$$0 = \int_{\mathcal{R}} \nabla \cdot \mathbf{v} dV = \oint_{\partial \mathcal{R}} \mathbf{v} \cdot \hat{\mathbf{n}} dS. \quad (5.64)$$

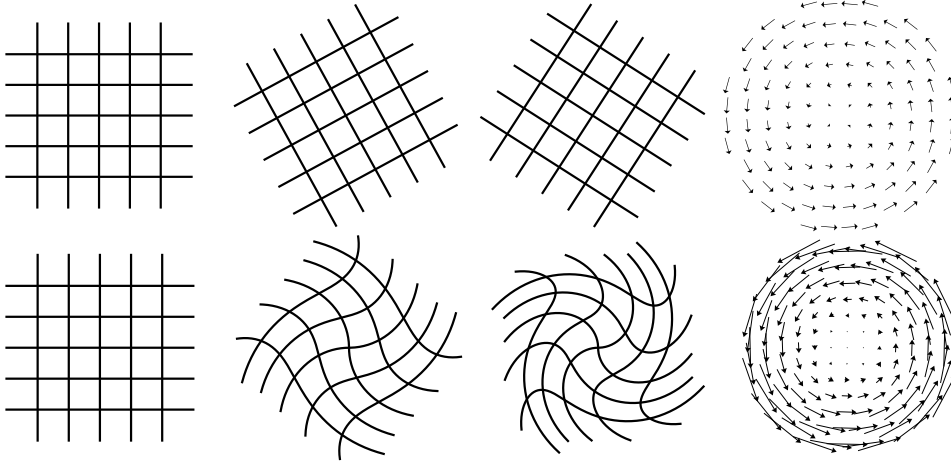


FIGURE 5.4: Illustrating the rotation and straining of fluid patches in a two-dimensional circular and non-divergent flow with non-dimensional velocity, $\mathbf{v} = f(|\mathbf{x}|) \hat{\mathbf{z}} \times \mathbf{x} = f(|\mathbf{x}|) (x \hat{\mathbf{y}} - y \hat{\mathbf{x}}) = f(|\mathbf{x}|) \hat{\vartheta}$, where $\mathbf{x} = x \hat{\mathbf{x}} + y \hat{\mathbf{y}}$ is the position vector for a fluid particle relative to the origin (at center of the panels), and $\hat{\vartheta}$ is the angular unit vector pointed counter-clockwise relative to the positive x -axis. As discussed in Section 5.6, the area of each fluid patch remains fixed as it moves with the non-divergent flow. The top row shows a rigid rotational flow (pure rotation with zero strain) with $f(|\mathbf{x}|) = 1$, with time increasing to the right and with the right-most column showing the rigid rotating fluid flow. The bottom row shows the result from a rotating and straining flow with $f(|\mathbf{x}|) = \sqrt{x^2 + y^2}$. Thanks to Kentaro Hanson for providing the Python notebook to generate the grid advection panels.

Importantly, this result holds only when integrating around the boundary of the closed volume, $\partial\mathcal{R}$. It does not necessarily mean that $\mathbf{v} \cdot \hat{\mathbf{n}} = 0$ holds at every point along the boundary. Indeed, when the boundary is time dependent, then $\mathbf{v} \cdot \hat{\mathbf{n}} \neq 0$ generally holds along the boundary.

Making use of equation (5.64) allows us to write

$$\frac{d}{dt} \left[\int_{\mathcal{R}} dV \right] = \oint_{\partial\mathcal{R}} \mathbf{v}^{(b)} \cdot \hat{\mathbf{n}} dS = - \oint_{\partial\mathcal{R}} (\mathbf{v} - \mathbf{v}^{(b)}) \cdot \hat{\mathbf{n}} dS. \quad (5.65)$$

This result is identical to the mass budget equation (4.47) for the special case of a constant reference density appropriate for a Boussinesq ocean. The dia-surface transport, $(\mathbf{v} - \mathbf{v}^{(b)}) \cdot \hat{\mathbf{n}} dS$, measures the volume per time crossing the boundary of the region, whether that region has a static or moving boundary. For example, if the boundary is the ocean free surface, then we can make use of the surface kinematic boundary condition (5.4).

5.7 Meridional-depth circulation

Geophysical fluid flows are generally three-dimensional. However, it is sometimes useful to summarize aspects of that flow by integrating the mass transport over one of the directions. A common approach is to integrate over the zonal direction either between two solid-wall boundaries (as in an ocean basin) or over a periodic domain (as in the atmosphere or within the Southern Ocean). Doing so leaves a two-dimensional transport in the meridional-depth plane

$$V^\rho = \int_{x_1}^{x_2} \rho v dx \quad \text{and} \quad W^\rho = \int_{x_1}^{x_2} \rho w dx, \quad (5.66)$$

where

$$x_1 = x_1(y, z) \quad \text{and} \quad x_2 = x_2(y, z) \quad (5.67)$$

are expressions for the zonal boundaries as a function of (y, z) , with Figure 5.5 offering a schematic. In some cases the zonal direction is periodic, as in the case of the global zonally integrated circulation in the atmosphere or for the Drake Passage latitudes in the Southern Ocean. In such cases we can dispense with x_1 and x_2 as the integration extends around the periodic domain. In other cases the basin has zonal boundaries, as in the Atlantic and Indian-Pacific oceans, and as depicted in Figure 5.5. In this section we derive the **meridional-depth streamfunction** for the zonally integrated flow, with a streamfunction available when the zonally integrated flow is non-divergent.

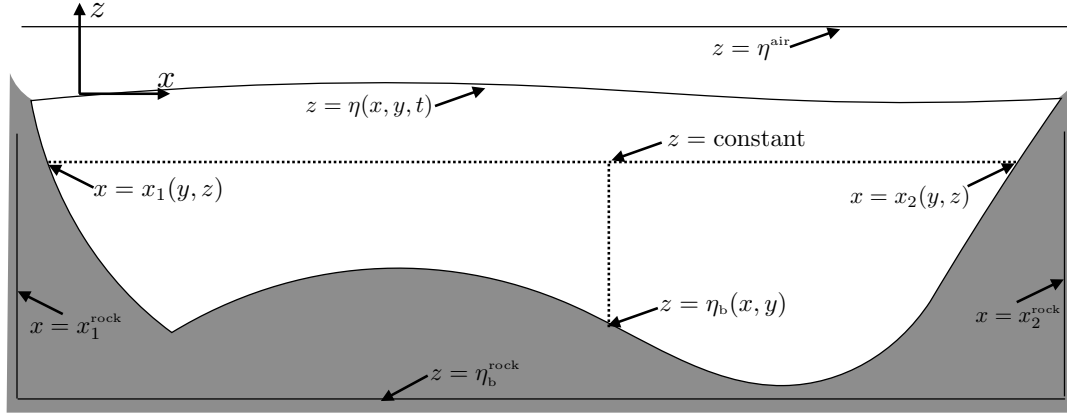


FIGURE 5.5: Geometry needed to compute the **meridional-depth streamfunction**. The zonal boundaries are written $x = x_1(y, z)$ and $x = x_2(y, z)$, which are generally functions of latitude and vertical position. The bottom is written as $z = \eta_b(x, y)$ and the vertical position of an arbitrary constant depth surface is written $z = \text{constant}$. We also display the constant zonal positions, $x_{1,2}^{\text{rock}}$, which are fully within the rock, as well as the bottom position, η_b^{rock} , which is also within the rock. These rock coordinates allow us to dispense with much of the kinematic formalities needed to compute the streamfunction, so long as the fluid flow taken as zero inside the rock.

5.7.1 The zonally integrated transport is non-divergent

By writing the functions $x_1(y, z)$ and $x_2(y, z)$, we must assume that the normal direction along the boundary everywhere has a nonzero and single-signed projection in the \hat{x} direction. If that is indeed the case (we dispense with this assumption below), then we can write the normal direction as

$$\hat{n}_i = \frac{\nabla(x - x_i)}{|\nabla(x - x_i)|} = \frac{\hat{x} - \hat{y}\partial_y x_i - \hat{z}\partial_z x_i}{\sqrt{1 + (\partial_y x_i)^2 + (\partial_z x_i)^2}}, \quad (5.68)$$

for boundaries $i = 1, 2$. Furthermore, the no-normal flow boundary condition at the bottom (Section 3.6.1) takes on the form

$$\mathbf{v} \cdot \hat{n}_i = 0 \implies u = v\partial_y x_i + w\partial_z x_i \quad \text{at } x = x_i(y, z). \quad (5.69)$$

We make use of this boundary condition in this section to prove that the zonally integrated flow is non-divergent.

To see how to create a streamfunction, consider the zonal integrated area transport for a non-divergent flow⁷

$$V(y, z, t) = \int_{x_1(y, z)}^{x_2(y, z)} v(x', y, z, t) dx' \quad \text{and} \quad W(y, z, t) = \int_{x_1(y, z)}^{x_2(y, z)} w(x', y, z, t) dx'. \quad (5.70)$$

⁷The case for a steady compressible flow follows analogously since in that case $\nabla \cdot (\rho \mathbf{v}) = 0$, in which case we would consider $(\rho v, \rho w)$ rather than (v, w) .

Taking the meridional derivative of the meridional transport, and making use of Leibniz's rule and the non-divergence condition, leads to

$$\frac{\partial V}{\partial y} = \frac{\partial}{\partial y} \left[\int_{x_1}^{x_2} v(x', y, z) dx \right] \quad (5.71a)$$

$$= v(x_2) \partial_y x_2 - v(x_1) \partial_y x_1 + \int_{x_1}^{x_2} \frac{\partial v}{\partial y} dx \quad (5.71b)$$

$$= v(x_2) \partial_y x_2 - v(x_1) \partial_y x_1 - \int_{x_1}^{x_2} \left[\frac{\partial u}{\partial x} + \frac{\partial w}{\partial z} \right] dx \quad (5.71c)$$

$$= -[u - v \partial_y x - w \partial_z x]_{x=x_2} + [u - v \partial_y x - w \partial_z x]_{x=x_1} - \frac{\partial}{\partial z} \int_{x_1}^{x_2} w(x', y, z) dx \quad (5.71d)$$

$$= -\frac{\partial W}{\partial z}. \quad (5.71e)$$

To reach the final equality we made use of the no-normal flow boundary condition in the form of equation (5.69), so that the boundary terms vanish identically. We thus conclude that the zonally integrated transport is non-divergent

$$\frac{\partial V}{\partial y} + \frac{\partial W}{\partial z} = 0. \quad (5.72)$$

5.7.2 Meridional-depth streamfunction

As a consequence of the non-divergence condition (5.72), we can introduce a meridional-depth streamfunction

$$\Psi(y, z, t) = - \int_{\eta_b^{\text{rock}}}^z V(y, z', t) dz' = - \int_{\eta_b^{\text{rock}}}^z \left[\int_{x_1(y, z')}^{x_2(y, z')} v(x', y, z', t) dx' \right] dz', \quad (5.73)$$

whose derivatives specify the zonally integrated flow. An idealized version of the meridional-depth circulation is shown in Figure 5.6, with this circulation in the form of an overturning cell. Note that the z dependence for the streamfunction (5.73) arises just from the upper limit of the vertical integral. Furthermore, the lower limit of $z = \eta_b^{\text{rock}}$ is a spatial constant that is chosen so that the lower limit on the integral is beneath the fluid anywhere in the full domain, with the convention that there is zero transport for any region below the fluid bottom (i.e., no fluid transport in rock). This specification for the lower integration limit ensures that the streamfunction has its spatial dependence just on (y, z) . We further discuss this extension into the rock in Section 5.7.4.

5.7.3 Verifying that Ψ is a streamfunction

It is a useful exercise to verify that Ψ as defined by equation (5.73) is indeed a streamfunction for the zonally integrated flow. Suppressing the time dependence for notational brevity, we first show that

$$\frac{\partial \Psi}{\partial z} = -\frac{\partial}{\partial z} \left[\int_{\eta_b^{\text{rock}}}^z V(y, z') dz' \right] = -V(y, z), \quad (5.74)$$

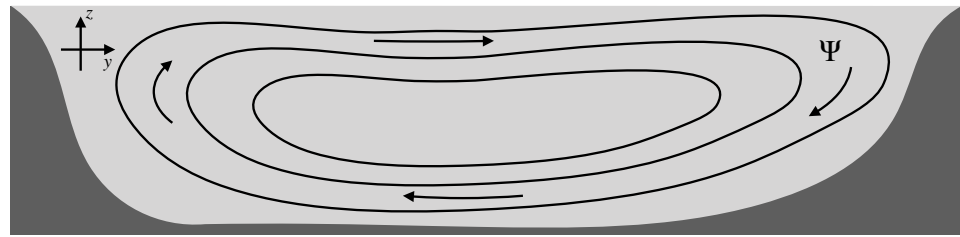


FIGURE 5.6: An idealized depiction of a steady meridional-depth overturning circulation for the zonally integrated flow. Shown here are streamlines (isolines of constant Ψ) for the zonally integrated flow between two solid boundaries or over a zonally periodic domain. The flow is assumed to be non-divergent, as per equation (5.72). In the upper reaches of the fluid, flow moves northward (positive y), with downward motion as it reaches the northern boundary, then southward motion at depth and eventual return towards the surface near the southern boundary.

where we used Leibniz's rule and noted that only the upper integration limit is a function of z . For the meridional derivative we have

$$\frac{\partial \Psi}{\partial y} = - \int_{\eta_b^{\text{rock}}}^z \frac{\partial V(y, z')}{\partial y} dz' = \int_{\eta_b^{\text{rock}}}^z \frac{\partial W(y, z')}{\partial z'} dz' = W(y, z), \quad (5.75)$$

where we used the non-divergent condition (5.72), and we also set

$$W(z = \eta_b^{\text{rock}}) = 0, \quad (5.76)$$

which follows from our convention that η_b^{rock} is below the deepest fluid region. Also, we are able to move the $\partial/\partial y$ derivative across the lower limit of the integral since η_b^{rock} is a constant. We have thus shown that Ψ is a streamfunction since its derivatives equal to the zonally integrated flow.

To evaluate the streamfunction (5.73) at the ocean surface, $z = \eta(x, y, t)$, we follow a method similar to how we deal with the bottom. Namely, introduce a constant η^{air} that is larger than any value of $\eta(x, y, t)$ and with the convention that the transport is zero in regions above the ocean surface. In this case the streamfunction computed across the full depth of the domain is given by minus the net meridional transport across the chosen latitude

$$\Psi(y, z = \eta^{\text{air}}) = - \int_{\eta_b^{\text{rock}}}^{\eta^{\text{air}}} V dz' = - \int_{\eta_b^{\text{rock}}}^{\eta^{\text{air}}} \left[\int_{x_1}^{x_2} v dx \right] dz'. \quad (5.77)$$

Volume conservation means that this transport vanishes in the steady state but it is generally nonzero in the presence of transients or boundary volume fluxes.

5.7.4 Generalizing to arbitrary domains

The method of extending the integration into the rock, and thus transforming a spatially dependent integration limit to a constant, serves to capture the flow while simplifying the practical calculation of the streamfunction. Indeed, it is a necessary method for computing the streamfunction in realistic domains such as those where the zonal boundaries are not monotonic functions of latitude or depth. A further generalization is found by introducing zonal rock coordinate values, $x_{1,2}^{\text{rock}}$, which are fully outside of the ocean fluid domain as depicted in Figure 5.5. Making use of these values allows us to write the streamfunction (5.73) in the equivalent

form

$$\Psi(y, z, t) = - \int_{x_1^{\text{rock}}}^{x_2^{\text{rock}}} \left[\int_{\eta_b(x', y)}^z v(x', y, z', t) dz' \right] dx'. \quad (5.78)$$

Relative to equation (5.73), we moved the zonal integral to the outside and vertical integral to the inside. Reference to Figure 5.5 offers a pictorial explanation for why this integral is identical to equation (5.73). The streamfunction expression (5.78) offers a more suitable framework for studying circulation partitioned according to surfaces of constant generalized vertical coordinate rather than constant depth. That formulation requires kinematics arising from use of a [generalized vertical coordinate](#), with its discussion provided in VOLUME 3.

5.7.5 $\Psi(y, z)$ does not generally delineate particle pathlines

In Section 1.8 we showed that a fluid particle pathline equals to a streamline when the flow is steady, and then in Section 5.4.1 we showed that streamfunction isolines are streamlines. One might then be led to infer that for a steady flow, the meridional-depth streamfunction delineates fluid particle pathlines in the y - z plane. That inference, however, is generally wrong. The reason is that that zonal integration removes spatial degrees of freedom that can hide crucial flow properties.

Two examples are the Ferrel Cell in the atmosphere ([Andrews et al., 1987](#)) and overturning circulation in the Southern Ocean ([Döös and Webb, 1994](#)) (see [Karoly et al. \(1997\)](#) for a unified discussion of their streamfunctions). For both of these circulations, fluid particles in the fluid interior are mostly confined to constant potential density or specific entropy surfaces. Since these surfaces are not flat, and generally have slopes in the zonal direction, then closed north-south motion on such surfaces can appear as closed isolines when projected into the meridional-depth plane. The accumulation of such motions on vertically stacked potential density surfaces creates a single closed meridional-depth streamfunction contour. This closed streamfunction contour suggests that fluid particle motion extends from near the top of the fluid column to near the bottom of the fluid column. In fact, no such motion occurs for a single fluid particle since the potential density surfaces generally do not extend from the top to bottom of the column.

This example motivates the study of overturning circulation as projected onto potential density coordinates (for the ocean) or isentropic coordinates (for the atmosphere). The associated circulation streamfunctions expose flow properties that are complementary to the meridional-depth streamfunction. We postpone the development of such streamfunctions until VOLUME 3, after developing the kinematics of a [generalized vertical coordinate](#).

5.8 Kinematic free surface equation

We here derive the volume budget over a column of fluid. This budget provides a kinematic expression for the free surface evolution in a non-divergent flow.

5.8.1 Derivation

Vertically integrate the constraint, $\nabla \cdot \mathbf{v} = 0$, over the depth of an ocean column, from $z = \eta_b(x, y)$ at the bottom to $z = \eta(x, y, t)$ at the free surface and use the bottom and surface kinematic

boundary conditions. This calculation yields

$$0 = \int_{\eta_b}^{\eta} \nabla \cdot \mathbf{v} dz \quad (5.79a)$$

$$= w(\eta) - w(\eta_b) + \int_{\eta_b}^{\eta} \nabla \cdot \mathbf{u} dz \quad (5.79b)$$

$$= w(\eta) - w(\eta_b) + \nabla \cdot \left[\int_{\eta_b}^{\eta} \mathbf{u} dz \right] - \mathbf{u}(\eta) \cdot \nabla \eta + \mathbf{u}(\eta_b) \cdot \nabla \eta_b \quad (5.79c)$$

$$= [w(\eta) - \mathbf{u}(\eta) \cdot \nabla \eta] - [w(\eta_b) - \mathbf{u}(\eta_b) \cdot \nabla \eta_b] + \nabla \cdot \left[\int_{\eta_b}^{\eta} \mathbf{u} dz \right], \quad (5.79d)$$

where we made use of Leibniz's Rule to move the horizontal divergence outside of the integral. We now make use of the surface kinematic boundary condition (5.5) and the bottom no-flow condition

$$w(\eta) - \mathbf{u} \cdot \nabla \eta = -Q_m / \rho_o + \partial_t \eta \quad z = \eta \quad (5.80a)$$

$$w = \mathbf{u} \cdot \nabla \eta_b \quad z = \eta_b \quad (5.80b)$$

to render the free surface equation for a fluid with a non-divergent flow

$$\partial_t \eta = Q_m / \rho_o - \nabla \cdot \mathbf{U}, \quad (5.81)$$

where

$$\mathbf{U} = \int_{\eta_b}^{\eta} \mathbf{u} dz \quad (5.82)$$

is the depth integrated horizontal transport. For the special case of a steady state with zero boundary mass flux, the depth integrated flow is non-divergent

$$\nabla \cdot \mathbf{U} = 0 \quad \text{if } Q_m = 0 \text{ and } \partial \eta / \partial t = 0. \quad (5.83)$$

5.8.2 Comments

Comparing to the surface kinematic boundary condition

Recall that we can write the surface kinematic boundary condition for a non-divergent flow in the special form of equation (5.6). Comparing to the free surface equation (5.81) renders the identity

$$\partial_t \eta - Q_m / \rho_o = -\nabla \cdot \mathbf{U} = \nabla \cdot [(z - \eta) \mathbf{v}], \quad (5.84)$$

where the final expression is evaluated at $z = \eta$ after evaluating the divergence.

Concerning the evolution of sea level

Comparing the free surface equation (5.81) holding for a non-divergent flow to the free surface equation (3.101) holding for a divergent flow indicates that the non-divergent case is missing a contribution from the material changes in density

$$\frac{\partial \eta}{\partial t} = \frac{Q_m}{\rho_o} - \nabla \cdot \mathbf{U} \quad \text{Boussinesq ocean } (\nabla \cdot \mathbf{v} = 0) \quad (5.85a)$$

$$\frac{\partial \eta}{\partial t} = \frac{Q_m}{\rho(\eta)} - \nabla \cdot \mathbf{U} - \int_{\eta_b}^{\eta} \frac{1}{\rho} \frac{D\rho}{Dt} dz \quad \text{non-Boussinesq ocean } (\nabla \cdot \mathbf{v} \neq 0). \quad (5.85b)$$

The material time changes to density arise from mixing and boundary fluxes of buoyancy. The particular absence of an impact from surface buoyancy fluxes means that the free surface in a Boussinesq ocean is not impacted by global thermal expansion, such as that arising from ocean warming. [Greatbatch \(1994\)](#) and [Griffies and Greatbatch \(2012\)](#) provide a recipe for diagnostically addressing this formulation limitation, thus enabling a study of global mean sea level with Boussinesq ocean models.



5.9 Exercises

EXERCISE 5.1: NON-DIVERGENT AND IRROTATIONAL FLOW IN POLAR COORDINATES

Consider the following two-dimensional velocity field written using polar coordinates (VOLUME 1)

$$\mathbf{u}(r, \vartheta) = \hat{\mathbf{r}} U (1 - a^2/r^2) \cos \vartheta - \hat{\boldsymbol{\vartheta}} U (1 + a^2/r^2) \sin \vartheta, \quad (5.86)$$

with U and a constants.

- (a) Show that the flow is non-divergent, $\nabla \cdot \mathbf{u} = 0$.
- (b) Show that the flow is irrotational, $\nabla \times \mathbf{u} = 0$.

EXERCISE 5.2: NON-DIVERGENT FLOW AND TRAJECTORIES

This exercise is based on Q1.8 of [Johnson \(1997\)](#). Consider a fluid particle trajectory given by

$$\mathbf{X}(T) = X_0 e^{\alpha T} \hat{\mathbf{x}} + Y_0 e^{\beta T} \hat{\mathbf{y}} + Z_0 e^{\gamma T} \hat{\mathbf{z}} = X(T) \hat{\mathbf{x}} + Y(T) \hat{\mathbf{y}} + Z(T) \hat{\mathbf{z}}, \quad (5.87)$$

where \mathbf{X}_0 is the initial particle position, and α, β, γ are constants with dimensions of inverse time.

- (a) Show that the Eulerian velocity field, \mathbf{v} , is steady so that it is independent of time, $\mathbf{v}(\mathbf{x})$.
- (b) What condition ensures that the flow is non-divergent, $\nabla \cdot \mathbf{v} = 0$?

EXERCISE 5.3: FLUID PARTICLE DISPLACEMENT IN A WAVE

Consider a two-dimensional non-divergent flow, and assume the zonal flow is constant while the meridional flow is a wave traveling in the zonal direction

$$\mathbf{u} = U \hat{\mathbf{x}} + V \sin(k x - \omega t) \hat{\mathbf{y}}, \quad (5.88)$$

with U, V constant speeds, $k > 0$ is the wavenumber, and $\omega > 0$ is the wave's angular frequency. Assume the initial position for a fluid particle is given by $\mathbf{X}(T=0) = (X_0, Y_0)$.

- (a) Since the flow is horizontally non-divergent, it has a streamfunction, $\mathbf{u} = \hat{\mathbf{z}} \times \nabla \psi$. Determine $\psi(x, y, t)$. Comment on its connection to particle trajectories.
- (b) What is the zonal fluid particle position, $X(T)$, in this flow, where $T = t$ is the time measured in the fluid particle (Lagrangian) reference frame?
- (c) What is the meridional fluid particle position, $Y(T)$, in this flow? Hint: check to be sure the solution satisfies the initial condition. Introduce the wave phase speed when writing the solution, $c = \omega/k > 0$.
- (d) Discuss the trajectory of a fluid particle when the wave's phase speed approaches the background flow speed, $c \rightarrow U$.
- (e) Write the fluid particle trajectory equations in the frame moving with the wave. Hint: to help keep signs correct, it is useful to follow the space-time transformation formalism

used in Section 1.6 for the Galilean transformation, only here we transfer to the frame defined by the wave.

- (f) Express the streamfunction in terms of the wave frame coordinates, $\bar{\psi}(\bar{x}, \bar{y}, \bar{t})$. Comment on its relation to particle trajectories.

EXERCISE 5.4: STREAMLINES FOR CELLULAR FLOW

Sketch the velocity field for this streamfunction

$$\psi(x, y) = A \sin(kx) \sin ly, \quad (5.89)$$

where (k, l) are the zonal and meridional components to the wavevector, respectively. Hint: assume any convenient value for k, l and the amplitude, A , but indicate what values were chosen. Furthermore, show vectors so that the sense of the flow is clear.

EXERCISE 5.5: ZERO NET AREA TRANSPORT THROUGH STATIC CLOSED CURVE

For a two-dimensional non-divergent flow, show that there is zero net area transport of fluid crossing an arbitrary static and simply connected closed curve. Consequently, the area remains unchanged for any closed region moving with the fluid flow. Note that in two space dimensions, the area transport of fluid across a line has dimensions $L^2 T^{-1}$, thus representing an area transport.

EXERCISE 5.6: ZERO NET VOLUME TRANSPORT THROUGH STATIC CLOSED SURFACE

For a three-dimensional non-divergent flow, show that there is zero net volume transport of fluid crossing an arbitrary static and simply connected closed surface within the fluid interior. Note that in three space dimensions, the transport of fluid across a surface has dimensions $L^3 T^{-1}$, thus representing a volume transport.

EXERCISE 5.7: NET FLUID TRANSPORT ACROSS AN ARBITRARY SURFACE

Consider flow in a container with static sides/bottom. Draw an arbitrary static surface, \mathcal{S} , within the fluid from one side of the container to the other as in Figure 5.7. Integrate the fluid volume transport over the surface, $\int_{\mathcal{S}} \mathbf{v} \cdot \hat{\mathbf{n}} d\mathcal{S}$.

- (a) For a non-divergent flow, show that the volume transport, $\int_{\mathcal{S}} \mathbf{v} \cdot \hat{\mathbf{n}} d\mathcal{S}$, vanishes. That is, the net volume transport across the surface is zero.
- (b) Specialize the above result to a horizontal surface so that we see there is zero integrated vertical volume transport across the surface, $\int_{\mathcal{S}} w dx dy = 0$. Discuss these results.
- (c) Rework part (a) for the case of a compressible fluid so that fluid elements conserve their mass rather than their volume, in which case mass continuity is given by equation (3.10)

$$\frac{1}{\rho} \frac{D\rho}{Dt} = -\nabla \cdot \mathbf{v}. \quad (5.90)$$

Again, we are to compute the volume transport across a surface, but now for the case of a compressible flow rather than non-divergent flow.

EXERCISE 5.8: RIGID-BODY ROTATION

Consider a velocity field corresponding to a time-independent rigid-body rotation on a plane

$$\mathbf{u} = \Omega \hat{z} \times \mathbf{x} = \Omega (-y \hat{x} + x \hat{y}), \quad (5.91)$$

where $\Omega > 0$ is a constant rotation rate.

- (a) Compute the relative vorticity, $\boldsymbol{\omega} = \nabla \times \mathbf{u}$.

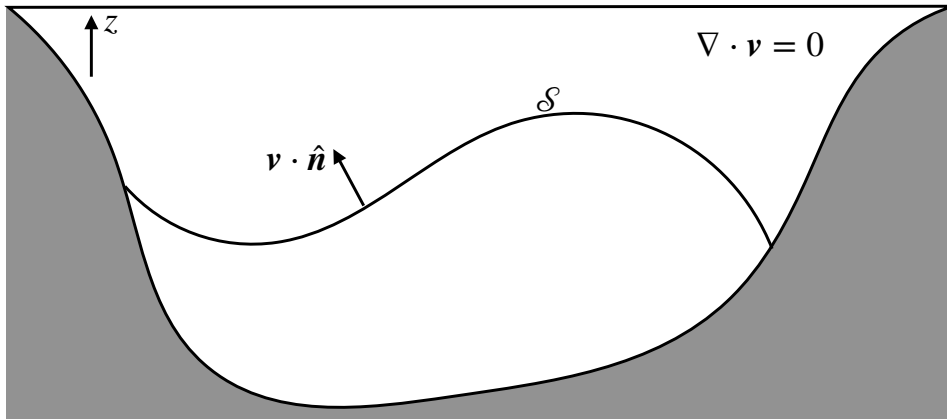


FIGURE 5.7: Schematic for exercise 5.7, whereby we show that the net flow vanishes across a static surface, \mathcal{S} , that extends from one boundary to the other within a non-divergent flow.

- (b) Compute the streamfunction $\mathbf{u} = \hat{z} \times \nabla\psi$. Draw streamfunction contours; i.e., lines of constant streamfunction. Put arrows to orient the flow along the streamlines.
- (c) Describe the geometry of material lines. Hint: since the velocity field is time-independent, material parcel trajectories are coincident with streamlines.

EXERCISE 5.9: ALTERNATIVE FORM OF MERIDIONAL-DEPTH STREAMFUNCTION

In equation (5.73), we introduced the meridional-depth overturning streamfunction

$$\Psi(y, z, t) = - \int_{\eta_b^{\min}}^z V(y, z', t) dz'. \quad (5.92)$$

Show that an alternative streamfunction is given by

$$\Gamma(y, z, t) = \int_{y_s}^y W(y', z, t) dy', \quad (5.93)$$

where y_s is a constant latitude southward of the southern-most latitude where fluid exists. That is, show that

$$\frac{\partial \Gamma}{\partial y} = W \quad \text{and} \quad \frac{\partial \Gamma}{\partial z} = -V. \quad (5.94)$$

EXERCISE 5.10: VOLUME TRANSPORT THROUGH STREAMTUBE ENDS

Recall our discussion of streamtubes in Section 1.8.2 (see in particular Figure 1.5). Show that for a non-divergent flow field, the volume transport (volume per time) through the two streamtube ends balances

$$\int_{\mathcal{S}_1} \mathbf{v} \cdot \hat{\mathbf{n}}_1 d\mathcal{S} + \int_{\mathcal{S}_2} \mathbf{v} \cdot \hat{\mathbf{n}}_2 d\mathcal{S} = 0, \quad (5.95)$$

where $\hat{\mathbf{n}}_1$ and $\hat{\mathbf{n}}_2$ are the outward normals at the two end caps \mathcal{S}_1 and \mathcal{S}_2 . Since the end caps have oppositely directed outward normals, equation (5.95) says that the volume transport entering one streamtube end equals to that leaving the other end. Furthermore, the area of the streamtube is inversely proportional to the local normal velocity, so that flow speeds up when moving through a narrower region of the tube.

The identity (5.95) holds whether the flow is steady or not. Yet for an unsteady flow, streamlines and pathlines are not generally equivalent. So although the volume transport through the two ends is the same, the material contained in that transport is not necessarily

the same. That is, the pathlines of fluid particles are not necessarily parallel to streamlines, so that fluid particles can generally cross the streamtube boundaries.

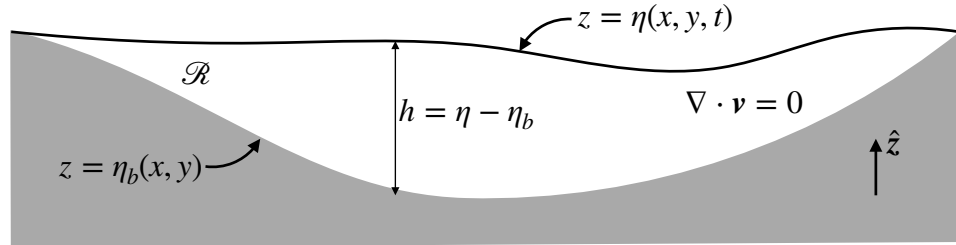


FIGURE 5.8: Schematic for exercise 5.11 with $z = \eta(x, y, t)$ the free surface at the top of the fluid. This exercise shows that the area integrated time tendency for the free surface vanishes in the absence of mass transport across the free surface.

EXERCISE 5.11: AREA AVERAGE OF FREE SURFACE TIME TENDENCY

Consider a non-divergent ocean flow bounded by a free upper surface and a solid bottom. Let $z = \eta_b(x, y)$ be the vertical position of the static bottom, and $z = \eta(x, y, t)$ be the position of the transient free surface, so that the thickness of the layer is $h = -\eta_b + \eta$ (see Figure 5.8). The horizontal extent of the layer is a function of time, and is defined by a vanishing thickness $h = -\eta_b + \eta = 0$ (e.g., ocean water reaching the shoreline). Assume no material crosses either the surface or bottom boundaries, so that both boundaries are material surfaces. Show that the free surface has a time derivative, $\partial\eta/\partial t$, whose area average vanishes. Discuss this result.

EXERCISE 5.12: VOLUME INTEGRAL OF THE NON-DIVERGENT CARTESIAN VELOCITY FIELD

Consider a non-divergent ocean flow in Cartesian coordinates bounded by a free upper surface and a solid bottom over a domain \mathcal{R} . Let $z = \eta_b(x, y)$ be the vertical position of the static bottom, and $z = \eta(x, y, t)$ be the position of the transient free surface as in Figure 5.8. Prove that the domain integral of the velocity is given by

$$\int_{\mathcal{R}} \mathbf{v} dV = \int_{z=\eta} \mathbf{x} (\mathbf{v} \cdot \hat{\mathbf{n}}) d\mathcal{S} = \int_{z=\eta} \mathbf{x} (\partial_t \eta - Q_m / \rho_0) dx dy. \quad (5.96)$$

Hint: Use the [kinematic boundary conditions](#) from Section 5.3. Note that for simplicity we assume Cartesian coordinates.

EXERCISE 5.13: VERIFYING THAT Ψ IS A STREAMFUNCTION

In Section 5.7.3 we verified that the meridional-depth streamfunction, Ψ , is indeed a streamfunction when it is written in the form of equation (5.73). Provide an analogous derivation to show that the alternative expression in equation (5.78) is indeed also a streamfunction. Hint: the derivation closely follows that in Section 5.7.3.



Part II

Thermodynamics

Thermodynamics is a phenomenological discipline focused on relations between macroscopic properties of physical systems, in particular how those properties change as the system transitions from one equilibrium state to another. Thermodynamics is a necessary ingredient for understanding the stability, evolution, and transformation of macroscopic systems, with such topics at the heart of geophysical fluid mechanics. In this part of the book we develop elements of equilibrium thermodynamics relevant to a multi-component fluid in a gravity field. We limit concern to a single phase of matter (liquid or gas), noting that a more complete treatment for geophysical fluids must consider multiple phases and their transitions.

We focus on classical thermodynamics, which means we are generally concerned with **macrostates** of a fluid system, with each macrostate specified by a few macroscopic properties such as temperature, pressure, and matter concentration. For our purposes, a macrostate is synonymous with **thermodynamic state**. This nomenclature must be modified when discussing statistical mechanics and quantum mechanics, whereby the complementary notion of a microstate takes on a far more central role than considered in this book.

The name “thermodynamics” suggests that the discipline concerns how heat moves through a system. Indeed, that topic formed the focus of the subject in the 19th century, as exemplified by [Maxwell \(1872\)](#). However, treatments following the formulation from Gibbs generally focus on energy and entropy, from which temperature is a derived **intensive property**. Energy and entropy are logically distinct concepts that together form the basis for thermodynamics. Energy is a concept borrowed from mechanics. **Internal energy** refers to the energy of microscopic (molecular) degrees of freedom, with this energy the concern of Chapter 6 where we focus on transitions between thermodynamic equilibrium states in the absence of gravity. In Chapter 7 we extend the equilibrium theory to include a geopotential, as relevant for geophysical fluids.

Our study of thermodynamics is incompletely addressed in this part of the book. Further treatment concerns the melding of thermodynamics with the mechanics describing macroscopic fluid motion. After introducing the basics of momentum and mechanical energy for macroscopic motion in Chapter 8, we return to thermodynamics in Chapter 10 as applied to a moving fluid. That study necessarily moves beyond the restrictions of equilibrium thermodynamics considered in Chapters 6 and 7, but only slightly. The key assumption we make in Chapter 10 is that each fluid element is locally within thermodynamic equilibrium. The assumption of **local thermodynamic equilibrium** allows us to bring forward the key facets of equilibrium thermodynamics to the nonequilibrium thermodynamics required for moving fluids.

Thermodynamics is a deep subject whose subtleties rarely cease to puzzle and amaze both the novice and expert. For some perspective, consider the following reflections from two physics giants on the enduring nature of thermodynamics.

Thermodynamics is a funny subject. The first time you go through it, you do not understand it at all. The second time you go through it, you think you understand it, except for one or two points. The third time you go through it, you know you do not understand it, but by that time you are so used to the subject it does not bother you anymore. *Attributed to Arnold Sommerfeld, unknown source*

A theory is the more impressive the greater the simplicity of its premises, the more different kinds of things it relates, and the more extended is its area of applicability. Therefore the deep impression which classical thermodynamics made upon me. It is the only physical theory of universal content concerning which I am convinced that, within the framework of the applicability of its basic concepts, it will never be overthrown. [Einstein \(1970\)](#)

The mathematics in this chapter rely mostly on the basics of partial differentiation, with specific topics discussed in appendices to Chapter 6.

Chapter 6

EQUILIBRIUM THERMODYNAMICS

We here study equilibrium thermodynamics with special emphasis on the needs for geophysical fluids. Thermodynamics is conceptually subtle, thus making this chapter relatively long on words.

CHAPTER GUIDE

Our treatment is consistent with [Reif \(1965\)](#), chapter 2 of [Landau and Lifshitz \(1980\)](#), [Callen \(1985\)](#), and chapter 2 of [Ebeling and Feistel \(2011\)](#). Mathematical tools required for thermodynamics include partial differential calculus from VOLUME 1, and we offer particular mathematical tools in appendices at the end of this chapter.

6.1	Conceptual foundations	166
6.1.1	Thermodynamic equilibrium	167
6.1.2	Exchanges between thermodynamic systems	167
6.1.3	Extensive and intensive properties	169
6.1.4	Thermodynamic configuration space	169
6.1.5	Reversible processes and quasi-static processes	170
6.1.6	Internal energy and total energy	171
6.1.7	Postulates of thermodynamics	171
6.2	Materially closed systems	173
6.2.1	First law of thermodynamics	173
6.2.2	The nature of working and heating	173
6.2.3	Mechanical work from pressure	174
6.2.4	Entropy and the quasi-static transfer of internal degrees of freedom	176
6.2.5	Gibbs' fundamental thermodynamic relation	176
6.2.6	Using the Gibbs relation for computing entropy changes	177
6.2.7	Partial derivatives	178
6.2.8	Entropy and thermodynamic processes	179
6.2.9	Properties of thermodynamic equilibrium	180
6.3	Characterizing materially open systems	181
6.3.1	Scaling of extensive thermodynamic functions	182
6.3.2	Chemical potential and the Euler form	182
6.3.3	Molar mass and molar chemical potential	183
6.3.4	Chemical work and the Gibbs-Duhem relation	183
6.3.5	Gibbs potential	184
6.3.6	Extensive functions of $(T, p, M^{(n)})$	185
6.4	Thermodynamic equilibrium with matter flow	186
6.5	Materially open systems with fixed total mass	187

6.5.1	Matter concentrations	187
6.5.2	Fundamental thermodynamic relation per unit mass	187
6.5.3	Seawater as a binary fluid	188
6.5.4	Further study	189
6.6	Thermodynamic potentials	189
6.6.1	Equations of state	190
6.6.2	Internal energy	190
6.6.3	Entropy	191
6.6.4	Enthalpy	191
6.6.5	Gibbs potential	192
6.6.6	Chemical potential and the Gibbs potential	193
6.6.7	A diagram for quick reference	194
6.7	Response functions	195
6.7.1	Specific heat capacities	195
6.7.2	Thermal expansion coefficient	196
6.7.3	Haline contraction coefficient	196
6.7.4	Speed of sound (acoustic) waves	196
6.8	Maxwell relations for single component fluids	196
6.8.1	Maxwell relation from internal energy	197
6.8.2	Summary of the Maxwell relations	197
6.9	Appendix: partial differential identities	197
6.9.1	Slope of curve defined by $d\Psi = 0$ and $dz = 0$	198
6.9.2	Slope of curve defined by $d\Psi = 0$ and $dx = 0$ or $dy = 0$	198
6.9.3	Triple product identity	198
6.9.4	Further study	199
6.10	Appendix: exact and inexact differentials	199
6.10.1	Exact differentials	199
6.10.2	Inexact differentials	200
6.10.3	Integrating factors	200
6.10.4	An example using the velocity field	200
6.10.5	A hiker climbing a mountain	201
6.11	Appendix: Euler's theorem for homogeneous functions	201
6.12	Appendix: Legendre transformations	202
6.12.1	Operational perspective	202
6.12.2	Geometrical presentation	203
6.12.3	Example	204
6.12.4	Further study	204
6.13	Exercises	204

6.1 Conceptual foundations

In our study of equilibrium thermodynamics, we are concerned with macroscopic fluid systems whose evolution tends toward states whose properties are determined by intrinsic factors rather than depending on memory of previous external influences. When in such **macrostates**, the physical system is said to be in **thermodynamic equilibrium**. When a constraint is modified, the system moves through a sequence of macrostates as it evolves towards its new thermodynamic equilibrium, with the time evolution through such macrostates referred to as a **process**. One aim for thermodynamics is the determination of a new thermodynamic equilibrium after the modification of a constraint.

Any macrostate is comprised of a huge number of microscopic degrees of freedom that comprise a particular **microstate**. The allure of thermodynamics is that it can describe

macroscopic systems, and the process of moving from one thermodynamic equilibria to another, using just a handful of macroscopically measurable properties without directly accessing information about the microstates.

6.1.1 Thermodynamic equilibrium

Equilibrium thermodynamics is the study of physical systems within a **thermodynamic equilibrium**, and how these systems transit from one thermodynamic equilibria to another through a **quasi-static process**. We explore the defining characteristics of thermodynamic equilibrium within this chapter. At a basic level, a system in thermodynamic equilibrium could remain in that state for all time, with details of the equilibrium dependent on the constraints imposed on the system. When constraints are modified, then a system generally transitions to another thermodynamic equilibria. Note that “for all time” is a loaded term. More precisely, we mean “for a time extremely long compared to any time scale relevant to the physical system under consideration”.

A system in thermodynamic equilibrium experiences no time changes to the system’s macroscopic properties. However, a mechanical **steady state** is not necessarily a thermodynamic equilibrium. For example, consider a region of fluid with nonzero heat fluxes yet with no heat flux convergence so the temperature of the region does not change. As we see in this chapter, a temporally constant temperature is a signature of a macroscopic steady state, whereas the flow of heat is the sign of thermodynamic disequilibrium. The distinction is sometimes subtle and always important.

To provide motivation for the study of thermodynamic equilibrium, consider an **isolated system**, defined as a physical system that does not exchange heat, matter, or mechanical forces with its surroundings, though possibly experiencing **body forces** such as from gravity. Given sufficient time, all isolated systems reach their thermodynamic equilibrium consistent with the constraints and forces on the system. Geophysical fluids are routinely exposed to mechanical and thermal interactions with their surrounding environment, and as such as they are not isolated. Even so, it is useful to understand the basic properties of isolated systems and their corresponding thermodynamic equilibrium, as doing so provides the starting point for understanding how systems deviate from thermodynamic equilibrium. Furthermore, a fundamental assumption of thermodynamics applied to moving fluids is that each **fluid element** is in a **local thermodynamic equilibrium**, even while the macroscopic fluid is not in a global thermodynamic equilibrium. Hence, we are motivated to study equilibrium thermodynamics since it forms the foundations for a study of moving fluids, even when those moving fluids are globally far from thermodynamic equilibrium.

6.1.2 Exchanges between thermodynamic systems

In the study of thermodynamics it is important to precisely characterize how a physical system interacts with its surrounding environment through mechanical, thermal, and material interactions and exchanges. An infinitesimal **fluid element**, and the integrated accumulation of fluid elements over finite fluid regions, constitute the physical systems we are concerned with in our study of thermodynamics. Furthermore, we are concerned with fluid elements that routinely interact mechanically with their surroundings so that they are mechanically open; i.e., they feel pressure from the surrounding environment. Hence, we here focus on characterizing how a physical system interacts thermally and materially with its surroundings, with Figure 6.1 depicting the three interactions of concern.

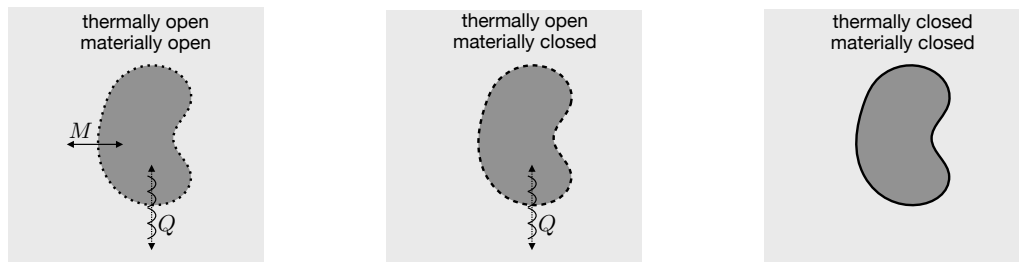


FIGURE 6.1: Depicting the three kinds of thermodynamic exchanges considered in this chapter. The central dark shaded region constitutes the thermodynamic system under consideration, such as a fluid element, with the surrounding lighter shaded region constituting the local surrounding environment, such as other fluid elements. The first panel shows the case where the system and local environment are open to exchanges of both heat (diabatic exchanges) and matter. This is the case holding for a real fluid element, though with the fluid element defined to have constant mass (but not a constant matter content). The middle panel shows the case that is closed to matter exchange but open to heat exchange. This case is not commonly studied in fluid mechanics, but it forms a useful intermediate system for pedagogical purposes in this chapter. The final panel shows the case where the system and environment are closed to heat exchange (adiabatic) and to matter exchange.

- **THERMALLY OPEN (DIABATIC) AND MATERIALLY OPEN:** An open physical system exchanges matter, thermodynamic properties, and mechanical forces with its surrounding environment. All naturally occurring fluid systems are open in this manner.
- **THERMALLY OPEN (DIABATIC) AND MATERIALLY CLOSED:** We have occasion to consider a thermodynamic system that is mechanically and thermally open yet materially closed. Such systems maintain a fixed matter content yet exchange thermal and mechanical properties with their surrounding environment. This case is not commonly studied in fluid mechanics, but it forms a useful intermediate system for pedagogical purposes in this chapter.
- **THERMALLY CLOSED (ADIABATIC) AND MATERIALLY CLOSED:** We sometimes consider a thermodynamic system that is both materially closed and thermally closed and yet mechanically open. In fluid mechanics, such systems constitute **fluid parcels**, defined as infinitesimal regions that maintain fixed matter and fixed thermal properties yet move according to the mechanical forces acting on the parcel. A **perfect fluid** is a continuum of infinitesimal material fluid parcels.

Again, each of the above interactions is mechanically open, so that the system is exposed to mechanical forces, either contact forces such as pressure and friction or body forces as arise from the planetary gravity, Coriolis, and centrifugal accelerations. For pedagogical purposes we first study thermodynamics of fluid elements that are thermally open yet materially closed and then extend to fluid elements that are both thermally and materially open.

As a somewhat overloaded terminology, “adiabatic” in fluid mechanics is often used for a process that is both thermally closed and materially closed. Indeed, it is rare to have a natural process in fluids that is thermally closed yet materially open. The reason is that the exchange of matter typically occurs along with the exchange of heat. Even so, we maintain the distinction for pedagogical purposes in our formulation. That is, adiabatic here just means thermally closed, so that it implies nothing explicitly or implicitly regarding the nature of material exchanges.

6.1.3 Extensive and intensive properties

We distinguish between thermodynamic properties according to whether they are an **extensive property** or an **intensive property**. Extensive properties scale with the size of the system, with examples including mass, internal energy and entropy. Mathematically, we say that functions representing extensive properties scale with a power 1 with the size of the system. We return to this mathematical point in Section 6.11 when discussing the degree of homogeneity for a function.

A **homogeneous fluid** is one in which each **intensive property** is a spatial constant throughout the fluid, with example intensive properties including temperature, pressure, and chemical potential. Hence, intensive properties do not scale with the size of a system, so that intensive properties are scale invariant and thus scale with power 0 as the size of the system changes. In the absence of an externally imposed force field such as gravity, intensive properties are uniform for systems in thermodynamic equilibrium (we show this property in Sections 6.2.9 and 7.2.2). However, as discussed in Section 7.2, hydrostatic balance is realized in thermodynamic equilibrium for a fluid in an externally imposed gravity field, in which case pressure is not uniform.

Extensive and intensive properties come as conjugate pairs in thermodynamics, whereby intensive properties always multiply their conjugate extensive property (e.g., pressure-volume and temperature-entropy) when appearing in the various forms of the first law of thermodynamics. In this chapter, extensive properties are labeled with a superscript e (except for the mass and volume), with this label *not* a tensor index. In Section 6.5 we introduce the internal energy per mass and entropy per mass, as doing so is most convenient when studying thermodynamic systems of fixed mass, such as a fluid element. In this manner we can convert the extensive properties to their specific (per mass) form in which case we drop the e superscript. It is the specific form of extensive properties that provides a straightforward transfer to the study of constant mass fluid elements that move with the fluid flow.

6.1.4 Thermodynamic configuration space

As seen in our study of classical mechanics in VOLUME 1, the physical configuration of a mechanical system is specified by the spatial position and velocity for each particle (Lagrangian mechanics), or equivalently the spatial positions and momenta (Hamiltonian mechanics). An equilibrium thermodynamic system is specified by a suite of continuous thermodynamic properties that define coordinates for a point within **thermodynamic configuration space**, also referred to as the thermodynamic state space. Each point in thermodynamic configuration space specifies a particular thermodynamic equilibrium state, and it makes no statement about the geographical positions of the material.¹ Paths within thermodynamic configuration space are built from the **locus** of infinitesimal quasi-static processes that lead from one equilibrium state to another. Processes that are not quasi-static are not represented in thermodynamic configuration space. Note that we commonly depict thermodynamic configuration space using diagrams with orthogonal axes for the thermodynamic properties. However, there is no notion of distance or angle between points in thermodynamic configuration space since there is no **metric** tensor. Mathematically, we say that thermodynamic configuration space comprises a **differentiable manifold**.²

¹We follow Section 4.2 of [Callen \(1985\)](#) in this presentation of thermodynamic configuration space.

²A summary of the mathematical structure of equilibrium thermodynamics can be found in [this online tutorial from Salamon et al.](#) Note that there are some formulations of thermodynamics that do introduce a metric through properties of the entropy. In so doing, these formulations transform the differentiable manifold to

6.1.5 Reversible processes and quasi-static processes

We here introduce two canonical processes that form the basis for much of our thinking about how a physical system transitions between two thermodynamic equilibria.

Reversible processes have zero net change to entropy

In our discussion of time reversal in VOLUME 1, we noted that classical particle motion is time reversal symmetric in the absence of friction. Indeed, mechanically reversible processes have no physical means to distinguish the direction of time. Hence, an animation of the motion looks sensible when viewed either forward or backward in time.

We here extend the notion of mechanical reversibility to thermodynamic processes. Namely, a thermodynamically **reversible process** can traverse an infinitesimal path through thermodynamic configuration space in either direction. It follows that a reversible process continuously moves between thermodynamic equilibria, which in turn means that the **locus** of reversible processes traces out a continuous path through thermodynamic configuration space. As seen in Section 6.2.8, the net entropy of a physical system plus its surrounding environment remains unchanged by reversible processes, whereas irreversible processes are characterized by an increase in the net entropy.

Quasi-static processes allow for nonzero net change to entropy

Like a reversible process, a **quasi-static process** moves continuously between two infinitesimally close thermodynamic equilibrium states, so the locus of quasi-static processes traces out a path in thermodynamic configuration space. However, a quasi-static process can be either reversible or irreversible. If a quasi-static process is irreversible, then its path in thermodynamic configuration space is in a direction that increases the net entropy of the system plus environment, with this sign-definite entropy increase one statement of the **second law of thermodynamics**. In this manner, all reversible processes are quasi-static, and yet not all quasi-static processes are irreversible. Stated differently, quasi-static describes the kinematic character of the process (infinitesimally slow, near-equilibrium), and reversible adds a restriction that the process generates no net entropy.

A quasi-static process is fully defined by its continuous path through thermodynamic configuration space. Hence, it does not involve time or rates of change. Evidently, a quasi-static process is not a real physical process. However, we can use a real physical process to approximate a quasi-static process, so long as the quasi-static process has a monotonically nondecreasing entropy. For example, consider a quasi-static path that moves from point *A* to point *B* in thermodynamic configuration space. Approximating this path with a real physical process involves intermediate states that are not necessarily in thermodynamic equilibrium, so that the intermediate states are not representable by points in a thermodynamic configuration space. The accuracy of the approximation is a function of the rate to which thermodynamic equilibrium is approached, which itself is a function of the degree to which constraints are modified as the real physical system moves from *A* to *B*.

a Riemannian manifold. There are tradeoffs when doing so, with [Andresen et al. \(1988\)](#) offering a survey of the tradeoffs. Here, we follow the geometric approach of Gibbs as articulated in the book by [Callen \(1985\)](#).

Thermodynamic equilibrium is required to define thermodynamic properties

We are afforded the means to unambiguously measure thermodynamic properties (e.g., temperature, pressure, chemical potential) only when a physical system is in thermodynamic equilibrium. Hence, when a system traverses a quasi-static path through thermodynamic configuration space, its properties are well defined, whereas the properties are fuzzy when a system is out of thermodynamic equilibrium. This importance placed on thermodynamic equilibrium is of clear concern when applying thermodynamics to a moving geophysical fluid, in which case the fluid is generally far from equilibrium. To make headway, however, we introduce the hypothesis of [local thermodynamic equilibrium](#), which is the foundation upon which equilibrium thermodynamics is extended to evolving continuous media such as a fluid.

6.1.6 Internal energy and total energy

In the Prologue to this book (see VOLUME 1), we presented elements of the continuum approximation, where we emphasized the huge number of microscopic (molecular) degrees of freedom that are averaged over when describing a fluid as a continuous media. [Internal energy](#) embodies the energy of microscopic degrees of freedom not explicitly considered in a macroscopic continuum treatment. Internal energy is not readily accessed nor harnessed, which contrasts to the mechanical energy of macroscopic motion.

For a simple [ideal gas](#) (Section 7.5), internal energy arises from the translational kinetic energy of molecular motion, as well as degrees of freedom associated with rotation and vibration. Kinetic theory applied to a simple ideal gas suggests that we conceive of internal energy as [thermal energy](#). That is, we idealize molecules as point masses whose kinetic energy is directly related to temperature, and with the internal energy of an ideal gas directly proportional to temperature. However, for a general fluid, particularly for liquids, the internal energy is more than a measure of the kinetic energy of molecules, as real molecules exhibit intermolecular potential energy arising from molecular interactions.

In general, the concept of internal energy is rather slippery. We are thus motivated to sidestep internal when getting serious about quantitative notions, such as when studying energetics of fluid flow in Chapter 10. We do so by appealing to the conservation of [total energy](#) as postulated in Section 6.1.7. Even so, to lay the foundations we largely focus on internal energy in this chapter.

6.1.7 Postulates of thermodynamics

Thermodynamics is not a first principles theory, though it does have its roots in statistical mechanics. We follow [Callen \(1985\)](#) by building thermodynamics from a set of postulates from which deductive results are derived. The following postulates render a logical basis for the subject, with the bulk of this chapter and Chapter 7 exemplifying these postulates and developing implications.³

- ★ THERMODYNAMIC EQUILIBRIUM: There exists states of [thermodynamic equilibrium](#) that are completely characterized macroscopically by a few extensive properties, including internal energy, volume, and mass (or mole number). For each thermodynamic equilibrium there exists a scalar intensive property, called the [thermodynamic temperature](#), or more

³The interested reader may wish to consider the conceptually distinct approach of [Reif \(1965\)](#), who develops thermodynamics from a statistical physics perspective. The postulational approach is further pursued by [Lieb and Yngvason \(2000\)](#) and [Thess \(2011\)](#).

briefly the temperature, that is uniquely defined. Furthermore, the temperature has the same value for two systems in thermodynamic equilibrium with one another.

- * **ZEROTH LAW OF THERMODYNAMICS:** When two physical systems, A and B , are each separately in thermodynamic equilibrium with a third system, C , then the systems A and B are also in thermodynamic equilibrium with one another. This property is referred to as the [zeroth law of thermodynamics](#).
- * **MAXIMUM ENTROPY:** [Entropy](#) is an extensive property of a macrostate.⁴ The values assumed by the other extensive properties are those that maximize the entropy over the manifold of constrained thermodynamic equilibrium states. This postulate of [maximum entropy](#) is fundamental to how we determine properties of thermodynamic equilibria.
- * **ENTROPY INCREASES:** The entropy of a composite macroscopic system is additive over the constituent subsystems.⁵ Furthermore, entropy is a continuous and differential function that is a monotonically increasing function of the internal energy. This postulate is fundamental to how we use thermodynamics for composite systems such as a fluid.
- * **TOTAL ENERGY IS CONSERVED:** The total energy of a thermodynamic system is locally (in space and time) conserved while undergoing a thermodynamic process. This property constitutes the [first law of thermodynamics](#). For a macroscopic fluid, total energy is the sum of the internal energy arising from microscopic degrees of freedom plus the mechanical energy of macroscopic degrees of freedom. In this chapter, as well as Chapter 7, we are mostly concerned with internal energy, whereas Chapters 8 and 10 extend the discussion to include mechanical energy. Space and time locality of total energy conservation means that physical processes are not allowed in which total energy disappears from one point in space or time only to reappear at a distant point. As a corollary, we are afforded a local budget equation for total energy, whereby energy is transferred from one form to another and with particular forms of this budget equation a topic of Chapter 10.
- * **THIRD LAW OF THERMODYNAMICS:** Internal energy and entropy are extensive scalar quantities that are finite for finite sized systems and bounded from below. In the limit of zero thermodynamic temperature for single-phase systems (single state of matter), the derivatives of entropy with respect to extensive variables disappear asymptotically. Many take the zero temperature limit to have zero entropy, though statistical fluctuations break this assumption (see page 51 of [Ebeling and Feistel \(2011\)](#) for discussion). We have little direct use for the third law, though it takes on an important role when considering quantum statistical mechanics.⁶

The two postulates concerning entropy (entropy maximum and entropy increasing) constitute the [second law of thermodynamics](#). The following early expressions also appear for the second law.⁷

- Clausius (1850): A cooler object never heats a hotter object.
- Kelvin (1851): There are no heat engines whose only result is to cause a single heat reservoir to lose energy through cooling and perform an equal amount of work.

⁴Energy is well defined for both microstates and macrostates, whereas entropy is only defined for macrostates.

⁵In Exercise 6.1 we see what additivity implies for the functional form of the entropy differences between two equilibrium states.

⁶Section 4.5 of [Lemons \(2013\)](#) provides a pedagogical discussion of some key points related to the third law.

⁷See chapter 1 of [Lemons \(2013\)](#) for more on these expressions of the second law.

Statistical mechanics reveals the statistical nature of entropy and the second law. In Sections 6.2.9 and 7.2.2, we see how entropy provides the basis for determining properties at thermodynamic equilibrium, and for how systems approach equilibrium. We make further use of the second law in Chapter 10 to constrain certain processes acting in a multi-component fluid.

6.2 Materially closed systems

We here apply the foundational concepts from Section 6.1 to develop thermodynamic relations for a materially closed physical system.

6.2.1 First law of thermodynamics

The first law of thermodynamics for a materially closed physical system establishes a relationship between the internal energy of two infinitesimally close thermodynamic equilibrium states, the work done to or by the system, and the thermal energy exchanged between the system and its surrounding environment. The first law takes on the mathematical form

$$dJ^e = dW + dQ \quad \text{materially closed.} \quad (6.1)$$

In this equation, dJ^e is the **exact differential** of the internal energy, measuring the difference in the internal energy between two thermodynamic equilibria. The term dW is the **inexact differential** measuring the change to the internal energy due to work applied to the system (**working**). Finally, dQ is the inexact differential measuring the change to the internal energy due to thermal energy transferred to the system (**heating**). We only consider mechanical work in this book, though note that there are other forms of work such as those arising from electromagnetic forces.

The first law of thermodynamics is a statement of energy conservation for a physical system, where the exact differential of internal energy, dJ^e , arises from working and heating applied to the system or by the system. It is a statement about internal energy differences, with the actual value not determined. It is not a full statement of energy conservation since, in the form of equation (6.1), we have ignored the kinetic energy associated with macroscopic movement and the potential energy due to placement within a force field such as gravity. This assumption is relaxed in Chapter 10, where we include mechanical energy in addition to internal energy, with their sum being the **total energy** of a moving geophysical fluid.

6.2.2 The nature of working and heating

Working and **heating** are both path-dependent (history dependent) thermodynamic processes that transform a system from one thermodynamic state to another. Infinitesimal amounts of working and heating are mathematically represented by an **inexact differential** as denoted by the d symbol. It is remarkable that the first law in equation (6.6) shows that the sum of two inexact differentials equals an exact differential.

The internal energy is a **state function**, meaning that it is a property of the thermodynamic state of a system and it is not a function of the path history taken to reach that state. The path independent nature of changes to internal energy is reflected by its exact differential, dJ^e , appearing in the first law equation (6.1). This is a key property of any thermodynamic state function (there are more introduced later), with its changes computed only through information

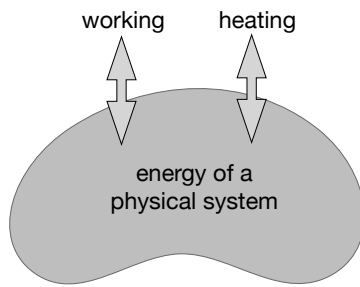


FIGURE 6.2: Working and heating refer to energy transition processes that affect a change in energy of a system. Work is a synonym for the energy change associated with working, and heat is a synonym for the energy change due to heating. Here we depict how working and heating affect the energy of a system. The two-way arrows indicate that working and heating can either increase or decrease the energy, depending on whether working and heating are done on or by the system.

about the initial and final states; no information is needed about the path taken to reach these states.

Working and heating denote actions applied to a system (they are verbs) rather than properties of a system (they are not nouns). As depicted in Figure 6.2, they are energy in transition. The terms “work” and “heat” are often used instead of “working” and “heating”. Indeed, we will often make use of that language in this book, but only in reference to the amount of energy gained or lost through working and heating; i.e., as energy differences. An overly relaxed usage of these terms can spuriously lead one to seek information concerning the “work content” or “heat content” of a physical system. So in summary, working and heating refer to energy transition processes that affect a change in energy of a system. Work is a synonym for the energy change associated with working, and heat is a synonym for the energy change due to heating.

These points are particularly relevant when asking questions about the heat transported by the macroscopic motion of a fluid (with dimensions energy per time and SI units of Watt = Joule per second). One is then led to analyze a heat budget, in which it is tempting to define the “heat content” of a fluid element or fluid region according to its integrated temperature, mass, and heat capacity. But the notion of heat content spuriously conflates a thermodynamic process (heating) with a thermodynamic state property (enthalpy; Section 6.6.4). Furthermore, any definition of heat content (more precisely, the enthalpy) is ambiguous due to the arbitrariness of the temperature scale (e.g., Celsius scale versus Kelvin scale). Only enthalpy differences have a physical meaning in our study of classical thermodynamics.⁸ Therefore, when examining heat transport, care should be exercised if also including the notion of heat content. One way to detect if there is a conceptual error is to ask whether a particular conclusion is modified by changing the temperature scale. If so, then one should revisit assumptions of the analysis since the results might be unphysical unless coupled to relevant qualifiers.

6.2.3 Mechanical work from pressure

As forces do work on a physical system they change its internal energy and mechanical energy. We are here concerned only with the effects on internal energy, though note that mechanical changes that alter internal energy are generally balanced by compensating changes to mechanical energy (see Section 10.6). One way to perform mechanical work is via changes to the volume of

⁸In quantum statistical mechanics, we encounter the third law, largely promoted by Max Planck, in which we ascribe an absolute value for entropy based on its value at zero thermodynamic temperature. See section 4.5 of [Lemons \(2013\)](#) for more on the third law.

a fluid element through the action of pressure (a contact force per area) on the boundary of the fluid element. For example, if a fluid element increases its volume, it must do work against the surrounding environment to overcome the compressive force from pressure.

When volume changes occur quasi-statically, then we can write the **pressure work** in the mathematical form

$$dW = -p dV, \quad (6.2)$$

where p is the pressure that acts on the boundaries of the fluid element. The assumption that the mechanical process is quasi-static allows us to unambiguously define pressure acting on the system, and thus to write equation (6.2) for the work. The negative sign arises since the compression of a fluid element into a smaller volume, $dV < 0$, requires positive mechanical work be applied to the fluid element, $dW > 0$. The mathematical form of pressure work derives from the general form of mechanical work given by

$$\text{work} = \text{force} \times \text{distance} = \text{force}/\text{area} \times \text{distance} \times \text{area} = \text{force}/\text{area} \times \text{volume}. \quad (6.3)$$

Stated alternatively, we note that pressure is a force per unit area acting on a surface, and the product of the surface area and its normal displacement is the volume swept out during a time increment.

We offer the following further points in regards to the expression (6.2) for mechanical work from pressure.

- Let us use some material from our study of pressure in Part III of this volume to further justify equation (6.2) for pressure work. For that purpose, introduce an oriented infinitesimal area, $\hat{n} dS$, with \hat{n} the surface normal direction. The pressure force acting on this area is given by $-p \hat{n} dS$, with the minus sign corresponding to a compressive force. Over an infinitesimal time increment, the work done by pressure to move this area by an increment, dx , is given by

$$-p dx \cdot \hat{n} dS = -p dV, \quad (6.4)$$

where we identified the infinitesimal volume swept out during the time increment as

$$dV = dx \cdot \hat{n} dS. \quad (6.5)$$

- Pressure is an **intensive property** that measures the intensity of a force (per area) that is conjugate to the extensive property, V . In general, work applied to a thermodynamic system, thus leading to a change in the internal energy, takes on the form of an intensive property multiplying the change of an **extensive property**.
- From a mathematical perspective, pressure is the **integrating factor** that connects the **inexact differential**, dW , to the **exact differential**, dV . We summarize the mathematics of inexact differentials in Section 6.10.
- For a **quasi-static process**, pressure changes the internal energy of a fluid through the pressure work according to equation (6.2). As seen in Section 10.2, pressure also changes the kinetic energy of a moving fluid by changing the fluid speed. When combining the internal energy and mechanical energy budgets in Section 10.6, we see how pressure affects the total energy of a fluid element.

- Surface tension acting on fluid interfaces can give rise to mechanical work. We generally ignore surface tension when interested just in scales larger than a few centimeters (see Section 9.9).

6.2.4 Entropy and the quasi-static transfer of internal degrees of freedom

The internal energy of a thermodynamic system can change when the molecular degrees of freedom are energized. For a materially closed system whose internal energy changes in a quasi-static manner, we consider the thermal energy change as relates to entropy changes via

$$dQ = T dS^e \quad \text{materially closed.} \quad (6.6)$$

T is the **thermodynamic temperature** (measured relative to absolute zero) and it is an intensive property whereas S^e is the extensive form of entropy. Entropy is an extensive state function so that T provides the integrating factor connecting the inexact differential, dQ , to the exact differential, dS^e . A nonzero dQ in a geophysical fluid can arise from radiative fluxes external to the fluid element; internal sources from viscous friction; and the exchange of thermal energy through the mixing of fluid properties. Since heating has dimensions of energy, the entropy has dimensions of energy per temperature.

6.2.5 Gibbs' fundamental thermodynamic relation

We summarize the discussion of this section by writing the first law for quasi-static materially closed processes

$$dJ^e = -p dV + T dS^e \quad \text{quasi-static materially closed processes.} \quad (6.7)$$

This equation is known as the **Gibbs relation**, or more commonly the **fundamental thermodynamic relation**, here expressed for quasi-static materially closed processes that connect one thermodynamic equilibrium state to another. That is, Gibbs' fundamental thermodynamic relation is a constraint maintained between macroscopic properties that connect infinitesimally close thermodynamic equilibria via quasi-static processes. Assuming a quasi-static process enables us to write the first law in terms of the intensive properties, p, T , and their conjugate extensive properties, V, S^e , rather than the more general expression (6.1) in terms of the inexact working and heating processes, dW and dQ . Furthermore, the Gibbs relation (6.7) suggests that we interpret minus the pressure as the amount of internal energy required to add one unit of volume to the system while holding entropy fixed. Likewise, temperature is the internal energy required to add one unit of entropy to the system while holding volume fixed.

Since internal energy and entropy are thermodynamic state functions, their difference between any two thermodynamic equilibria can be computed using the Gibbs' relation regardless how the system actually transitioned from one equilibrium state to another. For example, if the system transitions via irreversible processes, we can still compute the difference in internal energy and entropy by imagining the locus of quasi-static processes that connect the two equilibria. This approach is one of the key practical applications of Gibbs' relation, since we generally have no operational means to compute the irreversible working or heating, and yet we can still compute the changes to thermodynamic state functions through assuming the transition occurred via a quasi-static process. Correspondingly, the fundamental thermodynamic relation is an integrable differential equation, with a solution found by performing a path integral along a quasi-static path within thermodynamic configuration space from an initial equilibrium

state to a final equilibrium state. The solution provides the finite difference between the two equilibrium states for one of the extensive properties, internal energy or entropy.

All differentials within the fundamental thermodynamic relation (6.7) are exact differentials of state functions. This property is a result of assuming the thermodynamic processes are quasi-static, in which case we can determine the integrating factors pressure and temperature to thus replace the inexact differentials dW and dQ with exact differentials. Even with the quasi-static restriction, equation (6.7) offers great utility (with its extension to materially open systems given in Section 6.5). We are only concerned with quasi-static changes to fluid elements in this book. Hence, the fundamental thermodynamic relation (6.7) provides the central expression of the first law of thermodynamics for our purposes. In particular, it provides the starting point for our extension in Chapter 10 of the first law to moving fluid elements, in which we replace the exact differential operator, d , with the material time derivative, D/Dt .

It follows from the Gibbs relation (6.7) that the internal energy is a natural function of volume and entropy

$$dJ^e = -p dV + T dS^e \implies J^e = J^e(V, S^e). \quad (6.8)$$

Conversely, the entropy for a materially closed system is naturally a function of volume and internal energy

$$T dS^e = dJ^e + p dV \implies S^e = S^e(V, J^e). \quad (6.9)$$

We see that both of the extensive thermodynamic state properties, J^e and S^e , are functions of extensive properties, with such dependence having implications for the scaling discussed in Section 6.3.1. Furthermore, we note that both J^e and S^e are functions of the volume of a system, but not of the shape. This behavior is strictly only appropriate for fluids, and it ignores effects from interfaces. Both of these assumptions are suitable for our study of geophysical fluid flows.

6.2.6 Using the Gibbs relation for computing entropy changes

Our distinction between quasi-static processes and reversible processes, first introduced in Section 6.1.5, follows the treatments given by [Callen \(1985\)](#) (sections 4.2 and 4.3), [Reif \(1965\)](#) (sections 2.9 and 2.10), and [Lemons \(2013\)](#) (section 1.2). The distinction is particularly important when computing the difference in entropy between equilibrium states as depicted in Figure 6.3. In this figure, any two states can be connected by the locus of infinitesimal quasi-static processes (either reversible or irreversible). For example, equilibrium state C has a higher entropy than states A and B , so state C can only be reached from A or B by irreversible processes. In contrast, states A and B have the same entropy, so they are connected by reversible processes.

How can we compute the entropy difference between equilibrium states? Since entropy is a thermodynamic state property, the entropy difference between two equilibria is path independent. That is, we do not need to be concerned with the actual process used to reach any particular thermodynamic equilibrium state. Rather, we only need to know that the state is in equilibrium. So if we know the thermodynamic properties of two equilibrium states, then we can construct any suitable quasi-static process to connect the two equilibria, such as depicted here between states A and C . Since the processes used to create this path are quasi-static, we can integrate Gibbs' fundamental thermodynamic relation (6.7) along the quasi-static path, thus computing the entropy change. We provide a detailed example of these ideas in Exercise 6.3 by analytically computing the entropy change arising from the free and adiabatic expansion of an ideal gas.

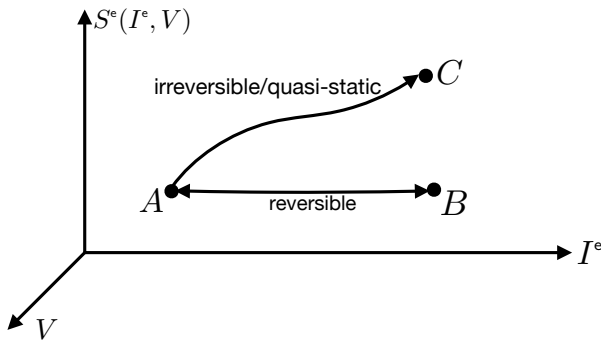


FIGURE 6.3: An example thermodynamic configuration space for an isolated physical system, as defined by the entropy, internal energy, and volume. Each point in thermodynamic configuration space is a particular thermodynamic equilibrium of the system. Here we focus on three equilibrium states, A , B , and C . Since equilibrium states A and B have the same entropy, they can be connected by a path built from the locus of infinitesimal reversible processes, each of which keep entropy unchanged. The straight path shown here between A and B has a double-headed arrow, since reversible processes can proceed in either direction. In contrast, states A and C have different entropies. Hence, the path from A to C shown here is built from the locus of irreversible quasi-static processes that connect infinitesimally close thermodynamic equilibria. The second of thermodynamics says we can only transit from A to C , the direction of increasing entropy, rather than in the opposite direction. So in summary, since thermodynamic configuration space can only depict thermodynamic equilibria, any path drawn in this space is built from the locus of infinitesimal quasi-static processes (that can be either reversible or irreversible). It follows that the difference in thermodynamic state properties for any two points in this space can be computed by integrating the Gibbs fundamental thermodynamic relation (6.7) along a quasi-static path.

6.2.7 Partial derivatives

The fundamental thermodynamic relation (6.8) appears in terms of internal energy, which is written as a natural function of the extensive properties volume and entropy. We arrive at two partial derivative identities by expanding the exact differential of internal energy⁹

$$d\mathcal{I}^e = \left[\frac{\partial \mathcal{I}^e}{\partial V} \right]_{S^e, M} dV + \left[\frac{\partial \mathcal{I}^e}{\partial S^e} \right]_{V, M} dS^e, \quad (6.10)$$

and then identifying this expression with the fundamental thermodynamic relation (6.8) to reveal

$$\left[\frac{\partial \mathcal{I}^e}{\partial S^e} \right]_{V, M} = T \quad (6.11)$$

$$\left[\frac{\partial \mathcal{I}^e}{\partial V} \right]_{S^e, M} = -p. \quad (6.12)$$

Each equation relates an intensive property (right hand side) to the partial derivative of internal energy with respect to an extensive property. Furthermore, since each of the extensive properties is a homogeneous function of degree one, then it follows that the intensive properties are homogeneous functions of degree zero. That is, the intensive properties, T and p , do not scale with the size of the system. Rather, intensive properties are scale invariant. We arrive at analogous partial derivative identities for entropy, $S^e(V, \mathcal{I}^e)$, by expanding its exact differential

⁹The M subscript on the partial derivatives in equation (6.10) refer to the fixing of the matter concentration since the thermodynamic system is assumed to be closed to matter exchange. This constraint is relaxed in Section 6.3.

and then comparing to equation (6.9)

$$\left[\frac{\partial S^e}{\partial J^e} \right]_{V,M} = \frac{1}{T} \quad (6.13)$$

$$\left[\frac{\partial S^e}{\partial V} \right]_{J^e,M} = \frac{p}{T}. \quad (6.14)$$

Recall that partial derivatives are defined with the complement variables held fixed during the differentiation. Hence, so long as we are clear about functional dependence, extra subscripts such as those exposed in equations (6.11)-(6.12) are not needed for the partial derivatives. Nonetheless, traditional thermodynamic notation exposes all of the subscripts in order to remain explicit about the dependent and independent variables. Such notation, though clumsy, can be essential when in the midst of manipulations with thermodynamic potentials and their derivatives.

6.2.8 Entropy and thermodynamic processes

We have already introduced the notions of reversible and irreversible processes in Section 6.1.5. Here we bring summarize these points and connect them to entropy.

A process that increases the net entropy is irreversible

A **reversible process** can, at each stage, go either forward or backward, thus possessing time reversal symmetry. In the absence of non-conservative forces (e.g., friction), Newton's laws of mechanics are reversible. For example, one observes nothing unphysical about the motion of an ideal pendulum with time moving backward rather than forward.¹⁰ A reversible process does not alter the net entropy of a physical system plus its surrounding environment. In contrast, the net entropy changes in the presence of an **irreversible process**, with the **second law of thermodynamics** stating that the net entropy change is positive.

Reversible thermodynamic processes are quasi-static and yet not all quasi-static processes are reversible. For example, a process that involves friction can evolve quasi-statically and yet such processes are irreversible since they increase the net entropy. So quasi-static is a property of how a system changes, whereas reversibility is a statement about changes to both the system and its surrounding environment. Any natural process is irreversible, with irreversibility providing an arrow for time evolution by breaking the symmetry between past and future.

Reversible exchange of heat via heat baths

The exact differential of entropy, when undergoing a quasi-static process in a materially closed system, is given by $dS^e = dQ/T$, with $T > 0$ (recall T is the Kelvin thermodynamic temperature). Evidently, the entropy differential, dS^e , has the same sign as the heating differential, dQ/T . Furthermore, entropy for a materially closed system undergoing quasi-static changes remains unchanged in the absence of heating.¹¹

The idealization of a heat bath allows us to conceive of reversible heating; i.e., heating without change in net entropy for a thermodynamic system plus the heat bath. Heat baths

¹⁰We discuss time-reversal symmetry in VOLUME 1. We also consider time symmetry for the perfect fluid equations (Euler equations) in Exercise 9.6.

¹¹As exemplified by the study of the adiabatic and free expansion of a gas in Exercise 6.3, irreversible changes lead to entropy increases even if the process is adiabatic.

are held at a fixed temperature, which is the idealization of the case when the surrounding environment is arbitrarily larger than the thermodynamic system under consideration. Now imagine exchanging heat between a thermodynamic system and a series of heat baths to progressively alter the system's temperature by the differential, dT . In each exchange of heat, the entropy of the system plus heat bath is constructed to remain unchanged since we are exchanging an equal magnitude of entropy between them

$$dS_{\text{net}}^e = dS_{\text{system}}^e + dS_{\text{bath}}^e = dQ/T - dQ/T = 0. \quad (6.15)$$

To reverse the process, we merely reverse the heat exchanges between the thermodynamic system and the heat baths.

A comment on statistical mechanics

As noted above, when any thermodynamic process occurs irreversibly there is a net increase in entropy of the universe, which is a statement of the second law of thermodynamics. In statistical mechanics, entropy is computed by counting the number of microstates accessible to any given macrostate. Reversible processes do not modify the number of accessible microstates so there is zero change in the entropy. In contrast, irreversible processes increase entropy by increasing the number of accessible microstates.¹²

6.2.9 Properties of thermodynamic equilibrium

Consider two systems labelled¹³ by α and β that are separately in thermodynamic equilibrium with internal energies, \mathcal{I}_α^e , \mathcal{I}_β^e , and volumes, V_α , V_β . Allow these two systems to interact mechanically and thermally, but do not allow for any exchange of matter. Allow the interaction processes to be either reversible or irreversible, but assume the interactions conserve the total internal energy and volume of the combined system. Hence, the system maintains the following constraints during the interaction process

$$d(\mathcal{I}_\alpha^e + \mathcal{I}_\beta^e) = 0 \quad \text{and} \quad d(V_\alpha + V_\beta) = 0. \quad (6.16)$$

When the composite system reaches thermodynamic equilibrium, the entropy maximum postulate forming the second law of thermodynamics (Section 6.1.7) means that

$$dS^e = d(S_\alpha^e + S_\beta^e) = 0 \quad (6.17)$$

for the combined composite system. Importantly, this condition holds only at equilibrium, whereas the constraints (6.16) hold throughout the process of reaching equilibrium. From equation (6.9) we know that entropy is naturally a function of volume and internal energy so that

$$dS^e = \left[\frac{\partial S_\alpha^e}{\partial \mathcal{I}_\alpha^e} \right]_{V_\alpha, M_\alpha} d\mathcal{I}_\alpha^e + \left[\frac{\partial S_\alpha^e}{\partial V_\alpha} \right]_{\mathcal{I}_\alpha^e, M_\alpha} dV_\alpha + \left[\frac{\partial S_\beta^e}{\partial \mathcal{I}_\beta^e} \right]_{V_\beta, M_\beta} d\mathcal{I}_\beta^e + \left[\frac{\partial S_\beta^e}{\partial V_\beta} \right]_{\mathcal{I}_\beta^e, M_\beta} dV_\beta \quad (6.18a)$$

$$= \frac{1}{T_\alpha} d\mathcal{I}_\alpha^e + \frac{p_\alpha}{T_\alpha} dV_\alpha + \frac{1}{T_\beta} d\mathcal{I}_\beta^e + \frac{p_\beta}{T_\beta} dV_\beta \quad (6.18b)$$

¹²The books by [Reif \(1965\)](#) and [Callen \(1985\)](#) provide pedagogical, and somewhat complementary, treatments of statistical thermodynamics.

¹³The labels α and β are not tensor labels. Instead, they merely label the system under consideration.

$$= \left[\frac{1}{T_\alpha} - \frac{1}{T_\beta} \right] dJ_\alpha^e + \left[\frac{p_\alpha}{T_\alpha} - \frac{p_\beta}{T_\beta} \right] dV_\alpha, \quad (6.18c)$$

where we used the partial derivative identities (6.13) and (6.14) for the second equality, and the constraints (6.16) for the final equality. Again, $dS^e = 0$ at thermodynamic equilibrium, and this condition holds for arbitrary and independent dJ_α^e and dV_α . We are thus led to the thermal and mechanical equilibrium conditions

$$T_\alpha = T_\beta \quad \text{and} \quad p_\alpha = p_\beta \quad \text{thermodynamic equilibrium.} \quad (6.19)$$

That is, the temperature and pressure are uniform when the composite system reaches thermodynamic equilibrium.¹⁴

To understand how the two systems thermally approach thermodynamic equilibrium, assume the volumes of the two systems are fixed so that there is no mechanical work from pressure. Furthermore, assume the two systems are initially separated by an adiabatic wall with initial temperatures $T_\alpha^{\text{init}} > T_\beta^{\text{init}}$. Now allow for the flow of heat by switching from an adiabatic wall to a diathermal wall. Since the temperature differs for the two systems, they are mutually out of equilibrium. Heat flows in a manner to bring the two systems into equilibrium, during which time entropy of the composite system increases. At the new equilibrium, temperature is uniform and entropy has reached its maximum within the constraints imposed on the composite system. At a time instant after the wall changes from adiabatic to diathermal, the infinitesimal entropy change takes the form

$$dS^e = \left[\frac{1}{T_\alpha^{\text{init}}} - \frac{1}{T_\beta^{\text{init}}} \right] dJ_\alpha^e > 0, \quad (6.20)$$

where the inequality follows from the second law of thermodynamics (Section 6.1.7). If $T_\alpha^{\text{init}} > T_\beta^{\text{init}}$, then an increase in entropy requires $dJ_\alpha^e < 0$, which means that heat leaves the system α and flows to the system β . Hence, as the composite system approaches thermodynamic equilibrium, heat flows from the region with higher temperature to the region with lower temperature. This result, deduced from the second law of thermodynamics, accords with common experience.

In regards to the time scale for equilibration, note that mechanical equilibrium (equality of pressure) generally arises much sooner than thermal equilibrium (equality of temperature). The reason is that mechanical equilibrium is facilitated by force imbalances that lead to macroscopic motion (e.g., acoustic waves), whereas thermal equilibrium arises from microscopic motion (e.g., molecular diffusion). This time scale separation means that real fluid systems, experiencing forcing and dissipation, are far closer to mechanical equilibrium than thermal equilibrium.

6.3 Characterizing materially open systems

A thermodynamic system is generally open to the transfer of matter across its boundaries. We here summarize methods used to characterize systems and processes that allow for the movement of matter, with extensive use of Euler's theorem for homogeneous functions presented in Section 6.11.

¹⁴As seen in Chapter 7, pressure at thermodynamic equilibrium is not a uniform constant for a system within a gravity field. Rather, pressure is in hydrostatic balance.

6.3.1 Scaling of extensive thermodynamic functions

Both the internal energy, \mathcal{J}^e , and entropy, \mathcal{S}^e , are extensive properties of a fluid system. Consequently, the transfer of matter across the system boundaries leads to an additive change in \mathcal{J}^e and \mathcal{S}^e . The internal energy and entropy thus have their natural functional dependencies (6.8) and (6.9) extended to include the matter content

$$\mathcal{J}^e = \mathcal{J}^e(V, \mathcal{S}^e, M^{(n)}) \quad \text{and} \quad \mathcal{S}^e = \mathcal{S}^e(V, \mathcal{J}^e, M^{(n)}), \quad (6.21)$$

where the $M^{(n)}$ argument is shorthand for the $n = 1, \dots, N$ matter constituents.

What happens when we scale the system by an arbitrary parameter λ ? Under this scale operation, the extensive variables, \mathcal{J}^e , \mathcal{S}^e , as well as the volume, V , and masses, $M^{(n)}$, scale by the same scale factor. The relation (6.21) thus leads to the scaling

$$\lambda \mathcal{J}^e(V, \mathcal{S}^e, M^{(n)}) = \mathcal{J}^e(\lambda V, \lambda \mathcal{S}^e, \lambda M^{(n)}) \quad \text{and} \quad \lambda \mathcal{S}^e(V, \mathcal{J}^e, M^{(n)}) = \mathcal{S}^e(\lambda V, \lambda \mathcal{J}^e, \lambda M^{(n)}), \quad (6.22)$$

thus revealing that $\mathcal{J}^e(V, \mathcal{S}^e, M^{(n)})$ and $\mathcal{S}^e(\lambda V, \lambda \mathcal{J}^e, \lambda M^{(n)})$ are homogeneous functions of degree one. Making use of Euler's theorem (6.135) with $\gamma = 1$ leads to

$$\mathcal{J}^e(V, \mathcal{S}^e, M^{(n)}) = V \left[\frac{\partial \mathcal{J}^e}{\partial V} \right]_{\mathcal{S}^e, M^{(n)}} + \mathcal{S}^e \left[\frac{\partial \mathcal{J}^e}{\partial \mathcal{S}^e} \right]_{V, M^{(n)}} + \sum_{n=1}^N M^{(n)} \left[\frac{\partial \mathcal{J}^e}{\partial M^{(n)}} \right]_{V, \mathcal{S}^e, M^{(m \neq n)}} \quad (6.23a)$$

$$\mathcal{S}^e(V, \mathcal{J}^e, M^{(n)}) = V \left[\frac{\partial \mathcal{S}^e}{\partial V} \right]_{\mathcal{J}^e, M^{(n)}} + \mathcal{J}^e \left[\frac{\partial \mathcal{S}^e}{\partial \mathcal{J}^e} \right]_{V, M^{(n)}} + \sum_{n=1}^N M^{(n)} \left[\frac{\partial \mathcal{S}^e}{\partial M^{(n)}} \right]_{V, \mathcal{J}^e, M^{(m \neq n)}}. \quad (6.23b)$$

These are very special expressions for the internal energy and entropy that are of great use throughout thermodynamics.¹⁵

6.3.2 Chemical potential and the Euler form

We can further massage the results (6.23a) and (6.23b) by making use of the partial derivative identities from Section 6.2.7 to render

$$\mathcal{J}^e = -pV + T\mathcal{S}^e + \sum_{n=1}^N M^{(n)} \left[\frac{\partial \mathcal{J}^e}{\partial M^{(n)}} \right]_{V, \mathcal{S}^e, M^{(m \neq n)}} \quad (6.24)$$

$$T\mathcal{S}^e = pV + \mathcal{J}^e + \sum_{n=1}^N T M^{(n)} \left[\frac{\partial \mathcal{S}^e}{\partial M^{(n)}} \right]_{V, \mathcal{J}^e, M^{(m \neq n)}}. \quad (6.25)$$

Self-consistency requires

$$\left[\frac{\partial \mathcal{J}^e}{\partial M^{(n)}} \right]_{V, \mathcal{S}^e} = -T \left[\frac{\partial \mathcal{S}^e}{\partial M^{(n)}} \right]_{V, \mathcal{J}^e, M^{(m \neq n)}}, \quad (6.26)$$

which motivates defining the **chemical potential**

$$\mu^{(n)} \equiv \left[\frac{\partial \mathcal{J}^e}{\partial M^{(n)}} \right]_{V, \mathcal{S}^e, M^{(m \neq n)}} = -T \left[\frac{\partial \mathcal{S}^e}{\partial M^{(n)}} \right]_{V, \mathcal{J}^e, M^{(m \neq n)}} \quad (6.27)$$

¹⁵Note that the $M^{(n)}$ subscript on the partial derivatives in equations (6.23a) and (6.23b) (the ones not appearing as part of summations) is a shorthand for holding all matter constituent masses fixed while computing the partial derivative.

thus leading to

$$\mathcal{I}^e = T \mathcal{S}^e - p V + \sum_{n=1}^N \mu^{(n)} M^{(n)} \iff T \mathcal{S}^e = \mathcal{I}^e + p V - \sum_{n=1}^N \mu^{(n)} M^{(n)}. \quad (6.28)$$

These expressions provide the internal energy and entropy as homogeneous first-order function of its extensive and intensive variables, and they are referred to as their **Euler form**.

By definition, the chemical potential, $\mu^{(n)}$, is an intensive property that measures the change in the internal energy, \mathcal{I}^e , when altering the mass, $M^{(n)}$, of the constituent n , while fixing the entropy, volume, and mass of the other components. Equivalently, it is minus the temperature weighted change in the entropy, \mathcal{S}^e , when altering the mass, $M^{(n)}$ while fixing the volume, internal energy, and mass of the other components. We can define a chemical potential for a single component system, in which it is the change arising from altering the mass of the system. Despite its name, the chemical potential does not necessarily refer to the existence of chemical reactions, though we note that it does appear prominently in the thermodynamics of chemical reactions (e.g., [Atkins and de Paula \(2006\)](#)).

6.3.3 Molar mass and molar chemical potential

It is sometimes convenient to write the mass of a constituent as the product of the number of moles, $N^{(n)}$, and the mass per mole, $M^{(n)}$ (the *molar mass*), so that

$$M^{(n)} = N^{(n)} M^{(n)} \quad \text{no implied sum.} \quad (6.29)$$

In this way, an infinitesimal mass change is given by

$$dM = \sum_{n=1}^N dM^{(n)} = \sum_{n=1}^N d(N^{(n)} M^{(n)}) = \sum_{n=1}^N M^{(n)} dN^{(n)}, \quad (6.30)$$

so that mass changes are signalled by changes in the number of moles. We furthermore note the identity (no implied sum)

$$M^{(n)} \mu^{(n)} = M^{(n)} \left[\frac{\partial \mathcal{I}^e}{\partial M^{(n)}} \right]_{V, \mathcal{S}^e, M^{(m \neq n)}} = N^{(n)} M^{(n)} \left[\frac{\partial \mathcal{I}^e}{\partial (N^{(n)} M^{(n)})} \right]_{V, \mathcal{S}^e, N^{(m \neq n)}} = N^{(n)} \tilde{\mu}^{(n)}, \quad (6.31)$$

where we defined the molar chemical potential determined according to mole number

$$\tilde{\mu}^{(n)} = \left[\frac{\partial \mathcal{I}^e}{\partial N^{(n)}} \right]_{V, \mathcal{S}^e, N^{(m \neq n)}} = M^{(n)} \mu^{(n)}. \quad (6.32)$$

We are similarly led to the identities (no implied sum)

$$M^{(n)} d\mu^{(n)} = N^{(n)} d\tilde{\mu}^{(n)} \quad \text{and} \quad \mu^{(n)} dM^{(n)} = \tilde{\mu}^{(n)} dN^{(n)}. \quad (6.33)$$

6.3.4 Chemical work and the Gibbs-Duhem relation

Changes to the matter composition of a system changes the internal energy through **chemical work**, written as $d\mathcal{C}$. If the changes to the matter composition occur quasi-statically then the

chemical work is written

$$d\mathcal{C} = \sum_{n=1}^N \mu^{(n)} dM^{(n)} = \sum_{n=1}^N \tilde{\mu}^{(n)} dN^{(n)}, \quad (6.34)$$

so that the chemical potential is the integrating factor connecting the inexact differential measuring the chemical work to the exact differential change in matter content. The chemical potential is the energy absorbed or released due to an infinitesimal change in the matter content. As shown in Section 7.2.2, matter in a mixture tends to move from regions of high chemical potential to lower chemical potential, thus motivating the name “potential” in analog to the gravitational potential.

The inclusion of chemical work brings the first law of thermodynamics to the form

$$d\mathcal{I}^e = d\mathcal{W} + d\mathcal{Q} + d\mathcal{C} \quad \text{general processes} \quad (6.35a)$$

$$d\mathcal{I}^e = -p dV + T dS^e + \sum_{n=1}^N \mu^{(n)} dM^{(n)} \quad \text{quasi-static processes.} \quad (6.35b)$$

Use of the quasi-static form of the first law (6.35b) along with the differential of the result (6.28) leads to the Gibbs-Duhem relation¹⁶

$$S^e dT - V dp + \sum_{n=1}^N M^{(n)} d\mu^{(n)} = 0. \quad (6.36)$$

The Gibbs-Duhem relation describes how changes in the intensive variables (temperature, pressure, and chemical potential) are dependent on values for the extensive variables (entropy, volume, and matter composition) for a physical system at thermodynamic equilibrium. As a corollary we see that for processes occurring at constant temperature and pressure that

$$\sum_{n=1}^N M^{(n)} d\mu^{(n)} = \sum_{n=1}^N N^{(n)} d\tilde{\mu}^{(n)} = 0 \quad \text{constant } T, p. \quad (6.37)$$

6.3.5 Gibbs potential

We offer a formal study of thermodynamic potentials in Section 6.6. Among those, we find **Gibbs potential** of particular use for geophysical fluid mechanics and thus introduce it here

$$\mathcal{G}^e = \mathcal{I}^e - T S^e + p V = \sum_{n=1}^N \mu^{(n)} M^{(n)}. \quad (6.38)$$

The reason that the Gibbs potential is so useful is that it is a natural function of temperature, pressure, and matter content,

$$\mathcal{G}^e = \mathcal{G}^e(T, p, M^{(n)}), \quad (6.39)$$

with $T, p, M^{(n)}$ readily measured fluid properties. This convenient functional dependence is confirmed by taking the differential, $d\mathcal{G}^e$, and using the fundamental thermodynamic relation (6.35b) to find

$$d\mathcal{G}^e = -S^e dT + V dp + \sum_{n=1}^N \mu^{(n)} dM^{(n)}. \quad (6.40)$$

¹⁶In Exercise 6.4 we work through the derivation of Gibbs-Duhem (6.36) in a bit more detail.

In turn, we can derive the following partial derivatives,

$$\left[\frac{\partial \mathcal{G}^e}{\partial T} \right]_{p, M^{(n)}} = -\mathcal{S}^e \quad \text{and} \quad \left[\frac{\partial \mathcal{G}^e}{\partial p} \right]_{T, M^{(n)}} = V \quad \text{and} \quad \left[\frac{\partial \mathcal{G}^e}{\partial M^{(n)}} \right]_{p, T, M^{(m \neq n)}} = \mu^{(n)}. \quad (6.41)$$

We also have the following second partial derivative identities

$$\left[\frac{\partial \mu^{(n)}}{\partial p} \right]_{T, M^{(m)}} = \frac{\partial}{\partial p} \left[\frac{\partial \mathcal{G}^e}{\partial M^{(n)}} \right]_{p, T, M^{(m \neq n)}} \quad (6.42a)$$

$$= \frac{\partial}{\partial M^{(n)}} \left[\frac{\partial \mathcal{G}^e}{\partial p} \right]_{p, T, M^{(m \neq n)}} \quad (6.42b)$$

$$= \left[\frac{\partial V}{\partial M^{(n)}} \right]_{p, T, M^{(m \neq n)}} \quad (6.42c)$$

as well as

$$\left[\frac{\partial \mu^{(n)}}{\partial T} \right]_{p, M^{(m)}} = \frac{\partial}{\partial T} \left[\frac{\partial \mathcal{G}^e}{\partial M^{(n)}} \right]_{p, T, M^{(m \neq n)}} \quad (6.43a)$$

$$= \frac{\partial}{\partial M^{(n)}} \left[\frac{\partial \mathcal{G}^e}{\partial T} \right]_{p, M^{(m)}} \quad (6.43b)$$

$$= - \left[\frac{\partial \mathcal{S}^e}{\partial M^{(n)}} \right]_{p, T, M^{(m \neq n)}}. \quad (6.43c)$$

The second derivative identities are particular examples of a [Maxwell relation](#), with Maxwell relations resulting from commutativity of the partial derivative operation.

6.3.6 Extensive functions of $(T, p, M^{(n)})$

Just as for the internal energy and entropy, the Gibbs function, $\mathcal{G}^e(T, p, M^{(n)})$, is an extensive function. Since the temperature and pressure are both intensive properties, we follow the scale analysis from Section 6.3.1 to arrive at the Euler form of the Gibbs function

$$\mathcal{G}^e(T, p, M^{(n)}) = \sum_{n=1}^N M^{(n)} \left[\frac{\partial \mathcal{G}^e}{\partial M^{(n)}} \right]_{p, T, M^{(m \neq n)}} = \sum_{n=1}^N \mu^{(n)} M^{(n)}, \quad (6.44)$$

which is consistent with the definition (6.38). Indeed, any extensive property written as a function of $(T, p, M^{(n)})$ can be written in the same fashion. For example, the internal energy, entropy, and volume take the form

$$\mathcal{I}^e(T, p, M^{(n)}) = \sum_{n=1}^N M^{(n)} \left[\frac{\partial \mathcal{I}^e}{\partial M^{(n)}} \right]_{p, T, M^{(m \neq n)}} = \sum_{n=1}^N \mathcal{N}^{(n)} \left[\frac{\partial \mathcal{I}^e}{\partial \mathcal{N}^{(n)}} \right]_{p, T, \mathcal{N}^{(m \neq n)}} \quad (6.45a)$$

$$\mathcal{S}^e(T, p, M^{(n)}) = \sum_{n=1}^N M^{(n)} \left[\frac{\partial \mathcal{S}^e}{\partial M^{(n)}} \right]_{p, T, M^{(m \neq n)}} = \sum_{n=1}^N \mathcal{N}^{(n)} \left[\frac{\partial \mathcal{S}^e}{\partial \mathcal{N}^{(n)}} \right]_{p, T, \mathcal{N}^{(m \neq n)}} \quad (6.45b)$$

$$V(T, p, M^{(n)}) = \sum_{n=1}^N M^{(n)} \left[\frac{\partial V}{\partial M^{(n)}} \right]_{p, T, M^{(m \neq n)}} = \sum_{n=1}^N \mathcal{N}^{(n)} \left[\frac{\partial V}{\partial \mathcal{N}^{(n)}} \right]_{p, T, \mathcal{N}^{(m \neq n)}}. \quad (6.45c)$$

The partial derivatives, $[\partial(\mathcal{G}^e, \mathcal{I}^e, \mathcal{S}^e, V)/\partial N^{(n)}]_{p,T,N_m \neq n}$, are intensive properties known as the *partial Gibbs potential*, *partial internal energy*, *partial entropy*, and *partial volume*. These relations mean that we can regard each of the extensive quantities as the sum of contributions from each of the material components as determined by their partial properties. For the particular case of a single matter component we have

$$\mathcal{G}^e(T, p, M) = M \left[\frac{\partial \mathcal{G}^e}{\partial M} \right]_{p,T} = \mu M \quad (6.46a)$$

$$\mathcal{I}^e(T, p, M) = M \left[\frac{\partial \mathcal{I}^e}{\partial M} \right]_{p,T} = N \left[\frac{\partial \mathcal{I}^e}{\partial N} \right]_{p,T} \quad (6.46b)$$

$$\mathcal{S}^e(T, p, M) = M \left[\frac{\partial \mathcal{S}^e}{\partial M} \right]_{p,T} = N \left[\frac{\partial \mathcal{S}^e}{\partial N} \right]_{p,T} \quad (6.46c)$$

$$V(T, p, M) = M \left[\frac{\partial V}{\partial M} \right]_{p,T} = N \left[\frac{\partial V}{\partial N} \right]_{p,T}. \quad (6.46d)$$

6.4 Thermodynamic equilibrium with matter flow

Consider a single-component fluid ($N = 1$) that consists of two regions or systems, labelled by α and β , with each of these two systems separately in thermodynamic equilibrium. Assume the composite system is enclosed in a container with fixed volume, $V_\alpha + V_\beta = V$. Allow the two systems to interact thermally, mechanically, and materially. What are the properties of thermodynamic equilibrium for the composite system, $\alpha \oplus \beta$?

To answer this question, we follow the procedure in Section 6.2.9, here considering the case where matter flows between the systems in addition to thermal transfer and mechanical interactions. Such processes occur as the composite system approaches thermodynamic equilibrium. Initially, the α and β systems are separately in thermodynamic equilibrium with internal energies, $(\mathcal{I}_\alpha^e, \mathcal{I}_\beta^e)$, volumes, (V_α, V_β) , and masses, (M_α, M_β) . During the process of reaching thermodynamic equilibrium, the internal energy, volume, and mass of the composite system remains constant so that¹⁷

$$d(\mathcal{I}_\alpha^e + \mathcal{I}_\beta^e) = 0 \quad \text{and} \quad d(V_\alpha + V_\beta) = 0 \quad \text{and} \quad d(M_\alpha + M_\beta) = 0. \quad (6.47)$$

From equation (6.21) we know that entropy is a natural function of volume, internal energy, and mass of each matter constituent. With only a single matter constituent we have

$$d\mathcal{S}^e = \frac{1}{T_\alpha} d\mathcal{I}_\alpha^e + \frac{p_\alpha}{T_\alpha} dV_\alpha - \frac{\mu_\alpha}{T_\alpha} dM_\alpha + \frac{1}{T_\beta} d\mathcal{I}_\beta^e + \frac{p_\beta}{T_\beta} dV_\beta - \frac{\mu_\beta}{T_\beta} dM_\beta \quad (6.48a)$$

$$= \left[\frac{1}{T_\alpha} - \frac{1}{T_\beta} \right] d\mathcal{I}_\alpha^e + \left[\frac{p_\alpha}{T_\alpha} - \frac{p_\beta}{T_\beta} \right] dV_\alpha - \left[\frac{\mu_\alpha}{T_\alpha} - \frac{\mu_\beta}{T_\beta} \right] dM_\alpha, \quad (6.48b)$$

where we used the partial derivative identities (6.13), (6.14), and (6.27). As before, $d\mathcal{S}^e = 0$ at thermodynamic equilibrium, and this condition holds for arbitrary and independent $d\mathcal{I}_\alpha^e$, dV_α , and dM_α . We are thus led to the thermal, mechanical, and material conditions for thermodynamic equilibrium

$$T_\alpha = T_\beta \quad \text{and} \quad p_\alpha = p_\beta \quad \text{and} \quad \mu_\alpha = \mu_\beta. \quad (6.49)$$

¹⁷We here assume there is no macroscopic mechanical energy, so that the total energy is the internal energy. In Section 10.7 we relax this assumption by considering macroscopic motion.

That is, the temperature, pressure, and chemical potential are uniform when the composite system reaches thermodynamic equilibrium. Note that this thermodynamic equilibrium condition means that each term in the Gibbs-Duhem relation (6.36) separately vanishes. Furthermore, since the Gibbs potential equals to the mass times the chemical potential for a single component system (equation (6.44)), equality of the chemical potentials at equilibrium means that

$$\mu_\alpha = \mu_\beta \implies \frac{\mathcal{G}_\alpha^e}{M_\alpha} = \frac{\mathcal{G}_\beta^e}{M_\beta}. \quad (6.50)$$

As for the direction of heat flow discussed in Section 6.2.9, we can determine the direction for matter flow as the composite system, $\alpha \oplus \beta$, approaches thermodynamic equilibrium. For this purpose, assume the temperature and volumes are already uniform, but the matter content initially differs. At the instance the two systems start interacting, the entropy differential is given by

$$T dS^e = -(\mu_\alpha - \mu_\beta) dM_\alpha > 0, \quad (6.51)$$

where T is the equilibrium temperature of the two systems, and where the inequality holds according to the second law of thermodynamics (Section 6.1.7). If $\mu_\alpha > \mu_\beta$, then this inequality requires $dM_\alpha < 0$. Hence, in the process of approaching thermodynamic equilibrium, matter flows from regions of high chemical potential to regions of low chemical potential. This behavior allows us to consider the chemical potential in a manner directly akin to temperature. That is, temperature differences measure the potential for heat to be fluxed, and likewise chemical potential differences measure the potential for matter to be fluxed. The chemical potential is central to the study of changes in matter states (e.g., solid to liquid, liquid to gas), as well as for chemical reactions (e.g., [Guggenheim, 1967](#); [Atkins and de Paula, 2006](#)).

6.5 Materially open systems with fixed total mass

In our study of geophysical fluids, we make use of a continuum of fluid elements. Each fluid element is open mechanically, thermally, and materially while maintaining constant mass as it quasi-statically evolves through local thermodynamic equilibrium states. Hence, when formulating the equations of linear irreversible thermodynamics in Chapter 10, we make use of thermodynamic equations written in their “per unit mass” form. Here we present these equations, as well as extend our understanding of the formalism.

6.5.1 Matter concentrations

We generally make use of matter or tracer concentration as written

$$C^{(n)} = M^{(n)}/M \implies \sum_{n=1}^N C^{(n)} = 1, \quad (6.52)$$

with the constant mass constraint $\sum_{n=1}^N C^{(n)} = 1$ meaning that only $N - 1$ of the concentrations are linearly independent.

6.5.2 Fundamental thermodynamic relation per unit mass

We scale away the mass of the system by setting the scale factor $\lambda = M^{-1}$ in our discussion in Section 6.3.1 of how extensive properties scale. The result is the *specific* (per mass) versions of

the extensive properties

$$\mathcal{J}^e = M \mathcal{J} \quad (6.53a)$$

$$\mathcal{S}^e = M \mathcal{S} \quad (6.53b)$$

$$V = M/\rho = M \nu_s \quad (6.53c)$$

$$M^{(n)} = M C^{(n)}, \quad (6.53d)$$

where

$$\nu_s = 1/\rho \quad (6.54)$$

is the specific volume and the total mass, M , is held fixed. In the equality (6.53d), $C^{(n)}$ is the mass fraction or concentration of species, n , in the fluid (Section 6.5.1). Substituting the specific quantities (6.53a)-(6.53d) into the fundamental thermodynamic relation (6.35b) leads to the fundamental thermodynamic relation in terms of specific thermodynamic quantities

$$d\mathcal{J} = T d\mathcal{S} - p d\rho^{-1} + \sum_n \mu^{(n)} dC^{(n)}. \quad (6.55)$$

This is the form of the fundamental thermodynamic relation most commonly used in this book. Again, this relation holds for quasi-static processes where the total mass of the system is fixed, thus making it relevant for our study of constant mass fluid elements in Chapter 10.

6.5.3 Seawater as a binary fluid

The atmosphere is a multi-component and multi-phase fluid that is well approximated as a mixture of water vapor and dry air. However, we do not consider moist atmospheric processes in this book nor do we consider phases changes. In contrast, there are many occasions in this book that require us to consider seawater as a binary fluid system of salt dissolved in fresh water so that their concentrations satisfy the constraint¹⁸

$$C^{\text{salt}} + C^{\text{water}} = 1 \implies dC^{\text{water}} = -dC^{\text{salt}}. \quad (6.56)$$

We are thus able to write the Gibbs fundamental thermodynamic relation (6.55) in the form

$$d\mathcal{J} = T d\mathcal{S} - p d\rho^{-1} + \mu^{\text{water}} dC^{\text{water}} + \mu^{\text{salt}} dC^{\text{salt}} \quad (6.57a)$$

$$= T d\mathcal{S} - p d\rho^{-1} + \mu dC, \quad (6.57b)$$

where

$$C = C^{\text{salt}} \quad (6.58)$$

is the concentration of salt (mass of salt per mass of seawater), and

$$\mu = \mu^{\text{salt}} - \mu^{\text{water}} \quad (6.59)$$

¹⁸Salt in the ocean is largely comprised of chloride ions, sodium ions, sulphate ions, magnesium ions, calcium ions, potassium ions, and hydro-carbonate ions. The composition of the principal ions in seawater is roughly a constant, thus allowing us to be concerned only with the “salt” content and concentration rather than that for the individual components. In turn, we can accurately consider seawater as a two-component fluid comprised of fresh water and salt. See Section 1.4 of [Kamenkovich \(1977\)](#), Section 3.1 of [Gill \(1982\)](#), Section 1.2 of [Olbers et al. \(2012\)](#), or Section 1.4 of [Vallis \(2017\)](#) for more details.

is the relative chemical potential for seawater, often referred to as the **seawater chemical potential**. We return in Section 6.59 to discuss how the chemical potentials are computed according to partial derivatives of the Gibbs potential, which is the preferred method for the ocean and atmosphere.

The **absolute salinity**, S , with units parts per thousand (gram per kilogram), is related to C^{salt} via

$$S = 1000 C^{\text{salt}}. \quad (6.60)$$

The range of absolute salinity in the ocean (roughly $0 \leq S \leq 40$) is more convenient than the range of C^{salt} , making salinity more commonly used in ocean physics.

6.5.4 Further study

Chapters 1 and 2 of [Olbers et al. \(2012\)](#) provide a more complete suite of thermodynamic relations for seawater.

6.6 Thermodynamic potentials

As mentioned in Section 6.2.2, internal energy and entropy are two examples of a **state function** (functions only of the current state). We now introduce additional state functions, also known as **thermodynamic potentials**. They are related by the Euler form equation (6.28), here written in its specific expression as appropriate for constant mass fluid elements

$$\mathcal{I} = T \mathcal{S} - p \nu_s + \sum_{n=1}^N \mu^{(n)} C^{(n)} \iff T \mathcal{S} = \mathcal{I} + p \nu_s - \sum_{n=1}^N \mu^{(n)} C^{(n)}. \quad (6.61)$$

Each thermodynamic potential is a natural function of certain other thermodynamic variables, as determined by the fundamental thermodynamic relation. Furthermore, the intensive variables, T and p , are derived via partial derivatives of the thermodynamic potentials.

It is notable that the experimentalist generally has access to measuring the intensive variables rather than their conjugate variables, with temperature and entropy a primary example. Namely, it is generally not possible to directly measure entropy whereas temperature is routinely measured. Hence, for a practical use of equilibrium thermodynamics we seek reformulations whereby we can select which variables are mathematically independent. This reformulation is realized by making use of a **Legendre transformation**, which then leads to the introduction of alternative thermodynamic potentials. Importantly, the introduction of alternative thermodynamic potentials introduces no new fundamental information. However, the practice of thermodynamics is greatly facilitated through the Legendre transformation to new potentials, and it is for this reason that Legendre transformations are commonly employed in thermodynamics. For the mathematically curious, we provide a primer on Legendre transformations in the appendix Section 6.12.

In deriving new thermodynamic potentials, we specialize to the case of a binary fluid, which is the most common case for the ocean and atmosphere. If there are more than two matter constituents, then the term μdC appearing in these formula become $\sum_{n=1}^N \mu^{(n)} dC^{(n)}$. Partial derivatives are also modified accordingly.

As a point of practice, it is very important to commit to a single choice for the thermodynamic potential when manipulating thermodynamic equations. The reason is that functional

dependencies change when switching to a different thermodynamic potential, thus exposing oneself to mistakes when swapping formulations midstream.

6.6.1 Equations of state

Equations (6.11), (6.12), and (6.27) provide expressions for intensive properties, T , p , and $\mu^{(n)}$, in terms of the partial derivatives of the internal energy in terms of extensive functions S^e , V , and $M^{(n)}$. Hence, we can write T , p , and $\mu^{(n)}$ in the functional form

$$T = T(S^e, V, M^{(m)}) \quad \text{and} \quad p = p(S^e, V, M^{(m)}) \quad \text{and} \quad \mu^{(n)} = \mu^{(n)}(S^e, V, M^{(m)}). \quad (6.62)$$

Each of these equations is a particular example of an [equation of state](#), which offer constraints that must be satisfied by the thermodynamic variables when in thermodynamic equilibrium. Knowledge of all the equations of state is equivalent to knowledge of the fundamental thermodynamic relation (6.35b). In the following, we develop similar equations of state based on other thermodynamic potentials.

6.6.2 Internal energy

Recall the fundamental thermodynamic relation (6.57b) written for a binary fluid

$$d\mathcal{I} = T dS - p d\nu_s + \mu dC. \quad (6.63)$$

Equation (6.63) identifies the specific internal energy, \mathcal{I} , as a natural function of specific entropy, S , specific volume, ν_s , and matter concentration, C ,

$$\mathcal{I} = \mathcal{I}(S, \nu_s, C). \quad (6.64)$$

Knowledge of the fundamental thermodynamic relation (6.63) allows us to derive a variety of thermodynamic relations via partial differentiation. For example, we can identify the intensive variables

$$\left[\frac{\partial \mathcal{I}}{\partial S} \right]_{\nu_s, C} = T \quad \text{and} \quad \left[\frac{\partial \mathcal{I}}{\partial \nu_s} \right]_{S, C} = -p \quad \text{and} \quad \left[\frac{\partial \mathcal{I}}{\partial C} \right]_{S, \nu_s} = \mu, \quad (6.65)$$

which are the specific (per mass) forms of equations (6.11), (6.12), and (6.27).

Evidently, the three equations contained in equation (6.65) provide a relation between the intensive properties, T, p, μ , as derivatives of a function, the internal energy, which is itself a function $\mathcal{I}(S, \nu_s, C)$. Hence, we may consider T, p, μ each as a function of (S, ν_s, C) , and thus write

$$T = T(S, \nu_s, C) \quad \text{and} \quad p = p(S, \nu_s, C) \quad \text{and} \quad \mu = \mu(S, \nu_s, C), \quad (6.66)$$

which are the equations of state (6.62) written in terms of specific (per mass) quantities. In turn, the exact differentials of the intensive properties are

$$dT = \left[\frac{\partial T}{\partial S} \right]_{\nu_s, C} dS + \left[\frac{\partial T}{\partial \nu_s} \right]_{C, S} d\nu_s + \left[\frac{\partial T}{\partial C} \right]_{S, \nu_s} dC \quad (6.67)$$

$$dp = \left[\frac{\partial p}{\partial S} \right]_{\nu_s, C} dS + \left[\frac{\partial p}{\partial \nu_s} \right]_{C, S} d\nu_s + \left[\frac{\partial p}{\partial C} \right]_{S, \nu_s} dC \quad (6.68)$$

$$\mu = \mu(\mathcal{S}, \nu_s, C) \implies d\mu = \left[\frac{\partial \mu}{\partial \mathcal{S}} \right]_{\nu_s, C} d\mathcal{S} + \left[\frac{\partial \mu}{\partial \nu_s} \right]_{C, \mathcal{S}} d\nu_s + \left[\frac{\partial \mu}{\partial C} \right]_{\mathcal{S}, \nu_s} dC. \quad (6.69)$$

6.6.3 Entropy

Rearrangement of the fundamental thermodynamic relation (6.63) leads to the exact differential for specific entropy

$$d\mathcal{S} = \frac{1}{T} d\mathcal{J} + \frac{p}{T} d\nu_s - \frac{\mu}{T} dC. \quad (6.70)$$

In this form, specific entropy has the functional dependence

$$\mathcal{S} = \mathcal{S}(\mathcal{J}, \nu_s, C), \quad (6.71)$$

whose knowledge provides yet another form of the fundamental equation of state. This functional dependence, along with equation (6.70), lead to the following identities for the intensive properties

$$\left[\frac{\partial \mathcal{S}}{\partial \mathcal{J}} \right]_{\nu_s, C} = \frac{1}{T} \quad \text{and} \quad \left[\frac{\partial \mathcal{S}}{\partial \nu_s} \right]_{\mathcal{J}, C} = \frac{p}{T} \quad \text{and} \quad \left[\frac{\partial \mathcal{S}}{\partial C} \right]_{\mathcal{J}, \nu_s} = -\frac{\mu}{T}. \quad (6.72)$$

As for internal energy in Section 6.6.2, equation (6.72) provides a relation between T, p, μ as derivatives of a function, the entropy, which is itself a function $\mathcal{S}(\mathcal{J}, \nu_s, C)$. Hence, we may consider T, p, μ as each a function of (\mathcal{J}, ν_s, C) to thus write the equations of state

$$T = T(\mathcal{J}, \nu_s, C) \quad \text{and} \quad p = p(\mathcal{J}, \nu_s, C) \quad \text{and} \quad \mu = \mu(\mathcal{J}, \nu_s, C). \quad (6.73)$$

6.6.4 Enthalpy

Thus far we have worked only with the fundamental thermodynamic relation (6.63). We now introduce the specific enthalpy through use of our first Legendre transformation

$$\mathcal{H} = \mathcal{J} - \nu_s \left[\frac{\partial \mathcal{J}}{\partial \nu_s} \right]_{S, C^{(n)}} = \mathcal{J} + \nu_s p = T \mathcal{S} + \sum_{n=1}^N \mu^{(n)} C^{(n)}. \quad (6.74)$$

The first equality is a Legendre transformation and the second equality made use of the partial derivative identity from equation (6.65) relating internal energy to pressure. Finally, the third equality made use of the Euler form equation (6.61). Specializing to the case of a binary fluid, such as the ocean or atmosphere, and use of the fundamental thermodynamic relation (6.63), leads to the exact differential for enthalpy

$$d\mathcal{H} = d\mathcal{J} + d(p \nu_s) \quad (6.75a)$$

$$= T d\mathcal{S} - p d\nu_s + \mu dC + p d\nu_s + \nu_s dp \quad (6.75b)$$

$$= T d\mathcal{S} + \nu_s dp + \mu dC. \quad (6.75c)$$

Recall that for quasi-static processes, $T d\mathcal{S}$ equals to the thermal energy added to a fluid element. Hence, for processes occurring at constant pressure and constant matter content, changes in enthalpy are determined by the thermal energy added to the system. This connection motivates the name *heat function* sometimes applied to enthalpy (e.g., page 4 of [Landau and Lifshitz \(1987\)](#)).

Equation (6.75c) is the Gibb's fundamental thermodynamic relation written with enthalpy rather than internal energy. Evidently, the Legendre transformation (6.74) renders a functional dependence for enthalpy

$$\mathcal{H} = \mathcal{H}(\mathcal{S}, p, C), \quad (6.76)$$

which in turn leads to the following partial derivative identities

$$\left[\frac{\partial \mathcal{H}}{\partial \mathcal{S}} \right]_{p,C} = T \quad \text{and} \quad \left[\frac{\partial \mathcal{H}}{\partial p} \right]_{\mathcal{S},C} = \nu_s \quad \text{and} \quad \left[\frac{\partial \mathcal{H}}{\partial C} \right]_{\mathcal{S},p} = \mu. \quad (6.77)$$

As for internal energy in Section 6.6.2, equations (6.77) provide a relation between T, ν_s, μ as derivatives of a function, the enthalpy, which is itself a function $\mathcal{H}(\mathcal{S}, p, C)$. Hence, we may consider T, ν_s, μ as each a function of (\mathcal{S}, p, C) to thus render the following equations of state

$$T = T(\mathcal{S}, p, C) \quad \text{and} \quad \nu_s = \nu_s(\mathcal{S}, p, C) \quad \text{and} \quad \mu = \mu(\mathcal{S}, p, C). \quad (6.78)$$

For the following reasons, enthalpy's functional dependence (6.76) is more convenient for studies of geophysical fluids than that for internal energy, $\mathcal{I}(\mathcal{S}, \nu_s, C)$, or for entropy $\mathcal{S}(\mathcal{I}, \nu_s, C)$.

- In the laboratory or field, we generally have direct mechanical means for measuring pressure in a fluid, whereas specific volume requires indirect methods involving the equation of state for density discussed in Section 14.3.
- The interaction between fluid elements typically occurs at near constant pressure. Hence, fluid elements exchange both their entropy and enthalpy when the exchange occurs at constant pressure.
- Specific entropy remains constant when following a fluid element in the absence of mixing or other irreversible effects. Correspondingly, enthalpy remains constant for constant pressure motion without mixing. Conversely, in the presence of mixing at constant pressure, fluid elements mix their specific enthalpy, specific entropy, and tracer concentration.

6.6.5 Gibbs potential

The Gibbs potential is defined by the Legendre transformation

$$\mathcal{G} = \mathcal{H} - \mathcal{S} \left[\frac{\partial \mathcal{H}}{\partial \mathcal{S}} \right]_{p,C} = \mathcal{H} - \mathcal{S} T = \sum_{n=1}^N \mu^{(n)} C^{(n)}, \quad (6.79)$$

where the final equality made use of equation (6.61). The exact differential of the Gibbs potential is given by

$$d\mathcal{G} = d\mathcal{H} - d(T\mathcal{S}) \quad (6.80a)$$

$$= T d\mathcal{S} + \nu_s dp + \mu dC - T d\mathcal{S} - \mathcal{S} dT \quad (6.80b)$$

$$= -\mathcal{S} dT + \nu_s dp + \mu dC, \quad (6.80c)$$

where we made use of the fundamental thermodynamic relation (6.75c) written in terms of enthalpy. The Gibbs potential has the functional dependence

$$\mathcal{G} = \mathcal{G}(T, p, C), \quad (6.81)$$

which leads to the partial derivatives identities

$$\left[\frac{\partial \mathcal{G}}{\partial T} \right]_{p,C} = -\mathcal{S} \quad \text{and} \quad \left[\frac{\partial \mathcal{G}}{\partial p} \right]_{T,C} = \nu_s \quad \text{and} \quad \left[\frac{\partial \mathcal{G}}{\partial C} \right]_{T,p} = \mu. \quad (6.82)$$

As for internal energy in Section 6.6.2, equations (6.82) provide a relation between \mathcal{S}, ν_s, μ as derivatives of a function, the Gibbs potential, which is itself a function $\mathcal{G}(T, p, C)$. Hence, we may consider \mathcal{S}, ν_s, μ each as a function of (T, p, C) to render the following functional relations

$$\mathcal{S} = \mathcal{S}(T, p, C) \quad \text{and} \quad \nu_s = \nu_s(T, p, C) \quad \text{and} \quad \mu = \mu(T, p, C). \quad (6.83)$$

The form of the fundamental dependencies (6.81), and the associated equations of state (6.83), are often used in fluid mechanics and physical chemistry. The reason is that temperature, pressure, and concentration are readily measured in the laboratory and the environment. We can thus measure the partial derivatives of \mathcal{G} , and the functional dependence (6.83) provides a convenient means to express \mathcal{S}, ν_s , and μ (e.g., see the adiabatic lapse rate discussion in Section 7.3).

Given its convenient functional dependence, the Gibbs potential plays a central role in developing the thermodynamics of seawater as formulated by [Feistel \(1993\)](#) and codified by [IOC et al. \(2010\)](#). We thus endeavor to exhibit how quantities (e.g., response functions as in Section 6.7) can be computed based on knowledge of the Gibbs potential and its partial derivatives. For example, use of equation (6.82) renders the Legendre transformation expression for the enthalpy

$$\mathcal{H} = \mathcal{G} + T\mathcal{S} = \mathcal{G} - T \left[\frac{\partial \mathcal{G}}{\partial T} \right]_{p,C}. \quad (6.84)$$

6.6.6 Chemical potential and the Gibbs potential

Throughout this section we have displayed equations for the chemical potential of a binary fluid in terms of the partial derivatives of the thermodynamic potentials, such as equation (6.82) using the Gibbs potential. Here we consider some details that lead to further understanding of the partial derivatives. We start by writing the chemical potential of fresh water and salt as contained within seawater in terms of the partial derivatives of the extensive Gibbs potential

$$\mu^{\text{water}} = \left[\frac{\partial \mathcal{G}^e}{\partial M^{\text{water}}} \right]_{T,p,M^{\text{salt}}} \quad \text{and} \quad \mu^{\text{salt}} = \left[\frac{\partial \mathcal{G}^e}{\partial M^{\text{salt}}} \right]_{T,p,M^{\text{water}}}. \quad (6.85)$$

The total mass of a sample of seawater is given by $M = M^{\text{water}} + M^{\text{salt}}$. Consequently, to compute these partial derivatives requires us to alter the mass of the sample as we hold the mass of one component fixed while varying the mass of the other component. This sort of partial derivative is less convenient for our purposes since we prefer to work with constant mass samples, such as we encounter with constant mass fluid elements. For that purpose we introduce the specific Gibbs potential, in which case the chemical potential of fresh water is

$$\mu^{\text{water}} = \left[\frac{\partial \mathcal{G}^e}{\partial M^{\text{water}}} \right]_{T,p,M^{\text{salt}}} = \left[\frac{\partial (M \mathcal{G})}{\partial M^{\text{water}}} \right]_{T,p,M^{\text{salt}}} = \mathcal{G} + M \left[\frac{\partial \mathcal{G}}{\partial M^{\text{water}}} \right]_{T,p,M^{\text{salt}}}. \quad (6.86)$$

The specific Gibbs potential is a natural function of $T, p, C^{(n)}$, and since $C^{\text{water}} + C^{\text{salt}} = 1$ we can write the Gibbs potential in terms of just one of the concentrations, typically chosen as

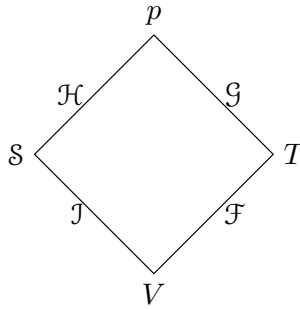


FIGURE 6.4: A diagram that offers a quick reference to determine the natural functional dependencies of thermodynamic potentials, here drawn for a materially closed system. Starting from the lower left side, we have specific internal energy surrounded by its natural variables, entropy and volume, $J(S, \nu_s)$. Moving around in a clockwise direction we find enthalpy, $H(S, p)$, the Gibbs's potential, $G(T, p)$, and the Helmholtz potential (Exercise 6.7), $F(T, \nu_s)$.

C^{salt} . We are thus led to

$$\mu^{\text{water}} = G + M \left[\frac{\partial G}{\partial M^{\text{water}}} \right]_{T,p,M^{\text{salt}}} \quad (6.87\text{a})$$

$$= G + M \left[\frac{\partial G}{\partial C^{\text{water}}} \right]_{T,p} \left[\frac{\partial C^{\text{water}}}{\partial M^{\text{water}}} \right]_{M^{\text{salt}}} \quad (6.87\text{b})$$

where the concentration partial derivative is given by

$$\left[\frac{\partial C^{\text{water}}}{\partial M^{\text{water}}} \right]_{M^{\text{salt}}} = \left[\frac{\partial}{\partial M^{\text{water}}} \right]_{M^{\text{salt}}} \left[\frac{M^{\text{water}}}{M^{\text{water}} + M^{\text{salt}}} \right] = \frac{C^{\text{salt}}}{M}, \quad (6.88)$$

thus leading to the chemical potential of fresh water within seawater

$$\mu^{\text{water}} = G + C^{\text{salt}} \left[\frac{\partial G}{\partial C^{\text{water}}} \right]_{T,p} = G - C^{\text{salt}} \left[\frac{\partial G}{\partial C^{\text{salt}}} \right]_{T,p}. \quad (6.89)$$

We are thus able to work with the specific Gibbs function for a constant mass fluid element and compute its concentration partial derivative. Similar manipulations lead to the chemical potential for salt within seawater

$$\mu^{\text{salt}} = G + C^{\text{water}} \left[\frac{\partial G}{\partial C^{\text{salt}}} \right]_{T,p} = G + (1 - C^{\text{salt}}) \left[\frac{\partial G}{\partial C^{\text{salt}}} \right]_{T,p}. \quad (6.90)$$

We are thus led to the seawater chemical potential

$$\mu = \mu^{\text{salt}} - \mu^{\text{water}} = \left[\frac{\partial G}{\partial C^{\text{salt}}} \right]_{T,p}, \quad (6.91)$$

which agrees with equation (6.82).

6.6.7 A diagram for quick reference

Figure 6.4 provides a diagram that can be useful to help remember the various functional dependencies of thermodynamic potentials. There are many such diagrams, some more complete and thus more complex.

6.7 Response functions

Response functions measure the change in a thermodynamic property as the system is forced in some manner. We here introduce the [heat capacity](#), [thermal expansion coefficient](#), and [haline contraction coefficient](#), which are three response functions commonly encountered in ocean and atmospheric fluid mechanics.

6.7.1 Specific heat capacities

The heat capacity measures the change in heat associated with a change in temperature at constant matter composition. There are two distinct heat capacities generally considered in fluid mechanics: one with specific volume held fixed and the other with pressure held fixed

$$c_v \equiv \frac{1}{M} \left[\frac{dQ}{dT} \right]_{\nu_s, C} \quad \text{SI units m}^2 \text{ s}^{-2} \text{ K}^{-1}. \quad (6.92)$$

$$c_p \equiv \frac{1}{M} \left[\frac{dQ}{dT} \right]_{p, C} \quad \text{SI units m}^2 \text{ s}^{-2} \text{ K}^{-1}. \quad (6.93)$$

Each of these quantities are specific heat capacities since we have divided by the mass. If heating occurs quasi-statically, we can make use of the equation (6.6) that relates heating and entropy, applied here in its specific (per mass) form $M^{-1} dQ = T dS$. The result is a state function form of the specific heat capacities

$$c_v = T \left[\frac{\partial S}{\partial T} \right]_{\nu_s, C} = -T \left[\frac{\partial}{\partial T} \right]_{\nu_s, C} \left[\frac{\partial G}{\partial T} \right]_{p, C} \quad (6.94)$$

$$c_p = T \left[\frac{\partial S}{\partial T} \right]_{p, C} = -T \left[\frac{\partial}{\partial T} \right]_{p, C} \left[\frac{\partial G}{\partial T} \right]_{p, C} \quad (6.95)$$

where the second equalities in both of the above equations introduced the Gibbs potential according to equation (6.82). Furthermore, we can make use of the fundamental thermodynamic relation (6.55) with specific volume and matter concentration held fixed to yield

$$c_v = T \left[\frac{\partial S}{\partial T} \right]_{\nu_s, C} = \left[\frac{\partial I}{\partial T} \right]_{\nu_s, C}. \quad (6.96)$$

The second form of c_v motivates the name *internal energy capacity* rather than heat capacity at fixed volume. Equation (6.96) implies that internal energy, for a process occurring at constant specific volume and constant tracer concentration, can be written in terms of a *caloric equation of state*

$$I = I(T) \quad \text{constant } \nu_s \text{ and } C. \quad (6.97)$$

Making use of the fundamental thermodynamic relation (6.75c) written in terms of enthalpy leads to the constant pressure heat capacity

$$c_p = T \left[\frac{\partial S}{\partial T} \right]_{p, C} = \left[\frac{\partial I}{\partial T} \right]_{p, C} + p \left[\frac{\partial \nu_s}{\partial T} \right]_{p, C} = \left[\frac{\partial H}{\partial T} \right]_{p, C}. \quad (6.98)$$

The constant pressure heat capacity is equivalently referred to as the *enthalpy capacity*.

6.7.2 Thermal expansion coefficient

The thermal expansion coefficient measures relative changes in density as temperature changes at constant pressure and concentration

$$\alpha_T = -\frac{1}{\rho} \left[\frac{\partial \rho}{\partial T} \right]_{p,C} = \frac{1}{\nu_s} \left[\frac{\partial \nu_s}{\partial T} \right]_{p,C} = \frac{1}{(\partial G/\partial p)_{T,C}} \left[\frac{\partial}{\partial T} \right]_{p,C} \left[\frac{\partial G}{\partial p} \right]_{T,C} \quad (6.99)$$

where the final equality introduced the Gibbs function according to equation (6.82). The minus sign in the definition is introduced since density typically reduces when temperature increases, so that for most substances $\alpha_T > 0$. Freshwater near its freezing point is an important counter-example, with $\alpha_T < 0$ allowing for solid ice to float on liquid water.

6.7.3 Haline contraction coefficient

A similar response function measures changes to density arising from changes in the salt concentration (salinity) in seawater

$$\beta_S = \frac{1}{\rho} \left[\frac{\partial \rho}{\partial S} \right]_{p,T} = -\frac{1}{\nu_s} \left[\frac{\partial \nu_s}{\partial S} \right]_{p,T} = -\frac{1}{(\partial G/\partial p)_{T,S}} \left[\frac{\partial}{\partial S} \right]_{T,p} \left[\frac{\partial G}{\partial p} \right]_{T,S} \quad (6.100)$$

where $S = 1000 C$ is the salinity (6.60). Seawater density typically increases (fluid element volume contracts) when salinity increases, so that $\beta_S > 0$.

6.7.4 Speed of sound (acoustic) waves

Changes in density with respect to pressure at a fixed entropy define the inverse squared sound speed

$$\frac{1}{c_s^2} = \left[\frac{\partial \rho}{\partial p} \right]_S = -\frac{1}{(\nu_s)^2} \left[\frac{\partial \nu_s}{\partial p} \right]_S = -\frac{1}{[(\partial G/\partial p)_{T,S}]^2} \left[\frac{\partial}{\partial p} \right]_S \left[\frac{\partial G}{\partial p} \right]_{T,S}. \quad (6.101)$$

The sound speed is a strong function of pressure, generally increasing with higher pressure, as well as temperature, generally decreasing with lower temperature. For the ocean, these two effects compete when moving into the ocean interior. In the upper 500 m to 1000 m, decreasing temperatures cause the sound speed to reduce whereas at deeper regions the higher pressures overcome the temperature effect thus increasing the sound speed. The result is a sound speed minimum between 500 m and 1000 m. The sound speed minimum and the associated acoustic waveguide play an important role in ocean acoustics, in particular for how certain whales are able to communicate across ocean basins. We consider the sound speed for an ideal gas in Section 7.5.8.

6.8 Maxwell relations for single component fluids

Thermodynamics makes use of basic properties of exact differentials for the purpose of developing identities between partial derivatives. Maxwell relations refer to a suite of partial derivative identities that follow from the equality of mixed second partial derivatives of thermodynamic potentials. We already made use of some Maxwell relations in Section 6.3.5 when discussing the Gibbs potential, and we use another in Section 7.3 for expressing the adiabatic lapse rate in terms of readily measurable thermo-mechanical properties. In this section we develop the

Maxwell relations encountered with single component fluids, with similar relations readily derived for multi-component fluids.

6.8.1 Maxwell relation from internal energy

As seen from Section 6.6.2, the natural functional dependence for internal energy in a single-component fluid is given by its fundamental thermodynamic relation (6.63)

$$d\mathcal{I} = \left[\frac{\partial \mathcal{I}}{\partial S} \right]_{\nu_s} dS + \left[\frac{\partial \mathcal{I}}{\partial \nu_s} \right]_S d\nu_s = T dS - p d\nu_s \implies \mathcal{I} = \mathcal{I}(S, \nu_s). \quad (6.102)$$

The mixed second partial derivatives are equal

$$\left[\frac{\partial}{\partial \nu_s} \right]_{S,C} \left[\frac{\partial}{\partial S} \right]_{\nu_s,C} \mathcal{I} = \left[\frac{\partial}{\partial S} \right]_{\nu_s,C} \left[\frac{\partial}{\partial \nu_s} \right]_{S,C} \mathcal{I}, \quad (6.103)$$

so that, via the fundamental thermodynamic relation (6.102), we have the Maxwell relation

$$\left[\frac{\partial T}{\partial \nu_s} \right]_S = - \left[\frac{\partial p}{\partial S} \right]_{\nu_s}. \quad (6.104)$$

6.8.2 Summary of the Maxwell relations

The other thermodynamic potentials, and their associated fundamental thermodynamical relations, lead to further Maxwell relations as summarized here

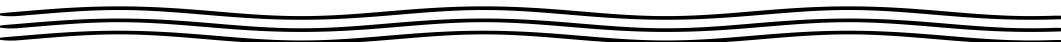
$$d\mathcal{J} = T dS - p d\nu_s \implies \left[\frac{\partial T}{\partial \nu_s} \right]_S = - \left[\frac{\partial p}{\partial S} \right]_{\nu_s} \quad (6.105)$$

$$d\mathcal{H} = T dS + \nu_s dp \implies \left[\frac{\partial T}{\partial p} \right]_S = \left[\frac{\partial \nu_s}{\partial S} \right]_p \quad (6.106)$$

$$d\mathcal{G} = -S dT + \nu_s dp \implies \left[\frac{\partial S}{\partial p} \right]_T = - \left[\frac{\partial \nu_s}{\partial T} \right]_p. \quad (6.107)$$

$$d\mathcal{F} = -S dT - p d\nu_s \implies \left[\frac{\partial S}{\partial \nu_s} \right]_T = \left[\frac{\partial p}{\partial T} \right]_{\nu_s}. \quad (6.108)$$

These four Maxwell relations for single-component fluids involve permutations on cross derivatives of (T, S) and (p, ν_s) . In statistical mechanics, (T, S) determine the density of accessible microscopic states forming the thermodynamic system, whereas (p, ν_s) involves an external control parameter and its corresponding generalized force.



6.9 Appendix: partial differential identities

As discussed in Section 6.1.4, the mathematics of thermodynamics consists of calculus on a differentiable manifold. To make thermodynamics of practical use requires skills with manipulating partial differential relations. We briefly encountered such manipulations with the Maxwell relations in Section 6.8, as well as the discussion of thermodynamic potentials in Section 6.6. A successful use of such manipulations requires care to maintain consistent functional

dependencies while performing partial derivative operations. In this section we derive some expressions commonly found in these manipulations in hopes of removing some of their mystery. For this purpose we consider a scalar function, Ψ , of three independent variables, (x, y, z) . Although this notation suggests Cartesian spatial coordinates, the independent variables relevant for thermodynamics are those that describe the thermodynamic configuration space as discussed in Section 6.6 when formulating the variety of thermodynamic potentials.

6.9.1 Slope of curve defined by $d\Psi = 0$ and $dz = 0$

Consider processes occurring on a surface of constant Ψ , in which case the condition,

$$d\Psi = 0, \quad (6.109)$$

acts as a constraint on the independent variables, (x, y, z) , so that

$$d\Psi = \left[\frac{\partial \Psi}{\partial x} \right]_{y,z} dx + \left[\frac{\partial \Psi}{\partial y} \right]_{y,x} dy + \left[\frac{\partial \Psi}{\partial z} \right]_{z,y} dz = 0. \quad (6.110)$$

In particular, we seek information about how x and y vary along the constant Ψ surface when z is also held constant, in which case

$$dz = 0 \quad \text{and} \quad d\Psi = 0 \implies \left[\frac{\partial \Psi}{\partial x} \right]_{y,z} dx = - \left[\frac{\partial \Psi}{\partial y} \right]_{y,x} dy. \quad (6.111)$$

We are thus led to the expression for the slope of the curve in the (x, y) -plane that is formed by the intersection of that plane with the constant Ψ surface

$$\left[\frac{\partial x}{\partial y} \right]_{\Psi,z} = - \frac{(\partial \Psi / \partial y)_{x,z}}{(\partial \Psi / \partial x)_{y,z}}. \quad (6.112)$$

The same manipulations also determine the inverse slope, in which case

$$\left[\frac{\partial y}{\partial x} \right]_{\Psi,z} = - \frac{(\partial \Psi / \partial x)_{y,z}}{(\partial \Psi / \partial y)_{x,z}} = \frac{1}{(\partial x / \partial y)_{\Psi,z}}. \quad (6.113)$$

6.9.2 Slope of curve defined by $d\Psi = 0$ and $dx = 0$ or $dy = 0$

The identical manipulations used above for $dz = 0$ can separately be repeated for $dx = 0$ and $dy = 0$, thus resulting in the identities

$$\left[\frac{\partial z}{\partial y} \right]_{\Psi,x} = - \frac{(\partial \Psi / \partial y)_{z,x}}{(\partial \Psi / \partial z)_{y,x}} = \frac{1}{(\partial y / \partial z)_{\Psi,x}} \quad (6.114a)$$

$$\left[\frac{\partial x}{\partial z} \right]_{\Psi,y} = - \frac{(\partial \Psi / \partial z)_{x,y}}{(\partial \Psi / \partial x)_{z,y}} = \frac{1}{(\partial z / \partial x)_{\Psi,y}}. \quad (6.114b)$$

6.9.3 Triple product identity

Now return to the constraint, $d\Psi = 0$, which allows us to eliminate one of the three independent variables in terms of the others, for example,

$$d\Psi = 0 \implies z = z(x, y), \quad (6.115)$$

so that

$$dz = \left[\frac{\partial z}{\partial x} \right]_{\Psi,y} dx + \left[\frac{\partial z}{\partial y} \right]_{\Psi,x} dy. \quad (6.116)$$

We again seek information about how x and y vary along the constant Ψ surface when z is also held constant, in which case

$$dz = 0 \implies \left[\frac{\partial x}{\partial y} \right]_{\Psi,z} = -\frac{(\partial z/\partial y)_{\Psi,x}}{(\partial z/\partial x)_{\Psi,y}}. \quad (6.117)$$

Rearrangement, along with the slope identity (6.114a), leads to the remarkably versatile triple product identity

$$\left[\frac{\partial z}{\partial x} \right]_{\Psi,y} \left[\frac{\partial y}{\partial z} \right]_{\Psi,x} \left[\frac{\partial x}{\partial y} \right]_{\Psi,z} = -1. \quad (6.118)$$

6.9.4 Further study

Appendix A of [Callen \(1985\)](#) works through a number of very useful elementary identities involving partial derivative operations, including those presented here. We also encounter these identities when studying generalized vertical coordinates in VOLUME 3 of this book.

6.10 Appendix: exact and inexact differentials

In this appendix we present a primer on exact differentials and inexact differentials, with both appearing throughout the study of equilibrium thermodynamics.

6.10.1 Exact differentials

Consider an arbitrary scalar function of space, $F(\mathbf{x})$, written as a function of Cartesian coordinates, \mathbf{x} . A differential increment for that function, computed between two close points \mathbf{x} and $\mathbf{x} + d\mathbf{x}$, is given by

$$dF(\mathbf{x}) = F(\mathbf{x} + d\mathbf{x}) - F(\mathbf{x}) = d\mathbf{x} \cdot \nabla F, \quad (6.119)$$

where we dropped higher order terms due to the infinitesimal nature of the increments. It follows that we can determine the finite increment between two points through integration

$$F(\mathbf{x}_B) - F(\mathbf{x}_A) = \int_{\mathbf{x}_A}^{\mathbf{x}_B} dF(\mathbf{x}) = \int_{\mathbf{x}_A}^{\mathbf{x}_B} d\mathbf{x} \cdot \nabla F. \quad (6.120)$$

These results are familiar from elementary calculus, with the increment, dF , given by equation (6.119) termed an [exact differential](#). Importantly, the finite increment, $F(\mathbf{x}_B) - F(\mathbf{x}_A)$, depends only on the endpoint values of F . It does not depend on the path taken to go from \mathbf{x}_A to \mathbf{x}_B . Correspondingly, the integral of an exact differential vanishes when computed around a closed loop

$$\oint dF = 0. \quad (6.121)$$

Now consider a differential expression written as

$$\mathbf{A} \cdot d\mathbf{x} = A dx + B dy + C dz, \quad (6.122)$$

where $\mathbf{A} = A \hat{\mathbf{x}} + B \hat{\mathbf{y}} + C \hat{\mathbf{z}}$ is a vector represented using Cartesian coordinates. If $\nabla \times \mathbf{A} = 0$, then \mathbf{A} can be written as the gradient of a scalar

$$\nabla \times \mathbf{A} = 0 \implies \mathbf{A} = \nabla F, \quad (6.123)$$

in which case we have an exact differential expression

$$\mathbf{A} \cdot d\mathbf{x} = \nabla F \cdot d\mathbf{x} = dF. \quad (6.124)$$

We conclude that the differential $dF = \mathbf{A} \cdot d\mathbf{x}$ is exact if

$$\nabla \times \mathbf{A} = 0 \implies dF = \mathbf{A} \cdot d\mathbf{x} \quad \text{exact differential.} \quad (6.125)$$

6.10.2 Inexact differentials

If $\nabla \times \mathbf{A} \neq 0$, then $\mathbf{A} \cdot d\mathbf{x}$ is termed an **inexact differential**. We make use of the following notation for inexact differentials,

$$dG = \mathbf{A} \cdot d\mathbf{x}, \quad (6.126)$$

(note the symbol d for the inexact differential). Notably, the path integral of an inexact differential depends on the path taken between the endpoints. Correspondingly, the integral of an inexact differential around a closed loop does not generally vanish

$$\oint dG \neq 0. \quad (6.127)$$

6.10.3 Integrating factors

Consider again the inexact differential, $dG = \mathbf{A} \cdot d\mathbf{x}$, and assume there exists a scalar function, ϕ , so that the product, $\phi^{-1} dG$, is exact. For ϕ to exist it must be such that

$$\nabla \times (\mathbf{A} \phi^{-1}) = 0. \quad (6.128)$$

Consequently, we can write

$$\mathbf{A} = \phi \nabla F, \quad (6.129)$$

so that

$$dG = \mathbf{A} \cdot d\mathbf{x} = \phi \nabla F \cdot d\mathbf{x} = \phi dF. \quad (6.130)$$

The function, ϕ , is known as an **integrating factor**. As seen in Section 6.2.3, pressure is the integrating factor for mechanical work, temperature is the integrating factor for heating, and the **chemical potential** is the integrating factor for chemical work.

6.10.4 An example using the velocity field

Consider the scalar product, $\mathbf{v} \cdot d\mathbf{x}$, where \mathbf{v} is the velocity field for a fluid and $d\mathbf{x}$ is a differential increment in space directed along a path and represented using Cartesian coordinates. Furthermore, introduce the curl of the velocity, which defines the vorticity, $\boldsymbol{\omega} = \nabla \times \mathbf{v}$. For cases where the vorticity vanishes, $\boldsymbol{\omega} = 0$, then $d\Psi = \mathbf{v} \cdot d\mathbf{x}$ is an exact differential. Consequently, Stokes' theorem means that the circulation vanishes for an irrotational velocity field computed

around an arbitrary closed loop

$$\mathcal{C} \equiv \oint_{\partial S} \mathbf{v} \cdot d\mathbf{x} = \int_S \boldsymbol{\omega} \cdot \hat{\mathbf{n}} dS = 0. \quad (6.131)$$

Another way to see this result is to note that a vanishing curl means that the velocity field can be expressed as the gradient of a scalar, $\mathbf{v} = \nabla\psi$, so that $d\Psi = \nabla\psi \cdot d\mathbf{x}$, which is manifestly exact.

6.10.5 A hiker climbing a mountain

Consider a hiker climbing a mountain. The mechanical work exurted by the hiker, which is force applied over a distance, is a function of the path taken. Some paths are smooth and well marked, whereas others are rough and poorly marked. Likewise, the frictional heating (of the hiker's feet, for example) depend on details of the path (and the shoes!). So although the start and finish points are fixed, the work exerted and heat generated in going between these points is a function of the path.

In contrast, the change in gravitational potential energy between the start and finish points is a function only of the elevation difference between the start and finish points. It does not depend on the path between the points. So the gravitational potential energy increment is an exact differential, with the potential energy for each point a function of the elevation at the point and not, instead, determined by the path to that point.

6.11 Appendix: Euler's theorem for homogeneous functions

We make use of Euler's theorem for homogeneous functions in our discussion of thermodynamic properties, particularly when examining materially open systems starting at Section 6.3. We here prove Euler's theorem by considering a suite of Q independent variables, X_1, X_2, \dots, X_Q , and an arbitrary function of these variables, $F(X_1, X_2, \dots, X_Q)$. We say that this function is a homogeneous function of degree γ if the following property holds

$$F(\lambda X_1, \lambda X_2, \dots, \lambda X_Q) = \lambda^\gamma F(X_1, X_2, \dots, X_Q), \quad (6.132)$$

with λ an arbitrary scalar. The left hand side is the function evaluated with each of the independent variables scaled by the same number, λ . The right hand side is the function evaluated with the unscaled variables, but multiplied by the scale raised to the power γ .

A particularly remarkable and useful property of such functions can be found by taking $\partial/\partial\lambda$ on both sides of the identity (6.132). The left hand side has the following partial derivative, as found through the chain rule

$$\begin{aligned} \frac{\partial F(\lambda X_1, \lambda X_2, \dots, \lambda X_Q)}{\partial \lambda} &= \frac{\partial F(X_1, X_2, \dots, X_Q)}{\partial X_1} \frac{\partial(\lambda X_1)}{\partial \lambda} + \dots + \frac{\partial F(X_1, X_2, \dots, X_Q)}{\partial X_Q} \frac{\partial(\lambda X_Q)}{\partial \lambda} \\ &= \sum_{q=1}^Q \left[\frac{\partial F(X_1, X_2, \dots, X_Q)}{\partial X_q} \right]_{X_r \neq q} X_q \end{aligned} \quad (6.133)$$

The derivative of the right hand side of equation (6.132) is given by

$$\frac{\partial[\lambda^\gamma F(X_1, X_2, \dots, X_Q)]}{\partial \lambda} = \gamma \lambda^{\gamma-1} F(X_1, X_2, \dots, X_Q). \quad (6.134)$$

Bringing these results together leads to Euler's theorem for homogeneous functions, which is found by setting $\lambda = 1$

$$\sum_{q=1}^Q X_q \left[\frac{\partial F(X_1, X_2, \dots, X_Q)}{\partial X_q} \right]_{X_r \neq q} = \gamma F(X_1, X_2, \dots, X_Q). \quad (6.135)$$

As we find in this chapter, an intensive property is represented by a homogeneous function of degree $\gamma = 0$, meaning such properties are scale invariant. For example, a bucket of homogeneous water has the same temperature whether or not we remove an arbitrary sample of the water. In contrast, an extensive property is represented by a homogeneous function of degree $\gamma = 1$. In Section 6.3 we develop thermodynamic implications of such mathematical properties for materially open systems.

6.12 Appendix: Legendre transformations

As seen in Section 6.6, there are a suite of thermodynamic potentials that allow us to explore thermodynamics through the lens of distinct independent variables. Switching between thermodynamic potentials and corresponding independent variables is enabled by the Legendre transformation. We here offer the mathematical basics, starting with an operational perspective and then providing a geometrical view.

6.12.1 Operational perspective

Consider a function, $Y = Y(X)$, that has an explicit dependence on the independent variable, X , and assume this function has a continuous derivative, which we write as

$$P = \frac{dY}{dX}. \quad (6.136)$$

Furthermore, assume that there is a one-to-one relation between X and P , which can be ensured if the second derivative never vanishes, $d^2Y/dX^2 \neq 0$.

Now define a new function through a Legendre transformation

$$\Psi = Y - X(dY/dX) = Y - X P. \quad (6.137)$$

What is the functional dependence of Ψ ? To answer this question requires us to compute the differential of Ψ

$$d\Psi = dY - P dX - X dP = -X dP, \quad (6.138)$$

which follows since

$$dY = (dY/dX) dX = P dX. \quad (6.139)$$

We thus find that

$$d\Psi = -X dP \implies \Psi = \Psi(P), \quad (6.140)$$

so that the Legendre transformation has allowed us to move from the function, $Y(X)$, to the function, $\Psi(P)$. Although these two functions have distinct functional dependencies, since there is a one-to-one relation between X and P , then there is equal information contained in $Y(X)$ and $\Psi(P)$. Motivation for using one or the other function is based on subjective reasons, such as whether an experimentalist has more control over X or P as independent variables.

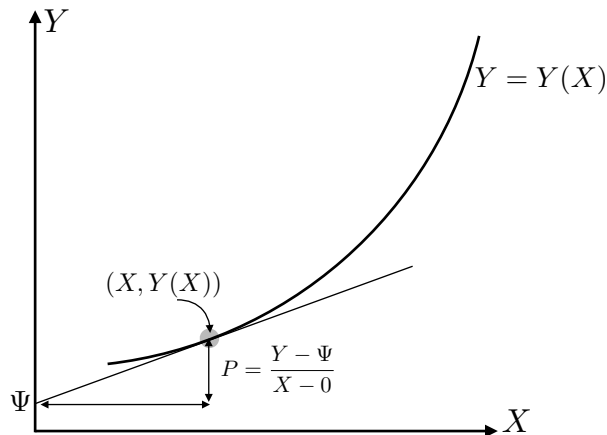


FIGURE 6.5: Illustrating the geometry of the Legendre transformation according to the discussion in Section 6.12.2. For each point, X , on the real line, the functional relation, $Y = Y(X)$, specifies the position, (X, Y) , of a point on the X - Y plane. Another way to specify the same point is to provide the slope, $P = dY/dX$, and Y -intercept, $\Psi = Y - PX$, for a line passing through that point. The envelope of all such lines, $\Psi(P)$, then provides the same information as the original function, $Y(X)$.

Another, somewhat longer, way to derive the above result is to write Y as an implicit function of P through

$$Y = Y(X) = Y[X(P)], \quad (6.141)$$

so that

$$dX = \frac{dX}{dP} dP \quad X \text{ and } P \text{ are 1-to-1 related} \quad (6.142a)$$

$$dY = \frac{dY}{dX} \frac{dX}{dP} dP = P \frac{dX}{dP} dP \quad \text{chain rule and } P = dY/dX. \quad (6.142b)$$

Use of these identities in equation (6.138) again renders $d\Psi = -X dP$.

The assumption of a non-vanishing second derivative holds for thermodynamic functions since such functions are either convex (also called concave up) ($d^2Y/dX^2 > 0$), or concave ($d^2Y/dX^2 < 0$) functions of their natural variables. For example, in a system with fixed matter concentration, entropy is concave in internal energy whereas internal energy is convex in entropy. An important exception to this result holds at critical points, where the second derivative vanishes. As discussed in Chapter 8 of [Callen \(1985\)](#), such points are central to determining the stability of thermodynamic equilibria.

6.12.2 Geometrical presentation

For each point, X , on the real line, the functional relation, $Y = Y(X)$, specifies the position, (X, Y) , of a point on the X - Y plane. As illustrated in Figure 6.5, there is another means to specify the same point. Namely, we can provide the envelope of tangent lines to each point along the curve, $Y = Y(X)$, along with the Y -intercept of these tangent lines. The tangent lines at each point, X , are specified by the slope, P , as given by

$$P = \frac{Y - \Psi}{X - 0} \implies \Psi = Y - X P, \quad (6.143)$$

with Ψ the intercept along the Y -axis. We thus have the Legendre transformation as a special realization of line geometry in a plane, with the envelope of such lines providing the same

information as the original function. The following quote from Section 5-2 of [Callen \(1985\)](#) provides a summary of the geometrical idea.

Just as every point in the plane is described by the two numbers X and Y , so every straight line in the plane can be described by two numbers, P and Ψ , where P is the slope of the line and Ψ is the intercept along the Y -axis. Then just as the relation, $Y = Y(X)$, selects a subset of all possible points (X, Y) , a relation $\Psi = \Psi(P)$ selects a subset of all possible lines (P, Ψ) . A knowledge of the intercepts, Ψ , of the tangent lines as a function of the slopes, P , enables us to construct the family of tangent lines and thence the curve of which they are an envelope. Thus the relation, $\Psi = \Psi(P)$ is completely equivalent to $Y = Y(X)$.

6.12.3 Example

Consider a parabola, $Y(X) = X^2$, in which case $P = dY/dX = 2X$ so that the Legendre transformation yields

$$\Psi = Y - P X = X^2 - 2X^2 = -(P/2)^2, \quad (6.144)$$

as well as the differential

$$d\Psi = -P dP/2 = -X dP. \quad (6.145)$$

With $dP/dX = d^2Y/dX^2 = 2$, we know there is a one-to-one relation between X and P since the second derivative never vanishes.

6.12.4 Further study

Section 5-2 of [Callen \(1985\)](#) provides a thorough discussion of Legendre transformations, from which the geometrical presentation is adapted. It is notable that in analytical mechanics (see VOLUME 4 of this book), Lagrangian dynamics and Hamiltonian dynamics are connected via a Legendre transformation.



6.13 Exercises

EXERCISE 6.1: ADDITIVITY PROPERTY OF ENTROPY

In developing the notion of entropy from basic postulates, one is led to assume entropy changes are additive. Namely, when a physical system undergoes a physical process, the entropy change for the full system, dS^e , equals to the sum of the entropy change for the system decomposed into arbitrary subsystems

$$dS^e = \sum_{n=1}^N dS_n^e. \quad (6.146)$$

Consider how this assumption plays out for a heat reservoir with temperature, T , that gains or loses a quantity of heat, $d\Omega$. For the full system, the entropy change can only be a function of the temperature and the heating

$$dS^e = f(T, d\Omega). \quad (6.147)$$

Now decompose the system into its N identical subsystems, so that each subsystem experiences $N^{-1} dQ$ heating. For the additive property to hold, we must have this entropy change satisfying

$$dS^e = f(T, dQ) = N f(T, N^{-1} dQ). \quad (6.148)$$

Show that this condition can only be satisfied by

$$f(T, dQ) = g(T) dQ, \quad (6.149)$$

where $g(T)$ remains to be determined. That is, additivity means that the entropy change must be split into the product of the heating times a function of temperature.

EXERCISE 6.2: ENTROPY DIFFERENCE BETWEEN TWO THERMODYNAMIC EQUILIBRIA

Consider two thermodynamic equilibrium states, A and B , for an isolated system as depicted in Figure 6.6. Assuming the physical system is a simple ideal gas, compute the entropy difference

$$\Delta S^e = S_B^e - S_A^e. \quad (6.150)$$

Note that we explore properties of an [ideal gas](#) atmosphere in Section 7.5. We do not require all of that material for this exercise. Instead, we only need to know that for an ideal gas in thermodynamic equilibrium, its thermodynamic properties are constrained to satisfy the [equation of state](#),

$$pV = n^{\text{mole}} R^g T, \quad (6.151)$$

as discussed in Section 7.5.1. Also, we need to know that the internal energy of a simple ideal gas is given by

$$J^e = c_v T, \quad (6.152)$$

where c_v is a constant heat capacity.

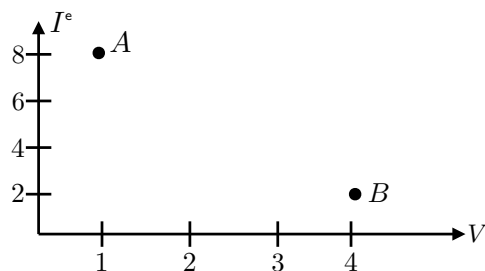


FIGURE 6.6: We here depict the J^e - V plane from the thermodynamic configuration space of a physical system. Points A and B are two thermodynamic equilibrium states whose volume and internal energy are given by $A(1, 8)$ and $B(4, 2)$ using arbitrary energy and volume units.

EXERCISE 6.3: ADIABATIC FREE EXPANSION OF A SIMPLE IDEAL GAS

In Figure 6.7 we depict a simple ideal gas in thermodynamic equilibrium within an insulated container of volume, V , with the gas having an initial temperature, T , and pressure, p . We allow this gas to freely expand into another insulated and evacuated container with volume, $2V$, where it reaches its new thermodynamic equilibrium state in the volume $2V$. Note that an evacuated container is a vacuum, so that it has no gas and a vanishing pressure, $p = 0$. Assume no heat is exchanged with the environment before, during, and after the free expansion process (all stages are adiabatic), and assume the system is materially closed (no exchange of matter).

Make use of the properties of an ideal gas as given in the writeup of Exercise 6.2.

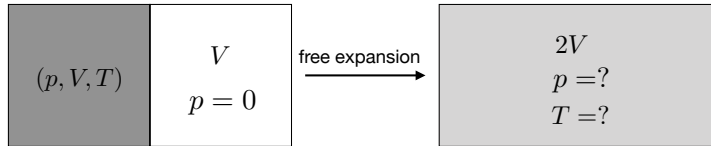


FIGURE 6.7: Illustrating the adiabatic free expansion of a simple ideal gas for Exercise 6.3. The left panel shows the initial equilibrium state, with the gas having properties (p, V, T) . This gas is next to an equal volume that is evacuated and so has $p = 0$. The right panel shows the final equilibrium state, in which the gas has freely expanded to the volume, $2V$. The process is assumed to occur adiabatically. We are asked to determine properties of the expanded gas after it reaches thermodynamic equilibrium.

- (a) Is the free expansion process reversible? Is it quasi-static? Discuss.
- (b) Has there been any mechanical work done during the free expansion?
- (c) Is the temperature at the final thermodynamic equilibrium different from temperature of the initial thermodynamic equilibrium? Hint: recall the first law of thermodynamics for a materially closed system. Also note that the internal energy of an ideal gas is directly proportional to the temperature.
- (d) Is there an entropy change as a result of the free expansion process? If so, then compute it. Hint: keep in mind that entropy is a state function.
- (e) Discuss how entropy can change even though the process is adiabatic.

EXERCISE 6.4: DERIVATION OF THE GIBBS-DUHEM RELATION

Show all of the steps leading to the Gibbs-Duhem relation (6.36).

EXERCISE 6.5: CHEMICAL POTENTIAL IDENTITY

As seen in Section 10.5.6, we have need to consider the partial derivative

$$\left[\frac{\partial \mathcal{H}}{\partial C} \right]_{T,p} \quad (6.153)$$

when determining the chemical work done by mixing within a fluid. Prove the identity

$$\left[\frac{\partial \mathcal{H}}{\partial C} \right]_{T,p} = \left[\frac{\partial \mathcal{H}}{\partial C} \right]_{S,p} - T \left[\frac{\partial \mu}{\partial T} \right]_{C,p} = \mu - T \left[\frac{\partial \mu}{\partial T} \right]_{C,p}. \quad (6.154)$$

Hint: as seen in Section 6.6.4, the natural functional dependence for enthalpy is $\mathcal{H}(S, p, C)$, whereas in Section 6.6.5 we found the natural function dependence of the Gibbs potential to be $\mathcal{G}(T, p, C)$. Equate the exact differential expressions for enthalpy using the two functional dependencies $\mathcal{H}(S, p, C)$ and $\mathcal{G}(T, p, C)$, and then derive a Maxwell relation based on the fundamental thermodynamic relation written in terms of the Gibbs potential.

EXERCISE 6.6: EXAMPLE LEGENDRE TRANSFORMATION

Using the notation from Section 6.12, consider a function, $Y(X) = A e^{BX}$. What is its Legendre transformed partner, $\Psi(P)$?

EXERCISE 6.7: HELMHOLTZ FREE ENERGY

Follow the analysis in Section 6.6 for the Helmholtz free energy, which is defined by the Legendre transformation

$$\mathcal{F} = \mathcal{I} - T \mathcal{S} = -p \nu_s + \sum_{n=1}^N \mu^{(n)} C^{(n)}, \quad (6.155)$$

where the second equality made use of equation (6.61).



Chapter 7

THERMODYNAMICS WITH A GEOPOTENTIAL

In this chapter we extend the equilibrium thermodynamics from Chapter 6 to allow for gravitational effects as embodied by the geopotential (which also includes the planetary centrifugal acceleration). Thermodynamic equilibrium of a fluid within a constant gravitational field is consistent with mechanical equilibrium; i.e., the fluid is in exact hydrostatic balance. We develop certain properties of hydrostatic fluids, such as the adiabatic lapse rate, potential temperature, and a variety of identities holding for an ideal gas (which is a useful approximation for the atmosphere).

It is notable that the hydrostatic balance is very useful for the atmosphere and ocean, particularly at the large scales, even though these fluids are moving and so not in exact hydrostatic balance. It is for this reason that the thermodynamics of a hydrostatic fluid is also useful for fluids in approximate hydrostatic balance.

Furthermore, it is notable that the relations derived in this chapter are suitable for atmosphere and ocean flows that are not in thermodynamic equilibrium, as evidenced by an *in situ* temperature that is not uniform throughout the fluid. The reason we can use equilibrium thermodynamic relations is that moving geophysical fluids largely satisfy the assumption of local thermodynamic equilibrium, in which infinitesimal fluid elements are in thermodynamic equilibrium even while finite fluid regions are not. This assumption allows us to ascribe thermodynamic properties to each point within the continuum fluid.

CHAPTER GUIDE

For discussions of thermodynamics in the presence of gravity, we consulted Chapter 9 of *Guggenheim* (1967), §25 of *Landau and Lifshitz* (1980), and Section 1.8 of *Kamenkovich* (1977). Many of the relations derived in this chapter also appear in atmospheric dynamics books, such as *Holton and Hakim* (2013).

7.1	Loose threads	210
7.2	Thermodynamic equilibrium with a geopotential	210
7.2.1	The First law of thermodynamics	210
7.2.2	Thermodynamic equilibrium with varying volume	211
7.2.3	Thermodynamic equilibrium with fixed volume	211
7.2.4	Vertical salinity gradient at thermodynamic equilibrium	212
7.2.5	Thermodynamic equilibrium for geophysical fluid flows?	213
7.2.6	Further study	214
7.3	Adiabatic lapse rate	214
7.3.1	Isentropic rearrangement	214

7.3.2	Thermodynamic formulation	215
7.3.3	Adiabatic lapse rate for pressure changes	216
7.3.4	Adiabatic lapse rate for height changes	216
7.3.5	Further study	216
7.4	Potential temperature	217
7.4.1	Motivating the definition of potential properties	217
7.4.2	Temperature changes from pressure changes	218
7.4.3	Defining the potential temperature	218
7.4.4	Potential temperature and specific entropy	219
7.5	Thermodynamic relations for a simple ideal gas	220
7.5.1	Equation of state	220
7.5.2	Internal energy	221
7.5.3	Heat capacity	222
7.5.4	Enthalpy	223
7.5.5	Thermal expansion coefficient	223
7.5.6	Fundamental thermodynamic relations	223
7.5.7	Isothermal compressibility	223
7.5.8	Sound speed	224
7.5.9	Adiabatic lapse rate	224
7.5.10	Geopotential thickness	224
7.5.11	Potential temperature	226
7.5.12	Further study	227
7.6	Exercises	227

7.1 Loose threads

- Exercise working through statistical mechanics of ideal gas in gravity field. Follow [Kubo \(1965\)](#), Chapter 2, Problem 3. Make the point of this being another way to derive hydrostatic balance as an equilibrium thermodynamic solution. Note that $T=\text{constant}$, which holds even in a gravity field. So the atmosphere has an exponential density profile.

7.2 Thermodynamic equilibrium with a geopotential

What are the properties of thermodynamic equilibrium in the presence of a [geopotential](#)? To answer this question, we here consider a single-component fluid system in the presence of a static geopotential, Φ , which represents the accelerations from both planetary gravity and planetary centrifugal. Throughout this analysis, we assume the acceleration arising from the geopotential is prescribed and is thus not affected by the mass of the thermodynamic system placed in the geopotential field. Furthermore, we assume the force from the geopotential is terrestrial, so that it is weak enough to ignore general relativistic effects.¹

7.2.1 The First law of thermodynamics

As seen in Section 6.2.3, a thermodynamic system subjected to a pressure field undergoes pressure work as its volume changes. Analogously, when the mass of a thermodynamic system

¹The relevant non-dimensional ratio is given by Φ/c^2 , with c the speed of light. See [Santiago and Visser \(2018\)](#) for a concise review of how gravity leads to a spatially dependent temperature in thermal equilibrium through Tolman's temperature gradient. These considerations are important when Φ/c^2 is order unity. For terrestrial purposes, $\Phi/c^2 \lll 1$, so that relativistic gravitational effects are entirely negligible.

changes within a geopotential field, then it is subjected to geopotential work, which takes the form

$$dW^{\text{geo}} = \Phi dM. \quad (7.1)$$

We thus see that the geopotential is an intensive property with mass its corresponding extensive property. Consequently, the first law for a quasi-static process is modified from equation (6.35b) to now read

$$d\mathcal{I}^e = -p dV + T dS^e + (\mu + \Phi) dM \iff dS^e = T^{-1} [p dV + d\mathcal{I}^e - (\mu + \Phi) dM], \quad (7.2)$$

where μ is the chemical potential in the absence of a geopotential

$$\left[\frac{\partial \mathcal{I}^e}{\partial M} \right]_{V, S^e} = \mu + \Phi \quad \text{and} \quad \left[\frac{\partial \mathcal{I}^e}{\partial M} \right]_{V, S^e, \Phi=0} = \mu. \quad (7.3)$$

The corresponding Gibbs-Duhem relation (6.36) now takes on the form

$$-V dp + S^e dT + M d(\mu + \Phi) = 0. \quad (7.4)$$

7.2.2 Thermodynamic equilibrium with varying volume

Following our discussion in Section 6.4, we consider two adjoining fluid regions that are allowed to adjust toward thermodynamic equilibrium in the presence of a geopotential field. The entropy differential in equation (6.48b) now takes on the form

$$dS^e = \left[\frac{1}{T_\alpha} - \frac{1}{T_\beta} \right] d\mathcal{I}_\alpha^e + \left[\frac{p_\alpha}{T_\alpha} - \frac{p_\beta}{T_\beta} \right] dV_\alpha - \left[\frac{\mu_\alpha + \Phi_\alpha}{T_\alpha} - \frac{\mu_\beta + \Phi_\beta}{T_\beta} \right] dM_\alpha, \quad (7.5)$$

which follows from the constraints (6.47) that assume fixed internal energy, mass, and volume for the composite system $\alpha \oplus \beta$. Equilibrium is characterized by $dS^e = 0$, which leads to a uniform temperature, as for the case with uniform Φ . A further extension of Section 6.4 suggests that $dp = 0$ and $d(\mu + \Phi) = 0$ at equilibrium. However, our understanding of fluid statics leads us to expect pressure to vary according to the hydrostatic balance discussed in Section 8.6. That is, a uniform pressure does not arise for equilibrium with a nonuniform geopotential. For that purpose we consider different constraints.

7.2.3 Thermodynamic equilibrium with fixed volume

To recover hydrostatic balance at thermodynamic equilibrium, consider the case with each volume remaining fixed. In this manner we have

$$d(\mathcal{I}_\alpha^e + \mathcal{I}_\beta^e) = 0 \quad \text{and} \quad dV_\alpha = dV_\beta = 0 \quad \text{and} \quad d(M_\alpha + M_\beta) = 0. \quad (7.6)$$

An example consists of two vertically positioned fluid boxes, with $\nabla\Phi$ defining the local vertical direction and with adjustment towards equilibrium consisting of mass moving from one box to the other. By fixing each of the region volumes, pressure does no work so that internal energy changes only through entropy and mass changes

$$d\mathcal{I}^e = T dS^e + (\mu + \Phi) dM \iff dS^e = T^{-1} [d\mathcal{I}^e - (\mu + \Phi) dM]. \quad (7.7)$$

Correspondingly, we find that thermodynamic equilibrium results when

$$dT = 0 \quad \text{and} \quad d(\mu + \Phi) = 0. \quad (7.8)$$

To interpret the equilibrium condition, $d(\mu + \Phi) = 0$, take the derivative with respect to geopotential, holding temperature and mass fixed, to render

$$\left[\frac{\partial \mu}{\partial \Phi} \right]_{T,M} = -1. \quad (7.9)$$

Using our understanding of fluid statics, we anticipate the hydrostatic balance and so assume that pressure at thermodynamic equilibrium is a monotonic function of the geopotential, Φ , so that

$$\left[\frac{\partial \mu}{\partial \Phi} \right]_{T,M} = \left[\frac{\partial \mu}{\partial p} \right]_{T,M} \left[\frac{dp}{d\Phi} \right]_{T,M} = -1. \quad (7.10)$$

Making use of the Maxwell relation (6.42c) and the identity (6.46d) leads to

$$\left[\frac{\partial \mu}{\partial p} \right]_{T,M} = V/M = 1/\rho, \quad (7.11)$$

where $\rho = M/V$ is the mass density. Using this result in equation (7.10) then leads to

$$\left[\frac{dp}{d\Phi} \right]_{T,M} = -\rho, \quad (7.12)$$

so that we recover an expression of hydrostatic balance

$$dp = -\rho d\Phi. \quad (7.13)$$

Hydrostatic balance says that the pressure differential is directly related to the geopotential differential, with the proportionality determined by mass density. The minus sign means that pressure increases when moving towards lower geopotential. We thus conclude that thermodynamic equilibrium in a geopotential field consists of a uniform temperature with pressure satisfying the exact hydrostatic balance (7.13).

7.2.4 Vertical salinity gradient at thermodynamic equilibrium

Consider the case of seawater as approximated by a two-component fluid, so that the entropy differential is given by

$$dS^e = T^{-1} [p dV + dJ^e - (\mu^{\text{salt}} + \Phi) dM^{\text{salt}} - (\mu^{\text{water}} + \Phi) dM^{\text{water}}]. \quad (7.14)$$

Separately holding the salt and freshwater masses fixed,² we apply the same formalism as pursued in Section 7.2.3 for a single component fluid, thus leading to

$$dT = 0 \quad \text{and} \quad d(\mu^{\text{salt}} + \Phi) = 0 \quad \text{and} \quad d(\mu^{\text{water}} + \Phi) = 0. \quad (7.15)$$

²This constraint is appropriate since we are looking for the entropy extrema for an isolated system with no boundary fluxes of either salt or freshwater.

Subtracting the second and third equilibrium condition leads to the equilibrium condition for the seawater chemical potential,

$$d(\mu^{\text{salt}} - \mu^{\text{water}}) = d\mu = 0. \quad (7.16)$$

Now recall the seawater chemical potential is given by equation (6.91) in terms of the salinity derivative of the specific Gibbs potential

$$\mu = \mu^{\text{salt}} - \mu^{\text{water}} = \left[\frac{\partial \mathcal{G}}{\partial S} \right]_{T,p}, \quad (7.17)$$

where $S = C_{\text{salt}}$ is the salt concentration. Hence, we may consider the seawater chemical potential to be a function of the temperature, pressure, and salt concentration

$$\mu = \mu(T, p, S). \quad (7.18)$$

The equilibrium conditions, $dT = 0$ and $d\mu = 0$, lead to

$$\frac{\partial \mu}{\partial S} dS + \frac{\partial \mu}{\partial p} dp = 0. \quad (7.19)$$

The hydrostatic relation $dp = -\rho d\Phi$ leads to

$$\frac{\partial \mu}{\partial S} \frac{dS}{d\Phi} = \rho \frac{\partial \mu}{\partial p}. \quad (7.20)$$

Assuming the geopotential takes on the simple form, $\Phi = g z$, then

$$\frac{\partial \mu}{\partial S} \frac{dS}{dz} = g \rho \frac{\partial \mu}{\partial p}. \quad (7.21)$$

We thus conclude that at thermodynamic equilibrium, the salinity maintains a nonzero geopotential gradient whereas the *in situ* temperature is uniform.

7.2.5 Thermodynamic equilibrium for geophysical fluid flows?

A vertically independent *in situ* temperature is not observed in the large-scale ocean or atmosphere (scales larger than fluid elements). Likewise, as noted on page 28 of [Kamenkovich \(1977\)](#), the vertical salinity gradient implied by the equilibrium relation (7.20) is not observed in the ocean. Both results put into question the relevance of *thermodynamic equilibrium* for geophysical fluids at the macroscale. Why is this? It is notable that this question was also examined by Maxwell, as evidenced by page 299 of [Maxwell \(1872\)](#), with his conclusions (reached in consultation with Lord Kelvin), largely consistent with the following discussion.

Thermodynamic equilibrium is realized through the action of molecular diffusion. As noted in Section 6.1 and throughout Chapter 10, fluids maintain *local thermodynamic equilibrium* at the scale of fluid elements (roughly 10^{-4} m), even for fluid elements undergoing turbulent fluid motion. However, molecular diffusion is far too slow to bring the large-scale atmosphere and ocean to a near thermodynamic equilibrium, which would require molecular diffusion to counteract diurnal and seasonal solar heating that push the larger scales out of thermodynamic equilibrium. Solar forcing also leads, through fluid instabilities, to the generation of turbulent motions. So the question becomes whether mixing from turbulent motion (i.e., turbulent

diffusion) can act as a highly efficient form of molecular diffusion to bring the atmosphere and ocean toward thermodynamic equilibrium at the large scales?

Answering this question requires us to draw upon some characteristics of turbulent diffusion.³ It also relies on basic properties of conservative tracers to be discussed more fully in Section 10.11, with potential temperature (Section 7.4) a near conservative tracer in the atmosphere and Conservative Temperature in the ocean (Section 10.10). A turbulent flow, even one with homogeneous and isotropic statistical properties, is a time evolving flow, whereas thermodynamic equilibrium is macroscopically static. So a statistically equilibrated turbulent flow is a non-equilibrium steady state, not a thermodynamic equilibrium state. Furthermore, conservative tracers are mixed by turbulent flows over length scales larger than fluid elements. But homogenizing such tracers does not homogenize *in situ* temperature in a geophysical fluid, since *in situ* temperature is not a conservative tracer due to its dependence on pressure, and pressure is not homogeneous within a gravity field.⁴

As a result, an atmosphere with a vertically homogeneous potential temperature has a vertically dependent *in situ* temperature (see discussion of lapse rate in Section 7.3). Likewise, an ocean with a vertically homogeneous Conservative Temperature and salinity has a vertically dependent *in situ* temperature. So while turbulent diffusion is highly efficient at homogenizing conservative scalar properties, this does not translate to homogenization of *in situ* temperature. We conclude that turbulent diffusion does not lead toward thermodynamic equilibrium in geophysical fluids.

7.2.6 Further study

The presentation in this section largely follows §25 of *Landau and Lifshitz* (1980) and Section 1.8 of *Kamenkovich* (1977).

7.3 Adiabatic lapse rate

The temperature of a fluid can change without the transfer of heat. This adiabatic temperature change arises when the fluid pressure changes. We here introduce the adiabatic lapse rate, which measures the vertical variations in temperature for a static fluid placed in a gravity field. There are two lapse rates commonly considered: one related to height and one related to pressure. We introduce some manipulations commonly performed with thermodynamic state functions and their partial derivatives, with the goal of expressing the lapse rate in terms of commonly measured response functions.

7.3.1 Isentropic rearrangement

Consider a finite region of a static fluid in a gravitational field. Assume the fluid is initially in a horizontal layer in thermodynamic equilibrium so that it has a uniform *in situ* temperature. Now rearrange the fluid into a vertical column, and do so without changing the entropy; i.e., without the transfer of heat across the fluid boundary (adiabatically) and without mixing any of its matter constituents. Performing this rearrangement raises the center of mass of the fluid

³See *Tennekes and Lumley* (1972) and chapter 13 in *Vallis* (2017) for a more complete treatment of turbulence.

⁴In section 10.10 we derive the evolution equation for *in situ* temperature as based on the first law of thermodynamics, thus revealing its connection to pressure. We also discuss general principles of conservative tracers in Section 10.11.

and thus increases the gravitational potential energy. This process requires mechanical work against the gravitational field.

Gravity makes pressure at the bottom of the vertical fluid column greater than at the top. This pressure difference modifies the temperature in the column, thus putting the fluid out of global thermodynamic equilibrium. We seek a general expression for how changes in pressure affects changes in temperature for a static fluid, with the pressure changes imparted reversibly and adiabatically so that entropy does not change. Mathematically, we seek an expression for the partial derivative

$$\hat{\Gamma} \equiv \left[\frac{\partial T}{\partial p} \right]_{C,S}, \quad (7.22)$$

which is known as the **adiabatic lapse rate**. The adiabatic lapse rate can be measured directly, with empirical expressions fit to laboratory measurements. Additionally, it is convenient to express it in terms of other thermodynamic response functions in order to garner further physical insight. The necessary manipulations form the bulk of this section, and they provide useful exposure to the variety of manipulations encountered with thermodynamics.

7.3.2 Thermodynamic formulation

When matter concentration of a fluid element is held fixed, the equation of state (6.83) allows us to consider entropy as a function of temperature and pressure so that

$$dS = \left[\frac{\partial S}{\partial T} \right]_p dT + \left[\frac{\partial S}{\partial p} \right]_T dp. \quad (7.23)$$

Substituting the definition of heat capacity from equation (6.95) leads to

$$T dS = c_p dT + T \left[\frac{\partial S}{\partial p} \right]_T dp. \quad (7.24)$$

It is useful to eliminate $(\partial S / \partial p)_T$ in favor of a more easily measurable quantity. For that purpose we make use of the Maxwell relation (6.107) to write

$$\left[\frac{\partial S}{\partial p} \right]_T = - \left[\frac{\partial \nu_s}{\partial T} \right]_p. \quad (7.25)$$

Introducing the thermal expansion coefficient (6.99) yields an expression for entropy changes in terms of temperature and pressure changes

$$T dS = c_p dT - T \left[\frac{\partial \nu_s}{\partial T} \right]_p dp = c_p dT - \left[\frac{T \alpha_T}{\rho} \right] dp. \quad (7.26)$$

Since c_p and α_T are readily measurable response functions, the expression (7.26) is a useful means to compute infinitesimal entropy changes when matter concentration is held constant.

7.3.3 Adiabatic lapse rate for pressure changes

Equation (7.26) means that the change in temperature associated with changes in pressure, with $dS = 0$ and $dC = 0$, can be written

$$\hat{\Gamma} = \left[\frac{\partial T}{\partial p} \right]_{C,S} = \frac{T \alpha_T}{\rho c_p}. \quad (7.27)$$

This relation holds for any form of pressure changes, such as those due to hydrostatic pressure changes or pressure fluctuations in an acoustic wave. Temperature indeed changes when pressure changes, even though there has been no heat exchanged with the environment. With $\hat{\Gamma}$ so defined, we can write the entropy change in equation (7.26) as

$$T dS = c_p (dT - \hat{\Gamma} dp). \quad (7.28)$$

The term $dT - \hat{\Gamma} dp$ subtracts from the *in situ* temperature differential the pressure induced changes in temperature. In Section 7.4 we introduce the [potential temperature](#), which is defined just for the purpose of removing changes due to pressure.

7.3.4 Adiabatic lapse rate for height changes

A static fluid in a gravity field is in exact hydrostatic balance, whereby the pressure at a point equals to the weight per area above that point (Section 8.6). Hydrostatic balance in a constant gravity field maintains the following relation between the pressure differential and the vertical differential

$$dp = -g \rho dz. \quad (7.29)$$

Use of the chain rule within the lapse rate expression (7.27) leads to

$$\Gamma = \left[\frac{\partial T}{\partial z} \right]_{C,S} = \left[\frac{\partial T}{\partial p} \right]_{C,S} \left[\frac{\partial p}{\partial z} \right] = -\rho g \left[\frac{T \alpha_T}{\rho c_p} \right] = -\frac{g T \alpha_T}{c_p}. \quad (7.30)$$

This form for the lapse rates measures the change in temperature (the *lapse*) within a constant composition fluid element as it is isentropically moved vertically through a hydrostatic pressure field.

7.3.5 Further study

In Section 7.5.9 we consider the adiabatic lapse rate for the special case of a simple ideal gas. For this gas, the internal energy of a fluid element is represented entirely by its temperature, and pressure is caused solely by molecular thermal motion. For water, however, molecular interaction energies are important, and pressure arises not only from thermal motion but also from interaction forces of the densely packed molecules. These differences between the behavior of water and a perfect gas are examined by [McDougall and Feistel \(2003\)](#) in terms of molecular dynamics. In particular, they note that the lapse rate, being proportional to the thermal expansion coefficient, can be negative when the thermal expansion is negative. A negative thermal expansion coefficient occurs in cool fresh water, such as the Baltic Sea, whereby its temperature decreases as work is done on the fluid element as pressure increases.

The addition of water to the atmosphere modifies the lapse rate, as the air is then no longer well approximated by an ideal gas. Chapter 18 of [Vallis \(2017\)](#) offers a pedagogical discussion of the thermodynamics of a moist tropical atmosphere.

7.4 Potential temperature

As discussed in Section 7.2, thermodynamic equilibrium of a fluid in a geopotential field sees the hydrostatic pressure balancing the weight of fluid. Thermodynamic equilibrium is also characterized by a uniform *in situ temperature* temperature, T , which requires removal of the temperature gradient associated with the adiabatic lapse rate discussed in Section 7.3. The molecular diffusive processes (see Section 10.10) that homogenize *in situ* temperature are very slow, so that geophysical fluids are rarely in thermodynamic equilibrium. We here introduce the notion of *potential temperature*, which offers a measure of temperature that removes the adiabatic lapse rate. With some qualifiers discussed below, turbulent mixing processes active in geophysical fluids lead to a nearly homogenous potential temperature. As such, potential temperature is a more practical thermodynamic tracer than *in situ* temperature.

7.4.1 Motivating the definition of potential properties

Heating and cooling of the ocean occur predominantly near the ocean surface.⁵ In contrast, transport in the ocean interior is nearly adiabatic and isohaline (i.e., nearly isentropic). The physical picture is suggested whereby the surface ocean boundary layer experiences irreversible processes that set characteristics of water masses that move quasi-reversibly within the ocean interior. As a means to characterize and thus to label these waters, oceanographers prefer to use properties that maintain constant values when moving within the quasi-isentropic ocean interior. Salinity is a good label for this purpose since it is only altered by mixing between waters of varying concentrations, and in turn it is materially constant in the absence of mixing.⁶ This behavior constitutes a basic property of material tracers, which are tracers that measure the mass of a constituent per mass of a fluid sample. However, it is *not* a property of the *in situ* temperature, T , which changes even in the absence of mixing due to pressure effects. We are thus motivated to seek a thermodynamic property that evolves analogously to material tracers, so that it can be used as a second material label for fluid elements. A similar motivation stems from the analysis of atmospheric motions.

A thermodynamic property that remains constant when a fluid element is moved from one pressure to another, without the transfer of heat or matter and without any kinetic energy dissipation, is said to be a *potential property*. *Potential temperature* is the example that concerns us in this section. As we will see, in some special cases the potential temperature is directly proportional to the specific entropy. More practically, it offers a means to estimate the heat transport within a geophysical fluid.

Conservative Temperature, Θ , is another potential property discussed in Section 10.10, with Conservative Temperature defined as the potential enthalpy divided by a constant heat capacity. As detailed in [McDougall \(2003\)](#), Conservative Temperature provides a more convenient and accurate measure of heat transport in a geophysical fluid than potential temperature. As such, Θ is now more commonly used in applications than potential temperature, θ , ([McDougall et al., 2021](#)).

⁵Geothermal heating at the ocean bottom is a notable exception, and it can be very large over regions next to the crustal vents. However, when averaged over larger scales, geothermal heating is far smaller than radiative and turbulent heating at the ocean surface.

⁶There are nuances concerning what we mean by “salinity”, with details given by [IOC et al. \(2010\)](#) (in particular, see Sections A.8 and A.9). We are not directly concerned with these nuances in this book, though note that they are important for ocean measurements and the interpretation of salinity as used in numerical ocean models ([McDougall et al., 2021](#)).

7.4.2 Temperature changes from pressure changes

Motion of a fluid element, without exchange of heat (adiabatic) or matter (constant concentration), generally changes the pressure of the fluid element. In turn, this motion causes the *in situ* temperature to have a differential that is in proportion to the adiabatic lapse rate given by (Section 7.3)

$$dT = \hat{\Gamma} dp. \quad (7.31)$$

Consequently, and as already noted, the *in situ* temperature is not a useful thermodynamic variable to label fluid elements since it changes even for adiabatic and constant concentration processes. Instead, it is more useful to remove the adiabatic pressure effects. This is the key reason for introducing potential temperature.

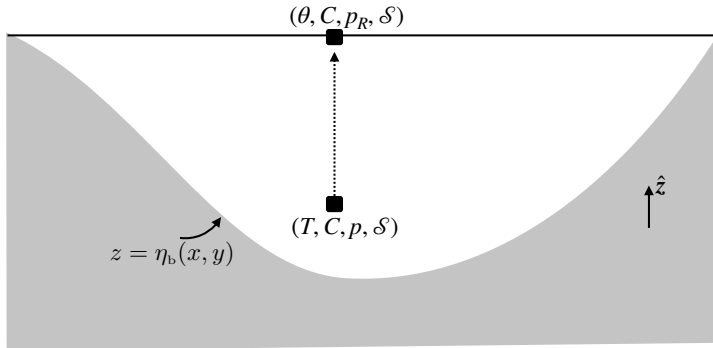


FIGURE 7.1: Potential temperature is the *in situ* temperature that a fluid element of fixed material composition would have if isentropically displaced from its *in situ* pressure to a reference pressure, p_R . The schematic here depicts that displacement for a seawater fluid element with *in situ* temperature, T , salinity, $S = 1000\text{C}$, pressure, p , and specific entropy, S . The element is moved to the ocean surface with the standard sea level atmospheric pressure providing the reference pressure.

7.4.3 Defining the potential temperature

Operationally, the potential temperature is based on removing adiabatic pressure effects from *in situ* temperature. That is, potential temperature is defined as the *in situ* temperature that a fluid element of fixed material composition would have if it were isentropically transported from its *in situ* pressure to a reference pressure p_R , with the reference pressure typically taken at the ocean/land surface (see Figure 7.1). Mathematically, the potential temperature, θ , is the reference temperature obtained via integration of $dT = \hat{\Gamma} dp$ for an isentropic *in situ* temperature change with respect to pressure

$$\int_{\theta}^T dT' = \int_{p_R}^p \hat{\Gamma}(T', p', C) dp' \implies T = \theta(T, p_R, C) + \int_{p_R}^p \hat{\Gamma}(T, p', C) dp', \quad (7.32)$$

with $\hat{\Gamma}$ the lapse rate defined in terms of pressure changes in equation (7.27). By definition, the *in situ* temperature, T , equals the potential temperature, θ , at the reference pressure, $p = p_R$. Elsewhere, they differ by an amount determined by the adiabatic lapse rate. Furthermore, we see that

$$\left[\frac{\partial T}{\partial p} \right]_{C,S} = \left[\frac{\partial \theta}{\partial p} \right]_{C,S} + \hat{\Gamma}. \quad (7.33)$$

However, by definition

$$\left[\frac{\partial T}{\partial p} \right]_{C,s} = \hat{\Gamma} \quad (7.34)$$

so that

$$\left[\frac{\partial \theta}{\partial p} \right]_{C,s} = 0. \quad (7.35)$$

That is, by construction, the potential temperature depends explicitly on the concentration, C , and *in situ* temperature, T , and has a parametric dependence on the reference pressure. It has no explicit dependence on the *in situ* pressure when holding tracer concentration and entropy fixed. Finally, we emphasize that the potential temperature is a function of tracer concentration, C . Hence, the potential temperature generally changes if the tracer concentration changes. For example, potential temperature in the ocean changes if the salinity changes.

7.4.4 Potential temperature and specific entropy

An alternative definition of the potential temperature follows by noting that the entropy of a fluid element remains unchanged as it is reversibly moved to the reference pressure. Consequently, writing entropy as a function of the *in situ* temperature, pressure, and matter concentration as in equation (6.83)

$$S = S(T, p, C) \quad (7.36)$$

leads to the defining identity for potential temperature

$$S = S(T, p, C) = S(\theta, p_R, C). \quad (7.37)$$

This relation directly connects changes in entropy to changes in potential temperature

$$dS = \left[\frac{\partial S(\theta, p_R, C)}{\partial \theta} \right]_C d\theta. \quad (7.38)$$

Consequently, the reversible transport of a fluid element with constant matter concentration ($dC = 0$) occurs with both a constant specific entropy and constant potential temperature.

We can go even further than the relation (7.38) by recalling that equation (7.28) relates the differential of specific entropy to temperature and pressure

$$T dS = c_p (dT - \hat{\Gamma} dp), \quad (7.39)$$

where $\hat{\Gamma}$ is the adiabatic lapse rate defined in terms of pressure changes (equation (7.27)), and we set $dC = 0$ since we are holding concentration fixed. To relate $dT - \hat{\Gamma} dp$ to $d\theta$ we write the potential temperature equation (7.32) in the form

$$\theta(T, p_R, C) = T - \int_{p_R}^p \hat{\Gamma}(T, p', C) dp' = T - \Psi(T, p, C, p_R), \quad (7.40)$$

so that the differentials are related by

$$d\theta = dT - d\Psi. \quad (7.41)$$

We evaluate $d\Psi$ using the chain rule and then specialize to the case of constant composition

and with a fixed reference pressure

$$d\Psi = \frac{\partial\Psi}{\partial T} dT + \frac{\partial\Psi}{\partial p} dp + \frac{\partial\Psi}{\partial C} dC + \frac{\partial\Psi}{\partial p_R} dp_R \quad (7.42a)$$

$$= \frac{\partial\Psi}{\partial T} dT + \frac{\partial\Psi}{\partial p} dp \quad (7.42b)$$

$$\equiv \left[\int_{p_R}^p \frac{\partial \hat{\Gamma}(T, p', C)}{\partial T} dp' \right] dT + \hat{\Gamma}(T, p, C) dp. \quad (7.42c)$$

Evaluating this differentials at the reference pressure removes the integral so that

$$d\Psi = \hat{\Gamma}(T, p_R, C) dp, \quad (7.43)$$

in which case the potential temperature differential is

$$d\theta = dT - \hat{\Gamma}(T, p_R, C) dp. \quad (7.44)$$

Making use of this relation in equation (7.39) renders an expression for the entropy differential in terms of the potential temperature differential

$$dS = c_p \theta^{-1} d\theta \quad p = p_R \text{ and } dC = 0. \quad (7.45)$$

Although evaluated at the reference pressure, as part of exercise 10.5 we see that this relation holds for an ideal gas at all pressures. Furthermore, as part of exercise 10.6 we see that this relation also holds for all pressures in certain liquids.

7.5 Thermodynamic relations for a simple ideal gas

In an **ideal gas**, we ignore the potential energy of intermolecular interaction forces between molecules. Also, the molecules in an ideal gas are assumed to occupy zero volume (i.e., they are point particles), although they do collide elastically. As a result, the internal energy of an ideal gas is just due to translation, rotation, and vibration of molecules. We refer to a **simple ideal gas** as an ideal gas where the internal energy is a linear function of temperature.

In this section we develop a variety of thermodynamic relations for a simple ideal gas atmosphere in mechanical equilibrium characterized by the exact hydrostatic balance. Furthermore, we assume the fluid is locally in a thermodynamic equilibrium although it is generally not globally in equilibrium (so there is a nonzero lapse rate). Although the real atmosphere is moving, and thus not in exact hydrostatic balance, nor is the real atmosphere a simple ideal gas, it turns out that the relations established here provide a reasonably accurate depiction of the atmosphere's thermodynamic state. Furthermore, by exposing these relations for the ideal gas, we further our understanding of the thermodynamic relations established earlier in this chapter.

7.5.1 Equation of state

At thermodynamic equilibrium (here assumed to be locally maintained for each fluid element), the thermodynamic properties of an **ideal gas** are constrained to satisfy the following **equation of state**

$$pV = n^{\text{mole}} R^g T, \quad (7.46)$$

where p is the pressure, V is the volume, n^{mole} is the number of moles of the gas,

$$R^g = 8.314 \text{ J mole}^{-1} \text{ K}^{-1} = 8.314 \text{ kg m}^2 \text{ s}^{-2} \text{ mole}^{-1} \text{ K}^{-1} \quad (7.47)$$

is the **universal gas constant**, and T is the absolute temperature in Kelvin. The number of moles equals to the mass, M , of the gas divided by the mass per mole, M^{mole}

$$n^{\text{mole}} = M/M^{\text{mole}}. \quad (7.48)$$

The mass density, $\rho = M/V$, is thus given by

$$\rho = \frac{p M^{\text{mole}}}{T R^g} \equiv \frac{p}{T R^M}, \quad (7.49)$$

where

$$R^M = R^g/M^{\text{mole}} \quad (7.50)$$

is the **specific gas constant** as defined by the universal gas constant normalized by the molar mass for the constituent. For air we have the molar mass

$$M^{\text{air}} = 28.8 \times 10^{-3} \text{ kg mole}^{-1} \quad (7.51)$$

so that air's specific gas constant is

$$R^{\text{air}} = \frac{R^g}{M^{\text{air}}} = \frac{8.314 \text{ kg m}^2 \text{ s}^{-2} \text{ mole}^{-1} \text{ K}^{-1}}{28.8 \times 10^{-3} \text{ kg mole}^{-1}} = 2.938 \times 10^2 \text{ m}^2 \text{ s}^{-2} \text{ K}^{-1}. \quad (7.52)$$

Equation (7.49) shows that the mass density of a thermodynamically equilibrated ideal gas is directly proportional to the pressure: increasing pressure increases density. In contrast, mass density is inversely proportional to the temperature: increases in temperature lead to lower mass density. This behavior for the ideal gas density is reflected in certain real gases and liquids.⁷

7.5.2 Internal energy

An ideal gas is comprised of molecules that interact only through elastic collisions. There are no inter-molecular forces. Furthermore, the volume of the individual molecules is ignored in comparison to the volume of empty space between the molecules, so they are approximated as point masses. Consequently, the internal energy for an ideal gas is independent of density and of the matter concentration. It is hence a function only of the temperature, which measures the kinetic energy of the elastic point molecules

$$J = J(T) \quad \text{ideal gas.} \quad (7.53)$$

Consequently, the exact differential of internal energy for an ideal gas is

$$dJ = c_v dT. \quad (7.54)$$

⁷A notable counter-example is water near its freezing point, which becomes more dense as temperature rises. This anomalous behavior is why a body of water freezes from the top down rather than from the bottom up.

The appearance of c_v , the constant volume specific heat capacity discussed in Section 6.7.1, arises in order for the ideal gas internal energy to satisfy the general equation (6.96). The heat capacity for an ideal gas is generally a function of temperature. However, for many applications it is sufficient to consider a simple ideal gas, in which c_v is a constant so that

$$\mathcal{I} = c_v T + \text{constant} \quad \text{simple ideal gas.} \quad (7.55)$$

The arbitrary constant of integration is generally set to zero so that the internal energy vanishes at absolute zero, $T = 0 \text{ K}$.

7.5.3 Heat capacity

The heat capacity is a constant for a simple ideal gas (equation (7.55)). Results from statistical mechanics show that the thermal/internal energy per molecule equals to $k_B T/2$ per excited molecular degree of freedom, where

$$k_B = 1.3806 \times 10^{-23} \text{ kg m}^2 \text{ s}^{-2} \text{ K}^{-1} \quad (7.56)$$

is the Boltzmann constant. Dry air is mostly comprised of the diatomic molecules, N_2 and O_2 . Diatomic molecules at temperatures of the lower atmosphere have two rotational and three translational degrees of freedom,⁸ so that $\mathcal{I}_{\text{molecule}} = 5 k_B T/2$.

We convert this energy per molecule to an energy per mole of diatomic molecules by multiplying by Avogadro's number

$$\mathcal{I}_{\text{mole diatomic}} = 5 A^v k_B T/2 = 5 R^g T/2, \quad (7.57)$$

where the universal gas constant is given by

$$R^g = A^v k_B \quad (7.58a)$$

$$= (6.022 \times 10^{23} \text{ mole}^{-1}) (1.3806 \times 10^{-23} \text{ m}^2 \text{ kg s}^{-2} \text{ K}^{-1}) \quad (7.58b)$$

$$= 8.314 \text{ kg m}^2 \text{ s}^{-2} \text{ mole}^{-1} \text{ K}^{-1}. \quad (7.58c)$$

Finally, dividing by the molar mass for dry air

$$M^{\text{air}} = 0.028 \text{ kg mole}^{-1} \quad (7.59)$$

leads to the simple ideal gas approximation to the dry air heat capacity

$$c_v = \frac{5 R^g}{2 M^{\text{air}}} = 742 \text{ m}^2 \text{ s}^{-2} \text{ K}^{-1}. \quad (7.60)$$

The measured heat capacity for dry air at standard temperature (300 K) is $718 \text{ m}^2 \text{ s}^{-2} \text{ K}^{-1}$, so the simple ideal gas estimate is only $(742 - 718)/718 = 3.3\%$ too large.

⁸At high temperatures, two vibrational degrees of freedom are also excited so that $\mathcal{I}_{\text{molecule}} = 7 k_B T/2$ at high temperatures.

7.5.4 Enthalpy

The enthalpy is generally given by equation (6.74), which for a simple ideal gas takes the form

$$\mathcal{H} = \mathcal{I} + p/\rho = c_v T + \frac{T R^g}{M^{\text{mole}}} = T(c_v + R^M) \quad (7.61)$$

where $R^M = R^g/M^{\text{mole}}$ (equation (7.50)) is the specific gas constant for the gas. Recall that the constant pressure heat capacity is given by equation (6.98)

$$c_p = T \left[\frac{\partial \mathcal{S}}{\partial T} \right]_{p,C} = \left[\frac{\partial \mathcal{H}}{\partial T} \right]_{p,C}. \quad (7.62)$$

Consequently, for a simple ideal gas we have

$$c_p = c_v + R^M \quad \text{and} \quad \mathcal{H} = c_p T. \quad (7.63)$$

7.5.5 Thermal expansion coefficient

The thermal expansion coefficient for an ideal gas is given by

$$\alpha_T = -\frac{1}{\rho} \frac{\partial \rho}{\partial T} = \frac{1}{T}. \quad (7.64)$$

Evidently, as temperature increases the ideal gas thermal expansion decreases.

7.5.6 Fundamental thermodynamic relations

The fundamental thermodynamic relation, written in terms of internal energy (equation (6.57b)) and enthalpy (equation (6.74)), are given by

$$d\mathcal{I} = T d\mathcal{S} - p d\nu_s + \mu dC \quad (7.65)$$

$$d\mathcal{H} = T d\mathcal{S} + \nu_s dp + \mu dC. \quad (7.66)$$

For a simple ideal gas these relations take the form

$$c_v dT = T d\mathcal{S} - p d\nu_s + \mu dC \quad (7.67)$$

$$c_p dT = T d\mathcal{S} + \nu_s dp + \mu dC. \quad (7.68)$$

7.5.7 Isothermal compressibility

The isothermal compressibility measures the change in volume when holding the temperature and matter concentration fixed and it is determined by the partial derivatives

$$-\frac{1}{V} \left[\frac{\partial V}{\partial p} \right]_{T,C} = \frac{1}{\rho} \left[\frac{\partial \rho}{\partial p} \right]_{T,C}. \quad (7.69)$$

For an ideal gas the compressibility is given by

$$-\frac{1}{V} \left[\frac{\partial V}{\partial p} \right]_{T,C} = \frac{1}{p}, \quad (7.70)$$

so that the compressibility decreases when pressure increases.

7.5.8 Sound speed

Sound travels through a fluid through compression and expansion of the fluid media. So we expect the sound speed to be related to the compressibility. But rather than the isothermal compressibility considered above, sound waves are largely adiabatic waves so that the entropy is constant. We are thus in need of the isentropic compressibility to compute the sound speed. That is, as defined by equation (6.101), the sound speed is the pressure derivative of density computed with entropy and matter concentration held fixed. We make use of the fundamental relations (7.67) and (7.68), with $dS = 0$ and $dC = 0$ to have

$$\frac{c_v}{c_p} = \frac{p}{\rho} \left[\frac{\partial \rho}{\partial p} \right]_{S,C} = (p/\rho) c_s^{-2} \implies c_s^2 = (p/\rho)(c_p/c_v) = T R^M (c_p/c_v). \quad (7.71)$$

For an ideal diatomic gas, such as nitrogen and oxygen, the ratio $c_p/c_v = 7/5$. Taking $R^M = 2.938 \times 10^2 \text{ m}^2 \text{ s}^{-2} \text{ K}^{-1}$ for air from equation (7.52) then leads to

$$c_s \approx 350 \text{ m s}^{-1} \quad \text{for } T = 300 \text{ K}. \quad (7.72)$$

7.5.9 Adiabatic lapse rate

The thermal expansion coefficient from equation (7.64) is given by $\alpha_T = T^{-1}$, so that the lapse rates are

$$\hat{\Gamma} = \frac{1}{\rho c_p} \quad \text{and} \quad \Gamma = -\frac{g}{c_p}. \quad (7.73)$$

The measured specific heat capacity for a dry atmosphere at standard temperature (300 K) is

$$c_p = 1005 \text{ m}^2 \text{ s}^{-2} \text{ K}^{-1} \quad (7.74)$$

so that the adiabatic lapse rate for a dry atmosphere is roughly

$$\Gamma_d = -9.8 \text{ K}/(1000 \text{ m}). \quad (7.75)$$

Hence, the *in situ* temperature decreases by nearly 10 K when rising 1000 m in a dry and ideal gas atmosphere.

7.5.10 Geopotential thickness

We now establish basic relations for a static atmosphere satisfying the hydrostatic balance. These relations also hold to a very good approximation for the large-scale atmosphere given the dominance of approximate hydrostatic balance for these scales (see Section 11.2).

Relations for an atmosphere with varying temperature

Integrating the hydrostatic balance equation (7.13) renders an expression for the pressure on a geopotential, Φ_1 ,

$$p(\Phi_1) = \int_{\Phi_1}^{\infty} \rho(\Phi) d\Phi, \quad (7.76)$$

where we assumed that $p(\Phi_2 = \infty) = 0$. Use of the ideal gas law brings the integrand to the form

$$d\Phi = -\rho^{-1} dp = -T R^{\text{air}} p^{-1} dp. \quad (7.77)$$

Using this expression in equation (7.76) leads to the **hypso**metric equation, which provides the geopotential thickness between two pressure isosurfaces

$$\Phi(z_2) - \Phi(z_1) = -R^{\text{air}} \int_{p_1}^{p_2} T d(\ln p). \quad (7.78)$$

Recall that $dp < 0$ if $dz > 0$ since the hydrostatic pressure decreases when moving up in the atmosphere. We define the **geopotential height** according to

$$Z = \Phi/g, \quad (7.79)$$

where g is the gravitational acceleration at sea level. The geopotential height is close to the geometric height in the troposphere and lower stratosphere. The hypsometric equation (7.78) says that the geopotential thickness between two isobars is

$$Z_2 - Z_1 = \frac{R^{\text{air}}}{g} \int_{p_2}^{p_1} T d(\ln p). \quad (7.80)$$

Defining the layer mean temperature

$$\langle T \rangle = \frac{\int_{p_2}^{p_1} T d(\ln p)}{\int_{p_2}^{p_1} d(\ln p)} \quad (7.81)$$

and the layer mean **scale height**

$$H = \frac{R^{\text{air}} \langle T \rangle}{g} \quad (7.82)$$

leads to the **geopotential thickness**

$$Z_2 - Z_1 = -H \ln(p_2/p_1). \quad (7.83)$$

The geopotential thickness is thus directly proportional to the mean temperature within the pressure layer, with thicker layers, for example, associated with higher mean temperatures.

We can invert the geopotential thickness relation (7.83) for the pressures to render

$$p_1 = p_2 e^{(Z_2 - Z_1)/H} = p_2 e^{(Z_2 - Z_1)g/(R^{\text{air}} \langle T \rangle)}. \quad (7.84)$$

This relation, or more commonly its simplified version (7.88) discussed below, is sometimes referred to as the **law of atmospheres** or the **barometric law**. The scale height is a function of pressure through its dependence on the layer averaged temperature in equation (7.82). Note that the pressure, p_1 , is larger under a column of warm air than under the same column with cool air.

Relations for an atmosphere with a constant temperature

For the special case of an atmosphere with a constant temperature, T , then the scale height is a constant⁹

$$H_{\text{const}} = R^{\text{air}} T_{\text{const}}/g. \quad (7.85)$$

⁹As we saw earlier in this chapter, an atmosphere has uniform *in situ* temperature at thermodynamic equilibrium. However, the effects from turbulent motions, even very modest turbulent motions, readily break thermodynamic equilibrium.

Setting $T_{\text{const}} = 300 \text{ K}$ and using the specific gas constant for air from equation (7.52) leads to the scale height

$$H_{\text{const}} = \frac{2.938 \times 10^2 \text{ m}^2 \text{ s}^{-2} \text{ K}^{-1} \times 300 \text{ K}}{9.8 \text{ m s}^{-2}} \approx 9 \times 10^3 \text{ m}. \quad (7.86)$$

It is furthermore convenient to set $Z_2 = 0$ with $p_2 = p_{\text{slp}}$ the sea level pressure, whose global average is

$$\langle p_{\text{slp}} \rangle = 101.325 \times 10^3 \text{ N m}^{-2}. \quad (7.87)$$

The pressure in an isothermal atmosphere thus decreases exponentially with geopotential height according to the scale height

$$p(Z) = \langle p_{\text{slp}} \rangle \exp(-Z/H_{\text{const}}). \quad (7.88)$$

7.5.11 Potential temperature

The fundamental thermodynamic relation for a simple ideal gas (7.68) takes on the following form for an isentropic change

$$c_p dT = \nu_s dp. \quad (7.89)$$

Dividing both sides by temperature and using the ideal gas relation

$$\frac{\nu_s}{T} = \frac{R^M}{p} \quad (7.90)$$

leads to

$$c_p d(\ln T) = R^M d(\ln p). \quad (7.91)$$

Since c_p and R^M are constants, we can integrate this relation from the reference pressure to an arbitrary pressure

$$c_p \int_{\theta}^T d(\ln T) = R^M \int_{p_R}^p d(\ln p), \quad (7.92)$$

which renders the explicit expression for the potential temperature of a simple ideal gas

$$\theta = T \left[\frac{p_R}{p} \right]^{R^M/c_p} \quad \text{where} \quad c_p = \frac{7 R^M}{2}, \quad (7.93)$$

with c_p the constant pressure heat capacity of a simple ideal gas of diatomic molecules (Section 7.5.3). In some treatments (e.g., Exercise 7.6) it is useful to introduce the Exner function

$$\Pi = \frac{c_p T}{\theta} = c_p \left[\frac{p}{p_R} \right]^{R^M/c_p}. \quad (7.94)$$

In Exercise 7.5 we show that $\partial\theta/\partial p = 0$ for the ideal gas, thus exemplifying the removal of explicit pressure effects from the potential temperature. Furthermore, it follows from equation (7.93) that the potential temperature differential is related to temperature and pressure differentials via

$$\frac{\delta\theta}{\theta} = \frac{\delta T}{T} - \frac{\delta p}{p}. \quad (7.95)$$

In particular, if the differential is computed between points in space within a fluid at a particular

time instance, then we are led to the relationship between spatial gradients

$$\frac{\nabla \theta}{\theta} = \frac{\nabla T}{T} - \frac{\nabla p}{p}. \quad (7.96)$$

7.5.12 Further study

Atmospheric sciences and dynamic meteorology books have thorough discussions of ideal gas thermodynamics. Some of the material in section 2.7 of *Holton and Hakim (2013)* was used in the present section.



7.6 Exercises

EXERCISE 7.1: CONSTRAINT FOR ISENTROPIC PROCESSES WITH SIMPLE IDEAL GASES

Show that for a simple ideal gas, isentropic processes (i.e., processes that are both adiabatic and of constant matter concentration) are constrained so that

$$p \nu_s^{c_p/c_v} = \text{constant}, \quad (7.97)$$

where $\nu_s = \rho^{-1}$ is the specific volume.

EXERCISE 7.2: ENTROPY FUNCTION FOR SIMPLE IDEAL GAS

Following the results from Section 7.5, determine the expression for the specific entropy of a simple ideal gas with a single matter constituent.

EXERCISE 7.3: GEOPOTENTIAL HEIGHT

The **geopotential height** is the height above the earth of a chosen pressure surface.

- (a) Show that an ideal gas atmosphere in exact hydrostatic balance with a uniform lapse rate

$$\frac{dT}{dz} = -|\Gamma| = \text{constant} \quad (7.98)$$

has a geopotential height at a pressure p given by

$$z = \frac{T_0}{|\Gamma|} \left[1 - \left(\frac{p_0}{p} \right)^{-R^M |\Gamma| / g} \right], \quad (7.99)$$

where T_0 is the temperature at $z = 0$.

- (b) For an isothermal atmosphere, obtain an expression for the geopotential height as a function of pressure, and show that this result is consistent with the expression (7.99) in the appropriate limit.

EXERCISE 7.4: DENSITY FOR A THERMODYNAMICALLY EQUILIBRATED IDEAL GAS ATMOSPHERE

As seen in Section 7.2, the *in situ* temperature, T , is uniform for a thermodynamically equilibrated atmosphere. Assuming the atmosphere is an ideal gas, derive an expression for the density as a function of height for an atmosphere with uniform T .

EXERCISE 7.5: POTENTIAL TEMPERATURE FOR AN IDEAL GAS

Show that $\partial\theta/\partial p = 0$ for the potential temperature of an ideal gas given by equation (7.93)

$$\theta = T \left[\frac{p_R}{p} \right]^{R^M/c_p}. \quad (7.100)$$

Hint: remember that $\partial T/\partial p \neq 0$ since the partial derivative is computed with other variables fixed.

EXERCISE 7.6: THERMODYNAMIC RELATIONS FOR AN ATMOSPHERE

In this exercise, we establish some relations for an ideal gas atmosphere, and one relation holding for an arbitrary equation of state. We make the following assumptions.

- The gravitational acceleration is constant throughout the full depth of the atmosphere. This assumption becomes questionable when integrating to the top of the atmosphere.
- Ignore differences in the horizontal cross-sectional area of a fluid column at the bottom and top of the atmosphere arising from the spherical nature of the planet. See Exercise 8.5 for more on this issue.
- An exactly hydrostatic atmosphere has zero horizontal gradients. An approximate hydrostatic balance has horizontal pressure gradients that force flows, but the vertical pressure gradient remains balanced by the gravity force just like in an exact hydrostatic state. These points are detailed in 11, but we should be able to do the present exercise in the absence of that chapter.

- (a) PRESSURE-HEIGHT IDENTITY: Prove the following identity and state your assumptions

$$\int_0^{p_s} z \, dp = \int_{z=0}^{z_{\text{top}}} p \, dz. \quad (7.101)$$

This identity will be of use for some of the following questions.

- (b) IDEAL GAS $\mathcal{I} + \Phi$ INTEGRATED OVER DEPTH OF A HYDROSTATIC ATMOSPHERE: For an ideal gas atmosphere in exact hydrostatic balance, show that the integral of the gravitational potential energy plus internal energy from the surface to the top of the atmosphere is equal to the integral of the enthalpy of the atmosphere

$$\int_0^{z_{\text{top}}} (\Phi + \mathcal{I}) \rho \, dz = \int_0^{z_{\text{top}}} \mathcal{H} \rho \, dz, \quad (7.102)$$

where

$$\mathcal{H} = p \alpha + \mathcal{I} \quad (7.103)$$

is the enthalpy per mass,

$$\Phi = g z \quad (7.104)$$

is the simple form of the geopotential, which is also the gravitational potential energy per mass, and \mathcal{I} is the internal energy per mass. The height integral extends from the surface where $z = 0$, to the top of the atmosphere where $z = z_{\text{top}}$.

- (c) VERTICAL DERIVATIVE OF DRY STATIC ENERGY: For an ideal gas atmosphere in hydrostatic balance, show that

$$\frac{d\sigma}{dz} = \Pi \frac{d\theta}{dz}, \quad (7.105)$$

where

$$\sigma = \mathcal{H} + \Phi \quad (7.106)$$

is the dry static energy and

$$\Pi = c_p (T/\theta) \quad (7.107)$$

is the *Exner function* introduced in equation (7.94).

- (d) FIRST IDENTITY FOR HORIZONTAL PRESSURE GRADIENT: For an ideal gas atmosphere (either hydrostatic or non-hydrostatic), derive the following expression for the pressure gradient acceleration

$$-\frac{1}{\rho} \nabla p = -\theta \nabla \Pi. \quad (7.108)$$

It then follows that for any instant in time, we have the relation between differentials

$$\rho^{-1} dp = \theta d\Pi. \quad (7.109)$$

- (e) SECOND IDENTITY FOR HORIZONTAL PRESSURE GRADIENT: For an ideal gas atmosphere (either hydrostatic or non-hydrostatic), derive the following expression for the pressure gradient acceleration

$$-\frac{1}{\rho} \nabla p = -\frac{c_s^2}{\rho \theta} \nabla(\rho \theta), \quad (7.110)$$

where c_s is the sound speed.

- (f) $\mathcal{I} + \Phi$ INTEGRATED OVER DEPTH OF A HYDROSTATIC ATMOSPHERE: Show that for a hydrostatic atmosphere with an arbitrary equation of state

$$\int_0^{p_s} (\Phi + \mathcal{I}) dp = \int_0^{p_s} \mathcal{H} dp. \quad (7.111)$$

That is, show that the relation in the first part of this problem holds even without making the ideal gas assumption.

EXERCISE 7.7: UNIT KNUDSEN NUMBER

From VOLUME 1 of this book, we define the **Knudsen number** as the ratio $\text{Kn} = L_{\text{mfp}}/L_{\text{macro}}$, where $L_{\text{macro}} \approx 10^{-4}$ m is the macroscopic length scale used in the discussion of the continuum approximation, and L_{mfp} is the molecular mean free path. Throughout this exercise make use of $p_{\text{stand}} = 101.325 \times 10^3$ Pa for standard atmospheric pressure. We also need some of the relations from kinetic theory given in the Prologue chapter in VOLUME 1.

- Consider a mole of an isothermal and ideal gas atmosphere of $T = 300\text{K}$ with a constant gravitational acceleration. At what pressure is the Knudsen number unity? Write your answer as a fraction of standard sea atmospheric pressure, p_{stand} .
- Compute the altitude corresponding to the above pressure, assuming the sea level pressure is p_{slp} and the geopotential is $\Phi = g z$. Hint: make use of results from Section 7.5.10.
- Assuming $p = p_{\text{stand}}$, at what temperature is $\text{Kn} = 1$? Hint: assume the ideal gas law holds regardless the temperature.
- Comment on at least one atmospherically inaccurate assumption made during this exercise.



Part III

Dynamics

Dynamics is the area of mechanics that examines the causes of motion. Following a Newtonian approach, to understand the cause of motion requires an understanding of forces.¹⁰ We thus focus in this part of the book on studying the variety of forces acting on a moving geophysical fluid. Throughout our study, we encounter a suite of theoretical concepts that form the foundations of geophysical fluid dynamics. Our presentation typically moves from the general to the specific, with each chapter written in a manner that allows it to be picked up without relying too much on other chapters. The general to specific presentation allows us to establish general principles based on fundamental concepts and to then see how those concept manifest in specific contexts.

Forces of concern in geophysical fluid mechanics include the body force acting on a fluid element from the earth's gravity field along with the contact forces from pressure and friction that act between adjacent fluid elements. Additionally, by choosing to work in a non-inertial rotating terrestrial reference frame, we encounter body forces from the Coriolis and planetary centrifugal accelerations, just as encountered for geophysical particle mechanics studied in VOLUME 1 of this book. Each of these forces play important roles in determining the diversity of geophysical fluid motion, and their analysis leads to dynamical insights into the nature and causes of fluid motion. We observe that forces in fluids are commonly inferred from kinematic properties of the motion, thus making use of the fluid kinematics encountered in VOLUME 1.

SUMMARY OF THE DYNAMICS CHAPTERS

We start the development of dynamics by formulating the equations of motion (linear momentum and angular momentum) in Chapter 8 using Newtonian methods. In subsequent chapters we study the forces appearing in these equations, including friction (Chapter 9), pressure (Chapter 12), and buoyancy (Chapter 14). Buoyancy is the vertical pressure force, arising from density inhomogeneities, that are not balanced by gravity. As such, our study of buoyancy focuses on vertical forces, which contrasts to our study of pressure form stresses in Chapter 12, which focus on horizontal forces.

When studying buoyancy in Chapter 14, we make use of an equation of state that provides the mass density of a fluid element as a function of thermodynamical properties such as temperature, pressure, and matter concentration. In Chapter 10 we study the flow of energy through the fluid, including both mechanical energy of the macroscopic fluid and the internal energy of the molecular degrees of freedom. We thus study how mechanical energy is exchanged with internal energy in the presence of work done by pressure and heat generated by friction.

Chapters 11 and 13 introduce a variety of approximate equations that allow us to focus on selected dynamical regimes by filtering away selected phenomena. It is here that we encounter the hydrostatic approximation and the Boussinesq ocean approximation, both of which are commonly used for large-scale models of the ocean and atmosphere. Approximate balances are further examined in Chapter 15, where we study the mechanics of a rapidly rotating fluid. We here encounter the geostrophic balance, which is a diagnostic balance appropriate for describing large-scale geophysical flows in which the horizontal pressure acceleration is balanced by the Coriolis acceleration. Geostrophic balance is one of the variety of balances considered in Chapter 16, which introduces balanced flow regimes pertaining to horizontal motions. Chapter 17 examines the physics of an Ekman boundary layer in which the Coriolis acceleration balances vertical friction.

¹⁰An alternative to Newtonian mechanics is provided by Hamilton's principle, which primarily focuses on energy rather than forces. In VOLUME 4 of this book, we make use of Hamilton's principle for describing motion of classical particles and geophysical fluids.

Throughout this book, we generally assume a constant effective gravitational acceleration. However, routine daily observations of the ocean encounter tidal motions arising from spatial-temporal variations of the gravity field. We thus take a brief look in Section 11.6 at formulating the equations of geophysical fluid mechanics in the presence of a space and time dependent gravitational acceleration.

MATHEMATICS AND KINEMATICS IN THIS PART

In this part of the book we encounter a broad suite of physical concepts. Fortunately, their presentation requires relatively modest mathematical tools. As a result, we make use, almost exclusively, of Cartesian tensors and Cartesian vector calculus from VOLUME 1, and Eulerian fluid kinematics also from VOLUME 1.

Chapter 8

MOMENTUM

We here formulate the mechanical equations for linear momentum and axial angular momentum for geophysical fluid motions. We derive these equations of [geophysical fluid dynamics](#) (GFD) using Newton's laws of motion applied to a gravitationally stratified fluid continuum moving on a rotating planet where the rotation rate is constant in time. Relative to the point particle, the new dynamical feature afforded to the continuum concerns contact stresses between fluid elements, thus comprising the pressure and frictional forces from local mechanical interactions. We provide some discussion of the basic features of these equations, with particular emphasis on the constraints imposed by an axial angular momentum conserving flow.

READER'S GUIDE TO THIS CHAPTER

We make use of results from point particle mechanics and fluid kinematics as studied in [VOLUME 1](#). In Section 8.2 we consider integrals of the linear momentum and forces over finite regions when forming the finite volume ([weak formulation](#)) momentum budget. These integral expressions hold for Cartesian tensors, such as for the [planetary Cartesian coordinates](#) or the [tangent plane Cartesian coordinates](#) from Section 8.5. Extra tools from tensor analysis, beyond that considered in this book, are needed to extend these integrals to general tensors (e.g., see Chapter 2 of [Tromp \(2025a\)](#)). However, the strong form equations throughout this chapter hold for general tensors, and we display the Cartesian and spherical representations.

8.1	Loose threads	236
8.2	Linear momentum equation	236
8.2.1	Body forces	236
8.2.2	Contact forces	237
8.2.3	Kinetic stress tensor	239
8.2.4	Equation of motion	239
8.2.5	Linear momentum for finite regions	239
8.2.6	Advective form	241
8.2.7	Momentum equation with gravity in a rotating reference frame	241
8.2.8	Euler equation for perfect fluid motion	242
8.2.9	Further study	242
8.3	Spherical/geopotential coordinates	243
8.4	Vector-invariant velocity equation	244
8.4.1	Dynamic pressure	245
8.4.2	Magnus acceleration	246
8.4.3	Nonlinear accelerations for some example flows	246

8.5	The tangent plane approximation	246
8.5.1	Basics of the tangent plane approximation	247
8.5.2	Tangent plane is a geopotential approximation	248
8.5.3	Traditional approximation and the f -plane	248
8.5.4	β -plane approximation	248
8.5.5	Comments and caveats	249
8.6	Exact hydrostatic balance	249
8.6.1	Properties of exact hydrostatic balance	249
8.6.2	Comparison to approximate hydrostatic balance	250
8.6.3	Hydrostatic balance in a variable gravity field	251
8.7	Axial angular momentum	252
8.7.1	Axial angular momentum equation	252
8.7.2	Axial angular momentum conserving motion of a ring of air	253
8.7.3	Conditions for steady circulation	255
8.7.4	Further study	255
8.8	Exercises	255

8.1 Loose threads

- Exercise to derive the vector-invariant velocity equation using spherical coordinates.

8.2 Linear momentum equation

We here develop Newton's second law for a continuous fluid region, thus deriving the budget for linear momentum. We present the momentum budget over both a finite volume region of the fluid ([weak formulation](#)) and for an infinitesimal fluid element ([strong formulation](#)). We assume Cartesian tensors for an Eulerian region, and comment on the equations using general Eulerian coordinates as well as a Lagrangian fluid element.

8.2.1 Body forces

Forces acting on an arbitrary Eulerian region, \mathcal{R} , of a continuous matter distribution are of two general types. The first involves forces that originate from outside of the matter and act throughout the body, thus motivating the names [external forces](#) or [body forces](#). Examples relevant to our studies include gravitational forces (including the planetary gravitational force as well as astronomical tidal forces), as well as the planetary Coriolis force and planetary centrifugal force (both due to the rotating planetary reference frame). The net body force acting on a finite volume of continuum matter is the volume integral of the body force per unit mass, \mathbf{f}_{body} , multiplied by the mass of the matter

$$\mathbf{F}_{\text{body}} = \int_{\mathcal{R}} \mathbf{f}_{\text{body}} \rho dV. \quad (8.1)$$

For example, the effective gravitational force (combination of central gravity plus planetary centrifugal) acting on a region of fluid is given by

$$\mathbf{F}_{\text{geo}} = \int_{\mathcal{R}} \mathbf{g} \rho dV = - \int_{\mathcal{R}} \nabla \Phi \rho dV, \quad (8.2)$$

where $\mathbf{g} = -\nabla\Phi$ is the effective acceleration arising from the gradient of the geopotential, Φ , studied in VOLUME 1 of this book. Likewise, the Coriolis force acting on the fluid region is given by

$$\mathbf{F}_{\text{coriolis}} = -2 \int_{\mathcal{R}} (\boldsymbol{\Omega} \times \mathbf{v}) \rho dV. \quad (8.3)$$

These body forces have the same appearance as for the point particle, with the only difference being the material is now continuous rather than a point mass, thus requiring an integral over the fluid region.

8.2.2 Contact forces

The second kind of forces are **contact forces**, such as pressure forces and frictional forces. Contact forces are molecular in origin and have only local extent.¹ In continuum mechanics, a contact force per unit area is referred to as a **traction**. A contact force can be resolved into its normal component (proportional to the pressure force) and tangential component (known as a shear force). Mathematically, we compute the net contact force exerted on the region by area integrating the **stress tensor** projected onto the normal direction along the region boundary (i.e., by area integrating the traction)

$$\mathbf{F}_{\text{contact}} = \oint_{\partial\mathcal{R}} \mathbf{T} \cdot \hat{\mathbf{n}} d\mathcal{S}, \quad (8.4)$$

where $\hat{\mathbf{n}}$ is the outward normal direction orienting the domain boundary with $d\mathcal{S}$ the associated area element, and \mathbf{T} is the **stress tensor**, which is a second order tensor that organizes the stresses acting in the fluid. We have more to say about the stress tensor in the following as well as in Chapter 9. For now, we must be satisfied with equation (8.4) providing the definition of a contact force.

Contact forces acts on a continuum fluid element through the nonzero spatial extent of fluid elements, with this spatial extent allowing for interactions between adjacent fluid elements. Point particles do not experience contact forces since point particles have no spatial extent. Hence, contact forces represent a fundamentally new feature, conceptually and operationally, to the fluid dynamical equations relative to the equations of point particles.

Stresses from friction and pressure

As detailed in Chapter 9, there are two types of stress that concern us: diagonal stresses associated with reversible momentum exchange through **pressure**, and stresses associated with the irreversible exchange of momentum through friction. Hence, it is convenient to decompose the stress tensor components according to

$$T^{ab} = \mathbb{T}^{ab} - p g^{ab}. \quad (8.5)$$

In this equation, p is the mechanical pressure, which is a force per unit area acting in a compressive manner on the area of a surface; i.e., it is a normal force. The second order tensor, g^{ab} , is a chosen coordinate representation of the inverse **metric tensor** and it equals to the **Kronecker delta** when choosing Cartesian coordinates in Euclidean space. The **friction stress tensor** is written \mathbb{T}^{ab} . It is also known as the **deviatoric stress tensor**, and it arises solely from deviations to the case of a static fluid where stress is due solely to pressure. The friction stress

¹See Chapter 2 of [Pride \(2025\)](#) for discussion of the molecular origin of contact forces.

tensor has zero trace (hence the name deviatoric stress tensor), with mechanical pressure arising from the trace of the full stress tensor.

Substitution of the stress tensor (8.5) into the contact force expression (8.4) leads to

$$\mathbf{F}_{\text{contact}} = \oint_{\partial\mathcal{R}} (\mathbb{T} \cdot \hat{\mathbf{n}} - p \hat{\mathbf{n}}) dS, \quad (8.6)$$

where the integral is taken over the bounding surface of the domain whose outward normal is $\hat{\mathbf{n}}$. Given this expression for contact forces acting on the boundary of a fluid domain, it is seen that positive pressure ($p > 0$) acts in the direction opposite to the surface's outward normal so that pressure always acts in a compressive manner. Deviatoric stresses create more general forces on the bounding surface, which can have compressive, expansive, shearing, and/or rotational characteristics.

Exchange of momentum between fluid elements

We mathematically represent the exchange of momentum between fluid elements via a symmetric stress tensor, with symmetry implied by statements about angular momentum conservation (detailed in Section 9.4). The divergence of the stress tensor then leads to a force acting on the fluid element. The forces arising from molecular viscosity provide an irreversible exchange of momentum that reduce the kinetic energy of fluid elements (Section 10.2.3). This process is dissipative and thus referred to as friction. Furthermore, when averaging over turbulent realizations of a fluid, the impacts on the mean flow are generally far larger than those associated with molecular viscosity, with these exchanges commonly parameterized via a symmetric stress tensor.

A gauge symmetry of pressure force

The contribution from pressure in the contact force (8.6) remains invariant if pressure is shifted by an arbitrary function of time

$$p(\mathbf{x}, t) \rightarrow p(\mathbf{x}, t) + F(t). \quad (8.7)$$

We see this invariance by noting that

$$\oint_{\partial\mathcal{R}} F(t) \hat{\mathbf{n}} dS = F(t) \oint_{\partial\mathcal{R}} \hat{\mathbf{n}} dS = 0, \quad (8.8)$$

where the final equality follows from a corollary of the [divergence theorem](#). Briefly, through the divergence theorem we know that

$$\oint_{\partial\mathcal{R}} p \hat{\mathbf{n}} dS = \int_{\mathcal{R}} \nabla p dV, \quad (8.9)$$

so that if pressure is shifted by a spatial constant then the pressure gradient body force remains unchanged, as will the integrated pressure contact force.

We refer to this invariance of the pressure force as a [gauge symmetry](#). It means that motion of the fluid remains unchanged if pressure is modified by a spatial constant that can generally be a function of time.

8.2.3 Kinetic stress tensor

The final contribution to the finite volume momentum budget arises from the transport of momentum across the grid cell faces, which takes the form of a contact force due to fluid motion

$$\mathbf{F}_{\text{motion}} = - \oint_{\partial\mathcal{R}} (\rho \mathbf{v} \otimes \mathbf{v}) \cdot \hat{\mathbf{n}} d\mathcal{S} = \oint_{\partial\mathcal{R}} \mathbb{T}^{\text{kinetic}} \cdot \hat{\mathbf{n}} d\mathcal{S}, \quad (8.10)$$

where we introduced the **kinetic stress tensor**

$$\mathbb{T}^{\text{kinetic}} = -\rho \mathbf{v} \otimes \mathbf{v}, \quad (8.11)$$

where $\mathbf{v} \otimes \mathbf{v}$ is the tensor product of the velocity with itself. The kinetic stress tensor arises from the mechanical interactions between moving fluid elements. The turbulent contribution to the mechanical stress is known as the **Reynolds stress tensor**.

8.2.4 Equation of motion

The linear momentum of a fluid region is given by

$$\mathbf{P} = \int_{\mathcal{R}} \mathbf{v} \rho dV. \quad (8.12)$$

Applying Newton's law of motion to the continuum leads to the finite volume equation of motion for the Eulerian region

$$\frac{d}{dt} \int_{\mathcal{R}} \mathbf{v} \rho dV = \int_{\mathcal{R}} \rho \mathbf{f}_{\text{body}} dV + \oint_{\partial\mathcal{R}} (\mathbf{T} - \rho \mathbf{v} \otimes \mathbf{v}) \cdot \hat{\mathbf{n}} d\mathcal{S}. \quad (8.13)$$

Applying the divergence theorem to the boundary integral yields

$$\frac{d}{dt} \int_{\mathcal{R}} \rho \mathbf{v} dV = \int_{\mathcal{R}} (\rho \mathbf{f}_{\text{body}} - \nabla \cdot (\rho \mathbf{v} \otimes \mathbf{v}) + \nabla \cdot \mathbf{T}) dV, \quad (8.14)$$

where we brought the contact forces into the volume integral through exposing the divergence of the stress tensors. Finally, since the Eulerian region is arbitrary and static, we have the strong form equation of motion given by the **flux-form conservation law** for momentum

$$\partial_t(\rho \mathbf{v}) + \nabla \cdot (\rho \mathbf{v} \otimes \mathbf{v}) = \rho \mathbf{f}_{\text{body}} + \nabla \cdot \mathbf{T}. \quad (8.15)$$

In Figure 8.1 we illustrate the contributions to the momentum budget (8.14) for an Eulerian region using Cartesian coordinates. Note that although we focused on Cartesian Eulerian coordinates for the derivation of equation (8.15), the equation holds for arbitrary Eulerian coordinates if we simply interpret the divergence operator as the covariant divergence.

8.2.5 Linear momentum for finite regions

Consider the budget of linear momentum for an arbitrary region, \mathcal{R} , moving in an arbitrary manner within the fluid and as described by Cartesian coordinates. For this purpose we make use of the **Leibniz-Reynolds transport theorem**

$$\frac{d}{dt} \left[\int_{\mathcal{R}} \varphi dV \right] = \int_{\mathcal{R}} \frac{\partial \varphi}{\partial t} dV + \oint_{\partial\mathcal{R}} \varphi \mathbf{v}^{(b)} \cdot \hat{\mathbf{n}} d\mathcal{S}, \quad (8.16)$$

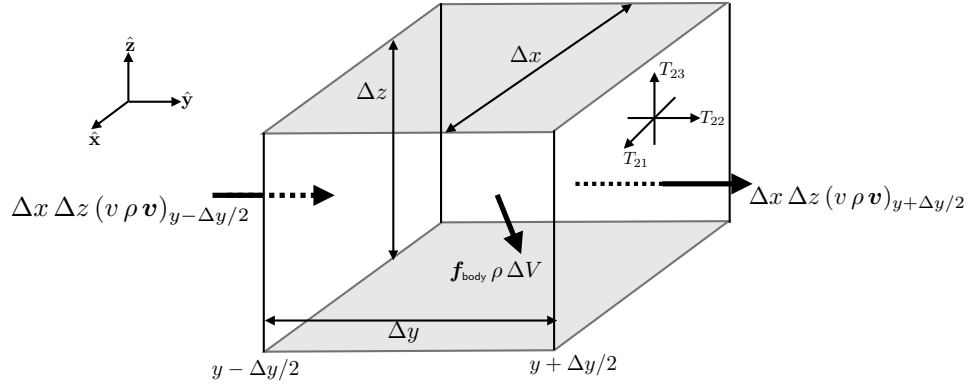


FIGURE 8.1: A finite sized region used to illustrate the budget of momentum for an Eulerian region (fixed in space) using Cartesian coordinates, here emphasizing the transport in the \hat{y} direction. Across each face we have the advective transport of momentum, with the transport crossing in the \hat{y} direction given by $\Delta x \Delta z (v \rho \mathbf{v})_{y \pm \Delta y/2}$. In addition, each cell face experiences a stress that provides a force per area directed within the cell face (strains) and perpendicular to the cell face (normal stresses). These stresses include the effects from both pressure (as part of the normal stress) and friction (proportional to the strains). Finally, the body force, $\rho \mathbf{f}_{\text{body}} dV$, acts over the full extent of the cell, with this term including the body force from gravity, planetary centrifugal, and planetary Coriolis.

where $\mathbf{v}^{(b)}$ is the velocity of the region boundary, $\partial\mathcal{R}$, with $\hat{\mathbf{n}}$ the outward normal along the boundary. Applying this result to a component of the linear momentum per volume, $\varphi = \rho v^m$ (assuming Cartesian tensors), and making use of the flux-form Eulerian momentum equation (8.15) leads to

$$\frac{d}{dt} \left[\int_{\mathcal{R}} \rho v^m dV \right] = \int_{\mathcal{R}} \partial_t (\rho v^m) dV + \oint_{\partial\mathcal{R}} (\rho v^m) \mathbf{v}^{(b)} \cdot \hat{\mathbf{n}} dS \quad (8.17a)$$

$$= \int_{\mathcal{R}} [\rho f^m + \partial_n (T^{mn} - \rho v^m v^n)] dV + \oint_{\partial\mathcal{R}} (\rho v^m) \mathbf{v}^{(b)} \cdot \hat{\mathbf{n}} dS \quad (8.17b)$$

$$= \int_{\mathcal{R}} \rho f^m dV + \oint_{\partial\mathcal{R}} (T^{mn} - \rho v^m v^n) \hat{\mathbf{n}}_n dS + \oint_{\partial\mathcal{R}} (\rho v^m) \mathbf{v}^{(b)} \cdot \hat{\mathbf{n}} dS \quad (8.17c)$$

$$= \int_{\mathcal{R}} \rho f^m dV + \oint_{\partial\mathcal{R}} [T^{mn} + \rho v^m (v^{(b)n} - v^n)] \hat{\mathbf{n}}_n dS. \quad (8.17d)$$

We can write this relation as

$$\frac{d}{dt} \left[\int_{\mathcal{R}} \rho \mathbf{v} dV \right] = \int_{\mathcal{R}} \rho \mathbf{f}_{\text{body}} dV + \oint_{\partial\mathcal{R}} [\mathbf{T} + \rho \mathbf{v} \otimes (\mathbf{v}^{(b)} - \mathbf{v})] \cdot \hat{\mathbf{n}} dS, \quad (8.18)$$

thus revealing that the evolution of linear momentum over an arbitrary region is affected by the volume integrated body force acting over the region, plus the stresses acting on the region boundary. The boundary stresses have contributions from pressure and friction. Additionally, the boundary stresses have a contribution from the kinetic stress arising from advection of linear momentum across the region boundary, and with advection computed relative to motion of the boundary. In Section 9.8 we specialize the budget (8.18) to an infinitesimally thin interface. That analysis is then used to develop stress conditions for a surface within a single fluid media, as well as the stress condition at the boundary between two fluids.

We refer to a **Lagrangian region** as one that moves so that the surface velocity and barycentric velocity satisfy $\mathbf{v}^{(b)} \cdot \hat{\mathbf{n}} = \mathbf{v} \cdot \hat{\mathbf{n}}$, in which case the kinetic stress is eliminated from the finite volume momentum budget (8.18). We denote a Lagrangian region by writing $\mathcal{R}(\mathbf{v})$ to emphasize

that the region moves with the barycentric fluid velocity, \mathbf{v} . For this case the linear momentum is only affected by body forces as well as stresses (pressure and friction) contained in the stress tensor

$$(\mathbf{v} - \mathbf{v}^{(b)}) \cdot \hat{\mathbf{n}} = 0 \implies \frac{d}{dt} \left[\int_{\mathcal{R}(\mathbf{v})} \rho \mathbf{v} dV \right] = \int_{\mathcal{R}(\mathbf{v})} \rho \mathbf{f}_{\text{body}} dV + \oint_{\partial \mathcal{R}(\mathbf{v})} \mathbf{T} \cdot \hat{\mathbf{n}} dS. \quad (8.19)$$

This relation is [Reynolds transport theorem](#) applied to linear momentum.

8.2.6 Advection form

Making use of arbitrary Eulerian coordinates, we introduce the material time derivative with the covariant derivative operator (rather than partial derivative)

$$\rho \frac{Dv^a}{Dt} = \rho (\partial_t + v^b \nabla_b) v^a \quad (8.20a)$$

$$= \rho \partial_t v^a + \rho \nabla_b (v^b v^a) - \rho v^a \nabla_b v^b \quad (8.20b)$$

$$= \rho [\partial_t v^a + \nabla_b (v^b v^a)] + v^a (\partial_t \rho + v^b \nabla_b \rho) \quad (8.20c)$$

$$= \partial_t (\rho v^a) + \nabla_b (\rho v^a v^b), \quad (8.20d)$$

where we made use of the mass [continuity equation](#)

$$\partial_t \rho + \nabla \cdot (\rho \mathbf{v}) = 0. \quad (8.21)$$

We are thus led to the advective form of the momentum equation (8.15)

$$\rho \frac{D\mathbf{v}}{Dt} = \rho \mathbf{f}_{\text{body}} + \nabla \cdot \mathbf{T}. \quad (8.22)$$

Evidently, the advective form absorbs contributions from the kinetic stress into the material time derivative operator. Equation (8.22) is a continuum expression of Newton's equation of motion, and it is sometimes referred to as [Cauchy equation of motion](#). It is the strong form expression of momentum conservation that has its corresponding weak form given by equation (8.19)

8.2.7 Momentum equation with gravity in a rotating reference frame

We now specialize the momentum equation (8.22) to suit the needs of geophysical fluid mechanics. We first write the stress tensor in terms of the deviatoric component from friction and a diagonal component from pressure (equation (8.6))

$$\rho \frac{D\mathbf{v}}{Dt} = \rho \mathbf{f}_{\text{body}} - \nabla p + \nabla \cdot \mathbb{T}. \quad (8.23)$$

Next, move to a rotating terrestrial reference frame and thus expose the Coriolis acceleration and the effective gravitational force

$$\rho \frac{D\mathbf{v}}{Dt} + 2\rho \boldsymbol{\Omega} \times \mathbf{v} = -\rho \nabla \Phi - \nabla p + \nabla \cdot \mathbb{T}. \quad (8.24)$$

Note that we often find it convenient to write the divergence of the friction stress tensor as

$$\nabla \cdot \mathbb{T} = \rho \mathbf{F}, \quad (8.25)$$

with \mathbf{F} the frictional acceleration. In this case, the equation of motion (8.24) takes on

$$\rho \frac{D\mathbf{v}}{Dt} + 2\rho \boldsymbol{\Omega} \times \mathbf{v} = -\rho \nabla \Phi - \nabla p + \rho \mathbf{F}, \quad (8.26)$$

or the equivalent flux-form

$$\partial_t(\rho \mathbf{v}) + \nabla \cdot (\rho \mathbf{v} \otimes \mathbf{v}) + 2\rho \boldsymbol{\Omega} \times \mathbf{v} = -\rho \nabla \Phi - \nabla p + \rho \mathbf{F}. \quad (8.27)$$

Note that these forms for the equation of motion arise from extracting the rigid-body motion of the basis vectors to define the Coriolis acceleration. Any remaining changes to the basis vectors arise from motion of the fluid relative to the rigid-body rotating reference frame, and thus appear when expanding the material time derivative. These equations offer a suitable starting point for studies of geophysical fluid dynamics. They are sometimes referred to as the [Navier-Stokes equation](#). However, that name is more commonly applied to the non-rotating case with a specific form for the friction operator (see Section 9.6.7). We thus refer to equations (8.24), (8.26), and (8.27) as Newton's law of motion for a rotating fluid.²

8.2.8 Euler equation for perfect fluid motion

The inviscid form of the momentum equation (8.23) is known as the [Euler equation](#) of perfect fluid mechanics

$$\rho \frac{D\mathbf{v}}{Dt} = \rho \mathbf{f}_{\text{body}} - \nabla p, \quad (8.28)$$

where the body force is conservative. That is, the Euler equation is concerned just with fluid motion in the absence of dissipative processes. The inviscid form of the momentum equation (8.24) leads to the Euler equation in the presence of rotation and gravitation

$$\rho \frac{D\mathbf{v}}{Dt} + 2\rho \boldsymbol{\Omega} \times \mathbf{v} = -\rho \nabla \Phi - \nabla p. \quad (8.29)$$

Many features of geophysical fluid motion are well understood by ignoring frictional dissipation, in which case we work with a particular form of the Euler equation. The reason we can ignore friction relates to the huge length scales for much of the geophysical flows we are concerned with in this book, in which the effects from molecular viscosity are far too weak to have a direct impact. So although molecular viscosity is necessary to close the energy budget for geophysical flows, it does not directly impact on flow regimes that concern most attention in this book. We further comment on this point when discussing the [Reynolds number](#) in Section 9.7, and we comment more on the Euler equation in Section 9.6.7.

8.2.9 Further study

Chapter 5 of [Aris \(1962\)](#) offers an insightful discussion of continuum mechanics as applied to a fluid. Section 2.2 [Vallis \(2017\)](#) provides a derivation of the dynamical equations of motion for the atmosphere and ocean, similar to the approach given here. [Lautrup \(2005\)](#) provides

²The Navier-Stokes equations were first derived by Claude-Louis Navier in 1822 and later independently derived by George Stokes in 1845.

many nuggets of understanding for concepts such as body and contact forces. We offer further discussion of the mathematics and physics of stress in Chapters 9 and 12.

8.3 Spherical/geopotential coordinates

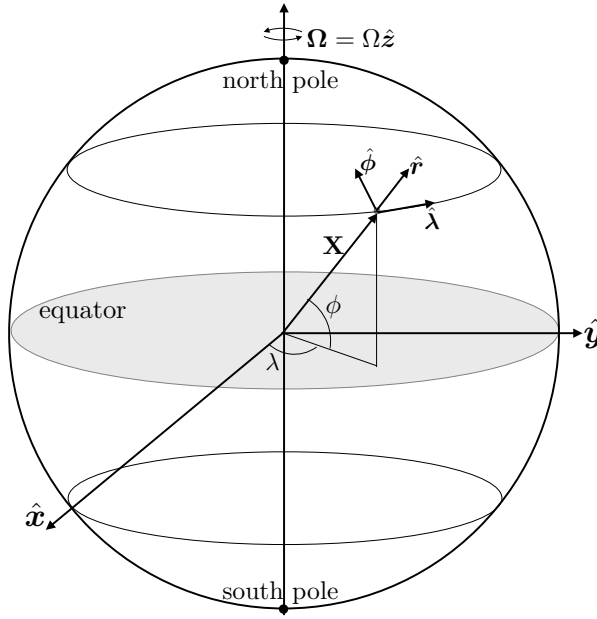


FIGURE 8.2: Geometry and notation for motion around a rotating sphere using planetary spherical and planetary Cartesian coordinates. For geophysical applications, the sphere rotates counter-clockwise when looking down from the north polar axis and it has an angular speed Ω . The planetary Cartesian triad of orthonormal basis vectors, $(\hat{x}, \hat{y}, \hat{z})$ points along the orthogonal axes and rotates with the sphere. The planetary spherical triad (also rotating with the sphere) of orthonormal non-coordinate basis vectors, $(\hat{\lambda}, \hat{\phi}, \hat{r})$, makes use of the longitudinal unit vector $\hat{\lambda}$, which points in the longitudinal direction (positive eastward), the latitudinal unit vector $\hat{\phi}$, which points in the latitudinal direction (positive northward) and the radial unit vector \hat{r} , which point in the radial direction (positive away from the center).

Geophysical fluids move on a rotating planet with the planet commonly assumed to have an oblate spherical geometry, though with the equations approximated by their spherical form when using the geopotential vertical coordinate. To display the equations of motion, we make use of the acceleration as derived for a point particle in VOLUME 1 using the geopotential coordinate to measure radial distances from the center of the sphere, as well as the longitude and latitude angular coordinates defined by Figure 8.2. The point particle time derivative, which is computed following the particle, translates into a material time derivative for fluid elements. We are thus led to the spherical/geopotential equations of motion

$$\frac{Du}{Dt} + \frac{u(w - v \tan \phi)}{r} + 2\Omega(w \cos \phi - v \sin \phi) = -\frac{1}{\rho r \cos \phi} \frac{\partial p}{\partial \lambda} + F^\lambda \quad (8.30)$$

$$\frac{Dv}{Dt} + \frac{v w + u^2 \tan \phi}{r} + 2\Omega u \sin \phi = -\frac{1}{\rho r} \frac{\partial p}{\partial \phi} + F^\phi \quad (8.31)$$

$$\frac{Dw}{Dt} - \frac{u^2 + v^2}{r} - 2\Omega u \cos \phi = -g - \frac{1}{\rho} \frac{\partial p}{\partial r} + F^r, \quad (8.32)$$

where we introduced the spherical components to the friction acceleration

$$\mathbf{F} = F^\lambda \hat{\lambda} + F^\phi \hat{\phi} + F^r \hat{r}, \quad (8.33)$$

which is determined by the divergence of the frictional stress tensor. We also note the spherical coordinate form for the gradient operator

$$\nabla = \frac{\hat{\lambda}}{r \cos \phi} \frac{\partial}{\partial \lambda} + \frac{\hat{\phi}}{r} \frac{\partial}{\partial \phi} + \hat{r} \frac{\partial}{\partial r}, \quad (8.34)$$

as well as the material time derivative operator acting on each of the velocity components

$$\frac{D}{Dt} = \frac{\partial}{\partial t} + \mathbf{v} \cdot \nabla = \frac{\partial}{\partial t} + \frac{u}{r \cos \phi} \frac{\partial}{\partial \lambda} + \frac{v}{r} \frac{\partial}{\partial \phi} + w \frac{\partial}{\partial r}. \quad (8.35)$$

We can write the spherical momentum equations in a bit more compact form by introducing the spherical coordinate velocity field

$$\mathbf{v} = \mathbf{u} + \hat{r} w = u \hat{\lambda} + v \hat{\phi} + w \hat{r} \quad (8.36)$$

and the corresponding spherical coordinate acceleration

$$\mathbf{A}_{\text{sphere}} = \frac{Du}{Dt} \hat{\lambda} + \frac{Dv}{Dt} \hat{\phi} + \frac{Dw}{Dt} \hat{r}. \quad (8.37)$$

We also introduce the metric acceleration to render

$$\rho \frac{D\mathbf{v}}{Dt} + 2\rho \boldsymbol{\Omega} \times \mathbf{v} = -\rho \nabla \Phi - \nabla p + \rho \mathbf{F}, \quad (8.38)$$

where we have the acceleration relative to the rotating frame

$$\frac{D\mathbf{v}}{Dt} = \mathbf{A}_{\text{sphere}} + \frac{1}{r} [u \tan \phi (\hat{r} \times \mathbf{v}) + w \mathbf{u} - \hat{r} \mathbf{u} \cdot \mathbf{u}]. \quad (8.39)$$

For some purposes it is convenient to combine one piece of the metric acceleration to the Coriolis acceleration to yield

$$\mathbf{A}_{\text{sphere}} + \frac{1}{r} [w \mathbf{u} - \hat{r} \mathbf{u} \cdot \mathbf{u}] + \left[2\boldsymbol{\Omega} + \frac{u \tan \phi \hat{r}}{r} \right] \times \mathbf{v} = -\nabla \Phi - \rho^{-1} \nabla p + \mathbf{F}. \quad (8.40)$$

8.4 Vector-invariant velocity equation

There are many occasions to make use of an alternative form of the equation of motion that swaps out the material time derivative in favor of the vorticity and kinetic energy. For that purpose we make use of the identity for the nonlinear self-advection term derived in the vector calculus chapter of VOLUME 1

$$(\mathbf{v} \cdot \nabla) \mathbf{v} = \boldsymbol{\omega} \times \mathbf{v} + \nabla(\mathbf{v} \cdot \mathbf{v})/2, \quad (8.41)$$

where $\boldsymbol{\omega} = \nabla \times \mathbf{v}$ is the vorticity. We derive the corresponding **vector invariant** form of the velocity equation using Cartesian coordinates and then invoke general coordinate invariance to

extend the result to arbitrary coordinates.³ Making use of equation (8.41) thus leads to the material acceleration

$$\frac{D\mathbf{v}}{Dt} = \frac{\partial \mathbf{v}}{\partial t} + \boldsymbol{\omega} \times \mathbf{v} + \nabla(\mathbf{v} \cdot \mathbf{v})/2 \quad (8.42)$$

so that the momentum equation (8.24) becomes the **vector invariant** velocity equation

$$\frac{\partial \mathbf{v}}{\partial t} + (2\boldsymbol{\Omega} + \boldsymbol{\omega}) \times \mathbf{v} = -\nabla(\Phi + \mathbf{v} \cdot \mathbf{v}/2) + \rho^{-1}(-\nabla p + \nabla \cdot \mathbb{T}). \quad (8.43)$$

The name *vector-invariant* is motivated since the form of this equation remains unchanged when using Cartesian or spherical coordinates.

8.4.1 Dynamic pressure

The vector-invariant velocity equation (8.43) is mathematically equivalent to the momentum equation (8.24). Even so, it provides a more convenient means to derive Bernoulli's theorem in Section 10.8.3 and the vorticity equation studied in VOLUME 3. Furthermore, it highlights certain physical processes affecting Eulerian accelerations that are not obviously seen from the momentum equation. One such process is the **dynamic pressure**, which arises from the kinetic energy per mass appearing in the velocity equation (8.43). Gradients in the kinetic energy per mass contribute a dynamical pressure gradient that accelerates the fluid down the kinetic energy gradient, from regions of high kinetic energy per mass to regions of low kinetic energy per mass. To help understand this process, consider a Boussinesq ocean (Chapter 13), in which case the density factor is a constant, $\rho = \rho_0$, so that we can write the accelerations from pressure and kinetic energy as

$$-(1/\rho_0) \nabla p - \nabla(\mathbf{v} \cdot \mathbf{v}/2) = -\rho_0^{-1} \nabla(p + \rho_0 \mathbf{v} \cdot \mathbf{v}/2) \equiv -\rho_0^{-1} \nabla p_{\text{stag}}. \quad (8.44)$$

In this equation we defined the **stagnation pressure** (page 149 of *Kundu et al. (2016)*), also called the *total head* (Section 3.1 of *Saffman (1992)*)

$$p_{\text{stag}} \equiv p + \rho_0 \mathbf{v} \cdot \mathbf{v}/2, \quad (8.45)$$

which is the sum of the mechanical pressure, p , plus the dynamic pressure, $\rho_0 \mathbf{v} \cdot \mathbf{v}/2$.

The stagnation pressure is the mechanical pressure required to keep the local acceleration unchanged if the dynamic pressure is set to zero as per a stagnant fluid. This situation arises in practice in a device known as a *Pitot tube* used to measure the speed of flow in a pipe, with the Pitot tube making use of the Bernoulli theorem formulated in Section 10.8. Stagnation points also arise at special points along solid objects within a moving fluid, such as wings. The dynamic pressure, $\rho_0 \mathbf{v} \cdot \mathbf{v}/2$, provides an isotropic force per area in addition to mechanical pressure, p . Hence, the stagnation pressure is the total isotropic contact force per area, thus motivating some treatments to refer the stagnation pressure as the *total pressure*.⁴

³See Exercise 8.1 for a derivation using general Eulerian coordinates.

⁴In many applications, the mechanical pressure, p , is referred to as the *static pressure* so that the total/stagnation pressure is the sum of the static plus dynamic pressures. See section 4.9 of *Kundu et al. (2016)* for more discussion.

8.4.2 Magnus acceleration

The acceleration, $-\boldsymbol{\omega} \times \mathbf{v}$, appearing in the velocity equation (8.43) couples vorticity and velocity. This acceleration is known as the **Magnus acceleration**. Since it acts only when there is both motion and vorticity, it is sometimes referred to as a *vortex force*.⁵ Evidently, the Magnus acceleration deflects a spinning fluid element in a direction perpendicular to its trajectory in a manner analogous to the Coriolis acceleration.⁶

8.4.3 Nonlinear accelerations for some example flows

We here consider some example two-dimensional velocities to help garner insights into the nonlinear accelerations. First note that there are certain flows where the self-advection term vanishes identically so that

$$(\mathbf{v} \cdot \nabla) \mathbf{v} = 0 \implies \boldsymbol{\omega} \times \mathbf{v} + \nabla(\mathbf{v} \cdot \mathbf{v})/2 = 0. \quad (8.46)$$

One example is a zonal flow with a meridional shear

$$\mathbf{v} = u(y) \hat{\mathbf{x}}, \quad (8.47)$$

in which case the self-advection vanishes, $(\mathbf{v} \cdot \nabla) \mathbf{v} = 0$, so that

$$\boldsymbol{\omega} = -\partial_y u \hat{\mathbf{z}} \quad \text{and} \quad \boldsymbol{\omega} \times \mathbf{v} = -u \partial_y u \hat{\mathbf{y}} \quad \text{and} \quad \nabla(\mathbf{v} \cdot \mathbf{v}/2) = u \partial_y u \hat{\mathbf{y}}. \quad (8.48)$$

An example flow with a nonzero self-advection is given by the two-dimensional flow of an ideal vortex

$$\mathbf{u} = \hat{\mathbf{z}} \times \nabla \psi = \gamma (-y \hat{\mathbf{x}} + x \hat{\mathbf{y}}), \quad (8.49)$$

where $\gamma > 0$ is a constant with dimensions of inverse time.⁷ This flow has zero horizontal divergence, $\nabla \cdot \mathbf{u} = 0$, and constant vorticity

$$\hat{\mathbf{z}} \cdot \boldsymbol{\omega} = \zeta = 2\gamma. \quad (8.50)$$

The accelerations from self-advection, Magnus, and dynamic pressure are given by

$$-(\mathbf{u} \cdot \nabla) \mathbf{u} = \gamma^2 \mathbf{x} \quad \text{and} \quad -\boldsymbol{\omega} \times \mathbf{v} = 2\gamma^2 \mathbf{x} \quad \text{and} \quad -\nabla(\mathbf{u} \cdot \mathbf{u}/2) = -\gamma^2 \mathbf{x}. \quad (8.51)$$

In Figure 8.3 we depict these three accelerations, along with the velocity field. Notice how the Magnus acceleration acts to the right of the flow, whereas the acceleration from the dynamic pressure gradient partially opposes the Magnus acceleration.

8.5 The tangent plane approximation

Spherical coordinates are suited for the study of planetary fluid dynamics for cases where the fluid samples the earth's curvature. However, spherical coordinates are more complicated to work with than Cartesian coordinates. We are thus led to consider the utility of an idealized **tangent**

⁵Chapter 3 of [Saffman \(1992\)](#) pursues this interpretation in studying the forces acting on and by vortices.

⁶Besides causing a moving and spinning fluid element to deflect, the Magnus acceleration provides the mechanism whereby a solid spinning body immersed in a moving fluid is deflected, such as commonly experienced by spinning balls used for baseball, tennis, and cricket.

⁷We made use of this velocity in VOLUME 1 for our study of kinematics in two-dimensional flow.

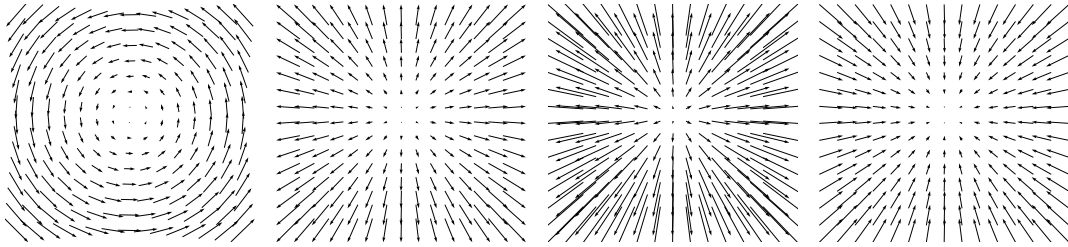


FIGURE 8.3: Illustrating the various nonlinear accelerations contributing to the velocity time tendency as per the vector-invariant velocity equation (8.43). Far left panel: the two-dimensional non-divergent velocity, $\mathbf{u} = \gamma(-y\hat{\mathbf{x}} + x\hat{\mathbf{y}})$. Middle left panel: self-advection acceleration $-(\mathbf{u} \cdot \nabla)\mathbf{u} = \gamma^2 \mathbf{x}$. Middle right panel: Magnus acceleration $-\boldsymbol{\omega} \times \mathbf{u} = 2\gamma^2 \mathbf{x}$. Far right panel: dynamic pressure gradient acceleration, $-\nabla(\mathbf{u}^2/2) = -\gamma^2 \mathbf{x}$. Notice that the Magnus acceleration acts to the right of the flow, whereas the acceleration from the dynamic pressure gradient partially opposes the Magnus acceleration. The sum of the Magnus acceleration and dynamic pressure gradient acceleration equals to the acceleration from self-advection. In each panel we set $\gamma = 1$ and used arbitrary units.

plane configuration as part of a hierarchy of theoretical models to help understand geophysical fluid motion. This motivation leads to the **f-plane** and **beta-plane (β -plane)** approximations, which are the two cases of the tangent plane approximation considered in this book. It is important to note that the tangent plane approximation is not based on assuming a locally flat sphere. Rather, the tangent plane approximation is based on assuming a locally flat geopotential. We further comment on this subtle, but important, distinction in Sections 8.5.2 and 8.5.5.

8.5.1 Basics of the tangent plane approximation

Consider a position at latitude, $\phi = \phi_0$, and introduce a local Cartesian set of coordinates according to

$$(x, y, z) = (R_e \lambda \cos \phi_0, R_e (\phi - \phi_0), z) \quad (8.52)$$

$$(\hat{\mathbf{x}}, \hat{\mathbf{y}}, \hat{\mathbf{z}}) = (\hat{\lambda}, \hat{\phi}, \hat{r}), \quad (8.53)$$

where z is the vertical position from the earth surface. Use of these Cartesian coordinates leads to the following inviscid equations of motion local to $\phi = \phi_0$

$$\frac{Du}{Dt} + 2(\Omega^y w - \Omega^z v) = -\frac{1}{\rho} \frac{\partial p}{\partial x} \quad (8.54a)$$

$$\frac{Dv}{Dt} + 2(\Omega^z u - \Omega^x w) = -\frac{1}{\rho} \frac{\partial p}{\partial y} \quad (8.54b)$$

$$\frac{Dw}{Dt} + 2(\Omega^x v - \Omega^y u) = -\frac{1}{\rho} \frac{\partial p}{\partial z} - g, \quad (8.54c)$$

with planetary rotational vector components

$$\boldsymbol{\Omega} = \Omega (\cos \phi_0 \hat{\mathbf{y}} + \sin \phi_0 \hat{\mathbf{z}}). \quad (8.55)$$

Note the absence of metric terms due to the use of Cartesian coordinates on a flat geometry.

8.5.2 Tangent plane is a geopotential approximation

As formulated above, the tangent plane approximation originates from the geopotential vertical coordinate system rather than the spherical coordinates. In geopotential coordinates, the effective gravitational acceleration (central gravity plus planetary centrifugal) is aligned with the local vertical direction. Correspondingly, the resulting tangent plane equations have the effective gravitational force aligned in the \hat{z} direction. This very convenient property of the geopotential coordinate system was discussed in VOLUME 1.

In contrast, when studying motion in a rotating tank, such as in Section 11.5, it is convenient to separately account for the gravitational acceleration and rotating reference frame's centrifugal acceleration, so that both accelerations appear explicitly in the fluid equation of motion. It is thus important to distinguish the tangent plane equations (which absorb the rotating reference frame's centrifugal acceleration into the effective gravity acceleration) from the equations used for a rotating fluid in a laboratory tank (which separately account for gravity and centrifugal).⁸

8.5.3 Traditional approximation and the f -plane

The traditional approximation is discussed in Section 11.1.3, where we justify retaining only the local vertical component of the rotation vector for the study of large-scale planetary flows, thus resulting in

$$D\mathbf{u}/Dt + f \hat{z} \times \mathbf{u} = -\rho^{-1} \nabla_h p \quad \text{and} \quad Dw/Dt = -\rho^{-1} \partial_z p - g. \quad (8.56)$$

The f -plane makes further use of a constant Coriolis parameter

$$f = 2\Omega \sin \phi_o \equiv f_o. \quad (8.57)$$

The f -plane approximation is the simplest model for the study of fluid motion from within a rotating reference frame using a locally flat geopotential. It thus provides an end member in the hierarchy of theoretical models of geophysical fluid flows affected by the Coriolis acceleration.

8.5.4 β -plane approximation

As studied in VOLUME 5, Rossby waves are planetary scale waves that sample the earth's curvature. The latitudinal dependence of the Coriolis parameter (i.e., differential rotation) is the essential ingredient for their existence. To capture Rossby waves on a tangent plane requires the meridional gradient of the Coriolis parameter, with a linear dependence sufficient

$$f = f_o + R_e^{-1} (2\Omega \cos \phi_o) (y - y_o). \quad (8.58)$$

The β -plane approximation only depends on the meridional gradient of the Coriolis parameter, in which case we more succinctly write

$$f = f_o + \beta y \quad \text{and} \quad \beta = R_e^{-1} \partial_\phi f = (2\Omega/R_e) \cos \phi_o, \quad (8.59)$$

⁸As noted by [Durran \(1993\)](#), confusion can arise when forgetting this distinction.

thus ignoring the constant $-(2\Omega \cos \phi_0) y_0 / R_e$.⁹ Observe that the β -plane approximation is formally valid so long as the horizontal scale of motion, L , is not too large, in which case we require

$$\beta L \ll |f_0|. \quad (8.60)$$

This condition is assumed in our study of quasi-geostrophy in VOLUME 3.

8.5.5 Comments and caveats

We emphasized that the [tangent plane](#) assumes a locally flat geopotential, so that the gravitational acceleration remains locally vertical. Additionally, for the [traditional approximation](#) we retain only the local vertical component of the planetary rotation vector, which leads to a simpler expression for the Coriolis acceleration. It is tempting to extrapolate the dynamics on a tangent plane to an infinite plane. However, doing so certainly breaks the assumption built into the truncated Taylor series used to mathematically justify the tangent plane approximation. Furthermore, it leads to the unphysical situation of an infinite flat rotating plane without a centrifugal acceleration to distinguish a center of rotation. Additionally, an infinite β -plane leads to an unbounded rotation rate.

8.6 Exact hydrostatic balance

We are mostly interested in moving fluids within this book. Even so, it is useful to expose the signature of a static fluid supporting the trivial solution, $\mathbf{v} = 0$. The equation of motion (8.24) has an exact static solution so long as the pressure gradient force balances the effective gravitational force

$$\nabla p = -\rho \nabla \Phi, \quad (8.61)$$

and where the frictional stress tensor has zero divergence. Equation (8.61) constitutes the exact form of the [hydrostatic balance](#). As justified in Section 11.2, the hydrostatic balance is a very good approximation for the vertical momentum equation in large-scale geophysical fluids even when those fluids are moving. We will thus commonly make the [hydrostatic approximation](#) for moving fluids. For the current considerations, we are interested in a static fluid, in which case the hydrostatic balance (8.61) is an exact solution.

8.6.1 Properties of exact hydrostatic balance

We make the following observations of the exact hydrostatic balance.

- Since ∇p is directly proportional to $\nabla \Phi$, surfaces of constant pressure (*isobars*) in a static fluid correspond to surfaces of constant geopotential.
- Since the curl of the pressure gradient vanishes, a static fluid maintains its density gradients parallel to geopotential gradients

$$\nabla \rho \times \nabla \Phi = 0, \quad (8.62)$$

⁹We could choose to absorb the constant, $-(2\Omega \cos \phi_0) y_0 / R_e$, into the definition of f_0 . But that choice is typically not made since the f -plane generally uses $f_0 = 2\Omega \sin \phi$, and adding just the term βy for the β -plane makes for a more direct comparison between results on the f -plane and the corresponding β -plane.

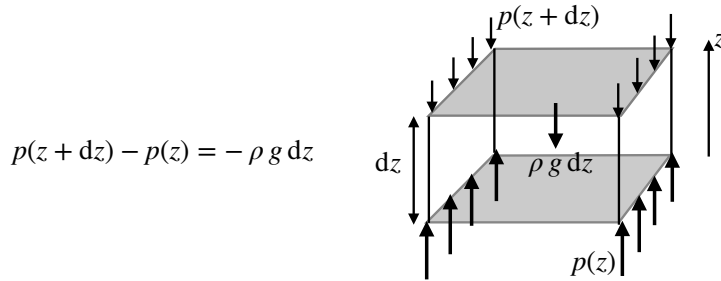


FIGURE 8.4: Illustrating the forces acting in a hydrostatically balanced fluid layer placed in a geopotential field $\Phi = g z$ with g constant. The layer has an infinitesimal thickness, $dz > 0$, density, ρ , and horizontal cross-sectional area, dA . The pressure force acting on the top and bottom of the layer are compressive. Hence, the pressure force at the top of the layer acts downward, $\mathbf{F}^{\text{press}}(z + dz) = -\hat{z} p(z + dz) dA$, whereas the pressure force at the bottom of the layer acts upward, $\mathbf{F}^{\text{press}}(z) = +\hat{z} p(z) dA$. In a hydrostatically balanced fluid, the difference in pressure across the layer is exactly balanced by the weight per area of fluid within the layer. Consequently, $p(z + dz) - p(z) = -g \rho(z) dz$, so that pressure at the top of the layer is less than that at the bottom.

which in turn means that density surfaces are parallel to geopotentials so that

$$\rho = \rho(\Phi) \quad \text{static fluid.} \quad (8.63)$$

For the geopotential $\Phi = g z$, a static fluid is realized if the density depends only on the vertical position

$$\rho = \rho(z) \quad \text{static fluid with } \Phi = g z. \quad (8.64)$$

If the density gradient has any component perpendicular to $\nabla\Phi$, then pressure forces will affect fluid flow thus implying that the fluid is not in an exact hydrostatic balance.

- Projecting both sides of equation (8.61) onto an infinitesimal space increment, $d\mathbf{x}$, renders

$$d\mathbf{x} \cdot \nabla p = -\rho d\mathbf{x} \cdot \nabla\Phi \implies \frac{dp}{d\Phi} = -\rho. \quad (8.65)$$

Hence, the difference in hydrostatic pressure between any two geopotentials is given by the integral

$$p(\Phi_2) - p(\Phi_1) = - \int_{\Phi_1}^{\Phi_2} \rho(\Phi) d\Phi. \quad (8.66)$$

If $\Phi = g z$ then we recover

$$p(z_2) - p(z_1) = -g \int_{z_1}^{z_2} \rho(z) dz, \quad (8.67)$$

so that the difference in hydrostatic pressure between two geopotentials is given by the weight per horizontal area of fluid between the two geopotentials. This relation is illustrated for an infinitesimally thin layer in Figure 8.4.

8.6.2 Comparison to approximate hydrostatic balance

A static fluid in a gravitational field exhibits hydrostatic balance whereby pressure at a point is a function solely of the geopotential, in which case $p = p(z)$ when $\Phi = g z$. Correspondingly, $dp/dz = -\rho g$, which means that we determine hydrostatic pressure at a point by computing the weight per horizontal area of fluid above that point. Likewise, density is just a function of

geopotential since $\nabla\rho \times \nabla\Phi = 0$.

For an approximate hydrostatic fluid, pressure is a function of space and time, $p = p(\mathbf{x}, t)$, as is density, $\rho = \rho(\mathbf{x}, t)$. Hence, we are no longer ensured that pressure and density isolines are parallel. However, the approximate hydrostatic fluid retains a vertical pressure gradient given by

$$\frac{\partial p}{\partial z} = -\rho g \quad \text{approximate hydrostatic.} \quad (8.68)$$

Hence, column by column, the pressure at a point in an approximate hydrostatic fluid is determined by the weight per horizontal area of fluid above that point. This key property is thus shared between fluids in exact and approximate hydrostatic balance. In Chapter 11 we have much more to say about fluid flows maintaining approximate hydrostatic balance.

8.6.3 Hydrostatic balance in a variable gravity field

For much of this book, we assume the gravitational field is fixed and prescribed. This assumption is based on the [shallow fluid approximation](#), in which we assume the thickness of the atmosphere and ocean are tiny relative to the planet's radius. But for studies of the full atmosphere, or for the study of gaseous planets and stars, we can no longer make the shallow fluid approximation. We here take a brief tangent to describe hydrostatic balance without assuming a shallow fluid, so that the gravity field is affected by the fluid itself.

Recalling our study of Newtonian gravity in VOLUME 1, we know that the gravitational potential satisfies [Poisson's equation](#)

$$\nabla^2\Phi = 4\pi G \rho. \quad (8.69)$$

For a fluid in hydrostatic balance, pressure is related to the geopotential via equation (8.61)

$$\nabla p = -\rho \nabla\Phi = \rho \mathbf{g}, \quad (8.70)$$

where $\mathbf{g} = -\nabla\Phi$ is the gravitational acceleration. We are thus led to the elliptic equation for pressure

$$\nabla \cdot (\rho^{-1} \nabla p) = -4\pi G \rho. \quad (8.71)$$

It is notable that the gravitational field depends on the mass density, ρ , which in turn is a function of pressure, which is itself dependent on gravity.

Barotropic fluid

A [barotropic fluid](#) has pressure a function just of density, $p = p(\rho)$, so that

$$\nabla \times (\rho^{-1} \nabla p) = 0, \quad (8.72)$$

which means we can introduce the [pressure potential](#) that satisfies

$$\nabla\Phi_p = \rho^{-1} \nabla p. \quad (8.73)$$

The Poisson equation (8.71) thus takes the form

$$\nabla^2\Phi_p = -4\pi G \rho. \quad (8.74)$$

Spherically symmetric mass density

For a spherically symmetric mass density, the hydrostatic balance and Poisson equation reduce to

$$\frac{dp(r)}{dr} = -\rho(r) g(r) = -\rho(r) G M(r)/r^2 \quad (8.75a)$$

$$\frac{1}{r^2} \frac{d}{dr} \left[\frac{r^2}{\rho} \frac{dp(r)}{dr} \right] = -4\pi G \rho(r). \quad (8.75b)$$

If the central density is finite and approximately $\rho \approx \rho_c$, then the mass for a tiny radius around the core is $M(r) \approx 4\pi r^3 \rho_c/3$. Hence, the hydrostatic balance (8.75a) leads to the radial pressure derivative

$$dp/dr \approx -4\pi G \rho_c^2 r/3, \quad (8.76)$$

so that the pressure has zero radial derivative at the center of the sphere. We consider the outer edge of the planet (or star) to be at a radius where the density vanishes, at which point the pressure also vanishes if the planet is surrounded by a vacuum.

Further study

More discussion of these ideas, at the level of that considered here, can be found in Chapter 6 of [Lautrup \(2005\)](#).

8.7 Axial angular momentum

Moving from our study of linear momentum thus far in this chapter, we now consider the axial angular momentum of a fluid element. In VOLUME 1, we studied many facets of angular momentum for a particle moving around a rotating planet. Much of that discussion holds for the fluid element, in particular the relation between axial angular momentum and the Coriolis acceleration. Yet there are some differences that arise from the extended nature of the fluid continuum, thus supporting contact forces such as pressure. In this section we explore facets of angular momentum for a perfect fluid. Refer to Figure 8.2 for orientation and notation.

8.7.1 Axial angular momentum equation

Following our discussion of a point particle in VOLUME 1, the axial angular momentum of a fluid element is given by

$$L^z = (\rho \delta V) r_\perp (u + r_\perp \Omega) \equiv (\rho \delta V) l^z \quad (8.77)$$

where

$$l^z = r_\perp (u + r_\perp \Omega) \quad (8.78)$$

is the axial angular momentum per unit mass, and the distance to the polar rotation axis,

$$r_\perp = r \cos \phi, \quad (8.79)$$

is the moment-arm for determining the torques acting on a fluid element. Making use of the zonal momentum equation (8.30), as well as the material time derivative of the moment arm

$$\frac{Dr_{\perp}}{Dt} = \frac{Dr}{Dt} \cos \phi - r \frac{D\phi}{Dt} \sin \phi = w \cos \phi - v \sin \phi, \quad (8.80)$$

we find the material time change

$$\frac{Dl^z}{Dt} = (u + 2\Omega r_{\perp}) \frac{Dr_{\perp}}{Dt} + r_{\perp} \frac{Du}{Dt} \quad (8.81a)$$

$$= (u + 2\Omega r_{\perp}) \frac{Dr_{\perp}}{Dt} + (u + 2\Omega r_{\perp})(v \sin \phi - w \cos \phi) - \frac{1}{\rho} \frac{\partial p}{\partial \lambda} \quad (8.81b)$$

$$= (u + 2\Omega r_{\perp}) \left[\frac{Dr_{\perp}}{Dt} + v \sin \phi - w \cos \phi \right] - \frac{1}{\rho} \frac{\partial p}{\partial \lambda} \quad (8.81c)$$

$$= -\frac{1}{\rho} \frac{\partial p}{\partial \lambda}. \quad (8.81d)$$

We are thus led to the evolution of axial angular momentum per mass

$$\rho \frac{Dl^z}{Dt} = -\frac{\partial p}{\partial \lambda} \implies \frac{\partial(\rho l^z)}{\partial t} + \nabla \cdot (\rho l^z \mathbf{v}) = -\frac{\partial p}{\partial \lambda}. \quad (8.82)$$

In the absence of a zonal pressure gradient, the axial angular momentum for a fluid element is materially invariant, which is a result also shared with the point particle. Certain of the physical constraints for motion of the point particle also hold for the fluid element. In particular, we can equate the zonal Coriolis acceleration to the zonal acceleration induced by axial angular momentum conservation. For example, a fluid element initially at rest in a fluid with zero zonal pressure gradient will zonally accelerate when moved meridionally (e.g., as from a meridional pressure gradient) according to the needs of axial angular momentum conservation.

8.7.2 Axial angular momentum conserving motion of a ring of air

Atmospheric and oceanic flows rarely experience a zero zonal pressure gradient. However, on a smooth spherical planet with zonal periodicity, a zonal integral removes the zonally integrated zonal pressure gradient,

$$\int_0^{2\pi} \partial_{\lambda} p d\lambda = 0. \quad (8.83)$$

Hence, we expect that the zonally integrated inviscid flow of a homogeneous ring of fluid (with fixed latitude and radius) on a smooth planet preserves its axial angular momentum

$$\frac{d}{dt} \int_0^{2\pi} \rho l^z r \cos \phi d\lambda = \int_0^{2\pi} \rho \frac{Dl^z}{Dt} r \cos \phi d\lambda = - \int_0^{2\pi} \frac{\partial p}{\partial \lambda} r \cos \phi d\lambda = 0. \quad (8.84)$$

We consider some thought experiments to illustrate the zonal fluid motion induced by axial angular momentum conservation, with these considerations having their analog in the more extensive discussion of point particle thought experiments considered in VOLUME 1.

Consider a latitudinal ring of constant mass inviscid fluid circling the earth at latitude ϕ_A and radial position r_A . If the ring is at rest in the rotating terrestrial reference frame, the angular momentum per mass for this ring is due to just the rigid-body motion of the planet,

$$l^z = \Omega (r_A \cos \phi_A)^2. \quad (8.85)$$

Altering either the latitude (to ϕ_B) or radial position (to r_B) induces a corresponding zonal velocity, $u_B \neq 0$, that maintains fixed axial angular momentum

$$l^z = \Omega (r_A \cos \phi_A)^2 = r_B \cos \phi_B (u_B + \Omega r_B \cos \phi_B), \quad (8.86)$$

which means that

$$u_B = \Omega \frac{(r_A \cos \phi_A)^2 - (r_B \cos \phi_B)^2}{r_B \cos \phi_B}. \quad (8.87)$$

For example, moving the ring vertically to a radial distance, $r_B \neq r_A$, while maintaining a constant latitude, $\phi_B = \phi_A$, induces a zonal velocity

$$u_B = \Omega \cos \phi_A \frac{r_A^2 - r_B^2}{r_B}. \quad (8.88)$$

If the new radial position is less than the original, so that $r_A^2 > r_B^2$, then axial angular momentum conservation induces an eastward zonal velocity ($u_B > 0$); i.e., westerly winds. The opposite happens for an increase in the radial position. If we instead change the latitudinal position of the ring ($\phi_A \neq \phi_B$) while keeping the radial position fixed ($r_A = r_B$), then axial angular momentum conservation induces the zonal velocity

$$u_B = r_A \Omega \frac{\cos^2 \phi_A - \cos^2 \phi_B}{\cos \phi_B}. \quad (8.89)$$

Since $-\pi/2 \leq \phi \leq \pi/2$, we know that $\cos \phi \geq 0$ on the sphere, and $\cos \phi$ decreases moving poleward in either hemisphere. Hence, poleward latitudinal motion that preserves axial angular momentum induces eastward flow ($u_B > 0$), whereas equatorward latitudinal motion induces westward flow ($u_B < 0$).

How realistic is it to have coherent rings of inviscid air circulating around the planet at all latitudes? To answer this question we insert some numbers for a ring of radius R_e that starts with zero relative velocity at the equator, $\phi_A = 0$, in which case equation (8.89) reduces to

$$u_B = r_A \Omega \frac{\sin^2 \phi_B}{\cos \phi_B}. \quad (8.90)$$

This zonal flow is sometimes referred to as the axial angular momentum conserving flow. The westerly winds induced by axial angular momentum conserving motion have the following speeds at a selection of latitudes

$$u(10^\circ) = 14 \text{ m s}^{-1} \quad u(20^\circ) = 58 \text{ m s}^{-1} \quad u(30^\circ) = 134 \text{ m s}^{-1}. \quad (8.91)$$

The values at higher latitudes grow unbounded since $\cos \phi \rightarrow 0$ as the poles are approached. So there is a problem with an idealized theory of atmospheric circulation based on axial angular momentum conserving rings of air.

Even without detailed knowledge of flow instabilities studied in VOLUME 5, we can imagine that an axial angular momentum conserving flow will eventually go unstable and thus break the assumptions of axial symmetry. Such instabilities introduce eddying motion that present torques leading to non-conservation of axial angular momentum. Further investigation (e.g., [Held and Hou \(1980\)](#)) reveals that inviscid axial angular momentum conserving ideas extend only so far as the [Hadley circulation](#), which extends only to the middle latitudes.

8.7.3 Conditions for steady circulation

Now consider the conditions required to realize a steady circulation, in which

$$\nabla \cdot (\rho l^z \mathbf{v}) = -\partial_\lambda p \quad \text{and} \quad \nabla \cdot (\rho \mathbf{v}) = 0. \quad (8.92)$$

By integrating the steady mass continuity equation over a region south of an arbitrary latitude, $\phi = \phi_n$, we find a vanishing integrated mass transported across the latitude, so long as there is zero vertical transport across the top ($r = r_{\text{top}}$) and bottom ($r = R_e$) boundaries. That is, across any latitude, northward mass transport must be balanced by the same amount of southward mass transport. It is notable that these conditions hold for flows with and without friction. The same conclusions result for the steady angular momentum budget over the same region, though in this case we are ignoring friction that would otherwise affect the budget particularly near the earth surface.

8.7.4 Further study

This section only touched upon the broad topic of the axial angular momentum budget for the atmosphere, which includes features of the Hadley Cell and Ferrel Cell. Entry points to this topic can be found in Section 10.3 of [Holton and Hakim \(2013\)](#), Section 8.2 of [Marshall and Plumb \(2008\)](#), and Chapter 14 of [Vallis \(2017\)](#), as well as the milestone study from [Held and Hou \(1980\)](#).

In Section 12.5 we consider the zonally integrated axial angular momentum budget for the ocean with a sloping solid-earth bottom boundary as well as an upper free surface. For the ocean, the flow is distinctively not axially symmetric (outside the latitude of the Drake Passage), given the advent of land-sea boundaries. Even so, the study reveals the important role for boundary form stresses (Section 12.1) in affecting the angular momentum, in addition to boundary frictional stresses. We also pursue a study of axial angular momentum in the two-dimensional non-divergent barotropic model in VOLUME 3, with the present discussion anticipating many of those results.



8.8 Exercises

EXERCISE 8.1: VECTOR-INVARIANT USING GENERAL EULERIAN COORDINATES

Derive the identity (8.41) using general Eulerian coordinates and the covariant derivative studied in VOLUME 1.

EXERCISE 8.2: PRESSURE SOLUTION TO EULER'S EQUATION

This exercise is adapted from Q1.10 of [Johnson \(1997\)](#). Consider the Euler equation (8.29) in a non-rotating reference frame (zero Coriolis) and with constant density

$$\rho \frac{D\mathbf{v}}{Dt} = -\nabla p - \rho g \hat{\mathbf{z}}. \quad (8.93)$$

Assume the Cartesian velocity field is given by

$$\mathbf{v}(\mathbf{x}, t) = \tau^{-2} (\hat{\mathbf{x}} x t + \hat{\mathbf{y}} y t - 2 \hat{\mathbf{z}} z t), \quad (8.94)$$

where τ is a constant with dimensions of time.

- Show that the velocity field is non-divergent, $\nabla \cdot \mathbf{v} = 0$.
- Find the pressure field, $p(\mathbf{x}, t)$, satisfying $p(\mathbf{x} = 0, t) = P_0(t)$.

EXERCISE 8.3: CONDITIONS FOR UNIFORM FLOW WITHOUT GRAVITY AND ROTATION

Consider the Euler equation (8.29) in the absence of rotation (zero Coriolis) and gravitation (free space fluid)

$$\rho \frac{D\mathbf{v}}{Dt} = -\nabla p. \quad (8.95)$$

Ignore all boundaries throughout this exercise, and assume density is a uniform constant.

- What equation does the pressure need to satisfy to ensure $\mathbf{v} \equiv \mathbf{v}_0$, where \mathbf{v}_0 is a constant in space and time?
- What equation does the pressure need to satisfy to ensure $\partial_t(\nabla \cdot \mathbf{v}) = 0$?

EXERCISE 8.4: HYDROSTATIC BALANCE IN A CONTAINER WITH TWO LIQUIDS

Figure 8.5 depicts a flat bottom container with two immiscible liquids of densities $\rho_1 < \rho_2$ and corresponding thicknesses h_1 and h_2 , with the lighter fluid resting on top of the heavier fluid. Now vertically insert a smooth open ended tube into the liquid. As the tube's lower end approaches the bottom of the container, the liquid within the tube must rest at the same level as the liquid outside the tube. The reason is the top of the tube is open to the same atmosphere as the container. Convince yourself of this result.

Now remove the top liquid layer but keep the heavier lower layer, in which we have the tube containing liquid with density ρ_2 to a height h_2 above the bottom. Next, pour the lighter fluid into the container to the thickness h_1 , but do not let any of the light fluid enter the tube. How high will the lower layer rise within the tube when reaching static equilibrium? Assume the atmospheric pressure is a horizontal constant. Hint: this is a very simple exercise.

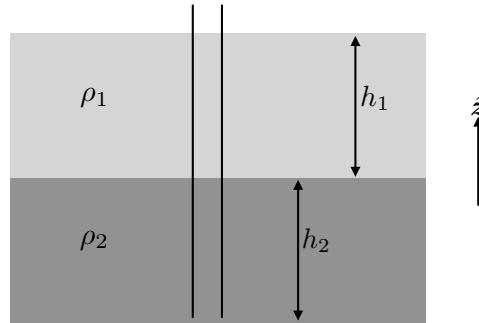


FIGURE 8.5: A container with two immiscible liquids of densities $\rho_1 < \rho_2$ and thicknesses h_1 and h_2 , which is considered in Exercise 8.4. A smooth tube with both ends open is then placed in the container, with the tube bottom near the bottom of the container.

EXERCISE 8.5: HYDROSTATIC BALANCE IN SPHERICAL COORDINATES

Figure 8.6 depicts a solid angle sector of a sphere, extending from radius $r = r_A$ to $r = \infty$. Assume the fluid is in hydrostatic balance and that all mass is spherically symmetric, so that the density, gravitational acceleration, and pressure are functions only of the radius. We know that the hydrostatic balance at a point is given by $dp/dr = -\rho(r) g(r)$. Is the area integrated pressure around the sphere at radius, $r = r_A$, equal to the weight of fluid above this radius? Assume that $\rho(r) g(r)$ falls off faster than r^{-3} as the radius increases, and that $p(r = \infty) = 0$.

EXERCISE 8.6: DIAGNOSING THE PRESSURE FOR A GIVEN FLOW

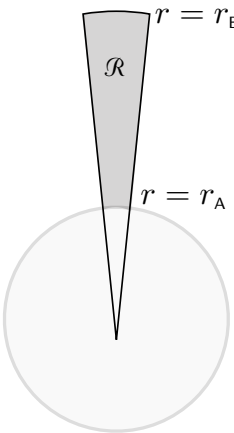


FIGURE 8.6: A fluid within a spherical region, \mathcal{R} , as depicted for Exercise 8.5. Is the area integrated pressure at radius, $r = r_A$, equal to the weight of fluid above this radius? Assume that $\rho(r) g(r)$ falls off faster than r^{-3} as the radius increases, and that $p(r = \infty) = 0$.

Consider a two-dimensional perfect fluid with constant density, ρ , that satisfies the Euler equation in the absence of planetary rotation

$$\rho \frac{D\mathbf{u}}{Dt} = -\nabla_h p. \quad (8.96)$$

Provide a suitable pressure (to within a constant) that corresponds to the following steady (i.e., time independent) velocity fields, with $\gamma > 0$ a constant having dimensions inverse time, and $\mathbf{x} = \hat{\mathbf{x}}x + \hat{\mathbf{y}}y$ the horizontal position vector. Consider the following hints: (i) check your physical dimensions, (ii) check that $\nabla \times [(\mathbf{u} \cdot \nabla)\mathbf{u}] = 0$, (iii) check that $\nabla \cdot \mathbf{u} = 0$, which is required since ρ is a constant.

- (a) $\mathbf{u} = \gamma \mathbf{x}$
- (b) $\mathbf{u} = -\gamma \hat{\mathbf{z}} \times \mathbf{x}$
- (c) $\mathbf{u} = \gamma (x \hat{\mathbf{x}} - y \hat{\mathbf{y}})$.

EXERCISE 8.7: THEOREM OF STRESS MEANS ([Aris \(1962\)](#) EXERCISE 5.12.2)

Make use of Cauchy's equation of motion (8.22) and the divergence theorem to prove the following identity (known as the *theorem of stress means*)

$$\oint_{\partial\mathcal{R}} \Psi T^{pq} \hat{n}_q dS = \int_{\mathcal{R}} \left[T^{pq} \partial_q \Psi + \rho \Psi \left(\frac{Dv^p}{Dt} - f^p \right) \right] dV, \quad (8.97)$$

where Ψ is an arbitrary differentiable function, and \hat{n}_q is the q 'th component of the outward normal on $\partial\mathcal{R}$. This theorem finds use in certain formulations of continuum mechanics. Assume Cartesian tensors.

EXERCISE 8.8: AREA OF A STEADY 1D LAMINAR JET EMANATING FROM A DOWNWARD NOZZLE
 Consider a steady state laminar jet of constant density and inviscid water emanating from a downward facing nozzle with a constant prescribed volume flow rate, Q (dimensions volume per time). Ignore surface tension and assume the air pressure acting on the surface of the jet is constant all along the jet. You can solve this exercise by making use of the steady vertical momentum equation and the steady mass continuity equation.

- (a) Explain why we can set $dp/dz = 0$ within the jet once it leaves the nozzle.
- (b) Determine an expression for the area of the jet, $A(z)$, as a function of distance, z , from

the nozzle, with the nozzle placed at $z = 0$ and $z < 0$ a position beneath the nozzle. In addition to z , your expression will contain Q , g , and $A(0)$.

- (c) Is the area of the jet getting smaller or larger as the water moves downward away from the nozzle? Does this answer agree with your experience?
- (d) If the downward speed of water at the nozzle is $w(0) = 0.5 \text{ m s}^{-1}$, then at what vertical position, z , is the area of the jet four times different than at $z = 0$?

EXERCISE 8.9: ROSSBY EFFECT

Consider a horizontal region of fluid whose velocity is rotationally symmetric and depth independent

$$\mathbf{u} = \boldsymbol{\Gamma} \times \mathbf{r}, \quad (8.98)$$

where

$$\boldsymbol{\Gamma} = \Gamma(r) \hat{\mathbf{z}} \quad (8.99)$$

is an angular velocity, $\hat{\mathbf{z}}$ is the vertical direction, and r is the radial distance to the origin. Furthermore, let $\Gamma(r)$ vanish for radial distances $r \geq R$ for some radius R . Let the fluid be moving on a β -plane with Coriolis parameter $f = f_0 + \beta y = f_0 + \beta r \sin \vartheta$, where ϑ is the polar angle relative to the x -axis. Derive an integral expression for the Coriolis acceleration integrated over this fluid region. Discuss the direction of the acceleration.

You may find the following hints of use.

- The resulting integrated Coriolis acceleration is solely in the $\hat{\mathbf{y}}$ direction, and it vanishes when $\beta = 0$.
- The answer is given in [Rossby \(1948\)](#), and is sometimes known as the Rossby effect.
- We further consider such interactions between rotating fluid motion and the Coriolis parameter in VOLUME 3 when studying the [beta-drift \(\$\beta\$ -drift\)](#) of axially symmetric vortices. There, we find that the beta drift leads to a northwestward drift rather than the northward drift from the Rossby effect. The reason for the discrepancy is that [Rossby \(1948\)](#) ignored pressure effects that set up a secondary flow that induces westward drift, in addition to Rossby's northward drift. For this exercise, we ignore these pressure effects, just like Rossby did.

EXERCISE 8.10: CENTER OF MASS TRANSPORT THEOREM

Consider a field, ψ , that satisfies the standard conservation law

$$\rho \frac{D\psi}{Dt} = -\nabla \cdot \mathbf{J}, \quad (8.100)$$

within a region, $\mathcal{R}(\mathbf{v})$, that moves with the fluid flow. We here derive some results that hold for Cartesian coordinates.

- (a) Prove the transport theorem valid for Cartesian tensors

$$\frac{d}{dt} \int_{\mathcal{R}(\mathbf{v})} \psi \mathbf{x} \rho dV = \int_{\mathcal{R}(\mathbf{v})} (\mathbf{J} + \rho \psi \mathbf{v}) dV - \oint_{\partial \mathcal{R}(\mathbf{v})} \mathbf{x} (\hat{\mathbf{n}} \cdot \mathbf{J}) dS. \quad (8.101)$$

Hint: multiply both sides of equation (8.100) by x^m .

- (b) Offer an interpretation of equation (8.101). Hint: first consider the special case that the total ψ -stuff, defined by $\Psi \equiv \int_{\mathcal{R}(\mathbf{v})} \psi \rho dV$, is constant when following the flow. Further hint: consider the more specialized case of $\psi = 1$ and $\mathbf{J} = 0$.

EXERCISE 8.11: VORTICITY AND THE MERIDIONAL DERIVATIVE OF ANGULAR MOMENTUM
Vorticity is the curl of the velocity field, $\nabla \times \mathbf{v}$, and we study its mechanics in **VOLUME 3**. Making use of spherical coordinates from **VOLUME 1**, we find the radial component of vorticity is

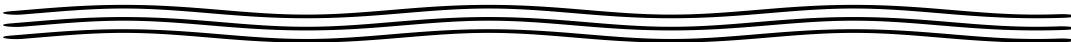
$$\zeta = (r \cos \phi)^{-1} [\partial_\lambda v - \partial_\phi(u \cos \phi)]. \quad (8.102)$$

Derive a relation for purely zonal flow ($v = 0$) between the vorticity and the meridional derivative of the axial angular momentum.

EXERCISE 8.12: EQUATIONS IN CYLINDRICAL-POLAR COORDINATES

The spherical/geopotential equations from Section 8.3 are appropriate when studying motion on the rotating planet. However, there are questions that warrant the use of cylindrical-polar coordinates (see the orthogonal coordinates chapter in **VOLUME 1**). We have in mind here the study of vortices or tropical cyclones. Each of these cases suggest the use of cylindrical-polar coordinates with the origin at the center of the vortex. Note that we are not making the tangent plane approximation here, so that centrifugal terms should appear explicitly in the equations of motion.

- (a) Write the velocity using cylindrical-polar coordinates.
- (b) Write the acceleration using cylindrical-polar coordinates.
- (c) Write the momentum equation using cylindrical-polar coordinates. Discuss the terms appearing in those equations.
- (d) Write the equation for the axial angular momentum relative to a vertical axis through the origin. Discuss this equation relative to that holding for axial angular momentum around the planet's rotational axis as discussed in Section 8.7.
- (e) Assume $\nabla \cdot (\rho \mathbf{v}) = 0$ as well as axial symmetry. Write the equation for the streamfunction, ψ , for circulation in the radial-vertical plane. What are its physical dimensions?



Chapter 9

STRESS

We introduced contact forces in Chapter 8 when deriving the fluid equations of motion. In the present chapter we dive deeper into the study of contact forces and their corresponding stresses. We also discuss conditions placed on stress and velocity at boundaries. We organize fluid stresses into a second order Cauchy stress tensor and further decompose this stress into isotropic or normal stresses (pressure), which are the only stresses supported by perfect fluids, and the additional tangential or shearing stresses that arise in real fluids due to viscosity.

CHAPTER GUIDE

Understanding the mathematical and physical aspects of stress is important for the suite of fluid models studied in this book. Because the subject involves vectors and tensors, it can require more patience than analogous chapters that discuss scalar fields. To make the formalism less mathematically intense, we employ Cartesian tensors throughout. Books on continuum mechanics provide detailed and thorough discussions of stress. The presentation in chapter 9 of [Lautrup \(2005\)](#) is compatible with the presentation in this chapter.

9.1	Introduction to stresses in fluids	262
9.2	Cauchy's stress principle and Newton's laws	263
9.2.1	Cauchy's stress principle	263
9.2.2	Newton's third law and local equilibrium of stresses	264
9.2.3	Comments on the local equilibrium relation	265
9.2.4	Historical comments	266
9.3	The stress tensor	267
9.3.1	The stress tetrahedron	267
9.3.2	The stress tensor and stress vector	267
9.3.3	Stress is a tensor	269
9.4	Angular momentum and the stress tensor	269
9.4.1	Basic formulation	270
9.4.2	Physical interpretation	270
9.4.3	Symmetry of the stress tensor	271
9.5	Forces and torques in an exact hydrostatic fluid	271
9.5.1	Force balance	272
9.5.2	Pressure force balance for a homogeneous fluid	272
9.5.3	Torque balance	274
9.6	Constitutive relation between stress and strain rate	275
9.6.1	Thermodynamic pressure and mechanical pressure	276

9.6.2	Couette flow and the frictional stress tensor	276
9.6.3	D'Alembert's theorem for perfect fluids	277
9.6.4	Guidance from Galilean invariance	278
9.6.5	A comment on Rayleigh drag	278
9.6.6	Constitutive relation for Newtonian fluids	278
9.6.7	Navier-Stokes and Euler equations	281
9.6.8	No-slip boundary conditions on solid boundaries	282
9.6.9	Laplacian friction in terms of vorticity and divergence	282
9.6.10	Frictional stresses in a sheared flow	283
9.6.11	The net stress tensor	284
9.6.12	Comments and further study	284
9.7	Reynolds number and flow regimes	284
9.7.1	Non-dimensional Navier-Stokes	284
9.7.2	Ratio of inertial to frictional accelerations	285
9.7.3	Reynolds numbers for geophysical flows	285
9.7.4	Further study	287
9.8	Stress on an interface	287
9.8.1	General formulation	287
9.8.2	Solid material boundary	288
9.8.3	No-slip condition at a static boundary	289
9.8.4	Lagrangian interface	289
9.8.5	Permeable interface	290
9.8.6	Summary comments	290
9.8.7	Comments on boundary layers	291
9.9	Surface tension	291
9.9.1	Capillary tube	292
9.9.2	Force balance on an air-water interface	292
9.9.3	Young-Laplace formula	294
9.9.4	Soluble gas bubbles inside water	296
9.9.5	When we can ignore surface tension	297
9.9.6	Further study	297
9.10	Exercises	297

9.1 Introduction to stresses in fluids

As a continuous region of matter, a fluid element experiences two kinds of forces: **body forces** and **contact forces**. Body forces act throughout the fluid element and arise from a force field whose source is external to the fluid. The accumulated effects from body forces within a fluid region result from volume integrating the body forces over the region. In geophysical fluid mechanics, we are concerned with body forces from the effective gravitational acceleration (central gravity plus planetary centrifugal) and the body force from the planetary Coriolis acceleration.

Contact forces are the focus of this chapter, with such forces arising from intermolecular forces within the fluid media. Macroscopically, they give rise to the local exchange of dynamical properties between fluid elements, and they represent a fundamental distinction between forces acting on a fluid element and those acting on a point particle. Dividing the contact force by the area upon which it acts leads to the **Cauchy's stress vector**. As a force per unit area, stresses are associated with two directions: the direction of the force and the direction normal to the area acted upon by the force. Correspondingly, stresses acting on a fluid element are naturally

organized into a second order stress tensor.¹ Details of the stress tensor govern the dynamic response of a continuous media to kinematic and thermodynamic properties of the media. Consequently, the equations of continuum mechanics posed by Cauchy find their specialization when prescribing the stress tensor, with this specification known as a **constitutive relation**.

We distinguish two types of mechanical stresses acting within a fluid: a **normal stress** and a **tangential stress**, with tangential stresses also called **shear stresses**. Pressure is the canonical normal stress that acts normal to any surface within a fluid, and with pressure acting in a compressive manner. The ability of a fluid to resist compression is a function of the fluid's compressibility. Fluids flow in the presence of tangential or shear stresses, with viscous friction acting to resist such motion.

Contact forces, which are given by the Cauchy stress times an area element, satisfy **Newton's third law**, also known as the action/reaction law.² Hence, the net contact force acting on a finite region arises just from the contact forces acting at the region boundary. This property of contact forces means that a mechanically isolated region of a continuous media (i.e., a region unaffected by external forces or boundary contact forces) does not spontaneously translate its center of mass. Similarly, symmetry of the stress tensor means that an isolated region does not spontaneously alter its angular momentum.

Surface tension is a stress that acts on the boundaries of a fluid media, such as the boundary between air and water. Surface tension is unique in this chapter in that it does *not* satisfy **Newton's third law**. As shown in Section 9.9, surface tension is generally negligible for length scales larger than a few centimeters. Even so, the effects of surface tension are important if studying physical processes associated with air-sea interactions, such as tracer, heat, and momentum exchange through bubbles, droplets, and capillary waves.

9.2 Cauchy's stress principle and Newton's laws

We here develop some general properties of contact forces and the associated stresses, and we do so by considering an arbitrary smooth and simply closed region, \mathcal{R} , of fluid with volume $V = \int_{\mathcal{R}} dV$ and mass $M = \int_{\mathcal{R}} \rho dV$ (Figure 9.1). Furthermore, let $\partial\mathcal{R}$ be the bounding surface for the region, and let $\hat{\mathbf{n}}$ be the outward normal at a point on the boundary.

9.2.1 Cauchy's stress principle

The bounding surface of a fluid region experiences mechanical interactions with the surrounding fluid continuum (due to molecular forces) and these interactions lead to contact forces acting on the boundary. Let $\boldsymbol{\tau}$ be the stress vector (force per unit area) acting at a point on $\partial\mathcal{R}$. **Cauchy's stress principle** asserts that the stress vector is a function of the position, time, and boundary normal

$$\boldsymbol{\tau} = \boldsymbol{\tau}(\mathbf{x}, t, \hat{\mathbf{n}}). \quad (9.1)$$

The dependence on the boundary normal in equation (9.1) means that the stress acting on a surface is generally a function of the orientation of that surface. This form of the stress trivially holds for an exactly hydrostatic fluid where the stress vector is proportional to the pressure (Section 8.6). Furthermore, the stress from pressure is oriented along the inward normal, thus

¹In the language of continuum mechanics, we here work exclusively with the Cauchy stress tensor. See Section 1.22 of [Tromp \(2025a\)](#) for more details.

²See the Newtonian mechanics chapter in VOLUME 1 for more on Newton's third law.

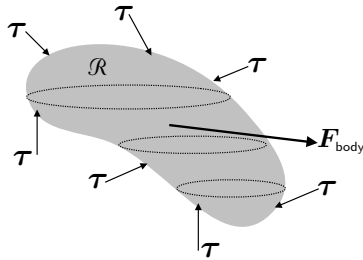


FIGURE 9.1: Schematic of the net body force, \mathbf{F}_{body} , acting on a finite region of fluid, plus the accumulation of stress vectors, τ , acting on the region boundaries. The net body force is determined by a volume integral of the body force (gravity, planetary centrifugal, and planetary Coriolis) acting at each point within the volume. In contrast, the volume integral of the stress divergence reduces to an area integral of the stress over the region boundary. Stress arises from pressure (compressive and normal) and strains (which lead to a stress via [constitutive relation](#)). The contribution from pressure to horizontal accelerations is referred to as [form stress](#). The form stress coming from the bottom boundary is called the [topographic form stress](#). The form stress appearing at the air-sea boundary is the [atmospheric form stress](#) if considering ocean dynamics and [oceanic form stress](#) if considering atmospheric dynamics. We study form stress in Chapter 12.

reflecting the purely compressive nature of pressure

$$\boldsymbol{\tau} = -p(\mathbf{x}, t) \hat{\mathbf{n}} \quad \text{static fluid.} \quad (9.2)$$

Cauchy's stress principle is sensible for points within the fluid media, and its relevance has been supported by experimental studies over the time since Cauchy made this assertion in the 1820s. Furthermore, it holds for pressure and viscous stresses at the interface between fluid media or at solid-earth boundaries. However, Cauchy's stress principle does not hold for [surface tension](#), which is proportional to the curvature of the surface separating two fluid media (e.g., atmosphere and ocean), where curvature involves spatial gradients of the normal vector. As discussed in Section 9.9, surface tension is important for length scales on the order of centimeters, and as such play a minor role in this book. Hence, with the single exception of surface tension, we rely on Cauchy's stress principle to formulate the fluid dynamical equations.

9.2.2 Newton's third law and local equilibrium of stresses

Newton's second law says that in an inertial reference frame, unbalanced forces acting on a physical system affect a time change to the linear momentum. Consider a region, $\mathcal{R}(\mathbf{v})$, whose fluid elements follow the [barycentric velocity](#). Newton's second law then states that the material time evolution of the region's linear momentum is given by

$$\frac{d}{dt} \int_{\mathcal{R}(\mathbf{v})} \mathbf{v} \rho dV = \int_{\mathcal{R}(\mathbf{v})} \mathbf{f}_{\text{body}} \rho dV + \oint_{\partial\mathcal{R}(\mathbf{v})} \boldsymbol{\tau} d\mathcal{S}, \quad (9.3)$$

where $\int_{\mathcal{R}(\mathbf{v})} \mathbf{f}_{\text{body}} \rho dV$ is the domain integrated body force. To develop a general property for the contact forces, consider this balance for a region whose size gets infinitesimally small. Assuming the integrands for the two volume integrals are well behaved (i.e., smooth and bounded) as the region size goes to zero, we see that the volume integrals are proportional to L^3 , where L is a length scale measuring the size of the region (e.g., side for a cubical region or diameter for a spherical region). In the same manner, we assume the stresses are well behaved in the case of an infinitesimal region. However, the integral of the contact forces goes to zero at the slower rate that is proportional to L^2 . Self-consistency for the balance (9.3) over a region of

infinitesimal size thus requires the contact forces to satisfy the limiting behavior

$$\lim_{L \rightarrow 0} \frac{1}{L^2} \oint_{\partial \mathcal{R}(v)} \boldsymbol{\tau} d\mathcal{S} = 0. \quad (9.4)$$

This behavior means that contact forces at a point in the fluid must be in local equilibrium. Equation (9.4) is sometimes referred to as [Cauchy's fundamental lemma](#).

A direct implication of the local equilibrium statement is that stress vectors that respect Cauchy's principle (9.1) satisfy

$$\boldsymbol{\tau}(\mathbf{x}, t, \hat{\mathbf{n}}) = -\boldsymbol{\tau}(\mathbf{x}, t, -\hat{\mathbf{n}}). \quad (9.5)$$

For example, the stress vector on one side of a surface is equal and oppositely directed to the stress vector acting on the other side. This equation is an expression of [Newton's third law](#), here written in terms of the stresses acting in a continuous media. It is of fundamental importance throughout our study of contact forces and their associated stresses acting within the fluid and at boundaries. We thus see how an application of Newton's second law, the linear momentum principle (9.3) for a continuous media, leads to a statement of Newton's third law in the form of equation (9.5) holding for contact forces.

As an example of the above ideas, the simplest stress we consider in this chapter is that from pressure, with pressure acting solely in a compressive manner so that the stress vector takes the form

$$\boldsymbol{\tau}_{\text{press}}(\mathbf{x}, t, \hat{\mathbf{n}}) = -p(\mathbf{x}, t) \hat{\mathbf{n}}. \quad (9.6)$$

This stress trivially satisfies the Newton's third law relation (9.5) since

$$\boldsymbol{\tau}_{\text{press}}(\mathbf{x}, t, \hat{\mathbf{n}}) = -\boldsymbol{\tau}_{\text{press}}(\mathbf{x}, t, -\hat{\mathbf{n}}). \quad (9.7)$$

9.2.3 Comments on the local equilibrium relation

The local equilibrium relation (9.4), and the corresponding expression of Newton's third law, (9.5), might suggest that stresses cannot lead to motion. However, that suggestion is incorrect since stresses integrated over a finite region can lead to a net force that causes motion. That is, local/pointwise mechanical equilibrium does not imply mechanical equilibrium for finite regions. Furthermore, since contact forces within the domain interior cancel pointwise, the local equilibrium relation (9.4) says that the net contact force acting on the region arises only from the area integrated stresses acting on the region boundary.

To further emphasize the above point, consider an ocean region bounded at its bottom by the solid earth and its upper surface by an atmosphere of nonzero mass. Variations (divergences) in stresses over finite regions within the ocean fluid lead to accelerations and thus to motion. However, when integrated over the full ocean domain, all stresses cancel from the interior of the fluid. Consequently, the net contact force acting on the full ocean domain reduces to the contact force acting just on the ocean boundaries. The boundary contact forces arise from mechanical interactions with the solid-earth and the overlying atmosphere. The center of mass for the ocean basin remains static if the accumulation of forces sum to zero, which includes the contact forces acting over its boundaries plus the volume integrated body forces from effective gravity (central gravity plus planetary centrifugal) and planetary Coriolis.

In Figure 9.2 we illustrate the net pressure force acting on an arbitrary fluid domain. Pressure acts solely in a compressive manner as directed along the inward normal to the domain.

Area integration over a domain boundary renders the net pressure force acting on the domain

$$\mathbf{F}^{\text{press}} = - \oint_{\partial\mathcal{R}} p \hat{\mathbf{n}} d\mathcal{S} = - \int_{\mathcal{R}} \nabla p dV, \quad (9.8)$$

where the second equality follows from application of Gauss's [divergence theorem](#) for a scalar field. When decomposed according to coordinate axes, the pressure force acting on the boundary has a component in both the vertical and horizontal directions, thus contributing to both vertical and horizontal accelerations. The vertical accelerations are closely balanced by the weight of fluid, with exact balance in the case of a hydrostatic fluid. The horizontal stresses from pressure are known as [form stress](#). This name arises since the stress depends on the form, or shape, of the surface on which pressure acts.

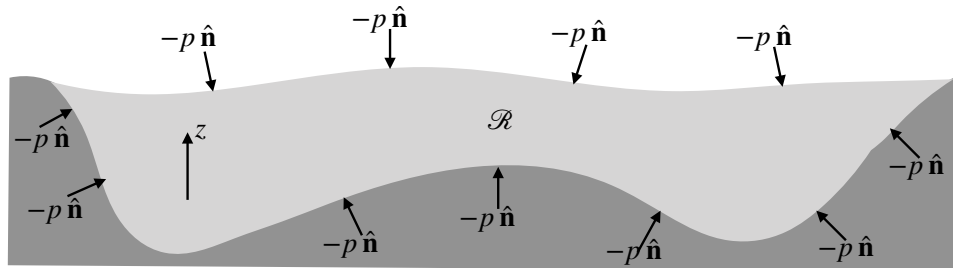


FIGURE 9.2: Schematic of contact forces from pressure acting on the boundaries to an ocean domain. Pressure forces are directed according to minus the local normal since pressure is a compressive force aligned with the inward normal direction. As with all contact forces, the pressure forces acting in the interior of the ocean are locally in mechanical equilibrium. Hence, when integrated over the global domain the net pressure forces only arise at the domain boundaries. That is, the net pressure force acting on the full ocean domain arises only at the interface between the solid-earth and the ocean, plus the interface between the atmosphere and the ocean. Note that the pressure force has a component in both the vertical and horizontal directions as per the orientation of the local normal vector. Further boundary stresses arise from viscous exchange, which generally have components perpendicular to the boundary normal; i.e., tangential to the boundary. Such stresses also satisfy Newton's third law.

9.2.4 Historical comments

We find it useful to quote from [Truesdell \(1952\)](#), who provides the following description of [Cauchy's stress principle](#) as given by equation (9.1).

Upon any imagined closed surface, \mathcal{S} , there exists a distribution of stress vectors, $\boldsymbol{\tau}$, whose resultant and moment are equivalent to those of the actual forces of material continuity exerted by the material outside \mathcal{S} upon that inside.

Worded in this manner, we can understand the relation between Newton's third law and Cauchy's stress principle. The profound nature of Cauchy's stress principle is further articulated, again from [Truesdell \(1952\)](#).

[Cauchy's stress principle] has the simplicity of genius. Its profound originality can be grasped only when one realizes that a whole century of brilliant geometers had treated very special elastic problems in very complicated and sometimes incorrect ways without ever hitting upon this basic idea, which immediately became the foundation of the mechanics of distributed media.

9.3 The stress tensor

Cauchy's stress principle reduces the mathematical complexity of describing stress vectors. A further implication of this principle leads to Cauchy's theorem, which states that the stress vector, which is a function of space, time, and normal direction, can be expressed in terms of a stress tensor (a function of space and time) projected into the direction of the normal. The purpose of this section is to provide arguments supporting this theorem, with these arguments largely following the original from Cauchy in 1827.

9.3.1 The stress tetrahedron

Consider the tetrahedron fluid region shown in Figure 9.3, where three of the four sides are aligned according to the Cartesian coordinate axes and the fourth side has an outward normal, $\hat{\mathbf{n}} = (\hat{n}_1, \hat{n}_2, \hat{n}_3)$, projecting into all three directions. In the limit that the tetrahedron size goes to zero, local equilibrium of the contact forces (as per Cauchy's fundamental lemma (9.4)) means that

$$-\sum_{m=1}^3 \boldsymbol{\tau}^{(m)} dA_m + \boldsymbol{\tau}^{\hat{\mathbf{n}}} dA = 0, \quad (9.9)$$

where we use the shorthand expression for the outward normal directed stress vector

$$\boldsymbol{\tau}(\mathbf{x}, t, \hat{\mathbf{n}}) = \boldsymbol{\tau}^{\hat{\mathbf{n}}}. \quad (9.10)$$

In equation (9.9), $\boldsymbol{\tau}^{(m)} dA_m$ (no implied summation) is the contact force vector acting on the face with outward normal parallel to the corresponding coordinate axis, and $\boldsymbol{\tau}^{\hat{\mathbf{n}}} dA$ is the contact force acting on the slanted face with outward normal, $\hat{\mathbf{n}}$. The minus sign arises for the summation term since the outward normals for these three faces point in the negative coordinate directions, and our convention is for $\boldsymbol{\tau}^{(m)}$ to align with the positive coordinate directions. The areas for each face are related to the slanted face area through

$$dA_m = \hat{n}_m dA, \quad (9.11)$$

so that the local equilibrium relation (9.9) becomes

$$\boldsymbol{\tau}^{\hat{\mathbf{n}}} = \sum_{m=1}^3 \hat{n}_m \boldsymbol{\tau}^{(m)}. \quad (9.12)$$

9.3.2 The stress tensor and stress vector

Equation (9.12) can be organized into a matrix-vector equation

$$\begin{bmatrix} (\boldsymbol{\tau}^{\hat{\mathbf{n}}})^1 & (\boldsymbol{\tau}^{\hat{\mathbf{n}}})^2 & (\boldsymbol{\tau}^{\hat{\mathbf{n}}})^3 \end{bmatrix} = \begin{bmatrix} \hat{n}_1 & \hat{n}_2 & \hat{n}_3 \end{bmatrix} \begin{bmatrix} \tau^{(1)1} & \tau^{(1)2} & \tau^{(1)3} \\ \tau^{(2)1} & \tau^{(2)2} & \tau^{(2)3} \\ \tau^{(3)1} & \tau^{(3)2} & \tau^{(3)3} \end{bmatrix}, \quad (9.13)$$

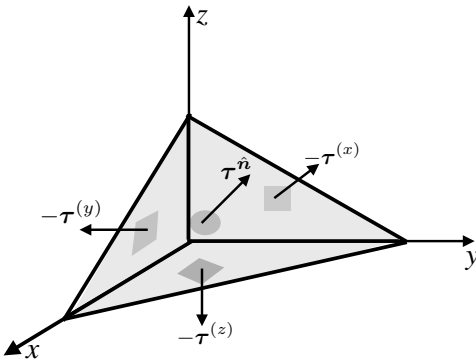


FIGURE 9.3: Cauchy's tetrahedron region of fluid with stresses acting on the four faces. Note that the stresses are not necessarily directed normal to the faces. Local equilibrium of stresses (as per Cauchy's fundamental lemma (9.4)) means that the accumulation of these four stresses around the region adds to zero as the region volume goes to zero.

where each matrix element is the n -component of the m -stress $\boldsymbol{\tau}^{(m)}$. We introduce a less cumbersome notation by writing

$$\begin{bmatrix} (\boldsymbol{\tau}^{\hat{n}})^1 & (\boldsymbol{\tau}^{\hat{n}})^2 & (\boldsymbol{\tau}^{\hat{n}})^3 \end{bmatrix} = \begin{bmatrix} \hat{n}_1 & \hat{n}_2 & \hat{n}_3 \end{bmatrix} \begin{bmatrix} T^{11} & T^{12} & T^{13} \\ T^{21} & T^{22} & T^{23} \\ T^{31} & T^{32} & T^{33} \end{bmatrix}, \quad (9.14)$$

so that T^{mn} measures the force per area in the n -direction along a surface whose outward normal points in the m -direction, as depicted in Figure 9.4. Making use of T^{mn} in the expression (9.12) leads to

$$(\boldsymbol{\tau}^{\hat{n}})^n = \sum_{m=1}^3 \hat{n}_m T^{mn}, \quad (9.15)$$

which can be written more succinctly as

$$\boldsymbol{\tau}^{\hat{n}} = \hat{\mathbf{n}} \cdot \mathbf{T}. \quad (9.16)$$

We thus see that the stress vector that acts on a surface that is oriented according to a normal vector, $\hat{\mathbf{n}}$, equals to the projection of the stress tensor, \mathbf{T} , onto the normal vector. Evidently, $\boldsymbol{\tau}^{\hat{n}}$ is a vector with components within the tangent plane of the surface, as well as normal to the surface. Exposing functional dependence to equation (9.16) reveals

$$\boldsymbol{\tau}^{\hat{n}}(\mathbf{x}, t, \hat{\mathbf{n}}) = \hat{\mathbf{n}} \cdot \mathbf{T}(\mathbf{x}, t), \quad (9.17)$$

which manifests Cauchy's theorem. Namely, the stress vector $\boldsymbol{\tau}^{\hat{n}}$, which is a function of $(\mathbf{x}, t, \hat{\mathbf{n}})$, has been decomposed into a stress tensor, \mathbf{T} , which is a function of (\mathbf{x}, t) , as well as the projection of the stress tensor into a direction $\hat{\mathbf{n}}$. Finally, note a common example concerns the case of a vertical normal direction, $\hat{\mathbf{n}} = \hat{\mathbf{z}}$, as for the stress acting on a nearly horizontal sea surface. In this case the stress vector is

$$\boldsymbol{\tau}^{\hat{\mathbf{z}}} = \hat{\mathbf{x}} T^{31} + \hat{\mathbf{y}} T^{32} + \hat{\mathbf{z}} T^{33}. \quad (9.18)$$

The horizontal components are key to the transfer of horizontal stress between the atmosphere and ocean, thus providing a mechanical forcing to the ocean circulation. The vertical stress

is less important particularly for hydrostatic fluids whose vertical momentum equation is dominated by hydrostatic balance.

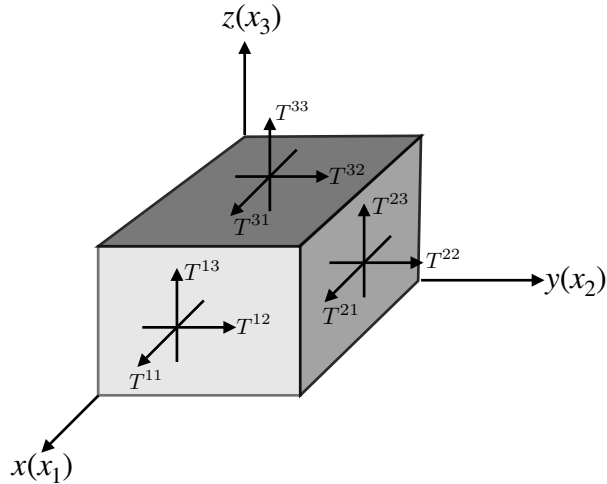


FIGURE 9.4: Illustrating the components to the stress tensor, T^{mn} and how they are organized according to the coordinate axes. The component T^{mn} is the stress that points in the n -direction along the face with outward normal in the m -direction.

9.3.3 Stress is a tensor

How do we know that T^{mn} form the components to a tensor rather than just being elements of a 3×3 matrix? To answer this question we note that each component of \mathbf{T} is a force per area, with force a vector and area orientable by its outward normal. As it is built from vectors, which are first order tensors, we suspect that \mathbf{T} should be a proper second order tensor. This suspicion is supported by the [quotient rule](#) from tensor analysis, which means that equation (9.15) indeed yields T^{mn} that are components to a second order tensor. Through the power of tensor analysis, we thus see that our considerations, based on the rather contrived tetrahedron region in Figure 9.3, hold for an arbitrary region described by an arbitrary coordinate system.

9.4 Angular momentum and the stress tensor

The linear momentum principle afforded by Newton's law of motion allowed us to deduce the local equilibrium property (9.4) of the stress. We here derive a constraint placed on the stress tensor that is imposed by studying angular momentum. Phenomenologically, we observe that geophysical fluids, as with most common fluids, experience torques only as the moments of body forces acting throughout the volume of a fluid region, or as moments of contact forces acting on the surface bounding the fluid region. We now make use of this observation to deduce symmetry of the stress tensor.³

³Page 11 of [Batchelor \(1967\)](#) and Section 5.13 of [Aris \(1962\)](#) offer brief discussions of fluids in which internal force couples lead to torques distinct from those considered here, and in which the stress tensor has an anti-symmetric component. [Dahler and Scriven \(1961\)](#) provide a more thorough account of such *polar materials*. Internal sources of angular momentum are studied in solid mechanics, with Section 5.3 of [Malvern \(1969\)](#) offering a discussion. See also Example 8.21 of [?](#) and Example 8.21 of [Tromp \(2025b\)](#) for presentations of intrinsic spin using differential forms.

9.4.1 Basic formulation

Consider a constant mass fluid element that has a Cartesian position \mathbf{x} relative to an arbitrary origin. The angular momentum of the fluid element with respect to the origin is

$$\mathbf{L} = \rho \delta V (\mathbf{x} \times \mathbf{v}), \quad (9.19)$$

and its material time evolution is

$$\frac{D\mathbf{L}}{Dt} = \rho \delta V \mathbf{x} \times \frac{D\mathbf{v}}{Dt}, \quad (9.20)$$

which follows since $D(\rho \delta V)/Dt = 0$, $D\mathbf{x}/Dt = \mathbf{v}$, and $\mathbf{v} \times \mathbf{v} = 0$. Making use of Cauchy's form for the equation of motion (8.22)

$$\rho \frac{D\mathbf{v}}{Dt} = \rho \mathbf{f}_{\text{body}} + \nabla \cdot \mathbf{T} \quad (9.21)$$

allows us to write the angular momentum evolution as

$$\frac{D\mathbf{L}}{Dt} = \delta V \mathbf{x} \times (\rho \mathbf{f}_{\text{body}} + \nabla \cdot \mathbf{T}). \quad (9.22)$$

The first term arises from body forces (e.g., central gravity, planetary centrifugal, and Coriolis) and the second term arises from the divergence of stresses. Expanding the stress divergence term renders

$$\left[\frac{D\mathbf{L}_m}{Dt} \right]_{\text{stress}} = \delta V \epsilon_{mnp} x^n (\nabla \cdot \mathbf{T})^p \quad (9.23a)$$

$$= \delta V \epsilon_{mnp} x^n \partial_q T^{pq} \quad (9.23b)$$

$$= \delta V \epsilon_{mnp} [\partial_q (x^n T^{pq}) - (\partial_q x^n) T^{pq}] \quad (9.23c)$$

$$= \delta V \epsilon_{mnp} [\partial_q (x^n T^{pq}) - T^{pn}], \quad (9.23d)$$

where the final equality follows since $\partial_q x^n = \delta^n{}_q$. Note that for brevity we dropped the **body** notation on the body force vector. Bringing this result back into the full expression (9.22) leads to

$$\frac{D\mathbf{L}_m}{Dt} = \delta V \epsilon_{mnp} [\rho x^n f^p + \partial_q (x^n T^{pq}) - T^{pn}]. \quad (9.24)$$

9.4.2 Physical interpretation

To facilitate a physical interpretation of the terms appearing in the angular momentum equation (9.24), integrate over an arbitrary Lagrangian region (region moving with the barycentric velocity, \mathbf{v}) so that

$$\frac{d}{dt} \int_{\mathcal{R}(\mathbf{v})} L_m = \int_{\mathcal{R}(\mathbf{v})} \epsilon_{mnp} [\rho x^n f^p + \partial_q (x^n T^{pq}) - T^{pn}] dV. \quad (9.25)$$

As noted earlier, the first term on the right hand side arises from torques due to body forces acting over the region

$$\int_{\mathcal{R}(\mathbf{v})} \epsilon_{mnp} (\rho x^n f^p) dV = \int_{\mathcal{R}(\mathbf{v})} (\mathbf{x} \times \mathbf{f}_{\text{body}})_m \rho dV. \quad (9.26)$$

The second term on the right hand side of equation (9.25) can be transferred into a surface integral using the divergence theorem

$$\int_{\mathcal{R}(\mathbf{v})} \epsilon_{mnp} \partial_q (x^n T^{pq}) dV = \int_{\partial \mathcal{R}(\mathbf{v})} \epsilon_{mnp} x^n T^{pq} \hat{n}_q d\mathcal{S} = \int_{\partial \mathcal{R}(\mathbf{v})} (\mathbf{x} \times \boldsymbol{\tau})_m d\mathcal{S}, \quad (9.27)$$

where \hat{n}_q is the q 'th component of the outward normal direction on the region boundary, $\partial \mathcal{R}(\mathbf{v})$, and

$$\tau^p = T^{pq} \hat{n}_q \quad (9.28)$$

is the p 'th component to the stress vector that is normal to $\hat{\mathbf{n}}$ (see equation (9.16)). Hence, the second term is the contribution to angular momentum evolution due to torques arising from the moment of contact forces acting on the region boundary.

9.4.3 Symmetry of the stress tensor

As noted at the start of this section, geophysical fluids have their angular momentum affected by torques arising from the moment of body forces acting throughout the fluid region, plus the moment of contact forces acting on the region boundary. There is a third term in equation (9.24) that does not fit into either category, and it is given by the volume integral

$$-\int_{\mathcal{R}(\mathbf{v})} \epsilon_{mnp} T^{pn} dV = \int_{\mathcal{R}(\mathbf{v})} \epsilon_{mpn} T^{pn} dV \equiv \int_{\mathcal{R}(\mathbf{v})} T_m^\times dV, \quad (9.29)$$

where we defined

$$T_m^\times = \epsilon_{mpn} T^{pn}. \quad (9.30)$$

This term contributes a volume source to angular momentum and yet it is *not* associated with body forces. We might refer to it as a *torque density* (torque source per volume). As already noted, such torque sources are *not* relevant for geophysical fluids, in which case we conclude that geophysical fluids are affected only by symmetric stress tensors

$$T^{mn} = T^{nm} \implies \epsilon_{mnp} T^{np} = 0. \quad (9.31)$$

Symmetry of the stress tensor is a central property of the stresses acting on geophysical fluids, so we only consider symmetric stress tensors throughout this book.

9.5 Forces and torques in an exact hydrostatic fluid

In this section we return to the study of a static fluid in a gravitational field originally considered in Section 8.6. The exact solution is known as exact hydrostatic balance, which is distinguished from the approximate hydrostatic balance appropriate for moving geophysical fluids under certain scaling regimes (Section 11.2). For a static fluid, all forces and all torques sum to zero at any point. Similarly, the integrated forces and integrated torques acting on any finite fluid region also vanish. The static fluid offers useful practice in applying the formalism of continuum mechanics to a system where we know the answer (i.e., nothing moves). Furthermore, there are interesting and important applications of these ideas, such as in the building of dams and underwater structures, both of which we certainly hope will remain static!

9.5.1 Force balance

The force balance in an exact hydrostatic fluid was addressed in Section 8.6 where we deduced the following relation between the pressure gradient and geopotential gradient

$$\nabla p = -\rho \nabla \Phi. \quad (9.32)$$

This equality holds at every point within the fluid, and as such it is a **strong formulation** of the hydrostatic balance.⁴ Integrating over a finite fluid region, \mathcal{R} , and using the divergence theorem for scalar fields renders the finite volume (**weak formulation**) of hydrostatic balance

$$\int_{\mathcal{R}} \rho \nabla \Phi \, dV = - \int_{\mathcal{R}} \nabla p \, dV = - \oint_{\partial \mathcal{R}} p \hat{\mathbf{n}} \, dS. \quad (9.33)$$

Expanding the above relations for the special case of $\Phi = g z$ leads to the differential statements

$$0 = \hat{\mathbf{x}} \cdot \nabla p = \hat{\mathbf{y}} \cdot \nabla p \quad \text{and} \quad \rho g = -\hat{\mathbf{z}} \cdot \nabla p, \quad (9.34)$$

with the first two equations implying that the exact hydrostatic pressure is only a function of z . The corresponding weak form of hydrostatic balance reads

$$g M = - \int_{\mathcal{R}} \nabla p \cdot \hat{\mathbf{z}} \, dV = - \oint_{\partial \mathcal{R}} p (\hat{\mathbf{n}} \cdot \hat{\mathbf{z}}) \, dS, \quad (9.35)$$

where $M = \int_{\mathcal{R}} \rho \, dV$ is the mass in the fluid region, and the weak form of horizontal balances are

$$0 = \int_{\mathcal{R}} \nabla p \cdot \hat{\mathbf{x}} \, dV = \oint_{\partial \mathcal{R}} p (\hat{\mathbf{n}} \cdot \hat{\mathbf{x}}) \, dS \quad (9.36a)$$

$$0 = \int_{\mathcal{R}} \nabla p \cdot \hat{\mathbf{y}} \, dV = \oint_{\partial \mathcal{R}} p (\hat{\mathbf{n}} \cdot \hat{\mathbf{y}}) \, dS. \quad (9.36b)$$

We emphasize that these finite volume balances hold for any arbitrarily shaped region within a static fluid.

9.5.2 Pressure force balance for a homogeneous fluid

To further our understanding of the pressure force balances in a static fluid, consider a constant density static ocean sitting under a massless atmosphere, in which case the hydrostatic pressure is

$$p = -\rho g z, \quad (9.37)$$

where $z < 0$ for the ocean. Now examine the pressure forces acting on the three sides of the triangle in Figure 9.5. This geometry is simple enough to explicitly compute the pressure forces, thus confirming the general properties in equations (9.35), (9.36a), and (9.36b).

The outward normal vectors along the three triangle faces are given by

$$\hat{\mathbf{n}}_A = +\hat{\mathbf{y}} \quad \text{and} \quad \hat{\mathbf{n}}_B = -\hat{\mathbf{z}} \quad \text{and} \quad \hat{\mathbf{n}}_C = \hat{\mathbf{z}} \cos \varphi - \hat{\mathbf{y}} \sin \varphi, \quad (9.38)$$

⁴The weak formulation provides integral relations whereas the strong formulation provides differential relations.

where

$$\tan \varphi = \frac{z_2 - z_1}{y_2 - y_1} = \frac{\Delta z}{\Delta y} \quad (9.39)$$

is the slope of the hypotenuse relative to the horizontal. The integrated pressure force along the vertical face is thus given by

$$\mathbf{F}_A^{\text{press}} = - \int p \hat{\mathbf{n}}_A dS = \hat{\mathbf{y}} \Delta x \int_{z_1}^{z_2} \rho g z dz = \hat{\mathbf{y}} (\rho g/2) (z_2 + z_1) \Delta z \Delta x, \quad (9.40)$$

where Δx is the thickness of the triangle in the \hat{x} direction into the page. Note that $\mathbf{F}_A^{\text{press}}$ points in the $-\hat{\mathbf{y}}$ direction since $z_2 + z_1 < 0$. Likewise, the integrated pressure force along the horizontal face is given by

$$\mathbf{F}_B^{\text{press}} = - \int p \hat{\mathbf{n}}_B dS = -\hat{\mathbf{z}} \Delta x \int_{y_1}^{y_2} \rho g z_1 dy = -\hat{\mathbf{z}} \rho g z_1 \Delta y \Delta x, \quad (9.41)$$

which points upward since $z_1 < 0$.

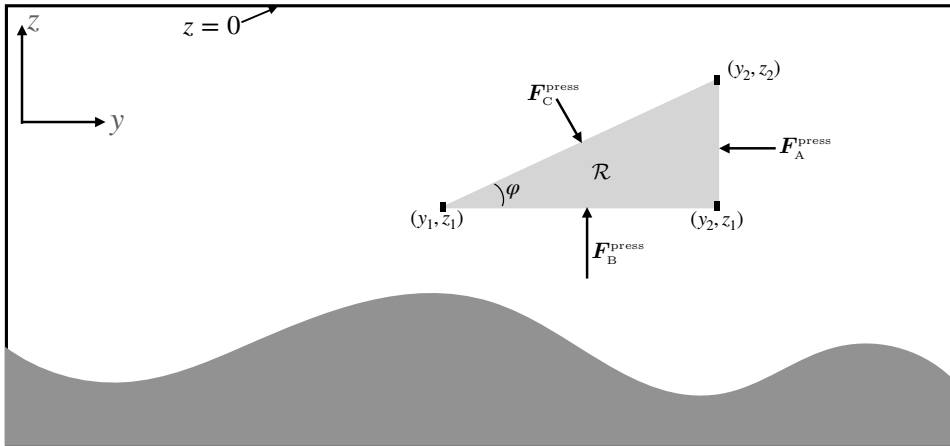


FIGURE 9.5: A right triangle region of fluid in a static ocean where $z < 0$. The positions for the three corners are shown as (y_1, z_1) , (y_2, z_1) , and (y_2, z_2) , along with the pressure forces acting on the three sides. In exact hydrostatic balance, the area integrated pressure force acting over the triangle boundary vanishes, $-\oint_{\mathcal{R}} p \hat{\mathbf{n}} dS = 0$. If the density of the fluid is assumed constant, then we can analytically compute the force balance as detailed in Section 9.5.2.

The integrated pressure force along the sloped hypotenuse face, C , requires a bit of trigonometry. For this purpose we write vertical position along the hypotenuse as

$$z = \eta(y) = z_2 - (y_2 - y) \tan \varphi, \quad (9.42)$$

so that the horizontal projection of the surface area is given by equation (12.4)

$$dS = |\nabla(z - \eta)| dx dy = \frac{dx dy}{|\cos \varphi|}. \quad (9.43)$$

Hence, the integrated pressure force on the hypotenuse is given by

$$\mathbf{F}_C^{\text{press}} = - \int p \hat{\mathbf{n}}_C dS \quad (9.44a)$$

$$= \frac{\hat{\mathbf{n}}_c}{\cos \varphi} \Delta x \int_{y_1}^{y_2} \rho g \eta(y) dy \quad (9.44b)$$

$$= (\hat{\mathbf{z}} - \hat{\mathbf{y}} \tan \varphi) \rho g \Delta x [z_2 \Delta y - y_2 \Delta z - (1/2)(y_1 + y_2) \Delta y \tan \varphi] \quad (9.44c)$$

$$= (\hat{\mathbf{z}} - \hat{\mathbf{y}} \tan \varphi) \rho g \Delta x [z_2 \Delta y - y_2 \Delta z + (y_1 + y_2) \Delta z / 2] \quad (9.44d)$$

$$= (\hat{\mathbf{z}} - \hat{\mathbf{y}} \tan \varphi) \rho g \Delta x \Delta y (z_1 + z_2) / 2. \quad (9.44e)$$

Bringing these results together renders the net pressure forces in the two directions

$$\hat{\mathbf{y}} \cdot (\mathbf{F}_A^{\text{press}} + \mathbf{F}_B^{\text{press}} + \mathbf{F}_C^{\text{press}}) = (\rho g \Delta x / 2) [(z_1 + z_2) \Delta z - \tan \varphi (z_1 + z_2) \Delta y] = 0 \quad (9.45a)$$

$$\hat{\mathbf{z}} \cdot (\mathbf{F}_A^{\text{press}} + \mathbf{F}_B^{\text{press}} + \mathbf{F}_C^{\text{press}}) = \rho g \Delta x \Delta y \Delta z / 2 = M g, \quad (9.45b)$$

where the mass of the triangle is given by

$$M = \rho \Delta x \Delta y \Delta z / 2. \quad (9.46)$$

We thus see that the area integrated horizontal pressure forces vanish, whereas the area integrated vertical pressure force balances the weight of the fluid. Again, these results are expected given the general expressions (9.35), (9.36a), and (9.36b) of force balance. Even so, being able to explicitly compute the pressure forces acting around a region, and to confirm the general force balances, is a useful means to become familiar with hydrostatic pressure.

9.5.3 Torque balance

Torques arise in the presence of force *couplets*, which in turn lead to time changes in the angular momentum. In our discussion of the stress tensor in Section 9.4, we saw that a symmetric stress tensor removes volume sources of torque; i.e., there are no internal sources of force couplets. So the only means to impart a nonzero torque is for force couplets to arise from body forces (forces originating outside of the fluid region) and from contact forces that act between fluid elements within the region. In this section, we show that in a static fluid, the net torque vanishes both at an arbitrary point in the fluid as well as when integrated over an arbitrary region.

Strong form: zero torques acting on a fluid element

The torque is the moment of a force computed about a chosen origin. For a static geophysical fluid, the torque acting on a fluid element is given by the moment of the pressure force plus the moment of the effective gravity force (central gravity plus planetary centrifugal)

$$\mathbf{x} \times \mathbf{f}_{\text{body}} \rho \delta V = \mathbf{x} \times (-\rho^{-1} \nabla p - \nabla \Phi) \rho \delta V. \quad (9.47)$$

As seen in Section 9.5.1, the pressure and effective gravitational forces exactly balance at each point with a static fluid so that $\nabla p = -\rho \nabla \Phi$. Hence, there can be no torques at each point since there are no net forces at each point.

Weak form: zero torques acting on a finite fluid region

To show that the torque vanishes for a finite fluid region, we can merely integrate the fluid element result (9.47) over the finite region. Since the integral of zero is still zero, there are no torques on the region. An alternative approach makes use of the weak formulation by following the discussion in Section 9.4.2. In this approach, we start by writing the time change in angular

momentum acting on a static fluid region

$$\frac{d}{dt} \int_{\mathcal{R}} \mathbf{L} = \int_{\mathcal{R}} [\mathbf{x} \times (-\rho \nabla \Phi)] dV + \oint_{\partial \mathcal{R}} [\mathbf{x} \times (-\hat{\mathbf{n}} p)] dS. \quad (9.48)$$

Note that although the discussion in Section 9.4.2 focused on a Lagrangian region, $\mathcal{R}(\mathbf{v})$, there is no distinction here between Lagrangian and Eulerian since the fluid is static.

The pressure contribution in equation (9.48) is written in its contact force form, which is appropriate for a weak formulation. However, to compare its contribution to the torque with that from effective gravity requires us to convert the area integral to a volume integral. For that purpose we use Cartesian tensor notation and expose full details

$$\oint_{\partial \mathcal{R}} (\hat{\mathbf{n}} \times \mathbf{x})_a p dS = \epsilon_{abc} \oint_{\partial \mathcal{R}} \hat{n}^b x^c p dS \quad \text{permutation symbol} \quad (9.49a)$$

$$= \epsilon_{abc} \int_{\mathcal{R}} \partial^b (x^c p) dV \quad \text{divergence theorem} \quad (9.49b)$$

$$= \epsilon_{abc} \int_{\mathcal{R}} (\delta^{bc} p + x^c \partial^b p) dV \quad \text{product rule} \quad (9.49c)$$

$$= \epsilon_{abc} \int_{\mathcal{R}} x^c \partial^b p dV \quad \epsilon_{abc} \delta^{bc} = 0 \quad (9.49d)$$

$$= -\epsilon_{acb} \int_{\mathcal{R}} x^c \partial^b p dV \quad \epsilon_{abc} = -\epsilon_{acb} \quad (9.49e)$$

$$= - \int_{\mathcal{R}} (\mathbf{x} \times \nabla p)_a dV \quad \text{vector cross product notation.} \quad (9.49f)$$

This result then brings the angular momentum equation (9.48) to the form

$$\frac{d}{dt} \int_{\mathcal{R}} \mathbf{L} = \int_{\mathcal{R}} [\mathbf{x} \times (-\rho \nabla \Phi - \nabla p)] dV. \quad (9.50)$$

At this point we can invoke the strong form force balance in equation (9.32), thus revealing that the integrand on the right hand side vanishes at each point in the fluid. However, this approach is no different than starting from the strong formulation of the torques in equation (9.47) and integrating over a finite region. An alternative approach, remaining fully within the weak formulation, states that if the region's angular momentum remains constant, then that defines a region experiencing zero net torque. This approach is the same as taken for the force balance, whereby we say that a fluid region experiencing no acceleration is one that has zero net forces acting on it. Hence, for a region with time invariant angular momentum we are led to the finite volume (weak form) torque balance

$$\int_{\mathcal{R}} [\mathbf{x} \times (\rho \nabla \Phi + \nabla p)] dV = 0 \implies \int_{\mathcal{R}} (\mathbf{x} \times \rho \nabla \Phi) dV = - \int_{\partial \mathcal{R}} (\mathbf{x} \times \hat{\mathbf{n}} p) dS, \quad (9.51)$$

with this balance the direct analog of the weak form force balances given by equations (9.35), (9.36a), and (9.36b).

9.6 Constitutive relation between stress and strain rate

Thus far we have offered a rather general treatment of stress, developing its properties according to the conservation of linear momentum and angular momentum. We now develop a [constitutive](#)

relation that connects stress to properties of the fluid as well as kinematic properties of the flow.

9.6.1 Thermodynamic pressure and mechanical pressure

Consider a fluid in which the stress on an area element is always normal to the area element and is independent of the orientation. This fluid is in hydrostatic balance and the corresponding isotropic stress tensor and stress vector are written⁵

$$T^{mn} = -p \delta^{mn} \iff \mathbf{T} \cdot \hat{\mathbf{n}} = -p \hat{\mathbf{n}}, \quad (9.52)$$

where p is the hydrostatic pressure field. Since the pressure introduced here arises from purely mechanical considerations, we refer to it as the mechanical pressure. For a compressible fluid at rest, we can identify the mechanical pressure with the thermodynamic pressure encountered in our study of equilibrium thermodynamics in Chapter 6. Furthermore, if we assume that local thermodynamic equilibrium is maintained for fluid elements within a moving fluid, then we are motivated to continue making this identification between mechanical pressure and thermodynamical pressure (see Section 4.5 of *Kundu et al. (2016)* or Section 1.10 of *Salmon (1998)*).

When the fluid flow is non-divergent, we lose the connection between mechanical pressure and thermodynamical pressure, even when the fluid is at rest. The reason is that a non-divergent fluid flow is unable to do pressure work on a fluid element since the flow cannot change the fluid element's volume. Hence, for non-divergent flow there is no connection between pressure and changes to internal energy as per the first law of thermodynamics (Section 6.2). A non-divergent flow only has need to consider mechanical pressure as revealed through the measurement of stresses. Furthermore, the mechanical pressure instantaneously conforms to the needs of non-divergence throughout the fluid (see Section 13.3). In Section 13.8 we develop the energetic implications for flows that are non-divergent.

9.6.2 Couette flow and the frictional stress tensor

Couette flow arises when fluid is placed between two long and straight concentric cylinders that can rotate. Relative motion between the two cylinders leads to fluid motion. For example, if the inner surface rotates, then fluid next to the cylinder wall will move with the cylinder. Any normal stresses on the fluid imparted by the cylinders are directed toward the cylinder axis and so cannot render any tangential motion. This elegant experiment proves that fluid motion can be induced by purely tangential stresses. Furthermore, the tangential stress imparted by the inner cylinder transfers through the fluid to the outer cylinder. Indeed, if the inner cylinder rotates at a constant rate, then eventually the whole fluid-cylinder system rotates as a solid body. Couette flow thus exhibits how real fluids can support tangential stresses in response to tangential strains, thus providing a clear distinction from a perfect fluid where only normal stresses (i.e., pressure) are supported.

As evidenced by the Couette flow, a moving fluid has a more complex stress relation than a static fluid. In particular, the presence of tangential stresses in the fluid provides evidence for

⁵Pascal's law says that pressure in a static fluid is an isotropic force per area. A proof of Pascal's law follows as a special case of the proof in Section 9.3.1 making use of Cauchy's fundamental lemma to relate the stress vector to the stress tensor.

an additional piece to the stress tensor that we write as

$$T^{mn} = -p \delta^{mn} + \mathbb{T}^{mn} \iff \mathbf{T} = -p \mathbb{I} + \mathbb{T}. \quad (9.53)$$

The pressure term remains isotropic as for a fluid at rest, thus imparting normal stresses. The additional tensor, \mathbb{T} , is referred to as the **friction stress tensor**.⁶ The friction tensor captures the irreversible exchanges of momentum between moving (relative to one another) fluid elements, such as in Couette flow, with the irreversible momentum exchange supported by fluid viscosity. Viscosity is assumed to be identically zero in a perfect fluid, so that a perfect fluid can only support normal stresses from pressure even when the perfect fluid has relative motion.

As noted above, we assume the frictional stress tensor vanishes when there is zero relative motion within the fluid.⁷ The physical idea is that fluid strains are needed to generate friction between fluid elements to support the transfer of momentum through the presence of viscosity. The determination of frictional stresses from kinematic properties (such as strain) requires a **constitutive relation**. The constitutive relation commonly used for geophysical fluids follows that for a **Newtonian fluid**, which is a particular type of *Stokesian fluid* whose frictional stresses are assumed to be linearly proportional to the strain rate.

The each diagonal stress, $T^1{}_1$, $T^2{}_2$, and $T^3{}_3$, are a **normal stress**, whereas the off-diagonal elements are **shear stresses**. The sum of the normal stresses forms the trace of the stress tensor and is given by

$$T^q{}_q = T^1{}_1 + T^2{}_2 + T^3{}_3 = -3p + \mathbb{T}^q{}_q. \quad (9.54)$$

If $\mathbb{T}^q{}_q = 0$ then \mathbb{T} is known as a **deviatoric stress tensor**. As discussed in Section 9.6.6, a deviatoric friction tensor is consistent with the assumption of equal mechanical and thermodynamical pressures.

9.6.3 D'Alembert's theorem for perfect fluids

Consider a finite impermeable solid body placed in a steady fluid flow, with the flow assumed to be uniform upstream and downstream. A particular realization is an arbitrarily long pipe flow with a solid object in the middle of the pipe. **D'Alembert's theorem** says that the force exerted by a perfect fluid on the solid body has no component along the direction of the pipe's central axis. A proof of this theorem, as provided in Section 13 of [Meyer \(1971\)](#), makes use of basic insights into momentum balances.

D'Alembert's theorem suggests a behavior that is contrary to common experience. Namely, a solid object placed in a real fluid flow experiences a net force in the direction of the fluid flow, so that there is a transfer of momentum between the fluid and the object. Consequently, D'Alembert's theorem became known as **D'Alembert's paradox**, thus motivating research during the 19th and early 20th centuries to understand stresses acting between a fluid and solid. It further put into question the ability to consider a fluid with arbitrarily small, but nonzero, viscosity as approximately a perfect fluid.

The nonzero viscosity present in real fluid supports tangential/shearing stresses, which then contribute in addition to the normal (pressure) stresses already present in perfect fluids. It is the shearing stresses, no matter how small in magnitude (but nonzero), that lead to a net force on the solid body. These ideas highlight the subtle nature of taking the limit of vanishing

⁶Some refer to the friction tensor as the viscous tensor. We eschew that name to reduce confusion with the viscosity tensor, which is a fourth order tensor appearing in the stress-strain constitutive relation. See Section 4.5 of [Kundu et al. \(2016\)](#) and Chapter 17 in [Griffies \(2004\)](#) for a discussion of the viscosity tensor.

⁷This assumption is part of those needed for a Stokes fluid as discussed in Section 5.21 of [Aris \(1962\)](#).

viscosity. Namely, a real fluid, no matter how small its viscosity (so long as it is nonzero), displays fundamentally distinct behavior near solid boundaries relative to the perfect fluid (whose viscosity is identically zero). We return to this point in Section 9.6.7 when discussing the relation between the Navier-Stokes equation and the Euler equation.

9.6.4 Guidance from Galilean invariance

Consider a fluid in uniform motion in free space. Performing a Galilean transformation allows us to move to a reference frame where the fluid is static. Through Galilean invariance we expect the dynamics to remain unchanged. Since we assume friction vanishes when the fluid is static (as per a Stokesian fluid), Galilean invariance implies that the frictional stresses vanish when the fluid undergoes uniform motion in any direction.

Uniform motion of fluid elements is reflected in zero velocity gradients, which offers a key insight into how friction depends on strains. Namely, these considerations suggest that the friction tensor is a function of gradients in the velocity field, $\partial_m v^n$. Furthermore, as the stress tensor must be symmetric (Section 9.4), a sensible expression for the friction tensor is one that is linearly proportional to the strain rate tensor studied in VOLUME 1. Symmetry of the friction tensor thus removes any dependence on the rotation tensor.⁸ A fluid that has a linear constitutive relation between stress and the strain rate is known as a Newtonian fluid. Furthermore, this constitutive relation takes the same mathematical form as Hooke's law used in the study of elastic materials.⁹

9.6.5 A comment on Rayleigh drag

Rayleigh drag is a particular form of friction that makes use of the acceleration

$$\mathbf{F}_{\text{Rayleigh}} = -\gamma \mathbf{v}, \quad (9.55)$$

where $\gamma > 0$ is an inverse time scale. Rayleigh drag is *not* Galilean invariant since it decelerates all flows, even uniformly moving flows, towards rest where rest is defined by a particular laboratory frame. Furthermore, Rayleigh drag is not equal to the divergence of a frictional stress tensor, and so it does not arise from a contact stress. Even so, it has found some use for rudimentary purposes, particularly when aiming to derive analytic expressions for how friction acts on flows in a bulk sense.

9.6.6 Constitutive relation for Newtonian fluids

There are many details involved with deriving the constitutive relation for a Newtonian fluid, with discussions provided in Section G of [Serrin \(1959\)](#), Chapter 5 of [Aris \(1962\)](#), Section 3.1 of [Segel \(1987\)](#), and Section 4.5 of [Kundu et al. \(2016\)](#) for general fluids, and Chapter 17 and 18 of [Griffies \(2004\)](#) for hydrostatic fluids with particular focus on the ocean. We here offer a taste of these considerations by starting with the constitutive relation

$$\mathbb{T}^{mn} = \rho (2\nu S^{mn} + \lambda \nabla \cdot \mathbf{v} \delta^{mn}), \quad (9.56)$$

⁸The absence of a dependence on the rotation tensor is to be expected, since this tensor renders a rigid rotation on fluid elements, thus inducing no change in the distance between fluid particles.

⁹In fact, Hooke's Law provides a linear relationship between stress and strain, whereas for Newtonian fluids we consider a linear relationship between stress and strain rate.

with S^{mn} the components to the strain rate tensor introduced in VOLUME 1, and whose trace equals to the velocity divergence

$$S^q_q = \nabla \cdot \mathbf{v}. \quad (9.57)$$

The first contribution to the frictional stress (9.56) includes the strain tensor multiplied by the **first kinematic viscosity**, $\nu > 0$ (dimensions of squared length per time). The second contribution arises just from flow divergence as scaled by a **second kinematic viscosity**, λ . The sum

$$\nu_{\text{bulk}} = \rho(\lambda + 2\nu/3) \quad (9.58)$$

is known as the **bulk viscosity**, which, as discussed in the following, will be set to zero. Finally, one sometimes finds it more convenient to work with the **dynamic viscosity**

$$\mu_{\text{vsc}} = \rho\nu. \quad (9.59)$$

Deviatoric friction tensor

As noted in Section 9.6.1, the pressure appearing in the stress tensor is a mechanical pressure that equals to minus one-third the trace of the stress tensor when the fluid is at rest

$$T^q_q = -3p \quad \text{static fluid.} \quad (9.60)$$

We assume that the frictional stress tensor does not alter this trace, so that the frictional stress tensor has zero trace and so it is a **deviatoric stress tensor**¹⁰

$$\mathbb{T}^q_q = 0 = 3\nu_{\text{bulk}}\nabla \cdot \mathbf{v} \implies \lambda = -2\nu/3, \quad (9.61)$$

so that the total stress tensor is given by

$$T^{mn} = -\delta^{mn}p + 2\mu_{\text{vsc}}S_{\text{dev}}^{mn} \quad \text{with} \quad S_{\text{dev}}^{mn} = S^{mn} - \delta^{mn}S^q_q/3, \quad (9.62)$$

where S_{dev} is the **deviatoric strain rate tensor**. We next offer arguments for why the friction tensor used for geophysical flows should have zero trace.

Equality of the mechanical and thermodynamic pressures

The frictional stress tensor (9.56) is not the precise form typically used in geophysical fluid modeling. Instead, the velocity divergence term is generally dropped even for compressible flows, and the viscosity is anisotropic and more generally takes the form of a fourth order *viscosity tensor* (see Chapter 17 and 18 of [Griffies \(2004\)](#) for the ocean). Furthermore, what is generally respected in most geophysical applications is the deviatoric nature of the friction tensor. That property is maintained since it is consistent with our assumption in Section 9.6.1 that the mechanical pressure equals to the thermodynamic pressure.

To see this equality between the pressures, introduce the mechanical pressure, p^{mech} , according to the trace of the stress tensor

$$T^q_q = -3p_{\text{mech}}. \quad (9.63)$$

That is, mechanical pressure is minus one-third the trace of the stress tensor whether the fluid is at rest or in motion. We can, in principle, measure this pressure by measuring the stresses.

¹⁰A second order tensor in 3-dimensions, \mathbb{E} , has a *deviator*, \mathbb{D} , with components given by $\mathbb{D}^m_n = \mathbb{E}^m_n - (1/3)\delta^m_n\mathbb{E}^q_q$. By construction, the trace of the deviator vanishes: $\mathbb{D}^q_q = 0$.

If we now return to the general form of the stress tensor

$$T^{mn} = -\delta^{mn} p + \rho (\lambda \nabla \cdot \mathbf{v} \delta^{mn} + 2\nu S^{mn}), \quad (9.64)$$

with p here given by the thermodynamic pressure, then the trace is

$$T^q_q = -3p + \rho (3\lambda + 2\nu) \nabla \cdot \mathbf{v}. \quad (9.65)$$

Setting the two traces (9.63) and (9.65) equal then leads to

$$p_{\text{mech}} - p = -\nu_{\text{bulk}} \nabla \cdot \mathbf{v}. \quad (9.66)$$

Hence, in regions where the flow converges, the mechanical pressure is greater than the thermodynamical pressure, $p_{\text{mech}} > p$, whereas where flow diverges then $p_{\text{mech}} < p$.

Stokes assumed $p = p_{\text{mech}}$ by taking a zero bulk viscosity, and he used arguments from kinetic theory of gases to support that choice.¹¹ This choice is generally taken for geophysical fluid applications, largely based on the assumption of local thermodynamic equilibrium mentioned in Section 9.6.1, and by noting that the flows are predominantly close to divergence-free.

Local thermodynamical equilibrium is not a good assumption in supersonic flows (e.g., shock waves), in which case $p \neq p_{\text{mech}}$ and the bulk viscosity is nonzero. Correspondingly, the divergence term and the second kinematic viscosity, $\lambda \neq -2\nu/3$, are important. Additionally, the second viscosity is important when concerned with the damping of acoustic waves (e.g., sounds absorption). Neither topics are considered in this book so that we have no further concern for the second viscosity.

Frictional force per volume

Taking the mechanical and thermodynamic pressures equal, so that the second kinematical viscosity satisfies equation (9.61), renders the frictional force per volume as given by the divergence of the frictional stress tensor

$$\rho F^n = \partial_m \mathbb{T}^{mn} = 2 \partial_m (\mu_{\text{vsc}} S_{\text{dev}}^{mn}). \quad (9.67)$$

The special case of a Boussinesq ocean with $\nabla \cdot \mathbf{v} = 0$

For a Boussinesq ocean (Chapter 13), the viscous friction (9.67) simplifies to

$$\rho_o F^n = 2 \rho_o \partial_m (\nu S^{mn}). \quad (9.68)$$

To reach this equality we set the dynamic viscosity to $\mu_{\text{vsc}} = \rho_o \nu$, with ρ_o the constant Boussinesq reference density. Furthermore, as studied in Chapter 13, the Boussinesq ocean has a non-divergent flow field so that $\nabla \cdot \mathbf{v} = \partial_m v^m = 0$, in which case

$$S_{\text{dev}}^{mn} = S^{mn} \quad \text{if } \nabla \cdot \mathbf{v} = 0. \quad (9.69)$$

Finally, for the case of a constant kinematic viscosity, we have the Boussinesq result reducing

¹¹As noted in Section 62 of [Serrin \(1959\)](#), Stokes later admitted to having little confidence in this argument.

to the Laplacian form, which is seen by

$$\nu^{-1} F^n = 2 \partial_m S^m{}_n \quad (9.70a)$$

$$= \partial_m (\partial_n v^m) + \partial_m (\partial_n v^m)^T \quad (9.70b)$$

$$= \partial_n (\partial_m v^m) + \partial_m \partial^m v_n \quad (9.70c)$$

$$= \nabla^2 v_n, \quad (9.70d)$$

with equation (9.70c) the topic of Exercise 9.4. We thus find that

$$\mathbf{F} = \nu \nabla^2 \mathbf{v}, \quad (9.71)$$

which is a form that we routinely make use of for scale analysis, such as when introducing the Reynolds number in Section 9.7.

9.6.7 Navier-Stokes and Euler equations

The Navier-Stokes equation is a special form of the momentum equation found by assuming a Newtonian constitutive relation. In this case the Navier-Stokes momentum equation (8.24), in the presence of rotation and gravity, takes on the form

$$\rho \frac{D\mathbf{v}}{Dt} + 2\rho \boldsymbol{\Omega} \times \mathbf{v} = -\rho \nabla \Phi - \nabla p + \nabla \cdot (2\mu_{vsc} S_{dev}), \quad (9.72)$$

where we set the friction tensor equal to $\mathbb{T} = 2\mu_{vsc} S_{dev}$. Quite often when examining the mathematical properties of the Navier-Stokes equation, one assumes the flow to be non-divergent, in which case $S_{dev} = S$ since $S^q{}_q = \nabla \cdot \mathbf{v} = 0$. A further simplification occurs by assuming a constant density, ρ , and constant kinematic viscosity, ν , in which case the friction tensor reduces to the Laplacian form (9.71) so that the Navier-Stokes equation becomes

$$\frac{D\mathbf{v}}{Dt} + 2\boldsymbol{\Omega} \times \mathbf{v} = -\nabla \Phi - \rho^{-1} \nabla p + \nu \nabla^2 \mathbf{v}. \quad (9.73)$$

This form, or even simpler when ignoring rotation and gravity, is commonly studied by mathematicians concerned with existence and uniqueness properties of fluid flow solutions (e.g., see [Doering and Gibbon \(1995\)](#)). When assuming the fluid to be perfect, so that there are no viscous forces, the momentum equation is referred to as the Euler equation¹²

$$\frac{D\mathbf{v}}{Dt} + 2\boldsymbol{\Omega} \times \mathbf{v} = -\nabla \Phi - \rho^{-1} \nabla p. \quad (9.74)$$

It is tempting to consider the Euler equations to be a continuous limit of the Navier-Stokes equation as the viscosity goes to zero. However, there is a key distinction between the two equations. Namely, the Navier-Stokes equations admit solutions that display statistically equilibrated turbulent motions, whereby energy cascades to the small scales through vortex stretching in three dimensional flows. This energy is ultimately dissipated by viscosity at the small spatial scales, and this mechanism holds no matter how small the viscosity, so long as it is nonzero. In contrast, for the Euler equations, with identically zero viscosity, energy cannot be dissipated at the small scales so that an equilibrium turbulent cascade is unavailable.

¹²Note that some authors refer to the Euler equations only in the case of a perfect fluid that has no body force, so that both rotation and gravitation vanish.

9.6.8 No-slip boundary conditions on solid boundaries

Another fundamental distinction between the Euler equation and Navier-Stokes equation concerns the boundary conditions. For the Navier-Stokes equation, the presence of a second order operator (the Laplacian), weighted by the viscosity, signals a distinct behavior of the flow next to boundaries. The Euler equation can only maintain a no-normal flow kinematic boundary condition at a boundary, with the kinematics detailed in VOLUME 1. Yet the viscous fluid described by the Navier-Stokes equation must satisfy an additional boundary condition.

Evidence based on research in the 19th and 20th centuries suggests that fluids, such as air and water, adhere to solid boundaries and thus satisfy the **no-slip boundary condition**.¹³ Writing $\hat{\mathbf{n}}$ as the outward normal along the solid boundary, a no-slip boundary condition at a stationary solid boundary means that the flow has a zero component in the direction tangent to the boundary

$$\mathbf{v} - \hat{\mathbf{n}}(\hat{\mathbf{n}} \cdot \mathbf{v}) = 0 \quad \text{for points at the solid boundary.} \quad (9.75)$$

When combined with the kinematic boundary condition, $\hat{\mathbf{n}} \cdot \mathbf{v} = 0$, we find that a no-slip boundary condition requires the fluid velocity to vanish at the solid boundary.¹⁴ This boundary condition has basic implications for how stress acts between fluids and solids. We have more to say concerning this boundary condition in Section 9.8.¹⁵

9.6.9 Laplacian friction in terms of vorticity and divergence

The Laplacian friction operator with a constant viscosity is afforded the following decomposition

$$\nu^{-1} F^n = \partial_m(\partial^m v^n) \quad (9.76a)$$

$$= \partial_m(\partial^m v^n - \partial^n v^m + \partial^n v^m) \quad (9.76b)$$

$$= \partial_m(\partial^m v^n - \partial^n v^m) + \partial^n(\partial_m v^m) \quad (9.76c)$$

$$= 2\partial_m R^{nm} + \partial^n \nabla \cdot \mathbf{v} \quad (9.76d)$$

$$= -\partial_m(\epsilon^{nmp} \omega_p) + \partial^n \nabla \cdot \mathbf{v} \quad (9.76e)$$

$$= -\epsilon^{nmp} \partial_m \omega_p + \partial^n \nabla \cdot \mathbf{v} \quad (9.76f)$$

$$= -(\nabla \times \boldsymbol{\omega})^n + \partial^n \nabla \cdot \mathbf{v}. \quad (9.76g)$$

In the fourth equality we introduced the **rotation tensor**

$$R^{nm} = (1/2)(\partial^m v^n - \partial^n v^m), \quad (9.77)$$

which is related to the vorticity, $\boldsymbol{\omega} = \nabla \times \mathbf{v}$, via

$$R^{nm} = -\epsilon^{nmp} \omega_p / 2. \quad (9.78)$$

¹³As discussed in the historical essay by [Anderson \(2005\)](#), it was the work of Prandtl in 1905 that first exposed the fundamental nature of the no-slip boundary condition, and its role in establishing boundary layers around solid bodies immersed in a fluid flow.

¹⁴More generally, if the solid boundary is moving, then the no-slip condition means that there is zero relative flow between the fluid and solid.

¹⁵See also the comments and footnote on page 86 of [Segel \(1987\)](#) as well as pages 83-84 of [Meyer \(1971\)](#).

These manipulations have served to decompose the Laplacian viscous acceleration, with a constant viscosity, into the two terms

$$\mathbf{F} = \nu [-\nabla \times \boldsymbol{\omega} + \nabla(\nabla \cdot \mathbf{v})]. \quad (9.79)$$

The Laplacian friction acceleration is thus due to the curl of the vorticity plus gradients in the velocity divergence. Many geophysical flows are dominated by vorticity, with the divergence relatively small. Indeed, the Boussinesq ocean discussed in Chapter 13 has $\nabla \cdot \mathbf{v} = 0$, in which case frictional acceleration arises only when the vorticity has a nonzero curl. Correspondingly, irrotational flows (where $\boldsymbol{\omega} = 0$) that are also non-divergent have zero Laplacian frictional acceleration.

9.6.10 Frictional stresses in a sheared flow

As a means to connect the above ideas in this section to the Couette flow discussed in Section 9.6.2, consider a non-divergent velocity that only has a zonal component with a vertical shear (Figure 9.6)

$$\mathbf{v} = u(z) \hat{x}. \quad (9.80)$$

In this case the only nonzero components to the strain rate tensor are due to the vertical shear, $S^1_3 = S_3^1 = \partial_z u / 2$. Now consider a horizontal area whose outward normal is parallel to the \hat{z} direction. The frictional force acting on that area is given by the area integral of the frictional stress

$$\mathbf{F}_{\text{area}} = \int \mathbb{T} \cdot \hat{n} dS = \int \mathbb{T} \cdot \hat{z} dx dy = \rho \frac{\hat{x}}{2} \nu A \frac{\partial u}{\partial z}, \quad (9.81)$$

where $A = \int dx dy$ is the horizontal area, and where we used the constant reference density, ρ , for a Boussinesq ocean.

Momentum is deposited in regions where there is a divergence in the stress, in which case momentum is transferred from regions of high vertical shear to low vertical shear. At a point, the momentum is affected by the divergence of the friction stress at that point. For $\mathbf{v} = u(z) \hat{x}$ we have

$$\left[\frac{\partial(\rho v_m)}{\partial t} \right]_{\text{viscous}} = \partial_n \mathbb{T}^n_m \Rightarrow \left[\frac{\partial(\rho u)}{\partial t} \right]_{\text{viscous}} = \partial_z (\mu_{\text{vsc}} \partial_z u), \quad (9.82)$$

so that zonal momentum is preferentially deposited to or removed from regions with high vertical curvature in the zonal velocity. Spatial variations in the dynamic viscosity, $\mu_{\text{vsc}} = \rho \nu$, also contribute to the patterns of viscous friction.

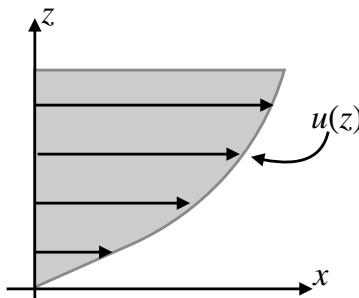


FIGURE 9.6: Sample profile of zonal velocity possessing a vertical shear: $\mathbf{v} = u(z) \hat{x}$ and with a no-slip boundary condition at $z = 0$. The resulting zonal frictional stress arises from the nonzero vertical shear in the presence of viscosity.

9.6.11 The net stress tensor

Combining the frictional stress tensor with pressure and kinetic stress yields the flux-form momentum equation (8.27)

$$\frac{\partial(\rho \mathbf{v})}{\partial t} + 2\rho \boldsymbol{\Omega} \times \mathbf{v} + \rho \nabla \Phi = \nabla \cdot \mathbf{T}^{\text{net}}, \quad (9.83)$$

where we introduced the [net stress tensor](#)

$$\mathbf{T}^{\text{net}} = -p \mathbb{I} - \rho \mathbf{v} \otimes \mathbf{v} + \mathbb{T} = \begin{bmatrix} -p - \rho u^2 + \mathbb{T}_{11} & -\rho u v + \mathbb{T}_{12} & -\rho u w + \mathbb{T}_{13} \\ -\rho u v + \mathbb{T}_{12} & -p - \rho v^2 + \mathbb{T}_{22} & -\rho v w + \mathbb{T}_{23} \\ -\rho u w + \mathbb{T}_{13} & -\rho v w + \mathbb{T}_{23} & -p - \rho w^2 + \mathbb{T}_{33} \end{bmatrix}. \quad (9.84)$$

The left hand side of the momentum equation (9.83) includes the local time tendency plus the body forces from Coriolis and effective gravity. The right hand side is the divergence of the net stress tensor, with this tensor combining the pressure stress, kinetic stress, and frictional stress. Varieties of the net stress tensor appear in subsequent chapters of this book, with details dependent on the chosen approximations.

9.6.12 Comments and further study

There are more elaborate constitutive relations between the frictional stress tensor and strain rate tensor than those considered in this section. The most general form for a Newtonian fluid introduces a fourth-order viscosity tensor as in Section 4.5 of [Kundu et al. \(2016\)](#) and Chapter 17 in [Griffies \(2004\)](#). We also recommend the presentation of stress in Chapter 5 of [Aris \(1962\)](#).

Geophysical fluids such as air and water are generally well treated using Newtonian constitutive relations. However, there are some geophysical turbulence theories that propose a non-Newtonian constitutive relation for part of their closures, whereby the constitutive relation makes use of products of the strain rate tensor for computing stress. [Anstey and Zanna \(2017\)](#) offer a compelling approach with a subgrid scale stress tensor that is non-Newtonian and furthermore contains a non-zero trace, thus resulting in a modification to the mechanical pressure. Additional nonlinear relations can arise when the viscous tensor is a function of the flow, such as with the Smagorinsky scheme commonly used for Large Eddy Simulations (LES) (see [Smagorinsky \(1993\)](#) or Chapter 18 of [Griffies \(2004\)](#)).

9.7 Reynolds number and flow regimes

How important is friction relative to other terms in the momentum equation? In particular, how does it compare to the material acceleration? We consider that question in the context of the non-rotating and constant density Navier-Stokes equations with a constant viscosity, ρ ,

$$\frac{\partial \mathbf{v}}{\partial t} + (\mathbf{v} \cdot \nabla) \mathbf{v} = -\rho^{-1} \nabla p + \nu \nabla^2 \mathbf{v}. \quad (9.85)$$

9.7.1 Non-dimensional Navier-Stokes

We non-dimensionalize the Navier-Stokes equation (9.85) to garner an understanding of relative magnitudes of the various terms. For that purpose, introduce the dimensional scales and

corresponding non-dimensional fields

$$L = \text{length scale} \quad U = \text{velocity scale} \quad P = \text{pressure scale} \quad T = \text{time scale}, \quad (9.86)$$

so that equation (9.85) takes the form

$$\frac{\partial \hat{\mathbf{v}}}{\partial \hat{t}} + \frac{U T}{L} (\hat{\mathbf{v}} \cdot \hat{\nabla}) \hat{\mathbf{v}} = -\frac{T P}{\rho U L} \hat{\nabla} \hat{p} + \frac{T \nu}{L^2} \hat{\nabla}^2 \hat{\mathbf{v}}, \quad (9.87)$$

where the hat fields are non-dimensional and defined according to

$$\nabla = L^{-1} \hat{\nabla} \quad \partial_t = T^{-1} \partial_{\hat{t}} \quad \mathbf{v} = U \hat{\mathbf{v}} \quad p = P \hat{p}. \quad (9.88)$$

9.7.2 Ratio of inertial to frictional accelerations

We are concerned with three dimensional flows with only a single length and velocity scale, L and U . For the time scale we assume that it is determined by the fluid particle time scale, which is the **advection time scale**

$$T = L/U. \quad (9.89)$$

Furthermore, we assume that the scale of mechanical pressure is comparable to the dynamical stress induced by the flow itself, thus leading to the **dynamical pressure scaling**¹⁶

$$P = \rho U^2. \quad (9.90)$$

These assumed scales for time and pressure bring the non-dimensional Navier-Stokes equation (9.87) into the rather tidy form

$$\frac{\partial \hat{\mathbf{v}}}{\partial \hat{t}} + (\hat{\mathbf{v}} \cdot \hat{\nabla}) \hat{\mathbf{v}} = -\hat{\nabla} \hat{p} + \frac{1}{\text{Re}} \hat{\nabla}^2 \hat{\mathbf{v}}. \quad (9.91)$$

Flow regimes of the non-dimensional Navier-Stokes equation are specified by the non-dimensional number, $\text{Re} = L U / \nu$, which is the **Reynolds number**. By definition, the Reynolds number is the ratio of scales for material (inertial) acceleration to frictional acceleration

$$\text{Re} = \frac{\text{inertial accelerations}}{\text{frictional accelerations}} = \frac{U/T}{\nu U/L^2} = \frac{L^2/T}{\nu} = \frac{L U}{\nu}. \quad (9.92)$$

9.7.3 Reynolds numbers for geophysical flows

Laboratory experiments with flow around and within various objects indicate the following regimes of flow as a function of the Reynolds number:

$$\text{Re} \sim \begin{cases} \leq 10^2 & \text{laminar} \\ 10^2 - 10^3 & \text{quasi-periodic flow} \\ 10^3 - 10^4 & \text{transition to turbulence} \\ \geq 10^4 & \text{fully turbulent.} \end{cases} \quad (9.93)$$

These numbers are fuzzy given their dependence on geometry of the objects placed in the flow and their characteristic length scale. What is more general concerns the behavior of the flow,

¹⁶When considering flows close to geostrophic balance, we find that pressure scales as $\rho f U L$, where f is the Coriolis parameter, which is distinct from the ρU^2 scaling found for flows not feeling the Coriolis acceleration.

with a transition from laminar to turbulent typically occurring as the flow moves from relatively low Reynolds number to high Reynolds number.

For a given molecular kinematic viscosity, the Reynolds number is dependent on the velocity and length scales. Let us consider some examples. First, place a finger into a flowing stream of water, such as in a gentle mountain creek. Let the length scale for the finger be 10^{-2} m and the stream flow at a speed of $U \approx 0.1 - 1$ m s⁻¹. With the kinematic viscosity of water given by (page 75 of [Gill \(1982\)](#))

$$\nu_{\text{water}} = 10^{-6} \text{ m}^2 \text{ s}^{-1}, \quad (9.94)$$

our finger poking into the mountain stream is associated with a flow Reynolds number on the order of

$$\text{Re}_{\text{finger in stream}} = 10^3 - 10^4. \quad (9.95)$$

Evidently, mountain stream flow around a finger is at the lower end of the turbulent regime. We thus expect to see slightly turbulent whirls and eddies downstream from the finger.

Now consider an oceanographic length scale given by a Gulf Stream ring (see Figure 15.1) in which $L \approx 10^5$ m. Assuming the flow speed is on the same order as the mountain stream (good assumption) leads to a huge Reynolds number for Gulf Stream flow

$$\text{Re}_{\text{Gulf Stream}} = 10^{10} - 10^{11}. \quad (9.96)$$

For the atmosphere, we take $L = 10^6$ m for a typical atmospheric weather system, $U = 10$ m s⁻¹ for the speed, and

$$\nu_{\text{air}} = 1.4 \times 10^{-5} \text{ m}^2 \text{ s}^{-1}, \quad (9.97)$$

for the kinematic viscosity of air at standard pressure (page 75 of [Gill \(1982\)](#)). Given the larger length and velocity scales, the Reynolds number for large-scale atmospheric circulation features is

$$\text{Re}_{\text{weather system}} = 10^{12}. \quad (9.98)$$

Note that these large Reynolds numbers are associated with horizontal scales of geophysical flows. Vertical motions have much smaller L and U , so that the Reynolds number for vertical motions are significantly smaller than horizontal scales. Even so, the associated Reynolds numbers typically put the flow in a highly turbulent regime. The Reynolds numbers in geophysical fluid flows are huge relative to typical values found in engineering flows. The large values arise from the large geophysical length scales of the flows. Large Reynolds numbers signal the minor role that molecular viscosity plays in large-scale geophysical fluid flows, which explains why so much of geophysical fluid mechanics (outside of boundary layers) is concerned with inviscid flows.

A fundamental feature of large Reynolds number flow is the presence of turbulent motions. Turbulent flows are highly nonlinear and affect a transfer of mechanical energy across length and time scales. This cascade leads to the dissipation of mechanical energy at the small scales. It is at the small scales that flow curvature can be large enough for the relatively tiny values of molecular viscosity to dissipate mechanical energy, thus preventing an [ultraviolet catastrophe](#); i.e., preventing the unbounded pile up of mechanical energy at the smallest scales.¹⁷ So molecular viscosity is necessary to properly close the mechanical energy budget in geophysical flows. However, the precise value of the molecular viscosity (and by extension the precise form of the viscous operator) is generally considered of little consequence to the behavior of large scale geophysical flows.

¹⁷Ultraviolet refers to the high wavenumber end of the flow spectrum. The name refers to the violet part of the visible electromagnetic spectrum, which has a higher wavenumber than the infrared part of the spectrum.

9.7.4 Further study

The ocean and atmosphere exhibit a huge variety of turbulent regimes, from the macroturbulence of quasi-geostrophic eddies to the fine scale turbulence of boundary layers. Turbulence is not directly considered in this book. However, certain of its implications are identified in various places given that it is so basic to the ocean and atmosphere flows. [Vallis \(2017\)](#) offers a pedagogical entry point for the physics and maths of geophysical fluid turbulence.

9.8 Stress on an interface

In this section we study the stress acting on an interface. This analysis applies to an arbitrary surface within a single media as well as for the boundary interface separating a liquid and a gas (air-sea boundary) or between a fluid and a rigid boundary (air-land or ocean-land). We ignore the effects from surface tension discussed in Section 9.9 since we are interested in length scales on the order of meters or larger (see in particular Section 9.9.5).

9.8.1 General formulation

Formulation of the stress boundary conditions follows from applying the finite volume momentum equation (8.18) to a tiny cylindrical region straddling a moving interface such as that shown in Figure 9.7. The sides of the cylinder have thickness h and the top and bottom have area δS . In the limit that the cylinder thickness goes to zero, the volume integrals in equation (8.18) vanish under the assumption of a smooth velocity field on both sides of the interface as well as smooth body forces. We are thus left with the constraint that the area integrated contact forces must vanish when integrated around the cylinder boundary

$$\oint_{\partial \text{cylinder}} [\mathbf{T} + \rho \mathbf{v} \otimes (\mathbf{v}^{(b)} - \mathbf{v})] \cdot \hat{\mathbf{n}} dS = \oint_{\partial \text{cylinder}} [-p \mathbb{I} + \mathbb{T} + \rho \mathbf{v} \otimes (\mathbf{v}^{(b)} - \mathbf{v})] \cdot \hat{\mathbf{n}} dS = 0. \quad (9.99)$$

The end-caps on the cylinder vanish as $h \rightarrow 0$, in which case we have no constraint based on the stresses acting on the end-caps. Instead, the $h \rightarrow 0$ limit leads us to conclude that the contact force on one side of the interface is equal and opposite to that on the other side. This condition is a direct statement of the [Newton's third law](#) as manifest via the local equilibrium of stresses (i.e., [Cauchy's fundamental lemma](#)) discussed in Section 9.2.2. For the stresses acting on the interface in Figure 9.7, this equilibrium states that

$$[-p_A \mathbb{I} + \mathbb{T}^A + \rho_A \mathbf{v}_A \otimes (\mathbf{v}^{(b)} - \mathbf{v}_A)] \cdot \hat{\mathbf{n}}_A + [-p_B \mathbb{I} + \mathbb{T}^B + \rho_B \mathbf{v}_B \otimes (\mathbf{v}^{(b)} - \mathbf{v}_B)] \cdot \hat{\mathbf{n}}_B = 0. \quad (9.100)$$

Setting $\hat{\mathbf{n}} = \hat{\mathbf{n}}_B = -\hat{\mathbf{n}}_A$ leads to

$$[-p_A \mathbb{I} + \mathbb{T}^A + \rho_A \mathbf{v}_A \otimes (\mathbf{v}^{(b)} - \mathbf{v}_A)] \cdot \hat{\mathbf{n}} = [-p_B \mathbb{I} + \mathbb{T}^B + \rho_B \mathbf{v}_B \otimes (\mathbf{v}^{(b)} - \mathbf{v}_B)] \cdot \hat{\mathbf{n}}, \quad (9.101)$$

which is an expanded expression of Newton's third law given by equation (9.5). Recall that we are ignoring surface tension, which means there is no pressure jump across the interface (see Section 9.9). Hence, setting $p_A = p_B$ allows us to cancel pressure thus leaving an interface stress condition involving just the frictional stress and kinetic stress

$$[\mathbb{T}^A + \rho_A \mathbf{v}_A \otimes (\mathbf{v}^{(b)} - \mathbf{v}_A)] \cdot \hat{\mathbf{n}} = [\mathbb{T}^B + \rho_B \mathbf{v}_B \otimes (\mathbf{v}^{(b)} - \mathbf{v}_B)] \cdot \hat{\mathbf{n}}, \quad (9.102)$$

which is sometimes more suitably written as

$$(\mathbb{T}^A - \mathbb{T}^B) \cdot \hat{\mathbf{n}} = \mathbf{v}_B [\rho_B (\mathbf{v}^{(b)} - \mathbf{v}_B) \cdot \hat{\mathbf{n}}] - \mathbf{v}_A [\rho_A (\mathbf{v}^{(b)} - \mathbf{v}_A) \cdot \hat{\mathbf{n}}]. \quad (9.103)$$

Recall from Section 9.3 that $\mathbb{T}^A \cdot \hat{\mathbf{n}}$ and $\mathbb{T}^B \cdot \hat{\mathbf{n}}$ pick out that portion of the frictional stress tensor that acts on a surface whose outward normal is $\hat{\mathbf{n}}$. We now consider some examples to help understand the boundary condition (9.103).

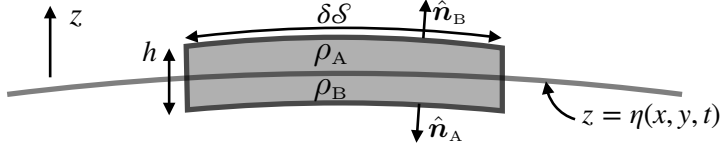


FIGURE 9.7: An infinitesimal region used in formulating the stress boundary condition at an interface. The interface can be one that separates two fluid regions with densities ρ_A and ρ_B . It can also represent the boundary between a fluid (region A) and solid (region B). The interface generally moves with velocity $\mathbf{v}^{(b)}$. We orient the interface through the outward normals according to (recall h is infinitesimal) $\hat{\mathbf{n}} = \hat{\mathbf{n}}_B = -\hat{\mathbf{n}}_A$, so that the outward normal for region A points into region B whereas the outward normal for region B points into region A. For this particular interface, the normal direction has a nonzero projection in the vertical, $\hat{\mathbf{n}} \cdot \hat{\mathbf{z}} \neq 0$, thus allowing us to define the interface vertical position according to $z = \eta(x, y, t)$. This interface represents an idealized geometry useful to formulate the stress condition at the boundary between fluid media, such as the air-sea interface, fluid-land interface, or interior fluid interface (e.g., buoyancy surface). The single geometric assumption is that there are no overturning motions so that $\hat{\mathbf{n}} \cdot \hat{\mathbf{z}} \neq 0$, with this assumption based on convenience. The stress condition is general and so does not require this assumption.

9.8.2 Solid material boundary

Consider a solid material boundary through which no matter crosses. Let region B be the solid side of the interface and region A the fluid side (region A is either the ocean or atmosphere). The material nature of the boundary means that no matter crosses it, in which case the material kinematic boundary condition from VOLUME 1 yields

$$(\mathbf{v}^{(b)} - \mathbf{v}_A) \cdot \hat{\mathbf{n}} = (\mathbf{v}^{(b)} - \mathbf{v}_B) \cdot \hat{\mathbf{n}} = 0. \quad (9.104)$$

A nonzero $\mathbf{v}^{(b)}$ corresponds here to a moving solid boundary, such as the region next to the grounding line of an ice-shelf. More commonly, in geophysical fluid applications we have $\mathbf{v}^{(b)} = 0$ for solid boundaries. In either case, there is no contribution from the kinetic stress so that the stress condition (9.102) reduces to

$$\mathbb{T}^A \cdot \hat{\mathbf{n}} = \mathbb{T}^B \cdot \hat{\mathbf{n}} \iff \mathbb{T}^A \cdot \hat{\mathbf{n}}_A = -\mathbb{T}^B \cdot \hat{\mathbf{n}}_B. \quad (9.105)$$

This identity is consistent with

$$\mathbb{T}^A \cdot \hat{\mathbf{n}} = \boldsymbol{\tau}^{\text{fricA}}(\mathbf{x}, t, \hat{\mathbf{n}}) = -\boldsymbol{\tau}^{\text{fricA}}(\mathbf{x}, t, -\hat{\mathbf{n}}) = \mathbb{T}^B \cdot \hat{\mathbf{n}} = \boldsymbol{\tau}^{\text{fricB}}(\mathbf{x}, t, \hat{\mathbf{n}}), \quad (9.106)$$

which expresses Newton's third law in the form of Cauchy's principle in equation (9.5). Hence, the frictional force imparted by the land on the fluid is equal and opposite to that imparted by the fluid on the land.

9.8.3 No-slip condition at a static boundary

At solid boundaries, the kinematic boundary condition sets the normal component of the velocity to zero¹⁸

$$\mathbf{v} \cdot \hat{\mathbf{n}} = 0 \quad \text{kinematic no-flux condition on static material boundary.} \quad (9.107)$$

However, kinematics is unable to specify the tangential component of the velocity along a solid boundary. Following the discussion from Section 9.6.8, we invoke the **no-slip boundary condition** to specify the tangential component.

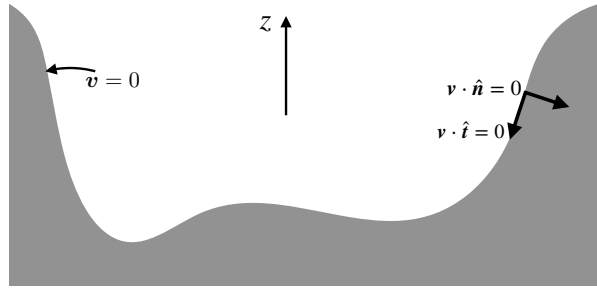


FIGURE 9.8: The no-slip boundary condition means that fluid has a zero tangential velocity component at the solid-fluid boundary, $\mathbf{v} \cdot \hat{\mathbf{t}} = 0$. Together, the kinematic no-normal flow boundary condition, $\mathbf{v} \cdot \hat{\mathbf{n}} = 0$, plus the dynamic no-slip boundary condition, $\mathbf{v} \cdot \hat{\mathbf{t}} = 0$, mean that the fluid sticks to the solid boundary. That is, the fluid particle velocity vanishes at a solid boundary when the no-slip condition holds.

That is, a fluid at the solid-fluid interface has a velocity matching that of the solid so that the fluid sticks to the solid boundary as depicted in Figure 9.8. The no-slip boundary condition means that both the normal and tangential components of the fluid velocity vanish next to static solid boundaries

$$\mathbf{v} \cdot \hat{\mathbf{n}} = \mathbf{v} \cdot \hat{\mathbf{t}} = 0 \quad \text{no-slip condition on static solid boundaries.} \quad (9.108)$$

The no-slip boundary condition gives rise to an exchange of momentum between the solid and fluid, with this exchange mediated by viscosity. This boundary condition is the origin of the tangential stresses found in the **Couette flow** discussed in Section 9.6.2. In the absence of viscous friction, as per an inviscid perfect fluid, the no-slip boundary condition cannot be imposed since doing so would mathematically over-specify the flow. Consequently, for inviscid fluids the tangential component of the velocity remains unspecified at solid boundaries.

9.8.4 Lagrangian interface

Consider a Lagrangian interface within the fluid, with this interface defined so that

$$(\mathbf{v}^{(b)} - \mathbf{v}_A) \cdot \hat{\mathbf{n}} = (\mathbf{v}^{(b)} - \mathbf{v}_B) \cdot \hat{\mathbf{n}} = 0. \quad (9.109)$$

This condition is identical to the solid material boundary condition (9.104), so that the kinetic stress contribution to equation (9.102) vanishes. We thus have the frictional stress condition (9.105) and a Newton's third law interpretation (9.106), yet now the frictional transfer takes place between two regions of the same fluid.

¹⁸For convenience we here assume the solid boundary is static. Generalizations to moving solid boundaries are straightforward, requiring one to merely replace \mathbf{v} with $\mathbf{v} - \mathbf{v}^{(b)}$ in the results of this subsection.

9.8.5 Permeable interface

Now allow for the interface to be permeable to matter, with matter conservation meaning that

$$\rho_A (\mathbf{v}_A - \mathbf{v}^{(b)}) \cdot \hat{\mathbf{n}} = \rho_B (\mathbf{v}_B - \mathbf{v}^{(b)}) \cdot \hat{\mathbf{n}}. \quad (9.110)$$

The kinetic stress thus adds to the frictional contribution in the stress boundary condition (9.102), with the kinetic stress providing a transfer of momentum across the interface through the transfer of matter that carries a nonzero linear momentum. Rearrangement of the stress boundary condition (9.102) with use of mass conservation (9.110) leads to

$$(\mathbb{T}^A - \mathbb{T}^B) \cdot \hat{\mathbf{n}} = (\mathbf{v}_A - \mathbf{v}_B) [\rho_A (\mathbf{v}_A - \mathbf{v}^{(b)}) \cdot \hat{\mathbf{n}}]. \quad (9.111)$$

We unpack this boundary condition by considering two cases.

Single continuous fluid media

If the interface is within a single continuous fluid media, then $\mathbf{v}_A = \mathbf{v}_B$ so that the frictional stress tensor boundary condition (9.105) again holds: $(\mathbb{T}^A - \mathbb{T}^B) \cdot \hat{\mathbf{n}} = 0$.

Air-sea boundary interface

Consider now the air-sea boundary where region B is the ocean and region A the atmosphere. Introduce the dia-surface mass flux according to the kinematic boundary conditions discussed in VOLUME 1,

$$\rho_A (\mathbf{v}_A - \mathbf{v}^{(b)}) \cdot \hat{\mathbf{n}} = \rho_B (\mathbf{v}_B - \mathbf{v}^{(b)}) \cdot \hat{\mathbf{n}} = -Q_m, \quad (9.112)$$

where Q_m is the mass per time per surface area crossing the boundary. The minus sign is implied by the convention that $Q_m > 0$ means that mass enters the ocean side of the interface and leaves the atmosphere side. In this case, the stress boundary condition (9.111) takes the form

$$(\mathbb{T}^{\text{air}} - \mathbb{T}^{\text{oce}}) \cdot \hat{\mathbf{n}} = -(\mathbf{v}_{\text{atm}} - \mathbf{v}_{\text{oce}}) Q_m. \quad (9.113)$$

We might consider the velocity of the atmosphere to be unequal to that of the ocean, in which case the surface normal projection of the frictional stress tensor satisfies a jump condition in the presence of mass transport across the air-sea interface. However, following Section 1.9 of *Batchelor* (1967), available evidence suggests that when approaching the boundary interface, the velocity of the two media match, both their normal and tangential components. In this case we again return to the friction boundary condition (9.105), in which the normal projection of the frictional stress tensors match, even in the presence of mass transport across the boundary.

9.8.6 Summary comments

There are three terms in the general expression for the stress boundary condition (9.101), with contributions from pressure, friction, and kinetic stress. In the absence of surface tension (Section 9.9), pressure is continuous at the interface; i.e., its value is the same on both sides of the interface. In the absence of mass transport across the interface, then we find a continuous kinetic stress at the interface that then leads to a continuous frictional stress. However, mass transport crossing the interface leads to a jump in the friction for those cases where velocity has a jump across the interface. Even so, empirical evidence suggests that the velocity has no jump across the interface, in which case there is no jump in the normal stress.

The subject of boundary conditions for momentum are not simple, particularly in the presence of mass transport across the boundary. We have only briefly touched on the topic, with similar discussions provided by Section 1.9 of [Batchelor \(1967\)](#) and Section 4.10 of [Kundu et al. \(2016\)](#). Specialized treatments are needed when pursuing these topics in more detail.

9.8.7 Comments on boundary layers

A fundamental advance in the relevance of fluid mechanics for describing observed flows came from the 20th century work of Prandtl and others who noted the central role of viscosity, even the tiny molecular values, in forming boundary layers when fluids flow next to rigid bodies.¹⁹ Prandtl's work focused on flows around airplane wings, thus supporting the development of aerodynamics as a scientific and engineering discipline. The key ideas transfer to geophysical flows where boundary layers form in the atmosphere and ocean as these fluids interact with the solid earth. Boundary layers also form where the atmosphere and ocean interact with one another.

A key facet of geophysical boundary layers concerns the dominance of turbulence in producing an eddy viscosity that is many orders larger than molecular viscosity. Indeed, molecular viscosity plays a role only in a very small region (the laminar subregion) immediately adjacent to the boundary. In contrast, the bulk of the boundary layer is dominated by turbulent flows. In Chapter 17 we study geophysical boundary layers that are affected by pressure, Coriolis, and turbulence induced friction. The role of rotation distinguishes geophysical boundary layers from engineering applications. The associated [Ekman boundary layer](#) is crucial for understanding circulation and transport in both the atmosphere and ocean.

9.9 Surface tension

Surface tension arises from the anisotropic forces acting on molecules that are within a mean free path distance from the surface between two immiscible liquids, between a liquid and gas, or between a fluid and a solid. Energetically, surface tension arises since molecules have a preference for locations within the bulk of the fluid (surrounded by identical neighbors) rather than at the boundary (where it encounters fewer identical neighbors). Surface tension acts to resist forces that act to increase the surface area, and it has many physical consequences that are part of our common experience. For example, it allows certain insects to walk on water even though their body density is greater than water. It also accounts for the predominantly spherical shape of rain drops and gas bubbles in liquids. As we study in VOLUME 5, surface tension gives rise to capillary waves when there is a very slight breeze on the ocean surface, or when a tiny stone is thrown into a still pond (gravity waves dominate for larger stones). In the present section we focus on the mechanics of surface tension. Note that a first principles understanding of surface tension involves tools from physical chemistry that are outside of the scope of this book. Here, we develop the subject phenomenologically.

¹⁹For a historical treatment of boundary layer theory see [Anderson \(2005\)](#), or for a pedagogical study see [Tennekes and Lumley \(1972\)](#). The associated mathematical methods of singular perturbation theory and matched asymptotic expansions (e.g., [Van Dyke \(1975\)](#)) offer an example of how the study of physical systems can spawn the development of new mathematical methods.

9.9.1 Capillary tube

Atmospheric pressure at the earth's surface is roughly $p_{\text{atm}} = 10^5 \text{ N m}^{-2}$. As we saw in Section 9.6, pressure acts normal to a surface regardless the surface orientation. So fill a container of water whose weight per horizontal area is less than the atmospheric pressure, $\rho g h < p_{\text{atm}}$ and turn the container upside-down as in Figure 9.9. Does the water spill from the container? Common experience with drinking glasses indicate that water will spill. But what about containers with a very small cross-sectional area such as the pipettes used in chemistry laboratories? Pipettes, or more generally capillary tubes, hold the liquid regardless the orientation. They do so since their cross-sectional area is small enough to allow forces from surface tension to overcome gravitational instabilities acting at the liquid-gas interface. We return to this point in VOLUME 5 when studying the [Rayleigh–Taylor instability](#) in the presence of surface tension. In the remainder of this section we discuss elements of surface tension with the goal to develop intuition as well as to determine the length scales where it becomes important.

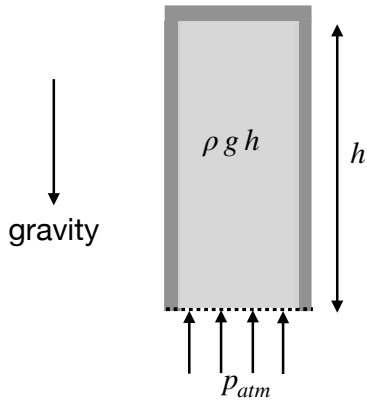


FIGURE 9.9: A container of water with density ρ and height h is placed upside-down. Atmospheric pressure, p_{atm} , will support water with thickness $h < p_{\text{atm}}/(\rho g) \approx 10 \text{ m}$ if the cross-sectional area of the container is small enough to allow for surface tension to overcome the gravitationally unstable waves that otherwise allow water to spill from the container. The liquid-gas interface supports both gravity waves and capillary waves, both of which are studied in VOLUME 5. If the wavelength is small enough then surface tension suppresses the growth of unstable gravity waves so that the liquid remains within the capillary tube. However, for longer waves allowed by increasing the cross-sectional area, then fluctuations allow the gravitational instability to overcome surface tension, thus breaking the interface and releasing water.

9.9.2 Force balance on an air-water interface

Consider two fluids with distinct densities. Air and water provide one example of special importance to understanding physics at the ocean-atmosphere boundary. Another example concerns two immiscible layers of water within the ocean or two layers of air within the atmosphere. For molecules well within either of the fluid regions, the intermolecular forces are statistically isotropic. In contrast, intermolecular forces are not isotropic for molecules within a mean free path distance from the interface.²⁰ Attractive (cohesive) intermolecular (van der Waals) forces dominate within a liquid whereas gas molecules generally feel more repulsive forces. Hence, a liquid molecule within the liquid-gas interface preferentially experiences an

²⁰As discussed in the Prologue in VOLUME 1, the mean free path is a statistical measure of the distance a molecule moves before hitting another molecule.

attractive force towards the liquid side of the interface, as depicted in Figure 9.10. Surface tension arises from the cohesive force per area acting between molecules in a direction that parallels the interface, with surface tension acting to resist perturbations to the interface shape.

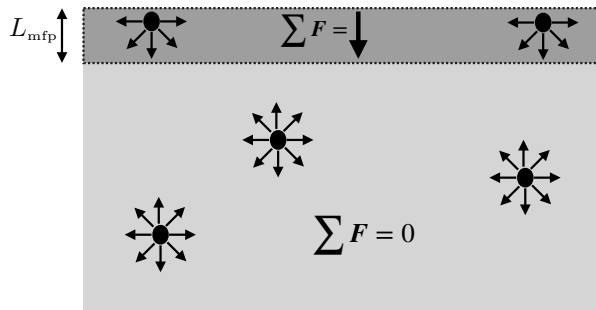


FIGURE 9.10: Surface tension at a liquid-gas interface arises from the anisotropic cohesive forces acting on liquid molecules within a mean-free-path distance, L_{mfp} , from the interface, which contrasts to the isotropic cohesive forces acting away from the interface. The net intermolecular force vanishes for interior molecules, whereas the net force acts inward on molecules at the interface. Surface tension refers to the cohesive force per area acting between molecules in a direction that is parallel to the interface.

Anisotropic attractive intermolecular forces cause the interface between the two fluids to behave as a stretched membrane that experiences a tensile force resisting any stretching of the interface. The magnitude of the tensile force per unit length (or energy per unit area) is the **surface tension**, γ (SI units $\text{N m}^{-1} = \text{kg s}^{-2}$), which measures the force needed to change the interface a unit length. Equivalently, the surface tension is the energy per area needed to change the surface area. The surface tension is a property of the two fluids, including their temperature, as well as any impurities that might be included on the interface; e.g., oil on the surface of water effects properties of the capillary waves found on the air-sea interface. In the following we focus on the liquid-gas example to be specific and to expose issues that arise in studies of the air-sea interface. For a liquid-gas interface surrounding a liquid drop, the tensile force acts to curve the interface towards the liquid into a spherical shape.

The tensile force along a line segment is directed normal to the line and tangent to the interface

$$\mathbf{f}_{\text{interface}} = -\gamma \hat{\mathbf{n}} \times \delta \mathbf{x}, \quad (9.114)$$

where $\hat{\mathbf{n}}$ is a normal vector pointing towards the center of the curved interface, and $\delta \mathbf{x}$ is a line element oriented so that the normal $\hat{\mathbf{n}}$ points to the left facing in the direction of the line increment. Figure 9.11 depicts the surface tensile forces acting on the surface of a spherical bubble of water. Note that it is sometimes useful to consider the product γdS as the work (units of $\text{N m}^{-1} = \text{Joule}$) required to create an area, dS , on the interface. We make use of this energetic perspective in Section 9.9.3.

To develop an expression for the pressure jump across the liquid-gas interface, consider a spherical droplet of radius R shown in Figure 9.11 and focus on the circular cross-section cut through the center of the sphere. The net tensile force acting on the circumference of the circle is

$$\mathbf{F}_{\text{circle}} = \oint_{\text{circle}} \mathbf{f}_{\text{interface}} = - \oint_{\text{circle}} \gamma \hat{\mathbf{n}} \times \delta \mathbf{x} = -2\pi R \gamma \hat{\mathbf{z}}. \quad (9.115)$$

Equilibrium of the spherical droplet is realized by a pressure jump across the circular cross-

sectional area

$$\pi R^2 (p_{\text{in}} - p_{\text{out}}) = 2\pi R \gamma \implies (p_{\text{in}} - p_{\text{out}}) = 2\gamma/R. \quad (9.116)$$

Hence, the pressure jump is determined by the surface tension (a property of the two fluids) and the curvature of the sphere, R , which is also the radius of curvature for the sphere. Pressure is higher inside of the sphere (i.e., on the concave side of the interface), with this pressure required to balance the pressure outside the sphere plus the surface tension. Notably, equilibrium for smaller bubbles (with $R \rightarrow 0$) requires a larger pressure difference than for larger bubbles.

The pressure jump is known as the **capillary pressure**. It arises from surface tension and curvature of the interface. The relation (9.116) is a special case of the **Young-Laplace formula**, specialized here to a sphere.

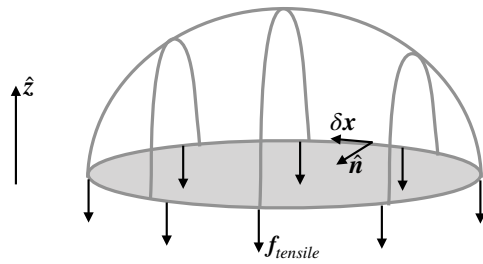


FIGURE 9.11: Surface tension on a spherical water droplet, with water on the inside of the sphere and air on the outside. The tensile forces act parallel to the spherical interface between the water and air. When cutting a circular cross-section as shown here, the surface tensile force acts downward. In equilibrium, the net tensile forces acting downward along the circumference of the hemisphere ($2\pi R \gamma$) are balanced by a pressure jump across the droplet, with the interior pressure larger than the exterior pressure. Focusing on the circular cross-section, this area remains static so long as $2\pi R \gamma = \pi R^2 (p_{\text{in}} - p_{\text{out}})$, leading to a pressure jump across the droplet interface $p_{\text{in}} - p_{\text{out}} = 2\gamma/R$. This result is general: namely, according to the Young-Laplace formula (9.126), pressure is greater on the concave side of the interface than on the convex side.

9.9.3 Young-Laplace formula

We garner added insight into the physics of surface tension by considering the energetics required to enable a virtual displacement of a surface through a pressure field along with the work required to change the area of the surface. The resulting **Young-Laplace formula** expresses the pressure jump in terms of the surface tension and the principle radii of curvature for the surface.

Consider a horizontal surface depicted in Figure 9.12 that represents the interface separating fluid-A from fluid-B, with \hat{n} a unit normal vector oriented from fluid-A to fluid-B. Now consider a virtual displacement of each point along the interface by an infinitesimal distance, $\delta h = \eta(x, y, t)$, with $\hat{n} \delta h$ connecting points on the initial position of the interface to the displaced position, where $\delta h > 0$ if the displacement is directed towards fluid-B and $\delta h < 0$ if directed towards fluid-A. The (signed) volume swept out by an infinitesimal area, dA , is given by $\delta h dA$. There are two forms of work required to move the surface: pressure work required to change the fluid volume and area work required to change the surface area. The pressure work is given by

$$\mathcal{W}_{\text{vol}} = -p_A \delta V_A - p_B \delta V_B = (p_B - p_A) \delta V_A = (p_B - p_A) \delta h dA, \quad (9.117)$$

where we set $\delta V_A = -\delta V_B = \delta h dA$. For example, if $p_B > p_A$ and the displacement is into fluid-B ($\delta h > 0$), then $\mathcal{W}_{\text{vol}} > 0$. We thus find that $\mathcal{W}_{\text{vol}} > 0$ to displace the surface into the

fluid region with higher pressure, whereas $\mathcal{W}_{\text{vol}} < 0$ if displacing the interface into a region with lower pressure.

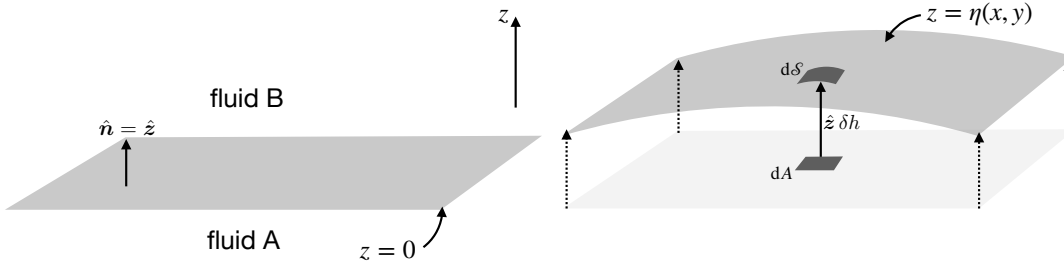


FIGURE 9.12: Left panel: initial position of a material interface separating two fluid regions, fluid-A and fluid-B. Right panel: infinitesimal displacement of the interface sweeps out a volume in space, here depicted with the interface moving upward. To determine the volume, extend a unit normal vector, \hat{n} , from the initial interface position and pointing towards fluid-B. For this example, $\hat{n} = \hat{z}$. Let $\delta h = \eta$ be the distance along that normal to the new position, with $\delta h > 0$ if the displacement moves towards fluid-B and $\delta h < 0$ for displacements pointing to fluid-A. We assume that displacements at each interface point can move independently of adjacent points, so that the interface area generally changes. The Young-Laplace formula (9.126) says that the pressure jumps when crossing an interface that is subject to surface tension, with pressure higher on the concave side. In this example, Young-Laplace says pressure is higher on the Fluid-A side since that it is the concave side.

In the presence of surface tension, work is needed to change to the interface area

$$\mathcal{W}_{\text{area}} = \gamma \delta A, \quad (9.118)$$

where δA is the change in area of an infinitesimal element on the interface

$$\delta A = dS - dA \quad (9.119a)$$

$$= dA \left[\sqrt{1 + (\nabla \delta h)^2} - 1 \right] \quad (9.119b)$$

$$\approx dA (\nabla \delta h)^2 / 2. \quad (9.119c)$$

To reach this result we made use of kinematics from VOLUME 1 that relates the area of an infinitesimal element on a curved surface to the area of its horizontal projection. We next make use of the surface curvature detailed in the vector calculus chapter in VOLUME 1 where we find that the vertical displacement is given, for small displacements, by

$$-\delta h \approx \frac{1}{2} R_1^{-1} (\mathbf{x} \cdot \mathbf{e}_1)^2 + \frac{1}{2} R_2^{-1} (\mathbf{x} \cdot \mathbf{e}_2)^2. \quad (9.120)$$

R_1^{-1}, R_2^{-1} are the eigenvalues and $\mathbf{e}_1, \mathbf{e}_2$ are the corresponding eigenvectors of the matrix of second partial derivatives of $\delta h(x, y)$, whereas the inverse eigenvalues, R_1, R_2 , are the radii of curvature of the displaced surface. To get signs correct, it is important to note that the radius of curvature is positive if the surface curves towards the outward normal direction, and negative otherwise. For the example depicted in the right panel of Figure 9.12, both radii of curvature are negative since the surface curves away from the outward normal (pointing from A to B). This convention explains the minus sign on the left side of equation (9.120).

Orienting the Cartesian axes along the eigenvector directions renders

$$(\nabla \delta h)^2 \approx (x/R_1)^2 + (y/R_2)^2 = (-\delta h) \left[\frac{1}{R_1} + \frac{1}{R_2} \right], \quad (9.121)$$

where we set

$$(-\delta h)/R_1 = (x/R_1)^2 \quad \text{and} \quad (-\delta h)/R_2 = (y/R_2)^2. \quad (9.122)$$

We are thus led to the area difference

$$\delta A \approx dA (-\delta h) \left[\frac{1}{R_1} + \frac{1}{R_2} \right]. \quad (9.123)$$

Note that $\delta A > 0$ whether displacing the surface into a concave or convex direction, since the sign of δh accounts for the sign of the radii of curvature. For small displacements of the surface from its horizontal position, we again make use of the calculus discussion from VOLUME 1 to connect the radii of curvature for a surface with the Laplacian of the displacement of the surface, in which case equation (9.123) takes on the form

$$\delta A \approx -dA \delta h \nabla^2(\delta h). \quad (9.124)$$

Total work for the interface displacement is given by the sum of the area work and volume work

$$\mathcal{W}_{\text{area}} + \mathcal{W}_{\text{vol}} = dA \delta h [-\gamma(R_1^{-1} + R_2^{-1}) + p_B - p_A] = dA \delta h [-\gamma \nabla^2 \eta + p_B - p_A], \quad (9.125)$$

and equilibrium results if the net work vanishes, in which case

$$p_B - p_A = \gamma(R_1^{-1} + R_2^{-1}) = \gamma \nabla^2 \eta, \quad (9.126)$$

where we set $\delta h = \eta$ as per Figure 9.12. This equation is the [Young-Laplace formula](#), which reduces to equation (9.116) if $R_1 = R_2$ as for a sphere. It says that there is a pressure jump, known as the [capillary pressure](#), across an interface as given by the surface tension times the sum of the inverse principle radii of curvature, or equivalently the surface tension times the Laplacian of the displacement. To help remember signs, note that the Young-Laplace formula (9.126) says that the pressure on the concave side of an interface is higher than on the convex side. Hence, pressure is higher on the inside of a bubble/droplet. For the example depicted in Figure 9.12, $\nabla^2 \eta < 0$ since the surface is a local maximum, in which case $p_A > p_B$ since fluid A is on the concave side of the interface.

9.9.4 Soluble gas bubbles inside water

The previous considerations hold whether there is liquid or gas inside a spherical bubble or drop. As an example, consider a spherical gas bubble of radius $R = 10^{-6}$ m inside water and make use of the air-water surface tension $\gamma = 0.072 \text{ N m}^{-1} = 0.072 \text{ kg s}^{-2}$. We thus find the pressure jump is

$$p_{\text{in}} - p_{\text{out}} = 2\gamma/R \approx 144 \times 10^3 \text{ N m}^{-2} = 1.42 p_{\text{atm}}, \quad (9.127)$$

where $p_{\text{atm}} = 1.01 \times 10^5 \text{ N m}^{-2}$ is standard atmospheric pressure. If the gas inside the bubble is water soluble, then the enhanced pressure inside the bubble will induce more gas to dissolve in the water, which in turn will cause the bubble to shrink and thus increase the pressure inside the bubble. Small bubbles of soluble gases can thus be squeezed towards zero radius by the effects of surface tension induced pressure.

9.9.5 When we can ignore surface tension

The sizable pressure jump (9.127) arises from the tiny radius of curvature of the bubble, with the pressure jump decreasing as the bubble radius increases. Rather than a bubble, consider an ocean surface capillary-gravity wave (see VOLUME 5), such as those observed from a boat. Such waves may have wavelength on the order of 10^{-2} m or longer. If we set the radius of curvature to $R \sim 10^{-2}$ m, then equation (9.127) finds an entirely negligible pressure jump of $\Delta p \approx 10^{-4} p_a$.

Most geophysical fluid motion of concern in this book is associated with material interfaces having a radius of curvature on the order of meters or larger. It is for this reason that surface tension is generally ignored when studying geophysical fluid motion. That is, we can safely assume there is no pressure jump when approaching an interface between two fluid media, or between a fluid and a solid boundary. This discussion then justifies the approach considered in Section 9.8 when studying stresses at interfaces, in which we applied Newton's third law for pressure at the interface.

Even so, the role of surface tension is central to the fundamental mechanisms of how matter, momentum, and energy are transferred across the air-sea interface. Relatedly, as we show in VOLUME 5, capillary waves arise from surface tension, with capillary waves the initial response of the ocean free surface upon the imposition of a wind stress.

9.9.6 Further study

This [30-minute video](#) from Prof. Trefethen provides a pedagogical summary of surface tension. The upside-down container of water in Figure 9.9 is based on a discussion of capillary-gravity waves in Section 3.1.3 of [Falkovich \(2011\)](#). We study capillary-gravity waves in VOLUME 5. Section 1.9 of [Batchelor \(1967\)](#) discusses how surface tension acts between two fluid media, with that discussion extended into his Section 3.3 to develop boundary conditions for velocity and stress. The bubble example in Section 9.9.4 is taken from Section 1.3 of [Kundu et al. \(2016\)](#). Section 4.10 of [Kundu et al. \(2016\)](#) provides a detailed accounting of the force balance at an interface, offering more details than found in [Batchelor \(1967\)](#). The energetic arguments used to derive the Young-Laplace formula follows Section 61 of [Landau and Lifshitz \(1987\)](#). Section 46 of [Fetter and Walecka \(2003\)](#) discuss the dynamics of membranes under tension. Chapter 8 of [Lautrup \(2005\)](#) provides a thorough and pedagogical discussion of surface tension and associated phenomena.



9.10 Exercises

EXERCISE 9.1: HYDROSTATIC PRESSURE UNDER AN ICE SHELF

Figure 9.13 depicts an idealized ice shelf cavity, whereby a tongue of land ice extends out over the ocean. Assume the ocean is in exact hydrostatic balance so there is no fluid flow. What is the pressure at point *A* relative to point *B*? Note that these two points are the same distance from the resting ocean surface.

EXERCISE 9.2: PRESSURE FORCE ON A SPHERE AND A HEMISPHERE

Refer to Figure 9.14 for this exercise.

- What is the net vertical pressure force acting on the sphere due to the surrounding fluid?

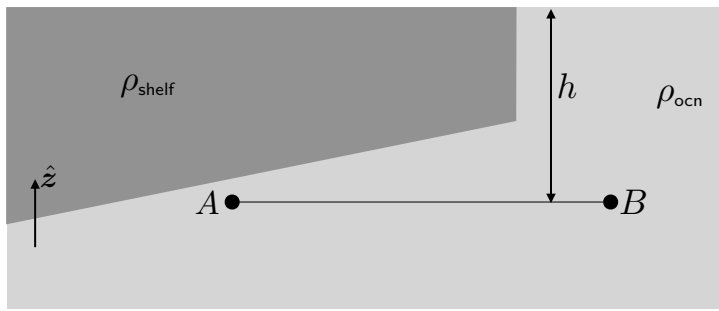


FIGURE 9.13: Geometry of an idealized ice shelf, with the ice having density, ρ_{shelf} , and the ocean having density, ρ_{ocn} . The two points, A and B , are each the same distance, h , from the ocean surface, yet point A is within the ice shelf cavity whereas point B is outside the shelf.

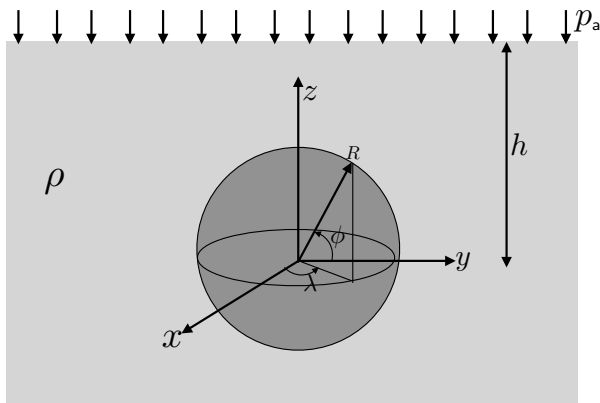


FIGURE 9.14: A solid sphere of radius, R , within a hydrostatic fluid of uniform density, ρ , and with the center of the sphere a distance $h > R$ from the fluid surface. A uniform applied atmospheric pressure, p_a , is applied to the fluid surface at $z = h$, where we set $z = 0$ at the sphere center.

- (b) What is the net horizontal pressure force vector from the surrounding fluid?
- (c) Assume that only the $y > 0$ portion of the sphere sits within the fluid ($0 \leq \lambda \leq \pi$ and $-\pi/2 \leq \phi \leq \pi/2$), whereas the $y < 0$ portion is outside of the fluid ($\pi \leq \lambda \leq 2\pi$ and $-\pi/2 \leq \phi \leq \pi/2$). For example, consider a hemispherical light on the side of a swimming pool. What is the net horizontal force vector on the hemispherical region that sits within the fluid?

EXERCISE 9.3: FORCE BALANCE FOR A NON-ACCELERATING TANGENT PLANE OCEAN

Consider an ocean basin, \mathcal{R} , on the rotating tangent plane as in Figure 9.2, with bottom interface separating the ocean fluid from the solid-earth, and upper interface separating the ocean fluid from the atmosphere, and where the atmosphere has a nonzero mass.²¹ Assume no matter crosses the ocean boundaries; i.e., no evaporation, precipitation, nor river runoff. Hence, the ocean domain maintains a fixed mass

$$M = \int_{\mathcal{R}} \rho dV \quad (9.128)$$

as well as fixed matter. In this case, the ocean domain is materially closed and so its center of

²¹In some applications it is suitable to assume a zero mass atmosphere. For this exercise, however, we do not make that assumption.

mass position

$$\mathbf{X}_{\text{com}} = M^{-1} \int_{\mathcal{R}} \mathbf{x} \rho dV \quad (9.129)$$

has a velocity given by

$$\frac{d\mathbf{X}_{\text{com}}}{dt} = M^{-1} \int_{\mathcal{R}} \mathbf{v} \rho dV, \quad (9.130)$$

and corresponding acceleration

$$\frac{d^2\mathbf{X}_{\text{com}}}{dt^2} = M^{-1} \int_{\mathcal{R}} \frac{D\mathbf{v}}{Dt} \rho dV. \quad (9.131)$$

Apply a horizontal stress over the ocean surface with a stress vector $\boldsymbol{\tau}^{\text{surf}}$. This stress leads to motion of the ocean fluid. Allow for the ocean bottom to exchange momentum with the static solid-earth through a horizontal bottom turbulent stress, $\boldsymbol{\tau}^{\text{bott}}$. Assume there are no vertical components to $\boldsymbol{\tau}^{\text{surf}}$ and $\boldsymbol{\tau}^{\text{bott}}$. Also use Cartesian coordinates so that Cartesian vector/tensor analysis is sufficient for this tangent plane analysis.

- (a) What is the force balance for the full ocean domain if the center of mass experiences no acceleration. Express the corresponding force balance in words and in equations. Expose the contact forces arising from pressure and from turbulent stresses, as well as the body forces from Coriolis and gravity. The answer should be generally stated, with no need for specific details. Hint: consider Figure 9.2 and include the missing forces to this diagram. Mathematically express the force balance as an integral expression as per the [weak formulation](#) of fluid mechanics.
- (b) Express the vertical component of the force balance assuming the fluid is in an approximate hydrostatic balance, meaning that the pressure and gravitational forces are balanced.²²
- (c) Consider an ocean without any turbulent contact stresses at the boundaries, $\boldsymbol{\tau}^{\text{surf}} = \boldsymbol{\tau}^{\text{bott}} = 0$ and assume there is no motion anywhere in the fluid. What integral constraints are satisfied by the horizontal components of the pressure contact force? Hint: recall equations [equations \(9.36a\)](#) and [\(9.36b\)](#). Also note assume that the free surface is flat, which is consistent with the absence of motion.
- (d) Assume the ocean is on an f -plane (Section 8.5) so that $\boldsymbol{\Omega} = \hat{\mathbf{z}} \Omega = \hat{\mathbf{z}} (f/2)$ is a constant vector. Also assume that the center of mass velocity vanishes, $\int_{\mathcal{R}} \rho \mathbf{v} dV = 0$. Discuss the resulting zonal and meridional force balance. Hint: one of the forces appearing in part (a) now vanishes.

EXERCISE 9.4: STEP IN THE DERIVATION OF LAPLACIAN FRICTION

Verify equation [\(9.70c\)](#) used to derive the Cartesian Laplacian friction operator used for the Boussinesq fluid with a constant viscosity.

EXERCISE 9.5: THOUGHT EXPERIMENT IN SUPPORT OF SYMMETRIC STRESS TENSORS

To further support the conclusion in Section 9.4.3 concerning a symmetric stress tensor, consider a particular component of the torque density, such as the vertical

$$T_3^{\times} = \epsilon_{3pn} T^{pn} = T^{12} - T^{21}, \quad (9.132)$$

²²In Section 11.2 we provide a discussion of when this approximation is appropriate for moving fluids. That discussion is not needed for the current exercise. Instead, we merely assume the vertical momentum balance is hydrostatic.

with the corresponding torque applied to a fluid element given by

$$T_3^\times \delta V = (T^{12} - T^{21}) \delta x \delta y \delta z. \quad (9.133)$$

What sort of angular acceleration is induced by this torque when computed relative to the fluid element center?

Hint: To answer this question, assume the fluid element is moving as a rigid body so that we can compute its angular acceleration by dividing the torque by the moment of inertia for the fluid element. The moment of inertia depends on the shape of the element, which is unspecified. Even so, we can estimate the moment of inertia computed relative to a vertical axis through the center of the element

$$I_3 = \alpha [(\delta x)^2 + (\delta y)^2] \rho \delta x \delta y \delta z, \quad (9.134)$$

where α is a dimensionless geometric factor.

EXERCISE 9.6: PROPERTIES UNDER TIME REVERSAL²³

Make an animation of a dynamical system over a period of time, and then play the animation backwards in time. Is there anything about the time reversed animation to indicate it is not physically realizable? If not, then the dynamical system possesses symmetry under the reversal of time. We considered this question in VOLUME 1 when studying the motion of a point particle. Here we ask the same question for the perfect fluid satisfying the Euler equation (9.74) in a rotating reference frame, in which we show there is time symmetry. We then show that time reversal symmetry is broken by viscous friction in the Navier-Stokes equation (9.73).

- (a) Consider a particular solution, $\mathbf{v}(\mathbf{x}, t)$, to the Euler equation in a rotating reference frame in either free space (i.e., no boundaries) or with static material boundaries where the flow satisfies the no normal flow boundary condition, $\mathbf{v} \cdot \hat{\mathbf{n}} = 0$. What transformation properties for the pressure, $p(\mathbf{x}, t)$, density, $\rho(\mathbf{x}, t)$, geopotential, $\Phi(\mathbf{x}, t)$, and rotation, $\boldsymbol{\Omega}$, are sufficient for $\mathbf{v}^*(\mathbf{x}, t^*) = -\mathbf{v}(\mathbf{x}, -t)$ to be a solution? That is, by running time backwards, and changing the sign of the velocity, does this flow also satisfy the Euler equations?
- (b) Real fluids are not time reversible. For example, water leaving a tea pot does turn around and reenter the pot. Also, if air were a perfect fluid then one could only survive through breathing in a cross-wind since otherwise we would breath in the same air we just breathed out. Even though perfect fluids suffer from unrealistic features, it is of interest to expose symmetries of the Euler equations and to then study how these symmetries are broken. To see how dissipation breaks time reversal symmetry, consider the Laplacian viscous friction acceleration appearing in the Navier-Stokes equation (9.73)

$$\mathbf{F} = \nu \nabla^2 \mathbf{v}, \quad (9.135)$$

where $\nu > 0$ is the kinematic viscosity. Examine the symmetry of this operator under time reversal, assuming the $\nu > 0$ for both time directions.



²³This exercise was inspired by the discussion on page 77 of Meyer (1971), with the added feature here of the Coriolis acceleration.

Chapter 10

ENERGY AND ENTROPY

In this chapter we study the energetics of fluid flow. In particular, we are concerned with how energy is partitioned between the mechanical energy of macroscopic motion and the internal energy associated with internal degrees of freedom. To fully specify energy in fluid flows requires us to study the flow of entropy and the associated constraints arising from the second law of thermodynamics. For this purpose we extend the equilibrium thermodynamics of Chapters 6 and 7 to include time dependent moving fluid phenomena. Making this transition requires the hypothesis of local thermodynamic equilibrium.

READER'S GUIDE FOR THIS CHAPTER

This chapter builds from the thermodynamics of Chapters 6 and 7, the momentum dynamics of Chapter 8, and study of friction from Chapter 9. In addition to developing the budgets for mechanical energy and total energy (mechanical plus internal), we derive budgets for entropy and potential enthalpy. A particularly important practical outcome of this chapter concerns the equation for potential enthalpy or [Conservative Temperature](#), with this equation completing the suite of fundamental equations describing the evolution of a geophysical fluid. We work with Cartesian tensors to reduce the mathematical overhead.

10.1	Potential energy from the effective gravitational field	303
10.1.1	Potential energy and hydrostatic pressure	303
10.1.2	Material evolution	303
10.1.3	Flux-form potential energy equation	304
10.1.4	Reference geopotential	304
10.1.5	Evolution of regionally integrated potential energy	304
10.1.6	Potential energy for an ocean domain	305
10.1.7	Potential energy and vertical stratification	306
10.1.8	Potential energy and mixing	306
10.2	Kinetic energy of macroscopic motion	307
10.2.1	Kinetic energy budget from Cauchy's equation	308
10.2.2	Kinetic energy budget for a geophysical fluid	308
10.2.3	Frictional dissipation of kinetic energy	309
10.2.4	Further study	311
10.3	Mechanical energy budget	311
10.3.1	Differential mechanical energy budget	311
10.3.2	Mechanical energy budget for a finite volume	312
10.4	Hypothesis of local thermodynamic equilibrium	312
10.4.1	Elements of the local thermodynamic equilibrium hypothesis	312
10.4.2	Heuristic arguments for local equilibration	313

10.5 Thermodynamics of a moving fluid	314
10.5.1 Concerning the transition to a continuous fluid	314
10.5.2 Space-time derivatives and thermodynamic partial derivatives	315
10.5.3 A cautionary remark for thermodynamic partial derivatives	316
10.5.4 First law for a moving fluid element	316
10.5.5 Enthalpy budget	317
10.5.6 Thermal and chemical processes and fluxes	318
10.5.7 First law in terms of potential temperature	319
10.5.8 Materially constant specific entropy for a perfect fluid	319
10.5.9 Further study	319
10.6 Budget for total energy	319
10.6.1 Postulating the budget for total energy	320
10.6.2 First law of thermodynamics for a moving fluid	320
10.6.3 Joule heating from friction	321
10.6.4 Comments on gauge symmetry	321
10.6.5 Further study	322
10.7 Thermodynamic equilibrium with macroscopic motion	322
10.7.1 Deriving the equilibrium conditions	322
10.7.2 Further study	323
10.8 Bernoulli's theorem	323
10.8.1 Bernoulli potential	323
10.8.2 Mechanical injection work	324
10.8.3 Bernoulli's theorem for a steady perfect fluid	324
10.8.4 Traditional derivation of Bernoulli's theorem	325
10.8.5 Steady flow in a pipe	326
10.8.6 Steady flow over a topographic bump	328
10.8.7 Further study	329
10.9 Entropy budget for the ocean	329
10.9.1 Non-advective entropy flux and entropy source	330
10.9.2 Constraints from the second law of thermodynamics	332
10.9.3 A summary presentation	334
10.9.4 Comments	335
10.9.5 Further study	335
10.10 Temperature evolution	335
10.10.1 Evolution of <i>in situ</i> temperature	336
10.10.2 Evolution of potential temperature	337
10.10.3 Conservative Temperature for the ocean	337
10.10.4 Alternative functional dependencies for specific enthalpy	339
10.10.5 Comments and further study	339
10.11 Conservation laws and potential properties	339
10.11.1 Flux-form conservation laws	340
10.11.2 Conservation laws that are not flux-form	340
10.11.3 Non-material or wave-like transport of properties	340
10.11.4 Material and non-material conservation laws	341
10.11.5 Concerning potential properties	342
10.11.6 Further study	342
10.12 Equations for rotating and stratified fluids	342
10.13 Exercises	344

10.1 Potential energy from the effective gravitational field

Geophysical fluids move within an effective gravitational field created by the rotating massive planet. In this section we study the potential energy of a fluid element and fluid regions within the prescribed effective gravitational field. In particular, we consider the relatively simple form for the effective gravitational acceleration given by the geopotential,

$$\Phi = g z, \quad (10.1)$$

where the acceleration, g , includes effects from both the planet's central gravity field plus the planetary centrifugal acceleration (see VOLUME 1).¹

10.1.1 Potential energy and hydrostatic pressure

The potential energy of a fluid element of mass, $\rho \delta V$, within a prescribed geopotential field, Φ , is given by $\Phi \rho \delta V$, so that the potential energy of a finite fluid region is the integral

$$\int_{\mathcal{R}} \rho \Phi dV = \int \left[\int_{z_a}^{z_b} \rho \Phi dz \right] dA. \quad (10.2)$$

The right expression extracted the potential energy per horizontal area of a vertical fluid column integrated between $z_a \leq z \leq z_b$. For a hydrostatic fluid column (Section 8.6), we can express the potential energy per area in terms of a pressure integrated geopotential via the coordinate change

$$dp = -g \rho dz, \quad (10.3)$$

so that²

$$g \int_{z_a}^{z_b} \rho z dz = - \int_{p_a}^{p_b} z dp = -g^{-1} \int_{p_a}^{p_b} \Phi dp, \quad (10.4)$$

where $p_a = p(z_a)$ and $p_b = p(z_b)$. Alternatively, we can write

$$g \int_{z_a}^{z_b} \rho z dz = - \int_{z_a}^{z_b} (\partial_z p) z dz = -(p_b z_b - p_a z_a) + \int_{z_a}^{z_b} p dz. \quad (10.5)$$

Both expressions (10.4) and (10.5) connect hydrostatic pressure to the potential energy per horizontal area.

10.1.2 Material evolution

We now focus on how potential energy of a constant mass fluid element changes in time, in which case we consider the material time derivative

$$\frac{D(\Phi \rho \delta V)}{Dt} = \rho \delta V \frac{D\Phi}{Dt}, \quad (10.6)$$

where $D(\rho \delta V)/Dt = 0$ since the fluid element has a constant mass. The material time derivative for the geopotential

$$\frac{D\Phi}{Dt} = \frac{\partial \Phi}{\partial t} + \mathbf{v} \cdot \nabla \Phi, \quad (10.7)$$

¹We offer some discussion of astronomical tide producing forces in our discussion of gravity in VOLUME 1 as well as in Section 11.6, whereby the geopotential is a more complicated function of space and time, $\Phi(\mathbf{x}, t)$.

²We considered similar manipulations in Exercise 7.6.

contains a local time dependence that arises from astronomical tide forcing or movement of mass on the planet (Section 11.6). As further explored in Section 10.3, the advective term represents an exchange of mechanical energy between the kinetic energy contained in fluid motion and the potential energy due to the fluid being within a gravitational field. This energy exchange arises when fluid moves across surfaces of constant geopotential. For example, motion up the geopotential gradient, $\mathbf{v} \cdot \nabla \Phi > 0$, increases potential energy and motion down the geopotential gradient decreases potential energy. With the geopotential $\Phi = g z$, we have

$$\mathbf{v} \cdot \nabla \Phi = g w, \quad (10.8)$$

so that vertically upward motion ($w > 0$) increases potential energy.

10.1.3 Flux-form potential energy equation

Another way to reveal the same ideas is to write the density weighted material time derivative of the geopotential

$$\rho \frac{D\Phi}{Dt} = \partial_t(\rho \Phi) + \nabla \cdot (\rho \mathbf{v} \Phi). \quad (10.9)$$

For the simple geopotential, $\Phi = g z$, we thus find

$$\rho \frac{D\Phi}{Dt} = \rho g w \iff \partial_t(\rho \Phi) + \nabla \cdot (\rho \mathbf{v} \Phi) = \rho g w. \quad (10.10)$$

10.1.4 Reference geopotential

There is no change to the energetics if we modify the gravitational reference state by modifying the geopotential

$$\Phi \rightarrow \Phi + \Phi_r \quad (10.11)$$

with Φ_r an arbitrary constant. In particular, this offset has no effect on the evolution of gravitational potential energy of the constant mass fluid element since

$$\frac{D(\Phi_r \rho \delta V)}{Dt} = \Phi_r \frac{D(\rho \delta V)}{Dt} = 0. \quad (10.12)$$

Hence, as is well known from classical particle mechanics, it is not the value of the gravitational potential energy that is important, but instead it is the space and time changes that affect energetics.

10.1.5 Evolution of regionally integrated potential energy

Consider the evolution of the gravitational potential energy integrated over a finite region, \mathcal{R} . If the fluid region is closed to mass transport, as per a material boundary, then we can make use of the Leibniz-Reynolds transport theorem (see VOLUME 1) to write

$$\frac{d}{dt} \int_{\mathcal{R}} \Phi \rho dV = \int_{\mathcal{R}} \frac{D\Phi}{Dt} \rho dV, \quad (10.13)$$

which is an extension of the material evolution equation (10.6). If the region is open to material mass transport, we make further use of Leibniz-Reynolds to find

$$\frac{d}{dt} \int_{\mathcal{R}} \Phi \rho dV = \int_{\mathcal{R}} \frac{\partial(\rho \Phi)}{\partial t} dV + \oint_{\partial\mathcal{R}} \rho \Phi \mathbf{v}^{(b)} \cdot \hat{\mathbf{n}} d\mathcal{S} \quad (10.14a)$$

$$= \int_{\mathcal{R}} \left[\rho \frac{D\Phi}{Dt} - \nabla \cdot (\rho \Phi \mathbf{v}) \right] dV + \oint_{\partial\mathcal{R}} \rho \Phi \mathbf{v}^{(b)} \cdot \hat{\mathbf{n}} d\mathcal{S} \quad (10.14b)$$

$$= \int_{\mathcal{R}} \rho \frac{D\Phi}{Dt} dV + \oint_{\partial\mathcal{R}} \rho \Phi (\mathbf{v}^{(b)} - \mathbf{v}) \cdot \hat{\mathbf{n}} d\mathcal{S} \quad (10.14c)$$

$$= \int_{\mathcal{R}} g \rho w dV + \oint_{\partial\mathcal{R}} \rho \Phi (\mathbf{v}^{(b)} - \mathbf{v}) \cdot \hat{\mathbf{n}} d\mathcal{S}, \quad (10.14d)$$

where $\mathbf{v}^{(b)}$ is the velocity of a point on the boundary of the domain. The evolution thus consists of the mass integrated material time evolution of the geopotential, plus a surface term that contributes to the transport of the geopotential across the regional boundaries. For the simple geopeontial used here, the material evolution of the geopotential is given by the domain integrated $g \rho w$.

10.1.6 Potential energy for an ocean domain

Now assume the finite region is a vertical column of ocean fluid with fixed horizontal cross-section that extends g from the ocean surface to the ocean bottom. In this case we have horizontal transport across the vertical column bounds, plus vertical transport of mass across the ocean free surface. For the free surface we make use of the surface kinematic boundary condition from VOLUME 1 to write

$$\int_{z=\eta} \rho \Phi (\mathbf{v}^{(b)} - \mathbf{v}) \cdot \hat{\mathbf{n}} d\mathcal{S} = \int_{z=\eta} Q_m \Phi dA. \quad (10.15)$$

In this equation, Q_m is the mass per time per horizontal area of matter crossing the ocean free surface at $z = \eta$, where $Q_m > 0$ for matter entering the ocean domain, and $d\mathcal{S}$ is the area element on the free surface with dA its horizontal projection. As noted in Section 10.1.4, we can add a constant to the geopotential without affecting the energetics, which is here seen by noting that mass conservation means that

$$\frac{d}{dt} \int \rho dV = - \int_{\mathcal{R}} \nabla \cdot [\rho (\mathbf{v} - \mathbf{v}^{(b)})] dV, \quad (10.16)$$

which results from setting $\Phi = 1$ in equation (10.14d). In general, we expect the transfer of mass across the surface boundary to affect the gravitational potential energy both because it adds or removes mass to the ocean domain, and because it affects the geopotential. To help interpret the sign from the boundary term, it is useful to define the reference state geopotential so that $\Phi > 0$ at the ocean surface, no matter what the value of η . We can do so by defining the reference geopotential at or below the ocean bottom. In this case, adding mass increases the gravitational potential energy and removing mass reduces it.

Consider the special case of a geopotential $\Phi = g z$, so returning to a $z = 0$ reference state, in which case the global ocean potential energy equation is written

$$\frac{d}{dt} \int \rho z dV = \int \rho w dV + \int Q_m \eta dA, \quad (10.17)$$

where we cancelled the constant gravitational acceleration. Now decompose Q_m and η into their global area means and deviations

$$Q_m = \overline{Q_m} + Q'_m \quad \text{and} \quad \eta = \bar{\eta} + \eta', \quad (10.18)$$

so that

$$g \int Q_m \eta \, dA = g \overline{Q_m} \bar{\eta} A + g \int Q'_m \eta' \, dA. \quad (10.19)$$

As before, the $\overline{Q_m} \bar{\eta}$ term alters potential energy relative to the arbitrary reference state, here taken as $z = 0$. The area correlation term increases potential energy in regions where $Q'_m \eta' > 0$, which acts to increase the relative deviation of the free surface from its mean value. That is, $Q'_m \eta' > 0$ in regions where $Q'_m > 0$ and $\eta' > 0$ as well as in regions where $Q'_m < 0$ and $\eta' < 0$. Conversely, the correlation term reduces potential energy where Q'_m and η' are anti-correlated, which acts to decrease the relative deviation of the free surface height.

10.1.7 Potential energy and vertical stratification

Consider the potential energy of a region of horizontally homogeneous fluid centered at a vertical position, $z = z_c$, and with constant horizontal cross-sectional area, A . Assuming we do not move vertically far away from the central position, we can write the density in the linear form

$$\rho(z) = \rho(z_c) + \frac{d\rho(z_c)}{dz} (z - z_c) \equiv \rho_c - K(z - z_c), \quad (10.20)$$

where $K = -d\rho(z_c)/dz > 0$ is a shorthand for the vertical density gradient at the central point. The potential energy per volume ($\Delta V = A \Delta z$) for fluid in the vertical region $z \in [z_c - \Delta z/2, z_c + \Delta z/2]$ is given by

$$(g/\Delta z) \int z \rho \, dz = (g/\Delta z) \int_{z_c - \Delta z/2}^{z_c + \Delta z/2} [\rho_c - K(z - z_c)] z \, dz \quad (10.21a)$$

$$= g \rho_c z_c - g K (\Delta z)^2 / 12. \quad (10.21b)$$

We thus see that the gravitational potential energy decreases as the vertical stratification, $K > 0$, increases, with the maximum potential energy when the stratification vanishes, $K = 0$. As seen in Section 10.1.8, potential energy is maximized when $K = 0$ since the center of mass moves vertically upward as the stratification reduces to zero.

10.1.8 Potential energy and mixing

Consider a fluid in exact hydrostatic balance (Section 8.6) with a gravitationally stable vertical stratification where light fluid is above heavy fluid.³ Now introduce a physical process, such as vertical mixing associated with a kinetic energy source, that reduces the vertical stratification. Reducing vertical stratification requires mixing to move heavy fluid up and light fluid down. In so doing, the kinetic energy supporting the mixing is converted into gravitational potential energy since the center of mass for the fluid column rises.

We can formulate this thought experiment by considering a column of seawater that is vertically stratified in salinity, S , and Conservative Temperature, Θ , and another column that

³In Section 14.5 we provide a more precise discussion of gravitational stability.

is vertically unstratified with constant values, S_m and Θ_m .⁴ We assume the mass of the two columns is the same so that the bottom pressure, p_b , and surface pressure, p_a , are the same for the two columns. However, the volumes will generally differ since the density differs, so that the two free surfaces, η and η_m , differ. Assuming a geopotential for the homogenized column, $\Phi = g z_m$, leads to the integrated potential energy

$$g \int_{\eta_b}^{\eta_m} \rho(S_m, \Theta_m, p) z_m dz_m = - \int_{p_b}^{p_a} z_m dp, \quad (10.22)$$

where we used the hydrostatic balance to write

$$dp = -g \rho(S_m, \Theta_m, p) dz_m. \quad (10.23)$$

Likewise, the stratified column has an integrated potential energy

$$g \int_{\eta_b}^{\eta} \rho(S, \Theta, p) z dz = - \int_{p_b}^{p_a} z dp, \quad (10.24)$$

so that the difference between the gravitational potential energies per horizontal area in the two columns is given by

$$g \int_{\eta_b}^{\eta_m} \rho(S_m, \Theta_m, p) z dz - g \int_{\eta_b}^{\eta} \rho(S, \Theta, p) z dz = \int_{p_a}^{p_b} (z_m - z) dp = (p_b - p_a) (\bar{z}_m - \bar{z}). \quad (10.25)$$

In this equation we introduced the center of mass positions for the vertically homogeneous column, \bar{z}_m , and the stratified column, \bar{z} , defined by

$$\bar{z}_m = \frac{1}{p_b - p_a} \int_{p_a}^{p_b} z_m dp \quad \text{and} \quad \bar{z} = \frac{1}{p_b - p_a} \int_{p_a}^{p_b} z dp. \quad (10.26)$$

There are two contributions to the potential energy difference in equation (10.25). The first is the mass per horizontal area, as measured by the difference in bottom pressure and applied surface pressure, $(p_b - p_a)/g > 0$. The second is the difference between the center of mass for the two columns, $\bar{z}_m - \bar{z}$, which is a positive number since homogenizing a fluid column moves heavier water up and lighter water down so that $\bar{z}_m > \bar{z}$. Hence, the potential energy of the homogenized column is larger than the stratified column. We develop more experience with the energetics of mixing in Exercise 10.1.

10.2 Kinetic energy of macroscopic motion

Mechanical energy is a dynamical property formed by adding the energy due to the macroscopic motion of fluid elements (kinetic energy) to the potential energy arising from the position of a fluid element within the geopotential field. Here, we develop the budget for kinetic energy and then the full mechanical energy (kinetic plus potential) in Section 10.3.

⁴See Section 14.3 for discussion of the seawater equation of state. For present purposes it is sufficient to know that seawater density is a function of the material tracer S , the thermodynamic tracer, Θ , and pressure, p . When a column is vertically homogenized that means S and Θ are constant throughout the column. However, pressure remains hydrostatic and thus is not vertically constant. Since density is a function of pressure, it too retains a vertical gradient.

10.2.1 Kinetic energy budget from Cauchy's equation

We start the analysis by considering general features of the kinetic energy budget as seen from Cauchy's equation of motion (8.22)

$$\rho \frac{D\mathbf{v}}{Dt} = \rho \mathbf{f}_{\text{body}} + \nabla \cdot (-p \mathbb{I} + \mathbb{T}), \quad (10.27)$$

with a body force per mass, \mathbf{f}_{body} , and contact stress from pressure, p , and the symmetric frictional stress tensor, \mathbb{T} . Taking the scalar product with the fluid velocity, \mathbf{v} , leads to

$$\rho \frac{D\mathcal{K}}{Dt} = \rho \mathbf{v} \cdot \mathbf{f}_{\text{body}} + v^n \partial_m (-p \delta^m_n + \mathbb{T}^m_n), \quad (10.28)$$

where

$$\mathcal{K} = \mathbf{v} \cdot \mathbf{v} / 2 = \delta_{mn} v^m v^n / 2 \quad (10.29)$$

is the kinetic energy per mass. We thus see that the kinetic energy of a fluid element is affected by work done by the body forces, $\rho \mathbf{v} \cdot \mathbf{f}_{\text{body}}$, along with work done by stresses through both pressure and friction.

Rearranging the stress term in equation (10.28) leads to

$$\rho \frac{D\mathcal{K}}{Dt} = \rho \mathbf{v} \cdot \mathbf{f}_{\text{body}} + \nabla \cdot (-p \mathbf{v} + \mathbf{v} \cdot \mathbb{T}) + p \nabla \cdot \mathbf{v} - (\partial_m v^n) \mathbb{T}^m_n. \quad (10.30)$$

The contribution from $\nabla \cdot (-p \mathbf{v} + \mathbf{v} \cdot \mathbb{T})$ is the divergence of a flux arising from pressure and viscous stress, whereas the term, $p \nabla \cdot \mathbf{v}$, arises from pressure work done on a fluid element as it changes volume. For the final term in equation (10.30), as note that the frictional stress tensor is symmetric so that

$$(\partial_m v^n) \mathbb{T}^m_n = S^m_n \mathbb{T}^m_n \quad (10.31)$$

where we introduced the strain rate tensor

$$2 S^m_n = \partial_m v^n + (\partial_m v^n)^T = \partial_m v^n + \partial^n v_m. \quad (10.32)$$

As shown in Section 10.2.3, the frictional stress tensors resulting from the constitutive relations in Section 9.6 result in a non-negative $S^m_n \mathbb{T}^m_n$, in which case frictional stresses dissipate (reduce) kinetic energy.

10.2.2 Kinetic energy budget for a geophysical fluid

We now develop the kinetic energy budget for a fluid in a rotating reference frame, in which case the body force is provided by the effective gravity and Coriolis. For this purpose we make use of the momentum equation (8.24)s

$$\rho \frac{D\mathbf{v}}{Dt} + 2 \rho \boldsymbol{\Omega} \times \mathbf{v} = -\rho \nabla \Phi + \nabla \cdot (-p \mathbb{I} + \mathbb{T}) \quad (10.33a)$$

$$= -\rho \nabla \Phi - \nabla p + \rho \mathbf{F}, \quad (10.33b)$$

where we wrote

$$\mathbf{F} = \rho^{-1} \nabla \cdot \mathbb{T} \quad (10.34)$$

for acceleration due to viscous friction that arises from the divergence of the frictional stress tensor. Taking the scalar product of \mathbf{v} with the momentum equation in the form of equation

(10.33b) renders

$$\rho \frac{D\mathcal{K}}{Dt} = -\rho \mathbf{v} \cdot \nabla \Phi - \mathbf{v} \cdot \nabla p + \rho \mathbf{v} \cdot \mathbf{F}. \quad (10.35)$$

We thus see that the kinetic energy of a fluid element is affected by work done by the geopotential, $-\rho \mathbf{v} \cdot \nabla \Phi$, along with work done by stresses through both pressure and friction. We examine these mechanical processes in the following.

Contribution from the geopotential

Kinetic energy increases for motion directed down the geopotential gradient

$$\mathbf{v} \cdot \nabla \Phi < 0 \implies \text{increases kinetic energy}. \quad (10.36)$$

For example, with a simple geopotential, $\Phi = g z$, kinetic energy increases where the vertical velocity is downward,

$$w < 0 \implies -w g \rho > 0 \longleftrightarrow \text{downward motion increases } \mathcal{K} \text{ of a fluid element}. \quad (10.37)$$

As seen in Section 10.1.2, this increase in kinetic energy due to motion down the geopotential gradient is exactly balanced by a decrease in gravitational potential energy. That is, an increase in kinetic energy through motion down the geopotential comes at the cost of a decrease in the gravitational potential energy. This exact conversion between kinetic energy and potential energy is also seen in VOLUME 1 when studying point particle dynamics.

Contribution from the pressure gradient body force

Kinetic energy increases in regions where the velocity projects down the pressure gradient,

$$\mathbf{v} \cdot \nabla p < 0 \implies \text{increase kinetic energy}, \quad (10.38)$$

thus resulting in an increase in fluid speed imparted by the pressure gradient force. Conversely, kinetic energy is reduced in regions where the flow is directed up the pressure gradient. It is notable that geostrophic flows, studied in Section 15.4, have a velocity given by

$$\mathbf{v}_g = (g \rho)^{-1} \hat{\mathbf{z}} \times \nabla p. \quad (10.39)$$

Consequently, geostrophic flows have $\mathbf{v}_g \cdot \nabla p = 0$, so that the pressure gradient force has no impact on the horizontal kinetic energy of a geostrophic fluid.

Contribution from friction

Kinetic energy is reduced in regions where the velocity has a negative projection onto the direction of the friction vector, $\rho \mathbf{v} \cdot \mathbf{F} < 0$. As detailed in Section 10.2.3, the friction arising from a viscous stress tensor appropriate for a Newtonian fluid gives rise to two contributions to kinetic energy: the divergence of a viscous flux plus a sign-definite sink.

10.2.3 Frictional dissipation of kinetic energy

We here detail the role of friction on kinetic energy

$$\text{friction power per volume} = \rho \mathbf{v} \cdot \mathbf{F} = \mathbf{v} \cdot (\nabla \cdot \mathbb{T}), \quad (10.40)$$

which is the frictional power per volume (energy per time per volume) that modifies the kinetic energy per volume of a fluid element, and with the frictional stress tensor, \mathbb{T} , determined by the constitutive equation (9.62). We anticipated this contribution in the general discussion of Section 10.2.1, and here provide details.

To proceed, expose Cartesian tensor labels to have

$$\rho \mathbf{v} \cdot \mathbf{F} = v_m \rho F^m \quad (10.41a)$$

$$= v_m \partial_n \mathbb{T}^{nm} \quad (10.41b)$$

$$= 2 v_m \partial_n (\rho \nu S_{\text{dev}}^{mn}) \quad (10.41c)$$

$$= 2 \partial_n (\rho \nu v_m S_{\text{dev}}^{mn}) - 2 \rho \nu \partial_n v_m S_{\text{dev}}^{mn} \quad (10.41d)$$

$$= 2 \nabla \cdot (\rho \nu \mathbf{v} \cdot \mathbf{S}_{\text{dev}}) - 2 \rho \nu S_{mn} S_{\text{dev}}^{mn}, \quad (10.41e)$$

where we recall from Section 9.6.6 that the **deviatoric strain rate tensor** has elements given by

$$S_{\text{dev}}^{mn} = S^{mn} - \delta^{mn} S^q_q / 3 \quad \text{with} \quad S^q_q = \nabla \cdot \mathbf{v}. \quad (10.42)$$

To reach equation (10.41e) required the identity

$$2 \partial_n v_m S_{\text{dev}}^{mn} = (\partial_n v_m + \partial_m v_n) S_{\text{dev}}^{mn} + (\partial_n v_m - \partial_m v_n) S_{\text{dev}}^{mn} = 2 S_{mn} S_{\text{dev}}^{mn}, \quad (10.43)$$

where

$$(\partial_n v_m - \partial_m v_n) S_{\text{dev}}^{mn} = 2 R_{mn} S_{\text{dev}}^{mn} = 0 \quad (10.44)$$

due to symmetry of the deviatoric strain rate tensor, $S_{\text{dev}}^{mn} = S_{\text{dev}}^{nm}$, and anti-symmetry of the **rotation tensor**, $R_{mn} = -R_{nm}$. We show that the second term in equation (10.41e) is non-negative by noting that

$$0 \leq \mathbf{S}_{\text{dev}} : \mathbf{S}_{\text{dev}} \quad (10.45a)$$

$$= (S_{\text{dev}})_{mn} S_{\text{dev}}^{mn} \quad (10.45b)$$

$$= (S_{mn} - \delta_{mn} S^q_q / 3) (S^{mn} - \delta^{mn} S^p_p / 3) \quad (10.45c)$$

$$= S_{mn} S^{mn} + \delta_{mn} \delta^{mn} S^q_q S^p_p / 9 - 2 S_{mn} \delta^{mn} S^q_q / 3 \quad (10.45d)$$

$$= S_{mn} S^{mn} - (S^q_q)^2 / 3 \quad (10.45e)$$

$$= S_{mn} (S^{mn} - \delta^{mn} S^q_q / 3) \quad (10.45f)$$

$$= S_{mn} S_{\text{dev}}^{mn}. \quad (10.45g)$$

We are thus left with the friction contribution to kinetic energy evolution

$$\rho \mathbf{v} \cdot \mathbf{F} = 2 \nabla \cdot (\rho \nu \mathbf{v} \cdot \mathbf{S}_{\text{dev}}) - 2 \rho \nu S_{\text{dev}} : S_{\text{dev}}. \quad (10.46)$$

We interpret the two contributions to the frictional power in equation (10.46) as

$$\rho \mathbf{v} \cdot \mathbf{F} = \text{divergence of viscous flux} - \text{viscous dissipation}. \quad (10.47)$$

The divergence theorem means that when integrated over the full domain, the divergence of the viscous flux becomes a contribution from boundary stresses, and boundary stresses can either increase or decrease kinetic energy according to details of the boundary processes. In contrast, the sign-definite dissipation term provides a sink to the kinetic energy at each point

in the fluid interior. This frictional dissipation is commonly written

$$\epsilon \equiv [\mathbf{v} \cdot \mathbf{F}]_{\text{dissipate}} = 2\nu \mathbf{S}_{\text{dev}} : \mathbf{S}_{\text{dev}} \geq 0. \quad (10.48)$$

The dimensions of ϵ are $\text{L}^2 \text{T}^{-3}$, which in SI units are $\text{m}^2 \text{s}^{-3} = \text{W kg}^{-1}$. We thus refer to ϵ as the kinetic energy dissipation per mass arising from viscous effects. It is also sometimes referred to as the viscous power per mass.⁵

10.2.4 Further study

The study of physical processes contributing to kinetic energy dissipation is central to the study of ocean mixing. The review by [MacKinnon et al. \(2013\)](#) provides a pedagogical starting point for this active area of ocean physics.

As shown in Section 17.8 of [Griffies \(2004\)](#), we can relate the global integral of the kinetic energy dissipation to the friction vector by taking the functional derivative of the dissipation with respect to the velocity field. This connection follows from the self-adjoint nature of the friction operator and it can be a useful mathematical framework for developing numerical discretizations as in [Griffies and Hallberg \(2000\)](#).

10.3 Mechanical energy budget

We here develop the budget, both differential and integral, for mechanical energy of a moving fluid.

10.3.1 Differential mechanical energy budget

Adding the material time evolution equations for kinetic energy per mass (equation (10.35)) and potential energy per mass (equation (10.10)) leads to the material time derivative of the mechanical energy per mass

$$\rho \frac{D\mathcal{M}}{Dt} = -\mathbf{v} \cdot \nabla p + 2\nabla \cdot (\rho\nu \mathbf{v} \cdot \mathbf{S}_{\text{dev}}) + \rho(-\epsilon + \partial_t \Phi) \quad (10.49a)$$

$$= -\nabla \cdot (p\mathbf{v} - 2\rho\nu \mathbf{v} \cdot \mathbf{S}_{\text{dev}}) + p\nabla \cdot \mathbf{v} + \rho(-\epsilon + \partial_t \Phi) \quad (10.49b)$$

$$= -\nabla \cdot \mathbf{J}^{\text{mech}} + p\nabla \cdot \mathbf{v} + \rho(-\epsilon + \partial_t \Phi), \quad (10.49c)$$

where

$$\mathcal{M} = \mathcal{K} + \Phi \quad (10.50)$$

is the mechanical energy per mass of a fluid element. Equation (10.49c) introduced the mechanical energy flux

$$\mathbf{J}^{\text{mech}} = p\mathbf{v} - 2\rho\nu \mathbf{v} \cdot \mathbf{S}_{\text{dev}} = -\mathbf{v} \cdot (-p\mathbb{I} + \mathbb{T}) = -\mathbf{v} \cdot \mathbf{T}, \quad (10.51)$$

where \mathbf{T} is the stress tensor for a Newtonian fluid given by equation (9.62). We can write the material time evolution equation (10.52) as a flux-form conservation equation

$$\partial_t(\rho\mathcal{M}) + \nabla \cdot (\rho\mathcal{M}\mathbf{v} + \mathbf{J}^{\text{mech}}) = p\nabla \cdot \mathbf{v} + \rho(-\epsilon + \partial_t \Phi). \quad (10.52)$$

⁵To be sure one trusts the nomenclature, it is useful to expand the Einstein summation convention to show that $\mathbf{S}_{\text{dev}} : \mathbf{S}_{\text{dev}}$ is the sum of nine perfect squares, thus ensuring that $\epsilon \geq 0$.

Equation (10.49c) says that the material evolution of mechanical energy per mass arises from the convergence of the mechanical energy flux, \mathbf{J}^{mech} , plus the work done by pressure in a fluid with non-zero flow divergence, along with frictional dissipation (more discussed in Section 10.6.3), and time changes to the geopotential. Furthermore, as shown when studying total energy in Section 10.6, mechanical energy is exchanged with internal energy through pressure work and frictional dissipation. This exchange provides the fundamental link between the mechanical energy of macroscopic motion and the internal energy of microscopic degrees of freedom. As already anticipated, there is a cancellation of the mechanical energy exchanged between kinetic and potential energy due to motion through the geopotential field. However, the time-dependent geopotential provides a source of mechanical energy arising from processes external to the fluid, such as astronomical effects that drive tidal motions.

10.3.2 Mechanical energy budget for a finite volume

To derive the finite volume mechanical energy budget, we make use of the Leibniz-Reynolds transport theorem (see VOLUME 1) and the flux-form mechanical energy budget (10.52), thus leading to

$$\frac{d}{dt} \left[\int_{\mathcal{R}} \rho \mathcal{M} dV \right] = - \oint_{\partial\mathcal{R}} \rho \mathcal{M} (\mathbf{v} - \mathbf{v}^{(b)}) \cdot \hat{\mathbf{n}} dS - \oint_{\partial\mathcal{R}} \mathbf{J}^{\text{mech}} \cdot \hat{\mathbf{n}} dS + \int_{\mathcal{R}} [p \nabla \cdot \mathbf{v} + \rho (-\epsilon + \partial_t \Phi)] dV. \quad (10.53)$$

The first term on the right hand side arises from the advective transport of mechanical energy across the moving boundary. The second term arises from the boundary work done by pressure and viscous stresses, with equation (10.51) yielding the equivalent expression in terms of the stress tensor

$$- \oint_{\partial\mathcal{R}} \mathbf{J}^{\text{mech}} \cdot \hat{\mathbf{n}} dS = \oint_{\partial\mathcal{R}} \mathbf{v} \cdot \mathbf{T} \cdot \hat{\mathbf{n}} dS. \quad (10.54)$$

The third term in equation (10.53) is a volume source arising from pressure work applied to each fluid element, viscous dissipation, and time tendencies in the geopotential.

10.4 Hypothesis of local thermodynamic equilibrium

We make use of the hypothesis of local thermodynamic equilibrium in Section 10.5 to couple the equilibrium thermodynamics in Chapters 6 and 7 to fluids in macroscopic motion. This hypothesis presumes that macroscopic fluid motion is decomposed into a continuum of tiny moving regions, each referred to as a **fluid element** and each assumed to be in local thermodynamic equilibrium. For a perfect fluid, macroscopic motion does not alter the entropy for a fluid element. That is, in the absence of mixing of fluid elements, advective transport is a reversible process. In contrast, mixing of properties between real fluid elements is irreversible and thus increases entropy.

10.4.1 Elements of the local thermodynamic equilibrium hypothesis

For a real fluid, any finite sized region is generally out of thermodynamic equilibrium, as evidenced, say, by a non-uniform temperature over macroscopic length scales. Even so, the **local thermodynamic equilibrium** hypothesis assumes that infinitesimal fluid elements are in local

thermodynamic equilibrium, thus affording the means to determine intensive thermodynamic properties (e.g., temperature, pressure, chemical potential) at each point within the fluid continuum. Furthermore, the hypothesis means that the functional dependence of state functions (e.g., internal energy, entropy, enthalpy) remains the same for the moving fluid as they are for thermodynamic equilibrium. This particular implication of the hypothesis provides the key operational means for extending to a moving fluid the differential relations developed for equilibrium thermodynamics in Chapters 6 and 7.

Theoretical foundations for the hypothesis of local thermodynamic equilibrium are rather difficult and somewhat unresolved. Indeed, many presentations postulate that the equations of equilibrium thermodynamics can be extended to moving continuous media, with justification provided *a posteriori* based on the resulting implications (e.g., Section III.2 of *DeGroot and Mazur (1984)*). We follow this approach here.⁶ The hypothesis has proven successful for the atmosphere and ocean motions studied in this book, so that we accept it without concern.⁷ Further discussion of the hypothesis of local thermodynamic equilibrium can be found in Section 49 of *Landau and Lifshitz (1987)*, chapter 5 of *Huang (1987)*, and Section 19.2 of *Woods (1975)*.⁸

10.4.2 Heuristic arguments for local equilibration

How does local thermodynamic equilibration come about, and how well should we expect it to be satisfied? If we assume a fluid element has length scale $L_{\text{macro}} = 10^{-4}$ m, as motivated by the discussion of the continuum approximation in the Prologue chapter in VOLUME 1, then the question reduces to determining the time scale for a fluid element to have its mechanical and thermodynamical properties homogenized. We consider mechanical equilibrium to be related to the time scales for pressure to equilibrate, whereas thermodynamic equilibrium requires the additional considerations of material and thermal diffusion.

Pressure signals are transmitted by acoustic waves at the sound speed, c_s , (studied in VOLUME 5), so that we assume pressure equilibration times are proportional to L_{macro}/c_s . The sound speed for air at room temperature is roughly 350 m s⁻¹, so that pressure fluctuations are transmitted across an air element in roughly 3×10^{-7} s. The sound speed is about five times larger in water, thus leading to roughly 6×10^{-8} s for the pressure signal to cross an element of water. Both of these time scales are extremely tiny from a macroscopic perspective, thus supporting the assumption that pressure is rapidly equilibrated over the length scales of a fluid element.

The time scale for homogenization of temperature and matter concentrations are given by $L_{\text{macro}}^2/\kappa$, where κ is the respective molecular kinematic diffusivity for temperature or matter, which is on the order of 10^{-6} m² s⁻¹ to 10^{-5} m² s⁻¹. Hence, the time scale for a fluid element to homogenize its temperature and tracer concentration, through molecular diffusion, is $10^{-3} - 10^{-2}$ s. This time scale is far larger than the pressure time scale, yet it is still small relative to typical macroscopic processes associated with fluid motion.

⁶The hypothesis of local thermodynamic equilibrium can be motivated by noting that the microscopic motions of molecules have a much shorter equilibration time scale relative to the longer time scale of macroscopic processes of interest for fluid flow (see the Prologue chapter in VOLUME 1). Even so, pursuit of that motivation has some nuances that go beyond our goals. Hence, our perspective is pragmatic, in which we assume local thermodynamic equilibrium and see what it implies.

⁷The hypothesis of local thermodynamic equilibrium is questionable for rarefied gas dynamics of the upper atmosphere, which is a subject outside the scope of this book.

⁸The extension of equilibrium thermodynamics to a moving fluid falls under the discipline of quasi-equilibrium thermodynamics, also referred to as linear irreversible thermodynamics. The term “linear” in the name refers to an assumption that the system is close to thermodynamic equilibrium throughout its motion so that thermodynamic fluxes are linear functions of the gradients of the thermodynamic state variables.

10.5 Thermodynamics of a moving fluid

In this section we extend the formalism of equilibrium thermodynamics from Chapters 6 and 7 to the case of a moving fluid. We can make this extension by invoking the hypothesis of local **thermodynamic equilibrium** discussed in Section 10.4. Namely, the fluid is treated as a continuum of infinitesimal **fluid elements**, each evolving through a sequence of **quasi-static processes** and remaining internally in thermodynamic equilibrium at each time instance. Under this hypothesis, we can apply Gibb's **fundamental thermodynamic relation** (6.57b) to each element of a two-component fluid such as seawater or the atmosphere:

$$d\mathcal{J} = T dS - p d(1/\rho) + \mu dC. \quad (10.55)$$

This equation expresses the first law of thermodynamics for a **quasi-static process**, thus relating the exact differential of specific internal energy, \mathcal{J} , to the specific entropy, S , specific volume, $1/\rho$, and matter concentration, C , along with the thermodynamic temperature, T , the pressure, p , and the relative chemical potential, μ .

Geophysical fluids are exposed to mechanical and thermal processes that support macroscopic fluid motion. By making the local thermodynamic equilibrium hypothesis, we assume that each fluid element is in local thermodynamic equilibrium and separately satisfies the fundamental thermodynamic relation (10.55) as it evolves quasi-statically. We furthermore assume that the thermodynamic potentials for the moving fluid have a functional dependence on their state variables that is the same as found in equilibrium thermodynamics. This assumption is basic to our ability to maintain a field theoretic description of the continuum. Namely, there is no objective definition of a fluid element. Instead, they are infinitesimal regions of a continuum. The uniform functional form ensures that thermodynamic potentials vary smoothly in space and time, allowing us to take their derivatives and to construct continuous field equations.

10.5.1 Concerning the transition to a continuous fluid

For a continuum fluid, each of the thermodynamic properties in the fundamental thermodynamic relation (10.55) are continuous functions of space and time. Furthermore, equation (10.55) provides a relation between **exact differentials** as detailed in Section 6.10. As exact differentials of continuous fields, we can make use of the space and time differentials to write

$$d\Psi = \Psi(\mathbf{x} + d\mathbf{x}, t + dt) - \Psi(\mathbf{x}, t) = dt \partial_t \Psi + d\mathbf{x} \cdot \nabla \Psi, \quad (10.56)$$

where Ψ is one of the thermodynamic properties, dt is the time differential, and $d\mathbf{x}$ is the vector of space differentials. We are led to the total time derivative for a property following an arbitrary trajectory, $\mathbf{x} = \mathbf{X}(t)$

$$\frac{d\Psi}{dt} = \frac{\partial\Psi}{\partial t} + \frac{d\mathbf{X}}{dt} \cdot \nabla \Psi. \quad (10.57)$$

Restricting the trajectory to that defined by a fluid particle, so that $\mathbf{v} = d\mathbf{X}/dt$, renders the **material time derivative**

$$\frac{D\Psi}{Dt} = \frac{\partial\Psi}{\partial t} + \mathbf{v} \cdot \nabla \Psi. \quad (10.58)$$

We make use of this result in Section 10.5.4 to transition the quasi-static relation (10.55) to a moving fluid.

10.5.2 Space-time derivatives and thermodynamic partial derivatives

We need one more piece of formalism prior to transitioning the quasi-static relation (10.55) to a moving fluid. For this purpose, consider the particular case of specific enthalpy, in which case

$$\mathcal{H} = \mathcal{H}(\mathbf{x}, t) = \mathcal{H}[S(\mathbf{x}, t), p(\mathbf{x}, t), C(\mathbf{x}, t)], \quad (10.59)$$

where the second equality exposed the natural functional dependence based on the fundamental thermodynamic relation (6.75c)

$$d\mathcal{H} = T dS + (1/\rho) dp + \mu dC, \quad (10.60)$$

which holds for transitions between equilibrium states (Section 6.6.4). Again, this same functional dependence is assumed to hold for the case of an evolving fluid, so long as the time scales for macroscopic evolution are much longer than the time scales for reaching local thermodynamic equilibrium (see Section 10.4.2). We next make use of the chain-rule to render the spatial gradient

$$\nabla \mathcal{H} = \left[\frac{\partial \mathcal{H}}{\partial S} \right]_{p,C} \nabla S + \left[\frac{\partial \mathcal{H}}{\partial p} \right]_{S,C} \nabla p + \left[\frac{\partial \mathcal{H}}{\partial C} \right]_{S,p} \nabla C. \quad (10.61)$$

This spatial gradient probes properties of the field, $\mathcal{H}(\mathbf{x}, t)$, which is a function of three other fields, $S(\mathbf{x}, t), p(\mathbf{x}, t), C(\mathbf{x}, t)$. From this field theoretic perspective, the thermodynamic partial derivatives are computed by holding the value of the complement thermodynamic properties fixed at a particular point in space and time. For example, exposing space and time positions renders the awkward, yet unambiguous, expression

$$\left[\frac{\partial \mathcal{H}}{\partial S} \right]_{p,C} = \left[\frac{\partial \mathcal{H}[S(\mathbf{x}, t), p(\mathbf{x}, t), C(\mathbf{x}, t)]}{\partial S(\mathbf{x}, t)} \right]_{p(\mathbf{x}, t), C(\mathbf{x}, t)}. \quad (10.62)$$

We next apply the thermodynamic partial derivative identities (6.77) to write

$$\left[\frac{\partial \mathcal{H}}{\partial S} \right]_{p,C} = \left[\frac{\partial \mathcal{H}[S(\mathbf{x}, t), p(\mathbf{x}, t), C(\mathbf{x}, t)]}{\partial S(\mathbf{x}, t)} \right]_{p(\mathbf{x}, t), C(\mathbf{x}, t)} = T(\mathbf{x}, t) \quad (10.63a)$$

$$\left[\frac{\partial \mathcal{H}}{\partial p} \right]_{S,C} = \left[\frac{\partial \mathcal{H}[S(\mathbf{x}, t), p(\mathbf{x}, t), C(\mathbf{x}, t)]}{\partial p(\mathbf{x}, t)} \right]_{S(\mathbf{x}, t), C(\mathbf{x}, t)} = 1/\rho(\mathbf{x}, t) \quad (10.63b)$$

$$\left[\frac{\partial \mathcal{H}}{\partial C} \right]_{S,p} = \left[\frac{\partial \mathcal{H}[S(\mathbf{x}, t), p(\mathbf{x}, t), C(\mathbf{x}, t)]}{\partial C(\mathbf{x}, t)} \right]_{S(\mathbf{x}, t), p(\mathbf{x}, t)} = \mu(\mathbf{x}, t), \quad (10.63c)$$

thus leading to⁹

$$\nabla \mathcal{H} = T \nabla S + \rho^{-1} \nabla p + \mu \nabla C. \quad (10.64)$$

⁹Equation (10.64) is used on page 193 of *Landau and Lifshitz* (1987) as part of their derivation of the entropy budget for a moving fluid in the presence of heat conduction. It is also used on their page 229 to derive energetics for a fluid with both heat conduction and matter diffusion. See also their page 4 for more general discussion of how equilibrium thermodynamic relations imply relations between the space and time structure of thermodynamic functions in a moving fluid. Other treatments in the literature typically gloss over the transition of the fundamental thermodynamic relation of equilibrium thermodynamics to the quasi-equilibrium thermodynamics needed for moving fluids.

An analogous relation also holds for time derivatives, in which case

$$\partial_t \mathcal{H} = T \partial_t \mathcal{S} + \rho^{-1} \partial_t p + \mu \partial_t C. \quad (10.65)$$

We thus find a direct connection between exact differentials satisfied by the fundamental thermodynamic relations in equilibrium thermodynamics (Chapters 6 and 7), and partial derivatives in both space and time. Such connections prove particularly useful in connecting between the mechanical force from pressure and gradients in thermodynamic properties. That is, the identity (10.64) offers an alternative means to express the pressure gradient acceleration appearing in the momentum equation (e.g., equation (8.23))¹⁰

$$-\rho^{-1} \nabla p = -\nabla \mathcal{H} + T \nabla \mathcal{S} + \mu \nabla C. \quad (10.66)$$

10.5.3 A cautionary remark for thermodynamic partial derivatives

A common confusion arises when it is unclear whether a mathematical expression represents an equilibrium thermodynamic relation between thermodynamic variables, such as in the fundamental thermodynamic relation (10.55), or a relation involving space-time field representations of thermodynamic properties. The distinction is particularly important when considering derivatives and integrals since it is necessary to know what variables are held fixed in the process of performing the operations.

For example, consider the middle relation in equation (6.82), which says that the partial derivative of the Gibbs potential with respect to pressure, holding temperature and tracer concentration fixed, equals to the specific volume

$$\left[\frac{\partial \mathcal{G}(T, p, C)}{\partial p} \right]_{T,C} = \nu_s = \rho^{-1}. \quad (10.67)$$

However, if we encounter the Gibbs potential as a space-time dynamical field, and we use pressure as a generalized vertical coordinate so that $\mathcal{G} = \mathcal{G}(x, y, p, t)$, then we might need to compute the distinct partial derivative

$$\left[\frac{\partial \mathcal{G}}{\partial p} \right]_{x,y,t} \neq \left[\frac{\partial \mathcal{G}}{\partial p} \right]_{T,C}. \quad (10.68)$$

These two partial derivatives are distinct since varying pressure at a fixed (x, y, t) is distinct from varying pressure at a fixed T, C . One example where this distinction is particularly crucial is when examining energetics of a Boussinesq ocean in Section 13.6.

10.5.4 First law for a moving fluid element

Sections 10.5.1 and 10.5.2 provide the key operational means for developing the equations of quasi-equilibrium thermodynamics, in which we apply the equilibrium thermodynamic relations to a moving and evolving continuum of infinitesimal fluid elements. Consequently, the fundamental thermodynamic relation (10.55), which is the first law for a quasi-static process transitioning between thermodynamic equilibria, becomes for a moving fluid element

$$\frac{D\mathcal{J}}{Dt} = T \frac{D\mathcal{S}}{Dt} + \frac{p}{\rho^2} \frac{D\rho}{Dt} + \mu \frac{DC}{Dt}. \quad (10.69)$$

¹⁰We make use of the identity (10.66) for studies of circulation and potential vorticity in VOLUME 3.

Making use of the space and time derivative results from Section 10.5.2 leads to the gradient and Eulerian time derivative identities

$$\nabla \mathcal{J} = T \nabla S + p \rho^{-2} \nabla \rho + \mu \nabla C \quad (10.70a)$$

$$\partial_t \mathcal{J} = T \partial_t S + p \rho^{-2} \partial_t \rho + \mu \partial_t C. \quad (10.70b)$$

We can recast the first law (10.69) by recalling that mass conservation as studied in VOLUME 1 means that changes in the volume of a fluid element are related to density changes via

$$\frac{1}{\delta V} \frac{D(\delta V)}{Dt} = \frac{1}{\nu_s} \frac{D\nu_s}{Dt} = -\frac{1}{\rho} \frac{D\rho}{Dt}. \quad (10.71)$$

Hence, equation (10.69) can be written

$$\delta M \frac{D\mathcal{J}}{Dt} = T \delta M \frac{DS}{Dt} - p \frac{D(\delta V)}{Dt} + \mu \delta M \frac{DC}{Dt}, \quad (10.72)$$

where $\delta M = \rho \delta V$ is the mass of the fluid element. Since the mass of the fluid element is constant when following a material fluid particle trajectory, equation (10.72) is the fluid element extension of the first law given by equation (10.55). Alternatively, we can express the material time changes to the volume of a fluid element in terms of the divergence of the velocity field,

$$\frac{1}{\delta V} \frac{D(\delta V)}{Dt} = \nabla \cdot \mathbf{v} \quad (10.73)$$

to write

$$\frac{D\mathcal{J}}{Dt} = T \frac{DS}{Dt} - (p/\rho) \nabla \cdot \mathbf{v} + \mu \frac{DC}{Dt}. \quad (10.74)$$

Processes affecting internal energy that appear on the right hand side are (i) entropy production, whose form is developed in Sections 10.6 and 10.9, (ii) mechanical work from pressure modifying the volume of the fluid element, and (iii) mixing (chemical work) through the exchange of matter constituents between fluid elements.

10.5.5 Enthalpy budget

It is often more convenient to consider the specific enthalpy (Section 6.6.4),

$$\mathcal{H} = \mathcal{J} + p/\rho = \mathcal{J} + p \nu_s. \quad (10.75)$$

Making use of mass continuity equation ($\partial_t \rho + \nabla \cdot (\rho \mathbf{v}) = 0$) and the internal energy equation (10.74) yield

$$\frac{D\mathcal{H}}{Dt} = \frac{D\mathcal{J}}{Dt} + \frac{1}{\rho} \frac{Dp}{Dt} - \frac{p}{\rho^2} \frac{D\rho}{Dt} \implies \frac{D\mathcal{H}}{Dt} = T \frac{DS}{Dt} + \frac{1}{\rho} \frac{Dp}{Dt} + \mu \frac{DC}{Dt}, \quad (10.76)$$

with the second expression consistent with equations (10.64) and (10.65) for the gradient and local time tendency of the specific enthalpy.

The specific enthalpy equation (10.76) says that for constant pressure processes, material time changes to specific enthalpy of a moving fluid element arise just from those processes that give rise to changes in specific entropy and changes in matter concentration

$$\frac{Dp}{Dt} = 0 \implies \frac{D\mathcal{H}}{Dt} = T \frac{DS}{Dt} + \mu \frac{DC}{Dt}. \quad (10.77)$$

Since many boundary processes occur approximately at near constant pressure (e.g., air-sea fluxes), this result motivates formulating boundary fluxes of matter and thermal energy in terms of enthalpy fluxes rather than internal energy fluxes. Also, the mixing of fluid elements occurs locally in space so that pressure of fluid elements is the same when they mix, again making enthalpy a useful thermodynamic potential for the study of mixing.

10.5.6 Thermal and chemical processes and fluxes

The internal energy of a fluid element is modified by the diabatic transfer of thermal energy. We are generally concerned with two thermal fluxes, one due to conduction and one due to radiation

$$\mathbf{J}^{\text{therm}} = \mathbf{J}^{\text{cond}} + \mathbf{J}^{\text{rad}}. \quad (10.78)$$

Details of the radiant flux require topics outside our scope so we leave it unspecified. However, we consider forms for heat conduction in Section 10.9, with the simplest form being Fourier's law of conduction whereby \mathbf{J}^{cond} is directed down the temperature gradient.

The internal energy of a fluid element also changes through changes in the matter concentration. This change occurs when fluid elements mix at constant pressure. As mentioned in Section 10.5.5, enthalpy is the proper thermodynamic potential to consider for examining the mixing of matter concentrations. We thus assume that the transfer of chemical energy associated with a matter flux, \mathbf{J}^C , leads to a corresponding chemical energy flux given by

$$\mathbf{J}^{\text{chem}} = \left[\frac{\partial \mathcal{H}}{\partial C} \right]_{T,p} \mathbf{J}^C. \quad (10.79)$$

The enthalpy partial derivative is computed at constant pressure and temperature so to isolate the energy change associated just with mixing of matter. It is important to distinguish this partial derivative with the distinct derivative that leads to the chemical potential as in equation (6.77)

$$\left[\frac{\partial \mathcal{H}}{\partial C} \right]_{S,p} = \mu. \quad (10.80)$$

As shown by Exercise 6.5, the two partial derivatives are related by

$$\left[\frac{\partial \mathcal{H}}{\partial C} \right]_{T,p} = \mu - T \left[\frac{\partial \mu}{\partial T} \right]_{p,C}, \quad (10.81)$$

so that

$$\mathbf{J}^{\text{chem}} = \left[\mu - T \left[\frac{\partial \mu}{\partial T} \right]_{p,C} \right] \mathbf{J}^C. \quad (10.82)$$

We make use of this relation when studying the entropy budget in Section 10.9.

Details of the thermal and chemical fluxes are undetermined at this point. We garner further insights through studying the entropy budget and second law of thermodynamics in Section 10.9, as well as the budget for total energy in Section 10.6. It is remarkable how far the first and second laws of thermodynamics can be used to constrain the molecular flux laws.¹¹

¹¹Geophysical fluid flows are dominated by turbulence. Hence, it would be far more powerful to develop laws of thermodynamics to constrain turbulence fluxes rather than molecular fluxes. The difficulty with this aspiration is that turbulence is a property of the flow whereas the laws of thermodynamics, as formulated in this chapter, are associated with properties of the fluid. Properties of the flow are far less universal and thus require examination for each of the many regimes of turbulence found in geophysical fluids.

10.5.7 First law in terms of potential temperature

Equation (7.45) says that the change in entropy for a fluid element moving with constant matter concentration and at the reference pressure, p_R , is given in terms of the potential temperature

$$\frac{D\theta}{Dt} = \frac{c_p}{\theta} \frac{D\theta}{Dt}. \quad (10.83)$$

For a single-component fluid, the potential temperature equals to the *in situ* temperature when $p = p_R$, in which case

$$c_p \frac{D\theta}{Dt} = \theta \frac{D\theta}{Dt} \quad \text{at } p = p_R \text{ and } dC = 0. \quad (10.84)$$

In general, this relation has little practical value since a fluid element generally does not maintain pressure at the reference pressure. Even so, in Exercise 10.5 we see that this relation holds at all pressures for the special case of an ideal gas, and in Exercise 10.6 we see it also holds for some liquids at all pressures.

10.5.8 Materially constant specific entropy for a perfect fluid

Each material fluid parcel within a perfect fluid maintains a constant specific entropy given that it experiences no dissipation (friction is absent), maintains a constant composition (mixing is absent), and encounters no heating (adiabatic). Consequently, specific entropy for each fluid element is reversibly stirred through advection

$$\frac{D\theta}{Dt} = \frac{\partial \theta}{\partial t} + \mathbf{v} \cdot \nabla \theta = 0. \quad (10.85)$$

A perfect fluid generally admits nonzero gradients of specific entropy, even as each fluid parcel moves without altering its specific entropy. The homentropic fluid is a special case where the entropy is a space-time constant throughout the fluid domain.

10.5.9 Further study

DeGroot and Mazur (1984) provide an authoritative accounting of quasi-equilibrium thermodynamics as applied to continuum matter such as a fluid. *Gregg (1984)* and *Davis (1994)* apply these methods to small-scale mixing in the ocean. Slightly different formulations can be found in *Landau and Lifshitz (1987)* and *Batchelor (1967)*.

10.6 Budget for total energy

In our study of point particle mechanics in VOLUME 1, we found that a point particle conserves its mechanical energy in the absence of friction. In contrast, the mechanical energy for a fluid element is not materially constant even when only conservative forces act on the element. The reason is that for the continuum fluid, there is a conversion between mechanical energy and internal energy as pressure does work to alter the volume of fluid elements. Additionally, any frictional dissipation of kinetic energy acts to irreversibly convert some kinetic energy to internal energy through Joule heating (Section 10.6.3).

We thus see that if there is an energy conservation principle for moving fluids, then it must involve internal energy along with mechanical energy. For this reason, we here combine the mechanical energy budget from Section 10.3 with the internal energy budget from Section 10.5,

thus rendering the budget for **total energy** of a fluid element. Furthermore, we postulate that the domain integrated total energy changes only due to boundary effects, as well as possible changes in the geopotential via astronomical effects. This assumption then leads to further specifications of the processes contributing to the budgets for internal energy and enthalpy.

10.6.1 Postulating the budget for total energy

In their specific (per mass) forms, the total energy, \mathcal{E} , of a fluid element is the sum of the internal energy, \mathcal{I} , associated with internal degrees of freedom, plus the mechanical energy, \mathcal{M} , arising from macroscopic motion, with the mechanical energy the sum of the kinetic energy plus potential energy

$$\mathcal{E} = \mathcal{I} + \mathcal{M} = \mathcal{I} + \mathcal{K} + \Phi. \quad (10.86)$$

We postulate that \mathcal{E} satisfies a conservation law whereby it is affected only by the convergence of a total energy flux, plus a source due to temporal changes in the geopotential

$$\rho \frac{D\mathcal{E}}{Dt} = -\nabla \cdot \mathbf{J}^\varepsilon + \rho \partial_t \Phi. \quad (10.87)$$

Correspondingly, the flux-form equation for total energy is

$$\frac{\partial(\rho\mathcal{E})}{\partial t} + \nabla \cdot (\rho \mathbf{v} \mathcal{E} + \mathbf{J}^\varepsilon) = \rho \partial_t \Phi. \quad (10.88)$$

The flux of total energy is given by

$$\rho \mathbf{v} \mathcal{E} + \mathbf{J}^\varepsilon = \rho \mathbf{v} \mathcal{E} + \mathbf{J}^{\text{therm}} + \mathbf{J}^{\text{chem}} + \mathbf{J}^{\text{mech}} \quad (10.89a)$$

$$= \rho \mathbf{v} \mathcal{E} + \mathbf{J}^{\text{therm}} + \mathbf{J}^{\text{chem}} - \mathbf{v} \cdot (-p \mathbb{I} + \mathbb{T}) \quad (10.89b)$$

$$= \rho \mathbf{v} (\mathcal{E} + p/\rho) + \mathbf{J}^{\text{therm}} + \mathbf{J}^{\text{chem}} - \mathbf{v} \cdot \mathbb{T}, \quad (10.89c)$$

where $\mathbf{J}^{\text{therm}}$ and \mathbf{J}^{chem} were discussed in Section 10.5.6, and \mathbf{J}^{mech} was derived in Section 10.3. We have more to say concerning the flux of total energy in Section 10.8 when studying the Bernoulli potential.

We are led to postulate the total energy equation (10.87) through assuming that $\int_{\mathcal{R}} \rho \mathcal{E} dV$ remains constant in time for a region, \mathcal{R} , that is closed to thermal, material, and mechanical interactions, and one where the geopotential is constant in time. This assumption is based on our understanding of molecular and atomic mechanics.

10.6.2 First law of thermodynamics for a moving fluid

We now have the total energy budget as postulated in the form of equation (10.87), along with the mechanical energy budget derived in equation (10.52). Subtracting the two yields the internal energy budget

$$\rho \frac{D(\mathcal{E} - \mathcal{M})}{Dt} = \rho \frac{D\mathcal{I}}{Dt} = -\nabla \cdot (\mathbf{J}^{\text{therm}} + \mathbf{J}^{\text{chem}}) - p \nabla \cdot \mathbf{v} + \rho \epsilon. \quad (10.90)$$

This equation provides yet another expression for the **first law of thermodynamics** for a moving fluid element. It says that the internal energy of a fluid element is modified through the convergence of thermal and chemical fluxes, pressure work that alters the volume of a fluid element, and frictional dissipation through viscosity. Both the pressure work and frictional

dissipation are exchanged with mechanical energy, and so they appear with opposite signs in the budget for mechanical energy. We specify the thermal and chemical fluxes in Section 10.9 when studying the entropy budget, where the second law of thermodynamics provides constraints on these fluxes.

We can make use of the enthalpy equation (10.76) to render the enthalpy budget

$$\rho \frac{D\mathcal{H}}{Dt} - \frac{Dp}{Dt} = -\nabla \cdot (\mathbf{J}^{\text{therm}} + \mathbf{J}^{\text{chem}}) + \rho \epsilon. \quad (10.91)$$

This equation is used in Section 10.10 when studying the evolution of temperature.

10.6.3 Joule heating from friction

Frictional dissipation, $\epsilon > 0$, measures the conversion of kinetic energy into heat, and it is thus a conversion from mechanical energy to internal energy

$$\dot{Q}_{\text{Joule}} \equiv \epsilon. \quad (10.92)$$

This term is referred to as **Joule heating** in analog to the process that occurs in electrical circuits. The Joule heating of a fluid by molecular viscosity is larger in regions where the fluid strains are larger, signalling a more efficient transfer of power to the microscales where molecular viscosity can act on the flow.

In the ocean interior, measurements indicate that $\epsilon \approx 10^{-9} \text{ W kg}^{-1}$. Dividing by $c_p = 3900 \text{ J kg}^{-1} \text{ K}^{-1}$ leads to a heating rate of less than $10^{-3} \text{ K century}^{-1}$, which is a very small rate of ocean heating. Consequently, ocean Joule heating has a negligible role in the ocean heat budget and as such is generally ignored. Atmospheric flows are roughly two orders faster so that the kinetic energy per mass is four orders larger. The larger flow speeds lead to larger shears thus creating larger viscous dissipation that reaches roughly $\epsilon \approx 2 \text{ W m}^{-2}$ globally averaged. Hence, Joule heating is an important part of the global atmosphere enthalpy budget ([Becker, 2003](#)).

10.6.4 Comments on gauge symmetry

Consider again the flux-form equation for total energy (10.88). It is notable that the time tendency for the total energy remains unchanged if we shift the flux of total energy by a curl,

$$\rho \mathcal{E} \mathbf{v} + \mathbf{J}^\varepsilon \rightarrow \rho \mathcal{E} \mathbf{v} + \mathbf{J}^\varepsilon + \nabla \times \mathbf{G}, \quad (10.93)$$

with \mathbf{G} referred to as a **gauge function**. This arbitrariness in the definition of total energy flux represents a **gauge symmetry**. We conclude that the energy flux has no unique local physical meaning. Instead, it is only the convergence of the energy flux that has an unambiguous meaning given by its role in affecting a time change to the energy at a point in space.

We also encounter this form of a **gauge symmetry** in the potential vorticity flux discussed in VOLUME 3, as well as the vector streamfunction for a non-divergent flow in VOLUME 1. In some cases we can exploit the symmetry to our subjective desires, such as for choosing the potential vorticity. However, we know of no strategic use of gauge symmetry for the study of energy budgets.

10.6.5 Further study

The postulate of globally integrated total energy conservation in Section 10.6.1, and the associated discussion of energy budgets, follow that from Section 33 of [Serrin \(1959\)](#), Section II.4 of [DeGroot and Mazur \(1984\)](#), Chapter 14 of [Callen \(1985\)](#), Sections 49 and 58 of [Landau and Lifshitz \(1987\)](#), Chapters 3 and 4 of [Müller \(2006\)](#), Appendix B of [IOC et al. \(2010\)](#), Section 2.4 of [Olbers et al. \(2012\)](#), Chapter 1 of [Vallis \(2017\)](#), and Section 13.5.5 of [Thorne and Blandford \(2017\)](#).

10.7 Thermodynamic equilibrium with macroscopic motion

We derived the properties of a [local thermodynamic equilibrium](#) in Section 6.2.9 for a single component fluid, and in Section 7.2 for a binary fluid in the presence of a geopotential. We here extend those discussions to the case of a finite region of a fluid undergoing macroscopic motion in the absence of gravity. We assume no external forces or torques, so that the total linear momentum and total angular momentum remain constant. As in our earlier discussions, we derive the properties of thermodynamic equilibrium by assuming entropy is an extremum at equilibrium. Furthermore, the extremum must be consistent with the variety of conserved quantities, thus motivating the use of Lagrange multipliers as part of the formalism needed to determine the extremum.

10.7.1 Deriving the equilibrium conditions

To focus on the allowed macroscopic motion, we ignore external fields such as from gravity, in which case the total energy is the sum of the internal energy plus kinetic energy

$$\mathcal{E}^e = \mathcal{I}^e + P^2/(2M), \quad (10.94)$$

where $\mathbf{P} = M\mathbf{v}$ is the linear momentum of the system with velocity \mathbf{v} and mass M , and $P^2 = \mathbf{P} \cdot \mathbf{P}$ is the squared momentum. If the macroscopic system is materially and mechanically closed then total energy remains constant, as does the linear momentum and angular momentum. Thermodynamic equilibrium is realized by maximizing the function

$$\Psi = \mathcal{S}^e + \mathbf{A} \cdot \mathbf{P} + \mathbf{B} \cdot (\mathbf{x} \times \mathbf{P}), \quad (10.95)$$

where \mathbf{x} is the position of the macroscopic system, and the vectors \mathbf{A} and \mathbf{B} are constant Lagrange multipliers. Note that for convenience we assume the system to be macroscopically small but microscopically large (e.g., a fluid element) so that we can assign a single position to the system.

Should entropy be a function of the total energy (which is a constant of the motion) or remain a function of just the internal energy? To answer this question we appeal to the statistical interpretation of entropy whereby the number of microstates corresponding to a particular macrostate is invariant under a [Galilean transformation](#). The local rest state, where total energy equals to internal energy, is thus sufficient for defining the functional dependence¹²

$$\mathcal{S}^e = \mathcal{S}^e(V, \mathcal{I}^e) = \mathcal{S}^e[V, \mathcal{E}^e - P^2/(2M)]. \quad (10.96)$$

¹²See the footnote on page 36 of [Landau and Lifshitz \(1980\)](#) for more discussion of this point.

Hence, maximizing Ψ with respect to the linear momentum component, P^m , requires the derivative

$$\left[\frac{\partial S^e}{\partial P_m} \right]_V = \left[\frac{\partial S^e}{\partial J^e} \right]_V \frac{\partial J^e}{\partial P_m} = -\frac{1}{T} \frac{P^m}{M} = -\frac{v^m}{T}, \quad (10.97)$$

so that the macroscopic velocity at equilibrium is

$$\frac{\partial \Psi}{\partial P_m} = 0 \implies \mathbf{v} = T(\mathbf{A} + \mathbf{B} \times \mathbf{x}). \quad (10.98)$$

With temperature uniform throughout the macroscopic system at thermodynamic equilibrium, we find a velocity decomposed into a uniform translation plus a rigid-body rotation. That is, a closed macroscopic system in thermodynamic equilibrium can, at most, exhibit uniform translation plus rigid-body rotation. More general macroscopic motion is not possible when the system is in thermodynamic equilibrium. Furthermore, note that each component of the strain rate tensor vanishes for uniform translation plus a rigid-body rotation (see VOLUME 1). For the Newtonian fluids considered in this book, a zero strain rate tensor means there are no frictional stresses (Section 9.6.6), thus ensuring no frictionally generated entropy.

The [Cauchy-Stokes decomposition theorem](#) from VOLUME 1 shows that at each time instance, motion of a fluid element can be kinematically decomposed into translation, rotation, and dilation. Dilation occurs through mechanical work. In its absence, and without heating or mixing, the fluid element moves through sequences of translations and rotations that maintain thermodynamic equilibrium. With dilation, heating, and/or matter mixing, we conceive of a moving fluid as a continuum of fluid elements that, on a time scale that is tiny relative to macroscopic processes, adjusts to thermodynamic equilibrium in response to interactions with the surrounding fluid environment.

10.7.2 Further study

We here followed the discussion of §10 in [Landau and Lifshitz \(1980\)](#). See also a complementary discussion in Section 1.8 of [Kamenkovich \(1977\)](#), who considers a two-component fluid in the presence of gravity.

10.8 Bernoulli's theorem

The total energy equation (10.87) reveals that the material time change for the total energy of a fluid element is affected by the convergence of pressure times velocity. Hence, even in the absence of irreversible processes (i.e., a perfect fluid) and with a time-independent geopotential, the total energy of a fluid element is not materially invariant. The pressure flux, $p\mathbf{v}$, is a fundamental contribution to energy within the continuum. As shown in this section, it is the pressure work required for the fluid element to mechanically exist within the continuum. We thus refer to $p\mathbf{v}$ as the mechanical [injection work](#). This conceptualization of $p\mathbf{v}$ arises in the context of exploring the remarkably versatile [Bernoulli's theorem](#), which is particularly useful in diagnosing energetic properties of steady flows.

10.8.1 Bernoulli potential

Consider the flux-form equation for the total energy, (10.88), written here as

$$\partial_t(\rho\mathcal{E}) + \nabla \cdot [\rho\mathbf{v}(\mathcal{E} + p/\rho) + \mathbf{J}^{\text{therm}} + \mathbf{J}^{\text{chem}} - \mathbf{v} \cdot \mathbb{T}] = \rho\partial_t\Phi. \quad (10.99)$$

The left hand side indicates that total energy of a fluid element is locally modified by the advective transport of the quantity

$$\mathcal{E} + p/\rho = (\mathcal{K} + \Phi) + (\mathcal{J} + p/\rho) = \mathcal{M} + \mathcal{H} \equiv \mathcal{B}, \quad (10.100)$$

where we introduced the [Bernoulli potential](#), which is the sum of the mechanical energy per mass plus the enthalpy per mass

$$\mathcal{B} = \mathcal{M} + \mathcal{H} = \mathcal{K} + \Phi + \mathcal{J} + p/\rho. \quad (10.101)$$

For a perfect fluid there is no irreversible transfer of heat, matter, or momentum so that

$$\text{perfect fluid} \implies \mathbf{J}^{\text{therm}} = 0 \quad \text{and} \quad \mathbf{J}^{\text{chem}} = 0 \quad \text{and} \quad \mathbb{T} = 0. \quad (10.102)$$

Hence, we see that integration over a region with zero boundary transfer of $\mathbf{v} \cdot \mathcal{B}$ leads to the conservation of total energy for a perfect fluid with a time independent geopotential. Note that for some purposes it can be useful to write the total energy equation (10.99) as an equation for the Bernoulli function, which takes the form

$$\partial_t(\rho \mathcal{B}) + \nabla \cdot [\rho \mathbf{v} \cdot \mathcal{B} + \mathbf{J}^{\text{therm}} + \mathbf{J}^{\text{chem}} - \mathbf{v} \cdot \mathbb{T}] = \partial_t p + \rho \partial_t \Phi. \quad (10.103)$$

10.8.2 Mechanical injection work

Why is $\rho \mathcal{E}$ affected by the convergence of $\rho \mathbf{v} \cdot \mathcal{B}$ rather than the convergence of $\rho \mathbf{v} \cdot \mathcal{E}$? To answer this question,¹³ again note that the Bernoulli potential is the sum of the total energy per mass of a fluid element, \mathcal{E} , plus the term p/ρ . So what is p/ρ ? Imagine carving out a tiny region from within a continuous fluid with pressure, p , and specific volume, $1/\rho$, leaving behind a “hole”. The mechanical work required to carve out this hole is precisely equal to p/ρ . Correspondingly, we interpret p/ρ as the mechanical work required to inject a unit mass of fluid with specific volume $1/\rho$ into a region with pressure p . We thus refer to p/ρ as the [injection work](#), and we in turn see that specific enthalpy, $\mathcal{H} = \mathcal{J} + p/\rho$ (equation (10.75)), measures the internal energy plus the mechanical work required for a fluid element to exist within a continuum.

We can support the above interpretation by considering the flux, $\rho \mathbf{v} \cdot \mathcal{B}$, in a perfect fluid that penetrates a static closed fluid region

$$\oint_{\partial\mathcal{R}} \rho \mathbf{v} \cdot \hat{\mathbf{n}} \, d\mathcal{S} = \oint_{\partial\mathcal{R}} \rho \mathbf{v} \cdot \hat{\mathbf{n}} \, d\mathcal{S} + \oint_{\partial\mathcal{R}} p \mathbf{v} \cdot \hat{\mathbf{n}} \, d\mathcal{S}. \quad (10.104)$$

The first term on the right hand side is the flux of total energy (mechanical plus internal) that penetrates the region boundary, $\partial\mathcal{R}$. The second term is the mechanical work done by pressure acting on the boundary. The example in Section 10.8.5 further supports this perspective, whereby we develop the energetics of a control volume of fluid moving through a pipe.

10.8.3 Bernoulli's theorem for a steady perfect fluid

Consider a perfect fluid flow in steady state (vanishing Eulerian time derivatives). Steady state mass continuity means that

$$\partial_t \rho = -\nabla \cdot (\rho \mathbf{v}) = 0. \quad (10.105)$$

¹³The argument presented here follows Section 13.5.4 of [Thorne and Blandford \(2017\)](#) as well as Section 6 of [Landau and Lifshitz \(1987\)](#).

This relation, along with a steady state energy in equation (10.99) (absent friction, heating, mixing, and with a time-independent geopotential), means that the steady state velocity field is locally tangent to isosurfaces of the Bernoulli potential

$$\mathbf{v} \cdot \nabla \mathcal{B} = 0. \quad (10.106)$$

We thus see that the Bernoulli potential is constant along streamlines in a steady perfect fluid, which is a result known as [Bernoulli's theorem](#). Hence, as the steady flow moves along a streamline, there is an exchange between the total energy per mass, \mathcal{E} , and the injection work, p/ρ , such that their sum remains constant.

A constant Bernoulli potential for steady flow is used frequently in engineering fluid dynamics to interpret flow around objects, such as for flow around a wing, in which case the sum $p + \rho \mathbf{v}^2/2$ is sometimes referred to as the [total pressure](#) or [stagnation pressure](#). It leads to a realization of [Bernoulli's principle](#), whereby in regions of steady flows with relatively low pressure, the energy per mass is relatively large, whereas the converse holds in regions of high pressure. The change in energy is largely due to a change in the kinetic energy, so that flow is fast in regions of low pressure (e.g., top of the wing, flow around a train moving through a tunnel) and slow in regions of high pressure (e.g., bottom of the wing).¹⁴ That is, the Bernoulli principle provides an energetic expression for why a fluid slows down when moving into a region of relatively high pressure, and speeds up when moving to a region of low pressure.

10.8.4 Traditional derivation of Bernoulli's theorem

For completeness we offer a second derivation of Bernoulli's theorem that follows a more traditional route and reveals some useful manipulations. For this purpose, convert the advective-form momentum equation (8.24) into its vector-invariant form as in Section 8.4 by making use of the vector identity

$$\boldsymbol{\omega} \times \mathbf{v} = -\mathcal{K} + (\mathbf{v} \cdot \nabla) \mathbf{v}, \quad (10.107)$$

where $\boldsymbol{\omega} = \nabla \times \mathbf{v}$ is the vorticity. This identity allows us to eliminate velocity self-advection in favor of the [vorticity](#) and kinetic energy per mass

$$\partial_t \mathbf{v} + \boldsymbol{\omega}_a \times \mathbf{v} = -\rho^{-1} \nabla p - \nabla \mathcal{M}, \quad (10.108)$$

where

$$\boldsymbol{\omega}_a = \boldsymbol{\omega} + 2\boldsymbol{\Omega} \quad (10.109)$$

is the [absolute vorticity](#) and we set the irreversible terms to zero since we are assuming a perfect fluid. Hence, the Eulerian time evolution for the kinetic energy per mass is given by

$$\partial_t \mathcal{K} = -\rho^{-1} \mathbf{v} \cdot \nabla p - \mathbf{v} \cdot \nabla \mathcal{M}, \quad (10.110)$$

where we set $\mathbf{v} \cdot (\boldsymbol{\omega}_a \times \mathbf{v}) = 0$.

For Bernoulli's theorem we are interested in the steady state, with a steady kinetic energy per mass realized by the balance

$$\rho^{-1} \mathbf{v} \cdot \nabla p = -\mathbf{v} \cdot \nabla \mathcal{M}. \quad (10.111)$$

¹⁴See [this discussion and video](#) for why it is physically incorrect to use Bernoulli's theorem for explaining the lift on an airplane wing.

We can connect this steady state balance to the Bernoulli potential by noting that for a steady perfect and single-component fluid, equation (10.66) allows us to write

$$\rho^{-1} \mathbf{v} \cdot \nabla p = \mathbf{v} \cdot (\nabla \mathcal{H} - T \nabla \mathcal{S}). \quad (10.112)$$

Combining with equation (10.111) renders

$$\mathbf{v} \cdot (\nabla \mathcal{H} + \nabla \mathcal{M} - T \nabla \mathcal{S}) = \mathbf{v} \cdot (\nabla \mathcal{B} - T \nabla \mathcal{S}) = 0. \quad (10.113)$$

A perfect fluid maintains materially constant specific entropy (Section 10.5.8), which in a steady state means that

$$\mathbf{v} \cdot \nabla \mathcal{S} = 0 \quad \text{and} \quad \mathbf{v} \cdot \nabla \mathcal{B} = 0 \quad \iff \text{steady state perfect fluid.} \quad (10.114)$$

That is, for a steady perfect fluid the velocity is aligned with isosurfaces of specific entropy and Bernoulli potential.

10.8.5 Steady flow in a pipe

To help further understand Bernoulli's theorem and the contribution from the mechanical work provided by pressure forces, consider the steady flow of a constant density perfect fluid in a frictionless pipe as depicted in Figure 10.1. For this system, Bernoulli's theorem says that the following simplified form of the Bernoulli potential is constant for flow along a streamline

$$\mathcal{B} = \mathbf{v}^2/2 + p/\rho + g z = \text{constant}. \quad (10.115)$$

Note that internal energy dropped out since for a constant density fluid the internal energy is a constant and so plays no role in the energetics. Equation (10.115) means that there is a precise balance between the kinetic energy per mass, injection work, and geopotential for a steady and constant density fluid. For example, for flow following a constant geopotential, pressure is relatively low in regions of large kinetic energy whereas pressure is relatively high in regions of small kinetic energy. We further pursue this understanding by showing that the statement (10.115) of Bernoulli's theorem can be derived through traditional energetic arguments, whereby the mechanical work done on the fluid system equals to the system's change in kinetic energy, thus manifesting the [work-energy theorem](#).

For this purpose, let the system under examination be a control volume of fluid as described in the caption to Figure 10.1, and examine the work done on the control volume over an arbitrary time increment, Δt . During this time, a mass of fluid given by

$$M = \rho A_1 u_1 \Delta t = \rho A_2 u_2 \Delta t, \quad (10.116)$$

moves through the pipe, with $A_1 u_1 = A_2 u_2$ following from volume conservation, and we assumed that the $u_{1,2} = \Delta x_{1,2}/\Delta t$ measures the average velocity across the pipe cross-section. Mechanical work is applied to the fluid in the control volume by pressure acting on the end caps (contact force) and by gravity acting throughout the fluid (body force).

- **PRESSURE WORK:** At the left end cap, pressure from fluid to the left of the control volume does work on the control volume by the amount $p_1 A_1 \Delta x_1 = p_1 M/\rho$. On the right end, the control volume does work on the fluid to its right, which means that a negative work is applied to the control volume in the amount $-p_2 A_2 \Delta x_2 = -p_2 M/\rho$.

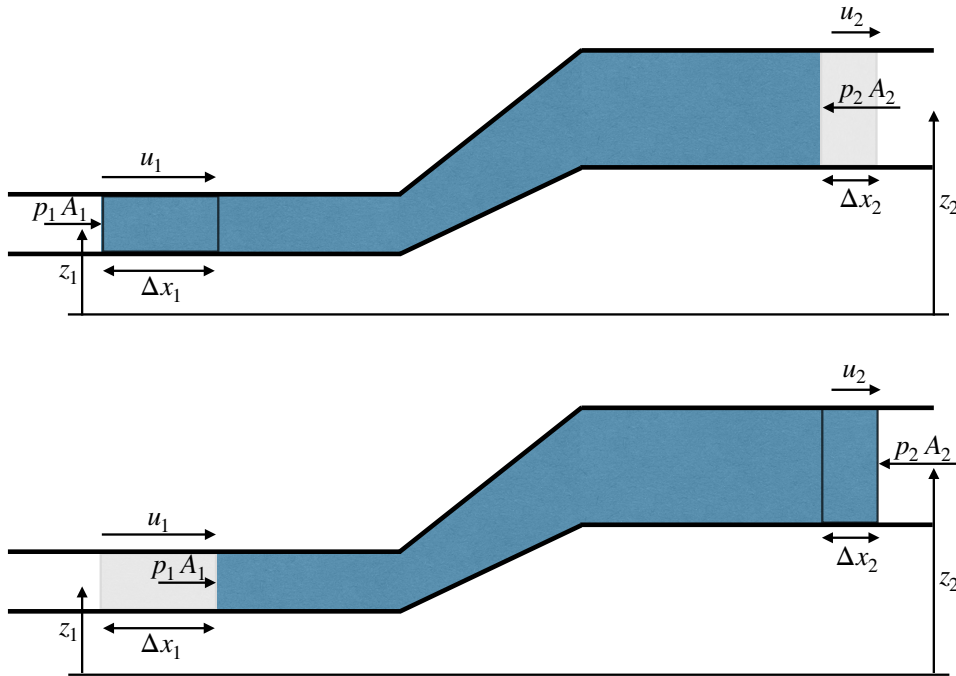


FIGURE 10.1: An example to illustrate the basic physics of Bernoulli's theorem and pressure work, whereby we depict the flow of a perfect and constant density fluid from left to right in a pipe of variable cross-section and variable height. We study the energetics of a control volume (dark blue region) moving with the fluid. The top panel shows the control volume at one time and the lower panel shows the control volume at a time Δt later, after which a mass of fluid, M , has moved through the system. Volume conservation means that $(u_1 \Delta t) A_1 = (u_2 \Delta t) A_2$, where $\Delta x_{1,2}$ is the horizontal displacement of the fluid plug over time Δt , $u_{1,2}$ is the cross-sectional area average velocity, $A_{1,2}$ is the pipe cross-sectional area, and $M = \rho \Delta x_1 A_1 = \rho \Delta x_2 A_2$ is the mass of fluid moving over the Δt time increment. Pressure forces, $p_{1,2}$, at the end caps point inward (compressive), with pressure on the left larger than that on the right to support the fluid moving to the right. As the fluid moves upward it increases its gravitational potential energy and in so doing the fluid does work against gravity.

- GRAVITATIONAL WORK: Fluid downstream at the right end is higher than fluid upstream on the left end. The control volume must do work against gravity to achieve this altitude increase and this work is given by $-g M (z_2 - z_1)$.

As the fluid moves from left to right, the control volume changes its kinetic energy by the amount $(M/2)(u_2^2 - u_1^2)$. Equating this kinetic energy change to the work applied to the control volume renders

$$(1/2)(u_2^2 - u_1^2) = (1/\rho)(p_1 - p_2) - g(z_2 - z_1), \quad (10.117)$$

where the mass, M , dropped out. Rearrangement then leads to

$$u^2/2 + p/\rho + g z = \text{constant}, \quad (10.118)$$

which is a statement of Bernoulli's theorem (10.115).

Making use of volume conservation allows us to rearrange equation (10.117) to determine the pressure difference between the left and right end of the pipe

$$p_1 - p_2 = \rho g (z_2 - z_1) - (\rho/2) u_1^2 [1 - (A_1/A_2)^2]. \quad (10.119)$$

To help understand this result, consider two special cases starting with $A_1 = A_2$. We see that for equal cross-sectional areas, the pressure drop equals to the increase in gravitational potential

energy,

$$p_1 - p_2 = \rho g (z_2 - z_1) > 0 \quad \text{with } A_2 = A_1, \quad (10.120)$$

so that the pressure work equals to the gravitational work required to lift the fluid. Next consider $z_2 = z_1$ so that there is no change in gravitational potential energy but there is a change in cross-sectional area, in which case

$$p_1 - p_2 = -(\rho/2) u_1^2 [1 - (A_1/A_2)^2] < 0 \quad \text{with } z_2 = z_1. \quad (10.121)$$

In this case there is a pressure increase as the fluid moves into a region with larger cross-sectional area ($A_2 > A_1$). This pressure increase slows the fluid speed, which accords with volume conservation.

These examples support our understanding of how pressure provides mechanical work on fluid control volume boundaries, with that work required to maintain conservation of mechanical energy (seen in the above case with $A_2 = A_1$) and conservation of volume (see in the above case with $z_2 = z_1$). Indeed, taking the control volume to be a tiny fluid element furthers our understanding of the p/ρ injection work contribution to the Bernoulli potential (10.100).

10.8.6 Steady flow over a topographic bump

We build from the discussion of steady pipe flow in Section 10.8.5 by describing a more geophysically relevant case of steady single-component perfect fluid flowing over a topographic bump. In Figure 10.2 we illustrate this flow in the absence of rotation. As the fluid moves over the bump, it speeds up in order to maintain volume continuity. In regions of faster flow, Bernoulli's theorem (10.115) says that the pressure is lower, which is realized here by a lowering of the sea surface height over the bump. For a small bump, we can imagine that the flow remains symmetric with respect to the bump, so that the flow downstream of the bump is a reflection of the upstream flow. To maintain steady flow in the presence of a larger bump requires a larger pressure drop, which will eventually break the symmetry between downstream and upstream. For an even larger topographic bump, we find there is no way to satisfy Bernoulli's theorem, in which case the flow transitions into a time dependent [hydraulic jump](#).

As for the pipe flow, the steady flow maintains two flow constants: the volume flow rate and the simplified form of the Bernoulli potential in equation (10.115)

$$\mathcal{T} = v h \Delta \quad \text{and} \quad \mathcal{B} = v^2/2 + p/\rho + g z, \quad (10.122)$$

where h is the thickness of the layer and Δ the width in the direction perpendicular to the flow. Also, recall that the Bernoulli potential is a constant along a particular streamline. However, for a constant density layer the Bernoulli potential is independent of depth, as we illustrate below. For simplicity we assume the flow is only a function of the along-stream coordinate, y , and furthermore assume the pressure on the upper interface is a uniform constant p_a . We also assume the top and bottom interfaces of the layer are material, which then means they are each streamlines.

It is more convenient to work with the flow rate, $\mathcal{T} = v h \Delta$, than the velocity, v , in which case the Bernoulli potential is given by

$$\mathcal{B} = \mathcal{T}^2/(2 h^2 \Delta^2) + p/\rho + g z. \quad (10.123)$$

Far upstream of the bump the layer thickness takes on its unperturbed value, H , so that the

Bernoulli potential along the surface streamline at $z = H$ is given by

$$\mathcal{B} = \mathcal{T}^2/(2H^2\Delta^2) + p_a/\rho + gH. \quad (10.124)$$

Notice how every term on the right hand side is positive, so that $\mathcal{B} > 0$. Also notice that the Bernoulli potential along the bottom streamline takes the same value

$$\mathcal{B} = \mathcal{T}^2/(2H^2\Delta^2) + p_b/\rho = \mathcal{T}^2/(2H^2\Delta^2) + (p_a + \rho h H)/\rho, \quad (10.125)$$

which results since the layer has constant density. Now express the Bernoulli potential in a region affected by the bump, in which case

$$\mathcal{B} = \mathcal{T}^2/(2h^2\Delta^2) + p_a/\rho + g\eta = \mathcal{T}^2/(2h^2\Delta^2) + p_a/\rho + g(h + \eta_b). \quad (10.126)$$

We observe that

$$\mathcal{B} - g\eta_b = \mathcal{T}^2/(2h^2\Delta^2) + p_a/\rho + gh \geq 0, \quad (10.127)$$

with this quantity referred to as the *Bernoulli head*. The condition $\mathcal{B} - g\eta_b \geq 0$ holds so long as the flow maintains the assumptions of Bernoulli's theorem. However, if the topography is too tall, then $\mathcal{B} - g\eta_b \leq 0$, in which case the flow can no longer satisfy the Bernoulli theorem. This result leads us to define a critical topography height

$$\eta_b^{\text{crit}} = \mathcal{B}/g = \mathcal{T}^2/(2H^2\Delta^2g) + p_a/(\rho g) + H. \quad (10.128)$$

When topography is larger than this height, the flow cannot reach a steady state and/or the flow develops a dependence on the direction perpendicular to the page. In either case, the assumptions of Bernoulli's theorem breakdown.

10.8.7 Further study

For an examination of Bernoulli's theorem for flows in a non-rotating reference frame, such as flow in laminar boundary layers, see [this video](#) from Prof. Shapiro. Chapter 3 of [Acheson \(1990\)](#) and the text from [Pratt and Whitehead \(2008\)](#) make use of Bernoulli's theorem for understanding flows over obstacles with and without the Coriolis acceleration, with Section 1.4 of [Pratt and Whitehead \(2008\)](#) forming the basis for the discussion in Section 10.8.6. See also Exercise 8.6 of [Klinger and Haine \(2019\)](#).

10.9 Entropy budget for the ocean

In this section we consider the entropy budget for the ocean and make use of the [second law of thermodynamics](#) to infer specific forms for the thermal and chemical fluxes introduced in Section 10.5.6. The discussion also holds for the atmosphere in the absence of phase transitions, though we focus on the ocean application to be specific. Hence, the matter concentration in this section is the salt concentration for seawater.

The entropy budget follows by rearranging the enthalpy equation (10.76)

$$T\rho\frac{D\mathcal{S}}{Dt} = \rho\frac{D\mathcal{H}}{Dt} - \frac{Dp}{Dt} - \mu\rho\frac{DC}{Dt}, \quad (10.129)$$

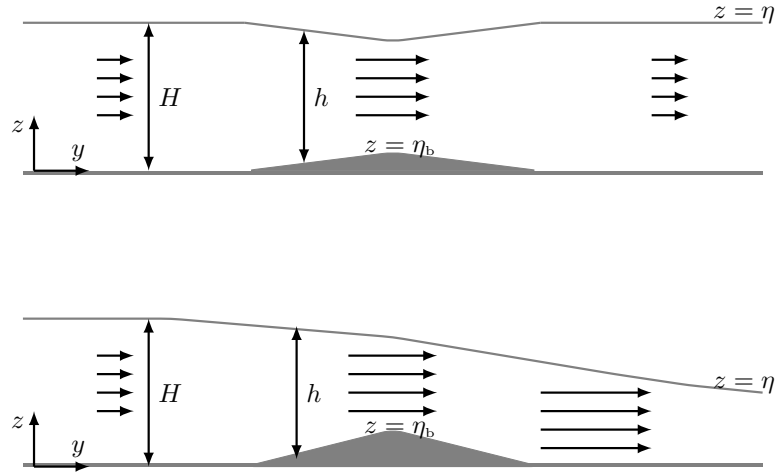


FIGURE 10.2: Depicting steady flow of a single-component fluid with constant density, ρ , flowing over a topographic bump and viewed from a non-rotating reference frame so there is no Coriolis acceleration. We assume all properties are a function only of the along-stream position, y , and $z = 0$ is taken at the position of a flat topography. For steady flow of a constant density fluid, the volume transport, \mathcal{T} , is constant and given by $\mathcal{T} = v h \Delta$, where Δ is the width of the flow in the direction perpendicular to the page, and $h = \eta - \eta_b$ is the layer thickness. The simplified form of the Bernoulli potential given by equation (10.115) is also constant along any streamline, $\mathcal{B} = v^2/2 + p/\rho + g z = \text{constant}$. The top panel shows the flow for a very small topographic bump, so that the flow is symmetric around the bump. The lower panel show flow for a larger bump that requires more fluid upstream of the bump to support enough pressure drop for steady flow to make it over the bump.

with the enthalpy budget in the form (10.91) yielding

$$T \rho \frac{D\mathcal{S}}{Dt} = -\nabla \cdot (\mathbf{J}^{\text{therm}} + \mathbf{J}^{\text{chem}}) + \rho \epsilon + \mu \nabla \cdot \mathbf{J}^C, \quad (10.130)$$

where we wrote the tracer equation as

$$\rho \frac{DC}{Dt} = -\nabla \cdot \mathbf{J}^C, \quad (10.131)$$

for some tracer flux, \mathbf{J}^C . Through manipulations pursued in Section 10.9.1, we identify a non-advection entropy flux and a corresponding entropy source. This form of the entropy budget is useful since we can then invoke the second law of thermodynamics to insist that the entropy source is non-negative, and that statement renders some constraints on the thermal and chemical fluxes.

10.9.1 Non-advection entropy flux and entropy source

To start the manipulations, divide the entropy equation (10.130) by T and rewrite in terms of a flux convergence plus a source

$$\rho \frac{D\mathcal{S}}{Dt} = -\nabla \cdot \left[\frac{\mathbf{J}^{\text{therm}} + \mathbf{J}^{\text{chem}} - \mu \mathbf{J}^C}{T} \right] + \nabla(1/T) \cdot (\mathbf{J}^{\text{therm}} + \mathbf{J}^{\text{chem}} - \mu \mathbf{J}^C) - (\mathbf{J}^C/T) \cdot \nabla \mu + \frac{\rho \epsilon}{T}. \quad (10.132)$$

Recall from the identity (10.81) that we can write the chemical energy flux as

$$\mathbf{J}^{\text{chem}} = \left[\frac{\partial \mathcal{H}}{\partial C} \right]_{T,p} \mathbf{J}^C = \left[\mu - T \left[\frac{\partial \mu}{\partial T} \right]_{C,p} \right] \mathbf{J}^C = (\mu - T \mu_T) \mathbf{J}^C, \quad (10.133)$$

where we introduced a shorthand for the third equality. This identity then leads to

$$\mathbf{J}^{\text{chem}} - \mu \mathbf{J}^C = -T \mu_T \mathbf{J}^C, \quad (10.134)$$

in which case the entropy equation (10.132) becomes

$$\rho \frac{D\mathcal{S}}{Dt} = -\nabla \cdot \left[\frac{\mathbf{J}^{\text{therm}} - T \mu_T \mathbf{J}^C}{T} \right] + \nabla(1/T) \cdot (\mathbf{J}^{\text{therm}} - T \mu_T \mathbf{J}^C) - (\mathbf{J}^C/T) \cdot \nabla \mu + \frac{\rho \epsilon}{T}. \quad (10.135)$$

We thus identify the non-advection entropy flux

$$\mathbf{J}^s = \frac{\mathbf{J}^{\text{therm}}}{T} - \left[\frac{\partial \mu}{\partial T} \right]_{p,C} \mathbf{J}^C = \frac{\mathbf{J}^{\text{therm}}}{T} + \left[\frac{\partial \mathcal{S}}{\partial C} \right]_{T,p} \mathbf{J}^C, \quad (10.136)$$

where the second equality made use of the Maxwell relation

$$-\left[\frac{\partial \mathcal{S}}{\partial C} \right]_{T,p} = \left[\frac{\partial \mu}{\partial T} \right]_{p,C}, \quad (10.137)$$

which is derived as part of the solution to Exercise 6.5. The additional terms comprise the entropy source

$$\Sigma^s = \frac{\rho \epsilon}{T} + \nabla(1/T) \cdot (\mathbf{J}^{\text{therm}} - T \mu_T \mathbf{J}^C) - (\mathbf{J}^C \cdot \nabla \mu)/T \quad (10.138a)$$

$$= \frac{\rho \epsilon}{T} + \frac{\nabla T}{T^2} \cdot (T \mu_T \mathbf{J}^C - \mathbf{J}^{\text{therm}}) - (\mathbf{J}^C \cdot \nabla \mu)/T \quad (10.138b)$$

$$= \frac{\rho \epsilon}{T} - \frac{\nabla T \cdot \mathbf{J}^{\text{therm}}}{T^2} + \frac{\mathbf{J}^C \cdot (\mu_T \nabla T - \nabla \mu)}{T} \quad (10.138c)$$

$$= \frac{\rho \epsilon}{T} - \frac{\nabla T \cdot \mathbf{J}^{\text{therm}}}{T^2} - \frac{\mathbf{J}^C \cdot (\mu_C \nabla C + \mu_p \nabla p)}{T} \quad (10.138d)$$

$$= \frac{\rho \epsilon}{T} - \frac{\nabla T \cdot \mathbf{J}^{\text{therm}}}{T^2} - \frac{\mathbf{J}^C}{T} \cdot \left[\left[\frac{\partial \mu}{\partial C} \right]_{T,p} \nabla C + \left[\frac{\partial \mu}{\partial p} \right]_{T,C} \nabla p \right], \quad (10.138e)$$

where we wrote the gradient of the chemical potential, $\mu(T, p, C)$, as

$$\nabla \mu = \left[\frac{\partial \mu}{\partial T} \right]_{p,C} \nabla T + \left[\frac{\partial \mu}{\partial p} \right]_{T,C} \nabla p + \left[\frac{\partial \mu}{\partial C} \right]_{T,p} \nabla C = \mu_T \nabla T + \mu_p \nabla p + \mu_C \nabla C. \quad (10.139)$$

The non-advection entropy flux (10.136) arises from the thermal and chemical fluxes, and the entropy source (10.138e) includes contributions from those fluxes as well as the frictional dissipation of mechanical energy.

10.9.2 Constraints from the second law of thermodynamics

The second law of thermodynamics states that the entropy source is non-negative¹⁵

$$\Sigma^s \geq 0. \quad (10.140)$$

This condition imposes constraints on the frictional dissipation, thermal flux, and tracer flux. Since frictional dissipation in Newtonian fluids (equation (10.48)) is non-negative, $\epsilon \geq 0$, we make use of the second law to constrain just the thermal flux and tracer flux. Furthermore, recall from equation (10.78) that the thermal flux is comprised of a radiant flux and conductive flux. We assume that radiant flux is determined by processes external to the fluid (e.g., shortwave radiation that penetrates into the upper ocean). We thus use the second law to constrain just the conductive portion of the thermal flux along with the tracer flux. That is, from the entropy source (10.138e) we have the second law constraint

$$-\nabla T \cdot \mathbf{J}^{\text{cond}} - T \mu_C \mathbf{J}^C \cdot \left[\nabla C + \frac{\mu_p}{\mu_C} \nabla p \right] \geq 0. \quad (10.141)$$

This constraint can be satisfied by assuming the conductive and tracer fluxes are of the form

$$\rho^{-1} \mathbf{J}^{\text{cond}} = -c_p \kappa_T \nabla T - \kappa_{TC} \left[\nabla C + \frac{\mu_p}{\mu_C} \nabla p \right] \quad (10.142a)$$

$$\rho^{-1} \mathbf{J}^C = -\kappa_C \left[\nabla C + \frac{\mu_p}{\mu_C} \nabla p \right] - \kappa_{CT} \nabla T. \quad (10.142b)$$

The variety of molecular fluxes

The first term in the conductive thermal flux (10.142a) is known as Fourier's law of conduction

$$\mathbf{J}_{\text{Fourier}}^{\text{cond}} = -\rho c_p \kappa_T \nabla T, \quad (10.143)$$

in which case the conductive thermal flux is directed down the gradient of the *in situ* temperature. The second term leads to a conductive thermal flux in the presence of matter concentration gradients and pressure gradients, and this process is known as the Dufour effect

$$\mathbf{J}_{\text{Dufour}}^{\text{cond}} = -\rho \kappa_{TC} \left[\nabla C + \frac{\mu_p}{\mu_C} \nabla p \right]. \quad (10.144)$$

The first term in the matter flux (10.142b) is known as Fick's law of diffusion

$$\mathbf{J}_{\text{Fick}}^C = -\rho \kappa_C \nabla C. \quad (10.145)$$

The second term in the matter flux (10.142b) is known as barodiffusion

$$\mathbf{J}_{\text{barodiff}}^C = -(\rho \kappa_{CT} \mu_p / \mu_C) \nabla p, \quad (10.146)$$

¹⁵In Exercise 10.10 we discuss Boltzmann's H-theorem, which provides one means to prove that entropy increases as a system approaches thermodynamic equilibrium.

which is a matter flux arising from a pressure gradient. Finally, the matter flux arising from temperature gradients is known as the **Soret effect**

$$\mathbf{J}_{\text{Soret}}^C = -\rho \kappa_{CT} \nabla T. \quad (10.147)$$

Thermodynamic equilibrium and the vertical gradient of salinity

In Section 7.2, we learned that thermodynamic equilibrium for a fluid in a gravity field leads to a uniform temperature, T , and a pressure in exact hydrostatic balance. The salt flux must vanish in thermodynamic equilibrium, but in the presence of a pressure gradient we have a nonzero vertical salinity gradient from equation (10.142b) given by

$$\frac{dC}{dz} = -\frac{\mu_p}{\mu_C} \frac{dp}{dz} = \frac{\mu_p \rho g}{\mu_C}. \quad (10.148)$$

This relation is identical to equation (7.21) resulting from our study of conditions for thermodynamic equilibrium of a binary fluid in a gravity field. It is satisfying to see the same thermodynamic equilibrium condition arise from the rather different path taken here.

Invoking Onsager reciprocity condition

The **Onsager reciprocity conditions**¹⁶ are now invoked to relate the two off-diagonal coefficients according to

$$T \mu_C \kappa_{CT} = \kappa_{TC}, \quad (10.149)$$

which brings the entropy condition to the form

$$c_p \kappa_T |\nabla T|^2 + \kappa_C \mu_C T \left| \nabla C + \frac{\mu_p}{\mu_C} \nabla p \right|^2 + 2 \kappa_{TC} \nabla T \cdot \left[\nabla C + \frac{\mu_p}{\mu_C} \nabla p \right] \geq 0. \quad (10.150)$$

This condition then constrains the phenomenological constants κ_C , κ_T and κ_{TC} so that

$$|\kappa_{TC}|^2 \leq \kappa_T \kappa_C c_p T \mu_S. \quad (10.151)$$

Comments on measurements

The cross-diffusion coefficients, κ_{TC} and κ_{CT} , are both measured to be very small for seawater, so that the **Dufour effect** and **Soret effect** are commonly ignored. Furthermore, in an ocean in thermodynamic equilibrium, the vertical salinity gradient implied by equation (10.148) is roughly 3 g kg^{-1} per 1000 m. This vertical salinity gradient is far larger than measured in the ocean, thus providing evidence that turbulent fluxes, even in the ocean interior, dominate over molecular fluxes. That is, the observed ocean has sufficient turbulence to keep it well away from thermodynamic equilibrium.

¹⁶See Chapter 14 of [Callen \(1985\)](#) for more on the Onsager reciprocity conditions, along with their underlying dynamical connections.

10.9.3 A summary presentation

We here summarize the previous material by skipping details for the entropy flux, thermal flux, and matter flux. For this purpose, write the budget for the total energy in the form

$$\rho \frac{D\mathcal{E}}{Dt} = -\nabla \cdot (p\mathbf{v} - \mathbf{v} \cdot \mathbb{T}) + \rho \left[-\epsilon + T \frac{D\mathcal{S}}{Dt} + \mu \frac{DC}{Dt} \right] + \rho \partial_t \Phi. \quad (10.152)$$

Now assume that the specific entropy and matter concentration satisfy the evolution equations

$$\rho \frac{D\mathcal{S}}{Dt} = -\nabla \cdot \mathbf{J}^s + \Sigma^s \quad \text{and} \quad \rho \frac{DC}{Dt} = -\nabla \cdot \mathbf{J}^C, \quad (10.153)$$

thus rendering

$$\rho \left[T \frac{D\mathcal{S}}{Dt} + \mu \frac{DC}{Dt} \right] = -T \nabla \cdot \mathbf{J}^s + T \Sigma^s - \mu \nabla \cdot \mathbf{J}^C \quad (10.154a)$$

$$= -\nabla \cdot (T \mathbf{J}^s + \mu \mathbf{J}^C) + \nabla T \cdot \mathbf{J}^s + \nabla \mu \cdot \mathbf{J}^C + T \Sigma^s, \quad (10.154b)$$

which then brings the total energy equation (10.152) into the form

$$\rho \frac{D\mathcal{E}}{Dt} = -\nabla \cdot (p\mathbf{v} - \mathbf{v} \cdot \mathbb{T} + T \mathbf{J}^s + \mu \mathbf{J}^C) + [-\rho \epsilon + \nabla T \cdot \mathbf{J}^s + \nabla \mu \cdot \mathbf{J}^C + T \Sigma^s] + \rho \partial_t \Phi. \quad (10.155)$$

We now postulate that the globally integrated total energy is constant in the absence of boundary processes and with a time independent geopotential. In the presence of mechanical dissipation and matter constituent mixing, a necessary condition for such global energy conservation is for the specific entropy source to take the form

$$T \Sigma^s = \rho \epsilon - \nabla T \cdot \mathbf{J}^s - \nabla \mu \cdot \mathbf{J}^C. \quad (10.156)$$

That is, the entropy source arises from frictional dissipation, entropy mixing, and matter mixing. With this form for the entropy source, the total energy budget (10.155) is given by the material form and the equivalent flux-form expressions

$$\rho \frac{D\mathcal{E}}{Dt} = -\nabla \cdot (p\mathbf{v} - \mathbf{v} \cdot \mathbb{T} + T \mathbf{J}^s + \mu \mathbf{J}^C) + \rho \partial_t \Phi \quad (10.157a)$$

$$\frac{\partial(\rho\mathcal{E})}{\partial t} = -\nabla \cdot (\mathcal{E}\mathbf{v} + p\mathbf{v} - \mathbf{v} \cdot \mathbb{T} + T \mathbf{J}^s + \mu \mathbf{J}^C) + \rho \partial_t \Phi. \quad (10.157b)$$

The modified form of the internal energy budget (10.74) is found by subtracting the mechanical energy budget (10.52) from the total energy budget (10.157a)

$$\rho \frac{D\mathcal{J}}{Dt} = \rho \frac{D(\mathcal{E} - \mathcal{M})}{Dt} = -p \nabla \cdot \mathbf{v} - \nabla \cdot (T \mathbf{J}^s + \mu \mathbf{J}^C) + \rho \epsilon. \quad (10.158)$$

The corresponding enthalpy budget (10.76) is given by

$$\rho \frac{D\mathcal{H}}{Dt} - \frac{Dp}{Dt} = -\nabla \cdot (T \mathbf{J}^s + \mu \mathbf{J}^C) + \rho \epsilon = -\nabla \cdot \mathbf{J}^H + \rho \epsilon. \quad (10.159)$$

In the second equality we defined the enthalpy flux

$$\mathbf{J}^H = T \mathbf{J}^s + \mu \mathbf{J}^C \quad (10.160a)$$

$$= \mathbf{J}^{\text{therm}} - T \left[\frac{\partial \mu}{\partial T} \right]_{p,C} \mathbf{J}^C + \mu \mathbf{J}^C \quad (10.160\text{b})$$

$$= \mathbf{J}^{\text{therm}} + \left[\frac{\partial \mathcal{H}}{\partial C} \right]_{T,p} \mathbf{J}^C \quad (10.160\text{c})$$

$$= \mathbf{J}^{\text{therm}} + \mathbf{J}^{\text{chem}}, \quad (10.160\text{d})$$

where we used equation (10.136) for the entropy flux, \mathbf{J}^s , equation (10.133) for the chemical flux, \mathbf{J}^{chem} , and the thermodynamic identity (10.81) for the third equality. Furthermore, recall that the thermal flux, $\mathbf{J}^{\text{therm}}$, is the sum of a conductive plus radiative contribution as per equation (10.78).

10.9.4 Comments

It is remarkable how the second law of thermodynamics predicts new physical processes through considering the various forms that the thermal and matter fluxes can take to ensure a positive entropy source. [Caldwell \(1973\)](#) and [Caldwell and Eide \(1981\)](#) estimate the Soret effect for seawater, where they propose some relevance of this effect in quiescent ocean regions with strong gradients. In contrast, for liquids the Dufour effect is about 1000 times smaller than Fickian heat conduction and so it is safely ignored throughout the ocean. [McDougall and Turner \(1982\)](#) and [McDougall \(1983\)](#) studied double-diffusive convection in the presence of cross-diffusion, extending the ocean applications to arbitrary solutions with a pair of solutes. None of these studies consider the role of pressure gradients in generating fluxes.

For most purposes of ocean physics, the fluxes considered in this section are far smaller than those induced by turbulent flow processes. In this case, the flux relations reduce to the Fickian and Fourier expressions yet with turbulent exchange coefficients rather than their molecular values. Turbulence thus makes molecular diffusive processes generally negligible for the ocean. Indeed, we already made this conclusion when noting that thermodynamic equilibrium implies a sizable vertical salinity gradient as given by equation (10.148). Whereas turbulence acts to produce a homogenous salinity (as well as potential temperature and potential enthalpy), molecular diffusion leads to a rather large vertical salinity gradient. Since the vertical salinity gradient implied by thermodynamic equilibrium is much larger than that measured in the ocean, we conclude that the ocean is far from a thermodynamic equilibrium.

10.9.5 Further study

Much of our presentation in this section followed that from Sections 2.4 and 2.5 from [Olbers et al. \(2012\)](#) and Appendix B of [IOC et al. \(2010\)](#). [Graham and McDougall \(2013\)](#) extend these ideas to a turbulent ocean. The physical ideas underlying the Onsager reciprocity conditions are lucidly discussed in Chapter 14 of [Callen \(1985\)](#).

10.10 Temperature evolution

In specifying the state of a fluid element it is sensible to make use of the temperature, pressure, and tracer concentration given that these state properties are readily measured in the laboratory and environment. Furthermore, these properties are the natural variables for the Gibbs potential (Section 6.6.5). Hence, given values for (T, p, C) we can determine the Gibbs potential and then determine all other thermodynamic properties by taking partial derivatives.

How do we specify the evolution of (T, p, C) for a fluid element? Evolution of the matter concentration follows from the tracer equation (an advection-diffusion equation) as developed in VOLUME 1. Pressure measures the compressive stress acting on each fluid element (Section 9.6), with its specification depending on the dominant dynamical balances (see Section 10.12). Temperature reflects the energy of the internal microscopic degrees of freedom within a fluid element, with its evolution the subject of this section. We show how Conservative Temperature, Θ , rather than *in situ* temperature, T , or potential temperature, θ , offers the simplest prognostic equation of the three temperature variables. The key reason is that Θ evolves almost precisely like a material tracer, driven by the convergence of fluxes, whereas the equations for T and θ contain extra source terms in addition to flux convergences.

10.10.1 Evolution of *in situ* temperature

In developing the temperature equation it is useful to start from the prognostic equation for enthalpy as developed in Sections 10.5.5. For that purpose we write the enthalpy equation (10.159) as

$$\rho \frac{D\mathcal{H}}{Dt} = \frac{Dp}{Dt} - \nabla \cdot \mathbf{J}^{\mathcal{H}} + \rho \epsilon, \quad (10.161)$$

with the enthalpy flux, $\mathbf{J}^{\mathcal{H}}$, written in terms of the entropy and tracer fluxes as per equation (10.160d).

To reveal a prognostic equation for temperature, we write enthalpy as a function of (T, p, C) so that

$$\frac{D\mathcal{H}}{Dt} = \left[\frac{\partial \mathcal{H}}{\partial T} \right]_{p,C} \frac{DT}{Dt} + \left[\frac{\partial \mathcal{H}}{\partial p} \right]_{T,C} \frac{Dp}{Dt} + \left[\frac{\partial \mathcal{H}}{\partial C} \right]_{T,p} \frac{DC}{Dt}. \quad (10.162)$$

The partial derivatives can be related to response functions via the following. First, the specific heat capacity at constant pressure is given by equation (6.98)

$$\left[\frac{\partial \mathcal{H}}{\partial T} \right]_{p,C} = c_p. \quad (10.163)$$

Next, we make use of the Gibbs potential identities in Section 6.6.5 to write

$$\left[\frac{\partial \mathcal{H}}{\partial p} \right]_{T,C} = \left[\frac{\partial \mathcal{G}}{\partial p} \right]_{T,C} - T \left[\frac{\partial}{\partial p} \right]_{T,C} \left[\frac{\partial \mathcal{G}}{\partial T} \right]_{p,C} \quad (10.164a)$$

$$= \nu_s - T \left[\frac{\partial}{\partial T} \right]_{p,C} \left[\frac{\partial \mathcal{G}}{\partial p} \right]_{T,C} \quad (10.164b)$$

$$= \nu_s - T \left[\frac{\partial \nu_s}{\partial T} \right]_{p,C} \quad (10.164c)$$

$$= \nu_s (1 - T \alpha_T), \quad (10.164d)$$

where α_T is the thermal expansion coefficient given by equation (6.99). Use of these identities in the enthalpy equation (10.162) and rearrangement leads to the *in situ* temperature equation

$$c_p \rho \frac{DT}{Dt} = -\nabla \cdot \mathbf{J}^{\mathcal{H}} + \left[\frac{\partial \mathcal{H}}{\partial C} \right]_{T,p} \nabla \cdot \mathbf{J}^C + \alpha_T T \frac{Dp}{Dt} + \rho \epsilon. \quad (10.165)$$

The *in situ* temperature of a fluid element thus evolves according to convergence of the enthalpy fluxes, divergence of matter concentration fluxes, material time changes to pressure, and

frictional dissipation. We can massage this expression a bit more by introducing the enthalpy flux (10.160c) so that

$$c_p \rho \frac{DT}{Dt} = -\nabla \cdot \mathbf{J}^{\text{therm}} - \mathbf{J}^C \cdot \nabla \left[\frac{\partial \mathcal{H}}{\partial C} \right]_{T,p} + \alpha_T T \frac{Dp}{Dt} + \rho \epsilon, \quad (10.166)$$

where constraints on the conductive portion of the thermal flux were discussed in Section 10.9.2.

10.10.2 Evolution of potential temperature

We can convert the *in situ* temperature equation (10.165) into a version of the potential temperature equation by recalling the expression (7.27) for the lapse rate

$$\hat{\Gamma} = \left[\frac{\partial T}{\partial p} \right]_{C,S} = \frac{T \alpha_T}{\rho c_p} \quad (10.167)$$

so that equation (10.165) takes the form

$$c_p \rho \left[\frac{DT}{Dt} - \hat{\Gamma} \frac{Dp}{Dt} \right] = -\nabla \cdot \mathbf{J}^{\mathcal{H}} + \left[\frac{\partial \mathcal{H}}{\partial C} \right]_{T,p} \nabla \cdot \mathbf{J}^C + \rho \epsilon. \quad (10.168)$$

Making use of the definition (7.32) for potential temperature renders

$$c_p \rho \frac{D\theta}{Dt} = -\nabla \cdot \mathbf{J}^{\mathcal{H}} + \left[\frac{\partial \mathcal{H}}{\partial C} \right]_{T,p} \nabla \cdot \mathbf{J}^C + \rho \epsilon. \quad (10.169)$$

As expected, pressure changes are removed from the evolution equation for potential temperature.

10.10.3 Conservative Temperature for the ocean

Rather than expressing enthalpy as a function $\mathcal{H}(T, p, C)$, we make use of its natural coordinate dependence $\mathcal{H}(S, p, C)$ from Section 6.6.4, which leads to the enthalpy equation in the form (10.159)

$$\rho \frac{D\mathcal{H}}{Dt} = \frac{Dp}{Dt} - \nabla \cdot \mathbf{J}^{\mathcal{H}} + \rho \epsilon. \quad (10.170)$$

The pressure term arises just like for *in situ* temperature. Its presence suggests we introduce the **potential enthalpy**.

Potential enthalpy and Conservative Temperature

The potential enthalpy is defined as the enthalpy of a fluid element moved to a reference pressure, p_R , while maintaining fixed specific entropy and fixed tracer concentration

$$\mathcal{H}^{\text{pot}}(S, C) = \mathcal{H}(S, p_R, C). \quad (10.171)$$

As for potential temperature (Section 7.4.3), it is most convenient to take p_R as the standard atmospheric pressure, thus corresponding to the standard pressure at the air-sea interface. This definition parallels that for potential temperature given by equation (7.37). It is also motivated by the exchange of enthalpy (heat) across the air-sea boundary, thus providing a natural means to study coupled air-sea processes.

By construction, the material time derivative of potential enthalpy is given by

$$\rho \frac{D\mathcal{H}^{\text{pot}}}{Dt} = \rho \left[\frac{\partial \mathcal{H}^{\text{pot}}}{\partial S} \right]_C \frac{DS}{Dt} + \rho \left[\frac{\partial \mathcal{H}^{\text{pot}}}{\partial C} \right]_S \frac{DC}{Dt} \quad (10.172a)$$

$$= \theta (-\nabla \cdot \mathbf{J}^S + \Sigma^S) - \mu_R \nabla \cdot \mathbf{J}^C \quad (10.172b)$$

$$= (\theta/T) [\rho \epsilon - \nabla \cdot \mathbf{J}^{\mathcal{H}}] - [\mu_R - (\theta/T) \mu] \nabla \cdot \mathbf{J}^C, \quad (10.172c)$$

where we set

$$\theta = \left[\frac{\partial \mathcal{H}^{\text{pot}}}{\partial S} \right]_C \quad \text{and} \quad \mu_R = \left[\frac{\partial \mathcal{H}^{\text{pot}}}{\partial C} \right]_S, \quad (10.173)$$

used equation (10.156) for the entropy source, Σ^S , and equation (10.160a) for the enthalpy flux, $\mathbf{J}^{\mathcal{H}}$. Now define the **Conservative Temperature**, Θ , via

$$c_p^{\text{ref}} \Theta \equiv \mathcal{H}^{\text{pot}}(S, C) = \mathcal{H}(S, p_R, C), \quad (10.174)$$

where c_p^{ref} is a reference specific heat capacity. For the ocean, [McDougall \(2003\)](#) proposed that c_p^{ref} be chosen so that $\Theta = \theta$ at a salinity of 35 parts per thousand. Furthermore, [McDougall \(2003\)](#) argued that the terms driving material time changes to the potential enthalpy in equation (10.172c) are well approximated for the ocean by just the convergence of the enthalpy flux. Hence, the Conservative Temperature satisfies, to a very good approximation, the source-free tracer equation¹⁷

$$\rho c_p^{\text{ref}} \frac{D\Theta}{Dt} = -\nabla \cdot \mathbf{J}^{\mathcal{H}}. \quad (10.175)$$

Key points regarding the Conservative Temperature equation

The Conservative Temperature equation (10.175) is mathematically identical to the material tracer equation, and as such it offers an elegant means to prognose thermodynamic properties of the fluid and to perform budget analyses. We further emphasize two points in regards to this equation relative to the potential temperature equation (10.169).

- The source terms (those not associated with flux convergences) on the right hand side of the potential temperature equation (10.169) are much larger than those in the Conservative Temperature equation (10.175). In particular, [McDougall \(2003\)](#) and [Graham and McDougall \(2013\)](#) showed that the potential temperature sources are roughly 100 times larger in certain regions of the ocean than the Conservative Temperature sources.
- The heat capacity, c_p^{ref} , that appears in the Conservative Temperature equation is a fixed constant, by construction. This feature contrasts to the space-time variable heat capacity, c_p , appearing in both the *in situ* temperature equation (10.165) and potential temperature equation (10.169). The space-time variations of c_p are not negligible (e.g., order 5% for the global ocean), thus making the non-constant heat capacity required for the T and θ equations very inconvenient for purposes of budget analyses (see [McDougall et al. \(2021\)](#) for more on this point).

We close by noting that the enthalpy flux, $\mathbf{J}^{\mathcal{H}}$, is related to the entropy flux and concentration flux as per equation (10.160d). As discussed in Section 2.6 of [Olbers et al. \(2012\)](#), the dominant terms appearing in this flux arise from entropy, which itself is largely due to fluxes of temperature. Consequently, the flux $\mathbf{J}^{\mathcal{H}}$ is well approximated as a flux just of Θ .

¹⁷See [McDougall \(2003\)](#) for the necessary arguments supporting the approximate equation (10.175).

10.10.4 Alternative functional dependencies for specific enthalpy

Thus far in this section, we have considered specific enthalpy to be a function of (T, p, C) as well as its natural functional dependence, (S, p, C) . The introduction of potential temperature and Conservative Temperature allow us to consider two more functional dependencies

$$\mathcal{H} = \mathcal{H}^{\text{natural}}(S, p, C) = \mathcal{H}^T(T, p, C) = \mathcal{H}^\theta(\theta, p, C) = \mathcal{H}^\Theta(\Theta, p, C). \quad (10.176)$$

We use distinct notations for the functions since they each return specific enthalpy yet when fed distinct input. Given the more common use of either potential temperature or Conservative Temperature in atmosphere and ocean sciences, the final two functional dependencies are most commonly used in practice. Note that for brevity, we often drop the extra notation adorning the specific enthalpy symbol, except where confusion may arise. As an example of the above functional dependence, consider the exact differential of specific enthalpy when written using the (Θ, p, C) dependence, in which

$$d\mathcal{H} = \left[\frac{\partial \mathcal{H}^\Theta}{\partial \Theta} \right]_{p,C} d\Theta + \left[\frac{\partial \mathcal{H}^\Theta}{\partial p} \right]_{\Theta,C} dp + \left[\frac{\partial \mathcal{H}^\Theta}{\partial C} \right]_{\Theta,p} dC \quad (10.177a)$$

$$= \left[\frac{\partial \mathcal{H}^\Theta}{\partial \Theta} \right]_{p,C} d\Theta + \rho^{-1} dp + \left[\frac{\partial \mathcal{H}^\Theta}{\partial C} \right]_{\Theta,p} dC, \quad (10.177b)$$

where we set

$$\rho^{-1} = \left[\frac{\partial \mathcal{H}^\Theta}{\partial p} \right]_{\Theta,C}, \quad (10.178)$$

which is a generalization of the partial derivative (6.77) holding for the natural functional dependence. Further discussion of the other partial derivatives are provided in [Graham and McDougall \(2013\)](#) as well as Appendices A.10 and A.11 of [IOC et al. \(2010\)](#).

10.10.5 Comments and further study

We skipped many details in the derivation of the Conservative Temperature equation (10.175), so that the interested reader must consult the more complete discussion given in Section 2.6 of [Olbers et al. \(2012\)](#), which is itself based on [McDougall \(2003\)](#) and [Graham and McDougall \(2013\)](#).

Considerations for the atmosphere involve phase changes (liquid-vapor and liquid-solid), with the associated latent heat exchanges leading order contributions to the enthalpy budget (see [Lauritzen et al. \(2022\)](#) for a comprehensive review). Additionally, the role of frictional dissipation is not negligible in the atmosphere whereas it is negligible in the ocean (see Section 10.6.3).

10.11 Conservation laws and potential properties

A central facet of theoretical physics concerns the development of concepts and tools to expose conservation laws and their underlying symmetries. We routinely make use of such laws in geophysical fluid mechanics to provide constraints on the fluid motion and to study budgets of corresponding properties to help understand fundamental processes. As such, conservation laws offer great physical insight and predictive utility. We close this chapter by summarizing some conceptual points concerning conservation laws. In particular, we identify the need to distinguish

laws that involve just the convergence of a flux from those that also include non-conservative “source” terms. We also distinguish between material and non-material conservation laws, in which properties satisfying material conservation laws are materially invariant in the absence of local mixing processes.

10.11.1 Flux-form conservation laws

Certain scalar properties studied in fluid mechanics satisfy conservation laws that are written as

$$\rho \frac{D\psi}{Dt} = -\nabla \cdot \mathbf{J} \iff \frac{\partial(\rho\psi)}{\partial t} = -\nabla \cdot (\rho \mathbf{v}\psi + \mathbf{J}). \quad (10.179)$$

The right hand side of the flux-form expression (second equation) involves a flux that is comprised of an advective term, $\rho \mathbf{v}\psi$, plus a non-advective term, \mathbf{J} . Examples of conservation laws of this type include the material tracer concentration, $\psi = C$, as in equation (10.185); the Conservative Temperature, $\psi = \Theta$, as in equation (10.186); the total energy, $\psi = \mathcal{E}$, in the absence of astronomical forces, as in equation (10.157b); and the potential vorticity, $\psi = Q$, studied in VOLUME 3. In our study of tracer budgets in VOLUME 1, we saw how the Leibniz-Reynolds transport theorem connects this differential equation to finite volume budgets for the integral of ψ -stuff within a region, $\int_{\mathcal{R}} \psi \rho dV$.

Conservation laws of the form (10.179) are a direct consequence of the local conservation of ψ -stuff within the fluid. That is, the amount of ψ -stuff changes at a point only through the local convergence of fluxes onto that point, and likewise for a finite region. Such conservation laws are consistent with basic notions of causality and locality that appear throughout physics, with a discussion of such conservation laws offered in Section 27-1 of [Feynman et al. \(1963\)](#).

10.11.2 Conservation laws that are not flux-form

The presence of source/sinks are relevant for chemical and biogeochemical reactions, whereby matter is converted from one form to another. Such processes are not mathematically represented as the convergence of a flux. As such, they are not contained in the conservation law (10.179) and they are correspondingly referred to as [non-conservative process](#). Even without chemical reactions, not all fluid properties satisfy flux-form conservation laws of the form (10.179). For example, linear momentum of a fluid element is affected by pressure, planetary Coriolis, and effective gravity, and these processes are not represented as the convergence of a flux.

As discussed in both VOLUME 1 and VOLUME 4, conservation laws are associated with symmetries of the physical system. Correspondingly, non-conservative terms appearing in an evolution equation often reflect the breaking of a symmetry. For example, motion around a sphere does not conserve linear momentum even in the absence of forces, whereas linear momentum is conserved for free motion in a planar geometry.

10.11.3 Non-material or wave-like transport of properties

Pressure is of particular note since pressure perturbations travel through a compressible fluid via acoustic waves (see VOLUME 5), or, in the case of a non-divergent flow, a pressure perturbation is felt globally and instantaneously as reflected in the elliptic Poisson equation satisfied by pressure (Section 13.3). More generally, the wave mediated transfer of forces, or other fluid properties such as momentum or mechanical energy, is an example of a non-material transfer; i.e., a transfer of information not arising from the transfer of matter. Non-material wave

mediated transfer often occurs much faster than material transfer, with matter transport only mediated through advection and diffusion. Correspondingly, material substances (and potential enthalpy) are not directly affected by wave transport. Rather, waves affect material substances only so far as they affect advection and diffusion.

10.11.4 Material and non-material conservation laws

Mass invariance for a fluid element reflects matter conservation in classical physics, which in turn motivates the kinematic perspective pursued throughout this book that follows fluid elements whose mass remains constant. Relatedly, in the absence of mixing, the matter content of the fluid element remains invariant so that its tracer concentration is materially constant

$$\rho \frac{DC}{Dt} = 0. \quad (10.180)$$

For example, in the absence of mixing, the salt content of seawater and the water content of moist air are materially constant, so that the salt concentration and water concentration in a fluid element remain constant. Correspondingly, in the presence of mixing between two fluid elements, the net material tracer in the combined fluid element equals to the sum of the tracer content in the contributing elements. We refer to a fluid property satisfying such conservation laws as a [materially conservative property](#).

What about fluid properties that satisfy a local flux-form conservation law of the form (10.179), and yet do not remain materially invariant in the absence of mixing? For example, consider the total energy, \mathcal{E} , from Section 10.6. Even in the absence of mixing (an entropy source) and with time independent body forces (i.e., constant effective gravity), the mechanical work from pressure modifies the internal energy of the fluid element via the energy equation (10.157a)

$$\rho \frac{D\mathcal{E}}{Dt} = -\nabla \cdot (p \mathbf{v}). \quad (10.181)$$

Pressure work means that when two fluid elements are combined, the total energy of the combined fluid, \mathcal{E}_{12} , is not generally equal to the sum of their separate total energies,

$$\mathcal{E}_{12} \neq \mathcal{E}_1 + \mathcal{E}_2. \quad (10.182)$$

So although total energy is locally conserved in the sense that it satisfies a local flux-form conservation law, it does not satisfy a material-like conservation law. We say that total energy is a [non-materially conservative property](#). Notably, when integrated globally over a domain closed to energy fluxes, including mechanical energy fluxes (meaning there is no pressure work applied to the domain boundaries), and when there are no time dependent astronomical forces, then the domain integrated total energy, $\int \rho \mathcal{E} dV$, remains constant. This [global conservation](#) law means that the total energy is conserved globally. Conservation laws for non-materially conserved properties, such as total energy, offer a less powerful constraint on fluid motion than the material conservation laws. Even so, global conservation can be of great use when studying energy transformations within a closed domain.

We summarize the above discussion by noting that for a fluid property to satisfy a [local conservation](#) law, it is necessary that the density weighted material derivative of that property be given by the convergence of a flux as in equation (10.179). A [materially conservative property](#) must, furthermore, have its flux convergence vanish in the absence of mixing processes that are local in space and time, such as for a diffusive flux proportional to the tracer gradient.

In contrast, the pressure flux convergence acting to modify total energy, $-\nabla \cdot (p\mathbf{v})$, can be nonzero even in regions where there is no mixing of matter since pressure is transported by waves (Section 10.11.3). So although total energy is locally conserved, its flux is dependent on non-local processes as mediated by waves, so that total energy satisfies a non-material conservation law.

10.11.5 Concerning potential properties

As introduced in Sections 7.4 and 10.10.3, to study fluid mixing it is useful to work with scalar fields that are not affected by adiabatic and isentropic pressure work. For this reason, rather than *in situ* temperature, we prefer to work with potential temperature, θ , or Conservative Temperature, Θ , both of which are potential properties as discussed in Section 7.4.1. Some potential properties are also endowed with the local conservation property discussed above, which makes local budgets available just like for a material tracer. For example, Conservative Temperature is very well approximated as a conservative property, with its non-flux form sources far smaller than potential temperature (Section 10.10.3). In contrast, neither *in situ* temperature nor total energy are potential properties since an adiabatic and isentropic change in pressure alters the *in situ* temperature and total energy of a fluid element.

10.11.6 Further study

Much from this section is motivated by the more extensive discussion in Sections A.8 and A.9 of [IOC et al. \(2010\)](#).

10.12 Equations for rotating and stratified fluids

We close this chapter by summarizing the physical content of the suite of partial differential equations describing rotating and stratified fluids.

$$\rho \frac{D\mathbf{v}}{Dt} + 2\rho\boldsymbol{\Omega} \times \mathbf{v} = -\rho\nabla\Phi - \nabla p + \nabla \cdot \mathbb{T} \quad \text{momentum} \quad (10.183)$$

$$\frac{D\rho}{Dt} = -\rho\nabla \cdot \mathbf{v} \quad \text{mass continuity} \quad (10.184)$$

$$\rho \frac{DC}{Dt} = -\nabla \cdot \mathbf{J}^C \quad \text{matter conservation} \quad (10.185)$$

$$\rho \frac{D\Theta}{Dt} = -\nabla \cdot \mathbf{J}^\Theta \quad \text{potential enthalpy conservation} \quad (10.186)$$

$$\rho = \rho(C, \Theta, p) \quad \text{equation of state.} \quad (10.187)$$

It is a testament to the success of classical continuum mechanics that these equations are of use for describing fluid phenomena from the millimetre scale to the planetary scale. We summarize the following terms in these equations.

- **LINEAR MOMENTUM AND VELOCITY:** Newton's second law of motion, as developed for a fluid in Chapter 8, provides the prognostic equation for the velocity field, \mathbf{v} . Each of the three velocity components evolves according to its respective dynamical equation (10.183). As noted at the end of Section 8.2.4, we write the momentum equation in the form (10.183) by separating the time dependence of the basis vectors into a term arising from rigid-body rotation (which leads to planetary Coriolis and planetary centrifugal

accelerations) and a term arising from the motion of the fluid relative to the rotating sphere (which leads to the metric acceleration when using non-Cartesian coordinates).

- MASS CONSERVATION: Kinematics provides a constraint on the velocity field according to the needs of mass conservation for a fluid element, with this constraint leading to the continuity equation (10.184).
- MATERIAL TRACER CONSERVATION: Kinematic constraints from the conservation of matter leads to the material tracer equation (10.185). Evolution is determined by the convergence of tracer fluxes, \mathbf{J} , with this flux specified by molecular diffusion, or through other parameterized processes when sampling flow on scales larger than millimetres (VOLUME 4).
- THERMODYNAMIC TRACER: The Conservative Temperature, Θ , (Section 10.10.3), evolves according to the convergence of fluxes, just like a material tracer.
- DENSITY: The *in situ* density can be updated in time via mass continuity (equation (10.184)) or via knowledge of (C, Θ, p) . We discuss the many forms of density for the ocean and atmosphere in Section 14.3.
- PRESSURE: There is no prognostic equation for pressure. Rather, pressure is diagnosed based on knowledge of other fields. Here are sketches of how that diagnostic calculation is performed.
 - For an ideal gas, pressure is diagnosed from the ideal gas relation (7.49) using the density and temperature.
 - For fluid flow maintaining an approximate hydrostatic balance (Section 11.2), pressure is diagnosed at a point through knowledge of the weight per area above the point.
 - For a non-divergent fluid flow as per the oceanic Boussinesq ocean (Chapter 13), pressure is no longer connected thermodynamically to partial derivatives of the thermodynamic potentials (Section 6.6). Instead, pressure is a purely mechanical property that is determined kinematically by the non-divergence constraint. In particular, for a non-hydrostatic Boussinesq fluid, pressure is diagnosed by solving a Poisson equation derived from taking the divergence of the momentum equation (see Section 13.3).
- GEOPOTENTIAL: The geopotential, Φ , is a function of the mass distribution of the planet and any relevant astronomical bodies, as well as the planetary centrifugal acceleration. The simple geopotential is generally used in this book, with the single exception of Section 11.6 where we develop the equations for astronomical tides. The simple geopotential is specified by both the radial position (to give the height above an arbitrary reference level) plus the latitude (to give the planetary centrifugal potential) (VOLUME 1). For geophysical fluid studies, the reference level is generally taken at the level of a resting sea surface. We thus often write the radial coordinate as

$$r = R_e + z \tag{10.188}$$

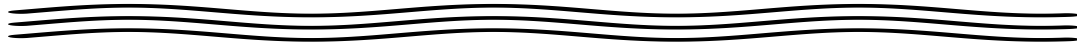
where $R_e = 6.371 \times 10^6$ m is the radius of a sphere whose volume approximates that of the earth, and z is the geopotential coordinate measuring the height above sea level.

- EARTH'S SPIN: The earth's angular velocity, Ω , is time constant for geophysical fluid studies of concern here, and it has magnitude $\Omega = 7.2921 \times 10^{-5} \text{ s}^{-1}$ due to the planet's spin around its axis plus its orbit around the sun.
- FRICTION: The friction vector,

$$\rho \mathbf{F} = \nabla \cdot \mathbb{T}, \quad (10.189)$$

is the divergence of a symmetric and trace-free deviatoric friction tensor, \mathbb{T} (Section 9.6). The friction tensor is determined through a constitutive relation as a function of the strain and viscous properties.

- KINEMATIC AND DYNAMIC BOUNDARY CONDITIONS: Kinematic and dynamic boundary conditions consist of the exchange of matter, momentum, and enthalpy with the surrounding media, such as the solid earth or another fluid component (e.g., atmosphere-ocean exchange). We discuss the boundary conditions in various places within these volumes.



10.13 Exercises

EXERCISE 10.1: ENERGETICS OF OCEAN MIXING

In this exercise we develop some basics for the energetics of mixing, thus providing more experience with the ideas developed in Section 10.1.8. We do so by examining a vertical column of seawater with uniform horizontal cross-sectional area, A . Let the initial conditions consist of two homogeneous regions stacked vertically, with thickness h_n , mass M_n , density ρ_n , Conservative Temperature Θ_n , and salinity S_n , where $n = 1$ is the lower region and $n = 2$ the upper region. Assume this column to be stably stratified so that $\Delta\rho = \rho_1 - \rho_2 > 0$. We then completely mix the two regions to produce a homogeneous column of fluid of mass M , salinity S , and Conservative Temperature Θ . We ignore pressure effects on density, so that the density is uniform in the two regions prior to mixing, and uniform in the full column after mixing. The conservation of mass, conservation of salt, and conservation of potential enthalpy (heat), mean that these scalar properties remain the same before and after the mixing, thus allowing us to compute the properties of the homogenized column

$$M = M_1 + M_2 \quad \text{and} \quad M\Theta = M_1\Theta_1 + M_2\Theta_2 \quad \text{and} \quad MS = M_1S_1 + M_2S_2. \quad (10.190)$$

- Compute the gravitational potential energy of the initial seawater column, taking the bottom of the column as the zero reference level.
- Compute the gravitational potential energy of the fluid column after homogenization. Verify that the gravitational potential energy of the homogenized column is greater than the initial column. For this question, assume the final thickness of the column equals to the sum of the initial thicknesses. This assumption is not exact but is very accurate for our purposes. An exact calculation is given in our study of sea level in VOLUME 5, where we consider a thought experiment with buckets of seawater.
- If the same amount of energy used to increase the gravitational potential energy was instead used to increase kinetic energy of the homogenized fluid, what is the expression for the change in squared velocity? Write your expression in terms of the thicknesses, h_n , and densities, ρ_n .

- (d) If the change in gravitational potential energy were converted to potential enthalpy of the homogenized fluid, what is the expression for the increase in Conservative Temperature, Θ ? Again, write your expression in terms of the thicknesses, h_n , and densities, ρ_n .
- (e) Compute the change in speed and change in Conservative Temperature for the previous parts of this exercise using the following values for a region of seawater: $c_p = 3992.1 \text{ J kg}^{-1} \text{ K}^{-1}$, $\rho_1 = 1020 \text{ kg m}^{-3}$, $\Delta\rho = 1 \text{ kg m}^{-3}$, $h_1 = 1 \text{ m}$, and $h_2 = 1 \text{ m}$.

EXERCISE 10.2: A MODIFIED FRICTIONAL STRESS TENSOR

Following the methods from Section 10.2.3, assume viscous friction in the momentum equation takes the form

$$\rho \mathbf{F} = \partial_n(\rho \nu \partial_n \mathbf{v}), \quad (10.191)$$

with $\nu > 0$ a scalar kinematic viscosity (generally non-constant). This friction operator corresponds to the frictional stress tensor

$$\mathbb{T}_{nm} = \rho \nu \partial_n v_m. \quad (10.192)$$

- (a) Show that when integrated over the full domain

$$\int \mathbf{F} \cdot \mathbf{v} \rho dV < 0, \quad (10.193)$$

where boundary terms are ignored. Hence, the global integrated kinetic energy is dissipated (reduced) through the impacts of viscosity in the interior of the domain. Note that for this exercise, it is sufficient to assume Cartesian tensors.

- (b) What property does the assumed \mathbb{T}_{nm} in equation (10.192) *not* satisfy, thus making it unsuitable as a frictional stress tensor? Discuss according to what we studied in Section 9.4.

EXERCISE 10.3: INTEGRATED FRICTIONAL DISSIPATION FOR AN INCOMPRESSIBLE FLUID

Consider an incompressible fluid ($\nabla \cdot \mathbf{v} = 0$ along with ρ is constant) with constant viscosity, $\nu > 0$. Assume the fluid is contained in a region, \mathcal{R} , whose boundary, $\partial\mathcal{R}$, is static. Also assume the velocity satisfies the no-slip condition on $\partial\mathcal{R}$, as relevant for a viscous fluid. Show that the frictional dissipation of kinetic energy (Section 10.2.3) has a global integral

$$\int_{\mathcal{R}} \mathbf{v} \cdot \mathbf{F} \rho dV = -\nu \int_{\mathcal{R}} |\boldsymbol{\omega}|^2 \rho dV, \quad (10.194)$$

where $\boldsymbol{\omega} = \nabla \times \mathbf{v}$ is the vorticity. This result shows that the globally integrated viscous dissipation vanishes for an irrotational and non-divergent flow contained in a region with no-slip walls.

EXERCISE 10.4: MECHANICAL ENERGY FOR A PERFECT FLUID WITH ZERO FLOW DIVERGENCE

Consider a non-divergent flow ($\nabla \cdot \mathbf{v} = 0$), as in the Boussinesq ocean studied in Chapter 13. In this case, pressure does no work on fluid elements since each element maintains a constant volume.¹⁸ Furthermore, assume the fluid is perfect and so it has zero viscous stresses. Finally, assume the geopotential is constant in time ($\partial_t \Phi = 0$). Interpret the resulting finite volume mechanical energy budget from Section 10.3.2. In particular, is there a pressure work term on this finite region?

¹⁸In studying the kinematics of non-divergent flows in VOLUME 1, we showed that $\nabla \cdot \mathbf{v} = 0$ means that fluid elements maintain a materially constant volume.

EXERCISE 10.5: THERMODYNAMIC MANIPULATIONS FOR IDEAL GASES

This question develops some manipulations with the potential temperature.

- (a) Beginning with the expression (7.93) for potential temperature of an ideal gas, show that

$$d\theta = \frac{\theta}{T} \left[dT - \frac{\nu_s}{c_p} dp \right]. \quad (10.195)$$

- (b) Given the result (10.195), show that an ideal gas satisfies the following relation

$$T dS = \frac{c_p T}{\theta} d\theta. \quad (10.196)$$

Whereas the relation (7.45) holds for a general fluid only at the reference pressure, this exercise shows that it holds for an ideal gas at all pressures. As a result, a moving fluid of ideal gas satisfies the material time relation

$$T \frac{D\dot{S}}{Dt} = \frac{c_p T}{\theta} \frac{D\theta}{Dt} \Rightarrow \frac{c_p T}{\theta} \frac{D\theta}{Dt} = \dot{Q}. \quad (10.197)$$

EXERCISE 10.6: THERMODYNAMIC MANIPULATIONS FOR A LIQUID

Consider seawater with specific entropy given by (see Section 1.7.2 of [Vallis \(2017\)](#))

$$S(S, T, p) = S_0 + c_{po} \ln(T/T_o) [1 + \beta_s^* (S - S_o)] - \alpha_o p \left[\beta_T + \beta_T \gamma^* \frac{p}{2} + \beta_T^* (T - T_o) \right], \quad (10.198)$$

and corresponding specific heat capacity at constant pressure

$$c_p(S, T, p) = c_{po} [1 + \beta_s^* (S - S_o)] - \alpha_o p \beta_T^* T. \quad (10.199)$$

In these equations, T is the *in situ* temperature, S is the salinity, and p is the *in situ* pressure. All other terms on the right hand side to these expressions are empirical constants. Verify that the specific entropy differential for a fluid element with constant composition is given by

$$\theta dS = c_p(S, \theta, p_R) d\theta, \quad (10.200)$$

where θ is the potential temperature and p_R is the corresponding reference pressure. Consequently, we can write for a moving fluid element

$$\dot{Q} = \frac{c_p T}{\theta} \frac{D\theta}{Dt}, \quad (10.201)$$

where we evaluate the non-constant heat capacity at $c_p(S, \theta, p_R)$. We see that certain liquids have an expression for heating that is analogous to that for an ideal gas, with the ideal gas case discussed in Exercise 10.5. Hint: Make use of the identity (7.37).

EXERCISE 10.7: BERNOULLI THEOREM AND TWO SHEETS OF PAPER (EXERCISE 1.22 OF [Sutherland \(2010\)](#))

Hold two sheets of paper from their top edge so they are two fingers-widths apart. Blow between the two sheets. Do they separate or come together. Explain what happens in terms of the physics discussed in this chapter. Hint: make use of the simplest form of Bernoulli's theorem from Section 10.8.

EXERCISE 10.8: DYNAMICALLY INCONSISTENT VELOCITY

Consider the two dimensional non-divergent vector field

$$\mathbf{u} = \Gamma (y^2 \hat{\mathbf{x}} + x^2 \hat{\mathbf{y}}), \quad (10.202)$$

with Γ a constant of dimensions $L^{-1} T^{-1}$. In this exercise we will show that \mathbf{u} it *cannot* be a physically realizable velocity field.

- (a) Assuming \mathbf{u} is a velocity field for two-dimensional fluid flow, then determine the pressure field giving rise to this velocity. Assume a constant density, non-rotating reference frame, zero friction, and no boundary effects. Do so by making use of the Bernoulli theorem in equation (10.115) for horizontal (constant z) flow, and thus provide the expression for pressure, and express that pressure along a streamline. Hint: compute the streamfunction corresponding to the velocity, and choose a convenient streamline upon which to evaluate the pressure.
- (b) Now make use of the momentum equation to find the pressure gradient. Attempt to integrate this equation to then find the pressure field. You should reach an inconsistency. Given this inconsistency, what can you conclude about the physical realizability of the given \mathbf{u} as a velocity vector? Discuss. Hint: recall the discussion of exact differentials in Section 6.10.

EXERCISE 10.9: CROCCO'S THEOREM

Prove that the spatial gradient of the Bernoulli potential for a single-component steady state perfect fluid can be written

$$\mathcal{B} = T \nabla \mathcal{S} + \mathbf{v} \times \boldsymbol{\omega}_a. \quad (10.203)$$

This result is known as Crocco's Theorem ([Crocco, 1937](#)). We derive two conclusions from this theorem. First, in a steady state, there is a nonzero vorticity non-parallel to the velocity whenever $\mathcal{B} \neq T \nabla \mathcal{S}$:

$$\mathbf{v} \times \boldsymbol{\omega}_a = \mathcal{B} - T \nabla \mathcal{S}. \quad (10.204)$$

Second, it means that the velocity for a single-component perfect fluid in steady state is aligned parallel to isosurfaces of both the Bernoulli potential and the specific entropy

$$\mathbf{v} \cdot \nabla \mathcal{B} = T \mathbf{v} \cdot \nabla \mathcal{S}. \quad (10.205)$$

Hint: to help formulate the proof, study the discussion in Section 10.8.3 where we showed that the Bernoulli potential is constant along a steady flow streamline in a perfect fluid. Also recall equation (10.112), which is valid for a steady state and applied here to a single-component fluid.

EXERCISE 10.10: BOLTZMANN'S H-THEOREM

An isolated physical system in [thermodynamic equilibrium](#) is equally likely to be in any of its accessible microstates. This statement is known as the [postulate of equal *a priori* probabilities](#). It follows that if an isolated physical system is not equally likely to be found in any of its accessible microstates, then this system cannot be in thermodynamic equilibrium. Rather, it will spontaneously evolve towards thermodynamic equilibrium. The [second law of thermodynamics](#) states that entropy increases during this evolution, thus providing an arrow for time. In this exercise, which follows Appendix A.12 of [Reif \(1965\)](#), we step through the [H-theorem](#) of [Boltzmann \(1966\)](#), which presents a mathematical argument for the increase in entropy in the context of the kinetic theory of gases. This celebrated theorem provided the first connection between entropy, a purely macroscopic property, to the dynamics of molecules.

Consider an isolated macroscopic physical system and let $P_r(t)$ be the normalized probability that the system can be found in any of its $r = 1, N$ microstates, where N is on the order of Avogadro's number and with $\sum_r P_r(t) = 1$. Let $W_{rs} \geq 0$ be the transition probability per unit time that the system transitions from state r to state s , and assume the dynamical laws (e.g., Newton's laws) specifying W_{rs} are reversible, so that

$$W_{rs} = W_{sr}. \quad (10.206)$$

The probability, $P_r(t)$, increases in time if the system transitions to r from s , whereas it decreases if the transitions occur in the opposite direction. We thus have the change in time for the probability given by the following equation

$$\frac{dP_r}{dt} = \sum_s [P_s W_{sr} - P_r W_{rs}] = \sum_s W_{rs}(P_s - P_r), \quad (10.207)$$

which is known as a master equation in statistical physics. Now introduce the quantity H defined as the expectation of the natural log of the probability

$$H \equiv \sum_r P_r \ln P_r, \quad (10.208)$$

which is the information entropy of [Shannon \(1948\)](#) and [Jaynes \(1957\)](#). Prove that

$$\frac{dH}{dt} \leq 0, \quad (10.209)$$

with the equal sign holding if $P_r = P_s$ for all accessible microstates. If we identify the extensive version of entropy as

$$S^e = -k_B H = -k_B \sum_r P_r \ln P_r, \quad (10.210)$$

then $dH/dt \leq 0$ proves that entropy increases as the system transitions toward equilibrium, with equilibrium characterized by having all microstates equally likely.



Chapter 11

HYDROSTATIC FLOWS

The ocean and atmosphere thermo-hydrodynamical equations (10.183)-(10.187) explain a huge range of phenomena. Yet by encapsulating so many physical scales of motion and associated dynamical processes, the equations are difficult to manage when studying a focused dynamical regime. Therefore, it is common to approximate or filter the equations to remove scales that are not of direct interest to the problem at hand, thus enabling a more telescopic view of the dynamics. The [hydrostatic primitive equations](#) provide an important example of this approach.

For a moving fluid with scales of motion that maintain a small vertical to horizontal aspect ratio, the vertical pressure gradient and gravitational acceleration individually remain far larger than other accelerations acting on a fluid element. In this case, the vertical momentum equation, even for the moving fluid, satisfies the [hydrostatic approximation](#) column-by-column. We thus have a flow whereby each vertical column is in hydrostatic balance, and yet there are horizontal pressure gradients that drive horizontal motion. Correspondingly, there is also vertical motion. In this chapter, we study the many facets of this approximately hydrostatic flow.

We also here discuss facets of a space-time dependent gravity field, as relevant for ocean tides, and how it affects the equations of motion, including the hydrostatic balance.

READER'S GUIDE TO THIS CHAPTER

The column-by-column hydrostatic balance found in the approximate hydrostatic flow is ubiquitous in large-scale fluid flows in the atmosphere and ocean. We thus make extensive use in this book of the corresponding expressions for the pressure gradients holding for such flows. The [hydrostatic primitive equations](#) have been very useful in the study of ocean and atmosphere circulation since their introduction in the 1950s. We make use of these equations throughout our study of geophysical fluid mechanics.

11.1	The hydrostatic primitive equations	350
11.1.1	Hydrostatic approximation	350
11.1.2	Shallow fluid approximation	351
11.1.3	Traditional approximation	351
11.1.4	Summary of the hydrostatic primitive equations	352
11.1.5	Flux-form mechanical energy budget	353
11.1.6	Depth integrated mechanical energy budget	353
11.1.7	Comments and further study	354
11.2	Elements of approximate hydrostatic pressure	355
11.2.1	Expressions for the hydrostatic pressure	355
11.2.2	Evolution of hydrostatic pressure	356
11.2.3	Heuristic scaling	357

11.2.4	Removal of a dynamically irrelevant background state	358
11.2.5	Ocean dynamic topography	359
11.2.6	Surfaces of atmospheric geopotential height and pressure	360
11.2.7	Concerning vertical motion	361
11.2.8	Further study	361
11.3	Horizontal pressure gradients	361
11.3.1	Top down horizontal pressure gradient	361
11.3.2	Bottom up horizontal pressure gradient	363
11.4	Balancing internal and external pressure gradients	364
11.4.1	Horizontal hydrostatic pressure gradient in a mass conserving fluid	365
11.4.2	Balanced pressure gradients above a level of no motion	366
11.4.3	Balanced pressure gradients above a sloping side boundary	368
11.5	Homogeneous fluid in a rotating tank	371
11.5.1	What about the planet's rotation?	372
11.5.2	Formulating the equations of motion	372
11.5.3	Rigid-body rotation and parabolic free surface shape	373
11.5.4	Further study	375
11.6	Space-time dependent gravity field	375
11.6.1	Simple geopotential	375
11.6.2	General geopotential	375
11.6.3	Momentum equation	376
11.6.4	Hydrostatic primitive equations	376
11.6.5	Depth independent perturbed geopotential	377
11.7	Exercises	377

11.1 The hydrostatic primitive equations

The [hydrostatic primitive equations](#) provide a set of approximate equations for use in studying large-scale atmospheric and oceanic fluid mechanics. Indeed, nearly all numerical models of the large-scale atmospheric and oceanic circulation are based on the primitive equations. They make use of the following three approximations.

11.1.1 Hydrostatic approximation

As discussed in Section 8.6, a static fluid in a gravity field maintains an exact [hydrostatic balance](#), whereby the pressure at a point equals to the weight per area of fluid above that point. As shown in Section 11.2, the hydrostatic balance is very closely maintained column-by-column for the large scales in a moving geophysical fluid. Hence, it is appropriate for many purposes to take the [hydrostatic approximation](#) for the vertical momentum equation, with this approximation central to the study of large-scale geophysical fluid mechanics.

The hydrostatic approximation results in a balance within the vertical momentum equation (8.32) between the vertical pressure gradient and the effective gravitational force

$$\frac{\partial p}{\partial r} = -\rho g, \quad (11.1)$$

with this balance holding separately for each vertical column. Notably, there are no viscous or turbulent terms appearing in the hydrostatic balance.

Vertical integration of this equation, while assuming g is constant, renders a diagnostic expression for the hydrostatic pressure at a point as a function of the weight per horizontal

area above the point

$$p(r, \lambda, \phi, t) = p(r_0, \lambda, \phi, t) - g \int_{r_0}^r \rho(r', \lambda, \phi, t) dr'. \quad (11.2)$$

Note that we exposed the horizontal space dependence along with the time dependence for the density and hence the hydrostatic pressure. That is, an approximate hydrostatic fluid flow has horizontal pressure gradients as well as time dependence.

We emphasize that in making the hydrostatic approximation, we are *not* assuming that vertical motion vanishes. In fact, there is vertical motion. But with the hydrostatic approximation, the vertical motion is not prognosed by the vertical momentum equation. Instead, it must be diagnosed via the constraints imposed on the motion. We have more comment on this point in Section 11.2.7. Furthermore, there are no other terms appearing in the vertical momentum equation, so that we retain just the vertical pressure gradient acceleration and the gravitational acceleration. Friction or boundary turbulent stresses do not appear in the hydrostatic balance, whereas they generally do appear in the non-hydrostatic vertical momentum equation.

11.1.2 Shallow fluid approximation

The ocean and atmosphere each form a fluid shell that envelops the outer portion of the planet. The thickness of these fluids is small relative to the Earth's radius. The **shallow fluid approximation**¹ builds this scale separation into the equations of motion by setting the radial coordinate equal to the Earth's radius

$$r = R_e + z \approx R_e. \quad (11.3)$$

This approximation is made where r appears as a multiplier, but not as a derivative operator. For example, the spherical coordinate gradient operator (8.34) takes the approximate form

$$\nabla = \frac{\hat{\lambda}}{r \cos \phi} \frac{\partial}{\partial \lambda} + \frac{\hat{\phi}}{r} \frac{\partial}{\partial \phi} + \hat{r} \frac{\partial}{\partial r} \approx \frac{\hat{\lambda}}{R_e \cos \phi} \frac{\partial}{\partial \lambda} + \frac{\hat{\phi}}{R_e} \frac{\partial}{\partial \phi} + \hat{r} \frac{\partial}{\partial r}. \quad (11.4)$$

The shallow fluid approximation proves useful when computing the depth integrated fluid mechanical equations for studies where we wish to remove the vertical degrees of freedom. Examples include the depth integrated mechanical energy in Section 11.1.6, the depth integrated momentum equation in Section 12.4, the depth integrated angular momentum equation in Section 12.5, and the depth integrated vorticity equations studied in VOLUME 3.

11.1.3 Traditional approximation

The **traditional approximation** comprises three approximations that come as a package in order to maintain physical consistency.

Coriolis acceleration

The traditional approximation sets to zero the Coriolis accelerations in the horizontal momentum equations that involve the vertical velocity. We are thus concerned only with the local vertical

¹The shallow fluid approximation is distinct from the shallow water approximation.

component of the Earth's angular rotation vector (see VOLUME 1)

$$\boldsymbol{\Omega} = \Omega \hat{\mathbf{Z}} = \Omega (\hat{\phi} \cos \phi \hat{\mathbf{r}} + \hat{\mathbf{r}} \sin \phi) \rightarrow \Omega \sin \phi \hat{\mathbf{r}} = \mathbf{f}/2, \quad (11.5)$$

where

$$\mathbf{f} = (2 \Omega \sin \phi) \hat{\mathbf{r}} \quad (11.6)$$

is the planetary Coriolis parameter and $\hat{\mathbf{Z}}$ is the vertical direction through the north pole for the planetary Cartesian coordinate system (Figure 8.2).²

Metric terms

The traditional approximation also drops the metric terms, uw/r and vw/r , associated with the vertical velocity as they appear in the horizontal momentum equations (8.30) and (8.31). These terms are generally smaller than the other terms since w is much smaller than the horizontal velocity for large-scale geophysical fluid flow.

Physical consistency

The shallow fluid approximation and both parts of the traditional approximation must be taken together in order to maintain a consistent energy and angular momentum conservation principle for the resulting equations. As shown in Exercise 11.3, taking one but not the other approximation leads to a physically inconsistent set of equations

11.1.4 Summary of the hydrostatic primitive equations

The above approximations lead to the [hydrostatic primitive equations](#) written in spherical coordinates

$$\frac{Du}{Dt} - \frac{uv \tan \phi}{R_e} - fv = -\frac{1}{\rho R_e \cos \phi} \frac{\partial p}{\partial \lambda} + F^\lambda \quad (11.7)$$

$$\frac{Dv}{Dt} + \frac{u^2 \tan \phi}{R_e} + fu = -\frac{1}{\rho R_e} \frac{\partial p}{\partial \phi} + F^\phi \quad (11.8)$$

$$\frac{\partial p}{\partial z} = -g \rho, \quad (11.9)$$

where the gradient operator is given by equation (11.4). We can write these equations in the vector form

$$\rho \frac{D\mathbf{u}}{Dt} + (f + u \tan \phi / R_e) \hat{\mathbf{z}} \times \rho \mathbf{u} = -\rho \nabla \Phi - \nabla p + \rho \mathbf{F}, \quad (11.10)$$

where

$$\mathbf{F} = \hat{\lambda} F^\lambda + \hat{\phi} F^\phi \quad (11.11)$$

is the horizontal friction acceleration, and the vertical component of equation (11.10) is the hydrostatic balance. Furthermore, the material time derivative in this equation represents just the relative acceleration

$$\frac{D\mathbf{u}}{Dt} = \hat{\lambda} \frac{Du}{Dt} + \hat{\phi} \frac{Dv}{Dt}. \quad (11.12)$$

²We use the capital $\hat{\mathbf{Z}}$ to distinguish this north pole unit vector from the local $\hat{\mathbf{z}} = \hat{\mathbf{r}}$ unit vector pointing vertically relative to a tangent plane discussed in Section 8.5.

11.1.5 Flux-form mechanical energy budget

For fluid flow maintaining the approximate hydrostatic approximation, the kinetic energy is dominated by horizontal motion. Indeed, as we now show, the proper form of the kinetic energy is precisely that contained just in the horizontal motions. We do so by taking the scalar product of the horizontal velocity with the momentum equation (11.10) to render

$$\rho \frac{D\mathcal{K}^{\text{hyd}}}{Dt} = -\rho \mathbf{u} \cdot \nabla \Phi - \mathbf{u} \cdot \nabla p + \rho \mathbf{u} \cdot \mathbf{F}, \quad (11.13)$$

where we introduced the hydrostatic kinetic energy per mass

$$\mathcal{K}^{\text{hyd}} = \mathbf{u} \cdot \mathbf{u}/2. \quad (11.14)$$

Making use of the hydrostatic balance in the presence of a simple geopotential, $\Phi = g z$ (so that $\mathbf{u} \cdot \nabla \Phi = 0$), leads to

$$\rho \frac{D\mathcal{K}^{\text{hyd}}}{Dt} = -(\mathbf{v} \cdot \nabla p - w \partial_z p) + \rho \mathbf{u} \cdot \mathbf{F} \quad (11.15a)$$

$$= -\nabla \cdot (\mathbf{v} p) + p \nabla \cdot \mathbf{v} - w g \rho + \rho \mathbf{u} \cdot \mathbf{F}, \quad (11.15b)$$

which leads to the flux-form conservation equation for kinetic energy

$$\partial_t(\rho \mathcal{K}^{\text{hyd}}) + \nabla \cdot [\mathbf{v} (\rho \mathcal{K}^{\text{hyd}} + p)] = p \nabla \cdot \mathbf{v} - \rho g w + \rho \mathbf{u} \cdot \mathbf{F}. \quad (11.16)$$

Furthermore, $\Phi = g z$ means that

$$\rho D\Phi/Dt = \partial_t(\rho \Phi) + \nabla \cdot (\rho \mathbf{v} \Phi) = \rho g w, \quad (11.17)$$

in which case the flux-form equation for the mechanical energy per mass, \mathcal{M}^{hyd} , is given by

$$\partial_t(\rho \mathcal{M}^{\text{hyd}}) + \nabla \cdot [\rho \mathbf{v} (\mathcal{M}^{\text{hyd}} + p/\rho)] = p \nabla \cdot \mathbf{v} + \rho \mathbf{u} \cdot \mathbf{F}, \quad (11.18)$$

where

$$\mathcal{M}^{\text{hyd}} = \mathcal{K}^{\text{hyd}} + \Phi = \mathbf{u} \cdot \mathbf{u}/2 + g z. \quad (11.19)$$

Equation (11.18) compares to the non-hydrostatic mechanical energy equation (10.52). The key difference is that the kinetic energy per mass is here just given by the horizontal flow (11.14). Additionally, the friction vector for the hydrostatic flow is horizontal. Otherwise, the physical interpretation of the mechanical energy budget accords with that for the non-hydrostatic flow given in Section 10.3.

11.1.6 Depth integrated mechanical energy budget

We here extend the analysis from Section 11.1.5 to derive the depth integrated mechanical energy budget for the hydrostatic primitive equations. We here integrate over the depth of an ocean column, whereas for an atmospheric column we let the surface go to infinity. The kinetic energy per area contained in the horizontal flow as integrated over a column is given by

$$\int_{\eta_b}^{\eta} \rho \mathcal{K}^{\text{hyd}} dz = \frac{1}{2} \int_{\eta_b}^{\eta} \rho \mathbf{u} \cdot \mathbf{u} dz. \quad (11.20)$$

Leibniz's rule leads to the time tendency

$$\frac{d}{dt} \int_{\eta_b}^{\eta} \rho \mathcal{K}^{hyd} dz = \partial_t \eta [\rho \mathcal{K}^{hyd}]_{z=\eta} + \int_{\eta_b}^{\eta} \partial_t (\rho \mathcal{K}^{hyd}) dz. \quad (11.21)$$

Making use of the kinetic energy equation (11.16) as well as Leibniz's rule gives the budget

$$\begin{aligned} \frac{d}{dt} \int_{\eta_b}^{\eta} \rho \mathcal{K}^{hyd} dz &= [\rho \mathcal{K}^{hyd} + p_a]_{z=\eta} (\partial_t \eta - w + \mathbf{u} \cdot \nabla \eta)_{z=\eta} + [\rho \mathcal{K}^{hyd} + p_b]_{z=\eta_b} (w - \mathbf{u} \cdot \nabla \eta_b)_{z=\eta_b} \\ &\quad - \nabla_h \cdot \left(\rho \mathbf{u} \mathcal{K}^{hyd} + \mathbf{u} p \right) dz + \int_{\eta_b}^{\eta} (p \nabla \cdot \mathbf{v} - \rho g w + \rho \mathbf{u} \cdot \mathbf{F}) dz. \end{aligned} \quad (11.22)$$

Note that when bringing ∇_h outside the vertical integral, besides making use of Leibniz's rule, we also assumed ∇_h is itself independent of z , which is trivially the case with Cartesian coordinates. However, for spherical coordinates the assumption requires the [shallow fluid approximation](#) so that the r^{-1} appearing in the gradient operator is replaced by R_e^{-1} as per equation (11.4). It is here that we see that the depth integrated equations are most usefully posed when working with the hydrostatic primitive equations.

The bottom and surface kinematic boundary conditions from VOLUME 1 then give the depth-integrated kinetic energy budget

$$\begin{aligned} \frac{d}{dt} \int_{\eta_b}^{\eta} \rho \mathcal{K}^{hyd} dz &= \\ Q_m [\mathcal{K}^{hyd} + p_a/\rho]_{z=\eta} - \nabla_h \cdot \int_{\eta_b}^{\eta} &(\rho \mathbf{u} \mathcal{K}^{hyd} + \mathbf{u} p) dz + \int_{\eta_b}^{\eta} (p \nabla \cdot \mathbf{v} - \rho g w + \rho \mathbf{u} \cdot \mathbf{F}) dz. \end{aligned} \quad (11.23)$$

The first term on the right hand side arises from the mass transport across the ocean surface, along with the applied surface pressure. The second term is the horizontal convergence of the depth integrated flux of kinetic energy plus pressure. The final term is the depth integral of the buoyancy conversion term, pressure work, plus frictional work. Similar manipulations starting from the flux-form mechanical energy budget (11.18) lead to the depth integrated budget

$$\begin{aligned} \frac{d}{dt} \int_{\eta_b}^{\eta} \rho \mathcal{M}^{hyd} dz &= \\ Q_m [\mathcal{M}^{hyd} + p_a/\rho]_{z=\eta} - \nabla_h \cdot \int_{\eta_b}^{\eta} &(\rho \mathbf{u} \mathcal{M}^{hyd} + \mathbf{u} p) dz + \int_{\eta_b}^{\eta} (p \nabla \cdot \mathbf{v} + \rho \mathbf{u} \cdot \mathbf{F}) dz, \end{aligned} \quad (11.24)$$

where we see that the buoyancy conversion term cancels.

11.1.7 Comments and further study

The [hydrostatic primitive equations](#) make use of the momentum equations, which contrasts to *non-primitive* equation methods that develop evolution equations for the vorticity and divergence. [Smagorinsky \(1963\)](#) was an early proponent of the hydrostatic primitive equations for use in studying the large-scale ocean and atmospheric circulation. These equations form the basis for many general circulation models of the atmosphere and ocean. However, it is notable that finer resolution simulations, that admit strong vertical motions, must make use of the non-hydrostatic primitive equations. Non-hydrostatic simulations are particularly relevant when studying clouds in the atmosphere and fine-scale mixing in the ocean, with both of these

processes involving nontrivial vertical accelerations that break the hydrostatic approximation. These models sometimes also time step the momentum equations, in which case they are referred to as the [non-hydrostatic primitive equations](#).

11.2 Elements of approximate hydrostatic pressure

For a static fluid with identically zero net acceleration, the vertical pressure gradient precisely balances the weight of fluid to thus realize exact [hydrostatic balance](#). We discussed this static solution to the equations of motion in Sections 8.6 and 9.5. For a moving fluid with scales of motion that maintain a small vertical to horizontal aspect ratio, the presentation in this section reveals that the vertical pressure gradient and gravitational acceleration individually remain far larger than other accelerations acting on a fluid element. In this case, the vertical momentum equation, even for the moving fluid, remains approximately in hydrostatic balance column-by-column. We thus have a fluid flow whereby each vertical fluid column is in hydrostatic balance, and yet there are horizontal pressure gradients that drive motion. In this section we study aspects of such approximately hydrostatic fluid flows.

For simplicity in this section we make use of Cartesian coordinates rather than the spherical coordinates used in Section 11.1.

11.2.1 Expressions for the hydrostatic pressure

Making the hydrostatic approximation in the vertical momentum equation leads to the local balance

$$\partial_z p = -\rho g. \quad (11.25)$$

Vertically integrating upward from a point within the ocean to the ocean surface leads to the hydrostatic pressure

$$p(x, y, z, t) = p_a(x, y, t) + g \int_z^\eta \rho(x, y, z', t) dz'. \quad (11.26)$$

In this equation we wrote $p(\eta) = p_a$ for the pressure at the ocean free surface, $z = \eta(x, y, t)$, arising from the weight of the overlying atmosphere or sea ice; i.e., this is the applied pressure acting on the top of the ocean fluid. A similar integration applies to the atmosphere

$$p(x, y, z, t) = g \int_z^{z_{\text{top}}} \rho(x, y, z', t) dz', \quad (11.27)$$

where $z = z_{\text{top}}$ is the top of the atmosphere, sometimes approximated by $z_{\text{top}} = \infty$. For both the ocean and the atmosphere, we assume g remains a constant over the vertical extent of the fluid, which is a sensible approximation even for the top of the atmosphere.³

In both the ocean and atmosphere, the hydrostatic pressure at a vertical position, z , equals to the weight per horizontal area of matter above that position, with equations (11.26) and (11.27) providing explicit expressions in terms of *in situ* density and boundary contributions. These expressions offer a great simplification for how we determine pressure relative to the non-hydrostatic case. The remainder of this section provides example implications.

³See [Staniforth \(2022\)](#) for a more accurate calculation of the gravitational acceleration for use in global atmosphere and ocean models.

11.2.2 Evolution of hydrostatic pressure

We expect that hydrostatic pressure evolves according to the convergence of mass onto the column of fluid above that point. The ocean hydrostatic pressure also changes due to time changes in the applied upper boundary pressure. Here we derive mathematical expressions that support these expectations, with Figure 11.1 providing a schematic.

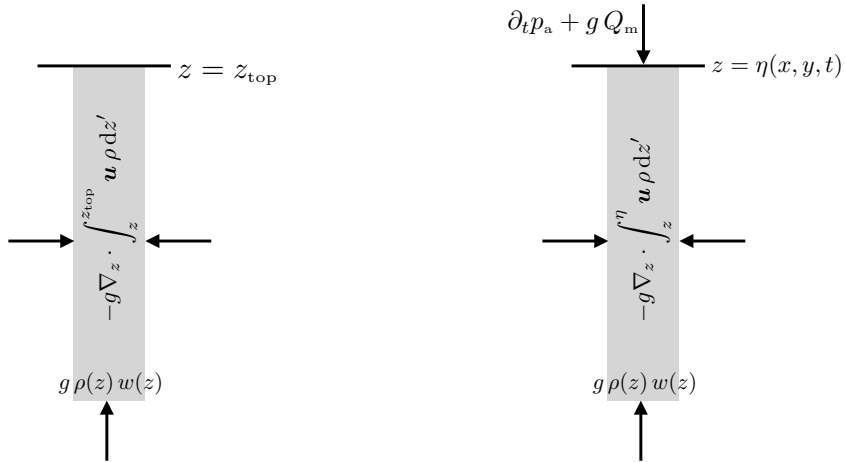


FIGURE 11.1: Evolution of hydrostatic pressure for a vertical position in the atmosphere (left panel) and ocean (right panel) according to equations (11.29) and (11.31a). Hydrostatic pressure at a vertical position, z , which here is the bottom of the fluid column, arises from the convergence of mass onto the column over the region above z . The ocean column also has a contribution from the time tendency of applied surface pressure plus the mass of coming across the top boundary. For the atmosphere as assume the top boundary is at $z_{\text{top}} = \infty$ and so there is no mass coming across that boundary.

Hydrostatic pressure in the atmosphere

A time derivative of the atmospheric hydrostatic pressure (11.27) renders

$$\partial_t p = g \int_z^{z_{\text{top}}} \partial_t \rho(x, y, z', t) dz'. \quad (11.28)$$

Note the absence of a time derivative on z_{top} . We ensure this time derivative is not relevant by setting z_{top} to a constant value well above anything of physical relevance; e.g., $z_{\text{top}} \approx \infty$. In Exercise 11.1 we introduce the [mass continuity](#) equation to derive

$$\partial_t p = g \rho(z) w(z) - g \nabla_h \cdot \int_z^{z_{\text{top}}} \mathbf{u} \rho dz'. \quad (11.29)$$

As anticipated, the hydrostatic pressure at a point changes according to the convergence of mass onto the column above that point, as can occur through motion across the bottom and through the side, with this equation illustrated in Figure 11.1.

Hydrostatic pressure in the ocean

The derivation for the ocean requires some more work since the ocean free surface is a permeable space and time dependent function. A time derivative of the ocean pressure expression (11.26)

renders

$$\partial_t p = \partial_t p_a + g \rho(\eta) \partial_t \eta + g \int_z^\eta \partial_t \rho(x, y, z', t) dz', \quad (11.30)$$

where we made use of Leibniz's rule to take the time derivative of the upper limit at $z = \eta(x, y, t)$, and with the shorthand $\rho(\eta) = \rho(x, y, z = \eta, t)$. In Exercise 11.1 we perform the necessary steps to derive

$$\partial_t p = \partial_t p_a + g \rho(z) w(z) + g Q_m - g \nabla_h \cdot \int_z^\eta \mathbf{u} \rho dz', \quad (11.31a)$$

with this equation illustrated in Figure 11.1. The first term on the right hand side arises from time fluctuations of the applied pressure at $z = \eta$. The second and third terms measure the vertical convergence of mass onto the column of fluid sitting above the vertical position, with $\rho(z) w(z)$ the mass flux entering the column from below and Q_m the mass flux entering from across the free surface. The final term arises from the vertically integrated horizontal mass transport converging onto the column above the position of interest.

11.2.3 Heuristic scaling

We here present a scale analysis to justify the hydrostatic approximation. This analysis serves to introduce a common method used in fluid mechanics to identify those processes that may be dominant for a particular flow regime. In particular, the flow regime of interest here occurs for motion with a small vertical to horizontal aspect ratio

$$\alpha_{\text{aspect}} \equiv H/L \ll 1. \quad (11.32)$$

Here, the scale H a typical length scale for vertical motion, whereas L is the horizontal length scale of the motion. This small aspect ratio regime is fundamental to the large-scale circulation of the ocean and atmosphere. As the hydrostatic approximation is concerned with the force balances in a fluid column, it is sufficient to ignore rotation when performing a scale analysis.

Consider the vertical momentum equation (8.54c) from the tangent plane and traditional approximations (Section 8.5), along with the associated scales for the various terms

$$\frac{Dw}{Dt} = -\frac{1}{\rho} \frac{\partial p}{\partial z} - g \quad (11.33a)$$

$$\frac{W}{T} + \frac{UW}{L} + \frac{WW}{H} = -\frac{1}{\rho} \frac{\partial p}{\partial z} - g. \quad (11.33b)$$

In the second equation we introduced the following scales for the terms appearing on the left hand side of the first equation.

- L is the horizontal scale of the motion.
- H is the vertical scale of the motion.
- W is the vertical velocity scale.
- U is the horizontal velocity scale. For this analysis we do not distinguish between the zonal and meridional velocity scales, writing U for both. This assumption is not always valid, such as when scaling for jet stream or equatorial flows, both of which have larger zonal speeds than meridional.

- T is the time scale of the motion. We assume that the time scale is determined by horizontal advection; i.e., we use an [advection time scale](#)⁴ so that $T \sim L/U$.

Each of these scales emerge from the flow, and as such we refer to them as [emergent scales](#). They are scales that we choose to focus on as part of the analysis. To get a sense for the numbers, consider large-scale atmospheric flows with $W = 10^{-2} \text{ m s}^{-1}$, $L = 10^5 \text{ m}$, $H = 10^3 \text{ m}$, $U = 10 \text{ m s}^{-1}$. These numbers lead to the time scale, $T = L/U = 10^4 \text{ s}$, and to the values for the vertical momentum equation

$$10^{-6} \text{ m s}^{-2} \sim -\frac{1}{\rho} \frac{\partial p}{\partial z} - g. \quad (11.34)$$

With $g \sim 10 \text{ m s}^{-2}$, the only term that can balance the gravitational acceleration is the vertical pressure gradient. A similar analysis holds for large-scale ocean flows where we set $W = 10^{-3} \text{ m s}^{-1}$, $L = 10^3 \text{ m}$, $H = 10^1 \text{ m}$, $U = 10^{-1} \text{ m s}^{-1}$. These numbers lead to a time scale, $T = L/U = 10^4 \text{ s}$, and to

$$10^{-7} \text{ m s}^{-2} \sim -\frac{1}{\rho} \frac{\partial p}{\partial z} - g. \quad (11.35)$$

In either case, large scale motion maintains an approximate hydrostatic balance whereby $\partial p/\partial z = -\rho g$.

We offer a more formal scale analysis in Section 13.2, making use of the oceanic Boussinesq equations derived in Chapter 13. For the remainder of this section we explore certain properties of a fluid flow maintaining an approximate hydrostatic balance.

11.2.4 Removal of a dynamically irrelevant background state

The previous analysis pointed to the dominance of the hydrostatic balance in the vertical momentum equation for large scale motions. However, is that analysis sufficient to understand what causes motion? To help answer that question, consider a density field that is decomposed into a constant, ρ_0 , plus a deviation

$$\rho(\mathbf{x}, t) = \rho_0 + \rho'(\mathbf{x}, t), \quad (11.36)$$

with a corresponding decomposition of the pressure field

$$p(\mathbf{x}, t) = p_0(z) + p'(\mathbf{x}, t) \quad \text{with} \quad \frac{dp_0}{dz} = -\rho_0 g. \quad (11.37)$$

That is, the pressure is decomposed into a background [static pressure](#) field that is just a function of z , plus a deviation from the background pressure. In this case, the non-rotating vertical momentum equation takes the form

$$\rho \frac{Dw}{Dt} = -\frac{\partial p'}{\partial z} - \left[\frac{dp_0}{dz} + \rho_0 g \right] = -\frac{\partial p'}{\partial z}. \quad (11.38)$$

We thus see that the exact hydrostatically balanced background pressure, $p_0(z)$, has no dynamical implications. Correspondingly, to garner a more relevant scaling for the hydrostatic balance it is appropriate to ask whether the dynamically active pressure, p' , is approximately hydrostatic.

⁴This assumption for time scale is not always appropriate, such as for studies of waves where we may instead consider time scales according to a wave speed and wave length.

For flows with small aspect ratios, the vertical momentum equation remains approximately hydrostatic even when removing the dynamically inactive background pressure field. So our intuition about hydrostatic dominance holds unchanged even for the dynamical pressure. The formal justification of this approximation is nicely framed within the Boussinesq equations of Chapter 13 since the pressure force in these equations exposes just the dynamically active pressure. We thus postpone further discussion of hydrostatic scaling until Section 13.2.

11.2.5 Ocean dynamic topography

There are occasions in ocean physics where it is useful to study the thickness of a layer bounded below by an isobar in the ocean interior and above by the free surface, as depicted in Figure 11.2)

$$D(p) = \eta - z(p). \quad (11.39)$$

Assuming a hydrostatic balance for each fluid column allows us to relate this expression to the vertical integral between two pressure surfaces of the specific volume, ρ^{-1}

$$D(p) = \int_{z(p)}^{\eta} dz = g^{-1} \int_{p_a}^p \frac{dp'}{\rho}, \quad (11.40)$$

where the second step used the hydrostatic balance and absorbed a minus sign by swapping integral limits. We refer to the thickness, $D(p)$, as the **dynamic topography** with respect to a reference pressure, p , and it is also known as the **steric sea level**.

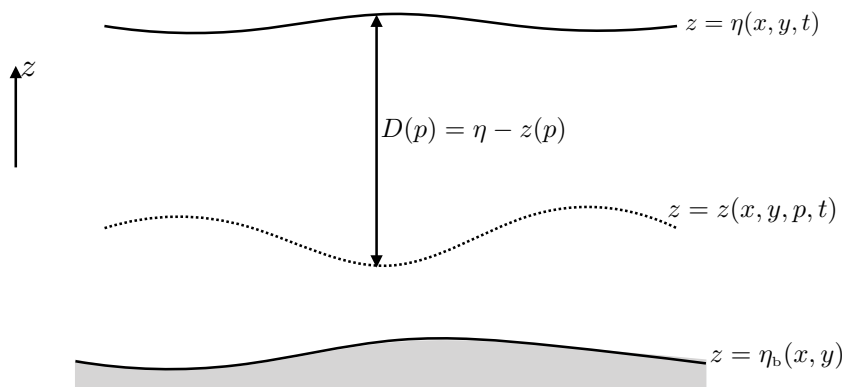


FIGURE 11.2: The ocean dynamic topography, $D(p) = \eta - z(p)$, is the thickness of a layer from the sea surface at $z = \eta(x, y, t)$ to the vertical position of a constant pressure surface, $z = z(x, y, p, t)$.

Evolution of the dynamic topography arises from changes in the pressure applied to the free surface as well as changes in the specific volume

$$g \frac{\partial D(p)}{\partial t} = -\frac{1}{\rho(\eta)} \frac{\partial p_a}{\partial t} + \int_{p_a}^p \frac{\partial \rho^{-1}}{\partial t} dp. \quad (11.41)$$

Importantly, the time derivative here acts on the specific volume when computed on surfaces of constant pressure. If the depth, $z(p)$, of the constant pressure surface is static, then the evolution of layer thickness, $D(p)$, is identical to the sea surface, η . In general, there is no such static pressure level, thus making the time tendencies differ, though certain situations warrant this approximation.

11.2.6 Surfaces of atmospheric geopotential height and pressure

In Section 7.5.10 we computed the [geopotential height](#) within an exact hydrostatic and ideal gas atmosphere. We here apply those results to the case of approximate hydrostatic and ideal gas columns, making use of equation (7.83) for the difference in geopotential height between two constant pressure surfaces (isobars)

$$Z_2 - Z_1 = -(R^{\text{air}} \langle T \rangle / g) \ln(p_2/p_1). \quad (11.42)$$

In this equation, $\langle T \rangle$ is the mean temperature within the column as computed according to equation (7.81), and R^{air} is the specific gas constant for air given by equation (7.52). The [geopotential thickness](#) (11.42) is positive when the isobars have $p_2 < p_1$. This situation holds when level-2 sits at a higher altitude in the atmosphere than level-1, since the hydrostatic pressure decreases moving upward.

The geopotential thickness (11.42) is directly proportional to the column mean temperature, so that a warmer column is thicker. This result is expected since for a given mass of air, a warmer column is less dense and so isobars are higher over warmer hydrostatic air columns than cooler columns. Correspondingly, when moving horizontally along a constant geopotential surface (constant z), we encounter higher pressure when moving into a region of warmer air. This situation is entirely analogous to that studied later in Figure 11.4 when studying the horizontal pressure difference between two hydrostatic and equal mass columns of seawater. We can see this property mathematically by using equation (11.42) to compute the [law of atmospheres](#) or the [barometric law](#) (also encountered in Section 7.5.10)

$$p_1 = p_2 e^{(Z_2 - Z_1)g/(R^{\text{air}} \langle T \rangle)}, \quad (11.43)$$

thus revealing that p_1 is larger in regions where $\langle T \rangle$ is larger.

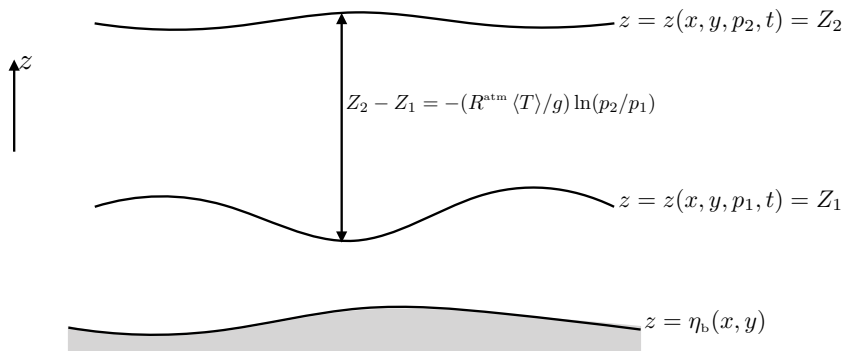


FIGURE 11.3: Geopotential thickness for a layer of an ideal gas atmosphere located between two constant pressure surfaces as given by equation (11.42): $Z_2 - Z_1 = -(R^{\text{air}} \langle T \rangle / g) \ln(p_2/p_1)$. When the flow is approximately hydrostatic, then $p_2 < p_1$ so that the thickness of the layer is positive. Also notice that the layer thickness increases when the column averaged temperature, $\langle T \rangle$, increases. Correspondingly, when moving horizontally along a constant geopotential surface (fixed z), we encounter higher pressure when moving into a region of warmer air and lower pressure when moving into a region of colder air, which is seen from the pressure equation (11.43).

11.2.7 Concerning vertical motion

Unbalanced vertical accelerations still exist in an approximate hydrostatic flow.⁵ Yet these vertical accelerations are not seen in the prognostic equations, since the vertical momentum equation is just the local hydrostatic balance. Hence, rather than compute vertical motion prognostically, vertical motion in an approximate hydrostatic flow must be diagnosed through constraints on the motion.

For example, volume continuity discussed in Section 13.1.4 provides a constraint in a three-dimensionally non-divergent flow ($\nabla \cdot \mathbf{v} = 0$). In this flow, a horizontal velocity divergence, $\nabla_h \cdot \mathbf{u} > 0$, is balanced by vertical velocity convergence, $-\partial_z w = \nabla_h \cdot \mathbf{u} > 0$. There are vertical pressure forces that give rise to the vertical motion, and they are precisely those pressure forces needed to maintain a non-divergent flow. In a hydrostatic flow, we do not directly compute these forces for the purpose of prognosing vertical accelerations. Rather, the vertical acceleration is inferred through the $\nabla \cdot \mathbf{v} = 0$ kinematic constraint. Even so, the forces can be diagnosed given the velocity and the accelerations.

11.2.8 Further study

Section 2.7.4 in [Vallis \(2017\)](#) provides examples of scales over which the hydrostatic relation remains a useful approximation in geophysical fluid flows. Further discussions of dynamic topography are given in Appendix B.4 of [Griffies et al. \(2014\)](#) as well as in [Tomczak and Godfrey \(1994\)](#). This [8-minute video from Prof. Hogg](#) offers a pedagogical introduction to hydrostatic pressure.

11.3 Horizontal pressure gradients

In contrast to an exact hydrostatic fluid, where there is no fluid motion, there are generally horizontal pressure gradients in an approximate hydrostatic fluid flow, and these horizontal gradients drive horizontal motion. Such horizontal pressure gradients can arise from horizontal differences in the mass density. We refer to such pressure gradients as [internal pressure gradients](#) since they arise from density gradients internal to the fluid. Internal pressure gradients are sometimes referred to as [baroclinic pressure gradients](#). Horizontal pressure gradients can also arise from horizontal gradients in the total mass of a fluid column, with such pressure gradients referred to as [external pressure gradients](#). External pressure gradients are sometimes referred to as [barotropic pressure gradients](#).

In developing an understanding of the horizontal pressure accelerations in an approximate hydrostatic flow, it is useful to examine the variety of expressions for the pressure gradient, which is the purpose of this section. We make use of these expressions for case studies in Section 11.4. Note that we couch the language for the ocean case, though the atmosphere case can be readily found through simplifying the ocean expressions.

11.3.1 Top down horizontal pressure gradient

Here we examine the horizontal pressure gradient in an approximate hydrostatic flow, and do so by integrating from the top down. This approach complements that in Section 11.3.2, which starts from the bottom and integrates up.

⁵By “unbalanced”, we here mean accelerations that are not hydrostatically balanced.

External and internal contributions to the horizontal pressure gradient

Recall equation (11.26), which expresses the hydrostatic pressure at a point within the ocean

$$p(x, y, z, t) = p_a(x, y, t) + g \int_z^\eta \rho(x, y, z', t) dz'. \quad (11.44)$$

In this equation, $p_a = p[x, y, z = \eta(x, y, t), t]$ is the pressure applied to the ocean free surface at $z = \eta(x, y, t)$ from any mass above the ocean, such as the atmosphere or cryosphere. In some idealized cases we assume the media above the ocean is massless, in which case $p_a = 0$. Now introduce the globally referenced [Archimedean buoyancy](#) (see Chapter 14) as defined by

$$b = -g(\rho - \rho_0)/\rho_0, \quad (11.45)$$

in which case the hydrostatic pressure is

$$p = -g \rho_0 z + g \rho_0 [\eta + p_a/(g \rho_0)] - \rho_0 \int_z^\eta b dz'. \quad (11.46)$$

The first term on the right hand side is a background pressure that increases moving downward. However, this background pressure has no horizontal dependence and so it does not contribute to the horizontal pressure gradient. In contrast, the second and third terms have horizontal gradients and are thus sometimes referred to as the [dynamical pressure](#). The second term arises from the free surface height plus the applied surface pressure. This term is uniformly felt throughout the fluid column since it has no vertical dependence. The free surface term is the product of the large number, $g \rho_0$, times a small free surface undulation, η . The third term arises from buoyancy within the fluid computed relative to the constant background density, ρ_0 , and this term is a function of vertical position. Furthermore, it is the vertical integral over a generally large depth range of the buoyancy, and it can be of comparable magnitude to the second term.

The horizontal gradient of the hydrostatic pressure (11.46) is given by

$$\nabla_h p = \underbrace{\nabla_h p_a + g \rho(\eta) \nabla_h \eta}_{\text{external contribution}} - \underbrace{\rho_0 \int_z^\eta \nabla_h b dz'}_{\text{internal contribution}} = \underbrace{\nabla_h p_a + g \rho(\eta) \nabla_h \eta}_{\text{external contribution}} + \underbrace{g \int_z^\eta \nabla_h \rho dz'}_{\text{internal contribution}}. \quad (11.47)$$

The internal contribution to the pressure gradient arises from horizontal gradients in Archimedean buoyancy that are integrated vertically over the region above the point of interest. The external contribution acts throughout the vertical fluid column since it is only a function of horizontal position and time. Every point within the fluid column instantly feels this term whenever there is a gradient in the applied surface pressure, the surface height, or the surface buoyancy, with $\rho_0[g - b(\eta)] = g \rho(\eta)$.

Mathematical comments regarding the external contribution

Observe that the external contributions to the horizontal pressure gradient in equation (11.47) are all functions of horizontal position and time, so there is no z dependence to hold fixed when computing ∇_h on these terms. Even so, we sometimes retain the ∇_h notation to align with that required to denote a horizontal gradient operator acting on three dimensional fields, such as buoyancy, $b(x, y, z, t)$, and density, $\rho(x, y, z, t)$.

To exemplify this comment, observe that the external contribution can be written as the

horizontal pressure gradient evaluated at the ocean surface⁶

$$(\nabla_h p)_{z=\eta} = \nabla_h p_a + g \rho(\eta) \nabla_h \eta. \quad (11.48)$$

Hence, the pressure gradient in equation (11.47) can be written in the succinct form

$$\nabla_h p = (\nabla_h p)_{z=\eta} - \rho_0 \int_z^\eta \nabla_h b \, dz' = (\nabla_h p)_{z=\eta} + g \int_z^\eta \nabla_h \rho \, dz'. \quad (11.49)$$

Observe that the component of the horizontal pressure gradient in a direction tangent to the free surface arises just from the $\nabla_h p_a$ term.

Mathematically, equation (11.48) decomposes the horizontal pressure gradient into the horizontal gradient of pressure along the curved free surface (the $\nabla_h p_a$ term), plus a term that accounts for curvature of the free surface (the $g \rho(\eta) \nabla_h \eta$ term). As seen in VOLUME 3, this decomposition of the horizontal pressure gradient, made throughout the fluid column, is a key step needed to formulate the equations of motion using generalized vertical coordinates.

11.3.2 Bottom up horizontal pressure gradient

It is sometimes useful to work with the bottom pressure and bottom topography, rather than the free surface height. For this purpose we invert the formulation from Section 11.3.1 by introducing the bottom pressure

$$p_b = p_a + g \int_{\eta_b}^{\eta} \rho \, dz, \quad (11.50)$$

in which case

$$p = p_a + g \int_z^{\eta} \rho \, dz \quad (11.51a)$$

$$= p_a + g \int_{\eta_b}^{\eta} \rho \, dz - g \int_{\eta_b}^z \rho \, dz \quad (11.51b)$$

$$= p_b - g \int_{\eta_b}^z (\rho - \rho_0 + \rho_0) \, dz \quad (11.51c)$$

$$= p_b - g \rho_0 (z - \eta_b) + \rho_0 \int_{\eta_b}^z b \, dz', \quad (11.51d)$$

so that the corresponding expression for the horizontal hydrostatic pressure gradient is

$$\nabla_h p = \underbrace{\nabla_h p_b + g \rho(\eta_b) \nabla_h \eta_b}_{\text{external contribution}} + \underbrace{\rho_0 \int_{\eta_b}^z \nabla_h b \, dz'}_{\text{internal contribution}} = \underbrace{\nabla_h p_b + g \rho(\eta_b) \nabla_h \eta_b}_{\text{external contribution}} - \underbrace{g \int_{\eta_b}^z \nabla_h \rho \, dz'}_{\text{internal contribution}}. \quad (11.52)$$

The horizontal pressure gradient at the bottom

Just as for the pressure gradient expression (11.47), observe that equation (11.52) decomposes the horizontal pressure gradient into an external and internal contribution. The internal contribution arises from gradients in the buoyancy as integrated below the depth of interest. The external contributions arise from gradients in the bottom pressure, which measures the

⁶Namely, all terms in equation (11.48) are a function just of the horizontal position computed along the $z = \eta(x, y, t)$ ocean surface, so that we could write ∇ rather than ∇_h . Yet on the left hand side it is important to write ∇_h , since we are evaluating the horizontal pressure gradient at the surface.

mass per area of fluid within the column, plus gradients in the bottom topography as weighted by the bottom buoyancy (11.58). The external contribution can be written as the horizontal pressure gradient evaluated at the ocean bottom

$$(\nabla_h p)_{z=\eta_b} = \nabla_h p_b + g \rho(\eta_b) \nabla_h \eta_b, \quad (11.53)$$

which accords with equation (11.48) for the horizontal pressure gradient evaluated at the ocean surface. Evidently, the horizontal pressure gradient at the ocean bottom equals to the gradient of the bottom pressure, plus a term that accounts for the bottom slope. Furthermore, the component of the horizontal pressure gradient in a direction tangent to the ocean bottom arises just from the $\nabla_h p_b$ term. Finally, we make use of expression (11.53) to produce a more succinct form of the horizontal pressure gradient (11.52)

$$\nabla_h p = (\nabla_h p)_{z=\eta_b} + \rho_o \int_{\eta_b}^z \nabla_h b \, dz' = (\nabla_h p)_{z=\eta_b} - g \int_{\eta_b}^z \nabla_h \rho \, dz'. \quad (11.54)$$

Further decomposing the bottom pressure contribution

The bottom pressure contribution to equations (11.52) and (11.54) is generally dominated by gradients in the bottom topography. These gradients are static and so it can be useful to isolate the bottom topography by taking the horizontal gradient of equation (11.50) to find

$$\nabla_h p_b = \nabla p_a + g \rho(\eta) \nabla \eta - g \rho(\eta_b) \nabla \eta_b + g \int_{\eta_b}^{\eta} \nabla_h \rho \, dz \quad (11.55a)$$

$$= \left[\nabla p_a + g \rho(\eta) \nabla \eta - b(\eta_b) \nabla \eta_b + g \int_{\eta_b}^{\eta} \nabla_h \rho \, dz \right] - g \rho_o \nabla \eta_b, \quad (11.55b)$$

in which case we write the bottom pressure gradient as

$$\nabla_h p_b = \nabla_h p'_b - g \rho_o \nabla_h \eta_b, \quad (11.56)$$

so that the horizontal pressure gradient takes the form

$$\nabla_h p = \underbrace{\nabla_h p'_b - \rho_o b(\eta_b) \nabla_h \eta_b}_{\text{external contribution}} + \underbrace{\rho_o \int_{\eta_b}^z \nabla_h b \, dz'}_{\text{internal contribution}}, \quad (11.57)$$

where we introduced the bottom buoyancy via

$$\rho_o [g - b(\eta_b)] \nabla \eta_b = g \rho(\eta_b) \nabla \eta_b. \quad (11.58)$$

11.4 Balancing internal and external pressure gradients

In this section we work through a set of case studies by considering a given density configuration that sets up an internal pressure gradient, and then seek a sea level configuration that establishes an external pressure gradient to balance the internal pressure gradient, thus leading to a net zero horizontal pressure gradient. We do not seek reasons for why the internal and external pressure gradients balance, which require more than the hydrostatics used in this chapter. Rather, we consider the balanced state as a useful means to further an understanding of hydrostatic pressure. We are also motivated by noting that many ocean flows maintain a partial balance

between internal and external pressure gradients along certain surfaces, which motivates the notion of a [level of no motion](#), thus making the balanced state a useful starting point for examining the more complete dynamics of a particular flow.

As the starting point for these considerations, recall the expressions for the horizontal pressure gradient along the ocean surface (equation (11.48)) and ocean bottom (equation (11.53)). Here we list these equalities again, along with expressions that follow from evaluating equation (11.49) at the ocean bottom and equation (11.54) at the ocean surface

$$(\nabla_h p)_{z=\eta} = \nabla_h p_a + g \rho(\eta) \nabla_h \eta = (\nabla_h p)_{z=\eta_b} - g \int_{\eta_b}^{\eta} \nabla_h \rho dz \quad (11.59a)$$

$$(\nabla_h p)_{z=\eta_b} = \nabla_h p_b + g \rho(\eta_b) \nabla_h \eta_b = (\nabla_h p)_{z=\eta} + g \int_{\eta_b}^{\eta} \nabla_h \rho dz. \quad (11.59b)$$

11.4.1 Horizontal hydrostatic pressure gradient in a mass conserving fluid

As a warm-up to the continuous cases to follow, we work through an example emblematic of how one determines the sign for horizontal pressure gradients in an approximate hydrostatic balance. The example is posed for equal mass columns of mass conserving fluid in a bounded fluid layer, such as the ocean, but these considerations hold for the atmosphere where the upper boundary is the top of the atmosphere (i.e., effectively unbounded). We assume the flat bottom of the layer has a constant pressure so that the horizontal pressure gradient vanishes along the bottom, thus offering a particular example of the [level of no motion](#).

Two columns with equal mass yet different densities

Consider two adjacent columns of seawater with equal mass but with distinct density; assume the density in each column is constant throughout the respective columns; and assume the atmospheric pressure is equal above the two water columns. Figure 11.4 offers a schematic, where we make the additional assumption that the two columns sit on a flat bottom. We can imagine setting up this configuration by starting with uniform density water, then warming the water in column B more than column A while maintaining constant mass in the two columns. This process sets up a horizontal density gradient with an associated horizontal gradient in the hydrostatic pressure. Furthermore, the less dense water in column B occupies more volume so that its free surface sits higher

$$\rho_B < \rho_A \implies \eta_B > \eta_A. \quad (11.60)$$

What is the sign of the horizontal hydrostatic pressure gradient? As we show in the following, column B (the low density column) has larger hydrostatic pressure than column A (the high density column) for every point in the column, except at the bottom where the two bottom pressures are identical since the two columns have equal mass. The bottom thus represents a [level of no motion](#).

Computing pressure starting from the equal bottom pressures

Since the two columns have equal mass and equal cross-sectional area, the hydrostatic pressures (weight per unit area) at the bottom of the two columns are equal and given by

$$p_b = g \rho_A (\eta_A - \eta_b) = g \rho_B (\eta_B - \eta_b), \quad (11.61)$$

where $z = \eta_b(x, y)$ is the vertical position at the bottom, $z = \eta_A(x, y, t)$ is the top of column A, and $z = \eta_B(x, y, t)$ is the top of column B. Since the bottom pressures are identical, there is no horizontal pressure gradient at the bottom so that all pressure gradients exist above the bottom.

The hydrostatic pressure at an arbitrary position within column A is given by

$$p_A(z) = g \rho_A (\eta_A - z) = p_b - g \rho_A (-\eta_b + z), \quad (11.62)$$

where we only expose here the z dependence to reduce clutter. The second equality arose by substituting the bottom pressure from equation (11.61) to eliminate the surface height η_A . Doing so is useful since we know that $\eta_A \neq \eta_B$, and yet the bottom pressure is the same for the two columns. The same approach for pressure in column B yields

$$p_B(z) = g \rho_B (\eta_B - z) = p_b - g \rho_B (-\eta_b + z). \quad (11.63)$$

We can now take the difference between the two hydrostatic pressures to find

$$p_B(z) - p_A(z) = g (-\eta_b + z) (\rho_A - \rho_B) > 0. \quad (11.64)$$

Since $\rho_A > \rho_B$ and $z \geq \eta_b$ we see that at any point above the bottom, the hydrostatic pressure in column B (the lighter column) is greater than that in column A (the denser column). This horizontal difference in the hydrostatic pressure renders a force pointing from column B to column A. Vertically integrating this pressure difference over the thickness of column A leads to the net force per horizontal length

$$\mathbf{F}_{B \rightarrow A} = \int_{\eta_b}^{\eta_A} [p_B(z) - p_A(z)] dz = (g/2) (\rho_A - \rho_B) (\eta_A - \eta_b)^2 > 0. \quad (11.65)$$

Inferring pressure gradients starting from the top

Another way to understand why the pressure force points from column B to column A is to note that at the top of both columns the pressures are the same (and equal to the uniform atmospheric pressure). However, since column B sits higher than column A, as we move down from $z = \eta_B$ the pressure increases in column B immediately, whereas the pressure in column A remains at the atmospheric pressure until entering the water column at $z = \eta_A < \eta_B$. So it is clear that the pressure in column B is greater than A starting from the surface and moving down. Since the two bottom pressures are equal, then we infer the pressure isolines as drawn in Figure 11.4.

11.4.2 Balanced pressure gradients above a level of no motion

Consider the case in which there is zero horizontal pressure gradient along a constant geopotential surface

$$z = \eta_{nm}. \quad (11.66)$$

We might find this configuration to be a relevant approximation of the sluggish flows in the deep ocean where flow can be much weaker than the upper ocean, thus corresponding to relatively weak horizontal pressure gradients. Along this level there is zero horizontal geostrophic flow.⁷

⁷As studied in Chapter 15, geostrophic flow arises from a balance between the Coriolis acceleration and the horizontal pressure gradient acceleration. Hence, if there is a depth along which there is zero horizontal pressure

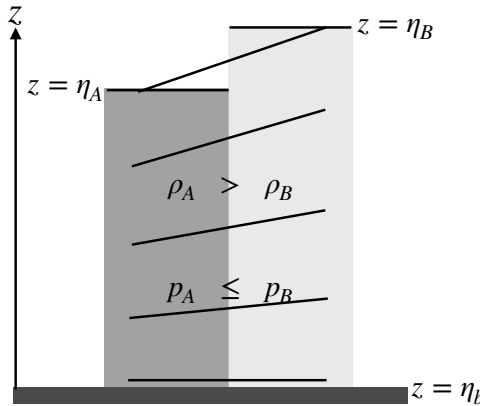


FIGURE 11.4: Two seawater columns on a flat bottom with equal mass but different densities with $\rho_A > \rho_B$. We assume the atmosphere above the columns has the same pressure over both columns, thus offering zero horizontal pressure force. Furthermore, the horizontal cross-sectional area of the two columns are the same so that the less dense water in column B has more volume and thus a greater thickness: $\eta_B > \eta_A$. Since the column masses are the same, the hydrostatic pressures (weight per horizontal area) at the bottom of the two columns are equal: $p_A(z = \eta_b) = p_B(z = \eta_b) = p_b$. In ocean parlance, the bottom offers a [level of no motion](#) from which to reference the pressure field. At any vertical position, z , above the bottom, equation (11.64) shows that the hydrostatic pressure in column B is greater than A : $p_B(z) - p_A(z) = g(-\eta_b + z)(\rho_A - \rho_B) > 0$. The horizontal gradient in hydrostatic pressure thus points from column B towards column A . The solid lines show lines of constant pressure (isobars), which are horizontal next to the bottom but which slope upward to the right moving towards the surface. This configuration provides is useful to compare this schematic to Figure 15.4, which discusses the depth dependence of the horizontal gradient in hydrostatic pressure as per $\partial(\nabla_h p)/\partial z = -g \nabla_h \rho$.

What is required from the hydrostatic pressure field to realize this level of no motion? Based on the expressions (11.49) and (11.54), the pressure field must satisfy

$$0 = (\nabla_h p)_{z=\eta_{nm}} = (\nabla_h p)_{z=\eta} + g \int_{\eta_{nm}}^{\eta} \nabla_h \rho \, dz = (\nabla_h p)_{z=\eta_b} - g \int_{\eta_b}^{\eta_{nm}} \nabla_h \rho \, dz. \quad (11.67)$$

Each of these equations expresses a compensation or balance between external and internal contributions to the pressure gradient so that

$$(\nabla_h p)_{z=\eta} = -g \int_{\eta_{nm}}^{\eta} \nabla_h \rho \, dz \quad (11.68a)$$

$$(\nabla_h p)_{z=\eta_b} = g \int_{\eta_b}^{\eta_{nm}} \nabla_h \rho \, dz. \quad (11.68b)$$

In Figure 11.5 we illustrate the compensation (11.68a) that results if an external pressure gradient from a sloping sea level exactly balances the internal pressure gradient from horizontal density gradients so that

$$\rho(\eta) \nabla_h \eta = - \int_{\eta_{nm}}^{\eta} \nabla_h \rho \, dz. \quad (11.69)$$

This equation allows us to estimate the scale for the free surface slope by writing

$$\rho_0 |\nabla_h \eta| \sim H |\nabla_h \rho| = (H \rho_0 / g) |S N^2|, \quad (11.70)$$

where S is the slope of the density surfaces relative to the horizontal, $H = \eta - \eta_{nm}$ is the depth of the fluid, and N^2 is the squared buoyancy frequency. Assuming $|S| \approx 10^{-3}$, $H \approx 3 \times 10^3$ m, gradient, then there is a corresponding zero horizontal geostrophic flow.

and $N^2 \approx 10^{-6} \text{ s}^{-2}$ leads to the free surface slope

$$|\nabla_h \eta| \approx 10^{-7}. \quad (11.71)$$

Evidently, the free surface slope is much smaller (roughly 10^{-3} times smaller) than that of the interior density surfaces. We see this relative slopes again when studying the reduced gravity model as part of shallow water theory in VOLUME 3.

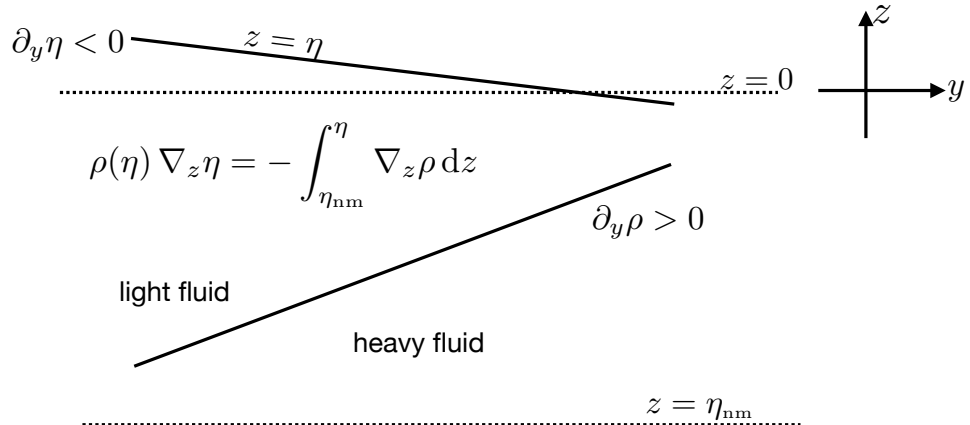


FIGURE 11.5: Illustrating the balance of internal and external horizontal pressure gradients that is needed to realize a level of zero horizontal pressure gradient at $z = \eta_{nm}$ (i.e., a *level of no motion*), and thus a level with zero geostrophic flow. The balance shown here is taken from equation (11.68a) with a zero applied pressure gradient, $\nabla p_a = 0$. Hence, compensation is between an external pressure gradient from the sea level that exactly balances the internal pressure gradient from horizontal density gradients. The relative slope of the free surface is exaggerated here, with actual slopes scaling as in equation (11.71), which are generally much smaller (roughly 10^{-3} smaller) than the slope of density surfaces.

11.4.3 Balanced pressure gradients above a sloping side boundary

We now extend the example from Section 11.4.2 to study the case of compensated internal and external pressure gradients in the presence of a sloping coastal side boundary. Just like over a flat bottom, realizing this compensation requires a sea level gradient to produce the external pressure gradient to balance the internal pressure gradient caused by the density field. As we find here, typical coastal density gradients, with lighter waters near the coast, leads to sea level rise near the coast and with this rise referred to as *steric setup*. The analysis is motivated by the studies of *Holland-Hansen (1934)*, *Csanady (1979)* and *Bingham and Hughes (2012)*. Note that to pursue an analytical calculation requires a number of common approximations. These approximations are often not accurate for realistic flows. However, they lead to expressions whose relevance can be tested. Furthermore, in Exercise 15.5 we slightly extend these results to account for any nonzero bottom geostrophic flows.

Idealized coastal density and topography

To enable an analytical calculation, consider a static density given by⁸

$$\rho(y, z) = \rho_0 + \rho'(y, z) \quad \text{with } |\rho'| \ll \rho_0, \quad (11.72)$$

⁸There is nothing special about (y, z) dependence, so that these arguments hold also for (x, z) dependence as well.

and a bottom topography that is a monotonic function of the off-shore distance,

$$z = \eta_b(y) \quad \text{with } \partial_y \eta_b < 0. \quad (11.73)$$

An example coastal density configuration is depicted in Figure 11.6, whereby the topography deepens off-shore, $\partial_y \eta_b < 0$, and with lighter water next to the coast as might occur from freshening and warming in the shallow coastal waters. Along-shore gradients (in the \hat{x} -direction) are typically far weaker than across shore gradients (in the \hat{y} -direction). This observation then motivates assuming all fields to have zero ∂_x .

Depth of no motion intersecting a bottom of no motion

Assume a depth of no-motion at $z = \eta_{nm}$ that intersects the sloping coastal bottom at $z = \eta_b(y_{nm})$ as in Figure 11.6. Furthermore, assume there is no horizontal pressure gradient all along the bottom, from $y = y_{nm}$ to the coastline at $y = 0$, so that the bottom becomes a sloped surface of no geostrophic motion. Although there are many cases where geostrophic currents are nonzero next to sloping bottoms, it is useful to consider the no motion case as a baseline. Doing so facilitates diagnostic calculations reflective of the approach used for the open ocean away from coasts and thus forms a baseline dynamical balance. Equation (11.59b) then says that at each position along the bottom, from $y = y_{nm}$ to $y = 0$, the horizontal pressure at the sea surface balances the depth integrated horizontal density gradient

$$(\partial_y p)_{z=\eta} = -g \int_{\eta_b}^{\eta} \partial_y \rho \, dz. \quad (11.74)$$

Integrating to find the steric setup along a coast

To derive an approximation for the sea level at the coast relative to the interior, assume the surface density is a constant ($\rho(\eta) \approx \rho_0$), and the atmospheric pressure is constant ($\nabla p_a = 0$), which, with equation (11.59a), then renders

$$\partial_y \eta = -\frac{1}{\rho_0} \int_{\eta_b}^{\eta} \partial_y \rho \, dz. \quad (11.75)$$

This equation says that if density increases away from the coast, then sea level rises toward the coast, which, as already noted, we refer to as a **steric setup** of coastal sea level.

With one further approximation, equation (11.75) can be integrated to provide an explicit expression for the steric sea level at the coast, relative to sea level away from the coast. For that purpose, set the upper limit on the right hand side integral to 0, thus yielding

$$\partial_y \eta = -\frac{1}{\rho_0} \int_{\eta_b}^0 \partial_y \rho \, dz. \quad (11.76)$$

Now integrate this equation from the coast at $y = 0$ to the off-shore position at $y = y_{nm}$, so that

$$\eta(0) - \eta(y_{nm}) = \frac{1}{\rho_0} \int_0^{y_{nm}} \left[\int_{\eta_b(y)}^0 \partial_y \rho(y, z) \, dz \right] dy. \quad (11.77)$$

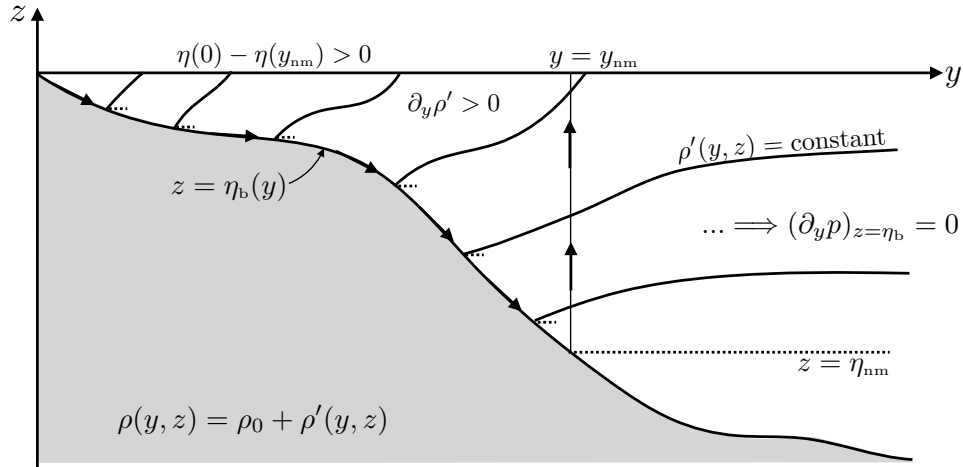


FIGURE 11.6: Density field in a region next to a coastal shelf and slope, illustrating the typical case with lighter water next to the coast, such as from freshening and warming in the shallow coastal waters. Along-shore density gradients (in the \hat{x} -direction) are typically far weaker than across-shore gradients (in the \hat{y} -direction), so that we assume $\partial_x = 0$ for all fields. If there are no geostrophic currents at the bottom, so that $(\nabla_b p)_{z=\eta_b} = 0$ (indicated by the short horizontal dotted lines next to the bottom), then there is an exact compensation of external and internal pressure gradients as given in Section 11.4.2 and as illustrated by Figure 11.5. This pressure compensation is arrived at by sea level rising next to the coast. The arrows along the bottom and the vertical line at $y = y_{nm}$ refer to the integration sense for the steric calculations of $\eta(y = 0)$ (equation (11.81)) and $\eta(y = y_{nm})$ (equation (11.79)). Although many continental slope regions have nonzero flow at the bottom, the calculation of coastal steric setup assuming $(\nabla_b p)_{z=\eta_b} = 0$ offers a useful starting point for interpreting coastal sea level patterns.

Pulling the ∂_y derivative across the vertical integral, and using Leibniz's rule, leads to

$$\eta(0) - \eta(y_{nm}) = \frac{1}{\rho_0} \int_0^{y_{nm}} \left[\frac{\partial}{\partial y} \int_{\eta_b(y)}^0 \rho(y, z) dz + \rho(y, z = \eta_b) \partial_y \eta_b \right] dy. \quad (11.78)$$

Since $\eta_b(y = 0) = 0$ (sea level vanishes at the shoreline), the first integral on the right hand side is given by

$$\frac{1}{\rho_0} \int_0^{y_{nm}} \left[\frac{\partial}{\partial y} \int_{\eta_b(y)}^0 \rho(y, z) dz \right] dy = \frac{1}{\rho_0} \int_{\eta_b(y_{nm})}^0 \rho(y_{nm}, z) dz, \quad (11.79)$$

which is an integral that extends from the bottom at $\eta(y = y_{nm})$ up to $z = 0$, as depicted in Figure 11.6. This integral is an approximate expression for the bottom pressure via

$$\int_{\eta_b(y_{nm})}^0 \rho(y_{nm}, z) dz = \int_{\eta_b}^\eta \rho(y_{nm}, z) dz - \int_0^\eta \rho(y_{nm}, z) dz \quad (11.80a)$$

$$= p_b(y_{nm})/g - \int_0^\eta \rho(y_{nm}, z) dz \quad (11.80b)$$

$$\approx p_b(y_{nm})/g. \quad (11.80c)$$

The second integral in equation (11.78) is given by

$$\frac{1}{\rho_0} \int_0^{y_{nm}} \rho[y, z = \eta_b(y)] \partial_y \eta_b dy = -\frac{1}{\rho_0} \int_0^{\eta_b(y_{nm})} \rho_b d\eta_b, \quad (11.81)$$

where we set

$$d\eta_b = -(\partial_y \eta_b) dy, \quad (11.82)$$

which follows since η_b is a monotonic function of y , and with the minus sign accounting for $\partial_y \eta_b < 0$ as assumed for Figure 11.6. The left hand integral in equation (11.81) is a y -integral of the bottom density times the topographic slope, integrated from the coastal position at $y = 0$ to the off-shore position at $y = y_{nm}$. The right hand side is the bottom density, $\rho_b = \rho[y, z = \eta_b(y)]$, integrated along the bottom from $\eta_b(0) = 0$ to $\eta_b(y = y_{nm})$, as depicted by the arrows along the bottom in Figure 11.6. This integral can be thought of as a laying down onto the bottom of the usual vertical integral used to compute the hydrostatic pressure.⁹

Bringing terms together allows us to write equation (11.78) as

$$\eta(0) - \eta(y_{nm}) = -\frac{1}{\rho_0} \int_{\eta_b(y_{nm})}^0 \rho_b d\eta_b + \frac{1}{\rho_0} \int_{\eta_b(y_{nm})}^0 \rho(y_{nm}, z) dz \quad (11.83a)$$

$$\approx -\frac{1}{\rho_0} \int_{\eta_b(y_{nm})}^0 \rho_b d\eta_b + p_b(y_{nm})/(g \rho_0). \quad (11.83b)$$

As noted earlier, a low density near to the coast contributes to $\eta(0) - \eta(y_{nm}) > 0$. The various assumptions needed to derive equations (11.83a) and (11.83b) render these equations an approximation for more realistic sea levels near coasts. Even so, they offer relatively simple expressions that only requires density and topography information, and as such offer a useful starting point for interpreting sea level patterns next to coasts and on continental shelves. In particular, the direct contributions to sea level from winds are missing from this formulation, so that deviations from steric setup typically signal contributions from winds. In Exercise 15.5 we provide a slight extension to incorporate a nonzero horizontal pressure gradient at the bottom, and an associated geostrophically balanced bottom flow.

11.5 Homogeneous fluid in a rotating tank

As an application of the ideas developed in this chapter and in earlier chapters, we develop the equations for a homogeneous fluid in a rotating tank such as occurs in laboratory studies of rotating fluids. One point of departure from planetary applications concerns the choice of vertical coordinate. Recall we introduced the **geopotential** in our study of planetary particle mechanics in VOLUME 1, with surfaces of constant geopotential having a constant effective gravitational force (sum of central gravity plus planetary centrifugal). Correspondingly, we introduced geopotential coordinates to simplify the equations for planetary fluid dynamics. In contrast, for the rotating tank we do not make use of geopotential coordinates. Instead, we expose the centrifugal acceleration (due to rotation of the tank), which allows for a clear display of the parabolic shape for the free surface when the fluid is in rigid-body motion.

⁹Note that [Csanady \(1979\)](#) and [Bingham and Hughes \(2012\)](#) refer to the integral (11.81) as a line integral computed along the bottom. However, it is not the sort of line integral considered in our study of vector calculus in VOLUME 1. The reason is that the integrand, ρ_b , is weighted by the bottom increment, $d\eta_b = -(\partial_y \eta_b) dy$, rather than the arc-length along the bottom, $ds = dy \sqrt{1 + (\partial_y \eta_b)^2}$. The bottom increment only includes the change in depth moving horizontally up the slope.

11.5.1 What about the planet's rotation?

Do we need to worry about the planet's rotation? To answer this question, consider a typical record player with an angular speed of 45 revolutions per minute

$$\Omega_{\text{record}} = 0.75 \text{ s}^{-1}. \quad (11.84)$$

This angular speed is roughly 10^4 times faster than the magnitude of the Earth's [angular velocity](#), $7.29 \times 10^{-5} \text{ s}^{-1}$. For a tank rotating at a rate on the same order as a record player, we are justified ignoring the rotating Earth in comparison to the rotating tank. That is, we can safely ignore planetary Coriolis and planetary centrifugal accelerations, allowing us to instead focus on the non-inertial accelerations arising just from the tank rotating on a laboratory turntable.

11.5.2 Formulating the equations of motion

In an inertial reference frame, a fluid element feels the gravitational force, pressure force, and friction, thus leading to the Cartesian coordinate equations of motion

$$\frac{Du_I}{Dt} = -\frac{1}{\rho} \frac{\partial p}{\partial x} + F^x \quad (11.85)$$

$$\frac{Dv_I}{Dt} = -\frac{1}{\rho} \frac{\partial p}{\partial y} + F^y \quad (11.86)$$

$$\frac{Dw_I}{Dt} = -\frac{1}{\rho} \frac{\partial p}{\partial z} - g + F^z, \quad (11.87)$$

where \mathbf{v}_I is the inertial velocity, ρ is the constant density, and we orient the coordinates so that the z -axis extends vertically upward from the center of the tank and parallel to the gravity acceleration. Correspondingly, the rotation vector for the tank is

$$\boldsymbol{\Omega} = \Omega \hat{\mathbf{z}} = (f/2) \hat{\mathbf{z}}. \quad (11.88)$$

To derive the rotating frame equations, return to some of the particle kinematics from VOLUME 1, in which we write the position of a fluid particle as

$$\mathbf{X}(t) = X \hat{\mathbf{x}} + Y \hat{\mathbf{y}} + Z \hat{\mathbf{z}}. \quad (11.89)$$

We assume that the Cartesian unit vectors are fixed in the rotating frame and thus move as a rigid-body with the rotating tank. The inertial velocity is thus given by

$$\frac{d\mathbf{X}}{dt} = \left[\frac{dX}{dt} \right] \hat{\mathbf{x}} + \left[\frac{dY}{dt} \right] \hat{\mathbf{y}} + \left[\frac{dZ}{dt} \right] \hat{\mathbf{z}} + \boldsymbol{\Omega} \times \mathbf{X}. \quad (11.90)$$

Correspondingly, the acceleration is given by

$$\frac{d^2\mathbf{X}}{dt^2} = \left[\frac{d^2X}{dt^2} \right] \hat{\mathbf{x}} + \left[\frac{d^2Y}{dt^2} \right] \hat{\mathbf{y}} + \left[\frac{d^2Z}{dt^2} \right] \hat{\mathbf{z}} + 2 \boldsymbol{\Omega} \times \mathbf{v} + \boldsymbol{\Omega} \times (\boldsymbol{\Omega} \times \mathbf{X}), \quad (11.91)$$

where we defined the rotating frame Cartesian velocity as

$$\mathbf{v} = \left[\frac{dx}{dt} \right] \hat{\mathbf{x}} + \left[\frac{dy}{dt} \right] \hat{\mathbf{y}} + \left[\frac{dz}{dt} \right] \hat{\mathbf{z}}. \quad (11.92)$$

Setting the inertial acceleration equal to the inertial force per mass leads to the equations of motion in the rotating frame

$$\frac{Du}{Dt} - 2\Omega v = -\frac{1}{\rho} \frac{\partial p}{\partial x} + \Omega^2 x + F^x \quad (11.93)$$

$$\frac{Dv}{Dt} + 2\Omega u = -\frac{1}{\rho} \frac{\partial p}{\partial y} + \Omega^2 y + F^y \quad (11.94)$$

$$\frac{Dw}{Dt} = -\frac{1}{\rho} \frac{\partial p}{\partial z} - g + F^z, \quad (11.95)$$

which take on the vector form

$$\frac{D\mathbf{v}}{Dt} + f \hat{\mathbf{z}} \times \mathbf{v} = -\nabla [p/\rho + gz - \Omega^2(x^2 + y^2)/2] + \mathbf{F}. \quad (11.96)$$

As expected, we encounter both a Coriolis and centrifugal acceleration due to the rotation of the tank.

11.5.3 Rigid-body rotation and parabolic free surface shape

Consider a fluid at rest in a non-rotating tank, and then start the tank rotating. As in our discussion of Couette flow in Section 9.6.2, viscous effects transfer motion from the outside tank wall (where a no-slip boundary condition makes the fluid move with the wall) into the interior of the fluid. Given sufficient time and a constant rotation rate, the fluid reaches a steady state in rigid-body motion. Recall that rigid-body motion means that the velocity vanishes in the rotating reference frame.

As an application of the above equations of motion, we here determine the shape of the upper free surface for this steady rigid-body motion, offering two related derivations. Note that when the fluid reaches rigid-body motion, all strains vanish within the fluid so that frictional stresses vanish (see Section 9.6). Hence, the steady force balance is fully inviscid although the steady state required viscosity to reach it. The ability to ignore friction in the steady state greatly simplifies the analysis.

Component equations of motion

The velocity and acceleration in the rotating frame are zero when the fluid is in rigid-body motion. The vertical momentum equation (11.95) thus reduces to the approximate hydrostatic balance

$$\frac{\partial p}{\partial z} = -\rho g. \quad (11.97)$$

In general we do not have hydrostatic balance for motion in a tank that deviates from rigid-body. However, when that motion is close to a rigid-body rotation, then the fluid is in an approximate hydrostatic balance. As seen in Section 11.2, this situation corresponds to the large-scale ocean and atmosphere.

Hydrostatic balance with a constant density means that the pressure is a linear function of depth

$$p(x, y, z) = \rho g (\eta - z), \quad (11.98)$$

where $z = \eta(x, y)$ is the vertical position of the free surface. The horizontal momentum equations (11.93)-(11.94) reduce to a balance between the pressure gradient and centrifugal

accelerations

$$\frac{\partial p}{\partial x} = \rho x \Omega^2 \quad \text{and} \quad \frac{\partial p}{\partial y} = \rho y \Omega^2. \quad (11.99)$$

Pressure thus increases when moving radially away from the center. Substituting in the pressure as given by the hydrostatic relation (11.98) leads to relations satisfied by the free surface when in rigid-body motion

$$g \frac{\partial \eta}{\partial x} = x \Omega^2 \quad \text{and} \quad g \frac{\partial \eta}{\partial y} = y \Omega^2. \quad (11.100)$$

Integration leads to the quadratic expression for the free surface

$$\eta = \eta(0) + \frac{\Omega^2 (x^2 + y^2)}{2 g}, \quad (11.101)$$

where $\eta(0)$ is the free surface at the center of the tank where $x = y = 0$. The rigid-body rotating fluid thus has a quadratic free surface with the height of the surface increasing away from the center, as depicted in Figure 11.7. Notice how the fluid density dropped out from the problem, so that this parabolic shape holds for any homogeneous fluid in rigid-body motion.

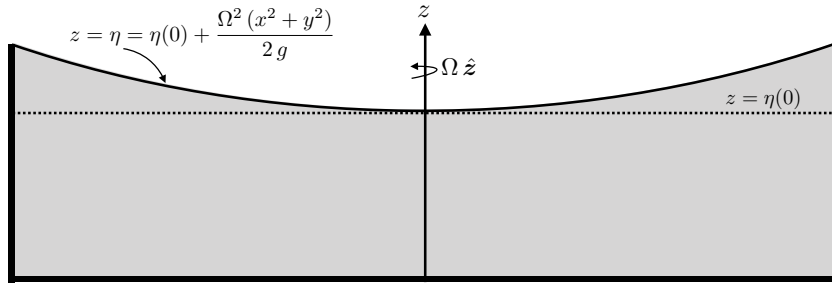


FIGURE 11.7: Rotating tank of homogeneous fluid that has reached a steady state with a parabolic free surface.

Vector force balance

A more telescopic means to determine the free surface shape is to set the forces to zero on the right hand side of the vector equation of motion (11.96) so that

$$p/\rho + g z - \Omega^2 (x^2 + y^2)/2 = p_o/\rho, \quad (11.102)$$

where p_o is a constant pressure to be specified below. Furthermore, we set friction to zero since the fluid is in rigid-body motion, in which case the strain rate tensor vanishes. Everywhere along the free surface, with $z = \eta$, the pressure equals to that applied to the free surface by the overlying media, $p = p_a$ (e.g., atmospheric pressure). Hence, setting $z = \eta$ in equation (11.102) and solving for η yields

$$\eta = \frac{p_o - p_a}{\rho g} + \frac{\Omega^2 (x^2 + y^2)}{2 g}. \quad (11.103)$$

For simplicity, assume the applied pressure is spatially constant. Hence, setting p_o according to the free surface at $x = y = 0$ brings the free surface to the parabolic form in equation (11.101)

$$\frac{p_o - p_a}{\rho g} = \eta(0) \implies \eta = \eta(0) + \frac{\Omega^2 (x^2 + y^2)}{2 g}. \quad (11.104)$$

11.5.4 Further study

We study the angular momentum for the shallow water version of this system in VOLUME 3. See section 6.6.4 of [Marshall and Plumb \(2008\)](#) for more discussion of laboratory rotating tank experiments.

11.6 Space-time dependent gravity field

We here formulate the dynamical equations for a geophysical fluid in the presence of a space and time dependent gravitational acceleration. This formulation has application to the study of astronomical tides in the ocean, and we rely on the presentation of tidal accelerations in the Newtonian mechanics chapter from VOLUME 1. In addition to tides, climate warming is making it increasingly relevant to study how ocean sea level responds to changes in mass distributions associated with melting land ice. Hence, the nontrivial impact that melting land glaciers has on the Earth's geoid and Earth's rotation ([Farrell and Clark, 1976](#); [Mitrovica et al., 2001](#); [Kopp et al., 2010](#)) further motivates developing the dynamical equations of a liquid ocean in the presence of a space-time dependent gravity.

11.6.1 Simple geopotential

As detailed in our study of particle mechanics in VOLUME 1, the effective gravitational field incorporates the effects from the central gravity field plus the planetary centrifugal acceleration. The effective gravitational field is conservative, so that the gravitational acceleration of a fluid element can be represented as the gradient of a scalar

$$\mathbf{g} = -\nabla\Phi, \quad (11.105)$$

with Φ the geopotential. In most applications of this book, the local vertical direction is denoted by

$$z = r - R_e, \quad (11.106)$$

with $z = 0$ the geopotential surface corresponding to a resting ocean and $R_e = 6.367 \times 10^6$ m the average radius of the Earth. The geopotential in this case is given by

$$\Phi = \Phi_0 = g z, \quad (11.107)$$

with $g \approx 9.8 \text{ m s}^{-2}$ the typical value used for the gravitational acceleration at the Earth's surface.

11.6.2 General geopotential

Consider a generalized geopotential written in the form

$$\Phi = \Phi_0(r) + \Phi_1(r, \lambda, \phi, t), \quad (11.108)$$

where $\Phi_0(r)$ is the geopotential given by equation (11.107), and Φ_1 incorporates perturbations to the geopotential. For the study of ocean tides, the structure of Φ_1 arises from astronomical perturbations to the Earth's gravity field. The calculation of ocean tides arising from astronomical forcing is formulated with a space-time dependent geopotential as in equation (11.108),

with the radial dependence of Φ_1 neglected (e.g., Section 9.8 in [Gill, 1982](#)). [Arbic et al. \(2004\)](#) provide a discussion of global tide modeling.

Nontrivial Φ_1 variations also arise from perturbations in terrestrial masses, such as the melting of land ice such as that occurring on Greenland or Antarctica due to climate warming. These mass distribution changes lead to changes in the Earth's gravitational field, its rotational moment of inertia, and the deformation of the crust ([GRD](#), as in [Gregory et al. \(2019\)](#)). Each of these effects lead to modifications in the [static equilibrium sea level](#). In contrast to ocean tides, GFM perturbations associated with melting land ice are not periodic nor readily predictable. Furthermore, as evidenced by Figure 1 of [Mitrovica et al. \(2001\)](#), the amplitude of static equilibrium sea level changes can be far greater than typical open ocean tide fluctuations.

11.6.3 Momentum equation

We start from the inviscid momentum equation from Section [8.2.7](#) for a fluid in a rotating reference frame and within a gravitational field

$$\rho \frac{D\mathbf{v}}{Dt} + 2\boldsymbol{\Omega} \times \rho \mathbf{v} = -\nabla p - \rho \nabla \Phi. \quad (11.109)$$

In writing the momentum equation in this form, we have chosen to retain an orientation afforded by the unperturbed geopotential, $\Phi_0(r)$, which are surfaces of constant z . This approach reflects that commonly used to study ocean tides. In the presence of a perturbed geopotential, Φ_1 , the “horizontal” directions defined by surfaces of constant z are no longer parallel to geopotential surfaces. We thus may interpret the sum $\nabla_h p + \rho \nabla_h \Phi$ as an orientation of the pressure gradient along surfaces of constant geopotential, where the geopotential is determined by $\Phi = \Phi_0 + \Phi_1$, rather than just the unperturbed geopotential Φ_0 .

11.6.4 Hydrostatic primitive equations

As detailed in Section [11.1](#), the hydrostatic primitive equations reduce the vertical momentum equation to its static inviscid form, which is the hydrostatic balance

$$\frac{\partial p}{\partial z} = -\rho \frac{\partial \Phi}{\partial z} = -\rho(g + \partial_z \Phi_1). \quad (11.110)$$

The hydrostatic balance is modified from its traditional form for cases where the perturbation geopotential Φ_1 exhibits nontrivial depth dependence. Correspondingly, the horizontal momentum equation (making the Traditional Approximation from Section [11.1](#)) takes the form

$$\rho \frac{D\mathbf{u}}{Dt} + \hat{\mathbf{z}} f \times \rho \mathbf{u} = -(\rho \nabla_h \Phi_1 + \nabla_h p) \quad (11.111)$$

where ∇_h is the horizontal gradient taken on surfaces of constant z . In their oceanic Boussinesq form (Chapter [13](#)), the inviscid horizontal momentum equation becomes

$$\frac{D\mathbf{u}}{Dt} + \hat{\mathbf{z}} f \times \mathbf{u} = -(1/\rho_0) (\rho_0 \nabla_h \Phi_1 + \nabla_h p) \quad (11.112)$$

where ρ_0 is the constant reference density for a Boussinesq fluid. The Boussinesq form makes the addition of a perturbed geopotential quite straightforward, in which it is gradients in $\rho_0 \Phi_1 + p$ that take the place of gradients in pressure p .

11.6.5 Depth independent perturbed geopotential

A particularly simple form of Φ_1 occurs when it is depth independent,

$$\Phi_1 = \Phi_1(\lambda, \phi, t), \quad (11.113)$$

in which case the hydrostatic balance (11.110) returns to its traditional form $\partial_z p = -\rho g$. This form is motivated by the scale analysis considered in VOLUME 1, where we find that the radial component of the Earth's gravitational field greatly exceeds that from the Moon or other celestial bodies, so that it is the lateral variation in the gravitational acceleration that drive tidal motions. In this case it is convenient to write the geopotential as

$$\Phi_1 = -g h, \quad (11.114)$$

with $h = h(\lambda, \phi, t)$ the perturbed geopotential height field. The full geopotential is thus written

$$\Phi = g(z - h), \quad (11.115)$$

with this form revealing that the zero of the geopotential is now set by $z = h$ rather than $z = 0$. In the study of ocean tides, h is referred to as the **equilibrium tide**. In geodesy, h is referred to as the **static equilibrium sea level**.

Since the perturbed geopotential is depth independent, it only affects the depth integrated horizontal momentum, and it does so through the term

$$-\int_{\eta_b}^{\eta} \nabla_h \Phi_1 dz = g \int_{\eta_b}^{\eta} \nabla_h h dz = g(-\eta_b + \eta) \nabla_h h. \quad (11.116)$$

Hence, modifications to the geopotential as embodied by the perturbed geopotential height field, $h = h(\lambda, \phi, t)$, are isolated to their impacts on the horizontal pressure gradients acting on the depth integrated horizontal momentum.



11.7 Exercises

EXERCISE 11.1: EVOLUTION OF HYDROSTATIC PRESSURE

In this exercise we derive the evolution equations for the hydrostatic pressure at a vertical position in both the atmosphere and the ocean, thus filling in some of the mathematical steps from Section 11.2.2. For both cases we take the time derivative of the hydrostatic pressure expression, use Leibniz's rule, mass continuity, and the kinematic boundary conditions. Note that for the atmosphere, z_{top} is a constant height that is often approximated as $z_{\text{top}} = \infty$.

- (a) Derive equation (11.29) for the atmosphere.
- (b) Derive equation (11.31a) for the ocean.

EXERCISE 11.2: INVERSE BAROMETER SEA LEVEL

A zero horizontal pressure gradient at the ocean surface, in the presence of an applied surface pressure, is known as an **inverse barometer** sea level, whereby from equation (11.59a) we have

$$(\nabla_h p)_{z=\eta} = \nabla_h p_a + g \rho(\eta) \nabla_h \eta = 0. \quad (11.117)$$

Assuming that $\rho(\eta)$ a constant, show that the inverse barometer sea level is depressed under an atmospheric high pressure (where $\nabla_h^2 p_a < 0$) and it rises under an atmospheric low (where $\nabla_h^2 p_a > 0$), with Figure 11.8 providing a schematic. This result is rather intuitive, with the anomalously high atmospheric pressure load acting to depress the ocean free surface, and an anomalously low atmospheric pressure acting to raise the ocean free surface. The inverse barometer sea level plays an important role in tropical storms that impact on the coast, since the atmospheric pressure is anomalously low at the center of the storm so that the sea level is anomalously high.

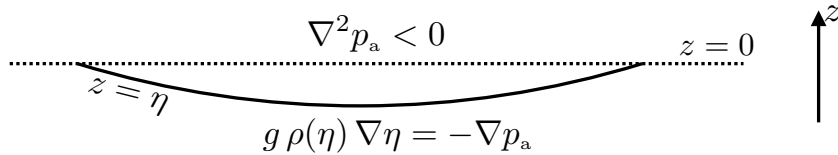


FIGURE 11.8: Illustrating the inverse barometer response of the ocean free surface under an atmospheric high pressure where $\nabla^2 p_a < 0$, so that the inverse barometer sea level is depressed according to equation (??).

EXERCISE 11.3: PRIMITIVE EQUATIONS AND AXIAL ANGULAR MOMENTUM

The axial angular momentum of a fluid element satisfying the primitive equations is given by

$$L^z = (\rho \delta V) R_\perp (u + R_\perp \Omega) \equiv (\rho \delta V) l^z \quad (11.118)$$

where

$$R_\perp = R_e \cos \phi \quad (11.119)$$

is the distance from the polar rotation axis to a point on the sphere with radius R_e , and

$$l^z = R_\perp (u + R_\perp \Omega) \quad (11.120)$$

is the angular momentum per unit mass. For this exercise, we develop some results for the axial angular momentum in the primitive equations. For this purpose, it can be useful to recall the discussion of axial angular momentum in Section 8.7, in which we did not assume primitive equations.

- (a) Consider a constant mass fluid element in the absence of friction. Show that the primitive equation zonal momentum equation (11.7) implies that the material evolution of axial angular momentum per mass is given by

$$\frac{Dl^z}{Dt} = -\frac{1}{\rho} \frac{\partial p}{\partial \lambda}. \quad (11.121)$$

- (b) Assume the zonal pressure gradient vanishes. Move the fluid element vertically while maintaining a fixed latitude. What happens to the zonal momentum of this primitive equation fluid element? Hint: be sure to remain within the “world” of the primitive equations.
- (c) Give a very brief symmetry argument for why the axial angular momentum is materially conserved when $\partial p / \partial \lambda = 0$. Hint: recall the discussion of Noether’s theorem in the discussion of angular momentum in VOLUME 1.
- (d) Consider the material evolution of primitive equation axial angular momentum per mass in the case where the zonal momentum equation retains the unapproximated form of

the Coriolis acceleration. Discuss the resulting material evolution equation. Does this equation make sense based on the symmetry argument given in the previous part of this exercise?

EXERCISE 11.4: MASS BALANCE FOR A HYDROSTATIC OCEAN COLUMN

Show that for a hydrostatic fluid flow, the mass balance for a fluid column takes the form

$$\partial_t(p_b - p_a) = -g \nabla \cdot \mathbf{U}^\rho + g Q_m, \quad (11.122)$$

where

$$\mathbf{U}^\rho = \int_{\eta_b}^{\eta} \mathbf{u} \rho dz \quad (11.123)$$

is the depth integrated horizontal mass transport,

$$p_b = p_a + g \int_{\eta_b}^{\eta} \rho dz \quad (11.124)$$

is the hydrostatic pressure at the ocean bottom, and $p_a(x, y, t)$ is the pressure applied to the ocean surface from the overlying atmosphere or sea ice.

EXERCISE 11.5: EVOLUTION OF ATMOSPHERIC BOTTOM HYDROSTATIC PRESSURE

In deriving equation (11.29) we assumed the lower limit on the integral to be a horizontal constant. However, when integrating over the full atmospheric column, the lower limit varies horizontally given that the Earth boundary is not flat. Return to equation (??) and derive the evolution equation for the bottom pressure

$$\partial_t p_b = -g \nabla_h \cdot \mathbf{U}^\rho, \quad (11.125)$$

where

$$p_b(x, y, t) = p[x, y, z = \eta_b(x, y), t] \quad (11.126)$$

is the atmospheric pressure at the solid Earth at $z = \eta_b(x, y)$,

$$\mathbf{U}^\rho = \int_{\eta_b}^{z_{\text{top}}} \mathbf{u} \rho dz' \quad (11.127)$$

is the depth integrated horizontal mass transport, and z_{top} is the vertical position of the atmospheric top that is assumed to be independent of horizontal position.



Chapter 12

PRESSURE FORM STRESS

As introduced in our discussion of Cauchy's stress principle in Section 9.2, pressure form stress is the horizontal stress arising from pressure that acts on a sloped surface or interface. As a contact force per area, Newton's third law describes how form stress renders a transfer of pressure forces across interfaces, with pressure form stress affecting a vertical transfer of horizontal pressure forces. Hence, it provides an inviscid/reversible mechanism for the vertical transfer of horizontal momentum, thus complementing the vertical transfer associated with viscosity in the presence of tangential shear stresses (Section 9.6.2).

In this chapter we study pressure form stress as it appears on a variety of interfaces encountered in geophysical fluids. We then develop two case studies to expose the role of pressure form stress in the force balances affecting motion of an ocean fluid column. The first case study is concerned with the evolution of vertically integrated horizontal linear momentum per mass. The second case study focuses on the axial angular momentum budget as a framework to study the dominant force balances in ocean channel flow and ocean gyre flow.

CHAPTER GUIDE

We here build from the study of stresses in Chapter 9, with an understanding of pressure form stress greatly enhancing our understanding of horizontal forces acting in geophysical fluids. The basic concepts presented here hold whether the pressure is non-hydrostatic or hydrostatic, since we are only concerned with pressure as a mechanical force per area. The focus on horizontal forces in this chapter complements our studies in Chapter 14, whereby the net vertical acceleration from pressure and gravitational forces is repackaged into the buoyancy force.

Rather than provide a suite of exercises at the chapter's end, we offer two extended case studies (Sections 12.4 and 12.5) examining the linear momentum and axial angular momentum budgets as computed over finite domains. Besides providing many mathematical details, these case studies illustrate how fluids are affected by the variety of form stresses that act within the fluid and at the fluid boundaries. The reader is encouraged to work through all details to appreciate the mathematical and physical questions that arise when performing such finite volume budgets.

12.1 Pressure form stresses at an interface	382
12.1.1 Concerning the sign of a form stress	383
12.1.2 Mathematical expression for form stress	384
12.1.3 Comments	385

12.2	Form stresses on solid-fluid boundaries	386
12.2.1	Zonally symmetric ridge	386
12.2.2	Form stress transfer between the fluid and its boundaries	386
12.2.3	Decomposing topographic form stress	388
12.3	Interfacial form stress	389
12.3.1	Interfacial form stresses transferred between layers	389
12.3.2	Zonally integrated interfacial form stress	391
12.3.3	Comments	392
12.4	Case study: momentum budget for the primitive equations	392
12.4.1	Flux-form horizontal momentum equation	392
12.4.2	Leibniz's rule for the inertial and Coriolis accelerations	393
12.4.3	External and internal decomposition of the kinetic stress	393
12.4.4	Decomposing the depth integrated horizontal pressure gradient	394
12.4.5	Depth integrated momentum equation	396
12.4.6	Zonally integrated zonal momentum balance	397
12.4.7	Balances when $\nabla \cdot \mathbf{U}^p = 0$	398
12.5	Case study: axial angular momentum budget	399
12.5.1	Anticipating the budget	399
12.5.2	Axial angular momentum	400
12.5.3	Depth integrated axial angular momentum budget	400
12.5.4	Atmospheric and topographic form stresses	401
12.5.5	Turbulent stresses at the surface and bottom	401
12.5.6	Summary budget for column integrated axial angular momentum	402
12.5.7	Steady domain integrated balance	403
12.5.8	Form stress versus dual form stress	404
12.5.9	Steady zonal and depth integrated budget	404
12.5.10	Southern Ocean balances	404
12.5.11	Topographic form stress and ocean gyres	405
12.5.12	Further study	406

12.1 Pressure form stresses at an interface

As depicted in Figure 12.1, there are three surfaces or interfaces across which we commonly study form stresses in geophysical fluids.

- **ATMOSPHERE-OCEAN FORM STRESS:** A form stress occurs at the air-sea interface. From the perspective of the ocean, the nonzero atmospheric pressure applied to the sea surface (the [sea level pressure](#)) provides a pressure acting on the sloped upper ocean free surface, thus rendering an [atmospheric form stress](#) acting on the ocean. Through [Newton's third law](#), this form stress is met by the equal in magnitude but oppositely directed [oceanic form stress](#) acting on the atmosphere.
- **INTERIOR FLUID INTERFACIAL FORM STRESS:** A form stress occurs on an internal interface within the fluid, and we study this [interfacial form stress](#) in Section 12.3. Although the interface is arbitrary, it is dynamically very interesting to study form stresses acting on buoyancy isosurfaces. The reason is that buoyancy interfaces are directly connected to the geostrophic motion studied in Chapter 15. In particular, in Section 15.7 we study form stresses associated with buoyancy interfaces found in geostrophic flows.
- **FLUID-TOPOGRAPHY FORM STRESS:** A form stress exists at a solid/fluid boundary, at which the ocean or atmosphere impart a pressure force on the solid earth. Through

Newton's third law, the pressure force imparted by the fluid on the solid earth is met equally in magnitude but oppositely in direction by a force provided by the solid earth onto the fluid. The horizontal projection of this force per area acting from the earth on the fluid is the [topographic form stress](#) and it is considered in Section 12.2.

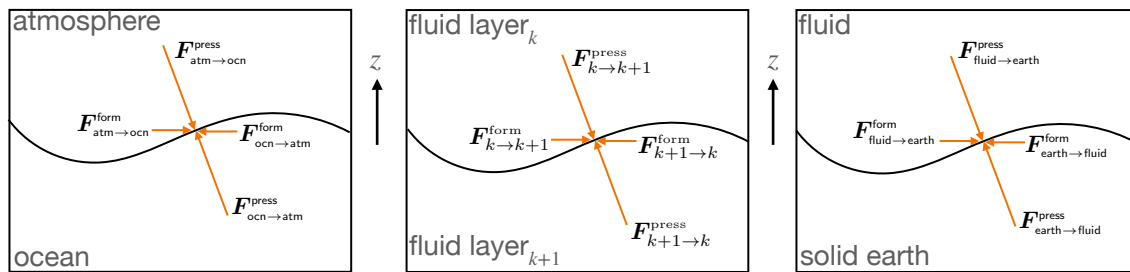


FIGURE 12.1: Illustrating the three interfaces of concern in geophysical fluid mechanics for the discussion of form stresses. Continuity of pressure at the interface, through [Newton's third law](#), means that the form stress on one side of the interface is equal and opposite to that acting on the other side. Left panel: a curved atmosphere-ocean interface leads to an atmospheric form stress acting on the ocean, $\mathbf{F}_{\text{atm} \rightarrow \text{ocn}}^{\text{form}}$, and its equal and opposite oceanic form stress acting on the atmosphere, $\mathbf{F}_{\text{ocn} \rightarrow \text{atm}}^{\text{form}} = -\mathbf{F}_{\text{atm} \rightarrow \text{ocn}}^{\text{form}}$. Middle panel: a curved interior ocean interface (e.g., a buoyancy surface) leads to an interfacial form stress acting on the lower layer, $\mathbf{F}_{k \rightarrow k+1}^{\text{form}}$, and its equal and opposite interfacial form stress acting on the upper layer, $\mathbf{F}_{k+1 \rightarrow k}^{\text{form}} = -\mathbf{F}_{k \rightarrow k+1}^{\text{form}}$. Right panel: a curved fluid-solid earth interface leads to a fluid form stress acting on the solid earth, $\mathbf{F}_{\text{fluid} \rightarrow \text{earth}}^{\text{form}}$, and its equal and opposite oceanic form stress acting on the fluid, $\mathbf{F}_{\text{earth} \rightarrow \text{fluid}}^{\text{form}} = -\mathbf{F}_{\text{fluid} \rightarrow \text{earth}}^{\text{form}}$. The magnitude of the form stresses is a function of the pressure acting at the interface as well as the slope of the interface. For example, all else being equal, we find that a steeper slope leads to a larger form stress magnitude.

12.1.1 Concerning the sign of a form stress

As a vector, pressure form stress has a direction and a magnitude, with three examples depicted in Figure 12.1. Keeping track of the direction can be confusing if it is unclear who is the giver of the form stress and who is the receiver. To help in understanding the sign, imagine pushing against a heavy rock or boulder. If there is no motion, then you exert a force on the rock in one direction whereas, through [Newton's third law](#), the rock exerts an equal and opposite force on you. Clarity is realized by specifying the origin of the force in order to determine its sign. For example, as illustrated in Figure 12.2, is one concerned with the force applied by the ocean bottom pressure onto the earth (liquid ocean is giver and solid earth is receiver), or instead with the force from the earth applied onto the ocean fluid (earth is giver and ocean is receiver)? These forces have equal magnitude but opposite direction. Knowing the direction requires knowing the force giver and/or the force receiver.

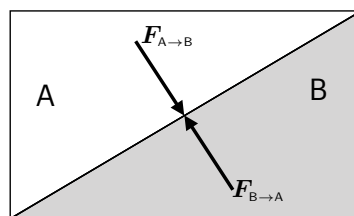


FIGURE 12.2: Contact forces, such as pressure, satisfy Newton's third law. Hence, the contact force at a point imparted by region A onto region B, $\mathbf{F}_{A \rightarrow B}$, is equal and opposite to the force imparted by region B onto region A so that $\mathbf{F}_{A \rightarrow B} = -\mathbf{F}_{B \rightarrow A}$.

12.1.2 Mathematical expression for form stress

To expose the mathematics of form stress, consider a surface, \mathcal{S} , such as that shown in Figure 12.3. To kinematically decompose the pressure force, assume the surface has no vertical portion. This assumption is not necessary to define a form stress, but it is convenient for our purposes of providing a mathematical expression. Furthermore, the assumption is commonly satisfied for geophysical surfaces of interest with large-scale fluid mechanics.

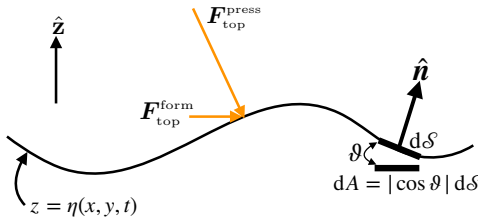


FIGURE 12.3: The pressure force acting on an arbitrary surface is given by $\mathbf{F}^{\text{press}} = -p \hat{n} d\mathcal{S}$, where $d\mathcal{S}$ is the surface area element. We here depict the pressure acting on the top side of a surface, $\mathbf{F}_{\text{top}}^{\text{press}}$. Through Newton's third law, the pressure force vector acting on the top side of the interface is equal and opposite to the pressure force acting on the bottom side: $\mathbf{F}_{\text{top}}^{\text{press}} = -\mathbf{F}_{\text{low}}^{\text{press}}$. The horizontal component of this force vector arises from the slope of the surface; i.e., its geometric form. We thus refer to the horizontal pressure force per area as the **form stress**, with the corresponding horizontal pressure force satisfying Newton's third law, $\mathbf{F}_{\text{top}}^{\text{form}} = -\mathbf{F}_{\text{low}}^{\text{form}}$. The area element on the surface, $d\mathcal{S}$, has a horizontal projection given by $dA = dx dy = \cos \vartheta d\mathcal{S}$, with the angle assumed to be within the range $-\pi/2 < \vartheta < \pi/2$ so that the surface is nowhere vertical.

Assuming the surface has no vertical sections allows us to write the vertical position of a point on the surface as¹

$$z = \eta(x, y, t). \quad (12.1)$$

The outward normal pointing away from the top side of the surface is given by

$$\hat{n}_{\text{top}} = \frac{\nabla(z - \eta)}{|\nabla(z - \eta)|} = \frac{\hat{z} - \nabla\eta}{\sqrt{1 + |\nabla\eta|^2}}. \quad (12.2)$$

Multiplying the pressure times the horizontal area element on the surface, $d\mathcal{S}$, leads to the net pressure force acting at a point on the top side of the surface

$$\mathbf{F}^{\text{press}} = -p \hat{n}_{\text{top}} d\mathcal{S} = -p (\hat{z} - \nabla\eta) dA = -p (-\partial_x \eta \hat{x} - \partial_y \eta \hat{y} + \hat{z}) dA. \quad (12.3)$$

In this equation we used the identity

$$d\mathcal{S} = |\nabla(z - \eta)| dA = \sqrt{1 + |\nabla\eta|^2} dA, \quad (12.4)$$

with

$$dA = dx dy \quad (12.5)$$

the horizontal projection of the surface area element (see Figure 12.3). We identify the form stress acting on the top side of this interface as

$$\text{pressure form stress acting on top side of interface} \equiv p \nabla\eta. \quad (12.6)$$

The name follows since the stress is determined by the “form” of the surface as measured by its

¹We discuss this sort of analytic geometry in the vector calculus chapter of VOLUME 1.

slope, $\nabla\eta$. We can thus write the pressure force acting on the top side of the surface as the sum of a vertical pressure force plus a horizontal pressure form stress

$$\mathbf{F}_{\text{top}}^{\text{press}} = \hat{\mathbf{z}} [\hat{\mathbf{z}} \cdot \mathbf{F}_{\text{top}}^{\text{press}}] + \mathbf{F}_{\text{top}}^{\text{form}} = p (-\hat{\mathbf{z}} + \nabla\eta) \, dA \quad \text{pressure force on top side of interface.} \quad (12.7)$$

Newton's third law, as manifested by Cauchy's fundamental lemma (Section 9.2) says that there is a local mechanical equilibrium of pressure contact forces at each point within a continuous media. Additionally, as seen in our discussion of stress on an interface in Section 9.8, this local mechanical equilibrium holds for pressure forces acting on interfaces separating two fluids, such as the atmosphere and ocean, as well as a fluid and the solid earth. Thus, the contact pressure force acting on the lower side of the interface is equal in magnitude but oppositely directed to the contact force acting on the top side (see Section 9.6.2)

$$\mathbf{F}_{\text{low}}^{\text{press}} = \hat{\mathbf{z}} [\hat{\mathbf{z}} \cdot \mathbf{F}_{\text{low}}^{\text{press}}] + \mathbf{F}_{\text{low}}^{\text{form}} = p (+\hat{\mathbf{z}} - \nabla\eta) \, dA \quad \text{pressure force on lower side of interface.} \quad (12.8)$$

12.1.3 Comments

We here offer some comments on pressure form stress.

For stress is not a mysterious notion

The form stress, particularly interfacial form stress, can appear mysterious in some presentations. Part of the reason is that it sometimes appears seemingly without prior motivation as part of mathematical manipulations of the momentum equation, typically as part of an integrated force balance. We illustrate these manipulations in Sections 12.2, 12.3, and 12.5, yet aim to offer sufficient physical motivation to help guide the maths. Another reason for the mystery is that the signs ascribed to form stress are often not clearly specified, with such ambiguities motivating the somewhat pedantic discussion in Section 12.1.1.

Unbalanced form stresses and motion

Consider a container filled with water at rest. The horizontal pressure forces acting on the container sides are pressure form stresses between the water and the container. As discussed in Section 9.5, without motion we know that the form stresses balance over the whole of the fluid-container boundary, whereas horizontal motion occurs if the form stresses are out of balance. Quite generally, when concerned with fluid motion, we are interested in processes that lead to unbalanced form stresses. For example, when studying bottom topographic form stresses in the ocean, the bulk of the form stress acts to merely hold the ocean water within the ocean basin. The dynamically active portion of the topographic form stress, associated with fluid motion, is a small residual of the total form stress. Careful analysis is required to diagnose dynamically relevant patterns, with [Molemaker et al. \(2015\)](#) and [Gula et al. \(2015\)](#) presenting one method.

Dual form stress is not the same as the form stress

Observe that

$$p \nabla\eta = \nabla(\eta p) - \eta \nabla p. \quad (12.9)$$

Much of the literature refers to $-\eta \nabla p$ as the form stress, thus in effect ignoring the $\nabla(\eta p)$ gradient. Instead, we refer to $-\eta \nabla p$ as the **dual form stress**. As emphasized in Section 12.4.4,

$-\eta \nabla p$ is not a pressure form stress. So even though both the form stress and dual form stress have dimensions of a force per area, the dual form stress does not act to accelerate a fluid element through Newton's equation of motion.

The confusion between form stress and dual form stress originates from the common application of zonal averages when studying momentum budgets for zonally symmetric channels. In this case we may wish to study the dynamics of the zonally averaged flow, in which we have the identity

$$\oint p \partial_x \eta \, dx = - \int \eta \partial_x p \, dx. \quad (12.10)$$

Hence, the zonally integrated form stress (left hand side) equals to the zonally integrated dual form stress (right hand side). However, care must be exercised in applying this identity in non-zonally periodic domains (we further pursue this point in Section 12.4). Even more fundamentally, $p \nabla \eta \neq -\eta \nabla p$. Consequently, it is generally necessary to distinguish the pressure form stress, which is a horizontal force per area that acts to accelerate fluid elements through Newton's law of motion, from the dual form stress, which does not appear in Newton's equation of motion.

12.2 Form stresses on solid-fluid boundaries

In this section we focus on form stress arising from the shape of the solid earth interface with the atmosphere and ocean; i.e., the *fluid-topographic form stress*. As we are normally interested in the form stress applied to the fluid, we focus on the *topographic form stress*. We also encounter the form stress associated with undulations in the ocean free surface and the atmospheric pressure at that interface, with the *atmospheric form stress* the horizontal pressure stress imparted to the ocean from the atmosphere, and the *oceanic form stress* the horizontal pressure stress imparted to the atmosphere from the ocean.

12.2.1 Zonally symmetric ridge

In Figure 12.4 we depict an idealized ridge with an example oceanic pressure field to illustrate the nature of topographic form stress acting on the ocean. Rather than assuming exact hydrostatic equilibrium as in Figure 9.5, with zero horizontal pressure gradients, we here consider pressure to be higher to the west of the ridge than to the east. Since the ridge is assumed to be symmetric in the zonal direction, we conclude that the topographic form stress, which acts just at the fluid-solid interface, is higher on the west side of the ridge than on the east. In turn, the net topographic form stress acting on the fluid is to the west, whereas the net oceanic form stress acting on the solid earth is to the east. We encounter this situation in Section 12.5.10 when studying the force balances for steady circulation in a zonally periodic channel.

12.2.2 Form stress transfer between the fluid and its boundaries

We now illustrate how topographic form stress appears mathematically in the study of momentum balances acting on a fluid. For definiteness, consider a column of ocean fluid extending from the bottom at $z = \eta_b(x, y)$ to the free surface at $z = \eta(x, y, t)$, and focus on the zonal force balance such as depicted in Figure 12.4. In computing the acceleration acting on this column at a particular horizontal position, we need to determine the depth integrated zonal

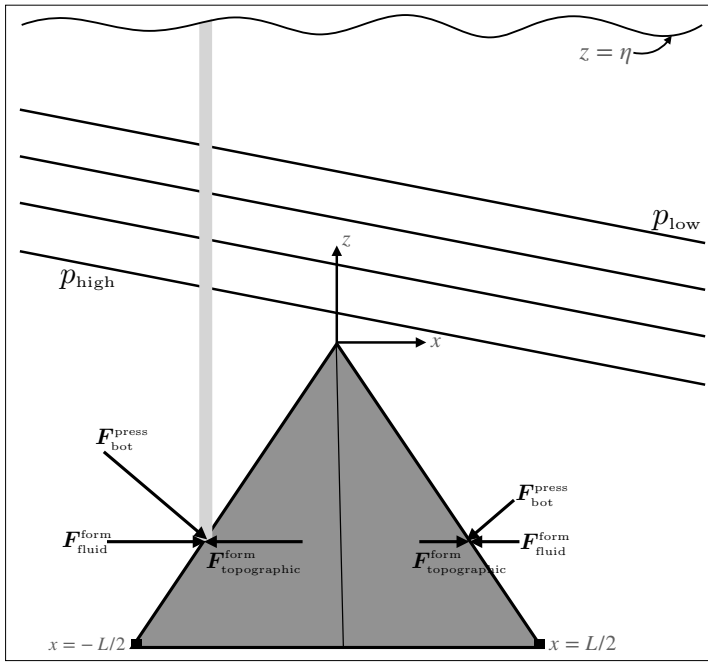


FIGURE 12.4: Depicting contact forces acting at a fluid-solid interface. The topographic form stress acts on the fluid and the equal in magnitude but oppositely directed fluid form stress acts on the solid earth. In this illustration the topography is assumed to be a ridge in the shape of an equilateral triangle. We also assume there is higher pressure to the west of the ridge than to the east as per the zonal balance discussed in Figure 12.8 for a Southern Ocean ridge. Hence, the topographic form stress has a larger magnitude on the western side of the ridge than on the eastern side. When integrated over the full ridge, we find a net westward topographic form stress acting on the fluid and a net eastward fluid form stress acting on the solid earth. If the ridge was free to move, it would move to the east. The thin gray column extends from the solid earth bottom to the ocean free surface. As this column sits on the western side of the ridge, topographic form stress provides a westward acceleration at the column bottom. The net acceleration of the column is determined by integrating the contact forces around the column boundary, plus the body forces integrated over the column interior. We study the axial angular momentum budget for a fluid column in Section 12.5, with form stresses appearing in that budget.

pressure gradient

$$\text{depth integrated zonal pressure gradient} = - \int_{\eta_b}^{\eta} \frac{\partial p}{\partial x} dz. \quad (12.11)$$

We expose the contact force version of the pressure force by making use of Leibniz's rule to write

$$-\int_{\eta_b}^{\eta} \frac{\partial p}{\partial x} dz = \underbrace{-\frac{\partial}{\partial x} \int_{\eta_b}^{\eta} p dz}_{\text{zonal deriv depth integrated pressure}} + \underbrace{\frac{\partial \eta}{\partial x} p_a}_{\text{atmospheric form stress}} - \underbrace{\frac{\partial \eta_b}{\partial x} p_b}_{\text{topographic form stress}}, \quad (12.12)$$

where p_a is the pressure applied to the ocean at its surface, $z = \eta$, and p_b is the pressure at the ocean bottom, $z = \eta_b$. The decomposition identifies the following three pressure contributions to the pressure force acting on the fluid column.

- ZONAL DERIVATIVE OF THE COLUMN INTEGRATED PRESSURE: The first term in equation (12.12) arises from the zonal derivative of pressure across the vertical sides of the column

$$\text{zonal derivative of layer integrated pressure} = -\frac{\partial}{\partial x} \int_{\eta_b}^{\eta} p dz. \quad (12.13)$$

This term leads to a net eastward acceleration if the depth integrated pressure is higher to the west than the east.

- ATMOSPHERIC FORM STRESS AT THE FREE SURFACE: In the presence of a sloping free surface interface, equation (12.12) reveals that if $\partial\eta/\partial x \neq 0$, then the atmospheric pressure, p_a , imparts an atmospheric form stress onto the ocean

$$\text{zonal atmospheric form stress acting on ocean} = \frac{\partial\eta}{\partial x} p_a. \quad (12.14)$$

For example, if the free surface slopes up to the east, $\partial\eta/\partial x > 0$, then the atmosphere provides a positive (eastward) zonal form stress onto the ocean. In turn, through Newton's third law, the ocean provides a westward zonal form stress to the atmosphere.

- TOPOGRAPHIC FORM STRESS ON OCEAN: Equation (12.12) also reveals that the bottom pressure, p_b , present at $z = \eta_b$, imparts a form stress to the solid earth

$$\text{zonal oceanic form stress acting on solid earth} = \frac{\partial\eta_b}{\partial x} p_b. \quad (12.15)$$

In turn, through Newton's third law, the topographic form stress acting on the ocean is equal in magnitude but oppositely directed

$$\text{zonal topographic form stress acting on ocean} = -\frac{\partial\eta_b}{\partial x} p_b. \quad (12.16)$$

For example, if the bottom rises to the east, so that $\partial\eta_b/\partial x > 0$, then the oceanic form stress acting on the solid earth is eastward whereas the topographic form stress acting on the ocean is westward. As a check, we verify that the signs of these form stresses are consistent with those in Figure 12.4.

12.2.3 Decomposing topographic form stress

We follow the approach used in Section 11.3.2 to decompose the contributions to the bottom pressure. Assuming the fluid maintains an approximate hydrostatic balance, and focusing on the oceanic case, allows us to decompose the bottom pressure according to

$$p_b = p_a + g \int_{\eta_b}^{\eta} \rho dz \quad (12.17a)$$

$$= \underbrace{g \rho_a [\eta + p_a / (g \rho_a)]}_{\text{external}} - \underbrace{g \rho_a \eta_b}_{\text{topog}} + \underbrace{g \int_{\eta_b}^{\eta} (\rho - \rho_a) dz}_{\text{internal}} \quad (12.17b)$$

$$\equiv p_{\text{ext}} + p_{\text{top}} + p_{\text{int}}. \quad (12.17c)$$

We refer to the contribution from applied surface pressure plus surface height undulations as *external*, whereas those arising from density deviations relative to a constant reference density

are termed *internal*. There is a further contribution from bottom topography itself.

Multiplying the decomposed pressure (12.17c) by the slope of the bottom topography renders an expression for the various contributions to topographic form stress

$$-p_b \nabla \eta_b = -p_{\text{ext}} \nabla \eta_b - p_{\text{top}} \nabla \eta_b - p_{\text{int}} \nabla \eta_b. \quad (12.18)$$

The topographic term is static whereas the other two terms are time dependent. External contributions arise from undulations in the free surface as well as the applied pressure. This contribution fluctuates due to motions occurring on the relatively rapid time scales associated with external gravity waves or atmospheric pressure fluctuations such as through synoptic weather patterns. Internal contributions arise from the relatively slow internal movements of density surfaces, such as from internal gravity waves or even slower motions due to advection and diffusion. The study from [McCabe et al. \(2006\)](#) pursues this decomposition of the topographic form stress as part of their analysis of flow around a headland.

12.3 Interfacial form stress

In this section we focus on the form stress acting at an interface within the fluid itself, which is known as the **interfacial form stress**. As part of this discussion we expose some of the common manipulations found when considering finite volume integrated momentum budgets, whereby we decompose the horizontal pressure gradient acceleration acting on an infinitesimal column of fluid within the layer, as depicted in Figure 12.5. These manipulations are analogous to those considered in Section 12.2 for the topographic and atmospheric form stresses.

12.3.1 Interfacial form stresses transferred between layers

When studying the momentum of a column of fluid within a chosen layer, we need to compute the depth integrated zonal pressure gradient over a layer at a particular horizontal point

$$\text{layer integrated zonal pressure gradient} = - \int_{\eta_{k+1/2}}^{\eta_{k-1/2}} \frac{\partial p}{\partial x} dz, \quad (12.19)$$

where $z = \eta_{k-1/2}(x, y, t)$ is the vertical position for the interface at the top of the fluid layer and $z = \eta_{k+1/2}(x, y, t)$ is the vertical position for the bottom interface. If the layer integrated pressure gradient is downgradient to the east, then pressure accelerates the column to the east, and conversely when the layer integrated pressure gradient is downgradient to the west.

Although the depth integrated pressure gradient expression (12.19) is straightforward to understand, we also find it useful to consider the complementary perspective by studying the contact force version of the pressure acceleration. Proceeding as in Section 12.2 for topographic and atmospheric form stresses, we make use of Leibniz's Rule for a fluid layer

$$-\int_{\eta_{k+1/2}}^{\eta_{k-1/2}} \frac{\partial p}{\partial x} dz = \underbrace{-\frac{\partial}{\partial x} \int_{\eta_{k+1/2}}^{\eta_{k-1/2}} p dz}_{\text{zonal deriv layer integrated pressure}} + \underbrace{\frac{\partial \eta_{k-1/2}}{\partial x} p_{k-1/2}}_{\text{IFS at } k-1/2 \text{ interface}} - \underbrace{\frac{\partial \eta_{k+1/2}}{\partial x} p_{k+1/2}}_{\text{IFS at } k+1/2 \text{ interface}}, \quad (12.20)$$

where we introduced the pressures acting at a point on the interfaces

$$p_{k-1/2} = p(x, y, z = \eta_{k-1/2}, t) \quad \text{and} \quad p_{k+1/2} = p(x, y, z = \eta_{k+1/2}, t). \quad (12.21)$$

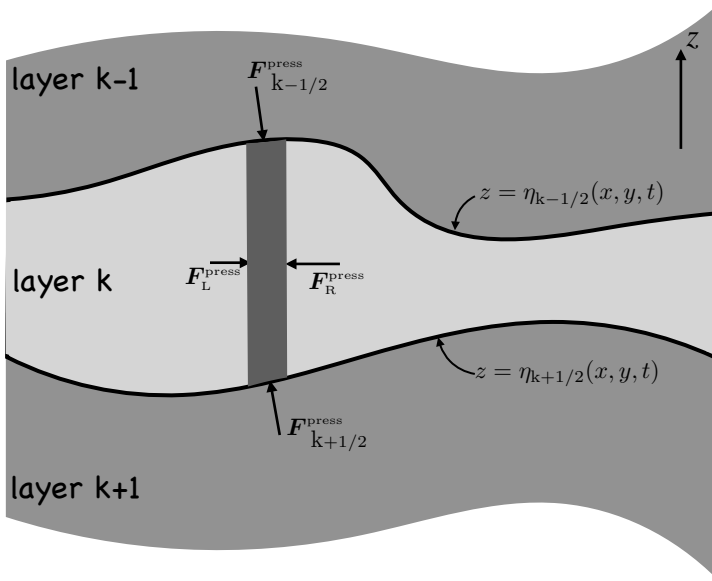


FIGURE 12.5: A schematic of the contact pressure force per area acting on the boundaries of a vertical column within a fluid layer. The horizontal cross-sectional area of the column is depth independent. The interface at the lower boundary is at the vertical position $z = \eta_{k+1/2}(x, y, t)$, and the upper interface is at $z = \eta_{k-1/2}(x, y, t)$. In accordance with Newton's third law, pressures are continuous across each of the $\eta_{k\pm 1/2}$ layer interfaces so that the pressure forces are equal in magnitude yet oppositely directed on the opposite sides to the interfaces. The boundaries of the dark gray columnar region feel a contact pressure force acting inward, as per the compressive nature of pressure. The left side of the column experiences a pressure, p_L ; the right side experiences the pressure, p_R ; the upper interface has a pressure, $p_{k-1/2}$, acting between the layer $k - 1$ and layer k , and the lower interface has a pressure, $p_{k+1/2}$, acting between the layer $k + 1$ and layer k . The **interfacial form stress (IFS)** is the name given to the horizontal pressure stress acting on the upper and lower layer interfaces. Through Newton's third law, the **IFS** imparted to layer k at the $z = \eta_{k-1/2}$ interface is equal and opposite to the **IFS** imparted to layer $k - 1$ at this same interface. The same holds for the **IFS** at the $k + 1/2$ interface. It is common to define the layers according to buoyancy (see Section 15.7) given its direct connection to pressure and dynamics. Even so, the ideas of pressure contact forces are generic and thus hold for arbitrarily defined layers. This figure is adapted from Figure A1 in [Loose et al. \(2023\)](#).

The decomposition identifies the following three pressure contributions, analogous to the decomposition in Section 12.2 for the topographic and atmospheric form stresses.

- **ZONAL DERIVATIVE OF THE COLUMN INTEGRATED PRESSURE:** The first term arises from the zonal derivative of pressure across the vertical sides of the column within the layer

$$\text{zonal derivative of layer integrated pressure} = -\frac{\partial}{\partial x} \int_{\eta_{k+1/2}}^{\eta_{k-1/2}} p \, dz. \quad (12.22)$$

- **INTERFACIAL FORM STRESS AT UPPER INTERFACE:** The pressure at the $z = \eta_{k-1/2}$ interface is given by $p_{k-1/2}$. In the presence of a sloping interface, $\partial \eta_{k-1/2} / \partial x \neq 0$, this pressure imparts the following interfacial form stress (IFS) to layer-k:

$$\text{IFS on layer-}k \text{ from the } \eta_{k-1/2} \text{ interface} = \frac{\partial \eta_{k-1/2}}{\partial x} p_{k-1/2}. \quad (12.23)$$

For example, if the upper layer interface slopes up to the east, $\partial \eta_{k-1/2} / \partial x > 0$, then the interfacial form stress provides a positive (eastward) zonal force to layer-k. In turn, through Newton's third law, the layer above, labelled $k - 1$, feels an interfacial form stress

directed to the west.

- INTERFACIAL FORM STRESS AT LOWER INTERFACE: The pressure, $p_{k+1/2}$, present at the $z = \eta_{k+1/2}$ interface imparts an interfacial form stress to layer-k given by

$$\text{IFS on layer-}k \text{ from } \eta_{k+1/2} \text{ interface} = -\frac{\partial \eta_{k+1/2}}{\partial x} p_{k+1/2}. \quad (12.24)$$

For example, if the layer slopes down to the east, $\partial \eta_{k+1/2} / \partial x < 0$, then the interfacial form stress accelerates layer-k to the east. In turn, through Newton's third law, the interfacial form stress acts to accelerate the layer below, labelled $k + 1$, to the west.

Now apply the above to a column of ocean fluid, and extend the integration to include the full ocean column from the free upper surface to the rigid solid earth bottom. Evidently, all the intermediate interfacial form stresses vanish in the depth integral, with this cancellation a result of Newton's third law. Hence, accumulation of the interfacial form stresses throughout the ocean column leaves only the interfacial form stress at the top ($z = \eta$) and at the bottom ($z = \eta_b$). The corresponding boundary form stresses arise from mechanical interactions with the atmosphere ($z = \eta$) and solid earth ($z = \eta_b$), as discussed in Section 12.2. This result was already encountered in a more general context of contact forces in Section 9.2. It also arises in our analysis of the depth integrated axial angular momentum budget in Section 12.5.

12.3.2 Zonally integrated interfacial form stress

Besides studying the force acting on a column at a particular horizontal position, it is interesting to study the net zonal force acting on the layer. For pressure, we thus need to consider the zonal integral of the layer integrated zonal pressure gradient

$$-\int \left[\int_{\eta_{k+1/2}}^{\eta_{k-1/2}} \frac{\partial p}{\partial x} dz \right] dx = \int \left[-\frac{\partial}{\partial x} \int_{\eta_{k+1/2}}^{\eta_{k-1/2}} p dz + \frac{\partial \eta_{k-1/2}}{\partial x} p_{k-1/2} - \frac{\partial \eta_{k+1/2}}{\partial x} p_{k+1/2} \right] dx. \quad (12.25)$$

If the domain is zonally periodic or is bounded by sloping shorelines (see Figure 12.6 discussed in Section 12.4.6), then the first term vanishes so that the zonally integrated pressure acting on the layer arises just from the interfacial form stresses

$$-\int \left[\int_{\eta_{k+1/2}}^{\eta_{k-1/2}} \frac{\partial p}{\partial x} dz \right] dx = \int \left[\frac{\partial \eta_{k-1/2}}{\partial x} p_{k-1/2} - \frac{\partial \eta_{k+1/2}}{\partial x} p_{k+1/2} \right] dx. \quad (12.26)$$

This zonal integral is only affected by zonal anomalies for the layer vertical positions and pressures

$$-\int \left[\int_{\eta_{k+1/2}}^{\eta_{k-1/2}} \frac{\partial p}{\partial x} dz \right] dx = \int \left[\frac{\partial \eta'_{k-1/2}}{\partial x} p'_{k-1/2} - \frac{\partial \eta'_{k+1/2}}{\partial x} p'_{k+1/2} \right] dx \quad (12.27a)$$

$$= \int \left[-\eta'_{k-1/2} \frac{\partial p'_{k-1/2}}{\partial x} + \eta'_{k+1/2} \frac{\partial p'_{k+1/2}}{\partial x} \right] dx, \quad (12.27b)$$

where primes denote deviations from the zonal mean. In Section 12.5.9 we offer details to prove that it is only the zonal anomalies that contribute to the zonal integral in a zonally periodic channel, or for domains with sloping shorelines. Furthermore, note that for the second equality we introduced the alternative dual form stress expressions afforded by zonal periodicity or zonal

sloped shorelines. We offer cautionary remarks on this replacement in Section 12.5.8 regarding this second equality.

12.3.3 Comments

Interfacial form stress acts on any arbitrary surface drawn in a fluid. Interfaces defined by buoyancy surfaces make the connection between the general concepts presented here to geostrophic mechanics, and they do so given the connection between buoyancy slopes and thermal wind (Section 15.4.3). Most studies of interfacial form stress are thus concerned with isopycnal interfacial form stress, with a discussion given in Section 15.7.

12.4 Case study: momentum budget for the primitive equations

In this section we develop the evolution equation for the depth integrated horizontal momentum per volume in a column of ocean fluid

$$\mathbf{U}^\rho = \int_{\eta_b}^{\eta} \rho \mathbf{u} dz, \quad (12.28)$$

extending from the ocean bottom at $z = \eta_b(x, y)$ to the ocean surface at $z = \eta(x, y, t)$. As we see, the evolution equation exposes how form stresses acting at the ocean surface and ocean bottom contribute to the column force balance. A study of the depth integrated momentum equation is commonly considered when the ocean fluid maintains an approximate hydrostatic balance (see Sections 11.2 and 13.2), and the shallow fluid approximation (Section 11.1.2). These two approximations constitute the hydrostatic primitive equations (Section 11.1), which we assume holds in this section.

An important technical feature of the primitive equations is that the horizontal gradient operator, ∇_h , is depth independent, which is a property we use to develop the budget equations in this section. In particular, we need this assumption for equation (12.31c) below. We also made use of this property of ∇_h in Section 11.1.6 to derive the depth integrated kinetic energy budget for the primitive equations.

12.4.1 Flux-form horizontal momentum equation

Our starting point is the flux-form horizontal momentum equation (8.27) as specialized to a simple geopotential, $\Phi = g z$,

$$\partial_t(\rho \mathbf{u}) + \nabla \cdot [\rho \mathbf{v} \otimes \mathbf{u}] + f \hat{z} \times (\rho \mathbf{u}) = -\nabla_h p + \rho \mathbf{F}. \quad (12.29)$$

In this equation, $\rho \mathbf{F}$ is the horizontal friction vector, and the tensor product provides components to the kinetic stress tensor (Section 8.2.3)

$$\rho [\mathbf{v} \otimes \mathbf{u}]_{mi} = \rho v_m u_i = -\mathbb{T}_{mi}^{\text{kinetic}} \quad (12.30)$$

with $m = 1, 2, 3$ for the velocity vector, \mathbf{v} , whereas $i = 1, 2$ (for the horizontal velocity vector, \mathbf{u} , extending just over the horizontal range).

12.4.2 Leibniz's rule for the inertial and Coriolis accelerations

Leibniz's rule renders the following expressions for the depth integrated inertial acceleration and Coriolis acceleration

$$\int_{\eta_b}^{\eta} \frac{\partial(\rho \mathbf{u})}{\partial t} dz = \partial_t \mathbf{U}^\rho - [\rho \mathbf{u} \partial_t \eta]_{z=\eta} \quad (12.31a)$$

$$\int_{\eta_b}^{\eta} \frac{\partial(w \rho \mathbf{u})}{\partial z} dz = [w \rho \mathbf{u}]_{z=\eta} - [w \rho \mathbf{u}]_{z=\eta_b} \quad (12.31b)$$

$$\int_{\eta_b}^{\eta} \nabla_h \cdot [\rho \mathbf{u} \otimes \mathbf{u}] dz = \nabla_h \cdot \left[\int_{\eta_b}^{\eta} \rho \mathbf{u} \otimes \mathbf{u} dz \right] - [\mathbf{u} \cdot \nabla \eta (\rho \mathbf{u})]_{z=\eta} + [\mathbf{u} \cdot \nabla \eta_b (\rho \mathbf{u})]_{z=\eta_b} \quad (12.31c)$$

$$\int_{\eta_b}^{\eta} f \hat{\mathbf{z}} \times (\rho \mathbf{u}) dz = f \hat{\mathbf{z}} \times \mathbf{U}^\rho. \quad (12.31d)$$

Use of the surface and bottom kinematic boundary conditions from VOLUME 1

$$\partial_t \eta + \mathbf{u} \cdot \nabla \eta = w + \rho^{-1} Q_m \quad \text{for } z = \eta \quad (12.32a)$$

$$\mathbf{u} \cdot \nabla \eta_b = w \quad \text{for } z = \eta_b \quad (12.32b)$$

leads to the depth integrated inertial and Coriolis accelerations

$$\begin{aligned} \int_{\eta_b}^{\eta} [\partial_t(\rho \mathbf{u}) + \nabla \cdot (\mathbf{v} \otimes (\rho \mathbf{u})) + f \hat{\mathbf{z}} \times \rho \mathbf{u}] dz \\ = (\partial_t + f \hat{\mathbf{z}} \times) \mathbf{U}^\rho - \mathbf{u}(\eta) Q_m - \nabla_h \cdot \int_{\eta_b}^{\eta} \mathbb{T}_{\text{hor}}^{\text{kinetic}} dz, \end{aligned} \quad (12.33)$$

where we introduced the horizontal kinetic stress tensor

$$\mathbb{T}_{\text{hor}}^{\text{kinetic}} = -\rho \mathbf{u} \otimes \mathbf{u}. \quad (12.34)$$

12.4.3 External and internal decomposition of the kinetic stress

For some applications it can be useful to introduce the density weighted depth averaged horizontal velocity

$$\bar{\mathbf{u}} = \frac{\int_{\eta_b}^{\eta} \rho \mathbf{u} dz}{\int_{\eta_b}^{\eta} \rho dz} = \frac{\mathbf{U}^\rho}{(p_b - p_s)/g}, \quad (12.35)$$

where p_b is the hydrostatic pressure at the ocean bottom, and p_s is the pressure applied to the ocean surface. The depth averaged velocity is referred to as the [external velocity](#), whereas the deviation from the depth average

$$\mathbf{u}' = \mathbf{u} - \bar{\mathbf{u}}, \quad (12.36)$$

is referred to it as the [internal velocity](#).² It follows by definition that the internal velocity has a zero density weighted vertical integral

$$\int_{\eta_b}^{\eta} \rho \mathbf{u}' dz = \int_{\eta_b}^{\eta} \rho (\mathbf{u} - \bar{\mathbf{u}}) dz = 0. \quad (12.37)$$

²It is also common in the ocean physics literature to refer to \mathbf{u}' as the [baroclinic velocity](#) and $\bar{\mathbf{u}}$ as the [barotropic velocity](#). We avoid that nomenclature since we prefer to use baroclinic and barotropic in reference to vorticity mechanics in VOLUME 3.

Consequently, by making use of $\mathbf{u} = \bar{\mathbf{u}} + \mathbf{u}'$ we find the depth integrated kinetic stress

$$\int_{\eta_b}^{\eta} \mathbb{T}_{\text{hor}}^{\text{kinetic}} dz = -g^{-1} (p_b - p_a) [\bar{\mathbf{u}} \otimes \bar{\mathbf{u}} + \overline{\mathbf{u}' \otimes \mathbf{u}'}. \quad (12.38)$$

Note that absence of cross-terms (i.e., no internal-external correlation terms) appearing in the depth integrated stress (12.38). In this manner we have separated the contributions from kinetic stresses due to depth averaged horizontal velocities from those arising from depth-dependent horizontal velocities.

12.4.4 Decomposing the depth integrated horizontal pressure gradient

We here consider the depth integrated pressure and the corresponding depth integrated horizontal pressure gradient

$$P = \int_{\eta_b}^{\eta} p dz \quad \text{and} \quad \int_{\eta_b}^{\eta} \nabla_h p dz. \quad (12.39)$$

Assuming each fluid column maintains an approximate hydrostatic balance allows us to decompose these integrals into elemental constituents. Doing so offers insights into the way pressure accelerates the fluid.

Depth integrated pressure and its connection to the potential energy

Write the depth integrated pressure as

$$P = \int_{\eta_b}^{\eta} p dz = \int_{\eta_b}^{\eta} [d(pz) - z dp] = p_a \eta - p_b \eta_b + \mathcal{P}, \quad (12.40)$$

where we used the hydrostatic balance for a vertical fluid column to write³ $dp = -g \rho dz$, and we introduced the potential energy per horizontal area of a fluid column

$$\mathcal{P} = \int_{\eta_b}^{\eta} g \rho z dz. \quad (12.41)$$

Equation (12.40) decomposes the depth integrated pressure into a contribution from the applied surface pressure acting at the free surface, the bottom pressure acting at the bottom, and the potential energy per horizontal area of a fluid column.

Depth integrated horizontal pressure gradient

For the depth integrated horizontal pressure gradient, we start by using Leibniz's rule to render

$$\nabla_h P = \nabla_h \int_{\eta_b}^{\eta} p dz = p_a \nabla_h \eta - p_b \nabla_h \eta_b + \int_{\eta_b}^{\eta} \nabla_h p dz. \quad (12.42)$$

³More generally, the differential of pressure is given by $dp = \nabla p \cdot d\mathbf{x}$ when probing three-dimensional spatial increments, $d\mathbf{x}$. However, the integral in equation (12.40) is vertical, in which case $dp = (\partial p / \partial z) dz$. For the approximate hydrostatic fluid we thus have the transformation $dp = -g \rho dz$.

Making use of the decomposition (12.40) leads to

$$-\int_{\eta_b}^{\eta} \nabla_h p dz = -\nabla_h P + p_a \nabla_h \eta - p_b \nabla_h \eta_b \quad (12.43a)$$

$$= -\nabla_h [p_a \eta - p_b \eta_b + \mathcal{P}] + p_a \nabla_h \eta - p_b \nabla_h \eta_b \quad (12.43b)$$

$$= -\nabla_h \mathcal{P} - \eta \nabla_h p_a + \eta_b \nabla_h p_b. \quad (12.43c)$$

These are very important results and so worth writing in a single identity

$$-\int_{\eta_b}^{\eta} \nabla_h p dz = -\nabla_h P + p_a \nabla_h \eta - p_b \nabla_h \eta_b = -\nabla_h \mathcal{P} - \eta \nabla_h p_a + \eta_b \nabla_h p_b. \quad (12.44)$$

Equation (12.43a) exposes contributions from minus the horizontal gradient of the depth integrated pressure plus surface and bottom **form stresses**

$$\text{minus gradient of } \int_{\eta_b}^{\eta} p dz + \text{boundary form stresses} = -\nabla_h P + p_a \nabla_h \eta - p_b \nabla_h \eta_b. \quad (12.45)$$

As a complement, equation (12.43c) exposes contributions from the gradient of the potential energy plus those from the **dual form stresses**

$$\text{minus gradient of } \int_{\eta_b}^{\eta} g \rho z dz + \text{boundary dual form stresses} = -\nabla_h \mathcal{P} - \eta \nabla_h p_a + \eta_b \nabla_h p_b. \quad (12.46)$$

As noted in Section 12.1.3, it is common for the literature to confuse form stresses with dual form stresses, along with contributions from depth integrated pressure and the potential energy. The role of these pressures is further studied for the axial angular momentum budget in Section 12.5, and furthermore within the column vorticity balances studied in VOLUME 3.

Pressure balances for motionless flow that is exactly hydrostatic

As discussed in Section 8.6, the horizontal pressure gradient everywhere vanishes for a fluid in exact hydrostatic balance, $\nabla_h p = 0$. Correspondingly, the free surface and surface applied pressure are spatially constant in order to maintain zero pressure gradients throughout the fluid. For the depth integral pressure gradient, the decompositions (12.43a) and (12.43c) lead to the exact hydrostatic fluid identities maintained at each vertical fluid column

$$\nabla_h P = -p_b \nabla_h \eta_b \quad (12.47a)$$

$$\nabla_h \mathcal{P} = \eta_b \nabla_h p_b. \quad (12.47b)$$

The first identity says that the horizontal gradient of the depth integrated hydrostatic pressure exactly balances the topographic form stress. The second identity says that the horizontal gradient of the potential energy per area balances the dual topographic form stress.

Since the curl of the left hand side vanishes for both of equation (12.47a) and (12.47b), we find that the bottom pressure must be aligned with the bottom topography in order to maintain zero flow

$$\hat{z} \cdot (\nabla \eta_b \times \nabla p_b) = 0. \quad (12.48)$$

In the language of vorticity (VOLUME 3), we say that there is no bottom pressure torque when the flow is exactly hydrostatic. Conversely, nonzero flow is signaled by a misalignment of the contours of constant bottom pressure and bottom topography. We can also arrive at the identity (12.48) by taking the horizontal derivative of the bottom pressure. Since the fluid is static we

have a spatially constant free surface and applied pressure, and a density that is horizontally uniform. Consequently,

$$\nabla_h p_b = g \nabla_h \int_{\eta_b}^{\eta} \rho dz = -g \rho(z = \eta_b) \nabla_h \eta_b, \quad (12.49)$$

thus revealing that bottom pressure contours are indeed parallel to bottom topography contours when the fluid is in exact hydrostatic balance.

12.4.5 Depth integrated momentum equation

Bringing the pieces together leads to the depth integrated horizontal momentum equation for an approximate hydrostatic fluid

$$(\partial_t + f \hat{z} \times) \mathbf{U}^\rho = \mathbf{u}(\eta) Q_m + p_a \nabla_h \eta - p_b \nabla_h \eta_b - \nabla_h P + \nabla_h \cdot \left[\int_{\eta_b}^{\eta} \mathbb{T}_{\text{hor}}^{\text{kinetic}} dz \right] + \int_{\eta_b}^{\eta} \rho \mathbf{F} dz. \quad (12.50)$$

In this equation we exposed minus the gradient of the depth integrated pressure along with the boundary form stresses, as per equation (12.43a). We could just as well have chosen to expose minus the gradient of the potential energy along with the boundary dual form stresses, as per equation (12.43c), in which case

$$(\partial_t + f \hat{z} \times) \mathbf{U}^\rho = \mathbf{u}(\eta) Q_m - \eta \nabla_h p_a + \eta_b \nabla_h p_b - \nabla_h \mathcal{P} + \nabla_h \cdot \left[\int_{\eta_b}^{\eta} \mathbb{T}_{\text{hor}}^{\text{kinetic}} dz \right] + \int_{\eta_b}^{\eta} \rho \mathbf{F} dz. \quad (12.51)$$

For many applications we focus on the vertical divergence of horizontal frictional stress plus a term arising from horizontal strains, in which case

$$\int_{\eta_b}^{\eta} \rho \mathbf{F} dz = \int_{\eta_b}^{\eta} (\rho \mathbf{F}^h + \partial_z \boldsymbol{\tau}) dz = \mathbf{D} + \boldsymbol{\tau}^\eta - \boldsymbol{\tau}^{\eta_b} \equiv \mathbf{D} + \Delta \boldsymbol{\tau}, \quad (12.52)$$

where $\boldsymbol{\tau}^\eta$ is the horizontal stress vector at the surface (e.g., wind stress on the ocean surface), $\boldsymbol{\tau}^{\eta_b}$ is the horizontal stress vector at the bottom (e.g., turbulent drag at the fluid-solid earth boundary), and

$$\mathbf{D} = \int_{\eta_b}^{\eta} \rho \mathbf{F}^h dz \quad (12.53)$$

is the depth integrated friction arising from horizontal stresses within the fluid interior (e.g., viscous stresses as in Section 9.6). In this case the horizontal momentum equation (12.51) takes on the equivalent forms

$$(\partial_t + f \hat{z} \times) \mathbf{U}^\rho = \mathbf{u}(\eta) Q_m + p_a \nabla_h \eta - p_b \nabla_h \eta_b - \nabla_h P + \mathbf{A} + \mathbf{D} + \Delta \boldsymbol{\tau} \quad (12.54a)$$

$$(\partial_t + f \hat{z} \times) \mathbf{U}^\rho = \mathbf{u}(\eta) Q_m - \eta \nabla_h p_a + \eta_b \nabla_h p_b - \nabla_h \mathcal{P} + \mathbf{A} + \mathbf{D} + \Delta \boldsymbol{\tau}, \quad (12.54b)$$

where we introduced the shorthand for the nonlinear kinetic stress term

$$\mathbf{A} \equiv \nabla_h \cdot \left[\int_{\eta_b}^{\eta} \mathbb{T}_{\text{hor}}^{\text{kinetic}} dz \right] = -\nabla_h \cdot \left[\int_{\eta_b}^{\eta} \rho \mathbf{u} \otimes \mathbf{u} dz \right]. \quad (12.55)$$

12.4.6 Zonally integrated zonal momentum balance

Zonal integration and zonal averaging offer a common means to summarize elements of the flow, particularly in the atmosphere where zonal motions are much stronger than meridional due to the earth's rotation and the differential solar heating of the planet. Additionally, zonal averaging is of particular interest in the Southern Ocean, where the Drake Passage latitudes offer a zonally unbounded domain for ocean circulation. Even for zonally bounded ocean domains where gyre circulations occur, it is of interest to zonally integrate across the domain to study balances leading to meridional motion across the chosen latitude. We are thus motivated to integrate zonally across the full extent of the domain, with the resulting boundary contributions dependent on the geometry and topology of the domain.

Three canonical domains

We illustrate three canonical domains in Figure 12.6. For the zonally periodic domain, the zonal integral of any zonal derivative vanishes so that, for example,

$$\oint \partial_x P dx = 0, \quad (12.56)$$

where we write $\oint dx$ for integration over a zonally periodic domain. Additionally, zonal derivatives vanish for a zonally bounded domain with sloping shorelines

$$\int \partial_x P dx = \Delta P = 0. \quad (12.57)$$

The reason this integral vanishes is that any depth integrated quantity, such as P , vanishes at the shoreline edge merely since the layer thickness vanishes at the shoreline edge. The same result holds for any other depth integrated quantity, including depth integrated axial angular momentum, mass transport, and potential energy.

It is only for the zonally bounded domain with vertical sidewalls (third panel in Figure 12.6) that we are unable to drop the zonal integral of the zonal pressure gradient. We observe that vertical sidewalls are common for numerical models and many theories of the ocean circulation. However, vertical sidewalls are the exception in Nature. For this reason, in the following we focus on the more geophysically relevant periodic configuration and the sloping shoreline configuration.

Zonally integrated meridional mass transport

A zonal integral, either over a periodic domain or a domain with vanishing layer thickness along the shoreline, renders an expression for the meridional transport across the zonal-depth section

$$f \int V^\rho dx = \int [p_a \partial_x \eta - p_b \partial_x \eta_b - \partial_t U^\rho - u(\eta) Q_m + (\mathbf{A} + \mathbf{D} + \Delta\boldsymbol{\tau}) \cdot \hat{\mathbf{x}}] dx, \quad (12.58)$$

where we set $\int \partial_x P dx = \int \partial_x \mathcal{P} dx = 0$. Note that the Coriolis parameter was pulled outside the zonal integral since it is constant along a constant latitude line. As discussed in Section 12.5, this equation, or its analog for the axial angular momentum, provides a useful framework for studies of momentum balances in both the Southern Ocean and in ocean gyres. For the special case of a steady state in the absence of surface mass fluxes, so that $\partial_t U^\rho = 0$ and $Q_m = 0$, and for a domain closed in the north and south, so that steady mass conservation renders

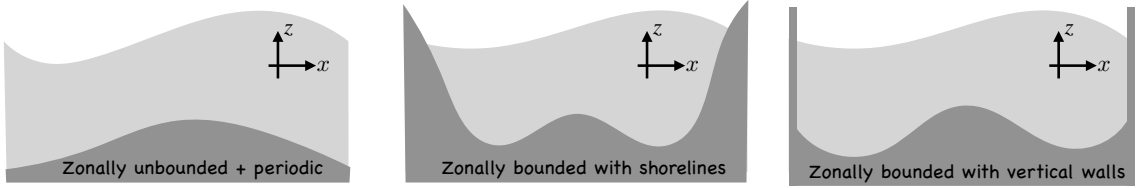


FIGURE 12.6: Three canonical zonal topologies/geometries considered in the study of fluid flow, particularly ocean flows. The light portion of each panel represents the fluid whereas the darker portion is the solid earth bottom topography. Left panel: zonally unbounded and periodic channel. Here, the topography, surface boundary forcing, and flow are zonally periodic. Middle panel: zonally bounded region where the zonal bounds occur along sloping shorelines at which the fluid thickness vanishes. The horizontal position of the vanishing thickness is time dependent since the fluid can move up and down the shoreline. Right panel: zonally bounded region where the fluid encounters a vertical sidewall so that the horizontal position of the fluid boundary is fixed, and so there is no horizontal position where the fluid thickness vanishes. Fixed vertical sidewall boundaries are commonly found in numerical model simulations and tacitly assumed in many theoretical treatments. Even so, vertical sidewall boundaries are uncommon in Nature.

$\int V^\rho dx = 0$, then the balance (12.58) simplifies to

$$\int [p_a \partial_x \eta - p_b \partial_x \eta_b + (\mathbf{A} + \mathbf{D} + \Delta\boldsymbol{\tau}) \cdot \hat{\mathbf{x}}] dx = 0. \quad (12.59)$$

For those cases where nonlinear terms and interior friction are small, we find a balance between pressure form stresses at the boundaries plus boundary turbulent stresses. We defer to Section 12.5 any further remarks on this case.

12.4.7 Balances when $\nabla \cdot \mathbf{U}^\rho = 0$

There are many occasions in which the depth integrated flow is close to non-divergent, $\nabla \cdot \mathbf{U}^\rho = 0$. Such occurs particularly at the large scale and for cases where we neglect the mass transport across the ocean surface, $Q_m = 0$. Following the kinematics of non-divergent flows from VOLUME 1, we introduce a **streamfunction** so that

$$\mathbf{U}^\rho = \hat{\mathbf{z}} \times \nabla_h \Psi, \quad (12.60)$$

with the streamfunction, Ψ , having dimensions of mass per time. Use of the transport streamfunction brings the Coriolis contribution to the form

$$f \hat{\mathbf{z}} \times \mathbf{U}^\rho = f \hat{\mathbf{z}} \times (\hat{\mathbf{z}} \times \nabla_h \Psi) = -f \nabla_h \Psi, \quad (12.61)$$

so that the momentum equations (12.54a) (12.54b) become

$$\partial_t \mathbf{U}^\rho = f \nabla_h \Psi + p_a \nabla_h \eta - p_b \nabla_h \eta_b - \nabla_h P + \mathbf{A} + \mathbf{D} + \Delta\boldsymbol{\tau}. \quad (12.62a)$$

$$\partial_t \mathbf{U}^\rho = f \nabla_h \Psi - \eta \nabla_h p_a + \eta_b \nabla_h p_b - \nabla_h \mathcal{P} + \mathbf{A} + \mathbf{D} + \Delta\boldsymbol{\tau} \quad (12.62b)$$

To reach a steady flow requires the following balances

$$-f \nabla_h \Psi = p_a \nabla_h \eta - p_b \nabla_h \eta_b - \nabla_h P + \mathbf{A} + \mathbf{D} + \Delta\boldsymbol{\tau} \quad (12.63a)$$

$$-f \nabla_h \Psi = -\eta \nabla_h p_a + \eta_b \nabla_h p_b - \nabla_h \mathcal{P} + \mathbf{A} + \mathbf{D} + \Delta\boldsymbol{\tau}. \quad (12.63b)$$

For some analysis it can be useful to project equation (12.63a) into the horizontal direction tangent to the bottom topography, denoted by the unit vector $\hat{\mathbf{t}}$. Doing so eliminates the $p_b \nabla_h \eta_b$ term to have the steady along-topography flow balance

$$-f \hat{\mathbf{t}} \cdot \nabla_h \Psi = \hat{\mathbf{t}} \cdot (p_a \nabla_h \eta - \nabla_h P + \mathbf{A} + \mathbf{D} + \Delta\tau). \quad (12.64)$$

12.5 Case study: axial angular momentum budget

We here develop the column integrated budget for axial angular momentum in an ocean region, such as shown in Figure 12.7. We then further specialize the budget by zonally integrating. The analysis shares features with the depth integrated linear momentum balance developed in Section 12.4. As in that discussion, we here assume the primitive equations (Section 11.1) so that the horizontal gradient operator is independent of depth (as for Sections 11.1.6 and 12.4, we need this assumption for equation (12.69b) below).

There is a close relation between the zonal momentum and axial angular momentum, with details provided in our study of geophysical particle dynamics in VOLUME 1. We choose to here study axial angular momentum since it has a slightly simpler budget (equation (12.65) discussed below) than the corresponding budget equation (12.54a) for zonal linear momentum. The simpler budget follows since axial angular momentum is directly connected to the axial symmetry of the rotating spherical planet through Noether's theorem.

To add a bit more generality to the analysis, we make use of spherical coordinates, though doing so offers only a modest degree of extra details beyond Cartesian coordinates. Although here focused on the ocean, many of the concepts and methods are directly relevant to a study of atmospheric axial angular momentum as introduced in Section 8.7 and discussed in Section 10.3 of [Holton and Hakim \(2013\)](#).

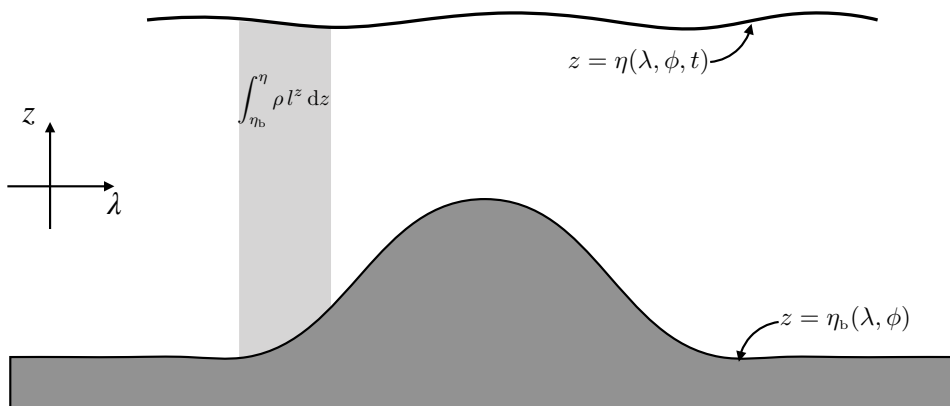


FIGURE 12.7: Schematic of the axial angular momentum for a fluid column, here depicted moving in an ocean with a topographic bump. In Section 12.5 we develop the budget for the depth and zonal integrated axial angular momentum in the ocean, where we see that the axial angular momentum is affected by a variety of boundary processes as well as interior transports and pressures.

12.5.1 Anticipating the budget

Before diving into the mathematical formulation, let us use some of the understanding gleaned from earlier sections of this chapter to anticipate the basic results. Doing so offers a framework

to guide the maths, and to double check that the maths indeed renders a physically sensible budget.

For this purpose, consider a column of fluid such as shown in Figure 12.7. The forces acting on that column arise from contact forces (pressure stress, kinetic stress, and frictional stress) acting on the boundary (sides, top, and bottom), and body forces acting throughout the column (from effective gravity and Coriolis). There are further avenues for momentum to be transported across the ocean surface as part of the mass transported by rain, evaporation, and rivers. Each of these transports of momentum correspond to forces that contribute a torque to the fluid column computed relative to the earth's rotational axis, thus modifying the axial angular momentum of the fluid column. In the following development, we mathematically express the variety of forces and corresponding torques, thus building up the axial angular momentum budget.

12.5.2 Axial angular momentum

The axial angular momentum budget for a fluid element follows that developed in Section 8.7, here written with the addition of zonal friction

$$\rho \frac{Dl^z}{Dt} = -\frac{\partial p}{\partial \lambda} + r_{\perp} \rho F^{\lambda}, \quad (12.65)$$

where

$$l^z = r_{\perp} (u + r_{\perp} \Omega) \quad (12.66)$$

is the axial angular momentum per unit mass, and

$$r_{\perp} = r \cos \phi \quad (12.67)$$

is the distance to the polar rotation axis (the moment arm). For the primitive equations we set the radial position, r , to the earth radius, R_e , in the following.⁴ Use of the mass continuity equation leads to the Eulerian flux-form budget

$$\partial_t(\rho l^z) + \nabla \cdot (\rho \mathbf{v} l^z) = -\partial_{\lambda} p + r_{\perp} \rho F^{\lambda}, \quad (12.68)$$

with $l^z \rho dz$ the angular momentum per unit horizontal area. We use this form for the local budget to develop the depth integrated axial angular momentum budget.

12.5.3 Depth integrated axial angular momentum budget

Vertically integrating equation (12.68) over a column of ocean fluid renders a budget for the column-integrated axial angular momentum. As in Section 12.4.2, we here make use of Leibniz's rule to reach the following identities that expose boundary contributions

$$\int_{\eta_b}^{\eta} \frac{\partial(\rho l^z)}{\partial t} dz = \frac{\partial}{\partial t} \left[\int_{\eta_b}^{\eta} \rho l^z dz \right] - \left[\rho l^z \frac{\partial \eta}{\partial t} \right]_{z=\eta} \quad (12.69a)$$

$$\int_{\eta_b}^{\eta} \nabla_h \cdot (\rho \mathbf{u} l^z) dz = \nabla_h \cdot \left[\int_{\eta_b}^{\eta} \rho \mathbf{u} l^z dz \right] - [\rho l^z \mathbf{u} \cdot \nabla \eta]_{z=\eta} + [\rho l^z \mathbf{u} \cdot \nabla \eta_b]_{z=\eta_b} \quad (12.69b)$$

$$\int_{\eta_b}^{\eta} \frac{\partial(\rho w l^z)}{\partial z} dz = [w \rho l^z]_{z=\eta} - [w \rho l^z]_{z=\eta_b}. \quad (12.69c)$$

⁴See also Exercise 11.3.

Equation (12.69b) made use of the primitive equations whereby the horizontal divergence operator is depth independent. The surface and bottom kinematic boundary conditions from VOLUME 1 allow us to reach a reasonably tidy expression

$$\frac{\partial}{\partial t} \left[\int_{\eta_b}^{\eta} l^z \rho dz \right] = [l^z Q_m]_{z=\eta} - \nabla_h \cdot \left[\int_{\eta_b}^{\eta} l^z \mathbf{u} \rho dz \right] + \int_{\eta_b}^{\eta} \left[-\frac{\partial p}{\partial \lambda} + r_{\perp} \rho F^{\lambda} \right] dz. \quad (12.70)$$

The left hand side of the budget equation (12.70) is the time tendency for the depth integrated axial angular momentum per horizontal area in a horizontally fixed fluid column. This time tendency arises from the convergence of horizontal advection of axial angular momentum plus torques due to surface boundary mass fluxes, depth integrated zonal pressure gradients, and depth integrated irreversible stresses. This mathematical expression of the budget meets our expectations based on our understanding of the physical principles discussed in Section 12.5.1.

12.5.4 Atmospheric and topographic form stresses

We can further unpack the contribution from pressure in the budget (12.70) by making use of Leibniz's rule to write

$$-\int_{\eta_b}^{\eta} \frac{\partial p}{\partial \lambda} dz = -\frac{\partial P}{\partial \lambda} + p_a \frac{\partial \eta}{\partial \lambda} - p_b \frac{\partial \eta_b}{\partial \lambda}, \quad (12.71a)$$

where P is the depth-integrated pressure given by equation (12.39). We studied this decomposition of the pressure force in Section 12.2 and encountered it in Section 12.4.4. Again, we see that the depth integrated zonal pressure gradient has been decomposed into three terms: (i) zonal pressure differences integrated across the depth of the column, (ii) form stress imparted to the ocean from the atmospheric pressure, (iii) form stress imparted by the solid earth bottom topography onto the ocean.

12.5.5 Turbulent stresses at the surface and bottom

For turbulent stresses, we focus on the vertical transfer of zonal momentum arising from the vertical shear of horizontal stresses

$$\rho F^{\lambda} = \frac{\partial \tau^{\lambda}}{\partial z}, \quad (12.72)$$

where τ^{λ} is the zonal component to the stress vector.⁵ When integrated vertically over an ocean column, $\int_{\eta_b}^{\eta} \rho F^{\lambda} dz$, this friction arises from stresses acting in the ocean surface and bottom boundary/Ekman layers (Chapter 17), where the stress arises from turbulent motions that transfer momentum vertically through these layers.

For the friction contribution, we make use of the primitive equations so that the axial moment-arm is approximated by its value at the ocean surface

$$r_{\perp} = r \cos \phi = (z + R) \cos \phi \approx R \cos \phi = R_{\perp}, \quad (12.73)$$

as per the shallow fluid approximation built into the hydrostatic primitive equations discussed in Section 11.1. This assumption allows us to write the frictional contribution to the angular

⁵As seen in equation (12.53), there are other turbulent terms associated with interior Reynolds stresses arising from horizontal shears. We omit these terms for the present analysis.

momentum budget (12.70) in the form

$$\int_{\eta_b}^{\eta} r_{\perp} \rho F^{\lambda} dz \approx R_{\perp} \int_{\eta_b}^{\eta} \rho F^{\lambda} dz = R_{\perp} (\tau_{atm}^{\lambda} - \tau_{bot}^{\lambda}). \quad (12.74)$$

The final expression introduced τ_{atm}^{λ} , which is the zonal component to the stress acting on the ocean surface imparted through interactions between the ocean and the overlying atmosphere and/or ice. The signs are such that $\tau_{atm}^{\lambda} > 0$ transfers an eastward momentum to the ocean such as via a westerly wind stress. Likewise, the stress τ_{bot}^{λ} is the zonal stress at the ocean bottom imparted through interactions between the ocean and the solid-earth. The signs are such that $\tau_{bot}^{\lambda} > 0$ reflects the transfer of eastward momentum from the ocean to the solid-earth, or conversely the transfer of westward momentum from the earth to the ocean. The net contribution from vertical friction is thus given by the moment arm, R_{\perp} , multiplied by the difference in boundary stresses.

12.5.6 Summary budget for column integrated axial angular momentum

Bringing all the pieces together leads to the depth integrated axial angular momentum budget

$$\frac{\partial}{\partial t} \left[\int_{\eta_b}^{\eta} l^z \rho dz \right] = -\nabla_h \cdot \left[\int_{\eta_b}^{\eta} l^z \mathbf{u} \rho dz \right] - \frac{\partial P}{\partial \lambda} + [l^z Q_m]_{z=\eta} + p_a \frac{\partial \eta}{\partial \lambda} - p_b \frac{\partial \eta_b}{\partial \lambda} + R_{\perp} (\tau_{atm}^{\lambda} - \tau_{bot}^{\lambda}). \quad (12.75)$$

Other than assuming a specific form of the frictional stress given by equation (12.72), this result is the exact budget for the axial angular momentum in a column of ocean fluid satisfying the primitive equations.

Removing zonal means

We further isolate the processes contributing to the budget (12.75) by introducing the zonal mean operator

$$\bar{A} \equiv \frac{1}{L(\phi)} \int A d\lambda, \quad (12.76)$$

where

$$L(\phi) = (R_e \cos \phi) \Delta \lambda = R_{\perp} \Delta \lambda \quad (12.77)$$

is the zonal length of the domain as a function of latitude, ϕ , and $\Delta \lambda$ is the zonal extent of the domain in radians. For a domain that circles the planet, then $\Delta \lambda = 2\pi$. Other domains are possible, such as those in Figure 12.6. The corresponding zonal anomalies to the depth integrated pressure, sea surface height, and bottom topography are thus given by

$$P' = P - \bar{P} \quad \text{and} \quad \eta' = \eta - \bar{\eta} \quad \text{and} \quad \eta'_b = \eta_b - \bar{\eta}_b, \quad (12.78)$$

in which case equation (12.75) takes the form

$$\frac{\partial}{\partial t} \left[\int_{\eta_b}^{\eta} l^z \rho dz \right] = -\nabla_h \cdot \left[\int_{\eta_b}^{\eta} l^z \mathbf{u} \rho dz \right] - \frac{\partial P'}{\partial \lambda} + [l^z Q_m]_{z=\eta} + p_a \frac{\partial \eta'}{\partial \lambda} - p_b \frac{\partial \eta'_b}{\partial \lambda} + R_{\perp} (\tau_{atm}^{\lambda} - \tau_{bot}^{\lambda}). \quad (12.79)$$

Steady state balance

Steady state balances are of particular interest when studying the large-scale low frequency circulation. A steady state holds for the angular momentum budget (12.79) so long as the following balance is maintained

$$\nabla_h \cdot \left[\int_{\eta_b}^{\eta} l^z \mathbf{u} \rho dz \right] = -\frac{\partial P'}{\partial \lambda} + [l^z Q_m]_{z=\eta} + p_a \frac{\partial \eta'}{\partial \lambda} - p_b \frac{\partial \eta'_b}{\partial \lambda} + R_{\perp} (\tau_{atm}^{\lambda} - \tau_{bot}^{\lambda}). \quad (12.80)$$

Consequently, a steady state is realized if the horizontal divergence of depth integrated axial angular momentum advection (left hand side) is balanced by torques created by the variety of physical processes on the right hand side. We further examine these physical processes by studying the zonally integrated budget.

12.5.7 Steady domain integrated balance

Consider the area integral of the steady state balance (12.80) over the full ocean domain that is either periodic and/or has sloping side boundaries. In this case the divergence of the angular momentum transport integrates to zero, so that we are left with the balance

$$\int_{\phi_s}^{\phi_n} \left(\int_{\lambda_w(\phi)}^{\lambda_e(\phi)} \left[[l^z Q_m]_{z=\eta} + p'_a \frac{\partial \eta'}{\partial \lambda} - p'_b \frac{\partial \eta'_b}{\partial \lambda} + R_{\perp} (\tau_{atm}^{\lambda} - \tau_{bot}^{\lambda}) \right] d\lambda \right) R_e^2 \cos \phi d\phi = 0. \quad (12.81)$$

In computing the area integral, we chose to first integrate over the longitudinal domain, $\lambda_w(\phi) \leq \lambda \leq \lambda_e(\phi)$, which is a function of latitude, and then to integrate over the full latitudinal domain, $\phi_s \leq \phi \leq \phi_n$. In most applications the surface mass term, $[l^z Q_m]_{z=\eta}$, is smaller than the other terms, in which case the balance is between the boundary form stresses and the boundary turbulent stresses.

In the angular momentum balance (12.81), we introduced the zonal anomalies for the applied surface pressure and the bottom pressure

$$p'_a(\lambda, \phi) = p_a(\lambda, \phi) - \bar{p}_a(\phi) \quad \text{and} \quad p'_b(\lambda, \phi) = p_b(\lambda, \phi) - \bar{p}_b(\phi). \quad (12.82)$$

We can introduce these anomalous fields since their zonal averages do not contribute to the budgets in either the periodic or sloping shoreline domains. To verify this property, note that

$$\int \bar{p}_a \frac{\partial \eta'}{\partial \lambda} d\lambda = \int \frac{\partial (\bar{p}_a \eta')}{\partial \lambda} d\lambda = 0. \quad (12.83)$$

For a periodic domain this term vanishes by inspection. For a zonally bounded domain with a sloping shoreline, it also vanishes since $\eta' = 0$ at the edge of the shoreline. Likewise, the bottom pressure term satisfies

$$\int \bar{p}_b \frac{\partial \eta'_b}{\partial \lambda} d\lambda = \int \frac{\partial (\bar{p}_b \eta'_b)}{\partial \lambda} d\lambda = 0, \quad (12.84)$$

which follows either by periodicity or since $\eta'_b = 0$ along the edge of a sloping shoreline. In conclusion, we see that it is only the zonal anomalies of the atmospheric and bottom pressures, and free surface and bottom topography, that impact the zonal mean zonal momentum balance (12.86) for the periodic and sloping shoreline domains.

12.5.8 Form stress versus dual form stress

We can further exploit symmetry of the periodic domain and sloping shoreline domain by writing the form stresses in equation (12.86) in an alternative manner that makes use of the dual form stress

$$\int \left[p'_a \frac{\partial \eta'}{\partial \lambda} - p'_b \frac{\partial \eta'_b}{\partial \lambda} \right] d\lambda = \int \left[-\frac{\partial p'_a}{\partial \lambda} \eta' + \frac{\partial p'_b}{\partial \lambda} \eta'_b \right] d\lambda. \quad (12.85)$$

Diagnostics of zonally integrated form stress can be more convenient using one form or the other, depending on dataset or numerical model framework. We have a choice since the zonal integral is the same, and that freedom is afforded since the spatial integral removes local information that appears as a total zonal derivative. However, we offer two caveats in this regard.

- The identity (12.85) does not hold for the bounded domain with vertical sidewalls (third panel of Figure 12.6). If working in such a domain and if one chooses to study patterns based on the right hand side dual form stress, then its zonal integral will not agree with that of the form stress on the left hand side. Correspondingly, physical interpretations based on the dual form stress are questionable.
- Although the zonal integrals in equation (12.85) agree for the periodic domain and sloping shoreline domain, there is no local identity between terms on the left hand side and right hand side. So if one wishes to make a statement about patterns of local form stresses acting on the depth integrated axial angular momentum, then it is necessary to return to the form stress appearing on the left hand side of equation (12.85).

12.5.9 Steady zonal and depth integrated budget

Now consider just a zonal integral of the steady angular momentum budget (12.80), again over a domain that is either periodic or has sloping shorelines (Figure 12.6). In both of these cases, we are left with the zonal and depth integrated steady angular momentum budget

$$\frac{1}{R \cos \phi} \int \frac{\partial}{\partial \phi} \left[\int_{\eta_b}^{\eta} l^z v \rho dz \right] d\lambda = \int \left[[l^z Q_m]_{z=\eta} + p'_a \frac{\partial \eta'}{\partial \lambda} - p'_b \frac{\partial \eta'_b}{\partial \lambda} + R_{\perp} (\tau_{atm}^{\lambda} - \tau_{bot}^{\lambda}) \right] d\lambda. \quad (12.86)$$

The meridional divergence of the advective transport of angular momentum is balanced, in the steady state, by the boundary terms on the right hand side.

12.5.10 Southern Ocean balances

Under certain cases the primary balance in equation (12.86) is between the form stress and boundary turbulent stress, whereby

$$\oint \left[p'_a \frac{\partial \eta'}{\partial \lambda} + R_{\perp} \tau_{atm}^{\lambda} \right] d\lambda \approx \oint \left[p'_b \frac{\partial \eta'_b}{\partial \lambda} + R_{\perp} \tau_{bot}^{\lambda} \right] d\lambda. \quad (12.87)$$

For much of the large-scale Southern Ocean circulation, the primary balance is even simpler: it is a balance between surface wind stress and topographic form stress

$$\oint \tau_{atm}^{\lambda} d\lambda \approx \oint p'_b \frac{1}{R_{\perp}} \frac{\partial \eta'_b}{\partial \lambda} d\lambda = - \oint \eta'_b \frac{1}{R_{\perp}} \frac{\partial p'_b}{\partial \lambda} d\lambda, \quad (12.88)$$

with this balance exemplified in Figure 12.8. We now state in words what this balance means in the presence of a net eastward wind stress, $\oint \tau_{atm}^{\lambda} d\lambda > 0$. The equivalent expressions on the

right hand side allow complementary perspectives.

- For the first equality in equation (12.88) we see that a balance is realized if on the upwind side of a topographic bump there is an anomalously high bottom pressure, with the opposite on the downwind side. Correspondingly, there is a net westward topographic form stress imparted by the solid earth onto the ocean that balances the eastward surface wind stress imparted by the atmosphere onto the ocean.
- The second equality in equation (12.88) reveals that for $\eta'_b > 0$ (topographic ridge), a steady angular momentum balance is maintained so long as the bottom pressure decreases across the ridge from west to east, just as depicted in Figure 12.8.

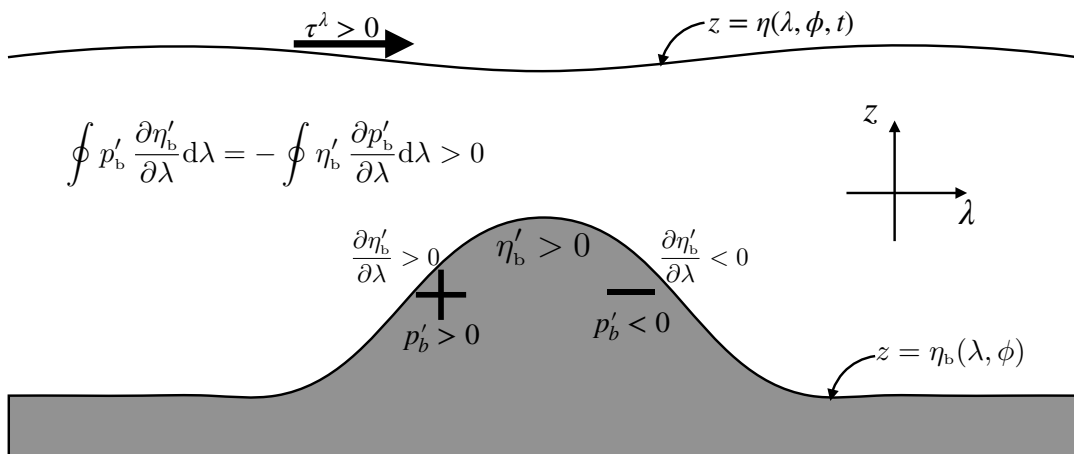


FIGURE 12.8: Depicting the balance between zonal wind stress and topographic form stress for a southern hemisphere zonally periodic ocean channel. For an eastward wind stress, the flow reaches a steady state if the upwind side of a topographic bump sees an anomalously high bottom pressure whereas on the downwind side it is anomalously low. The form stress imparted by the ocean onto the solid earth is eastward since the bottom pressure is higher in the west and lower in the east. Conversely, Newton's third law tells us that the topographic form stress imparted by the solid earth onto the ocean is westward. In this manner, the eastward force imparted by the atmosphere onto the ocean through wind stress is balanced by a westward topographic form stress imparted by the solid earth onto the ocean. Furthermore, the eastward bottom pressure gradient leads to a northward depth integrated geostrophic transport above the southern hemisphere ridge. Signs are swapped when flow moves over a depression, in which a westward bottom pressure gradient leads to southward geostrophic transport over the depression. We revisit these dynamical processes for the shallow water fluid in VOLUME 3.

12.5.11 Topographic form stress and ocean gyres

Hughes (2000) and *Hughes and de Cueves* (2001) are notable for having emphasized the importance of bottom topographic form stress, and the associated bottom pressure torque appearing in the vorticity equation studied in VOLUME 3. The key role for topographic form stress is well appreciated for channel flows since the work of *Munk and Palmén* (1951) who studied the Southern Ocean steady force balances (see also *Webb and de Cueves* (2007) for studies of the transient case). However, *Hughes* (2000) and *Hughes and de Cueves* (2001) showed that it is central even for steady ocean gyre circulations when allowing for sloping sides rather than vertical sides. Hence, sloping sides for the gyre domain allow for a steady momentum balance to occur between bottom form stress and wind stress, and a steady vorticity balance to occur between bottom pressure torque and wind stress curl. As a result, topographic

form stress and bottom pressure torques allow for a mostly inviscid balance in ocean gyres much like for the zonally re-entrant Southern Ocean.

12.5.12 Further study

Elements of this section are based on [Hughes \(2000\)](#) and [Hughes and de Cueves \(2001\)](#), as well as the analogous discussion of the global atmospheric axial angular momentum budget developed in Section 10.3 of [Holton and Hakim \(2013\)](#). [Straub \(1993\)](#) provides an analogous analysis with a focus on the Southern Ocean. The physical processes establishing the balances noted for the Southern Ocean remain under investigation, with further resources to the literature including Section 21.7 of [Vallis \(2017\)](#), and the reviews by [Rintoul et al. \(2001\)](#), [Rintoul and Naveira Garabato \(2013\)](#), and [Rintoul \(2018\)](#). We further revisit this balance for the shallow water system in VOLUME 3.



Chapter 13

BOUSSINESQ OCEAN

The **Mach number** is the ratio of the fluid particle speed to the speed of sound waves, and in some areas of fluid mechanics the Mach number reaches unity or larger.¹ In such flows it is important to consider the influence of compressibility since the large flow speeds can lead to nontrivial local density changes through the convergence of advective mass fluxes.

Many of the geophysical flows studied in this book, particularly ocean flows, have tiny Mach numbers. Hence, their local density changes are generally much smaller than the mean density. Yet even with a small Mach number, pressure can play a nontrivial role in affecting density changes for those cases where motions extend over vertical distances comparable to the **scale height**. For the atmosphere, the scale height (Section 7.5.10) is roughly 10 km, whereas the ocean's scale height is generally deeper than the ocean. For this reason, compressibility effects can be important for atmospheric motions, whereas they can be neglected for many purposes of ocean fluid mechanics.

Because compressibility effects are relatively weak in the ocean, the ocean velocity field is nearly non-divergent, thus allowing for use of the volume conserving flow kinematics studied in VOLUME 1. Even with this approximation, it is crucial to note that the ocean is not an incompressible fluid since density is not uniform. Hence, an approximate theory for ocean circulation, one that incorporates effects from horizontal and vertical density variations (i.e., **thermohaline effects**), requires more than the mechanics of an incompressible fluid.² It is for this purpose that we here develop the equations for a **Boussinesq ocean**, which sit somewhere between the equations of a fully compressible fluid (i.e., **non-Boussinesq** fluids) and incompressible flows.

READER'S GUIDE TO THIS CHAPTER

We here derive the Boussinesq ocean equations and explore their physical properties, including energetics. The Boussinesq ocean has broader application than just to the ocean, with many characteristics also holding for atmospheric flow satisfying the anelastic approximation (see Section 2.5 of [Vallis \(2017\)](#)). Furthermore, the Boussinesq ocean provides the starting point for many of the geophysical fluid models found later in this book. This is a relatively long chapter due to the broad use of the Boussinesq ocean in this book, which in

¹When a jet airplane or rocket moves at a speed greater than Mach one, such super-sonic motion generates a spectacularly loud and powerful sonic boom. When studying acoustics in VOLUME 5, we see precisely how a density fluctuation is related to the Mach number. For purposes of the present chapter, density fluctuations are very small and thus correspond to a tiny Mach number.

²The fluid mechanics of constant density fluids is sometimes referred to as **hydrodynamics**. Certain idealized models of geophysical fluid mechanics follow the approaches of hydrodynamics; e.g., the single layer of constant density shallow water fluid. However, horizontal and vertical density variations are crucial for many atmosphere and ocean flows, and it is for such flows that we make use of the Boussinesq ocean equations.

turn motivates us to explore many of its facets.

13.1	The Boussinesq ocean approximation	409
13.1.1	Isolating the dynamically active pressure field	409
13.1.2	Boussinesq momentum equation	411
13.1.3	A vorticity motivation to set ρ constant	411
13.1.4	Mass continuity	412
13.1.5	Version I of the Boussinesq ocean equations	412
13.1.6	Version II of the Boussinesq ocean equations	414
13.1.7	Boussinesq inertial mass is not the gravitational mass	414
13.1.8	Summary points	415
13.1.9	Further study	416
13.2	Scaling for the hydrostatic approximation	417
13.2.1	Stratified non-rotating Boussinesq ocean equations	417
13.2.2	Non-dimensionalization	417
13.2.3	Specifying the scales	418
13.2.4	Non-dimensional Boussinesq equations of motion	419
13.2.5	The Froude number	419
13.2.6	Horizontal hydrostatic pressure gradient	420
13.2.7	Evolution of hydrostatic pressure	421
13.3	How pressure enforces non-divergent flow	421
13.3.1	Poisson equation for pressure	422
13.3.2	Boundary conditions	422
13.3.3	Characterizing the pressure sources	424
13.3.4	Comments and further study	425
13.4	Helmholtz decomposing the velocity equation	426
13.4.1	Helmholtz decomposition	426
13.4.2	The pressure equation	427
13.4.3	The vorticity equation	427
13.4.4	The velocity equation	427
13.4.5	Comments	427
13.5	Tracer budgets in Eulerian regions	428
13.5.1	Formulating the budget equation	428
13.5.2	Interpreting advective tracer contributions	429
13.5.3	A rectangular region example	429
13.5.4	Comments	430
13.6	Mechanical energy analysis: part I	430
13.6.1	Governing equations	431
13.6.2	Kinetic energy	431
13.6.3	Potential energy and mechanical energy	432
13.6.4	Finite volume mechanical energy budget	433
13.7	Boussinesq energetics with dissipation	434
13.7.1	Forms for the buoyancy flux	434
13.7.2	Mechanical forcing and dissipation	435
13.7.3	Governing equations with molecular friction and diffusion	436
13.7.4	Kinetic energy evolution	437
13.7.5	Frictional dissipation	437
13.7.6	Domain integrated kinetic energy	437
13.7.7	Potential energy evolution	438
13.7.8	Mechanical energy	440
13.7.9	Conditions required for a steady state mechanical energy	440
13.7.10	Further reading	441

13.8 Mechanical energy analysis: part II	441
13.8.1 Boussinesq dynamic enthalpy	441
13.8.2 Regionally integrated Boussinesq dynamic enthalpy	443
13.8.3 Density derivatives	444
13.8.4 Comments	446
13.9 Available potential energy	447
13.9.1 Analytic continuation of buoyancy surfaces	448
13.9.2 The dual relation between height and buoyancy	451
13.9.3 Exact expression for APE	452
13.9.4 Approximate expression for APE	453
13.9.5 Comments	455
13.10 Exercises	456

13.1 The Boussinesq ocean approximation

For the ocean, density deviates no more than a few percent relative to the volume mean density. Although small, ocean density deviations act over large distances and are crucial for driving large-scale circulations. Such [thermohaline effects](#) derive their driving force from space and time variations in temperature and salinity that affect density and, in turn, modify the pressure. A key reason that small density changes can be so pivotal is that the density variations are multiplied by the relatively large gravitational acceleration when computing pressure.

The equations for a Boussinesq ocean provide a systematic means to ignore small density deviations where it is safe to do so dynamically, while retaining density variations where they are critical such as when multiplied by gravity. The Boussinesq ocean makes use of (a slightly modified) compressible thermodynamics plus an incompressible kinematics. The use of compressible thermodynamics allows for thermohaline processes to modify density and thus pressure and circulation, while the incompressible kinematics removes sound waves from the prognostic flow field and renders the volume of a fluid element materially invariant.

Stated in slightly different words, the Boussinesq ocean's prognostic velocity is non-divergent, thus representing an incompressible flow, and yet the Boussinesq ocean fluid admits density variations, as for a compressible fluid. Hence, the Boussinesq ocean describes the incompressible flow of a compressible fluid. This pithy definition exemplifies the important distinction between a [fluid property](#) and a [flow property](#). Since the flow is non-divergent, pressure in the Boussinesq ocean is not the [thermodynamic pressure](#) that appears in the compressible non-Boussinesq fluid. Rather, Boussinesq pressure is a purely [mechanical pressure](#) that acts as the Lagrange multiplier to constrain the Boussinesq flow to remain non-divergent.³

13.1.1 Isolating the dynamically active pressure field

Pressure in a vertically stratified fluid can be decomposed into a static background hydrostatic pressure plus a deviation from the background pressure. We made use of this decomposition in Section 11.2.4 when developing a scaling for the hydrostatic approximation. The decomposition holds even when the fluid is non-hydrostatic. We consider the background pressure to be a function just of depth and as such it is determined by a static and horizontally homogeneous background density field. We are motivated to introduce this decomposition given that the background hydrostatic pressure field (again, it is just a function of depth) is dynamically

³We see this role for pressure as a Lagrange multiplier when studying Hamilton's principle for a Boussinesq ocean in VOLUME 4. See also Section 59A of [Serrin \(1959\)](#) for more on pressure in a non-divergent flow.

inactive (as shown below). This decomposition is exact and motivated by the desire to isolate the dynamically active part of the equations of motion.

To achieve the pressure decomposition, start by decomposing density according to

$$\rho(\mathbf{x}, t) = \rho_*(z) + \rho'(\mathbf{x}, t) \quad (13.1)$$

where the deviation density is much smaller than the reference density

$$\rho' \ll \rho_*. \quad (13.2)$$

The following formulation for the momentum equation holds for the general case of $\rho_*(z)$. However, we note in Section 13.1.2 that setting $\rho_*(z) = \rho_*$ is motivated for studies of potential vorticity in the Boussinesq ocean. Indeed, a space and time constant reference density is generally synonymous with the Boussinesq ocean equations.⁴

The corresponding decomposition of pressure is given by the sum of a static and depth dependent background pressure, $p_*(z)$, and a deviation pressure, $p'(\mathbf{x}, t)$,

$$p(\mathbf{x}, t) = p_*(z) + p'(\mathbf{x}, t). \quad (13.3)$$

The background pressure is assumed to be in hydrostatic balance with the reference density

$$\frac{dp_*}{dz} = -\rho_* g, \quad (13.4)$$

with p_* and ρ_* both static. We offer the following points to clarify the decomposition of pressure in equation (13.3).

- Assuming the background pressure, $p_*(z)$, to be hydrostatic does *not* imply that the full pressure, $p(\mathbf{x}, t)$, is also hydrostatic. Rather, the decomposition merely serves to remove that portion of the pressure field that plays no role in establishing motion (we see this property below). So this decomposition holds whether the full pressure is approximately hydrostatic or fully non-hydrostatic.
- Furthermore, if $p(\mathbf{x}, t)$ is in an approximate hydrostatic balance (Section 11.2), the decomposition (13.3) does *not* remove all of the hydrostatic pressure from $p(\mathbf{x}, t)$. Rather, $p'(\mathbf{x}, t)$ is generally nonzero whether $p(\mathbf{x}, t)$ is in an approximate hydrostatic balance or fully non-hydrostatic.

With the above density and pressure decompositions, the momentum equation

$$\rho \left[\frac{D\mathbf{v}}{Dt} + 2\boldsymbol{\Omega} \times \mathbf{v} \right] = -\nabla p - \hat{\mathbf{z}} g \rho \quad (13.5)$$

takes the equivalent form

$$(\rho_* + \rho') \left[\frac{D\mathbf{v}}{Dt} + 2\boldsymbol{\Omega} \times \mathbf{v} \right] = -\nabla p' - g \rho' \hat{\mathbf{z}} - \left[\frac{dp_*}{dz} + \rho_* g \right] \hat{\mathbf{z}} \quad (13.6a)$$

$$= -\nabla p' - g \rho' \hat{\mathbf{z}}, \quad (13.6b)$$

where we used the hydrostatic balance (13.4) for the second equality. We thus see that the background hydrostatic pressure, $p_*(z)$, leads to no motion since it drops out from the

⁴Exercise 13.5 offers a modest means to generalize this assumption.

momentum equation. The gradient pressure force is thus determined solely by the gradient of p' .

13.1.2 Boussinesq momentum equation

To develop the Boussinesq momentum equation, divide the momentum equation (13.6b) by the density, $\rho = \rho_0 + \rho'$, and write the pressure and gravity terms as

$$\frac{\nabla p' + g \rho' \hat{z}}{\rho_0 + \rho'} = \frac{\nabla p' + g \rho' \hat{z}}{\rho_0 + \rho'} \left[\frac{\rho_0 - \rho'}{\rho_0 - \rho'} \right] = \frac{\nabla p' + g \rho' \hat{z}}{\rho_0^2 - (\rho')^2} (\rho_0 - \rho') \approx \frac{\nabla p' + g \rho' \hat{z}}{\rho_0}, \quad (13.7)$$

where the final approximation results from dropping all terms that are second order in deviation quantities. This approximation then leads to the Boussinesq momentum equation

$$\frac{D\mathbf{v}}{Dt} + 2\boldsymbol{\Omega} \times \mathbf{v} = -\frac{1}{\rho_0} \nabla p' + b \hat{z}, \quad (13.8)$$

where we introduced the globally referenced Archimedean buoyancy (Chapter 14) as defined relative to the constant background density

$$b = -\frac{g \rho'}{\rho_0} = -\frac{g (\rho - \rho_0)}{\rho_0}. \quad (13.9)$$

Hence, the globally referenced Archimedean buoyancy is positive when the *in situ* density is less than the reference density so that $\rho' = \rho - \rho_0 < 0$. That is, $b > 0$ when the fluid element is lighter (more buoyant) than the background reference density. Buoyancy is the product of the gravitational acceleration, which is a relatively large term, and the small number ρ'/ρ_0 . Their product is generally not small so that it generally cannot be neglected from the momentum equation. This is a key point in deriving Boussinesq ocean equations that contain dynamical processes arising from horizontal buoyancy gradients.

In the special case of a space and time constant reference density, $\rho_0(z) = \rho_0$, it is convenient to introduce the shorthand for the deviation pressure normalized by the reference density

$$\varphi = \frac{p'}{\rho_0} = \frac{p - p_0(z)}{\rho_0}. \quad (13.10)$$

In this case the Boussinesq momentum equation takes the rather tidy form

$$\frac{D\mathbf{v}}{Dt} + 2\boldsymbol{\Omega} \times \mathbf{v} = -\nabla \varphi + b \hat{z}. \quad (13.11)$$

13.1.3 A vorticity motivation to set ρ_0 constant

We now anticipate a discussion of vorticity and potential vorticity from VOLUME 3 to motivate setting $\rho_0(z)$ to a constant. This paragraph is not critical for the remainder of this chapter, but worth returning to after studying vorticity and baroclinicity for the Boussinesq fluid in VOLUME 3. For that purpose, note that the form of the pressure gradient acceleration found in equation (13.11) is particularly useful given that the curl of the right hand side eliminates pressure from the vorticity equation. In contrast, for the more general form with $\rho_0(z)$ in equation (13.8), the Boussinesq baroclinicity vector has a contribution from both pressure and buoyancy (we derive

equation (13.12) in an exercise in VOLUME 3)

$$\mathbf{B} = \nabla \left[b - \frac{p'}{\rho_0^2} \frac{d\rho}{dz} \right] \times \hat{\mathbf{z}}. \quad (13.12)$$

The additional pressure contribution complicates the development of potential vorticity whereby we wish to have $\mathbf{B} \cdot \nabla b = 0$. We are thus motivated to use a space and time constant reference density so that $d\rho_0/dz = 0$. Following this motivation, we generally assume ρ_0 is a constant in this book. Even so, in Exercise 13.5 we discuss a middle ground by defining a slightly more general buoyancy field while retaining a constant ρ_0 .

13.1.4 Mass continuity

When decomposing density according to equation (13.1), the mass continuity equation

$$\frac{D\rho}{Dt} = -\rho \nabla \cdot \mathbf{v}, \quad (13.13)$$

takes the form

$$\frac{D\rho'}{Dt} = -(\rho_0 + \rho') (\nabla_h \cdot \mathbf{u} + \partial_z w). \quad (13.14)$$

For many geophysical flows, the material time derivative on the left hand side is much smaller than either of the two terms appearing on the right hand side. To help formalize this observation it is useful to introduce a time scale for the various terms in this equation

$$\left| \frac{1}{\rho} \frac{D\rho'}{Dt} \right| \sim \frac{1}{T_\rho} \quad |\partial_x u| \sim T_u^{-1} \quad |\partial_y v| \sim T_v^{-1} \quad |\partial_z w| \sim T_w^{-1}. \quad (13.15)$$

Quite often we find flows in which the time scales associated with the spatial deformations of the flow, in the direction of the flow, are much smaller than time scales for the material changes in density, whereby

$$T_u^{-1}, T_v^{-1}, T_w^{-1} \gg T_\rho^{-1}. \quad (13.16)$$

In this case the only way for the mass balance equation (13.14) to hold is for the three terms contributing to the divergence to balance one another

$$\partial_x u + \partial_y v + \partial_z w \approx 0. \quad (13.17)$$

Taking this balance to the limit motivates setting the velocity field for the Boussinesq ocean to be non-divergent

$$\nabla_h \cdot \mathbf{u} + \partial_z w = \nabla \cdot \mathbf{v} = 0. \quad (13.18)$$

Note that for density stratified flows we generally find the horizontal divergence of the horizontal velocity balancing the vertical convergence of the vertical velocity. For a Boussinesq ocean this balance is exact

$$\nabla_h \cdot \mathbf{u} = -\partial_z w. \quad (13.19)$$

13.1.5 Version I of the Boussinesq ocean equations

The first form of the oceanic Boussinesq equations emphasizes the role of buoyancy computed relative to a reference state of constant density, $\rho = \rho_0$. This form facilitates a focus on that portion of the pressure field giving rise to internal or baroclinic pressure gradients; i.e., those

pressure gradients that generate motion independent of free surface undulations. The oceanic Boussinesq equations thus take the form

$$\frac{D\mathbf{v}}{Dt} + 2\boldsymbol{\Omega} \times \mathbf{v} = -\nabla\varphi + b\hat{\mathbf{z}} + \mathbf{F} \quad \text{velocity equation} \quad (13.20a)$$

$$\nabla \cdot \mathbf{v} = 0 \quad \text{continuity equation} \quad (13.20b)$$

$$\frac{Db}{Dt} = \dot{b} \quad \text{buoyancy equation} \quad (13.20c)$$

$$b = -\frac{g\rho'}{\rho_0} = -\frac{g(\rho - \rho_0)}{\rho_0} \quad \text{buoyancy defined} \quad (13.20d)$$

$$\varphi = \frac{p'}{\rho_0} = \frac{p - p_0(z)}{\rho_0} \quad \text{dynamic pressure defined} \quad (13.20e)$$

$$\rho = \rho_0(1 - \alpha\Theta + \beta S) \quad \text{linear equation of state} \quad (13.20f)$$

$$\frac{dp_0}{dz} = -\rho_0 g \quad \text{background hydrostatic pressure.} \quad (13.20g)$$

We offer the following comments on these equations.

- MATERIAL EVOLUTION OF BUOYANCY: The term \dot{b} on the right hand side of the buoyancy equation (13.20c) is a placeholder for any process leading to a material change in buoyancy, such as diffusion or sources. We further discuss $\dot{b} \neq 0$ in Section 13.7.1.
- EQUATION OF STATE: The equation of state, (13.20f), is written as a linear function of salinity and Conservative Temperature, with the thermal expansion coefficient, α , and haline contraction coefficient, β , assumed constant.⁵ This form for the equation of state eliminates processes such as cabbeling and thermobaricity, which are discussed in our study of ocean buoyancy in VOLUME 5. These processes are important for certain features of the ocean, thus prompting the more general equation set written in Section 13.1.6. However, the linear equation of state is sufficient for many of our studies in this book, as is the further simplified form with zero haline contraction, $\beta = 0$.
- APPROXIMATE HYDROSTATIC BALANCE: Most numerical models of the large-scale ocean circulation assume the flow maintains an approximate hydrostatic balance. Assuming this balance holds in the velocity equation (13.20a) leads to the split into a horizontal velocity equation plus a vertical hydrostatic balance

$$\frac{Du}{Dt} + 2\boldsymbol{\Omega} \times \mathbf{v} = -\nabla_h\varphi + \mathbf{F}^h \quad \text{horizontal velocity equation} \quad (13.21a)$$

$$\frac{\partial\varphi}{\partial z} = b \quad \text{approximate hydrostatic balance,} \quad (13.21b)$$

where ∇_h is the horizontal gradient operator and \mathbf{F}^h is the horizontal frictional acceleration. As emphasized in Section 11.1 when deriving the hydrostatic primitive equations, the approximate hydrostatic balance leads to a vertical velocity equation with no friction nor Coriolis contribution. Rather, when making the hydrostatic approximation we just retain a balance between the vertical pressure gradient and gravity/buoyancy.

⁵It is unfortunate that β is used for two prominent but very distinct properties of geophysical fluids. First, it is the meridional derivative of the Coriolis parameter: $\beta = \partial_y f$. Second, it is the haline contraction coefficient: $\beta = \rho^{-1} \partial \rho / \partial S$. These distinct uses will be clearly defined so to avoid confusion.

13.1.6 Version II of the Boussinesq ocean equations

The Boussinesq equations (13.20a)-(13.20g) are suited for many purposes in this book. However, the following form is better suited to studying or simulating realistic Boussinesq ocean flows, with such flows involving separate prognostic equations for salinity and Conservative Temperature rather than a single prognostic equation for buoyancy. We are thus motivated to consider the Boussinesq ocean equations in the form

$$\frac{D\mathbf{v}}{Dt} + 2\boldsymbol{\Omega} \times \mathbf{v} = -(1/\rho_0) (\nabla p + \rho \nabla \Phi) + \mathbf{F} \quad \text{velocity equation} \quad (13.22a)$$

$$\nabla \cdot \mathbf{v} = 0 \quad \text{continuity equation} \quad (13.22b)$$

$$\frac{DS}{Dt} = \dot{S} \quad \text{salinity equation} \quad (13.22c)$$

$$\frac{D\Theta}{Dt} = \dot{\Theta} \quad \text{Conservative Temperature equation} \quad (13.22d)$$

$$\rho = \rho(S, \Theta, \Phi) \quad \text{equation of state.} \quad (13.22e)$$

We make the following comments concerning these equations.

- **GEOPOTENTIAL:** The geopotential is here considered to be a function of space and time, as relevant when studying the role of astronomical tidal forcing or changes to the mass distribution of the planet

$$\Phi = \Phi(\mathbf{x}, t). \quad (13.23)$$

- **EQUATION OF STATE:** The equation of state is a function of salinity, Conservative Temperature, and geopotential, thus allowing for processes such as cabelling and thermobaricity (VOLUME 5). Furthermore, the pressure dependence in the equation of state is computed as per a homogeneous and resting hydrostatic fluid

$$\rho(S, \Theta, \Phi) = \rho(S, \Theta, p = -\rho_0 \Phi). \quad (13.24)$$

In Section 13.8 we provide an energetic argument for why it is appropriate to take this functional form rather than the more general form discussed in Section 14.3, in which density is a function of the full *in situ* pressure: $\rho = \rho(S, \Theta, p)$.

- **HYDROSTATIC APPROXIMATION:** As for version I of the Boussinesq ocean equations, we here list the equations when making the hydrostatic approximation in the vertical momentum equation, in which case the velocity equation (13.22a) splits into a horizontal velocity equation and hydrostatic balance

$$\frac{D\mathbf{u}}{Dt} + 2\boldsymbol{\Omega} \times \mathbf{v} = -(1/\rho_0) (\nabla_h p + \rho \nabla_h \Phi) + \mathbf{F}^h \quad \text{horizontal velocity equation} \quad (13.25a)$$

$$\frac{\partial p}{\partial z} = -g \rho \quad \text{hydrostatic balance.} \quad (13.25b)$$

13.1.7 Boussinesq inertial mass is not the gravitational mass

The **inertial mass** is the mass multiplying acceleration on the right hand side Newton's law of motion, $\mathbf{F} = m \mathbf{a}$, and it is correspondingly used to measure kinetic energy. The **gravitational mass** is the mass used to compute the gravitational force, and so it is the mass used when computing weight, buoyancy, and gravitational potential energy. The **principle of equivalence**,

originating from the work of Galileo and forming a key element to Einstein's relativity theory, states that the gravitational mass and the inertial mass are the same. The principle of equivalence is embedded into the use of Newtonian mechanics, so much so that we routinely assume that inertial mass and gravitational mass are identical.

A Boussinesq ocean fluid element materially conserves its volume since the velocity is non-divergent. In turn, the inertial mass of a Boussinesq fluid element is measured by multiplying its volume by the constant reference density, ρ_0 . In contrast, whenever there is a gravitational acceleration multiplying density, the Boussinesq fluid element retains the full *in situ* density to measure the weight of the fluid element. Use of *in situ* density for the gravitational mass ensures an accurate representation of the gravitational force, hydrostatic pressure (Section 13.2.7), buoyancy (Chapter 14) and the gravitational potential energy (Sections 13.6 and 13.8). These considerations reveal that the Boussinesq ocean *does not* respect the principle of equivalence since it distinguishes between the inertial mass and the gravitational mass.

The following offers a summary of various properties of a Boussinesq fluid element related to its distinct inertial mass and gravitational mass:

$$\text{inertial mass density} = \rho_0 \quad (13.26a)$$

$$\text{inertial mass} = \rho_0 \delta V \quad (13.26b)$$

$$\text{linear momentum} = \mathbf{v} \rho_0 \delta V \quad (13.26c)$$

$$\text{kinetic energy} = \rho_0 \delta V \mathbf{v} \cdot \mathbf{v} / 2 \quad (13.26d)$$

$$\text{tracer mass} = C \rho_0 \delta V \quad (13.26e)$$

$$\text{enthalpy content} = c_p \Theta \rho_0 \delta V \quad (13.26f)$$

$$\text{gravitational mass density} = \rho \quad (13.26g)$$

$$\text{gravitational mass} = \rho \delta V \quad (13.26h)$$

$$\text{gravitational force (weight)} = -\rho \delta V \nabla \Phi \quad (13.26i)$$

$$\text{gravitational force (weight) with simple geopotential} = -g \rho \delta V \hat{\mathbf{z}} \quad (13.26j)$$

$$\text{gravitational potential energy} = \Phi \rho \delta V \quad (13.26k)$$

$$\text{gravitational potential energy with simple geopotential} = g z \rho \delta V. \quad (13.26l)$$

13.1.8 Summary points

We close this section by summarizing a number of conceptual points characterizing the Boussinesq ocean. It is useful to return to this list to help dispel common confusions.

Divergent and non-divergent velocity components

The velocity that results from the Boussinesq momentum equation (i.e., the prognostic Boussinesq velocity) is non-divergent. This is the velocity used for transport as per the material time derivative operator. Additionally, there is a divergent velocity field, \mathbf{v}^d , that balances the material evolution of density

$$\frac{1}{\rho'} \frac{D\rho'}{Dt} = -\nabla \cdot \mathbf{v}^d \neq 0. \quad (13.27)$$

The divergent velocity is not used for any of the Boussinesq dynamical equations. Nonetheless, $\mathbf{v}^d \neq 0$, as its divergence balances the material evolution of density according to equation (13.27). Consequently, there are acoustic waves (VOLUME 5) supported by \mathbf{v}^d in the Boussinesq ocean.

Concerning density evolution and thermohaline circulation

The use of a non-divergent velocity for the Boussinesq ocean equations does not mean that the material time evolution of ρ vanishes. Instead, the scaling in Section 13.1.4 focuses just on the mass continuity equation. We must additionally acknowledge that as temperature and salinity evolve, so too does *in situ* density as determined through the equation of state. Indeed, equation (13.27) provides one expression for this evolution. Changes to density translate into changes in pressure, which in turn drive the large-scale circulation through [thermohaline effects](#).

The thermodynamic equation for Conservative Temperature is needed to determine density. There are various forms for the relation between temperature and density that depend on thermodynamic assumptions. We discuss the flavors for density in Section 14.3. For purposes of realistic ocean modeling, an accurate expression for density is critical, whereas for idealized modeling it is common to assume density equals to a constant times the temperature.

Buoyancy

We note the rather trivial point that there is identically zero buoyancy (Chapter 14), $b = -g(\rho - \rho_0)/\rho_0$, in a fully homogeneous fluid where density is constant, $\rho = \rho_0$, everywhere. Hence, for an exactly incompressible fluid, where density is a fixed and uniform constant, there are no buoyancy forces. Such fluids serve many purposes, as exemplified by studies of a single layer of shallow water fluid later in this book. However, buoyancy forces are of primary importance for many other purposes in geophysical fluid mechanics. The Boussinesq ocean accounts for buoyancy forces, and the changes arising from processes such as heating and freshening, while making use of the more convenient kinematics of a non-divergent flow. We have far more to say concerning buoyancy in Chapter 14.

Distinguishing the Boussinesq ocean from the traditional Boussinesq approximation

The Boussinesq ocean equations are more general than the traditional Boussinesq approximation considered in other areas of fluid mechanics (e.g., [Chandrasekhar, 1961](#)). In particular, the traditional Boussinesq approximation assumes a linear equation of state. However, as we saw in Section 13.1.6, the Boussinesq ocean generally has a nonlinear equation of state, which is essential for realistic ocean circulation studies.

Connection to anelastic atmosphere

The atmosphere is far more compressible than the ocean, so that density variations cannot be neglected and the divergent nature of the velocity is important. However, there are some cases in which an atmospheric analog to the oceanic Boussinesq approximation can be useful. The analog is known as the [anelastic approximation](#) and it is mathematically isomorphic to the oceanic Boussinesq approximation, in which case $\nabla \cdot (\rho \mathbf{v}) = 0$ is assumed. Section 2.5 of [Vallis \(2017\)](#) offers more details for the atmospheric anelastic approximation.

13.1.9 Further study

Section 2.4 of [Vallis \(2017\)](#) offers more details to show that density variations are small within the ocean. Further discussion of the Boussinesq ocean approximation can be found in Section 9.3 of [Griffies and Adcroft \(2008\)](#). This video [from SciencePrimer](#) provides a concise summary of ocean circulation arising from differences in density created by [thermohaline effects](#).

13.2 Scaling for the hydrostatic approximation

In Section 11.2 we considered a rudimentary scale analysis justifying the hydrostatic approximation for large-scale ocean and atmospheric flow. However, in that discussion we noted the need to remove a dynamically inactive hydrostatic pressure before addressing the question of whether the dynamically active pressure field is indeed approximately hydrostatic. That decomposition of pressure was performed in Section 13.1.1 as part of deriving the Boussinesq ocean equations. Hence, it is convenient to now return to the question of hydrostatic scaling within the context of the perfect non-rotating Boussinesq ocean equations.

13.2.1 Stratified non-rotating Boussinesq ocean equations

The continuously stratified perfect Boussinesq equations in a non-rotating reference frame are

$$\frac{D\mathbf{u}}{Dt} = -\nabla_h \varphi \quad \text{and} \quad \frac{Dw}{Dt} = -\frac{\partial \varphi}{\partial z} + b \quad \text{and} \quad \nabla \cdot \mathbf{v} = 0 \quad \text{and} \quad \frac{Db}{Dt} = 0. \quad (13.28)$$

To help isolate the dynamically important portion of pressure, we proceed much like in Section 13.1.1 whereby buoyancy is written

$$b = b'(x, y, z, t) + \tilde{b}(z). \quad (13.29)$$

The static buoyancy, $\tilde{b}(z)$, encompasses a background stratification that is in hydrostatic balance with its corresponding portion of the pressure field

$$\frac{d\tilde{\varphi}}{dz} = \tilde{b}(z). \quad (13.30)$$

The Boussinesq equations thus take the form

$$\frac{D\mathbf{u}}{Dt} = -\nabla_h \varphi' \quad \text{and} \quad \frac{Dw}{Dt} = -\frac{\partial \varphi'}{\partial z} + b' \quad \text{and} \quad \nabla \cdot \mathbf{v} = 0 \quad \text{and} \quad \frac{Db'}{Dt} = -w N^2, \quad (13.31)$$

where

$$N^2 = \frac{d\tilde{b}}{dz} \quad (13.32)$$

is the squared [buoyancy frequency](#) of the background vertical stratification.⁶ The decomposition into a background stratification helps to isolate the dynamical portion of the horizontal pressure gradient by removing a static depth dependent background. It also allows us to consider the dynamically interesting, but simpler, case in which the background stratification dominates those perturbations around it.

13.2.2 Non-dimensionalization

Now introduce the dimensional scales (in uppercase) and corresponding non-dimensional quantities (with hats)

$$(x, y) = L(\hat{x}, \hat{y}) \quad z = H\hat{z} \quad \mathbf{u} = U\hat{\mathbf{u}} \quad w = W\hat{w} \quad (13.33)$$

$$t = T\hat{t} \quad \varphi' = \Phi\hat{\varphi}' \quad b' = B\hat{b}' \quad N^2 = \bar{N}^2\hat{N}^2, \quad (13.34)$$

⁶We discuss buoyancy frequency in Section 14.6. For present purposes, we merely note that it provides a measure of the vertical stratification of density, with $N^2 > 0$ for a gravitationally stable density stratification.

which yields the equations of motion

$$\frac{U}{T} \frac{\partial \hat{u}}{\partial \hat{t}} + \frac{U^2}{L} \hat{u} \frac{\partial \hat{u}}{\partial \hat{x}} + \frac{U^2}{L} \hat{v} \frac{\partial \hat{u}}{\partial \hat{y}} + \frac{UW}{H} \hat{w} \frac{\partial \hat{u}}{\partial \hat{z}} = -\frac{\Phi}{L} \frac{\partial \hat{\varphi}'}{\partial \hat{x}} \quad (13.35a)$$

$$\frac{U}{T} \frac{\partial \hat{v}}{\partial \hat{t}} + \frac{U^2}{L} \hat{u} \frac{\partial \hat{v}}{\partial \hat{x}} + \frac{U^2}{L} \hat{v} \frac{\partial \hat{v}}{\partial \hat{y}} + \frac{UW}{H} \hat{w} \frac{\partial \hat{v}}{\partial \hat{z}} = -\frac{\Phi}{L} \frac{\partial \hat{\varphi}'}{\partial \hat{y}} \quad (13.35b)$$

$$\frac{W}{T} \frac{\partial \hat{w}}{\partial \hat{t}} + \frac{UW}{L} \hat{u} \frac{\partial \hat{w}}{\partial \hat{x}} + \frac{UW}{L} \hat{v} \frac{\partial \hat{w}}{\partial \hat{y}} + \frac{WW}{H} \hat{w} \frac{\partial \hat{w}}{\partial \hat{z}} = -\frac{\Phi}{H} \frac{\partial \hat{\varphi}'}{\partial \hat{z}} + B \hat{b}' \quad (13.35c)$$

$$\frac{B}{T} \frac{\partial \hat{b}'}{\partial \hat{t}} + \frac{UB}{L} \hat{u} \frac{\partial \hat{b}'}{\partial \hat{x}} + \frac{UB}{L} \hat{v} \frac{\partial \hat{b}'}{\partial \hat{y}} + \frac{WB}{H} \hat{w} \frac{\partial \hat{b}'}{\partial \hat{z}} = -W \bar{N}^2 \hat{w} \hat{N}^2 \quad (13.35d)$$

$$\frac{U}{L} \frac{\partial \hat{u}}{\partial \hat{x}} + \frac{U}{L} \frac{\partial \hat{v}}{\partial \hat{y}} + \frac{W}{H} \frac{\partial \hat{w}}{\partial \hat{z}} = 0. \quad (13.35e)$$

13.2.3 Specifying the scales

We assume the following choices for scales based on the flow regimes of interest.

- **TIME SCALE:** Assume that the time scale is determined by the horizontal velocity scale and the horizontal length scale

$$T = L/U. \quad (13.36)$$

That is, we make use of a horizontal **advection time scale**.

- **VERTICAL VELOCITY:** It is common to assume the vertical velocity scales according to the continuity equation

$$\nabla_h \cdot \mathbf{u} + \partial_z w = 0 \implies W = U \frac{H}{L} \equiv U \alpha_{\text{aspect}}, \quad (13.37)$$

where the final equality introduced the vertical to horizontal **aspect ratio**, α_{aspect} . However, vertical density stratification acts to suppress vertical motion so that we introduce a non-dimensional number, ϵ

$$w = W \hat{w} = \epsilon \left[\frac{HU}{L} \right] \hat{w}. \quad (13.38)$$

In Section 13.2.5 we motivate choosing ϵ as the squared **Froude number**.

- **PRESSURE:** Scale the pressure according to the non-rotating balance of the material time change in horizontal velocity and the horizontal pressure gradient

$$\frac{U}{T} + \frac{UU}{L} = \frac{\Phi}{L} \implies \Phi = U^2. \quad (13.39)$$

We made use of this **dynamical pressure scaling** in Section 9.7.2 when non-dimensionalizing the Navier-Stokes equation in a non-rotating reference frame. For flows in a rotating reference frame that are in near geostrophic balance, we find that pressure instead scales with the Coriolis acceleration as per the geostrophic balance (e.g., Sections 17.3.2).

- **BUOYANCY:** We choose to scale buoyancy according to the hydrostatic balance

$$B = \frac{\Phi}{H} = \frac{U^2}{H}, \quad (13.40)$$

which is motivated by the importance of hydrostatic pressure in geophysical flows.

13.2.4 Non-dimensional Boussinesq equations of motion

With these choices, the equations of motion (13.35a)-(13.35e) take on the non-dimensional form

$$\frac{D\hat{\mathbf{u}}}{Dt} = -\hat{\nabla}\hat{\varphi}' \quad (13.41)$$

$$\epsilon \alpha_{\text{aspect}}^2 \frac{D\hat{w}}{Dt} = -\frac{\partial \hat{\varphi}'}{\partial \hat{z}} + \hat{b}' \quad (13.42)$$

$$\left[\frac{U^2}{N^2 H^2} \right] \frac{D\hat{b}'}{Dt} + \epsilon \hat{N}^2 \hat{w} = 0 \quad (13.43)$$

$$\hat{\nabla} \cdot \hat{\mathbf{u}} + \epsilon \frac{\partial \hat{w}}{\partial \hat{z}} = 0 \quad (13.44)$$

where we introduced the non-dimensional material time derivative

$$\frac{D}{Dt} = \frac{\partial}{\partial \hat{t}} + \hat{\mathbf{u}} \cdot \hat{\nabla}_z + \epsilon \hat{w} \frac{\partial}{\partial \hat{z}}. \quad (13.45)$$

13.2.5 The Froude number

At this point we make a choice for the parameter, ϵ , noting that there are many choices that one could consider. For our interests it is suitable to set ϵ equal to the squared [Froude number](#)

$$\epsilon = \text{Fr}^2 = \frac{U^2}{N^2 H^2}. \quad (13.46)$$

The Froude number measures the relative strength of vertical shears (i.e., vertical derivatives) of the horizontal velocity, U/H , versus the buoyancy stratification, N . Alternatively, it measures the ratio of the horizontal speed for a fluid particle, U , to an internal gravity wave speed, NH (we study internal gravity waves in [VOLUME 5](#)). Large Froude numbers indicate large fluid particle speeds relative to wave speeds, with $\text{Fr} > 1$ an indicator of hydraulic instability.⁷ In contrast, a relatively strong stratification (N^2 large) corresponds to a small Froude number and to flow that is stabilized by vertical stratification. Note that the squared Froude number is the inverse of the [Richardson number](#)

$$\text{Ri} = \text{Fr}^{-2} = \frac{N^2 H^2}{U^2}. \quad (13.47)$$

It is a matter of taste whether one works with Fr or Ri .

The choice (13.46) leads to the vertical velocity scale

$$W = \text{Fr}^2 \left[\frac{HU}{L} \right]. \quad (13.48)$$

For $\text{Fr} < 1$, which is the case for stably stratified fluids, this result means that stratification reduces the scale for the vertical velocity. The corresponding non-dimensional Boussinesq equations take the form

$$\frac{D\hat{\mathbf{u}}}{Dt} = -\hat{\nabla}_z \hat{\varphi}' \quad (13.49)$$

⁷In [VOLUME 5](#) we briefly discuss a hydraulic instability as part of the discussion of shallow water waves.

$$\text{Fr}^2 \alpha_{\text{aspect}}^2 \frac{\text{D}\widehat{w}}{\text{D}\widehat{t}} = -\frac{\partial \widehat{\varphi}'}{\partial \widehat{z}} + \widehat{b}' \quad (13.50)$$

$$\frac{\widehat{\text{D}}\widehat{b}'}{\widehat{\text{D}\widehat{t}}} + \widehat{N}^2 \widehat{w} = 0 \quad (13.51)$$

$$\widehat{\nabla} \cdot \widehat{\mathbf{u}} + \text{Fr}^2 \frac{\partial \widehat{w}}{\partial \widehat{z}} = 0. \quad (13.52)$$

The condition for hydrostatic balance in a stratified fluid thus takes the form

$$\text{Fr}^2 \alpha_{\text{aspect}}^2 \ll 1. \quad (13.53)$$

This result supports our initial suspicion that stratification suppresses vertical motion, thus reducing the vertical acceleration terms that break hydrostatic balance. That is, hydrostatic balance is more readily achieved for a stratified flow than for an unstratified flow. Note also that the horizontal divergence of the horizontal flow is reduced by the presence of stratification, which thus leads to a horizontal flow that is nearly non-divergent

$$\left| \widehat{\nabla} \cdot \widehat{\mathbf{u}} \right| = \left| \text{Fr}^2 \frac{\partial \widehat{w}}{\partial \widehat{z}} \right| \ll \left| \frac{\partial \widehat{w}}{\partial \widehat{z}} \right|. \quad (13.54)$$

Finally, this scaling reveals how the hydrostatic approximation becomes less accurate when $\text{Fr}^2 \alpha_{\text{aspect}}^2 \sim 1$, which occurs when stratification is weak and/or the aspect ratio order unity.

13.2.6 Horizontal hydrostatic pressure gradient

In Section 11.4.1 we studied the horizontal pressure gradient between two columns of constant density for a hydrostatic fluid. In that example, the two columns have equal mass, so the fluid is non-Boussinesq. Here, we consider the same example for a Boussinesq ocean, where volume is conserved rather than mass.

The expression for the hydrostatic pressure at a point within the fluid takes on the same form as that for a non-Boussinesq fluid (Section 11.2.1)

$$p_h(x, y, z, t) = p_a(x, y, t) + g \int_z^\eta \rho(x, y, z', t) dz', \quad (13.55)$$

and the horizontal pressure gradient is thus given by

$$\nabla_h p_h = \nabla_h p_a + g \rho(\eta) \nabla_h \eta + g \int_z^\eta \nabla_h \rho dz'. \quad (13.56)$$

For many studies with a Boussinesq ocean, we are interested in the horizontal pressure gradients in the presence of a rigid lid ocean surface whereby $\eta = 0$. In this case we compute the **internal pressure gradient** (also referred to as the **baroclinic pressure gradient**)

$$\nabla_h p_h = g \int_z^0 \nabla_h \rho dz' \quad \text{rigid lid ocean.} \quad (13.57)$$

Hence, the internal horizontal pressure gradient at a vertical position, z , equals to the horizontal density gradient vertically integrated above that point. For example, if density increases poleward, then so too does the internal hydrostatic pressure.

13.2.7 Evolution of hydrostatic pressure

In Section 11.2.2 we developed the Eulerian evolution equation for hydrostatic pressure in a non-Boussinesq fluid. Here we discuss the evolution in a Boussinesq ocean. To do so we take the Eulerian time tendency of the hydrostatic pressure (13.55), in which case

$$\partial_t p = \partial_t p_a + g \rho(\eta) \partial_t \eta + \int_z^\eta \partial_t \rho(x, y, z', t) dz'. \quad (13.58)$$

This equation holds for both the Boussinesq ocean and the non-Boussinesq ocean.

For the mass conserving non-Boussinesq ocean, we can use [mass continuity](#) to set $\partial_t \rho = -\nabla \cdot (\mathbf{v} \rho)$ in (13.58). Use of Leibniz's rule then reveals that the hydrostatic pressure evolves due to the convergence of mass onto the fluid column above that point (see Section 11.2.2 for the derivation). This result is expected since the hydrostatic pressure at a point is the weight per area of fluid above that point.

For a Boussinesq ocean, the volume conserving kinematics means that we cannot replace $\partial_t \rho$ in (13.58) with $-\nabla \cdot (\mathbf{v} \rho)$. Correspondingly, the weight of a fluid column can change merely through *in situ* density changes, so that the weight can change even if the matter content remains fixed, such as through heating.

For the Boussinesq case, note that energetic consistency from Section 13.8 means that the *in situ* density in a Boussinesq ocean has the functional dependence, $\rho(S, \Theta, \Phi)$, with Φ the geopotential. Hence, the Eulerian time derivative of density is given by

$$\partial_t \rho = (\partial \rho / \partial S) \partial_t S + (\partial \rho / \partial \Theta) \partial_t \Theta + (\partial \rho / \partial \Phi) \partial_t \Phi. \quad (13.59)$$

With a simple geopotential, $\Phi = g z$, we have $\partial_t \Phi = 0$ since the Eulerian time derivative is computed at fixed (x, y, z) . This result leads to the time changes in the hydrostatic pressure for a Boussinesq ocean

$$\partial_t p = \partial_t p_a + g \rho(\eta) \partial_t \eta + \int_z^\eta [(\partial \rho / \partial S) \partial_t S + (\partial \rho / \partial \Theta) \partial_t \Theta] dz'. \quad (13.60)$$

This equation reveals the direct dependence of the hydrostatic pressure on changes in S and Θ . Hence, heating and freshening, which alter the *in situ* density, directly alter the hydrostatic pressure in a Boussinesq ocean by altering the fluid's weight per area. This result contrasts to the mass conserving non-Boussinesq fluid, whose weight per area changes only through changes to its mass per area.

13.3 How pressure enforces non-divergent flow

Return now to the case of a non-hydrostatic fluid and consider the Boussinesq momentum equation (13.22a) written in the tangent plane form

$$\rho_0 (\partial_t + \mathbf{v} \cdot \nabla) \mathbf{v} + f \mathbf{z} \times \rho_0 \mathbf{v} = -\nabla p - \rho_0 g \hat{\mathbf{z}} + \rho_0 \mathbf{F}. \quad (13.61)$$

The non-divergence constraint on the velocity, $\nabla \cdot \mathbf{v} = 0$, must be maintained at each point in the fluid and at each time instance. How is that constraint maintained? As we show in this section, pressure provides the force that maintains non-divergence. Furthermore, pressure is determined through solving an elliptic boundary value problem. Elliptic partial differential equations transfer information instantaneously. Physically, this situation corresponds to the

transition from a compressible non-Boussinesq fluid, in which pressure signals propagate via acoustic waves (VOLUME 5), to the non-divergent flow of a Boussinesq ocean, in which pressure adjusts instantaneously just as if the acoustic waves traveled at infinite speed. The Boussinesq ocean sits between the compressible fluid and incompressible flow. That is, the Boussinesq prognostic velocity is non-divergent, and so it does not support acoustic waves, whereas the full velocity is divergent (Section 13.1.8), and this divergent portion supports acoustic waves, although such waves are never felt by the Boussinesq dynamical fields.

13.3.1 Poisson equation for pressure

To derive the pressure equation, we find it convenient to expose Cartesian tensor labels on the momentum equation (13.61)

$$\partial_t v^m + v^n \partial_n v^m + f \epsilon^{mnp} \delta_{3n} v_p = -\partial^m p/\rho_0 - \delta^{3m} g \rho/\rho_0 + F^m. \quad (13.62)$$

The time derivative is eliminated by taking the divergence through contracting with the operator ∂_m ,

$$\partial_m \partial_t v^m = \partial_t \partial_m v^m = 0, \quad (13.63)$$

thus leading to

$$-\nabla^2 p/\rho_0 = \partial_m (v^n \partial_n v^m + f \epsilon^{m3p} v_p + \delta^{3m} g \rho/\rho_0 - F^m), \quad (13.64)$$

where the Laplacian operator is

$$\nabla^2 = \partial_m \partial^m. \quad (13.65)$$

Equation (13.64) can be written as **Poisson's equation**

$$-\nabla^2 p = \rho_0 \nabla \cdot \mathbf{D}, \quad (13.66)$$

with the vector \mathbf{D} given by the accelerations sans that from pressure

$$D^m = v^n \partial_n v^m + f \epsilon^{m3p} v_p + \delta^{3m} g \rho/\rho_0 - F^m \quad (13.67a)$$

$$\mathbf{D} = (\mathbf{v} \cdot \nabla) \mathbf{v} + f \hat{\mathbf{z}} \times \mathbf{v} + g (\rho/\rho_0) \hat{\mathbf{z}} - \mathbf{F}. \quad (13.67b)$$

We choose to maintain the minus sign on the left hand side of equation (13.66) so that a positive divergence ($\nabla \cdot \mathbf{D} > 0$) represents a positive source for p . We can see this sign by considering a sinusoidal pressure perturbation, in which case

$$-\nabla^2 p \propto p, \quad (13.68)$$

so that a positive source, $-\nabla^2 p = \rho_0 \nabla \cdot \mathbf{D} > 0$, leads to a local positive pressure anomaly, and conversely for a negative source.

13.3.2 Boundary conditions

To derive the boundary conditions for the Poisson equation (13.66), we find it useful to write the velocity equation as

$$\partial_t \mathbf{v} = -\nabla p/\rho_0 - \mathbf{D}. \quad (13.69)$$

We consider a variety of boundaries in the following.

Static material surface

For a static material boundary we can make use of the no normal flow kinematic boundary condition, in which case

$$\hat{\mathbf{n}} \cdot \partial_t \mathbf{v} = \partial_t (\hat{\mathbf{n}} \cdot \mathbf{v}) = 0 \implies (\nabla p + \rho_0 \mathbf{D}) \cdot \hat{\mathbf{n}} = 0 \quad \text{for static material boundaries.} \quad (13.70)$$

This boundary condition takes the form

$$\hat{\mathbf{n}} \cdot \nabla p = -\rho_0 \mathbf{D} \cdot \hat{\mathbf{n}} \quad \text{for static material boundaries.} \quad (13.71)$$

Hence, maintenance of the no normal flow condition along a static material boundary requires a corresponding **Neumann boundary condition** for pressure.

Consider the case of $\hat{\mathbf{n}} = -\hat{\mathbf{z}}$ along a flat solid boundary at $z = \eta_b$. In this case

$$-\rho_0 \mathbf{D} \cdot \hat{\mathbf{n}} = g \rho - \hat{\mathbf{z}} \cdot \mathbf{F}, \quad (13.72)$$

so that along the boundary we have

$$-\rho_0 \mathbf{D} \cdot \hat{\mathbf{n}} = \rho_0 \hat{\mathbf{z}} \cdot [(\mathbf{v} \cdot \nabla) \mathbf{v} + g (\rho/\rho_0) \hat{\mathbf{z}} - \mathbf{F}] = g \rho - \hat{\mathbf{z}} \cdot \mathbf{F}, \quad (13.73)$$

where

$$\hat{\mathbf{z}} \cdot [(\mathbf{v} \cdot \nabla) \mathbf{v}] = (\mathbf{v} \cdot \nabla) w = 0, \quad (13.74)$$

since $w = 0$ on the flat solid boundary at $z = \eta_b$. We are thus led to the pressure boundary condition (13.71)

$$-\partial_z p = \rho g - \hat{\mathbf{z}} \cdot \mathbf{F} \quad \text{at } z = \eta_b. \quad (13.75)$$

Rigid lid ocean surface

For many purposes it is sufficient to assume the upper ocean surface is rigid and flat ($z = \eta = 0$), in which case we follow the approach taken for the flat bottom boundary condition (13.75) to find the boundary condition

$$\partial_z p = -\rho g + \rho_0 \hat{\mathbf{z}} \cdot \mathbf{F} \quad \text{at } z = 0. \quad (13.76)$$

Free upper ocean surface

The ocean free surface is generally dynamic and permeable, so that the velocity does not satisfy a no normal flow condition along this surface.⁸ To develop the pressure boundary condition at the free surface, we invoke a dynamical principle rather than a kinematic principle. Namely, we invoke continuity of pressure across an interface, which follows from Newton's third law (recall our discussion of stress along an interface in Section 9.8). Hence, the pressure condition at the ocean free surface is the **Dirichlet boundary condition**

$$p = p_a \quad \text{at } z = \eta(x, y, t), \quad (13.77)$$

where p_a is the pressure applied to the ocean surface from the overlying atmosphere or cryosphere.

⁸See the discussion of the kinematic boundary condition in VOLUME 1.

13.3.3 Characterizing the pressure sources

The right hand side of the Poisson equation (13.66)

$$-\nabla^2 p = \rho_o \nabla \cdot \mathbf{D}, \quad (13.78)$$

contains four sources. We here separately study the pressure resulting from these sources, borrowing from the treatment given in VOLUME 3 when studying the kinematically simpler horizontally non-divergent barotropic model. As we find, three of the pressure sources contribute to non-hydrostatic pressures and one to hydrostatic pressure. These pressure sources are *associated* with the pressure perturbations rather than *causing* the perturbations.

Divergence of self-advection

The first source is given by the divergence of self-advection, which can be written

$$-\rho_o^{-1} \nabla^2 p_{\text{self advect}} = \nabla \cdot \mathbf{D}_{\text{self advect}} \quad (13.79a)$$

$$= \partial_n(v^m \partial_m v^n) \quad (13.79b)$$

$$= (\partial_n v^m) (\partial_m v^n) + v^m (\partial_n \partial_m v^n) \quad (13.79c)$$

$$= (\partial_n v^m) (\partial_m v^n), \quad (13.79d)$$

where we set

$$v^m \partial_n \partial_m v^n = v^m \partial_m \partial_n v^n = 0 \quad (13.80)$$

since $\partial_n v^n = 0$ follows from the non-divergent nature of the flow. Furthermore, introducing the **velocity gradient tensor**

$$G^m{}_n = \partial_n v^m, \quad (13.81)$$

and its decomposition into the symmetric strain rate tensor, \mathbf{S} , and the anti-symmetric rotation tensor, \mathbf{R} , renders

$$\nabla \cdot \mathbf{D}_{\text{self advect}} = \mathbf{G} : \mathbf{G}^\top = (\mathbf{S} + \mathbf{R}) : (\mathbf{S} + \mathbf{R})^\top = (\mathbf{S} + \mathbf{R}) : (\mathbf{S} - \mathbf{R}) = \underbrace{\mathbf{S} : \mathbf{S}}_{\text{splat}} - \underbrace{\mathbf{R} : \mathbf{R}}_{\text{spin}}. \quad (13.82)$$

The vorticity or spin source provides a negative source to $-\nabla^2 p_{\text{self advect}}$. In contrast, the contribution from strain, sometimes referred to as **splat**, provides a positive source.⁹ As detailed for horizontally non-divergent barotropic flow in VOLUME 3, we understand why there is a negative pressure source from vortical (spinning) motion since, to retain a non-divergent flow, pressure must counteract the centrifugal acceleration arising from curved fluid motion. Likewise, a positive pressure source associated with straining motion is needed to counteract the convergent accelerations induced by strains.

Divergence of the Coriolis acceleration

The divergence of the Coriolis acceleration introduces a pressure source given by

$$-\rho_o^{-1} \nabla \cdot \nabla p_{\text{coriolis}} = \nabla \cdot \mathbf{D}_{\text{coriolis}} = \nabla \cdot (f \hat{z} \times \mathbf{v}) = \beta u - f \zeta, \quad (13.83)$$

⁹The whimsically named **splat** source is so-named since it is large when a fluid element is squashed in a manner increasing fluid strains, akin to how strains appear when a fluid impacts or “splats” against a solid obstacle. Imagine a water balloon thrown against a wall.

where $\zeta = \partial_x v - \partial_y u$ is the vertical component to the relative vorticity, and $\beta = \partial_y f$ is the planetary vorticity gradient. To help understand the $f\zeta$ term, consider two-dimensional flow with a cyclonic relative vorticity so that $f\zeta > 0$. Cyclonic flow feels an associated centrifugal acceleration directed “outward”. To maintain a non-divergent two-dimensional flow requires an oppositely directed “inward” pressure gradient force. Hence, such rotating flow induces a low pressure source as a means to counteract the centrifugal acceleration

$$-\nabla \cdot \nabla p_{\text{coriolis}} < 0. \quad (13.84)$$

Again, see VOLUME 3 for more discussion of this source as found in the horizontally non-divergent barotropic fluid.

Divergence of the gravitational force per volume

The divergence of the gravitational force per volume is given by

$$-\nabla \cdot \nabla p_{\text{gravity}} = \rho_0 \nabla \cdot \mathbf{D}_{\text{gravity}} = \nabla \cdot (g \rho \hat{\mathbf{z}}) = g \partial_z \rho. \quad (13.85)$$

The associated pressure gradient is that arising from the local hydrostatic component of the pressure field in which

$$\nabla \cdot (-\nabla p_{\text{gravity}} + g \rho \hat{\mathbf{z}}) = 0. \quad (13.86)$$

In regions where density decreases upward, $\partial_z \rho < 0$, a compressible fluid element that conserves its mass will expand when moving upward into less dense fluid. For a non-divergent flow that conserves the volume of fluid elements, there must be a counteracting force from pressure to halt the expansion of a fluid element. This counteracting force arises from the hydrostatic component to the pressure field that acts inward to squeeze the fluid element, with this pressure force originating from the negative pressure source, $-\nabla^2 p_{\text{gravity}} = g \partial_z \rho < 0$.

Divergence of the friction vector

The third source arises from the divergence of friction,

$$-\nabla \cdot \nabla p_{\text{friction}} = \rho_0 \nabla \cdot \mathbf{D}_{\text{friction}} = -\rho_0 \nabla \cdot \mathbf{F}. \quad (13.87)$$

With interior fluid friction arising from a nonzero strain rate (Section 9.6), we expect this pressure source to be most important in regions of large strains. Indeed, for a non-divergent flow feeling only molecular viscosity, the friction operator is given by (see Section 9.6.7)

$$\mathbf{F} = \nu \nabla^2 \mathbf{v}, \quad (13.88)$$

where $\nu > 0$ is a constant molecular viscosity. In this case $\nabla \cdot \mathbf{F} = 0$, so that viscous friction does not contribute a pressure source. More general cases are considered in applications where the molecular viscosity is replaced by a flow dependent eddy viscosity so that $\nabla \cdot \mathbf{F} \neq 0$. For the case of a converging frictional acceleration, $\nabla \cdot \mathbf{F} < 0$, friction then leads to a positive pressure source, and vice versa for $\nabla \cdot \mathbf{F} > 0$.

13.3.4 Comments and further study

The gravitational source contributes a local hydrostatic component to the pressure field, whereas the other three sources contribute non-hydrostatic pressure sources. In many applications,

such as general circulation modeling of the ocean and atmosphere, the fluid is assumed to be approximately hydrostatic (Chapter 11). In this case vertical motion is diagnosed rather than prognosed, and the non-hydrostatic component of pressure is never needed to evolve the fluid motion. Even so, vertical derivatives in the non-hydrostatic pressure provide the vertical force needed for vertical accelerations. We have more to say on vertical motion in Section 14.11.

Markowski and Richardson (2010) provide lucid discussions of pressure forces acting in geophysical fluids. In particular their Section 2.5 inspired much of the current section.

13.4 Helmholtz decomposing the velocity equation

In this section we introduce some mathematical properties of the velocity equation for a Boussinesq ocean in a simply connected ocean domain, \mathcal{R} , with boundary, $\partial\mathcal{R}$. For this purpose, we again write the velocity equation (13.61) in the form

$$\partial_t \mathbf{v} = -\nabla p/\rho_0 - \mathbf{D}, \quad (13.89)$$

where \mathbf{D} , as given by equation (13.67b), contains the various accelerations sans the pressure gradient

$$\mathbf{D} = (\mathbf{v} \cdot \nabla) \mathbf{v} + f \hat{\mathbf{z}} \times \mathbf{v} + g(\rho/\rho_0) \hat{\mathbf{z}} - \mathbf{F}. \quad (13.90)$$

13.4.1 Helmholtz decomposition

The Helmholtz decomposition from VOLUME 5 says that on a simply connected domain, an arbitrary vector, such as the acceleration \mathbf{D} , can be decomposed as

$$\mathbf{D} = \mathbf{D}^{\text{rot}} + \mathbf{D}^{\text{div}}, \quad (13.91)$$

where the two vectors on the right hand side satisfy

$$\nabla \cdot \mathbf{D}^{\text{rot}} = 0 \quad \text{and} \quad \nabla \times \mathbf{D}^{\text{rot}} \neq 0 \quad \mathbf{D}^{\text{rot}} \text{ is divergent-free} \quad (13.92a)$$

$$\nabla \times \mathbf{D}^{\text{div}} = 0 \quad \text{and} \quad \nabla \cdot \mathbf{D}^{\text{div}} \neq 0 \quad \mathbf{D}^{\text{div}} \text{ is curl-free.} \quad (13.92b)$$

We make use of the Helmholtz decomposition for a Boussinesq ocean by noting that the non-divergent velocity only has a rotational contribution

$$\mathbf{v} = \mathbf{v}^{\text{rot}}, \quad (13.93)$$

whereas the pressure gradient only has a divergent component

$$\nabla p = (\nabla p)^{\text{div}}. \quad (13.94)$$

In contrast, the acceleration, \mathbf{D} , generally has a rotational component and a divergent component, as written in equation (13.91). It also has a harmonic component that we can readily set to zero for a simply connected domain, but which is generally nonzero in non-simple domains such as an ocean with islands.

13.4.2 The pressure equation

Making use of the Helmholtz decomposition (13.91) brings the velocity equation (13.89) into the form

$$\partial_t \mathbf{v} = -\nabla p/\rho_0 - \mathbf{D}^{\text{rot}} - \mathbf{D}^{\text{div}}. \quad (13.95)$$

The accelerations, $\partial_t \mathbf{v}$, and \mathbf{D}^{rot} , are each divergent-free. In contrast, the accelerations, $-\nabla p/\rho_0$ and \mathbf{D}^{div} , each have nonzero divergence. Self-consistency is maintained if the sum, $\nabla p/\rho_0 + \mathbf{D}^{\text{div}}$, has zero divergence so that

$$\nabla \cdot (\nabla p/\rho_0 + \mathbf{D}^{\text{div}}) = 0 \implies -\nabla^2 p = \rho_0 \nabla \cdot \mathbf{D}^{\text{div}} = \rho_0 \nabla \cdot \mathbf{D}. \quad (13.96)$$

This is the Poisson equation for the pressure field already derived in Section 13.3.1. We go one further step by observing that $\nabla p/\rho_0 + \mathbf{D}^{\text{div}}$ is both curl-free and divergent-free, which we write as

$$\nabla p/\rho_0 + \mathbf{D}^{\text{div}} = \mathbf{H} \quad \text{with} \quad \nabla \cdot \mathbf{H} = \nabla \times \mathbf{H} = 0. \quad (13.97)$$

13.4.3 The vorticity equation

The accelerations, $\nabla p/\rho_0$ and \mathbf{D}^{div} , are each curl-free. In contrast, the accelerations, $\partial_t \mathbf{v}$ and \mathbf{D}^{rot} , each have nonzero curl. Self-consistency thus requires the sum, $\partial_t \mathbf{v} + \mathbf{D}^{\text{rot}}$, to be curl-free

$$\nabla \times (\partial_t \mathbf{v} + \mathbf{D}^{\text{rot}}) = 0 \implies \partial_t (\nabla \times \mathbf{v}) = -\nabla \times \mathbf{D}^{\text{rot}}, \quad (13.98)$$

which is the relative vorticity equation that we further study in VOLUME 3. Going one step further we note that the vector $\partial_t \mathbf{v} + \mathbf{D}^{\text{rot}}$ is both curl-free and divergent-free, which we write as

$$\partial_t \mathbf{v} + \mathbf{D}^{\text{rot}} = \mathbf{I} \quad \text{with} \quad \nabla \cdot \mathbf{I} = \nabla \times \mathbf{I} = 0. \quad (13.99)$$

13.4.4 The velocity equation

The above considerations have led us to the pressure gradient equation (13.97) and the velocity tendency equation (13.99)

$$\nabla p/\rho_0 + \mathbf{D}^{\text{div}} = \mathbf{H} \quad (13.100)$$

$$\partial_t \mathbf{v} + \mathbf{D}^{\text{rot}} = \mathbf{I}, \quad (13.101)$$

where both \mathbf{H} and \mathbf{I} are divergent-free and curl-free. Adding these two equations leads to

$$\partial_t \mathbf{v} = -\nabla p/\rho_0 - \mathbf{D}^{\text{rot}} - \mathbf{D}^{\text{div}} + \mathbf{H} + \mathbf{I}, \quad (13.102)$$

with this form of the velocity equation equivalent to the original Helmholtz decomposed equation (13.95) if we set

$$\mathbf{H} + \mathbf{I} = 0. \quad (13.103)$$

13.4.5 Comments

This section was inspired by [Marshall and Pillar \(2011\)](#), who applied a Helmholtz decomposition to study the variety of accelerations appearing in the Boussinesq velocity equation. A particularly revealing result of this decomposition, when setting $\mathbf{H} = \mathbf{I} = 0$, is the ability to make a 1-to-1

connection between terms in the Helmholtz decomposed velocity equation with terms in the relative vorticity equation. This correspondence can support dynamical understanding.

13.5 Tracer budgets in Eulerian regions

We are commonly interested in the tracer budget for a fluid region, and we examined a variety of regions when studying tracers in VOLUME 1 for a non-Boussinesq fluid. Here, we expose issues that arise for tracer budgets in a Boussinesq ocean. We specialize to the study of an Eulerian region, \mathcal{R} , and emphasize how the non-divergent flow constrains the advective tracer transport and affects changes to the volume integrated tracer content.

13.5.1 Formulating the budget equation

Consider a tracer concentration, C , and compute its net content over an Eulerian region, \mathcal{R}

$$\rho_0 \int_{\mathcal{R}} C \, dV = \rho_0 V \langle C \rangle, \quad (13.104)$$

where C satisfies the Boussinesq tracer equation

$$\partial_t(\rho_0 C) + \nabla \cdot (\rho_0 C \mathbf{v} + \mathbf{J}) = 0, \quad (13.105)$$

and

$$\langle C \rangle = \frac{\int_{\mathcal{R}} C \, dV}{\int_{\mathcal{R}} dV} = \frac{1}{V} \int_{\mathcal{R}} C \, dV \quad (13.106)$$

is the volume averaged tracer concentration within the Eulerian region with fixed volume, $V = \int_{\mathcal{R}} dV$. Following from the discussion of tracer budgets in VOLUME 1, we have

$$\rho_0 \frac{d(V \langle C \rangle)}{dt} = \rho_0 V \frac{d\langle C \rangle}{dt} \quad (13.107a)$$

$$= \rho_0 \frac{d}{dt} \int_{\mathcal{R}} C \, dV \quad (13.107b)$$

$$= \int_{\mathcal{R}} \frac{\partial(\rho_0 C)}{\partial t} \, dV \quad (13.107c)$$

$$= - \int_{\mathcal{R}} \nabla \cdot (\rho_0 C \mathbf{v} + \mathbf{J}) \, dV \quad (13.107d)$$

$$= - \oint_{\partial\mathcal{R}} (\rho_0 C \mathbf{v} + \mathbf{J}) \cdot \hat{\mathbf{n}} \, d\mathcal{S}, \quad (13.107e)$$

where we used the divergence theorem on the final equality, with $\partial\mathcal{R}$ the boundary of \mathcal{R} and with outward normal direction, $\hat{\mathbf{n}}$. Changes in the total tracer contained within the region arise from the convergence of boundary fluxes due to the non-advectional flux, \mathbf{J} , plus convergence of the advective tracer flux, $\rho_0 C \mathbf{v}$. Since the region volume is constant in time, changes in the total tracer content directly affect the volume averaged tracer concentration, $\langle C \rangle$.

At any point along the boundary, the tracer content is modified if there is a non-advectional flux, \mathbf{J} , directed across the boundary. There is no *a priori* constraint on \mathbf{J} , with local properties determining its sign and magnitude. In contrast, contributions from the boundary advective flux are constrained due to the non-divergent nature of the Boussinesq velocity, which we discuss next.

13.5.2 Interpreting advective tracer contributions

As seen by equation (13.107e), any advective flux, $\rho \mathbf{v} C$, that is directed into the region adds tracer to the region, whereas a flux directed outward reduces the region's tracer content. However, because the velocity is non-divergent, the tracer contained within the region is unaffected if we modify the advective tracer flux along the boundary by adding a number that is constant over the region \mathcal{R} . We see this property for any closed Eulerian region by writing

$$0 = \int_{\mathcal{R}} \nabla \cdot \mathbf{v} dV = \oint_{\partial\mathcal{R}} \mathbf{v} \cdot \hat{\mathbf{n}} d\mathcal{S}. \quad (13.108)$$

Hence, the velocity is, at each time instance, constrained so that the non-divergent flow cannot lead to the accumulation of fluid within any closed and static region. Correspondingly, the amount of fluid entering \mathcal{R} exactly and instantaneously balances the amount of fluid leaving \mathcal{R} . We can thus add any spatial constant, k , to the advective flux without affecting the net change in tracer content

$$\oint_{\partial\mathcal{R}} (C + k) \mathbf{v} \cdot \hat{\mathbf{n}} d\mathcal{S} = \oint_{\partial\mathcal{R}} C \mathbf{v} \cdot \hat{\mathbf{n}} d\mathcal{S} + k \oint_{\partial\mathcal{R}} \mathbf{v} \cdot \hat{\mathbf{n}} d\mathcal{S} = \oint_{\partial\mathcal{R}} C \mathbf{v} \cdot \hat{\mathbf{n}} d\mathcal{S}. \quad (13.109)$$

Boundary advection occurring with $C = k$ has no affect on the net tracer within a region.

To help interpret the role of advective fluxes on integrated tracer content, we find it useful to set the arbitrary spatial constant to $k = -\langle C \rangle$. In this manner, the advective contribution to the tracer budget takes the form

$$V \left[\frac{d\langle C \rangle}{dt} \right]_{\text{advective}} = - \oint_{\partial\mathcal{R}} C \mathbf{v} \cdot \hat{\mathbf{n}} d\mathcal{S} = - \oint_{\partial\mathcal{R}} (C - \langle C \rangle) \mathbf{v} \cdot \hat{\mathbf{n}} d\mathcal{S}. \quad (13.110)$$

Hence, advective transport through the region boundary changes the region integrated C , and thus the volume mean $\langle C \rangle$, only if the boundary transport occurs with C values that differ from the region average, $\langle C \rangle$.

13.5.3 A rectangular region example

Consider the rectangular region of Figure 13.1 that is closed along its bottom, northern, eastern, and western boundaries, yet that is open along its top boundary and southern boundary. Specify flow along the southern boundary to be northward and let it bring fluid into the region with $C_{\text{south}} > \langle C \rangle$, thus acting to increase $\langle C \rangle$. Due to the non-divergent nature of the velocity, the northward transport of fluid through the southern boundary is exactly balanced by a vertically upward transport of fluid out of the top boundary. What does that vertical transport of fluid imply about changes to $\langle C \rangle$? The answer depends on the tracer concentration on the top boundary.

- If $C_{\text{top}} > \langle C \rangle$, then the relatively high values of tracer that leave through the top boundary act to decrease the net C within the region, thus counteracting the contribution of $C_{\text{south}} > \langle C \rangle$ that enters through the southern boundary. For the special case of equal C transports through the two boundaries, then there is no accumulation of C within the region so that $\langle C \rangle$ remains unchanged.
- If $C_{\text{top}} = \langle C \rangle$, then $\langle C \rangle$ increases due to the transport of C through the southern boundary, with no net transport across the top boundary.

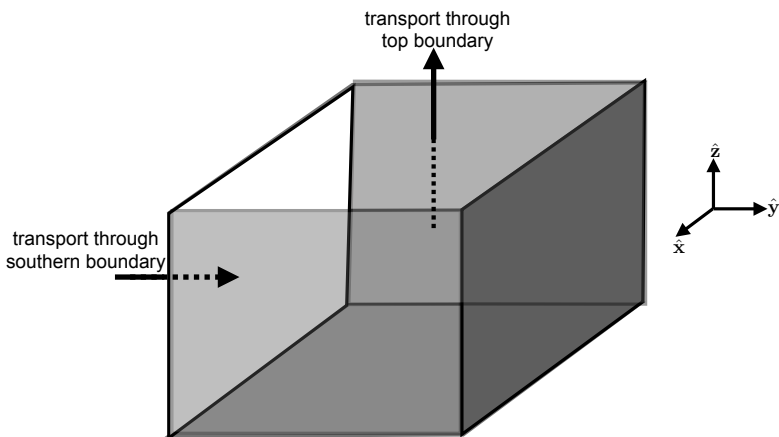


FIGURE 13.1: A rectangular ocean region for considering the tracer budget in a Boussinesq ocean. We assume the only open boundaries of the region are along the southern boundary and top boundary, with the remaining boundaries closed. Note that the top boundary can generally be within the ocean interior, and so does not need to be the top of the ocean. The non-divergent nature of the flow means that any fluid entering through the southern boundary must leave through the top boundary, and conversely. This constraint on the flow impacts on how the advective tracer transport affects changes to the volume integrated tracer within the region.

- If $C_{\text{top}} < \langle C \rangle$, then the vertical transport of $C_{\text{top}} < \langle C \rangle$ increases $\langle C \rangle$ acting just like the $C_{\text{south}} > \langle C \rangle$ fluid that enters through the southern boundary. That is, we can increase $\langle C \rangle$ in the region by bringing fluid into the domain with C greater than $\langle C \rangle$, or by exporting fluid with C less than $\langle C \rangle$.

13.5.4 Comments

Constraints introduced by the non-divergent nature of the Boussinesq ocean render subtleties to the physical interpretation of how tracer fluxes affect the budget of tracer within a region. These constraints are absent from the non-Boussinesq fluid, whose flow is generally divergent. The discussion in this section was motivated by Appendix B of [Gregory \(2000\)](#), who studied heat (enthalpy) budgets within a numerical Boussinesq ocean circulation model.

13.6 Mechanical energy analysis: part I

The volume of a fluid element in a non-divergent flow remains materially invariant even as pressure acts on the element. Hence, pressure cannot perform mechanical work on the fluid. Consequently, a non-divergent flow supports no pressure work conversion between internal energy and kinetic energy, which contrasts to the case in a non-Boussinesq fluid (see Section 10.3). In this section we formulate a mechanical energy budget for the Boussinesq ocean, and find that this budget is closed for a perfect fluid so long as the geopotential is time-independent and there are no boundary effects. Many of the steps are directly analogous to those in a non-Boussinesq fluid detailed in Chapter 10, though with some important distinctions that are emphasized in this section as well as Section 13.8.

13.6.1 Governing equations

We develop the mechanical energy budget for an unforced non-hydrostatic Boussinesq ocean with density a function only of salinity and Conservative Temperature,

$$\rho = \rho(S, \Theta). \quad (13.111)$$

The more general pressure-dependent equation of state is considered in Section 13.8. Furthermore, we work with the velocity, density, and continuity equations in the form

$$\rho_0 \left[\frac{D\mathbf{v}}{Dt} + 2\boldsymbol{\Omega} \times \mathbf{v} \right] = -\nabla p - \rho \nabla \Phi \quad (13.112a)$$

$$\frac{D\rho}{Dt} = \frac{\partial \rho}{\partial S} \frac{DS}{Dt} + \frac{\partial \rho}{\partial \Theta} \frac{D\Theta}{Dt} = \dot{\rho} \quad (13.112b)$$

$$\nabla \cdot \mathbf{v} = 0. \quad (13.112c)$$

Note that the geopotential, Φ , is generally a function of space and time, $\Phi = \Phi(\mathbf{x}, t)$, with this dependence appropriate when studying astronomical tides or mass inhomogeneities creating spatial variations in the gravity field.

13.6.2 Kinetic energy

To obtain a kinetic energy equation, start by taking the dot product of the velocity, \mathbf{v} , and the momentum equation (13.112a) and note that the Coriolis acceleration drops out since it is orthogonal to the velocity

$$\mathbf{v} \cdot (2\boldsymbol{\Omega} \times \mathbf{v}) = 0. \quad (13.113)$$

The material time derivative takes the form

$$v^n \delta_{mn} [\partial_t v^m + (\mathbf{v} \cdot \nabla) v^m] = (\partial_t + \mathbf{v} \cdot \nabla) \mathcal{K} = \frac{D\mathcal{K}}{Dt}, \quad (13.114)$$

where we introduced the kinetic energy per mass

$$\mathcal{K} = \delta_{mn} v^m v^n / 2 = \mathbf{v} \cdot \mathbf{v} / 2. \quad (13.115)$$

The equation for the Boussinesq kinetic energy per volume thus takes the form

$$\rho_0 \frac{D\mathcal{K}}{Dt} = -\mathbf{v} \cdot \nabla p - \rho \mathbf{v} \cdot \nabla \Phi. \quad (13.116)$$

Alternatively, we can write this equation in the flux-form

$$\partial_t (\rho_0 \mathcal{K}) + \nabla \cdot [\mathbf{v} (\rho_0 \mathcal{K} + p)] = -\rho \mathbf{v} \cdot \nabla \Phi, \quad (13.117)$$

where we used $\nabla \cdot \mathbf{v} = 0$ to write $\mathbf{v} \cdot \nabla p = \nabla \cdot (\mathbf{v} p)$. Note that in Exercise 13.6 we show that the kinetic energy evolution derived here for the non-hydrostatic fluid holds also for the hydrostatic fluid, yet with the kinetic energy in the hydrostatic fluid determined solely by the horizontal velocity.

The term, $-\rho \mathbf{v} \cdot \nabla \Phi$, in the kinetic energy equation (13.117) is a source/sink that arises from fluid motion crossing surfaces of constant geopotential. Moving a fluid element down the geopotential gradient ($\mathbf{v} \cdot \nabla \Phi < 0$) increases the kinetic energy, and conversely when the

fluid moves up the geopotential gradient. We sometimes refer to this process as **buoyancy work**, particularly when considered in the context of a vertically stratified fluid. We can further exemplify this term by taking the simplified form of the geopotential, $\Phi = g z$, in which $\mathbf{v} \cdot \nabla \Phi = g w$.

13.6.3 Potential energy and mechanical energy

We here develop the potential energy budget and then add to the kinetic energy to derive the mechanical energy budget.

Gravitational potential energy

A fluid element has a gravitational potential energy per mass given by the geopotential, Φ , which has a material time derivative

$$\frac{D\Phi}{Dt} = \partial_t \Phi + \mathbf{v} \cdot \nabla \Phi. \quad (13.118)$$

The time-dependent geopotential provides an external source of potential energy to the system. Additionally, motion moving up the gradient of the geopotential ($\mathbf{v} \cdot \nabla \Phi > 0$) increases the potential energy per mass, and conversely for motion down the geopotential gradient.

Mechanical energy budget

Adding the gravitational potential energy equation (13.118) to the kinetic energy equation (13.116) renders the material evolution

$$\rho \frac{D\mathcal{K}}{Dt} + \rho \frac{D\Phi}{Dt} = -\nabla \cdot (\mathbf{v} p) + \rho \partial_t \Phi. \quad (13.119)$$

Note how the buoyancy work source, $\rho \mathbf{v} \cdot \nabla \Phi$, dropped out from this budget. Consequently, this term provides a reversible transfer of mechanical energy between gravitational potential energy per volume and the kinetic energy per volume. We saw the same transfer in Section 10.3 when studying the mechanical energy budget for a non-Boussinesq fluid.

Equation (13.119) has nearly the same form as that for the non-Boussinesq fluid given by equation (10.52). However, for the Boussinesq ocean it does not lead to a flux-form conservation law for mechanical energy, even for the perfect fluid. Operationally, the derivations diverge at this point since for the non-Boussinesq fluid we make use of the **mass continuity** equation, $\partial_t \rho + \nabla \cdot (\mathbf{v} \rho) = 0$, to write the material evolution of density. In contrast, material density evolution in the Boussinesq ocean is determined by material changes in temperature, salinity, and pressure.

To develop a closed Boussinesq mechanical energy budget, add $\Phi D\rho/Dt = \Phi \dot{\rho}$ to both sides of equation (13.119) to render the material evolution for the mechanical energy per volume

$$\frac{D}{Dt} [\rho \mathcal{K} + \rho \Phi] = -\nabla \cdot (\mathbf{v} p) + \rho \partial_t \Phi + \dot{\rho} \Phi, \quad (13.120)$$

which has the flux-form expression

$$\partial_t (\rho_0 \mathcal{M}) + \nabla \cdot [\mathbf{v} (\rho_0 \mathcal{M} + p)] = \rho \partial_t \Phi + \dot{\rho} \Phi, \quad (13.121)$$

where we defined the Boussinesq mechanical energy per volume as

$$\rho_0 \mathcal{M} = \rho_0 \mathcal{K} + \rho \Phi. \quad (13.122)$$

Note the ρ_0 determining the kinetic energy per volume, whereas ρ determines the gravitational potential energy. These distinct density factors result from the distinction made in the Boussinesq ocean between inertial mass and gravitational mass. We discussed this point in the opening to this chapter, emphasizing how the Boussinesq ocean does not respect the principle of equivalence.

13.6.4 Finite volume mechanical energy budget

Recall that a scalar tracer concentration, C , satisfies a flux-form equation of the form (13.105)

$$\partial_t(\rho_0 C) + \nabla \cdot (\rho_0 C \mathbf{v} + \mathbf{J}) = 0, \quad (13.123)$$

where \mathbf{J} is a subgrid tracer flux. Comparing to the mechanical energy equation (13.121), we see that mechanical energy has a non-zero source on the right hand side that cannot be written as the divergence of a flux. Additionally, the tracer vector, \mathbf{J} , corresponds in the energy equation to the pressure flux, $p \mathbf{v}$. With these correspondences between the tracer equation and mechanical energy equation, we can make direct use of the Leibniz-Reynolds transport theorem from VOLUME 1 to render the finite volume mechanical energy budget

$$\frac{d}{dt} \left[\int_{\mathcal{R}} \rho_0 \mathcal{M} dV \right] = - \oint_{\partial\mathcal{R}} \rho_0 \mathcal{M} (\mathbf{v} - \mathbf{v}^{(b)}) \cdot \hat{\mathbf{n}} dS - \oint_{\partial\mathcal{R}} p \mathbf{v} \cdot \hat{\mathbf{n}} dS + \int_{\mathcal{R}} [\rho \partial_t \Phi + \dot{\rho} \Phi] dV, \quad (13.124)$$

where \mathcal{R} is the finite volume region, $\partial\mathcal{R}$ is its boundary, $\mathbf{v}^{(b)}$ is the velocity of a point on the boundary, and $\hat{\mathbf{n}}$ is the outward normal on the boundary. The first term on the right hand side arises from the advective transport of mechanical energy across the moving region boundary, taking into account the difference between the fluid velocity and boundary velocity. The second term arises from the work done by pressure on the boundary, and the final term arises from time dependence to the geopotential plus material changes in density. It is notable that the flow is non-divergent at each point, so that pressure cannot do work in the interior of the region. Even so, pressure can do work on the boundary of the region where $\mathbf{v} \cdot \hat{\mathbf{n}} \neq 0$. Observe that the budget (13.124) for a Boussinesq ocean corresponds to the budget (10.53) for a non-Boussinesq fluid.

A material region is characterized by $(\mathbf{v} - \mathbf{v}^{(b)}) \cdot \hat{\mathbf{n}} = 0$ on the boundaries, in which case there is no transport of mechanical energy across the boundary. We are thus left with the mechanical energy budget (13.124)

$$\frac{d}{dt} \left[\int_{\mathcal{R}} \rho_0 \mathcal{M} dV \right] = - \oint_{\partial\mathcal{R}} p \mathbf{v} \cdot \hat{\mathbf{n}} dS + \int_{\mathcal{R}} (\rho \partial_t \Phi + \dot{\rho} \Phi) dV. \quad (13.125)$$

Recall we are assuming $\rho = \rho(S, \Theta)$ in this section, so that

$$\dot{\rho} = (\partial\rho/\partial S) \dot{S} + (\partial\rho/\partial\Theta) \dot{\Theta}. \quad (13.126)$$

Hence, for a time-independent geopotential ($\partial_t \Phi = 0$) and in the absence of processes that contribute to a material evolution of S and Θ (i.e., $\dot{S} = 0$ and $\dot{\Theta} = 0$), then the finite volume Boussinesq mechanical energy for a material fluid region is affected only by pressure work on

the boundaries.¹⁰

13.7 Boussinesq energetics with dissipation

The ocean is a forced-dissipative system, with mechanical and buoyant forcing predominantly at the surface and bottom boundaries and mechanical dissipation via molecular viscosity. In this section we extend the discussion from Section 13.6 to here develop the mechanical energy budget in a Boussinesq ocean affected by forcing and dissipation. Much of this discussion represents a specialization of the more general presentation of energetics in Chapter 10, here focusing on the ocean interior and considering the addition of buoyancy sources.

In particular, we examine energetics for the Boussinesq ocean equations written in their form with Archimedean buoyancy

$$\mathrm{D}\boldsymbol{v}/\mathrm{D}t + 2\boldsymbol{\Omega} \times \boldsymbol{v} = -\nabla\varphi + \hat{\boldsymbol{z}}b + \nabla \cdot \mathbb{T}/\rho_0 \quad (13.127a)$$

$$Db/\mathrm{D}t = -\nabla \cdot \mathbf{F}^b + Q^b \quad (13.127b)$$

$$\nabla \cdot \boldsymbol{v} = 0. \quad (13.127c)$$

The term $\nabla \cdot \mathbb{T}/\rho_0$ is the divergence of a friction stress tensor, $-\nabla \cdot \mathbf{F}^b$ is the convergence of a buoyancy flux vector, and Q^b is a buoyancy source either at the boundaries or the interior. The new element in this discussion, relative to Chapter 10, concerns the role of the buoyancy flux. One operational point to note is that for all subgrid scale and boundary conditions in a Boussinesq ocean, appearances of the *in situ* density present in a non-Boussinesq fluids are here converted to the Boussinesq reference density, ρ_0 .

13.7.1 Forms for the buoyancy flux

Buoyancy flux for large-scale flows

For large-scale flows a particularly common form for the buoyancy flux is taken as

$$\mathbf{F}^b = -\kappa \partial_z b \hat{\boldsymbol{z}} + \boldsymbol{v}^* b. \quad (13.128)$$

The first term is a downgradient vertical diffusive flux with the vertical eddy diffusivity, $\kappa > 0$, a function of the flow state so that

$$\kappa = \kappa(\boldsymbol{x}, t). \quad (13.129)$$

The second term is an advective flux, where the advective velocity, $\boldsymbol{v}^* = (\boldsymbol{u}^*, w^*)$, is assumed to be non-divergent

$$\nabla \cdot \boldsymbol{v}^* = \nabla_h \cdot \boldsymbol{u}^* + \partial_z w^* = 0. \quad (13.130)$$

The velocity, \boldsymbol{v}^* , is commonly termed the eddy-induced velocity, with particular choices for its parameterization examined in VOLUME 4 as part of our study of parameterizations for subgrid scale tracer transport.

¹⁰Note that \dot{S} and $\dot{\Theta}$ are nonzero in the presence of boundary processes (e.g., heat fluxes, fresh water fluxes) and in the presence of mixing (e.g., as parameterized by diffusion).

Boundary conditions

The normal component of the buoyancy flux vanishes at boundaries

$$\hat{\mathbf{n}} \cdot \mathbf{F}^b = 0, \quad (13.131)$$

so that boundary buoyancy fluxes are assumed to sit within the source term, Q^b , via

$$Q^b = Q^{\text{surf}} \quad \text{at } z = \eta(x, y, t) \quad (13.132\text{a})$$

$$Q^b = Q^{\text{bot}} \quad \text{at } z = \eta_b(x, y) \quad (13.132\text{b})$$

$$\mathbf{v}^* \cdot \hat{\mathbf{n}} = 0 \quad \text{all boundaries,} \quad (13.132\text{c})$$

where Q^{surf} is the surface buoyancy flux, Q^{bot} is the bottom buoyancy flux (e.g., geothermal heating), and $\hat{\mathbf{n}}$ is the outward normal at the boundaries. Both Q^{surf} and Q^{bot} are positive when directed upward. In our discussion of ocean buoyancy in VOLUME 5, we detail the plethora of processes leading to boundary fluxes of buoyancy.

Molecular buoyancy flux assumed in this section

In the remainder of this section, we are most interested in the energetic role of molecular diffusion of buoyancy rather than turbulent mixing. In this case the buoyancy flux takes on the downgradient diffusive form

$$\mathbf{F}^b = -\kappa \nabla b, \quad (13.133)$$

with $\kappa > 0$ a constant kinematic diffusivity.

13.7.2 Mechanical forcing and dissipation

Following our discussion of frictional stresses in Section 9.6, we here write the frictional acceleration, \mathbf{F} , in the Boussinesq ocean as the divergence of the frictional stress tensor, \mathbb{T} ,

$$\rho_o \mathbf{F} = \nabla \cdot \mathbb{T}. \quad (13.134)$$

Friction in large scale flows

For many large scale flows, the dominant contribution to frictional stresses arises from the vertical divergence of horizontal subgrid stresses, in which case the horizontal frictional acceleration vector takes the form

$$\rho_o \mathbf{F}^h = \partial_z \boldsymbol{\tau} = \rho_o \frac{\partial}{\partial z} \left[\nu_{\text{eddy}} \frac{\partial \mathbf{u}}{\partial z} \right], \quad (13.135)$$

where

$$\boldsymbol{\tau} = \rho_o \nu_{\text{eddy}} \partial_z \mathbf{u} \quad (13.136)$$

is the horizontal turbulent stress vector whose vertical derivative contributes to the vertical transfer of horizontal momentum. Whereas the molecular viscosity, ν , is a function of the fluid composition (Section 9.6), the eddy viscosity, ν_{eddy} , is a function of the flow so that

$$\nu_{\text{eddy}} = \nu_{\text{eddy}}(\mathbf{x}, t) \geq 0. \quad (13.137)$$

The eddy viscosity is typically many orders of magnitude larger than the molecular viscosity in regions of strong turbulent mixing.

Boundary stresses

Boundary stresses are written as

$$\hat{\mathbf{n}} \cdot \mathbb{T} = \boldsymbol{\tau}^{\text{surf}} \quad \text{at } z = \eta(x, y, t) \quad (13.138\text{a})$$

$$(-\hat{\mathbf{n}}) \cdot \mathbb{T} = \boldsymbol{\tau}^{\text{bott}} \quad \text{at } z = \eta_b(x, y). \quad (13.138\text{b})$$

The surface boundary stress vector, $\boldsymbol{\tau}^{\text{surf}}$, arises from the transfer of momentum between the ocean and atmosphere (or the ocean and ice). In numerical modeling practice, this stress is computed by a boundary layer parameterization that ingests the momentum from the atmosphere or ice and computes a stress that is transferred to the ocean through these boundary conditions. As per Newton's third law (the action/reaction law; see Section 9.8), the stress imparted to the ocean is equal and opposite the stress imparted to the atmosphere at its lower boundary.

The bottom stress vector, $\boldsymbol{\tau}^{\text{bott}}$, is often parameterized via a quadratic bottom drag

$$\boldsymbol{\tau}^{\text{bott}} = -C_d \rho \mathbf{v} |\mathbf{v}|, \quad (13.139)$$

where $C_d > 0$ is a dimensionless **drag coefficient** that is sometimes assumed to be a function of the bottom topographic roughness. This bottom stress acts to drag the ocean bottom velocity towards a state of rest. It is equal and opposite to the frictional stress transferred to the solid earth from the ocean. Note that this bottom drag acts similarly to the linear Rayleigh drag in equation (9.55). However, the bottom drag in equation (13.139) is nonlinear, whereas the Rayleigh drag is linear

$$\mathbf{F}_{\text{Rayleigh}} = -\gamma \mathbf{v}. \quad (13.140)$$

Molecular Laplacian friction assumed in this section

In the following, we are most interested in the energetic role of molecular viscosity rather than turbulent viscosity. In this case the frictional acceleration takes on the form

$$\mathbf{F} = \nu \nabla^2 \mathbf{v}. \quad (13.141)$$

Additionally, we ignore all boundary contributions in order to focus on contributions from molecular viscosity.

13.7.3 Governing equations with molecular friction and diffusion

Assuming frictional acceleration given by molecular viscosity (13.141), and a buoyancy flux given by downgradient molecular diffusion (13.133), leads to the simplified form of the governing equations (13.127a)-(13.127c)

$$D\mathbf{v}/Dt + 2\boldsymbol{\Omega} \times \mathbf{v} = -\nabla\varphi + \hat{z} b + \nu \nabla^2 \mathbf{v} \quad (13.142\text{a})$$

$$Db/Dt = \kappa \nabla^2 b + Q^b \quad (13.142\text{b})$$

$$\nabla \cdot \mathbf{v} = 0. \quad (13.142\text{c})$$

These are the equations whose energetics are now examined.

13.7.4 Kinetic energy evolution

We obtain a kinetic energy evolution equation just like in Section 13.6.2, with a scalar product of the velocity equation with \mathbf{v} leading to

$$D\mathcal{K}/Dt = -\nabla \cdot (\mathbf{v} \varphi) + w b + \nu \mathbf{v} \cdot \nabla^2 \mathbf{v}, \quad (13.143)$$

where we used $\nabla \cdot \mathbf{v} = 0$ to write $\mathbf{v} \cdot \nabla \varphi = \nabla \cdot (\mathbf{v} \varphi)$. Equation (13.143) says that the kinetic energy per mass of a Boussinesq fluid element is modified due to the advection of pressure, vertical motion in a buoyancy stratified fluid, and the projection of the velocity onto the frictional acceleration.

13.7.5 Frictional dissipation

Use of Cartesian coordinates allows us to write the Laplacian acting on a vector as (see Section 9.6.9)

$$\nabla^2 \mathbf{v} = -\nabla \times \boldsymbol{\omega}, \quad (13.144)$$

which then brings the Laplacian friction to the form

$$-\mathbf{v} \cdot \nabla^2 \mathbf{v} = \mathbf{v} \cdot \nabla \times \boldsymbol{\omega} \quad (13.145a)$$

$$= v_m \epsilon^{mnp} \partial_n \omega_p \quad (13.145b)$$

$$= \partial_n (\epsilon^{mnp} v_m \omega_p) - \epsilon^{mnp} \omega_p \partial_n v_m \quad (13.145c)$$

$$= -\partial_n (\epsilon^{nmp} v_m \omega_p) + \epsilon^{nmp} (\partial_n v_m) \omega_p \quad (13.145d)$$

$$= -\partial_n (\mathbf{v} \times \boldsymbol{\omega})^n + \omega^p \omega_p \quad (13.145e)$$

$$= -\nabla \cdot (\mathbf{v} \times \boldsymbol{\omega}) + \boldsymbol{\omega} \cdot \boldsymbol{\omega}. \quad (13.145f)$$

The kinetic energy equation (13.143) can thus be written

$$D\mathcal{K}/Dt = -\nabla \cdot (\mathbf{v} \varphi) + w b - \nu \mathbf{v} \cdot (\nabla \times \boldsymbol{\omega}) \quad (13.146a)$$

$$= -\nabla \cdot [\mathbf{v} \varphi + \nu (\mathbf{v} \times \boldsymbol{\omega})] + w b - \nu \boldsymbol{\omega} \cdot \boldsymbol{\omega}. \quad (13.146b)$$

The physical dimensions for all terms in these equations are $L^2 T^{-3}$: squared length per cubed time, which is the dimensions of energy per mass per time.

13.7.6 Domain integrated kinetic energy

Consider a region of fluid with no boundary contributions. Performing a volume average over that region leads to

$$\frac{d}{dt} \langle \mathcal{K} \rangle = \langle w b \rangle - \epsilon, \quad (13.147)$$

where the angle-brackets denote volume averaging

$$\langle \psi \rangle = \frac{\int \psi dV}{\int dV}. \quad (13.148)$$

To reach equation (13.147), we dropped all boundary terms, including the term $\hat{\mathbf{n}} \cdot (\mathbf{v} \times \boldsymbol{\omega})$, and introduced

$$\epsilon = \frac{\nu \int \boldsymbol{\omega} \cdot \boldsymbol{\omega} dV}{\int dV} = \nu \langle \boldsymbol{\omega} \cdot \boldsymbol{\omega} \rangle \geq 0, \quad (13.149)$$

which is the volume averaged kinetic energy dissipation rate arising from viscous effects (dimensions of $L^2 T^{-3}$). We thus see that there is more kinetic energy dissipation for a Boussinesq flow with larger domain averaged $\omega \cdot \omega$.

Equation (13.147) says that the domain averaged kinetic energy per mass is reduced by viscous dissipation acting within the fluid domain. Furthermore, the averaged kinetic energy is increased in regions where buoyancy and vertical motion are positively correlated, $\langle w b \rangle > 0$, in which case light water preferentially moves vertically up and heavy water down. Conversely, the averaged kinetic energy is decreased when buoyancy and vertical motion are negatively correlated (light water preferentially moves down and heavy water up).

13.7.7 Potential energy evolution

Assuming the simple form of the geopotential, $\Phi = g z$, leads to

$$D\Phi/Dt = g w = \mathbf{v} \cdot \nabla \Phi = \nabla \cdot (\mathbf{v} \Phi), \quad (13.150)$$

where the second equality follows from the definition of the material derivative, and since $\partial\Phi/\partial t = 0$. Multiplying the buoyancy equation (13.127b) by Φ , and the Φ equation (13.150) by b , then adding, leads to

$$D(\Phi b)/Dt = g b w + \Phi(Q^b + \kappa \nabla^2 b) \quad (13.151a)$$

$$= g b w + \Phi Q^b + \nabla \cdot (\kappa \Phi \nabla b) - \kappa \nabla \Phi \cdot \nabla b \quad (13.151b)$$

$$= g b w + \Phi Q^b + \nabla \cdot (\Phi \kappa \nabla b) - g \kappa \partial_z b, \quad (13.151c)$$

so that

$$DP^b/Dt = -b w - g^{-1} \Phi Q^b - \nabla \cdot (g^{-1} \Phi \kappa \nabla b) + \kappa \partial_z b. \quad (13.152)$$

The product

$$P^b = -g^{-1} \Phi b = z g \delta\rho/\rho \quad (13.153)$$

is the gravitational potential energy per mass associated with the deviation of density from the Boussinesq reference density, ρ_0 . Equation (13.152) says that the gravitational potential energy per mass of a fluid element changes depending on the vertical motion of buoyancy (the $-b w$ term); from diabatic sources (the ΦQ^b term); from a total divergence associated with buoyancy diffusion; and from the vertical diffusive flux of buoyancy. The diabatic source and diffusion are both irreversible terms, whereas the vertical motion term is reversible.

Writing the material evolution (13.152) in its flux-form leads to the Eulerian balance equation for the potential energy per mass

$$\partial_t P^b + \nabla \cdot [\mathbf{v} P^b + g^{-1} \Phi \kappa \nabla b] = -b w - g^{-1} \Phi Q^b + \kappa \partial_z b. \quad (13.154)$$

Integrating over a region of constant volume and with zero boundary fluxes (other than fluxes associated with Q^b), leads to

$$\frac{d}{dt} \langle P^b \rangle = -\langle b w \rangle - g^{-1} \langle \Phi Q^b \rangle + \kappa \left\langle \frac{\partial b}{\partial z} \right\rangle. \quad (13.155)$$

The domain averaged potential energy per mass evolves according to the correlation between vertical motion and buoyancy; the correlation between heating and depth; and the domain averaged vertical diffusive flux of buoyancy. We now comment on the right hand side terms.

Downgradient diffusion in the vertical

In a stably stratified ocean, buoyancy is larger in the upper ocean than deeper ocean, in which case

$$\partial b / \partial z > 0 \quad \text{stably stratified.} \quad (13.156)$$

A downgradient vertical diffusive flux acts to homogenize in the vertical. Consequently, when acting on a stably stratified fluid, diffusion moves buoyancy down from the upper ocean (where buoyancy is large) into the interior ocean (where buoyancy is less). Conversely, it moves low buoyancy upward. Hence, diffusion makes the upper ocean less buoyant (heavier) and the deeper ocean more buoyant (lighter). We thus see that diffusion raises the ocean center of mass and as such it increases the domain averaged gravitational potential energy via equation (13.155). This result was already found in Section 10.1.7 when studying potential energy for a non-Boussinesq fluid.

As a further comment, recall from our discussion of tracer kinematics in VOLUME 1 that mixing (including diffusion) in a non-Boussinesq fluid does not move mass, but it generally does move volume. In contrast, for a Boussinesq ocean, diffusion does not move volume but it generally does move mass. We thus find that vertical diffusion in a Boussinesq ocean can raise the center of mass through buoyancy diffusion even while it does not cause any volume transport.

Diabatic heating

The diabatic heating term in equation (13.155), $-g^{-1}\langle\Phi Q^b\rangle$, increases potential energy if there is a positive correlation between vertical position, $-g^{-1}\Phi = -z$, and heating

$$-g^{-1}\langle\Phi Q^b\rangle = -\langle z Q^b \rangle > 0. \quad (13.157)$$

That is, domain averaged potential energy increases if heating, $Q^b > 0$, preferentially occurs in regions deeper than cooling. This situation is not typical in the ocean, where heating is generally shallower than cooling. Geothermal heating at the ocean bottom is perhaps the only example where heating is deeper than cooling.

Vertical motion

The vertical motion term appearing in equation (13.155),

$$bw = -g w \delta\rho/\rho_o \quad (13.158)$$

has a positive sign in the kinetic energy equation (13.143), whereas it has a negative sign in the potential energy equation (13.152). To help understand this term, consider the specific case of a negatively buoyant fluid element

$$b = -g \delta\rho/\rho_o < 0. \quad (13.159)$$

If this fluid element moves vertically upward, $w > 0$, the fluid acquires positive gravitational potential energy since relatively heavy water is moving upwards. This increase in potential energy is reflected in the term $-w b > 0$ appearing in the potential energy equation (13.152). This increase in gravitational potential energy is associated with a decrease in kinetic energy through the $w b < 0$ term appearing in equation (13.143). The conversion between potential and kinetic energy associated with the $w b$ term is a key process arising from vertical motion.

13.7.8 Mechanical energy

Adding the equation for kinetic energy per mass (13.143) to the potential energy equation (13.152) leads to the material evolution for the mechanical energy per mass

$$\frac{D(\mathcal{K} + P^b)}{Dt} = -\nabla \cdot [\mathbf{v} \varphi + \nu \mathbf{v} \times \boldsymbol{\omega} + g^{-1} \kappa \Phi \nabla b] - \nu \boldsymbol{\omega} \cdot \boldsymbol{\omega} - g^{-1} \Phi Q^b + \kappa \partial_z b. \quad (13.160)$$

Notice how the term $w b$ cancelled as it provides for a reversible transfer of mechanical energy between potential and kinetic energies. This reversible transfer has no effect on the mechanical energy. As emphasized by Gent (1993), frictional dissipation appears only in the equation for kinetic energy per mass (13.143), whereas buoyancy diffusion and sources only appear in the potential energy equation (13.152). When forming the mechanical energy equation, these terms appear together.

Writing the budget (13.160) in flux-form leads to

$$\partial_t(\mathcal{K} + P^b) = -\nabla \cdot [\mathbf{v} (\mathcal{K} + P^b + \varphi) + \nu \mathbf{v} \times \boldsymbol{\omega} + g^{-1} \kappa \Phi \nabla b] - \nu \boldsymbol{\omega} \cdot \boldsymbol{\omega} - g^{-1} \Phi Q^b + \kappa \partial_z b. \quad (13.161)$$

The sum $\mathcal{K} + P^b + \varphi$ appearing on the right hand side is the Bernoulli potential for the Boussinesq ocean (see Section 10.6 for the non-Boussinesq form of the Bernoulli potential). Integrating the local mechanical energy budget (13.161) over a region with constant volume, and dropping surface terms, leads to the domain averaged mechanical energy budget

$$\frac{d}{dt} \langle \mathcal{K} + P^b \rangle = -\epsilon - \langle z Q^b \rangle + \kappa \left\langle \frac{\partial b}{\partial z} \right\rangle. \quad (13.162)$$

13.7.9 Conditions required for a steady state mechanical energy

A steady state mechanical energy for the full ocean domain is realized if there is a balance between changes in domain averaged kinetic energy and changes in domain averaged potential energy

$$\frac{d\langle \mathcal{K} \rangle}{dt} = -\frac{d\langle P^b \rangle}{dt}. \quad (13.163)$$

Setting the domain integrated mechanical energy time tendency to zero in equation (13.162) leads to the balance

$$\epsilon = -\langle z Q^b \rangle + \kappa \left\langle \frac{\partial b}{\partial z} \right\rangle. \quad (13.164)$$

Recall from equation (13.149) that frictional dissipation is non-negative

$$\epsilon \geq 0. \quad (13.165)$$

Consequently, a steady state mechanical energy for the ocean domain requires the right hand side of equation (13.164) to be positive. Such occurs when heating is preferentially below cooling (equation (13.157)), and when the diffusive flux moves buoyancy downward. We already discussed the diffusive flux in relation to equation (13.156). For the heat source, observe that locating a cooling source above the warming source will engender an overturning circulation, thus providing a kinetic energy source to balance the sink from viscous dissipation.

13.7.10 Further reading

Elements of this material originate from [Paparella and Young \(2002\)](#), and with Chapter 21 of [Vallis \(2017\)](#) offering a pedagogical discussion.

13.8 Mechanical energy analysis: part II

In this section we build on the analysis from Section 13.6, here allowing density to be a function of salinity, Conservative Temperature, and pressure so that

$$\frac{D\rho}{Dt} = \frac{\partial\rho}{\partial S} \frac{DS}{Dt} + \frac{\partial\rho}{\partial\Theta} \frac{D\Theta}{Dt} + \frac{\partial\rho}{\partial p} \frac{Dp}{Dt}. \quad (13.166)$$

Density thus materially evolves even in the absence of mixing or diabatic processes since Dp/Dt is nonzero whenever flow crosses isobars. Hence, the flux-form mechanical energy equation (13.121) now takes on the form

$$\partial_t (\rho \mathcal{K} + \rho \Phi) + \nabla \cdot [\mathbf{v} (\rho \mathcal{K} + \rho \Phi + p)] = \rho \partial_t \Phi + \Phi \left[\frac{\partial\rho}{\partial S} \dot{S} + \frac{\partial\rho}{\partial\Theta} \dot{\Theta} + \frac{\partial\rho}{\partial p} \dot{p} \right]. \quad (13.167)$$

The right hand side terms provide sources that contribute to the evolution of mechanical energy. In the absence of mixing, diabatic processes, and with a time independent geopotential, the sources reduce to a term arising from motion across pressure surfaces. Such motion can occur for either reversible or irreversible processes. This pressure source term is rather awkward since it means the mechanical energy budget is not closed even when the flow is reversible (i.e., perfect fluid) and with time independent astronomical forces. We now follow the approach of [Young \(2010\)](#) to recover a closed Boussinesq mechanical energy budget by making use of a modified form of the gravitational potential energy.

13.8.1 Boussinesq dynamic enthalpy

In this section we introduce a new thermodynamic potential that, in effect, provides us with an integrating factor to render a closed Boussinesq mechanical energy budget. This potential is referred to as the **Boussinesq dynamic enthalpy**. Before considering it, we do a brief warm-up to refamiliarize ourselves with salient pieces of the thermodynamic formalism from Chapter 6.

Material time changes to a pressure integral of density

Consider a thermodynamic potential, $\tilde{\Pi}(S, \Theta, p | p_r)$, defined according to the pressure integral of the *in situ* density

$$\tilde{\Pi}(S, \Theta, p | p_r) \equiv \int_{p_r}^p \rho(S, \Theta, p') dp' \implies \left[\frac{\partial \tilde{\Pi}}{\partial p} \right]_{S, \Theta} = \rho(S, \Theta, p), \quad (13.168)$$

where p_r is an arbitrary constant reference pressure. The notation, $\tilde{\Pi}(S, \Theta, p | p_r)$, emphasizes that p_r is a specified parameter whereas S, Θ, p are coordinates in thermodynamic configuration space (see Section 6.1.4). The integral in equation (13.168) is computed over pressure in a thermodynamic configuration space rather than an integral over a region in \mathbf{x} -space.¹¹

¹¹This is an example where the discussion in Section 10.5.3 is key, whereby we must distinguish between fields in a thermodynamic configuration space versus fields in geographical space and time.

Accordingly, the infinitesimal increment of $\tilde{\Pi}$ is given by

$$\delta\tilde{\Pi} = \delta S \left[\frac{\partial \tilde{\Pi}}{\partial S} \right]_{\Theta,p} + \delta\Theta \left[\frac{\partial \tilde{\Pi}}{\partial \Theta} \right]_{S,p} + \delta p \left[\frac{\partial \tilde{\Pi}}{\partial p} \right]_{S,\Theta} \quad (13.169a)$$

$$= \delta S \left[\frac{\partial \tilde{\Pi}}{\partial S} \right]_{\Theta,p} + \delta\Theta \left[\frac{\partial \tilde{\Pi}}{\partial \Theta} \right]_{S,p} + \rho(S, \Theta, p) \delta p. \quad (13.169b)$$

If the increment is computed following a moving fluid element then we are led to the material time derivative

$$\frac{D\tilde{\Pi}}{Dt} = \frac{DS}{Dt} \left[\frac{\partial \tilde{\Pi}}{\partial S} \right]_{\Theta,p} + \frac{D\Theta}{Dt} \left[\frac{\partial \tilde{\Pi}}{\partial \Theta} \right]_{S,p} + \rho(S, \Theta, p) \frac{Dp}{Dt}. \quad (13.170)$$

Material time changes to a geopotential integral of density

Using the same formalism as above, now consider a thermodynamic potential that is a function of salinity, Conservative Temperature, and geopotential

$$\Pi(S, \Theta, \Phi | \Phi_r) \equiv \int_{\Phi_r}^{\Phi} \rho(S, \Theta, \Phi') d\Phi' \implies \left[\frac{\partial \Pi}{\partial \Phi} \right]_{S,\Theta} = \rho(S, \Theta, \Phi), \quad (13.171)$$

where Φ_r is an arbitrary constant reference geopotential. We offer the following three comments concerning Π .

- For density that is independent of the geopotential, then $\Pi dV = (\Phi - \Phi_r) \rho dV$, which is the gravitational potential energy relative to a reference state. We thus interpret $\Pi(S, \Theta, \Phi)$ as a generalized gravitational potential energy per volume.
- One might consider Π to be the difference in hydrostatic pressure between Φ and Φ_r as per equation (8.66). However, the integral in equation (8.66) occurs in x -space between two geopotentials and holding the (x, y) coordinates fixed during the integration, with that integration generally crossing surfaces of constant S and Θ . In contrast, integration in equation (13.171) is taken from Φ_r to Φ within thermodynamic configuration space so that S and Θ are fixed while performing the geopotential integral. In this manner, the geopotential, rather than pressure, provides a coordinate within a Boussinesq thermodynamic configuration space, along with S and Θ .
- [Young \(2010\)](#) provides motivation for calling Π the Boussinesq dynamic enthalpy.

Following the same formalism used to derive $D\tilde{\Pi}/Dt$ in equation (13.170), we here compute the material time derivative of the Boussinesq dynamic enthalpy

$$\frac{D\Pi}{Dt} = \frac{DS}{Dt} \left[\frac{\partial \Pi}{\partial S} \right]_{\Theta,\Phi} + \frac{D\Theta}{Dt} \left[\frac{\partial \Pi}{\partial \Theta} \right]_{S,\Phi} + \rho(S, \Theta, \Phi) \frac{D\Phi}{Dt}. \quad (13.172)$$

We now create a mechanical energy budget in the form

$$\frac{D}{Dt} [\rho_0 \mathcal{K} + \Pi] = -[\mathbf{v} \cdot \nabla p + \rho \mathbf{v} \cdot \nabla \Phi] + \dot{S} \left[\frac{\partial \Pi}{\partial S} \right]_{\Theta,\Phi} + \dot{\Theta} \left[\frac{\partial \Pi}{\partial \Theta} \right]_{S,\Phi} + \rho \frac{D\Phi}{Dt} \quad (13.173a)$$

$$= -[\mathbf{v} \cdot \nabla p + \rho \mathbf{v} \cdot \nabla \Phi] + \dot{S} \left[\frac{\partial \Pi}{\partial S} \right]_{\Theta, \Phi} + \dot{\Theta} \left[\frac{\partial \Pi}{\partial \Theta} \right]_{S, \Phi} + \rho (\partial_t \Phi + \mathbf{v} \cdot \nabla \Phi) \quad (13.173b)$$

$$= -\mathbf{v} \cdot \nabla p + \rho \partial_t \Phi + \dot{S} \left[\frac{\partial \Pi}{\partial S} \right]_{\Theta, \Phi} + \dot{\Theta} \left[\frac{\partial \Pi}{\partial \Theta} \right]_{S, \Phi}, \quad (13.173c)$$

whose flux-form expression is given by

$$\partial_t (\rho_0 \mathcal{K} + \Pi) + \nabla \cdot [\mathbf{v} \cdot (\rho_0 \mathcal{K} + \Pi + p)] = \rho \partial_t \Phi + \dot{S} \left[\frac{\partial \Pi}{\partial S} \right]_{\Theta, \Phi} + \dot{\Theta} \left[\frac{\partial \Pi}{\partial \Theta} \right]_{S, \Phi}. \quad (13.174)$$

We thus see that in the absence of irreversible effects, and with a time independent geopotential, we have succeeded in deriving a closed (i.e., flux-form) mechanical energy budget for a Boussinesq ocean, with

$$\rho_0 \mathcal{M} = \rho_0 \mathcal{K} + \Pi \xrightarrow{\rho = \rho(S, \Theta)} \rho_0 \mathcal{K} + \rho (\Phi - \Phi_r) \quad (13.175)$$

the appropriate Boussinesq expression for the mechanical energy per volume.

13.8.2 Regionally integrated Boussinesq dynamic enthalpy

Following the treatment for a non-Boussinesq fluid in Section 10.1.6, we here study evolution of the gravitational potential energy integrated over a finite region, \mathcal{R} , that is open to material mass transport. Rather than working with the geopotential as done for the non-Boussinesq fluid, we here follow the discussion in Section 13.8.1 by making use of the Boussinesq dynamic enthalpy, thus ensuring a closed mechanical energy budget.

Budget with the equation of state: $\rho = \rho(S, \Theta, \Phi)$

We make use the Leibniz-Reynolds transport theorem from VOLUME 1 to find

$$\frac{d}{dt} \int_{\mathcal{R}} \Pi dV = \int_{\mathcal{R}} \partial_t \Pi dV + \oint_{\partial \mathcal{R}} \Pi \mathbf{v}^{(b)} \cdot \hat{\mathbf{n}} d\mathcal{S} = \int_{\mathcal{R}} \frac{D\Pi}{Dt} dV + \oint_{\partial \mathcal{R}} \Pi (\mathbf{v}^{(b)} - \mathbf{v}) \cdot \hat{\mathbf{n}} d\mathcal{S}, \quad (13.176)$$

where $\mathbf{v}^{(b)}$ is the velocity of a point on the boundary of the domain, $\partial \mathcal{R}$. We expose contributions from irreversible processes leading to material time changes to S and Θ by making use of the identity (13.172)

$$\frac{d}{dt} \int_{\mathcal{R}} \Pi dV = \int_{\mathcal{R}} \left[\frac{DS}{Dt} \left[\frac{\partial \Pi}{\partial S} \right]_{\Theta, \Phi} + \frac{D\Theta}{Dt} \left[\frac{\partial \Pi}{\partial \Theta} \right]_{S, \Phi} + \rho \frac{D\Phi}{Dt} \right] dV + \oint_{\partial \mathcal{R}} \Pi (\mathbf{v}^{(b)} - \mathbf{v}) \cdot \hat{\mathbf{n}} d\mathcal{S}. \quad (13.177)$$

A constant can be added to the dynamic enthalpy without altering the energetics, which is seen by noting that volume conservation means that¹²

$$\frac{d}{dt} \int dV = - \int_{\partial \mathcal{R}} (\mathbf{v} - \mathbf{v}^{(b)}) \cdot \hat{\mathbf{n}} d\mathcal{S}. \quad (13.178)$$

If the region is a vertical column of fluid with fixed horizontal cross-section, extending from the ocean surface to the ocean bottom, then there is horizontal transport across the vertical boundaries, plus vertical transport of mass across the ocean free surface. For the free surface

¹²For equation (13.178), see the discussion of kinematics in VOLUME 1.

we make use of the surface kinematic boundary condition from VOLUME 1 to write

$$\int_{z=\eta} (\Pi/\rho) \rho (\mathbf{v}^{(\eta)} - \mathbf{v}) \cdot \hat{\mathbf{n}} d\mathcal{S} = \int_{z=\eta} (\Pi/\rho) Q_m dA. \quad (13.179)$$

In this equation, Q_m is the mass per time per horizontal area of matter crossing the ocean free surface at $z = \eta$ where $Q_m > 0$ for matter entering the ocean domain, and $d\mathcal{S}$ is the area element on the free surface with dA its horizontal projection.

Budget with the equation of state: $\rho = \rho(S, \Theta)$

For the special case of an equation of state independent of pressure, $\rho = \rho(S, \Theta)$ (Section 13.6), we have $\Pi = \rho(\Phi - \Phi_r)$ so that equation (13.177) reduces to

$$\frac{d}{dt} \int_{\mathcal{R}} \rho (\Phi - \Phi_r) dV = \int_{\mathcal{R}} \left[(\Phi - \Phi_r) \frac{D\rho}{Dt} + \rho \frac{D\Phi}{Dt} \right] dV + \oint_{\partial\mathcal{R}} [\rho (\Phi - \Phi_r) (\mathbf{v}^{(b)} - \mathbf{v})] \cdot \hat{\mathbf{n}} d\mathcal{S}. \quad (13.180)$$

Note that the reference geopotential, Φ_r , drops out since the Boussinesq form of the Leibniz-Reynolds transport theorem (i.e., equation (13.176) with ρ replacing Π) leads to the identity

$$\frac{d}{dt} \int_{\mathcal{R}} \rho dV = \int_{\mathcal{R}} \frac{D\rho}{Dt} dV + \oint_{\partial\mathcal{R}} \rho (\mathbf{v}^{(b)} - \mathbf{v}) \cdot \hat{\mathbf{n}} d\mathcal{S}. \quad (13.181)$$

This equation means that the gravitational mass for a region of Boussinesq ocean (left hand side) changes through boundary terms, as for a non-Boussinesq fluid, plus processes that lead to material time changes in S and Θ

$$\rho = \rho(S, \Theta) \implies \frac{D\rho}{Dt} = \frac{\partial \rho}{\partial S} \frac{DS}{Dt} + \frac{\partial \rho}{\partial \Theta} \frac{D\Theta}{Dt}. \quad (13.182)$$

We understand the presence of the \dot{S} and $\dot{\Theta}$ terms by noting that irreversible processes, such as mixing, do not alter volume in a Boussinesq ocean. Hence, if irreversible processes change density of a fluid element, then there must be a corresponding change in the gravitational mass of the element.

13.8.3 Density derivatives

When computing the derivatives of density, it is important to note whether the derivative is computed holding (Θ, S) fixed or holding (x, y) fixed. As seen here, this distinction can be confused for the Boussinesq ocean, especially when the geopotential takes the simple form $\Phi = gz$.

Vertical derivative of *in situ* density for a non-Boussinesq fluid

To motivate the discussion, recall the *in situ* density for a non-Boussinesq fluid is a function of the salinity, S , Conservative Temperature, Θ , and *in situ* pressure, p ,

$$\rho = \rho(S, \Theta, p), \quad (13.183)$$

so that its spatial gradient is

$$\nabla \rho = \left[\frac{\partial \rho}{\partial S} \right]_{\Theta, p} \nabla S + \left[\frac{\partial \rho}{\partial \Theta} \right]_{S, p} \nabla \Theta + \left[\frac{\partial \rho}{\partial p} \right]_{S, \Theta} \nabla p = \left[\frac{\partial \rho}{\partial S} \right]_{\Theta, p} \nabla S + \left[\frac{\partial \rho}{\partial \Theta} \right]_{S, p} \nabla \Theta + \frac{1}{c_s^2} \nabla p. \quad (13.184)$$

In the final step we introduced the inverse squared sound speed

$$\frac{1}{c_s^2} = \left[\frac{\partial \rho}{\partial p} \right]_{S,\Theta}, \quad (13.185)$$

which is the partial derivative of density holding S and Θ fixed. Equation (13.184) says that the spatial gradient of density on the left hand side is determined by the sum of three terms that arise from spatial gradients of (S, Θ, p) , each multiplied by their respective functional derivative of the equation of state for density. The vertical component of this equation arises when measuring vertical stratification, in which case

$$\left[\frac{\partial \rho}{\partial z} \right]_{x,y} = \left[\frac{\partial \rho}{\partial S} \right]_{\Theta,p} \left[\frac{\partial S}{\partial z} \right]_{x,y} + \left[\frac{\partial \rho}{\partial \Theta} \right]_{S,p} \left[\frac{\partial \Theta}{\partial z} \right]_{x,y} + \frac{1}{c_s^2} \left[\frac{\partial p}{\partial z} \right]_{x,y}, \quad (13.186)$$

with $\partial p / \partial z = -\rho g$ for a hydrostatic fluid. Note that we exposed the (x, y) labels on the left hand side partial derivative. As seen next, these extra labels are especially important for the case of the Boussinesq ocean.

Vertical derivative of *in situ* density for a Boussinesq ocean

As seen earlier in this section, the *in situ* density for an energetically consistent Boussinesq ocean has the functional dependence

$$\rho = \rho(S, \Theta, \Phi). \quad (13.187)$$

That is, the geopotential, Φ , replaces pressure in the functional dependence, with the equation of state evaluated with a pressure $p_{\text{eos}} = -\rho_0 \Phi$. Hence, the spatial gradient of *in situ* density for a Boussinesq ocean is

$$\nabla \rho = \left[\frac{\partial \rho}{\partial S} \right]_{\Theta,\Phi} \nabla S + \left[\frac{\partial \rho}{\partial \Theta} \right]_{S,\Phi} \nabla \Theta + \left[\frac{\partial \rho}{\partial \Phi} \right]_{S,\Theta} \nabla \Phi, \quad (13.188)$$

so that the vertical stratification is measured by

$$\left[\frac{\partial \rho}{\partial z} \right]_{x,y} = \left[\frac{\partial \rho}{\partial S} \right]_{\Theta,\Phi} \left[\frac{\partial S}{\partial z} \right]_{x,y} + \left[\frac{\partial \rho}{\partial \Theta} \right]_{S,\Phi} \left[\frac{\partial \Theta}{\partial z} \right]_{x,y} + \left[\frac{\partial \rho}{\partial \Phi} \right]_{S,\Theta} \left[\frac{\partial \Phi}{\partial z} \right]_{x,y}. \quad (13.189a)$$

This relation is analogous to the non-Boussinesq expression (13.186). In particular, the inverse squared sound speed for a Boussinesq ocean is given by

$$\left[\frac{\partial \rho}{\partial \Phi} \right]_{S,\Theta} = -\frac{\rho_0}{c_s^2}. \quad (13.190)$$

Although the prognostic flow is non-divergent for the Boussinesq ocean, the full velocity field is divergent (Section 13.1.8), thus supporting acoustic waves.

Now consider the special (and common) case of a simple geopotential, $\Phi = g z$, whereby the Boussinesq sound speed is given by

$$\left[\frac{\partial \rho}{\partial z} \right]_{S,\Theta} = -\frac{\rho_0 g}{c_s^2}, \quad (13.191)$$

and the vertical stratification derivative is given by

$$\left[\frac{\partial \rho}{\partial z} \right]_{x,y} = \left[\frac{\partial \rho}{\partial S} \right]_{\Theta,z} \left[\frac{\partial S}{\partial z} \right]_{x,y} + \left[\frac{\partial \rho}{\partial \Theta} \right]_{S,z} \left[\frac{\partial \Theta}{\partial z} \right]_{x,y} + \left[\frac{\partial \rho}{\partial z} \right]_{S,\Theta}. \quad (13.192)$$

We here see why attachment of subscripts to the partial derivatives is essential to avoid confusion, since

$$\left[\frac{\partial \rho}{\partial z} \right]_{x,y} \neq \left[\frac{\partial \rho}{\partial z} \right]_{S,\Theta}. \quad (13.193)$$

The left hand side vertical derivative is computed holding the horizontal position fixed, as appropriate for computing the vertical stratification, whereas the right hand side vertical derivative is computed with (S, Θ) fixed, as appropriate for computing the sound speed. These two derivatives are conceptually distinct, with equation (13.192) exposing the mathematical distinction.

Horizontal derivative of *in situ* density for a Boussinesq ocean

The horizontal portion of the gradient (13.188), computed along surfaces of constant geopotential, is given by

$$\nabla_h \rho = \left[\frac{\partial \rho}{\partial S} \right]_{\Theta,\Phi} \nabla_h S + \left[\frac{\partial \rho}{\partial \Theta} \right]_{S,\Phi} \nabla_h \Theta. \quad (13.194)$$

Hence, when the geopotential takes the simple form, $\Phi = g z$, then we have

$$\nabla_h \rho = \left[\frac{\partial \rho}{\partial S} \right]_{\Theta,z} \nabla_h S + \left[\frac{\partial \rho}{\partial \Theta} \right]_{S,z} \nabla_h \Theta. \quad (13.195)$$

In either case, we see that the horizontal density gradient in a Boussinesq ocean is determined by the horizontal gradients of the Conservative Temperature and salinity.

13.8.4 Comments

Decoupling mechanical energy from internal energy

There are further nuances required to unravel energetics of the Boussinesq ocean, with details provided by [Young \(2010\)](#). When encountering these details for the first time one may wonder why bother since the non-Boussinesq energetics discussed in Sections 10.3 and 10.6 are, by comparison, very straightforward. However, the difficulty with non-Boussinesq energetics arises from the internal energy. Namely, since many geophysical flows, particularly those in the ocean, have speeds that are tiny compared to molecular speeds (see discussion of kinetic theory in the Prologue of VOLUME 1), the mechanical energy associated with geophysical flow is tiny relative to the internal energy arising from molecular motions. So when studying the total energy budget for a non-Boussinesq fluid, that energy is dominated by the internal energy. As detailed in [Young \(2010\)](#), the oceanic Boussinesq approximation allows us to focus on the Boussinesq mechanical energy arising just from the fluid flow, and it does so by decoupling mechanical energy from internal energy.

General form of the geopotential

The treatments in [Young \(2010\)](#) and Section 2.4.3 of [Vallis \(2017\)](#) focus on the simple form of the geopotential, $\Phi = g z$, in which case it appears that density is an energetically consistent

Boussinesq ocean can at most have the space and time dependence

$$\rho = \rho[S(\mathbf{x}, t), \Theta(\mathbf{x}, t), p = -\rho_0 g z]. \quad (13.196)$$

However, the formalism developed by [Young \(2010\)](#) allows for a general geopotential, including those that arise from astronomical tidal forcing and from mass redistributions such as near ice shelves. In these cases we retain a consistent Boussinesq energetics with density of the more general form

$$\rho = \rho[S(\mathbf{x}, t), \Theta(\mathbf{x}, t), p = -\rho_0 \Phi(\mathbf{x}, t)]. \quad (13.197)$$

Distinct manifestations of irreversible processes

It is notable that the irreversible terms from \dot{S} and $\dot{\Theta}$ that appear in the mechanical energy equations (13.121), (13.173c) and (13.174) are absent from the non-Boussinesq budget in equation (10.52). Instead, for the non-Boussinesq fluid, the irreversible mixing processes manifest through their effects on flow convergence via the mass continuity equation

$$-\nabla \cdot \mathbf{v} = \frac{1}{\rho} \frac{D\rho}{Dt}. \quad (13.198)$$

Since the Boussinesq ocean has a zero flow divergence, the role of mixing on the potential energy budget appears elsewhere within the mechanical energy budget.

13.9 Available potential energy

The gravitational potential energy per mass of a fluid element, as measured relative to the $z = 0$ geopotential, is given by $g \rho z$ (when assuming a simple geopotential). But how much of that potential energy can be converted to kinetic energy? Not all of it since a state of zero potential energy means all of the fluid sits at the reference geopotential, which is not generally possible. In Section 13.6 we noted that $-g^{-1} b \Phi$ is the potential energy per mass relative to the constant density background state. Pursuing this idea one more step, consider a background or reference buoyancy, $b_{\text{ref}}(z)$, that has a non-zero depth dependence but with no horizontal dependence. Without any horizontal buoyancy gradients there are zero horizontal internal pressure gradients so that an initially static fluid remains static.¹³ Such fluids have a zero Boussinesq baroclinicity, $\mathbf{B} = -\hat{\mathbf{z}} \times \nabla b$, with baroclinicity providing a source for vorticity.¹⁴ A Boussinesq ocean with zero baroclinicity does not generate vorticity since its pressure gradients are perpendicular to buoyancy gradients, which are vertical for a reference state with $b = b_{\text{ref}}(z)$. These concepts from vorticity motivate us to compute the potential energy relative to a depth-dependent background buoyancy profile.

[Lorenz \(1955\)](#) suggested that a particularly relevant background buoyancy state is the one obtained by a reversible rearrangement or sorting of the original buoyancy to a state that has zero baroclinicity. A reversible rearrangement means there is no mixing when moving between the original state and the background state. The difference in gravitational potential energy between these two states is termed the available potential energy (APE), with the APE measuring the potential energy accessible for generating reversible motion.¹⁵ Figure 13.2

¹³External pressure gradients, such as from sea level gradients or applied pressure gradients, are also assumed zero.

¹⁴We provide a full treatment of baroclinicity in our study of vorticity in VOLUME 3.

¹⁵Strictly, this is the potential energy available for producing motion *if* the fluid is allowed to relax to a state with zero baroclinicity. Yet as seen in Chapter 15, rotating stratified fluids generally reach a steady

illustrates the basic concept. In the remainder of this section we provide details to support a quantitative understanding of available potential energy. We restrict attention to the perfect Boussinesq ocean with a linear equation of state, and ignore the role of mixing and the rather difficult nuances related with the nonlinear equation of state. We also assume a simply connected domain.

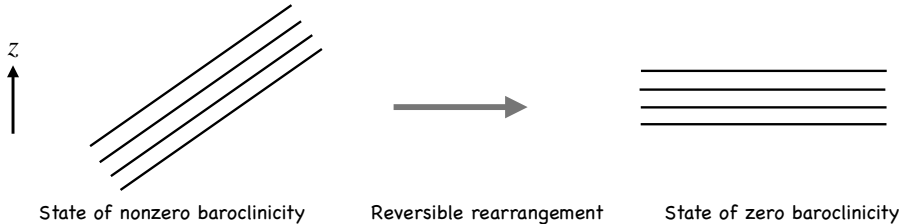


FIGURE 13.2: Isolines of constant buoyancy to illustrate the concept of available potential energy (APE) in a stably stratified Boussinesq ocean. The initial state (left panel) with non-zero baroclinicity ($\mathbf{B} = -\hat{\mathbf{z}} \times \nabla b$) is reversibly rearranged to have zero baroclinicity (right panel). The difference in gravitational potential energy between these two states defines the APE in the initial state. As shown in Section 13.9.3, the APE is a non-negative measure of the amount of gravitational potential energy that can, in principle, be reversibly converted to kinetic energy. Due to volume conservation and the absence of irreversible processes, the depth of a buoyancy surface in the background state shown in the right panel equals to the area average depth of the same buoyancy surface in the left panel (see Section 13.9.2).

13.9.1 Analytic continuation of buoyancy surfaces

An **outcrop** is the location at the ocean surface where a water property surface (e.g., an isopycnal, isotherm) meets the surface. Here we are concerned with outcrops of a buoyancy surface at the upper ocean boundary, along with the complement **incrop** of such surfaces at the solid-earth bottom boundary. Figure 13.3 illustrates such surfaces and their outcrops and incrops. When considering a fluid in a domain with geometric boundaries, and when describing properties of the fluid according to thermodynamic coordinates such as buoyancy, we must decide how to describe these surfaces in regions where they do not exist; i.e., where they are outcropped or incropped. We follow the *Lorenz convention* described in Lorenz (1955), Andrews (1983), Section 4 of Young (2012), and Appendix A of Ringler et al. (2017).

This goal might appear to be pointless. Namely, if the surface does not exist in a region, then why do we need to specify its properties? However, the “analytic continuation” of buoyancy surfaces is very useful when developing their kinematics, with particular use for available potential energy in Section 13.9.3. Such concerns have further applications for studies of water mass transformation arising from boundary buoyancy fluxes (e.g., see Nurser et al. (1999) along with the study of water mass analysis in VOLUME 5). Additionally, the buoyancy frequency along these surfaces is formally infinite since the extended buoyancy surfaces are squeezed into a zero thickness layer. Evidently, analytic continuation of buoyancy layers creates an infinite potential vorticity, which then leads to a potential vorticity Dirac delta sheet as discussed by Bretherton (1966) and Schneider et al. (2003) (see also our discussion of quasi-geostrophy in VOLUME 3). In the following we limit attention to domains with flat bottoms and vertical side-walls. Doing so removes the questions that arise with more general domains.

state (geostrophic balance) with nonzero baroclinicity (thermal wind). Even so, we ignore this concern by here following the standard treatment of available potential energy.

Buoyancy-area mean height of a buoyancy surface

Let $z = \eta(x, y, \mathcal{B}, t)$ be the vertical position (“height” for brief) of a surface with buoyancy, \mathcal{B} . We make use of the area mean height when formulating available potential energy. One way to define the area mean is to integrate $\eta(x, y, \mathcal{B}, t)$ over the area of the buoyancy surface and then divide by the area of the buoyancy surface

$$\overline{\eta(\mathcal{B}, t)}^{\text{buoyancy}} = \frac{\int_{\mathcal{B}} \eta(x, y, \mathcal{B}, t) dS}{\int_{\mathcal{B}} dS}, \quad (13.199)$$

where $\int_{\mathcal{B}} dS$ is the area integral over the \mathcal{B} buoyancy surface. Yet there are two problems with this area calculation. First, the area of a buoyancy surface is rather complicated to compute in practice, given that it can undulate, incrop, and outcrop. Second, the buoyancy surface area is time dependent thus making the area mean also time dependent.

Domain-area mean height of a buoyancy surface

An alternative method to compute the area mean height is to integrate over the area of the fluid domain

$$\overline{\eta(\mathcal{B})} = \frac{\int \eta(x, y, \mathcal{B}, t) dA}{\int dA}, \quad (13.200)$$

where

$$A = \int dA = \int_{\text{fluid domain}} dx dy \quad (13.201)$$

is the time-independent horizontal area of the fluid domain. Time-independence of the area is a plus. Yet by choosing the full domain area, we must specify the height of a buoyancy surface in those horizontal positions where the surface does not exist; i.e., where the surface outcrops or incrops. By doing so, we prove in Section 13.9.2 that the area mean height is time-independent for all buoyancy surfaces. This is another advantage of this approach. Finally, this area mean height satisfies the monotonicity property

$$\overline{\eta(\mathcal{B}_1)} > \overline{\eta(\mathcal{B}_2)} \quad \text{if} \quad \mathcal{B}_1 > \mathcal{B}_2. \quad (13.202)$$

That is, high buoyancy surfaces sit higher in the water column than low buoyancy surfaces. We make use of both the time-independence of the mean height and the monotonicity property when formulating the available potential energy in Section 13.9.3.

Analytic continuation of surface height at outcrops and incrops

So how do we specify the height in outcrop regions? Let us motivate a specification by considering a buoyancy surface that sits near the top of the domain; i.e., its buoyancy is near the domain maximum, b_{\max} . Assume this surface is not horizontal, with the surface $b = \mathcal{B}_{\text{outcrop}}$ in Figure 13.3 an example. Furthermore, let it cover less horizontal area than the full domain area. If we horizontally integrate just over regions where the surface does not outcrop, but still normalize by the total horizontal area of the domain, then the area mean height will be less than some of the other buoyancy surfaces whose buoyancy is less and yet whose horizontal area is more. As a result we will not satisfy the monotonicity property (13.202).

A way to recover monotonicity is to analytically continue the buoyancy surface along the upper boundary so that its height in the outcropped region is set to $\eta(x_{\text{outcrop}}, y_{\text{outcrop}}, \mathcal{B}_{\text{outcrop}}, t) = H$. Doing so then ensures that the domain-area mean height for buoyancy surfaces will approach H .

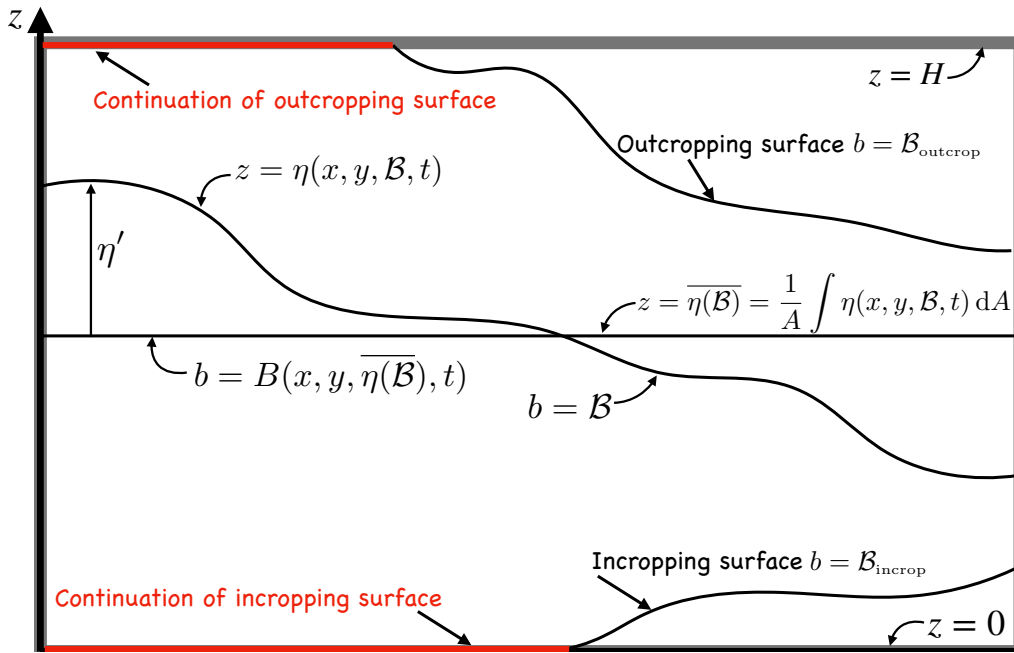


FIGURE 13.3: Geometry of buoyancy surfaces in a flat bottom box of perfect Boussinesq ocean with height H and horizontal area $\int dA = A$. Three representative buoyancy surfaces are shown: one that spans the full domain with $b = \mathcal{B}$, one that incrops at the bottom with $b = \mathcal{B}_{\text{incrop}}$, and one that outcrops at the surface with $b = \mathcal{B}_{\text{outcrop}}$. The vertical height of a buoyancy surface is $z = \eta(x, y, \mathcal{B}, t)$; its area average (which is time independent; see Section 13.9.2) is $\bar{\eta}(\mathcal{B}) = A^{-1} \int \eta(x, y, \mathcal{B}, t) dA$; and its corresponding anomalous height is $\eta'(x, y, \mathcal{B}, t) = \eta(x, y, \mathcal{B}, t) - \bar{\eta}(\mathcal{B})$. As a complement, a particular point on the $z = \bar{\eta}(\mathcal{B})$ height surface has buoyancy $b = B(x, y, \bar{\eta}(\mathcal{B}), t)$, which then leads to an anomalous buoyancy $b' = B(x, y, \bar{\eta}(\mathcal{B}), t) - \mathcal{B}$, where $B(x, y, \bar{\eta}(\mathcal{B}), t) = \mathcal{B}$ (see equation (13.206)). To allow the formalism to be transparent across all buoyancy surfaces, we set $\eta(x, y, \mathcal{B}_{\text{outcrop}}, t) = H$ in regions where the surface has outcropped, and $\eta(x, y, \mathcal{B}_{\text{incrop}}, t) = 0$ where the surface has incropped (denoted by the red lines). As a complement, we set $\partial z / \partial b = 1/N^2 = 0$ for regions where the surface has either incropped or outcropped, thus formally imposing an infinitely stratified extension of the incropped and outcropped surfaces across the top and bottom domain boundaries. Through this analytic continuation of the buoyancy surfaces, we are ensured that the area mean height of all buoyancy surfaces forms a monotonic sequence from 0 to H , with $\bar{\eta}(\mathcal{B}_1) > \bar{\eta}(\mathcal{B}_2)$ if $\mathcal{B}_1 > \mathcal{B}_2$. When focused on a single buoyancy surface, we can reduce notational clutter by writing, for example, $\bar{\eta}$ rather than $\bar{\eta}(\mathcal{B})$, as well as $b'(\bar{\eta}) = B(\bar{\eta}) - \mathcal{B}$, and $\eta' = \eta - \bar{\eta}$.

as their buoyancy approaches the maximum buoyancy. We provide an analogous continuation of the surface within the bottom boundary so that

$$\eta(x, y, \mathcal{B}, t) = \begin{cases} H & \text{if } (x, y) \in \text{outcrop region} \\ 0 & \text{if } (x, y) \in \text{incrop region} \\ \eta(x, y, \mathcal{B}, t) & \text{otherwise.} \end{cases} \quad (13.203)$$

These two continuations of the buoyancy surfaces ensures that the domain-area mean height of all buoyancy surfaces forms a monotonic sequence and that the sequence extends from $0 \leq \bar{\eta}(\mathcal{B}) \leq H$.

Analytic continuation of buoyancy stratification at outcrops and incrops

What does the analytic continuation (13.203) imply for buoyancy? As described, we allow all outcropped buoyancy surfaces to continue along the surface at $\eta = H$. All outcropped surfaces are thus squeezed into the infinitesimal upper fluid layer with buoyancy in that layer bounded

above by the domain maximum buoyancy, b_{\max} . Likewise, for the bottom of the domain we squeeze all incropped buoyancy surfaces into an infinitesimal layer bounded below by b_{\min} , the minimum buoyancy in the domain. Consequently, the upper and lower boundaries are formally capped by infinitely stratified shells in which the inverse squared buoyancy frequency vanishes.

13.9.2 The dual relation between height and buoyancy

In deriving an expression for the APE in Section 13.9.3, we find it useful to have relations between the unsorted and sorted buoyancy fields. We also make use of the dual relation between the height of a constant buoyancy surface and the buoyancy of a constant height surface. For this purpose we examine certain kinematic properties of buoyancy surfaces in a stably stratified box of a perfect Boussinesq ocean as in Figure 13.3.

Volume beneath a buoyancy surface using height coordinates

Making use of notation from Figure 13.3, the volume of fluid contained beneath an arbitrary buoyancy surface is

$$V(\mathcal{B}) = \int dA \int_0^{\eta(x,y,\mathcal{B},t)} dz = \int \eta(x, y, \mathcal{B}, t) dA = A \overline{\eta(\mathcal{B})}, \quad (13.204)$$

The following properties result from volume conservation in a perfect non-divergent flow in the absence of boundary fluxes, as derived in VOLUME 1 when studying the kinematics of non-divergent flows.

- The volume of fluid beneath an arbitrary buoyancy surface is time-independent, as is the area mean height of this surface. This property allowed us to drop the time argument from $V(\mathcal{B})$ and $\overline{\eta(\mathcal{B})}$ in equation (13.204).
- The area mean height of a buoyancy surface is identical to the height of the surface when it is reversibly rearranged to be horizontal.

To verify these properties, recall that buoyancy surfaces are material in a perfect fluid so that no fluid crosses them even as they fluctuate. It follows that the volume of fluid beneath an arbitrary buoyancy surface is time-independent. Since the horizontal area of the domain is time-independent, equation (13.204) also means that the area averaged height of the buoyancy surface is time-independent. Furthermore, any motion of a buoyancy surface in a perfect fluid is reversible, including motion that flattens the surface. Since its area mean height remains fixed, the area mean height equals to the height of the surface when it is flat.

Area mean buoyancy on a constant depth surface

As a further realization of the dual relation between height and buoyancy, note that the area average buoyancy, $b = B(x, y, z, t)$, along a constant height surface is also constant in time

$$\overline{B(z)} = A^{-1} \int B(x, y, z, t) dA = \text{time independent.} \quad (13.205)$$

This property follows since both buoyancy and volume are material constants following a fluid parcel in a perfect Boussinesq ocean. Hence, a fluid parcel carries both its buoyancy and volume unchanged so that the volume integrated buoyancy within any fluid region remains constant.

Correspondingly, the area integrated buoyancy along any fixed height surface remains constant. It also follows that the area mean buoyancy at $z = \eta(\mathcal{B})$ is \mathcal{B}

$$\overline{B[\eta(\mathcal{B})]} = A^{-1} \int B(x, y, z = \overline{\eta(\mathcal{B})}, t) dA = \mathcal{B}. \quad (13.206)$$

Volume beneath a buoyancy surface using buoyancy coordinates

Let us return to the volume beneath a buoyancy surface, only now use buoyancy coordinates to write

$$V(\mathcal{B}) = \int dA \int_0^{\eta(x,y,\mathcal{B},t)} dz = \int dA \int_{b(x,y,0,t)}^{\mathcal{B}} \frac{\partial z}{\partial b} db = \int dA \int_{b(x,y,0,t)}^{\mathcal{B}} \frac{db}{N^2} \quad (13.207)$$

where $b(x, y, 0, t)$ is the buoyancy at the bottom of the domain and

$$N^2 = \frac{\partial b}{\partial z} \quad (13.208)$$

is the squared buoyancy frequency. As noted in Section 13.9.1 and illustrated in Figure 13.3, we analytically continue the buoyancy surfaces into the surface and bottom boundaries so that

$$N^{-2}(x, y, \mathcal{B}) = \begin{cases} = 0 & \text{if } \mathcal{B} > b(x, y, H) \text{ (surface outcrop region)} \\ = 0 & \text{if } \mathcal{B} < b(x, y, 0) \text{ (bottom incrop region)} \\ = N^{-2}(x, y, \mathcal{B}) & \text{if } b(x, y, 0) \leq \mathcal{B} \leq b(x, y, H). \end{cases} \quad (13.209)$$

In this manner we can replace the lower limit in equation (13.207) with a constant buoyancy well below any buoyancy found in the domain, which we write as b_{\min} , so that

$$V(\mathcal{B}) = \int dA \int_{b_{\min}}^{\mathcal{B}} \frac{db}{N^2} = \int_{b_{\min}}^{\mathcal{B}} db \int \frac{dA}{N^2}. \quad (13.210)$$

Being able to commute the area and buoyancy integrals proves useful in the following.

13.9.3 Exact expression for APE

In this subsection we develop an expression for the APE of the perfect stably stratified Boussinesq ocean in a box. To start, consider the volume integrated gravitational potential energy per mass of the fluid in Figure 13.3, relative to a constant density background state with $\rho = \rho_0$

$$\mathcal{P} = - \int dA \int_0^H b z dz = -\frac{1}{2} \int dA \int_0^H b d(z^2). \quad (13.211)$$

Integration by parts leads to the equivalent expression

$$\mathcal{P} = -\frac{1}{2} \int dA \int_0^H d(b z^2) + \frac{1}{2} \int dA \int_{b(x,y,0)}^{b(x,y,H)} \eta^2(x, y, b) db \quad (13.212)$$

$$= -\frac{A H^2}{2} \overline{b(H)} + \frac{1}{2} \int dA \int_{b(x,y,0)}^{b(x,y,H)} \eta^2(x, y, b) db, \quad (13.213)$$

where $\overline{b(H)}$ is the area averaged buoyancy at the top of the fluid domain, $z = H$. As discussed in Section 13.9.1, integration over the finite domain using a buoyancy coordinate leads us to

set $\overline{b(H)} = b_{\max}$, the domain maximum buoyancy. Likewise, the second expression in equation (13.213) has its buoyancy integral range extended to b_{\min} and b_{\max} . By doing so we can swap the area and buoyancy integrals to render

$$\mathcal{P} = \frac{A}{2} \left[-H^2 b_{\max} + \int_{b_{\min}}^{b_{\max}} \overline{\eta^2(b)} db \right], \quad (13.214)$$

where $\overline{\eta^2(b)}$ is the area mean of the squared height of a buoyancy surface. The same calculation for the reference buoyancy, $b_{\text{ref}}(z)$, leads to

$$\mathcal{P}_{\text{ref}} = \frac{A}{2} \left[-H^2 b_{\max} + \int_{b_{\min}}^{b_{\max}} \overline{\eta(b)^2} db \right], \quad (13.215)$$

where we noted that the height of a reference buoyancy surface equals to the area mean of the corresponding buoyancy surface

$$\eta(b_{\text{ref}}) = \overline{\eta}(b = b_{\text{ref}}), \quad (13.216)$$

and the reference buoyancy at the surface boundary equals to the maximum buoyancy, $b_{\text{ref}}(H) = b_{\max}$.

Subtracting the gravitational potential energy of the reference/background state from the potential energy of the full state renders an expression for the available potential energy

$$\mathcal{P}_{\text{APE}} = \mathcal{P} - \mathcal{P}_{\text{ref}} = \frac{A}{2} \left[\int_{b_{\min}}^{b_{\max}} [\overline{\eta^2(b)} - \overline{\eta(b)^2}] db \right] = \int_{b_{\min}}^{b_{\max}} \overline{(\eta')^2} db \geq 0, \quad (13.217)$$

where (see Figure 13.3)

$$\eta(x, y, b, t) = \overline{\eta(b)} + \eta'(x, y, b, t). \quad (13.218)$$

The non-negative nature of the APE acknowledges that either a positive or negative undulation of a buoyancy surface gives rise to fluid motion.

Equation (13.217) is an exact expression for the APE of a perfect Boussinesq ocean in a flat bottom and simply connected domain. We encounter the same expression when studying the APE in a shallow water fluid in VOLUME 3. It is the natural expression when working in buoyancy coordinates, whereby the APE is determined by height variations of constant buoyancy surfaces.

13.9.4 Approximate expression for APE

When working with geopotential coordinates it is useful to obtain an approximate expression for the APE in terms of buoyancy variations on constant height surfaces. That is the subject of this subsection.

Approximate version of APE in terms of buoyancy fluctuations

To develop an approximate expression for the APE we write the height of a buoyancy surface, $\eta(\mathcal{B})$, in the form (see caption to Figure 13.3 to clarify signs)

$$\eta(\mathcal{B}) \approx \overline{\eta(\mathcal{B})} + \left[\frac{\partial z}{\partial b} \right]_{z=\bar{\eta}} [\mathcal{B} - B(\bar{\eta})] = \bar{\eta} - \frac{b'}{N^2} \approx \bar{\eta} - \frac{b'}{N_R^2}, \quad (13.219)$$

where the final step set $N^2(x, y, \bar{\eta}) \approx N_{\text{R}}^2(\bar{\eta})$, which is valid to the same order as the approximation. We are thus led to the approximate expression

$$\eta' = \eta - \bar{\eta} \approx -\frac{b'}{N_{\text{R}}^2} \quad (13.220)$$

so that the approximate APE is

$$\mathcal{P}_{\text{APE}} \approx A \left[\int_0^H \frac{(b')^2}{2 N_{\text{R}}^2} dz \right]. \quad (13.221)$$

This approximate expression is commonly used in practical calculations of APE, particularly when making use of field measurements (e.g., [Bishop et al. \(2020\)](#)).

Practical issues related to the sorted buoyancy profile

Figure 13.4 illustrates how to obtain the sorted buoyancy profile from a discretized version of a stably stratified fluid. The buoyancy of each cell is compared to that of all other cells and vertically stacked according to the relative buoyancy. The vertical position of the sorted grid cell is determined by accumulating the volume per horizontal area of the cell, starting from the bottom and moving up.

It is notable that cells with identical buoyancy lead to regions of zero vertical stratification in the sorted buoyancy profile. Such zero stratification regions commonly arise when sorting stratified fluid layers, where the buoyancy is constant within the layers. One is thus led to perform a vertical smoothing of the sorted profile to remove such unstratified regions, particularly if using the profile to define a background buoyancy frequency as required for the approximate APE calculation given by equation (13.221).

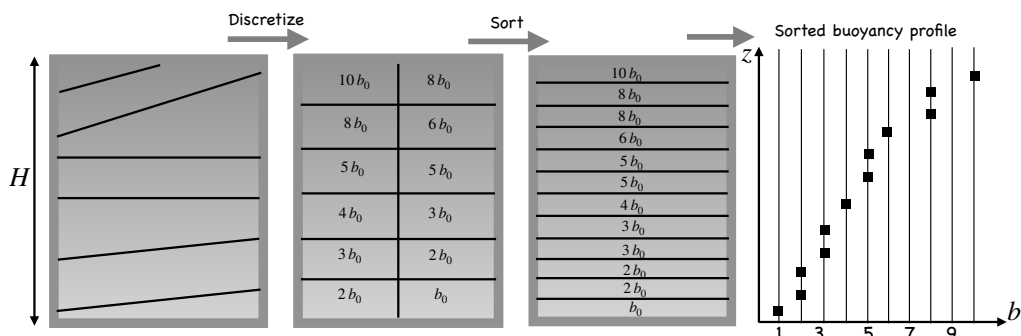


FIGURE 13.4: Illustrating how to sort buoyancy to determine the background or reference profile for computing APE. The first panel on the left shows a sample buoyancy field with black lines representing buoyancy isolines. The second panel shows a discretized version of the field, with b_0 a unit of buoyancy and each cell's buoyancy an integer multiple of b_0 . For simplicity we assume the horizontal area of the domain is depth independent and that each of the discrete grid cells has the same volume and horizontal area. The third panel shows the result of sorting the discrete buoyancy field, with the most buoyant fluid above the less buoyant fluid. During the sort, the cell's volume remains constant (Boussinesq ocean) and the accumulated volume per horizontal area determines the vertical position of the sorted cell. The final panel shows the sorted profile, $b_{\text{ref}}(z)$. Note that regions of zero lateral buoyancy gradient in the unsorted buoyancy field lead to vertically unstratified regions in the sorted buoyancy.

Budget for approximatae APE

To develop a budget for the approximate form of APE, start by considering the budget for buoyancy decomposed as

$$b(x, y, z, t) = b_{\text{ref}}(z) + b'(x, y, z, t), \quad (13.222)$$

so that the perfect fluid buoyancy equation takes on the form

$$\frac{Db}{Dt} = 0 \implies \frac{Db'}{Dt} = -w N_{\text{R}}^2. \quad (13.223)$$

Multiplying by b' leads to

$$\frac{D[(b')^2/2]}{Dt} = -w b' N_{\text{R}}^2, \quad (13.224)$$

and then dividing by N_{R}^2 renders

$$\frac{\partial P_{\text{APE}}}{\partial t} + \mathbf{v} \cdot \nabla P_{\text{APE}} = -w b' \left[1 - \frac{b'}{2} \frac{\partial(1/N_{\text{R}}^2)}{\partial z} \right], \quad (13.225)$$

where we defined the approximate APE per unit volume

$$P_{\text{APE}} = (1/2) [b'/N_{\text{R}}]^2. \quad (13.226)$$

In the case of a depth-independent reference buoyancy frequency, we see that the APE per unit volume materially evolves with a source $-w b'$, which is analogous to the potential energy evolution where the source is $-w b$. Now adding equation (13.225) to the kinetic energy equation (13.117) with $\Phi = g z$ leads to

$$\frac{\partial(\mathcal{K} + P_{\text{APE}})}{\partial t} + \mathbf{v} \cdot \nabla(\mathcal{K} + P_{\text{APE}} + p/\rho_{\text{o}}) = -w \left[g - b_{\text{ref}} - \frac{(b')^2}{2} \frac{\partial(1/N_{\text{R}}^2)}{\partial z} \right]. \quad (13.227)$$

Note that a global area average on any surface eliminates the $w(g - b_{\text{ref}})$ term since

$$\bar{w} = A^{-1} \int w \, dA = 0, \quad (13.228)$$

which follows from $\nabla \cdot \mathbf{v} = 0$ (this is an Exercise in the non-divergent kinematics chapter in VOLUME 1). Further simplifications arise with depth-independent N_{R} , with the corresponding space and time spectra studied by [Bühler et al. \(2014\)](#).

13.9.5 Comments

Elements of this section follow from Section 3.11.1 of [Vallis \(2017\)](#).

Available potential energy remains a compelling concept for many aspects of geophysical fluid studies. Unfortunately, for the ocean proves difficult to extend the formalism beyond the perfect fluid Boussinesq system considered here. Particular difficulties arise from the nonlinear equation of state for seawater and the nontrivial ocean geometry with distinct basins and enclosed seas. Further difficulties arise when considering the non-simply connected nature of the ocean domain.



13.10 Exercises

EXERCISE 13.1: DEPENDENCE ON REFERENCE DENSITY

Consider an inviscid Boussinesq ocean using a constant reference density, ρ_0 , and another inviscid Boussinesq ocean using a constant reference density, $\rho_1 \neq \rho_0$. Assume these two Boussinesq oceans start with an initial condition so that

$$\rho_0 \mathbf{v}_0 = \rho_1 \mathbf{v}_1, \quad (13.229)$$

and with pressure and buoyancy initialized so that

$$\rho_0 (-\nabla \varphi_0 + b_0 \hat{\mathbf{z}}) = \rho_1 (-\nabla \varphi_1 + b_1 \hat{\mathbf{z}}) = -\nabla p - g \rho \hat{\mathbf{z}}. \quad (13.230)$$

Derive an expression for the time tendency, $\partial_t(\rho_0 \mathbf{v}_0 - \rho_1 \mathbf{v}_1)$, thus revealing how the two Boussinesq oceans evolve differently.

EXERCISE 13.2: SYMMETRY UNDER A TIME-DEPENDENT TRANSLATION

In this exercise we consider the Euler equation in free space (no boundaries) where we focus only on the acceleration and the pressure gradient force. That is, we ignore any body forces from gravity and planetary rotation so that the Euler equation takes on the form

$$\rho_0 \frac{D\mathbf{v}}{Dt} = -\nabla p, \quad (13.231)$$

where we assume a Boussinesq ocean so that $\nabla \cdot \mathbf{v} = 0$.

Consider a shift in the reference frame used to describe the flow so that a coordinate position shifts according to

$$\mathbf{x} \rightarrow \mathbf{x} + \mathbf{c}(t), \quad (13.232)$$

where the vector \mathbf{c} is time dependent but has the same value for all points in space.

- (a) Is the shift (13.232) a [Galilean transformation](#)? Hint: recall the discussion of Galilean transformation in [VOLUME 1](#).
- (b) What happens to pressure in the new reference frame? Hint: consider the elliptic problem for pressure as discussed in [Section 13.3.1](#).
- (c) Write the equation of motion (13.231) in this new reference frame.

EXERCISE 13.3: GREEN'S FUNCTION EXPRESSION FOR PRESSURE

Consider the pressure equation from [Section 13.3](#) for the special case of a rigid lid upper ocean boundary

$$-\nabla^2 p = \rho_0 \nabla \cdot \mathbf{D} \quad \mathbf{x} \in \mathcal{R} \quad (13.233a)$$

$$\hat{\mathbf{n}} \cdot \nabla p = -\rho_0 \hat{\mathbf{n}} \cdot \mathbf{D} \quad \mathbf{x} \in \partial\mathcal{R}. \quad (13.233b)$$

If we know the vector \mathbf{D} , then the pressure boundary value problem is linear, thus enabling use of a [Green's function](#) method to determine an expression for pressure.¹⁶ In fact, the pressure is only determined up to a constant. Correspondingly, the discussion in [VOLUME 5](#) for the Poisson equation with Neumann boundary conditions shows that there is no Green's function for this boundary value problem. However, we can make use of the modified Green's function, \tilde{G} , that

¹⁶We study Green's functions in [VOLUME 5](#). Here, we present this exercise for those who have some prior knowledge of Green's functions, reserving a more pedagogical presentation for [VOLUME 5](#).

satisfies

$$-\nabla^2 \tilde{G}(\mathbf{x}|\mathbf{y}) = \delta(\mathbf{x} - \mathbf{y}) - 1/\mathcal{V} \quad \mathbf{x} \in \mathcal{R} \quad (13.234a)$$

$$\hat{\mathbf{n}} \cdot \nabla_x \tilde{G}(\mathbf{x}|\mathbf{y}) = 0 \quad \mathbf{x} \in \partial\mathcal{R}, \quad (13.234b)$$

where $\mathcal{V} = \int_{\mathcal{R}} dV$ is the domain volume. Determine an integral expression for the pressure field. Do so in a manner that decomposes the pressure into a harmonic portion satisfying $\nabla^2 p_{\text{harm}} = 0$, plus a deviation.

EXERCISE 13.4: STEADY PARALLEL SHEARED FLOW ON A TANGENT PLANE

Consider the non-divergent parallel sheared flow

$$\mathbf{v} = \hat{\mathbf{x}} u(y), \quad (13.235)$$

so that the flow is steady, zonal, and has a meridional dependence. Assume the flow is on a tangent plane as discussed in Section 8.5.

- (a) Show that this flow is an exact solution to the β -plane inviscid Boussinesq velocity equation.
- (b) Express the corresponding pressure gradient in terms of u and other terms.
- (c) Show that for an f -plane the stationary velocity can have an arbitrary orientation. Hint: it is sufficient to show that $\mathbf{v} = \hat{\mathbf{y}} v(x)$ is a stationary solution on the f -plane but not on the β -plane.

EXERCISE 13.5: A GENERALIZED BOUSSINESQ APPROXIMATION

In this exercise we derive a mild generalization to the Boussinesq approximation. This generalization facilitates a more accurate decomposition of pressure by introducing a new reference density, $\bar{\rho}(z)$, that is a static function of depth. The new decomposition also leads to a slightly modified buoyancy field.

The derivation starts with the usual decomposition of density using ρ_0 as a space and time constant

$$\rho(\mathbf{x}, t) = \rho_0 + \rho'(\mathbf{x}, t), \quad (13.236)$$

thus leading to the Boussinesq momentum equation

$$\frac{D\mathbf{v}}{Dt} + 2\boldsymbol{\Omega} \times \mathbf{v} = -\rho_0^{-1} (\nabla p + \hat{\mathbf{z}} g \rho). \quad (13.237)$$

But rather than take the traditional decomposition of the pressure and gravitational terms, we now write

$$\nabla p + \hat{\mathbf{z}} g \rho = \nabla[p - \bar{\rho}(z) + \bar{p}(z)] + \hat{\mathbf{z}} g [\rho - \bar{\rho}(z) + \bar{\rho}(z)] \quad (13.238a)$$

$$= \nabla[p - \bar{\rho}(z)] + \hat{\mathbf{z}} g [\rho - \bar{\rho}(z)]. \quad (13.238b)$$

This step introduced the density, $\bar{\rho}(z)$, and the corresponding hydrostatically balanced pressure

$$\frac{d\bar{p}(z)}{dz} = -g \bar{\rho}(z). \quad (13.239)$$

- (a) Show that the pressure is decomposed as

$$p(\mathbf{x}, t) = [p(\mathbf{x}, t) - \bar{p}(z)] + \bar{p}(z) = \rho_0 \tilde{\varphi} + \bar{p}(z). \quad (13.240)$$

What is $\tilde{\varphi}$?

- (b) Introduce a buoyancy

$$\tilde{b} = -\frac{g(\rho - \bar{\rho})}{\rho_0}, \quad (13.241)$$

defined relative to the depth-dependent background density, $\bar{\rho}(z)$, rather than the globally constant density ρ_0 . Show that the momentum equation is given by

$$\frac{D\mathbf{v}}{Dt} + 2\boldsymbol{\Omega} \times \mathbf{v} = -\nabla\tilde{\varphi} + \hat{\mathbf{z}}\tilde{b}. \quad (13.242)$$

- (c) Show that the baroclinicity vector appearing in the Boussinesq vorticity equation takes the form

$$\tilde{\mathbf{B}} = \nabla\tilde{b} \times \hat{\mathbf{z}}, \quad (13.243)$$

which is mathematically the same as with the traditional Boussinesq approximation from Section 13.1.2. We have thus succeeded in generalizing the pressure decomposition and buoyancy field, yet without corrupting the familiar Boussinesq vorticity dynamics.

EXERCISE 13.6: KINETIC ENERGY FOR A PERFECT HYDROSTATIC BOUSSINESQ FLUID

Consider a perfect hydrostatic Boussinesq ocean. Show that the kinetic energy per mass contained in the horizontal velocity,

$$\mathcal{K}_{\text{horz}} = \frac{\mathbf{u} \cdot \mathbf{u}}{2}, \quad (13.244)$$

satisfies the exact same equation as $\mathbf{v} \cdot \mathbf{v}/2$ does for a non-hydrostatic fluid, as given by equation (13.116). Assume the simple form for the geopotential, $\Phi = g z$.

EXERCISE 13.7: ENERGETICS FOR A PERFECT BOUSSINESQ OCEAN

In Section 13.6 we developed the energetic balances for a perfect Boussinesq ocean in a closed domain (domain where all boundary fluxes vanish). We here rederive the same energetics but using the momentum, buoyancy, and continuity equations in the form that exposes buoyancy

$$\frac{D\mathbf{v}}{Dt} + 2\boldsymbol{\Omega} \times \mathbf{v} = -\nabla\varphi + \hat{\mathbf{z}}b \quad (13.245a)$$

$$\frac{Db}{Dt} = 0 \quad (13.245b)$$

$$\nabla \cdot \mathbf{v} = 0 \quad (13.245c)$$

$$b = b(S, \Theta). \quad (13.245d)$$

Assume the simple form for the geopotential, $\Phi = g z$, and assume a closed and static domain (i.e., an Eulerian domain with no boundary contributions). To help physically interpret terms, remember to isolate the total divergence terms and the remainder. Hint: this exercise is a simplification of the material presented in Section 13.7.

- (a) Derive the material time evolution equation for the kinetic energy.
- (b) Derive the material time evolution equation for $P^b = -g^{-1}\Phi b = -b z$, with $\Phi = g z$. Interpret P^b and the processes that affect its material time evolution.
- (c) Derive the mechanical energy equation written in its flux-form, where we define the mechanical energy per volume as $\rho_0(\mathcal{K} + P^b)$. Note the presence of ρ_0 multiplying both \mathcal{K} and P^b . We thus derive an expression for $\rho_0 D(\mathcal{K} + P^b)/Dt$, and show that it is not affected by $w b$. Discuss.

- (d) Integrate the equation for the mechanical energy per mass to derive a global domain budget for mechanical energy. Discuss.

EXERCISE 13.8: KINETIC ENERGY AND THE HYDROSTATIC BOUSSINESQ EQUATIONS

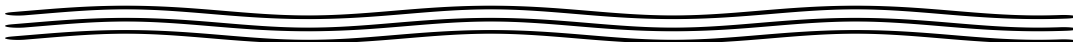
In this exercise we develop some properties of the kinetic energy for the hydrostatic Boussinesq equations listed in Section 13.1.5. We here assume the horizontal frictional acceleration is determined by vertical viscous friction in equation (13.135), and the stress boundary conditions are given by equations (13.138a) and (13.139).

- (a) Derive the flux-form expression for the kinetic energy budget.
- (b) Why does the kinetic energy only have contributions from the horizontal velocity components?
- (c) Discuss the role of vertical viscosity in transporting kinetic energy in the vertical.
- (d) Discuss the role of vertical viscosity in dissipating kinetic energy.
- (e) Discuss how wind stress and bottom drag impact the globally integrated kinetic energy.
Assume bottom drag in the form of equation (13.139).

EXERCISE 13.9: POTENTIAL ENERGY AND THE HYDROSTATIC BOUSSINESQ EQUATIONS

In this exercise we develop some properties of the gravitational potential energy for the hydrostatic Boussinesq equations stated in Section 13.1.5.

- (a) Derive the flux-form budget for gravitational potential energy written as $P^b = -g^{-1} \Phi b$ with $\Phi = g z$. Interpret P^b .
- (b) Discuss the role of the subgrid scale eddy-induced advection in this budget as given by equation (13.128). In particular, discuss its impact on the center of mass of the fluid.
- (c) Discuss the role of vertical diffusion in this budget as given by equation (13.128). In particular, discuss its impact on the center of mass of the fluid.
- (d) Integrate the gravitational potential energy budget over the global ocean. Discuss how the surface boundary buoyancy flux, Q^b , impacts on the global potential energy budget through impacts on the center of mass of the fluid. Ignore any bottom geothermal heating.



Chapter 14

BUOYANCY

A large portion of the vertical pressure force acting on a geophysical fluid element is balanced by the gravitational force, with a precise balance holding for an exact hydrostatic fluid. If there are vertically unbalanced density-induced pressure forces, then a fluid element experiences a vertical acceleration. The **buoyancy** of a fluid element is the unbalanced vertical acceleration from pressure that acts within a fluid environment that has density inhomogeneities and is placed within a gravity field. Correspondingly, the buoyancy of a fluid element vanishes in a fluid environment with a homogeneous density, even though each fluid element feels a gravitational force.¹ Buoyancy is a conceptually useful means to organize vertical forces from gravity and pressure in a fluid with varying density. Namely, if the vertical pressure forces acting on a fluid element are balanced by gravity, then the fluid element is neutrally buoyant; i.e., it floats. If these forces are unbalanced, then the fluid element has a nonzero vertical buoyant acceleration.

To introduce the concept of buoyancy, we study the static forces from gravity and hydrostatic pressure acting on a test region within a fluid environment. Besides being relevant to geophysical fluids, this study finds application to the buoyancy of bodies such as ships, balloons, icebergs, and marine life within their fluid environment.² We then examine the buoyancy of a **test fluid element**, and refer to this buoyancy as the **Archimedean buoyancy** of the fluid element. Examining the buoyancy of test fluid elements provides a venue to introduce static properties of geophysical fluids, such as gravitational stability, neutral directions, and neutral trajectories.

In addition to establishing properties of buoyancy within a static geophysical fluid using test fluid elements, we are interested in how gravity and pressure act to accelerate finite sized regions of fluid. For this purpose, we consider a more complete description that recognizes that a finite sized fluid element affects its surrounding fluid environment. This recognition leads to the concept of **effective buoyancy**. As with Archimedean buoyancy, the effective buoyancy is the net **static forces** acting to create vertical accelerations of a fluid element. More precisely, effective buoyancy is the vertical pressure acceleration acting on a fluid element that remains when setting all velocity dependent accelerations to zero (leaving only the static forces). As we find, the effective buoyancy has a contribution from Archimedean buoyancy, plus the vertical derivative of a pressure perturbation that depends only on the density field. This extra pressure perturbation represents the back-reaction on a fluid element due to the surrounding fluid environment.

¹Even though buoyancy vanishes in a constant density fluid, there can still be vertical accelerations due to nonzero flow convergences or divergences. For example, we encounter such accelerations when studying shallow water flow in VOLUME 3. Vertical acceleration of fluid elements also occurs in a constant density fluid, such as in the presence of the surface gravity waves and capillary waves studied in VOLUME 5.

²The Archimedean notion of buoyancy represents perhaps the most ancient of physical concepts in fluid mechanics. Archimedes was a mathematician, inventor, engineer, physicist, and astronomer who lived in Syracuse, Sicily from roughly 287 B.C.E to 212 B.C.E.

CHAPTER GUIDE

This chapter builds from the study of pressure in Chapters 8, 9, and 12. We also make use of the equations for a Boussinesq fluid derived in Chapter 13, in particular the Poisson equation satisfied by pressure in a non-divergent flow. An understanding of this chapter supports an understanding of how pressure and gravity work within a fluid with density inhomogeneities, thus creating vertical accelerations of fluid elements.

14.1	Loose threads	463
14.2	Buoyancy as the net static force	463
14.2.1	Gravity, pressure, and buoyancy	463
14.2.2	Moments of gravity and pressure	465
14.2.3	Buoyancy of geophysical fluids	466
14.2.4	Comments and further study	467
14.3	Mass density and its flavors	467
14.3.1	Equation of state for the atmosphere and ocean	467
14.3.2	Modified temperature variables	467
14.3.3	Differential and material time changes	468
14.3.4	Potential density	469
14.3.5	Linear equation of state for the ocean	470
14.3.6	Comments on density in a hydrostatic ocean	470
14.3.7	Further study	471
14.4	Archimedean buoyancy of a test fluid element	471
14.4.1	Locally referenced Archimedean buoyancy	471
14.4.2	Globally referenced Archimedean buoyancy	472
14.5	Buoyancy stratification and neutral directions	472
14.5.1	Two thought experiments	472
14.5.2	Comparing <i>in situ</i> densities	474
14.5.3	Neutral directions and the neutrality condition	475
14.5.4	Comments and further study	476
14.6	Buoyancy frequency and gravitational stability	476
14.6.1	Locally referenced potential density	478
14.6.2	Gravitational stability of an ideal gas atmosphere	478
14.6.3	Constant buoyancy frequency in idealized studies	479
14.7	Neutral helicity	480
14.7.1	Mathematical preliminaries	480
14.7.2	Neutral helicity is the reason neutral surfaces are ill-defined	482
14.7.3	Comments and further study	483
14.8	Neutral trajectories	483
14.8.1	Specifying the neutral trajectory	483
14.8.2	Velocity of the neutral trajectory	484
14.8.3	Geometric expressions	485
14.8.4	Summarizing the neutral relations	486
14.8.5	Comments	487
14.9	Pressure forces and vertical motion	487
14.9.1	Dynamically active and dynamically inactive pressures	488
14.9.2	Hydrostatic and non-hydrostatic pressures	488
14.9.3	Momentum equation for the Boussinesq ocean	489
14.10	Case study: test fluid elements in a homogeneous fluid	489
14.10.1	Equations of motion	490
14.10.2	Exact hydrostatic environment	490

14.10.3 An accelerating yet non-rotating environment	490
14.10.4 Rotating tank	492
14.11 Effective buoyancy and vertical accelerations	493
14.11.1 Poisson equations for $p' = p'_{\text{buoy}} + p'_{\text{flow}}$	493
14.11.2 Accelerations from effective buoyancy and fluid motion	495
14.11.3 Boundary value problems for the accelerations	496
14.11.4 Relative scales for effective and Archimedean buoyancies	498
14.11.5 Comments and further study	499
14.12 Exercises	500

14.1 Loose threads

- Provide some examples of b^{eff} fields in Section 14.11 as taken from [Tarshish et al. \(2018\)](#).
- Solution needed for Exercise 14.6.

14.2 Buoyancy as the net static force

In this section we introduce the concept of buoyancy as the net static force acting on a region of fluid, where **static forces** are those forces from gravity and hydrostatic pressure that are active in the absence of motion.

14.2.1 Gravity, pressure, and buoyancy

Consider an arbitrary finite region of matter, \mathcal{R} , referred to in the following as a test region and with density, ρ^{test} . Assume this test region is contained within a hydrostatic fluid environment as depicted in as in Figure 14.1. The gravitational body force acting on the test region is

$$\mathbf{F}^{\text{gravity}} = \int_{\mathcal{R}} \mathbf{g} \rho^{\text{test}} dV = -g \hat{\mathbf{z}} \int_{\mathcal{R}} \rho^{\text{test}} dV = -g M^{\text{test}} \hat{\mathbf{z}}, \quad (14.1)$$

where $M^{\text{test}} = \int_{\mathcal{R}} \rho^{\text{test}} dV$ is the test region's total mass, and we assumed the gravitational acceleration, $\mathbf{g} = -g \hat{\mathbf{z}}$, is a constant over the region. Notably, the gravitational force is independent of the fluid surrounding the region; it only depends on the mass of the region itself.

Because the test region is embedded within a fluid environment, there is a pressure contact force that acts on the region boundary, $\partial\mathcal{R}$, and it is given by the surface integral³

$$\mathbf{F}^{\text{press}} = - \oint_{\partial\mathcal{R}} p \hat{\mathbf{n}} d\mathcal{S}, \quad (14.2)$$

where p is the pressure of the fluid environment and $\hat{\mathbf{n}}$ is the outward normal on the boundary. Since the fluid environment is assumed to be in hydrostatic balance, the pressure is the same regardless the material within the region. If we assume the region is comprised of fluid itself

³In Chapter 5 of [Lautrup \(2005\)](#), the pressure force (14.2) is referred to as the buoyancy force. We instead define buoyancy as the net static forces acting on the test region as given by equation (14.4), with this terminology consistent with that in geophysical fluid mechanics.

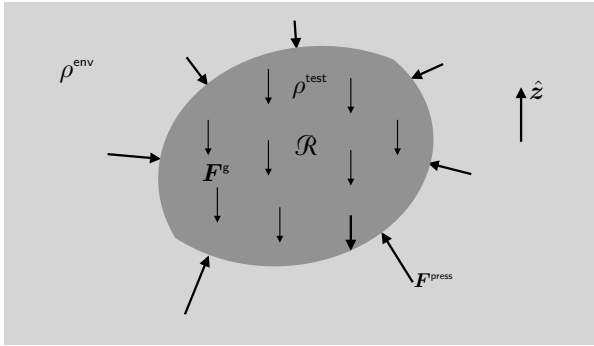


FIGURE 14.1: An arbitrary test region, \mathcal{R} , experiences a gravitational body force acting down and throughout the region, with this force determined by the mass density, ρ^{test} . The test region is surrounded by a fluid environment with density, ρ^{env} . Consequently, the test region experiences a contact pressure force acting on its bounding surface, $\partial\mathcal{R}$. If the fluid environment is in hydrostatic balance, then the pressure force acting on the test region is dependent only on properties of the fluid environment. This observation leads to [Archimedes' principle](#), in which the pressure force acting on the test region equals to the weight of fluid environment displaced by the region: $\mathbf{F}^{\text{press}} = -\oint_{\partial\mathcal{R}} p \hat{n} dS = -\int_{\mathcal{R}} \mathbf{g} \rho^{\text{env}} dV = g M^{\text{env}} \hat{z}$. Note that we assume the gravity field is fixed and unaffected by the test region itself. This assumption holds for our interests in geophysical fluid mechanics, but it is not an accurate assumption in the case of extremely massive (e.g., astronomical objects) that significantly alter the gravity field.

with density, ρ^{env} , then we have

$$\mathbf{F}^{\text{press}} = -\oint_{\partial\mathcal{R}} p \hat{n} dS \quad \text{pressure contact force} \quad (14.3a)$$

$$= -\int_{\mathcal{R}} \nabla p dV \quad \text{divergence theorem for scalars} \quad (14.3b)$$

$$= -\hat{z} \int_{\mathcal{R}} (dp/dz) dV \quad \text{hydrostatic balance so } p = p(z) \quad (14.3c)$$

$$= g \hat{z} \int_{\mathcal{R}} \rho^{\text{env}} dV \quad \text{hydrostatic balance so } dp/dz = -g \rho^{\text{env}} \quad (14.3d)$$

$$= g M^{\text{env}} \hat{z} \quad \text{fluid mass, } M^{\text{env}} = \int_{\mathcal{R}} \rho^{\text{env}} dV. \quad (14.3e)$$

The second equality arises from the divergence theorem (see VOLUME 1), allowing us to convert a surface integral of the pressure contact stress to the volume integral of the pressure gradient. The third and fourth equalities follow since the fluid environment is hydrostatic, in which case the pressure is a function just of the vertical position and $dp/dz = -g \rho^{\text{env}}$. The final equality reveals that the integrated pressure force acting on the test region equals to the weight of environmental fluid displaced by the region. This result is known as [Archimedes' principle](#).

The net force acting on the test region is given by the sum

$$\mathbf{F}^{\text{buoy}} = \mathbf{F}^{\text{gravity}} + \mathbf{F}^{\text{press}} = g \hat{z} (M^{\text{env}} - M^{\text{test}}) = g \hat{z} \int_{\mathcal{R}} (\rho^{\text{env}} - \rho^{\text{test}}) dV. \quad (14.4)$$

We refer to this net force, \mathbf{F}^{buoy} , that arises from the static forces from gravity and pressure, as the [buoyancy](#) force acting on the test region. If the mass of the displaced environmental fluid is greater than mass of the matter within the test region, then the buoyancy force is in the $+\hat{z}$ direction, in which case the test region rises. The case of a hot air balloon lifting off from ground level provides a familiar example. Conversely, if the mass of the displaced environmental fluid is less than the mass of the test region, then the buoyancy force is in the $-\hat{z}$ direction, in

which case the test region sinks. The case of a stone dropped into a lake provides a familiar example. Finally, if the masses are the same, then the test region has zero buoyancy force acting on it, in which case it is neutrally buoyant and floats within the fluid environment. The case of fish with swim bladders (e.g., trout or perch) provide a familiar example.⁴

14.2.2 Moments of gravity and pressure

We now investigate the torques acting on a fluid region due to gravity and pressure. These considerations are central to the stability of floating objects such as ships and icebergs. They also anticipate considerations of baroclinicity in the study of vorticity in VOLUME 3.

There are two forces acting on the region, one from gravity and one from pressure. We compute the moment of those forces (torques), relative to an arbitrary origin, according to the integrated vector products. The gravitational torque acting on the region is given by

$$\mathbf{M}^{\text{gravity}} = \int_{\mathcal{R}} \mathbf{x} \times \mathbf{g} \rho^{\text{test}} dV = -g \int_{\mathcal{R}} \mathbf{x} \times \hat{\mathbf{z}} \rho^{\text{test}} dV = g \hat{\mathbf{z}} \times \int_{\mathcal{R}} \mathbf{x} \rho^{\text{test}} dV = g M^{\text{test}} \hat{\mathbf{z}} \times \mathbf{x}^{\text{test}}, \quad (14.5)$$

where we introduced the region's center of mass position

$$\mathbf{x}^{\text{test}} = \frac{\int_{\mathcal{R}} \mathbf{x} \rho^{\text{test}} dV}{M^{\text{test}}}, \quad (14.6)$$

with \mathbf{x} the Cartesian coordinate relative to the origin. Evidently, the total gravitational torque acting on the region can be written as the torque due to the weight with a moment arm given by the region's center of mass position.

The pressure torque acting on the region is given by the surface integral

$$\mathbf{M}^{\text{press}} = - \oint_{\partial\mathcal{R}} p \mathbf{x} \times \hat{\mathbf{n}} dS. \quad (14.7)$$

We make use of a corollary of the divergence theorem in VOLUME 1 (see the vector calculus chapter), thus enabling us to write

$$\mathbf{M}^{\text{press}} = - \oint_{\partial\mathcal{R}} p \mathbf{x} \times \hat{\mathbf{n}} dS \quad (14.8a)$$

$$= \int_{\mathcal{R}} \nabla \times (p \mathbf{x}) dV \quad (14.8b)$$

$$= \int_{\mathcal{R}} (\nabla p \times \mathbf{x}) dV \quad (14.8c)$$

$$= -g \hat{\mathbf{z}} \times \int_{\mathcal{R}} \rho^{\text{env}} \mathbf{x} dV \quad (14.8d)$$

$$= -g M^{\text{env}} \hat{\mathbf{z}} \times \mathbf{x}^{\text{env}}, \quad (14.8e)$$

⁴Fish with swim bladders maintain neutral buoyancy by regulating the gas volume inside their bladder, thus keeping their average body density equal to that of the surrounding water. Such neutrally buoyant fish can float in place and so do not need to constantly swim to avoid sinking or rising. Not all marine animals are neutrally buoyant. For example, sharks and manta rays do not have a swim bladder, so they must keep moving in order to avoid sinking. Their movement provides a dynamical lift to counteract their slight negative buoyancy.

where the final equality introduced the center of mass coordinate for the displaced fluid⁵

$$\mathbf{x}^{\text{env}} = \frac{\int_{\mathcal{R}} \mathbf{x} \rho^{\text{env}} dV}{M^{\text{fluid}}}. \quad (14.9)$$

Evidently, the torque arising from the pressure acting on the region equals to the torque from the weight of the displaced fluid acting at the center of mass for the displaced fluid. This result is a corollary to Archimedes' principle and it is a key result in the study of stability of floating objects.

Adding the torques from gravity and pressure lead to the buoyancy torque

$$\mathbf{M}^{\text{buoy}} = \mathbf{M}^{\text{gravity}} + \mathbf{M}^{\text{press}} = g \hat{\mathbf{z}} \times (M^{\text{test}} \mathbf{x}^{\text{test}} - M^{\text{env}} \mathbf{x}^{\text{env}}). \quad (14.10)$$

If the object is floating then $M^{\text{test}} = M^{\text{env}}$, so that the buoyancy torque is

$$\mathbf{M}^{\text{buoy}} = g M^{\text{env}} \hat{\mathbf{z}} \times (\mathbf{x}^{\text{test}} - \mathbf{x}^{\text{env}}). \quad (14.11)$$

Notably, the difference, $\mathbf{x}^{\text{test}} - \mathbf{x}^{\text{env}}$, removes any dependence on the coordinate system's origin, so that this equation provides an objective statement about the buoyancy torque acting on the floating region. We see that the buoyancy torque vanishes only if the center of masses are aligned vertically. If they are misaligned, then the buoyancy torque causes the object to rotate. The questions about stability of that rotation is central to the study of ship engineering. Furthermore, a misaligned center of mass for the region and fluid anticipates our discussion of baroclinicity in the study of vorticity in VOLUME 3.

14.2.3 Buoyancy of geophysical fluids

When studying **buoyancy** of geophysical fluids, it is useful to write the buoyancy force as

$$\mathbf{F}^{\text{buoy}} = \hat{\mathbf{z}} \int_{\mathcal{R}} \mathbf{f}^{\text{buoy}} \rho^{\text{env}} dV, \quad (14.12)$$

where

$$\mathbf{f}^{\text{buoy}} = -\hat{\mathbf{z}} g (\rho^{\text{test}} - \rho^{\text{env}}) / \rho^{\text{env}} = b^{\text{loc}} \hat{\mathbf{z}}, \quad (14.13)$$

is the buoyancy acceleration at a point, and b^{loc} is the locally referenced buoyancy. In geophysical fluid parlance, we say that \mathbf{f}^{buoy} is the buoyancy acting on a test fluid element of density, ρ^{test} , arising from its placement in a fluid environment with local density, ρ^{env} . If the test fluid element has density greater than the fluid environment, $\rho^{\text{test}} > \rho^{\text{env}}$, then $b^{\text{loc}} < 0$ and the local buoyancy acceleration is negative (fluid element sinks). In contrast, if $\rho^{\text{test}} < \rho^{\text{env}}$ then $b^{\text{loc}} > 0$ and the buoyancy acceleration is positive (fluid element rises).

Considering the test fluid element as part of the fluid environment itself, then there is a nonzero buoyancy acceleration acting on a fluid element as a result of non-hydrostatic pressure forces, since any vertical acceleration of fluid element breaks the hydrostatic balance. We further examine non-hydrostatic pressure forces in Section 14.11.

⁵In chapter 5 of [Lautrup \(2005\)](#), he refers to $\mathbf{M}^{\text{press}}$ as the buoyancy moment. We instead use that term for the total torque acting on the region due to gravity plus pressure, as given in equations (14.10) and (14.11).

14.2.4 Comments and further study

Stable bodies that are fully immersed in the fluid, such as submarines, have their center of mass below the center of mass of the displaced fluid. In contrast, for regions that are floating, such as ships, the center of mass of the region sits above that of the displaced water. Chapter 5 of [Lautrup \(2005\)](#) provides a lucid introduction to the stability of floating objects, with direct applications to ships and icebergs.

In the remainder of this chapter we focus on the properties of a region of fluid within a fluid. We start by examining the buoyancy, or more precisely the [Archimedean buoyancy](#), of a [test fluid element](#), and then we introduce the [effective buoyancy](#) of a finite fluid region.

14.3 Mass density and its flavors

The density of a test fluid element is central to determining its buoyancy. The [equation of state](#) (Section 7.5.1) provides an expression for the mass density as a function of pressure, temperature, and material tracer concentration (salinity in the ocean and humidity in the atmosphere). In this section we derive salient properties of the equation of state as well as the related flavors of mass density used to study stratified fluid flows.

14.3.1 Equation of state for the atmosphere and ocean

The atmosphere and ocean are commonly approximated as two-component fluids (air and water vapor for the atmosphere; freshwater and salt for ocean). We thus write the *in situ* density as a function

$$\rho = \rho(S, T, p). \quad (14.14)$$

This [equation of state](#) is a function of the *in situ* temperature, T , the *in situ* pressure, p , and the *in situ* salinity (ocean) or humidity (atmosphere), S .⁶ The term [in situ](#) refers to a property measured locally at a point in the fluid. Such *in situ* properties contrast to a [potential property](#), which is based on referencing to a chosen pressure (e.g., potential temperature described in Section 7.4).

Liquids such as seawater have rather complex equations of states obtained from empirical fits to measurements. Part of the complexity arises from the multi-component nature of seawater (salt plus freshwater) as well as the nontrivial inter-molecular forces commonly found in liquids. In contrast, the dry atmosphere can, for many purposes, be well approximated as an ideal gas, which has a rather simple equation of state (see Section 7.5.1). Furthermore, even a moist atmosphere has an equation of state that can be massaged to look like that of an ideal gas (e.g., see Section 18.1 of [Vallis \(2017\)](#)). Hence, much of our discussion in this section is biased toward the ocean, where niceties of the equation of state are most important.

14.3.2 Modified temperature variables

As discussed in Section 7.4, the [in situ temperature](#) of a fluid element changes even if there is no heating applied to the element nor any changes to its material composition. Pressure changes provide a mechanical means for *in situ* temperature to change even in the presence of physical processes that are adiabatic and constant composition (e.g., laminar flow, linear

⁶For our purposes when discussing the ocean, we set $S = 1000 C$ with C the salt concentration, with this specification referred to as the [absolute salinity](#) by [IOC et al. \(2010\)](#). C generally has values around 0.035 so that S has values around 35.

waves). Is it possible to remove such pressure effects and still have a field that describes the “temperature” of a fluid element? That is, can we define a temperature-like field that is only modified by irreversible processes such as heating and mixing? This question is answered by defining **potential temperature**, θ , as well as potential enthalpy or **Conservative Temperature**, Θ . Details are provided for potential temperature in Section 7.4 and Conservative Temperature in Section 10.10. For now it is sufficient to note that the mass density can be written as a function salinity, potential temperature, and pressure

$$\rho = \rho(S, \theta, p), \quad (14.15)$$

or as a function of salinity, Conservative Temperature, and pressure

$$\rho = \rho(S, \Theta, p). \quad (14.16)$$

For most purposes throughout this book, it is not important to distinguish between potential temperature and Conservative Temperature.⁷ We choose to write Θ in most cases since Conservative Temperature offers the most general and self-consistent theoretical foundations for ocean thermodynamics, as per [McDougall \(2003\)](#) and [IOC et al. \(2010\)](#).

One comment on mathematical notation is key here. Namely, the functions $\rho(S, T, p)$, $\rho(S, \theta, p)$, and $\rho(S, \Theta, p)$ have distinct arguments and yet they all measure the same density. A more mathematically honest nomenclature distinguishes the functions by writing, say,

$$\rho = \mathcal{F}(S, T, p) = \mathcal{G}(S, \theta, p) = \mathcal{H}(S, \Theta, p). \quad (14.17)$$

However, we choose brevity in notation by allowing the functional dependence to signal the distinction. This overloaded notation is standard in the ocean physics literature, with care needed to ensure clarity in understanding.⁸

14.3.3 Differential and material time changes

To compute the buoyancy acting on a fluid element, we compare the *in situ* density of the test fluid element to that of its local surrounding fluid environment. To support that comparison, we must consider how *in situ* density in the fluid differs between two infinitesimally close points in the fluid. That is, we must compute the differential of *in situ* density.⁹ Given the functional dependence for the equation of state written in terms of S, Θ, p (equation (14.15)), the differential of *in situ* density is given by

$$d\rho = \left[\frac{\partial \rho}{\partial S} \right] dS + \left[\frac{\partial \rho}{\partial \Theta} \right] d\Theta + \left[\frac{\partial \rho}{\partial p} \right] dp \equiv \rho \beta dS - \rho \alpha d\Theta + c_s^{-2} dp. \quad (14.18)$$

The second equality introduced the following thermodynamic properties of the fluid¹⁰

$$\beta = \frac{1}{\rho} \left[\frac{\partial \rho}{\partial S} \right]_{\Theta, p} \quad \text{haline contraction coefficient} \quad (14.19)$$

⁷One case where the distinction is important concerns an ideal gas atmosphere as discussed in Section 14.6.2.

⁸We made note of this point when introducing scalar fields in the tensor algebra chapter in VOLUME 1.

⁹Recall we introduced differentials in Section 6.10. For the mathematically inclined reader, we say that equation (14.18) provides the exterior derivative of density.

¹⁰A property of the fluid is not a function of the fluid flow but instead is a function of the fluid state.

$$\alpha = -\frac{1}{\rho} \left[\frac{\partial \rho}{\partial \Theta} \right]_{S,p} \quad \text{thermal expansion coefficient} \quad (14.20)$$

$$c_s^2 = \left[\frac{\partial p}{\partial \rho} \right]_{S,\Theta} \quad \text{squared sound speed.} \quad (14.21)$$

The haline contraction coefficient, β , is considered for the ocean, where **haline** refers to salinity.¹¹

The density differential (14.18) leads to the material time change in the *in situ* density measured on a fluid particle trajectory

$$\frac{1}{\rho} \frac{D\rho}{Dt} = \beta \frac{DS}{Dt} - \alpha \frac{D\Theta}{Dt} + \frac{1}{\rho c_s^2} \frac{Dp}{Dt}. \quad (14.22)$$

In the absence of mixing, the Conservative Temperature and salinity are materially constant.¹² In this case, the material time evolution of the *in situ* density is affected only through adiabatic processes that lead to material time changes to the pressure

$$\frac{D\rho}{Dt} = \frac{1}{c_s^2} \frac{Dp}{Dt} \iff \text{adiabatic and isohaline changes.} \quad (14.23)$$

14.3.4 Potential density

As discussed in Section 14.3.2, the reversible motion of a perfect fluid element generally occurs with materially constant Conservative Temperature and materially constant tracer concentration. We thus find it convenient to combine the evolution of salinity and Conservative Temperature into the evolution of a single variable. **Potential density** is one such combination, which is defined as the density a fluid element has if reversibly moving the element to a chosen reference pressure

$$\varrho = \varrho(S, \Theta | p_{\text{ref}}) \equiv \rho(S, \Theta, p = p_{\text{ref}}). \quad (14.24)$$

Evidently, potential density is found by evaluating the equation of state for *in situ* density with the local value for S and Θ , yet with the pressure set to the fixed reference pressure, $p = p_{\text{ref}}$. Potential density is thus parametrically a function of the reference pressure. As for the Conservative Temperature, the reference pressure is often taken at sea level. However, as noted in a few paragraphs below, that choice is neither necessary nor universal.

Material evolution of potential density

With the definition (14.24), the material evolution of potential density is given by

$$\frac{1}{\varrho} \frac{D\varrho}{Dt} = \beta(S, \Theta, p = p_{\text{ref}}) \frac{DS}{Dt} - \alpha(S, \Theta, p = p_{\text{ref}}) \frac{D\Theta}{Dt}, \quad (14.25)$$

where

$$\beta(S, \Theta, p = p_{\text{ref}}) = \frac{1}{\varrho(S, \Theta, p = p_{\text{ref}})} \left[\frac{\partial \rho(S, \Theta, p_{\text{ref}})}{\partial S} \right]_{\Theta} \quad (14.26)$$

$$\alpha(S, \Theta, p = p_{\text{ref}}) = -\frac{1}{\varrho(S, \Theta, p = p_{\text{ref}})} \left[\frac{\partial \rho(S, \Theta, p_{\text{ref}})}{\partial \Theta} \right]_S \quad (14.27)$$

¹¹Note that in many chapters of this book, $\beta = \partial f / \partial y$ is the meridional derivative of the Coriolis parameter. We keep the two usages for β distinct so to avoid confusion.

¹²This statement has nuances that are discussed in Section 10.10 and in more detail in [IOC et al. \(2010\)](#). They can be ignored for present purposes.

are the haline contraction and thermal expansion coefficients evaluated at the reference pressure, $p = p_{\text{ref}}$. Since pressure is fixed at the reference value, there is no pressure derivative on the right hand side of equation (14.25). Conservative Temperature and salinity are materially constant for reversible processes; i.e., adiabatic motion that also maintains constant matter content (e.g., isohaline) for fluid elements. By construction, potential density is also materially constant for reversible processes since both terms on the right hand side of equation (14.25) vanish. This behavior is in contrast to *in situ* density, whose evolution is affected by pressure changes, as well as temperature and salinity changes (see equations (14.22) and (14.23)).

Reference pressures for ϱ and Θ

The reference pressure for the potential density is commonly assumed to be the same as for the Conservative Temperature (and potential temperature). This assumption is particularly the norm for the atmosphere, where the reference pressure is generally taken at the sea level. Likewise for the ocean, the potential temperature and Conservative Temperature are generally computed using a standard sea level reference pressure. However, there are many occasions in the ocean to consider potential density with larger reference pressures, such as when considering physical processes (e.g., mixing) within the ocean interior. Doing so is motivated by the nonlinear effects associated with the seawater equation of state. In this case, pressure effects prompt one to choose a reference pressure given by the *in situ* pressure of the analysis region. Even though it is common to choose a potential density reference pressure distinct from the surface pressure, the Conservative Temperature reference pressure generally remains at the surface. There is no fundamental problem with the use of distinct reference pressures for ϱ and Θ . In particular, all of the above properties of potential density remain unchanged.

14.3.5 Linear equation of state for the ocean

For certain purposes, it is useful to approximate the equation of state used to study ocean fluid mechanics. One common idealization is to compute density as a linear function of Conservative Temperature and salinity

$$\rho = \rho_0 [1 - \alpha (\Theta - \Theta_0) + \beta (S - S_0)], \quad (14.28)$$

where α , β , ρ_0 , Θ_0 , and S_0 are constants. An even further simplification is to set salinity to a space-time constant, so that density is just a linear function of Conservative Temperature. Alternatively, we may choose $\beta = 0$, in which case salinity is a passive tracer that has no impact on density.

14.3.6 Comments on density in a hydrostatic ocean

In an approximate hydrostatic fluid (Section 11.2), we only have access to the hydrostatic pressure. As such, density can only be computed as a function of hydrostatic pressure. Furthermore, density is generally a function of pressure whereas hydrostatic pressure is directly determined by the vertical integral of density. This self-referential situation is resolved for the Boussinesq ocean in which energetic consistency requires the seawater equation of state to use the geopotential defined pressure, $p_{\text{eos}} = -\rho_0 \Phi$, as the argument for density (Section 13.8). This pressure takes the static form, $p_{\text{eos}} = -\rho_0 g z$, for a simple geopotential. For the non-Boussinesq hydrostatic ocean, we can make use of pressure as the vertical coordinate, thus allowing for density to be evaluated at a pressure prescribed by the value of the vertical coordinate.

14.3.7 Further study

Chapter 1 of [Vallis \(2017\)](#) provides a pedagogical discussion of the equation of state for an ideal gas atmosphere and for seawater, as well as a discussion of the various flavors of density. See also Section 18.1 of [Vallis \(2017\)](#) for the equation of state for an ideal gas with water vapor. The seawater equation of state is detailed by [IOC et al. \(2010\)](#), with an overview provided by [McDougall et al. \(2013\)](#).

14.4 Archimedean buoyancy of a test fluid element

We now return to the notions of [Archimedean buoyancy](#) (sometimes abbreviated as “buoyancy”) of a test fluid element. Again, the Archimedean buoyancy is the sum of the static forces acting on a massive body, with the static forces arising from the body’s weight plus the pressure from the surrounding fluid environment. Also recall that a [test fluid element](#) does not alter the density field. Rather, it acts as a passive probe of the gravitational and pressure forces acting in the fluid.

14.4.1 Locally referenced Archimedean buoyancy

Consider the local definition of Archimedean buoyancy from equation (14.13)

$$b^{\text{loc}} = -g(\rho^{\text{test}} - \rho^{\text{env}})/\rho^{\text{env}} = g(1 - \rho^{\text{test}}/\rho^{\text{env}}), \quad (14.29)$$

where ρ^{env} is the local density of the fluid environment, and ρ^{test} is the density of the [test fluid element](#) within that environment. If the test fluid element has a density greater than the environment, then it has a negative locally referenced buoyancy, and vice versa.

In probing the Archimedean buoyancy of the fluid environment, we imagine moving the test fluid element from one point to another. Depending on the thought experiment, the test fluid element might retain all of its original properties during the movement, or those properties might be modified such as through mixing. Hence, in determining the buoyancy we determine the density, ρ^{test} , by specifying the test fluid element’s point of origin as well as how it is moved (e.g., with or without mixing?). Conventional approaches are specified later in this section. A key notion is that buoyancy as defined by equation (14.29) is a function of the path that the test fluid element takes to reach the environment point. This subjectivity lends ambiguity to the definition of local Archimedean buoyancy. We remove this ambiguity by asking specific questions. One central question we ask is if the test fluid element moves an infinitesimal distance while mixing its temperature and salinity with the environment, then what direction maintains a neutrally buoyant state for the test fluid element? This question forms the basis for defining [neutral directions](#) as studied in Section 14.5.

Working with locally referenced Archimedean buoyancy requires a redefinition of a reference state when moving from point to point within a fluid. The continuum of reference states allows for a local accounting of the gravitational stability and neutral directions. However, the re-referencing cannot be seamlessly incorporated into the equations of motion since at each point one needs to redefine the reference state. As an alternative means to garner local information about forces associated with density gradients, we examine the nature of the pressure force in our introduction to [effective buoyancy](#) in Section 14.11.

14.4.2 Globally referenced Archimedean buoyancy

The definition (14.29) accepts that buoyancy is a relative field. Hence, at each fluid point we redefine the environment to compare the density of the test fluid element. However, there are cases in which it is sufficient to define a globally constant environment with a constant reference density, ρ_{ref} . In this case we consider the global buoyancy as

$$b^{\text{glb}} = g(1 - \rho/\rho_{\text{ref}}), \quad (14.30)$$

where we compute ρ according to the local environmental density. This definition is particularly useful for idealized cases where the *in situ* density is not a function of pressure. In this case buoyancy is a function only of Conservative Temperature and salinity so that we can make use of potential density to measure buoyancy (as explained below).

Although the numerical value of b^{glb} is a function of the reference density, what is more relevant is the buoyancy of one fluid element relative to another

$$\Delta b^{\text{glb}} = -g(\Delta\rho/\rho_{\text{ref}}). \quad (14.31)$$

The sign of this relative buoyancy does not depend on the reference density, with the sign all that we need to conclude whether one fluid element is more buoyant than another. Furthermore, with a globally constant environmental density, the buoyancy becomes a local function of space. That is, we no longer compare the fluid element density to a changing local density. Instead, we compute the local density and compare it to the globally constant reference density. We can thus determine b^{glb} at a point through information available just at that point. That is, b^{glb} is a space-time local field. Correspondingly, we can map b^{glb} and determine the relative buoyancy of fluid elements anywhere in the fluid.

14.5 Buoyancy stratification and neutral directions

What are the Archimedean buoyant forces that act on a fluid element? We answer this question by using a test fluid element to probe the local fluid environment without disturbing the environment. We do not consider time changes in this section. Rather, we here examine a snapshot of the fluid environment and use test fluid elements to probe the buoyant properties of that environment. In Section 14.8 we extend the notions of the present section to include time changes.

In probing the buoyant properties of a fluid, we are led to introduce the notion of **neutral directions**, which are directions that a test fluid element can move without feeling any locally defined buoyant forces (*McDougall*, 1987a,b). The thought experiments that build an understanding of neutral directions are applicable to any continuously stratified fluid, thus serving to teach fundamental aspects of buoyancy in both the ocean and atmosphere.

14.5.1 Two thought experiments

As a fluid element moves through its surrounding fluid environment, it is exposed to a suite of physical processes that can modify its thermal, material, and mechanical properties; i.e., its Θ , S , and p . Modification of its pressure occurs through contact stresses with other fluid elements (Chapters 9 and 12). Modification of its thermal and material properties occurs through the mixing-induced exchange of heat and matter such as via diffusion (VOLUME 5). The exchange of thermal and material properties occurs in the presence of irreversible processes

whereas mechanical exchanges occur either reversibly (pressure exchange) or irreversibly (viscous exchange; Section 9.3).

The *in situ* density of a fluid element generally changes when it moves through the fluid environment, with the density change determined by how the element interacts with the surrounding fluid. We conceive of two complementary interactions for the purpose of examining the local Archimedean buoyancy of the test fluid element.

- **UNMIXED TEST FLUID ELEMENT:** Displace the test fluid element without changing Θ and S , yet allow p to equilibrate with the local environment. We imagine this adiabatic and isohaline (i.e., isentropic) displacement to occur by surrounding the test element with a thermally and materially impermeable elastic barrier so there is no thermal nor material mixing of the test element with the environment. Furthermore, assume the test fluid element mechanically equilibrates its pressure with the surrounding fluid, so that the surrounding fluid does reversible pressure-work (Section 6.2) on the test fluid element. The test fluid element's *in situ* density changes through the changing pressure of the local environment.
- **MIXED TEST FLUID ELEMENT:** The complement thought experiment considers the displacement of a test fluid element with its Θ , S , and p equilibrating with the local environment. Such equilibration requires a complete mixing of the test fluid element's Θ and S with the local environment, as well as the mechanical equilibration of its pressure. Notably, the mixed test fluid element represents a proxy for the local environmental properties, since its properties are identical to the local environment.

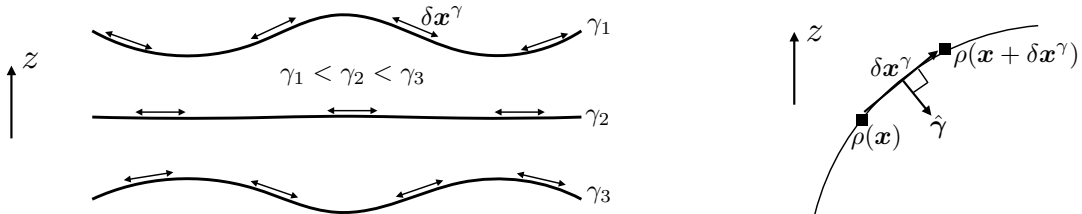
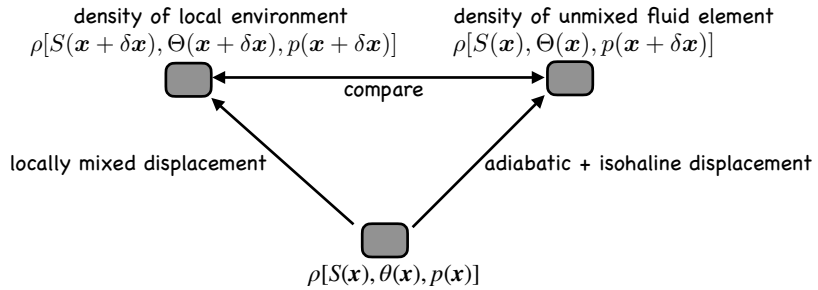


FIGURE 14.2: Depicting the notion of **neutral directions** within a stably stratified fluid. The left panel shows surfaces of constant γ , which represents a surface of constant buoyancy. For example, with a density field that is a function just of Θ , then γ surfaces are parallel to surfaces of constant Θ (see comment at end of Section 14.5.3). Reversible displacements of test fluid elements along a constant γ surface incur no local buoyancy acceleration; i.e., the test fluid element floats along neutral directions. At each point along a γ surface, a neutral direction is defined by directions within the local tangent to the surface. Note that for a fluid with a nonzero **neutral helicity** (Section 14.7), it is not possible to define such neutral surfaces globally. So this figure holds only for a vanishing neutral helicity. Even so, we can define a neutral direction locally, as per the right panel, which shows a zoomed view of a small region on a γ surface. Infinitesimal neutral displacements, $\delta\mathbf{x}^\gamma$, are displacements that satisfy $\delta\mathbf{x}^\gamma \cdot \hat{\gamma} = 0$, with this constraint leading to the **neutrality condition** (14.39). The **dianeutral direction**, $\hat{\gamma}$, is orthogonal to the local neutral direction, with the unit direction, $\hat{\gamma}$, given by equation (14.36). Again, the neutrality condition holds locally at each point in the fluid, so neutral directions are defined even for a fluid with a nonzero neutral helicity.

If we displace the unmixed test fluid element to a region where its *in situ* density differs from the local environment, then the fluid element feels a local Archimedean buoyant acceleration. However, as we show in this section, there are directions that the test fluid element can move that leave its local Archimedean buoyancy zero; i.e., where the test fluid element retains the same *in situ* density as the local environment and so remains neutrally buoyant. These directions are referred to as **neutral directions**. In effect, the test fluid element floats along a neutral direction. We illustrate this notion in Figure 14.2.

A complementary means to conceive of neutral directions is found by considering the mixed test fluid element. Again, as this test fluid element is displaced, it equilibrates its Θ and S (through mixing), and p (through mechanical interactions) with the local environment. This displacement is irreversible since it occurs via mixing, and an arbitrary displacement leads to a change in the fluid element's *in situ* density through changes in Θ , S , and p . However, if the mixed test element is displaced along the neutral direction, the mixing-induced changes from Θ and S exactly balance (as per the neutrality condition (14.39) derived below). In this manner, the only change to the *in situ* density arises from changes to the pressure felt by the test fluid element. Remarkably, when aligned along a neutral direction, these irreversible changes are identical to those felt by the reversibly displaced test fluid element along the same neutral direction. We conclude that the buoyant acceleration vanishes along a neutral direction for both the reversibly displaced (unmixed) test fluid element as well as for a irreversibly displaced (mixed) test fluid element.

14.5.2 Comparing *in situ* densities



$$\rho[S(\mathbf{x} + \delta\mathbf{x}^\gamma), \Theta(\mathbf{x} + \delta\mathbf{x}^\gamma), p(\mathbf{x} + \delta\mathbf{x}^\gamma)] = \rho[S(\mathbf{x}), \Theta(\mathbf{x}), p(\mathbf{x} + \delta\mathbf{x}^\gamma)] \implies \text{neutral direction}$$

FIGURE 14.3: Schematic of the two complementary thought experiments discussed in Section 14.5.2 used to determine neutral directions. The right path concerns a test fluid element that is thermally and materially closed but is mechanically open. Hence, as this test fluid element is displaced from its original location, \mathbf{x} , to a new position, $\mathbf{x} + \delta\mathbf{x}$, it equilibrates to the local pressure but retains the Θ and S of the origin. If the *in situ* density of the test fluid element is displaced along a direction where it maintains the same density as the local environment, then the locally defined Archimedean buoyancy vanishes and this displacement is aligned along a neutral direction. In this case, the displacement satisfies $\delta\mathbf{x}^\gamma \cdot \hat{\gamma} = 0$, as per the neutrality condition (14.39). The complement perspective is shown by the left path as defined by a test fluid element that locally mixes with its environment. If the mixing-induced changes in Θ precisely compensate the mixing-induced changes in S , according to the neutrality condition (14.39), then the *in situ* density change for this test fluid element arise only from changes in pressure. But that change is just like for the unmixed test element on the right path. In this manner, both the mixed and unmixed test fluid elements at $\mathbf{x} + \delta\mathbf{x}$ define the same neutral direction.

To make the above ideas mathematically precise, refer to Figure 14.3 as we consider an infinitesimal displacement, $\delta\mathbf{x}$, of a test fluid element and examine how its *in situ* density changes. First consider the fluid element that equilibrates (through mixing) its Θ , S , and p with the local environment along its displacement. As a result, its *in situ* density at the new location equals to that of the local environment, $\rho(\mathbf{x} + \delta\mathbf{x})$. To leading order, the difference in density between the original position and at the displaced position is computed according to the difference

$$\delta\rho = \rho(\mathbf{x} + \delta\mathbf{x}) - \rho(\mathbf{x}) \tag{14.32a}$$

$$= \rho[S(\mathbf{x} + \delta\mathbf{x}), \Theta(\mathbf{x} + \delta\mathbf{x}), p(\mathbf{x} + \delta\mathbf{x})] - \rho[S(\mathbf{x}), \Theta(\mathbf{x}), p(\mathbf{x})] \tag{14.32b}$$

$$\approx \delta\mathbf{x} \cdot \left[\frac{\partial\rho}{\partial\Theta} \nabla\Theta + \frac{\partial\rho}{\partial S} \nabla S + \frac{\partial\rho}{\partial p} \nabla p \right] \quad (14.32c)$$

$$= \rho \delta\mathbf{x} \cdot \left[-\alpha \nabla\Theta + \beta \nabla S + \frac{1}{\rho c_s^2} \nabla p \right]. \quad (14.32d)$$

For the unmixed test fluid element there is no exchange (no mixing) of Θ and S with its surrounding fluid environment. Hence, changes to density of the test fluid element arise just from pressure changes

$$\delta\rho_{\text{no mix}} = \rho(\mathbf{x} + \delta\mathbf{x})_{\text{no mix}} - \rho(\mathbf{x}) \quad (14.33a)$$

$$= \rho[S(\mathbf{x}), \Theta(\mathbf{x}), p(\mathbf{x} + \delta\mathbf{x})] - \rho[S(\mathbf{x}), \Theta(\mathbf{x}), p(\mathbf{x})] \quad (14.33b)$$

$$\approx \rho \delta\mathbf{x} \cdot \left[\frac{1}{\rho c_s^2} \nabla p \right]. \quad (14.33c)$$

Comparing the densities of the two displaced test fluid elements renders

$$\rho(\mathbf{x} + \delta\mathbf{x}) - \rho(\mathbf{x} + \delta\mathbf{x})_{\text{no mix}} = \delta\rho - \delta\rho_{\text{no mix}} \quad (14.34a)$$

$$= [\rho(\mathbf{x} + \delta\mathbf{x}) - \rho(\mathbf{x})] - [\rho(\mathbf{x} + \delta\mathbf{x})_{\text{no mix}} - \rho(\mathbf{x})] \quad (14.34b)$$

$$= \rho[S(\mathbf{x} + \delta\mathbf{x}), \Theta(\mathbf{x} + \delta\mathbf{x}), p(\mathbf{x} + \delta\mathbf{x})] - \rho[S(\mathbf{x}), \Theta(\mathbf{x}), p(\mathbf{x} + \delta\mathbf{x})] \quad (14.34c)$$

$$\approx \rho \delta\mathbf{x} \cdot [-\alpha \nabla\Theta + \beta \nabla S]. \quad (14.34d)$$

We discuss this result in the following.

14.5.3 Neutral directions and the neutrality condition

Following the thought experiments illustrated in Figure 14.3, we find that if the density of the displaced and unmixed test fluid element is the same as the local environment, then the particular displacement defines a neutral direction. From equation (14.34d) we define a displacement along a neutral direction as a displacement that satisfies

$$\delta\mathbf{x}^\gamma \cdot [-\alpha \nabla\Theta + \beta \nabla S] = \delta\mathbf{x}^\gamma \cdot \hat{\gamma} | -\alpha \nabla\Theta + \beta \nabla S | = 0, \quad (14.35)$$

where we introduced the normalized **dianeutral direction** given by

$$\hat{\gamma} = \frac{-\alpha \nabla\Theta + \beta \nabla S}{| -\alpha \nabla\Theta + \beta \nabla S |}, \quad (14.36)$$

which points in the direction of increasing density.¹³ Infinitesimal displacements, $\delta\mathbf{x}^\gamma$, that are orthogonal to the dianeutral direction, $\hat{\gamma}$, occur along a neutral direction

$$\delta\mathbf{x}^\gamma \cdot \hat{\gamma} = 0 \implies \text{displacement along a neutral direction.} \quad (14.37)$$

These displacements of the unmixed test fluid element lead to no difference in the *in situ* density between the local environment and the test fluid element. Hence, neutral displacements retain a vanishing local Archimedean buoyancy for the unmixed test fluid element. In contrast, displacements in the dianeutral direction alter the local buoyancy.

¹³Equation (4) in [McDougall et al. \(2014\)](#) makes use of the opposite sign convention so that their dianeutral direction points towards decreasing density. We instead choose $\hat{\gamma}$ pointing in the direction of increasing density, which follows the convention used for water mass transformation analysis, as studied in VOLUME 5.

Let us write the neutral displacement in the form

$$\delta\mathbf{x}^\gamma = \hat{\mathbf{t}}^\gamma \delta s, \quad (14.38)$$

where δs is the arc-length along the displacement and $\hat{\mathbf{t}}^\gamma$ is the unit direction pointing along the neutral displacement. We can thus write equation (14.35) as

$$\alpha \hat{\mathbf{t}}^\gamma \cdot \nabla \Theta = \beta \hat{\mathbf{t}}^\gamma \cdot \nabla S, \quad (14.39)$$

which we refer to as the **neutrality condition**. The neutrality condition means that the α weighted gradient of Θ exactly balances the β weighted gradient of S , if one aligns the gradients along a neutral direction. So when considering neutral directions from the perspective of the mixed test fluid element, the mixing-induced changes in Θ precisely compensate mixing-induced changes in S as per the neutrality condition (14.39). As a result, the *in situ* density of the mixed test fluid element changes only via changes to the pressure (since Θ and S changes are compensated), which is precisely how the unmixed test fluid element changes its *in situ* density.

As a corollary, for those cases in which $\nabla S = 0$, so that S is a spatial constant, then neutral directions are aligned parallel to surfaces of constant Θ . In such fluids, Θ measures Archimedean buoyancy so that fluid motion along surfaces of constant Θ feel no Archimedean buoyant acceleration. We mentioned this case in Figure 14.2.

14.5.4 Comments and further study

Neutral directions were introduced to ocean physics by [McDougall \(1987a,b\)](#), and they are the basis for how ocean physicists conceive of buoyancy stratification. Our discussion of neutral directions was inspired by the concise presentation in Section 2.7.2 of [Olbers et al. \(2012\)](#). Our study of vertical gravitational stability follows Section 3.6 of [Gill \(1982\)](#) as well as Section 2.10 of [Vallis \(2017\)](#). In an actual fluid, the movement of any fluid, even a tiny fluid element, modifies the surrounding fluid so that a test fluid element is a fiction. We return to this point in Section 14.11 when studying effective buoyancy.

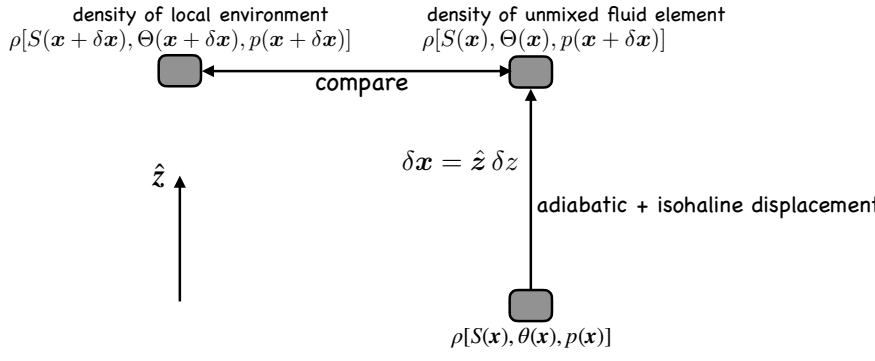
It is notable that our argument for the relevance of neutral displacements relied on the notion that physical processes are more “free” to act in directions that feel no resistance from buoyancy forces. More thorough arguments require the equations of motion. Alas, there is currently no fully dynamical argument for why the ocean prefers neutral displacements over arbitrary non-neutral displacements. However, empirical measurements of ocean mixing support the relevance of neutral directions for orienting tracer mixing within the ocean interior. More discussion of these points is given by [McDougall et al. \(2014\)](#), with mathematical implications presented in our study of tracer parameterizations in VOLUME 5.

14.6 Buoyancy frequency and gravitational stability

In Section 14.5 we considered a general spatial displacement, $\delta\mathbf{x}$, of a test fluid element, and determined conditions for this displacement to keep the locally defined Archimedean buoyancy at zero. In this section we ask a slightly different question, focusing on a vertical displacement of the test fluid element without mixing (Figure 14.4), where the difference between the environmental density and the unmixed test element’s density is

$$\rho(z + \delta z) - \rho(z + \delta z)_{\text{no mix}} = \rho \delta z (-\alpha \partial_z \Theta + \beta \partial_z S). \quad (14.40)$$

We seek an understanding of whether the vertical fluid column is gravitationally stable to such displacements. Since we assume there is no motion of the fluid, the stability calculation determines whether the column will exhibit a [static instability](#).¹⁴



$$\rho[S(x + \delta x), \Theta(x + \delta x), p(x + \delta x)] < \rho[S(x), \Theta(x), p(x + \delta x)] \implies \text{gravitationally stable}$$

$$\rho[S(x + \delta x), \Theta(x + \delta x), p(x + \delta x)] > \rho[S(x), \Theta(x), p(x + \delta x)] \implies \text{gravitationally unstable}$$

$$\rho[S(x + \delta x), \Theta(x + \delta x), p(x + \delta x)] = \rho[S(x), \Theta(x), p(x + \delta x)] \implies \text{gravitationally neutral}$$

FIGURE 14.4: Schematic of the calculation used to examine whether a fluid column is gravitationally stable under vertical displacement of a test fluid element, here realized by specializing the general displacement in Figure 14.3. An unmixed test fluid element (i.e., adiabatic and isohaline displacement) is displaced from its original location at a position \mathbf{x} to a position $\mathbf{x} + \delta\mathbf{x}$, with $\delta\mathbf{x} = \hat{\mathbf{z}} \delta z$ and $\delta z > 0$ in this figure. We compare the density of the displaced unmixed test fluid element with the local environment to determine whether the density stratification of the fluid environment is gravitationally stable ($N^2 > 0$), unstable ($N^2 < 0$), or neutrally stable ($N^2 = 0$).

Consider an upward displacement in equation (14.40) so that $\delta z > 0$. If the surrounding fluid environment has a lower density than the adiabatic and isohaline displaced test fluid element, $\rho(z + \delta z) < \rho(z + \delta z)_{\text{no mix}}$, then the test element feels a buoyant force returning it to the original vertical position. The restorative buoyant force per volume is written

$$g [\rho(z + \delta z) - \rho(z + \delta z)_{\text{no mix}}] = g \rho \delta z (-\alpha \partial_z \Theta + \beta \partial_z S) \equiv -N^2 \rho \delta z, \quad (14.41)$$

where we defined the squared [buoyancy frequency](#)

$$N^2 = g (\alpha \partial_z \Theta - \beta \partial_z S). \quad (14.42)$$

Gravitationally stable vertical motion results from a background density profile with $N^2 > 0$. In this case, the vertical displacement of an unmixed test fluid element moves the element into a region where buoyancy acts to return it to the original vertical position. This buoyant restoring force leads to buoyancy oscillations that can propagate as space-time patterns referred to as [internal gravity waves](#), which we study in VOLUME 5.

A gravitationally unstable profile, in which the fluid has higher density over lower, is signalled by $N^2 < 0$. In this case the displacement of an unmixed test fluid element results in an exponential growth associated with [gravitational instability](#). That is, when the fluid column has any location where $N^2 < 0$, a tiny vertical displacement of a test element leads to

¹⁴We study fluid instabilities in VOLUME 5 of this book, with most attention given to instabilities arising for fluid flows. The [static instability](#) considered in this section arises simply because the density profile has heavier fluid above lighter fluid, with gravity acting to overturn this fluid column to produce a stable vertical stratification.

an even larger displacement, thus causing the perturbation to grow. The resulting gravitational instability causes the fluid to overturn, with the result being that the overturning process returns the fluid column to a gravitational stable state with $N^2 > 0$.

14.6.1 Locally referenced potential density

Equation (14.42) defines the squared buoyancy frequency in terms of the vertical temperature and salinity gradients. This expression is identical to the vertical gradient of the potential density (14.24), when the reference pressure for density is taken local to the point where the buoyancy frequency is computed. That is, the vertical gradient of the **locally referenced potential density** provides a measure of the vertical stratification

$$N^2 = -g \left[\frac{1}{\varrho} \frac{\partial \varrho}{\partial z} \right]_{p_{\text{ref}}=p} = g \left[\alpha \frac{\partial \Theta}{\partial z} - \beta \frac{\partial S}{\partial z} \right]. \quad (14.43)$$

At a point in the fluid, the locally referenced potential density equals to the *in situ* density. However, when probing nearby points by displacing test fluid elements, and thus taking spatial variations into account, the two densities have distinct gradients. Namely, the gradient of the *in situ* density is affected by pressure gradients, whereas spatial gradients of the locally referenced potential density do not feel pressure effects.

14.6.2 Gravitational stability of an ideal gas atmosphere

We introduced the adiabatic lapse rate in Section 7.3 as a measure of how temperature varies as a function of pressure or depth. For an ideal gas atmosphere (Section 7.5), the temperature decreases when moving into a region of less pressure, and increases in regions of greater pressure. The squared buoyancy frequency for an ideal gas can be written (Exercise 14.2)

$$N^2 = \frac{g}{\theta} \frac{\partial \theta}{\partial z}. \quad (14.44)$$

The potential temperature for an ideal gas is given by equation (7.93)

$$\theta = T \left[\frac{p_{\text{ref}}}{p} \right]^{\varphi} \quad (14.45)$$

where

$$\varphi = R^M / c_p \quad (14.46)$$

is the dimensionless ratio of the specific gas constant to the heat capacity, both of which are constants for a simple ideal gas. Consequently, the squared buoyancy frequency takes the form

$$g^{-1} N^2 = \frac{\partial \ln \theta}{\partial z} = \frac{\partial \ln T}{\partial z} - \varphi \frac{\partial \ln p}{\partial z}. \quad (14.47)$$

Evidently, an *in situ* temperature that increases with height stabilizes the atmosphere, and a pressure that decreases with height also stabilizes. The more common situation is for an *in situ* temperature that decreases with height (e.g., it is typically colder on a mountain top than at sea level), with pressure also decreasing with height. Depending on the rate of their decrease, the atmosphere can be gravitationally stable (if temperature decreases gradually relative to pressure) or unstable.

For a hydrostatic fluid with a constant gravitational acceleration, the vertical derivative of pressure is given by (Section 11.2)

$$\frac{\partial p}{\partial z} = -\rho g, \quad (14.48)$$

so that pressure at a point in the fluid equals to the weight per area above that point (Section 8.6). Using this result leads to the squared buoyancy frequency for a hydrostatic ideal gas atmosphere

$$g^{-1} N^2 = \frac{\partial \ln T}{\partial z} + \frac{\varphi g \rho}{p} = \frac{1}{T} \left[\frac{\partial T}{\partial z} + \frac{g}{c_p} \right], \quad (14.49)$$

where we used the ideal gas relation $p = \rho T R^M$ for the final step. Equation (14.49) shows that the squared buoyancy frequency is positive (atmosphere is gravitationally stable) if the decrease with height of the *in situ* temperature is more gradual than the adiabatic lapse rate

$$N^2 = 0 \iff \partial_z T = \Gamma_d, \quad (14.50)$$

where for a dry ideal gas atmosphere (i.e., an atmosphere with no moisture and thus no phase changes),¹⁵ we find (see equation(7.75))

$$\Gamma_d = -g/c_p \approx -9.8 \text{ K/(1000 m)}. \quad (14.51)$$

Conversely, if the *in situ* temperature decreases upon ascent more quickly than the dry adiabatic lapse rate, then the vertical column is gravitationally unstable. In effect, the column becomes top heavy and subject to overturning. We summarize this gravitational stability criteria as follows:

$$\text{gravitationally stable} \quad N^2 > 0 \iff -\partial_z T < g/c_p \quad (14.52)$$

$$\text{gravitationally neutral} \quad N^2 = 0 \iff -\partial_z T = g/c_p \quad (14.53)$$

$$\text{gravitationally unstable} \quad N^2 < 0 \iff -\partial_z T > g/c_p, \quad (14.54)$$

with Figure 14.5 providing an illustration for three linear profiles of the *in situ* temperature.

14.6.3 Constant buoyancy frequency in idealized studies

In many idealized studies, pressure effects are ignored in the density, so that the squared buoyancy frequency is computed as the vertical derivative

$$N^2 = -\frac{g}{\rho} \frac{\partial \rho}{\partial z} \quad (14.55)$$

We thus see that if the density has the exponential structure

$$\rho(z) = \rho_0 e^{-z/H}, \quad (14.56)$$

then the squared buoyancy frequency is

$$N^2 = g/H. \quad (14.57)$$

¹⁵A moist atmosphere has a lapse rate that has a smaller magnitude.

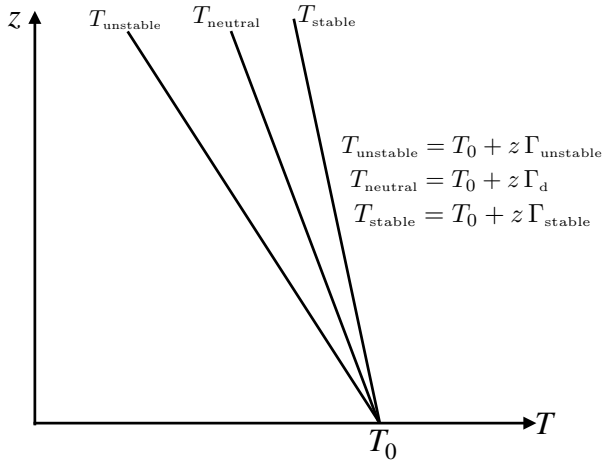


FIGURE 14.5: Three linear vertical profiles of *in situ* temperature in a dry ideal gas atmosphere. The neutrally stable profile has $T_{\text{neutral}} = T_0 + z \Gamma_d$, where $\Gamma_d = -g/c_p \approx -9.8 \text{ K/(1000 m)}$. A vertically unstable profile (heavy over light) has $T_{\text{unstable}} = T_0 + z \Gamma_{\text{unstable}}$ where $\Gamma_{\text{unstable}} < \Gamma_d = -g/c_p$. In contrast, the gravitationally stable atmosphere has $T_{\text{stable}} = T_0 + z \Gamma_{\text{stable}}$ where $\Gamma_{\text{stable}} > \Gamma_d = -g/c_p$.

For a Boussinesq ocean (Chapter 13), one typically computes the squared buoyancy frequency as

$$N_{\text{Bous}}^2 = -\frac{g}{\rho_0} \frac{\partial \rho}{\partial z} \quad (14.58)$$

so that the constant buoyancy frequency (14.57) arises from the linear density profile

$$\rho = \rho_0 (1 - z/H). \quad (14.59)$$

Evidently, the Boussinesq density profile (14.59) is an approximation to the non-Boussinesq profile (14.56) in the case of very large H . When studying thermodynamics we derived the atmospheric scale height in equation (7.86), in which $H \approx 10 \text{ km}$, which is within the troposphere. In contrast, the ocean scale depth is about an order of magnitude larger given the nearly incompressible nature of the ocean fluid, so that the scale depth for the ocean is well beneath the ocean bottom. This is yet another reason that the Boussinesq ocean is a useful approximation for many purposes of ocean mechanics.

14.7 Neutral helicity¹⁶

In our study of neutral directions in Section 14.5 we introduced the notion of a neutral displacement along [neutral directions](#). We here consider a topological property of neutral displacements and the dianeutral direction, with this property first identified by [McDougall and Jackett \(1988\)](#).

14.7.1 Mathematical preliminaries

Consider a continuous and nonzero vector field, $\mathbf{N}(\mathbf{x})$, and write its normalized version as

$$\hat{\mathbf{n}} = \mathbf{N}/|\mathbf{N}|. \quad (14.60)$$

¹⁶This section greatly benefited from input by Geoffrey Stanley.

Let \mathbf{N} define a smooth two-dimensional surface, \mathcal{S} , so that wherever \mathbf{N} is evaluated on \mathcal{S} then it is perpendicular to \mathcal{S} (see Figure 14.6 for an example). In general there is a continuum of such surfaces, yet we are here only interested in one of them. To be specific, assuming $\hat{\mathbf{n}} \cdot \hat{\mathbf{z}}$ is single-signed, let \mathcal{S} be defined by the accumulation of points, $\mathbf{x}_{\mathcal{S}} = x \hat{\mathbf{x}} + y \hat{\mathbf{y}} + \psi(x, y) \hat{\mathbf{z}}$, where $\psi(x, y)$ provides the vertical position of the surface as a continuous function of horizontal position.¹⁷ In this case,

$$\mathbf{N} = \hat{\mathbf{z}} - \nabla_h \psi = \hat{\mathbf{z}} - \hat{\mathbf{x}} \partial_x \psi - \hat{\mathbf{y}} \partial_y \psi \quad (14.61)$$

when evaluated on \mathcal{S} . In the following, we say that these sorts of surfaces are *well-defined* since they are smooth and everywhere have an outward normal direction.

Consider an arbitrary closed region, Ω , that lives on the surface, $\Omega \in \mathcal{S}$. Let $\hat{\mathbf{t}}$ be a unit tangent direction to the boundary of Ω and that is oriented counterclockwise around the boundary, $\partial\Omega$, as defined relative to \mathbf{N} (see Figure 14.6). Since $\mathbf{N} \cdot \hat{\mathbf{t}} = 0$ by construction, we can integrate this identity around $\partial\Omega$ to have

$$\oint_{\partial\Omega} \mathbf{N} \cdot \hat{\mathbf{t}} \, ds = 0 \implies \int_{\Omega} (\nabla \times \mathbf{N}) \cdot \hat{\mathbf{n}} \, d\mathcal{S} = 0, \quad (14.62)$$

where [Stokes' theorem](#) provides the second identity. Since the region, Ω , is arbitrary, the area integral in equation (14.62) vanishes only if the integrand is identically zero for each point on \mathcal{S} . We thus conclude:

$$\text{well-defined surface } \mathcal{S} \implies \mathcal{H} \equiv \mathbf{N} \cdot (\nabla \times \mathbf{N}) = 0. \quad (14.63)$$

The contrapositive also holds so that¹⁸

$$\mathcal{H} \neq 0 \implies \text{ill-defined surface } \mathcal{S}. \quad (14.64)$$

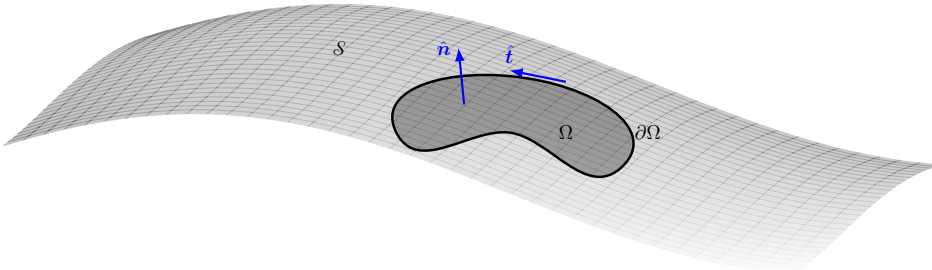


FIGURE 14.6: A smooth and orientable two-dimensional surface, \mathcal{S} , which we refer to as a “well-defined surface”. At each point on \mathcal{S} we can unambiguously define an outward normal, $+\hat{\mathbf{n}}$, and an inward normal, $-\hat{\mathbf{n}}$. Furthermore, we can consider an arbitrary simply connected closed region, Ω , with boundary $\partial\Omega$. The boundary is oriented by a unit tangent vector, $\hat{\mathbf{t}}$, that is perpendicular to the unit normal, $\hat{\mathbf{n}} \cdot \hat{\mathbf{t}} = 0$, and is oriented counterclockwise around $\partial\Omega$ according to $\hat{\mathbf{n}}$.

¹⁷We also consider such surfaces in [VOLUME 1](#) for studying kinematic boundary conditions satisfied by flow encountering a material surface.

¹⁸A contrapositive is a proposition or theorem formed by contradicting both the subject and predicate or both the hypothesis and conclusion of a given proposition or theorem. More succinctly, the proposition “if A then B” has the contrapositive “if not-B then not-A”. Likewise, the proposition has the converse “if B then A”, and it has the inverse “if not-A then not-B”.

14.7.2 Neutral helicity is the reason neutral surfaces are ill-defined

Now apply the above general results to the question of whether we can define a surface with its outward normal parallel to the dianeutral direction, $\hat{\gamma}$,

$$\mathbf{N} = -\alpha \nabla \Theta + \beta \nabla S = \hat{\gamma} | -\alpha \nabla \Theta + \beta \nabla S |. \quad (14.65)$$

If such a surface exists, we refer to it as a **neutral surface**, since at each point on the surface its local normal direction is $\hat{\gamma}$. From the discussion in Section 14.7.1 we know that neutral surfaces are well defined only if the **neutral helicity** vanishes, where the neutral helicity is

$$\mathcal{H}^\gamma = \mathbf{N} \cdot (\nabla \times \mathbf{N}) = (-\alpha \nabla \Theta + \beta \nabla S) \cdot [\nabla \times (-\alpha \nabla \Theta + \beta \nabla S)], \quad (14.66)$$

which can be written

$$\mathcal{H}^\gamma = (-\alpha \nabla \Theta + \beta \nabla S) \cdot [\nabla \times (-\alpha \nabla \Theta + \beta \nabla S)] \quad (14.67a)$$

$$= -\alpha \nabla \Theta \cdot (\nabla \times \beta \nabla S) - \beta \nabla S \cdot (\nabla \times \alpha \nabla \Theta) \quad (14.67b)$$

$$= -\alpha \nabla \Theta \cdot (\nabla \beta \times \nabla S) - \beta \nabla S \cdot (\nabla \alpha \times \nabla \Theta). \quad (14.67c)$$

Further expanding the spatial gradients of α and β

$$\nabla \alpha = (\partial \alpha / \partial \Theta) \nabla \Theta + (\partial \alpha / \partial S) \nabla S + (\partial \alpha / \partial p) \nabla p \quad (14.68a)$$

$$\nabla \beta = (\partial \beta / \partial \Theta) \nabla \Theta + (\partial \beta / \partial S) \nabla S + (\partial \beta / \partial p) \nabla p, \quad (14.68b)$$

then leads to

$$-\alpha \nabla \Theta \cdot (\nabla \beta \times \nabla S) = -\alpha \nabla \Theta \cdot (\partial_p \beta \nabla p \times \nabla S) = -\alpha \partial_p \beta \nabla p \cdot (\nabla S \times \nabla \Theta) \quad (14.69a)$$

$$-\beta \nabla S \cdot (\nabla \alpha \times \nabla \Theta) = -\beta \nabla S \cdot (\partial_p \alpha \nabla p \times \nabla \Theta) = \beta \partial_p \alpha \nabla p \cdot (\nabla S \times \nabla \Theta), \quad (14.69b)$$

which brings neutral helicity to the form

$$\mathcal{H}^\gamma = \nabla p \cdot (\nabla S \times \nabla \Theta) (\beta \partial_p \alpha - \alpha \partial_p \beta). \quad (14.70)$$

Introducing the thermobaricity parameter

$$\mathcal{T} = \beta \partial_p (\alpha / \beta) = \beta^{-1} (\beta \partial_p \alpha - \alpha \partial_p \beta) \quad (14.71)$$

renders the tidy result

$$\mathcal{H}^\gamma = \beta \mathcal{T} \nabla p \cdot (\nabla S \times \nabla \Theta). \quad (14.72)$$

A nonzero neutral helicity (14.72) is fundamentally related to a nonzero thermobaricity parameter \mathcal{T} . It is also associated with the non-zero volume for a parallelopiped in (Θ, S, p) space¹⁹

$$\nabla p \cdot (\nabla S \times \nabla \Theta) = \nabla \Theta \cdot (\nabla p \times \nabla S) = \nabla S \cdot (\nabla \Theta \times \nabla p), \quad (14.73)$$

with this volume a function of the (S, Θ, p) arrangement.

Returning to the question of whether a neutral surface is well-defined, we see that with $\mathcal{H}^\gamma \neq 0$ then neutral surfaces are ill-defined. What does this result mean in practice? Consider

¹⁹See the discussion in the Cartesian tensor algebra chapter (VOLUME 1) of the volume of a region defined by three vectors.

a stably stratified ocean where $\hat{\gamma} \cdot \hat{z} \neq 0$ everywhere. Even for this ocean we are unable to find any finite smooth surface, \mathcal{S}^γ , whose outward normal equals to $\hat{\gamma}$ everywhere on that surface. That is, we cannot find a single function, $\psi(x, y)$, where $\mathbf{N} = \hat{z} - \hat{x} \partial_x \psi - \hat{y} \partial_y \psi$ everywhere on \mathcal{S}^γ .

14.7.3 Comments and further study

Figure 14.6 provides an example smooth surface; i.e., a canonical well-defined surface. What does an ill-defined surface look like? [McDougall and Jackett \(1988\)](#) answered by noting that neutral paths possess a helical structure, with each closed loop in (S, Θ) space displaced vertically in pressure. This helical structure provides a source for irreversible (dianeutral) transformation of seawater. [Klocker and McDougall \(2010a,b\)](#) estimated the effects of this transformation on large-scale ocean overturning circulation. They found the effects from neutral helicity to be comparable to those from mixing, especially in the Southern Ocean.

[Bennett \(2019\)](#) discussed the geometry of neutral paths and made a connection to a theorem of Carathéodory developed in the context of thermodynamics. Additionally, [Stanley \(2019\)](#) showed that S and Θ (or ρ and p) on a neutral surface are functionally related but in a way that varies geographically. Stanley's topological analysis determined how different single-valued S - Θ relations in different geographic regions mesh together to form a globally continuous S - Θ relation. [Stanley et al. \(2021\)](#) then provided a corresponding method for determining approximate neutral surfaces. Such approximate neutral surfaces are globally well-defined, and with a local normal direction that is closely aligned with the dianeutral direction, $\hat{\gamma}$.

14.8 Neutral trajectories

We here extend the notion of neutral directions and neutral displacements considered in Section 14.5 to allow for time dependence. We thus consider a [neutral trajectory](#) as an infinitesimal path in a transient fluid where a test fluid element moves without feeling any net local buoyant force.

14.8.1 Specifying the neutral trajectory

We define a neutral trajectory according to the following algorithm, which generalizes the neutral direction algorithm from Section 14.5.3.

Consider two equal mass test fluid elements at points, \mathbf{x} and $\mathbf{x} + \delta\mathbf{x}$. Exchange these elements over a time increment, δt , without mixing (i.e., adiabatic and isohaline). If the exchange leaves the local *in situ* density and pressure unchanged at the two points, then the exchange occurs along a [neutral trajectory](#). The resulting infinitesimal displacement, $\delta\mathbf{x}^\gamma$, defines the neutral trajectory.²⁰ The rate of change along the neutral trajectory, $\mathbf{v}^\gamma = \delta\mathbf{x}^\gamma / \delta t$, defines the *neutral velocity*, \mathbf{v}^γ . As defined, neutral trajectories only have infinitesimal extents.

Stated differently, we examine infinitesimal displacements of a test fluid element, $\delta\mathbf{x}$, that occur without any mixing of S or Θ , and with the displacement realized over an infinitesimal time increment, $\delta t > 0$. If the displacement occurs along a neutral trajectory, written as $\delta\mathbf{x}^\gamma$, then at the new position the *in situ* density of the environment, $\rho(\mathbf{x} + \delta\mathbf{x}^\gamma, t + dt)$, is equal to that

²⁰We use the same notation, $\delta\mathbf{x}^\gamma$, as used for neutral displacements in Section 14.5. The two displacements are equal when ignoring time dependence.

of the element, $\rho[S(\mathbf{x}, t), \Theta(\mathbf{x}, t), p(\mathbf{x} + \delta\mathbf{x}^\gamma, t + \delta t)]$. We are thus led to the following condition that serves to implicitly define a neutral displacement

$$\underbrace{\rho[S(\mathbf{x}, t), \Theta(\mathbf{x}, t), p(\mathbf{x} + \delta\mathbf{x}^\gamma, t + \delta t)]}_{\text{in situ density of displaced element at incremented time}} = \underbrace{\rho[S(\mathbf{x} + \delta\mathbf{x}^\gamma, t + \delta t), \Theta(\mathbf{x} + \delta\mathbf{x}^\gamma, t + \delta t), p(\mathbf{x} + \delta\mathbf{x}^\gamma, t + \delta t)]}_{\text{in situ density of environmental at displaced location and incremented time}}. \quad (14.74)$$

This condition for a neutral displacement says that the *in situ* density of the environment at $(\mathbf{x} + \delta\mathbf{x}^\gamma, t + \delta t)$ (right hand side) equals to the *in situ* density of a test fluid element that is transported to $(\mathbf{x} + \delta\mathbf{x}^\gamma, t + \delta t)$, while holding S and Θ at the original (\mathbf{x}, t) values (left hand side).

14.8.2 Velocity of the neutral trajectory

The neutral trajectory condition (14.74) can be expressed as a differential relation by taking a leading order Taylor expansion of its left hand side

$$\rho[S(\mathbf{x}, t), \Theta(\mathbf{x}, t), p(\mathbf{x} + \delta\mathbf{x}^\gamma, t + \delta t)] = \rho(\mathbf{x}, t) + \frac{\partial \rho}{\partial p} \left[\delta\mathbf{x}^\gamma \cdot \nabla p + \frac{\partial p}{\partial t} \delta t \right], \quad (14.75)$$

as well as its right hand side

$$\begin{aligned} \rho[S(\mathbf{x} + \delta\mathbf{x}^\gamma, t + \delta t), \Theta(\mathbf{x} + \delta\mathbf{x}^\gamma, t + \delta t), p(\mathbf{x} + \delta\mathbf{x}^\gamma, t + \delta t)] &= \rho(\mathbf{x}, t) \\ &+ \frac{\partial \rho}{\partial p} \left[\delta\mathbf{x}^\gamma \cdot \nabla p + \frac{\partial p}{\partial t} \delta t \right] + \frac{\partial \rho}{\partial S} \left[\delta\mathbf{x}^\gamma \cdot \nabla S + \frac{\partial S}{\partial t} \delta t \right] + \frac{\partial \rho}{\partial \Theta} \left[\delta\mathbf{x}^\gamma \cdot \nabla \Theta + \frac{\partial \Theta}{\partial t} \delta t \right], \end{aligned} \quad (14.76)$$

and then inserting into the density condition (14.74) to render

$$\delta\mathbf{x}^\gamma \cdot (-\alpha \nabla \Theta + \beta \nabla S) + (-\alpha \partial_t \Theta + \beta \partial_t S) \delta t = 0. \quad (14.77)$$

Dividing by the time increment leads to the equivalent condition

$$\mathbf{v}^\gamma \cdot (-\alpha \nabla \Theta + \beta \nabla S) + (-\alpha \partial_t \Theta + \beta \partial_t S) = -\alpha \frac{D^\gamma \Theta}{Dt} + \beta \frac{D^\gamma S}{Dt} = 0, \quad (14.78)$$

where

$$\mathbf{v}^\gamma = \frac{\delta \mathbf{x}^\gamma}{\delta t} \quad (14.79)$$

defines the three-dimensional velocity vector along a neutral trajectory, and we introduced the corresponding time derivative following a neutral trajectory

$$\frac{D^\gamma}{Dt} = \frac{\partial}{\partial t} + \mathbf{v}^\gamma \cdot \nabla. \quad (14.80)$$

Notably, the neutral trajectory constraint (14.78) can be written as a relation between the pressure and density time derivatives along the neutral trajectory

$$\frac{\partial \rho}{\partial p} \frac{D^\gamma p}{Dt} = \frac{D^\gamma \rho}{Dt}. \quad (14.81)$$

We choose to focus on the form (14.78) in the following, since it exposes the tracers, S and Θ .

Equation (14.78) provides a time-dependent generalization of the neutrality condition (14.39) derived for a static ocean. This generalization says that for a neutral space-time trajectory, environmental changes in Θ encountered along the neutral trajectory are exactly compensated by environmental changes in S . Equation (14.78) also provides an explicit expression for the dianeutral component of the neutral velocity

$$\mathbf{v}^\gamma \cdot \hat{\gamma} = \frac{\alpha \partial_t \Theta - \beta \partial_t S}{|-\alpha \nabla \Theta + \beta \nabla S|}, \quad (14.82)$$

where we introduced the dianeutral unit direction from equation (14.65)

$$\hat{\gamma} = \frac{-\alpha \nabla \Theta + \beta \nabla S}{|-\alpha \nabla \Theta + \beta \nabla S|} = \frac{\mathbf{N}}{|\mathbf{N}|}. \quad (14.83)$$

14.8.3 Geometric expressions

Making use of the identity

$$\mathbf{v} \cdot \mathbf{N} = \mathbf{v} \cdot (-\alpha \nabla \Theta + \beta \nabla S), \quad (14.84)$$

along with equation (14.78) renders

$$\mathbf{N} \cdot (\mathbf{v} - \mathbf{v}^\gamma) = -\alpha \frac{D\Theta}{Dt} + \beta \frac{DS}{Dt}, \quad (14.85)$$

and further dividing by $|\mathbf{N}| = |-\alpha \nabla \Theta + \beta \nabla S|$ gives

$$(\mathbf{v} - \mathbf{v}^\gamma) \cdot \hat{\gamma} = \frac{-\alpha \dot{\Theta} + \beta \dot{S}}{|-\alpha \nabla \Theta + \beta \nabla S|}, \quad (14.86)$$

which compares to equation (14.82) for $\mathbf{v}^\gamma \cdot \hat{\gamma}$. The left hand side of equation (14.86) is familiar from our study in VOLUME 1 of kinematics of boundary conditions across surfaces. Here, we do not have a globally defined surface (due to helicity from Section 14.7). Yet we can consider an infinitesimal area element, $\delta\mathcal{S}$, that is oriented perpendicular to the dianeutral unit vector, $\hat{\gamma} \delta\mathcal{S}$. The volume per time of fluid crossing that tiny area element is given by

$$\text{volume per time of fluid crossing } \delta\mathcal{S} = (\mathbf{v} - \mathbf{v}^\gamma) \cdot \hat{\gamma} \delta\mathcal{S} = \frac{(-\alpha \dot{\Theta} + \beta \dot{S}) \delta\mathcal{S}}{|-\alpha \nabla \Theta + \beta \nabla S|}. \quad (14.87)$$

The right hand side is nonzero for cases where S and Θ experience material changes, and when those material changes are not compensated so that $\alpha \dot{\Theta} \neq \beta \dot{S}$. In such cases, equation (14.87) says that a fluid particle velocity, \mathbf{v} , and a neutral trajectory velocity, \mathbf{v}^γ , have distinct projections onto the dianeutral direction, $\hat{\gamma}$.

As illustrated in Figure 14.7, there are two ways for the right hand side of equation (14.87) to vanish. First, in the absence of any irreversible processes, so that $\dot{\Theta} = 0$ and $\dot{S} = 0$, then both Θ and S are materially invariant fluid properties and $\delta\mathcal{S}$ is a material area element. The second way is to have compensated irreversible processes so that $\alpha \dot{\Theta} = \beta \dot{S}$. This compensation is reminiscent of the compensation in equation (14.78) used to define the neutral velocity, \mathbf{v}^γ , via the motion of Θ and S surfaces as per equation (14.82). However, the condition $\alpha \dot{\Theta} = \beta \dot{S}$ concerns the irreversible processes acting on Θ and S , whereas equation (14.78) concerns a reversible thought experiment used to define neutral trajectories.

Neutral diffusion studied in VOLUME 5 is a physical process where the $\alpha \dot{\Theta} = \beta \dot{S}$ compon-

sation occurs, so long as the fluid has a linear equation of state (i.e., thermal expansion, α , and haline contraction, β , are constants). Yet compensation is broken when neutral diffusion occurs in the presence of a realistic (nonlinear) seawater equation of state, which introduces the processes of cabbeling and thermobaricity also discussed in VOLUME 5.

14.8.4 Summarizing the neutral relations

We here summarize the various relations for a neutral direction (infinitesimal displacement in a snapshot of the fluid) and a neutral trajectory (infinitesimal displacement within a transient fluid) by offering the geometrical perspective depicted in Figure 14.7.

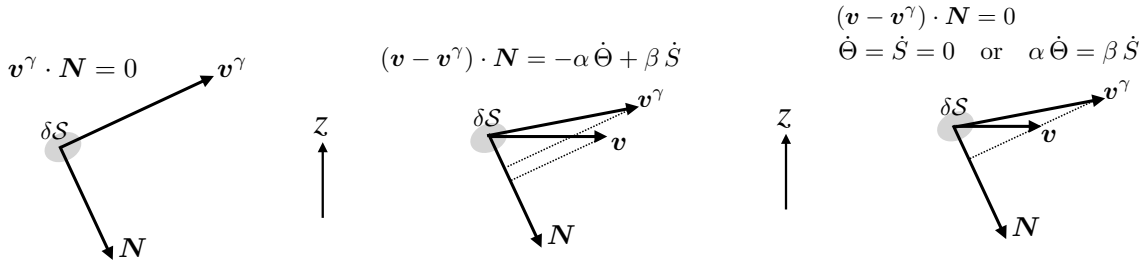


FIGURE 14.7: Depicting neutral directions and neutral trajectories. Left panel: for a time snapshot, as summarized by equation (14.88), then $\mathbf{v}^\gamma \cdot \dot{\gamma} = \mathbf{v}^\gamma \cdot \mathbf{N}/|\mathbf{N}| = 0$, thus defining the neutral trajectory as perpendicular to the dianeutral direction, with $\mathbf{N} = -\alpha \nabla \Theta + \beta \nabla S$. Middle panel: time dependent fluid with $(\mathbf{v} - \mathbf{v}^\gamma) \cdot \mathbf{N} = -\alpha \dot{\Theta} + \beta \dot{S}$ as per equation (14.89d). Right panel: time dependent fluid yet with either $\dot{\Theta} = \dot{S} = 0$, as when there are no irreversible mixing processes, or if those processes are compensated so that $\alpha \dot{\Theta} = \beta \dot{S}$, both of which render $(\mathbf{v}^\gamma - \mathbf{v}) \cdot \mathbf{N} = 0$.

Neutral direction

A neutral direction equals to a neutral trajectory in the special case of a static fluid, in which case Eulerian time derivatives vanish. In this case the constraint (14.77) reduces to the orthogonality condition

$$\delta \mathbf{x}^\gamma \cdot \dot{\gamma} = \delta t \mathbf{v}^\gamma \cdot \dot{\gamma} = 0. \quad (14.88)$$

Hence, for a static fluid, the neutral displacement, $\delta \mathbf{x}^\gamma = \delta t \mathbf{v}^\gamma$, and the corresponding neutral velocity, \mathbf{v}^γ , are everywhere orthogonal to the dianeutral vector, $\dot{\gamma}$. This condition is illustrated in the left panel of Figure 14.7.

Neutral trajectory

The conditions given in Sections 14.8.2 and 14.8.3 can be written in the following equivalent manners

$$\frac{D^\gamma \rho}{Dt} - \frac{\partial \rho}{\partial p} \frac{D^\gamma p}{Dt} = 0 \quad (14.89a)$$

$$-\alpha \frac{D^\gamma \Theta}{Dt} + \beta \frac{D^\gamma S}{Dt} = 0 \quad (14.89b)$$

$$-\alpha \partial_t \Theta + \beta \partial_t S + \mathbf{v}^\gamma \cdot (-\alpha \nabla \Theta + \beta \nabla S) = 0 \quad (14.89c)$$

$$(\mathbf{v} - \mathbf{v}^\gamma) \cdot \mathbf{N} = -\alpha \dot{\Theta} + \beta \dot{S}, \quad (14.89d)$$

with equation (14.89d) depicted by the right two panels of Figure 14.7. These equations reflect the need for a neutral trajectory, whose velocity is \mathbf{v}^γ , to weave its path within the time

dependent fluid environment. The special case with either $\dot{\Theta} = \dot{S} = 0$ (no irreversible processes) or $\alpha \dot{\Theta} = \beta \dot{S}$ (compensated irreversible processes) means that the neutral trajectory satisfies $(\mathbf{v} - \mathbf{v}^\gamma) \cdot \mathbf{N} = 0$, as depicted in the right panel of Figure 14.7.

14.8.5 Comments

By introducing time dependence we have enabled a step towards understanding how buoyancy works within an evolving fluid, thus moving beyond the time snapshot built into the neutral direction from Sections 14.5 and 14.7. Even so, the presentation in this section is limited in that it only considers infinitesimal excursions along a neutral trajectory. Indeed, this limitation is fundamental to the methods of neutral directions and neutral trajectories since they are designed to probe local buoyant forces; that is, the buoyancy of a test fluid element relative to its local environment. Moving beyond the infinitesimal trajectory leads to the concept of a test fluid element that remains coherent over a finite path while maintaining local mechanical equilibrium (i.e., pressure is equilibrated with the environment) and yet with fixed Θ and S . The finite trajectories for such fluid elements start along a neutral trajectory, but deviate upon moving further. [McDougall \(1987c\)](#) developed the mechanics of such fluid elements, with his study motivated by ocean coherent vortex structures such as reviewed by [McWilliams \(1985\)](#).

14.9 Pressure forces and vertical motion

As introduced in Section 11.2 and further detailed in Section 13.2, an approximate hydrostatic fluid is one in which the vertical pressure gradient locally balances the gravitational acceleration, with the horizontal gradient of hydrostatic pressure contributing to horizontal accelerations. Although vertical motion can occur in the approximately hydrostatic fluid, that motion is diagnosed rather than prognosed since the vertical momentum equation is reduced to local hydrostatic balance. For example, a diagnostic evaluation of the vertical velocity in a Boussinesq ocean is performed through vertically integrating the continuity equation, $\partial_z w = -\nabla_h \cdot \mathbf{u}$, along with the specification of w at one point within the vertical column.

As we see in equation (14.99c) derived below, the vertical derivative of the non-hydrostatic pressure is the only inviscid force contributing to a vertical acceleration. So even if the fluid satisfies the assumptions of approximate hydrostatic balance, it is the non-hydrostatic pressure force that enables vertical accelerations. That is, for the approximately hydrostatic fluid, the local hydrostatic balance holds, $\partial p / \partial z = -\rho g$, and yet there can still be a nonzero vertical acceleration, $Dw/Dt \neq 0$. This situation is directly analogous to the Boussinesq ocean as derived in Section 13.1. For the Boussinesq ocean, the prognostic velocity is non-divergent, $\nabla \cdot \mathbf{v} = 0$, and yet the fluid itself is compressible so that density has space and time variations, $D\rho/Dt \neq 0$.

We are concerned in this section with how pressure and gravity contribute to motion, and offer two methods to organize their accelerations starting from the momentum equation with the geopotential, $\Phi = g z$,

$$\rho D\mathbf{v}/Dt + 2\boldsymbol{\Omega} \times \rho \mathbf{v} = -\nabla p - g \rho \hat{\mathbf{z}} + \rho \mathbf{F}. \quad (14.90)$$

Analysis involving both methods serve complementary roles in understanding the nature of vertical accelerations.

14.9.1 Dynamically active and dynamically inactive pressures

Inspired by the formulation of the Boussinesq ocean equations in Section 13.1.1, we here organize the pressure and gravity accelerations by introducing a constant reference density, ρ_0 , along with a corresponding hydrostatically balanced reference pressure

$$p(\mathbf{x}, t) = p'(\mathbf{x}, t) + p_0(z) \quad \text{with} \quad dp_0/dz = -\rho_0 g. \quad (14.91)$$

By decomposing pressure as $p = p_0 + p'$, we expose the dynamically active portion of the pressure field, p' , by removing the dynamically inactive pressure, p_0 , from the momentum equation. Note that the dynamical pressure, p' , generally has both hydrostatic and non-hydrostatic contributions.

The decomposition (14.91) brings the pressure and gravity contributions on the right hand side of equation (14.90) into the form

$$\nabla p + \rho g \hat{\mathbf{z}} = \nabla p' - \rho_0 b \hat{\mathbf{z}}. \quad (14.92)$$

In this equation we introduced the globally referenced Archimedean buoyancy computed relative to the globally constant reference density, ρ_0 ,

$$b = -g(\rho - \rho_0)/\rho_0 = -g\rho'/\rho_0, \quad (14.93)$$

where

$$\rho' = \rho - \rho_0 \quad (14.94)$$

is the density deviation relative to the reference density.

14.9.2 Hydrostatic and non-hydrostatic pressures

The second decomposition of the pressure and gravity forces in equation (14.90) is based on splitting into a local hydrostatic pressure, p_h , and a non-hydrostatic pressure, p_{nh} ,

$$p = p_h + p_{nh} \quad \text{with} \quad \partial p_h / \partial z = -\rho g. \quad (14.95)$$

This decomposition is particularly useful when concerned with deviations from a local hydrostatic balance, which is central to the current analysis. However, it does not remove the global hydrostatic background pressure (i.e., the dynamically inactive pressure, $p_0(z)$), which can be seen by the identity

$$\partial p_h / \partial z = dp_0(z) / dz - \rho' g = dp_0(z) / dz + \rho_0 b. \quad (14.96)$$

With the pressure decomposition (14.95), the pressure and gravity contributions to the equation of motion take on the form

$$\nabla p + \rho g \hat{\mathbf{z}} = \nabla(p_h + p_{nh}) + \rho g \hat{\mathbf{z}} \quad (14.97a)$$

$$= \nabla_h(p_h + p_{nh}) + (\partial_z p_{nh} + \partial_z p_h + \rho g) \hat{\mathbf{z}} \quad (14.97b)$$

$$= \nabla_h p + \hat{\mathbf{z}} \partial_z p_{nh} \quad (14.97c)$$

$$= \nabla p_{nh} + \nabla_h p_h. \quad (14.97d)$$

Be mindful that the non-hydrostatic pressure is operated on by the full gradient operator, ∇ , whereas the hydrostatic pressure has just the horizontal gradient, ∇_h .

14.9.3 Momentum equation for the Boussinesq ocean

To further study how pressure and gravity lead to vertical motion, we find it convenient to assume a Boussinesq ocean so that the momentum equation (14.90) takes the form of equation (13.61)

$$\rho_o D\mathbf{v}/Dt + 2\boldsymbol{\Omega} \times \rho_o \mathbf{v} = -\nabla p - \rho g \hat{\mathbf{z}} + \rho_o \mathbf{F} \quad (14.98a)$$

$$= -\nabla p' + \rho_o b \hat{\mathbf{z}} + \rho_o \mathbf{F} \quad (14.98b)$$

$$= -\nabla p_{nh} - \nabla_h p_h + \rho_o \mathbf{F}. \quad (14.98c)$$

Focusing on the vertical velocity equation exposes processes leading to vertical accelerations of a fluid element (i.e., the vertical Lagrangian acceleration, Dw/Dt)

$$\rho_o Dw/Dt + \hat{\mathbf{z}} \cdot (2\boldsymbol{\Omega} \times \rho_o \mathbf{v}) = -\partial_z p - \rho g + \rho_o \mathbf{F} \cdot \hat{\mathbf{z}} \quad (14.99a)$$

$$= -\partial_z p' + \rho_o b + \rho_o \mathbf{F} \cdot \hat{\mathbf{z}} \quad (14.99b)$$

$$= -\partial_z p_{nh} + \rho_o \mathbf{F} \cdot \hat{\mathbf{z}}, \quad (14.99c)$$

In addition to the Coriolis acceleration on the left hand side, equation (14.99b) reveals that the vertical Lagrangian acceleration has contributions from the globally referenced Archimedean buoyancy, b , along with vertical gradients in the dynamical pressure, p' . From equation (14.99c) we see that the vertical Lagrangian acceleration has an inviscid contribution that arises solely from vertical derivatives in the non-hydrostatic pressure, p_{nh} . Note that when making either the tangent plane approximation (Section 8.5) or the traditional approximation (Section 11.1.3), the Coriolis acceleration is absent from the vertical momentum equation. The reason is that for both the tangent plane and the traditional approximation, the rotating reference frame is assumed to have an angular velocity oriented according to the local vertical, $\boldsymbol{\Omega} = \Omega \hat{\mathbf{z}}$.

14.10 Case study: test fluid elements in a homogeneous fluid

In this section we examine a case study focused on the motion of a test fluid element with nonzero Archimedean buoyancy and in the absence of mixing.²¹ We assume a tangent plane so that the Coriolis acceleration does not appear in the vertical momentum equation. Also, to avoid questions about local versus global buoyancy, and the associated questions about neutral directions, we assume the fluid environment has a constant and uniform density, ρ . A buoyancy force acts on the test fluid element if the fluid element has a density distinct from the environmental density.

In pursuing this analysis it is important to appreciate the nature of the corresponding thought experiments. Namely, we place a test fluid element somewhere in a prescribed fluid environment and examine how the environmental forces affect motion of the test fluid element. Importantly, we assume the environment is unaffected by the test fluid element, so that the contact forces remain fixed and prescribed. That is, the pressure and friction forces are unaffected by the test fluid element. This assumption is mechanically inconsistent since all fluid

²¹As noted in our study of fluid kinematics in VOLUME 1, in the absence of mixing then a fluid element is the same as a fluid parcel.

regions, no matter how small, affect the surrounding environment. Even so, results from the analysis are borne out for situations where we can safely ignore the environmental perturbations of real fluid elements. The analysis offers a useful warm-up to the study of effective buoyancy in Section 14.11.

14.10.1 Equations of motion

The equation of motion for a fluid element is given by

$$\rho D\mathbf{v}/Dt + 2\Omega \hat{\mathbf{z}} \times \rho \mathbf{v} = -\nabla p - g \rho \hat{\mathbf{z}} + \rho \mathbf{F}, \quad (14.100)$$

whereas the equation of motion for a test fluid element is

$$\rho^{\text{tfe}} \dot{\mathbf{v}}^{\text{tfe}} + 2\Omega \hat{\mathbf{z}} \times \rho^{\text{tfe}} \mathbf{v}^{\text{tfe}} = -\nabla p - g \rho^{\text{tfe}} \hat{\mathbf{z}} + \rho^{\text{tfe}} \mathbf{F}, \quad (14.101)$$

where ρ^{tfe} is the density of the test fluid element, \mathbf{v}^{tfe} is its velocity, and $\dot{\mathbf{v}}^{\text{tfe}}$ is its acceleration.²² As per our assumption stated earlier, both the pressure gradient and friction vector are the same for the fluid element and the test fluid element.

14.10.2 Exact hydrostatic environment

Consider a test fluid element in a fluid that is in exact hydrostatic equilibrium, so that there is no fluid motion. The test fluid element can only move vertically since all horizontal forces vanish. The vertical component of equation (14.101) yields

$$\rho^{\text{tfe}} \dot{w}^{\text{tfe}} = -dp/dz - g \rho^{\text{tfe}}. \quad (14.102)$$

The assumed exact hydrostatic background pressure gradient satisfies $dp/dz = -\rho g$, so that the test fluid element accelerates vertically according to

$$\rho^{\text{tfe}} \dot{w}^{\text{tfe}} = b \rho, \quad (14.103)$$

where we introduced the Archimedean buoyancy for the test fluid element, computed relative to the environmental fluid,

$$b = -g(\rho^{\text{tfe}} - \rho)/\rho. \quad (14.104)$$

Evidently, the test fluid element accelerates upward if it is lighter than the environment ($b > 0$), downward if heavier ($b < 0$), and remains stationary if neutrally buoyant ($b = 0$). This result accords with the study of Archimedean buoyancy from earlier sections.

14.10.3 An accelerating yet non-rotating environment

In VOLUME 1 we studied particle mechanics as viewed from an accelerated reference frame that is not rotating, such as for motion viewed in an accelerating train moving along a straight track. Here we place a tank of fluid (e.g., a tank of water) on a train car that experiences acceleration, \mathbf{A}^{tank} , such as depicted in Figure 14.8. Following the classical particle mechanics discussion in VOLUME 1, we find the equation of motion for the fluid in the tank is

$$\rho D\mathbf{v}/Dt = -\nabla p - \rho(g \hat{\mathbf{z}} + \mathbf{A}^{\text{tank}}) + \rho \mathbf{F}. \quad (14.105)$$

²²We write the acceleration as $\dot{\mathbf{v}}^{\text{tfe}}$ rather than $D\mathbf{v}^{\text{tfe}}/Dt$ since we are concerned with the motion of just a single test fluid element rather than a field of fluid elements.

We refer to $-\mathbf{A}^{\text{tank}}$ as the **non-inertial acceleration** that arises from the tank acceleration, and with $-\rho \mathbf{A}^{\text{tank}}$ the corresponding non-inertial force per volume acting on the fluid.²³ As a result of the non-inertial force, fluid piles up on the back side of the tank and is depleted from the front.

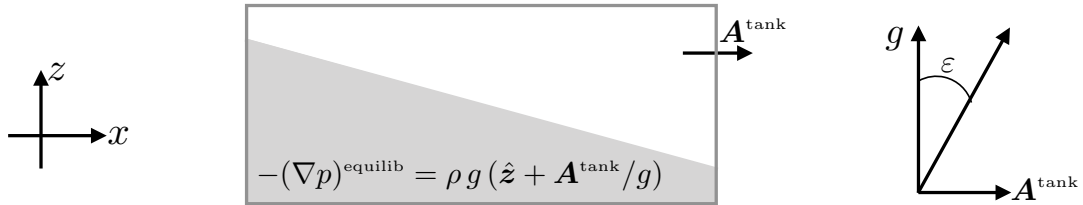


FIGURE 14.8: Left panel: A tank of homogeneous water on a train accelerating along a horizontal straight track, thus resulting in a pile up of the water at the back of the tank and depletion in the front. The water reaches a static equilibrium ($\mathbf{v} = 0$) when the pressure gradient acceleration balances both the gravitational acceleration and the train acceleration, $-(\nabla p)^{\text{equilib}} = \rho g (\hat{\mathbf{z}} + \mathbf{A}^{\text{tank}}/g)$. Right panel: Vector diagram for a positively buoyant test fluid element, with contributions from vertical buoyant acceleration and horizontal pressure gradient acceleration. The net acceleration on the test element acts at an angle to the vertical that is determined by the gravitational and train acceleration, making a slope, $\tan \varepsilon = |\mathbf{A}^{\text{tank}}|/g$, with the vertical. Notably, the positively buoyant test fluid element is accelerated vertically upward and horizontally in the *same* direction as the train's acceleration, whereas a negatively buoyant test fluid element is accelerated vertically downward and horizontally in the *opposite* direction as the acceleration. This thought experiment is readily verified by a helium balloon tied to the floor of an accelerating car, or a pendulum tied to the ceiling of the car.

The difference in fluid depth within the tank leads to a horizontal pressure gradient, with higher pressure at the back of the tank and lower in the front. There is no fluid motion (relative to the tank) if there is a balance between the horizontal pressure gradient and the tank acceleration, as well as a balance between the vertical pressure gradient and gravity,

$$-(\nabla p)^{\text{equilib}} = \rho g (\hat{\mathbf{z}} + \mathbf{A}^{\text{tank}}/g). \quad (14.106)$$

We can consider this result as exact hydrostatic balance but with a modified gravitational acceleration.²⁴

Motion of the test fluid element satisfies the equation

$$\rho^{\text{tfe}} \dot{\mathbf{v}}^{\text{tfe}} = -\nabla p - \rho^{\text{tfe}} (g \hat{\mathbf{z}} + \mathbf{A}^{\text{tank}}) + \rho^{\text{tfe}} \mathbf{F}. \quad (14.107)$$

Now consider the test fluid element that feels the equilibrated pressure gradient according to equation (14.106), in which case

$$\rho^{\text{tfe}} \dot{\mathbf{v}}^{\text{tfe}} = (\rho - \rho^{\text{tfe}}) (g \hat{\mathbf{z}} + \mathbf{A}^{\text{tank}}) = b \rho (\hat{\mathbf{z}} + \mathbf{A}^{\text{tank}}/g) = -(b/g) (\nabla p)^{\text{equilib}}. \quad (14.108)$$

Note that there is no frictional acceleration when there is no fluid motion, thus allowing us to set $\mathbf{F} = 0$. Evidently, the test fluid element accelerates along a line that is perpendicular to surfaces of constant pressure, thus making an angle with the vertical given by

$$\tan \varepsilon = |\mathbf{A}^{\text{tank}}|/g. \quad (14.109)$$

Acceleration of a positively buoyant test fluid element is sloped in the same direction as the

²³The minus sign accords with being pushed backward into a seat when a vehicle accelerates forward.

²⁴The principle of equivalence says we cannot distinguish between the acceleration of a reference frame and the acceleration from gravity. The result (14.106) supports this equivalence.

accelerating train, with this result readily verified by attaching a helium balloon to the floor of a train or car. Acceleration of the negatively buoyant test fluid element is sloped in the opposite direction as the accelerating train. This result accords with the discussion in VOLUME 1, in which a pendulum at rest in the accelerated train slopes opposite to the acceleration.

14.10.4 Rotating tank

In Section 11.5 we studied the motion of a homogeneous fluid in a rotating tank, whose equation of motion in the rotating reference frame is given by equation (11.96)

$$\rho \frac{D\mathbf{v}}{Dt} + 2\Omega \hat{\mathbf{z}} \times \rho \mathbf{v} = -\nabla [p + g z \rho - \Omega^2 \rho (x^2 + y^2)/2] + \rho \mathbf{F}. \quad (14.110)$$

The analogous equation for the test fluid element, again written in the rotating reference frame, is given by

$$\rho^{\text{tfe}} \dot{\mathbf{v}}^{\text{tfe}} + 2\Omega \hat{\mathbf{z}} \times \rho^{\text{tfe}} \mathbf{v}^{\text{tfe}} = -\nabla [p + g z \rho^{\text{tfe}} - \Omega^2 \rho^{\text{tfe}} (x^2 + y^2)/2] + \rho^{\text{tfe}} \mathbf{F}, \quad (14.111)$$

where we evaluate the position, $\mathbf{x} = \hat{\mathbf{x}} x + \hat{\mathbf{y}} y + \hat{\mathbf{z}} z$, according to the position of the test fluid element. At mechanical equilibrium, the fluid rotates as a rigid-body ($\mathbf{v} = 0$) with a parabolic free surface where the free surface is higher at the outer rim of the tank and lowest at the center. Furthermore, as the motion is rigid-body, the viscous friction vanishes. We thus find that the pressure gradient in the rigid-body rotating equilibrium satisfies

$$-(\nabla p)^{\text{equilb}} = \rho \nabla [g z - \Omega^2 (x^2 + y^2)/2] = g \rho [\hat{\mathbf{z}} - \Omega^2 (x \hat{\mathbf{x}} + y \hat{\mathbf{y}})/g] \equiv -\rho \mathbf{g}^{\text{rotate}}, \quad (14.112)$$

where the final equality defined the gravitational vector, $\mathbf{g}^{\text{rotate}}$, arising from the sum of the geopotential (central earth gravity plus planetary centrifugal) plus the centrifugal acceleration from the rotating tank. When placed in this mechanically equilibrated fluid environment, the test fluid element equation of motion (14.111) becomes

$$\rho^{\text{tfe}} \dot{\mathbf{v}}^{\text{tfe}} + 2\Omega \hat{\mathbf{z}} \times \rho^{\text{tfe}} \mathbf{v}^{\text{tfe}} = b \rho [\hat{\mathbf{z}} - \Omega^2 (\hat{\mathbf{x}} x + \hat{\mathbf{y}} y)/g] = -(\rho - \rho^{\text{tfe}}) \mathbf{g}^{\text{rotate}}. \quad (14.113)$$

Evidently, a positively buoyant test fluid element accelerates upward and toward the center of the tank. Furthermore, as it moves horizontally toward the tank center, the test fluid element picks up a Coriolis acceleration that deflects it to the right for counter-clockwise rotating tanks.

For the test fluid element, the ratio of the magnitudes of its Coriolis acceleration to the centrifugal acceleration is

$$\frac{\text{Coriolis}}{\text{centrifugal}} = \frac{2\rho^{\text{tfe}}}{\rho} \frac{g}{b} \frac{|\mathbf{u}^{\text{tfe}}|}{\Omega \sqrt{x^2 + y^2}} = \frac{2\rho^{\text{tfe}}}{\rho - \rho^{\text{tfe}}} \frac{|\mathbf{u}^{\text{tfe}}|}{\Omega \sqrt{x^2 + y^2}}. \quad (14.114)$$

Heavy test fluid elements, with small buoyancy, move toward the outer edge of the tank due to dominance of the centrifugal acceleration, whereas lighter test fluid elements concentrate toward the center. We can further reduce the influence of the Coriolis acceleration by changing the geometry to that of a long test tube to thus reduce $|\mathbf{u}^{\text{tfe}}|$, with this geometry used for centrifuges.

Is there a dynamically consistent motion in which the test fluid element has exactly zero horizontal material acceleration, $\dot{\mathbf{u}}^{\text{tfe}} = 0$? For this motion to occur requires a balance between

the Coriolis and centrifugal accelerations

$$2\Omega\rho^{tfe}(\hat{z}\times\mathbf{u}^{tfe})=-(b\rho\Omega^2/g)(\hat{x}x+\hat{y}y)\implies\mathbf{u}^{tfe}=[b\rho/(2g\rho^{tfe})](\boldsymbol{\Omega}\times\mathbf{x}). \quad (14.115)$$

However, this velocity field does not, in fact, have a zero acceleration since

$$\dot{\mathbf{u}}^{tfe}=[b\rho/(2g\rho^{tfe})](\boldsymbol{\Omega}\times\mathbf{u}^{tfe})\neq 0. \quad (14.116)$$

We conclude that there is no self-consistent free motion with $\dot{\mathbf{u}}^{tfe}=0$, much like the case of the test fluid element moving in the accelerating train studied in Section 14.10.3.

14.11 Effective buoyancy and vertical accelerations

In this section, we extend the discussion of Archimedean buoyancy by focusing on the vertical forces acting on a real fluid element, or more generally a finite sized fluid region, rather than on a test fluid element. To do so requires us to study, in some detail, the various forces appearing in the momentum equation. As a means to conceptually organize these forces, we introduce **static forces**, which are those forces not associated with fluid motion, plus **motional forces**, which are forces not associated with density inhomogeneities. Motional forces are specific to details of the velocity field, whereas static forces are deduced just from knowledge of the density field.

Effective buoyancy arises from the **static forces** acting on a fluid element. Although the effective buoyancy is in part comprised of Archimedean buoyancy, there are distinctions that arise through interactions between the fluid element and its surrounding environment. These interactions depend on the shape of the fluid region. As shown in this section (see in particular Figure 14.9), we find that fluid regions of different geometric shape can have different effective buoyancy even while they have the same Archimedean buoyancy.

To facilitate the analysis in this section, we consider a Boussinesq ocean, with the analysis also directly relevant to an anelastic atmosphere as considered by [Jeevanjee and Romps \(2015b\)](#). As explored in Section 13.3, pressure in a Boussinesq ocean constrains the velocity field to remain non-divergent. Furthermore, Boussinesq ocean pressure satisfies an the Poisson equation (an elliptic boundary value problem). We can decompose the pressure sources in the Poisson equation into physically distinct processes and the examine the associated pressure field. The task for this section is to derive the Poisson equations according to the various pressure sources, and then to discuss the physics of their associated vertical accelerations.

14.11.1 Poisson equations for $p'=p'_{buoy}+p'_{flow}$

The two decompositions of pressure described in Sections 14.9.1 and 14.9.2, as reflected in the Boussinesq velocity equations from Section 14.9.3, render two sets of corresponding Poisson equations for pressure. We here focus on the decomposition (14.98b), where the pressure and gravity accelerations appear in terms of the Archimedean buoyancy plus perturbation pressure. We defer until Section 14.11.3 an examination of the alternative decomposition into the local hydrostatic and non-hydrostatic pressures given by equation (14.98c).

Boundary value problem for the perturbation pressure, p'

We start by considering the Boussinesq momentum equation (14.98b)

$$\rho_0 (\partial_t + \mathbf{v} \cdot \nabla) \mathbf{v} + 2\boldsymbol{\Omega} \times \rho_0 \mathbf{v} = -\nabla p' + \rho_0 b \hat{\mathbf{z}} + \rho_0 \mathbf{F}. \quad (14.117)$$

As detailed in Section 13.3.1, the time tendency is eliminated by computing the divergence of this equation to render the Poisson equation for the perturbation pressure

$$-\nabla^2 p' = \rho_0 \nabla \cdot \mathbf{G}' = \rho_0 \nabla \cdot [(\mathbf{v} \cdot \nabla) \mathbf{v} + 2\boldsymbol{\Omega} \times \mathbf{v} - b \hat{\mathbf{z}} - \mathbf{F}], \quad (14.118)$$

where we introduced the vector,

$$\mathbf{G}' = (\mathbf{v} \cdot \nabla) \mathbf{v} + 2\boldsymbol{\Omega} \times \mathbf{v} - b \hat{\mathbf{z}} - \mathbf{F}, \quad (14.119)$$

whose divergence renders a source for the pressure field. We find it convenient to carry around a minus sign on the Laplacian operator since a positive source, $\rho_0 \nabla \cdot \mathbf{G}' > 0$, leads to a locally positive pressure signal (see Section 13.3.1 for more details on this point).

We require boundary conditions to fully specify the pressure, and for simplicity we assume material boundaries. In this case, the analysis considered in Section 13.3.2 renders the Neumann boundary condition

$$\hat{\mathbf{n}} \cdot \nabla p' = -\rho_0 \hat{\mathbf{n}} \cdot \mathbf{G}', \quad (14.120)$$

where $\hat{\mathbf{n}}$ is the outward normal along the boundary. We further simplify the analysis by assuming flat and rigid top and bottom boundaries along with horizontal boundaries that are either doubly periodic or infinite. Hence, along the top boundary, where $\hat{\mathbf{n}} = \hat{\mathbf{z}}$, pressure satisfies the Neumann boundary condition

$$\partial_z p' = -\rho_0 \hat{\mathbf{z}} \cdot \mathbf{G}' = \rho_0 (b + \mathbf{F} \cdot \hat{\mathbf{z}}) \quad \text{top boundary.} \quad (14.121)$$

To reach this result we noted that

$$\hat{\mathbf{z}} \cdot [(\mathbf{v} \cdot \nabla) \mathbf{v}] = (\mathbf{v} \cdot \nabla) (\hat{\mathbf{z}} \cdot \mathbf{v}) = 0, \quad (14.122)$$

since $\hat{\mathbf{z}} \cdot \mathbf{v} = w = 0$ along a rigid and material flat surface. The analogous result holds along the bottom boundary where $\hat{\mathbf{n}} = -\hat{\mathbf{z}}$ so that

$$\partial_z p' = \rho_0 \hat{\mathbf{z}} \cdot \mathbf{G}' = -\rho_0 (b + \mathbf{F} \cdot \hat{\mathbf{z}}) \quad \text{bottom boundary.} \quad (14.123)$$

Buoyancy induced pressure and flow induced pressure

The Laplacian operator is linear, with linearity affording the freedom to decompose the source in the Poisson equation (14.118), $\rho_0 \nabla \cdot \mathbf{G}'$, into physically distinct processes and then studying the pressures resulting from these processes. For this purpose we choose the following decomposition

$$-\nabla^2 p' \equiv -\nabla^2 (p'_{\text{buoy}} + p'_{\text{flow}}) \quad (14.124a)$$

$$-\nabla^2 p'_{\text{buoy}} = -\rho_0 \partial_z b \quad (14.124b)$$

$$-\nabla^2 p'_{\text{flow}} = \rho_0 \nabla \cdot [(\mathbf{v} \cdot \nabla) \mathbf{v} + 2\boldsymbol{\Omega} \times \mathbf{v} - \mathbf{F}]. \quad (14.124c)$$

The source term for the buoyancy pressure, p'_{buoy} , only involves the vertical derivative of the Archimedean buoyancy. Hence, there is no direct contribution from fluid motion on p'_{buoy} , with fluid motion only affecting p'_{buoy} indirectly through effects on $\partial_z b$. The converse holds for the pressure perturbation, p'_{flow} , which is sourced by fluid motion that gives rise to accelerations from self-advection, Coriolis, and friction. Hence, there is no direct impact from Archimedean buoyancy on p'_{flow} . The Neumann boundary conditions for these two pressures follows from the boundary conditions (14.121) and (14.123). For example, along the top boundary we have

$$\partial_z p'_{\text{buoy}} = \rho_0 b \quad \text{and} \quad \partial_z p'_{\text{flow}} = \rho_0 \hat{\mathbf{z}} \cdot \mathbf{F} \quad \text{top boundary conditions,} \quad (14.125)$$

with the same conditions holding along the bottom yet with a minus sign on the right hand side.

14.11.2 Accelerations from effective buoyancy and fluid motion

Having established the Poisson equations for the variety of pressures in Section 14.11.1, we now examine contributions to the vertical Lagrangian acceleration as given by equations (14.99b) and (14.99c). Emulating the decomposition used for pressure, we here decompose the vertical acceleration into conceptually distinct contributions from buoyancy and from fluid flow.

Vertical acceleration from effective buoyancy

Effective buoyancy is the first contribution to vertical Lagrangian acceleration, which is the vertical acceleration arising solely from the instantaneous mass/density field. Operationally, we deduce the effective buoyancy by instantaneously setting velocity to zero everywhere in the expression for the vertical acceleration

$$b^{\text{eff}} \equiv \left. \frac{Dw}{Dt} \right|_{v=0}. \quad (14.126)$$

Two conclusions follow directly from the operational definition of b^{eff} . First, as viscous friction only arises when there is relative fluid motion that lead to strains (Section 9.6.6), viscous friction does not contribute to the effective buoyancy. Next, we observe that any direct role for pressure in b^{eff} arises solely from the buoyancy pressure, p'_{buoy} . We make this conclusion since the Poisson equation (14.127) for the buoyancy pressure has a source that only depends on the instantaneous Archimedean buoyancy field, whereas it ignores all contributions from fluid flow. This dependence is precisely that defined for b^{eff} .

From the definition (14.126) we make use of equations (14.99b) and (14.99c) to unpack the variety of contributions to effective buoyancy

$$\rho_0 b^{\text{eff}} = \rho_0 b - \partial_z p' \Big|_{v=0} = -\partial_z p_{\text{nh}} \Big|_{v=0}. \quad (14.127)$$

The first equality identifies the difference between the effective buoyancy and the Archimedean buoyancy

$$\rho_0 (b^{\text{eff}} - b) = -\partial_z p'_{\text{buoy}}, \quad (14.128)$$

in which we set

$$\partial_z p' \Big|_{v=0} = \partial_z p_{\text{buoy}} \quad (14.129)$$

as per the discussion below equation (14.126). So equation (14.128) states that in the presence of a vertical gradient in the buoyancy pressure, then the Archimedean buoyancy is an incomplete

description of the vertical acceleration associated with the density field.

Equation (14.127) also reveals that the effective buoyancy is associated with that portion of the vertical gradient in the non-hydrostatic pressure that remains when $\mathbf{v} = 0$

$$\rho_o b^{\text{eff}} = -\partial_z p_{\text{nh}}|_{\mathbf{v}=0}. \quad (14.130)$$

This equation provides a generalization of the local hydrostatic balance, $\rho_o b = \partial_z(p_h - p_o)$ (equation (14.96)), so that we have the correspondence

$$\underbrace{\rho_o b = \partial_z(p_h - p_o)}_{\text{hydrostatic}} \longleftrightarrow \underbrace{\rho_o b^{\text{eff}} = -\partial_z p_{\text{nh}}|_{\mathbf{v}=0}}_{\text{non-hydrostatic}}. \quad (14.131)$$

Vertical acceleration from fluid flow

If one introduces an Archimedean buoyancy anomaly in a static fluid, then the initial vertical acceleration acting on the anomaly is given by its effective buoyancy, with this result following from the definition of effective buoyancy in equation (14.126). However, as the anomaly evolves, fluid motion is generated, at which point effective buoyancy is an incomplete measure of vertical acceleration. So in the presence of fluid motion we must also consider another term referred to as the **flow-induced vertical acceleration** or **motional forces**. Operationally, we deduce the flow-induced vertical acceleration by setting the density to a constant within the expression for the vertical acceleration

$$A_{\text{flow}} \equiv \frac{Dw}{Dt} \Big|_{\rho=\rho_o}. \quad (14.132)$$

As for the effective buoyancy in equation (14.126), the right hand side of equation (14.132) is evaluated using the full flow field at an instant, but with the accelerations evaluated with constant density at that instance. Since the Archimedean buoyancy vanishes when density has the uniform value, we know that

$$\rho_o A_{\text{flow}} = -\partial_z p'|_{\rho=\rho_o} + \rho_o \mathbf{F} \cdot \hat{\mathbf{z}} = -\partial_z p_{\text{nh}}|_{\rho=\rho_o} + \rho_o \mathbf{F} \cdot \hat{\mathbf{z}}. \quad (14.133)$$

Consequently, when the density field is uniform, $\rho = \rho_o$, then the vertical gradient of p' and p_{nh} are identical

$$\partial_z p'|_{\rho=\rho_o} = \partial_z p_{\text{nh}}|_{\rho=\rho_o}. \quad (14.134)$$

Furthermore, we identify the vertical gradient in $\partial_z p'|_{\rho=\rho_o}$ with the vertical gradient in the flow induced pressure, p'_{flow} , that satisfies the Poisson equation (14.124c). We thus have the identities

$$\partial_z p'|_{\rho=\rho_o} = \partial_z p'_{\text{flow}} = \partial_z p_{\text{nh}}|_{\rho=\rho_o}. \quad (14.135)$$

14.11.3 Boundary value problems for the accelerations

Following from the discussion in Section 14.11.2, we here derive the boundary value problems for the effective buoyancy and the flow induced acceleration.

Poisson equations for b^{eff} and A_{flow}

From equation (14.128) for the effective buoyancy and from the Poisson equation (14.124b) for the buoyancy pressure, we arrive at the Poisson equation for the effective buoyancy

$$\rho_0 b^{\text{eff}} = \rho_0 b - \partial_z p'_{\text{buoy}} \quad \text{and} \quad -\nabla^2 p'_{\text{buoy}} = -\rho_0 \partial_z b \implies -\nabla^2 b^{\text{eff}} = -\nabla_h^2 b. \quad (14.136)$$

Hence, the source for the effective buoyancy is the horizontal Laplacian of the Archimedean buoyancy. Correspondingly, the source for the difference, $b^{\text{eff}} - b$, is the vertical Laplacian of the Archimedean buoyancy

$$-\nabla^2(b^{\text{eff}} - b) = \partial_{zz} b. \quad (14.137)$$

We similarly derive the Poisson equation for the motional acceleration by making use of its operational definition (14.133) as well as the Poisson equation (14.124c) for the flow pressure

$$\begin{aligned} \rho_0 A_{\text{flow}} &= -\partial_z p'_{\text{flow}} + \rho_0 \mathbf{F} \cdot \hat{\mathbf{z}} \quad \text{and} \quad -\nabla^2 p'_{\text{flow}} = \rho_0 \nabla \cdot [(\mathbf{v} \cdot \nabla) \mathbf{v} + 2\boldsymbol{\Omega} \times \mathbf{v} - \mathbf{F}] \\ &\implies -\nabla^2 A_{\text{flow}} = -\partial_z \nabla \cdot [(\mathbf{v} \cdot \nabla) \mathbf{v} + 2\boldsymbol{\Omega} \times \mathbf{v} - \mathbf{F}] - \nabla^2(\mathbf{F} \cdot \hat{\mathbf{z}}). \end{aligned} \quad (14.138)$$

Boundary conditions

To completely specify the decomposition of vertical acceleration requires boundary conditions for the effective buoyancy, b^{eff} , and the motional acceleration, A_{flow} . Following our discussion of the Poisson equations in Section 14.11.1, we here only consider rigid and flat material upper and lower boundaries with no boundaries for the horizontal domain (either periodic or infinite horizontal domain). At the upper and lower boundaries we have $Dw/Dt = 0$, and this boundary condition holds whether $\mathbf{v} = 0$ or $\rho = \rho_0$, so that

$$b^{\text{eff}} = 0 \quad \text{and} \quad A_{\text{flow}} = 0 \quad \text{on rigid and flat boundaries.} \quad (14.139)$$

We are thus ensured that the net vertical acceleration is indeed the sum

$$\frac{Dw}{Dt} = A_{\text{flow}} + b^{\text{eff}}. \quad (14.140)$$

Poisson equation for the local non-hydrostatic pressure

We can also arrive at the above results by considering the momentum equation (14.98c) written using the decomposition of pressure into its local non-hydrostatic and local hydrostatic components

$$\rho_0 (\partial_t + \mathbf{v} \cdot \nabla) \mathbf{v} + 2\boldsymbol{\Omega} \times \rho_0 \mathbf{v} = -\nabla p_{nh} - \nabla_h p_h + \rho_0 \mathbf{F}. \quad (14.141)$$

A divergence of this equation leads to the Poisson equation for the non-hydrostatic pressure

$$-\nabla^2 p_{nh} = \nabla_h^2 p_h + \rho_0 \nabla \cdot [(\mathbf{v} \cdot \nabla) \mathbf{v} + 2\boldsymbol{\Omega} \times \mathbf{v} - \mathbf{F}]. \quad (14.142)$$

Taking a vertical derivative and use of the hydrostatic relation leads to the Poisson equation for the vertical derivative of the non-hydrostatic pressure

$$-\nabla^2(\partial_z p_{nh}) = -g \nabla_h^2 \rho + \rho_0 \partial_z \nabla \cdot [(\mathbf{v} \cdot \nabla) \mathbf{v} + 2\boldsymbol{\Omega} \times \mathbf{v} - \mathbf{F}]. \quad (14.143)$$

Setting $\mathbf{v} = 0$ in equation (14.142) renders the Poisson equation

$$-(\nabla^2 p_{nh})_{\mathbf{v}=0} = \nabla_h^2 p_h. \quad (14.144)$$

This equation says that the static portion of the non-hydrostatic pressure is sourced by the horizontal Laplacian of the hydrostatic pressure. Equivalently, the convergence of $(\nabla p_{nh})_{\mathbf{v}=0}$ is balanced by the divergence of the horizontal hydrostatic pressure gradient, $\nabla_h p_h$. Furthermore, setting $\mathbf{v} = 0$ in equation (14.143) yields the Poisson equation for the effective buoyancy

$$-\rho \nabla^2 b^{\text{eff}} = g \nabla_h^2 \rho \iff \nabla^2 b^{\text{eff}} = \nabla_h^2 b, \quad (14.145)$$

which accords with equation (14.136).

14.11.4 Relative scales for effective and Archimedean buoyancies

One way to emphasize the distinction between the effective buoyancy equation (14.145) and that for the Archimedean buoyancy is to compare their two elliptic equations

$$-\rho \nabla^2 b = g \nabla^2 \rho \quad \text{and} \quad -\rho \nabla^2 b^{\text{eff}} = g \nabla_h^2 \rho, \quad (14.146)$$

with the first equality following trivially by definition of Archimedean buoyancy, $b = -(g/\rho_0)(\rho - \rho_0)$. The different Laplacian operators acting on the source terms for b^{eff} and b means that these two buoyancy fields have different scales.

As an example of the distinct scales for b^{eff} and b , consider a cylindrically shaped Archimedean buoyancy anomaly (Figure 14.9) of scale B and with diameter D and height H . Given this information we seek a corresponding scale for the effective buoyancy, B_{eff} . Using the relation (14.145), and the cylindrical-polar coordinate version of the Laplacian operator from VOLUME 1, we have

$$\nabla^2 b^{\text{eff}} = \frac{1}{r} \frac{\partial}{\partial r} \left[r \frac{\partial b^{\text{eff}}}{\partial r} \right] + \frac{1}{r^2} \frac{\partial^2 b^{\text{eff}}}{\partial \vartheta^2} + \frac{\partial^2 b^{\text{eff}}}{\partial z^2} \quad \text{and} \quad \nabla_h^2 b = \frac{1}{r} \frac{\partial}{\partial r} \left[r \frac{\partial b}{\partial r} \right] + \frac{1}{r^2} \frac{\partial^2 b}{\partial \vartheta^2}, \quad (14.147)$$

where r is the radial distance from the cylinder axis, z the vertical coordinate along the cylinder axis, and ϑ the polar coordinate. We thus find the scalings

$$\nabla^2 b^{\text{eff}} \sim B_{\text{eff}} (D^{-2} + H^{-2}) \quad \text{and} \quad \nabla_h^2 b \sim B D^{-2}, \quad (14.148)$$

so that for a given Archimedean buoyancy anomaly scale, B , we find an associated effective buoyancy scale

$$B_{\text{eff}} = \frac{B}{1 + D^2/H^2}. \quad (14.149)$$

Evidently, the effective buoyancy scale is smaller than the Archimedean buoyancy scale. The effective buoyancy scale is smaller due to the pressure contribution that slows down any buoyant fluid element, with this pressure induced environmental back-reaction missing from the Archimedean buoyancy. Also observe that the effective buoyancy decreases when the ratio D/H increases. As a result, wide and flat “pancake” shaped buoyancy anomalies rise slower (with $B > 0$) than narrow “rocket shaped” anomalies. This result follows since a flat pancake anomaly must push aside more surrounding fluid as it moves vertically, whereas the narrow rocket shaped anomaly is more streamlined and thus more readily rises or falls.

As a buoyant fluid element moves vertically, it must displace the surrounding environmental

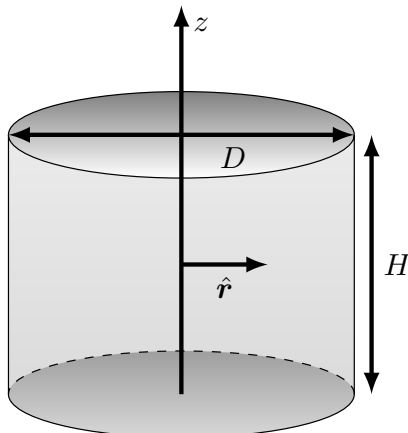


FIGURE 14.9: An Archimedean buoyancy anomaly of scale B here configured in the shape of a cylinder with diameter D and height H . Also shown are the vertical, z , and radial, r , axes for cylindrical-polar coordinates. In equation (14.149) we find the effective buoyancy for this anomaly scales as $B_{\text{eff}} = B/(1 + D^2/H^2)$, so that the effective buoyancy has a smaller magnitude than the Archimedean buoyancy. Also note that the magnitude of the effective buoyancy decreases as the diameter increases. This behavior reflects the need for a wide and flat buoyancy anomaly to push aside more surrounding fluid as it moves vertically, whereas a narrow and tall anomaly is more streamlined and so has less resistance to vertical motion.

fluid. The pressure contribution to the effective buoyancy accounts for the back-reaction of the environmental fluid on the buoyant fluid element. Since the Archimedean buoyancy ignores the back-reaction, it generally over estimates the magnitude of the vertical acceleration. By accounting for the pressure forces acting on the element from the surrounding fluid, the effective buoyancy offers a more accurate measure of the static vertical forces arising from density inhomogeneities.

14.11.5 Comments and further study

Studies from [Davies-Jones \(2003\)](#), [Doswell and Markowski \(2004\)](#), [Jeevanjee and Romps \(2015a,b\)](#) and [Tarshish et al. \(2018\)](#), point to the use of the effective buoyancy and the limitations of Archimedean buoyancy when studying buoyancy dominated motion, such as the early stages of a buoyant thermal in the atmosphere. Much of the material in this section was gleaned from these papers, particularly from [Jeevanjee and Romps \(2015a,b\)](#). Chapter 2 of [Markowski and Richardson \(2010\)](#) provides a pedagogical foundation for understanding pressure forces leading to vertical motion.

The structure of b^{eff} is distinct from the Archimedean buoyancy, b , with [Jeevanjee and Romps \(2015a\)](#) and [Tarshish et al. \(2018\)](#) providing examples where b and b^{eff} can even have opposite signs. Furthermore, [Tarshish et al. \(2018\)](#) made use of an analogy between the Poisson equation for b^{eff} and the Poisson equation for certain magnetostatics problems. The analogy allows for analytical expressions of b^{eff} for spherical and elliptical Archimedean buoyancy sources.



14.12 Exercises

EXERCISE 14.1: EXAMPLES OF BUOYANCY PERIOD

Using approximate but realistic values for the observed stratification, determine the buoyancy period ($T_b = 2\pi/N$) for

- mid-latitude troposphere
- stratosphere
- ocean thermocline
- ocean abyss.

Express the period in units of minutes, and provide references for where you obtained the observed stratification. Hint: for both the atmosphere and ocean, it is sufficient to assume stratification is dominated by potential temperature (or Conservative Temperature).

EXERCISE 14.2: BUOYANCY FREQUENCY FOR AN IDEAL GAS

Derive equation (14.44) for the squared buoyancy frequency of an ideal gas. Hint: first derive the expression for the potential density and then take its vertical derivative as per equation (14.43).

EXERCISE 14.3: VERTICAL INTEGRAL OF N^2

The expression for squared buoyancy frequency

$$N^2 = -g \left[\frac{\partial \ln \varrho}{\partial z} \right]_{p_{\text{ref}}=p} \quad (14.150)$$

makes it tempting to consider its vertical integral according to

$$-g^{-1} \int_{-H}^{\eta} N^2 dz \stackrel{?}{=} [\ln \varrho]_{\eta} - [\ln \varrho]_{-H}. \quad (14.151)$$

Discuss what is wrong with this equation. Under what conditions is it correct?

EXERCISE 14.4: MOMENTS OF GRAVITY AND PRESSURE WITH NON-CONSTANT GRAVITY

Generalize the discussion in Section 14.2.2 to the case of non-constant gravity field.

EXERCISE 14.5: WATER LEVEL OF A BOAT WITH AND WITHOUT A STONE

Consider a boat of mass M_b floating in constant density water, ρ_w , contained in a tank with vertical sidewalls and cross-sectional area A . Place a stone of mass M_s and density $\rho_s > \rho_w$ in the boat and measure the water level on the tank wall, h_1 . Then throw the stone into the water. What is the new water level, h_2 , as a function of h_1 and the other properties listed above? Does the water level rise or fall along the sides of the tank as a result of throwing the stone over the side? Hint: Watch [this Physics Girl video](#).

EXERCISE 14.6: FLOATING ICEBERG

In this exercise we consider the static equilibrium of an iceberg floating in seawater.

- Consider an iceberg as depicted in Figure 14.10. Assume static equilibrium for both the iceberg and the seawater, and assume the atmospheric pressure, p_a , is a uniform constant. Derive an expression for the thickness, h , of ice that sits within the water.

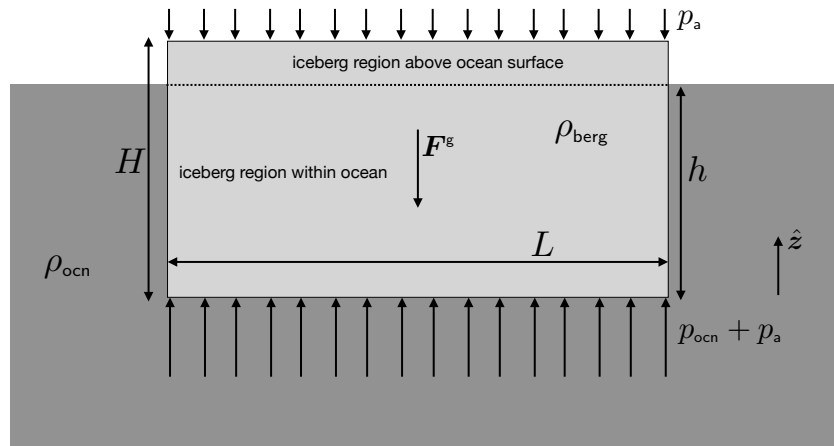


FIGURE 14.10: Schematic of a floating iceberg viewed from the side for use in Exercise 14.6. The iceberg has a constant density, ρ_{berg} , and the seawater has a constant density, $\rho_{\text{ocn}} > \rho_{\text{berg}}$. Assume the iceberg has a square base with sides L and vertical thickness H .

- (b) Consider an iceberg with non-uniform density, $\rho_{\text{berg}}(z)$, where $0 \leq z \leq H$ measures the position along the vertical axis of the iceberg, where $z = 0$ is the bottom and $z = H$ is the top. A non-uniform density might occur for cases where rocks are frozen into the ice. Depending on the density profile, the iceberg can be unstable to horizontal forces that cause the iceberg to flip over, particularly if L decreases to be on the order of H . Develop the stability criteria for this flipping instability using Archimedes' principle and the mechanics of angular momentum and torques. Hint: study chapter 5 of [Lautrup \(2005\)](#).

EXERCISE 14.7: THOUGHT EXPERIMENTS FOR EFFECTIVE BUOYANCY

We here examine some thought experiments for the purpose of developing an understanding of effective buoyancy. The thought experiments are somewhat trivial physically and yet they require us to confront basic assumptions, which is generally a useful exercise. Little if any mathematical analysis is expected here. Instead, we are looking for conceptual discussion of the thought experiments.

- (a) HORIZONTALLY UNSTRATIFIED DENSITY: Consider a horizontally unstratified density, $\rho = \rho(z)$, on a horizontally periodic domain with the fluid in hydrostatic equilibrium.
- (b) VERTICALLY UNSTRATIFIED DENSITY: Now consider a vertically unstratified density field, $\rho = \rho(x, y)$, so that the Archimedean buoyancy has no depth dependence. This vertically “neutrally buoyant” case commonly means that a fluid element can move vertically without feeling any buoyancy forces. Indeed, such is the case when referring to Archimedean buoyancy. What about effective buoyancy?



Chapter 15

GEOSTROPHY AND THERMAL WIND

Large-scale and low frequency flows in the atmosphere and ocean are strongly affected by planetary rotation. The inviscid balance for such flows is termed **geostrophy**, in which the planetary Coriolis acceleration balances the pressure gradient acceleration in the horizontal, while the vertical is in **hydrostatic balance**. In this chapter, we introduce salient features of geostrophically balanced flow and the associated **thermal wind balance**. These two diagnostic relations involve no time derivatives, and so cannot be used to predict the fluid flow evolution. However, they provide a very powerful framework for mechanically interpreting large-scale and low frequency flow in the atmosphere and ocean.

After studying the basic elements of rotating flow, we study the distinctive nature of isopycnal form stresses associated with geostrophically balanced eddy motions. Such form stresses are a key feature of the Earth's planetary energy balance, whereby positive buoyancy in the tropics is, in part, transported meridionally through the action of geostrophic eddies.

READER'S GUIDE TO THIS CHAPTER

This chapter assumes an understanding of the primitive equations from Chapter 11 and the Coriolis acceleration encountered in our study of Newtonian mechanics in VOLUME 1. The material in this chapter is fundamental to understanding the mechanics of large-scale flow in the atmosphere and ocean, and we make great use of it in the remainder of the book. We are not explicitly concerned with sphericity in this chapter, thus enabling the use of Cartesian vector calculus.

Much of the material in this chapter forms the basis for laminar theories of the large-scale ocean circulation in regions outside of the tropics. We further pursue these theories in VOLUME 3 by taking a deep dive into planetary geostrophic vorticity budgets. Further discussion of phenomenology is given in Chapter 7 of *Marshall and Plumb (2008)*. *Greenspan (1969)*, *Pedlosky (1996)*, *Samelson (2011)*, and chapters 19-22 of *Vallis (2017)* present ocean circulation theory through use of geophysical fluid dynamics.

We offer remarks on terminology in reference to flow directions. Ocean scientists generally speak of the direction of ocean currents, whereas atmospheric scientists refer to the direction from which air is sourced. Hence, for example, an ocean scientist refers to eastward currents (seawater flowing to the east), whereas an atmospheric scientist refers to westerly winds (air coming from the west and blowing to the east).

15.1 Loose threads	504
15.2 Primitive equations	504
15.3 The Rossby number	505

15.3.1	Scaling for the Rossby number	505
15.3.2	Ratio of material acceleration to Coriolis acceleration	506
15.3.3	Ratio of local time tendency to Coriolis acceleration	506
15.3.4	Rossby number for a kitchen sink	506
15.3.5	Rossby number for a Gulf Stream ring	506
15.4	Geostrophic balance	507
15.4.1	Geostrophic relation in geopotential coordinates	507
15.4.2	Cyclonic and anti-cyclonic flow orientation	508
15.4.3	Gradients in the density and hydrostatic pressure	509
15.4.4	Geostrophic relation in pressure coordinates	510
15.4.5	Further study	510
15.5	Planetary geostrophic mechanics	510
15.5.1	Planetary geostrophic equations	511
15.5.2	Planetary geostrophic vorticity equation	512
15.5.3	Taylor-Proudman and vertical stiffening	513
15.5.4	Meridional motion in response to vortex stretching and stress curls	514
15.5.5	The Sverdrup balance	515
15.6	Thermal wind balance	516
15.6.1	Relevant portion of density needed for thermal wind	517
15.6.2	Atmospheric jet stream and the Antarctic Circumpolar Current	517
15.6.3	Diagnosing geostrophic velocity from buoyancy	517
15.6.4	Thermal wind balance for the atmosphere	518
15.6.5	Thermal wind balance for a Boussinesq ocean	520
15.6.6	Thermal wind for a non-Boussinesq hydrostatic ocean	521
15.7	Isopycnal form stress from geostrophic eddies	523
15.7.1	Zonal mean zonal form stress on an isopycnal surface	523
15.7.2	Zonal mean zonal form stress acting on an isopycnal layer	525
15.7.3	Comments and further study	527
15.8	Exercises	528

15.1 Loose threads

- Max Nikurashin's work on topographic form stress in the Southern Ocean, and the lack of a direct connection to interfacial form stress. Unsure if this material is better here or in Chapter 12.

15.2 Primitive equations

Throughout this chapter we make use of the inviscid hydrostatic primitive equations derived in Section 11.1

$$[\partial_t + (\mathbf{v} \cdot \nabla)] \mathbf{u} + f \hat{\mathbf{z}} \times \mathbf{u} = -\rho^{-1} \nabla_h p \quad (15.1a)$$

$$\partial p / \partial z = -g \rho \quad (15.1b)$$

$$D\rho/Dt = -\rho \nabla \cdot \mathbf{v}, \quad (15.1c)$$

where the velocity vector is written using Cartesian coordinates

$$\mathbf{v} = \mathbf{u} + \hat{\mathbf{z}} w = \hat{\mathbf{x}} u + \hat{\mathbf{y}} v + \hat{\mathbf{z}} w, \quad (15.2)$$

and the horizontal gradient operator is

$$\nabla_h = \hat{\mathbf{x}} \partial_x + \hat{\mathbf{y}} \partial_y. \quad (15.3)$$

For some of the scale analysis in this chapter we assume a Boussinesq ocean (Section 13.1), in which case the mass continuity equation (15.1c) becomes the non-divergent condition on the velocity

$$\nabla \cdot \mathbf{v} = 0. \quad (15.4)$$

Furthermore, density for the Boussinesq horizontal momentum equation appears as a constant reference density, ρ_0 , and yet it retains its full form when appearing in the hydrostatic equation since it is there multiplied by the gravitational acceleration.

15.3 The Rossby number

Large-scale geophysical fluid flows are strongly influenced by the Earth's rotation. Indeed, the Earth can be considered a rapidly rotating planet for much of the observed large-scale motion of the ocean and atmosphere. There are two points to emphasize in this regard. First, much of the ocean and atmosphere motion is close to rigid-body rotation, in which weather patterns and ocean circulation are best viewed in the terrestrial reference frame on the rotating Earth (a non-inertial reference frame) rather than from an inertial reference frame fixed in space. Second, length scales directly experienced by humans are generally far too small to take a direct notice of the planetary rotation. This point is quantified by considering the **Rossby number**, which includes a horizontal length scale, a velocity length scale, and an angular rotation rate.

15.3.1 Scaling for the Rossby number

The Rossby number measures the ratio of the horizontal material acceleration (acceleration of a fluid particle) to the Coriolis acceleration. The material acceleration has two contributions: one from local time tendencies and one from advection. We expose typical characteristic scales for the horizontal acceleration of a fluid particle by writing

$$\frac{\partial \mathbf{u}}{\partial t} + (\mathbf{v} \cdot \nabla) \mathbf{u} \sim \frac{U}{T} + \frac{U^2}{L} + \frac{WU}{H}, \quad (15.5)$$

where U, W are typical horizontal and vertical velocity scales, L, H are typical horizontal and vertical length scales, and T is a typical time scale (recall a similar scale analysis for the hydrostatic balance in Section 11.2). Likewise, the Coriolis acceleration scales as

$$f \hat{\mathbf{z}} \times \mathbf{u} \sim f_0 U, \quad (15.6)$$

where f_0 is the scale for the Coriolis parameter. From the continuity equation for non-divergent flow ($\nabla \cdot \mathbf{v} = 0$) we see that the vertical and horizontal velocity scales are related by¹

$$W/H \sim U/L \implies W \sim U(H/L). \quad (15.7)$$

We are interested in flows where the ratio of the vertical to horizontal length scales, referred to as the **aspect ratio**, is small

$$\alpha_{\text{aspect}} = H/L \ll 1, \quad (15.8)$$

¹For divergent flows we can replace W with the scale for motion across hydrostatic pressure surfaces.

as per the hydrostatic approximation discussed in Section 11.2. Consequently, the vertical velocity scale is much less than the horizontal

$$W \ll U. \quad (15.9)$$

15.3.2 Ratio of material acceleration to Coriolis acceleration

Taking the ratio of the advection scale to the Coriolis scale leads to our first expression for the Rossby number

$$\text{Ro} = \frac{U^2/L}{f_0 U} = \frac{U}{f_0 L}. \quad (15.10)$$

For fixed scales U and L , the latitudinal variation of the Coriolis parameter makes the Rossby number smaller in magnitude near the poles than in the tropics.

15.3.3 Ratio of local time tendency to Coriolis acceleration

A complementary way to understand the Rossby number is to consider it as the ratio of the horizontal velocity's local time tendency to the Coriolis acceleration

$$\text{Ro} = \frac{U/T}{U f_0} = \frac{1/T}{f_0}. \quad (15.11)$$

Hence, the Rossby number is small for motions that have a frequency, T^{-1} , that is small compared to the [inertial frequency](#), f_0 . In both expressions (15.10) and (15.11) for the Rossby number, we associate $\text{Ro} \ll 1$ with flow regimes where the Earth's rotation plays a crucial role in the dynamics. With small Rossby number, both the local time derivative and the advective acceleration are smaller than the Coriolis acceleration.

15.3.4 Rossby number for a kitchen sink

Consider flow in a kitchen sink (left panel of Figure 15.1). Here, the length scale is $L = 1$ m (sink size) and the velocity scale is $U = 0.01 - 0.1$ m s $^{-1}$, thus giving a typical time scale for sink motion of $L/U \approx 10$ s – 100 s. Hence, at 30° latitude, where $f = 2\Omega \sin \phi = \Omega$, the Rossby number for fluid motion in a sink is

$$\text{Ro}_{\text{sink}} \approx 10^2 - 10^3. \quad (15.12)$$

The effects from planetary rotation are tiny on these length scales, so that the Coriolis force is negligible for kitchen sink fluid dynamics. Correspondingly, it is extremely difficult to experimentally determine a correlation between the hemisphere (northern or southern) to the rotational direction of water leaving a sink drain.

15.3.5 Rossby number for a Gulf Stream ring

For a Gulf Stream ring (right panel of Figure 15.1), the typical length scale is $L = 10^5$ m and velocity scale is $U = 0.1 - 1.0$ m s $^{-1}$, thus leading to a time scale $L/U \approx 10^5 - 10^6$ s. At 30° latitude the Rossby number is

$$\text{Ro}_{\text{ring}} \approx 10^{-2} - 10^{-1}. \quad (15.13)$$

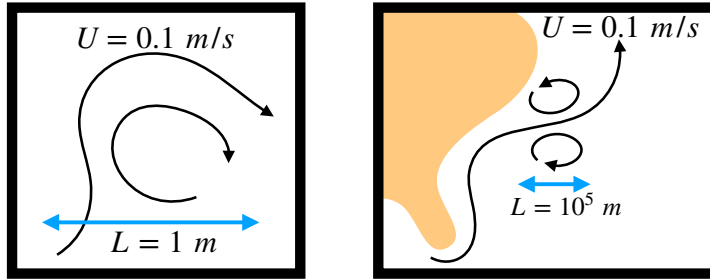


FIGURE 15.1: Estimating the Rossby number for flow in a kitchen sink (left panel) and rings spawned from the Gulf Stream (right panel). The kitchen sink has velocity scales on the order of $U \sim 0.01 - 0.1 \text{ m s}^{-1}$ whereas Gulf Stream rings have velocity scales on the order $U \sim 0.1 - 1.0 \text{ m s}^{-1}$. Their length scales are much more distinct, with the scale for a sink $L \sim 1 \text{ m}$ whereas for the Gulf Stream rings $L \sim 10^5 \text{ m}$. Taking the Coriolis parameter at 30° leads to $\text{Ro}_{\text{sink}} \sim 10^2 - 10^3$ and $\text{Ro}_{\text{ring}} \sim 10^{-2} - 10^{-1}$. The planetary Coriolis acceleration is central to Gulf Stream ring dynamics whereas it is utterly negligible for the kitchen sink.

Flow features of such large length scales can feel the planetary rotation so that the Coriolis acceleration is central to dynamics of Gulf Stream rings, as reflected in the small magnitude of the associated Rossby number.

15.4 Geostrophic balance

Under the influence of horizontal pressure forces, a fluid accelerates down the pressure gradient (movement from high pressure to low pressure). In the presence of rotation, a nonzero horizontal velocity couples to the Earth's rotation via the Coriolis parameter, f , thus giving rise to a nonzero horizontally oriented Coriolis acceleration $-f \hat{z} \times \mathbf{u}$. The Coriolis acceleration acts perpendicular to the fluid motion

$$\mathbf{u} \cdot (\hat{z} \times \mathbf{u}) = 0, \quad (15.14)$$

and as such it affects the fluid motion but does not alter kinetic energy; i.e., it does zero work on the fluid.² In the northern hemisphere where $f > 0$, the Coriolis acceleration acts to the right of the fluid motion. It follows that if the Coriolis and pressure gradient accelerations are balanced, then fluid flow is counter-clockwise around low pressure centers and clockwise around high pressure centers. In the southern hemisphere, where $f < 0$, the Coriolis acceleration acts in the opposite direction so that geostrophically balanced flow is oppositely oriented in the southern hemisphere relative to the north.

When the pressure acceleration balances the Coriolis acceleration, fluid motion is said to be in **geostrophic balance**. Geostrophically balanced flows in the atmosphere and ocean follow isobars (lines of constant pressure). Point particles also experience a Coriolis acceleration when viewed in a rotating reference frame. However, geostrophic balance is not afforded to particles since particles do not experience a pressure force that can balance the Coriolis force. Hence, the geostrophic balance is a distinctly fluid mechanical phenomena. Even so, in Figure 15.2 we offer a particle model to help understand the orientation of geostrophic flow.

15.4.1 Geostrophic relation in geopotential coordinates

When the Rossby number is small and friction is negligible, the leading order dynamical balance in the horizontal momentum equation (15.1a) is between the Coriolis acceleration and horizontal

²These characteristics of the Coriolis acceleration are directly analogous to the Lorentz force in electrodynamics ([Jackson, 1975](#)).

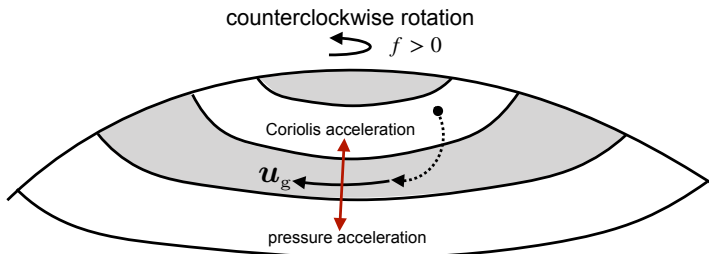


FIGURE 15.2: Geostrophic balance occurs in an inviscid fluid if the pressure gradient acceleration balances the Coriolis acceleration so that the net horizontal acceleration acting on a fluid element is zero. Here we depict a particle on a rotating and frictionless hill (analogous to a high pressure center) as a conceptual model to help understand geostrophic balance. As the particle moves downhill in the northern hemisphere, it picks up a rightward component to its trajectory as a result of the Coriolis acceleration that couples to motion. Equilibrium arises when the downhill gravitational acceleration balances the oppositely directed Coriolis acceleration.

pressure gradient acceleration

$$f \hat{\mathbf{z}} \times \mathbf{u}_g = -\rho^{-1} \nabla_h p, \quad (15.15)$$

with this equation known as **geostrophic balance**. The geostrophic balance equation leads to the expression for the geostrophic velocity³

$$\mathbf{u}_g = \frac{\hat{\mathbf{z}} \times \nabla_h p}{f \rho} \implies u_g = -\frac{1}{f \rho} \frac{\partial p}{\partial y} \quad \text{and} \quad v_g = \frac{1}{f \rho} \frac{\partial p}{\partial x}. \quad (15.16)$$

Note that the equator is special since the Coriolis parameter, $f = 2\Omega \sin \phi$, vanishes, thus precluding the relevance of geostrophy near the equator.

Equation (15.16) for the geostrophic velocity can be written as

$$\rho f \mathbf{u}_g = \hat{\mathbf{z}} \times \nabla_h p, \quad (15.17)$$

which suggests we interpret pressure as a streamfunction for $\rho f \mathbf{u}_g$. For the particular case of a Boussinesq ocean on an f -plane, in which we set ρ to the reference density ρ_0 and f is a constant, then we can write

$$\mathbf{u}_g = \hat{\mathbf{z}} \times \nabla_h [p/(\rho_0 f)]. \quad (15.18)$$

In this case $p/(\rho_0 f)$ is referred to as the **geostrophic streamfunction** for the f -plane Boussinesq geostrophic flow.

15.4.2 Cyclonic and anti-cyclonic flow orientation

If oriented in the same sense as the Earth's rotation (i.e., same sign of the Coriolis parameter), then rotational motion is said to be in a **cyclonic** sense. Oppositely oriented motion is **anti-cyclonic**. For example, geostrophic motion around a low pressure center in the northern hemisphere is counter-clockwise (Figure 15.3). Using the right hand rule, this motion represents a positively oriented rotation. Hence, with $f > 0$ in the north, counter-clockwise motion is cyclonic. In the southern hemisphere, geostrophic motion around a low pressure center is clockwise, which is a negatively oriented rotational motion (again, recall the right hand rule). In the south where $f < 0$, clockwise motion around a low pressure center represents cyclonic motion (Figure 15.3).

³We can write either ∇ or ∇_h in equation (15.16). The reason is that the $\hat{\mathbf{z}} \times$ operator selects only the horizontal portion of the gradient.

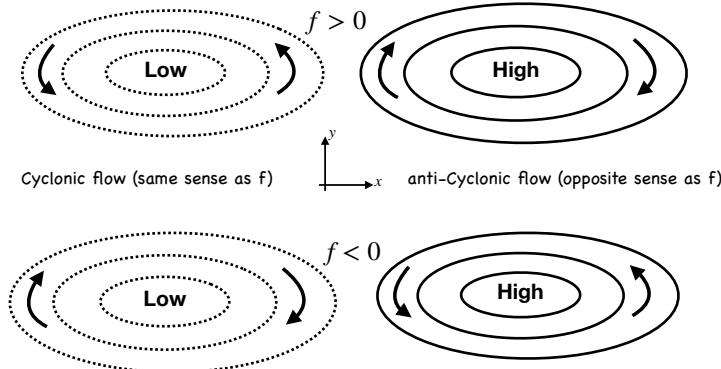


FIGURE 15.3: Geostrophic motion around low and high pressure centers in the northern hemisphere and southern hemisphere ($f = 2\Omega \sin \phi > 0$ in the north and $f < 0$ in the south). Upper panel: the counter-clockwise motion around the low pressure center in the northern hemisphere is in the same sense as the planetary rotation, and is thus termed **cyclonic**. Cyclonic motion around a low pressure in the southern hemisphere occurs in a clockwise direction, again corresponding to the direction of planetary rotation as viewed from the south. Geostrophic motion around a high pressure center is counter to the planetary rotation in both hemispheres, and is termed **anti-cyclonic**.

15.4.3 Gradients in the density and hydrostatic pressure

Horizontal momentum is affected by horizontal pressure gradient forces. Furthermore, the hydrostatic balance says that the vertical derivative of the horizontal pressure gradient is determined by horizontal density gradients

$$\frac{\partial(\nabla_h p)}{\partial z} = -g \nabla_h \rho. \quad (15.19)$$

Hence, in the presence of horizontal density gradients, the horizontal pressure gradient forces are depth dependent. Correspondingly, the horizontal velocity field experiences a depth dependent pressure force.

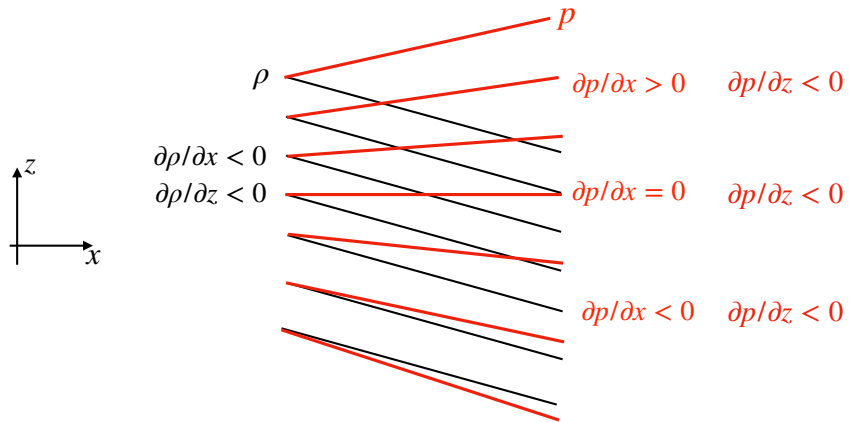


FIGURE 15.4: Horizontal density gradients support a vertical dependence to the horizontal gradient of the hydrostatic pressure via $\partial(\nabla_h p)/\partial z = -g \nabla_h \rho$. This figure depicts a vertically stable stratification of density ($\partial\rho/\partial z < 0$), along with pressure that decreases upward as per the hydrostatic balance ($\partial p/\partial z = -\rho g < 0$). Density is assumed to have a constant zonal gradient with $\partial\rho/\partial x < 0$, which leads to an increase in the zonal pressure gradient with height, $\partial(\partial p/\partial x)/\partial z > 0$. Depending on the thickness of the fluid column, the horizontal pressure gradient can change sign when moving up in the column, as shown here. Compare this figure to Figure 11.4, which discusses how to compute horizontal pressure gradients in a hydrostatic fluid.

We illustrate this depth dependence in Figure 15.4 with a depth independent horizontal

density gradient, $\partial\rho/\partial x = \text{constant} < 0$. This density gradient leads to a depth dependent horizontal gradient in the hydrostatic pressure. This figure also illustrates how the sign of the horizontal pressure gradient can change when moving in the vertical, depending on the value of the gradient at depth. It also illustrates how horizontal density gradients that are misaligned with pressure gradients lead to a nonzero **baroclinicity** vector

$$\mathbf{B} = \frac{\nabla\rho \times \nabla p}{\rho^2}. \quad (15.20)$$

As discussed in VOLUME 3 when studying vorticity, a nonzero baroclinicity (i.e., a misalignment of the density and pressure surfaces) imparts a “torque” on fluid elements that acts as a source for vorticity.

Depth dependence to the horizontal pressure gradient leads to a vertical shear in the horizontal geostrophic velocity

$$\frac{\partial(\rho f \mathbf{u}_g)}{\partial z} = \hat{z} \times \nabla(\partial p/\partial z) = -g \hat{z} \times \nabla\rho. \quad (15.21)$$

This connection between horizontal density gradients and vertical shears in the geostrophic velocity is known as the **thermal wind balance**, which we return to in Section 15.6.

15.4.4 Geostrophic relation in pressure coordinates

The hydrostatic balance

$$\partial p/\partial z = -\rho g \quad (15.22)$$

can be used to eliminate density from the geostrophic balance (15.15) to render

$$f \hat{z} \times \mathbf{u}_g = \frac{g \nabla_h p}{\partial p/\partial z}. \quad (15.23)$$

The right hand side is minus the lateral gradient of the geopotential, $\Phi = g z$, as computed along surfaces of constant pressure⁴

$$f \hat{z} \times \mathbf{u}_g = -\nabla_p \Phi \implies f \mathbf{u}_g = \hat{z} \times \nabla_p \Phi. \quad (15.24)$$

This is a useful expression of geostrophy for the compressible atmosphere.

15.4.5 Further study

Visualizations from rotating tank experiments offer a useful complement to the mathematical expressions presented here. For example, start around the 10 minute mark in [this video from Prof. Fultz](#).

15.5 Planetary geostrophic mechanics

We here introduce the equations for **planetary geostrophy(PG)**, which have found great use in describing elements of the large-scale laminar ocean circulation. We state the equations and

⁴In VOLUME 3 we study the mathematics of how to compute derivatives using generalized vertical coordinates, such as pressure. In particular, the formalism in that section reveals that $(\partial p/\partial x)_{y,z}/(\partial p/\partial z)_{x,y} = -(\partial z/\partial x)_{y,p} = -g^{-1} (\partial \Phi/\partial x)_{x,p}$, and likewise for the meridional derivative.

discuss their physical implications, deferring a systematic derivation for later. In particular, in VOLUME 3 we study the shallow water planetary geostrophic equations as well as the continuously stratified planetary geostrophic equations.

15.5.1 Planetary geostrophic equations

The governing equations for planetary geostrophy are based on the hydrostatic Boussinesq ocean equations stated in Section 13.1.6, with the assumption of a steady, linear, and frictional/geostrophic balance for the horizontal momentum

$$\rho_0 f (\hat{z} \times \mathbf{u}) = -\nabla_h p - \hat{z} (\partial_z p + \rho g) + \partial_z \boldsymbol{\tau} \quad (15.25a)$$

$$\nabla_h \cdot \mathbf{u} + \partial_z w = 0 \quad (15.25b)$$

$$Db/Dt = \dot{b}. \quad (15.25c)$$

The stress vector, $\boldsymbol{\tau}$, acts just in the horizontal directions so that the vertical component of the momentum equation (15.25a) is the hydrostatic balance

$$\partial_z p = -\rho g. \quad (15.26)$$

We now list some of the key physical attributes captured by these equations.

Velocity is determined by buoyancy

The only time derivative in the planetary geostrophic equations appears in the buoyancy equation (15.25c). All other equations are diagnostic. As the buoyancy evolves, the hydrostatic pressure changes and so too does the geostrophic velocity. Hence, the velocity is determined by the buoyancy field.

Planetary geostrophy admits no turbulence

The momentum equation is linear since planetary geostrophy drops the nonlinear advection of momentum. Turbulence relies on the nonlinear momentum advection. Hence, there is no turbulent flow described by the planetary geostrophic equations. Instead, planetary geostrophy is used to describe laminar ocean circulation at the large-scales.

Vertical transfer of horizontal momentum and subgrid scale parameterizations

We introduced a horizontal stress vector (dimensions of force per area) into the momentum equation

$$\boldsymbol{\tau} = (\tau^x, \tau^y, 0). \quad (15.27)$$

This stress is associated with vertical transfer of horizontal momentum in the ocean interior through vertical viscosity, as well as vertical transport of momentum between the atmosphere and ocean as well as between the solid-Earth and the ocean. The stress is enhanced by waves and turbulent features. However, such transient processes are not represented by planetary geostrophy. Hence, they must be parameterized, which generally leads to an enhanced vertical eddy viscosity relative to the molecular viscosity. In general, all models, either analytical or numerical, that are focused on planetary scale circulations do not resolve the scales over which molecular viscosity dominates the frictional dissipation. Consequently, it is necessary to provide

subgrid scale (SGS) parameterizations for the variety of physical processes that are unresolved by the model.

15.5.2 Planetary geostrophic vorticity equation

The vertical component of relative vorticity is

$$\zeta = \partial v / \partial x - \partial u / \partial y. \quad (15.28)$$

We study the many facets of vorticity in VOLUME 3. Here, we form the relative vorticity budget for the planetary geostrophic system by taking the curl of the momentum equation. Doing so provides insights into the mechanics of planetary geostrophic flow, which we deduce by considering various limits of the vorticity equation.

Curl of the PG momentum equation

Taking the curl of the momentum equation (15.25a), and rearranging terms, leads to the planetary geostrophic vorticity equation

$$-\rho_0 f \partial_z \mathbf{u} + \hat{\mathbf{z}} \rho_0 \nabla \cdot (f \mathbf{u}) = -g \nabla \times (\hat{\mathbf{z}} \rho) + \partial_z (\nabla \times \boldsymbol{\tau}). \quad (15.29)$$

Note that $\nabla \cdot (f \mathbf{u}) = \nabla_h \cdot (f \mathbf{u})$ since \mathbf{u} is the horizontal velocity vector. Introducing the globally referenced Archimedean buoyancy (Section 13.1.2)

$$b = -g (\rho - \rho_0) / \rho_0 \quad (15.30)$$

leads to

$$-f \partial_z \mathbf{u} + \hat{\mathbf{z}} \nabla_h \cdot (f \mathbf{u}) = \nabla \times (\hat{\mathbf{z}} b) + \partial_z (\nabla \times \boldsymbol{\tau} / \rho_0), \quad (15.31)$$

whose horizontal and vertical components are the following

$$f \partial_z \mathbf{u} = \hat{\mathbf{z}} \times \nabla b \quad (15.32a)$$

$$\nabla \cdot (f \mathbf{u}) = \partial_z [\hat{\mathbf{z}} \cdot (\nabla \times \boldsymbol{\tau} / \rho_0)]. \quad (15.32b)$$

In this section as well as Section 15.6 we study these equations by making a variety of simplifying assumptions.

Relative vorticity is absent from the PG vorticity equation

It is notable that there is no appearance of the relative vorticity, $\zeta = \partial_x v - \partial_y u$, in the planetary geostrophic vorticity equation (15.25a). The reason is that we dropped the material time derivative of velocity when forming the planetary geostrophic momentum equation (15.25a). By doing so, we eliminate ζ from the vorticity equation. Planetary geostrophy is valid for those cases where

$$|\zeta| \ll |f|, \quad (15.33)$$

which means the absolute vorticity (sum of planetary vorticity plus relative vorticity) is dominated by the planetary vorticity. We encounter more complete versions of the vorticity equation in VOLUME 3.

Rather than taking the curl of the planetary geostrophic momentum equation, we could have also derived the vorticity equation (15.31) by taking planetary geostrophic scaling in the

full vorticity equation. We choose here the path through the planetary geostrophic momentum equation since we have yet to discuss the full vorticity equation (again, this discussion is given in VOLUME 3).

15.5.3 Taylor-Proudman and vertical stiffening

Examination of the momentum equation (15.25a) reveals that inviscid planetary geostrophic flow on an f -plane is horizontally non-divergent

$$\nabla_h \cdot \mathbf{u} = 0 \quad f\text{-plane geostrophy.} \quad (15.34)$$

Use of the continuity equation (15.25b) means there is no vertical stretching of a vertical material line element⁵

$$\partial_z w = 0. \quad (15.35)$$

As shown in VOLUME 3, a vortex tube exhibits the same kinematics as a material line element. Hence, $\partial_z w = 0$ means there is no vertical stretching of a vortex tube in the inviscid planetary geostrophic fluid. This result has important implications that we now describe.

Flat bottom boundary and columnar motion

If there is a solid flat bottom to the domain, then the vertical velocity vanishes at that surface. With $\partial_z w = 0$ in the interior as well, then w vanishes throughout the domain. Hence, the fluid has zero vertical velocity, and motion occurs on horizontal planes perpendicular to the rotation axis; i.e., the flow is two-dimensional. We furthermore assume zero horizontal buoyancy gradients (i.e., homogeneous fluid), so that the horizontal portion of the vorticity equation (15.32a) implies that the horizontal velocity has zero vertical shear

$$\partial_z \mathbf{u} = 0 \quad f\text{-plane and homogeneous density.} \quad (15.36)$$

This result is known as the [Taylor-Proudman effect](#), with Figure 15.5 providing an illustration.⁶

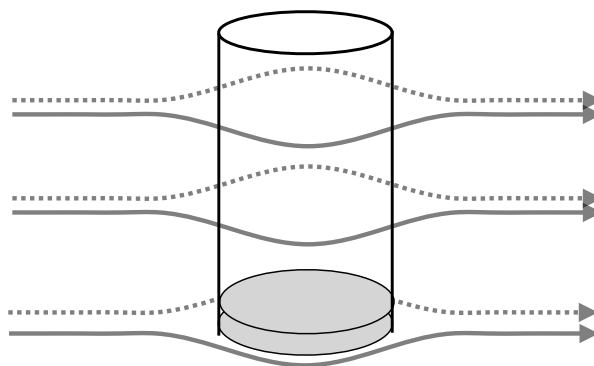


FIGURE 15.5: The [Taylor-Proudman effect](#), summarized by equation (15.36), says that steady horizontal flow is depth-independent when it occurs in a homogeneous and rapidly rotating fluid (i.e., geostrophically balanced flow) over a flat bottom (where $w = 0$). Hence, when the geostrophic flow encounters an obstacle anywhere in the column, such as the disk shown here at the bottom, then flow throughout the full depth coherently moves around the obstacle. The result is a vertically stiffened motion known as a [Taylor column](#).

⁵In our study of fluid kinematics in VOLUME 1, we study how vertical stretching of material line elements occurs in a flow with horizontal divergences.

⁶As we study in VOLUME 5, time-dependent establishment of the Taylor-Proudman effect is mediated by inertial waves.

Relevance to the ocean and atmosphere

In the ocean and atmosphere, the assumptions leading to the Taylor-Proudman effect are rarely satisfied due to the presence of stratification (i.e., vertical density variations), and a sloping solid Earth bottom. Nonetheless, there is a tendency for vertical velocities to be quite small due to the effects of rotation; even smaller than the non-divergent flow scaling $W/H \sim U/L$ would indicate (see Section 15.3.1). Additionally, there is a tendency for geostrophic turbulence to cascade energy into the **gravest vertical mode**; i.e., the largest vertical scale, especially in weakly stratified flows. This largest vertical scale mode is termed the **barotropic mode**, and motion of this mode is predominantly horizontal and depth independent. Smaller vertical scales of variation are captured by an infinite hierarchy of **baroclinic modes**. The process of moving kinetic energy of the flow from the baroclinic modes to the barotropic mode is referred to as **barotropization**.⁷

Further study of Taylor-Proudman

Rotating tank laboratory experiments offer a powerful means to explore the variety of rotating fluid mechanics relevant to the atmosphere and oceans. The following resources exemplify the Taylor-Proudman effect and the associated vertical stiffening of rotating fluids.

- One means to test Taylor-Proudman is to insert a dye into a rapidly rotating tank of unstratified water. After a few rotation periods the dye forms vertical sheets known as **Taylor curtains** whose center is along the rotation axis. The fluid is said to have a **vertical stiffness** due to the effects of rotation. Vertical stiffening in turn means that flow over a small obstacle is deflected throughout the column rather than just near the bump. This situation is depicted in Figure 15.5 and more vividly illustrated in [this video from the UCLA SpinLab](#).
- Near the 20 minute mark of [this video, also from UCLA](#), we see how vortices in a rotating fluid maintain their coherency much more than in a non-rotating fluid.
- Another laboratory test shown in [this video from Prof. Fultz](#) shows that a buoyant object (a ping pong ball) placed into a rotating tank rises much slower than in a non-rotating tank. The reason for the slower rise is that the ball must push up against the vertically stiffened fluid column when rotating, thus slowing its rise relative to when in a non-rotating fluid. Later in the same video, near the 16 minute mark, we see Taylor curtains in rotating fluids.

15.5.4 Meridional motion in response to vortex stretching and stresscurls

The vertical component to the vorticity balance is given by equation (15.32b), which can be written

$$\beta v = -f \nabla_h \cdot \mathbf{u} + \partial_z [\hat{\mathbf{z}} \cdot (\nabla \times \boldsymbol{\tau}/\rho_0)], \quad (15.37)$$

where

$$\beta = \partial_y f \quad (15.38)$$

⁷A compelling discussion of the cascade of energy from the baroclinic modes to barotropic mode is offered by [Smith and Vallis \(2001\)](#).

is the meridional derivative of the planetary vorticity.⁸ The continuity equation (15.25b) can be used to yield the following expression of the vorticity balance

$$\beta v = f \partial_z w + (1/\rho_0) \partial_z [\hat{z} \cdot (\nabla \times \boldsymbol{\tau})]. \quad (15.39)$$

The left hand side is the meridional advection of planetary vorticity, with $\beta > 0$ over the globe. The first term on the right hand side arises from vortex stretching by planetary vorticity; i.e., planetary induction or the [beta effect \(\$\beta\$ -effect\)](#) studied in VOLUME 3. The second term is the vertical divergence of the curl of the frictional stress.

Reading the vorticity equation (15.39) from right to left indicates that any process leading to a vorticity source via vortex stretching or vertically dependent frictional stress curls must be balanced by meridional motion. That is, the fluid responds to vortex stretching and vertically dependent stress curls by moving meridionally through the planetary vorticity field. In the frictional planetary geostrophic theory, meridional movement is the only means for fluid to respond to vorticity input since the fluid's vorticity is set by planetary vorticity (recall that for this theory, the relative vorticity is far smaller in magnitude than planetary vorticity). Reading equation (15.39) from left to right reveals that any meridional motion must be balanced by vortex stretching/squashing plus stress curls. For example, in the absence of the frictional stress term, poleward flow is balanced by stretching of a fluid column ($\partial_z w > 0$), whereas equatorial flow is balanced by squashing a column ($\partial_z w < 0$). In VOLUME 3, we provide a detailed study of the depth integrated vorticity equation (15.39), where we see how the depth integrated meridional flow is affected by stretching imparted by boundary torques. To get an initial taste for that study, we consider the Sverdrup balance in Section 15.5.5.

15.5.5 The Sverdrup balance

Depth integrating the vorticity balance (15.39) over the full depth of an ocean column leads to

$$\beta V = f [w(\eta) - w(\eta_b)] + \hat{z} \cdot \nabla \times [\boldsymbol{\tau}(\eta) - \boldsymbol{\tau}(\eta_b)] / \rho_0, \quad (15.40)$$

where

$$V = \int_{\eta_b}^{\eta} v \, dz \quad (15.41)$$

is the depth integrated meridional velocity. For the large-scale we generally assume the surface vertical velocity is relatively small, thus motivating $w(\eta) = 0$, which is the [rigid lid approximation](#). Further assuming a flat bottom allows us to drop the vertical velocity at the ocean bottom, $w(\eta_b) = 0$. Additionally, the surface turbulent stress from winds is often far larger than the bottom turbulent stress. These assumptions then lead to the [Sverdrup balance](#), which is a balance between the depth integrated meridional motion and the curl of the surface turbulent stress

$$\rho_0 \beta V_{\text{Sverdrup}} = \hat{z} \cdot \nabla \times \boldsymbol{\tau}(\eta) \quad \text{Sverdrup balance.} \quad (15.42)$$

Evidently, for Sverdrup balanced flow, vertically integrated meridional transport (left hand side) balances the wind stress curl (right hand side). In particular, a positive wind stress curl leads to northward vertically integrated flow.

As discussed in VOLUME 3, the most unrealistic aspect of the Sverdrup balance (15.42) concerns the assumption of vanishing $w(\eta_b)$, since $w(\eta_b)$ is generally non-negligible in regions

⁸ As studied in VOLUME 3, planetary rotation provides a vorticity, $\omega_{\text{planetary}} = f$, to fluids. Hence, the Coriolis parameter, f , is commonly referred to as the [planetary vorticity](#).

with sloping bottom boundaries and sizable bottom flows. Even so, the Sverdrup balance (15.42) is a useful place to start when studying the connection between wind stress curls and vertically integrated meridional transport. We also discuss a variant of the Sverdrup balance, known as the geostrophic Sverdrup balance, in VOLUME 3.

15.6 Thermal wind balance

Focusing now on the horizontal portion of the inviscid vorticity equation, as given by equation (15.32a), leads to the thermal wind balance (remember that $\nabla b = -(g/\rho_0) \nabla_h \rho$)

$$f \partial u / \partial z = -\nabla_h \times (\hat{z} b) = \hat{z} \times \nabla b = -(g/\rho_0) \hat{z} \times \nabla \rho, \quad (15.43)$$

which takes on the component form

$$f \partial_z u = -\partial_y b = (g/\rho_0) \partial_y \rho \quad \text{and} \quad f \partial_z v = \partial_x b = -(g/\rho_0) \partial_x \rho. \quad (15.44)$$

As seen already in Section 15.4.3, these relations can also be derived directly by taking the vertical derivative of the horizontal momentum equation (15.25a) and then using the horizontal gradient of the hydrostatic balance (15.26). In either case, the thermal wind balance (15.43) says that the horizontal geostrophic velocity possesses a vertical shear where the buoyancy field has a horizontal gradient. Buoyancy with a horizontal gradient leads to a baroclinic velocity as well as a nonzero baroclinicity vector that provides a source for vorticity (see VOLUME 3). Correspondingly, it is only the baroclinic (depth dependent) piece of geostrophic velocity that is related to horizontal buoyancy gradients. The depth-independent flow is not constrained by horizontal buoyancy gradients, which is the essence of the level of no motion problem in diagnostic oceanography.

The thermal wind shear (15.43) is rotated by $\pi/2$ relative to the direction of $\nabla_h b$. For the northern hemisphere ($f > 0$), the rotation is counter-clockwise so that, for example, with buoyancy increasing southward towards the equator, then the thermal wind increases upwards to the east. That is, the zonal geostrophic flow picks up a more eastward component moving upward. We illustrate this orientation in Figure 15.6, and consider further facets of this flow in Section 15.6.2.

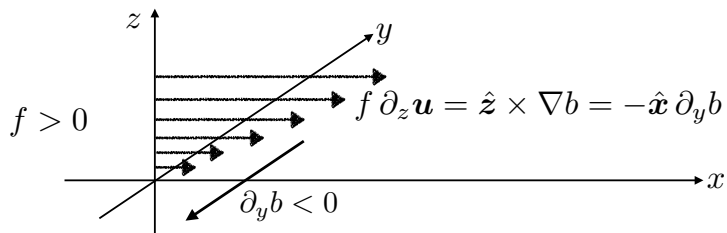


FIGURE 15.6: Orientation of the thermal wind shear for the northern hemisphere ($f > 0$). We depict a buoyancy that decreases to the north, so that $\nabla_h b = \hat{y} \partial_y b = -\hat{y} |\partial_y b|$. The corresponding geostrophic flow becomes more eastward moving vertically upward, as per the thermal wind relation $f \partial_z u = \hat{z} \times \nabla_h b = \hat{x} |\partial_y b|$. More generally, for a northern hemisphere geostrophic flow, the thermal wind shear is oriented with fluid of greater buoyancy to the right when facing in the direction of the shear, and fluid of lesser buoyancy to the left. For the southern hemisphere, the orientation is opposite given $f < 0$, so that a southern hemisphere geostrophic flow has a thermal wind shear oriented with fluid of greater buoyancy to the left. Evidently, in both hemispheres if there is more buoyant fluid towards the equator then that yields a corresponding geostrophic flow that becomes more eastward moving vertically upward.

15.6.1 Relevant portion of density needed for thermal wind

The thermal wind shear (15.43) depends only on the horizontal gradient of buoyancy or density. As seen in Section 15.6.4 for the atmosphere, Section 15.6.5 for the Boussinesq ocean, and Section 15.6.6 for the non-Boussinesq ocean, this property of the thermal wind shear means that we should focus on horizontal gradients of T computed on constant p surfaces (for the atmosphere), or on horizontal gradients of S and Θ (on constant z surfaces for the Boussinesq ocean and constant p surfaces for non-Boussinesq ocean). Consequently, when assessing the ability of a particular density field to drive thermal wind flow, we examine the T , S , and/or Θ fields rather than the *in situ* density field. Equivalently for the ocean, we examine the potential density (Section 14.3.4), with reference pressure taken at the local pressure.

These points are worth emphasizing since surfaces of constant T , S , and Θ in a compressible fluid generally have larger horizontal variability than constant *in situ* density surfaces. As such, one reaches misleading conclusions about the thermal wind flow if focusing on the *in situ* density field, whose quasi-horizontal surfaces might otherwise lead one to incorrectly conclude that the thermal wind shears are smaller than they actually are. We provide the necessary mathematical details to support these points in Sections 15.6.4, 15.6.5 and 15.6.6.

15.6.2 Atmospheric jet stream and the Antarctic Circumpolar Current

Due to the increased solar radiation reaching the equator relative to the poles, the zonal averaged temperature generally reduces when moving poleward. This poleward reduction in temperature corresponds to a poleward reduction in buoyancy. Also, for a stably stratified fluid, buoyancy increases upward. Figure 15.7 illustrates this situation.

A zonal average around a zonally symmetric solid-Earth boundary eliminates zonal derivatives and so renders the zonally averaged thermal wind relation

$$f \frac{\partial \bar{u}}{\partial z} = g \frac{\partial \bar{\rho}}{\partial y} = -\frac{\partial \bar{b}}{\partial y} > 0, \quad (15.45)$$

where $(\bar{\ })$ is the zonal mean operator. In the northern hemisphere, $\partial_y \bar{b} < 0$ (zonal mean buoyancy decreases towards the north), so that the zonal averaged thermal wind shear is positive, $\partial_z \bar{u} > 0$. For example, a westerly zonal wind (blowing to the east) strengthens with height (easterly thermal wind shear). In the Southern Hemisphere, $f < 0$, one finds a poleward decreasing buoyancy, $\partial_y \bar{b} > 0$. This buoyancy gradient corresponds to a eastward thermal wind shear, just like for the northern hemispere. Note that poleward movement, where $|f|$ increases, leads to a smaller thermal wind shear given the same buoyancy gradient.

15.6.3 Diagnosing geostrophic velocity from buoyancy

Vertical integration of the thermal wind relation (15.43) between two constant depth surfaces leads to

$$\mathbf{u}(z) = \mathbf{u}(z_{\text{ref}}) - f^{-1} \nabla_h \times \hat{\mathbf{z}} \int_{z_{\text{ref}}}^z b \, dz. \quad (15.46)$$

Hence, knowledge of the buoyancy field (e.g., through hydrographic measurements of temperature and salinity in the ocean), along with knowledge of the geostrophic velocity at a single depth, $\mathbf{u}(z_{\text{ref}})$, allows for determination of the full geostrophic velocity in terms of density. Unfortunately, specification of the unknown reference velocity is unavailable just from hydrographic

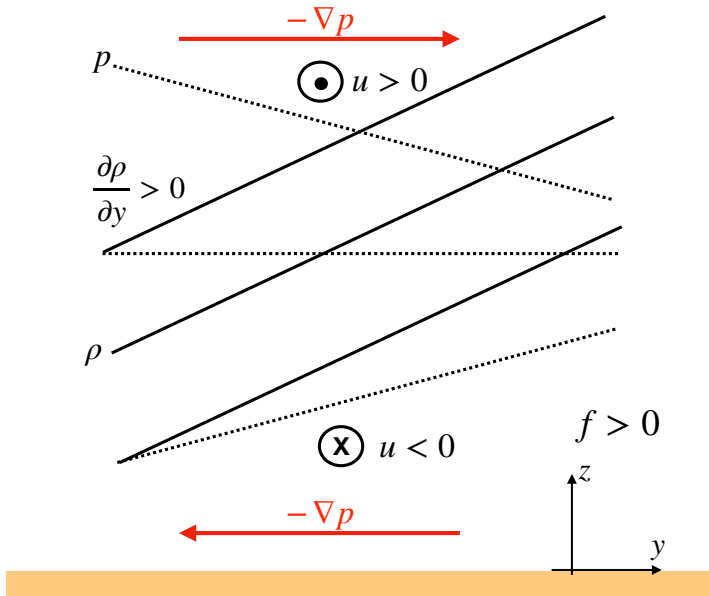


FIGURE 15.7: Schematic of the density (as per the discussion in Section 15.6.1) and hydrostatic pressure fields and the associated thermal wind balanced flow in the northern hemisphere ($f > 0$) with north to the right and east out of the page. We show surfaces of constant density (solid lines) and constant pressure (isobars; dashed lines). Density increases poleward ($\partial\rho/\partial y > 0$) so that, according to the discussion surrounding Figure 15.4, the meridional pressure gradient decreases when moving upward, $\partial(\partial p/\partial y)/\partial z = -g \partial_y \rho < 0$. We illustrate isobars with an equatorward directed downgradient pressure force at lower elevations ($-\partial p/\partial y < 0$) and poleward directed pressure force at higher elevations ($-\partial p/\partial y > 0$). The zonal geostrophic wind is in geostrophic balance with these pressure gradients, with a westward zonal flow at lower elevations (easterly winds) and eastward flow at higher elevations (westerly winds). This flow configuration creates an eastward vertical shear of the zonal geostrophic winds, $\partial u/\partial z > 0$.

measurements, thus leading to the [level of no motion](#) problem in diagnostic oceanography.⁹

15.6.4 Thermal wind balance for the atmosphere

The large-scale atmosphere is compressible and approximately in hydrostatic balance. The expression for geostrophic balance (15.24) in pressure coordinates is a suitable starting point to derive thermal wind for the atmosphere. For this purpose, we take the pressure derivative, $\partial/\partial p$, of (15.24) to render

$$f \frac{\partial \mathbf{u}}{\partial p} = \hat{\mathbf{z}} \times \nabla_p \left[\frac{\partial \Phi}{\partial p} \right], \quad (15.47)$$

with $\Phi = g z$ the geopotential. The hydrostatic relation $\partial p/\partial z = -\rho g$ takes the form

$$\frac{\partial p}{\partial \Phi} = -\rho \Rightarrow \frac{\partial \Phi}{\partial p} = -1/\rho \quad (15.48)$$

in which case

$$f \partial_p \mathbf{u} = -\hat{\mathbf{z}} \times \nabla_p (1/\rho). \quad (15.49)$$

⁹ [Gill \(1982\)](#) provides a discussion of the [level of no motion](#) (also referred to as the depth of no motion) problem arising in ocean circulation studies.

Ideal gas atmosphere

The specific volume takes the following form for an ideal gas atmosphere (see Section 7.5)

$$\rho^{-1} = R^M T/p. \quad (15.50)$$

Since the horizontal derivative in the thermal wind relation (15.49) is along pressure surfaces, we have

$$f \partial_p \mathbf{u} = -(R^M/p) (\hat{\mathbf{z}} \times \nabla_p T). \quad (15.51)$$

This expression gives rise to the name “thermal wind”, with vertical shears of the horizontal velocity generated by horizontal temperature gradients along isobars.

As for the ocean in equation (15.46), we vertically integrate the thermal wind expression (15.51), here between two pressure levels

$$\mathbf{u}(p_A) - \mathbf{u}(p_B) = f^{-1} R^M \hat{\mathbf{z}} \times \nabla_p \left[\int_{p_A}^{p_B} \frac{T dp}{p} \right], \quad (15.52)$$

where $p_A < p_B$, so that p_A is at a higher altitude than p_B . We define the thermal wind shear as the difference between the wind aloft (higher altitude and lower pressure) from that at a lower altitude (greater pressure)

$$\mathbf{u}_T = \mathbf{u}(p_A) - \mathbf{u}(p_B) \quad \text{with } p_A < p_B \quad (15.53)$$

so that

$$\mathbf{u}_T = (R^M/f) \hat{\mathbf{z}} \times \nabla_p \bar{T}^{\ln p}, \quad (15.54)$$

where we introduced the log-pressure weighted temperature between the two pressure surfaces

$$\bar{T}^{\ln p} = \int_{p_A}^{p_B} (T/p) dp. \quad (15.55)$$

Evidently, on the f -plane, equation (15.54) reveals that $R^M \bar{T}^{\ln p}/f$ is the streamfunction for the thermal wind shear.

Reconsider the previous example where the polar regions are colder than tropics, so that in the northern hemisphere on pressure surfaces, $\partial \bar{T}^{\ln p} / \partial y < 0$. Hence, the zonal westerly winds increase in magnitude with height. We depict this situation in Figure 15.8. Furthermore, the thermal wind shear points to the east. For a more general flow in the northern hemisphere, cold (less buoyant) air sits on the left side of the thermal wind shear and warm (buoyant) air on the right. The opposite orientation holds for the southern hemisphere since the Coriolis parameter is negative, $f < 0$.

Barotropic flow

Return to the thermal wind equation (15.49)

$$f \partial_p \mathbf{u} = -\hat{\mathbf{z}} \times \nabla_p (1/\rho) = \hat{\mathbf{z}} \times \rho^{-2} \nabla_p \rho. \quad (15.56)$$

For the special case of density a function just of the pressure, $\rho = \rho(p)$, then $\nabla_p \rho = 0$. This situation defines a **barotropic fluid**, which is characterized here by a horizontal geostrophic velocity with zero vertical variations. Note that we are here only concerned with the geostrophic flow. A density related to pressure through $\rho = \rho(p)$ can still support vertical variations of the

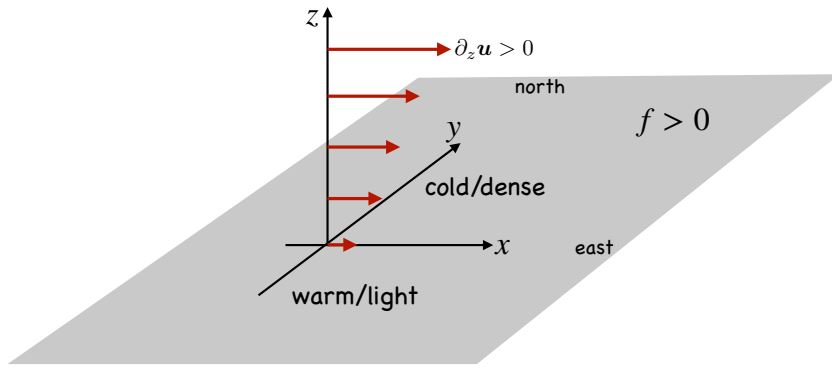


FIGURE 15.8: Thermal wind shear in the northern hemisphere ($f > 0$) middle latitude atmosphere, whereby cold/dense/less buoyant air sits to the north and warm/light/more buoyant air to the south. The zonal geostrophic winds increase to the east when rising in elevation, $\partial u / \partial z > 0$. We say that the zonal winds have an eastward thermal wind shear. In general, a geostrophic wind in the northern hemisphere atmosphere has cold/dense/less buoyant air to the left when facing downwind, whereas the opposite orientation holds for the southern hemisphere where $f < 0$.

ageostrophic flow.

We further discuss barotropic flow in VOLUME 3 as part of our study of vorticity. As detailed in that discussion, the general definition of a barotropic flow is one whereby the **baroclinicity** vector vanishes, $\mathbf{B} = \nabla p \times \nabla(1/\rho) = 0$. The functional relation $\rho = \rho(p)$ (equivalently $p = p(\rho)$) is a sufficient condition for vanishing baroclinicity. For a barotropic flow, there is no generation of vorticity through the twisting action imparted by density isosurfaces that deviate from pressure isosurfaces (isobars).

15.6.5 Thermal wind balance for a Boussinesq ocean

We here expose details for how to work with thermal wind in the ocean, accounting for the presence of both salinity and temperature in the equation of state, with this discussion following from that in Section 15.6.1. To start, consider the most general form of thermal wind according to equation (15.21)

$$f \frac{\partial(\rho \mathbf{u})}{\partial z} = -g \hat{\mathbf{z}} \times \nabla_h \rho. \quad (15.57)$$

Treatment of the *in situ* density depends on whether we consider a Boussinesq ocean (Chapter 13) versus a non-Boussinesq ocean. We here consider the Boussinesq ocean and then the non-Boussinesq ocean in Section 15.6.6.

For a Boussinesq ocean, the *in situ* density on the left hand side of equation (15.57) is set to the constant reference density, ρ_0 , in which case the thermal wind relation is given by

$$f \rho_0 \partial_z \mathbf{u} = -g \hat{\mathbf{z}} \times \nabla_h \rho. \quad (15.58)$$

Following from the discussion of Boussinesq energetics in Section 13.8.4, we know that the *in situ* density in a Boussinesq ocean takes the functional form of equation (13.197)

$$\rho = \rho[S(\mathbf{x}, t), \Theta(\mathbf{x}, t), p = -\rho_0 \Phi(\mathbf{x}, t)]. \quad (15.59)$$

For geostrophic flows we are generally only concerned with the simple geopotential, $\Phi(\mathbf{x}, t) = g z$, which defines the local vertical direction, $\hat{\mathbf{z}}$. Hence, $\hat{\mathbf{z}} \times \nabla_h \rho$ picks out the horizontal derivatives of the *in situ* density along surfaces of constant geopotential. We can thus express the horizontal

in situ density gradient as

$$\nabla_h \rho = \left[\frac{\partial \rho}{\partial S} \right]_{\Theta, \Phi} \nabla_h S + \left[\frac{\partial \rho}{\partial \Theta} \right]_{S, \Phi} \nabla_h \Theta = \rho_o (\beta \nabla_h S - \alpha \nabla_h \Theta), \quad (15.60)$$

where we introduced the Boussinesq form of the haline contraction and thermal expansion coefficients

$$\beta = \frac{1}{\rho_o} \left[\frac{\partial \rho}{\partial S} \right]_{\Theta, \Phi} \quad \text{and} \quad \alpha = -\frac{1}{\rho_o} \left[\frac{\partial \rho}{\partial \Theta} \right]_{S, \Phi}. \quad (15.61)$$

These results lead to the oceanic Boussinesq form of the thermal wind relation

$$f \partial_z \mathbf{u} = g \hat{\mathbf{z}} \times (\alpha \nabla_h \Theta - \beta \nabla_h S), \quad (15.62)$$

which decomposes the thermal wind shear into a contribution from a horizontal gradient in S and a horizontal gradient in Θ . In some treatments, the right hand side contribution is referred to as the horizontal gradient of the locally referenced potential density (see Section 14.6.1). Correspondingly, one generally finds that vertical sections of the potential density (referenced to a pressure near to that where computing thermal wind) provide a useful means to determine the magnitude and direction of the thermal wind shear; far more useful than sections of *in situ* density.

To help understand the geometry of the thermal wind equation (15.62), consider an ocean with a constant salinity and positive thermal expansion coefficient, so that

$$f \partial_z \mathbf{u} = g \alpha \hat{\mathbf{z}} \times \nabla_h \Theta \quad \text{if } \nabla S = 0. \quad (15.63)$$

Hence, in the northern hemisphere ($f > 0$) the thermal wind shear is oriented with relatively warm water to the right of the shear, just like that shown for the atmosphere in Figure 15.8 and more generally as discussed in Figure 15.6. More generally, with a non-constant salinity the thermal wind shear is oriented with more buoyant waters to the right (in northern hemisphere), as per the vector, $\alpha \nabla_h \Theta - \beta \nabla_h S$, appearing on the right hand side of the thermal wind equation (15.62). This vector is proportional to the horizontal components of the dianeutral unit vector introduced in Section 14.5.3 and given by

$$\hat{\gamma} = \frac{-\alpha \nabla \Theta + \beta \nabla S}{|-\alpha \nabla \Theta + \beta \nabla S|} \quad \text{so that} \quad \hat{\gamma}_{\text{horz}} = \frac{-\alpha \nabla_h \Theta + \beta \nabla_h S}{|-\alpha \nabla \Theta + \beta \nabla S|}. \quad (15.64)$$

Evidently, the vertical shear of the horizontal geostrophic velocity is perpendicular to the horizontal projection of the dianeutral unit vector, with this orientation shown in Figure 15.9.

15.6.6 Thermal wind for a non-Boussinesq hydrostatic ocean

We here expose details for how to work with thermal wind in a non-Boussinesq ocean, with this discussion following from that in Section 15.6.1. The formulation follows quite closely to a Boussinesq ocean, only now we start from the expression (15.49) for a compressible hydrostatic fluid using pressure as a vertical coordinate

$$\rho^2 f \partial_p \mathbf{u} = \hat{\mathbf{z}} \times \nabla_{hp} \rho. \quad (15.65)$$

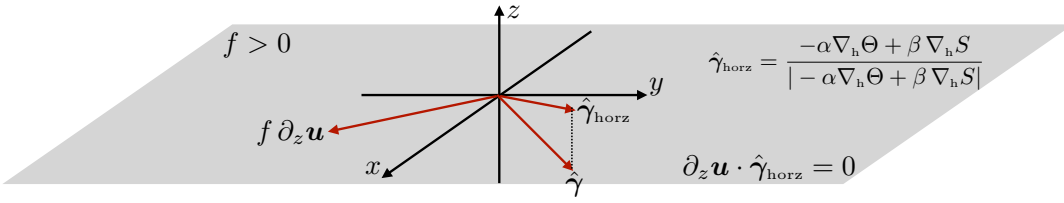


FIGURE 15.9: The thermal wind shear, $f \partial_z \mathbf{u}$, given by equation (15.62) is oriented perpendicular to the horizontal projection of the dianeutral unit vector given in equation (15.64). For example, with $\hat{\gamma}$ pointing towards less buoyant waters, the northern hemisphere thermal wind shear is oriented with more buoyant waters to the right when facing in the direction of the shear. For example, in an ocean with constant salinity, so that $\hat{\gamma}$ is normal to a constant Θ surface and pointing towards colder waters, then the thermal wind shear is oriented with warm water to the right of the shear. This orientation accords with that shown for the atmosphere in Figure 15.8 and more generally as per Figure 15.6.

For a non-Boussinesq ocean, we make use of the pressure dependence of the density so that

$$\rho = \rho[S(\mathbf{x}, t), \Theta(\mathbf{x}, t), p(\mathbf{x}, t)]. \quad (15.66)$$

The horizontal gradient operator, ∇_{hp} , in equation (15.65) is computed along surfaces of constant pressure so that

$$\nabla_{hp}\rho = \left[\frac{\partial \rho}{\partial S} \right]_{\Theta, p} \nabla_{hp}S + \left[\frac{\partial \rho}{\partial \Theta} \right]_{S, p} \nabla_{hp}\Theta = \rho (\beta \nabla_{hp}S - \alpha \nabla_{hp}\Theta), \quad (15.67)$$

where we introduced the non-Boussinesq form of the haline contraction and thermal expansion coefficients

$$\beta = \frac{1}{\rho} \left[\frac{\partial \rho}{\partial S} \right]_{\Theta, p} \quad \text{and} \quad \alpha = -\frac{1}{\rho} \left[\frac{\partial \rho}{\partial \Theta} \right]_{S, p}. \quad (15.68)$$

In this manner we can write the thermal wind relation (15.65) as

$$\rho f \partial_p \mathbf{u} = \hat{z} \times (\beta \nabla_{hp}S - \alpha \nabla_{hp}\Theta). \quad (15.69)$$

This expression is directly analogous to the Boussinesq form given by equation (15.62). Indeed, we can go one step further by using the chain rule and the hydrostatic relation to write

$$\partial_p \mathbf{u} = \frac{\partial \mathbf{u}}{\partial z} \frac{\partial z}{\partial p} = -(\rho g)^{-1} \frac{\partial \mathbf{u}}{\partial z}, \quad (15.70)$$

in which case the non-Boussinesq thermal wind takes on the form

$$f \partial_z \mathbf{u} = g \hat{z} \times (\alpha \nabla_{hp}\Theta - \beta \nabla_{hp}S). \quad (15.71)$$

Now, the key distinction from the Boussinesq form (15.62) is the appearance of a constant pressure derivative, ∇_{hp} , for the non-Boussinesq case, in contrast to the constant geopotential derivative, ∇_h , appearing in the Boussinesq case. Additionally, the non-Boussinesq case uses the distinct form of α and β given by equation (15.68) rather than the Boussinesq form in equation (15.61).

15.7 Isopycnal form stress from geostrophic eddies

As examined in Section 12.1, form stress is the horizontal stress arising from pressure acting on a sloped surface. The mathematical expression for the form stress acting on the top side of a surface is given by equation (12.6)

$$\Sigma_x^{\text{form}} = p \nabla_h \eta, \quad (15.72)$$

with the opposite sign for the form stress on the bottom side of the surface. Here, $z = \eta(x, y, t)$ is the vertical position of the surface (see Figure 12.3 or Figure 15.10). The net horizontal force from form stress is the area integral over the surface.

In this section we examine the zonal mean zonal form stress acting on an isopycnal surface (Section 15.7.1) and on an isopycnal layer (Section 15.7.2), each for an adiabatic, Boussinesq, hydrostatic ocean in geostrophic balance and within a zonally periodic channel of length L . We furthermore assume the fluid density is a linear function of Θ to remove compressibility effects and focus on the dynamics rather than also consider the thermodynamics. As we show, the zonal mean zonal form stress arising from geostrophically balanced fluctuations provide an eastward acceleration to the fluid. At the same time, these geostrophic eddies transport buoyancy and thickness/volume meridionally.

Although the channel geometry is relatively simple, it has applications to the middle latitude atmospheric circulation as well as for ocean circulation, particularly in the Southern Ocean where there is circumpolar channel-like flow within the Antarctic Circumpolar Current. Furthermore, the discussion exposes key elements of eddy-mean flow interactions, sharing points with the leading order generalized Lagrangian mean as well as the quasi-Stokes transport, both introduced in VOLUME 5.

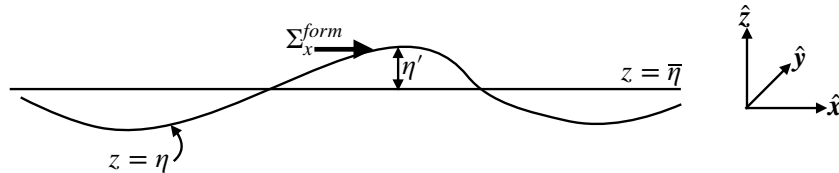


FIGURE 15.10: Schematic of the zonal form stress, Σ_x^{form} , acting on a surface whose zonal mean vertical position is $z = \bar{\eta}(y, t)$ and whose vertical position relative to the zonal mean is $z = \bar{\eta}(y, t) + \eta'(x, y, t)$.

15.7.1 Zonal mean zonal form stress on an isopycnal surface

We are here interested in the form stress acting on an isopycnal surface (constant buoyancy surface). Before specializing to an isopycnal, we decompose the form stress according to the zonal mean depth and its deviation from zonal mean (see Figure 15.10). Thereafter, specialization to an isopycnal surface in an adiabatic fluid connects the zonal mean form stress to the meridional eddy flux of buoyancy.

Zonal form stress on an arbitrary surface in a channel

The zonal mean vertical position of a surface is written

$$\bar{\eta}(y, t) = \frac{1}{L} \oint_0^L \eta(x, y, t) dx \quad (15.73)$$

and its corresponding zonal fluctuation is

$$\eta' = \eta - \bar{\eta}. \quad (15.74)$$

The zonal component of the form stress acting on this surface is thus given by

$$p \partial_x \eta = p(x, \bar{\eta} + \eta') \partial_x (\bar{\eta} + \eta') \quad (15.75a)$$

$$= p(x, \bar{\eta} + \eta') \partial_x \eta' \quad (15.75b)$$

$$\approx [p(x, \bar{\eta}) + \partial_z p(x, \bar{\eta}) \eta'] \partial_x \eta' \quad (15.75c)$$

$$= p(x, \bar{\eta}) \partial_x \eta' + \mathcal{O}(\eta')^2. \quad (15.75d)$$

Hence, to second order in fluctuations, η' , the zonal form stress acting on the surface equals to $p(x, \bar{\eta}) \partial_x \eta'$, where it is important to note that pressure is evaluated at the zonal mean depth, $z = \bar{\eta}$.

To within the same accuracy, the zonal integral of the zonal form stress is given by

$$\oint_0^L \Sigma_x^{\text{form}} dx \approx \oint_0^L p(\bar{\eta}) (\partial \eta' / \partial x) dx = - \oint_0^L \eta' [\partial p(\bar{\eta}) / \partial x] dx. \quad (15.76)$$

The final equality follows from zonal periodicity, which allows us to introduce the dual form stress inside the integral.¹⁰ Now assume the zonal pressure gradient at $\bar{\eta}$ is balanced by a meridional geostrophic velocity at the same vertical position

$$\partial p(\bar{\eta}) / \partial x = f \rho_o v(\bar{\eta}). \quad (15.77)$$

We can now decompose $v(\bar{\eta})$ into a mean and fluctuation,

$$v(\bar{\eta}) = \bar{v}(\bar{\eta}) + v'(\bar{\eta}), \quad (15.78)$$

so that

$$\oint_0^L \Sigma_x^{\text{form}} dx = -\rho_o f \oint_0^L \eta' v' dx, \quad (15.79)$$

where we noted that the Coriolis parameter is independent of zonal position and so can be pulled outside of the zonal integral. Hence, there is a nonzero zonal mean zonal form stress when there is a nonzero zonal correlation between fluctuations in the meridional velocity and the depth of the surface

$$\bar{\Sigma}_x^{\text{form}} = -\rho_o f \overline{v' \eta'}. \quad (15.80)$$

Geostrophic eddies affect a poleward buoyancy transport and eastward form stress

To further unpack the correlation appearing in equation (15.80), specialize to the case of an isopycnal surface in an adiabatic fluid. As shown in our discussion of generalized Lagrangian mean averaging in VOLUME 5, vertical fluctuations in the position of the isopycnal surfaces, relative to the zonal mean $\bar{\eta}$, are related to zonal fluctuations in the density

$$\eta' \approx -\frac{\rho'}{\partial \bar{\rho} / \partial z} = -\frac{b'}{N^2}, \quad (15.81)$$

¹⁰We discussed the relation between form stress and dual form stress in Section 12.4.4. The dual form stress here appears because the channel is zonally periodic. Hence, a zonal integral of the form stress equals (with a minus sign) to the zonal integral of the dual form stress.

where we introduced the squared buoyancy frequency of the zonal mean state, N^2 , as well as the fluctuating buoyancy, b' , via

$$N^2 = -\frac{g}{\rho_0} \frac{\partial \bar{\rho}}{\partial z} \quad \text{and} \quad b' = -\frac{g \rho'}{\rho_0}. \quad (15.82)$$

Equation (15.81) results from a leading order Taylor series relative to the zonal mean vertical position, $\bar{\eta}$. Making use of this result, we find the zonally averaged zonal form stress takes the form

$$\bar{\Sigma}_x^{\text{form}} = \frac{\rho_0 f}{N^2} \overline{v' b'}. \quad (15.83)$$

Again, the assumptions leading to equation (15.83) are (i) zonal periodicity, (ii) adiabatic and Boussinesq fluid, (iii) geostrophically balanced flow. Under these assumptions, the zonal mean zonal form stress acting on an isopycnal surface is proportional to the zonal correlation between fluctuations in the meridional velocity and the buoyancy. As we study in VOLUME 5, unstable waves satisfying the scalings of [quasi-geostrophy](#) (e.g., small Rossby number and large Richardson number) transport positive buoyancy (e.g., warm air/water) poleward and negative buoyancy (e.g., cold air/water) equatorward, thus ameliorating the equator-to-pole buoyancy difference established by solar radiation that preferentially warms the tropics. More generally, unstable quasi-geostrophic disturbances, such as those associated with [baroclinic instability](#), transport buoyancy down the horizontal buoyancy gradient. With buoyancy decreasing poleward, baroclinically unstable disturbances transport buoyancy poleward; so that $\overline{v' b'} > 0$. Correspondingly, these eddies produce a positive zonal mean zonal form stress

$$\bar{\Sigma}_x^{\text{form}} > 0. \quad (15.84)$$

Hence, in addition to transporting buoyancy poleward, geostrophic eddies provide a positive zonal mean force through zonal integrated form stress that accelerates the fluid in the eastward direction. These two properties of geostrophic eddies (poleward flux of positive buoyancy anomalies along with an eastward acceleration from form stress) are fundamental to the middle latitude atmospheric circulation as well as for ocean circulation, particularly within the channel-like Antarctic Circumpolar Current.

15.7.2 Zonal mean zonal form stress acting on an isopycnal layer

We offer another lens to understand the zonal mean zonal form stress by examining the form stress acting on a constant density layer of adiabatic Boussinesq fluid such as shown in Figure 15.11. This layered/isopycnal analysis anticipates some of the development considered for the stacked shallow water model and the isopycnal primitive equations in VOLUME 4.

Eastward layer eddy form stress and equatorward eddy thickness flux

The net form stress acting on the upper and lower layer interfaces in Figure 15.11 is given by

$$\Sigma^{\text{layer form}} = p_1 \nabla \eta_1 - p_2 \nabla \eta_2 \quad (15.85a)$$

$$= p(\eta + h/2) \nabla(\eta + h/2) - p(\eta - h/2) \nabla(\eta - h/2) \quad (15.85b)$$

$$\approx [p(\eta) - \rho g h/2] \nabla(\eta + h/2) - [p(\eta) + \rho g h/2] \nabla(\eta - h/2) \quad (15.85c)$$

$$= p \nabla h - \rho g h \nabla \eta \quad (15.85d)$$

$$= \nabla(p h) - h \nabla(p + \rho g \eta) \quad (15.85e)$$

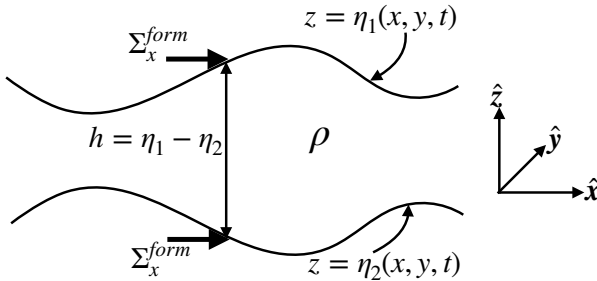


FIGURE 15.11: Schematic of a constant density layer of an adiabatic, hydrostatic, Boussinesq fluid with thickness $h(x, y, t) = \eta_1(x, y, t) - \eta_2(x, y, t) = (\eta + h/2) - (\eta - h/2)$, and uniform density $\rho = \text{constant}$. The east points to the right and north is oriented into the page. The zonal form stress, Σ_x^{form} , acting on the upper and lower interfaces at a horizontal position (x, y) are shown by the thick horizontal vectors. The zonal form stress is the horizontal component of the pressure force per area acting on the layer interfaces, with the sign of the form stress determined by the slope of the layer interface. For a zonally periodic fluid layer, the net zonal pressure force acting on the layer arises from the zonal form stress integrated over the layer interfaces.

$$= \nabla(p h) - \rho h \nabla M. \quad (15.85f)$$

In this relation we set $z = \eta$ for the vertical position at the center of the layer, introduced the **Montgomery potential**

$$M\rho_e = p + \rho g \eta, \quad (15.86)$$

and noted that ρ is a uniform constant layer potential density so that it commutes with the horizontal gradient operator computed along ρ surfaces. We also made use of the hydrostatic balance to approximate the interface pressures as

$$p(\eta + h/2) \approx p(\eta) + \frac{\partial p}{\partial z} \frac{h}{2} = p(\eta) - \rho g h/2 \quad (15.87a)$$

$$p(\eta - h/2) \approx p(\eta) - \frac{\partial p}{\partial z} \frac{h}{2} = p(\eta) + \rho g h/2. \quad (15.87b)$$

The zonal mean of the zonal layer form stress is thus given by the correlation between the layer thickness fluctuations and fluctuations in the zonal derivative of the Montgomery potential

$$\overline{\Sigma_x^{\text{layer form}}} = -\rho \overline{h' \partial M'/\partial x}, \quad (15.88)$$

where we set $\overline{\partial M/\partial x} = 0$ due to zonal periodicity. As seen in our study of the primitive equations in isopycnal vertical coordinates (VOLUME 3), the Montgomery potential is the geostrophic streamfunction in isopycnal coordinates, so that the fluctuating meridional geostrophic velocity is given by

$$f v' = \partial_x M'. \quad (15.89)$$

Consequently, the zonal mean zonal form stress acting on the layer equals to the correlation between the thickness fluctuations and fluctuations in the meridional geostrophic velocity

$$\overline{\Sigma_x^{\text{layer form}}} = -\rho f \overline{v' h'}. \quad (15.90)$$

Hence, as the geostrophic eddies provide a net eastward acceleration to the layer interfaces ($\overline{\Sigma_x^{\text{form}}} > 0$ as in equation (15.84)), they correspondingly provide a net eastward acceleration to the layer ($\overline{\Sigma_x^{\text{layer form}}} > 0$ as in equation (15.90)), thus moving volume meridionally within isopycnal layers so that positive thickness fluctuations are transported equatorward, $f v' \overline{h'} < 0$.

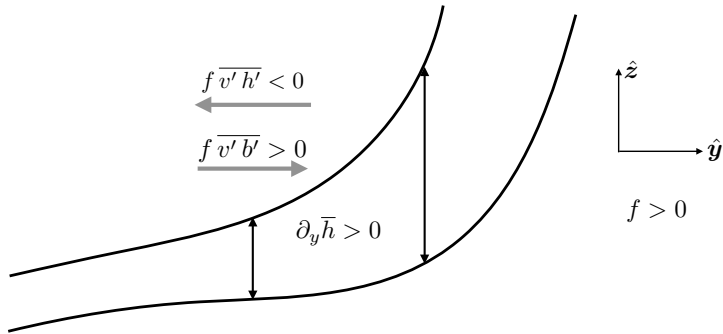


FIGURE 15.12: Illustrating the mean effects from baroclinic geostrophic eddies as they act to flux layer thickness downgradient ($f \bar{v}' \bar{h}' < 0$) and buoyancy poleward ($f \bar{v}' \bar{b}' > 0$). These processes result in the slumping or flattening of regions of steeply sloping isopycnals, thus reducing the available potential energy.

Downgradient thickness flux

To further understand the physics of the form stress in equation (15.90), parameterize the velocity-thickness eddy correlation, $\bar{v}' \bar{h}'$, by downgradient diffusion of thickness

$$\bar{v}' \bar{h}' = -\kappa \partial_y \bar{h}, \quad (15.91)$$

where $\kappa > 0$ is a nonzero kinematic diffusivity (dimensions of squared length per time). This parameterization is suggested by the work of [Gent and McWilliams \(1990\)](#) as discussed in the eddy parameterization chapter of VOLUME 4. As noted there, thickness diffusion as a parameterization reflects the general tendency of geostrophic eddies to reduce horizontal gradients in layer thickness as they reduce the available potential energy of the flow. In this case the zonal mean zonal form stress is

$$\bar{\Sigma}_x^{\text{layer form}} = \rho f \kappa \partial_y \bar{h}. \quad (15.92)$$

Figure 15.12 illustrates a northern hemisphere configuration where the zonal mean layer thickness increases to the north, $\partial_y \bar{h} > 0$. This density structure has a corresponding eastward zonal mean zonal form stress arising from parameterized geostrophic eddies acting on layer thickness. This situation corresponds to the case in Section 15.7.1, where we saw that geostrophic eddies preferentially transport positive buoyancy anomalies poleward and negative buoyancy anomalies equatorward. In the present analysis, meridional changes to the layer thickness correspond to a nonzero thermal wind shear. If layer thickness increases poleward, as for the case of weaker vertical stratification in the high latitudes, then the zonal velocity has a positive vertical shear, thus contributing an eastward zonal mean form stress.

15.7.3 Comments and further study

A key feature of geostrophic eddies exposed by this discussion concerns the connection between zonal form stress (providing an eastward force on the zonally periodic channel flow) and meridional eddy transport of buoyancy (positive buoyancy anomalies are transported poleward) and thickness (positive thickness anomalies are transported equatorward). The periodic channel domain is highly idealized. Nonetheless, the basic ideas form the roots for much of how we think about geostrophic eddies in the middle latitude atmosphere and the Southern Ocean. Further generalizations of the results in this section lead to the generalized Lagrangian mean, whose kinematic rudiments are discussed in VOLUME 4 as part of our study of tracer kinematics,

as well as the thickness weighted average studied in VOLUME 3 as part of the isopycnal models chapter.

The fundamental role of form stress in geostrophic turbulent flows is pedagogically treated by [Vallis \(2017\)](#). See, in particular, his Chapter 21 for a thorough and insightful discussion of circulation in the Southern Ocean. We also study form stress within the shallow water fluid in VOLUME 3, with that discussion complementing the presentation given here. We also touch on the notions of form stress when discussing the milestone paper from [Gent and McWilliams \(1990\)](#) as part of the VOLUME 4 chapter on eddy parameterizations. The ideas from [Gent and McWilliams \(1990\)](#) are foundational to how we think about the mean effects from baroclinic eddies in the ocean and atmosphere.



15.8 Exercises

EXERCISE 15.1: SMALL ROSSBY NUMBER AT HUMAN SCALES

Consider motion of a car at a speed $U \sim 10^5$ m hour $^{-1}$ and a length scale of $L \sim 10$ m. Furthermore, assume the car is moving at 30°N latitude so that $f_{\text{human}} = 2\Omega_{\text{human}} \sin \phi = \Omega_{\text{human}}$.

- (a) What is the rotation rate of the planet and corresponding rotation period, $T_{\text{human}} = 2\pi/\Omega_{\text{human}}$, required to render a unit Rossby number ($\text{Ro} = 1$) for the given “human” sized scales? Give resulting rotation rate in units of inverse seconds and period in seconds.
- (b) If the Earth rotated at the angular speed Ω_{human} , what would be the rigid-body speed for a point at rest on the Earth’s surface at the equator? Give result in units of meter per second.
- (c) How does the rigid-body speed compare to the speed of sound at standard atmospheric conditions? What about the root-mean-square speed for air molecules? Hint: read the chapter on the continuum approximation in VOLUME 1.
- (d) Discuss an astronomical object that has a very large rotational speed. Hint: 1993 Nobel Prize in physics.

EXERCISE 15.2: THE BETA SPIRAL

Consider a steady state Boussinesq planetary geostrophic fluid in the absence of mixing. Write the geostrophic velocity as

$$u = |\mathbf{u}| \cos \Delta \quad v = |\mathbf{u}| \sin \Delta, \quad (15.93)$$

where Δ is the angle measured counter-clockwise from east. Use thermal wind and the steady state perfect fluid buoyancy equation to determine an expression for $\partial \Delta / \partial z$. Show that for $f > 0$ (northern hemisphere) and $\partial b / \partial z = N^2 > 0$ (gravitationally stable fluid column; see Section 14.5), then $\partial \Delta / \partial z$ has opposite sign from the vertical velocity, w . This spiralling of the geostrophic velocity is known as the **beta spiral** in ocean physics.

EXERCISE 15.3: ALTERNATIVE FORM OF THERMAL WIND

Consider a fluid with density a function of pressure and potential temperature

$$\rho = \rho(\theta, p). \quad (15.94)$$

A physical realization of this equation of state is a lake. Show that the thermal wind shear for

a hydrostatic and non-Boussinesq fluid with this equation of state can be written in the form

$$\frac{\partial \mathbf{u}}{\partial z} = \left[\frac{N^2}{f \rho g} \right] (\hat{\mathbf{z}} \times \nabla_{h\theta} p), \quad (15.95)$$

where

$$N^2 = -\frac{g}{\rho} \frac{\partial \rho}{\partial \theta} \frac{\partial \theta}{\partial z} = g \alpha_\theta \frac{\partial \theta}{\partial z} > 0 \quad (15.96)$$

is the squared buoyancy frequency, assumed positive so that the fluid is gravitationally stable in the vertical (see Section 14.6). The term α_θ is the thermal expansion coefficient written in terms of potential temperature (Section 14.3.4),

$$\alpha_\theta = -(1/\rho) \partial \rho / \partial \theta > 0. \quad (15.97)$$

Finally, the horizontal gradient projected onto constant θ surfaces is given by¹¹

$$\nabla_{h\theta} = \hat{\mathbf{x}} \left[\frac{\partial}{\partial x} \right]_{y,\theta} + \hat{\mathbf{y}} \left[\frac{\partial}{\partial y} \right]_{x,\theta} \quad (15.98a)$$

$$= \nabla_h - \left[\frac{\nabla_h \theta}{\partial \theta / \partial z} \right] \frac{\partial}{\partial z}. \quad (15.98b)$$

Hint: This exercise requires careful use of the chain rule and the hydrostatic relation, along with the equations given in the problem statement. Furthermore, assume the fluid is fully compressible.

Hint: Some may wish to “warm-up” by showing that the result holds for the simpler equation of state $\rho = \rho(\theta)$. Some of the steps used for the simpler case are relevant for the case with $\rho = \rho(\theta, p)$.

EXERCISE 15.4: GEOSTROPHIC FLOW IN A ZONAL PERIODIC CHANNEL

Consider a constant inviscid geostrophic flow, $u > 0$, of a homogeneous fluid (constant density, ρ) in a zonal periodic channel on a northern hemisphere f -plane. Derive an expression for the free surface of the fluid layer, with $z = \eta$ the free surface, $z = 0$ the surface when the fluid is at rest. Draw a sketch.

EXERCISE 15.5: GEOSTROPHIC FLOW NEXT TO A SLOPING BOTTOM

In Section 11.4.3 we studied the steric setup of the sea surface height adjacent to a coast, including the general case of a sloping bottom. Revisit that analysis and now allow for a nonzero bottom geostrophically balanced flow, so that we no longer assume a zero horizontal pressure gradient next to the bottom. How are equations (11.83a) and (11.83b) extended to allow for a nonzero geostrophic flow next to the sloping bottom?



¹¹Generalized vertical coordinate horizontal gradients, such as $\nabla_{h\theta}$, are discussed in VOLUME 3, where we develop the mathematics of generalized vertical coordinates.

Chapter 16

TANGENT PLANE FLOWS

In this chapter we study a variety of inviscid tangent plane (horizontal) flow regimes characterized by a balance between a subset of terms appearing in the horizontal momentum equation. This study allows us to directly compare the geostrophically balanced flow of Chapter 15 to a variety of other balanced flows such as gradient wind and cyclostrophic balance, as well as inertial motion. We provide a categorization of the flow following natural coordinates (also referred to as intrinsic coordinates), which offer a concise means to compare the relative magnitudes of the Coriolis, pressure, and centrifugal accelerations acting on a fluid element moving horizontally.

READER'S GUIDE TO THIS CHAPTER

We make use of the hydrostatic primitive equations from Section 11.1, along with the Boussinesq ocean equations from Section 13.1. We also assume an understanding of the geostrophic balance from Chapter 15. Throughout this chapter we assume a tangent plane geometry and associated equations from Section 8.5, thus allowing for Cartesian coordinates. Also, we ignore all vertical motion, so that $\partial_z = 0$ and $\nabla_h \cdot \mathbf{u} = 0$. Some of this material is used in subsequent chapters, in particular Chapter 17 on Ekman mechanics as well as in VOLUME 3 for the study of quasi-geostrophy.

Recall from our study of effective gravity in VOLUME 1, motion on a geopotential surface incorporates the acceleration from both the central gravitational field and the planetary centrifugal acceleration. This property holds for the tangent plane approximation assumed in this chapter, whereby a geopotential is assumed to be horizontal. Consequently, planetary centrifugal acceleration is absorbed by the geopotential and so it does not explicitly appear here. We are thus concerned here with centrifugal accelerations arising from curved motion of the fluid itself, rather than to planetary rotation.

16.1 Horizontal flow using natural coordinates	532
16.1.1 Natural coordinates	532
16.1.2 Material acceleration	533
16.1.3 Centripetal and centrifugal accelerations	534
16.1.4 Coriolis and pressure gradient	535
16.1.5 Horizontal momentum equation and local Rossby number	535
16.1.6 Decomposition of the acceleration	536
16.1.7 Further study	537
16.2 Exact geostrophic balance	537
16.2.1 Steady f -plane flow	538
16.2.2 Steady β -plane flow	538
16.2.3 What about geostrophic balance with curved motion?	538

16.3	Inertial motion	539
16.3.1	Anti-cyclonic circular motion on f -plane	539
16.3.2	Period for inertial motion	540
16.3.3	Observing inertial motion	540
16.3.4	Inertial motion as Lagrangian fluid particle motion	541
16.3.5	“Inertial” motion does not refer to an inertial reference frame	541
16.3.6	Inertial motion on a sphere	541
16.4	Cyclostrophic balance	541
16.5	Gradient wind balance	543
16.5.1	Constraints on gradient wind flow	544
16.5.2	A variety of gradient wind flows	545
16.5.3	Comments	546
16.6	Exercises	546

16.1 Horizontal flow using natural coordinates

In this section we decompose the horizontal Boussinesq momentum equation into motion parallel to and motion perpendicular to the instantaneous trajectory of a fluid element moving along a constant geopotential surface. That is, we characterize the velocity and acceleration according to the local flow direction. Furthermore, we are only concerned with motion on a constant geopotential using the tangent plane approximation; i.e., horizontal motion.¹ The **natural coordinates** arising from this description exposes the centripetal/centrifugal acceleration that arises from curvature in the trajectory as measured by the radius of curvature. This non-inertial acceleration is distinct from the centrifugal acceleration that arises from planetary rotation, with planetary centrifugal acceleration already contained within the effective gravitational acceleration that acts in the local vertical direction (see discussion of effective gravity in VOLUME 1). We also decompose the accelerations from pressure, friction, and Coriolis into their natural coordinate components.

16.1.1 Natural coordinates

We make use of **natural coordinates** for our study of horizontal tangent plane motion. Natural coordinates (also **intrinsic coordinates**) are defined by a locally orthogonal set of unit vectors (see Figure 16.1)

$$\hat{z} = \hat{u} \times \hat{n} = \text{vertical direction} \quad (16.1a)$$

$$\hat{u} = \hat{n} \times \hat{z} = \text{tangent to horizontal velocity} \quad (16.1b)$$

$$\hat{n} = \hat{z} \times \hat{u} = \text{normal direction to the left of motion.} \quad (16.1c)$$

The unit vector, \hat{u} , is aligned with the horizontal velocity vector, so that

$$\mathbf{u} = |\mathbf{u}| \hat{u} = \frac{D\mathbf{s}}{Dt} \hat{u}, \quad (16.2)$$

where s is the arc-length measured along the trajectory² The unit vector, \hat{n} , is perpendicular to the velocity and points to the left of the trajectory facing downstream.

¹The two-dimensional motion considered here can be generalized to three-dimensional motion through use of the Serret-Frénet equations from differential geometry. An introduction to this approach for motion is provided by Section 20 of *Serrin* (1959) and Section 15.3.4 of *Dahlen and Tromp* (1998).

²See our discussion of line integrals in VOLUME 1 for more on the arc-length.

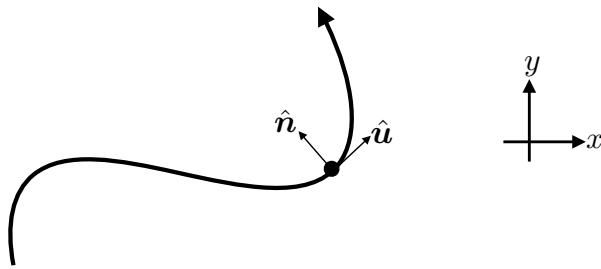


FIGURE 16.1: Illustrating the decomposition of horizontal motion of a fluid element into natural coordinates, as defined by a unit tangent vector, \hat{u} , pointing in the direction of the fluid element motion, and a unit normal vector, \hat{n} , pointing to the left of the motion facing downstream. The vertical direction is out of the page and satisfies $\hat{u} \times \hat{n} = \hat{z}$.

16.1.2 Material acceleration

When writing the velocity according to equation (16.2), we decompose the acceleration into the change in speed and change in direction

$$\frac{D\mathbf{u}}{Dt} = \frac{D|\mathbf{u}|}{Dt} \hat{u} + |\mathbf{u}| \frac{D\hat{u}}{Dt}. \quad (16.3)$$

Following our discussion in VOLUME 1 of rigid-body rotational motion, the magnitude of the direction change can be written in terms of the infinitesimal angle swept out by the motion as the fluid element moves along a trajectory

$$|\delta\hat{u}| = |\delta\vartheta|. \quad (16.4)$$

The infinitesimal angle swept out by the trajectory is related to the radius of curvature, R (Figure 16.2), and the arc-length increment, δs , traversed by the trajectory

$$\delta\vartheta = \frac{\delta s}{R}. \quad (16.5)$$

Finally, the infinitesimal change in tangent, $\delta\hat{u}$, is directed normal to the motion, which we see by noting

$$\hat{u} \cdot \hat{u} = 1 \implies \delta\hat{u} \cdot \hat{u} = 0. \quad (16.6)$$

That is, $\delta\hat{u}$ is orthogonal to \hat{u} , so that it points either parallel or anti-parallel to \hat{n} . Our convention is that \hat{n} points to the left of \hat{u} , so that if the trajectory turns to the left, then $\delta\hat{u}$ points parallel to \hat{n} , whereas if the trajectory turns to the right then $\delta\hat{u}$ points anti-parallel to \hat{n} . That is, $\delta\hat{u}$ always points towards the center of the circle used to compute the radius of curvature as in Figure 16.2.

Bringing these results together leads to the expression for the infinitesimal unit vector change

$$\delta\hat{u} = \hat{n} \frac{\delta s}{R}. \quad (16.7)$$

Our sign convention takes $R > 0$ for a fluid element turning in the direction of \hat{n} (to the left facing downstream) and $R < 0$ when turning opposite to \hat{n} (to the right facing downstream). Hence, the material time change is

$$\frac{D\hat{u}}{Dt} = \frac{D\hat{u}}{Ds} \frac{Ds}{Dt} = \frac{\hat{n}}{R} \frac{Ds}{Dt} = \frac{\hat{n}}{R} |\mathbf{u}|, \quad (16.8)$$

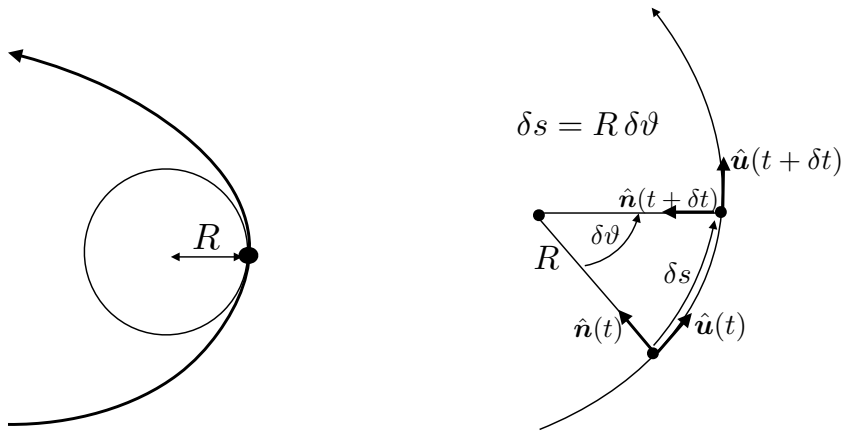


FIGURE 16.2: The left panel illustrates the radius of curvature associated with turning motion of a fluid element. The radius of curvature equals to the radius of a tangent circle (the **curvature circle**) that approximates, to second order accuracy, the trajectory at a particular point. The radius is smaller in magnitude when the trajectory is highly curved, whereas $|R| = \infty$ when the trajectory is straight. The radius is positive when the trajectory turns into the normal direction as depicted here (to the left; concave as defined by \hat{n}) and negative when turning in the opposite direction (to the right; convex as defined by \hat{n}). (For more on the mathematics of curvature, refer to the vector calculus chapter in VOLUME 1.) The right panel shows the time evolution of the unit vectors, \hat{u} and \hat{n} , along a trajectory, with these unit vectors oriented along (\hat{u}) and to the left (\hat{n}) of the motion. For simplicity, we depict motion on a circle, so that the radius of curvature, R , remains constant and is equal to the circle's radius. In general, the radius also changes along the trajectory.

where the speed is given by the time change of the arc-length along the trajectory

$$|\mathbf{u}| = \frac{Ds}{Dt}. \quad (16.9)$$

Combining these results renders the acceleration

$$\frac{D\mathbf{u}}{Dt} = \frac{D|\mathbf{u}|}{Dt} \hat{\mathbf{u}} + \frac{|\mathbf{u}|^2}{R} \hat{\mathbf{n}} = \frac{D^2s}{Dt^2} \hat{\mathbf{u}} + \frac{|\mathbf{u}|^2}{R} \hat{\mathbf{n}}. \quad (16.10)$$

The acceleration has thus been decomposed into the change in speed of the fluid element along the direction of the motion, plus the centripetal acceleration due to curvature of the trajectory. In Section 16.1.3 we justify referring to $\hat{\mathbf{n}} |\mathbf{u}|^2/R$ as the **centripetal** acceleration of the curved fluid motion.

16.1.3 Centripetal and centrifugal accelerations

The **centripetal** acceleration points towards the concave side of a turning trajectory: “centripetal” means “towards the center.” Its opposing partner, the **centrifugal** (“away from center”) acceleration points to the convex side (see Figure 16.3). So how do we interpret $\hat{\mathbf{n}} |\mathbf{u}|^2/R$? For motion turning to the left, towards $\hat{\mathbf{n}}$, the radius of curvature is positive, $R > 0$, so that $\hat{\mathbf{n}} |\mathbf{u}|^2/R$ points to the concave side of the trajectory (left side). For a trajectory turning to the right then $R < 0$, which again means that $\hat{\mathbf{n}} |\mathbf{u}|^2/R$ points to the concave side (now on the right). We conclude that the acceleration $\hat{\mathbf{n}} |\mathbf{u}|^2/R$ indeed represents a centripetal acceleration and $-\hat{\mathbf{n}} |\mathbf{u}|^2/R$ is the centrifugal acceleration.

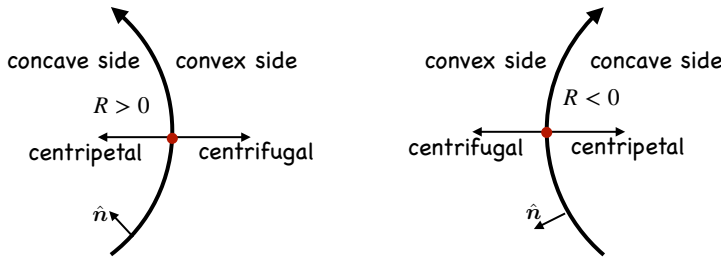


FIGURE 16.3: Centripetal acceleration of a turning fluid element, $\hat{n} |\mathbf{u}|^2/R$, points to the concave side of the curve (towards the center) whereas the centrifugal acceleration, $-\hat{n} |\mathbf{u}|^2/R$, points to the convex side (away from the center). The centripetal and centrifugal accelerations are paired action/reaction accelerations. The normal unit vector, \hat{n} , always points to the left of the motion, whereas the radius of curvature, R , is positive or negative depending on the direction of the turning motion. For a left turning trajectory (in direction of \hat{n}), the concave side is on the left and has positive radius of curvature, $R > 0$, whereas for the right turning trajectory (opposite direction of \hat{n}) the concave side is to the right with $R < 0$. To help remember the signs, note that centrifugal means “away from the center” whereas centripetal means “towards the center”. It is the centrifugal acceleration that pulls one away from the center of a merry-go-round whereas one’s arms and hands provide the balancing centripetal acceleration.

16.1.4 Coriolis and pressure gradient

The Coriolis acceleration takes the following form in natural coordinates

$$-f \hat{z} \times \mathbf{u} = -(\hat{z} \times \hat{\mathbf{u}}) f |\mathbf{u}| = -\hat{n} f |\mathbf{u}|, \quad (16.11)$$

so that the Coriolis acceleration always points to the right of the flow direction for $f > 0$. In contrast, the pressure gradient has two components

$$\nabla_h p = \hat{\mathbf{u}} (\hat{\mathbf{u}} \cdot \nabla_h p) + \hat{n} (\hat{n} \cdot \nabla_h p) = \hat{\mathbf{u}} \frac{\partial p}{\partial s} + \hat{n} \frac{\partial p}{\partial n}, \quad (16.12)$$

one pointing along the flow direction and one normal to the direction.

16.1.5 Horizontal momentum equation and local Rossby number

Bringing the above results together leads to the horizontal momentum equation as decomposed into natural coordinates

$$\frac{D|\mathbf{u}|}{Dt} = -\frac{1}{\rho_0} \frac{\partial p}{\partial s} + \mathbf{F} \cdot \hat{\mathbf{u}} \quad \text{motion in } \hat{\mathbf{u}} \text{ direction} \quad (16.13a)$$

$$\frac{|\mathbf{u}|^2}{R} + f |\mathbf{u}| = -\frac{1}{\rho_0} \frac{\partial p}{\partial n} + \mathbf{F} \cdot \hat{n} \quad \text{motion in } \hat{n} \text{ direction (perpendicular to } \hat{\mathbf{u}}\text{)}, \quad (16.13b)$$

where \mathbf{F} is the frictional acceleration and ρ_0 is the reference density for the Boussinesq ocean. These equations decompose the accelerations into those acting parallel to and normal to the trajectory. It is notable that the equation for the normal component is purely diagnostic; there is no time derivative in equation (16.13b). Instead, it is a balance containing accelerations from centripetal, Coriolis, normal pressure gradient, and normal component of friction. In the next few sections we consider certain limiting cases as revealed by the equations of motion (16.13a) and (16.13b). Friction remains zero in this chapter, yet it is nonzero in our study of Ekman mechanics in Chapter 17.

Steady frictionless flow

The frictionless balanced motions considered in this chapter all occur with a fixed velocity magnitude for the fluid element, so that the along-trajectory component of the momentum equation (16.13a) for frictionless motion reduces to

$$\frac{D|\mathbf{u}|}{Dt} = -\frac{1}{\rho_0} \frac{\partial p}{\partial s} = 0. \quad (16.14)$$

Hence, there is no pressure gradient along the direction of the fluid element motion. Correspondingly, the frictionless fluid motion preserves its kinetic energy

$$\frac{1}{2} \frac{D(\mathbf{u} \cdot \mathbf{u})}{Dt} = |\mathbf{u}| \frac{D|\mathbf{u}|}{Dt} = 0. \quad (16.15)$$

Local Rossby number

As discussed in Section 15.3, the Rossby number is the non-dimensional ratio of the acceleration from velocity advection to the Coriolis acceleration. In the normal component to the momentum equation (16.13b), we have the advection term manifest as the local centrifugal term. Following Chapter 1 of [van Heijst \(2010\)](#) we define the **local Rossby number** as the ratio of the centrifugal acceleration to the Coriolis acceleration

$$Ro_{\text{local}} = \frac{|\mathbf{u}|^2/R}{f/|\mathbf{u}|} = \frac{|\mathbf{u}|}{Rf}, \quad (16.16)$$

where, again, R is the radius of curvature for the motion. In this chapter we consider flow regimes characterized by values of Ro_{local} .

16.1.6 Decomposition of the acceleration

The horizontal equations of motion (16.13a) and (16.13b) offer a relatively simple and insightful description of the motion. We here provide a connection with the traditional Eulerian form of the equations of motion.

Advective form of the acceleration

The standard form of the material time derivative for horizontal motion is given by

$$\frac{\partial \mathbf{u}}{\partial t} + (\mathbf{u} \cdot \nabla_h) \mathbf{u} = \frac{D|\mathbf{u}|}{Dt} \hat{\mathbf{u}} + \frac{|\mathbf{u}|^2}{R} \hat{\mathbf{n}}, \quad (16.17)$$

so that

$$\hat{\mathbf{u}} \cdot \left[\frac{\partial \mathbf{u}}{\partial t} + (\mathbf{u} \cdot \nabla_h) \mathbf{u} \right] = \frac{D|\mathbf{u}|}{Dt} = -\frac{1}{\rho_0} \frac{\partial p}{\partial s} + \mathbf{F} \cdot \hat{\mathbf{u}} \quad (16.18a)$$

$$\hat{\mathbf{n}} \cdot \left[\frac{\partial \mathbf{u}}{\partial t} + (\mathbf{u} \cdot \nabla_h) \mathbf{u} \right] = \frac{|\mathbf{u}|^2}{R} = -f |\mathbf{u}| - \frac{1}{\rho_0} \frac{\partial p}{\partial n} + \mathbf{F} \cdot \hat{\mathbf{n}}. \quad (16.18b)$$

Depending on the information provided by a field measurement or numerical simulation, one might more readily diagnose the kinematic expressions on the left side of these equations or the force balances on the right side.

Further decompositions

There are further connections to be made between the Eulerian expressions of flow acceleration and forces, and those terms represented using natural coordinates that follow the flow. Some of these connections are the topic for Exercises 16.1 and 16.2

16.1.7 Further study

Chapter 8 in *Zdunkowski and Bott (2003)* and Section 3.2 of *Holton and Hakim (2013)* detail the use of natural coordinates for geophysical flows, with a similar decomposition provided in Section 7.10 of *Gill (1982)* and Section 2.9 of *Vallis (2017)*. Natural coordinates are also used in describing flows in non-rotating reference frames as in Section 20 of *Serrin (1959)* and as illustrated in [this video](#).

16.2 Exact geostrophic balance

Frictionless flow parallel to pressure contours experiences no pressure gradient ($\partial p / \partial s = 0$), so that the speed of a fluid element remains constant. Furthermore, if this motion occurs with an infinite radius of curvature (straight line motion parallel to pressure contours), then the force balance is between the normal pressure gradient and Coriolis. In this case the local Rossby number (16.16) vanishes

$$\text{Ro}_{\text{local}} = \frac{|\mathbf{u}|}{R f} = 0 \quad \text{if } |R| = \infty. \quad (16.19)$$

More precisely, exact geostrophic balance occurs under the following conditions.

- Fluid moves on a straight line so that the radius of curvature is infinite, $|R| = \infty$, thus making the centripetal acceleration and local Rossby number both vanish;
- Fluid moves along lines of constant pressure so that $\partial p / \partial s = 0$;
- Friction is zero.

In this case the equations of motion (16.13a) and (16.13b) take the form

$$\frac{D|\mathbf{u}|}{Dt} = 0 \quad (16.20a)$$

$$f |\mathbf{u}| = -\frac{1}{\rho_0} \frac{\partial p}{\partial n}. \quad (16.20b)$$

Equation (16.20a) says that the speed of a fluid element is constant, so that the horizontal kinetic energy likewise is constant. Equation (16.20b) says that the pressure gradient normal to the motion balances the Coriolis acceleration. We refer to this flow, depicted in Figure 16.4, as *exact geostrophic balance* since it is an exact solution under the above assumptions.

Writing the horizontal advection of speed in the form

$$\mathbf{u} \cdot \nabla_h |\mathbf{u}| = |\mathbf{u}| \hat{\mathbf{u}} \cdot \nabla_h |\mathbf{u}| = |\mathbf{u}| \frac{\partial |\mathbf{u}|}{\partial s}, \quad (16.21)$$

allows us to write the material constancy of the flow speed as

$$\frac{\partial |\mathbf{u}|}{\partial t} + |\mathbf{u}| \frac{\partial |\mathbf{u}|}{\partial s} = 0. \quad (16.22)$$

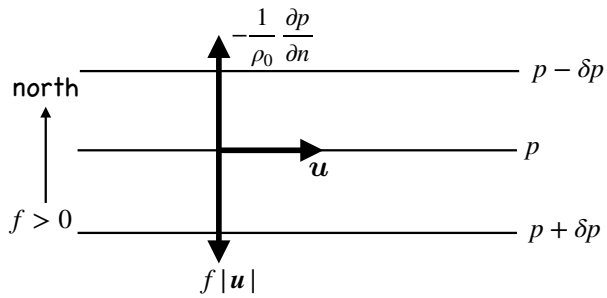


FIGURE 16.4: Exact geostrophic balance on a tangent plane occurs when the flow is horizontal, frictionless, straight, and follows contours of constant pressure. For this case the pressure gradient exactly balances the Coriolis acceleration so that the motion is perpendicular to both of these accelerations. We here depict motion assuming $f > 0$ as for the northern hemisphere. If flow is on an f -plane then the exact geostrophic balance is steady for any arbitrary flow direction. On a β -plane, steady exact geostrophic balance holds only for zonal flow.

Hence, a steady flow speed, with $\partial|\mathbf{u}|/\partial t = 0$, only holds for the exact geostrophic balance if the flow speed is fixed along each trajectory path

$$\frac{\partial|\mathbf{u}|}{\partial s} = 0 \implies \frac{\partial|\mathbf{u}|}{\partial t} = 0. \quad (16.23)$$

What is required for this condition to hold? We examine two cases, again restricted to a tangent plane.

16.2.1 Steady f -plane flow

Geostrophic motion on an f -plane is horizontally non-divergent (Section 15.4)

$$\nabla_h \cdot \mathbf{u} = \nabla_h \cdot (\hat{\mathbf{u}} |\mathbf{u}|) = 0. \quad (16.24)$$

Flow in a straight line, with each trajectory parallel to one another, has the trajectory direction independent of space. Hence, the non-divergent condition means that

$$0 = \nabla_h \cdot (\hat{\mathbf{u}} |\mathbf{u}|) = (\hat{\mathbf{u}} \cdot \nabla_h) |\mathbf{u}| = \frac{\partial|\mathbf{u}|}{\partial s}, \quad (16.25)$$

which proves that exact geostrophic flow on an f -plane is steady.

16.2.2 Steady β -plane flow

In Exercise 16.3 we show that exact geostrophic motion on the β -plane is steady only for trajectories that follow constant latitude lines; i.e., zonal trajectories as depicted in Figure 16.4.

16.2.3 What about geostrophic balance with curved motion?

The geostrophically balanced flows discussed in Chapter 15 generally have curvature, such as for the geostrophic motion around a pressure center as shown in Figure 15.3. But as emphasized by the natural coordinate decomposition as per equations (16.13a) and (16.13b), any curved motion has an associated centrifugal acceleration. So when speaking of geostrophic balance for flow that has a nonzero curvature, then the local Rossby number (16.16) is not precisely zero.

Rather, its magnitude is small but nonzero

$$|\text{Ro}_{\text{local}}| \ll 1 \quad \text{approximate geostrophic flow.} \quad (16.26)$$

When this limit is maintained, then it is sensible to ignore the centrifugal acceleration, which is commonly the case for large-scale flows. Even so, it is an approximation, with the centrifugal acceleration identically zero only for straight line motion on a plane.

16.3 Inertial motion

Inertial motion occurs under the following conditions:

- vanishing pressure gradient
- vanishing friction,

so that the equations of motion (16.13a) and (16.13b) take the form

$$\frac{\text{D}|\mathbf{u}|}{\text{Dt}} = 0 \quad (16.27\text{a})$$

$$\frac{|\mathbf{u}|^2}{R} + f |\mathbf{u}| = 0. \quad (16.27\text{b})$$

Equation (16.27a) says that inertial motion occurs with constant speed, whereas equation (16.27b) says that the motion maintains the balance between Coriolis and centrifugal accelerations

$$f |\mathbf{u}| = -\frac{|\mathbf{u}|^2}{R}. \quad (16.28)$$

Hence, local Rossby number has a unit magnitude

$$|\text{Ro}_{\text{local}}| = \frac{|\mathbf{u}|}{|R| |f|} = 1. \quad (16.29)$$

16.3.1 Anti-cyclonic circular motion on f -plane

To further understand inertial motion, rearrange equation (16.28) so that

$$f = -\frac{|\mathbf{u}|}{R}, \quad (16.30)$$

in which case the radius of curvature equals to the radius for the inertial circle

$$R = -|\mathbf{u}|/f. \quad (16.31)$$

Equation (16.30) can be satisfied in the northern hemisphere ($f > 0$) only for motion turning to the right (in which $R < 0$). The opposite orientation occurs in the southern hemisphere, where inertial motion turns to the left so that the radius of curvature is positive, $R = -|\mathbf{u}|/f > 0$ (see Figure 16.2 for the sign convention on the radius of curvature). Hence, inertial motion is oriented anti-cyclonically (orientated opposite to the earth's rotation). If the Coriolis parameter is constant, then the motion is circular, as depicted in Figure 16.5.

To emphasize the balance, return to equation (16.28) and recall that the Coriolis acceleration in the northern hemisphere points to the right when facing downstream, as per equation (16.11).

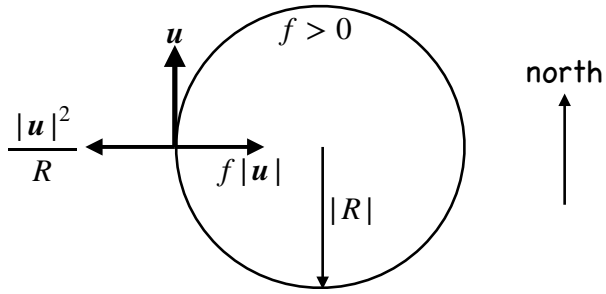


FIGURE 16.5: Inertial motion of a fluid on a plane occurs when the flow is horizontal, frictionless, and the motional centrifugal acceleration balances the planetary Coriolis acceleration in the presence of zero pressure gradient. We here depict motion assuming $f > 0$ as for the northern hemisphere, revealing that inertial motion is an anti-cyclonic circular motion with radius $|R| = |\mathbf{u}|/|f|$. The centrifugal acceleration, due to the motion of the fluid around the circle, is directed away from the center of the circle. The planetary Coriolis acceleration points to the right and toward the circle's center, thus providing the centripetal acceleration that balances the centrifugal acceleration. When turning to the right as in the northern hemisphere, the radius of curvature for the inertial circle is negative (see Figure 16.2 for sign convention), so that $R = -|\mathbf{u}|/f < 0$.

Hence, the balance (16.28) is between the Coriolis acceleration pointing to the right and the centrifugal acceleration pointing to the left. That is, the Coriolis acceleration provides the centripetal acceleration to balance the centrifugal acceleration.

16.3.2 Period for inertial motion

Equation (16.31) says that the speed of a fluid element is given by the radius of curvature times the magnitude of the Coriolis parameter

$$|\mathbf{u}| = |R f|. \quad (16.32)$$

The time for a fluid element to traverse an inertial circle is given by the circumference of the circle, $2\pi|R|$, divided by the constant speed, thus yielding the inertial period

$$T_{\text{inertial}} = \frac{2\pi|R|}{|\mathbf{u}|} = \frac{2\pi}{|f|}. \quad (16.33)$$

We encountered this inertial period in VOLUME 1 when studying inertial oscillations for a point particle.

16.3.3 Observing inertial motion

Inertial motion is rarely observed in the atmosphere since fluid motion nearly always occurs in the presence of a pressure gradient. In contrast, surface ocean flow is commonly generated by wind stresses that setup motion even in the absence of ocean pressure gradients. The moving fluid then engenders a planetary Coriolis acceleration, in which case there can be a balance between centrifugal and Coriolis for the moving ocean fluid. As a result, the observed surface ocean currents have nontrivial power within the inertial frequency band, rivaling energy contained in frequencies associated with astronomical tides (e.g., see Figure 3.3 of [Holton and Hakim \(2013\)](#)).

How large is an inertial circle? Consider a surface ocean current speed of $|\mathbf{u}| \sim 0.1 \text{ m s}^{-1}$, which is not atypical of current speeds outside of strong boundary currents or mesoscale eddies,

and assume the Coriolis parameter $f = 10^{-4} \text{ s}^{-1}$. In this case the inertial radius is

$$R_{\text{inertial}} \approx 10^3 \text{ m.} \quad (16.34)$$

Observations of inertial motion, such as that reproduced in Figure 8.3 of [Gill \(1982\)](#), confirm that the radii are indeed on the order of a few kilometers.

16.3.4 Inertial motion as Lagrangian fluid particle motion

The analysis in this section concerns a fluid element moving without feeling the impacts from pressure forces. The fluid thus exhibits the same force balance as the inertial motion of a point particle studied in VOLUME 1. So although we can measure inertial motion at a fixed point in space, the present considerations are Lagrangian in nature, focusing on motion of fluid elements. Furthermore, the inertial period refers to the time it takes for a fluid element to move around the inertial circle at its constant speed. It does not refer to the period of a wave, for example, and yet there are inertial waves encountered in VOLUME 5 that have this period. There are also inertia-gravity waves that have periods close to the inertial period (see again VOLUME 5 for the variety of discussions of inertial and inertia-gravity waves).

16.3.5 “Inertial” motion does not refer to an inertial reference frame

We make use of the term “inertial” when referring to inertial motion since both the Coriolis and centrifugal accelerations are nonzero only in the presence of motion; i.e., they require the inertia obtained by a moving massive body. Hence, “inertial motion” in this context does *not* refer to the motion viewed in an inertial reference frame.

16.3.6 Inertial motion on a sphere

In the analysis thus far, we have assumed an f -plane so that inertial motion is circular. Without solving the spherical equations for inertial motion we can anticipate what happens when such motion occurs on a sphere. As a fluid element moves to higher latitudes the magnitude of the Coriolis parameter increases, thus decreasing the radius of curvature and increasing the curvature. The opposite happens when moving equatorward. This effect of planetary sphericity leads to an egg-shaped pattern that does not close but instead drifts to the west. Now consider inertial motion that spans the equator. As the fluid crosses the equator, where $f = 0$, the radius of curvature is infinite so that the motion is straight. When moving away from the equator the Coriolis parameter increases in magnitude, which causes a fluid element to turn and close its path, again with a drift to the west. Motion north of the equator turns to the right whereas motion to the south turns left, so that inertial motion that spans the equator forms a figure-eight path. We illustrate this motion in Figure 16.6.

16.4 Cyclostrophic balance

Cyclostrophic balance occurs under the following conditions:

- fluid elements move along lines of constant pressure so that $\partial p / \partial s = 0$;
- vanishing Coriolis acceleration;
- vanishing friction.

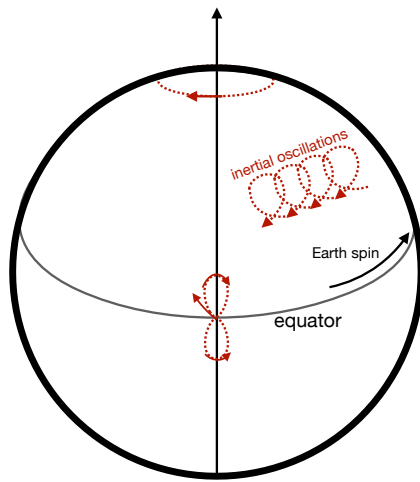


FIGURE 16.6: Depicting inertial motion on a sphere. As the fluid element moves poleward, f increases so that the radius of curvature decreases. Correspondingly, the fluid motion does not close, but instead the path drifts to the west. This westward drift holds for both hemispheres, where the sense of the motion is anti-cyclonic. The only closed and circular inertial motions are those that encircle the pole. Fluid elements that cross the equator exhibit a figure-eight pattern that also drifts to the west. This figure is adapted from Figure 4-14 of [von Arx \(1962\)](#).

The resulting tangent plane equations of motion (16.13a) and (16.13b) take the form

$$\frac{D|\mathbf{u}|}{Dt} = 0 \quad (16.35a)$$

$$\frac{|\mathbf{u}|^2}{R} = -\frac{1}{\rho_0} \frac{\partial p}{\partial n}. \quad (16.35b)$$

With a vanishing Coriolis acceleration we see that cyclostrophic balance corresponds to local Rossby number that has an infinite magnitude

$$|\text{Ro}_{\text{local}}| = \infty \quad \text{if } f = 0. \quad (16.36)$$

Approximate cyclostrophic balance holds when $|\text{Ro}_{\text{local}}| \gg 1$, but less than infinite.

Again, equation (16.35a) says that the speed is constant following a material fluid element. Equation (16.35b) says that cyclostrophic flow occurs when the centrifugal acceleration balances the pressure gradient, with the squared speed given by

$$|\mathbf{u}|^2 = -\frac{R}{\rho_0} \frac{\partial p}{\partial n}. \quad (16.37)$$

This equation can be satisfied for either clockwise or counter-clockwise motion around a low pressure center, as shown in Figure 16.7. For clockwise flow, the radius of curvature is negative, $R < 0$, whereas $\partial p / \partial n > 0$. The signs are swapped for counter-clockwise flow. Cyclostrophic balance cannot be maintained around a high pressure center. The reason is that if both the pressure and centrifugal accelerations point away from the circle's center, then they are unable to balance one another.

Cyclostrophic balance is relevant for scales on the order of a tornado, with a radius on the order of 300 m where tangential speeds are on the order of 30 m s^{-1} (see Section 3.2.4 of [Holton and Hakim \(2013\)](#)). For this flow scale, the Rossby number is on the order of 1000 at middle latitudes, thus justifying neglect of the Coriolis acceleration. Although tornadoes in

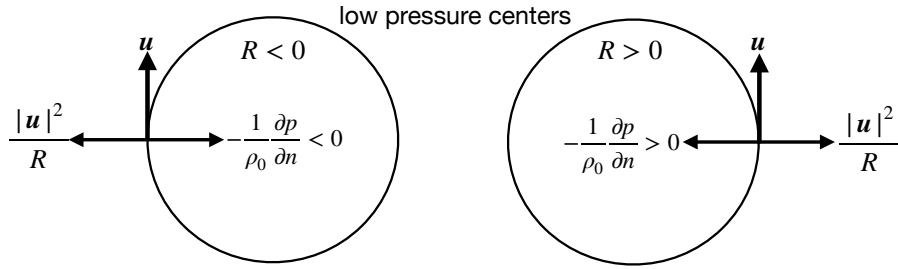


FIGURE 16.7: Cyclostrophic motion of a fluid on a tangent plane occurs when the flow is horizontal, non-rotating, frictionless, with constant speed, and where the outward directed centrifugal acceleration balances the inward directed pressure gradient normal to the flow. We here depict motion for clockwise and counter-clockwise cyclostrophic flow, both around a circular low pressure center so that $\partial p / \partial r > 0$ (pressure increasing radially outward). Recall that our convention from Section 16.1 is that the normal direction, \hat{n} , always points to the left of the flow direction. Left panel: clockwise motion with radius of curvature, $R < 0$, and with $\hat{n} = \hat{r}$ directed radially away from the center. The pressure gradient points into the center, so that $\hat{n} \cdot \nabla p = \partial p / \partial r > 0$, which means that $-\partial p / \partial n < 0$. Right panel: counter-clockwise motion with radius of curvature, $R > 0$, and with $\hat{n} = -\hat{r}$ directed radially into the center. The pressure gradient points to the center, so that $\hat{n} \cdot \nabla p = -\partial p / \partial r < 0$, which means the pressure acceleration satisfies $-\partial p / \partial n > 0$. Cyclostrophic balance does not occur for flow around a high pressure center. The reason is that for a high pressure center, the pressure and centrifugal acceleration will both point away from the center, in which case they are unable to balance one another.

cyclostrophic balance can rotate either clockwise or counter-clockwise, they are more often observed rotating cyclonically given that they are generally embedded within cyclonic storm systems. In contrast, smaller motions such as dust devils and water spouts are quite often seen rotating in either direction.

16.5 Gradient wind balance

Gradient wind balance occurs under the following conditions:

- fluid elements move along lines of constant pressure so that $\partial p / \partial s = 0$;
- vanishing friction.

The resulting equations of motion (16.13a) and (16.13b) take the form

$$\frac{D|\mathbf{u}|}{Dt} = 0 \quad (16.38a)$$

$$\frac{|\mathbf{u}|^2}{R} + f |\mathbf{u}| = -\frac{1}{\rho_0} \frac{\partial p}{\partial n}, \quad (16.38b)$$

Again, equation (16.38a) says that the speed is constant following a material fluid element. Equation (16.38b) says that gradient wind balanced flow occurs when the centrifugal and Coriolis accelerations balance the pressure gradient acting normal to the motion.

The local Rossby number is order unity for the gradient wind balance

$$|Ro_{local}| = \frac{|\mathbf{u}|}{|R| |f|} \sim 1, \quad (16.39)$$

meaning that both centrifugal and Coriolis accelerations are important as they balance the pressure gradient. Recall that the inertial motion from Section 16.3 has $|Ro_{local}| = 1$, which arises when the pressure gradient vanishes so that the Coriolis and centrifugal terms have equal but

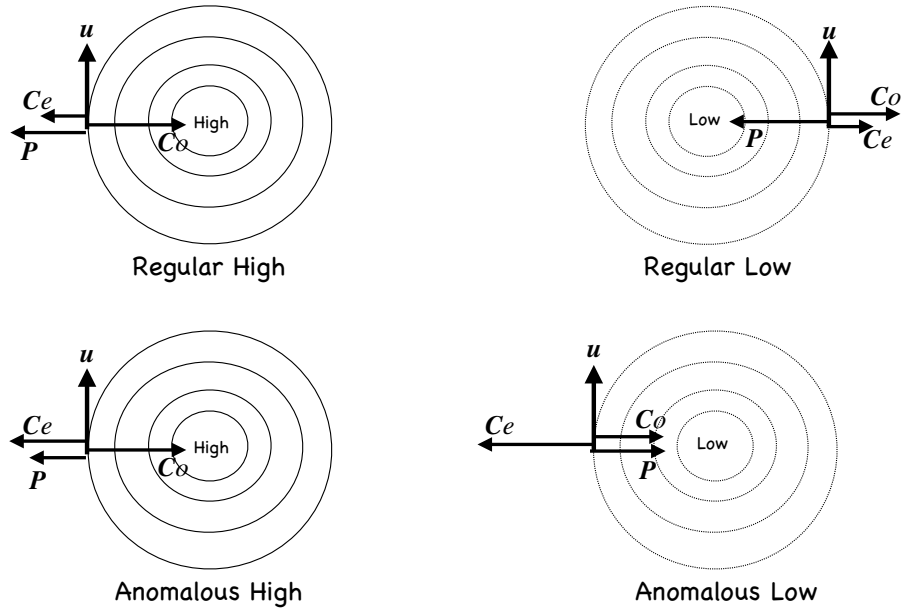


FIGURE 16.8: The variety of gradient wind balances available in the northern hemisphere ($f > 0$) around circular pressure centers. Gradient wind balance occurs when the flow is horizontal, frictionless, with constant speed, and where the centrifugal, pressure, and Coriolis accelerations balance under a variety of magnitudes. To reduce clutter, we use the following shorthand for the accelerations: $P = -\rho_0^{-1} \partial p / \partial n$, $Co = f |\mathbf{u}|$, and $Ce = |\mathbf{u}|^2 / R$. Upper left panel: motion around a regular high pressure center, whereby the centrifugal acceleration helps the pressure acceleration to balance the Coriolis acceleration. The pressure acceleration is larger in magnitude than the centrifugal. This flow is termed “regular” as it directly corresponds to geostrophic flow around a high pressure center. Lower left panel: motion around an anomalous high pressure center, whereby the centrifugal acceleration helps the pressure acceleration to balance the Coriolis acceleration, with the pressure acceleration smaller in magnitude than the centrifugal. This flow is termed “anomalous” as the pressure acceleration is subdominant to the centrifugal, in contrast to the case of a regular high. Upper right panel: motion around a regular low pressure center, whereby the Coriolis and centrifugal accelerations balance the pressure acceleration. Lower right panel: motion around an anomalous low pressure center, whereby the Coriolis and pressure accelerations balance the centrifugal acceleration. Note the opposite flow orientation between the regular and anomalous lows, whereas the regular and anomalous highs have the same flow orientation.

opposite magnitudes. The nonzero pressure gradient makes gradient wind flow fundamentally distinct from inertial motion.

16.5.1 Constraints on gradient wind flow

The quadratic formula leads to the following expression for the speed of gradient wind flow

$$|\mathbf{u}| = \frac{R}{2} \left[f \pm \sqrt{f^2 - \frac{4}{R} \frac{1}{\rho_0} \frac{\partial p}{\partial n}} \right]. \quad (16.40)$$

The speed is a real number if the pressure gradient, Coriolis parameter, and radius of curvature satisfy

$$f^2 > \frac{4}{R} \frac{1}{\rho_0} \frac{\partial p}{\partial n} \implies \frac{1}{\rho_0} \left| \frac{\partial p}{\partial n} \right| \leq \frac{|R| f^2}{4}. \quad (16.41)$$

This relation has direct implications for the structure of the pressure field depending on the sign of the radius of curvature. In particular, as seen in the following, this constraint implies that the pressure gradient at the center of a high pressure region must go to zero as the radius of curvature vanishes, which renders the pressure field relatively flat near the center of highs. In

contrast, there is no analogous limit for the magnitude of the pressure gradient approaching a low pressure center. This asymmetry between high and low pressures manifests in atmospheric flow with low pressure centers (cyclonic lows) having stronger magnitude than high pressure centers (anti-cyclonic highs).

16.5.2 A variety of gradient wind flows

We now identify the following force balances in the northern hemisphere ($f > 0$) available with a gradient wind balance. We provide schematics in Figure 16.8.

Regular and anomalous high pressure center (right turn with high pressure on right)

A regular high pressure occurs with $R < 0$, $\hat{\mathbf{n}} = \hat{\mathbf{r}}$, and $\partial p / \partial n = \partial p / \partial r \leq 0$. This case occurs with the centrifugal and pressure accelerations pointing away from the center, and these two accelerations balance the Coriolis acceleration that points to the high pressure center (upper left panel of Figure 16.8).

The inequality (16.41) provides a bound to the size of the pressure gradient since

$$\frac{1}{\rho_0} \frac{\partial p}{\partial n} \leq \frac{R f^2}{4} \text{ with } R \leq 0 \text{ and } \frac{\partial p}{\partial n} \leq 0 \implies \frac{1}{\rho_0} \left| \frac{\partial p}{\partial n} \right|_{\max} = \frac{|R| f^2}{4}. \quad (16.42)$$

That is, the pressure gradient for a regular high cannot be larger than this bound in order for there to be a gradient wind solution. Since $R \rightarrow 0$ as the center is approached, the normal pressure gradient, $\partial p / \partial n$, in turn must vanish towards the center. [Holton and Hakim \(2013\)](#) identifies two subcases for this balance depending on the relative size of the pressure and centrifugal accelerations, with the anomalous high the case where the pressure gradient acceleration is weaker than the centrifugal (lower left panel of Figure 16.8).

Regular low (left turn with low pressure on left)

This flow occurs with $R > 0$, $\hat{\mathbf{n}} = -\hat{\mathbf{r}}$, and $\partial p / \partial n = -\partial p / \partial r \leq 0$, so that the inequality (16.41) is always satisfied

$$\frac{1}{\rho_0} \frac{\partial p}{\partial n} \leq \frac{R f^2}{4} \text{ with } R \geq 0 \text{ and } \frac{\partial p}{\partial n} \leq 0 \implies \text{arbitrary size to } \left| \frac{\partial p}{\partial n} \right|. \quad (16.43)$$

Hence, there is no constraint imposed by gradient wind balance on the size of the pressure gradient magnitude, $|\partial p / \partial n|$. So the low pressure center can be arbitrarily strong and still maintain a gradient wind balance. Furthermore, the Coriolis and centrifugal accelerations point away from the low pressure center, and these two accelerations balance the pressure acceleration that points toward the center (upper right panel of Figure 16.8).

Anomalous low (right turn with low pressure on right)

This flow occurs with $R < 0$, $\hat{\mathbf{n}} = \hat{\mathbf{r}}$, and $\partial p / \partial n = \partial p / \partial r \geq 0$. This case occurs with the Coriolis and pressure accelerations pointing toward the low pressure center, and these two accelerations balance the centrifugal acceleration that points away from the center (lower right panel of Figure 16.8). As with the regular low, the inequality (16.41) provides no bound to the magnitude of the low pressure. Note the opposite orientation for the flow around an anomalous low relative to the regular low.

16.5.3 Comments

As noted in Section 3.2 of [Holton and Hakim \(2013\)](#), the difference between gradient wind speeds and geostrophic wind speeds is no more than 10% to 20% in middle latitude synoptic atmosphere flow. In the tropics, where geostrophy becomes less relevant, it is important to apply the gradient wind relation to capture the balanced flow states. Furthermore, [van Heijst \(2010\)](#) and Chapter 18 of [Cushman-Roisin and Beckers \(2011\)](#) make use of a gradient wind analysis for the study of ocean vortices. The deviations from geostrophy become important when considering relatively small ocean vortices and/or tropical vortices.



16.6 Exercises

EXERCISE 16.1: MECHANICAL EXPRESSIONS FOR THE RADIUS OF CURVATURE

The radius of curvature is a kinematic property of the flow. Determine expressions for the radius of curvature for fluid motion in terms of the Eulerian kinematics of the flow, as well as the dynamical forces acting on the flow. Simplify for steady flows and discuss.

EXERCISE 16.2: VECTOR-INVARIANT VELOCITY EQUATION

In Section 16.1, we decomposed the horizontal equations of motion into natural coordinates, and we did so by starting from the material time version of the velocity equation. Provide an analogous derivation using the [vector invariant](#) form of the velocity equation (see Section 8.4 for the three-dimensional case). Discuss the expression for the centripetal acceleration for steady flows.

EXERCISE 16.3: EXACT GEOSTROPHY ON A β -PLANE

Show mathematically that exact geostrophic motion on the β -plane is steady only for fluid flow that follows constant latitude lines; i.e., zonal flow as depicted in Figure 16.4.

EXERCISE 16.4: FLOWS THAT CANNOT BE IN GRADIENT WIND BALANCE

Show that there is no northern hemisphere gradient wind balanced flow in which the flow occurs in a counter-clockwise manner around a high pressure center. Draw a sketch with vectors for the corresponding accelerations. Similarly, show that there is no southern hemisphere gradient wind balanced flow in which the flow occurs in a clockwise manner around a high pressure center.

EXERCISE 16.5: HORIZONTAL DIVERGENCES

The exact geostrophic flow on the f -plane, as well as other balanced flows moving around circles, are all horizontally non-divergent. Discuss some physical processes that can introduce horizontal divergences.



Chapter 17

EKMAN MECHANICS

A [boundary layer](#) is a region of the fluid flow that is directly affected by boundaries. For geophysical applications we have in mind the solid-Earth boundary that interacts with both the ocean and atmosphere; the ocean-atmosphere boundary; the ocean-cryosphere boundary; and the atmosphere-cryosphere boundary. The fluid flow in geophysical boundary layers is generally very turbulent, thus causing rapid mixing and the transfer of properties within the boundary layer, along with the transport of properties between the boundary layer and the less turbulent fluid interior. Boundary layer physics is a well developed discipline of geophysical as well as engineering applications. Our treatment is relatively superficial by comparison to the focused treatments given by books such as [Tennekes and Lumley \(1972\)](#), [Stull \(1988\)](#), and [Thorpe \(2005\)](#).

We focus in this chapter on the rudiments of [Ekman mechanics](#), which is concerned with flow affected by accelerations from horizontal pressure gradients, vertical friction, and Coriolis, with particular attention given to regions near boundaries where turbulent friction is especially large and [Ekman boundary layers](#) form. The leading role for Coriolis acceleration causes Ekman boundary layers to exhibit behaviors quite distinct from their non-rotating cousins mentioned in Section 9.8.7. In particular, Ekman boundary layer flows are horizontally divergent, thus leading to the vertical exchange of fluid between the boundary layer and the fluid region outside of the boundary layer (i.e., the fluid interior). In so doing, the Ekman layer flow imparts a stretching and squeezing of interior fluid columns that strongly couples the boundary layer to vorticity and circulation of the fluid interior. This role for Ekman layers is especially crucial for the ocean general circulation.

READER'S GUIDE TO THIS CHAPTER

To introduce the subject we exhibit the role of friction in producing a down pressure gradient component to the flow, making use of natural coordinates from Chapter 16. In the remainder of this chapter, we focus on the mechanics of Ekman boundary layers, thus extending our understanding of strongly rotating flows introduced in Chapter 15. Ekman boundary layers are a key element in the study of ocean circulation, particularly the [wind-driven](#) circulation. We here borrow liberally from the material in Section 9.2 of [Gill \(1982\)](#), Section 6.2 of [Apel \(1987\)](#), Section 7.4 of [Marshall and Plumb \(2008\)](#), Chapter 8 of [Cushman-Roisin and Beckers \(2011\)](#), Section 5.7 of [Vallis \(2017\)](#), and materials from [Thorpe \(1988\)](#) and [Thorpe \(2005\)](#). A presentation consistent with engineering boundary layers can be found in Section 5.3 of [Tennekes and Lumley \(1972\)](#).

17.1	The dynamical balances	548
17.2	Horizontal balances in natural coordinates	549
17.2.1	Natural coordinates according to isobars	549
17.2.2	Geostrophic and Ekman balances	550
17.2.3	Rayleigh drag	551
17.2.4	Cross isobar flow driven by Rayleigh drag	552
17.2.5	Horizontal spiral plus vertical rising/sinking	553
17.2.6	Further study	553
17.3	Ekman number and Ekman layer thickness	554
17.3.1	Laplacian vertical friction	554
17.3.2	Non-dimensionalization	555
17.3.3	Defining the Ekman number and layer thickness	555
17.3.4	Estimates for the vertical eddy viscosity	556
17.4	Ocean surface Ekman layer	557
17.4.1	Horizontal mass transport within the Ekman layer	557
17.4.2	Example Ekman mass transports	559
17.4.3	Mass budget for the Ekman layer	559
17.4.4	Ekman layer coupled to the geostrophic interior	562
17.4.5	Further study	562
17.5	Bottom Ekman boundary layer	563
17.5.1	Horizontal mass transport within the Ekman layer	564
17.5.2	Mass budget for the bottom Ekman layer	565
17.5.3	An analytic bottom Ekman spiral velocity	565
17.5.4	Comments	569
17.6	Arrested bottom Ekman flows	569
17.6.1	Description of the adjustment	569
17.6.2	Applications	569
17.7	Exercises	571

17.1 The dynamical balances

Throughout this chapter we make use of a steady, linear, Boussinesq, hydrostatic primitive equations that maintain a balance between the horizontal accelerations from Coriolis, pressure, and friction

$$f \hat{z} \times \mathbf{u} = -\frac{1}{\rho_0} \nabla_h p + \mathbf{F}. \quad (17.1)$$

This balance is most relevant over large horizontal length scales as per the planetary geostrophic equations of Section 15.5.

The frictional acceleration, \mathbf{F} , of interest in this chapter arises from the vertical exchange of horizontal momentum between fluid layers. Turbulence induced viscous exchange is especially large in boundary regions such as the ocean surface, the atmospheric planetary boundary layer (i.e., atmosphere/land boundary), and the ocean bottom boundary layer. In such turbulent boundary layer regions we make use of the eddy viscosity, which is much larger than molecular values

$$\nu_{\text{eddy}} \gg \nu. \quad (17.2)$$

We have more to say regarding the mathematical form of the friction operator in Section 17.3.1.

For conceptual and mathematical convenience, we find it useful to separate the horizontal velocity into two components. The first is the geostrophic velocity defined by a balance between

the pressure gradient and Coriolis accelerations

$$f \hat{z} \times \mathbf{u}_g = -\frac{1}{\rho_0} \nabla_h p \implies \mathbf{u}_g = \frac{1}{f \rho_0} \hat{z} \times \nabla_h p. \quad (17.3)$$

We sometimes refer to \mathbf{u}_g as the [pressure driven velocity](#). The second is an [ageostrophic](#) or Ekman component defined by a balance between the frictional and Coriolis accelerations

$$f \hat{z} \times \mathbf{u}_e = \mathbf{F} \implies \mathbf{u}_e = -f^{-1} \hat{z} \times \mathbf{F}, \quad (17.4)$$

so that \mathbf{u}_e is the [frictional driven velocity](#).

This velocity decomposition has the appearance of superposing linearly independent flows, one geostrophic (pressure driven) and one ageostrophic (friction driven). However, the flows are coupled and thus not linearly independent. Namely, ageostrophic motions alter the pressure field which in turn affects the geostrophic flow. So the presence of friction and the associated ageostrophic flows lead to geostrophic flows differing from the inviscid case. Conversely, geostrophic flows affect the level of friction. Hence, the above decomposition does not reflect a physical decoupling of geostrophic and ageostrophic flows. Rather, it is only meant to help conceptually understand and describe the flow and the various force balances.

17.2 Horizontal balances in natural coordinates

Motion in Ekman boundary layers is both horizontal and vertical. Here, we introduce the role of friction for rotating fluid dynamics by just focusing on the horizontal motion on a tangent plane. In particular, we study balances occurring in horizontal flows that maintain a frictional geostrophic balance. As per the definition (17.3), geostrophic motion occurs along lines of constant pressure, with frictionally induced deviations crossing isobars and providing a down pressure gradient component to the fluid trajectory. Motivated by the discussion in Chapter 16, we make use of natural coordinates for the kinematics.

As a caveat, we note that our focus in this section on horizontal motions, and our assumption that $\partial_z = 0$, are not self-consistent in the presence of friction. The reason is that friction induces horizontal divergences that then lead to vertical flows. Even so, the following discussion provides a useful set of intuitive ideas that carry over to the more physically consistent discussion in the subsequent sections.

17.2.1 Natural coordinates according to isobars

We represent the horizontal flow according to [natural coordinates](#) defined along an arbitrary geopotential surface on a tangent plane. Instead of defining natural coordinates according to the flow direction, as done in Section 16.1 for the inviscid case, we here decompose the motion according to pressure contours (isobars). The unit vector, \hat{s} , is defined tangent to isobars in the horizontal plane and directed along the direction of geostrophic flow. We define the direction, \hat{n} , to be perpendicular to isobars and oriented down the horizontal pressure gradient

$$\hat{n} = -\frac{\nabla_h p}{|\nabla_h p|}. \quad (17.5)$$

As illustrated in Figure 17.1, in the northern hemisphere \hat{n} points to the left of the geostrophic velocity, whereas it is to the right in the southern hemisphere. We thus have the northern

hemisphere triplet of unit vectors

NORTHERN HEMISPHERE TRIPLET OF DIRECTIONS

$$\hat{z} = \hat{s} \times \hat{n} = \text{vertical direction} \quad (17.6a)$$

$$\hat{n} = \hat{z} \times \hat{s} = \text{down pressure gradient direction} \quad (17.6b)$$

$$\hat{s} = \hat{n} \times \hat{z} = \text{tangent to isobar in direction of geostrophic flow.} \quad (17.6c)$$

In the southern hemisphere, since \hat{n} points to the right of \hat{s} , the triplet of directions becomes

SOUTHERN HEMISPHERE TRIPLET OF DIRECTIONS

$$\hat{z} = \hat{n} \times \hat{s} = \text{vertical direction} \quad (17.7a)$$

$$\hat{n} = \hat{s} \times \hat{z} = \text{down pressure gradient direction} \quad (17.7b)$$

$$\hat{s} = \hat{z} \times \hat{n} = \text{tangent to isobar in direction of geostrophic flow.} \quad (17.7c)$$

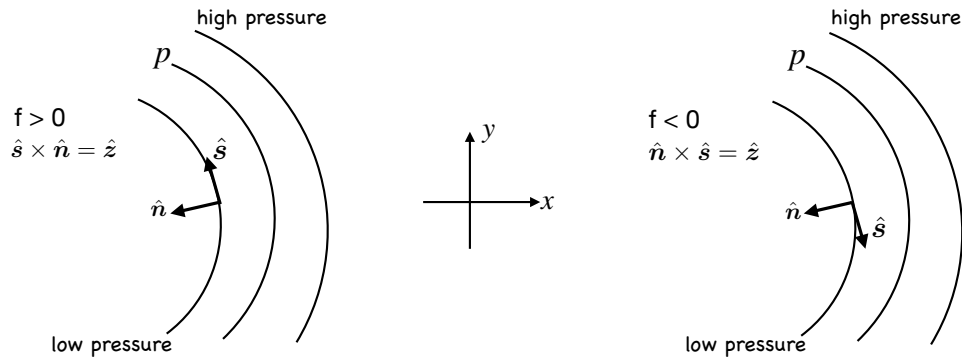


FIGURE 17.1: Natural coordinates defined along an arbitrary geopotential surface according to isobars in the horizontal plane, with the left panel for the northern hemisphere ($f > 0$) and right panel for the southern hemisphere ($f < 0$). The geostrophic flow is counter-clockwise around low pressure centers in the north and clockwise for the south. The normal direction, $\hat{n} = -\nabla_h p / |\nabla_h p|$, is oriented down the horizontal pressure gradient so that it points to the left of the geostrophic velocity (facing downstream) in the northern hemisphere and to the right in the southern hemisphere. The tangent direction, \hat{s} , points along the isobar in the direction of the geostrophic velocity.

17.2.2 Geostrophic and Ekman balances

We here express the geostrophic and Ekman velocities in terms of pressure and friction.

Geostrophic flow

The geostrophic velocity flows along isobars and so only has a component in the \hat{s} direction, as seen by writing

$$f \rho_o \mathbf{u}_g = \hat{z} \times \nabla_h p = \hat{n} \times \mathbf{z}. \quad (17.8)$$

Making use of the sign swap for \hat{s} as given by equations (17.6c) and (17.7c), we see that

$$\rho_o \hat{s} \cdot \mathbf{u}_g = |\nabla_h p|/f = |\nabla_h p|/|f| \quad \text{north, where } \hat{s} = \hat{n} \times \mathbf{z} \quad (17.9a)$$

$$\rho_o \hat{s} \cdot \mathbf{u}_g = -|\nabla_h p|/f = \nabla_h p/|f| \quad \text{south, where } \hat{s} = -\hat{n} \times \mathbf{z}. \quad (17.9b)$$

We thus find that for both hemispheres the geostrophic flow has a positive projection onto the flow direction,

$$\rho_0 \hat{s} \cdot \mathbf{u}_g = |\nabla_h p| / |f| > 0, \quad (17.10)$$

which is a result following from our construction of the \hat{s} direction.

Ekman flow

The horizontal Ekman velocity has a component both along and across isobars. For both the northern and southern hemispheres we have the following expressions

$$\hat{s} \cdot \mathbf{u}_e = |f|^{-1} \hat{n} \cdot \mathbf{F} \quad \text{and} \quad \hat{n} \cdot \mathbf{u}_e = -|f|^{-1} \hat{s} \cdot \mathbf{F}. \quad (17.11)$$

As expected, the Ekman velocity vanishes when the frictional acceleration vanishes, in which case the flow reduces to the geostrophic flow that moves along isobars so that $\hat{s} = \hat{\mathbf{u}}$. However, when there is a nonzero frictional acceleration aligned along isobars, that balances an Ekman velocity directed across isobars. Conversely, frictional accelerations aligned across isobars balance an Ekman velocity along isobars.

We arrive at a complementary perspective on the origin of cross-isobar flow through the following considerations. Without friction, the Coriolis and pressure gradient accelerations balance when the flow is geostrophic. In the presence of friction, the velocity is slowed so that the Coriolis acceleration weakens. If the pressure gradient acceleration is retained, as occurs if it is determined by large scale balances outside of the Ekman layer, then the Coriolis acceleration is unable to balance the pressure gradient. Consequently, flow is diverted from isobars and develops a component down the pressure gradient.

17.2.3 Rayleigh drag

The relative simplicity of Rayleigh drag facilitates analytical expressions for the Ekman velocity in terms of the geostrophic velocity (equation (17.10)). In doing so we are afforded an explicit illustration of how friction provides a cross-isobar component to the flow in the direction down the pressure gradient. Before developing the Ekman flows we here summarize elements of Rayleigh drag.

In Section 10.2.3 we studied how Rayleigh drag affects the kinetic energy budget. As a reminder, consider a frictional acceleration in the form of a Rayleigh drag acting on the velocity field

$$\mathbf{F} = -\frac{U_{\text{fric}} \mathbf{u}}{\delta} = -\gamma \mathbf{u}, \quad (17.12)$$

where δ is a vertical scale and U_{fric} is a friction velocity scale with dimensions $L T^{-1}$. The ratio

$$\gamma = \frac{U_{\text{fric}}}{\delta} \quad (17.13)$$

has dimensions T^{-1} and is an inverse spin-down time. That is, if only Rayleigh drag affected changes to the horizontal momentum, $\partial_t \mathbf{u} = -\gamma \mathbf{u}$, then the flow would exponentially come to a halt with an e-folding time, γ^{-1} . The drag is relatively large over rough surfaces, thus leading to a small e-folding time. In particular, drag on the lower atmospheric winds is larger over land than over the ocean. The reason is that trees, cities, and mountains dissipate more of the atmosphere's mechanical energy than interactions with the relatively smooth ocean surface.

Rayleigh drag dissipates all flow features, regardless of their spatial structure. That is,

Rayleigh drag does not prefer any particular length scales in the fluid flow. This lack of scale selectivity contrasts to the Laplacian friction discussed in Section 17.3.1, with Laplacian friction dissipating small spatial scales more strongly than large scales. Correspondingly, Rayleigh drag does not generally provide the means to produce a boundary layer.¹ Hence, when studying physics within the Ekman boundary layer in Section 17.3 we make use of Laplacian friction. But for now, Rayleigh drag provides a means to analytically illustrate the role of friction in producing spiral flows with non-zero horizontal divergence.

17.2.4 Cross isobar flow driven by Rayleigh drag

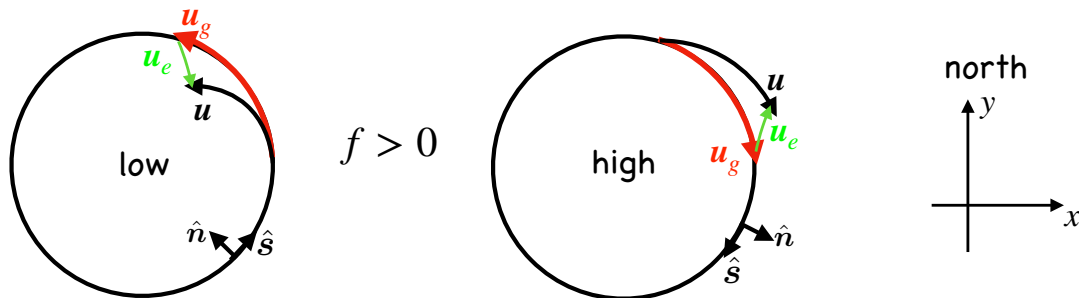


FIGURE 17.2: Illustrating frictional geostrophic flow in the northern hemisphere ($f > 0$). Left panel: geostrophic flow, \mathbf{u}_g , around a low pressure center is counter-clockwise and aligned with pressure isobars. Friction aligned along the isobars drives Ekman flow, \mathbf{u}_e , that has a component down the pressure gradient (normal to the geostrophic flow) as well as a component that is directed opposite the geostrophic flow. Consequently, the total velocity, $\mathbf{u}_g + \mathbf{u}_e$, spirals into the low pressure center. Right panel: the opposite oriented flow occurs around high pressure centers, where fluid spirals away from the high due to the cross-isobar flow driven by friction. By the definition given by equation (17.6b), the normal direction, $\hat{\mathbf{n}}$, is directed down the pressure gradient, whereas $\hat{\mathbf{s}}$ is tangent to the isobar and directed along the geostrophic flow direction.

Making use of the Rayleigh drag (17.12) brings the expressions (17.11) for the Ekman velocity into the form holding for both hemispheres

$$\hat{\mathbf{s}} \cdot \mathbf{u}_e = -(\gamma/|f|) \hat{\mathbf{n}} \cdot \mathbf{u}_e \quad (17.14a)$$

$$\hat{\mathbf{n}} \cdot \mathbf{u}_e = (\gamma/|f|) \hat{\mathbf{s}} \cdot (\mathbf{u}_e + \mathbf{u}_g). \quad (17.14b)$$

Rearrangement of these equations allows us to express the Ekman velocity in terms of the geostrophic velocity (equation (17.10)), with results for both hemispheres given by

$$\hat{\mathbf{n}} \cdot \mathbf{u}_e = \hat{\mathbf{s}} \cdot \mathbf{u}_g \left[\frac{\gamma |f|}{f^2 + \gamma^2} \right] = \frac{|\nabla_h p|}{\rho_0 |f|} \left[\frac{\gamma |f|}{f^2 + \gamma^2} \right] \quad (17.15a)$$

$$\hat{\mathbf{s}} \cdot \mathbf{u}_e = -\hat{\mathbf{s}} \cdot \mathbf{u}_g \left[\frac{\gamma^2}{\gamma^2 + f^2} \right] = -\frac{|\nabla_h p|}{\rho_0 |f|} \left[\frac{\gamma^2}{\gamma^2 + f^2} \right], \quad (17.15b)$$

where we used equation (17.10) to express the geostrophic velocity in terms of the normal pressure gradient and Coriolis parameter. The right hand expression in equation (17.15a) is positive, which means that the normal component to the Ekman velocity is directed down the horizontal pressure gradient

$$-\hat{\mathbf{n}} \cdot \mathbf{u}_e = \mathbf{u}_e \cdot \nabla_h p / |\nabla_h p| < 0, \quad (17.16)$$

¹In Section 17.3.3 we provide further discussion of what is needed mathematically and physically to produce a boundary layer.

so that this component is directed toward the low pressure. Since the right hand side of equation (17.15b) is negative, we conclude that the component of the Ekman velocity along the pressure isobar is directed opposite to the geostrophic velocity. We provide an example of an Ekman velocity in Figure 17.2 for the northern hemisphere.

Bringing all pieces together leads to the components for the total velocity, $\mathbf{u} = \mathbf{u}_g + \mathbf{u}_e$, and its squared magnitude

$$\hat{\mathbf{s}} \cdot \mathbf{u}_g = \frac{|\nabla_h p|}{|f|\rho_0} \quad \mathbf{u}_g \text{ is aligned with isobars} \quad (17.17a)$$

$$\hat{\mathbf{s}} \cdot \mathbf{u} = \hat{\mathbf{s}} \cdot \mathbf{u}_g \left[\frac{f^2}{f^2 + \gamma^2} \right] \quad \text{isobaric velocity component} \quad (17.17b)$$

$$\hat{\mathbf{n}} \cdot \mathbf{u} = (\gamma/|f|) \hat{\mathbf{s}} \cdot \mathbf{u} \quad \text{normal velocity component} \quad (17.17c)$$

$$(\hat{\mathbf{s}} \cdot \mathbf{u})^2 + (\hat{\mathbf{n}} \cdot \mathbf{u})^2 = \frac{(\hat{\mathbf{s}} \cdot \mathbf{u}_g)^2}{1 + (\gamma/f)^2} \quad \text{horizontal kinetic energy per mass.} \quad (17.17d)$$

The cross-isobar flow (equation (17.17c)) is directly driven by the Rayleigh drag, and it is directed down the normal pressure gradient so long as the flow has a positive projection onto the tangent direction

$$\hat{\mathbf{s}} \cdot \mathbf{u} > 0 \implies \hat{\mathbf{n}} \cdot \mathbf{u} > 0. \quad (17.18)$$

When flow is moving counter-clockwise around a low pressure in the northern hemisphere, where $\hat{\mathbf{n}}$ points toward the low pressure center, then Rayleigh drag causes the fluid to spiral into the low pressure center. Conversely, when flow is moving clockwise around a high pressure, with $\hat{\mathbf{n}}$ pointing away from the high pressure center, then Rayleigh drag causes the fluid to spiral away from the high pressure center. We depict these cases in Figure 17.2. Furthermore, equation (17.17d) shows that when $\gamma \neq 0$ the magnitude of the total flow is reduced relative to the geostrophic flow, thus reflecting the dissipation of kinetic energy arising from Rayleigh drag.²

17.2.5 Horizontal spiral plus vertical rising/sinking

Thus far, we have focused on the horizontal spiral motion as shown in Figure 17.2. Through continuity we infer a corresponding vertical motion induced by the convergence of mass into the low pressure center and the divergence of mass away from the high pressure center. Figure 17.3 illustrates the vertical motion in a bottom Ekman boundary layer of either the atmosphere or ocean whereby mass rises above a low pressure center in response to the horizontal convergence of mass in the Ekman layer. Conversely, mass diverges from the high pressure Ekman layer, with this divergence inducing a sinking motion over the high pressure to replace the diverging mass. In subsequent sections, we develop the formalism needed to compute the mass transport into and out of the Ekman boundary layer, thus moving beyond the limitations of the two-dimensional theory of the present section.

17.2.6 Further study

Our discussion of Ekman velocity arising from Rayleigh drag follows a similar treatment in Section 7.4 of *Marshall and Plumb (2008)*.

²See Section 10.2.3 for more on frictional dissipation of kinetic energy.

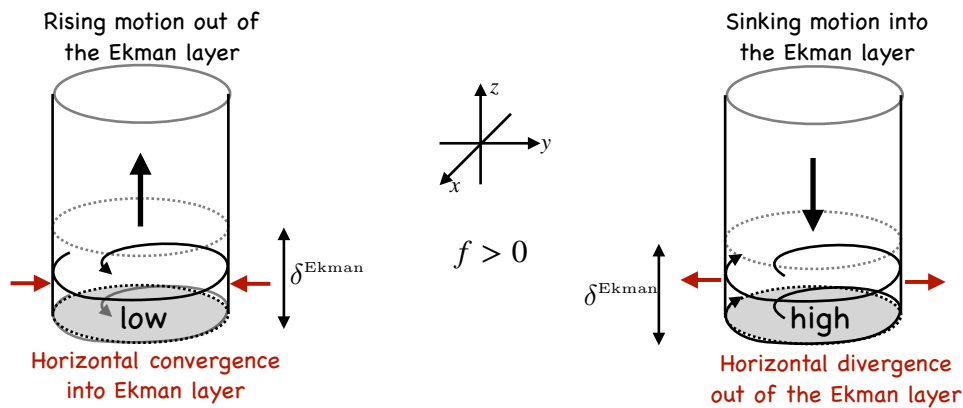


FIGURE 17.3: Illustrating the three-dimensional flow associated with Ekman layers in the northern hemisphere ($f > 0$) next to a bottom boundary (either the lower boundary of the atmosphere or bottom boundary of the ocean). This flow is inferred from the discussion in Section 17.2 and deduced in subsequent sections. Left panel: flow spiraling into a low pressure center creates convergence of mass into the Ekman layer. Mass continuity means that flow must vertically leave the Ekman layer to thus enter the interior fluid above. Right panel: flow spiraling away from a high pressure center creates divergence of mass away from the Ekman layer. Mass continuity means that flow must vertically sink into the Ekman layer from above. The Ekman layer thickness is denoted by δ^{Ekman} (Section 17.3). An analogous picture holds for the surface Ekman layer in the ocean, yet with the Ekman layer at the top of the column rather than the bottom.

17.3 Ekman number and Ekman layer thickness

Friction that is most prominent near surface and bottom boundaries arises from vertical shears in the horizontal velocity, with shears leading to flow instabilities and the development of turbulence and associated turbulent friction. There is no deductive theory for turbulent friction, so we must rely on empirical expressions. These expressions are typically based on a Laplacian viscous operator, partly motivated by the form arising from our brief discussion of kinetic theory and the continuum approximation in VOLUME 1. Most notably, this operator supports the development of a boundary layer through maintenance of both the no-slip (homogeneous Dirichlet) and stress (Neumann) boundary conditions.

17.3.1 Laplacian vertical friction

We introduced the Laplacian friction operator in Section 9.6.6 when studying stress in fluids. The Laplacian friction operator considered here is given in terms of the vertical shear of the horizontal stress vector

$$\mathbf{F}^{\text{viscous}} = \frac{1}{\rho} \frac{\partial \boldsymbol{\tau}}{\partial z} = \frac{\partial}{\partial z} \left[\nu_{\text{eddy}} \frac{\partial \mathbf{u}}{\partial z} \right], \quad (17.19)$$

with $\nu_{\text{eddy}} > 0$ a turbulent kinematic viscosity with dimensions $L^2 T^{-1}$. This form of the friction operator emulates the Laplacian operator representing molecular viscous friction (equation (9.71)). It is also the form most commonly used in theoretical and numerical models that focus on boundary layers where rotation is important.

Expanding the derivative in equation (17.19) reveals that the Laplacian friction is nonzero where there is curvature in the vertical profile of the horizontal velocity, and where there is vertical dependence to the viscosity and velocity

$$\mathbf{F}^{\text{viscous}} = \frac{\partial \nu_{\text{eddy}}}{\partial z} \frac{\partial \mathbf{u}}{\partial z} + \nu_{\text{eddy}} \frac{\partial^2 \mathbf{u}}{\partial z^2}. \quad (17.20)$$

The turbulent viscosity generally has a vertical dependence, with larger values in the boundary layer where turbulence is most energetic. This form of the friction preferentially acts on velocity exhibiting nontrivial vertical structure, thus acting to smooth any vertical dependence.

17.3.2 Non-dimensionalization

We non-dimensionalize the equations to isolate non-dimensional numbers affecting the flow regime. In particular, we identify the Ekman number as a measure of the importance of friction relative to rotation, with friction important where the Ekman number is order unity or larger, and unimportant where the Ekman number is much smaller than unity.³

We make use of the following scales and associated non-dimensional quantities

$$(x, y) = L(\hat{x}, \hat{y}) \quad z = H\hat{z} \quad (u, v) = U(\hat{u}, \hat{v}) \quad f = f_0 \hat{f} \quad p = P\hat{p} \quad (17.21)$$

where the hat terms are non-dimensional,⁴ and we introduced typical scales for horizontal length (L), vertical length (H), velocity (U), Coriolis parameter (f_0), and pressure (P). For the pressure scale we assume it follows geostrophic scaling so that it can be written⁵

$$P = f_0 \rho_0 U L. \quad (17.22)$$

Inserting the relations (17.21) into equation (17.1) leads to the non-dimensional frictional geostrophic equation

$$\hat{\mathbf{f}} \times \hat{\mathbf{u}} = -\hat{\nabla} \hat{p} + \frac{\mathbf{F}}{f_0 U}. \quad (17.23)$$

17.3.3 Defining the Ekman number and layer thickness

The **Ekman number** is a non-dimensional measure of the relative importance of the frictional acceleration due to vertical shears versus the Coriolis acceleration

$$Ek = \frac{\text{frictional acceleration from vertical shears}}{\text{Coriolis acceleration}}. \quad (17.24)$$

The Ekman number increases when there is more boundary layer turbulence, in which case the eddy viscosity, ν_{eddy} , is large relative to its small values in the interior region outside of the boundary layer. Additionally, the Ekman number increases when moving toward the equator, where the Coriolis parameter reduces.⁶

For the viscous stress form of Laplacian vertical frictional acceleration (equation (17.19))

$$\mathbf{F}^{\text{viscous}} = \frac{\nu_{\text{eddy}} U}{H^2} \frac{\partial^2 \hat{\mathbf{u}}}{\partial \hat{z}^2}, \quad (17.25)$$

³For flows where planetary rotation is not so important, the Reynolds number is the key non-dimensional number (Section 9.7) determining where viscous friction is important. Here, we are focused on rotationally dominant flows, in which case the Ekman number is the key for understanding planetary boundary layers.

⁴In Section 16.1.1 we defined $\hat{\mathbf{u}}$ as the unit vector pointing along the trajectory of a fluid element. In contrast, we here let $\hat{\mathbf{u}}$ be the non-dimensional horizontal velocity, with the widehat notation used here for non-dimensionalization to distinguish from the unit vector.

⁵Recall that in Section 13.2.3 we considered pressure in a non-rotating system to scale according to the dynamical pressure scale, U^2 , where U is a horizontal flow speed scale. In the presence of planetary rotation, the large-scale pressure field scales according to the geostrophic balance as per equation (17.22).

⁶When getting very close to the equator, our assumption of a frictional geostrophic balance breaks down so that other terms in the momentum equation, such as advection, become important.

the Ekman number is given by

$$\text{Ek} = \frac{\nu_{\text{eddy}}}{f_0 H^2}, \quad (17.26)$$

and the horizontal velocity equation (17.23) takes on the form

$$\hat{\mathbf{f}} \times \hat{\mathbf{u}} = -\hat{\nabla}_h \hat{p} + \text{Ek} \frac{\partial^2 \hat{\mathbf{u}}}{\partial z^2}. \quad (17.27)$$

If we take the vertical scale, H , equal to the length scale over which interior flow processes occur, then the Ekman number will be very small, even if the eddy viscosity is relatively large. In this case we conclude that friction is negligible, as indeed it is for many purposes where the boundary layer is not of concern.

However, the Ekman number multiplies the highest derivative in equation (17.27). So setting the Ekman number to zero represents a **singular limit**, whose mathematical meaning is that we change the order of the differential equation when setting $\text{Ek} = 0$. Reducing the order of the differential equation means we can only satisfy a reduced number of boundary conditions relative to the $\text{Ek} > 0$ case. In particular, with $\text{Ek} = 0$ we can no longer satisfy the no-slip condition at the solid-fluid boundary. In contrast, with any non-zero value of $\text{Ek} > 0$, no matter how small but nonzero, viscosity drags the flow to zero within a **boundary layer** where friction is leading order. We expect a boundary layer to form within a boundary layer thickness, $H = \delta^{\text{Ekman}}$, in which the Ekman number is order unity so where friction is of leading order importance

$$H = \delta^{\text{Ekman}} \implies \text{Ek} = \frac{\nu_{\text{eddy}}}{f_0 (\delta^{\text{Ekman}})^2} = 1. \quad (17.28)$$

Turning this equation around we see that the vertical scale, δ^{Ekman} , defines the viscous Ekman boundary layer thickness as a function of the eddy viscosity and Coriolis parameter

$$\text{Ek} = 1 \implies \delta^{\text{Ekman}} = \delta^{\text{viscous}} = \sqrt{\nu_{\text{eddy}} / f_0}. \quad (17.29)$$

17.3.4 Estimates for the vertical eddy viscosity

The eddy viscosity is not readily available from direct measurements or first principles. However, measuring the boundary layer thickness provides a means to infer a bulk kinematic viscosity for the boundary layer

$$\nu_{\text{eddy}} = f_0 (\delta^{\text{Ekman}})^2. \quad (17.30)$$

In the atmosphere, the boundary layer thickness is order 1000 m, so that at mid-latitudes, with $f_0 = 10^{-4}$ s⁻¹, we expect

$$\nu_{\text{eddy}}^{\text{atm}} \sim 10^2 \text{ m}^2 \text{ s}^{-1}, \quad (17.31)$$

whereas molecular viscosity for air is roughly 10⁻⁵ m² s⁻¹. In the ocean, the upper ocean boundary layer depth, outside of the deep convection regions, is roughly 50 m, in which case

$$\nu_{\text{eddy}}^{\text{ocn}} \sim 0.25 \text{ m}^2 \text{ s}^{-1}, \quad (17.32)$$

whereas the molecular viscosity for water is roughly 10⁻⁶ m² s⁻¹. Evidently, both eddy viscosities are many orders of magnitude larger than the corresponding molecular values.

17.4 Ocean surface Ekman layer

It is possible to establish integrated mass transport properties of the Ekman layer even without specifying details of the friction (i.e., the viscosity) or the stratification. The key ingredient is the boundary stress. This stress is commonly estimated for the surface ocean given information about the wind speed and atmospheric stratification. Hence, Ekman theory has found much application to studies of the wind-driven ocean circulation, with boundary layer integrated properties the most consequential and robust results from Ekman theory. We here focus on the ocean surface Ekman layer and then consider bottom Ekman boundaries for the atmosphere and ocean in Section 17.5.

Before starting, we emphasize that the stress is the key ingredient in computing properties of the Ekman layer. However, determining the stress is a nontrivial exercise in boundary layer physics, which is a difficult and uncertain topic outside our scope. Additionally, the turbulent boundary stress exchanged between the fluid and its boundary (either another fluid, ice, or the solid Earth) arises within Ekman boundary layers, where flow spirals relative to the geostrophic flow in the fluid interior (outside the Ekman boundary layer). So the boundary stress is generally rotated some amount relative to the interior geostrophic flow. We consider an analytic example of this rotation when studying the bottom Ekman layer in Section 17.5. For now, we simply recognize that the story is relatively simple when assuming the stress is given, but the stress itself can be rather difficult to accurately determine.

17.4.1 Horizontal mass transport within the Ekman layer

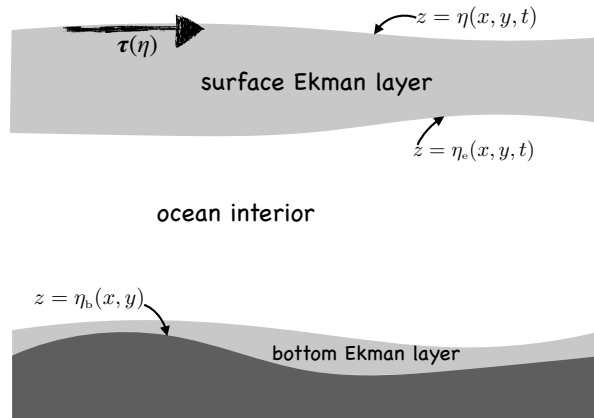


FIGURE 17.4: Ekman layer at the ocean surface, defined for vertical position $\eta_e(x, y, t) \leq z \leq \eta(x, y, t)$, with η_e specifying the Ekman layer bottom and η the free surface vertical position. Boundary stress from winds and/or sea ice imparts horizontal momentum to the upper ocean that is transmitted throughout the Ekman layer via the vertical divergence of turbulent horizontal shear stresses. As studied in Section 17.6, there is also a bottom Ekman layer created by stresses active next to the ocean bottom.

We are concerned with the mass budget for the ocean surface Ekman layer sitting between the lower boundary of the Ekman layer and the ocean free surface

$$\eta_e(x, y, t) \leq z \leq \eta(x, y, t), \quad (17.33)$$

as depicted in Figure 17.4. Knowledge of the mass budget has implications for how mechanical energy imparted to the boundary layer drives circulation within the interior of the ocean. This transport and associated circulation are how Ekman mechanics, limited to the boundary layer,

affect large-scale ocean circulation throughout the fluid column.

Integrating the horizontal Ekman balance (17.4) over the vertical scale of the Ekman layer leads to

$$\mathbf{M}_e = \int_{\eta_e}^{\eta} \rho_o \mathbf{u}_e dz \implies f \hat{\mathbf{z}} \times \mathbf{M}_e = \int_{\eta_e}^{\eta} \rho_o \mathbf{F} dz, \quad (17.34)$$

with \mathbf{M}_e the vertically integrated ageostrophic horizontal mass transport within the Ekman boundary layer. Assuming friction to be in the form of a vertical stress divergence as in equation (17.19) leads to the horizontal Ekman mass transport

$$\mathbf{M}_e = -f^{-1} \hat{\mathbf{z}} \times [\boldsymbol{\tau}(\eta) - \boldsymbol{\tau}(\eta_e)]. \quad (17.35)$$

Stress at the bottom of the Ekman layer, $\boldsymbol{\tau}(\eta_e)$, matches to the stress in the ocean interior. The stress in the fluid interior is generally much smaller than stress in the turbulent upper ocean surface, $\boldsymbol{\tau}(\eta)$, so that we can neglect $\boldsymbol{\tau}(\eta_e)$ when computing the mass transport. We are thus led to the expression for the surface stress induced ageostrophic horizontal mass transport within the upper ocean Ekman layer

$$\mathbf{M}_e = -f^{-1} \hat{\mathbf{z}} \times \boldsymbol{\tau}(\eta) = f^{-1} [\hat{\mathbf{x}} \tau^y(\eta) - \hat{\mathbf{y}} \tau^x(\eta)]. \quad (17.36)$$

The surface stress induced mass transport given by equation (17.36) is very useful in practice. Notably, we do not need to know the thickness of the Ekman layer. Rather, the mass transport is determined solely by the surface boundary stress.⁷ Furthermore, the horizontal mass transport within the Ekman layer is directed at right angles to the surface stress, as depicted in Figure 17.5, with mass transport to the right of the surface stress in the northern hemisphere and to the left in the southern hemisphere.

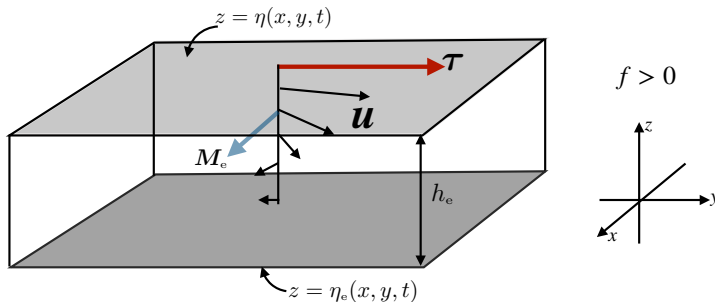


FIGURE 17.5: Horizontal transport integrated over the thickness of the surface ocean Ekman layer in the region $\eta_e(x, y, t) \leq z \leq \eta(x, y, t)$. The net mass transport is directed perpendicular to the boundary stress, oriented to the right in the northern hemisphere and to the left in the southern hemisphere. Here, the boundary stress, $\boldsymbol{\tau}$, is shown directed to the north so that in the northern hemisphere ($f > 0$), the vertically integrated horizontal Ekman transport, \mathbf{M}_e , is to the east. This perpendicular mass transport is the result of the vertically spiraling Ekman flow. Details of the Ekman spiral depend on ocean friction within the boundary layer as well as the stratification. However, the Ekman mass transport resulting from boundary stress is independent of the assumptions made about Ekman layer friction and stratification.

⁷As noted at the start of this section, determining the stress, $\boldsymbol{\tau}(\eta)$, transferred to the ocean requires information about the boundary layer processes in both the ocean and the adjoining media (either the atmosphere or cryosphere). Nevertheless, by expressing the mass transport, \mathbf{M}_e , in terms of the boundary stress provides a clear delineation of the causes for boundary layer transport. It has thus offered an important foundation for theories of wind-driven ocean circulation.

17.4.2 Example Ekman mass transports

Consider an example with an eastward zonal boundary stress, $\tau(\eta) = |\tau| \hat{\mathbf{x}}$ (i.e., westerly winds). In this case, the Ekman transport in the upper ocean is meridional

$$\mathbf{M}_e = -(|\tau|/f) \hat{\mathbf{y}} \quad (17.37)$$

which points equatorward in both hemispheres. Conversely, in the equatorial region where winds are predominantly from the east (easterly winds) so that $\tau(\eta) = -|\tau| \hat{\mathbf{x}}$, then the horizontal Ekman mass transport causes waters to move poleward away from (diverge from) the equator. Mass continuity is then satisfied by upwelling waters along the equator within the Ekman layer. We sketch the elements of this flow in Figure 17.6. Exercise 17.1 considers an analogous situation for a channel in the southern hemisphere, thus illustrating a basic feature of the wind-driven overturning circulation in the Southern Ocean.

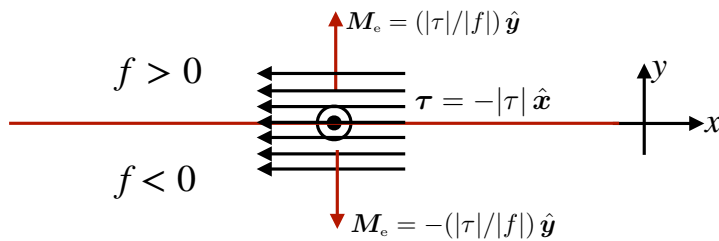


FIGURE 17.6: Easterly winds along the equator drive poleward horizontal mass transport within the upper ocean Ekman layer, as per equation (17.37). Furthermore, as discussed in Section 17.4.3, a steady state Ekman layer mass budget is typically realized by the upwelling of interior waters into the Ekman layer.

A second example concerns the case of a wind stress with a component aligned with a coastline as depicted in Figure 17.7. When the horizontal Ekman mass transport is directed away from the coast, a steady mass balance in the Ekman layer is associated with the upwelling of waters from beneath the Ekman layer (**Ekman suction**). Conversely when the horizontal mass transport is directed toward the coast, steady mass balance is realized by coastal downwelling (**Ekman pumping**). This process is very important for physical and biological features of the coastal ocean.

17.4.3 Mass budget for the Ekman layer

As seen in Figure 17.3, the horizontal transport of fluid within the Ekman layer induces a vertical transport into or out of the Ekman layer. To obtain a mathematical expression for the vertical transport, integrate the continuity equation $\nabla \cdot \mathbf{v} = 0$ over the vertical extent of the Ekman layer

$$\frac{\partial}{\partial x} \left[\int_{\eta_e}^{\eta} u \, dz \right] + \frac{\partial}{\partial y} \left[\int_{\eta_e}^{\eta} v \, dz \right] + [w(\eta) - \mathbf{u}(\eta) \cdot \nabla_h \eta] - [w(\eta_e) - \mathbf{u}(\eta_e) \cdot \nabla_h \eta_e] = 0. \quad (17.38)$$

For a Boussinesq ocean, the following kinematic boundary condition at the ocean free surface was derived in the discussion of non-divergent flows in VOLUME 1,

$$w + Q_m/\rho_0 = (\partial_t + \mathbf{u} \cdot \nabla_h) \eta \quad \text{at } z = \eta(x, y, t). \quad (17.39)$$

Similarly, at the bottom of the Ekman layer we measure the volume transport through this layer by computing the dia-surface transport, $w^{(\eta_e)}$, according to our study of kinematics in

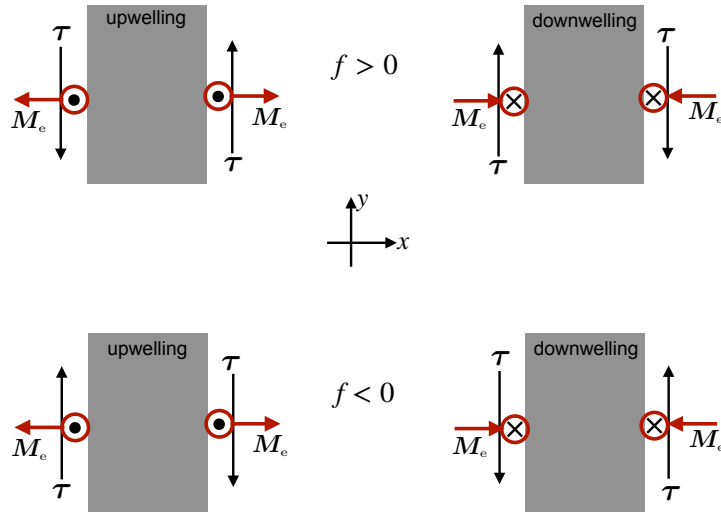


FIGURE 17.7: Wind stresses acting on the upper ocean with a component that is parallel to coastlines lead to horizontal mass transport away from or toward the coast. Mass continuity then leads to coastal upwelling or downwelling of waters into or out of the Ekman layer. Here we depict the various scenarios for the northern hemisphere (top row) and southern hemisphere (bottom row), with the gray regions representing land, the black vectors the wind stresses, and the red arrows the horizontal wind induced mass transports in the Ekman layer. This figure is adapted from Figure 4-24 of [von Arx \(1962\)](#).

VOLUME 1 (see the discussion of mixed layer kinematics)

$$w^{(\dot{\eta}_e)} = w - (\partial_t z + \mathbf{u} \cdot \nabla_h z) \quad \text{at } z = \eta_e(x, y, t). \quad (17.40)$$

The sign convention is such that $w^{(\dot{\eta}_e)} > 0$ means that volume enters (entrains into) the surface Ekman layer through its base, whereas $w^{(\dot{\eta}_e)} < 0$ means that volume leaves (detrains from) the surface Ekman layer base.

Using the kinematic boundary conditions (17.39) and (17.40) in the vertically integrated volume budget (17.38), and rearranging, leads to the Ekman layer mass budget

$$\rho_0 w^{(\dot{\eta}_e)} + Q_m = \rho_0 \partial h_e / \partial t + \nabla_h \cdot \mathbf{M}. \quad (17.41)$$

In this equation we wrote

$$h_e = \eta - \eta_e \quad (17.42)$$

for the thickness of the Ekman layer and

$$\mathbf{M} = \rho_0 \int_{\eta_e}^{\eta} \mathbf{u} dz \quad (17.43)$$

for the horizontal mass transport integrated over the Ekman layer. As a check on the above manipulations, let the Ekman layer go to the ocean bottom (so that $w^{(\dot{\eta}_e)} = 0$ and $\eta_e = \eta_b$), in which case the mass budget equation (17.41) correctly reduces to the kinematic free surface equation for the full ocean column⁸

$$\rho_0 \partial_t \eta = Q_m - \rho_0 \nabla \cdot \mathbf{U}, \quad (17.44)$$

with $\mathbf{U} = \int_{\eta_b}^{\eta} \mathbf{u} dz$ the vertically integrated horizontal velocity.

⁸Equation (17.44) is derived in our study of the kinematics of non-divergent flows in VOLUME 1.

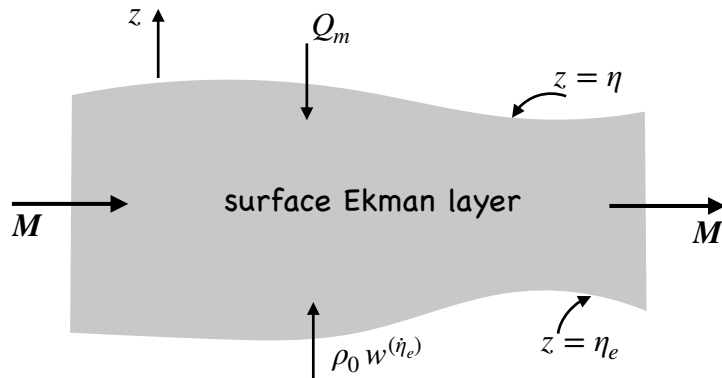


FIGURE 17.8: Mass budget over the surface Ekman layer of the ocean, with contributions from the surface mass flux, Q_m , flux through the bottom of the layer, $w^{(\dot{\eta}_e)}$, and vertically integrated horizontal flux, \mathbf{M} , within the layer. If there are any imbalances then the layer thickness will have a nonzero time tendency, $\partial_t h_e \neq 0$. Our sign convention is such as $w^{(\dot{\eta}_e)} > 0$ corresponds to water entering (entraining into) the Ekman layer (vertically upward motion) through the Ekman layer base at $z = \eta_e$, and likewise $Q_m > 0$ corresponds to water entering the Ekman layer through the free surface at $z = \eta$. Entrainment through the base of the Ekman layer is referred to as **Ekman suction** (or Ekman upwelling). The opposite case is referred to as **Ekman pumping** (or Ekman downwelling) when water leaves the Ekman layer and enters the ocean interior.

The horizontal mass transport given by equation (17.43) has a contribution from both the Ekman transport and remaining processes, such as geostrophic flow and ageostrophic flows not associated with Ekman. We write this mass transport in the form

$$\mathbf{M} = \mathbf{M}_e + \mathbf{M}_{\text{other}}. \quad (17.45)$$

The horizontal Ekman transport is determined by the boundary stress according to equation (17.36), with its divergence given by

$$\nabla_h \cdot \mathbf{M}_e = \hat{z} \cdot [\nabla_h \times (\boldsymbol{\tau}/f)]. \quad (17.46)$$

This result brings the Ekman layer mass budget (17.41) into the form

$$\rho_0 w^{(\dot{\eta}_e)} + Q_m = \rho_0 \partial_t h_e + \nabla_h \cdot \mathbf{M}_{\text{other}} + \hat{z} \cdot [\nabla_h \times (\boldsymbol{\tau}/f)]. \quad (17.47)$$

The left hand side of the layer mass budget (17.47) measures the mass transport crossing the bottom of the Ekman layer, $\rho_0 w^{(\dot{\eta}_e)}$, plus the transport crossing the free surface, Q_m . This transport balances a time change in the Ekman layer thickness (first right hand side term), plus the horizontal divergence of mass within the layer (associated with non-Ekman and Ekman). A steady state Ekman layer thickness, $\partial h_e / \partial t = 0$, is realized if the horizontal divergence of mass within the Ekman layer is exactly balanced by mass entering the Ekman layer through the top and/or bottom of the layer. We illustrate this budget in Figure 17.8. For example, in the equatorial case of Figure 17.6, the diverging horizontal Ekman layer flow induced by easterly winds (poleward Ekman transport on both sides of the equator) is balanced by water upwelling into the Ekman layer through the base, $w^{(\dot{\eta}_e)} > 0$, along with a generally smaller effects from surface mass fluxes through Q_m and possible other contributions through $\nabla_h \cdot \mathbf{M}_{\text{other}}$.

17.4.4 Ekman layer coupled to the geostrophic interior

The effects from boundary stress curl in equation (17.47) warrant particular attention whereby

$$\rho_0 w_{\text{Ekman}}^{(\dot{\eta}_e)} \equiv \nabla_h \cdot \mathbf{M}_e = \hat{z} \cdot [\nabla_h \times (\boldsymbol{\tau}/f)]. \quad (17.48)$$

The stress curl, as well as changes in f on the sphere, drive vertical motion through the base of the Ekman layer. The flow crossing the Ekman layer boundary acts to stretch or compress vertical fluid columns in the adjoining fluid interior. Interior fluid columns in a rotating fluid are stiffened through the [Taylor-Proudman effect](#) (Section 15.5.3). From our understanding of vorticity mechanics (VOLUME 3), particularly the notions of vortex stretching, we see that the Ekman induced stretching/compression of interior fluid columns leads to a change in vorticity of the fluid interior, and can then lead to meridional motion due to the [beta effect](#) (β -effect) (see discussion of [Sverdrup balance](#) in Section 15.5.4).

Consider an example with $\nabla_h \cdot \mathbf{M}_e = \hat{z} \cdot [\nabla_h \times (\boldsymbol{\tau}/f)] > 0$, so that winds induce a horizontal divergence of fluid within the Ekman layer. In a steady state, the interior flow accommodates this Ekman layer mass divergence by upwelling water through the Ekman layer base, $w^{(\dot{\eta}_e)} > 0$. This process of entraining interior water into the Ekman layer is known as [Ekman suction](#) (or Ekman upwelling when referring to the surface ocean Ekman layer). For the opposite case with $\nabla_h \cdot \mathbf{M}_e = \hat{z} \cdot [\nabla_h \times (\boldsymbol{\tau}/f)] < 0$, water leaves (detains) from the Ekman layer and moves into the interior region outside the boundary layer. Water detraining from the Ekman layer is known as [Ekman pumping](#) (or Ekman downwelling when referring to the surface ocean Ekman layer). As water diverges it produces a local low pressure so that the induced flow in the geostrophic interior is cyclonic around a region of Ekman divergence/upwelling. Conversely, the induced interior geostrophic flow is anti-cyclonic around a region of Ekman convergence/downwelling. Figure 17.9 illustrates the variety of cases found in the northern and southern hemispheres.

In the language of vorticity mechanics (VOLUME 3), Ekman upwelling (measured by $w^{(\dot{\eta}_e)} > 0$) into the surface Ekman boundary layer, leads to vortex stretching of interior fluid columns. Conversely, Ekman downwelling (with $w^{(\dot{\eta}_e)} < 0$) compresses the interior fluid columns. Vertical stiffening through the [Taylor-Proudman effect](#) within the geostrophic interior, coupled to Ekman induced vortex stretching/compression, makes what happens within the Ekman boundary layer of primary importance to the interior geostrophic flow. This coupling between the boundary layer and interior forms a key mechanism whereby mechanical forcing from surface boundary stress drives the [wind-driven](#) ocean circulation. It is notable that a primary role for the planetary Coriolis effect is required to enable a coupling between boundary layer and interior flow. In Figure 17.10 we offer a schematic of the circulation implied by Ekman dynamics in a homogeneous fluid on an f -plane, thus illustrating the coupling of the upper surface Ekman layer to the geostrophic interior and then to the bottom Ekman layer.

17.4.5 Further study

The following videos offer visuals to help develop further intuition for Ekman boundary flows.

- [This 4-minute video from Science Primer](#) provides an overview of how Ekman transport affects ocean circulation features near the coast and in open ocean gyres.
- [This video from MIT Earth, Atmospheric, and Planetary Sciences](#) illustrates the spiral flow found within an Ekman layer as realized in a rotating tank experiment.

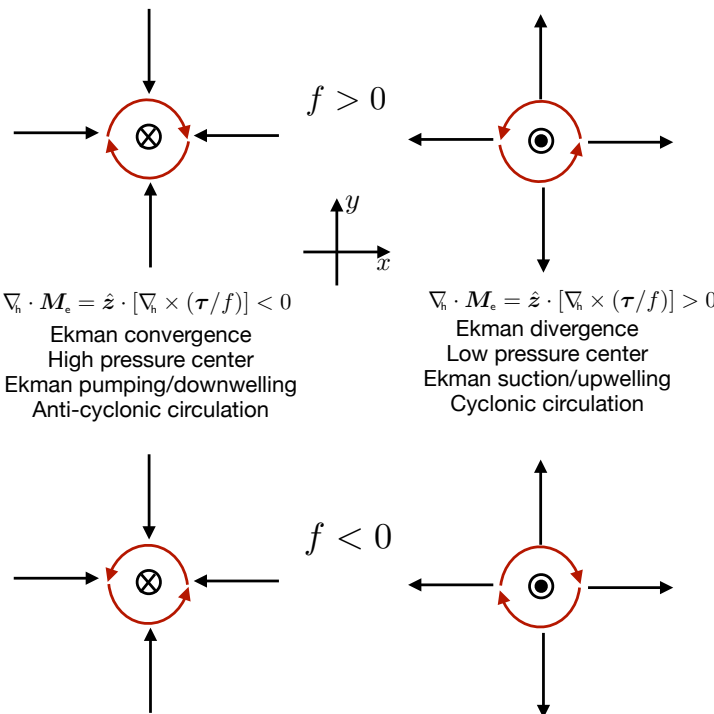


FIGURE 17.9: Plan view depicting the steady state horizontal and vertical transport in the surface ocean Ekman layer (ignoring the possible transport across the ocean surface from Q_m). The left column shows horizontal wind-induced convergence in the Ekman layer that induces vertical pumping/downwelling, where $\nabla_h \cdot \mathbf{M}_e = \hat{z} \cdot [\nabla_h \times (\boldsymbol{\tau}/f)] < 0$. The right column shows the horizontal divergence within the Ekman layer that is balanced by suction/upwelling, where $\nabla_h \cdot \mathbf{M}_e = \hat{z} \cdot [\nabla_h \times (\boldsymbol{\tau}/f)] > 0$. The top row is for the northern hemisphere ($f > 0$) and the bottom row is for the southern hemisphere ($f < 0$). The red arrows depict the sense for the induced geostrophic circulation in the interior just below the Ekman layer. Note that the horizontal Ekman transport is to the right of the red circulating flow in the northern hemisphere and to the left in the southern. Ekman pumping is associated with anti-cyclonic circulation (clockwise in the northern hemisphere and anti-clockwise in southern hemisphere). In contrast, Ekman suction is associated with cyclonic circulation. The circulation is supported by pressure gradients, with high pressure in regions of Ekman convergence, $\nabla_h \cdot \mathbf{M}_e < 0$, due to the accumulation of mass toward the center, thus giving rise to anti-cyclonic geostrophic flow in the interior. The opposite holds for regions of Ekman divergence, $\nabla_h \cdot \mathbf{M}_e > 0$, where water leaves the region thus leaving a low pressure center and inducing a cyclonic interior geostrophic flow.

- [This video from the UCLA SpinLab](#), near the 18 minute mark, shows how Ekman transport helps to explain the garbage patches found near the center of the ocean's sub-tropical gyres.
- [This video from the University of Chicago](#), starting near the 23 minute mark, provides examples of Ekman layers in a rotating tank. The other portions of this video exhibit many other novel aspects of rotating fluids and is highly recommended.

17.5 Bottom Ekman boundary layer

In this section we study the mechanics of a bottom Ekman boundary layer. For the mass transport, we merely translate the results from the upper ocean Ekman layer considered in Section 17.4, whereby the mass transports are specified by the bottom boundary stress. We go further in this analysis by also providing an analytic expression for the velocity profile within the Ekman layer, with the velocity profile allowing us to diagnose the bottom boundary stress according to the Neumann boundary condition placed on the horizontal velocity (equation

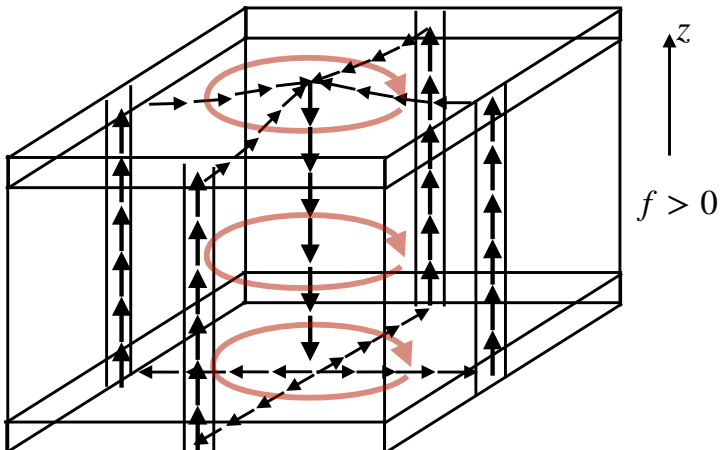


FIGURE 17.10: Schematic ocean Ekman gyre circulation in a rectangular box in the northern hemisphere f -plane as forced by an anti-cyclonic (clockwise) wind stress curl. The wind stress curl causes fluid to pile up in the center of the gyre and develop an anti-cyclonic flow. The horizontal convergence of mass toward the center of the gyre leads to downwelling into the gyre interior below the Ekman layer (as per the upper left panel of Figure 17.9). This downwelling water enters the geostrophic interior and further into the bottom Ekman layer. As discussed in Section 17.5, the downwelling water in the bottom Ekman layer causes a horizontal divergence of mass. Assuming the domain has fixed vertical side walls, continuity requires an upwelling along the outer portion of the gyre. If the wind stress is symmetric about the center of the domain, then so is the flow. However, axial symmetry is broken on the β -plane, in which flow is stronger on the western side of the gyre even if the wind remains symmetric about the domain center. We study such westward intensification of ocean gyres when studying vorticity in a shallow water fluid in VOLUME 3. This figure is adapted from Figure 6-15 of [von Arx \(1962\)](#).

(17.61) below).

17.5.1 Horizontal mass transport within the Ekman layer

Turning the derivation from Section 17.4.1 upside-down leads to a bottom horizontal Ekman mass transport

$$\mathbf{M}_e = \int_{\eta_b}^{\eta_e} \rho_o \mathbf{u}_e dz = -f^{-1} \hat{z} \times [\boldsymbol{\tau}(\eta_e) - \boldsymbol{\tau}(\eta_b)] \approx f^{-1} \hat{z} \times \boldsymbol{\tau}(\eta_b). \quad (17.49)$$

Note the sign swap relative to the upper Ekman layer transport in equation (17.36). Hence, the Ekman transport is directed to the left of the bottom stress in the northern hemisphere and to the right in the southern hemisphere. Care must be exercised when determining the stress, with examples given below, including an analytic example given in Section 17.5.3. In general, the stress is not aligned with the interior geostrophic flow, but is instead rotated by some amount.

Atmosphere-ocean Ekman layers

Consider the case where the bottom Ekman layer is the bottom of the atmosphere sitting over the ocean. The stress imparted to the bottom of the atmosphere is equal in magnitude yet oppositely directed to the stress acting on the upper ocean.⁹ Hence, the frictional stress induced mass transport (17.36) for the upper ocean Ekman layer is equal and opposite to the

⁹Recall our discussion of stress in Chapter 9, whereby stress on one side of an interface matches that on the other, which is a result following from Newton's third law.

frictional stress induced mass transport in the atmosphere Ekman layer

$$\mathbf{M}_e^{ocn} = -\mathbf{M}_e^{atm} \implies \mathbf{M}_e^{ocn} + \mathbf{M}_e^{atm} = 0. \quad (17.50)$$

Since the density of the atmosphere and ocean are quite different, the equal Ekman mass transports correspond to very different volume transports.

Ocean-solid Earth or atmosphere-solid Earth Ekman layer

Consider the bottom Ekman layer next to the solid Earth. Just like the atmosphere-ocean case, the stress imparted by the fluid on the Earth is equal and opposite to the stress by the Earth on the fluid. It is not generally simple to determine this stress, though we provide an example in Section 17.5.3 based on assuming information about the vertical viscosity profile within the boundary layer. From that example, we see that the stress is not directly aligned with the interior geostrophic flow just above the boundary layer. Instead, the stress is $\pi/4$ rotated to the left of the interior flow. The rotation is due to the spiraling structure of the boundary layer flow that gives rise to the stress.

17.5.2 Mass budget for the bottom Ekman layer

Following the derivation of the Ekman layer mass budget in Section 17.4.3, and assuming no mass enters through the solid Earth, we are led to the mass budget for the bottom Ekman boundary layer¹⁰

$$\rho_e w^{(\eta_e)} = \rho_e \partial_t h_e - \nabla_h \cdot \mathbf{M} \quad (17.51)$$

where $z = \eta_e(x, y, t)$ is the vertical position for the top of the bottom Ekman layer, and

$$h_e = \eta_e - \eta_b \quad (17.52)$$

is the Ekman layer thickness. For a steady state, the budget equation (17.51) says that the horizontal convergence of mass into the bottom Ekman boundary layer leads to a detrainment of mass from the Ekman layer into the interior fluid above (upwelling). Conversely, when fluid horizontally diverges from the bottom Ekman layer there is a balance from an entrainment (downwelling) of fluid from the interior into the bottom Ekman layer. This orientation for the mass transport is illustrated in Figure 17.3 as part of our earlier discussion.

17.5.3 An analytic bottom Ekman spiral velocity

When studying the bottom boundary layer for the atmosphere or the surface boundary layer for the ocean, we are generally afforded an estimate of the frictional boundary stress, $\tau(\eta)$. In turn, we can estimate the boundary stress induced mass transport and its divergence, and we can do so without making assumptions about the density profile or viscous stresses within the boundary layer. However, this estimate is less directly accessible for the ocean bottom Ekman layer, where we need $\tau(\eta_b)$ to determine the mass transport. We here take an alternative approach that produces an analytic profile for the velocity within the Ekman layer, so long as we know the viscosity within the boundary layer. Knowing the velocity profile then affords an estimate of the boundary stress. This approach requires a few assumptions that are not always

¹⁰Note the sign swap in the budget (17.51) in front of the horizontal transport term as compared to the surface boundary layer mass budget (17.41).

met, in particular it requires the viscosity. Even so, it provides physical insights that furthers an understanding of Ekman mechanics thus motivating the analysis.

Physical configuration

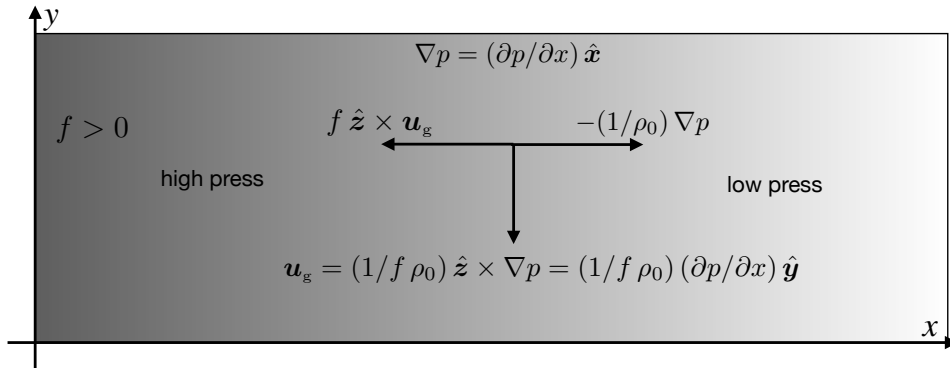


FIGURE 17.11: A southward geostrophic flow in the northern hemisphere ($f > 0$) induced by an eastward pressure gradient acceleration (low pressure to the east; $\partial p / \partial x < 0$) that balances a westward Coriolis acceleration.

We assume flow above the boundary layer is geostrophic and supported by a prescribed vertically independent pressure gradient

$$f \rho_0 \mathbf{u}_g = \hat{z} \times \nabla_h p. \quad (17.53)$$

A specific example is given by Figure 17.11, where a southward geostrophic flow in the northern hemisphere has an eastward pressure gradient acceleration (low pressure to the east) balanced by a westward Coriolis acceleration.

For flow within the bottom boundary layer, viscous stresses exchange horizontal momentum vertically between the inviscid geostrophic interior and the bottom no-slip condition. This viscous exchange slows the boundary layer velocity relative to the interior geostrophic velocity above the boundary layer. Since the pressure gradient is assumed to be vertically independent and prescribed, the slower velocity within the boundary layer means that the Coriolis acceleration is unable to balance the pressure gradient acceleration. This imbalance between pressure acceleration and Coriolis acceleration leads to a down pressure gradient component to the boundary layer velocity. As a result, the velocity spirals as we move downward toward the bottom.

We make the following assumptions to support deriving an analytic Ekman spiral velocity.

- The fluid within the Ekman layer has a constant density, ρ .
- The Coriolis parameter is a constant as per the f -plane.
- The prescribed pressure gradient is vertically independent so that the associated geostrophic velocity is vertically independent.
- The eddy viscosity is constant within the boundary layer and zero in the interior region above the boundary layer.
- The flow is steady.

The homogeneous density assumption is motivated by the rather small vertical scale of the bottom Ekman layer (tens of meters) relative to the horizontal scales over which density varies

in the ocean bottom (tens to hundreds of kilometers). Additionally, the boundary layer has turbulent mixing that acts to further homogenize the fluid. A constant viscosity is not always realistic since the turbulent viscosity is generally inhomogeneous within boundary layers. Even so, by assuming sufficient time for statistics to become stationary we can expect to make good use of the time averaged eddy viscosity.

Velocity profile within the Ekman layer

Bringing the above assumptions into the frictional geostrophic equations (17.1) leads to

$$f \hat{z} \times \mathbf{u} = -(1/\rho_0) \nabla_h p + \nu_{\text{eddy}} \partial_{zz} \mathbf{u} \quad \text{frictional geostrophy} \quad (17.54a)$$

$$\partial_z (\nabla_h p) = 0 \quad z\text{-independent horizontal pressure gradient} \quad (17.54b)$$

$$\mathbf{u}(\eta_b) = 0 \quad \text{no-slip bottom boundary condition} \quad (17.54c)$$

$$\mathbf{u}(\infty) = \mathbf{u}_g \quad \text{matching to geostrophic interior.} \quad (17.54d)$$

Decomposing the velocity into its geostrophic and ageostrophic components

$$\mathbf{u} = \mathbf{u}_g + \mathbf{u}_e, \quad (17.55)$$

leads to the equations for the Ekman velocity

$$f \hat{z} \times \mathbf{u}_e = \nu_{\text{eddy}} \partial_{zz} \mathbf{u}_e \quad (17.56a)$$

$$\mathbf{u}_e(\eta_b) = 0 \quad (17.56b)$$

$$\mathbf{u}_e(\infty) = 0. \quad (17.56c)$$

To reach this result we noted that the geostrophic velocity is vertically independent within the bottom boundary layer where the density is constant, so that the geostrophic velocity does not contribute to the viscous friction operator. Equation (17.56a) for the Ekman velocity can be converted to a fourth order differential equation, with the associated boundary conditions

$$(f^2 + \nu_{\text{eddy}}^2 \partial_{zzzz}) \mathbf{u}_e = 0 \quad (17.57a)$$

$$\mathbf{u}_e(\eta_b) = 0 \quad (17.57b)$$

$$\mathbf{u}_e(\infty) = 0. \quad (17.57c)$$

A solution to these equations renders the following velocity profile that holds both within the Ekman boundary layer and within the geostrophic interior

$$u(z) = u_g \left[1 - e^{-\Delta z/h_e} \cos(\Delta z/h_e) \right] - v_g e^{-\Delta z/h_e} \sin(\Delta z/h_e) \quad (17.58a)$$

$$v(z) = v_g \left[1 - e^{-\Delta z/h_e} \cos(\Delta z/h_e) \right] + u_g e^{-\Delta z/h_e} \sin(\Delta z/h_e) \quad (17.58b)$$

$$h_e^2 = 2 \nu_{\text{eddy}} / |f| \quad (17.58c)$$

$$\Delta z = z - \eta_b. \quad (17.58d)$$

The Ekman spiral and the bottom stress

The spiral velocity profile (17.58a)-(17.58b) vanishes at the bottom, $z = \eta_b \implies \Delta z = 0$, reflecting the no-slip bottom boundary condition. It also reduces to the interior geostrophic velocity at $\Delta z = \infty$. In moving downward through the boundary layer,

current deflects to the left of the interior geostrophic current for $f > 0$ and to the right with $f < 0$. This deflection is consistent with the schematic in Figure 17.10, with deflection turning the flow in the direction down the pressure gradient. Making use of the integral identities

$$\int_{\eta_b}^{\infty} e^{-\Delta z/h_e} \cos(\Delta z/h_e) d\Delta z = h_e/2 \quad \text{and} \quad \int_{\eta_b}^{\infty} e^{-\Delta z/h_e} \sin(\Delta z/h_e) d\Delta z = -h_e/2, \quad (17.59)$$

leads to the frictionally induced mass transport within the bottom Ekman layer

$$\mathbf{M}_e = \rho_0 \int_{\eta_b}^{\infty} \mathbf{u}_e dz \quad (17.60a)$$

$$= (h_e \rho_0/2) [-\hat{x}(u_g + v_g) + \hat{y}(u_g - v_g)] \quad (17.60b)$$

$$= f^{-1} \hat{z} \times \boldsymbol{\tau}(\eta_b). \quad (17.60c)$$

The equality (17.60c) arises from introducing the bottom stress according to the Ekman transport equation (17.49). Furthermore, the bottom stress is connected to the Neumann boundary condition placed on the horizontal velocity, thus leading to

$$\boldsymbol{\tau}(\eta_b) = \rho_0 \nu_{\text{eddy}} \left[\frac{\partial \mathbf{u}_e}{\partial z} \right]_{z=\eta_b} = (f h_e \rho_0/2) [\hat{x}(u_g - v_g) + \hat{y}(u_g + v_g)]. \quad (17.61)$$

Following from equation (17.51) we see that the bottom stress induced mass transport across the top of the bottom Ekman boundary layer is

$$\rho_0 w_{\text{Ekman}}^{(j_e)} = -\nabla_h \cdot \mathbf{M}_e = -\nabla \cdot [f^{-1} \hat{z} \times \boldsymbol{\tau}(\eta_b)] = (h_e \rho_0/2) \zeta_g, \quad (17.62)$$

where we made use of the assumed f -plane to set $\nabla_h \cdot \mathbf{u}_g = 0$, and we introduced the relative vorticity of the geostrophic flow

$$\zeta_g = \partial_x v_g - \partial_y u_g. \quad (17.63)$$

Hence, the relative vorticity of the interior geostrophic flow is proportional to the convergence of the horizontal mass transport within the bottom Ekman boundary layer. We illustrate the Ekman mass transport and bottom stress in Figure 17.12.

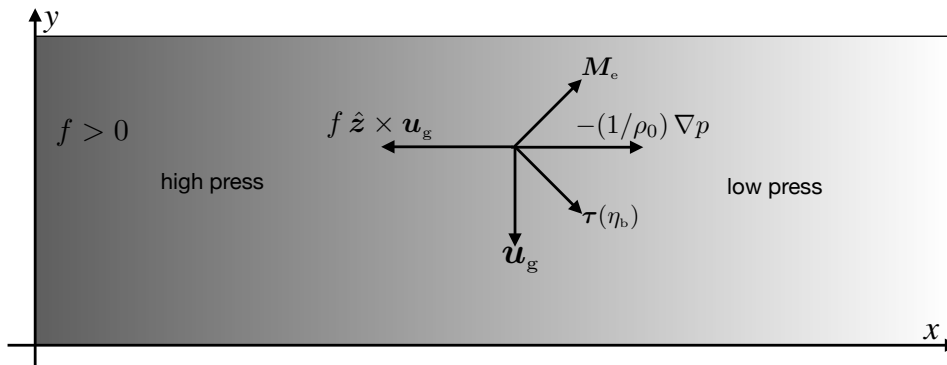


FIGURE 17.12: Mass transport and bottom stress in a homogeneous bottom Ekman layer on an f -plane in the northern hemisphere. Note how the boundary layer stress is directed $\pi/4$ radians to the left of the prescribed interior geostrophic velocity. Furthermore, the horizontal Ekman transport is itself $\pi/2$ radians to the left of the stress, which is then $3\pi/4$ to the left of the geostrophic velocity.

17.5.4 Comments

The Ekman spiral is a striking solution to the linear frictional geostrophic equations in a homogeneous fluid next to a flat no slip boundary. Section 5.7 of [Vallis \(2017\)](#) provides further discussion of the Ekman spiral solution discussed here. The spiral profile has been measured in the atmosphere and can be produced in the laboratory. However, it has proven difficult to measure in the ocean (see [Gnanadesikan and Weller \(1995\)](#) for an example). Even so, the effects from Ekman transport are robust features of the theory developed in this chapter, with those results independent of details for the vertical viscosity.

17.6 Arrested bottom Ekman flows

When studying the vertical velocity profile within the bottom boundary layer in Section 17.5, we assumed the density to be uniform within the boundary layer. [MacCready and Rhines \(1991, 1993\)](#), and [Garrett et al. \(1993\)](#) (building on earlier work from [Csanady \(1978\)](#)) questioned that assumption in their study of bottom boundary layers in the presence of a nonzero vertical density stratification next to sloping topography. They point out the remarkable possibility of a vanishing frictional stress within the sloping bottom boundary layer. That is, rather than nonzero friction leading to a zero flow next to the bottom, flow is arrested by a compensation of pressure gradient accelerations. The vanishing frictional stress motivates the term [slippery Ekman layer](#), whereas the equivalent term [arrested Ekman layer](#) refers to the zero boundary layer flow. We here briefly describe the arrested Ekman layer in reference to Figure 17.13.

17.6.1 Description of the adjustment

In both panels of Figure 17.13 we depict a prescribed vertically independent (barotropic) pressure acceleration that acts eastward and has a corresponding southward geostrophic flow ($f > 0$) and westward Coriolis acceleration. This configuration is identical to that shown in Figure 17.11 used for our study of the bottom Ekman spiral over a flat bottom. As the flow enters the bottom boundary layer it slows so that its Coriolis acceleration no longer balances the prescribed barotropic pressure gradient acceleration (we have seen this imbalance throughout this chapter). The bottom Ekman layer flow sends water cross-slope in the direction down the barotropic pressure gradient. In the configuration shown here, the cross-slope flow advects denser water upslope. In so doing, a horizontal depth-dependent (baroclinic) pressure acceleration develops adjacent to the bottom boundary layer, with the baroclinic pressure acceleration pointing opposite to the barotropic pressure acceleration. A steady state is realized when the two pressure accelerations balance within the boundary layer, in which case boundary layer flow halts.

It is remarkable that the dynamical balance for the arrested bottom boundary layer flow does not involve friction. Rather, arrest happens when the two pressure gradients balance and the Coriolis acceleration vanishes. That is, referring to the frictional geostrophic equation (17.1), each term separately vanishes in the arrested state.

17.6.2 Applications

[MacCready and Rhines \(1991, 1993\)](#) and [Garrett et al. \(1993\)](#) study the transient adjustment leading to the arrested state. They derive the expression for the time scale for adjustment to

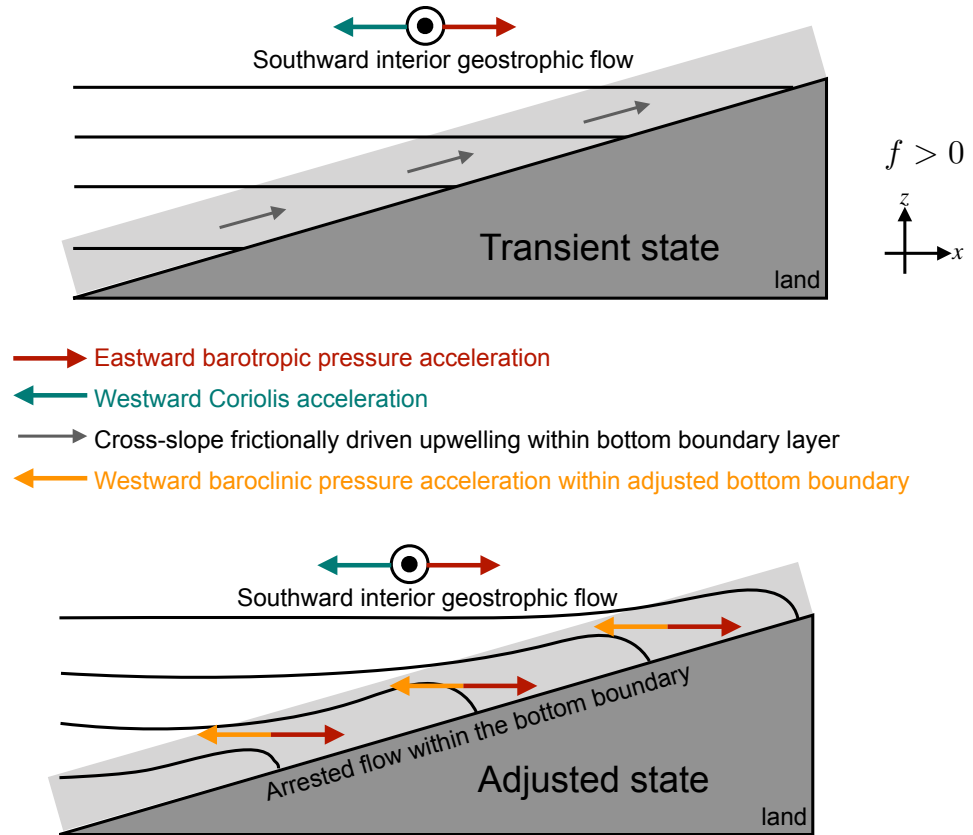


FIGURE 17.13: In both panels we depict a prescribed barotropic pressure acceleration that acts eastward and has a corresponding southward geostrophic flow and westward Coriolis acceleration. The solid black lines depict surfaces of constant buoyancy, also known as isopycnals (see Chapter 14). Top panel: As the flow enters the bottom boundary layer it slows so that its Coriolis acceleration no longer balances the barotropic pressure, thus sending water cross slope in the down pressure gradient direction. Bottom panel: The cross-slope movement of density creates a baroclinic pressure acceleration that counteracts the barotropic pressure acceleration. The steady state is realized when the two pressure accelerations balance, in which case flow within the boundary layer halts. In this halted state there are no frictional stresses since the flow halts, and with the halting arising from pressure effects rather than friction effects. Note that isopycnals are shown intersecting the solid boundary in a perpendicular direction, which is implied by the no-flux bottom boundary condition (in the absence of geothermal heating) as discussed in VOLUME 1 in our study of boundary conditions for tracers. Geostrophic flow in the opposite direction leads to downwelling along the bottom rather than upwelling. This figure is adapted from Figure 5 of [Wählin et al. \(2012\)](#).

the arrest state

$$T_{\text{arrest}} = \frac{|f|}{N^2 s^2}, \quad (17.64)$$

where s is the slope of the bottom topography and N^2 is the squared buoyancy frequency of the ambient water. The time is less in regions of strong stratification (N^2 relatively large), large topographic slopes (s^2 large), and low latitudes (f small). Conversely, the infinite time for either $N^2 = 0$ or $s^2 = 0$ indicates the need for both stratification and topographic slopes to render an arrest. Finally, we note the absence of any dissipation parameters (e.g., viscosity) from the time scale. Friction is needed to support the Ekman layer where flow crosses isobars, but the time to reach the arrested state is independent of friction.

[Wählin et al. \(2012\)](#) interpreted observations from the Amundsen Sea according to the arrested Ekman boundary layer and found T_{arrest} to be just a few hours. Additionally, the numerical model studies from [Spence et al. \(2017\)](#) and [Webb et al. \(2019\)](#) point to the ability

of barotropic shelf waves around Antarctica to provide an onshore directed barotropic pressure acceleration. Through the arrested Ekman layer mechanism described here, they find that the barotropic pressure is compensated through an upslope transport of relatively warm deep water in regions of the Antarctic Peninsula. Extensions and refinements of these ideas support an active area of ongoing research (e.g., [Wenegrat and Thomas, 2020](#); [Ruan et al., 2021](#); [Peterson and Callies, 2022](#)).



17.7 Exercises

EXERCISE 17.1: EKMAN MASS TRANSPORT IN A SOUTHERN CHANNEL

Consider a southern hemisphere zonally periodic channel (e.g., an idealized Southern Ocean) with a zonal wind stress that has a meridional dependence such as shown in Figure 17.14. Following the discussion in Sections 17.4.1 and 17.4.4, sketch the sense for the horizontal and vertical Ekman mass transport arising from this wind stress. Show the transport for regions to the north and to the south of the wind stress maximum. Ignore the β contribution by assuming the channel is not very wide and by noting that β is smaller in the high latitudes (as relevant to the Southern Ocean).

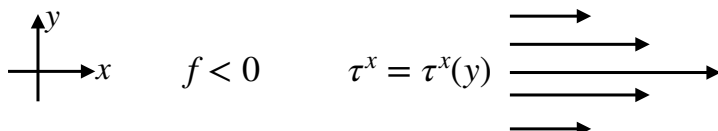


FIGURE 17.14: Zonal wind stress in a southern hemisphere zonally periodic channel with a maximum flanked by lower winds. What is the sense for the associated horizontal and vertical Ekman mass transport following from the discussion in Sections 17.4.1 and 17.4.4?

EXERCISE 17.2: RELATING EKMAN, ROSSBY, AND REYNOLDS NUMBERS

Under certain scalings, we can connect the Ekman number to the Rossby and Reynolds numbers. In detail, we have

$$\text{Ro} = \frac{U}{f_0 L} \quad \text{and} \quad \text{Ek} = \frac{\nu_{\text{eddy}}}{f_0 H^2} \quad \text{and} \quad \text{Re} = \frac{W H}{\nu_{\text{eddy}}}, \quad (17.65)$$

where

$$H = \text{vertical length scale} \quad (17.66a)$$

$$L = \text{horizontal length scale} \quad (17.66b)$$

$$U = \text{horizontal velocity scale} \quad (17.66c)$$

$$W = \text{vertical velocity scale.} \quad (17.66d)$$

and we defined the Reynolds number (Section 9.7) in terms of the vertical viscosity, vertical length scale, and vertical velocity scale. What is the ratio of the Rossby number to Reynolds if the flow is non-divergent?

EXERCISE 17.3: EKMAN BOUNDARY LAYERS AND RAYLEIGH DRAG

Rayleigh drag described in Section 17.2.3 allowed us to study the effects of friction on fluid trajectories. However, Rayleigh drag has no spatial derivatives, which contrasts to the Laplacian

friction from Section 17.3.1 and used elsewhere in this chapter. Comment on whether Rayleigh drag can support the no-slip boundary condition and the corresponding development of a boundary layer.

EXERCISE 17.4: MATH STEPS IN EKMAN BOUNDARY LAYER DERIVATION

In this exercise we fill in some of the mathematical steps for the bottom Ekman boundary layer calculation in Section 17.5.

- (a) Derive the fourth order differential equation (17.57a) from the second order equation (17.56a).
- (b) Verify that the Ekman spiral solution (17.58a)-(17.58d) is a solution to equation (17.57a) with the corresponding boundary conditions.



Part IV

End matter

Appendix A

GLOSSARY OF CONCEPTS AND TERMS

absolute salinity The absolute salinity is the mass fraction of salt within seawater, typically measured in parts per thousand. 189, 467

absolute vorticity The absolute vorticity is the sum of the relative vorticity, $\omega = \nabla \times \mathbf{v}$, plus the planetary vorticity, 2Ω . 325

action The action is the time integral of the Lagrangian density. Hamilton's principle states that the functional variation of the action is stationary for physically realized time evolution. xi

adiabatic An adiabatic process in a fluid occurs without the exchange of heat between fluid elements. In this manner, physical systems undergoing adiabatic processes are said to be thermally closed. “Adiabatic” in fluid mechanics is often used for a fluid element that is *both* thermally closed *and* materially closed. However, we maintain the distinction in our treatment in order to maintain consistency with the physics literature. 214

adiabatic lapse rate The adiabatic lapse rate measures the vertical variations in temperature for a static fluid placed in a gravity field. There are two lapse rates commonly considered: one related to height and one related to pressure. 214, 215, 479

advective time scale The advective time scale is given by $T = L/U$, where L is a typical length scale and U is a typical velocity scale for fluid particles. The advective time scale is commonly used for scale analysis of geophysical fluid flows. 285, 358, 418

ageostrophic Ageostrophic flow is any part of the flow field that is not in balance through geostrophy. In the context of Ekman mechanics, the ageostrophic flow is that flow directly affected by friction. In general, the ageostrophic flow has a nonzero horizontal divergence, which contrasts to the non-divergent horizontal flow for *f*-plane geostrophic flows. 549

anelastic approximation The anelastic approximation assumes $\nabla \cdot (\rho \mathbf{v}) = 0$, which is somewhat more relevant to the atmosphere than the Boussinesq case of $\nabla \cdot \mathbf{v} = 0$. We do not discuss the anelastic approximation in this book, preferring instead to focus on the Boussinesq ocean. 416

angular velocity Angular velocity measures the rotational velocity. It is oriented according to the right hand rule and it has magnitude generally measured in units of radians per second. The angular speed of the planet is mostly due to the planet's spin around its axis plus its orbit around the sun, and it has a value $\Omega = 7.2921 \times 10^{-5} \text{ s}^{-1}$. It is notable that finite rotations do not commute in three dimensional space. However, we can define the

angular velocity as a vector since it lives in the tangent space (Lie algebra), not in the rotation group itself (Lie group $SO(3)$). 344, 372

anti-cyclonic Anti-cyclonic refers to motion in the opposite sense as the planetary rotation, with the sense determined by viewing the rotating earth from above the poles. Geostrophic motion around a high pressure in the northern hemisphere occurs in a clockwise direction, which is anti-cyclonic. In contrast, geostrophic motion around a high pressure in the southern hemisphere occurs in an anti-clockwise direction, which is also anti-cyclonic. 508, 509

Archimedean buoyancy The Archimedean buoyancy is the buoyancy acting on a test fluid element computed relative to a reference buoyancy. We consider both a globally referenced density, thus leading to the globally referenced Archimedean buoyancy, $b = -g(\rho - \rho_0)/\rho_0$, as well as a locally referenced density, used to compute neutral directions. The Archimedean buoyancy of a test fluid element makes use of perhaps the most ancient of physical concepts in fluid mechanics. 362, 411, 461, 467, 471, 489

Archimedes' principle The net pressure contact force acting on a body within a fluid equals to the weight of fluid displaced by the body: $\mathbf{F}^{\text{press}} = -\oint_{\partial\mathcal{R}} p \hat{\mathbf{n}} d\mathcal{S} = \int_{\mathcal{R}} \mathbf{g} \rho^{\text{fluid}} dV = -g M^{\text{fluid}} \hat{\mathbf{z}}$. 464

arrested Ekman layer The arrested Ekman layer is a bottom boundary layer in which the cross-isobath Ekman transport driven by bottom stress is suppressed by a compensating barotropic pressure gradient, so that the boundary layer no longer exhibits the spiraling transport divergence but instead is halted or arrested in a nearly along isobath, nondivergent state. Arrested Ekman layers are informally referred to as slippery Ekman layers since the frictional stress vanishes. 569

aspect ratio The aspect ratio is the non-dimensional ratio of the vertical scales of motion, H , to the horizontal scales of motion, L , so that $\alpha_{\text{aspect}} \equiv H/L$. For flow that maintains an approximate hydrostatic balance, we have $\alpha_{\text{aspect}} \ll 1$, in which we say that hydrostatic flows have a small aspect ratio. 357, 418, 505

atmospheric form stress Atmospheric form stress is the contribution from atmospheric pressure acting to produce a horizontal ocean acceleration that acts at the interface between the ocean and atmosphere. This form stress is equal in magnitude to the oceanic form stress, but it is oppositely directed. 264, 382, 386

available potential energy The available potential energy (APE) is the difference in gravitational potential energy between an arbitrary state and a state reached by reversibly rearranging fluid to have zero baroclinicity. 447, 448, 527

Avogadro's number A mole of matter is defined as the mass of the material substance that contains Avogadro's number of that substance, where $A^\nu = 6.022 \times 10^{23} \text{ mole}^{-1}$. Avogadro's number is the proportionality constant converting from one molar mass of a substance to the mass of a substance. Avogadro's number is conventionally specified so that one mole of the carbon isotope, ^{12}C , contains exactly 12 grams. Hence, 12 grams of ^{12}C contains 6.022×10^{23} atoms of ^{12}C . Avogadro's number provides a connection between scales active in the microscopic world of atoms and molecules to the macroscopic world. 7, 222, 348

baroclinic instability Baroclinic instability is a fluid flow instability arising from the presence of baroclinicity in a thermal wind balanced flow. Baroclinic instability can be interpreted as a wave or global instability that arises from the constructive interference of vorticity waves. Baroclinic instability is formulated mathematically within quasi-geostrophy. 525

baroclinic modes The baroclinic mode is the first and higher eigenmode resulting from a vertical eigenmode decomposition of the primitive equations. There are a discrete infinity of baroclinic modes, with each higher mode possessing an additional zero crossing. 514

baroclinic pressure gradient A baroclinic pressure gradient arises from density gradients internal to the fluid. It is also known as an internal pressure gradient. 361, 420

baroclinic velocity The baroclinic velocity refers to the horizontal velocity minus the depth averaged horizontal velocity, with the average taken over the full depth of a fluid column. This velocity is also sometimes referred to as the internal velocity. 393, 516

baroclinicity Baroclinicity is the miss-alignment between density and pressure that renders a source for vorticity, $\mathbf{B} = -\nabla \times (\rho^{-1} \nabla p) = (\nabla \rho \times \nabla p)/\rho^2$. In a Boussinesq ocean, the baroclinicity vector arises just from horizontal gradients in the buoyancy, $\mathbf{B} = \nabla b \times \hat{z}$. 447, 510, 520

barodiffusion Barodiffusion is the diffusion of matter concentration due to pressure gradients. 332

barometric law The barometric law, also called the law of atmospheres, provides an expression for the pressure as a function of the geopotential thickness. It shows how the pressure exponentially decreases with altitude in the atmosphere, based on assuming a hydrostatic balance and ideal gas. 225, 360

barotropic fluid A barotropic fluid is one for which pressure is a function of density, $p = p(\rho)$, so that the baroclinicity vanishes, $\mathbf{B} = (\nabla \rho \times \nabla p)/\rho^2 = 0$. 251, 519

barotropic mode The barotropic mode is the zeroth eigenmode resulting from a vertical eigenmode decomposition of the primitive equations. It is sometimes referred to as the gravest vertical mode. For rigid lid models, the barotropic mode is depth independent. 514

barotropic pressure gradient A barotropic pressure gradient arises from gradients in the total mass of a fluid column. It is also referred to as an external pressure gradient. 361

barotropic velocity The barotropic velocity refers to the depth averaged horizontal velocity, averaged over the full depth of a fluid column. It is also referred to as the external velocity. 393

barotropization Barotropization refers to the process in freely evolving geostrophic turbulence whereby energy moves from higher baroclinic modes to the lowest modes, piling up at the barotropic mode. 514

barycenter The barycenter of a distribution of matter is the center of inertia for that matter. We choose the term barycentric velocity for \mathbf{v} to distinguish it from the molecular *center of mass velocity*, $\mathbf{v}^{(n)}$, of each material constituent. The barycentric velocity is the velocity we use when working with multi-component fluids. 118

barycentric velocity The barycentric velocity is the center of mass velocity for a fluid element.

The barycentric velocity plays the same role for multi-component fluids as the fluid parcel velocity does for single-component fluids. Differences between the barycentric velocity and the velocity of a specific fluid constituent can lead to the exchange of matter constituents across the boundary of the fluid element, with that exchange typically represented as diffusion. 21, 100, 115, 118, 121, 264

barystatic sealevel When freshwater enters the ocean, such as from melting continental ice sheets, it adds to the ocean mass and in turn increases global mean sea level. This change is referred to as **barystatic sealevel** change according to the sea level terminology paper from *Gregory et al. (2019)*. Although ocean salinity changes upon changing the freshwater content, the net effect on global mean sea level is almost entirely barystatic since the global halosteric effect is negligible. We can understand why the global halosteric effect is so tiny by recognizing that freshwater entering the ocean sees its salinity increase whilst the ambient seawater is itself freshened. These compensating salinity changes (which are often mistakenly ignored) have corresponding compensating sea level changes, thus bringing the global halosteric effect to near zero. 578

base manifold In continuum kinematics, we write the base or reference state of the continuum as \mathcal{B} , which defines a smooth base or reference manifold on which we can perform differential calculus. Each point of \mathcal{B} is specified by a value for the material (also Lagrangian) coordinate, a . 51, 93

Bernoulli potential The Bernoulli potential is the sum of the mechanical energy per mass plus the enthalpy per mass, $\mathcal{B} = \mathcal{M} + \mathcal{H} = \mathcal{K} + \Phi + \mathcal{I} + p/\rho$. For the Boussinesq ocean, the Bernoulli potential is $\mathcal{B} = \mathcal{K} + P^b + \varphi$. 324, 440

Bernoulli's principle The Bernoulli principle is a result of Bernoulli's theorem, whereby in regions of steady flows with relatively low pressure, the energy per mass is relatively large, whereas the converse holds in regions of high pressure. The change in energy is largely due to a change in the kinetic energy, so that flow is fast in regions of low pressure and slow in regions of high pressure. That is, the Bernoulli principle provides an energetic expression for why a fluid slows down when moving into a region of relatively high pressure, and speeds up when moving to a region of low pressure. 325

Bernoulli's theorem Bernoulli's theorem is a statement of total energy conservation for steady flows. Most commonly it appears for steady perfect fluid flows, in which the Bernoulli potential is constant along streamlines. For such steady perfect fluid flows, there is an exchange between the total energy per mass, \mathcal{E} , and the injection work, p/ρ , such that their sum remains constant along the streamline. 323, 325

beta effect (β -effect) The β -effect arises from the meridional dependence of the Coriolis parameter: $\beta = \partial_y f$, thus giving rise to differential rotation. The β -effect supports vorticity waves known as planetary Rossby waves. 515, 562

beta spiral The β -spiral refers to the spiralling of the geostrophic velocity when moving vertically within a column, and it arises from the effects of $\beta = \partial_y f$. 528

beta-drift (β -drift) The β -drift accounts for the northwestward drift of an ideal vortex due to differential rotation. The β -drift arises from pressure effects that set up a secondary flow

that induces westward drift, in addition to the northward drift from the Rossby effect.
258

beta-plane (β -plane) The β -plane is a tangent plane approximation (tangent to the geoid) that makes use of Cartesian coordinates for studying geophysical fluid motion local to a point on the rotating planet, and using a Coriolis parameter that is a linear function of latitude. Since motion is assumed to be on a constant geopotential, the β -plane makes use of the effective gravitational acceleration that includes both central gravity acceleration plus the planetary centrifugal acceleration. 247

body forces A body force acts throughout the extent of a fluid element, and it is synonymous with external force. Examples include the gravitational force, as well as the Coriolis and centrifugal forces arising from the rotating planetary reference frame. These forces are also known as long range forces. xix, 167, 236, 262

Boltzmann constant The Boltzmann constant, $k_B = 1.3806 \times 10^{-23} \text{ m}^2 \text{ kg s}^{-2} \text{ K}^{-1}$, relates the averaged kinetic energy of an ideal gas to the temperature of the gas. In so doing, it connects microscopic dynamical properties to macroscopic thermodynamic properties.
222

boundary layer A boundary layer is a region of the fluid flow that is directly affected by boundaries. For geophysical applications we have in mind the solid-earth boundary that interacts with both the ocean and atmosphere; the ocean-atmosphere boundary; the ocean-cryosphere boundary; and the atmosphere-cryosphere boundary. The fluid flow in geophysical boundary layers is generally very turbulent, thus causing rapid mixing and the transfer of properties within the boundary layer, along with the transport of properties between the boundary layer and the less turbulent fluid interior. The Ekman layer is a boundary layer of particular importance for geophysical flows, whereby the effects from the Coriolis acceleration are of importance. 547, 556

Boussinesq dynamic enthalpy The Boussinesq dynamic enthalpy is a thermodynamic potential introduced by [Young \(2010\)](#) for the analysis of energetics of a Boussinesq ocean. It is a generalization of the gravitational potential energy that allows for a closed mechanical energy budget even in the presence of a realistic seawater equation of state. 441, 442

Boussinesq ocean The Boussinesq ocean equations serve as a useful framework to study aspects of the ocean circulation, both large-scale and small-scale. The Boussinesq ocean's prognostic velocity is non-divergent, thus representing an incompressible flow, and yet the Boussinesq ocean fluid admits density variations, as for a compressible fluid. That is, the study of a Boussinesq ocean concerns the incompressible flow of a compressible fluid, thus exemplifying the important distinction between a fluid property versus a flow property. Since the flow is non-divergent, the pressure in the Boussinesq ocean is not the thermodynamic pressure found in the compressible non-Boussinesq fluid. Rather, Boussinesq pressure serves a purely mechanical role by acting as the Lagrange multiplier to constrain the Boussinesq flow to be non-divergent. The Boussinesq ocean has an inertial mass based on a constant reference density, ρ_0 , whereas the gravitational mass is based on the *in situ* density, ρ . Hence, the Boussinesq ocean does not respect the principle of equivalance, thus making it necessary to exercise special care when studying energetics of the Boussinesq ocean. 407

budget equations Much of this book is concerned with deriving and understanding equations that describe the evolution of fluid properties, with such equations (differential or integral) derived from physical principles such as Newton's laws of motion, Hamilton's principle of stationary action, Noether's theorem, thermodynamic laws, mass conservation, and vorticity mechanics. These are the budget equations that form the theoretical foundation of continuum mechanics. [ix](#)

bulk viscosity For a constitutive relation of the form $\mathbb{T}^{mn} = \rho(2\nu S^{mn} + \lambda \nabla \cdot \mathbf{v} \delta^{mn})$, we define $\nu_{\text{bulk}} = \rho(\lambda + 2\nu/3)$ as the bulk viscosity (dimensions of squared length per time). For all cases considered in this book, we set the bulk viscosity to zero, which is consistent with assuming the mechanical pressure equals to the thermodynamic pressure. [279](#)

buoyancy Buoyancy, or more precisely the Archimedean buoyancy, is the vertical force, acting on a region, \mathcal{R} , immersed in a fluid, with the forces those static forces from gravity and hydrostatic pressure. If the density of the displaced fluid is greater than the density of the matter within the region, $\rho^{\text{fluid}} > \rho^{\mathcal{R}}$, then the buoyancy force is in the $+\hat{z}$ direction, thus leading to a rising motion of the region. The converse happens if $\rho^{\text{fluid}} < \rho^{\mathcal{R}}$, in which case the region experiences a negative buoyancy force so that it sinks. If $\rho^{\text{fluid}} = \rho^{\mathcal{R}}$, then the region experiences zero buoyancy force so that the region is neutrally buoyant and it floats. When considering buoyancy of fluid elements, then we find a net positive or negative buoyancy arises only for a fluid environment with density inhomogeneities, so that the buoyancy of a fluid element vanishes in a fluid with a homogeneous density. [461](#), [464](#), [466](#)

buoyancy frequency The buoyancy frequency, N , provides a measure of the vertical stratification of denisty. It also provides a measure of the angular frequency for buoyancy oscillations. We compute the squared buoyancy frequency for the ocean via $N^2 = g(\alpha \partial_z \Theta - \beta \partial_z S)$, whereas the atmosphere typically computes it according to the vertical derivative of the potential temperature. If $N^2 < 0$ then the vertical column is gravitationally unstable. [417](#), [477](#)

buoyancy work The buoyancy work refers to the term, $-\rho \mathbf{v} \cdot \nabla \Phi$, appearing in the kinetic energy equation. For a simple geopotential it takes the form, $-\rho w g$. It refers to the work associated with the movement of a fluid element across geopotential surfaces. [432](#)

capillary pressure The capillary pressure is the pressure jump across a curved interface separating two fluids in the presence of surface tension. The pressure is larger on the concave side of the interface. [294](#), [296](#)

Cauchy equation of motion The Cauchy equation of motion is the expression of Newton's law of motion applied to continuous media such as a fluid. [241](#)

Cauchy's fundamental lemma Cauchy's fundamental lemma states that that contact forces at a point in the fluid must be in local equilibrium. This lemma is an expression of Newton's third law for a continuous media. [265](#), [287](#), [385](#)

Cauchy's stress principle Cauchy's stress principle asserts that the stress vector is a function of the position, time, and boundary normal: $\boldsymbol{\tau} = \boldsymbol{\tau}(\mathbf{x}, t, \hat{\mathbf{n}})$. The dependence on the boundary normal means that the stress acting on a surface is generally a function of the orientation of that surface. [263](#), [266](#), [267](#)

Cauchy's stress vector The Cauchy stress vector arises from dividing the contact force by the area upon which it acts. 262

Cauchy's theorem Cauchy's theorem states that the stress vector, which is a function of space, time, and normal direction, can be expressed in terms of a stress tensor (a function of space and time) projected into the direction of the normal. 267

Cauchy-Green strain tensor The Cauchy-Green strain tensor is the metric for Euclidean space represented using Lagrangian (material) coordinates, g_{IJ} . Furthermore, it is the representation when the Eulerian version of the metric tensor makes use of Cartesian coordinates, so that $g_{IJ} = F^i_I F^j_J \delta_{ij}$. Note that in Section 1.6 of [Tromp \(2025a\)](#), g_{IJ} is referred to as the *right Cauchy-Green deformation rate tensor*, which is the term also used in [Malvern \(1969\)](#). We use the term “strain” rather than “deformation” to help reduce confusion with the deformation matrix, F^i_I . 60

Cauchy-Stokes decomposition theorem The Cauchy-Stokes decomposition theorem says that the arbitrary motion of a region in a continuous media can be decomposed into a uniform translation, dilation along three perpendicular axes, plus a rigid body rotation. 74, 323

center of mass The center of mass is the position defined by the mass distribution of an object: $M \mathbf{x}_{\text{com}} = \int_{\mathcal{R}} \mathbf{x} \rho dV$, where $M = \int_{\mathcal{R}} \rho dV$ is the region’s mass. When considering the gravitational force on a region of matter, we sometimes refer to the center of mass as the center of gravity. 122, 465

centrifugal The centrifugal acceleration points towards the convex side of a turning trajectory; i.e., outward. Its opposing partner, the centripetal acceleration, points toward the center. The centrifugal acceleration arises from accelerated motion due to motion along a curved path. It is the centrifugal acceleration that pulls one away from the center of a merry-go-round whereas one’s arms and hands provide the balancing centripetal acceleration. For orbital motion, gravity provides the centripetal acceleration to counteract the centrifugal acceleration of the rotating planet. 531, 534

centripetal The centripetal acceleration points towards the concave side of a turning trajectory, with centripetal referring to the center. Its opposing partner, the centrifugal acceleration, points away from the center, thus pointing to the convex side of a curved trajectory. The centripetal acceleration is required to keep an object moving along a curved path. It is the centrifugal acceleration that pulls one away from the center of a merry-go-round whereas one’s arms and hands provide the balancing centripetal acceleration. For orbital motion, gravity provides the centripetal acceleration to counteract the centrifugal acceleration. 534

chemical potential The chemical potential, $\mu^{(n)}$, is an intensive property that measures the change in the internal energy, \mathcal{I}^e , when altering the mass, $M^{(n)}$, of the constituent n , while fixing the entropy, volume, and mass of the other components. Equivalently, it is minus the temperature weighted change in the entropy, \mathcal{S}^e , when altering the mass, $M^{(n)}$ while fixing the volume, internal energy, and mass of the other components. We can define a chemical potential for a single component system, in which it is the change arising from altering the mass of the system. Despite its name, the chemical potential does not necessarily refer to the existence of chemical reactions, though we note that it does appear prominently in the thermodynamics of chemical reactions. 182, 200

chemical work Chemical work refers to the change in internal energy arising from changes in matter composition. 183

compatibility Compatibility refers to the mathematical compatibility between the equations for tracer conservation and mass conservation. Compatibility manifests by the continuity equation for tracers reducing to the mass continuity equation when the tracer concentration is a uniform constant. Compatibility requires the non-advectional tracer fluxes to vanish when the tracer concentration is uniform, and for tracer boundary conditions to reduce to those for the fluid mass. 120

Conservative Temperature Conservative Temperature, Θ , is the potential enthalpy of a fluid element divided by a standard heat capacity. Conservative Temperature is far more conservative than potential temperature, θ . Hence, Θ is the preferred variable for measuring changes in heat within the ocean. 123, 124, 134, 214, 217, 301, 338, 468

conservative tracer Conservative tracers evolve via the convergence of advective and diffusive fluxes within the fluid interior, along with boundary conditions. Conservative tracers have no interior sources or sinks, so the net content of a conservative tracer over any finite volume domain is affected only through transport across boundaries. 214

constitutive relation A constitutive relation connects dynamics to kinematics. We make use of a generalization of Hooke's law to determine stress (a dynamical property) in terms of the strain rate tensor (a kinematic property), as mediated by the viscosity tensor. At a fundamental level, the constitutive relation is determined by properties of the material. However, turbulence closures are often written in terms of a constitutive relation determined by properties of the turbulent flow. 263, 264, 275, 277

contact force A contact force acts on the boundary of a fluid element, with examples including stresses from pressure and from friction. Contact forces are local forces. Contact forces are sometimes referred to as internal forces, since they arise from local interactions internal to the fluid, as distinct from body forces that arise from long range external forces that act throughout the body of a fluid element. Contact forces are also called tractions in some areas of continuum mechanics. Contact forces are molecular in origin, though we are unconcerned in this book with details of the molecular dynamics leading to these forces. Contact forces act on a region of a continuous media through the area integrated stresses acting on the boundary enclosing the region. xix, 237, 262, 381

continuity equation A continuity equation is a flux-form differential conservation law for intensive fluid properties that are typically expressed using the Eulerian kinematic perspective. Examples include the mass continuity equation for all constituents within a fluid sample, $\partial_t \rho + \nabla \cdot (\rho \mathbf{v}) = 0$, and the tracer continuity equation holding for individual matter constituents, $\partial_t (\rho C) + \nabla \cdot (\rho \mathbf{v} C + \mathbf{J}) = 0$. 89, 115, 241, 343

continuum approximation The continuum approximation assumes that mathematical limits for fluid volumes tending to zero are reached on length and time scales very large compared to molecular space and time scales. The temporal realization of the continuum approximation is based on recognizing that macroscopic motion associated with fluid flows (e.g., advection, waves, and mixing) evolves with time scales far longer than the time scales of molecular motions. Hence, from a macroscopic perspective, the continuum approximation leads us to assume that all fluid motions are continuous in both space and time. 2, 4, 19

continuum mechanics Continuum mechanics is the phenomenological study of how continuous matter moves through space and time. It formulates the mechanical partial differential equations based on conservation of matter and energy using continuous forms of Newton's laws and thermodynamics principles. [2](#)

Couette flow Couette flow arises when fluid is placed between two long and straight concentric cylinders that can rotate. Relative motion between the two cylinders leads to fluid motion. For example, if the inner surface rotates, then fluid next to the cylinder wall will move with the cylinder. Any normal stresses on the fluid imparted by the cylinders are directed toward the cylinder axis and so cannot render any tangential motion. [276](#), [289](#)

covariant derivative The covariant derivative is the generalization of the partial derivative operator that transforms as a $(0, 1)$ tensor with arbitrary coordinates. [29](#), [241](#)

curvature circle The curvature circle is a geometric construction used to compute the radius of curvature for a curve. More precisely, the radius of curvature equals to the radius of a tangent circle (the curvature circle) that approximates, to second order accuracy, the curve at a particular point. The radius is smaller in magnitude when the curve is highly curved, the radius goes to infinity as the curve straightens. [534](#)

cyclonic Cyclonic refers to motion in the same sense as the planetary rotation, with the sense determined by viewing the rotating earth from above the poles. Geostrophic motion around a low pressure in the northern hemisphere occurs in a counter-clockwise direction, which is cyclonic. In contrast, geostrophic motion around a low pressure in the southern hemisphere occurs in a clockwise direction, which is also cyclonic. [508](#), [509](#)

cyclostrophic balance Cyclostrophic balance refers to a steady horizontal balance between the pressure gradient and the motionally induced centrifugal acceleration found in the motion of a fluid parcel. It is commonly used for diagnostic purposes in studying tornadoes and other strongly eddying motions where the Rossby number is very large, and so we can ignore the effects from planetary Coriolis. [531](#)

D'Alembert's paradox D'Alembert's theorem suggests a behavior that is contrary to common experience. Namely, an object placed in a real fluid flow experiences a net force in the direction of the fluid flow, so that there is a transfer of momentum between the fluid and the solid body. Consequently, D'Alembert's theorem became known as D'Alembert's paradox. [277](#)

D'Alembert's theorem Consider a finite impermeable solid body placed in a steady fluid flow, with the flow assumed to be uniform upstream and downstream. A particular realization is an arbitrarily long pipe flow with a solid object in the middle of the pipe. D'Alembert's theorem says that the force exerted by a perfect fluid on the solid body has no component along the direction of the pipe's central axis. [277](#)

Deborah number The characterization of whether a material is a solid or fluid depends on the time scale of the macroscopic observation, t_{observe} , versus the time scale for the internal relaxations within the material, t_{relax} . The ratio $t_{\text{relax}}/t_{\text{observe}}$ is referred to as the Deborah number, Db . For the fluid mechanics considered in this book, we are concerned with tiny Deborah numbers, in which the relaxation time scales are determined by the relatively rapid molecular collisions that take place on time scales of order 10^{-10} s, whereas the

observation time scales are determined by macroscopic deformations that are $\approx 10^0$ s. In turn, rigid bodies have a zero Deborah number since the particles comprising the rigid body remain rigidly fixed relative to one another, so that $t_{\text{relax}} = 0$. 7

deformation Motion of the matter continuum provides a flow map that continuously and smoothly reshapes the continuum as time evolves. Deformation refers to this reshaping of the continuum, with deformation quantified through the deformation matrix computed from material space derivatives of the flow map. 47

deformation matrix Motion of the matter continuum provides a flow map that continuously and smoothly reshapes the continuum as time evolves. Deformation refers to this reshaping of the continuum, with deformation quantified through the deformation matrix computed from material space derivatives of the flow map. Mathematically, the deformation matrix is the transformation matrix moving between a -space (Lagrangian) and x -space (Eulerian) coordinates. 47, 55

deformation rate tensor The deformation rate tensor is another name for the strain rate tensor, which is the symmetric portion of the velocity gradient tensor. The strain rate tensor measures the ability of fluid flow to deform fluid elements through stretching, straining, and dilation. 47

deviatoric strain rate tensor The deviatoric strain rate tensor is given by $S_{\text{dev}}^{mn} = S^{mn} - \delta^{mn} S^q_q / 3$, so that it has zero trace, $S_{\text{dev}}^m = 0$. It is S_{dev} that appears in the constitutive relation for Newtonian fluids. 279, 310

deviatoric stress tensor The deviatoric stress tensor arises from relative motion (shears) within the fluid, and so represents deviations from the static case when stress is due solely to pressure (minus 1/3 times the trace of the stress tensor). Friction within Newtonian fluids (the only kind of fluids considered in this book) is contained within the deviatoric stress tensor, so that the deviatoric stress tensor is often called the deviatoric friction stress tensor. Mathematically, a second order tensor in 3-dimensions, \mathbb{E} , has a deviator, \mathbb{D} , with components given by $\mathbb{D}^{mn} = \mathbb{E}^{mn} - (1/3) \delta^{mn} \mathbb{E}^q_q$. By construction, the trace of the deviator vanishes: $\mathbb{D}^q_q = 0$. 237, 277, 279

diagnostic equation A diagnostic equation determines the value of a field at a particular time instance. An example is the non-divergence condition, $\nabla \cdot \mathbf{v} = 0$, satisfied by velocity in a Boussinesq ocean. There are generally no time derivatives appearing in diagnostic equations, though this property is generally a function of the chosen coordinate system. xi, 30

dianeutral direction The dianeutral direction points orthogonal to the neutral direction, with the dianeutral direction given by $\hat{\gamma} = (-\alpha \nabla \Theta + \beta \nabla S) / |-\alpha \nabla \Theta + \beta \nabla S|$. 473, 475

differentiable manifold A differentiable manifold is locally Euclidean and possess smoothness and continuous properties that allow one to perform differential calculus. A differentiable manifold is not necessarily equipped with a metric. For example, Gibbs' thermodynamic configuration space is a differentiable manifold that has no *a priori* metric structure. 169

differential rotation Using planetary Cartesian and spherical coordinates, earth's angular velocity vector is given by $\boldsymbol{\Omega} = \Omega \hat{\mathbf{z}} = \Omega (\hat{\phi} \cos \phi \hat{\mathbf{r}} + \hat{\mathbf{r}} \sin \phi)$. We see that the angular velocity vector has a spherical representation that is a function of latitudinal position, with

components in the local radial and local meridional directions. This spatial dependence to the local expression of planetary rotation is known as differential rotation. 248

diffusion Diffusion is the physical process by which a field, such as a tracer, spreads in space over time due to random motion, either from molecular chaos (molecular diffusion) or turbulent flows (turbulent diffusion). The net flux moves from regions of higher concentration to regions of lower concentration, thus moving down the concentration gradient. The mathematical equation describing diffusion is the canonical parabolic partial differential equation. 115

diffusion tensor The diffusion tensor is a second order symmetric and positive-definite tensor with dimensions of squared length per time. It is used to parameterize the downgradient eddy diffusive fluxes of tracers arising from turbulent motions. 135

diffusive flux The diffusion of tracer is derived by computing the convergence of the tracer diffusive flux, which is a flux that is directed down the tracer gradient and its strength is mediated by a diffusion tensor. 120

Dirac delta sheet The Dirac delta sheet refers to the ability to absorb the Neumann boundary condition into a modified interior source. By doing so, the boundary value problem has a modified interior source that is proportional to a Dirac delta (hence the term Dirac delta sheet), but it now has a homogeneous boundary condition. This reformulation of the Neumann boundary condition is commonly pursued in the geophysical fluids literature, such as when studying potential vorticity and for water mass analysis. 448

Dirichlet boundary condition The Dirichlet boundary condition prescribes the value of a function along the boundary. 423

divergence theorem The divergence theorem, also known as Gauss's divergence theorem, provides a relation between the volume integral of the divergence of a vector to the boundary integral of the vector projected onto the outward normal: $\int_{\mathcal{R}} \nabla \cdot \mathbf{F} dV = \oint_{\partial\mathcal{R}} \mathbf{F} \cdot \hat{\mathbf{n}} dS$. There are many corollaries to this theorem that we use in this book, one that says for Cartesian tensors that $\int_{\mathcal{R}} \nabla \phi dV = \oint_{\partial\mathcal{R}} \phi \hat{\mathbf{n}} dS$, which we use in formulating the effects from pressure in a weak formulation of the equations of motion. 90, 238, 266

drag coefficient The drag coefficients, C_d , is a non-dimensional number used to specify the stress boundary condition, commonly written in the nonlinear form as $\tau^{\text{bott}} = -C_d \rho \mathbf{v} |\mathbf{v}|$. 436

dual form stress The dual form stress, $-\eta \nabla p$, differs by a gradient from the form stress, $+p \nabla \eta$. Even though both have dimensions of a pressure, the dual form stress does not act to accelerate a fluid element. When integrated over a region where one can drop the gradient term, the integrated effects from the dual form stress equal to that from the form stress. However, it is not possible to make a local identification between the form stress and the dual form stress. 385, 395

Dufour effect The Dufour effect is a flux of heat that arises from matter concentration gradients and pressure gradients. 332, 333, 335

dynamic pressure The dynamic pressure is another name for the kinetic energy per mass as it appears in the vector-invariant velocity equation. Gradients in the kinetic energy per

mass contribute a dynamical pressure gradient that accelerates the fluid down the kinetic energy gradient, from regions of high kinetic energy per mass to regions of low kinetic energy per mass. 245

dynamic topography The dynamic topography is the thickness of a fluid layer bounded below by an isobar and above by the sea surface. It is commonly used for ocean circulation studies to map geostrophic flows. The ocean dynamic topography is also referred to as the steric sea level. 359

dynamic viscosity Dynamic viscosity is a fluid property that quantifies the fluid's resistance to shear, thus characterizing how much internal friction exists within the fluid when layers move relative to one another. The dimensions of dynamic viscosity are mass density $L^2 \text{ time}^{-1}$ = mass $L^{-1} \text{ time}^{-1}$. The kinematic viscosity equals to the dynamic viscosity divided by the density of the fluid. We typically work more in this book with kinematic viscosity than dynamic viscosity. 5, 279

dynamical pressure The dynamical pressure is that part of the hydrostatic pressure that has a horizontal gradient, and thus contributes to horizontal motion. It is not to be confused with the dynamic pressure, which is another name for the kinetic energy per mass as it appears in the vector-invariant velocity equation. 362

dynamical pressure scaling The dynamical pressure scaling is given by $P = \rho U^2$, where ρ is the mass density and U is the flow velocity scale. When considering flows close to geostrophic balance, we find that pressure scales as $P = \rho f U L$, where f is the Coriolis parameter. This scaling for pressure is distinct from the ρU^2 scaling found for flows not feeling the Coriolis acceleration. 285, 418

eddy diffusivity An eddy diffusivity is an emergent property of the flow that aims to capture the essential features of turbulent motion to irreversible mixing of tracers. Eddy diffusivities are typically far larger than molecular diffusivities, given the far more efficient nature of turbulent transport than molecular transport. 434

eddy viscosity An eddy viscosity is an emergent property of the flow that aims to capture the essential features of turbulent motion to irreversible mixing momentum. Eddy viscosities are typically far larger than molecular viscosities, given the far more efficient nature of turbulent transport than molecular transport. 435, 511

eddy-induced velocity An eddy-induced velocity is an emergent property of the flow that aims to capture the advective transport features of turbulent motion. Eddy-induced velocities are akin to Stokes' drifts, and they play an important role in parameterizations of geostrophic eddies. 434

effective buoyancy Effective buoyancy is the vertical acceleration acting on a fluid element that remains when setting all velocity dependent accelerations to zero (known as static forces). The effective buoyancy has a contribution from Archimedean buoyancy, plus the vertical derivative of a pressure perturbation that depends only on the density field. This extra pressure perturbation force is the back-reaction on a fluid element due to the surrounding fluid environment. 461, 467, 471, 493, 495

Ekman boundary layer An Ekman boundary layer arises from a balance between pressure, Coriolis, and turbulence induced friction. The role of rotation distinguishes geophysical boundary layers from engineering applications. The associated Ekman boundary layers are crucial for understanding circulation and transport in both the atmosphere and ocean. 291, 547

Ekman mechanics Ekman mechanics is concerned with geophysical fluid flow affected by accelerations from horizontal pressure gradients, vertical friction, and Coriolis, with particular attention given to regions near boundaries where turbulent friction is especially large. 547

Ekman number The Ekman number is the non-dimensional ratio of the relative importance of the frictional acceleration due to vertical shears versus the Coriolis acceleration. The Ekman number approaches unity within Ekman boundary layers, whereas it is tiny for regions outside the boundary layer. 555

Ekman pumping Detrainment of fluid out of the Ekman layer is referred to as Ekman pumping. When considering the surface boundary layer, Ekman pumping is commonly referred to as Ekman downwelling. It is of fundamental importance of dynamics of the large-scale ocean circulation. 559, 561, 562

Ekman suction Entrainment of fluid through into the Ekman boundary layer is referred to as Ekman suction. When considering the surface boundary layer, Ekman suction is commonly referred to as Ekman upwelling. It is of fundamental importance of dynamics of the large-scale ocean circulation, as well as for coastal flows. 559, 561, 562

elements pillar The elements pillar of geophysical fluid mechanics comprises the physical and mathematical formulation of conceptual models used to garner insight into rotating and stratified fluid motion. This pillar is concerned with setting the stage by deductively and descriptively exposing how physical concepts are mathematically expressed to describe geophysical fluid flows. ix

emergent phenomena pillar The emergent phenomena pillar of geophysical fluid mechanics studies solutions to equations that describe phenomena, such as waves, instabilities, turbulence, and general circulation, all of which emerge from the fundamental equations based on first principles. These phenomena can emerge in manners that are far from simple to understand deductively, particularly when considering nonlinear behavior such as turbulence. ix

emergent scale There are two general types of dimensional scales that we use to non-dimensionalize a mathematical physics equation. One is the emergent scale, which emerges from the flow itself. Emergent scales, such as the length scale and velocity scale of the flow, are specified by the subjective interest of the theorist though these scales are not under direct control. That is, we choose to focus on flows with a particular scale for purposes of examining the corresponding equations that describe that flow regime. A key example concerns our study of planetary geostrophy and quasi-geostrophy, where we choose to focus on flows of a particular scale where the Coriolis acceleration is of leading order importance. xii, 358

entrain Entrain refers to the movement of seawater from one density class to another, or the movement of seawaters across the base of the mixed layer. 107

entropy Entropy is an extensive property of a macrostate; it is not defined for microstates. In thermodynamic equilibrium, the values realized by the other extensive properties are those that maximize the entropy over the manifold of constrained thermodynamic equilibrium states. This postulate is fundamental to how we determine properties of thermodynamic equilibria. The entropy of a composite macroscopic system is additive over the constituent subsystems. Furthermore, entropy is a continuous and differential function that is a monotonically increasing function of the internal energy. This postulate is fundamental to how we use thermodynamics for composite systems such as a fluid. 172, 329

equation of state An equation of state expresses a constraint satisfied by thermodynamic variables in thermodynamic equilibrium. In geophysical fluid mechanics, we typically refer to the equation of state as an equation specifying the mass density of a fluid element in terms of thermodynamic state properties, such as temperature, tracer concentration, and pressure. The equation of state for the atmosphere is well approximated by the ideal gas equation, whereas the ocean has a nonlinear equation of state whose coefficients are fix by empirical measurements. 190, 205, 220, 467

equilibrium tide The equilibrium tide is the shape of the sea surface on a spherically symmetric and non-rotating planet with no land masses. It also assumes all transients have vanished, so that it is the shape of the sea surface assuming it responds instantaneously to astronomical gravity forcing. 377

Euler equation The Euler equation is the equation of motion for a perfect fluid, thus containing zero friction or other irreversible processes. We commonly make use of versions of the Euler equation in our studies, given that large-scale geophysical flows are not greatly affected by details of the molecular viscosity. 242, 281

Euler form The Euler form of a thermodynamic state property expresses that property as a first-order homogeneous function of its intensive and extensive variables. 183

Euler's theorem Euler's theorem for homogeneous functions provides precise relation between a function's homogeneity and its partial derivatives. We make use of this theorem in our study of mechanics, through the virial theorem, and in thermodynamics. 201, 202

Eulerian reference frame An Eulerian reference frame describes fluid motion relative to a fixed position (x -space), commonly referred to as the laboratory frame. This kinematic description measures fluid properties as the fluid streams by a fixed observer. It is not concerned with determining trajectories. Instead, Eulerian kinematics focuses on fluid properties as continuous fields that are functions of the space position, x , and time, t . 14, 17, 19

Eulerian time derivative The Eulerian time derivative is computed from a fixed position in space. It is sometimes referred to as the time tendency. Nonzero Eulerian time derivatives represent an evolving flow, whereas zero Eulerian time derivatives arise from steady state flows. 27

evolution equation An evolution equation determines the time tendency (Eulerian evolution) of a quantity such as the temperature or velocity. Terms in the prognostic equation are referred to as time tendencies. Evolution equations are also referred to as prognostic equations. x

exact differential An exact differential of a function, also called the exterior derivative, is written dF . The path integral of an exact differential depends only on the end points and so has no dependence on the path taken, $\int_A^B dF = F(B) - F(A)$. An example exact differential is given by $dF = \mathbf{A} \cdot d\mathbf{x}$ in which $\nabla \times \mathbf{A} = 0$. We make use of exact differentials of state functions in formulating the laws of equilibrium thermodynamics. 144, 173, 175, 199, 314

Exner function The Exner function is a thermodynamic quantity that relates pressure to temperature and potential temperature, which takes on a particularly simple form when assuming an ideal gas. 226

extensive property An extensive property of a physical system changes when the size of the material sample changes, with examples including particle number, mass, length, volume, kinetic energy, entropy, enthalpy, and linear momentum. Mathematically, extensive properties are represented by homogeneous functions of degree one. Extensive properties are to be compared to intensive properties, which are homogeneous functions of degree zero. 123, 169, 175, 202

external forces An external force acts throughout the extent of a fluid element and it arises from a force field that is external to the fluid element. It is synonymous with body force, with examples including the gravitational force, as well as the Coriolis and centrifugal forces arising from the rotating planetary reference frame. These forces are also known as long range forces. 236

external pressure gradient An external pressure gradient arises from gradients in the total mass of a fluid column. It is also referred to as a barotropic pressure gradient. 361

external scale There are two general types of dimensional scales that we use to non-dimensionalize a mathematical physics equation. One is the external scale, with examples in this book being the gravitational acceleration, Coriolis parameter, and specified background or reference state. External scales are set by the geophysical parameter regime in which the flow occurs, and as such they are under direct control of the theorist or experimentalist. The other scale is emergent, and is a property of the flow. xii

external velocity The external velocity refers to the depth averaged horizontal velocity, averaged over the full depth of a fluid column. It is also referred to as the barotropic velocity. 393

f-plane The *f*-plane is a tangent plane approximation (tangent to the geoid) that makes use of Cartesian coordinates for studying geophysical fluid motion local to a point on the rotating planet and using a constant Coriolis parameter. Since motion is assumed to be on a constant geopotential, the *f*-plane makes use of the effective gravitational acceleration that includes both central gravity acceleration plus the planetary centrifugal acceleration. 247

Fick's law of diffusion Fick's law of diffusion says that the diffusive flux of tracer concentration is given by a kinematic diffusivity times minus the gradient of the concentration, so that the flux is directed down the tracer concentration gradient. 332

first kinematic viscosity For a constitutive relation of the form $\mathbb{T}^{mn} = \rho(2\nu S^{mn} + \lambda \nabla \cdot \mathbf{v} \delta^{mn})$, $\nu > 0$ is the first kinematic viscosity (dimensions of squared length per time). 279

first law of thermodynamics The total energy of a thermodynamic system is locally (in space and time) conserved while undergoing a thermodynamic process. This property constitutes the *first law of thermodynamics*. For a macroscopic fluid, total energy is the sum of the internal energy arising from microscopic degrees of freedom plus the mechanical energy of macroscopic degrees of freedom. Space and time locality of total energy conservation means that physical processes are not allowed in which total energy disappears from one point in space or time only to reappear at a distant point. Note that energy is well defined for both microstates and macrostates, whereas entropy is only defined for macrostates. 172, 173, 320

flow map The flow map smoothly and continuously deforms the matter continuum through space as the fluid moves, and it is written as $\varphi(\mathbf{a}, T)$. The flow map provides the trajectory for the fluid particle specified by the material coordinate, \mathbf{a} . So in this sense we can consider the flow map as the accumulation of all fluid particle pathlines, and with its time derivative, $\partial_T \varphi(\mathbf{a}, T)$, providing the velocity of the fluid particle, $\partial_T \varphi(\mathbf{a}, T) = \mathbf{v}[\mathbf{x} = \varphi(\mathbf{a}, T), t = T] = \mathbf{v}^L(\mathbf{a}, T)$. The motion field is the reason there is a flow map, so that the nomenclature “motion field” and “flow map” are used interchangeably in this book since they both refer to movement of the continuum. 37, 47, 93

flow property A flow property is a property of the fluid flow. Examples include the non-divergent flow in a Boussinesq ocean and the turbulent diffusivity that is a function of the particular turbulent flow regime. 139, 409

flow-induced vertical acceleration Flow-induced vertical accelerations contribute to vertical acceleration of a fluid element as a result of motion itself. Operationally, we deduce the flow-induced vertical acceleration by setting the density to a constant within the vertical acceleration, so that $A_{\text{flow}} \equiv Dw/Dt|_{\rho=\rho_0}$. These accelerations arise in the study of effective buoyancy. We also refer to motional forces. 496

fluid element A fluid element is an infinitesimal deformable region of a real fluid that maintains a fixed mass but is exposed to the mixing/exchange of matter and thermodynamic properties with adjacent fluid elements. 22, 116, 167, 312, 314

fluid parcel Fluid parcel are infinitesimal deformable regions of a perfect fluid that maintain a fixed matter content and fixed thermodynamic properties, so that they have fixed mass and fixed enthalpy. 21, 168

fluid particle A material fluid particle is a zero dimensional mathematical point that follows motion of the continuous material fluid, with that motion specified by the velocity field. For a perfect fluid, fluid particles trace out integral curves of the velocity field, whereas for a real fluid the fluid particles provide integral curves for the barycentric velocity. The accumulation of a continuum of fluid particle trajectories define the pathlines that form the Lagrangian or material reference frame. 20, 47

fluid particle trajectories A fluid particle trajectory (also known as a pathline) is a curve in space that is traced out by a fluid particle as time moves forward. We are only concerned with smooth velocity fields, which allow for an unambiguous specification of the pathline (fluid particle trajectory) at each point of the fluid. Pathlines/trajectories are tangent to the velocity field at each point. Within the continuum approximation, there is a pathline/trajectory that passes through each point of space at each time instance. 37

fluid property A fluid property is a property of the fluid material, such as the density, molecular diffusivity, and thermal expansion coefficient. Fluid properties are independent of the flow. 139, 409

flux A flux of a physical quantity is a vector that measures the amount of that quantity traversing a unit area element perpendicular to the flux direction in unit time. The flux is related to the transport, whereby the flux is per unit area and the transport has the area multiplied. For example, the mass flux has dimensions $M\ L^{-2}\ T^{-1}$, whereas the mass transport has dimensions $M\ L^{-2}$. 89

flux-form conservation law A flux-form conservation law is a partial differential equation written in the form of a local time tendency of an intensive quantity that equals to (is driven by) the convergence of a flux. Such equations are generally written from an Eulerian perspective. Examples include the mass conservation equations, which are referred to as continuity equations, such as for the mass of all constituents within a fluid sample and for tracer continuity equations for individual matter constituents. 89, 124, 239

form stress Form stress is the contribution from pressure acting to give a horizontal acceleration. For a surface defined by $z = \eta(x, y, t)$, the form stress is given by $p \nabla_h \eta$ when acting on the top side of the surface, and $-p \nabla_h \eta$ on the bottom side. The name arises since the stress depends on the form, or shape, of the surface on which pressure acts. 264, 266, 381, 384, 395, 523

Fourier's law of conduction Fourier's law expresses the conductive flux of heat as proportional to a conductivity times the gradient of temperature, with the flux directed down the temperature gradient. The time changes to the temperature are given by the convergence of the downgradient flux. 318, 332

friction stress tensor The friction stress tensor arises from relative motion (shears) within the fluid, and it is often called the deviatoric stress tensor since its trace vanishes. 237, 277

frictional driven velocity The frictional driven velocity refers to that portion of the velocity that is directly driven by friction. In the context of Ekman mechanics, we have $\mathbf{u}_e = -f^{-1} \hat{\mathbf{z}} \times \mathbf{F}$, where \mathbf{F} is the friction acceleration. 549

Froude number The Froude number is the non-dimensional ratio of the fluid particle speed to the gravity wave speed. Froude number's larger than unity typically signal flow that is unstable to hydraulic jumps. For stratified flows, we also define the Froude number as a measure of the relative strength of vertical shears (i.e., vertical derivatives) of the horizontal velocity, U/H , versus the buoyancy stratification, N . For stratified flows, the squared Froude number equals to the inverse of the Richardson number. 418, 419

fundamental thermodynamic relation The fundamental thermodynamic relation, also known as the Gibbs relation, expresses the first law of thermodynamics in terms of quasi-static processes so that all terms are state variables. 176, 314

Galilean space-time Galilean space-time is the marriage of Euclidean space and Newtonian universal time. Galilean space-time is used throughout this book in our study of the non-relativistic motion of matter embedded in a background Euclidean space. 20

Galilean transformation A Galilean transformation is a linear transformation from one inertial reference frame to another, operationally realized by shifting the space coordinate by $\mathbf{x} \rightarrow \mathbf{x} + \mathbf{U}t$, where \mathbf{U} is a constant velocity. We generally expect the mechanical equations to be unchanged when undergoing a Galilean transformation, unless the forces have a dependence on the velocity. 30, 278, 322, 456

gauge function A gauge function is a physically unspecified function that is associated with a gauge symmetry. The simplest gauge function we encounter in this book is the arbitrary constant associated with streamfunctions for two-dimensional non-divergent flows. For three-dimensional non-divergent flows, gauge symmetry allows for an arbitrary gradient to be added to the vector streamfunction. We also encounter gauge functions when studying fluxes in flux-form Eulerian conservation laws. In these cases, is only the convergence of a flux that is physically relevant, so that the flux is arbitrary up to the curl of a vector function. 321

gauge symmetry A gauge symmetry arises from a redundancy in the mathematical description of a physical system. In fluid mechanics, there is a gauge symmetry associated with the ability to add a constant to the streamfunction in a horizontally non-divergent flow, with the constant not affecting the velocity field. For three dimensional non-divergent flow, the vector streamfunction is arbitrary up to the gradient of a scalar, with the details of this scalar irrelevant to the physics of the fluid flow. We also encounter gauge symmetries when defining the flux of a scalar field. Since the convergence of the flux affects time changes to the scalar, the flux is arbitrary up to the curl of a scalar. The presence of gauge symmetries affords us some freedom to choose a particular gauge to suite our subjective needs, with the choice not altering the objective physics. A standard reference for gauge symmetry, in the context of electromagnetism, is given in Section 27-4 in Volume II of *Feynman et al.* (1963). 144, 238, 321

generalized vertical coordinate A generalized vertical coordinate, σ , has a one-to-one invertible relation with the geopotential vertical coordinate, z , so that $\sigma = \sigma(x, y, z, t)$, and yet this coordinate is typically not orthogonal to the horizontal Cartesian coordinates. Generalized vertical coordinates are commonly used as the basis for numerical ocean and atmosphere models, and frequently used for theoretical formulations. 17, 26, 29, 129, 133, 155, 363, 529

geophysical fluid dynamics Geophysical fluid dynamics is a branch of fluid mechanics concerned with natural fluid motion on a rotating and gravitating body such as a planet or star. ix, 235

geophysical fluid mechanics Geophysical fluid mechanics is a branch of theoretical physics concerned with natural fluid motion on a rotating and gravitating body such as a planet or star, making use of concepts and methods from classical continuum mechanics and thermodynamics. vii

geopotential The geopotential for the rotating earth is the sum of the gravitational potential plus the potential from the planetary centrifugal acceleration. A resting ocean forms the shape of a geopotential, which is approximated as an oblate spheroid with slightly larger radius at the equator than the poles. 210, 237, 247, 303, 371

geopotential height The geopotential height equals to the geopotential divided by the gravitational acceleration. In atmospheric circulation studies it is often useful to know the geopotential thickness of a column bounded by isobars. [225](#), [227](#), [360](#)

geopotential thickness The geopotential thickness is the difference in geopotential height between two pressure levels, and it is commonly used in atmospheric circulation studies to diagnose geostrophic flow. [225](#), [360](#)

geostrophic balance The geostrophic balance is a diagnostic balance between the pressure gradient acceleration and the Coriolis acceleration. It is well maintained for the large-scale and low frequency middle to high latitude motions in the atmosphere and ocean. Geostrophic balance does not hold near the equator, since the Coriolis parameter vanishes there. [xi](#), [507](#), [508](#), [537](#)

geostrophic flow Geostrophic flow arises from a balance between the Coriolis acceleration and the horizontal pressure gradient acceleration. [366](#)

geostrophic streamfunction The geostrophic streamfunction is the streamfunction for the horizontal geostrophic flow. On the f -plane, pressure divided by density and the Coriolis parameter provides a streamfunction for the geostrophic velocity: $\mathbf{u}_g = \hat{\mathbf{z}} \times \nabla_h [p/(\rho_0 f)]$. [508](#)

geostrophic Sverdrup balance The geostrophic Sverdrup balance is the Sverdrup balance based on geostrophic flows. [516](#)

geostrophy Geostrophy is the state of being in geostrophic balance. [503](#)

Gibbs potential The Gibbs potential is a thermodynamic state property that is a natural function of temperature, pressure, and matter content. [184](#)

Gibbs relation The Gibbs relation, also known as the fundamental thermodynamic relation, expresses the first law of thermodynamics in terms of quasi-static processes so that all terms are state variables. [176](#)

Gibbs-Duhem The Gibbs-Duhem relation is a thermodynamic relation that describes how the changes in the intensive variables (temperature, pressure, and chemical potential) are dependent on values for the extensive variables (entropy, volume, and matter composition) for a physical system at thermodynamic equilibrium. It follows from the Euler form of internal energy and constrains how changes in one intensive variable affect the others. [184](#)

global conservation A property is said to be globally conserved if it remains constant in time over a region in the absence of boundary fluxes. [341](#)

global instabilities Global fluid instabilities arise from the constructive interference of waves and so involve the solution of an eigenvalue problem to determine properties of unstable waves. At most, a necessary condition can be derived to determine whether a global instability exists. Global instabilities are also referred to as wave instabilities. [xxi](#)

gradient wind Gradient wind balance refers to a steady balance in the horizontal tangent plane between the planetary Coriolis acceleration, motionally induced centrifugal acceleration, and the horizontal pressure gradient acceleration, as they act on a fluid parcel. It is commonly used to provide a diagnostic description of fluid motion with Rossby number near unity. [531](#)

gravest vertical mode The gravest vertical mode is the zeroth mode (barotropic mode) in a vertical eigenmode decomposition of the primitive equations. 514

gravitational instability A gravitationally unstable profile, in which the fluid has higher density over lower, is signalled by $N^2 < 0$. In this case the displacement of an unmixed test fluid element results in an exponential growth associated with a gravitational instability. That is, when the fluid column is vertically stratified with $N^2 < 0$, a tiny vertical displacement of a test element leads to an even larger displacement, thus causing the perturbation to grow. The resulting gravitational instability causes the fluid to overturn so that it returns the fluid column to a gravitational stable state. A gravitational instability is a particular type of static instability that is a function only of the static properties of the fluid, rather than properties of the flow. 477

gravitational mass The gravitational mass is the mass used to determine the gravitational force as part of Newton's law of gravity. The principle of equivalence says that this mass equals to the inertial mass that multiplies acceleration on the right hand side Newton's law of motion, $\mathbf{F} = m \mathbf{a}$. 414

Green's function The Green's function is the formal inverse of a linear differential operator. Knowledge of the Green's function allows one to write the solution to a linear differential equation as an integral, with the Green's function acting as a kernel. 120, 456

H-theorem Boltzmann's H-theorem is a foundational result in kinetic theory that explains how a gas evolves irreversibly toward thermodynamic equilibrium starting from time-reversible microscopic dynamics. The gas evolves irreversibly toward a state of maximum entropy, even though the underlying microscopic dynamics are time-reversible. 347

Hadley circulation Thermally direct (i.e., warm air rises and cold air descends) meridional-vertical overturning circulation in the atmosphere extending from the equatorial region (where warm and moist air rises) to the middle latitudes (where cooler and dry air descends). 254

haline Haline refers to the portion of seawater related to salinity. The term comes from the Greek word for salt. We thus refer to the haline contraction coefficient and the thermohaline (temperature and salinity) effects on ocean circulation. 469

haline contraction coefficient The haline expansion coefficient is a response function that measures the relative change in density as the salinity is altered while holding the pressure and temperature. It is typically positive, so that density increases as salinity increases. 195

harmonic function A harmonic function has zero Laplacian: $\nabla^2\psi = 0$. Harmonic functions satisfy the remarkable mean value property, whereby the value of a harmonic function at a point \mathbf{x} within an open region of a domain, \mathcal{R} , equals to the average of ψ taken over the surface of a sphere within \mathcal{R} that is centered at \mathbf{x} . 144

heat capacity The heat capacity is a thermodynamic response function that measures the change in heat as the temperature is changed, either at constant pressure (sometimes referred to as the enthalpy capacity) or at constant volume (sometimes referred to as the internal energy capacity). The heat capacity of a simple ideal gas is a constant, whereas for more realistic ideal gases it is a function of temperature. 195

heating Heating is the process of exchanging heat between thermodynamic systems. Heating modifies the internal energy as per the first law of thermodynamics. An infinitesimal amount of heating is mathematically expressed as dQ , with d identifying heating as an inexact differential process that transforms a system from one thermodynamic state to another, so that heating is a path-dependent process. Heating denotes an action applied to a system (a verb) rather than a property of a system (a noun). It is thermal energy *in transition* that arises at the boundary of a thermodynamic system. [173](#), [174](#)

Helmholtz decomposition In characterizing the kinematic properties of vector fields, such as the velocity vector for a moving fluid, [Helmholtz \(1867\)](#) introduced a method to decompose any vector into two distinct components whose properties are readily analyzed: one component vector has a zero divergence and the second vector has a zero curl. More formally, the Helmholtz decomposition says that any sufficiently smooth and rapidly decaying vector field can be decomposed uniquely into the sum of a gradient of a scalar potential and the curl of a vector potential. This Helmholtz decomposition, and its generalization to the Hodge decomposition, has extensive applications throughout fluid mechanics. [144](#), [426](#)

homentropic fluid A homentropic fluid has a space-time constant specific entropy throughout the fluid domain. [319](#)

homogeneous fluid A homogeneous fluid has all of its intensive properties a spatial constant throughout the fluid. [169](#)

homogeneous function Consider a suite of Q independent variables, X_1, X_2, \dots, X_Q , and an arbitrary function of these variables, $F(X_1, X_2, \dots, X_Q)$. We say that this function is a homogeneous function of degree γ if $F(\lambda X_1, \lambda X_2, \dots, \lambda X_Q) = \lambda^\gamma F(X_1, X_2, \dots, X_Q)$, with λ an arbitrary scalar. The left hand side is the function evaluated with each of the independent variables scaled by the same number, λ . The right hand side is the function evaluated with the unscaled variables, but multiplied by the scale raised to the power γ . Euler's theorem for homogeneous functions provides a precise relation between a function's homogeneity and its partial derivatives. We encounter properties of homogeneous functions when establishing the virial theorem in mechanics and when studying thermodynamic functions. [201](#)

Hooke's law Hooke's law provides a linear relationship between stress and strain in elastic media. The simplest form is for a linear harmonic oscillator, but more general forms are used in the study of elastic media. [278](#)

hydraulic jump A hydraulic jump occurs when fast supercritical flow (flow with speeds greater than the gravity wave speed) transitions to slower, deeper, subcritical flow (flow with speeds less than the gravity wave speed). The flow in a hydraulic jump is transient and generally quite turbulent. [328](#)

hydrodynamics A branch of fluid mechanics concerned with the flow of a homogeneous (constant density) incompressible fluid. [vii](#), [407](#)

hydrostatic approximation The hydrostatic balance is a diagnostic balance between the vertical pressure gradient force and the weight of fluid. The exact hydrostatic balance holds for a static fluid in a gravity field. The approximate hydrostatic balance holds quite well for

moving fluids with scales of motion such that the vertical scales are far smaller than the horizontal scales. 249, 349, 350

hydrostatic balance The hydrostatic balance is a diagnostic balance between the vertical pressure gradient force and the weight of fluid. The exact hydrostatic balance holds for a static fluid in a gravity field. The approximate hydrostatic balance holds quite well for moving fluids with scales of motion such that the vertical scales are far smaller than the horizontal scales. xi, 249, 271, 350, 355, 413, 503

hydrostatic primitive equations The hydrostatic primitive equations refer to the equations of motion for a fluid on a rotating planet, with the vertical momentum equation given by the hydrostatic balance. The horizontal equations are based on the traditional approximation in which the fluid thickness is much smaller than the planetary radius. The term “primitive” means that the prognostic dynamical field is the velocity rather than vorticity and divergence. Smagorinsky (1963) was an early proponent of the hydrostatic primitive equations for use in studying the large-scale ocean and atmospheric circulation. These equations form the basis for many general circulation models of the atmosphere and ocean. 349, 350, 352, 354

hypsometric equation The hypsometric equation provides the geopotential thickness between two pressure isosurfaces. 225

ideal gas An ideal gas satisfies the ideal gas law, which is based on assuming zero interactions between the point particle molecular degrees comprising the gas. The ideal gas law is a reasonably good approximation to air at standard temperature and pressure. 8, 171, 205, 220

in situ The term *in situ* is Latin for “in place”. We use it to specify the density, temperature, or other properties to mean properties measured at the location in space where they are taken. The *in situ* properties contrast to potential properties, such as potential density and potential temperature, which are computed by moving, without mixing, a fluid element to a specified reference pressure. 467

in situ temperature The *in situ* temperature is the temperature measured at a point within the fluid. 213, 214, 217, 467

incompressible flow Incompressible flow, also known as non-divergent flow, is defined by $\nabla \cdot \mathbf{v} = 0$. This flow is realized by the Boussinesq ocean, as well as fluid of constant density (and incompressible fluid). In two-dimensions, we consider the mechanics of horizontally non-divergent barotropic flow, whereby $\nabla \mathbf{u} = 0$. 139

incrop An incrop is the location at the sea floor where a water property surface (e.g., an isopycnal, isotherm) meets at the ocean bottom. 448

inertial frequency The inertial angular frequency is given by the Coriolis parameter, f . 506

inertial mass The inertial mass is the mass multiplying acceleration on the right hand side Newton’s law of motion, $\mathbf{F} = m \mathbf{a}$, and it is correspondingly used to measure kinetic energy. The principle of equivalence says that this mass equals to the gravitational used to compute the gravitational field using Newton’s law of gravity. 414

inertial motion Inertial motion refers to the horizontal motion of a fluid on a rotating planet where the only forces are the planetary Coriolis acceleration along with the motional centrifugal acceleration. 531, 539

inexact differential An inexact differential of a function is written dG . The path integral of an inexact differential depends on the path taken between the endpoints. Correspondingly, the closed loop integral of an inexact differential does not generally vanish: $\oint dG \neq 0$. An example inexact differential is given by $dG = \mathbf{A} \cdot d\mathbf{x}$ in which $\nabla \times \mathbf{A} \neq 0$. We make use of inexact differentials when studying how working and heating contribute to the first law of thermodynamics. 173, 175, 199, 200

information entropy Information entropy is used in statistical physics as a measure of the order/disorder of a probability distribution. It is proportional to the expectation value of the $\ln p$, where p is the probability density. It was originally introduced by [Boltzmann \(1966\)](#) in his proof of the H-theorem for kinetic theory of gases, and then by [Shannon \(1948\)](#) for information theory and [Jaynes \(1957\)](#) for statistical mechanics. 348

injection work The term, p/ρ , is a fundamental contribution to the flux of energy within the continuum. It is the pressure work required for the fluid element to mechanically exist within the continuum. We thus refer to p/ρ as the mechanical injection work. 323, 324

integral curve An integral curve is defined so that a given vector field is tangent to each point along the curve. For example, fluid particle trajectories are integral curves for the fluid velocity field. 20

integrating factor An integrating factor converts between an inexact and an exact differential. In thermodynamics, pressure is the integrating factor for mechanical work, temperature is the integrating factor for heating, and the chemical potential is the integrating factor for chemical work. 175, 200

intensive property An intensive property of a homogeneous physical system remains unchanged when the size of the material sample changes, with examples including mass density, tracer concentration, and Conservative Temperature. Mathematically, intensive properties are represented by homogeneous functions of degree zero. Intensive properties are to be compared to extensive properties, which are homogeneous functions of degree one. 123, 162, 169, 175, 202

interfacial form stress The interfacial form stress is the contribution from pressure that acts along an interface within a fluid to produce a horizontal acceleration. 382, 389, 390, 392

internal energy Internal energy refers to the energy of microscopic (molecular) degrees of freedom that are not explicitly resolved when working within the continuum approximation. Internal energy is not readily accessed nor harnessed, which contrasts to the mechanical energy of macroscopic motion. 162, 171

internal gravity waves An internal gravity wave is a transverse wave that is comprised of fluid particles undergoing a simple harmonic oscillation within a continuously and stably stratified buoyancy field. The angular frequency of the oscillation is determined by the buoyancy stratification and the sine of the angle the wave's group velocity makes with respect to the vertical (equivalently, the cosine of the angle the wave's phase velocity makes with horizontal). 477

internal pressure gradient An internal pressure gradient arises from density gradients internal to the fluid. It is also known as a baroclinic pressure gradient. 361, 420

internal velocity The internal velocity refers to the horizontal velocity minus the depth averaged horizontal velocity, with the average taken over the full depth of a fluid column. This velocity is also sometimes referred to as the baroclinic velocity. 393

intrinsic coordinates Intrinsic coordinates (also natural coordinates) refer to coordinates that are aligned along the flow direction and orthogonal to the flow. They are sometimes used as a means to kinematically decompose the flow into physically distinct components. In particular, they offer a concise means to compare the relative magnitudes of the Coriolis, pressure, and centrifugal accelerations acting on a fluid element moving horizontally 531, 532

inverse barometer A zero horizontal pressure gradient at the ocean surface, in the presence of an applied surface pressure, is known as an inverse barometer sea level, so that $(\nabla_h p)_{z=\eta} = \nabla_h p_a + g \rho(\eta) \nabla_h \eta = 0$. 377

irreversible process A physical process that results in the increase of entropy. Processes that increase the entropy of a fluid particle include the mixing of momentum such as through viscous friction; the mixing of matter such as through the diffusion of constituents in a multi-component fluid; and the mixing of enthalpy (diffusion of heat) in a fluid with variable temperature. vii, 179

isolated system An isolated does not exchange heat, matter, or mechanical forces with its surroundings, though it possibly does experience body forces such as from gravity or other external force fields. 167

isopycnal An isopycnal is a surface of constant potential density, which serves also as a surface of constant globally referenced Archimedean buoyancy. 523

Joule heating Joule heating, in the context of fluid mechanics, is the irreversible conversion of kinetic energy to internal energy through the process of viscous dissipation. 319, 321

kinematic boundary condition The kinematic boundary conditions arise from the kinematic constraints on fluid motion when encountering a boundary. The simplest kinematic boundary condition is the no-normal flow, in which $\mathbf{n} \cdot \mathbf{v} = 0$ for flow encountering a static and material boundary, such as the solid-earth, with $\hat{\mathbf{n}}$ the outward normal. When the boundary is material and yet moves, then $\mathbf{n} \cdot (\mathbf{v} - \mathbf{v}^{(b)}) = 0$, where $\mathbf{v}^{(b)}$ is the velocity of a point attached to the moving boundary. When the surface allows for fluid to cross, then the kinematic boundary condition is written $\rho(\mathbf{v} - \mathbf{v}^{(b)}) \cdot \hat{\mathbf{n}} = -Q_m$, where Q_m is the mass per time per area crossing the surface. If the boundary is the ocean surface, and the boundary is a monotonic function of vertical, then we can write the surface ocean kinematic boundary condition as $w + \rho^{-1} Q_m = (\partial_t + \mathbf{u} \cdot \nabla) \eta$, where $z = \eta(x, y, t)$ is the vertical position of the ocean free surface, and Q_m is the mass per time per horizontal area of fluid crossing the boundary. 99, 160

kinematic viscosity Kinematic viscosity is a fluid property that quantifies a the fluid's resistance to shear, thus characterizing how much internal friction exists within the fluid when layers move relative to one another. The dimensions of kinematic viscosity are $L^2 \text{ time}^{-1}$. The

kinematic viscosity equals to the dynamic viscosity divided by the density of the fluid. We typically work more in this book with kinematic viscosity than dynamic viscosity. 5

kinetic energy Kinetic energy of a fluid is a dynamical property arising from the macroscopic motion of the fluid. The kinetic energy for a fluid element of mass $\rho \delta V$ is given by $\frac{1}{2} \mathbf{v} \cdot \mathbf{v} \rho \delta V$, where \mathbf{v} is the fluid velocity. 307

kinetic stress tensor The kinetic stress tensor is a stress acting on an Eulerian region due to the transport of momentum across the boundary of that region, $\mathbb{T}^{\text{kinetic}} = -\rho \mathbf{v} \otimes \mathbf{v}$. In components, we have $(\mathbf{v} \otimes \mathbf{v})^{ab} = v^a v^b$. 239, 392

Knudsen number The Knudsen number, Kn , is ratio of the molecular mean free path to the macroscopic length scale. For this book, we are concerned with fluid conditions where the molecular mean free path is microscopic so that the Knudsen number is tiny, $\text{Kn} \ll 1$. 4, 229

Kronecker delta The Kronecker delta symbol, δ_{ab} , equals to unity if the indices $a = b$ and zero otherwise. The Kronecker delta is the Cartesian coordinate representation of the metric for Euclidean space using Cartesian coordinates. 60, 237

Lagrangian reference frame A Lagrangian reference frame is defined by motion of material fluid particles; i.e., it is a reference frame that is comoving with the continuum of fluid particles (a -space). The mechanical description aims to determine the continuum of trajectories, with each trajectory delineated by a continuous material coordinate that labels each fluid particle. The Lagrangian reference frame is non-inertial since fluid particles generally experience accelerations via changes to their speed and/or direction. 14, 17, 19, 47

Lagrangian region A Lagrangian region is a finite region within the fluid whereby every fluid particle in the region has a velocity given by the fluid velocity, \mathbf{v} , also known as the barycentric velocity. 122, 240

Lagrangian time derivative The Lagrangian time derivative measures the evolution of a fluid property along a trajectory defined by a fluid particle. This time derivative is also referred to as the material or substantive time derivative. 27

law of atmospheres The law of atmospheres, also called the barometric law, provides an expression for the pressure as a function of the geopotential thickness. It shows how the pressure exponentially decreases with altitude in the atmosphere, based on assuming a hydrostatic balance and ideal gas. 225, 360

Legendre transformation A Legendre transformation in thermodynamics and mechanics allows us to introduce new thermodynamic potentials that have modified natural functional dependencies. In thermodynamics, we can replace an extensive natural variable (like entropy or volume) in a thermodynamic potential with its conjugate intensive variable (temperature or pressure). Doing so is motivated if the new thermodynamic potential is more suited to experimental or theoretical conditions. The Lagrangian formulation of mechanics is related to the Hamiltonian formulation via a Legendre transformation. 189, 192, 202

Leibniz's rule Leibniz's rule provides the rule for differentiating integrals. 107–109, 112, 125, 131, 370, 387, 393

Leibniz-Reynolds transport theorem The Leibniz-Reynolds transport theorem provides the means to take the time derivative of an integrated fluid property, thus providing the basis for all finite-volume budgets within fluid mechanics. It serves to link the weak form (integral budgets) and strong form (differential budgets) of fluid mechanics. 19, 115, 125–127, 129, 131, 239, 304, 312, 340, 433, 443

level of no motion The level of no motion (also the depth of no motion) is an imagined level upon which there are no horizontal pressure gradients. This level is commonly used in diagnostic ocean studies where we do not have information about the absolute velocity, but instead only have information about the density field. We can then compute the geostrophic motion using thermal wind relative to the level of no motion. 365, 367, 516, 518

local conservation A local conservation law for a property, call it ψ -stuff, means that ψ changes at a point only through the local convergence of fluxes onto that point, and likewise for a finite region. Such conservation laws are consistent with basic notions of causality and locality that appear throughout physics, with a discussion of such conservation laws offered in Section 27-1 of *Feynman et al. (1963)*. 340, 341

local instabilities Local fluid instabilities are afforded a local necessary and sufficient condition to determine whether the fluid base state is unstable to perturbations. Gravitational instability provides the canonical example, along with centrifugal and symmetric instabilities. Local instabilities are also referred to as parcel instabilities. xxi

local Rossby number The local Rossby number is the non-dimensional ratio of the centrifugal acceleration due to relative motion to the planetary Coriolis acceleration: $\text{Ro}_{\text{local}} = (|\mathbf{u}|^2/R)/(f/|\mathbf{u}|) = |\mathbf{u}|/(R f)$, where R is the radius of curvature for the motion. 536

local thermodynamic equilibrium A fundamental assumption of thermodynamics applied to moving fluids is that each fluid element is in a local thermodynamic equilibrium, even while the macroscopic fluid has not reached its global thermodynamic equilibrium. This assumption is the basis for applying equilibrium thermodynamic relations to moving geophysical fluids, even when those moving fluids are globally far from thermodynamic equilibrium. 1, 6, 162, 167, 171, 209, 213, 276, 301, 312, 314, 322

locally referenced potential density The locally referenced potential density is numerically equal to the *in situ* density at each point in the fluid. However, when computing spatial gradients, we hold the pressure fixed so that the gradient only probes changes in salinity and temperature. The locally referenced potential density is used for computing gravitational stability and neutral directions. 478

locus A locus is the collection (or curve, surface, region, etc.) of points that follow from a specified relation. For example, the continuous path between two points in thermodynamic configuration space is built from the locus of infinitesimal quasi-static processes. 169, 170

Mach number The Mach number is the ratio of the fluid particle speed (flow speed) to the sound speed. For our studies we are only concerned with tiny Mach numbers. 407

macrostates In this book we focus on classical thermodynamics, which means we are generally concerned with macroscopic states of a fluid system; i.e., macrostate that is specified by a

few macroscopic properties such as temperature, pressure, and matter concentration. For our purposes, a macrostate is synonymous with thermodynamic state. This nomenclature must be modified when discussing statistical mechanics and quantum mechanics, whereby the complementary notion of a microstate takes on a far more central role than considered in this book. 162, 166

Magnus acceleration The Magnus acceleration appears in the vector-invariant velocity equation and has the mathematical form $-\boldsymbol{\omega} \times \mathbf{v}$. Since it acts only when there is both motion and vorticity, it is sometimes referred to as a *vortex force*. The Magnus acceleration is a nonlinear process that deflects a spinning fluid element in a direction perpendicular to its trajectory, in a manner analogous to the Coriolis acceleration. 246

mass conservation In our formulation of fluid mechanics, we assume that matter is neither created nor destroyed anywhere within the fluid continuum, and furthermore that the fluid remains in a single phase. These assumptions allow us to formulate differential and integral expressions for mass conservation. 87, 115

mass continuity The differential equation for mass conservation expressed as either a flux-form Eulerian conservation law: $\partial_t \rho + \nabla \cdot (\mathbf{v} \rho) = 0$ or through its material time evolution form: $D\rho/Dt = -\rho \nabla \cdot \mathbf{v}$. 89, 317, 356, 400, 412, 421, 432

material constant Same as material invariant. 124

material invariant The Lagrangian (material) time derivative vanishes for a property that is a material invariant. 30, 124

material time derivative The material time derivative measures the evolution of a fluid property along a trajectory defined by a fluid particle. This time derivative is also referred to as the Lagrangian or substantive time derivative. 27, 314

material tracers Fluids generally contain multiple matter constituents, and we refer to such matter constituents as material tracers, with examples being salinity and freshwater in the ocean, oxygen, nitrogen, and water vapor in the atmosphere. We measure the concentration of matter within a fluid element as the ratio of the mass of matter constituent to the mass of all constituents within the sample. The tracer concentration satisfies the tracer equation. 115

materially conservative property In the presence of mixing between two fluid elements, the net material tracer in the combined fluid element equals to the sum of the tracer content in the contributing elements. This property merely reflects matter conservation. Fluid properties that also satisfy this simple addition property are said to be materially conservative properties. To be materially conservative, a property must have its flux convergence vanish in the absence of mixing processes that are local in space and time. 341

maximum entropy Entropy is an extensive property of a macrostate. The values assumed by the other extensive properties are those that maximize the entropy over the manifold of constrained thermodynamic equilibrium states. This postulate is fundamental to how we determine properties of thermodynamic equilibria. 172

Maxwell relation Maxwell relations in thermodynamics arise from the equality of mixed partial derivatives of thermodynamic potentials. The Maxwell relations are commonly used for

thermodynamic manipulations that allow one to express quantities that are difficult to measure in terms of more readily measured quantities. 185

mechanical energy Mechanical energy of a fluid is a dynamical property formed by adding the energy due to motion of fluid elements (kinetic energy) to the energy arising from the position of a fluid element within the geopotential field (potential energy from the effective gravitational field). 307

mechanical energy flux The mechanical energy flux is given by $\mathbf{J}^{\text{mech}} = -\mathbf{v} \cdot \mathbf{T}$, where \mathbf{T} is the stress tensor consisting of pressure and friction. The convergence of the mechanical energy flux contributes to the evolution of mechanical energy of a moving fluid. 311

mechanical pressure Mechanical pressure is the pressure that appears along the diagonal of the stress tensor. In this book, the mechanical pressure equals to the thermodynamical pressure that appears in the equations for equilibrium thermodynamics. 276, 409

meridional-depth streamfunction The meridional-depth streamfunction, $\Psi(y, z)$, is the streamfunction for the non-divergent flow in the meridional-vertical plane. It is commonly used to summarize the three-dimensional overturning circulation in both the atmosphere and ocean. 152

metric A metric tensor is a symmetric second order tensor that provides the means to measure the distance between two points in space. The Kronecker delta is the Cartesian coordinate representation of the Euclidean space metric tensor. When working with alternative coordinates (e.g., spherical, generalized vertical coordinates), the coordinate representation becomes less trivial. 59, 169, 237

microstate Any macrostate is comprised of a huge number of microscopic degrees of freedom that comprise a particular microstate. 166

mole A mole is defined as the mass of a material substance that contains Avogadro's number of that substance, where $A^v = 6.022 \times 10^{23} \text{ mole}^{-1}$. Avogadro's number is conventionally specified so that one mole of the carbon isotope, ^{12}C , contains exactly 12 grams. Hence, 12 grams of ^{12}C contains 6.022×10^{23} atoms of ^{12}C . 7

momentum based viewpoint Determining the forces, either directly or indirectly, provides physical insight into the cause of fluid flow and its changes. This approach is referred to a momentum based viewpoint since it is based on working directly with the momentum equation (i.e., Newton's second law of motion). This viewpoint is distinct from a vorticity viewpoint whereby the primary concern is with terms contributing to the evolution of vorticity. x

Montgomery potential The Montgomery potential, $M = \varphi - bz$, satisfies the buoyancy coordinate form of the hydrostatic balance. The Montgomery potential plays a role for isopycnal coordinates that is directly analogous to pressure in geopotential coordinates. Correspondingly, the Montgomery potential is the geostrophic streamfunction in buoyancy coordinates. 526

motion field The motion field, $\boldsymbol{\varphi}$, is the mathematical object (or a "machine" using the language of [Misner et al. \(1973\)](#)) that generates a nonlinear time dependent and invertible flow map that continuously and smoothly reshapes the continuum as it moves through Euclidean

space as time evolves. The motion field is the reason there is a flow map, so that the nomenclature “motion field” and “flow map” are used interchangeably in this book. Both refer to movement of the continuum as time progresses. 47, 50, 93

motional forces The motional forces are terms contributing to vertical acceleration of a fluid element that arise from motion itself. Operationally, we deduce the motional vertical acceleration by setting the density to a constant within the expression for the vertical acceleration, so that $A_{\text{flow}} \equiv Dw/Dt|_{\rho=\rho_0}$. We also refer to flow-induced vertical accelerations. These forces arise in the study of effective buoyancy. 493, 496

natural coordinates Natural coordinates (also intrinsic coordinates) refer to coordinates that are aligned along the flow direction and orthogonal to the flow. They are sometimes used as a means to kinematically decompose the flow into physically distinct components. In particular, they offer a concise means to compare the relative magnitudes of the Coriolis, pressure, and centrifugal accelerations acting on a fluid element moving horizontally 531–533, 549

Navier-Stokes equation The Navier-Stokes equation is the basic equation of fluid mechanics that arises from specializing Cauchy’s equation of motion to have the stress tensor for a Newtonian fluid. Sometimes it refers to the equations in a rotating reference frame and so contains the Coriolis acceleration. 242, 281, 285

net stress tensor The net stress tensor is sum of the stress from pressure, kinetic stress, and friction: $\mathbf{T}^{\text{net}} = -p\mathbb{I} - \rho\mathbf{v} \otimes \mathbf{v} + \mathbb{T}$, with \mathbb{T} the friction tensor determined by a constitutive relation. 284

Neumann boundary condition The Neumann boundary condition prescribes the normal derivative of a function along the boundary. For tracers, the Neumann boundary condition is often referred to as the flux boundary condition since by prescribing the normal derivative we prescribe the flux. 423

neutral directions A neutral direction is a direction along which movement of a test fluid element leaves its local Archimedean buoyancy zero (i.e., where the test fluid element retains the same *in situ* density as the local environment), are directions where the fluid element remains neutrally buoyant. These directions are referred to as neutral directions. In effect, the test fluid element floats along a neutral direction. 471–473, 480

neutral helicity Neutral helicity is given by $\mathcal{H}^\gamma = \mathbf{N} \cdot (\nabla \times \mathbf{N}) = (-\alpha \nabla \Theta + \beta \nabla S) \cdot [\nabla \times (-\alpha \nabla \Theta + \beta \nabla S)]$. Neutral surfaces are well defined only if the neutral helicity vanishes, which is not the case for a realistic seawater equation of state. 473, 482

neutral surface A neutral surface is a surface whose outward normal is parallel to the dianeutral direction. Neutral surfaces exists only if the neutral helicity vanishes, which is not the case for a realistic seawater equation of state. 482

neutral trajectory Consider two equal mass test fluid elements at points, \mathbf{x} and $\mathbf{x} + \delta\mathbf{x}$. Exchange these elements over a time increment, δt , without mixing. If the exchange leaves the local *in situ* density and pressure unchanged at the two points, then the exchange occurs along a neutral trajectory. Correspondingly, neutral trajectories are infinitesimal paths in a transient fluid where a test fluid element moves without feeling any net local buoyant force. 483

neutrality condition The neutrality refers to the property of neutral directions that the α and β weighted gradients of Θ and S are exactly balanced when aligned along a neutral direction. So when considering neutral directions from the perspective of the mixed test fluid element, the mixing-induced changes in Θ precisely compensate mixing-induced changes in S as per the neutrality condition, $\alpha \hat{\mathbf{t}}^\gamma \cdot \nabla \Theta = \beta \hat{\mathbf{t}}^\gamma \cdot \nabla S$, where $\hat{\mathbf{t}}^\gamma$ is the unit direction pointing along the neutral displacement. 473, 476

Newton's third law To each action there is an equal and oppositely directed reaction. The third law holds for central forces, such as arise in Newtonian gravity and electrostatics. However, it does not hold for all forces, such as the Lorentz force acting on a moving charged particle. The strong form of Newton's third law is satisfied if the force of interaction between two particles is a central force (i.e., $(\mathbf{X}_{(i)} - \mathbf{X}_{(j)}) \times \mathbf{F}_{(ji)} = 0$) and it satisfies $\mathbf{F}_{(ij)} = -\mathbf{F}_{(ji)}$. The weak form of Newton's third law is satisfied if $\mathbf{F}_{(ij)} = -\mathbf{F}_{(ji)}$ whereas the force is not central. 263, 265, 287, 382, 383, 385

Newtonian fluid A Newtonian fluid has a linear relationship between frictional stress and strain as realized by a constant molecular viscosity. 277, 278

Newtonian time Newtonian time refers to the universal time, t , that is a monotonically increasing parameter that allows for the unambiguous distinction between past, present, and future. Hence, an event occurring at one point in space at time, t , also occurs at the same time everywhere else in space. Newtonian time is the time considered in this book since all motions are assumed to be at speeds well below that of light, so that relativistic effects are irrelevant. 20

no-slip boundary condition The no-slip boundary condition means that fluid adheres to solid boundaries due to the role of viscosity, so that there is zero relative flow between the fluid and solid. The no-slip boundary condition leads to boundary layer formation for fluids flows adjacent to solid boundaries. The no-slip boundary condition cannot be imposed for perfect fluids, since such fluids have no viscosity. As discussed in the historical essay by Anderson (2005), it was the work of Prandtl in 1905 that first exposed the fundamental nature of the no-slip boundary condition, and its role in establishing boundary layers around solid bodies immersed in a fluid flow. 282, 289, 373

Noether's theorem Noether's theorem states that for any symmetry of a physical system, there is a corresponding dynamical conservation law. For example, a classical particle system that exhibits Galilean symmetry maintains a constant linear momentum, constant mechanical energy, and constant angular momentum. A conservation law provides a dynamical constraint on the motion. The deduction of dynamical constraints is naturally arrived at using the methods of analytical mechanics, particularly through Hamilton's principle of stationary action. Noether's theorem is one of the most important foundational elements in 20th century mathematical physics. 15, 378, 399

non-advection flux A non-advection flux is any flux of a scalar field that is not advective, with the canonical example being a diffusive flux. 119, 121, 130, 134, 135

non-Boussinesq A non-Boussinesq fluid possesses the full gamut of compressibility effects. It contrasts to the Boussinesq ocean, which is quasi-compressible and whose prognostic flow field is non-divergent. 407, 529

non-conservative process A non-conservative process is a process that cannot be written as the convergence of a flux, but is instead written in the form of a source or sink in the budget equation for a property. 340

non-dimensionalization Non-dimensionalization is the process of removing all physical dimensions from an equation of motion, and in turn to identify a set of non-dimensional numbers that characterize a particular flow regime. xii

non-divergent flow Non-divergent flow is defined by $\nabla \cdot \mathbf{v} = 0$. This flow is realized by the Boussinesq ocean, which is the most general case of non-divergent flow. It is also realized by flow within a fluid of constant density. In two-dimensions, we consider the mechanics of horizontally non-divergent barotropic flow, whereby $\nabla \mathbf{u} = 0$. 139

non-hydrostatic primitive equations The non-hydrostatic primitive equations refer to the equations of motion for a fluid on a rotating planet that do *not* make the hydrostatic approximation for the vertical motion, and which time step velocity. These equations are suited for describing strong vertical motions, such as when studying clouds in the atmosphere and fine-scale mixing in the ocean. 355

non-inertial acceleration An accelerating reference frame is not an inertial frame. A non-inertial acceleration arises from describing motion within the non-inertial frame. The planetary Coriolis and planetary centrifugal accelerations are the canonical example non-inertial accelerations that arise in geophysical fluid mechanics. 491

non-materially conservative property Some fluid properties, such as the total energy, satisfy flux-form conservation laws, and so are globally conserved, and yet they are non-material. By non-material we mean that the total energy of two fluid elements, which added together, is not necessarily equal to the sum of the individual energies. For the case of total energy, it is the presence of pressure work that breaks the material nature of the property. To be materially conservative, a property must have its flux convergence vanish in the absence of mixing processes that are local in space and time. 341

normal stress Normal stresses act on a surface in a direction parallel to the surface normal direction. The normal stress can be compressive (positive stress) or tensile (negative stress). For our study of fluids, mechanical pressure is the negative of the mean normal stress and it is isotropic. The stress tensor organizes normal stresses and tangential stresses acting within a fluid, with normal stresses living along the diagonal to the stress tensor. Perfect fluids can only support normal stresses, whereas real fluids also have tangential stresses arising from viscosity in the presence of shearing strains. The ability of a fluid to resist compression is a function of the fluid's compressibility. 2, 263, 277

oceanic form stress Oceanic form stress is the contribution from ocean pressure acting to produce a horizontal atmospheric acceleration and that acts at the interface between the ocean and atmosphere. This form stress is equal in magnitude to the atmospheric form stress, but it is oppositely directed. 264, 382, 386

Onsager reciprocity conditions The Onsager reciprocity condition is a principle from nonequilibrium thermodynamics stating that, for systems close to thermodynamic equilibrium, the matrix of linear transport coefficients is symmetric (in the absence of magnetic fields). We make use of this condition to derive expressions for the molecular fluxes of temperature and matter in an ocean through use of the second law of thermodynamics. 333

outcrop An outcrop is the location at the ocean surface where a water property surface (e.g., an isopycnal, isotherm) meets at the surface. [448](#)

parcel A fluid parcel refers to an infinitesimal deformable region of a perfect fluid that maintain a fixed matter content and fixed thermodynamic properties, so that it has fixed mass and fixed enthalpy. [116](#)

parcel instabilities Parcel instabilities are afforded a local necessary and sufficient condition to determine whether the fluid base state is unstable to perturbations. Gravitational instability provides the canonical example, along with centrifugal and symmetric instabilities. Parcel instabilities are also referred to as local instabilities. [xxi](#)

Pascal's law Pascal's law says that pressure in a hydrostatic fluid is an isotropic force per area. [276](#)

passive tracer A passive tracer is a scalar field that satisfies the tracer equation, but it has zero impact on the velocity and is thus dynamically passive. Hence, a passive tracer provides a means to probe the advective-diffusive features of the flow without modifying it. [120](#)

pathlines A pathline, also known as a fluid particle trajectory, is a curve in space that is traced out by a fluid particle as time moves forward. We are only concerned with smooth velocity fields, which allow for an unambiguous specification of the pathline (trajectory) at each point of the fluid. Pathlines/trajectories are tangent to the velocity field at each point. Within the continuum approximation, there is a pathline/trajectory that passes through each point of space at each time instance. [37](#)

perfect fluid A fluid that flows in the absence of irreversible processes so that the motion is reversible and the specific entropy remains constant following a fluid particle. A perfect fluid is a continuum of infinitesimal material fluid parcels. Some authors use the term *ideal fluid*, but we eschew that term to avoid confusion with *ideal gas*. [vii](#), [168](#)

planetary Cartesian coordinates Planetary Cartesian coordinates are Cartesian coordinates with their origin at the planet center and that rotate with the planet. [235](#)

planetary geostrophy Planetary geostrophy refers to a set of equations based on assuming the Rossby number is small, thus reducing the velocity equation to the diagnostic frictional geostrophic balance along with boundary forcing from winds and bottom drag. Planetary geostrophy is commonly used to study the large-scale laminar ocean circulation. [510](#)

planetary vorticity Planetary vorticity refers to the vorticity imparted to every fluid due to its existence in a rotating planetary reference frame. [xix](#), [515](#)

Poisson's equation Poisson's equation, $\nabla^2 \Psi = \sigma$, is a linear elliptic partial differential equation where the Laplacian of a scalar function, Ψ , equals to a source term, σ . This equation arises in many contexts within geophysical fluid mechanics. [251](#), [422](#)

postulate of equal *a priori* probabilities An isolated physical system in thermodynamic equilibrium is equally likely to be in any of its accessible microstates. This statement is known as the postulate of equal *a priori* probabilities. It follows that if an isolated physical system is not equally likely to be found in any of its accessible microstates, then this system cannot be in thermodynamic equilibrium. Rather, it will spontaneously evolve

towards thermodynamic equilibrium. The second law of thermodynamics states that entropy increases during this evolution, thus providing an arrow for time. 347

potential density Potential density is the density of a fluid element moved to a reference pressure, p_R , while maintaining fixed specific entropy and fixed tracer concentration. For seawater, this movement is equivalent to fixed Conservative Temperature and fixed salinity, so that $\varrho(S, \Theta) = \rho(S, \Theta, p_R)$. 469

potential energy Potential energy of a fluid is a dynamical property arising from the presence of the fluid element within the gravitational field of the planet plus the centrifugal potential of the rotating planetary reference frame. It is sometimes referred to as the potential energy from the effective gravitational acceleration, or equivalently from the geopotential. The potential energy for a fluid element of mass $\rho \delta V$ is given by $\Phi \rho \delta V$, where Φ is the geopotential. 307

potential enthalpy Potential enthalpy is the enthalpy of a fluid element moved to a reference pressure, p_R , while maintaining fixed specific entropy and fixed tracer concentration: $\mathcal{H}^{\text{pot}}(S, C) = \mathcal{H}(S, p_R, C)$. It is used to define the Conservative Temperature, $c_p^{\text{ref}} \Theta \equiv \mathcal{H}^{\text{pot}}(S, C) = \mathcal{H}(S, p_R, C)$. 337

potential property A thermodynamic property that remains constant when a fluid element is moved from one pressure to another, without the transfer of heat or matter and without any kinetic energy dissipation, is said to be a potential property. Any material tracer, such as salinity, serves as a potential property. Conservative Temperature provides a very accurate potential property that directly measures the potential enthalpy of a fluid element. 217, 467

potential temperature Potential temperature, θ , is the temperature that a fluid element reaches after performing an adiabatic and constant concentration translation to a standard pressure. For the ocean and atmosphere, the standard pressure is generally taken as the standard surface pressure. 214, 216, 217, 319, 468

potential vorticity Potential vorticity is a strategically chosen component of the vorticity vector that melds mechanics (vorticity) to thermodynamics (stratification). Material conservation properties of potential vorticity render important constraints on fluid motion, thus promoting it as a primary field in the study of geophysical fluid mechanics. xix

pressure Mechanical pressure is the negative of the mean normal stress and it is isotropic. Thermodynamic pressure is that pressure is a macroscopic property that appears in the laws of thermodynamics. In our study of fluid mechanics, mechanical pressure and thermodynamic pressure are the same. 237

pressure driven velocity In the context of large-scale geophysical fluid mechanics, the pressure driven velocity is a velocity is another name for the geostrophic flow, where $f \rho \hat{z} \times \mathbf{u}_g = -\nabla_h p$. 549

pressure potential A barotropic fluid has $p = p(\rho)$, so that baroclinicity vanishes, $\mathbf{B} = -\nabla(\rho^{-1} \nabla p) = 0$. Hence, we can introduce the pressure potential, Φ_p , whereby $\nabla \Phi_p = \rho^{-1} \nabla p$. 251

pressure work The pressure work is the mechanical work done to a physical system through the effects from pressure acting to change the volume of the system. For an infinitesimal and quasi-static amount of pressure work, we have $dW = -p dV$, with dW the inexact differential amount of work, p the pressure (an intensive property), and dV the exact differential for the change in volume (an extensive property). The negative sign arises since the compression of a physical system into a smaller volume, $dV < 0$, requires positive mechanical work be applied to the system, $dW > 0$. 175

principle of equivalence The principle of equivalence states that the same mass, m , determines the gravitational force as well as any kinematic forces arising from acceleration. That is, in an inertial reference frame, $m\mathbf{g}$ is the gravitational force, and $m\ddot{\mathbf{X}}$ is the inertial force, with Newton's law yielding $\ddot{\mathbf{X}} = \mathbf{g}$. The principle of equivalence originates from the work of Galileo and it forms a key element to Einstein's relativity theory. 414, 433, 491

process In thermodynamics, when a constraint is removed, the physical system moves through a sequence of macrostates as it evolves towards its new equilibrium, with the time evolution through such macrostates referred to as a process. 166

prognostic equation A prognostic equation determines the time tendency (Eulerian evolution) of a quantity such as the temperature or velocity. Terms in the prognostic equation are referred to as time tendencies. A prognostic equation is also referred to as an evolution equation. x, xi, 30

quasi-equilibrium thermodynamics The application of equilibrium thermodynamic relations to a moving fluid that is globally out of equilibrium but is locally, at the level of infinitesimal fluid elements, in local thermodynamic equilibrium. 316

quasi-geostrophy Quasi-geostrophy refers to the theory whereby the horizontal geostrophic flow is evolved via the leading order effects from the ageostrophic flow. Quasi-geostrophy is formulated in terms of the quasi-geostrophic potential vorticity, from which the flow, pressure, and buoyancy can be diagnosed. The equations are formulated by taking an asymptotic expansion of the β -plane Boussinesq ocean equations with a small Rossby number and a large Richardson number. 525

quasi-static process Like a reversible process, a *quasi-static process* moves continuously between thermodynamic equilibrium states, so it traces out a path in thermodynamic configuration space. However, a quasi-static process can be either reversible or irreversible. If a quasi-static process is irreversible, then its path in thermodynamic configuration space is in a direction that increases the net entropy of the system plus environment, whereas if it is reversible then the path leaves the net entropy unchanged. In this manner, all reversible processes are quasi-static, and yet some quasi-static processes are irreversible. For moving fluids, we make the local thermodynamic equilibrium hypothesis, which means that macroscopic motion is very slow relative to the microscopic equilibration time inside each fluid element. In this manner, there can still be macroscopic motion even while each fluid element is assumed to be locally in thermodynamic equilibrium. 167, 170, 175, 314

quotient rule If the contraction of two objects yields a tensor, and if one of these objects is a tensor, then so too is the other. This quotient rule allows us to deduce the tensorial nature of an object based on whether that object is constructed from tensors. 269

Rayleigh drag Rayleigh drag is a particular form of friction that makes use of the acceleration, $-\gamma \mathbf{v}$, with γ^{-1} having dimensions of time. Rayleigh drag adds an acceleration that drags all flow towards a state of rest. Notably, Rayleigh drag has zero scale selectivity, which contrasts to Laplacian friction suggested by kinetic theory, whereby friction acts preferentially at the small scales. 278, 551

Rayleigh–Taylor instability A Rayleigh–Taylor occurs at the interface between two fluids of different densities when the lighter fluid pushes against the overlying heavier one in a gravitational field. This configuration is gravitationally unstable and leads to complex interpenetration of the fluids that is typically seen as spikes of heavy fluid descending and bubbles of light fluid rising. The Rayleigh-Taylor instability is partially stabilized in the presence of surface tension. 292

real fluid A fluid whose flow is affected by irreversible processes arising from momentum mixing (nonzero viscous friction); enthalpy mixing (nonzero diffusivity for temperature); matter mixing (nonzero diffusivity of matter constituents); and through sources such as radiation and chemical reactions. The specific entropy increases following a fluid particle moving in a real fluid. vii

reference manifold Same as base manifold. 51

response functions Response functions measure the change in a thermodynamic property as the system is forced in some manner. The heat capacity, thermal expansion coefficient, and haline contraction coefficient, are three response functions commonly encountered in ocean and atmospheric fluid mechanics. 195

reversible process A thermodynamically reversible process can traverse a path through thermodynamic configuraton space in either direction. It follows that a reversible process continuously moves between thermodynamic equilibria, which in turn means that a reversible process traces out a continuous path through thermodynamic configuration space. The net entropy of a physical system plus its surrounding environment remains unchanged by reversible processes, whereas irreversible processes are characterized by an increase in the net entropy. 170, 179

Reynolds number The Reynolds number is a non-dimensional number that measures the ratio of inertial acceleration to viscous acceleration: $Re = U L / \nu$, where U is a typical velocity scale, L a length scale, and ν the kinematic viscosity. 242, 285

Reynolds stress tensor The turbulent contribution to the kinetic stress tensor is known as the Reynolds stress tensor. 239

Reynolds transport theorem The Reynolds transport theorem is the Leibniz-Reynolds trans- port theorem applied to a Lagrangian region. 129, 241

Richardson number The Richardson number is the non-dimensional ratio of the vertical stratification to the vertical shear of the horizontal flow. The Richardson number appears throughout our study of stratified geophysical fluid flows. 419

rigid lid approximation The rigid lid approximation is a boundary condition that assumes vertical fluid velocity vanishes at the top boundary of the fluid column. It is commonly used for studies of the large-scale ocean circulation. 515

rigid-body motion Rigid body motion refers to the motion of a fluid in a manner where all fluid particles have a fixed relative position. Rigid-body motion of a fluid means that the fluid velocity vanishes in the rotating reference frame. All strains vanish for a fluid in rigid body motion, so that frictional stresses also vanish. 373, 374

Rossby effect The Rossby effect is a northward drift of vortices found in a rotating reference frame. 258

Rossby number The Rossby number is the non-dimensional ratio of the horizontal material acceleration (acceleration of a fluid particle) to the Coriolis acceleration. Geostrophic flows in the ocean and atmosphere are characterized by Rossby numbers much smaller than unity. The Rossby number offers a measure of the departure of the flow from solid body rotation, as determined by the radial component of the vorticity. 505

Rossby waves Rossby waves are dispersive waves that arise in a rotating reference frame with differential rotation, as for a rotating planet or the β -plane. They are typically studied via the quasi-geostrophic equations, and are sometimes referred to as vorticity waves. Also, long Rossby waves are supported by planetary geostrophic flows, which are Rossby waves in the limit where the horizontal wavenumber vanishes. Rossby waves play an important role in large-scale geophysical flows. 248

rotation tensor The rotation tensor is the anti-symmetric portion of the velocity gradient tensor, with elements given by twice the vorticity, $\mathbb{R}^{mn} = -\epsilon^{mnp} \omega_p/2$ with $\omega = \nabla \times \mathbf{v}$ the vorticity. The rotation tensor measures the ability of fluid flow to rotate without dilating fluid elements. 47, 73, 278, 282, 310, 424

scale height The scale height determines the e-folding height for pressure in the atmosphere or ocean. 225, 407

sea level pressure The sea level pressure is the atmospheric pressure at the level of the sea surface. 382

seawater chemical potential The seawater chemical potential, μ , is given by the difference in chemical potential for salt and freshwater, $\mu = \mu^{\text{salt}} - \mu^{\text{water}}$. 189

second kinematic viscosity For a constitutive relation of the form $\mathbb{T}^{mn} = \rho(2\nu S^{mn} + \lambda \nabla \cdot \mathbf{v} \delta^{mn})$, λ is the second kinematic viscosity (dimensions of squared length per time). 279

second law of thermodynamics The two postulates concerning entropy: entropy is maximized in thermodynamic equilibrium, and entropy is a non-decreasing function for thermodynamic processes, constitute the second law of thermodynamics. Statistical mechanics reveals the statistical nature of entropy and the second law. 123, 170, 172, 179, 329, 332, 335, 347

shallow fluid approximation The shallow fluid approximation is based on noting that for large-scale fluid mechanics of the atmosphere and ocean, the thickness of fluid is tiny relative to the radius of the planet. Hence, we write the radial coordinate equal to the earth's radius, $r = R_e + z \approx R_e$, where r appears as a multiplier (or divisor), but not as a derivative operator. The shallow fluid approximation is distinct from the shallow water approximation. 251, 351, 354

shallow water approximation The shallow water approximation assumes fluid to be vertically partitioned into homogeneous layers (with constant density), and with the pressure to be hydrostatic. As a result, fluid motion is comprised of vertically coherent columns moving within each layer, with the columns able to expand or contract according to horizontal flow convergence within each layer. 351

shear stresses The shear stress (also the tangential stress) is a stress acting within the plane of a surface, arising from shears. The stress tensor organizes normal stresses and shearing/-tangential stresses acting within a fluid, with shear stresses comprising the off-diagonal elements. 263, 277

simple ideal gas A simple ideal gas is an ideal gas in which the internal energy is a linear function of temperature, so that the heat capacities are constants. 220

singular limit A singular limit is a mathematical expression for a situation where a small parameter, if set to zero, eliminates the highest derivative operator from a differential equation. The common example for fluid mechanics is when the viscosity is set identically to zero, in which case the Laplacian friction operator is removed from the equations of motion, thus altering the boundary conditions that the flow satisfies. A singular limit fundamentally changes the structure of the solution. Namely, a flow with a positive viscosity, no matter how small but nonzero, supports boundary layer flows, whereas a zero viscosity perfect fluid flow has no boundary layer. 556

slippery Ekman layer The slippery Ekman layer is an informal name for the arrested Ekman layer, which is a bottom boundary layer in which the cross-isobath Ekman transport driven by bottom stress is suppressed by a compensating barotropic pressure gradient, so that the boundary layer no longer exhibits the spiraling transport divergence but instead is halted or arrested in a nearly along isobath, nondivergent state. Arrested Ekman layers are informally referred to as slippery Ekman layers since the frictional stress vanishes. 569

Soret effect The Soret effect is the diffusion of matter due to a temperature gradient. 333, 335

spatial manifold In continuum kinematics, as time progresses, the motion field smoothly and invertibly maps each point of the base manifold, \mathcal{B} , to a deformed state of the matter continuum. A point in the deformed state is described by a point in the spatial manifold, \mathcal{S} . 51, 93

specific gas constant The specific gas constant, R^M , equals to the universal gas constant divided by the mass per mole of the particular gas, $R^M = R^g/M^{\text{mole}}$. 221

specific volume The specific volume is the inverse of the mass density, $\nu_s = 1/\rho$, so that it measures the volume per mass. 188

splat Splat is given by the doubly-contracted strain rate tensor, \mathbf{S} : $\mathbf{S} = S^{mn} S_{mn} \geq 0$. This term appears as part of the source term for pressure in non-divergent flows. It is so-named since it is large when a fluid element is squashed in a manner increasing fluid strains, akin to how strains appear when a fluid impacts or “splats” against a solid obstacle. Imagine a water balloon thrown against a wall. 424

stagnation pressure The stagnation pressure, $p + \rho v^2/2$, is the mechanical pressure required to keep the local acceleration unchanged if the dynamic pressure is set to zero as per a stagnant fluid. This situation arises in practice in a device known as a Pitot tube used to measure the speed of flow in a pipe, with the Pitot tube making use of Bernoulli's theorem. The stagnation pressure is also referred to as the total pressure. 245, 325

state function A state function is a macroscopic property of the thermodynamic state of a system and not a function of the path history taken to reach that state. A state functions is also know as a thermodynamic potential. Internal energy, entropy, and enthalpy are three common state functions. 173, 189

static equilibrium sea level The static equilibrium sea level is the sea level that an ocean would take if the ocean was static, and so it formed a geopotential surface. The static equilibrium sea level is affected by mass distribution on the planet, which in turn affects the earth's gravitational field, its rotational moment of inertia, and the deformation of the crust (GRD, as in *Gregory et al. (2019)*). 376, 377

static forces In the context of buoyancy, we refer to static forces as those vertical forces acting on a fluid element that remain after setting to zero all velocity dependent accelerations. 461, 463, 493

static instability A static instability is a function of the static properties of the fluid, rather than properties of the flow. Gravitational instability is the common form of static instability considered in geophysical fluid mechanics. 477

static pressure In the analysis of flow, we often find it useful to decompose the pressure into a background static pressure field that is hydrostatic and just a function of z , plus a deviation from the background pressure. The static hydrostatic pressure only plays a role in supporting a constant background density field, and so it is dynamically irrelevant. 358

steady state For a steady state, the Eulerian time derivative vanishes for all fields, so that all fluid properties are time independent when measured in the laboratory frame. 30, 124, 167

steric sea level The steric sea level is the thickness of a fluid layer bounded below by an isobar and above by the sea surface. It is commonly used for ocean circulation studies to map geostrophic flows. The dynamic topography is also referred to as the ocean dynamic topography. 359

steric setup A steric setup refers to sea level rise near the coast that arises from the generally lower density near the coast. 368, 369

Stokes' theorem The vector calculus form of Stokes' theorem says that for a simply connected surface, $\oint_{\partial\Omega} \mathbf{A} \cdot d\mathbf{x} = \int_{\Omega} (\nabla \times \mathbf{A}) \cdot \hat{\mathbf{n}} d\mathcal{S}$, where \mathbf{A} is a vector, Ω is a simply connected surface with boundary $\partial\Omega$, $d\mathbf{x}$ is a line increment around the boundary, and $\hat{\mathbf{n}}$ is an outward normal to the surface and which defines the orientation. 146, 481

strain rate tensor The strain rate tensor, \mathbf{S} , is the symmetric portion of the velocity gradient tensor. The strain rate tensor measures the ability of fluid flow to deform fluid elements through stretching, straining, and dilation. 47, 278, 308, 424

streaklines A streakline is a curve obtained by connecting the positions for all fluid particles that emanate from a fixed point in space. We generally have no use for streaklines in our studies of geophysical flows, though they are often useful in laboratory experiments. 37, 39

streamfunction In two-dimensional non-divergent flow, we can define a streamfunction, whose curl yields the velocity field at each time instance. Consequently, isolines of the streamfunction are streamlines. The streamfunction is arbitrary up to a constant, thus representing a simple form of gauge symmetry. In three-dimensional non-divergent flow we can introduce a vector streamfunction, whose curl yields the velocity field. The vector streamfunction is arbitrary up to the gradient of a scalar field, which represents a form of gauge symmetry. 142, 398

streamlines A streamline is a curve in space that is tangent, at each time instance, to the fluid particle velocity. Streamlines and pathlines are identical only for steady flows, whereas they are generally distinct for unsteady flows. 37, 38

streamtube A streamtube is a bundle of streamlines crossing through an arbitrary closed curve. At each time instance, the flow velocity is tangent to the streamtube sides. Furthermore, when the flow is steady then streamlines are identical to material particle pathlines. Hence, a streamtube is a material tube for steady flow, in which case no fluid particles cross the streamtube boundary. 39

stress tensor The stress tensor is a second order tensor that organizes the stresses acting within a fluid. The stress tensor components have dimension of force per unit area, and each component is oriented by both the direction of the stress and the outward normal of the surface on which the stress acts. 237, 263, 268

strong formulation The strong formulation of the equations of fluid mechanics are given by partial differential equations, which assume smooth and continuous fields throughout the fluid domain. We always assume smooth and continuous fields, so that the strong and weak formulation are equivalent and connected via the Leibniz-Reynolds transport theorem. 131, 236, 272

subgrid scale Subgrid scale (SGS) refers to processes happening at scales smaller than the grid (length) scale of either a numerical model or field measurement. The parameterization of subgrid scale process remains an active area of ocean and atmospheric physics, given the importance of such processes for the large scale circulation. 434, 512

surface tension Surface tension is a stress that acts on the boundaries of a fluid media, such as the boundary between air and water. Surface tension does not satisfy Newton's third law. Surface tension arises from the anisotropic forces acting on molecules that are within a mean free path distance from the surface between two immiscible liquids, between a liquid and gas, or between a fluid and a solid. Energetically, surface tension arises since molecules have a preference for locations within the bulk of the fluid (surrounded by identical neighbors) rather than at the boundary (where it encounters fewer identical neighbors). Surface tension acts to resist forces that act to increase the surface area. The magnitude of the tensile force per unit length (or energy per unit area) is the surface tension, γ (SI units $N\ m^{-1} = kg\ s^{-2}$), which measures the force needed to change the interface a unit length. 263, 264, 291, 293

Sverdrup balance The Sverdrup balance is a diagnostic balance between vertically integrated meridional transport and the wind stress curl. In particular, a positive wind stress curl leads to northward vertically integrated flow. This balance helps to explain the steady equatorward ocean circulation appearing in the eastern portion of middle latitude gyres. xi, 515, 562

tangent plane The tangent plane makes use of Cartesian coordinates defined local to a point on the rotating planet. The f -plane and β -plane are the two common forms of the tangent plane approximation encountered in this book. It is important to note that the tangent plane approximation is not based on assuming a locally flat sphere. Rather, the tangent plane approximation as based on assuming a locally flat geopotential. 246, 249, 489, 531

tangent plane Cartesian coordinates Tangent plane Cartesian coordinates are Cartesian coordinates defined local to a point on the rotating planet, with the approximation based on assuming a locally flat geopotential. The f -plane and β -plane are the two forms of the tangent plane approximation encountered in this book. It is important to note that the tangent plane approximation is not based on assuming a locally flat sphere. Rather, the tangent plane approximation as based on assuming a locally flat geopotential. Consequently, the approximation makes use of the effective gravitational acceleration (minus the gradient of the geopotential) that includes both central gravity acceleration plus the planetary centrifugal acceleration. 235

tangential stress The tangential stress (also the shearing stress) is a stress acting within the plane of a surface, arising from shears and strains. The stress tensor organizes normal stresses and shearing/tangential stresses acting within a fluid. 263

Taylor column A Taylor column refers to a vertical column of fluid that is stiffened due to the effects of the rotating planet. Taylor columns are aligned with the axis of rotation, which for a spherical planet means they are aligned with the polar axis. 513

Taylor curtains One means to test Taylor-Proudman is to insert a dye into a rapidly rotating tank of unstratified water. After a few rotation periods the dye forms vertical sheets known as Taylor curtains whose center is along the rotation axis. The fluid is said to have a vertical stiffness due to the effects of rotation. Vertical stiffening in turn means that flow over a small obstacle is deflected throughout the column rather than just near the bump. 514

Taylor-Proudman effect The Taylor-Proudman effect refers to the vertical stiffening of fluid columns that appears in an unstratified, homogeneous, inviscid fluid in geostrophic balance. 513, 514, 562

tensor product A tensor product between two tensors produces a third tensor whose order is the sum of the terms. For example, the tensor product of two $(1, 0)$ vectors produces a $(2, 0)$ tensor, such as the second order kinetic stress tensor, $\mathbb{T}^{\text{kinetic}} = -\rho \mathbf{v} \otimes \mathbf{v}$. In components, we have $(\mathbf{v} \otimes \mathbf{v})^{ab} = v^a v^b$. The tensor product is an expression for tensors of the outer product from linear algebra. 392

test fluid element A test fluid element is a fluid element that has no effect on the surrounding fluid environment. It is used as a conceptual probe of real fluids much like the fluid particle. Yet unlike a fluid particle, the test fluid element has nonzero spatial extent

and it can exchange matter and energy with its surrounding environment. The test fluid element is of particular use when studying buoyancy. 23, 461, 467, 471, 489

thermal energy Kinetic theory applied to a simple ideal gas suggests that we conceive of internal energy as thermal energy. That is, we idealize molecules as point masses whose kinetic energy is directly related to temperature, and with the internal energy of an ideal gas directly proportional to temperature. However, for a general fluid, particularly for liquids, the internal energy is more than a measure of the kinetic energy of molecules, as real molecules exhibit intermolecular potential energy arising from molecular interactions. 171

thermal expansion coefficient The thermal expansion coefficient is a response function that measures minus the relative change in density as the temperature is altered while holding the pressure and matter concentration fixed. It is typically positive, so that density decreases as temperature increases. Freshwater near its freezing point is an important counterexample, where the negative thermal expansion coefficient allows for solid ice to float on liquid water. 195

thermal wind balance Thermal wind balance refers to diagnostic balance between the vertical shear in the horizontal geostrophic flows and horizontal gradient in the density field. 503, 510, 516

thermodynamic configuration space A thermodynamic system is specified by a suite of continuous thermodynamic properties. In this manner, we conceive of thermodynamic properties as defining coordinates for a point within thermodynamic configuration space, also referred to as thermodynamic state space. Each point in thermodynamic configuration space represents a particular thermodynamic equilibrium state. A continuous connection between two points in thermodynamic configuration space is afforded by the locus of infinitesimal quasi-static processes. Mathematically, thermodynamic configuration space is a differential manifold defined by the suite of macroscopic thermodynamic properties used to define the thermodynamic configuration. 169

thermodynamic equilibrium In our study of equilibrium thermodynamics, we are concerned with macroscopic fluid systems whose evolution tends toward states whose properties are determined by intrinsic factors rather than depending on memory of previous external influences. These particular macrostates are known as thermodynamic equilibria. At a basic level, a system in thermodynamic equilibrium could remain in that state for all time, with details of the equilibrium dependent on the constraints imposed on the system. When constraints are removed, then a system generally transitions to another thermodynamic equilibria. Note that “for all time” is a loaded term. More precisely, we mean “for a time extremely long compared to any time scale relevant to the physical system under consideration”. 166, 167, 171, 213, 347

thermodynamic potential A thermodynamic potential is a macroscopic property of the thermodynamic state of a system and not a function of the path history taken to reach that state. A thermodynamic potential is also known as a state function. Internal energy, entropy, and enthalpy are three common thermodynamic potentials. 189

thermodynamic pressure Thermodynamic pressure is the pressure that appears in the equations of equilibrium thermodynamics. In this book, the thermodynamic pressure equals to the

mechanical pressure, where the mechanical pressure appears along the diagonal of the stress tensor. 276, 409

thermodynamic state A thermodynamic state is the same as a macrostate. Namely, a physical system that is specified by a few macroscopic properties such as temperature, pressure, and tracer concentration. 162

thermodynamic temperature For each thermodynamic equilibrium there exists a scalar intensive property, called the thermodynamic temperature, or more briefly the temperature, that is uniquely defined. Furthermore, the temperature has the same value for two systems (absent external force fields) in thermodynamic equilibrium with one another. 171, 176

thermodynamics Thermodynamics is a phenomenological discipline focused on relations between macroscopic properties of physical systems, in particular how those properties change as the system transitions from one state to another. Thermodynamics is a necessary ingredient for understanding the stability, evolution, and transformation of macroscopic systems, with such topics at the heart of geophysical fluid mechanics. 162

thermohaline effects Thermohaline refers to the effects on density from temperature and salinity. Changes to ocean density due to changes in temperature and salinity play a lead role in large-scale ocean circulation through the accompanying effects on pressure. 407, 409, 416

time tendency Those terms in a prognostic Eulerian equation that contribute to the time evolution are referred to as time tendencies. For prognostic equations, knowledge of the processes contributing to the net time tendency enables a prediction of flow properties. x

topographic form stress Topographic form stress is the contribution from pressure acting to produce a horizontal acceleration and that acts at the interface between a fluid and solid-earth topography. Topographic form stress plays an important role in the force balance of flows next to sloping solid earth boundaries, such as in the Southern Ocean and western boundaries. 264, 383, 386

total energy Total energy for a classical fluid is the sum of the internal energy arising from microscopic degrees of freedom plus the mechanical energy of macroscopic degrees of freedom (kinetic plus potential). In developing the energetics of fluids, we postulate that the total energy is conserved for a mechanically, thermally, and materially closed physical system, with this postulate known as the first law of thermodynamics. 171, 173, 320

total pressure The total pressure, $p + \rho v^2/2$, is the mechanical pressure required to keep the local acceleration unchanged if the dynamic pressure is set to zero as per a stagnant fluid. This situation arises in practice in a device known as a *Pitot tube* used to measure the speed of flow in a pipe, with the Pitot tube making use of Bernoulli's theorem. The total pressure is also referred to as the stagnation pressure. 325

tracer equation The tracer equation is a partial differential equation describing the evolution of tracer fields, such as material tracers and thermodynamic tracers (potential enthalpy). Tracers are intensive scalar fluid properties that evolve through advection (in an Eulerian description), diffusion, and source/sinks. 115, 116

tracers Tracers refer to the general class of scalar fields that evolve via advection, diffusion, and source/sinks. Examples include the material tracers, salinity and humidity, and the

thermodynamic tracer potential enthalpy (Conservative Temperature). In the absence of source/sink terms, we say the tracer is conservative since its evolution depends only on the convergence of fluxes. 115

traction Traction is another name for contact force, with this term used in the continuum mechanics literature. Namely, with \mathbf{T} the stress tensor, the traction is the vector given by $\hat{\mathbf{n}} \cdot \mathbf{T}$, where $\hat{\mathbf{n}}$ is a normal direction. 237

traditional approximation The traditional approximation comprises three approximations that come as a package in order to maintain physical consistency. (A) It sets to zero the Coriolis terms in the horizontal momentum equations that involve the vertical velocity, thus retaining only the local vertical component of the earth's angular rotation vector. (B) It drops the metric terms, uw/r and vw/r , associated with the vertical velocity as they appear in the horizontal momentum equations. (C) The shallow fluid approximation and both parts of the traditional approximation must be taken together in order to maintain a consistent energy and angular momentum conservation principle for the resulting equations. 248, 249, 351, 489

transformation matrix The transformation matrix is the matrix of partial derivatives that provides the operational means to transform tensor components between one set of coordinates and another. For the coordinate transformation to be invertible, the Jacobian of the transformation matrix (i.e., its determinant) must never vanish. Although the transformation matrix carries two indices, it is not a tensor. Instead, it is a matrix operator used to transform from one set of basis vectors to another. 31, 55

transport A flux of a physical quantity is a vector that measures the amount of that quantity traversing a unit area element perpendicular to the flux direction in unit time. The transport is also a vector and it results from multiplying the flux by the area element perpendicular to the flux direction. So whereas the dimensions of a flux are physical quantity per area per time, the dimensions of transport are physical quantity per time. For example, the mass flux has dimensions $M L^{-2} T^{-1}$, whereas the mass transport has dimensions $M L^{-2}$. 88, 89

turbulence closure When we measure fluid motions in the laboratory or field, we generally do not measure the motions at scales on the order of $L_{macro} \approx 10^{-4}$ m. That is, our measurement devices generally have a spatial resolution coarser than L_{macro} , so that $L_{measure} \gg L_{macro}$. Likewise, numerical simulations are generally designed using discrete grids with length scales $L_{numerical} \gg L_{macro}$. The equations describing motions at the measurement/simulation length scales involve effects from fluctuations occurring at the smaller (unmeasured) scales. The reason for this coupling is that the fluid equations are nonlinear, and with the nonlinearities leading to an interaction across spatial scales. These fluctuations, generally associated with turbulent or chaotic motions, have statistical correlations that can play a role, sometimes a dominant role, in the evolution of flow features at the measured/simulated scales. The parameterization of these correlations in terms of measured/simulated motions constitutes the turbulence closure problem. 6

turbulent diffusion Diffusion is the physical process by which a field, such as a tracer, spreads in space over time due to random motion. Turbulent diffusion arises from random motion within a turbulent flow. The net flux moves from regions of higher concentration to regions of lower. The efficiency for diffusive transport in a turbulent fluid is many orders higher

than that from molecular diffusion. Chapter 13 in [Vallis \(2017\)](#) provides a pedagogical discussion of turbulent diffusion in geophysical flows. [214](#)

ultraviolet catastrophe Ultraviolet catastrophe refers to the unbounded pile up of mechanical energy at the smallest scales (highest wavenumbers), which occurs for inviscid fluids in the presence of a turbulent cascade. Viscosity removes the ultraviolet catastrophe from fluid motion, thus allowing for a turbulent equilibrium to be established in which forcing at the large scales is balanced by dissipation at the small scales. The name refers to the violet part of the visible electromagnetic spectrum, which has a higher wavenumber than the infrared part of the spectrum. [286](#)

universal gas constant The universal gas constant, R^g , has value $R^g = 8.314 \text{ J mole}^{-1} \text{ K}^{-1}$, and it appears in many thermodynamic expressions, such as the ideal gas law, $pV = n^{\text{mole}} R^g T$. It commonly appears divided by the molar mass of a gas, in which case we make use of the specific gas constant, $R^M = R^g/M\text{mole}$. [221](#), [222](#)

vector invariant The vector-invariant form of the velocity equation is based on replacing the material time derivative with the vorticity and kinetic energy, through use of the identity $(\mathbf{v} \cdot \nabla) \mathbf{v} = \boldsymbol{\omega} \times \mathbf{v} + \nabla(\mathbf{v} \cdot \mathbf{v})/2$, where $\boldsymbol{\omega} = \nabla \times \mathbf{v}$. [244](#), [245](#), [546](#)

velocity gradient tensor The velocity gradient tensor, \mathbf{G} , is the Eulerian means to quantify flow deformation. Its elements are the spatial derivatives of the velocity field. It is commonly decomposed into the symmetric strain rate tensor (also known as the deformation rate tensor) plus the anti-symmetric rotation tensor. [47](#), [71](#), [424](#)

velocity potential For irrotational horizontal flow, $\nabla \times \mathbf{u} = 0$, the velocity can be written as $\mathbf{u} = \nabla_h \phi$, where ϕ is the velocity potential. [144](#)

vertical stiffness Vertical stiffness of a fluid column results from the effects of the rotating reference frame, with the rotational axis aligning the fluid into Taylor columns. Vertical stiffening is synonymous with the Taylor-Proudman effect. [514](#)

vorticity Vorticity is the curl of the velocity, $\boldsymbol{\omega} = \nabla \times \mathbf{v}$. It plays a leading role in the study of geophysical fluid flows, where it is important to distinguish the relative vorticity, $\boldsymbol{\omega} = \nabla \times \mathbf{v}$, from the planetary vorticity, 2Ω . [xix](#), [325](#)

vorticity based viewpoint A variety of vorticity constraints offer the means to deduce flow properties without determining forces, thus prompting the **vorticity based viewpoint** that is distinct from the momentum-based approach, thus prompting the importance of vortex mechanics in geophysical fluid mechanics. [x](#), [618](#)

wave instabilities Wave instabilities arise from the constructive interference of waves and so involve the solution of an eigenvalue problem to determine properties of unstable waves. At most, a necessary condition can be derived to determine whether a wave instability exists. Wave instabilities are also referred to as global instabilities. [xxi](#)

weak formulation The weak formulation of the equations of fluid mechanics are given by integral differential equations, which can, under some circumstances, handle discontinuities in the flow fields. We always assume smooth and continuous fields, so that the strong and weak

formulation are equivalent and connected via the Leibniz-Reynolds transport theorem.
131, 235, 236, 272, 299

wind-driven The wind-driven ocean circulation refers to that part of the circulation primarily driven by the mechanical wind stresses. We are unable to fully decompose the circulation into wind-driven and thermohaline driven portions. Even so, for idealized theoretical studies one can focus on one part of the circulation or the other, with the theory of wind-driven circulation, and the corresponding Ekman and geostrophic mechanics, originating from the early days of ocean circulation theory via Stommel, Munk, and others. 547, 562

work-energy theorem The work-energy theorem of classical mechanics says that the net work done on a physical system over a time interval equals to the change in the kinetic energy.
326

working Working is the mechanical process of modifying the internal energy of a physical system. An infinitesimal amount of working is mathematically expressed as dW , with d identifying working as an inexact differential process that transforms a system from one thermodynamic state to another, so that working is a path-dependent process. We mostly focus on working via the effects from pressure-work, in which $dW = -p dV$, where p is the pressure and dV is the change in volume. Working denotes an action applied to a system (a verb) rather than a property of a system (a noun). It is mechanical energy *in transition* that arises at the boundary of a thermodynamic system. 173, 174

Young-Laplace formula The Young-Laplace formula provides an expression for the pressure jump across an interface with surface tension that separates two fluids. The pressure jump increases according to curvature of the interface. 294, 296

zeroth law of thermodynamics When two physical systems, A and B , are each separately in thermodynamic equilibrium with a third system, C , then the systems A and B are also in thermodynamic equilibrium with one another. This property is referred to as the zeroth law of thermodynamics. 172

Appendix B

LIST OF ACRONYMS

AI artificial intelligence xvii

APE available potential energy 447, 448, 451

GFD geophysical fluid dynamics ix, 235

GFM geophysical fluid mechanics vii, 376

GRD gravitational field, rotational moment of inertia, and deformation of the crust 376, 612

GVC generalized vertical coordinate xx

IFS interfacial form stress 390

PG planetary geostrophy 510, 512

SGS subgrid scale 512

Appendix C

LIST OF SYMBOLS

Many symbols encountered in this book are defined local to their usage and are not used far outside of that location. Many other symbols appear in a variety of places and are included in the tables given below. Additionally, we generally aim to respect the following conventions.

- Many symbols are adorned with extra labels. One usage exposes tensor indices, with tensor indices written using the slanted math font, such as F^i for the component i of the vector \mathbf{F} . Another usage expresses part of the name for the symbol, with the label written with the upright sans serif. Examples include the “ b ” in η_b for the position of the bottom solid boundary of a fluid domain, and the “ h ” in ∇_h for the horizontal gradient operator.
- We strive for unique symbols to represent distinct mathematical and/or physical objects. Yet that goal must confront the multitude of mathematical expressions appearing in this book. We have chosen, on rare occasions, to allow some symbols to carry multiple meanings. In such cases we emphasize the particular meaning of the symbol to help avoid confusion with its alternative meaning.

NON-DIMENSIONAL NUMBERS

SYMBOL	NAME	MEANING
Bu	Burger	$Bu = (\text{deformation radius}/\text{horizontal length scale of flow})^2 = (L_d/L)^2$
Db	Deborah	$Db = \text{relaxation time}/\text{observation time}$
Ek	Ekman	$Ek = \text{vertical frictional acceleration}/\text{planetary Coriolis acceleration}$
Fr	Froude	$Fr = \text{fluid particle speed}/\text{fluid wave speed} = U/c$
Ge	Geostrophic	$Ge = \text{horizontal accelerations from Coriolis}/\text{pressure acceleration} = f U L \rho_a/p$
Kn	Knudsen	$Kn = \text{molecular mean free path}/\text{macroscopic length scale}$
Ma	Mach	$Ma = \text{fluid particle speed}/\text{sound wave speed} = U/c_s$
Pr	Prandtl	$Pr = \text{viscosity}/\text{diffusivity} = \mu/\kappa$
Pe	Peclet	$Pe = \text{advective transport}/\text{diffusive transport} = U L/\kappa$
Re	Reynolds	$Re = \text{inertial acceleration}/\text{frictional acceleration} = U L/\nu$
Ri	Richardson	$Ri = \text{squared buoyancy frequency}/\text{squared vertical shear}$
Ro	Rossby	$Ro = \text{horizontal inertial acceleration}/\text{planetary Coriolis acceleration} = U/(f L)$

SYMBOL	MEANING
\mathcal{A}	wave action
$A^L(\mathbf{a}, T)$	Lagrangian representation of a fluid property as a function of material coordinates and time
\mathbf{a}	coordinate position for a fluid particle using arbitrary material/Lagrangian coordinates
\mathbf{A}, \mathbf{A}	second order skew symmetric tensor with elements satisfying $A^{mn} = -A^{nm}$
A^\vee	Avogadro's number: $A^\vee = 6.0222 \times 10^{23}$ mole $^{-1}$
\mathbf{B}	baroclinicity vector: $\mathbf{B} = \nabla\rho \times (-\rho^{-1} \nabla p) = (\nabla\rho \times \nabla p)/\rho^2$
\mathcal{B}	base (or reference) manifold for describing the space of continuum matter
b	Archimidean buoyancy with $b > 0$ for relatively light fluid: $b = -g(\rho - \rho_0)/\rho$
C	tracer concentration = mass of tracer per mass of fluid = tracer mass fraction
C_d	dimensionless bottom drag coefficient: $C_d > 0$
\mathcal{C}	circulation of velocity around the boundary of a surface $\mathcal{C} \equiv \oint_{\partial\mathcal{S}} \mathbf{v} \cdot d\mathbf{r}$
c_{grav}	shallow water gravity wave speed: $c_{\text{grav}} = \sqrt{g H}$
\mathbf{c}_g	wave group velocity, given by wavevector gradient of dispersion relation: $\mathbf{c}_g = \nabla_k \varpi(\mathbf{k})$
c_p	wave phase velocity: $\mathbf{c}_p = C_p \hat{\mathbf{k}}$
C_p	wave phase speed
c_s	sound speed: $c_s^{-2} = [\partial\rho/\partial p]_{\Theta,S}$
c_p	heat capacity at constant pressure: $c_p = [\partial\mathcal{H}/\partial T]_{p,C}$
\mathbf{E}, \mathbf{E}	second order eddy transport tensor for tracers, and with elements E^{mn}
$\mathbb{E}^1, \mathbb{E}^2, \mathbb{E}^3$	one (line), two (plane), and three dimensional Euclidean space
\mathcal{E}	total energy per mass of a fluid element = sum of internal plus mechanical energies
e_a	basis vectors for a chosen coordinate system, with index $a = 1, 2, 3$ for 3-dimensional space
e^a	basis one-forms for a chosen coordinate system, with index $a = 1, 2, 3$ for 3-dimensional space
f	Coriolis parameter, also the planetary vorticity: $f = 2\Omega \sin\phi$
f_\circ	Coriolis parameter at a particular latitude: $f_\circ = 2\Omega \sin\phi_0$
\mathbf{F}	frictional acceleration vector
$F^i{}_I$	deformation matrix, which transforms between \mathbf{x} -space (Eulerian) and \mathbf{a} -space (Lagrangian)
G	water mass transformation, with dimensions of mass per time
$G = G^{\text{grav}}$	Newton's gravitational constant: $G = 6.674 \times 10^{-11} \text{ N m}^2 \text{ kg}^{-2} = 6.674 \times 10^{-11} \text{ m}^3 \text{ kg}^{-1} \text{ s}^{-2}$
$G(\mathbf{x} \mathbf{x}_0)$	Green's function with \mathbf{x} the observation point (or field point) and \mathbf{x}_0 the source point
$\tilde{G}(\mathbf{x} \mathbf{x}_0)$	modified Green's function for Laplace's operator with Neumann boundary conditions
$G^\ddagger(\mathbf{x} \mathbf{x}_0)$	adjoint Green's function for non-self adjoint operators such as the diffusion operator
$\mathcal{G}(\mathbf{x} \mathbf{x}_0)$	free space Green's function; i.e., the Green's function without boundaries
\mathbf{G}	velocity gradient tensor with elements $G^i{}_j$
\mathcal{G}	Gibbs potential per mass of a fluid element
g_e	gravitational acceleration from central gravity due to just the mass of the planet
g	effective gravitational acceleration from central gravity + planetary centrifugal as evaluated at the Earth's surface: $g \approx 9.8 \text{ m s}^{-2}$

SYMBOL	MEANING
g'	reduced gravity defined between two shallow water layers: $g'_{k+1/2} = g(\rho_{k+1} - \rho_k)/\rho_{\text{ref}} \ll g$
\mathfrak{g}	metric tensor (symmetric positive definite second order tensor) with components \mathfrak{g}_{ab}
\mathbf{g}	square root of the metric tensor determinant: $\mathbf{g} = \sqrt{\det(\mathfrak{g}_{mn})}$
\mathbf{g}^E	square root of the metric tensor determinant using Eulerian coordinates: $\mathbf{g}^E = \sqrt{\det(\mathfrak{g}(\mathbf{x}))}$
\mathbf{g}^L	square root of the metric tensor determinant using Lagrangian coordinates: $\mathbf{g}^L = \sqrt{\det(\mathfrak{g}(\mathbf{a}, T))}$
h_k	layer thickness for a shallow water fluid: $h_k = \eta_{k-1/2} - \eta_{k+1/2} = \delta_k \eta_{k-1/2}$
h	layer thickness for a continuously stratified fluid: $h = \bar{h} \delta\sigma$
\mathbf{h}	specific thickness for a generalized vertical coordinate: $\mathbf{h} = \partial z / \partial \sigma = 1 / (\partial \sigma / \partial z)$
$\mathcal{H}(x)$	Heaviside step function: $\mathcal{H}(x) = 0$ for $x < 0$ whereas $\mathcal{H}(x) = 1$ for $x > 0$
H	vertical length scale of the flow under consideration
H	sometimes used as depth of the ocean bottom: $z = -H(x, y) = \eta_b(x, y)$
H	Hamiltonian energy function
\mathcal{H}	Hamiltonian density used in field theory; dimensions energy per volume (when in 3d space)
\mathcal{H}	enthalpy per mass of a fluid element
\mathbf{I}	unit tensor or Kronecker tensor: $\mathbf{I} = \delta^{ab} \mathbf{e}_a \otimes \mathbf{e}_b = \delta^a{}_b \mathbf{e}_a \otimes \mathbf{e}^b = \delta_a{}^b \mathbf{e}^a \otimes \mathbf{e}_b = \delta_{ab} \mathbf{e}^a \otimes \mathbf{e}^b$
\mathfrak{J}	internal energy per mass of a fluid element
i	$i = \sqrt{-1}$ used for imaginary numbers
i, j, k	tensor indices/labels for Eulerian coordinates
I, J, K	tensor indices/labels for Lagrangian coordinates
$\text{Im}[\cdot]$	imaginary part of a complex number; e.g., $\text{Im}[e^{-i\omega t}] = -\sin(\omega t)$
\mathbf{J}	tracer flux; for material tracers the dimensions are mass per time per area
\mathbf{k}	wavevector (dimensions inverse length) for a wave of wavelength $\Lambda = 2\pi/ \mathbf{k} $
$\hat{\mathbf{k}}$	unit vector in the direction of a wave: $\mathbf{k} = \hat{\mathbf{k}} \mathbf{k} $ (as distinct from the vertical unit vector, $\hat{\mathbf{z}}$)
$ \mathbf{k} $	wavenumber: $ \mathbf{k} = 2\pi/\Lambda$
K	kinetic energy for a particle of mass m : $K = m \mathbf{V} \cdot \mathbf{V}/2$
K	kinetic energy for a system of N particles, $\sum_{n=1}^N m^n \mathbf{V}^n \cdot \mathbf{V}^n$
\mathcal{K}	kinetic energy per mass of a fluid element arising from macroscopic motion: $\mathcal{K} = \mathbf{v} \cdot \mathbf{v}/2$
\mathcal{K}^{hyd}	kinetic energy per mass for an approximate hydrostatic flow: $\mathcal{K}^{\text{hyd}} = \mathbf{u} \cdot \mathbf{u}/2$
\mathcal{K}^{sw}	kinetic energy per horizontal area for a shallow water layer: $\mathcal{K}^{\text{sw}} = \rho h \mathbf{u} \cdot \mathbf{u}/2$
\mathbf{K}, \mathbf{K}'	positive and symmetric second order tensor parameterizing diffusive mixing
k	integer index to label a layer in a shallow water model with $k = 1, N$ layers ($k = 1$ is top layer)
k_B	Boltzmann constant: $k_B = 1.3806 \times 10^{-23} \text{ m}^2 \text{ kg s}^{-2} \text{ K}^{-1} = R^* / A^*$
k_R	Rossby height/depth: $k_R = \mathbf{k} N / f_0$ with horizontal wavenumber $ \mathbf{k} = \sqrt{k_x^2 + k_y^2}$
L	Lagrangian used in Lagrangian mechanics: kinetic minus potential energies: $L = K - P$
L	length scale for a particular physical feature and commonly used in scale analysis

LATIN SYMBOLS AND THEIR MEANING

SYMBOL	MEANING
\mathcal{L}	Lagrangian density used in field theory; dimensions energy per volume (when in 3d space)
L_d	deformation radius: (a) shallow water $L_d = \sqrt{g H}/f$; (b) continuous internal $L_d = H N/f$
\mathcal{M}	mechanical energy per mass of a fluid element arising from macroscopic motion
\mathcal{M}^{sw}	mechanical energy per area of a shallow water fluid column: $\mathcal{M}^{sw} = \mathcal{K}^{sw} + \mathcal{P}^{sw}$
\mathbf{M}	moment of inertia tensor
\mathbf{M}	potential momentum vector: $\mathbf{M} = \mathbf{u} + 2\boldsymbol{\Omega} \times \mathbf{X}$
M	Montgomery potential for continuously stratified fluid $M = \varphi - bz$
M	mass, as in the mass of a fluid region, $M = \int_{\mathcal{R}} \rho dV$
M_k^{dyn}	Montgomery potential for a shallow water layer: $M_k^{dyn} = \sum_{j=0}^{k-1} g_{j+1/2}^r \eta_{j+1/2}$
M^{air}	mass per mole of air: $M^{air} = 28.8 \times 10^{-3} \text{ kg mole}^{-1}$
N	buoyancy frequency
\mathcal{O}	order of magnitude
P	potential energy of a physical system, with corresponding force $\mathbf{F} = -\nabla P$
\mathcal{P}_k^{sw}	potential energy per horizontal area for a shallow water fluid: $\mathcal{P}_k^{sw} = g \rho_k \int_{\eta_{k+1/2}}^{\eta_{k-1/2}} z dz$
\mathcal{P}	phase of a wave
\mathcal{P}_σ	generalized momentum for discrete particle system: $\mathcal{P}_\sigma = \partial L / \partial \dot{\xi}^\sigma$
\mathcal{P}	generalized momentum density for continuous media: $\mathcal{P} = \partial \mathcal{L} / \partial (\partial_t \psi)$
\mathbf{P}	linear momentum of a physical system
p	pressure at a point in the fluid
p_a	pressure applied to the ocean surface from the atmosphere or cryosphere
p_b	pressure at the bottom of a fluid column, at the fluid-solid earth interface
p_{slp}	sea level pressure with an area average, $\langle p_{slp} \rangle = 101.325 \times 10^3 \text{ N m}^{-2}$
$p_{k-1/2}$	hydrostatic pressure at the layer interface with vertical position $z = \eta_{k-1/2}$
p_k^{dyn}	dynamic pressure in a shallow water layer: $p_k^{dyn} = \rho_{ref} \sum_{j=0}^{k-1} g_{j+1/2}^r \eta_{j+1/2}$
P_k	pressure integrated over a shallow water layer: $P_k \equiv \int_{\eta_{k+1/2}}^{\eta_{k-1/2}} p_k(z) dz = h_k (g \rho_k h_k / 2 + p_{k-1/2})$
Q	potential vorticity for continuously stratified (Ertel PV) or shallow water (Rossby PV)
q	quasi-geostrophic potential vorticity either for a continuous fluid or shallow water fluid
Q_m	mass flux (mass per horizontal area per time) across ocean surface: $Q_m > 0 \text{ enters ocean}$
\mathcal{Q}_m	mass flux (mass per surface area per time) across ocean surface: $\mathcal{Q}_m dS = Q_m dA$
Q_c	turbulent tracer flux (tracer per horiz area per time) across ocean surface: $Q_c > 0 \text{ enters ocean}$
\mathcal{Q}_c	turbulent tracer flux (tracer per surface area per time) across ocean surface: $QCcal dS = Q_c dA$
r	radial distance of a point relative to an origin
\mathbf{R}	rotation tensor: $2 R^m{}_n = \partial_n v^m - \partial^m v_n = -2 R_n{}^m$
\mathbb{R}^1	real number line
\mathbb{R}^2	two-dimensional space of real numbers
\mathbb{R}^3	three-dimensional space of real numbers
R	radius of a sphere

LATIN SYMBOLS AND THEIR MEANING

SYMBOL	MEANING
R_e	radius of sphere whose volume approximates that of the earth: $R_e = 6.371 \times 10^6 \text{ m}$
R^g	universal gas constant: $R^g = 8.314 \text{ J mole}^{-1} \text{ K}^{-1} = 8.314 \text{ kg m}^2 \text{ s}^{-2} \text{ mole}^{-1} \text{ K}^{-1}$
R^{air}	specific gas constant for air: $R^{\text{air}} = R^g/M^{\text{air}} = 2.938 \times 10^2 \text{ m}^2 \text{ s}^{-2} \text{ K}^{-1}$
\mathcal{R}	arbitrary region or manifold
$\mathcal{R}^a{}_b$	orthogonal rotation matrix
$\text{Re}[\cdot]$	real part of a complex number; e.g., $\text{Re}[e^{-i\omega t}] = \cos(\omega t)$
\mathcal{S}	spatial manifold
\mathcal{S}	entropy per mass of a fluid element
$\mathcal{S} = \mathcal{S}^{\text{action}}$	action: time integral of the Lagrangian: $\mathcal{S} = \int_{t_A}^{t_B} L \, dt$
\mathbf{S}	strain rate tensor: $2\mathbf{S} = \nabla \mathbf{v} + (\nabla \mathbf{v})^T$
\mathbf{S}^{dev}	deviatoric strain rate tensor: $\mathbf{S}^{\text{dev}} = \mathbf{S} - S^q_q/3$
S	salt concentration = mass of salt in a fluid element per mass of seawater
S	Absolute Salinity, generically referred to as salinity: $S = 1000 \mathcal{S}$
s	expression for a generic surface: $s = s(x, y, z, t)$.
s	arc-length along a curve $\mathbf{x}(s)$ with infinitesimal increment $ds = \sqrt{d\mathbf{x} \cdot d\mathbf{x}}$
\hat{s}	unit tangent to a curve, also written as $\hat{s} = \hat{\mathbf{t}}$ (see below)
sgn	sign function related to Heaviside step function via $\text{sgn}(x) = 2\mathcal{H}(x) - 1$
T'	absolute thermodynamic <i>in situ</i> temperature (Kelvin if in a thermodynamic equation)
T	time scale for a particular physical process and commonly used in scale analysis
T	time (universal Newtonian time) measured in the Lagrangian reference frame
t	time (universal Newtonian time) measured in the Eulerian reference frame
τ	general symbol for time as considered in the tensor analysis chapters
\mathbf{T}	stress tensor with natural elements $T^m{}_n$
$\mathbb{T}^{\text{kinetic}}$	kinetic stress tensor: $\mathbb{T}^{\text{kinetic}} = -\rho \mathbf{v} \otimes \mathbf{v}$
$\mathbb{T}^{\text{sw kinetic}}$	kinetic stress tensor for shallow water fluid: $\mathbb{T}^{\text{sw kinetic}} = -\rho \mathbf{u} \otimes \mathbf{u}$
$\hat{\mathbf{t}}$	unit tangent to a curve: $\hat{\mathbf{t}} = d\mathbf{x}/ds$, where s is the arc-length so that $ds = \sqrt{d\mathbf{x} \cdot d\mathbf{x}}$
\mathbf{u}	horizontal velocity of a fluid particle, with Cartesian representation: $\mathbf{u} = \hat{\mathbf{x}} u + \hat{\mathbf{y}} v$
U	horizontal velocity scale of the flow under consideration
\mathbf{U}	depth integrated horizontal velocity: $\mathbf{U} = \int_{\eta_b}^{\eta} \mathbf{u} \, dz$
V	volume, as in the volume of a fluid region, $V = \int_{\mathcal{R}} dV$
\mathbf{v}	velocity of a fluid particle: $\mathbf{v} = D\mathbf{x}/Dt$, with Cartesian components $\mathbf{v} = \hat{\mathbf{x}} u + \hat{\mathbf{y}} v + \hat{\mathbf{z}} w$
\mathbf{v}^*	eddy-induced velocity
\mathbf{v}^\dagger	residual velocity of a fluid particle: $\mathbf{v}^\dagger = \mathbf{v} + \mathbf{v}^*$
$\mathbf{v}^{(b)}$	velocity of a point on a region boundary
$\mathbf{v}^L(\mathbf{a}, T)$	Lagrangian velocity of a fluid particle so that $\mathbf{v}^L(\mathbf{a}, T) = \mathbf{v}[\mathbf{x} = \boldsymbol{\varphi}(\mathbf{a}, T), t = T]$
\mathbf{v}_I	velocity of a fluid particle measured in the inertial/absolute reference frame: $\mathbf{v}_I = \mathbf{v} + \boldsymbol{\Omega} \times \mathbf{x}$
W	vertical velocity scale of the flow under consideration
\mathcal{W}	on-shell action
w	vertical component to the velocity: $w = Dz/Dt$
w^{dia}	dia-surface flux = volume per surface area per time crossing a σ -surface: $w^{\text{dia}} = (1/ \nabla \sigma) \dot{\sigma}$
$w^{(\dot{\sigma})}$	dia-surface velocity = volume per <i>horizontal</i> area per time crossing σ -surface: $w^{(\dot{\sigma})} = \dot{\sigma} \partial z/\partial \sigma$

LATIN SYMBOLS AND THEIR MEANING

SYMBOL	MEANING
(x, y, z)	triplet of Cartesian coordinates
\mathbf{x}	spatial position as a line segment with an arrow pointing from an origin to the position of a particle
x	spatial position represented by either general coordinates or Cartesian coordinates
$\hat{\mathbf{x}}$	initial position for a fluid particle using arbitrary coordinates
$(\hat{\mathbf{x}}, \hat{\mathbf{y}}, \hat{\mathbf{z}})$	triplet of Cartesian unit vectors oriented in a righthand sense
$\mathbf{X}(t)$	position for a point particle defining a trajectory through space-time
$\mathbf{X}(\mathbf{a}, T)$	position of a material fluid particle expressed using material coordinates
z_σ	specific thickness for a generalized vertical coordinate: $z_\sigma = \partial z / \partial \sigma = h$

GREEK SYMBOLS AND THEIR MEANING

SYMBOL	MEANING
α	thermal expansion: $\alpha = -\rho^{-1} \partial \rho / \partial \theta$ or $\alpha = -\rho^{-1} \partial \rho / \partial \Theta$ or $\alpha = -\rho^{-1} \partial \rho / \partial T$
α_T	thermal expansion in terms of <i>in situ</i> temp: $\alpha = -\rho^{-1} \partial \rho / \partial T$
$\alpha^{(\Theta)}$	thermal expansion in terms of Conservative Temperature: $\alpha^{(\Theta)} = -\rho^{-1} \partial \rho / \partial \Theta$
α_{aspect}	aspect ratio; ratio of vertical to horizontal scales of the flow: $\alpha_{\text{aspect}} = H/L$
$\beta, \beta^{(S)}$	haline (saline) contraction coefficient: $\beta = \beta^{(S)} = \rho^{-1} \partial \rho / \partial S$
β	meridional derivative of planetary vorticity: $\beta = \partial_y f$
$\hat{\gamma}$	dianeutral unit direction perpendicular to the neutral tangent plane
δ_{ab}	Kronecker delta, which is the metric for Euclidean space with Cartesian coordinates
δ_b^a	components to the Kronecker tensor in arbitrary coordinates
ϵ	kinetic energy dissipation from viscosity (energy per time per mass)
ϵ_{ab}	components to the permutation symbol in two space dimensions
ϵ_{abc}	components to the permutation symbol in three space dimensions
ε_{abc}	components to the Levi-Civita symbol in three space dimensions: $\varepsilon_{abc} = \sqrt{\det(g_{ab})} \epsilon_{abc}$
ζ	vertical component to the relative vorticity; e.g., $\zeta = \partial_x v - \partial_y u$
ζ_a	vertical component to the absolute vorticity; e.g., $\zeta_a = f + \zeta$
η	vertical position of the free upper surface of a fluid domain: $z = \eta(x, y, t)$
η	vertical position of a generalized vertical coordinate surface: $z = \eta(x, y, \sigma, t)$, with σ the generalized vertical coordinate
$\eta_{k-1/2}$	vertical position of the top interface of the k shallow water layer
$\eta_{k+1/2}$	vertical position of the lower interface of the k shallow water layer
$\eta_b = -H$	vertical position of static solid-earth boundary: $z = \eta_b(x, y) = -H(x, y)$
θ	potential temperature
Θ	Conservative Temperature
κ	molecular kinematic diffusivity
κ_T	molecular diffusivity for <i>in situ</i> temperature in water: $\kappa_T = 1.4 \times 10^{-7} \text{ m}^2 \text{ s}^{-1}$
κ_S	molecular diffusivity for salt in water: $\kappa_S = 1.5 \times 10^{-9} \text{ m}^2 \text{ s}^{-1}$
κ_{eddy}	kinematic eddy diffusivity: $\kappa_{\text{eddy}} \gg \kappa$
Λ	wavelength of a wave: $\Lambda = 2\pi/ \mathbf{k} $, where \mathbf{k} is the wavevector and $ \mathbf{k} $ the wavenumber.
λ	reduced wavelength of a wave: $\lambda = \Lambda/(2\pi) = 1/ \mathbf{k} $.
λ	longitude on the sphere: $0 \leq \lambda \leq 2\pi$
μ_n	chemical potential for constituent n within a fluid (energy per mass)
$\tilde{\mu}_n$	chemical potential for constituent n within a fluid (energy per mole number)
μ	relative chemical potential for a binary fluid
μ	chemical potential for seawater: $\mu = \mu_{\text{salt}} - \mu_{\text{water}}$
μ_{vsc}	dynamic viscosity = $\rho \nu$
ν_s	specific volume: $\nu_s = \rho^{-1}$
ν	molecular kinematic viscosity
ν_{air}	molecular kinematic viscosity of air: $\nu_{\text{air}} \approx 1.3 \times 10^{-5} \text{ m}^2 \text{ s}^{-1}$
ν_{water}	molecular kinematic viscosity of fresh water: $\nu_{\text{water}} \approx 10^{-6} \text{ m}^2 \text{ s}^{-1}$
ν_{eddy}	eddy viscosity: $\nu_{\text{eddy}} \gg \nu$
ξ^a	a'th component to a generalized coordinate
Π	Exner function
Π	Boussinesq dynamic enthalpy

GREEK SYMBOLS AND THEIR MEANING

SYMBOL	MEANING
ρ	Eulerian <i>in situ</i> density (mass per volume) of a fluid element: $\rho = \rho(\mathbf{x}, t)$
ρ^L	mass density following a fluid particle trajectory (Lagrangian mass density): $\rho^L = \rho^L(\mathbf{a}, T)$
$\dot{\rho}^L$	initial mass density in Lagrangian space-time: $\dot{\rho}^L = \rho^L(\mathbf{a}, T = t_0)$
ρ_0	constant reference density used for the Boussinesq ocean
ρ_{ref}	constant reference density used for the shallow water fluid
ϱ	potential density referenced to a specified pressure
σ	generalized vertical coordinate, $\sigma = \sigma(x, y, z, t)$
τ	stress vector such as from winds or bottom stresses acting on the ocean
\mathbb{T}	frictional stress tensor
φ	pressure divided by the Boussinesq reference density: $\varphi = p/\rho_0$
φ	sometimes used as the variable for parameterizing a curve
ϕ	latitude on the sphere: $-\pi/2 \leq \phi \leq \phi/2$
Φ_e	gravitational potential from a spherical and homogeneous earth
Φ	geopotential from central gravity plus planetary centrifugal; also, potential energy per mass
Φ	inverse flow map that generates an inverse mapping of the fluid continuum: $\mathbf{a} = \Phi(\mathbf{x}, t)$
$\boldsymbol{\varphi}$	motion field that maps the fluid continuum as time evolves: $\mathbf{x} = \boldsymbol{\varphi}(\mathbf{a}, T)$
ψ	streamfunction for two-dimensional non-divergent flow: $\mathbf{u} = \hat{\mathbf{z}} \times \nabla \psi$
Ψ	vector streamfunction for three-dimensional non-divergent flow: $\mathbf{v} = \nabla \times \Psi$
ω	relative vorticity: $\boldsymbol{\omega} = \nabla \times \mathbf{v}$
ω	angular frequency for a wave so that the wave period is $2\pi/ \omega $
ϖ	dispersion relation for linear waves, relating angular frequency to the wavevector: $\omega = \varpi(\mathbf{k})$
Ω	angular velocity for a rotating reference frame
Ω	earth's angular velocity oriented through the north pole: $ \Omega = 7.2921 \times 10^{-5} \text{ s}^{-1}$

MATHEMATICAL OPERATIONS AND RELATIONS

SYMBOL	MEANING
$[\equiv]$	"has dimensions" for use in referring to the physical dimensions
\times	vector cross product
∇	covariant derivative operator, which acts on a (p, q) tensor to produce a $(p, q + 1)$ tensor.
∇	gradient operator
∇_h	horizontal gradient operator on constant z surface: $\nabla_h = \hat{\mathbf{x}} (\partial/\partial x)_z + \hat{\mathbf{y}} (\partial/\partial y)_z = \hat{\mathbf{x}} \partial_x + \hat{\mathbf{y}} \partial_y$
$\nabla \cdot$	divergence operator that acts on a vector to produce a scalar
$\nabla \times$	curl operator
∇_σ	horizontal gradient on constant σ -surface: $\nabla_\sigma = \hat{\mathbf{x}} (\partial/\partial x)_\sigma + \hat{\mathbf{y}} (\partial/\partial y)_\sigma$
$\partial/\partial\sigma$	vertical partial derivative with general vertical coordinate: $\partial_\sigma = \partial/\partial\sigma = \partial/\partial\sigma = (\partial z/\partial\sigma) \partial/\partial z$
$\partial/\partial t$	Eulerian time derivative acting at a fixed spatial position, \mathbf{x} , also written as ∂_t
$[\partial/\partial t]_\sigma$	time derivative computed on constant σ -surface
D/Dt	material, Lagrangian, or substantial time derivative following a fluid particle
D_r/Dt	time derivative following a ray (integral lines of the group velocity): $D_r/Dt = \partial/\partial t + \mathbf{c}_g \cdot \nabla$
D_g/Dt	time derivative following the horizontal geostrophic flow $D_g/Dt = \partial/\partial t + \mathbf{u}_g \cdot \nabla$
$\ddot{}$	inexact differential operator commonly found in thermodynamics
δ	virtual displacement (also the variation) for Lagrangian mechanics and Hamilton's principle
δ	differential increment that signals an object following the fluid flow
$\delta(x)$	one-dimensional Dirac delta with dimensions of inverse length
$\delta^{(2)}(\mathbf{x})$	two-dimensional Dirac delta with dimensions of inverse area
$\delta(\mathbf{x})$	three-dimensional Dirac delta with dimensions of inverse volume
$\delta(t)$	temporal Dirac delta with dimensions of inverse time
Δ	finite difference increment in space: $\Delta_x, \Delta_y, \Delta_z, \Delta_\sigma$
dA	infinitesimal horizontal area element: $dA = dx dy$
d^3a	infinitesimal region of material space: $d^3a = da db dc$
$d\mathcal{S}$	infinitesimal area element on a surface
dV	infinitesimal volume element, sometimes written $dV = d\mathbf{x}$
$d\mathbf{x}$	infinitesimal volume element, with Cartesian expression $d\mathbf{x} = dV = dx dy dz$
δV	infinitesimal volume for a region moving with the fluid (Lagrangian region)
$\int_{\mathcal{R}} dV$	volume integral over an arbitrary region, \mathcal{R}
$\int_{\mathcal{R}(\mathbf{v})} dV$	volume integral over a region following the fluid flow (Lagrangian integral)
$\int_{\mathcal{S}} d\mathcal{S}$	surface integral over an arbitrary surface \mathcal{S}
$\oint_{\partial\mathcal{R}} d\mathcal{S}$	surface integral over a closed surface $\partial\mathcal{R}$ that bounds the volume \mathcal{R}
$\oint d\ell$	closed line integral over a periodic domain
$\oint_{\partial\mathcal{S}} d\ell$	counter-clockwise closed line integral over the boundary of a surface, $\partial\mathcal{S}$
\sim	"similar to" or "scales as"
\approx	approximately equal to
$\dot{\Psi}$	time derivative following a trajectory; for fluid particle trajectories then, $\dot{\Psi} = D\Psi/Dt$

BIBLIOGRAPHY

- Acheson, D., *Elementary Fluid Dynamics*, Oxford Applied Mathematics and Computing Science Series, Oxford, Oxford, 1990. 329
- Anderson, J., Ludwig Prandtl's boundary layer, *Physics Today*, 58, 42–48, doi:10.1063/1.2169443, 2005. 282, 291, 604
- Anderson, P. W., More is different, *Science*, 177, 393–396, doi:10.1126/science.177.4047.39, 1972. ix
- Andresen, B., R. Berry, R. Gilmore, E. Ihrig, and P. Salamon, Thermodynamic geometry and the metrics of Weinhold and Gilmore, *Physical Review A*, 37(3), 845–848, doi:10.1103/PhysRevA.37.845, 1988. 170
- Andrews, D. G., A finite-amplitude Eliassen-Palm theorem in isentropic coordinates, *Journal of Atmospheric Sciences*, 40, 1877–1883, doi:10.1175/1520-0469(1983)040<1877:AFAEPT>2.0.CO;2, 1983. 448
- Andrews, D. G., J. R. Holton, and C. B. Leovy, *Middle Atmosphere Dynamics*, Academic Press, 1987. 155
- Anstey, J., and L. Zanna, A deformation-based parametrization of ocean mesoscale eddy Reynolds stresses, *Ocean Modelling*, 112, 99–111, 2017. 284
- Apel, J. R., *Principles of Ocean Physics*, International Geophysics Series, vol. 38, Academic Press, London, 1987. 547
- Arbic, B., S. T. Garner, R. W. Hallberg, and H. L. Simmons, The accuracy of surface elevations in forward global barotropic and baroclinic tide models, *Deep Sea Research*, 51, 3069—3101, 2004. 376
- Aris, R., *Vectors, Tensors and the Basic Equations of Fluid Mechanics*, Dover Publishing, New York, 1962. 40, 42, 48, 52, 74, 85, 115, 122, 242, 257, 269, 277, 278, 284
- Atkins, P., and J. de Paula, *Atkin's Physical Chemistry*, 8th ed., 1053 pp., W.H. Freeman and Co., 2006. 183, 187
- Badin, G., and F. Crisciani, *Variational formulation of fluid and geophysical fluid dynamics*, Springer International Publishing, Switzerland, 218 pages, 2018. xii, 33
- Batchelor, G. K., *An Introduction to Fluid Dynamics*, Cambridge University Press, Cambridge, England, 1967. 4, 11, 99, 269, 290, 291, 297, 319

- Becker, E., Frictional heating in global climate models, *Monthly Weather Review*, 131, 508–520, doi:10.1175/1520-0493(2003)131<0508:FHIGCM>2.0.CO;2, 2003. 321
- Bennett, A., The geometry of neutral paths, *Journal of Physical Oceanography*, 49, 3037–3044, doi:10.1175/JPO-D-19-0047.1, 2019. 483
- Bingham, R. J., and C. W. Hughes, Local diagnostics to estimate density-induced sea level variations over topography and along coastlines, *Journal of Geophysical Research*, 117, doi:10.1029/2011JC007276, 2012. 368, 371
- Bird, R. B., W. E. Stewart, and E. N. Lightfoot, *Transport Phenomena*, John Wiley and Sons, New York, 1960. 115
- Bishop, S., R. Small, and F. Bryan, The global sink of available potential energy by mesoscale air-sea interaction, *Journal of Advances in Modeling Earth Systems*, in review, 2020. 454
- Boltzmann, L., Further studies on the thermal equilibrium of gas molecules, in *Kinetic Theory, Vol. 2: Irreversible Processes*, edited by S. G. Brush, pp. 88–175, Pergamon Press, Oxford, english translation of Boltzmann (1872), “Weitere Studien über das Wärmegleichgewicht unter Gasmolekülen”, 1966. 347, 597
- Bretherton, F. P., Critical layer instability in baroclinic flows, *Quarterly Journal of the Royal Meteorological Society*, 92, 325–334, 1966. 448
- Bühler, O., J. Callies, and R. Ferrari, Wave–vortex decomposition of one-dimensional ship-track data, *Journal of Fluid Mechanics*, 756, 1007–1026, doi:10.1017/jfm.2014.488, 2014. 455
- Caldwell, D. R., Thermal and Fickian diffusion of sodium chloride in a solution of oceanic concentration, *Deep-Sea Research*, 20, 1029–1039, doi:10.1016/0011-7471(73)90073-9, 1973. 335
- Caldwell, D. R., and S. A. Eide, Soret coefficient and isothermal diffusivity of aqueous solutions of five principal salt constituents of seawater, *Deep-Sea Research*, 28A, 1605–1618, doi:10.1016/0198-0149(81)90100-X, 1981. 335
- Callen, H. B., *Thermodynamics and an Introduction to Thermostatics*, John Wiley and Sons, New York, 493 + xvi pp, 1985. 165, 169, 170, 171, 177, 180, 199, 203, 204, 322, 333, 335
- Chandrasekhar, S., *Hydrodynamic and Hydromagnetic Stability*, Dover Publications, New York, 654 pp, 1961. 416
- Crocco, L., Eine neue stromfunktion fur die erforschung der bewegung der gas emit rotation, *Zamm-zeitschrift Fur Angewandte Mathematik Und Mechanik*, 17, 1, doi:10.1002/ZAMM.19370170103, 1937. 347
- Csanady, G. T., Turbulent interface layers, *Journal of Geophysical Research*, 83(C5), 2329–2342, doi:10.1029/JC083iC05p02329, 1978. 569
- Csanady, G. T., The pressure field along the western margins of the North Atlantic, *Journal of Geophysical Research*, 84, 4905–4915, doi:10.1029/JC084iC08p04905, 1979. 368, 371
- Cushman-Roisin, B., and J.-M. Beckers, *Introduction to Geophysical Fluid Dynamics*, Academic-Press, Amsterdam, 828, 2011. 546, 547

- Dahlen, F. A., and J. Tromp, *Theoretical Global Seismology*, Princeton University Press, Princeton USA, 1998. 532
- Dahler, J., and L. Scriven, The angular momentum of continua, *Nature*, 4797, 36–37, 1961. 269
- Davies-Jones, R., An expression for effective buoyancy in surroundings with horizontal density gradients, *Journal of the Atmospheric Sciences*, 60, 2922–2925, doi:10.1175/1520-0469(2003)060,2922:AEFEBI.2.0.CO;2, 2003. 499
- Davis, R. E., Diapycnal mixing in the ocean: equations for large-scale budgets, *Journal of Physical Oceanography*, 24, 777–800, doi:10.1175/1520-0485(1994)024<0777:DMITOE>2.0.CO;2, 1994. 319
- DeGroot, S. R., and P. Mazur, *Non-Equilibrium Thermodynamics*, Dover Publications, New York, 510 pp, 1984. 115, 122, 313, 319, 322
- Doering, C., and J. Gibbon, *Applied analysis of the Navier-Stokes equations*, Cambridge University Press, Cambridge, UK, 217 pp, 1995. 281
- Döös, K., and D. J. Webb, The Deacon cell and the other meridional cells in the Southern Ocean, *Journal of Physical Oceanography*, 24, 429–442, doi:10.1175/1520-0485(1994)024<0429:TDCATO>2.0.CO;2, 1994. 155
- Doswell, C., and P. Markowski, Is bouyancy a relative quantity?, *Monthly Weather Review*, 132, 853–863, doi:10.1175/1520-0493(2004)132<0853:IBARQ>2.0.CO;2, 2004. 499
- Durran, D. R., Is the coriolis force really responsible for the inertial oscillation?, *Bulletin of the American Meteorological Society*, 74, 2179–2184, doi:10.1175/1520-0477(1993)074<2179:ITCFRR>2.0.CO;2, 1993. 248
- Ebeling, W., and R. Feistel, *Physics of Self-Organization and Evolution*, John Wiley & Sons, 2011. 165, 172
- Einstein, A., Autobiographical notes, in *Albert Einstein, Philosopher-Scientist*, edited by P. A. Schilpp, Library of Living Philosophers, p. 33, Cambridge University Press, 1970. 162
- Falkovich, G., *Fluid Mechanics: A short course for physicists*, Cambridge University Press, 167pp, 2011. 297
- Farrell, W., and J. Clark, On postglacial sea level, *Geophysical Journal of the Royal Astronomical Society*, 46, 646–667, 1976. 375
- Favre, A., Équations des gaz turbulents compressibles. Parts I and II., *Journel de Méchanic*, 4, 361–421, 1965. 137
- Feistel, R., Equilibrium thermodynamics of seawater revisited, *Progress in Oceanography*, 31, 101–179, 1993. 193
- Fetter, A. L., and J. D. Walecka, *Theoretical Mechanics of Particles and Continua*, Dover Publications, Mineola, New York, 570 pp, 2003. 297
- Feynman, R. P., R. B. Leighton, and M. L. Sands, *The Feynman lectures on physics*, Addison-Wesley Publishing Company, Reading, Mass, 1963. 340, 592, 600

Frisch, U., *Turbulence, the Legacy of A.N. Kolmogorov*, Cambridge University Press, 1995. 33

Frisch, U., and B. Villone, Cauchy's almost forgotten Lagrangian formulation of the Euler equation for 3D incompressible flow, *European Physical Journal*, 39, 325–351, doi:10.1140/epjh/e2014-50016-6, 2014. 67

Garrett, C., P. MacCready, and P. Rhines, Boundary mixing and arrested ekman layers: Rotating stratified flow near a sloping boundary, *Annual Review of Fluid Mechanics*, 25, 291–323, doi:10.1146/annurev.fl.25.010193.001451, 1993. 569

Gent, P., The energetically consistent shallow-water equations, *Journal of the Atmospheric Sciences*, 50, 1323–1325, doi:10.1175/1520-0469(1993)050<1323:TECSWE>2.0.CO;2, 1993. 440

Gent, P. R., and J. C. McWilliams, Isopycnal mixing in ocean circulation models, *Journal of Physical Oceanography*, 20, 150–155, doi:10.1175/1520-0485(1990)020<0150:IMIOCM>2.0.CO;2, 1990. 527, 528

Gill, A., *Atmosphere-Ocean Dynamics, International Geophysics Series*, vol. 30, Academic Press, London, 662 + xv pp, 1982. 5, 188, 286, 376, 476, 518, 537, 541, 547

Gnanadesikan, A., and R. Weller, Structure and instability of the ekman spiral in the presence of surface gravity waves, *Journal of Physical Oceanography*, 25, 3148–3171, doi:10.1175/1520-0485(1995)025<3148:SAIOTE>2.0.CO;2, 1995. 569

Graham, F., and T. McDougall, Quantifying the nonconservative production of Conservative Temperature, potential temperature, and entropy, *Journal of Physical Oceanography*, 43, 838–862, doi:10.1175/JPO-D-11-0188.1, 2013. 335, 338, 339

Greatbatch, R. J., A note on the representation of steric sea level in models that conserve volume rather than mass, *Journal of Geophysical Research*, 99, 12,767–12,771, doi:10.1029/94JC00847, 1994. 157

Greenspan, H. P., *The Theory of Rotating Fluids*, Cambridge University Press, Cambridge, UK, 1969. 503

Gregg, M. C., Entropy generation in the ocean by small-scale mixing, *Journal of Physical Oceanography*, 14, 688–711, 1984. 319

Gregory, J., Vertical heat transports in the ocean and their effect on time-dependent climate change, *Climate Dynamics*, 15, 501–515, doi:10.1007/s003820000059, 2000. 430

Gregory, J., S. M. Griffies, C. Hughes, J. Lowe, J. Church, I. Fukimori, N. Gomez, R. Kopp, F. Landerer, R. Ponte, D. Stammer, M. Tamisiea, and R. van den Wal, Concepts and terminology for sea level—mean, variability and change, both local and global, *Surveys in Geophysics*, 40, 1251–1289, doi:10.1007/s10712-019-09555-7, 2019. 376, 578, 612

Griffies, S. M., *Fundamentals of Ocean Climate Models*, Princeton University Press, Princeton, USA, 518+xxxiv pages, 2004. 137, 277, 278, 279, 284, 311

Griffies, S. M., and A. J. Adcroft, Formulating the equations for ocean models, in *Ocean Modeling in an Eddying Regime, Geophysical Monograph*, vol. 177, edited by M. Hecht and H. Hasumi, pp. 281–317, American Geophysical Union, 2008. 416

Griffies, S. M., and R. J. Greatbatch, Physical processes that impact the evolution of global mean sea level in ocean climate models, *Ocean Modelling*, 51, 37–72, doi:10.1016/j.ocemod.2012.04.003, 2012. 109, 157

Griffies, S. M., and R. Hallberg, Biharmonic friction with a Smagorinsky-like viscosity for use in large-scale eddy-permitting ocean models, *Monthly Weather Review*, 128, 2935–2946, doi:10.1175/1520-0493(2000)128<2935:BFWASL>2.0.CO;2, 2000. 311

Griffies, S. M., J. Yin, P. J. Durack, P. Goddard, S. Bates, E. Behrens, M. Bentsen, D. Bi, A. Biastoch, C. W. Böning, A. Bozec, C. Cassou, E. Chassignet, G. Danabasoglu, S. Danilov, C. Domingues, H. Drange, R. Farneti, E. Fernandez, R. J. Greatbatch, D. M. Holland, M. Ilicak, J. Lu, S. J. Marsland, A. Mishra, W. G. Large, K. Lorbacher, A. G. Nurser, D. Salas y Mélia, J. B. Palter, B. L. Samuels, J. Schröter, F. U. Schwarzkopf, D. Sidorenko, A.-M. Treguier, Y. Tseng, H. Tsujino, P. Uotila, S. Valcke, A. Voldoire, Q. Wang, M. Winton, and Z. Zhang, An assessment of global and regional sea level for years 1993–2007 in a suite of interannual CORE-II simulations, *Ocean Modelling*, 78, 35–89, doi:10.1016/j.ocemod.2014.03.004, 2014. 361

Griffies, S. M., A. Adcroft, and R. W. Hallberg, A primer on the vertical lagrangian-remap method in ocean models based on finite volume generalized vertical coordinates, *Journal of Advances in Modeling Earth Systems*, 12, doi:10.1029/2019MS001954, 2020. 19, 129

Guggenheim, E. A., *Thermodynamics: An Advanced Treatment for Chemists and Physicists*, 5th ed., North-Holland, Amsterdam, 390, 1967. 187, 209

Gula, J., M. Molemaker, and J. McWilliams, Gulf Stream dynamics along the southeastern U.S. seaboard, *Journal of Physical Oceanography*, 45, 690–715, doi:10.1175/JPO-D-14-0154.1, 2015. 385

Haine, T. W. N., S. M. Griffies, G. Gebbie, and W. Jiang, A review of Green's function methods for tracer timescales and pathways in ocean models, *Journal of Advances in Modeling Earth Systems (JAMES)*, 17, doi:10.1029/2024MS004637, 2025. 120

Held, I. M., and A. Y. Hou, Nonlinear axially symmetric circulations in a nearly inviscid atmosphere, *Journal of the Atmospheric Sciences*, 37(3), 515–533, doi:10.1175/1520-0469(1980)037<0515:NASCIA>2.0.CO;2, 1980. 254, 255

Holland-Hansen, B., The Sognefjord section: Oceanographic observations in the northernmost part of the North Sea and southern part of the Norwegian Sea, *James Johnstone Memorial Volume*, 1934. 368

Helmholtz, H., On integrals of the hydrodynamical equations, which express vortex-motion, *The London, Edinburgh, and Dublin Philosophical Magazine and Journal of Science*, 33, 485–512, doi:10.1080/14786446708639824, 1867. 595

Hesselberg, T., Die Gesetze der ausgeglichenen atmosphaerischen Bewegungen, *Beiträge der Physik der freien Atmosphäre*, 12, 141–160, 1926. 137

Holton, J. R., and G. J. Hakim, *An Introduction to Dynamic Meteorology*, 5th ed., Academic Press, Waltham, Mass, USA, 532 pp, 2013. 209, 227, 255, 399, 406, 537, 540, 542, 545, 546

Hoskins, B. J., and I. N. James, *Fluid Dynamics of the Midlatitude Atmosphere*, Wiley Blackwell, Chichester, UK, 2014. 82, 84

- Huang, K., *Statistical Mechanics*, John Wiley and Sons, New York, 493 pp, 1987. 1, 11, 313
- Hughes, C. W., A theoretical reason to expect inviscid western boundary currents in realistic oceans, *Ocean Modelling*, 2, 73–83, doi:10.1016/S1463-5003(00)00011-1, 2000. 405, 406
- Hughes, C. W., and B. de Cueves, Why western boundary currents in realistic oceans are inviscid: A link between form stress and bottom pressure torques, *Journal of Physical Oceanography*, 31, 2871–2885, 2001. 405, 406
- IOC, SCOR, and IAPSO, *The international thermodynamic equation of seawater-2010: calculation and use of thermodynamic properties*, Intergovernmental Oceanographic Commission, Manuals and Guides No. 56, UNESCO, doi:10.25607/OPB-1338, 196pp, 2010. 193, 217, 322, 335, 339, 342, 467, 468, 469, 471
- Jackson, J. D., *Classical Electrodynamics*, John Wiley and Sons, New York, USA, 848 pp, 1975. 507
- Jaynes, E. T., Information theory and statistical mechanics, *Physical Review*, 106(4), 620–630, doi:10.1103/PhysRev.106.620, 1957. 348, 597
- Jeevanjee, N., and D. Romps, Effective buoyancy, inertial pressure, and the mechanical generation of boundary layer mass flux by cold pools, *Journal of Atmospheric Sciences*, 72, 3199–3213, doi:10.1175/JAS-D-14-0349.1, 2015a. 499
- Jeevanjee, N., and D. Romps, Effective buoyancy at the surface and aloft, *Quarterly Journal of the Royal Meteorological Society*, 142, 811–820, doi:10.1002/qj.2683, 2015b. 493, 499
- Johnson, R. S., *A Modern Introduction fo the Mathematical Theory of Water Waves*, Cambridge Texts in Applied Mathematics, 1997. 43, 44, 157, 255
- Kamenkovich, V. M., *Fundamentals of Ocean Dynamics*, Elsevier Scientific Publishin Company, Amsterdam, 249 pp, 1977. 188, 209, 213, 214, 323
- Karoly, D. J., P. C. McIntosh, P. Berrisford, T. J. McDougall, and A. C. Hirst, Similarities of the Deacon cell in the Southern Ocean and Ferrel cells in the atmosphere, *Quarterly Journal of the Royal Meteorological Society*, 123, 519–526, doi:10.1002/qj.49712353813, 1997. 155
- Klinger, B., and T. Haine, *Ocean Circulation in Three Dimensions*, Cambridge University Press, 466, 2019. 329
- Klocker, A., and T. J. McDougall, Influence of the nonlinear equation of state on global estimates of dianeutral advection and diffusion, *Journal of Physical Oceanography*, 40, 1690–1709, doi:10.1175/2010JPO4303.1, 2010a. 483
- Klocker, A., and T. J. McDougall, Quantifying the consequences of the ill-defined nature of neutral surfaces, *Journal of Physical Oceanography*, 40, 1866—1880, doi:10.1175/2009JPO4212.1, 2010b. 483
- Kopp, R. E., J. X. Mitrovica, S. M. Griffies, J. Yin, C. C. Hay, and R. J. Stouffer, The impact of Greenland melt on regional sea level: a preliminary comparison of dynamic and static equilibrium effects, *Climatic Change Letters*, 103, 619–625, doi:10.1007/s10584-010-9935-1, 2010. 375

- Kreuzer, H. J., *Nonequilibrium thermodynamics and its statistical foundations*, 438 pp., Oxford Science Publications, New York, 1981. 115, 122
- Kubo, R., *Statistical Mechanics: An Advanced Course with Problems and Solutions*, North-Holland Publishing Company, Amsterdam, 1965. 210
- Kundu, P., I. Cohen, and D. Dowling, *Fluid Mechanics*, Academic Press, 921 + xxiv pp, 2016. 11, 42, 245, 276, 277, 278, 284, 291, 297
- Landau, L. D., and E. M. Lifshitz, *Statistical Physics: Part 1*, Pergamon Press, Oxford, UK, 544 pp, 1980. 165, 209, 214, 322, 323
- Landau, L. D., and E. M. Lifshitz, *Fluid Mechanics*, Pergamon Press, Oxford, UK, 539 pp, 1987. 191, 297, 313, 315, 319, 322, 324
- Lauritzen, P., N. Kevlahan, T. Toniazzo, C. Eldred, T. Dubos, A. Gassmann, V. Larson, C. Jablonowski, O. Guba, B. Shipway, B. Harrop, F. Lemarie, R. Tailleux, A. Herrington, W. Large, P. Rasch, A. Donahue, H. Wan, A. Conley, and J. Bacmeister, Reconciling and improving formulations for thermodynamics and conservation principles in Earth System Models (ESMs), *Journal of Advances in Modeling Earth Systems*, doi:10.1029/2022MS003117, 2022. 339
- Lautrup, B., *Physics of Continuous Matter: Exotic and Everyday Phenomena in the Macroscopic World*, Institute of Physics Publishing, Bristol and Philadelphia, 2005. 7, 242, 252, 261, 297, 463, 466, 467, 501
- Lemons, D. S., *A Student's Guide to Entropy*, Cambridge University Press, Cambridge, doi: 10.1017/CBO9780511984556, 2013. 172, 174, 177
- Lieb, E. H., and J. Yngvason, A fresh look at entropy and the second law of thermodynamics, *Physics Today*, 53, 32–37, doi:10.1063/1.883034, 2000. 171
- Lilly, J., Kinematics of a fluid ellipse in a linear flow, *Fluids*, 3(16), doi:10.3390/fluids3010016, 2018. 84
- Loose, N., G. M. Marques, A. Adcroft, S. Bachman, S. M. Griffies, I. Grooms, R. W. Hallberg, and M. Jansen, Comparing two parameterizations for the restratification effect of mesoscale eddies in an isopycnal ocean model, *Journal of Advances in Modeling Earth Systems (JAMES)*, 15, doi:10.1029/2022MS003518, 2023. 390
- Lorenz, E. N., Available potential energy and the maintenance of the general circulation, *Tellus*, 7, 157–167, 1955. 447, 448
- MacCready, P., and P. Rhines, Buoyant inhibition of ekman transport on a slope and its effect on stratified spin-up, *Journal of Fluid Mechanics*, 223, 631–661, doi:10.1017/S0022112091001581, 1991. 569
- MacCready, P., and P. Rhines, Slippery bottom boundary layers on a slope, *Journal of Physical Oceanography*, 23, 5–22, doi:10.1175/1520-0485(1993)023<0005:SSBLOA>2.0.CO;2, 1993. 569
- MacKinnon, J., Louis St. Laurent, and A. C. Naveira Garabato, Diapycnal mixing processes in the ocean interior, in *Ocean Circulation and Climate, 2nd Edition: A 21st century perspective, International Geophysics Series*, vol. 103, edited by G. Siedler, S. M. Griffies, J. Gould, and J. Church, pp. 159–183, Academic Press, doi:10.1016/B978-0-12-391851-2.00007-6, 2013. 311

- Malvern, L. E., *Introduction to the Mechanics of a Continuous Media*, Prentice-Hall, Englewood Cliffs, USA, 713pp, 1969. 14, 48, 55, 61, 269, 581
- Marion, J. B., and S. T. Thornton, *Classical Dynamics of Particles and Systems*, Harcourt Brace Jovanovich, San Diego, USA, 602 pp, 1988. x
- Markowski, P., and Y. Richardson, *Mesoscale Meteorology in Midlatitudes*, Wiley-Blackwell Publishers, Oxford, UK, 2010. 426, 499
- Marshall, D. P., and H. R. Pillar, Momentum balance of the wind-driven and meridional overturning circulation, *Journal of Physical Oceanography*, 41, 960–978, doi:10.1175/2011JPO4528.1, 2011. 427
- Marshall, J., and R. A. Plumb, *Atmosphere, Ocean, and Climate Dynamics*, 1st ed., Academic Press, Amsterdam, 319pp, 2008. 255, 375, 503, 547, 553
- Maxwell, J., *Theory of Heat*, 3rd ed., Longmans, Green, and Company, London, 313, 1872. 162, 213
- McCabe, R., P. MacCready, and G. Pawlak, Form drag due to flow separation at a headland, *Journal of Physical Oceanography*, 36, 2136–2152, doi:10.1175/JPO2966.1, 2006. 389
- McDougall, T., R. Feistel, and R. Pawlowicz, Thermodynamics of seawater, in *Ocean Circulation and Climate, 2nd Edition: A 21st Century Perspective, International Geophysics Series*, vol. 103, edited by G. Siedler, S. M. Griffies, J. Gould, and J. Church, pp. 141–158, Academic Press, 2013. 471
- McDougall, T. J., Double-diffusive convection caused by coupled molecular diffusion, *Journal of Fluid Mechanics*, 126, 379–397, doi:10.1017/S0022112083000221, 1983. 335
- McDougall, T. J., Neutral surfaces, *Journal of Physical Oceanography*, 17, 1950–1967, doi:10.1175/1520-0485(1987)017<1950:NS>2.0.CO;2, 1987a. 472, 476
- McDougall, T. J., Thermobaricity, cabbeling, and water-mass conversion, *Journal of Geophysical Research*, 92, 5448–5464, doi:10.1029/JC092iC05p05448, 1987b. 472, 476
- McDougall, T. J., The vertical motion of submesoscale coherent vortices across neutral surfaces, *Journal of Physical Oceanography*, 17, 2334–2342, 1987c. 487
- McDougall, T. J., Potential enthalpy: a conservative oceanic variable for evaluating heat content and heat fluxes, *Journal of Physical Oceanography*, 33, 945–963, doi:10.1175/1520-0485(2003)033<0945:PEACOV>2.0.CO;2, 2003. 217, 338, 339, 468
- McDougall, T. J., and R. Feistel, What causes the adiabatic lapse rate, *Deep-Sea Research*, 50, 1523–1535, 2003. 216
- McDougall, T. J., and D. R. Jackett, On the helical nature of neutral trajectories in the ocean, *Progress in Oceanography*, 20, 153–183, 1988. 480, 483
- McDougall, T. J., and J. S. Turner, The role of cross-diffusion on finger double-diffusive convection, *Nature*, 299, 812–814, doi:10.1038/299812a0, 1982. 335

McDougall, T. J., S. Groeskamp, and S. M. Griffies, On geometric aspects of interior ocean mixing, *Journal of Physical Oceanography*, 44, 2164–2175, doi:10.1175/JPO-D-13-0270.1, 2014. 475, 476

McDougall, T. J., P. M. Barker, R. M. Holmes, R. Pawlowicz, S. M. Griffies, and P. J. Durack, The interpretation of temperature and salinity variables in numerical ocean model output, and the calculation of heat fluxes and heat content, *Geoscientific Model Development*, 14, 6445–6466, doi:10.5194/gmd-14-6445-2021, 2021. 217, 338

McWilliams, J. C., Submesoscale, coherent vortices in the ocean, *Reviews of Geophysics*, 23, 165–182, 1985. 487

Mermin, N. D., What's wrong with these equations?, *Physics Today*, 42, 9–11, doi:10.1063/1.2811173, 1989. viii

Meyer, R., *Introduction to mathematical fluid dynamics*, Dover Publications, New York, 1971. 277, 282, 300

Misner, C., K. Thorne, and J. Wheeler, *Gravitation*, W.H. Freeman and Co., 1279 pages, 1973. 602

Mitrovica, J. X., M. E. Tamisiea, J. L. Davis, and G. A. Milne, Recent mass balance of polar ice sheets inferred from patterns of global sea-level change, *Nature*, 409, 1026–1029, 2001. 375, 376

Molemaker, M., J. McWilliams, and W. Dewar, Submesoscale instability and generation of mesoscale anticyclones near a separation of the California Undercurrent, *Journal of Physical Oceanography*, 45, 613–629, doi:10.1175/JPO-D-13-0225.1, 2015. 385

Müller, P., *The Equations of Oceanic Motions*, 1st ed., Cambridge University Press, Cambridge, 302pp, 2006. 322

Munk, W., and E. Palmén, Note on the dynamics of the Antarctic Circumpolar Current, *Tellus*, 3, 53–55, 1951. 405

Nurser, A. G., R. Marsh, and R. Williams, Diagnosing water mass formation from air-sea fluxes and surface mixing, *Journal of Physical Oceanography*, 29, 1468–1487, doi:10.1175/1520-0485(1999)029<1468:DWMFFA>2.0.CO;2, 1999. 448

Olbers, D. J., J. Willebrand, and C. Eden, *Ocean Dynamics*, 1st ed., Springer, Berlin, Germany, 704 pages, 2012. xii, 11, 188, 189, 322, 335, 338, 339, 476

Paparella, F., and W. R. Young, Horizontal convection is non-turbulent, *Journal of Fluid Mechanics*, 466, 205–214, doi:10.1017/S0022112002001313, 2002. 441

Pedlosky, J., *Ocean Circulation Theory*, Springer-Verlag, Berlin Heidelberg New York, 403 + xi pp, 1996. 503

Peterson, H. G., and J. Callies, Rapid spin up and spin down of flow along slopes, *Journal of Physical Oceanography*, doi:10.1175/JPO-D-21-0173.1, 2022. 571

Pope, S. B., *Turbulent Flows*, Cambridge Press, 2000. 11, 21, 33, 80

- Pratt, L. J., and J. A. Whitehead, *Rotating Hydraulics: Nonlinear Topographic Effects in the Ocean and Atmosphere*, 589 pp., Springer Science + Business Media, New York, 2008. 329
- Pride, S. R., *An Introduction to Continuum Physics*, Cambridge University Press, Cambridge, UK, 2025. 1, 237
- Reif, F., *Fundamentals of Statistical and Thermal Physics*, McGraw-Hill, New York, 1965. 1, 11, 165, 171, 177, 180, 347
- Reiner, M., The deborah number, *Physics Today*, 17, 62, doi:10.1063/1.3051374, 1964. 7
- Ringler, T., J. Saenz, P. Wolfram, and L. Van Roekel, A thickness-weighted average perspective of force balance in an idealized Circumpolar Current, *Journal of Physical Oceanography*, 47, 285–302, doi:10.1175/JPO-D-16-0096.1, 2017. 448
- Rintoul, S. R., The global influence of localized dynamics in the Southern Ocean, *Nature*, 558, 209–218, doi:10.1038/s41586-018-0182-3, 2018. 406
- Rintoul, S. R., and A. C. Naveira Garabato, Dynamics of the Southern Ocean circulation, in *Ocean Circulation and Climate, 2nd Edition: A 21st Century Perspective, International Geophysics Series*, vol. 103, edited by G. Siedler, S. M. Griffies, J. Gould, and J. Church, pp. 471–492, Academic Press, 2013. 406
- Rintoul, S. R., C. W. Hughes, and D. Olbers, The Antarctic Circumpolar Current system, in *Ocean Circulation and Climate, 1st Edition, International Geophysics Series*, vol. 103, edited by G. Siedler, J. Gould, and J. Church, pp. 271–301, Academic Press, 2001. 406
- Rossby, C.-G., On displacements and intensity changes of atmospheric vorticity, *Journal of Marine Research*, 7, 175–187, 1948. 258
- Ruan, X., J. O. Wenegrat, and J. Gula, Slippery bottom boundary layers: The loss of energy from the general circulation by bottom drag, *Geophysical Research Letters*, 48, doi:10.1029/2021GL094434, 2021. 571
- Saffman, P. G., *Vortex Dynamics*, Cambridge University Press, Cambridge, England, 1992. 245, 246
- Salmon, R., *Lectures on Geophysical Fluid Dynamics*, Oxford University Press, Oxford, England, 378 + xiii pp., 1998. xii, 1, 11, 48, 276
- Samelson, R., *The Theory of Large-Scale Ocean Circulation*, Cambridge University Press, Cambridge, UK, 193 pp., 2011. 503
- Santiago, J., and M. Visser, Gravity's universality: The physics underlying Tolman temperature gradients, *International Journal of Modern Physics D*, 27, doi:10.1142/S021827181846001X, 2018. 210
- Schneider, T., I. M. Held, and S. Garner, Boundary effects in potential vorticity dynamics, *Journal of Atmospheric Sciences*, 60, 1024–1040, doi:10.1175/1520-0469(2003)60<1024:BEIPVD>2.0.CO;2, 2003. 448
- Segel, L. A., *Mathematics Applied to Continuum Mechanics*, 590 pp., Dover Publications, 1987. 73, 74, 84, 278, 282

Serrin, J., Mathematical principles of classical fluid mechanics, in *Fluid Mechanics I*, edited by S. Flügge and C. Truesdell, pp. 125–263, Springer-Verlag, Berlin, 1959. 102, 278, 280, 322, 409, 532, 537

Shannon, C. E., A mathematical theory of communication, *Bell System Technical Journal*, 27(3), 379–423, doi:10.1002/j.1538-7305.1948.tb01338.x, reprinted with corrections in Bell Syst. Tech. J., 27, 623–656 (1948)., 1948. 348, 597

Smagorinsky, J., General circulation experiments with the primitive equations: I. The basic experiment, *Monthly Weather Review*, 91, 99–164, doi:10.1175/1520-0493(1963)091<0099:GCEWTP>2.3.CO;2, 1963. 354, 596

Smagorinsky, J., Some historical remarks on the use of nonlinear viscosities, in *Large Eddy Simulation of Complex Engineering and Geophysical Flows*, edited by B. Galperin and S. A. Orszag, pp. 3–36, Cambridge University Press, 1993. 284

Smith, K. S., and G. K. Vallis, The scales and equilibration of midocean eddies: freely evolving flow, *Journal of Physical Oceanography*, 31, 554–570, doi:10.1175/1520-0485(2001)031<0554:TSAEOM>2.0.CO;2, 2001. 514

Spence, P., R. M. Holmes, A. McC. Hogg, S. M. Griffies, K. D. Stewart, and M. H. England, Localized rapid warming of West Antarctic subsurface waters by remote winds, *Nature Climate Change*, doi:10.1038/NCLIMATE3335, 2017. 570

Staniforth, A. N., *Global Atmospheric and Oceanic Modelling*, Cambridge University Press, 2022. 355

Stanley, G. J., Neutral surface topology, *Ocean Modelling*, doi:10.1016/j.ocemod.2019.01.008, 2019. 483

Stanley, G. J., T. J. McDougall, and P. M. Barker, Algorithmic improvements to finding approximately neutral surfaces, *Journal of Advances in Modeling Earth Systems*, 13, doi:10.1029/2020MS002436, 2021. 483

Straub, D. N., On the transport and angular momentum balance of channel models of the Antarctic Circumpolar Current, *Journal of Physical Oceanography*, 23, 776–782, doi:10.1175/1520-0485(1993)023<0776:OTTAAM>2.0.CO;2, 1993. 406

Stull, R., *An Introduction to Boundary Layer Meteorology*, 670 pp., Kluwer Academic Publishers, 1988. 547

Sutherland, B. R., *Internal Gravity Waves*, Cambridge University Press, 2010. 346

Symon, K., *Mechanics*, Addison-Wesley Publishing Co., Reading, MA, USA, 639 pp, 1971. x

Tarshish, N., N. Jeevangee, and D. Lecoanet, Buoyant motion of a turbulent thermal, *Journal of the Atmospheric Sciences*, 75, 3233–3244, doi:10.1175/JAS-D-17-0371.1, 2018. 463, 499

Tennekes, H., and J. Lumley, *A First Course in Turbulence*, 300 pp., MIT Press, Cambridge, USA, 1972. 214, 291, 547

Thess, A., *The Entropy Principle: Thermodynamics for the Unsatisfied*, Springer-Verlag, Berlin, Heidelberg, 2011. 171

- Thorne, K., and R. Blandford, *Modern Classical Physics*, Princeton University Press, Princeton, USA, 1511 + xl pp, 2017. 322, 324
- Thorpe, S., The dynamics of the boundary layers of the deep ocean, *Science Progress*, 72, 189–206, 1988. 547
- Thorpe, S., *The Turbulent Ocean*, 439 pp., Cambridge University Press, Cambridge, UK, 2005. 547
- Tomczak, M., and J. S. Godfrey, *Regional Oceanography: An Introduction*, Pergamon Press, Oxford, England, 422 + vii pp, 1994. 361
- Tracy, E. R., A. J. Brizard, A. S. Richardson, and A. N. Kaufman, *Ray Tracing and Beyond: Phase Space Methods in Plasma Wave Theory*, Cambridge University Press, 2014. xv
- Tromp, J., *Theoretical and Computational Seismology*, Princeton University Press, Princeton, USA, 2025a. xv, 14, 48, 49, 50, 61, 66, 69, 95, 235, 263, 581
- Tromp, J., *A Geometrical Introduction to Tensor Calculus*, Princeton University Press, Princeton, USA, 2025b. 48, 50, 66, 269
- Truesdell, C., The mechanical foundations of elasticity and fluid dynamics, *Journal of Rational Mechanics and Analysis*, 1, 125–300, 1952. 266
- Truesdell, C., Notes on the history of the general equations of hydrodynamics, *American Mathematical Monthly*, 60, 445–458, doi:10.2307/2308407, 1953. 14, 17, 20
- Truesdell, C., *The kinematics of vorticity*, Dover Publications, Mineola, New York, 1954. 14, 15, 17, 20, 146
- Vallis, G. K., *Atmospheric and Oceanic Fluid Dynamics: Fundamentals and Large-scale Circulation*, 2nd ed., Cambridge University Press, Cambridge, 946 + xxv pp, 2017. 11, 188, 214, 216, 242, 255, 287, 322, 346, 361, 406, 407, 416, 441, 446, 455, 467, 471, 476, 503, 528, 537, 547, 569, 618
- Van Dyke, M., *Perturbation methods in fluid mechanics*, 1st ed., The Parabolic Press, Stanford, California, USA, 271, 1975. 291
- van Heijst, G., Dynamics of vortices in rotating and stratified flows, in *Fronts, Waves, and Vortices in Geophysical Flows*, Lecture notes in Physics 805, p. 192, Springer, 2010. 536, 546
- van Sebille, E., S. M. Griffies, R. Abernathey, T. Adams, P. Berloff, A. Biastoch, B. Blanke, E. Chassignet, Y. Cheng, C. Cotter, E. Deleersnijder, K. Döös, H. Drake, S. Drijfhout, S. Gary, A. Heemink, J. Kjellsson, I. Koszalka, M. Lange, C. Lique, G. MacGilchrist, R. Marsh, G. M. Adame, R. McAdam, F. Nencioli, C. Paris, M. Piggott, J. Polton, S. Rühs, S. Shah, M. Thomas, J. Wang, P. Wolfram, L. Zanna, and J. Zika, Lagrangian ocean analysis: fundamentals and practices, *Ocean Modelling*, 121, 49–75, doi:10.1016/j.ocemod.2017.11.008, 2018. 23
- von Arx, W. S., *An Introduction to Physical Oceanography*, Addison-Wesley Publishing Company, Reading, Massachusetts, USA, 422 pp, 1962. 542, 560, 564

- Wåhlin, A., R. Muench, L. Arneborg, G. Björk, H. Ha, S. Lee, and A. Alsén, Some implications of Ekman layer dynamics for cross-shelf exchange in the amundsen sea, *Journal of Physical Oceanography*, 42, 1461–1474, doi:10.1175/JPO-D-11-041.1, 2012. 570
- Webb, D., R. Holmes, P. Spence, and M. England, Barotropic Kelvin wave-induced bottom boundary layer warming along the West Antarctic Peninsula, *Journal of Geophysical Research: Oceans*, 124, 1595–1615, doi:10.1029/2018JC014227, 2019. 570
- Webb, D. J., and B. A. de Cueves, On the fast response of the Southern Ocean to changes in the zonal wind, *Ocean Science*, 3, 417–427, doi:10.5194/os-3-417-2007, 2007. 405
- Weiss, J., The dynamics of enstrophy transfer in two-dimensional hydrodynamics, *Physica D: Nonlinear Phenomena*, 48, 273–294, doi:10.1016/0167-2789(91)90088-Q, 1991. 84
- Wenegrat, J. O., and L. N. Thomas, Centrifugal and symmetric instability during ekman adjustment of the bottom boundary layer, *Journal of Physical Oceanography*, 50, 1793–1812, doi:10.1175/JPO-D-20-0027.1, 2020. 571
- Woods, L. C., *The Thermodynamics of Fluid Systems*, Oxford University Press, Oxford, UK, 359pp, 1975. 313
- Young, W. R., Stirring and mixing, in *WHOI 1999 Summer Study Program in Geophysical Fluid Dynamics*, Woods Hole Oceanographic Institute, 1999. 64
- Young, W. R., Dynamic enthalpy, Conservative Temperature, and the seawater Boussinesq approximation, *Journal of Physical Oceanography*, 40, 394–400, doi:10.1175/2009JPO4294.1, 2010. 441, 442, 446, 447, 579
- Young, W. R., An exact thickness-weighted average formulation of the Boussinesq equations, *Journal of Physical Oceanography*, 42, 692–707, doi:10.1175/JPO-D-11-0102.1, 2012. 448
- Zdunkowski, W., and A. Bott, *Dynamics of the Atmosphere: A Course in Theoretical Meteorology*, Cambridge University Press, Cambridge, UK, 719 pp, 2003. 537
- Zeitlin, V., *Geophysical Fluid Dynamics: Understanding (almost) everything with rotating shallow water models*, Oxford University Press, 2018. xix
- Zinnser, W., *Writing to Learn*, Harper Perennial, 1993. xiv

INDEX

- absolute salinity, 188, 467
- absolute temperature, 8
- acoustic waves, 340
 - Boussinesq ocean, 415
- action, xi
- action/reaction law, 262
- adiabatic, 167
- adiabatic lapse rate, 214, 478
- advection
 - reversible, 319
- advection operator, 27
- advection-diffusion equation, 134
- advective time, 285
- advective tracer flux, 119, 121
- ageostrophic velocity, 548
- air-water interface, 292
- anelastic approximation, 140, 416
- angular momentum, 269
- anti-cyclonic, 508
- approximate hydrostatic balance, 249
- arc length, 143
- Archimedean buoyancy, 411, 461
- area
 - evolution, 77, 79, 150
- arrested Ekman layer, 569
- aspect ratio, 357, 418, 419, 505
- association versus causation, xi, 424
- atmospheric form stress, 382, 386
- available potential energy, 447
 - approximate, 453
 - exact, 452
- Avogadro's number, 7
- axial angular momentum, 252
 - atmosphere, 254
- depth integrated, 400
 - ocean, 399
 - ring of air, 253
 - steady state, 403
- back-reaction, 461
- balances, xi
- baroclinic, 359, 516
 - pressure gradient, 361
- baroclinic instability, 525
- baroclinic velocity, 393
- baroclinicity, 447, 509, 520
- barodiffusion, 332
- barometric law, 225
- barotropic, 359
 - pressure gradient, 361
- barotropic velocity, 393, 519
- barotropization, 514
- barycenter, 118
- barycentric velocity, 20, 22, 115, 118, 121, 128, 264
- base manifold, 51, 93
- Bernoulli
 - head, 328
 - potential, 323
 - principle, 325
 - theorem, 324, 325
 - theorem for hydraulic control, 328
 - theorem for pipe flow, 326
- beta-plane approximation, 246, 248
- body forces, xix, 167, 168, 236, 262
- Boltzmann constant, 222
- Boltzmann's H-theorem, 347
- bottom
 - drag, 436
- boundary
 - layers, 291, 547, 548, 556

- stress, 436
velocity, 128
- Boussinesq approximation, 140
traditional, 416
- Boussinesq ocean, 139, 407, 409, 479, 504
density evolution, 415
dynamic enthalpy, 441, 442
energetics, 430, 458
equations, 412
generalized, 457
internal energy, 446
mass, 414
mass continuity, 412
momentum equation, 411
reference density, 141, 456
weight, 414
- budget analysis, ix, 123
- bulk viscosity, 278, 280
- buoyancy, 362, 461
effective, 493, 495
force, 464
frequency, 477
frequency for ideal gas, 478
globally referenced, 472
helium balloon, 489
homogeneous fluid, 416
relation to height, 451
sorting, 454
stratification, 472
work, 431
- cabbeling, 413
- caloric equation of state, 195
- capillary
capillary-gravity waves, 287
pressure, 294, 296
tube, 292
waves, 291
- Cauchy
fundamental lemma, 264
solution, 66, 67
stress principle, 263
theorem, 267
- Cauchy stress tensor, 262
- Cauchy stress vector, 262
- Cauchy-Green deformation tensor, 60
- Cauchy-Green strain tensor, 60
- Cauchy-Stokes decomposition, 74
- causal relations, ix
- causation versus association, 424
- center of mass motion, 109
- center of mass velocity, 118
- centrifugal acceleration, 371, 492, 532–534
- centrifuge, 492
- centripetal acceleration, 532–534
- channel flow, 523
- chemical energy flux, 318
- chemical potential, 182, 188, 193
- chemical reactions, 115
- chemical work, 183
- Christoffel symbols, 29
- circulation, 200
- compatibility
total mass + tracer mass, 120
- compression, 84
- conservation equation
flux-form, 124
material form, 124
- conservation law, 124
material, 341
non-material, 341
- conservation laws, 15, 339
- Conservative Temperature, 217, 335, 337, 467
- constitutive relation, 275, 277
- contact forces, xix, 168, 237, 262
- contact pressure force, 265
- continuity, 140
- continuity equation, 91, 115
- continuum approximation, 2, 4, 19
- continuum hypothesis, 2
- continuum mechanics, 2
- contrapositive proposition, 481
- convective time derivative, 27
- converse proposition, 481
- coordinate
general vertical, 25
material, 23–25, 52
position, 23
spatial, 52
- Couette flow, 276, 289
- couplet, 274
- covariant derivative
vector, 29
- Crocco's theorem, 347

- cross-diffusion, 122
curvature, 294
cyclonic, 508
cyclostrophic balance, 541
- D'Alembert
 paradox, 277
 theorem, 277
- Deborah number, 6
deformation matrix, 47, 55, 66
 discrete algorithm, 57
- deformation rate, 84
deformation rate tensor, 47, 71
- deformational flow, 83
delta sheets of potential vorticity, 448
- density, 468
depth of no motion, 517
developing flow, 27
- deviator, 279
deviatoric friction tensor, 279
deviatoric strain rate tensor, 279, 309
- deviatoric stress, 237, 277
- dia-surface transport, 134
- diabatic process, 167
- diagnostic equation, xi, 30
- dianeutral direction, 475
- diapycnal transport velocity, 107
- differentiable manifold, 169
- diffusive tracer flux, 119, 121, 128
- diffusivity
 eddy, 434
- dilatation, 80
- dilation, 74
- dimensional analysis, xii
- Dirichlet boundary condition, 423
- dissipation, 238, 310
- divergence, 282
- divergence theorem, 90
- diverging flow, 83
- drag coefficient, 436
- dual form stress, 385, 394, 404
- duality
 Eulerian and Lagrangian, 65
- Dufour effect, 332
- dynamic enthalpy, 441
- dynamic pressure, 245
- dynamic topography, 359
- dynamic viscosity, 278
- dynamical constraints, 15
dynamical pressure, 362
- Earth
 radius, 375
- eddy diffusivity, 434
- eddy viscosity, 435, 548
 Ekman layer, 556
- eddy-induced
 velocity, 434
- effective buoyancy, 461, 471, 493, 495
- effective gravity, 248
- Ekman
 arrested, 569
 balance, 548
 bottom layer, 563
 boundary layers, 291, 547, 548
 downwelling, 562
 horizontal transport, 557
 layer thickness, 556
 mass transport, 557
 mechanics, 547
 natural coordinates, 550
 number, 555
 ocean surface layer, 557
 pumping, 560, 562
 Rayleigh drag, 552
 spiral motion, 553
 suction, 560, 562
 transport, 559
 upwelling, 562
 velocity profile, 563
- emergent scales, xii
- energy
 dissipation of kinetic, 309
 dissipation of mechanical, 309
 gravitational potential, 303, 304, 306
 internal, 319
 internal budget, 320
 mechanical, 307, 311
 mechanical energy flux, 311
 total, 319
 total energy conservation, 334
- enthalpy, 191, 336
 budget, 317, 320, 334
 capacity, 195
- entrain, 107
- entropy, 171, 176, 179, 191

- budget, 329
flux, 330
maximum, 180
perfect fluid, 319
source, 330, 334
equation of motion, 239
rotating, 241
spherical, 243
equation of state, 190–192, 220, 467
Boussinesq ocean, 414
linear, 413
equilibrium tide, 377
Euler equation, 242, 281
time symmetry, 300
Euler form, 182
Euler's theorem, 201
Eulerian
duality with Lagrangian, 65
reference frame, 14, 19
region, 125
time derivative, 27
evolving flow, 27
exact differential, 144, 175, 176, 183, 199
hiker analogy, 201
exact geostrophic balance, 537
exact hydrostatic balance, 249
Exner function, 226, 228
extensive property, 115, 123, 169, 175
exterior derivative, 468
external
pressure, 388
pressure gradient, 361
velocity, 393
external forces, 262
external scales, xii
f-plane approximation, 246, 248
Ferrel Cell, 155
Fick's law of diffusion, 332
first kinematic viscosity, 278
first law of thermodynamics, 171, 173, 187, 320
moving fluid, 316
potential temperature, 319
flow lines, 37
flow map, 37, 47, 50, 93
flow versus fluid property, 139, 409
fluid
dynamics, xviii
element, 22, 116, 117, 121, 461
kinematics, xviii
material region, 22
parcel, 21, 116
particle, 20
particle trajectory, 24, 37
region, 23
fluid versus flow property, 139, 409
flux-form conservation law, 88, 339
force couplet, 274
forces
body, 167, 168, 236
contact, 237
form stress, 265, 394, 404
geostrophic eddies, 523
isopycnal layer, 525
isopycnal surface, 523
mathematical expression, 384
Fourier's heat law, 134
Fourier's law of conduction, 318, 332
friction
dissipation, 309, 321
driven velocity, 548
force, 280
vertical shear, 283
frictional
stress tensor, 276
Froude number, 418, 419
functional degrees of freedom, 140
fundamental
thermodynamic relation, 176
Galilean
invariance, 30, 278
transformation, 31, 32, 124
Galilean space-time, 20
gauge
function, 321
symmetry, 143, 146, 238, 321
general vertical coordinates, 25, 129
geopotential, 414
height, 224
height in ideal gas, 360
reference, 304
thickness, 224
geostrophic
balance, xi, 503, 507

- eddies, 523
exact balance, 537
Sverdrup balance, 515
geostrophic eddies, 525
geostrophic flow, 366
geostrophic streamfunction, 508
geostrophy
 pressure coordinates, 510
geothermal heating, 134
Gibbs potential, 184, 192, 210, 316
Gibbs relation, 176
Gibbs-Duhem, 183
global conservation, 341
global instability, *xxi*
gradient wind balance, 543
 regular high, 545
gravest vertical mode, 514
gravitational mass, 414
gravitational potential, 375
 general case, 375
gravitational potential energy, 303
 mixing, 306
 regional, 304
 stratification, 306
gravitational stability, 476
gravitational work, 210, 326
Green's function
 pressure equation, 456
Hadley circulation, 254
haline, 468
 contraction coefficient, 196, 468, 469
Hamilton's principle, xi
harmonic function, 144
heat capacity, 195
heat flow direction, 181
heat function, 191
heating, 173
height and buoyancy relation, 451
Helmholtz
 decomposition, 144, 426
 free energy, 206
homentropic fluid, 319
homogeneous
 fluid, 169
 function, 201
Hooke's Law, 278
hydraulic jump, 328
hydrodynamics, vii, 407
hydrostatic
 approximate balance, 249, 349, 350, 355, 414, 487
 approximate balance for ocean, 413
 background state, 358
 exact balance, 249, 271
 exact versus approximate, 250
 pressure, 355, 463
 pressure evolution, 356, 421
 pressure forces, 272
 primitive equations, 349, 350
 scaling, 357, 417
 torque balance, 274
 vertical motion, 351, 361
hypsometric equation, 224
ideal fluid, 21
ideal gas, 220
 adiabatic lapse rate, 224
 buoyancy frequency, 478
 compressibility, 223
 enthalpy, 223
 equation of state, 220
 geopotential thickness, 224
 heat capacity, 222
 internal energy, 221
 lapse rate, 478
 law, 8
 potential temperature, 226
 sound speed, 224
 thermal expansion coefficient, 223
in situ density, 469
in situ temperature, 217, 335
 evolution, 336
incompressible, 139
incompressible flow, 140
incropping buoyancy, 448
inertial
 frequency, 506
 motion, 539
 oscillation, 540
 reference frame, 14
inertial mass, 414
inexact differential, 173, 175, 176, 183, 200
 integrating factor, 200
information entropy, 347
injection work, 323

- instability
 global, [xxi](#)
 wave, [xxi](#)
- integral curve, [20](#), [38](#)
- integrating factor, [175](#), [176](#), [183](#), [200](#)
- intensive property, [115](#), [123](#), [169](#), [175](#), [312](#)
- interfacial form stress, [382](#), [389](#)
- intermolecular forces, [293](#)
- internal
 energy, [162](#), [171](#), [190](#), [319](#)
 energy and Boussinesq, [446](#)
 energy budget, [320](#)
 energy capacity, [195](#)
 forces, [237](#), [262](#)
 pressure, [388](#)
 pressure gradient, [361](#)
 velocity, [393](#)
- internal gravity waves, [477](#)
- intrinsic coordinates, [531](#)
- inverse barometer sea level, [377](#)
- inverse proposition, [481](#)
- irreversible process, [vii](#), [170](#), [179](#)
- irrotational
 flow, [145](#)
- isobar, [249](#)
- isolated system, [167](#)
- isopycnal, [107](#)
- Jacobian
 evolution, [81](#)
- Joule heating, [321](#)
- Joule unit of energy, [8](#)
- kinematic
 free surface equation, [107](#), [155](#)
 two-dimensional flow, [82](#)
 viscosity, [278](#)
- kinematic boundary condition, [99](#)
 buoyancy surface, [107](#)
 geometric derivation, [102](#)
 material interface, [102](#)
 moving material, [100](#)
 non-divergent flow, [141](#)
 ocean free surface, [106](#)
 permeable surface, [104](#)
 static material, [99](#)
- kinematics
 Eulerian, [17](#)
- Lagrangian, [17](#)
 motion field, [50](#)
 reference manifold, [51](#)
 referential description, [47](#), [51](#)
 relative description, [47](#)
 spatial manifold, [51](#)
 kinetic energy, [307](#)
 Boussinesq, [431](#)
 dissipation, [309](#), [310](#)
 hydrostatic Boussinesq, [458](#)
- kinetic stress, [392](#)
- kinetic theory, [7](#)
- Knudsen number, [4](#), [229](#)
- laboratory reference frame, [19](#)
- Lagrangian
 reference frame, [14](#), [19](#)
 region, [121](#)
 time derivative, [27](#)
- laminar subregion, [291](#)
- Laplacian friction, [554](#)
- law of atmospheres, [225](#)
- Legendre transformation, [189](#), [191](#), [192](#)
- Leibniz's rule, [107](#), [125](#)
- Leibniz-Reynolds transport theorem, [19](#), [125](#), [131](#)
- length scale
 gradient, [6](#)
 macroscopic, [3](#)
 mean free path, [3](#), [9](#)
 measurement, [6](#)
 molecular, [3](#)
 simulation, [6](#)
- level of no motion, [364](#)–[366](#)
- linear equation of state, [470](#)
- linear momentum
 finite volume, [239](#)
 Lagrangian volume, [240](#)
- local conservation, [340](#)
- local Rossby number, [536](#)
- local thermodynamic equilibrium, [1](#), [6](#), [171](#), [301](#), [312](#), [314](#)
- locally referenced potential density, [478](#)
- long range forces, [236](#)
- Lorenz convention, [448](#)
- Mach number, [407](#)
- macroscopically small, [1](#)

macrostate, 162
macrostates, 166
Magnus acceleration, 246
mapping the continuum, 50
mass
 gravitational, 414
 inertial, 414
mass budget, 128
 fluid column, 109, 110
 weak formulation, 117
mass conservation, 15, 93, 115
 arbitrary Eulerian region, 90
 Eulerian, 88
 finite Eulerian region, 88
 Jacobian derivation, 95
 Lagrangian, 91
 Lagrangian derivation, 96
 multi-components, 118
mass density, 467
mass flux, 88
mass flux through a surface, 104
material
 area evolution, 76
 closed system, 167, 173
 constant, 28, 124
 coordinate choices, 25
 coordinates, 24, 52
 curve, 65
 curve evolution, 66
 fluid parcel, 21
 invariance, 28, 30
 invariant, 124
 invariant volume, 140
 open system, 167
 surface, 29
 thickness evolution, 81
 volume evolution, 80
material time derivative, 27
 invariance, 33, 34
 space-time, 36
material tracers, 115
matter
 concentration, 187
 conservation, 339
 flow direction, 187
Maxwell relations, 184, 196
mean free path, 3

mechanical
 pressure, 276, 279
 work, 174
 work from geopotential, 210
mechanical energy, 307, 311
 Boussinesq, 430, 432, 441, 442
 dissipation, 286, 309
 finite volume, 312
membranes, 291
meridional
 overturning circulation, 151
metric acceleration, 244
metric tensor, 59, 60
microscopically large, 1
microstates, 166
molar mass, 183
mole, 7
molecular
 composition of air, 7
 composition of water, 7
 viscosity, 286
moment arm, 252
momentum
 axial angular, 252, 378
momentum equation
 natural coordinates, 535
 spherical, 243
momentum flux, 88
momentum-based, x
Montgomery potential, 525
motion field, 20, 47, 50, 93
motional forces, 493
natural coordinates, 531, 532
 isobars, 549
Navier-Stokes equation, 241, 281, 284
 non-dimensional, 284
 time asymmetric, 300
net stress tensor, 284
Neumann boundary condition, 135, 423
neutral
 directions, 471, 473
 helicity, 480
 surface, 482
neutral diffusion, 485
neutral direction, 486
neutral directions, 472
neutral trajectories, 483

- neutral trajectory velocity, 484
neutrality condition, 475
neutrally buoyant, 461, 464
Newton's
 equation of motion, 239
 third law, 262, 264, 287, 382
 third law and pressure, 265
Newtonian
 fluid, 277, 278
no normal flow boundary condition, 99
no-flux boundary condition, 134, 569
no-slip boundary condition, 282, 289
Noether's Theorem, 15
non-advection tracer flux, 119, 121
non-Boussinesq, 407, 479
non-Boussinesq steric effect, 108
non-conservative
 process, 340
non-dimensionalization, xii
 Ekman balance, 555
 hydrostatic approximation, 417
non-divergent
 velocity field, 140
non-hydrostatic
 primitive equations, 354
non-inertial acceleration, 490
non-inertial force, 490
non-Newtonian constitutive relations, 284
normal
 direction, 99
 evolution equation, 78
 solid-earth bottom, 100
 stress, 277
 vector, 143
normal stress, 263
nuclear reactions, 115

oceanic form stress, 382
outcropping buoyancy, 448
overturning
 Southern Ocean, 155
overturning streamfunction, 151

parameterizations, 6
partial
 entropy, 185
 internal energy, 185
 volumes, 185
passive
 tracer, 120
path integral
 path dependent, 173
pathlines, 37
 analog to car flow, 38
perfect fluid, vii, 21, 168
Pitot tube, 245
planetary
 beta effect, 514
 vorticity, xix, 514
planetary geostrophy, 510
 vorticity equation, 512
planetary vorticity, 514
Poisson equation
 pressure, 493
polar materials, 269
poleward buoyancy transport, 525
postulate of total energy conservation, 334
potential
 enthalpy, 217, 337
 property, 217, 467
 scalar properties, 342
potential density, 469
 locally referenced, 478
potential energy
 Boussinesq, 432
potential temperature, 216, 217, 226, 335, 467
 evolution, 337
 specific entropy, 219
potential vorticity
 delta sheet, 448
pressure
 boundary conditions, 422
 contact stress, 263
 driven velocity, 548
 dynamical pressure, 409
 external, 388
 internal, 388
 Lagrange multiplier, x
 mechanical, 276, 279
 Pascal unit, 8
 Poisson equation, 421
 stagnation, 325
 standard atmosphere, 8
 thermodynamic, 276

- thermodynamical, 279
total, 325
total head, 245
transport, 340
work, 174, 326
- pressure form stress, 265
- pressure gradient
baroclinic, 361
barotropic, 361
bottom, 365
external, 361, 362, 365
hydrostatic, 362, 365, 420, 509
ideal gas, 360
internal, 361, 362, 365, 420
- pressure scale
dynamical, 285, 418
- pressure source, 424
- primitive equations, 349, 350, 504
nomenclature, 354
- principle of equivalence, 414, 491
- prognostic equation, x, 30
- quasi-static process, 170, 179
- quotient rule, 269
- radius of curvature, 533, 539
- rarefied gas, 5
- Rayleigh drag, 278, 551
- real fluid, vii
- reduced gravity
model, 359
- reference
density, 141
geopotential, 304
pressure, 470
- reference manifold, 51
- referential description, 49
- region following the flow, 92
- response function, 195
- reversible process, 170, 179
- Reynolds number, 5, 285, 555, 571
atmosphere, 286
Gulf Stream rings, 286
turbulence, 285
- Reynolds transport theorem, 92, 97
linear momentum, 240
multi-component fluid, 129
- Richardson number, 419
- rigid body rotation, 74
rigid lid, 423
approximation, 515
- Rossby
effect, 258
- Rossby number, 505, 571
Gulf Stream ring, 506
kitchen sink, 506
local, 536
- Rossby waves, 248
- rotating tank, 371, 492, 514
parabolic free surface, 373
rigid-body motion, 373
- rotation, 47
- rotation tensor, 71, 73, 83, 278, 424
- rotational
flow, 83
- salinity, 188, 467
- scalar
streamfunction, 146
- scale analysis, xii, 417
- scale height, 224, 407
- scales
emergent, xii
external, xii
- sea level
thermal expansion, 156
- sea level pressure, 382
- seawater
chemical potential, 188, 193
- second kinematic viscosity, 278, 280
- second law of thermodynamics, 172, 176, 179, 180
- shallow fluid approximation, 351
- shear
flow, 457
strain, 84
stress, 277
- shear stress, 263
- simple ideal gas, 220, 221
- singular limit, 556
- slippery Ekman layer, 569
- slope of a surface, 105
- smooth velocity field, 37
- solenoidal velocity, 139
- Sorret effect, 332
- sorting buoyancy, 454

- sound speed, 196, 444, 468
ideal gas, 224
Southern Ocean overturning, 155
space increments
Eulerian, 65
Lagrangian, 65
space-time tensors, 36
spatial coordinates, 52
spatial manifold, 51, 93
specific
entropy, 219
gas constant for air, 220, 224
volume, 316
specific volume, 187
spin, 424
splat, 424
stagnation pressure, 245
standard
atmosphere, 8
pressure, 3
temperature, 3, 8
state function, 173
static
equilibrium sea level, 376, 377
forces, 461, 493
pressure, 358
static stability, 476

test
 charges, 20
 fluid element, 23, 461, 471, 489
 particles, 20
tetrahedron fluid region, 267
theorem of stress means, 257
thermal
 energy, 171
 equation of state, 467
 expansion coefficient, 196, 468, 469
thermal wind balance, 503, 510, 516
 Antarctic Circumpolar Current, 517
atmosphere, 518
 diagnostics, 517
 ocean, 520
 potential density, 520
thermobaricity, 413
thermodynamic
 configuration space, 169, 442
 integrating factor, 200
 laws, 171
 moving fluid, 314
 postulates, 171
 potential, 173, 189
 pressure, 276
 pressure in non-divergent flow, 276
 specific relations, 187
 state, 166
 systems exchanges, 167
 temperature, 171
thermodynamic equilibrium, 166, 167, 171,
 180, 186, 213, 217, 322
 fluid elements, 323
 macroscopic motion, 322
 salinity, 212, 333
 with geopotential, 210
thermodynamical
 pressure, 279
thermohaline circulation, 409, 416
thickness
 diffusion, 527
third law of thermodynamics, 171
tilting
 material lines, 72
time
 Newtonian, 20, 23
 notation for derivative, 98
 reversal symmetry, 300
 scale for molecular collisions, 10
 tendency, x, 27
 variety of derivatives, 131
topographic form stress, 382, 386
 components, 388
 zonal ridge, 386
tornado, 542
total
 energy, 171, 319
 pressure, 245
 time derivative, 26
tracer
 budget, 128, 133
 concentration, 118, 187
 mass flux, 118
 mechanics, xx, 15
 passive, 120
tracer boundary condition, 133
 air-sea boundary, 135
 bottom, 134
 no-normal derivative, 134
tracer equation, 115, 116, 118
 derived, 118
 Eulerian and Lagrangian forms, 119
tracers
 material, 115
traction, 237
traditional approximation, 248, 351
trajectory, 24, 37
transformation
 between material and spatial, 52
 Jacobian, 55
transformation matrix, 55
transition to turbulence, 285
translation, 74
transport
 streamfunction, 142, 398
 theorem for mechanical energy, 312
 theorem for scalar fields, 128
triple product identity, 198
turbulence, 213, 281, 285
turbulence closure, 6
turbulent
 cascade, 286
two-dimensional
 flow kinematics, 82

- ultraviolet catastrophe, 286
universal gas constant, 8, 220
vector
 streamfunction, 145
vector-invariant velocity equation, 244
velocity
 external, 393
 gradient tensor, 71
 harmonic potential, 148
 internal, 393
 molecular rms speed, 9
 potential, 144, 148
 surface, 100
velocity equation, 245
vertical
 Ekman transport, 559
 energetics with stratification, 306
 flow induced acceleration, 496
 gauge, 148
 shear, 72
 stiffness, 513, 514
 stratification, 476
viscosity, 277
 air, 5
 bulk, 278, 280
 dynamic, 5, 278
 eddy, 435
 first, 278
 kinematic, 5, 278
 second, 278, 280
 water, 5
viscosity tensor, 279
viscous
 dissipation, 310
 flux, 310
volume
 evolution, 79
volume budget
 column of water, 107
 material region, 92
volume evolution, 91, 128, 150
vortex
 force, 246
 lines, 72
vortical flow, 145
vorticity, 73, 82, 83, 200, 282, 325
 planetary geostrophic, 512
water mass, 217
wave
 acoustic, 415
 capillary, 291
 internal gravity, 477
wave instability, xxi
weak formulation, 19, 117, 131, 272, 274
well-defined surface, 480
wind-driven circulation, 562
wing flow, 325
work-energy theorem, 326
working, 173
world line, 20
Young-Laplace formula, 294, 296
 derivation, 294
zero buoyancy layer thickness, 448
zeroth law of thermodynamics, 171
zonal
 ridge and topographic form stress, 386